Aspects of Sway Frame Design and Ductility of Composite End Plate Connections

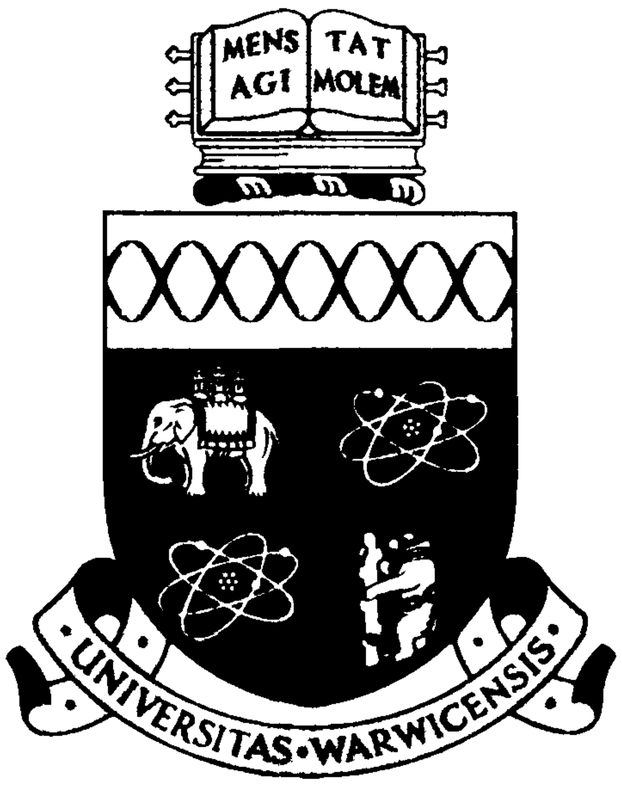

Nigel D Brown BEng(Hons)

Department of Engineering

University of Warwick

Thesis submitted to the University of Warwick for the degree of

Doctor of Philosophy

December 1995

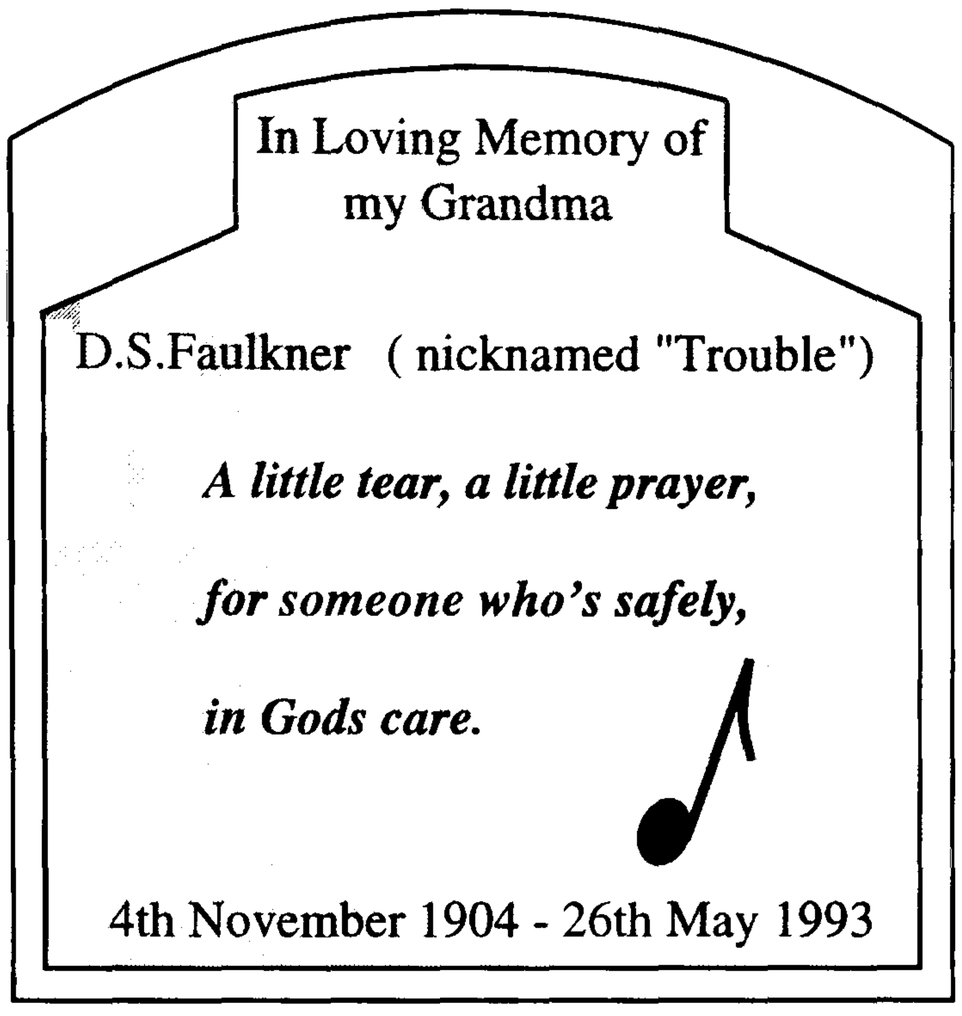
In Loving Memory of
my Grandma
D.S.Faulkner (nicknamed "Trouble")
A little tear, a little prayer,
for someone who's safely,
in Gods care.
4th November 1904 - 26th May 1993

Summary

This thesis reports work on two aspects of framed structures; part I is concerned with sway frames and part II with the ductility of composite flush end plate connections.

Part I has investigated the effect of adopting standardised end plate connections as the method of providing the load path between the structural members of a steelwork sway frame. Practical low to medium rise multi-storey frame geometries have been designed in accordance with limit state principles in conjunction with the Wind-Moment Method. Each frame was analysed by undertaking a second-order elastic-plastic computer analysis to ascertain their structural performance, with particular emphasis directed towards problems associated with stability and sway deflections. The computer simulation necessitated the formulation of a prediction equation that modeled the initial stiffness characteristics of the standard connections. This model has been verified by comparison with full scale experimental test results, mainly taken from the literature.

The investigation confirms that standardised end plate connections provide levels of stiffness and resistance which enable unbraced steel frames to be safely designed by the Wind-Moment method. There are however certain frame geometries where serviceability considerations dictate that stiffening to the frame would be necessary, if the standardised end plate connections were used.

Part II has investigated the ductility of five major axis composite flush end plate connections that incorporate nominally identical amounts of reinforcement in conjunction with either 457 or 533 serial size Universal Beams. Other variable parameters include end plate thickness and horizontal spacing of the rebars. The work was undertaken experimentally and the results analysed in the context of connection performance.

The results have shown that it will not prove difficult to ensure virtually rigid behaviour of the overall composite connection, despite the use of relatively thin end plates. Moreover, the experiments also show that the rotation capacity of composite connections in which 1% reinforcement is provided, would be sufficient to allow plastic methods of design to be used for composite beams with 457 serial size designations; however, ductility remains a problem when the depth of beam is further increased. To this end, an empirical model for assessment of ductility has been proposed, based on the observed deformation characteristics of the joint as a whole. This enables the total rotation capacity of one type of a composite connection to be determined when the failure occurs by fracture of the reinforcing bars.

Declaration

I declare that the work contained within this this is the result of my own investigations and has not been taken from any other research except where specific reference has been made. None of this work has been submitted for a higher qualification at any other establishment.

Acknowledgements

I am indepted to my supervisor, Dr D. Anderson, who has provided invaluable guidance, support and encouragement throughout the duration of this project.

I would also like to thank the Engineering and Physical Sciences Research Council (E.P.S.R.C.) and the Steel Construction Institute (S.C.I.), for providing the financial support for the project. Furthermore, my appreciation and gratitude is extended to the Civil Engineering Group at the University of Warwick, for the financial support during the dissertation period.

Also, I would like to extend my thanks to the workshop technicians at the University of Warwick, Messers C.W.Banks, C.J.Horsley (prior to his retirement in 1993), D.T.Smith and G.Hackett, for their skillful assistance and guidance during the construction and execution of the experimental programme. Furthermore, I would also like to thank the photographic technician of the Engineering Department, Mr G.H.Canham.

In addition, the guidance provided by Mr A. Hughes during the first part of this thesis, whilst working on secondment from Ove Arup and Partners at S.C.I., is greatfully acknowledged.

Finally, the loving support extended to me from my parents and my wife, have been a tower of inspiration and strength throughout the duration of my doctoral studies and is affectionately acknowledged.

Contents

Part II

Ductility of composite end plate connections

Appendices - Volume II

Notation

Upper case letters

A_s - Total steel area applicable to the reinforcement within the slab of a composite connection

A_{vc} - Shear area

B_{bf} - Width of the lower beam flange

B_{cf} - Width of the column flange

C_{bf} - Predicted compressive force acting through the lower beam flange

D - Depth of the beam member

D_b - Lever arm to the bolts measured from the base of the beam's flange

D_c - Depth of the column section

D_r - Lever arm to the reinforcement measured from the base of the beam's flange

E - Young's modulus for steel

E_{1t} - Vertical distance between the tensile bolts and the outermost surface of the top flange of the beam

F_b - Compressive resistance of the beam cross-section

F_{bc} - Flexibility of a bolted connection

F_c - Applied axial load in the member

F_{cf} - Flexibility of the column flange

F_{cw} - Flexibility of a column web panel

F_{ep} - Flexibility of the end plate

F_i - Force in a connection component

$F_{i.Rd}$ - Design resistance of a connection component

F_s - Tensile resistance of the concrete floor

F_t - Tensile resistance of the bolts to BS5950

G - Horizontal distance between bolt centres or the Shear modulus

H_t - Storey height

I - Second moment of area

I_b - Second moment of area applicable to a beam member

I_c - Second moment of area applicable to a cracked composite beam

I_{cf} - Second moment of area applicable to a single flange outstand

I_{ep} - Second moment of area applicable to the end plate

I_{uc} - Second moment of area applicable to an uncracked composite beam

K_{bc} - Stiffness of a bolted connection

K_i - Stiffness factor for a connection component

K_j - Connection stiffness

K_{ts} - Spring stiffness

L_E - Effective length

L_b - Lever arm to the centre of the top bolt row measured from the centre of the lower flange or span of beam

L_c - Cracked length of a continuous composite beam

L_f - Leg length of flange weld

L_{poc} - Distance between the the centre line of the column and the adjacent point of contraflexure at an internal span of a continuous beam

L_r - Lever arm to the centre of the reinforcement measured from the centre of the lower flange

L_{uc} - Uncracked length of a continuous composite beam

L_w - Leg length of web weld

L_1 - Length of reinforcement

L_2 - Slip at the slab/beam interface of a composite connection

$\bar{M}$ - Connection classification by strength

M_A - Moment at the left hand connection of an internal span of a continuous composite beam

M_B - Moment at the right hand connection of an internal span of a continuous composite beam

M_{AD} - External moment applicable to the cracked composite beam

M_{CD} - Internal moment applicable to the uncracked composite beam at mid span

M_{DA} - Internal moment applicable to the cracked composite beam

M_{DC} - Internal moment applicable to the uncracked composite beam

Mp_{conn} - Predicted moment of resistance for a composite connection

Mp_{steel} - Predicted moment of resistance of the bolted steelwork connection

Mp_{rein} - Predicted moment of resistance for a composite connection when only the reinforcement within the slab is considered

M_b - Lateral-torsional buckling resistance moment

M_j - Moment

$M_{pl.Rd}$ - Moment of resistance for a composite beam with respect to negative bending

M_{ult} - Moment of resistance for a composite connection determined experimentally

M_x - Largest column end moment

P - Axial load

P_b - Bolt spacing within the depth of the connected beam

P_c - Compression resistance of a column member

P_1 - Distance to the first shear stud measured from the face of the column

P_2 - Pitch of the shear studs along the hogging moment region of a composite beam

Q - Shear force

R_b - Tensile resistance of the bolts in accordance with Eurocode 3 : Annex J

R_f - Compressive resistance of the beam's lower flange

R_r - Tensile resistance of the reinforcement

$S_{j.init}$ - Connection's initial stiffness

S_b - Span of a composite beam

S_j - Secant stiffness

S_{rigid} - Rigid boundary applicable to the classification by rotation stiffness

S_1 - The vertical distance between the centre line of the top tension and the top of the upper beam flange

T - Bolt force in a steelwork connection

X_p - The depth of the plastic neutral axis below the upper beam flange

Lower case letters

a - Vertical distance between the centre line of the top bolt row and the centre line of the top beam flange

b - Vertical distance between the centre line of the top beam flange and the centre line of the slab reinforcement

b_c - Effective width of the concrete slab

b_{eff} - Effective breadth

d - Width of a single column flange outstand

d_c - The effective depth of a concrete slab

d_{ep} - The depth of the end plate

f_{yb} - Average yield stress applicable to the beam cross-section

f_{ybf} - Yield stress applicable to the lower beam flange

f_{ybw} - Yield stress applicable to the beam's web

f_{yr} - Yield stress applicable to the reinforcement

$f\left(\delta_{cf}\right)$ - Elongation of the reinforcement due to the column flange deformation

h - Vertical distance below the centre line of the top bolt row to the assumed point of rotation for a composite connection

h_1 - Lever arm from the highest bolt row in the connection to the centre of resistance of the compression zone

i - Number of tension bolt rows that have yielded under the connection moment

k - Secant stiffness applicable to a welded shear stud

k_1 - Stiffness of a column web panel

l - Length

l_a - Lever arm

m - Equivalent uniform moment factor

m_{cf} - Horizontal distance between the bolt position and the column web

m_{ep1} - Horizontal distance between the bolt position and the beam web

m_{ep2} - Vertical distance between the underside of the beam's tension flange and the tensile bolts

n - Number of shear studs provided within the hogging moment region of a composite beam

t - Thickness

t_{bf} - Thickness of the lower beam flange

t_{bw} - Thickness of the beam's web

t_{cf} - Thickness of the column flange

t_{cw} - Thickness of the column web

t_{ep} - Thickness of the end plate

tg - Tangent of an angle

r_b - Single bolt force acting through a column flange outstand

r_k - Root radius applicable to the column serial size

r_y - Radius of gyration about minor axis

u - Buckling parameter

v - Slenderness factor

z - Lever arm or depth of shear zone

Upper case Greek letters

Δ - Displacement

Δ_1 - Uncracked beam deflection

Δ_2 - Cracked beam deflection

Δ_l - Extension of the reinforcement

θ_A - Rotation at the left hand connection of an internal span of a continuous composite beam

θ_B -Rotation at the right hand connection of an internal span of a continuous composite beam

Lower case Greek letters

β - Geometrical or a bending moment distribution coefficient

γ - Flexibility factor

δ - Displacement

δ_{cf} - Column flange deformation

δ_{ep} - End plate deformation

ϵ - Strain in the reinforcement

η - Force ratio coefficient

λ_{LT} - Slenderness ratio

μ - Stiffness ratio

μ_i - Modification factor

ν - Poisson's ratio

τ - Uniform shear stress

τ_ϵ - Shear strain

ϕ_j - Angular rotation

ϕ_u - Predicted rotation capacity for a composite connection

ϕ_{ult} - Rotation capacity for a composite connection determined experimentally

Part I

Sway frame design incorporating standardised connections

Chapter 1

Wind-Moment design for unbraced frames

1.1 Introduction

For the design of unbraced frames, the traditional design approach has been to rely on the rotational stiffness of the connections to provide an adequate medium through which the stability of the structure can be assured. To analyse such a frame however, would be far from simple due to the inherent indeterminancy of the structure as a whole. Consequently, a design method was devised whereby the rotational stiffness of the connections was assumed to provide resistance to the horizontal forces only, and ignored moments developed in the connections under the action of gravity loads. This approach is termed the *Wind-Moment* or *Wind-Connection* Method[1] and offers an attractive approach for the design of unbraced structural steel frames.

The method derives its popularity as a result of rendering the frame statically determinate, thereby simplifying the analysis considerably. To achieve this transformation the following assumptions were adopted :

1. The beam members were treated as though they were simply supported

under the action of gravity loads. The connections were therefore assumed not to transfer any bending moments from the beams into the attached columns.

2. When analysing the frame under the actions of the horizontal forces, the connections between the beams and the columns possess full slope continuity with points of contraflexure at the mid-lengths of the structural members. This enables the internal moments and forces to be approximated by adopting the Portal Method of analysis[2].

The simplicity of the approach is illustrated in Figure 1.1. As a result of the internal moments and forces being independent of the relative stiffnesses between the structural members, time consuming re-analysis can be avoided.

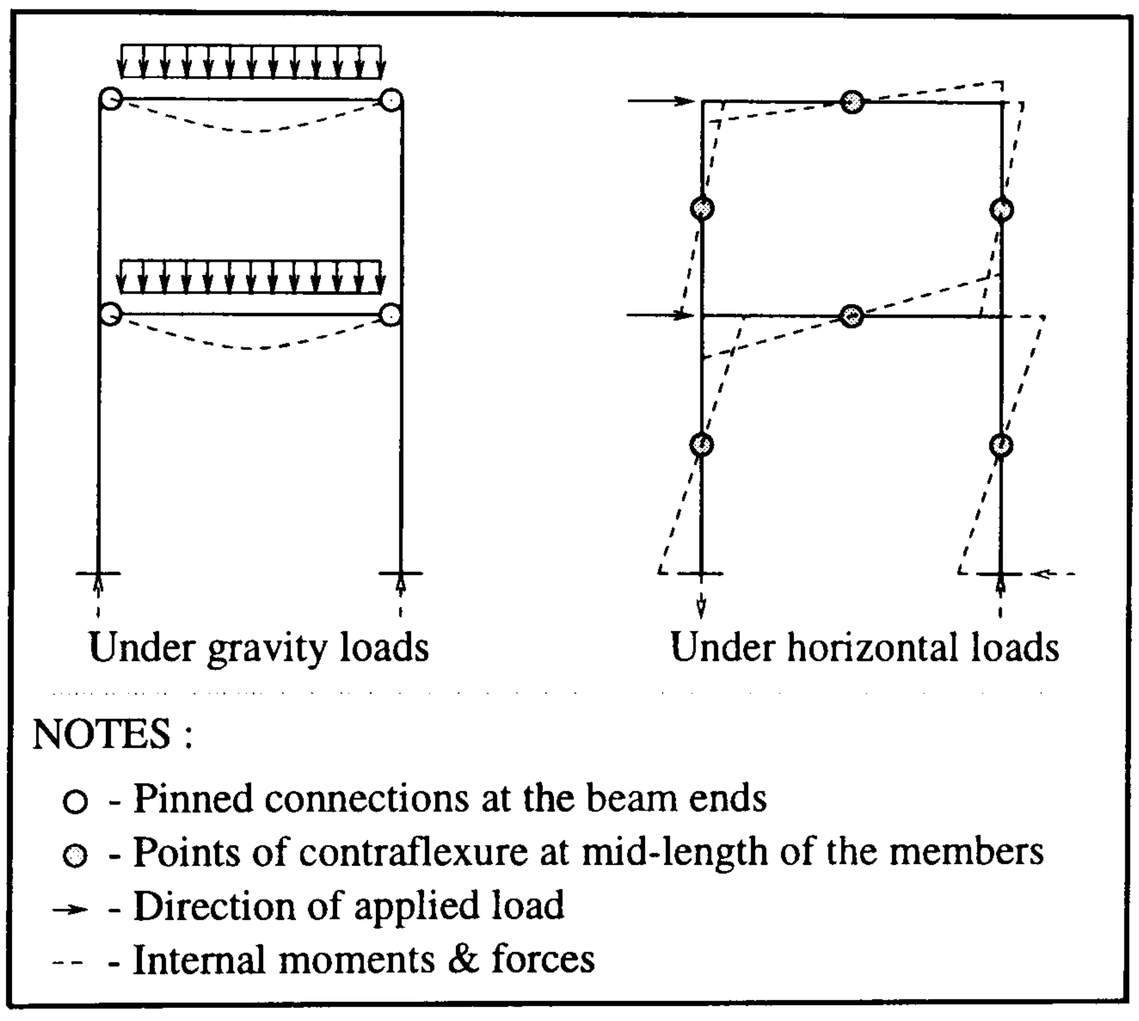

Figure 1.1: Simplifying assumption used by the Wind-Moment Method

Furthermore, since it is the mid span moment due to gravity load that controls the members size for low and medium-rise frames, the beam sections are generally the same size for all the floors which are intended for similar use and occupancy, thus simplifying the fabrication of the building. This is in contrast to fully-continuous construction with rigid joints, where it is not uncommon for the beam sections to differ throughout the height of the frame[3]. Additionally, advantages

are also forthcoming as a result of the connection's comparative weakness when compared to the strength of the beams, since web stiffening to the column, which is so often associated with rigid joints, can generally be avoided. The absence of stiffeners reduces fabrication costs and also provides greater freedom in the positioning and sizing of the beams which connect to the minor axis of the column.

To initiate the design sequence, the gravity load is considered in isolation from the horizontal force to enable the structural members and connections to be initially proportioned. The gravity and horizontal loads would then be combined in accordance with the appropriate design load cases and the initial design amended to withstand the combined effects. This would complete the design as far as the strength of the frame is concerned; however, further modification may be required following due consideration of sway deflections in accordance with serviceability requirements.

For serviceability, the connections are assumed to be rigid when calculating the sway deflections and then amplified by a multiplying factor to account for the influence of connection flexibility on the frame's response.

The design method described briefly above is not new and consequently, many buildings stand testimony to the acceptance that the above simplifications produce a satisfactory structural performance. In recent years however, the method has been regarded as a form of semi-rigid design and to this end theoretical studies in the mid 1980's [4, 5] and late 1980's [6, 7, 8] have been carried out. These studies have been fully described by their respective authors, from which the following conclusions have been drawn:

Beams

The assumption of having pinned connections at the ends of the beams results in these members being over designed. This over design is the consequence of the design method neglecting the true behaviour of the connections (see Figure 1.2).

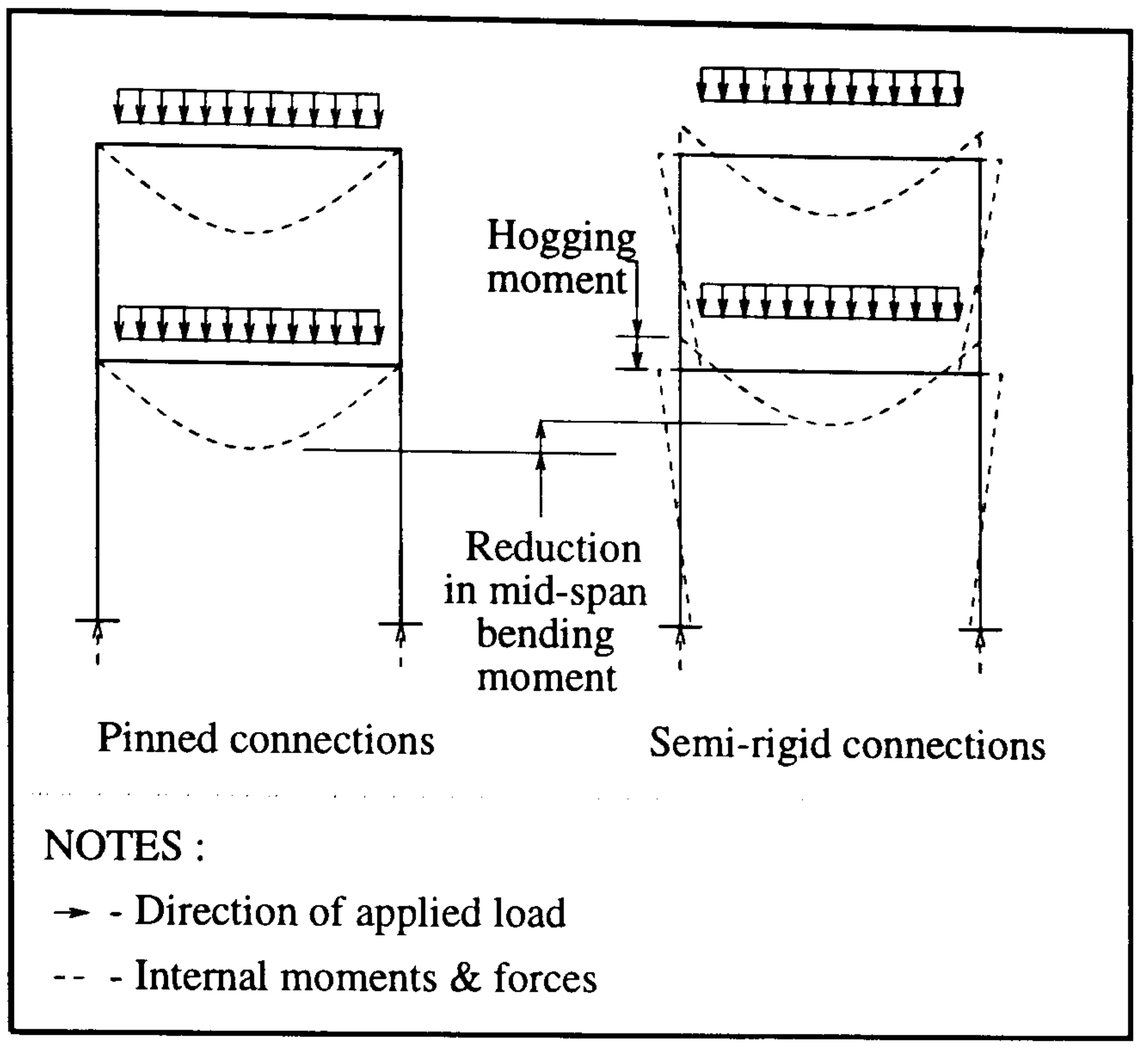

Figure 1.2: The effect of the true behaviour of the connections on the mid-span bending moment

The actual behaviour of the connections could be more accurately described as semi-rigid rather than pinned. Consequently, hogging bending moments would be developed at the support regions with the beneficial effect of reducing the bending moment at the centre of the beam.

Columns

The columns tend to be under designed, again as a consequence of the design method neglecting the true behaviour of the connections. The hogging moments that are developed at the connections have a detrimental effect on the column, since they will be generally required to resist greater moments than originally designed. In particular, the perimeter columns and other situations where unbalanced loading may be applied are the most vulnerable areas. However, it is thought that as the columns are also proportioned to resist the applied axial loads, the under design of these members is not as significant as the over design of the beams.

Connections

The connections generally tend to be under designed for the following reasons :

1. The hogging moment developed at the connections as a consequence of their true behaviour is neglected.

2. The additional moments that arise as result of the $P-\Delta$ effect are neglected (see Chapter 2, Figure 2.8).

3. The internal moment for at least one end of a beam would be in excess of that predicted by the method.

In addition to the above, it was generally accepted that the connections would have a lower moment capacity than the beam and therefore be classified as partial strength. This resulted from the connections being proportioned to resist end moments only, whereas the beams were governed by the much larger mid-span moment.

Frame stability

No direct allowance is made for the influence of the $P-\Delta$ effect on the internal moments and forces. However, they are indirectly considered for columns by adopting the effective length concept for the design of these members. This approach allows a column length to be used in design which is greater than its true length, for axes about which sway can occur. An effective length factor of 1.5 when considering major axis buckling, which is common in the design of fully continuous frames, has also been found to give satisfactory results with Wind-Moment frames[7]. However, since columns have been assumed to sway only about their major axis, an effective length factor equal to 1.0 is applied to minor axis buckling.

Despite the difference between the effective lengths for column buckling, for Universal Column sections, it was found that the minor axis controls the axial resistance of the member.

For low and medium-rise multi-storey frames, instability was not encountered below the design load level.

Sway deflections

The sway deflections of all the frames considered were larger than those predicted assuming the connections to be rigid. This is because of the semi-rigid and partial strength nature of the connections increasing the overall flexibility of the structures. To overcome this problem, a multiplying factor to the rigid deflections of 1.5 was recommended, since this amplification of the sway deflections was proved adequate in situations were the serviceability limit state governed the subsequent frame design[9].

Justification by rigid-plastic theory

The Wind-Moment Method can, in part, be justified by rigid-plastic theory[10]. as noted by Lay[11]. This theory describes the collapse condition as having the following characteristics :

1. A mechanism of plastic hinges has formed.

2. The internal moments and forces are in equilibrium with the applied loads.

3. Nowhere does the internal moment exceed the plastic moment of resistance.

The Lower-Bound Theorem then states *that the applied loads are less than or equal to the loads which collapse the frame,* and is applicable provided the second and third conditions are satisfied. The Wind-Moment Method meets these criteria required by this theorem and consequently produces safe designs. provided the frame also satisfies the assumptions of rigid-plastic theory. namely the effect of deflections on equilibrium can be neglected and collapse does not occur as a result of any form of buckling.

1.2 Analytical verification of the Wind-Moment method for unbraced design

A comprehensive verification of the Wind-Moment method was undertaken by Reading[1] in 1989. The objective of the study was to provide design rules which were consistent with limit state principles, to enable the method to be used in conjunction with BS5950, Part 1[12].

In essence, these design rules apply to steelwork structures which can be idealised as a series of unbraced plane frames which are effectively braced against out-of-plane sway at roof level and each subsequent floor level. Within each plane frame, the column sections were orientated such that loads in the plane of the frame tend to cause bending about the major axis. However, the scope of the rules was restricted, in terms of frame geometry and allowable loadings, to those adopted by the study (see Table 1.1).

			Minimum	Maximum
Frame geometry	Number of stories		**2**	**8**
	Number of bays		**1**	**4**
	Bay width (m)		**4.5**	**9.0**
	Bottom storey height (m)		**4.5**	**6.0**
	Storey height elsewhere (m)		**3.5**	**5.0**
	Bay width : storey height (bottom storey)		**0.75**	**2.00**
	Bay width : storey height (elsewhere)		**0.90**	**2.50**
	Greatest bay width : smallest bay width		**1.00**	**2.00**
	Clear span : storey height		**1.80**	**5.00**
Allowable loading	Dead load (kN/m^2)	Floors	**3.50**	**5.00**
		Roof	**4.00**	**7.50**
	Live load (kN/m^2)	Floors	**3.75**	**3.75**
		Roof	**1.50**	**1.50**
	Basic wind speed (m/s)		**37**	**52**

Table 1.1: Geometrical and loading restrictions imposed on Wind-Moment frames

The frames studied consisted of horizontal beams, which were arranged in

several grid formations, and vertical columns. The first grid arrangement consisted of the Wind-Moment frames alone resisting the full gravity load applied across the width of each bay, whereas alternatively, the second grid arrangement consisted of the additional provision of secondary beams positioned centrally between the adjacent Wind-Moment frames. Variations in the arrangements of the horizontal beams were incorporated into the study as a reflection of variations typically encountered in modern practice. Consequently, the inevitable change in corresponding design of these primary members, as a result of changing the load path within the frame as a whole, could additionally be considered.

Generally, for the majority of the frames considered, the bay width was kept constant over the complete height of the frame; however, in some instances an open-plan top storey was also investigated.

In total 120 different frame configurations were considered, in conjunction with the following two characteristic loading patterns:

1. Maximum gravity load combined with minimum wind load.

2. Minimum gravity load combined with maximum wind load.

The Wind loads were calculated in accordance with the British standard CP3 Chapter V, Part 2[13], and the gravity load is specified in Table 1.1.

Although it was recognised that considering only 120 configurations did not examine every possible combination of Wind-Moment frame which could be designed by the method, the selection adopted did encompass the extremes of frame geometry and loading, which were expected to provide the most critical appraisal of the method as a whole.

The largest range of studies took place on two storey frames comprising one and four bays in width. For each configuration considered, the specification was as follows: (i) The members were designed in UK Grade 50 steel, having a design strength equal to 355N/mm^2. (ii) The beam and column sections were chosen from the standard range of Universal Beam I-sections and Universal Column

H-sections respectively. (iii) The beam-to-column connections were extended end-plates, in UK Grade 43 steel of design strength 275N/mm^2. fastened to the column by M20 Grade 8.8 bolts. (iv) The column bases were taken to be fully-fixed. (v) The floor grid comprised primary beams only.

Furthermore, for each configuration detailed above, the following variations to the basic frames were additionally considered: (i) Members designed in Grade 43 steel. (ii) The extended end-plate connections were replaced by flush end-plates. (iii) Semi-rigid bases, modelled by assuming the base had a rotational stiffness equal to that of the attached column length.

Moreover, under the greatest intensity of gravity loading, bay widths of less than the maximum of 9m were also incorporated. This enabled a greater range of frame designs to be considered, thereby widening the scope of the study to embrace other configurations other than those applicable to the extremes of loading.

The final variation to the frame geometries considered so far, concerns the use of secondary beams. However, this particular arrangement was only adopted when the frames were being designed to resist the minimum amount of loading, since under these circumstances, the objective of the design was to obtain the smallest beams and columns. Clearly, this would be achieved by incorporating secondary beams as a consequence of the grid arrangement resulting in a further reduction in the gravity load carried by the beams forming part of the plane frame.

A third basic frame configuration consisting of an eight storey one bay frame was also considered. This was studied with all the variations given above, but only for the combination of maximum gravity load in conjunction with minimum wind load. The other combination of load was not considered, since preliminary calculations showed that under maximum wind load, such a slender frame was not suitable to be used as an unbraced structure, due to difficulty in designing the corresponding connections to resist the high wind moments.

In addition to the three basic frame types already described, two, four, six

and eight storey frames, all two bays in width, and a four storey, four bay frame were also investigated.

These frames were designed using the characteristics given earlier; however, the bay widths and column heights were kept constant throughout and were independent of the load case under consideration. To this end, the bay widths were fixed at 9m and storey heights of 4.5m and 3.5m were adopted to represent the bottom and upper storeys respectively.

The final frame configuration to be considered consisted of a two storey, two bay frame. This frame was designed to resist the maximum gravity in conjunction with the minimum wind load, as a consequence of the objective to investigate unequal bay widths, with or without open-plan top storeys.

1.2.1 Design to British codes of practice

Provisional design rules which are consistent with BS5950: Part 1 : 1990[12] guidelines for Simple Construction, were used to design each frame. These are summarised below:

Load combinations

The following load combinations, which are consistent with the requirements of BS5950, were applied to each frame.

1.4(Dead load) + 1.6(Imposed load) + Notional horizontal forces;

1.2(Dead load + Imposed load + Wind load);

1.4(Dead load + Wind load).

The notional horizontal forces were taken as 0.5% of the factored dead plus imposed load.

Internal moments and forces due to gravity load

The maximum beam moment at mid-span was calculated on the assumption that simply supported conditions are applicable over the full span of the beam

between centre lines of adjacent columns. However, in recognition of the fact that columns will generally receive a moment due to gravity load, as a consequence of the semi-rigid rather than pinned nature of the connections assumed, the beam end reaction is assumed to act a distance of 100mm from the face of the column, when determining the internal moments acting on the column. No account need be taken of such a moment in the design of the connections, since this moment is intended to make some allowance for the semi-rigid nature of the connections, which are only designed to resist shear.

When using BS5950, a further allowance may be optionally made for partial-fixity by assuming an end restraint moment equal to 10% of the maximum free moment in the beam. However, if this restraint moment is included at this stage, the connections should be designed to transmit the restraint moment to the columns, in addition to the vertical end reactions from the beam. This allowance was incorporated within the frame study.

Both the eccentricity moment and the 10% end restraint moment applied at any one storey height are divided equally between the respective upper and lower column lengths, provided these lengths do not differ by more than 50% in stiffness[12]. Furthermore, the moments are assumed to have no effect at the levels above and below that at which they are applied and consequently, dissipate to zero at the far ends of the column lengths.

Internal moments and forces due to wind load

The analysis was made by using the portal method of analysis. Consequently, points of contraflexure are assumed to be located at the mid-heights and lengths of the columns and beams respectively. In addition each bay acts as a simple portal, such that the total horizontal load can be divided between the bays in proportion to their spans.

Design of beams members

Since the Wind-Moment method can be justified in part by plastic theory, the corresponding beam members must be able to form plastic hinges and participate in collapse mechanisms. Consequently, to preclude premature failure of the members as a result of local buckling, the sections must be Class 1, Plastic.

Furthermore, to provide directional restraint to the columns, BS5950 requires the design moment of resistance of a beam member to be limited to 90% of the plastic moment of resistance. This does not however lead to an increase in the beams section when compared to simple design, since the design moment for the beam has also been reduced by 10% to take account of partial-fixity of the connections. Consequently, these two effects are mutually compensating.

Design of column members

For in-plane buckling, with bending about the major axis of the column, the effective length L_E was taken as 1.5 times the storey height, H_t.

For out-of-plane buckling, with bending about the minor axis, the provisional proposal was to take the effective length as $0.85H_t$. This was to take into account a small degree of restraint from the minor axis beams and their connections. However, this was changed to $1.0H_t$ as a result of the studies.

By the same reasoning as provided under the design of the beam members, the column sections should also be Class 1, Plastic sections.

To determine the lateral-torsional buckling resistance moment, an approximate slenderness ratio, equivalent to that used when designing columns in simple multi-storey construction was adopted (see equation 1.1).

$$\lambda_{LT} = \frac{0.5H_t}{r_y} \tag{1.1}$$

where:

r_y - Radius of gyration of the column section about its minor axis.

Finially, the following buckling check had to be satisfied by each of the column sections chosen (see equation 1.3).

$$\frac{F_c}{P_c} + \frac{M_x}{M_b} \leq 1.0 \tag{1.2}$$

where:

F_c - Applied axial load in the member

P_c - Compression resistance of column after taking account of its susceptibility to buckling

M_x - The largest column end moment

M_b - The lateral-torsional buckling resistance moment.

Design of connections

The design rules contained within BS5950[12], the Steel Designers Manual[2] and Manual on connections[14] were adopted where applicable to enable the connections to be sized.

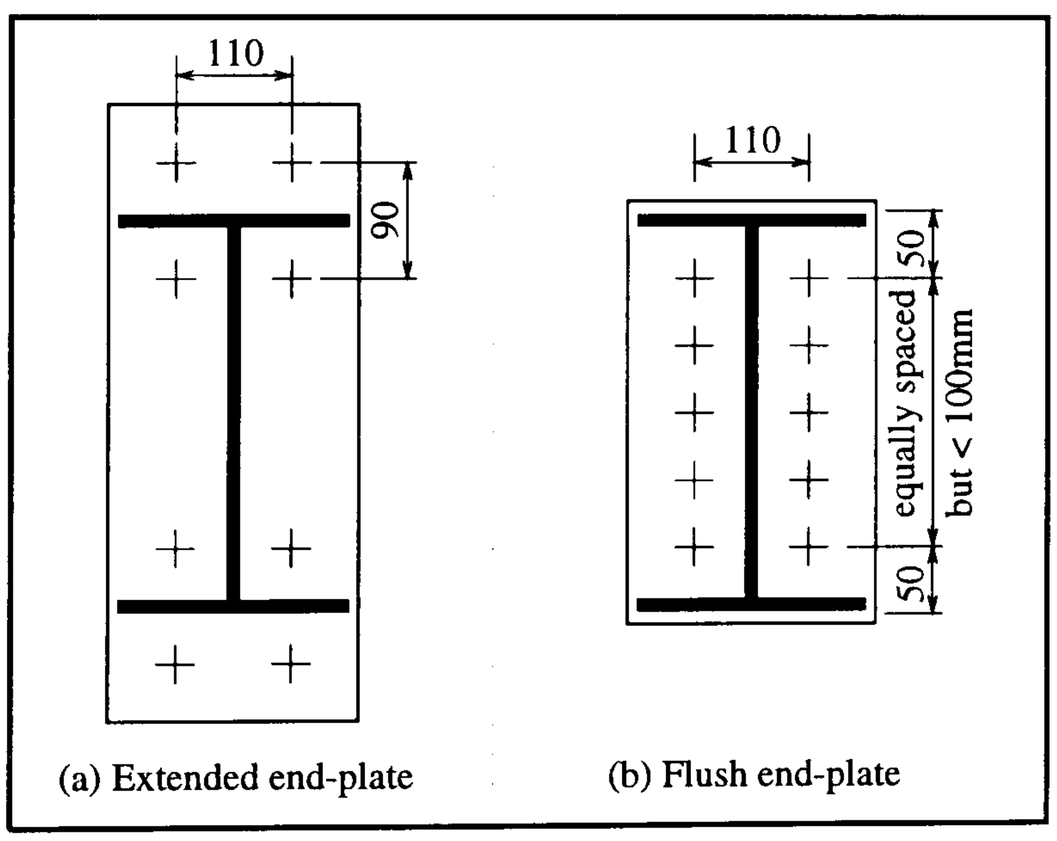

Figure 1.3: Connection details

The extended end plate connections consisted of four bolts symmetrically positioned around both beam flanges (see Figure 1.3(a)). The bolts and welds were designed by following the procedures contained within section 6 of BS5950[12]. whereas the end plates were designed elastically by limiting the stress to the

yield value[14]. Furthermore, the column's flange was checked by the method proposed by Horne and Morris[15], which considers the following two modes of failure. Firstly, simultaneous bolt fracture in conjunction with column yielding and secondly, column yielding alone. To complete the design, the column web was also checked in tension and shear.

The flush end-plate connections consisted of five bolt rows positioned symmetrically between the beams flanges (see Figure 1.3(b)). The bolts and welds were again designed in the same manner as described for the extended end plate connections; however, the thickness of the flush end plates was determined by using a model proposed by Horne and Morris[15]. This model was based on a T-stub arrangement with the tension bolts inducing double curvature.

1.2.2 Analytical procedure

An incremental second-order elastic-plastic procedure[16], in which the behavioural characteristics of the connections were represented by moment-rotation relationships, was adopted to analyse the frames designed as described above. The connection relationships were predicted by the method given in Eurocode 3[17], prior to its subsequent revision[18]. In addition, to provide an upper bound on the joint behaviour, the frames were also analysed assuming the connections were rigid and full strength.

The analysis represented the overall in-plane behaviour of the frame, thus enabling the deflections and internal moments and forces to be determined at load levels up to and including the collapse load. Consequently, the overall buckling check contained with BS5950 could be utilised to assess the lateral stability of the columns over each storey height.

$$\frac{F_c}{P_c} + \frac{mM_x}{M_b} \leq 1.0 \tag{1.3}$$

where:

m - Equivalent uniform moment factor.

For this check, the more precise relationship for calculating the slenderness ratio was utilised (see equation 1.4).

$$\lambda_{LT} = uv\left(\frac{H_t}{r_y}\right) \tag{1.4}$$

where:

u and v are parameters which depend on the section properties which influence the member's resistance to lateral-torsional buckling and are determined in accordance with Annex B of BS5950.

1.3 The need to re-verify the design method for Wind-Moment frames

Design rules which are consistent with BS5950: Part 1 : 1990[12]. together with a comprehensive commentary, have been published[1]. They were developed in conjunction with the analytical study described above, which was designed to investigate the behaviour of typical frames designed in accordance with Wind-Moment method[8]. The scope of the rules were therefore restricted, in terms of frame geometry and allowable loadings, to those adopted by the study (see Figure 1.1). Furthermore, the types of frames covered by the method were limited by the necessity to provide a suitable bracing system to prevent out-of-plane movement, about the minor axis of the columns members. This limitation is generally considered unwelcome and consequently, studies are being undertaken at present within the University of Warwick[19] to lift this undesirable restriction. Moreover, the design rules only apply to frames which employ either extended or flush end-plate beam-to-column connections, which invariably, as a consequence of the design method assuming little end restraint under the action of gravity loads, produces a connection strength lower than the adjacent beam members. Therefore the connections can be classified as partial-strength

in accordance with Eurocode 3[17]. This increases the likelihood of plastic hinges forming in these connections as the load increased. Therefore. to ensure that the assumptions made in design are not compromised, the connections must possess the necessary rotation capacity to enable moment redistribution to continue uninhibited until a hinge mechanism has formed. Although this assumption was also a requirement of the original verification described in section 1.2, it was recognised that this could not be guaranteed by the corresponding connection design methods adopted. Therefore, this has lead to the development of a range of standard ductile connections for Wind-Moment frames[20]. These connections achieve a ductile response whilst using the industry standard M20 or M24 Grade 8.8 bolts, by employing relatively thin end-plates (12-15mm) designed in accordance with Eurocode 3[18]. Consequently, they are more flexible than the typical connections used in the original analytical study[8], which were based on earlier design rules for moment connections[14, 15]. These rules tended to produce thicker end-plates than the proposed standard connections, and were based on the assumption that brittle modes of failure would be avoided mainly by using larger bolts and welds. Thus by incorporating the standard connections within the design of a Wind-Moment frame, the restraint to the columns would be reduced, which in turn would increase the second-order effects. The net effect on the frame's behaviour would therefore be a reduction in its overall stiffness, thus increasing its susceptibility to problems of instability. In addition, a further increase in the frames flexibility will also have a pronounced effect on the subsequent sway deflections under serviceability loadings. It was therefore necessary to repeat aspects of the original analytical study, to re-confirm the safety of Wind-Moment frames using the new standard connections. This re-validation is described in Chapter 4 within this thesis.

A secondary benefit of the repeated study has been the opportunity to model the stiffness of the connections used in the frame analysis more accurately. The original study used a preliminary version of Annex J, prepared during the drafting

of Eurocode 3. Work subsequently undertaken by Moore[21] however, concluded that the estimate of stiffness using this method was erratic and for thinner end-plates was consistently understated. This in part led to the annex being re-drafted[18], a process in progress during the period that this study was being undertaken. Consequently, a finalised version of the initial stiffness model now proposed to represent the connection behaviour (see Chapter 2) was unavailable; therefore an alternative initial stiffness prediction model was formulated by the author and verified using experimental test data (see Chapter 3).

1.4 Standardised connections for Wind-Moment Frames

Guidance for the design of unbraced frames in accordance with the Wind-Moment method was published by the Steel Construction Institute in 1991[1]. This publication covered all aspects of the method with the exception of providing specific design rules applicable to the connections. This omission has however, now been addressed by a separate volume entitled *Joints in Steel Construction - Moment Connections*, which has just been published[20]. Within this volume there is a specific chapter covering the design of suitable connections that can be incorporated directly into a Wind-Moment frame. The guidance is given in the form of standardised end-plate connections (see Figure 1.4), whose design is all but complete. Consequently, a few simple checks to ascertain the suitability of a designated connection to meet the required structural performance would be all that is incumbent on the designer to complete the frame specification.

For a connection to behave successfully in a Wind-Moment frame, it must be able to satisfy the following criteria. (i) The connection's moment capacity should be greater than the applied design moment, for both positive and negative applied bending moments. (ii) The connection should possess adequate rotational

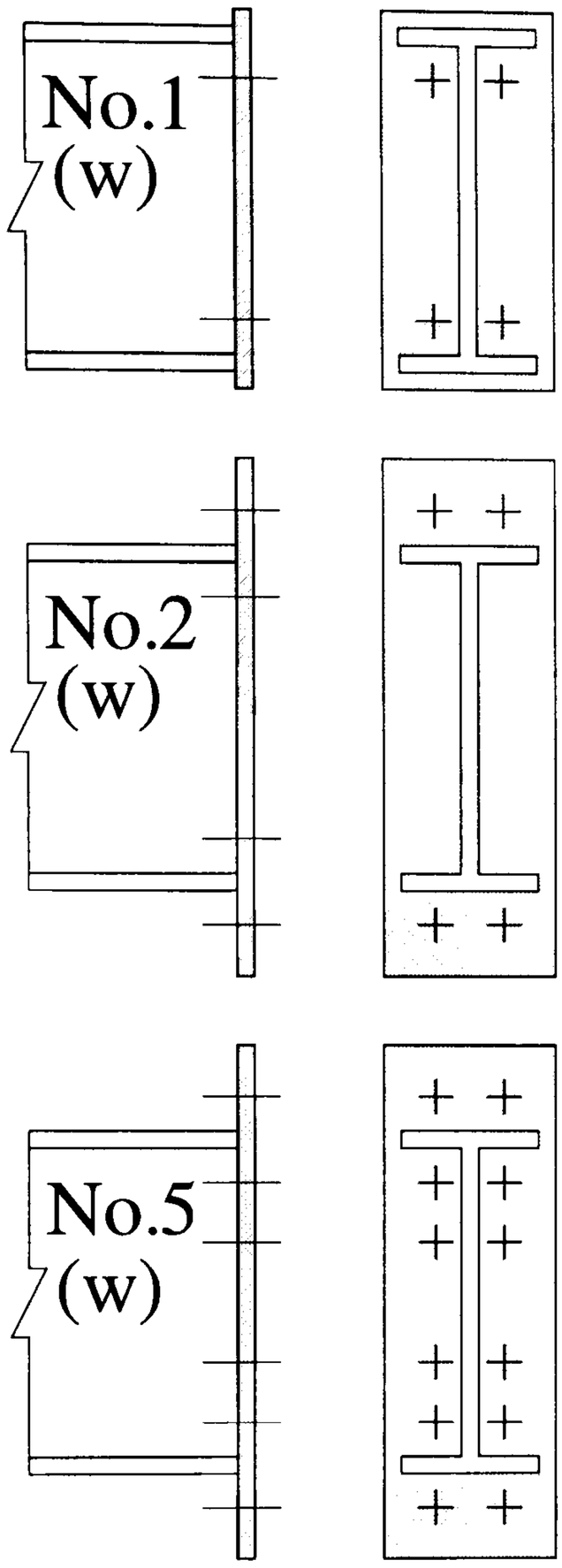

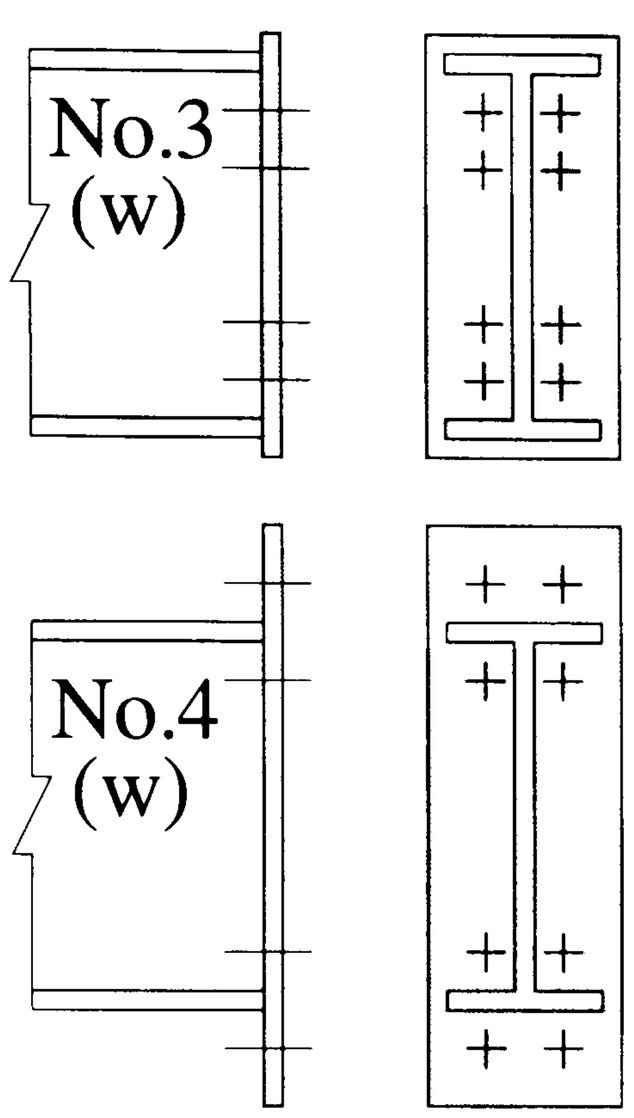

NOTES :

For dimensions & design tables see Appendix A

An additional bolt row may be provided for details 1,2 & 4 to increase the connections shear resistance

(w) - Connection available with an increased plate width to accomadate larger serial size beams

Not to scale

Standard connection	Type of end plate	Bolt size / end plate thickness	Universal beam range	Universal column range
1	flush	M20/12mm M24/15mm	254x102 - 762x267	202x203 - 356x368
2	extended	M20/15mm	254x102 - 533x210	202x203 - 356x368
2(w)		M24/20mm	457x191 - 762x267	
3	flush	M20/12mm	406x140 - 533x210	202x203 - 356x368
3(w)		M24/15mm	457x191 - 762x267	
4	extended	M20/12mm	254x102 - 533x210	202x203 - 356x368
4(w)		M24/15mm	457x191 - 762x267	
5	extended	M20/12mm	406x140 - 533x210	202x203 - 356x368
5(w)		M24/15mm	457x191 - 762x267	

Figure 1.4: Proposed standard end-plate connections

stiffness compatible with the assumptions made in the validation studies for the Wind-Moment method. (iii) The connections should possess sufficient rotation capacity (subsequently referred to as ductility) to enable the connection to act as a plastic hinge, in response to negative bending moments. (iv) The connection's shear resistance should be greater than the applied design shear force.

The ductility requirement is recognised as the single most important factor that distinguishes a Wind-Moment connection from the other more general moment resisting connections, and is achieved at the expense of strength and stiffness. These losses result from the necessity to use thin end plates to avoid brittle failure of the bolts, as a consequence of the standardisation process restricting the choice of bolt Grade to 8.8 and the bolt sizes to either M20 or M24.

Unfortunately, the connections ductility must not be compromised by incorporating refinements which would improve its corresponding strength and stiffness, such as substituting stronger material. If this happened, there would be a high risk of a tensile failure occurring through bolt fracture. This must be avoided, since the connection's mode of failure would be transformed into a mode which is emphatically non-ductile.

The ductility of a wind-moment connection is provided by designing the end-plate to deform essentially in double bending, to achieve a 'Mode 1' type of failure in accordance with the revised Annex J of Eurocode 3[18]. This was achieved by careful consideration of the thickness of the end-plate in relation to the size and strength of the bolts. To achieve this desired mode of failure, the end plate thickness would have to be limited to no more than half the corresponding bolt diameter[22]. Thus, the end result would be the achievement of an admirable ductile performance at unexceptable expense in terms of the connection's strength and stiffness. Consequently, the thickness adopted for the end plates was slightly greater than the maximum otherwise allowed to ensure Mode 1 failure; the thicknesses adopted were 12mm and 15mm for the M20 and M24 bolted connections respectively. The justification for this approach was initially one of engineering

judgement within the BCSA/SCI Connections Group, who collectively thought that adopting slightly thicker end plates would provide a more acceptable balance between the competing demands made on the connection, while remaining adequately ductile. This proposal has been subsequently born out by full scale experimental tests undertaken on a selection of the proposed connections at the University of Dundee[23, 24].

The technical interpretation of Eurocode 3 and the relevant annex, Annex J (revised), was undertaken by Hughes. Further details of the background work which led to the connections' publication is to be found elsewhere[22, 20]. The author's contribution to this aspect of the work was concerned with the production of validated computer software to produce the dimension and design tables for the standardised connections (see Appendix A). This work will be explained subsequently and was undertaken under the supervision of Hughes.

1.4.1 Production of the design and dimension tables

The computer software written for the production of the design and dimension tables was undertaken using a commercially available spreadsheet package entitled *Lotus 123*. This enabled the large amounts of data to be processed easily and the inevitable repetitive calculations to be completed with the minimum of complication.

For each connection detail, the design tables were split up into three spreadsheet programs, covering the connection's design moment of resistance, associated column limitations (explained below) and design shear resistance. The dimension tables were initially incorporated as part of the tables for the connections' design moment of resistance and separated at a later stage. Following this computation stage, each table was transferred directly into a word processor package, *Wordstar*, whereby the data was manipulated to produce the desired presentation. The advantage of this procedure was that once the data had been verified on the corresponding spreadsheet, the automatic process of transferring to the

word processor would minimise data corruption. The verification for the tables took the form of spot checks on every step of the calculation process, for each connection detail proposed.

Unfortunately, the following problem was encountered which threatened the automatic procedure outlined above. The output from each spreadsheet was too large, in the sense that each table occupied a greater proportion of the allocated space on the page than could be accommodated. One of the requirements laid down at the beginning of the project was the restriction on the total space necessary to present the design information. It was decreed that for each connection, all the design tables must be presented on a single side of A4 paper. This was to aid the designer by speeding up the process of connection choice, by having all the necessary information immediately to hand.

To overcome this set back, each spreedsheet was reduced to a sufficiently small size to enable the presentation objective to be met. The reduction necessary to achieve this goal however was prohibitive, since the clarity of the tables was severely compromised. The solution adopted was therefore to take the data from the spreadsheets and manually transfer it to the graphics package *Xfig*, which was available at the University of Warwick. In doing this, the data tables were easily sized to enable the presentation requirements to be fulfilled. To maintain confidence in the reliability of the data as a result of switching to a manual method of data transference, rigorous checking procedures were again implemented.

The use of the design tables, an example of which is shown in Figure 1.5, is discussed in detail in Chapter 4, which is additionally supplemented by a worked example (see Appendix B, Section B.3). The full set of design tables has been included in Appendix A of this thesis. The purpose of the following sections will therefore be to highlight some of the assumptions adopted in producing the design information. Further information with regard to the philosophy adopted in the design of the standardised connections may be obtained from the moment connections publication itself[20].

W4/24

Box 1

Moment Resistance

M.R. (in Nm) = 193 (h - 0.5 t_f + 40)

305 (h - 0.5 t_f - 60)

t_f (mm)	h (mm)	Serial Size Mass per metre	Moment Resistance kNm
		533 x 210	
21.3	544.6	122 b	256
18.8	539.5	109 b	254
17.4	536.7	101	253
15.6	533.1	92	251
13.2	528.3	82	250
		457 x 191	
19.6	467.4	98 b	218
17.7	463.6	89 bw	216
16.0	460.2	82	215
14.5	457.2	74	214
12.7	453.6	67	212
		457 x 152	
18.9	465.1	82 b	217
17.0	461.3	74	215
15.0	457.2	67	214
13.3	454.7	60	213
10.9	449.8	52	211
		406 x 178	
16.0	412.8	74	191
14.3	409.4	67	190
12.8	406.4	60	189
10.9	402.6	54	187
		406 x 140	
11.2	402.3	46	187
8.6	397.3	39	185
		356 x 171	
15.7	364.0	67	167
13.0	358.6	57	165
11.5	355.6	51	164
9.7	352.0	45	163
		356 x 127	
10.7	352.8	39	163
8.5	348.5	33	161
		305 x 165	
13.7	310.9	54	141
11.8	307.1	46	140
10.2	303.8	40	138
		305 x 127	
14.0	310.4	48	141
12.1	306.6	42	139
10.7	303.8	37	138
		305 x 102	
10.8	312.7	33	143
8.9	308.9	28	141
6.8	304.8	25	140
		254 x 146	
12.7	259.6	43	116
10.9	256.0	37	114
8.6	251.5	31	113
		254 x 102	
10.0	260.4	28	117
8.4	257.0	25	115
6.8	254.0	22	114

b - Where t_f > 18 use a butt weld to the flange

bw- If the beam is S275 use a butt weld to the flange

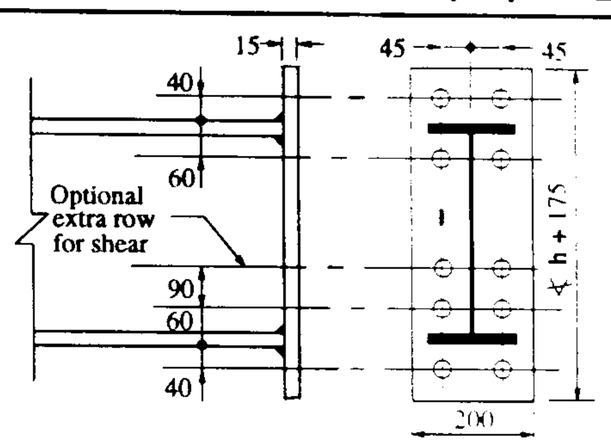

Box 2

Column Limitations

$\Sigma F_b \geq 509$ kN

See Note 2

S275					Grade	S355				
v	iv	iii	ii	i	Zone	i	ii	iii	iv	v
Web Tension	Web Crushing	Web Buckling	Web Shear	Flange Bending	**Serial Size** Mass per metre	Flange Bending	Web Shear	Web Buckling	Web Crushing	Web Tension
					356 x 368					
✓	✓	✓	✓	✓	202	✓	✓	✓	✓	✓
✓	✓	✓	940	✓	177	✓	✓	✓	✓	✓
✓	✓	✓	814	✓	153	✓	✓	✓	✓	✓
✓	✓	✓	691	✓	129	✓	892	✓	✓	✓
					305 x 305					
✓	✓	✓	✓	✓	283	✓	✓	✓	✓	✓
✓	✓	✓	✓	✓	240	✓	✓	✓	✓	✓
✓	✓	✓	✓	✓	198	✓	✓	✓	✓	✓
✓	✓	✓	905	✓	158	✓	✓	✓	✓	✓
✓	✓	✓	791	✓	137	✓	✓	✓	✓	✓
✓	✓	✓	681	✓	118	✓	879	✓	✓	✓
✓	✓	✓	565	✓	97	✓	730	✓	✓	✓
					254 x 254					
✓	✓	✓	935	✓	167	✓	✓	✓	✓	✓
✓	✓	✓	746	✓	132	✓	963	✓	✓	✓
✓	✓	✓	613	✓	107	✓	791	✓	✓	✓
✓	✓	✓	497*	✓	89	✓	642	✓	✓	✓
✓	■	■	406*	■	73	✓	525	✓	✓	✓
					203 x 203					
✓	✓	✓	497*	✓	86	✓	642	✓	✓	✓
✓	✓	✓	395*	✓	71	✓	510	✓	✓	✓
✓	■	■	349*	■	60	✓	451*	✓	✓	✓
✓	■	■	300*	■	52	■	387*	■	(■)	✓
✓	■	■	273*	■	46	■	353*	■	■	✓

* - Less than ΣF_b

(■)- Re - calculate

- Sections are not designated class 1

Box 3

Shear Resistance

See Note 4

340 kN

(optional extra row adds 265 kN)

Figure 1.5: Standard connection number 4 with M24 bolts

Moment resistance - box 1

The connection's moment resistance has been calculated on the assumption that the connecting column will either match the resistance of the end-plate, or will be reinforced to do so. In addition, the bolt forces have been calculated using the smallest beam section as the basis for design. This beam was adopted to produce a conservative estimate of the bolt forces used to calculate the connection's moment resistance. This simplifies the calculation to the consideration of the connection's lever arm only, at the expense of sacrificing a small proportion of the resistance.

Column limitations - box 2

This particular table covers all the Universal Columns that it was expected a designer may wish to use in Wind-Moment frames. The 152 universal column series was excluded, since it was thought that this column is so small as to be inappropriate for use in such a frame. The bolt force printed at the top of the table represents the summation of the maximum individual bolt forces that the corresponding connection could exert on the Universal Column section. Consequently this force was calculated using the largest beam section specified in the moment resistance table as the basis for design. This beam was adopted to enable the subsequent comparisons with column resistances, to be independent of variations of beam section. This simplification has the result of producing conservative assessments for the column limitations in all cases. The summation of the bolt forces are then systematically compared with the zones which may limit the column's resistance to withstand the applied connection forces. The limiting zones are web tension, crushing, buckling and shear and flange bending. This table was further simplified by the assumption that the interactions between axial force and bending moment could be ignored.

Shear resistance - box3

The resistance of the connection to vertical shear was calculated in accordance with Eurocode 3, and was based on the number of bolt rows available in the bottom half of the end-plate, which were assumed not to provide any tensile resistance to the connection. The total shear resistance of any connection was therefore a multiple of the number of bolt rows provided.

Refinements incorporated within the Moment Connections publication

There are several differences between the capacity tables shown in Appendix A and the moment connections publication[20]:

1. The notation used to reference a particular connection detail.

2. The overall presentation of the tables.

3. Standard detail number two, although given in Appendix A as an alternative, was dropped from the connection choices as a result of full scale tests undertaken by Bose[23]. These tests highlighted a brittle failure mode associated with the end plate itself, which fractured at the flange weld line. Consequently, this particular connection was not considered as an available choice during the frame study. Furthermore, from this series of tests it was also concluded that serial size beams greater than 686x254 should be excluded, since connections to larger beams failed in a non-ductile manner by the column web buckling at a rotation of less than 20mrads[23, 24]. However, this restriction does not effect the frame study reported in Chapter 4. since the largest beam considered was from the 686x254 range.

4. Refinements to the calculation procedures for effective lengths of bolt yield line patterns contained within the revised Annex J[18], were proposed after substantial work on the frame study had been completed. These modifications have lead to a small reduction in the allowable bolt force attributable

to the second bolt row of detail numbers 3 and 5. Consequently, the moment capacity of these details has been reduced in the publication by up to 10% and 5% for the M20 and M24 option respectively. Since standard detail number 3 has not been use for the study the reduction has no influence. However several frames incorporated detail 5 (see Appendix B, section B.2). It is thought by the author that since a connection's moment capacity in reality would be higher than that predicted[23, 24] the frames concerned need not be repeated to cater for the reduction.

5. The resistance of a column web to shear will be found to be greater in the moment connections publication. This is because in the author's calculations clause 5.4.6(2) of Eurocode 3 was used to calculate the shear area. The values now published use a lower shear area based on BS5950. However, this difference would have no significant influence on the study reported in Chapter 4, since when ever this limitation governed it was assumed that adequate reinforcing would be provided.

These modifications were undertaken by the Steel Construction Institute.

1.5 Benefits of standard connections in Wind-Moment frames

It is sometimes impossible and often difficult, functionally or architecturally, to accommodate suitably located bracing systems. Consequently, the design team would have to adopt an unbraced configuration to fulfill the structural requirements of the frame's specification. Unfortunately however, there is an economic penalty to consider for this type of design when compared to a braced alternative. This is the result of the increased complexity of the connections required by the unbraced frames, since moment connections are unavoidable.

However, it has been widely recognised that connection standardisation is

an important step forward to achieving not only economic benefits at the production stage, but also in the design office by simplifying the steelwork design process[25]. This has particular implications for unbraced frames where the moment connections by their very nature, require considerable time and effort to design, in comparison with simple joints. The standard connections for Wind-Moment frames included in the new publication[20] should therefore considerably ease the task of using this approach to design.

Chapter 2

Behavioural characteristics of bolted connections

2.1 Introduction

A straight-forward method of designing low to medium-rise unbraced steel frames has been briefly described in Chapter 1. This method relies on the rotational stiffness of the connections to provide an adequate medium through which the stability and lateral movement of the structure can be assured. Consequently, to enable the method to be validated using a second-order elastic-plastic approach necessitates the understanding of the true behaviour of the connections.

In the days when the design philosophy limited structural members to working stresses, such as those of BS449 [26], the connections were generally based on the ideal assumptions that they behaved either in a fully rigid manner, or as frictionless hinges. For a connection to behave rigidly necessitates full slope continuity between the adjoining members, in addition to moment due to gravity load being transmitted from the beams into the columns. Conversely, the frictionless hinge criteria is only satisfied when the beams act as simply supported members and therefore prevent any transfer of the moment. These assumptions simplify analysis considerably, but they do imply ideals of behaviour which, through ex-

perimental work, are known not to exist. In addition to such idealised behaviour, BS449 did recognise that the true characteristics of a connection lie somewhere in between. However, even during the late sixties, the computing software was insufficient to enable a realistic treatment of the connections to be considered for everyday design.

The subsequent development of more sophisticated software heralded a gradual change in the manner in which the connection behaviour was perceived. In parallel to this, the introduction of limit state design standards, such as BS5950 [12] and later Eurocode 3 [17], has lead to increased design guidance covering this specialised area. Therefore the modern day structural engineer is now able to consider the connections as an integral part of the design, instead of relying on the fabricators to fulfill this particular obligation.

To understand the implications of these changes on the analysis and subsequent performance of a structure, consideration of the fundamentals involved would be necessary. Therefore the following sections will introduce the concepts involved in the representation of the true connection behaviour, in a context appropriate for structural design.

In addition to the definitions given above for the idealised connection behaviour, the universally accepted term 'semi-rigid' will be used to define a connections behaviour where it falls somewhere in between the two idealised boundaries.

2.1.1 Moment-rotation characteristics

The purpose of a connection is to provide a path by which forces and moments can be transmitted between the individual structural members. For beam-to-column connections the 'forces' may include axial and shearing forces, bending moments and torsion. Torsion can usually be neglected for an in-plane study, since the twisting effect may be assumed to be prevented by a suitable out-of-plane bracing system. The axial and shearing deformations may also be generally neglected, since they are usually small in comparison to the rotational

deformation. Therefore, the properties of a beam-to-column connection that influence frame behaviour may be simplified to only the consideration of the rotational deformation [27].

The rotational deformation is traditionally expressed in the form of a moment-rotation characteristic, which relates a moment 'M_j' experienced by the connection to its corresponding angular rotation 'ϕ_j'. The angular rotation is defined as the change in angle of the end of the beam and the mating column face, from its original position (see Figure 2.1).

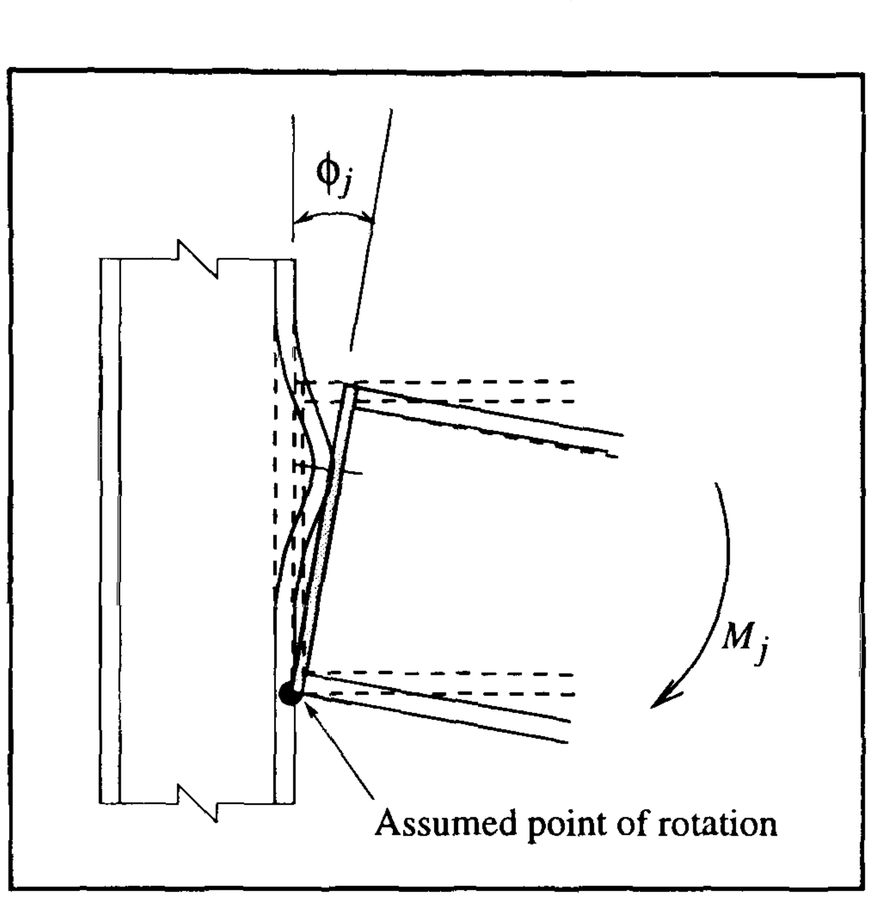

Figure 2.1: Angular rotation of a connection

From experimental work, a review of which can be found elsewhere [28. 29] it has been established that unique moment-rotation characteristics are produced for different types of connections. Even nominally identical connections show small differences in their behavioural characteristics.

The connection types which are commonly encountered in everyday design situations are end plate and cleated connections. These basic types of connection may be further sub-divided into the following categories. End plate connections include extended, flush and header plates, whereas cleated connections include flange cleats, web cleats and a combination of these cleats. The aforementioned connection types are illustrated in Figure 2.2, with typical examples of their moment-rotation characteristics to facilitate a comparison.

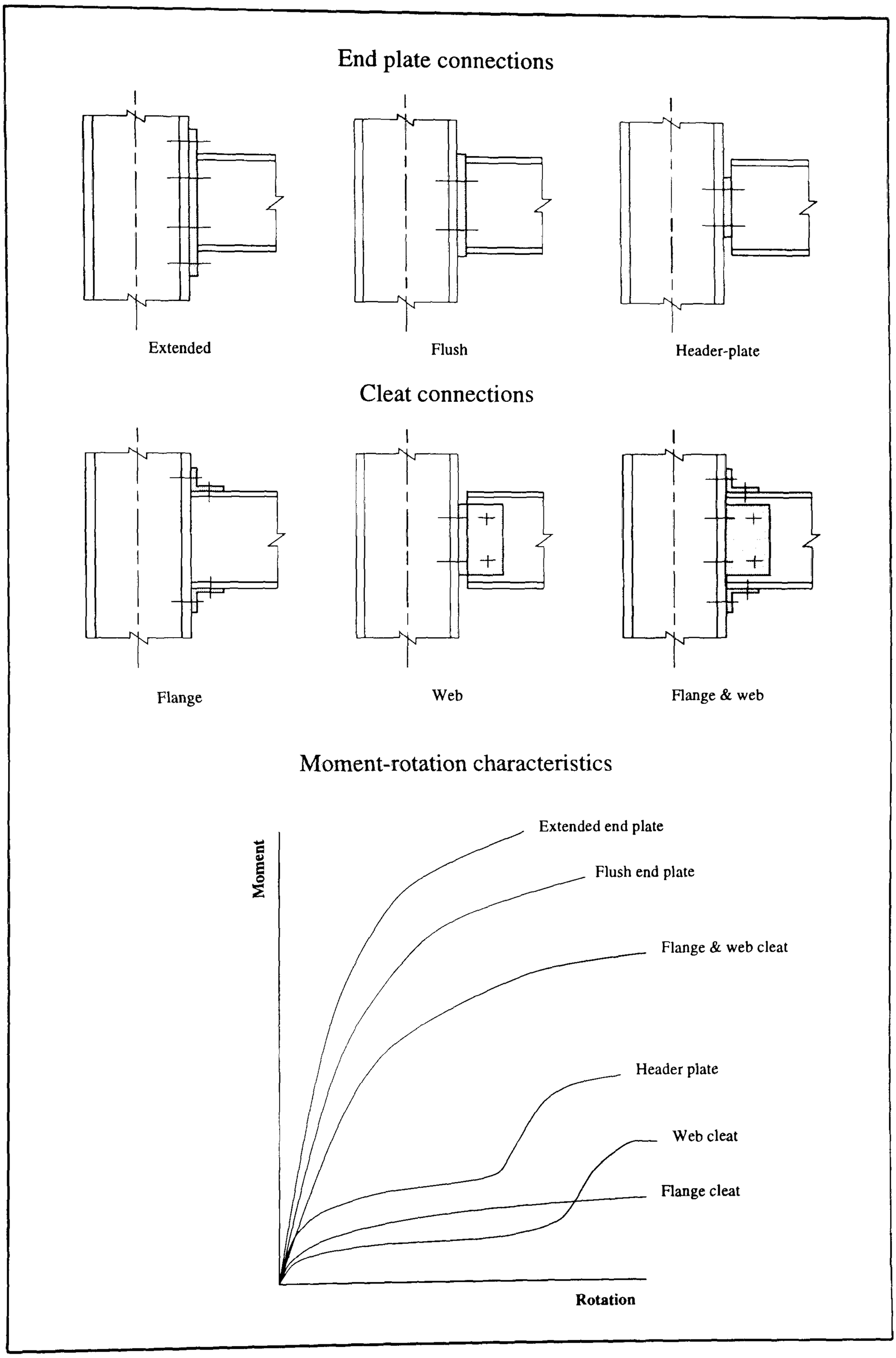

Figure 2.2: Connection types and their moment-rotation characteristics

The following distinguishing features can be identified from the characteristics shown in this figure. (i) The characteristics are essentially non-linear over their entire range. (ii) The maximum moment that the connection is able to resist is significantly influenced by the type of connection adopted. (iii) The characteristics fall in between the two ideals of behaviour, denoted by the vertical and horizontal axes representing the rigid and hinge assumptions respectively. (iv) Considerable variation can be seen in the amount of moment that can be sustained for a particular rotation. Conversely, the same is true for the corresponding rotation at a particular moment. In addition, another important feature of a connections behaviour which is not indicated by Figure 2.2, is illustrated by Figure 2.3. This particular characteristic was applicable to the author's first experimental test which was undertaken on a bare steel flush end plate connection (see Chapter 6, Figure 6.2).

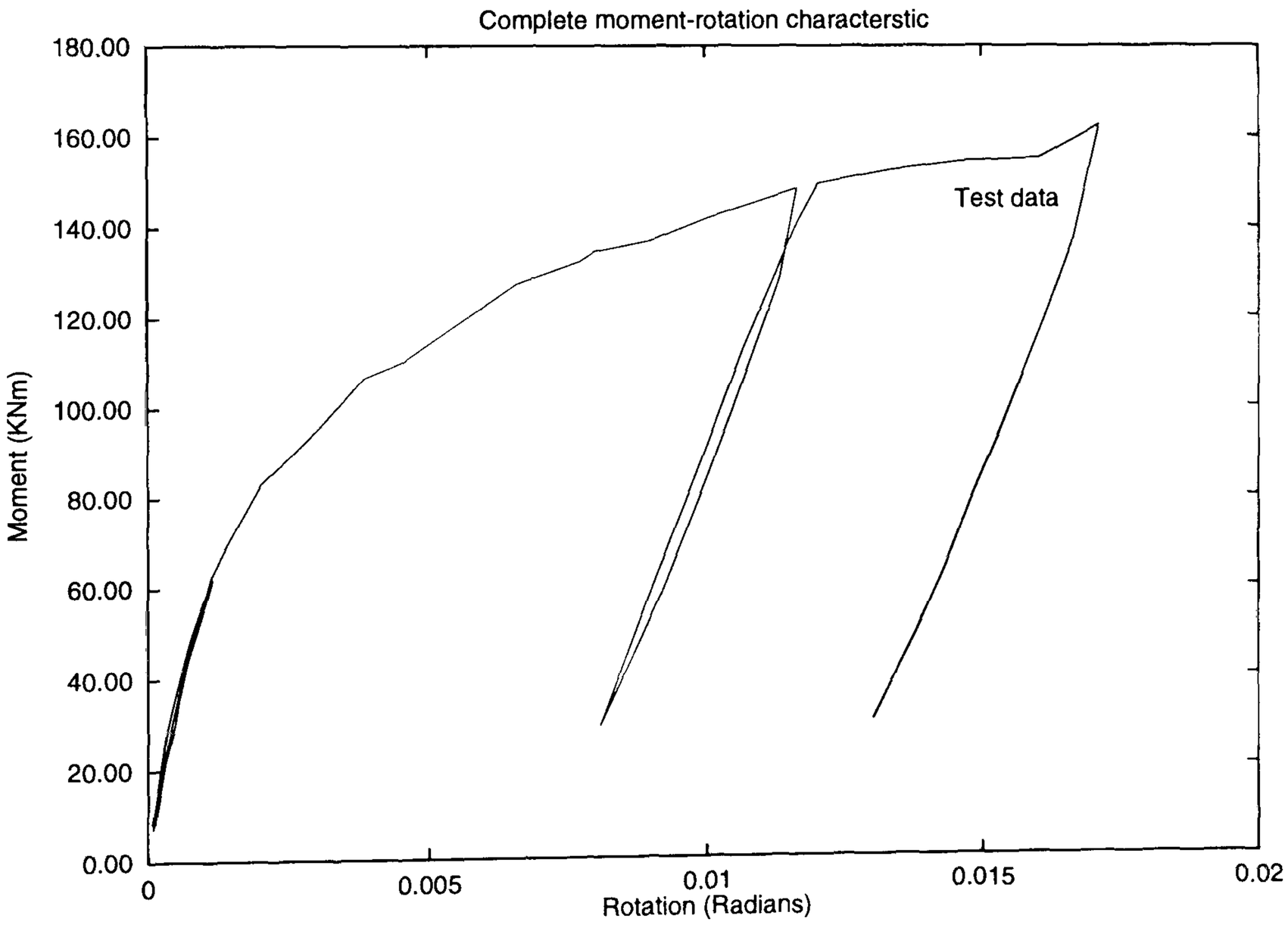

Figure 2.3: Unloading characteristic of connections

It can be seen from Figure 2.3 that at any stage, if the direction of rotation is reversed by reducing the applied moment, then the rotation recovers in an essen-

tially linear fashion that approximates to the initial slope of the characteristic.

It has been established by several researchers[30, 31, 32], that there are three fundamental properties of connection behaviour which would have a pronounced influence on the overall performance of a structure. Firstly, the connection's stiffness applicable to the level of moment that the connection must transmit. This is defined by the slope of the moment-rotation characteristic, which can assume one of three representations, namely the initial, tangent and secant stiffnesses (see Figure 2.4). It can be seen from this figure that the variation in the connection stiffness is considerable. It ranges from a maximum value corresponding to the initial portion of the characteristic and decreases as the moment increases.

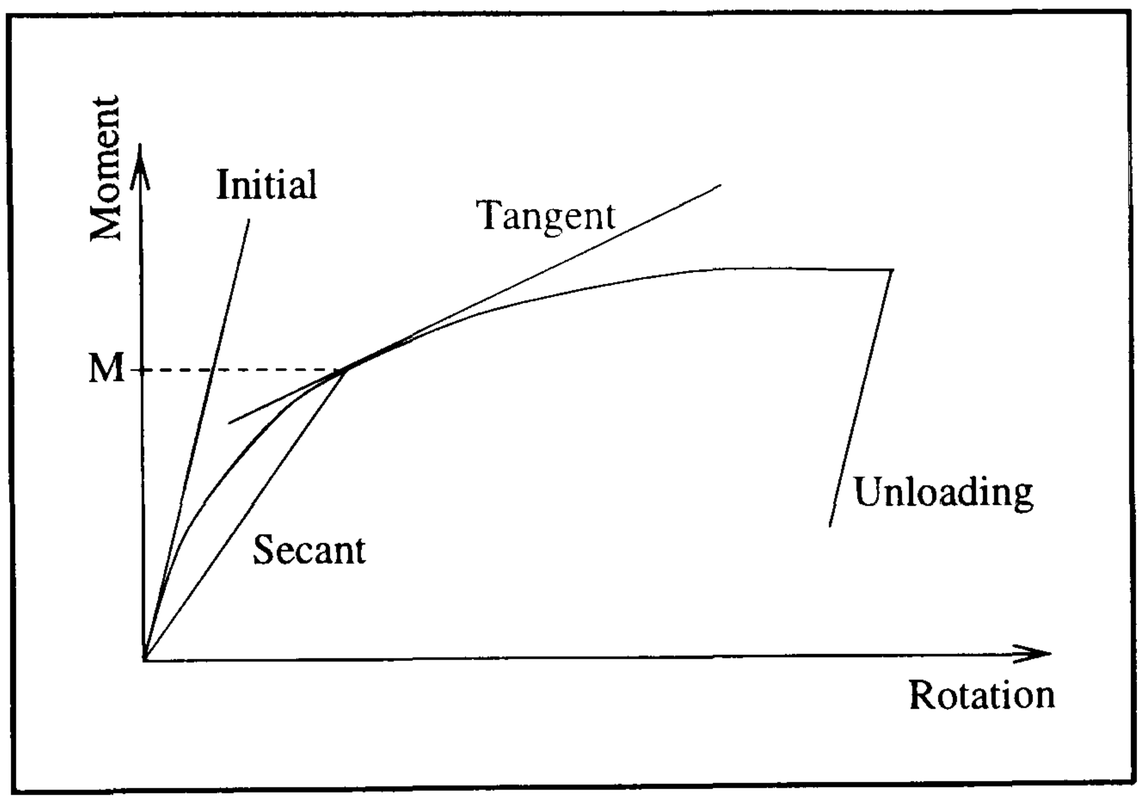

Figure 2.4: Representation of the connections stiffness

The final stiffness indicated in the figure is the unloading stiffness, which is applicable in situations were the connections are subjected to reverse loading sequences. Secondly, the connection's moment of resistance can be identified, corresponding to a pronounced reduction in stiffness, possibly by the characteristic becoming asymptopic to the horizontal, or by fracture of a component. Finally, the amount of ductility exhibited by the connection is important. The ductility is a measure of the rotational deformation sustained by the connection, and would be indicated by the maximum rotation achieved prior to loss of moment resistance or by brittle failure.

The factors which influence these fundamental properties are numerous and

in some instances complicated as a result of interactions occurring between the component parts of the connection. Consequently, the aim of the details listed below is to identify some of the more significant factors, which could be considered to contribute to the explanation for the non-linearity of the moment-rotation characteristic as a whole.

1. The localised yielding of individual components of the connection at different stages of loading.

2. Local buckling in the vicinity of the connection. This may occur in either the beam flanges, the beam and column webs, or in any combination.

3. The resistances of parts of the connection such as bolts and welds that may fail in a brittle manner.

4. The movements of the various constituent parts that make up the connection, relative to one another. During the loading process, irregular slips and movements occur, as a result of the various arrangements and combinations of bolts and structural shapes reacting together.

5. The thicknesses of the individual components that make up a particular connection, since this would have a pronounced effect on the overall geometrical changes caused by the application of the load patterns.

6. With certain connection types, such as header plate and web cleat connections, a marked step in the characteristic can be observed (see Figure 2.2). This step occurs when an initial gap existing between the end of the beam and the column face closes. However, the increase in stiffness cannot usually be capitalised upon, due to the amount of rotational deformation already sustained by the connection, causing the step to occur beyond the deformations that are associated with the theoretical collapse load of the frame[33].

The main problems faced by a designer who would like to take advantage of the particular properties of the connections in frame design, is incorporating them into the frame analysis. To ensure that equilibrium and compatibility are maintained requires a step-by-step computerised procedure which allows several iterations within each load step. The analysis is further complicated by the need to account for load patterns and lateral loads, which will create a situation whereby the connections on either end of a beam behave quite differently: some will be loading whilst others will be unloading. However, to enable such software to be written necessitates a suitable design model being developed.

To this end, many researchers have proposed models either adopting linear or non-linear techniques to predict the behavioural responses of the commonly available connections. A review of their varying approaches has been reported by Nethercot and Zandonini[34], and is summarised briefly below.

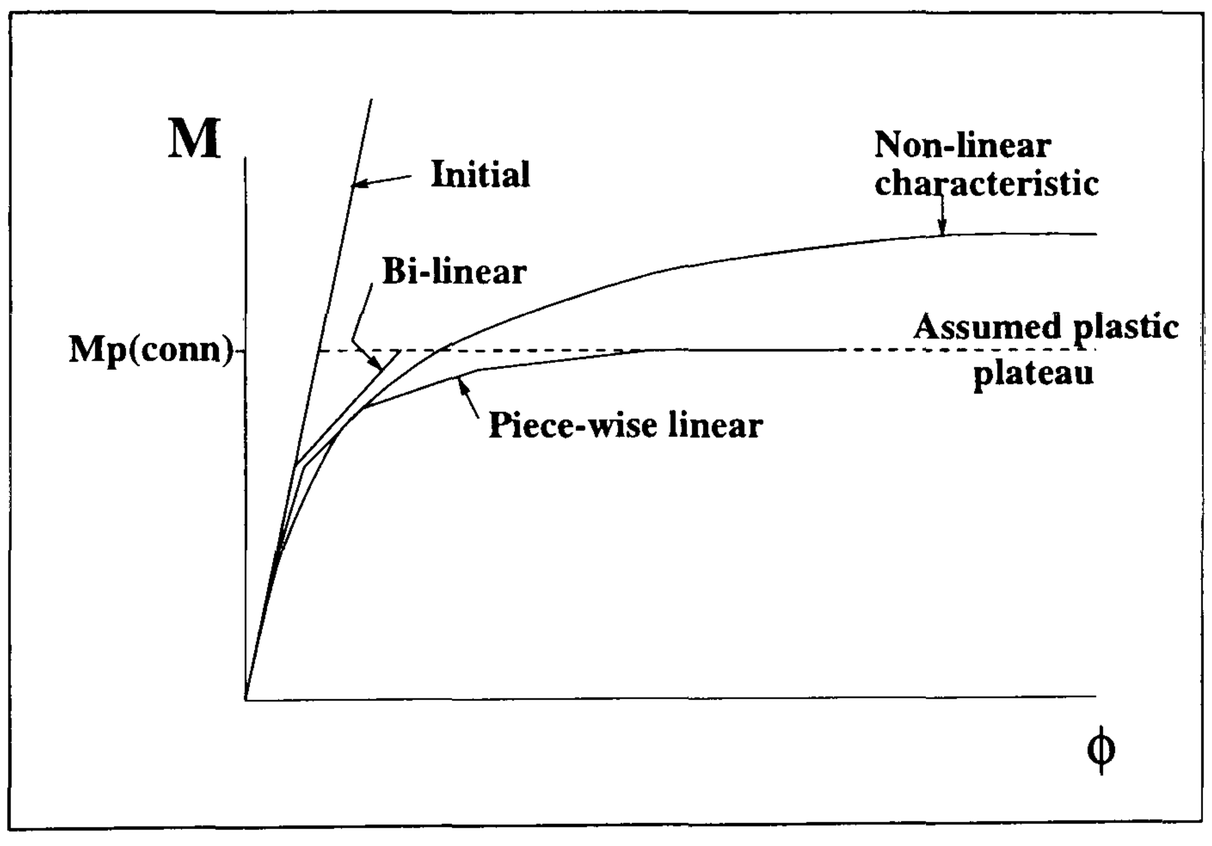

Figure 2.5: linear representations of connection behaviour

There are three types of linear representations which have been adopted by researchers and are illustrated in Figure 2.5. The simplest representation is that of a single straight line propagating from the origin and extending tangentially to the initial portion of the characteristic. This is known as the initial stiffness approach and models which conform to this methodology have been proposed by Rathbun[35] and Baker[36]. The main objection to its use as a

representative model, would be that the amount of rotational deformation sustained by the connection, may be underestimated for anything other than for very small applied moments. To improve on this model, Ang & Morris[37] and Lionberge & Weaver[38] proposed a bi-linear representation. Here the true characteristic is simplified to two straight lines. The first may represent the initial stiffness of the connection, but it is modified at a higher moment as a reflection of the non-linearality of the moment-rotation characteristic. As a further refinement, Poggi & Zandonini proposed a piece-wise approach[39]. For this model, several straight lines are predicted which intersect the characteristic at discrete locations. The philosophy here is to move with an increasing number of linear approximations to a far better representation of the non-linear characteristic.

The next level of complexity involves a completely non-linear approach using well-established mathematical techniques. These techniques include exponential[40, 41], polynomial[42, 43, 44], power series expressions[45], and cubic B-spline curves[46].

As an alternative method to those described so far, several researchers prefer to adopt a finite element model[47, 48]. As the name suggests, the connection is represented by a series of interconnecting elements with common boundary conditions at their interfaces. Matrix equations are then solved as the connection is loaded incrementally, to determine the corresponding element displacements and rotations during all phases of loading up to collapse.

In addition, mechanical models offer a further variation to represent connection behaviour. The principle behind this type of model is being able to divide the connection into a set of mechanical elements which may be interconnected via springs, to represent the behaviour under loading. Consequently, the overall accuracy of the approach relies on a sound understanding of the individual and interactive behaviour of the connection components, in addition to the accuracy of the assumed material properties. A model of this general form has been

proposed by Tschemmenegg[49] (see Figure 2.6).

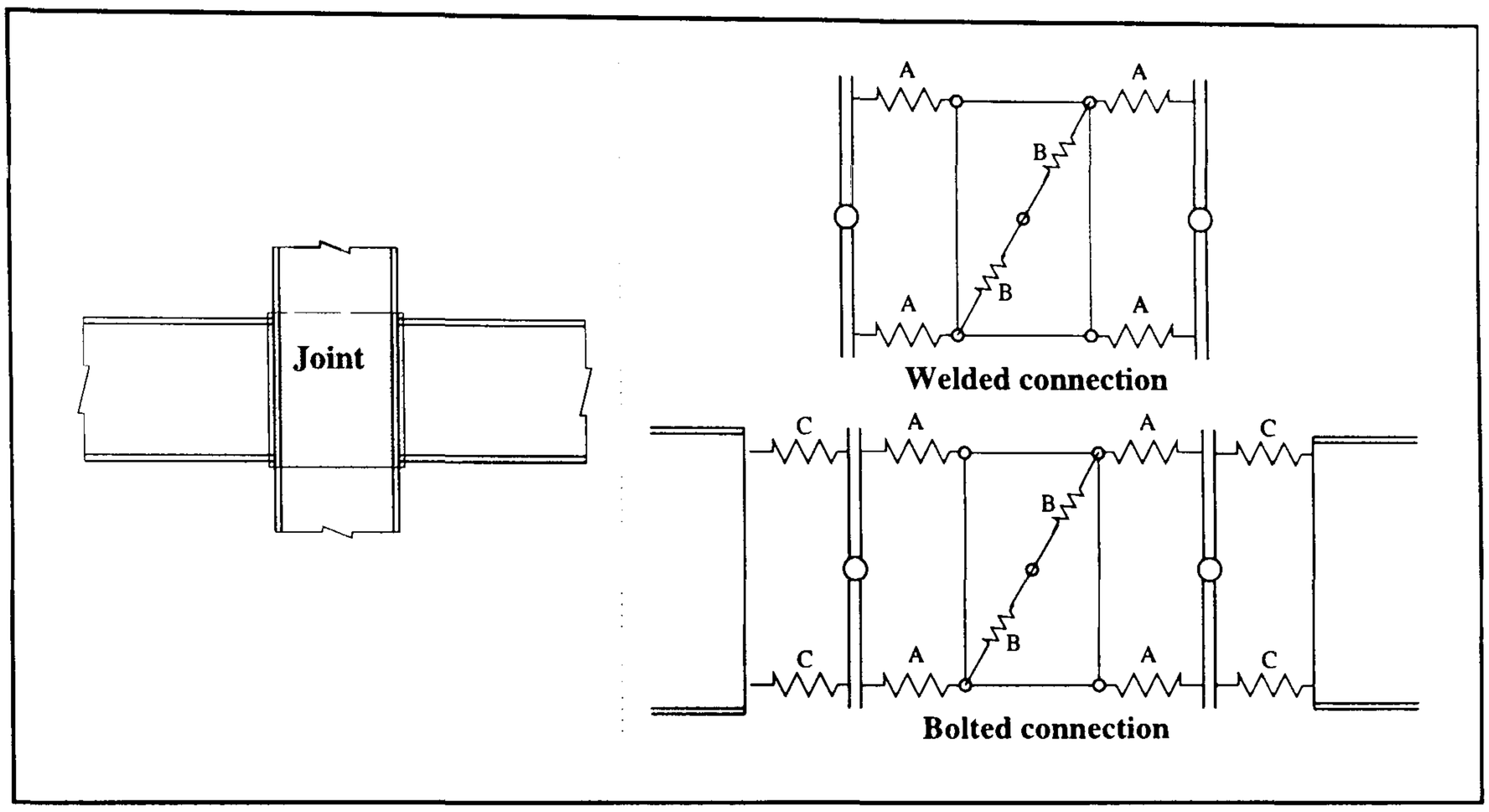

Figure 2.6: Mechanical model proposed by Tschemmenegg

where:

spring set A represent the load between the beam and the column;

spring set B represent the shear deformation in the column web panel; and

spring set C represent the additional deformations that would be present in a bolted connection.

Although from the above there appears to exist an abundance of information to predict a connection's behaviour, there was until recently a lack of practical advice in the form of design rules contained within the available codes of practice[12]. However, with the advent of the harmonised design codes across Europe, in particular Eurocode 3[18], the previously unresolved problems concerning the connection behaviour and subsequent representation are beginning to be addressed.

2.2 European codes of practice

There are nine codes of practice which make up the full range of Structural Eurocodes. The purpose of the following section will be to review the code

applicable to the design of steel structures, Eurocode 3[17], which will become available by the end of the century as a European standard and may supercede the British code of practice BS5950 Part 1: 1990[12].

Eurocode 3 ENV 1994-1-1

The advent of this standard has the potential to revolutionise the treatment of beam-to-column connections, since it is the only standard to provide practical design rules to enable a designer to represent the moment rotation-characteristics for a connection designed as part of a semi-rigid frame.

Initially the code requires the designer to classify the connections under the headings of strength and rigidity, since these two connection properties influence the type of global analysis which may be adopted for the frame as a whole (see Table 2.1).

Method of global analysis	Classification of the connections		
Elastic	Nominally pinned	Rigid	Semi-rigid
Rigid-plastic	Nominally pinned	Full strength	Partial strength
Elastic-plastic	Nominally pinned	Rigid & full strength	Semi-rigid & partial strength Semi-rigid & full strength Rigid & partial strength
Type of design adopted	*Simple*	*Continuous*	*Semi-continuous*

Table 2.1: Type of global analysis applicable to the connections classification

These types are

Elastic global analysis - This is based on the assumption that the stress-strain behaviour of the material is linear, whatever the stress level. First-order and second-order analyses are permitted; in which first-order theory assumes that

the initial geometry of the structure remains constant throughout the analysis, whereas second-order theory takes into account the influence of the deformation of the structure.

Rigid-plastic global analysis - In this type of analysis, elastic deformations of the members are neglected and plastic deformations are assumed to be concentrated at plastic hinge locations. Only first order analysis is permitted inless the frame being analysed conforms to the requirements necessary for the frame to be classified as a sway frame, clause 5.2.5.2, and the conditions of clause 5.2.6.3 are met.

Elastic-plastic global analysis - This has been further subdivided into:

1. Elastic-perfectly plastic - In this type of analysis, it is assumed that the cross-section remains fully elastic until the plastic resistance moment is reached and then becomes fully plastic. Plastic deformations are assumed to be concentrated at the plastic hinge locations.

2. Elasto-plastic - In this type of analysis, a bi-linear stress-strain relationship may be used, where the cross-section remains fully elastic until the stress in the extreme fibres reaches the yield strength. As the moment continues to increase, the section yields gradually as plasticity spreads across the cross-section and plastic deformations extend partially along the member.

Second-order effects - These effects collectively refer to the influence that the vertical loads have on the side sway stiffness of a column or frame, $P - \Delta$ effect, and the influence of the axial force on the flexural stiffness of a member, $P - \delta$ effect (see Figure 2.7).

2.2.1 Connection classification

Classification by strength

The strength classification aims to establish the corresponding resistance of a

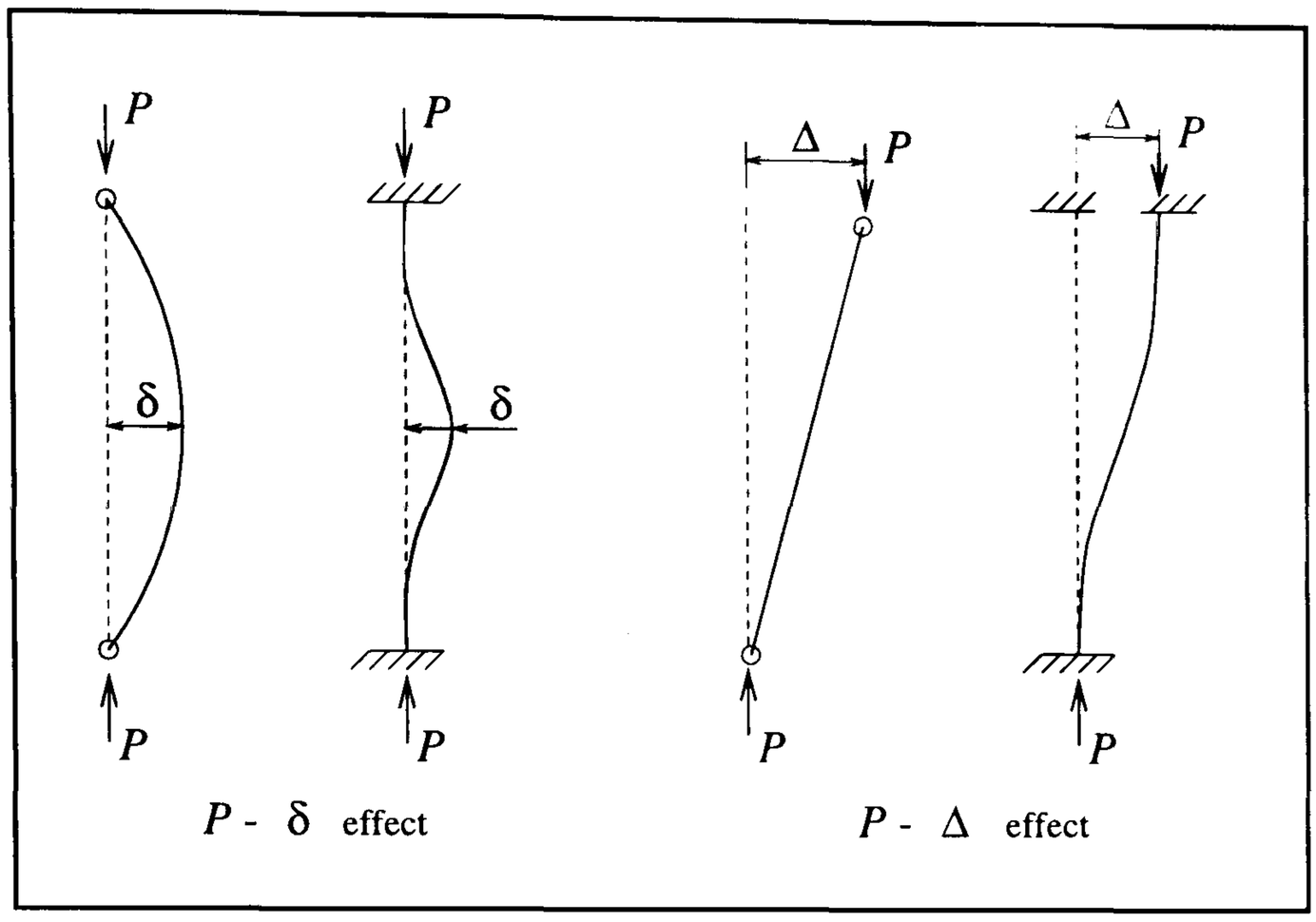

Figure 2.7: Second order effects

connection with respect to its connecting beam. There are three divisions within this classification which may be defined as follows.

1. Nominally pinned connections - This type of connection should be capable of transmitting the calculated design forces, without developing significant moments which might adversely affect members of the structure.

2. Partial strength connections - This type of connection should be capable of transmitting the calculated design forces and moments, but its design resistance would be lower than the connected beam. The rotation capacity of a partial strength connection which occurs at a plastic hinge location shall not be less than that needed to enable all the necessary plastic hinges to develop under the design loads. This rotation capacity may be vindicated by experimental evidence or through experience, whereby the connection's properties have been adequately proved.

3. Full strength connections - This type of connection should possess a design resistance in excess of the connected beam. Over-strength factors must be considered in situations where the rotation capacity is limited. However, if the design resistance of the connection is greater than 1.2 times the design

plastic resistance of the beam, the rotation capacity of the connection may be considered irrelevant. This is because it may then be assumed that any necessary plastic hinges will form in the beam in preference to the connection.

Classification by rigidity

The rigidity classification aims to categorise a connection's rotational behaviour. by establishing the degree of slope continuity that the connection can achieve. There are three divisions to this classification, which may be described as follows.

1. Nominally pinned connections - A nominally pinned connection shall be so designed that it cannot develop significant moments which might adversely affect members of the structure. This type of connection should be capable of transmitting the forces calculated in design and should be capable of accepting the resulting rotations. Furthermore, for a connection to behave as though nominally pinned, the revised Annex J (see section 2.3.1) states that its initial stiffness, $S_{j.init}$, should satisfy the requirements of equation 2.1.

$$S_{j.init} \leq \frac{EI_b}{2L_b} \tag{2.1}$$

where :

E - Young's modulus for steel

I_b - Second moment of area for the connecting beam

L_b - Length of the connecting beam.

2. Semi-rigid connections - This division encompasses all the connections which do not meet the criteria specified for the other divisions.

3. Rigid connections - This type of connection shall be so designed that its deformation has no significant influence on the distribution of internal forces

and moments in the structure. In addition. the connection must be capable of transmitting the forces and moments calculated in design.

Nominally pinned connections aside, to enable a connection's performance to be assessed in the context of the other two divisions, the code provides a limiting non-dimensional representation of a rigid beam-to-column connection characteristic (see figure 2.8).

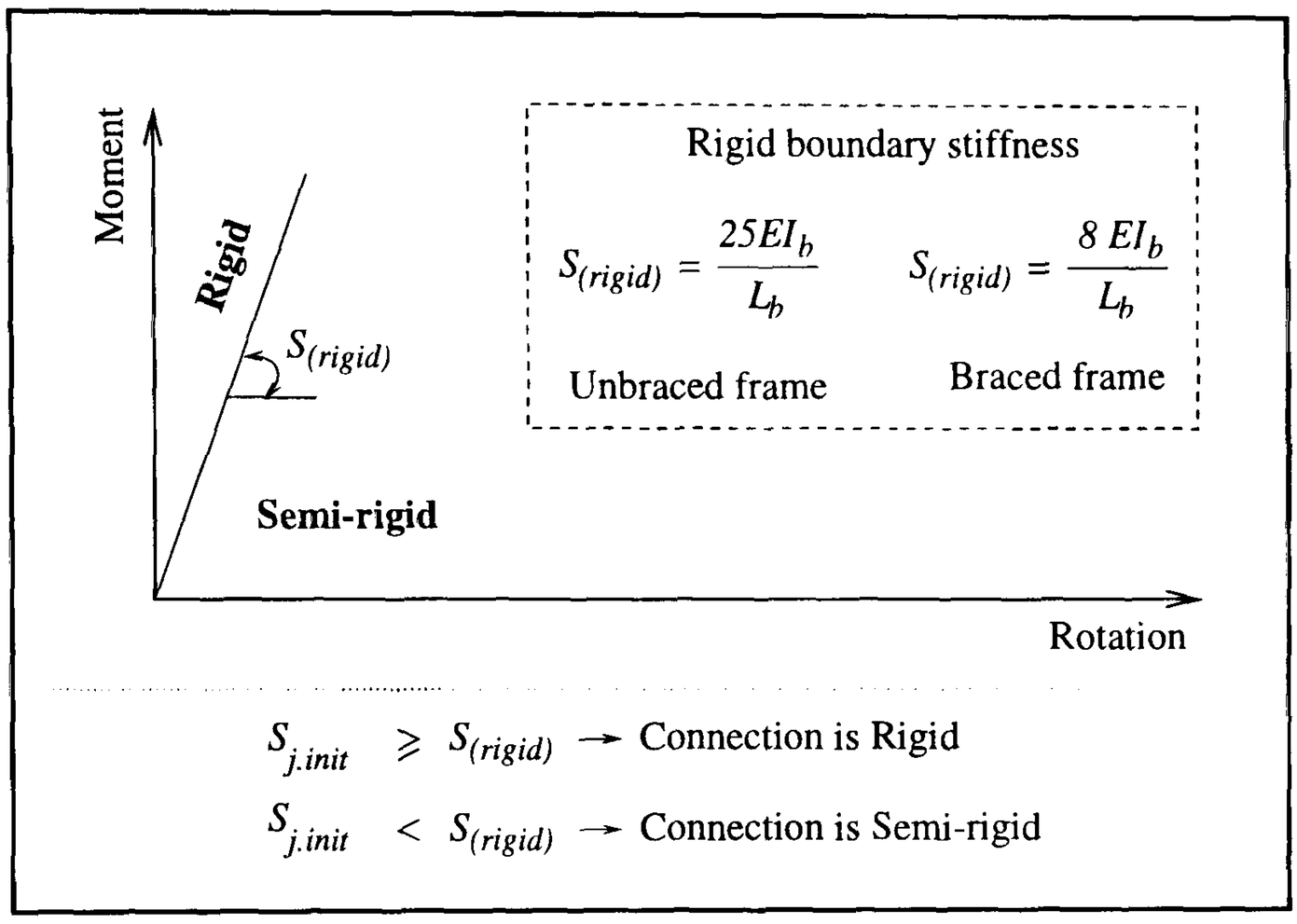

Figure 2.8: Eurocode 3 classification boundaries for rigid beam-to-column connections - revised Annex J[18]

The comparison then follows, whereby if the initial portion of the connection's characteristic lies above the solid line on the appropriate diagram, it may be considered as rigid; alternatively, if it lies below the line then it may be regarded as semi-rigid.

There is no interaction between the two classifications of strength and rigidity. Consequently, a connection may be classified as rigid or semi-rigid and at the same time be either partial or full strength.

2.2.2 Types of framing recognised by Eurocode 3

Three types of framing have been defined in Eurocode 3 and are used to

distinguish between frames which are either:

1. Semi-continuous, in which the structural properties of the connections need explicit consideration in the global analysis.

2. Continuous, in which the structural properties of the members need to be considered in the global analysis

3. Simple, in which the joints are not required to resist moments.

Eurocode 3 and the design rules for bolted connections therein[17] were used to predict the moment-rotational characteristics for Reading's analytical verification of the Wind-Moment method[8]. The objective of the study was to investigate the influence of incorporating semi-rigid connections, in comparison with the behaviour assumed by the method. As a consequence of using semi-rigid connections, the frames were classified as semi-continuous under the definitions listed above.

2.3 Model used by Reading

The true non-linear form of a connections characteristic is recognised by the code; however linearised approximations are permitted provided this approximate behaviour lies completely below the true form. This simplified representation is illustrated in Figure 2.9, which can be described as follows.

The characteristic may be assumed to be linear up to two thirds of the connection's moment of resistance. A second straight line then approximates the remaining curve up to the attainment of the connection's predicted moment of resistance, whereupon a plateau is substituted. This plateau is known as the plastic plateau and represents an ever-increasing rotation under a constant moment.

To predict this simplified characteristic, comprehensive rules are provided by an annex to the code, Annex J, which were specifically included to cover the de-

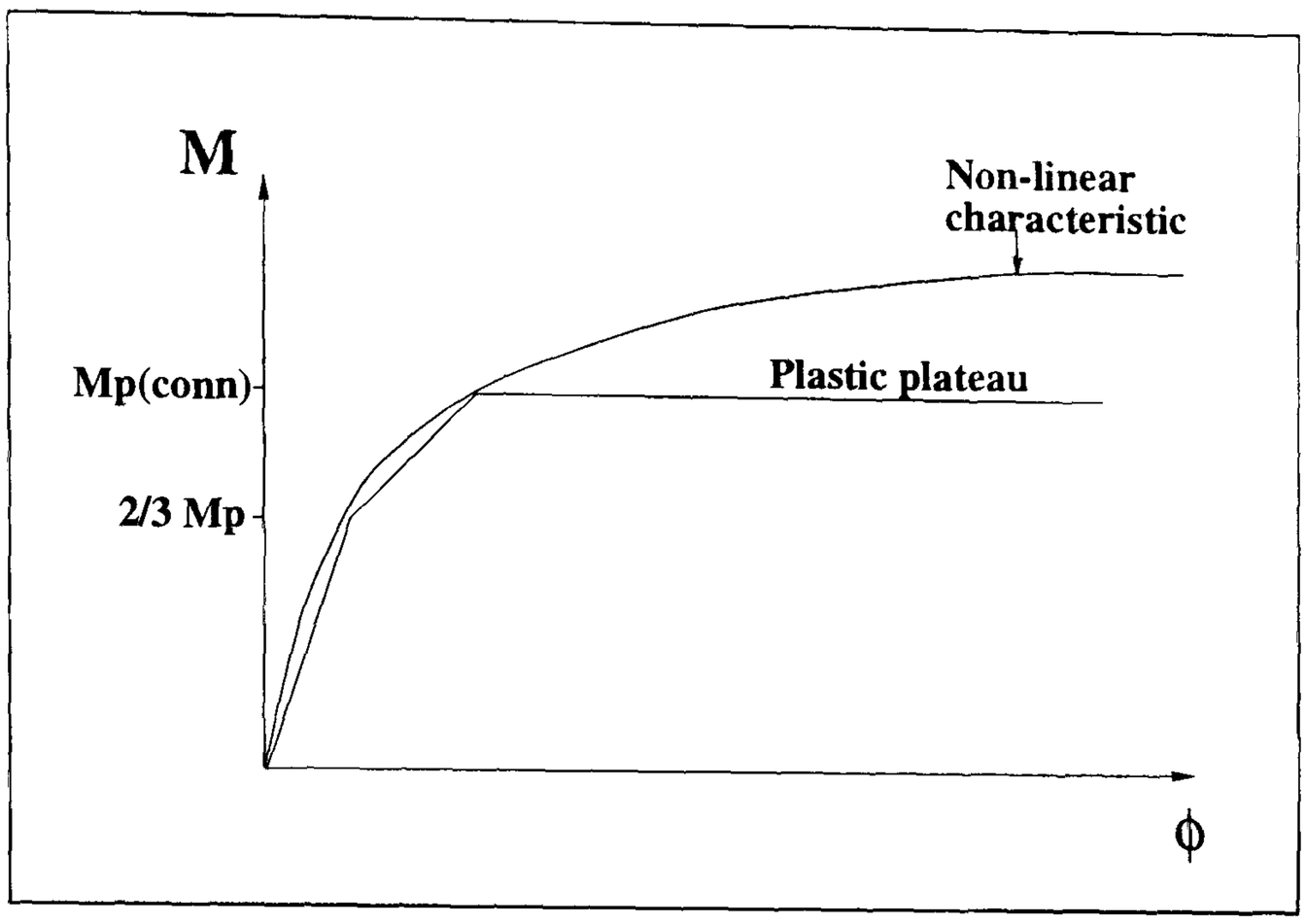

Figure 2.9: Simplified characteristic acceptable to Eurocode 3 part 1.1

sign of bolted beam-to-column connections. The procedures which have to be undertaken to enable the prediction of the connection's moment capacity to be calculated may be found elsewhere[8]. However, since the authors work described in Chapter 3 is concerned with the prediction of a connections rotational stiffness, it is appropriate to concentrate on this aspect of the behavioural characteristics.

2.3.1 Prediction equations for rotational stiffness of bolted end plate connections

Eurocode 3 - Annex J (prediction of rotational stiffness)

The model proposed by this annex takes the form of a mathematical expression (see equation 2.2), which aims to produce a secant stiffness S_j for specified values of the applied moment, particularly at two thirds of the connection's design moment of resistance and at the design moment of resistance itself.

A prediction model based on the need to predict a varying stiffness is a complicated task if a reliable assessment of a connections rotational stiffness is to be obtained. This complication is the result of the model having to compensate for the inevitable variability in plasticity which would be present in different areas

of the connection. The model, which is applicable to bolted end plates only, is represented by:

$$S_j = \frac{E{h_1}^2 t_{cw}}{\sum \frac{\mu_i}{k_i} \left[\frac{F_i}{F_{i.Rd}}\right]^2} \tag{2.2}$$

where :

h_1 = Lever arm from the highest bolt row in the connection, to the centre of resistance of the compression zone

μ_i = Modification factor

k_i = Stiffness factor for component i

F_i = Force in component i of the connection due to the applied moment

$F_{i.Rd}$ = Design resistance of component i of the connection.

The overall stiffness for a particular connection was predominantly a function of the parameter, k_i, and the ratio of force carried by the component to its design resistance, $\frac{F_i}{F_{i.Rd}}$. The components for which values of k_i were to be calculated are as follows:

1. The column flange in tension.

2. The end plate in tension.

3. The bolts in tension.

4. The column web in shear, tension and compression.

To evaluate the stiffness of the above components, guidance was given in the form of either constants or mathematical expressions.

During and after publication of ENV 1993-1-1, considerable comment was made from both practitioners and academics with regard to the useability and technical content of the annex. It was these comments that lead to a revised version of annex J[18] being prepared for inclusion in Eurocode 3 when it is published

as a European Standard. One of the major areas discussed was the acceptability of equation 2.2, to calculate the rotational stiffness of an end plate connection. It was concluded that the proposed equation did not always lead to consistent predictions[21] and should therefore be subsequently revised. In addition. some of the other objectives which were incorporated into the redrafted annex were an improvement of some of the detailed rules as a result of information obtained from recent investigations, and to further extend the rules to a wider range of joint types by permitting assemblies of individual components. Consequently, joints with bolted angle flange cleat connections are now included. although not considered any further in this thesis.

Eurocode 3 - Annex J(revised)

The code retains the recognition of the true form for the moment-rotation characteristic and the concept of linearised approximations. The difference comes in the methodology adopted for calculating the corresponding rotational stiffness for the connection. The model again has been expressed as a mathematical equation; however its aim has been simplified to the prediction of the connection's initial stiffness. This, in theory at least, should provide an improvement in the consistency of the resulting predictions, since connection plastification may now be neglected. This prediction alone may be deemed satisfactory to represent the rotational stiffness, provided that the design bending moment will not exceed two thirds of the connection's moment of resistance. However, if this criteria is not met, then the initial stiffness prediction would have to be modified to prevent the rotation at higher values of moment from being underestimated. Figure 2.10 illustrates the modification factor applicable for a bolted end plate connection in order to produce a bi-linear representation for the characteristic, for use in conjunction with elastic or elastic-plastic global analysis. Following modification, the model again assumes that a plastic plateau would follow the attainment of the connection's design moment of resistance.

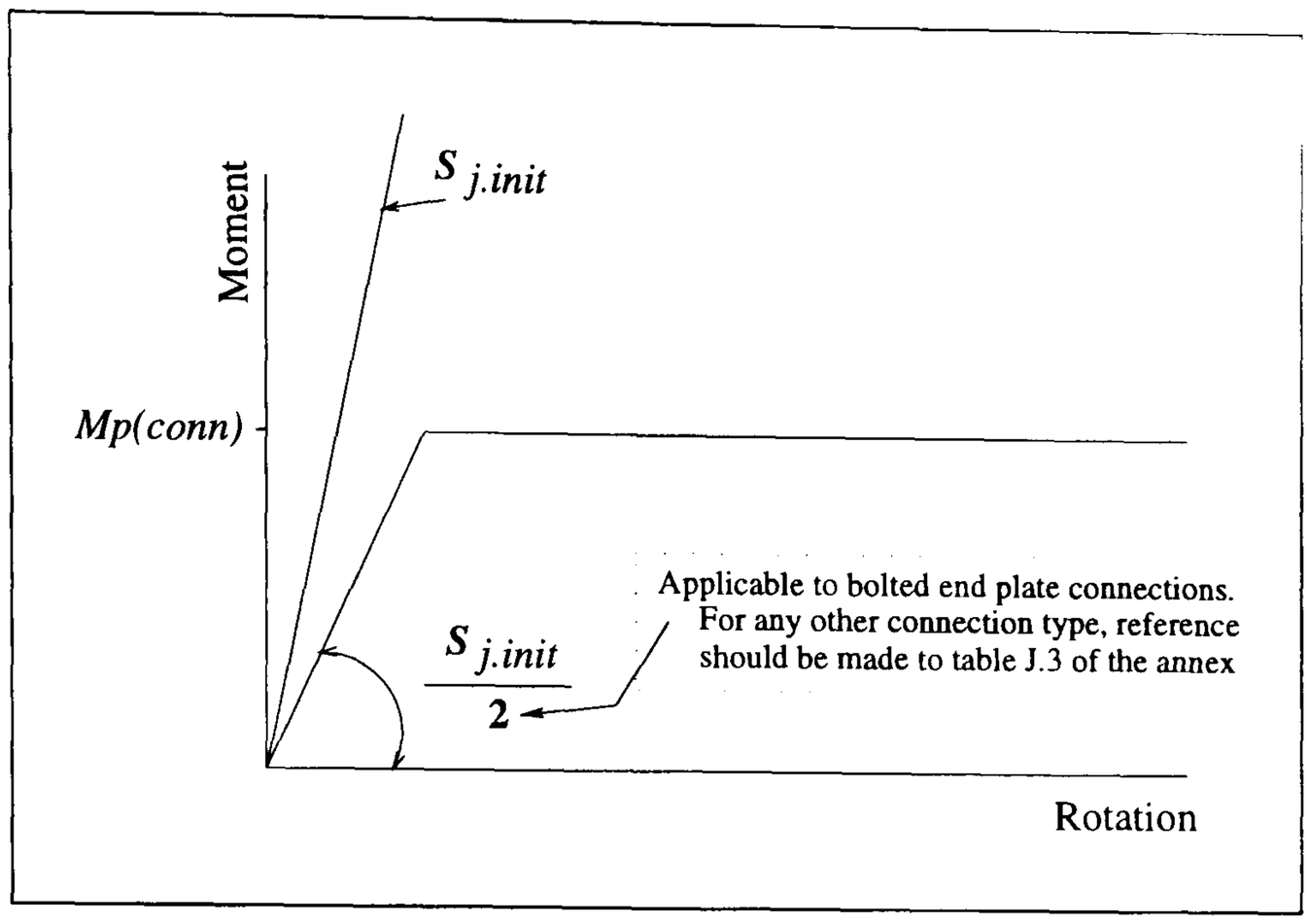

Figure 2.10: Bi-linear moment-rotation characteristic proposed by the revised Annex J

The revised equation for calculating the rotational stiffness, is shown by equation 2.3.

$$S_j = \frac{Ez^2}{\mu \sum_i \frac{1}{k_i}} \tag{2.3}$$

where :

k_i = the stiffness coefficient representing component i

z = lever arm

μ = the stiffness ratio $\left[\frac{1.5M_j}{Mp(conn)}\right]^{2.7}$ but ≥ 1.0

$S_{j.init}$ = the value of S_j at zero applied moment M_j.

The components which contribute to the calculation of k_i remain unaltered. However their calculation has been modified to reflect the change to an initial stiffness approach.

The author has undertaken a verification of this new prediction formulae for bolted extended and flush end plate connections (see Chapter 3), from which the following conclusions may be drawn.

1. The main contributions to the connections' flexibility were associated with the column web and the bolts, with the other components such as the end

plate and column flange, being of less significance.

2. The equation 2.3 over-predicted the initial stiffness for a flush end plate connection for 60% of the connections considered, rising to 75% of the connections considered for the extended end plate connections.

2.4 Moment-rotation characteristics suitable for unbraced design

2.4.1 Connection stiffness at ultimate limit state

To establish a moment-rotation characteristic which would be suitable for unbraced design, necessitates an appreciation of the connection's response under the various combinations of applied loadings. These applied loadings by definition, would consist of static loads caused by the weight of the structure in combination with any imposed loads, and dynamic wind loads. The different effects that these types of loadings have on the connection response, may be assessed by considering the typical frame shown in Figure 2.11a.

Following the application of the vertical load, the response of the connections are shown by Figure 2.11b. The moment-rotation characteristic for each connection follows the loading path up to the point where equilibrium of forces and moments in the frame are restored. This point is denoted 1 in the figure. It can also be seen that the moments and rotations at each connection are of the same magnitude, with the rotations being opposite signs. When the horizontal load is now applied to the frame, the connections respond quite differently (see Figure 2.11c). The effect of the horizontal load is to make the frame sway sideways. This sideways movement is resisted by the bending stiffness in the frame, by forcing the windward side of the beam to try and straighten. To achieve this, the windward connection would rotate in the opposite direction and unload, whereas the leeward side of the beam and consequently the leeward

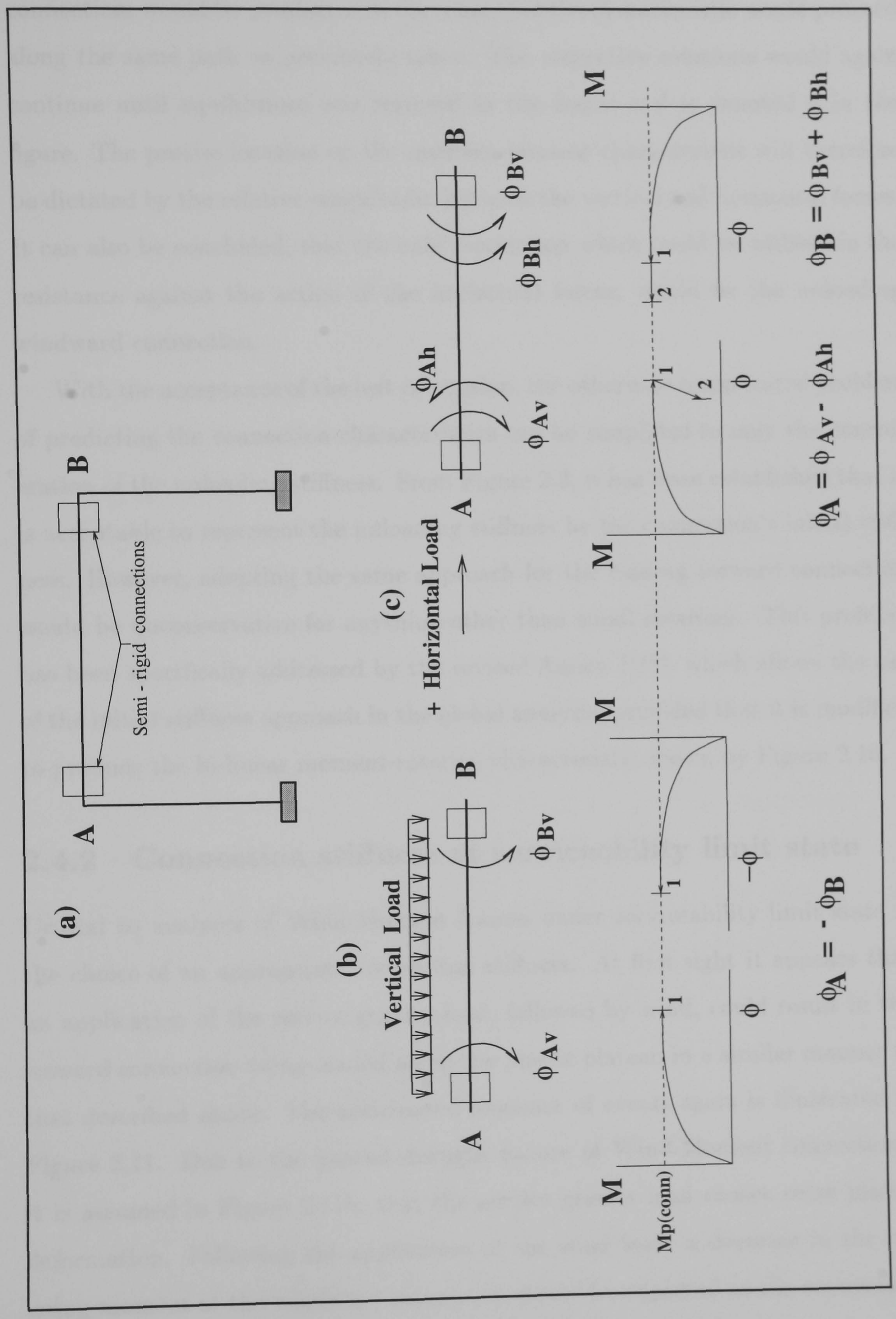

Figure 2.11: Connection response under applied loads

connection, would be unaffected in the sense that the characteristic would proceed along the same path as previously taken. The respective rotations would again continue until equilibrium was restored in the frame and is denoted 2 in the figure. The precise location on the moment-rotation characteristic will therefore be dictated by the relative magnitudes between the vertical and horizontal forces. It can also be concluded, that the only connection which could be utilised in the resistance against the action of the horizontal forces, would be the unloading windward connection.

With the acceptance of the last conclusion, the otherwise complicated problem of predicting the connection characteristics can be simplified to only the consideration of the unloading stiffness. From Figure 2.3, it has been established that it is acceptable to represent the unloading stiffness by the connection's initial stiffness. However, adopting the same approach for the loading leeward connection would be unconservative for anything other than small rotations. This problem has been specifically addressed by the revised Annex J[18], which allows the use of the initial stiffness approach in the global analysis, provided that it is modified to produce the bi-linear moment-rotation characteristic shown by Figure 2.10.

2.4.2 Connection stiffness at serviceability limit state

Crucial to analyses of Wind-Moment frames under serviceability limit state is the choice of an appropriate connection stiffness. At first sight it appears that an application of the service gravity load, followed by wind, could result in the leeward connection being loaded along the plastic plateau in a similar manner to that described above. The anticipated sequence of events again is illustrated in Figure 2.11. Due to the partial-strength nature of Wind-Moment connections, it is assumed in Figure 2.11b, that the service gravity load causes some plastic deformation. Following the application of the wind load, a decrease in the existing moment at the windward connection would be expected as the connection unloads; however, the plastic deformation on the leeward side 2.11b would con-

tinue. This implies that the same connection stiffness model which was adopted for the frames analysed under ultimate limit state, would again be applicable under serviceability conditions. However, there are three objections which could count against the view that the leeward connection should be treated as a plastic hinge.

Firstly, the approximation of the connection response as elastic-plastic, will result in the flexibility being increased above that shown by full scale test results. Figures 3.14 to 3.17 (see Chapter 3) show that the experimental behaviour of bolted connections would be far from a plastic plateau. Therefore, to treat a leeward connection as devoid of stiffness will over-estimate the flexibility of the frame. Furthermore, a deeper objection concerns the nature of wind loading itself.

The quasi-static equivalent wind loads used in design are just that; in reality buildings respond dynamically to wind by swaying to and fro, so that the shakedown process is symmetrical, irrespective of wind direction. Were it not so, one would see evidence of leaning buildings. Thus to determine sway deflections under service loading, the stiffness of each connection has been taken as its initial value, to represent the subsequent stiffness after shakedown.

The third objection to a more conservative approach arises from the nature of the sway limit itself. Design codes give recommended limits on deflection[17, 12], but as Eurocode 3 makes clear, they are not performance criteria; rather the limits are intended for comparison with results of calculations, usually on bare frames. The justification for these limits rests on the satisfactory performance of structures in practice. Some of these will have been designed by the Wind-Moment method; prior to the publication of reference [1] and consequently, the frames would have been designed without any allowance for connection flexibility.

It was therefore concluded that with the ability to calculate a reasonable estimate of the initial/unloading connection stiffness, it is appropriate to consider this value, but more conservative approaches should be avoided.

Summary

From the above, it has been shown that there are two different moment-rotation characteristics which are necessary to represent the connection response when considering unbraced design. Therefore to proceed with the frame study necessitated the production of a prediction equation that models the connection's initial stiffness. It is important to note however, that a too-stiff prediction of the connections initial stiffness must be avoided to prevent unconservative results from being obtained from the analysis, since it is this value that governs the frames sway at serviceability limit state and stability at ultimate limit state. Equation 2.3 was unavailable at the time the frame study was performed and therefore, the model described within Chapter 3 was developed by the author and adopted to enable the re-validation of the Wind-Moment method using the standard connections to be undertaken (see Chapter 4).

Chapter 3

Prediction equation to model the initial stiffness response for thin end plate connections

3.1 General

A method for determining the initial stiffness of flush and extended end plate connections is presented and verified empirically. The derivation of the equation was based on assumptions that are only valid for connections where the end plate is thin enough to allow the deformation characteristics to be ductile (see Chapter 1, section 1.4). The equation is not designed for general application to all types of end plate connections.

3.2 Derivation of the prediction equation

To enable the formulation of an initial stiffness prediction equation, the following were identified as the main parameters which would influence the connection's flexibility. Firstly, the end plate itself must play a significant role, since it has been designed to provide the connection with ductility and therefore is thin enough to

sustain considerable deformation without fracturing. Secondly, in a similar fashion to the end plate the connecting column flange was assumed to be the other main contributor, although it is recognised that its thickness is purely dependent upon the column section adopted, which would be chosen based on considerations of frame stability and strength and not in terms of adding flexibility to the connection. The prediction equation was therefore derived based primarily on the summation of these two individual flexibilities (see Figure 3.1).

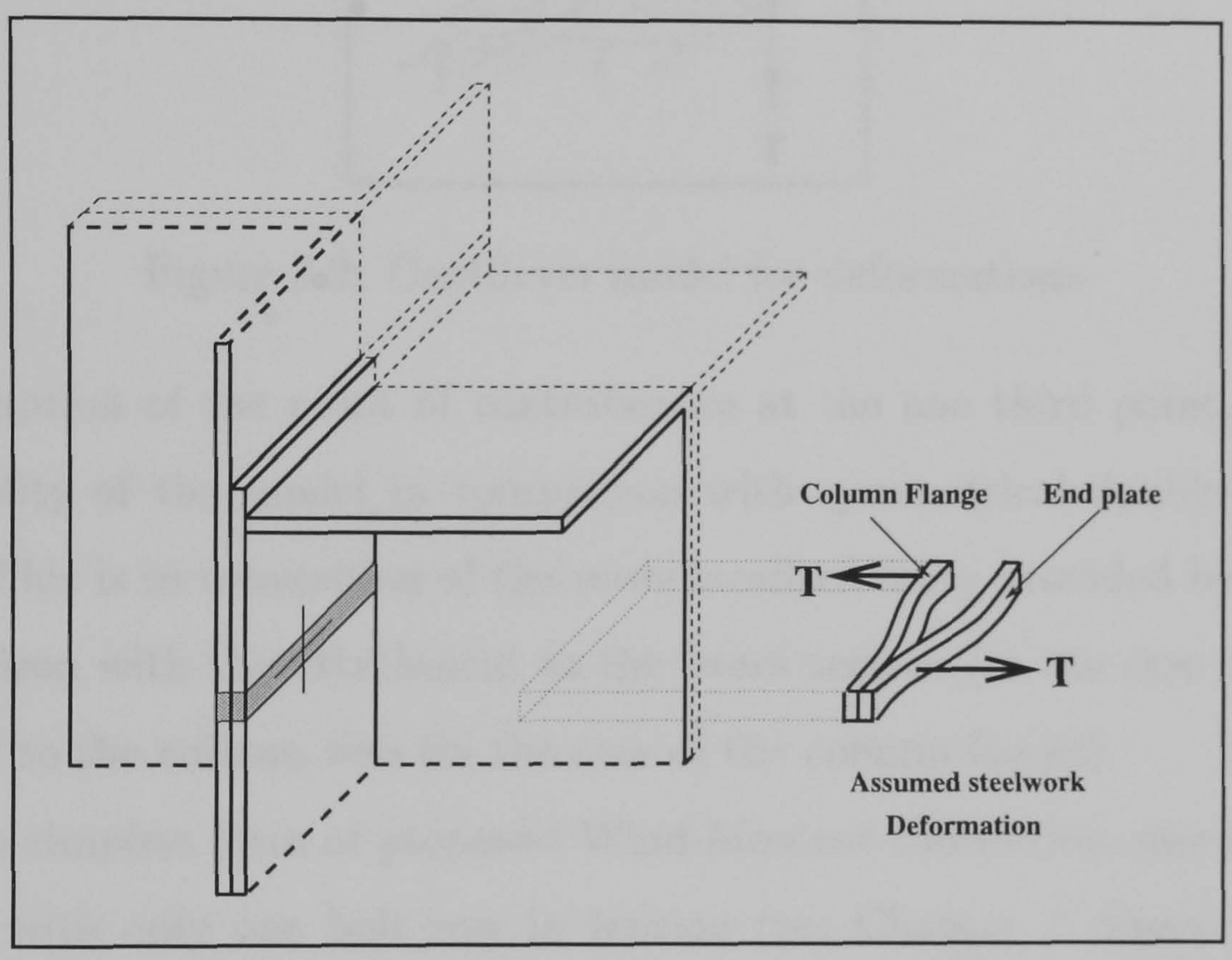

Figure 3.1: Deformation of the end plate and column flange

Any contribution to the flexibility of the connection caused by the other component parts was initially neglected. For example the bolts were assumed to be unextended as they possessed sufficient strength not to yield. However, their influence was recognised later by the inclusion of a coefficient to enhance the overall flexibility.

The end plate and column flange are held together by the tension bolts. Bending of the end plate occurs between the bolt position and the welds which attach the plate to the beam section (for simplicity in presentation, deformation between the bolts and the beam flange is not shown in Figure 3.1). Bending of the

column flange occurs between the bolt position and the root fillet between the flange outstand and the column web. For the initial behaviour, it was assumed that deformation of each component comprised the elastic response of two cantilevers whose tips provide a point of contraflexure in the total deformed shape of the component (see Figure 3.2).

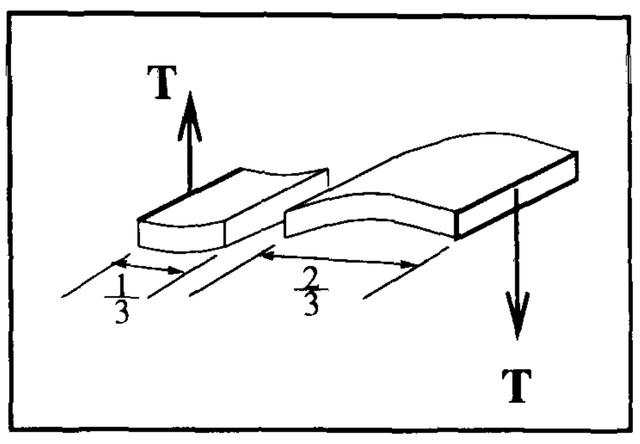

Figure 3.2: Cantilever model for deformations

The assumption of the point of contraflexure at the one third point, increases the flexibility of the model in comparison with symmetrical double-curvature bending. This is in recognition of the more localised fixity provided by the bolts in comparison with the attachment to the beam section (in the case of the end plate) and to the column web (in the case of the column flange).

For the simplest form of proposed Wind-Moment connection, namely a flush end plate with only one bolt row in tension (see Chapter 1, Figure 1.4), the revised Annex J[18], indicates that for the standard dimensions adopted for the bolt cross-centres and edge distances, the most likely yield line pattern to occur under these circumstances would have a circular configuration (see Figure 3.3).

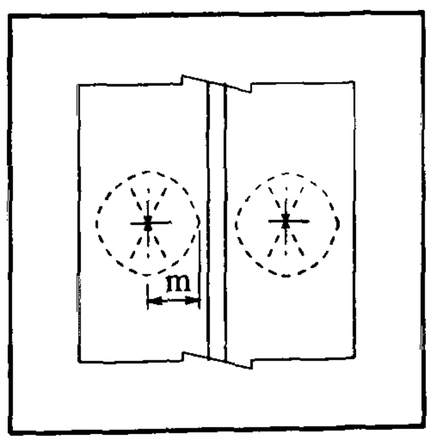

Figure 3.3: Circular yield line pattern as envisaged by Annex J

The dimension 'm' is defined as in the annex, as the distance from the bolt centre to 20% into the end plate-to-beam weld, or the root radius of the column

section. (The revised Annex J cited above will be subsequently referred to as Annex J).

To apply the cantilever model, the total length of the two cantilevers was taken as dimension 'm', as shown in Figure 3.4. It is more difficult though to estimate the corresponding equivalent breadth applicable to the cantilever model.

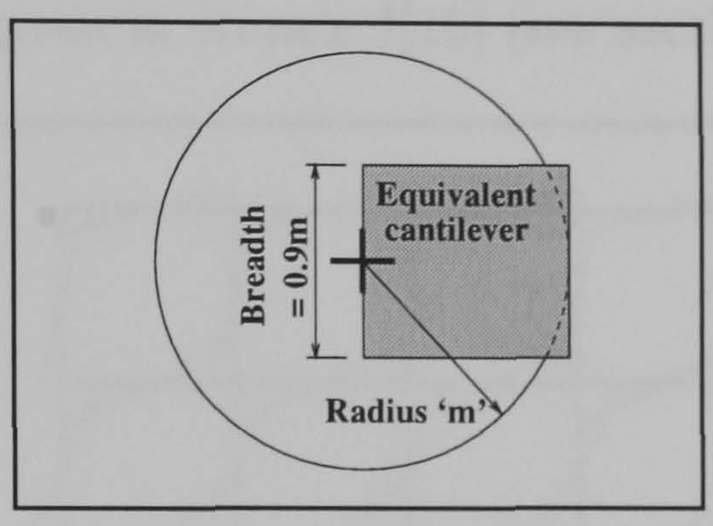

Figure 3.4: Equivalent length and breadth for the cantilever approximation

In view of the circular shape of the yield line pattern, it was assumed that the total breadth of the equivalent cantilevers would equal 0.9m (i.e. 0.45m each side of the centre line of the bolts, as shown in Figure 3.4).

The model ignores any flexibility arising from deformation of the column web panel in shear (see Figure 3.5) which arises in an external column, or in a column that is subjected to unbalanced loading.

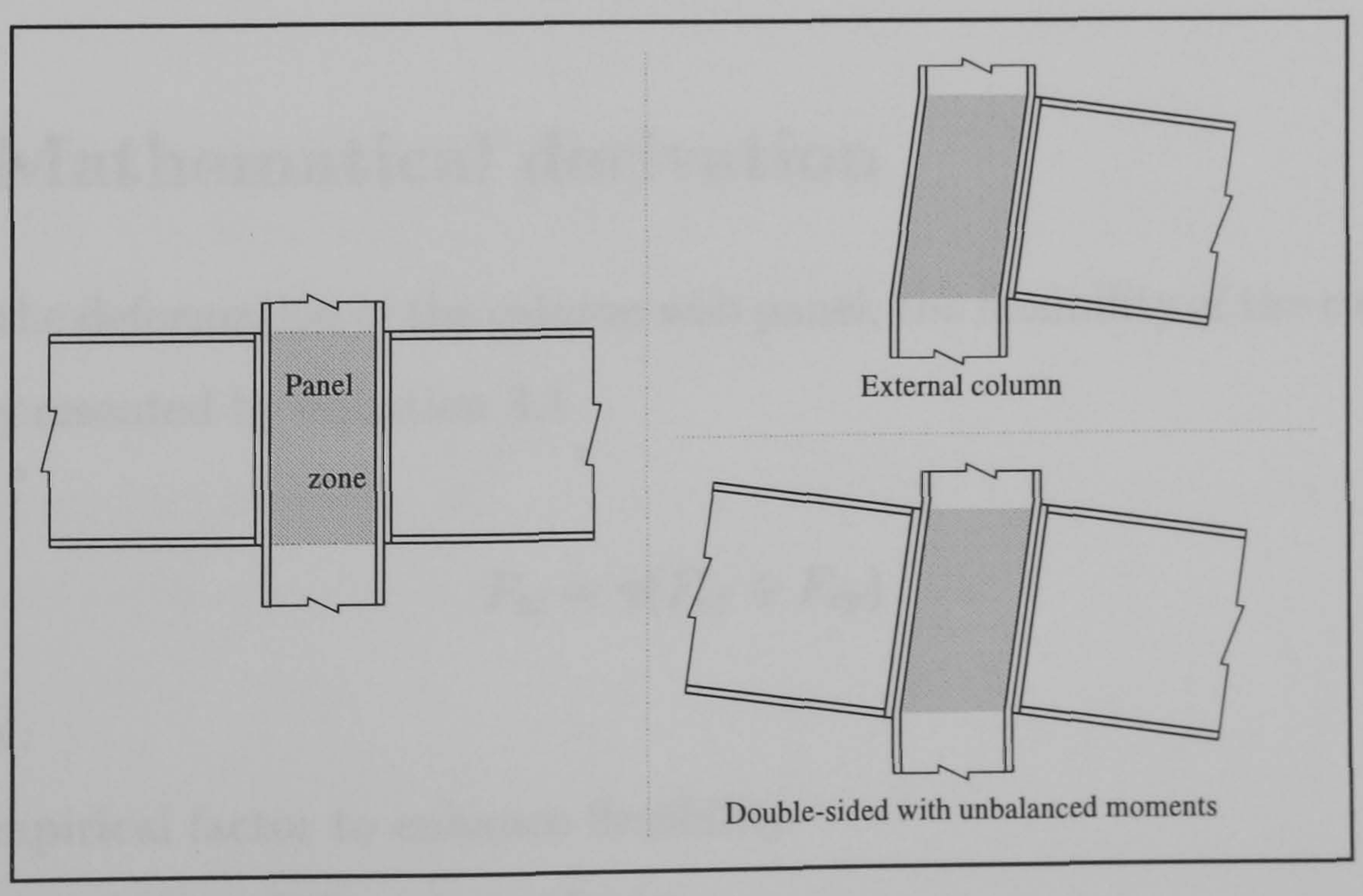

Figure 3.5: Column panel zone and associated deformations

Consequently, the experimental evidence used to validate the equation has been taken from balanced cruciform tests. However, due to the direction of the wind moments within a Wind-Moment frame, even the internal columns are subjected to unbalanced loading (see Figure 3.6). Therefore, the additional flexibility that would inevitably result will be accounted for by using the term for shear deformation of a column web given in Annex J[18] (see section 3.5).

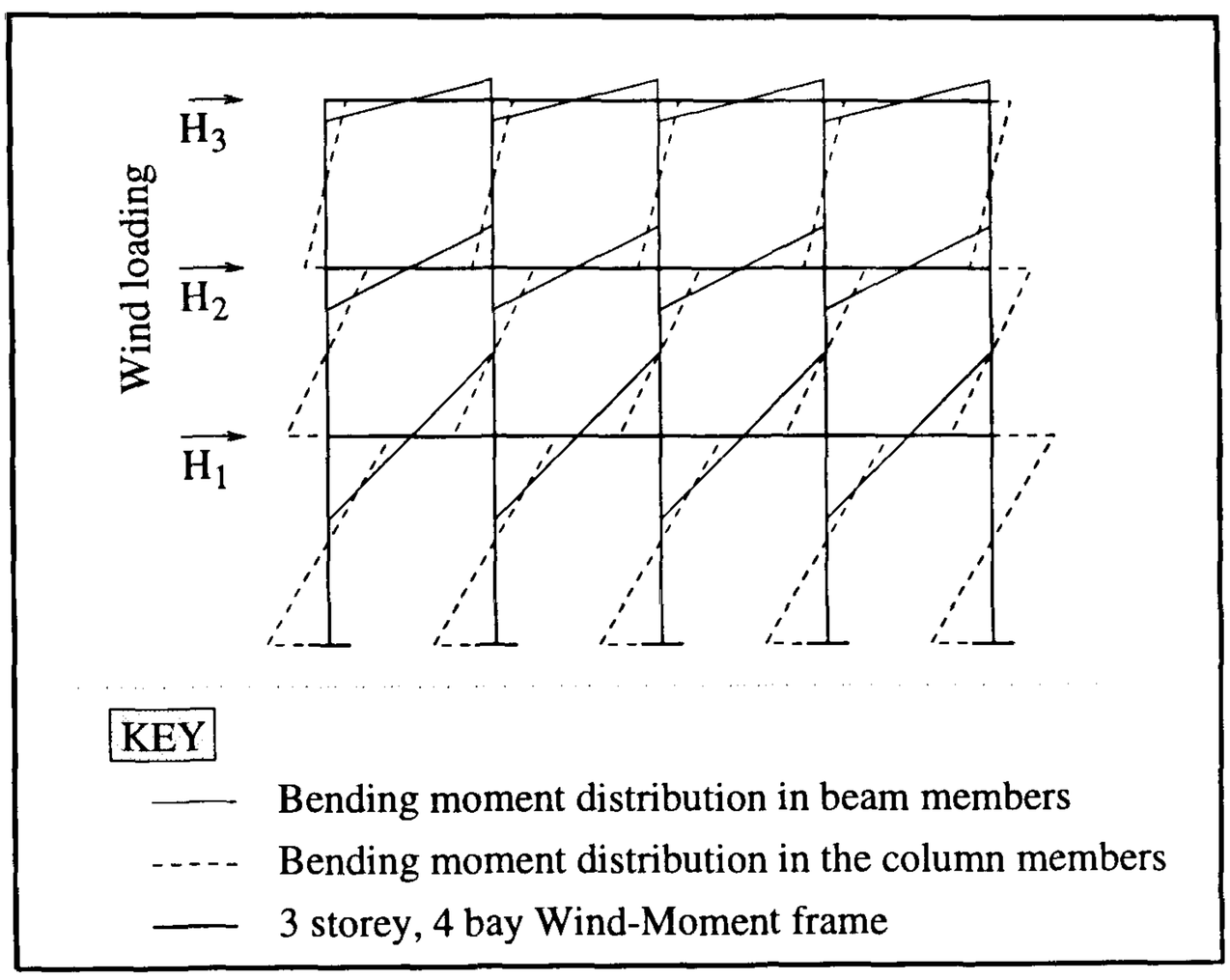

Figure 3.6: Bending moment distribution throughout a multi-bay Wind-Moment frame

3.3 Mathematical derivation

Ignoring the deformation of the column web panel, the flexibility of the connection can be represented by equation 3.1

$$F_{bc} = \gamma(F_{cf} + F_{ep}) \tag{3.1}$$

where :

γ - Empirical factor to enhance flexibility

F_{cf} - Flexibility of the column flange

F_{ep} - Flexibility of the end plate.

The flexibilities of the component parts can be calculated using the standard equation for the deflection of a cantilever. Thus, taking account of the assumed deformation characteristics of the column flange and end plate shown in Figure 3.2:

$$\Delta = \frac{Tl^3}{3EI}\left[\left(\frac{2}{3}\right)^3 + \left(\frac{1}{3}\right)^3\right] \tag{3.2}$$

Simplifying equation 3.2

$$\Delta = \frac{Tl^3}{9EI} \tag{3.3}$$

where :

T - Tensile force in one bolt

l - Length, denoted m_{cf} for the column flange and m_{ep} for the end plate

E - Young's Modulus for steel

I - Second moment of area.

For a rectangular plate the second moment of area is represented by equation 3.4.

$$I = \frac{b_{eff}t^3}{12} \tag{3.4}$$

where :

b_{eff} - The effective breadth of the plate

t - The thickness of the plate, denoted t_{cf} for the column flange and t_{ep} for the end plate.

To obtain an expression that represents flexibility of a component part 'i', substitute for I in equation 3.2 and divide through by T.

$$F_i = \frac{\Delta}{T} = \frac{l^3}{0.75Eb_{eff}t^3} \tag{3.5}$$

The flexibility of the column flange

The flexibility of the column flange is assumed to be entirely governed by the horizontal distance between the bolt position and the column web as denoted by m_{cf} in Figure 3.7.

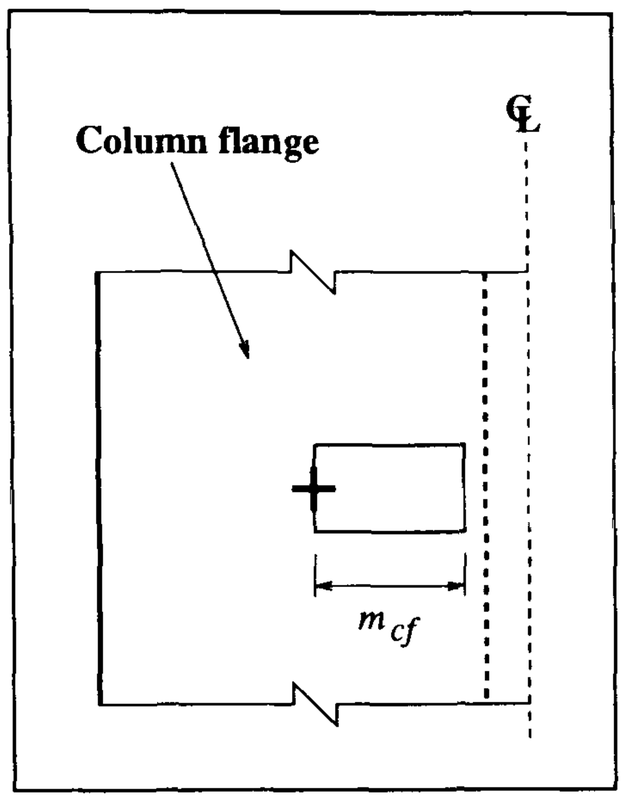

Figure 3.7: Cantilever length to represent the column flange

Therefore re-writing equation 3.5 for this component:

$$F_{cf} = \frac{\Delta_{cf}}{T} = \frac{m_{cf}^3}{0.75 E b_{eff} t_{cf}^3} \tag{3.6}$$

Assuming $b_{eff} = 0.9 m_{cf}$, as previously explained:

$$F_{cf} = \frac{\Delta_{cf}}{T} = \frac{m_{cf}^2}{0.675 E t_{cf}^3} \tag{3.7}$$

where :

$$m_{cf} = \frac{G}{2} - \frac{t_{cw}}{2} - 0.8 r_k,$$

G - Horizontal distance between the bolt centres

t_{cw} - Column web thickness

r_k - Root radius for the column section.

The flexibility of the end plate

The flexibility of a flush end plate will be influenced by the proximity of both the tension flange and the web of the connected beam section, to the tension bolts. This therefore introduces two possible lengths for the cantilever model, as shown in Figure 3.8. However, since the main resistance to the applied bending moment is provided by a beam's flanges, it is more appropriate to base the flexibility of the end plate on the distance between the tension flange and the tensile bolts. This distance is represented by m_{ep2} in Figure 3.8.

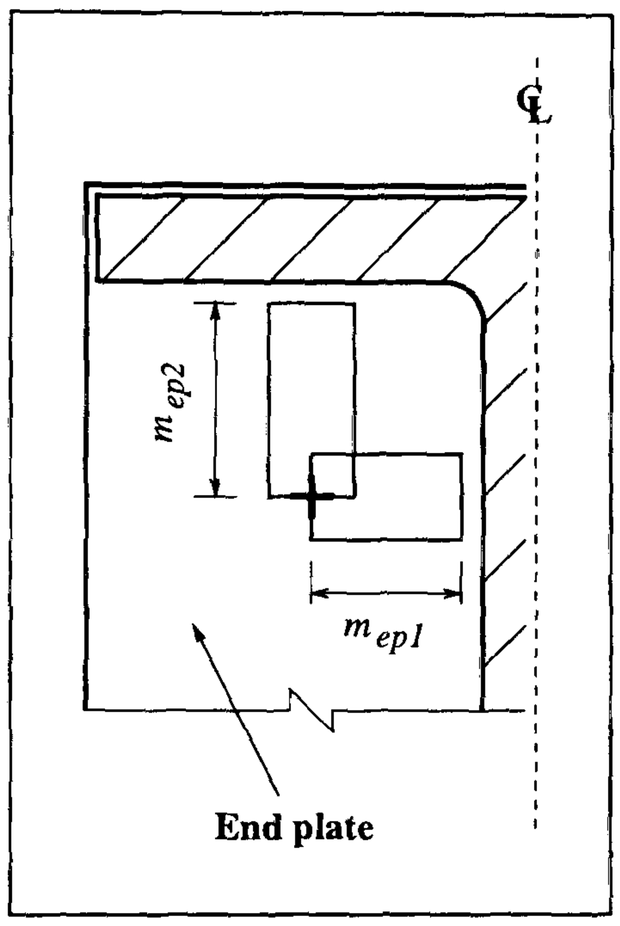

Figure 3.8: Alternative cantilever lengths to represent the end plate

It can be seen from equation 3.5 that the flexibility of the end plate is dependent on the cube of the length of the cantilever model, whereas in contrast, the stiffness varies linearly with the effective breadth. Therefore, as m_{ep1} and m_{ep2} are of roughly the same magnitude in the standard connections, the estimate of the corresponding stiffness is not strongly influenced by the choice of either m_{ep1} or m_{ep2}. Therefore, since the horizontal distance has been used when the column flange was being considered, it seemed appropriate to follow this lead and adopt m_{ep1} as the basis for calculating the effective breadth of the cantilever model in this situation. If, however, m_{ep2} is less than m_{ep1} then the former is taken. This is because these dimensions relate to the size of the circular yield-line pattern

(see Figure 3.3), which clearly cannot be bigger than the lesser of m_{ep1} and m_{ep2}.

Re-writing equation 3.5 in terms of the end plate dimensions:

$$F_{ep} = \frac{\Delta_{ep}}{T} = \frac{m_{ep2}^3}{0.75 E b_{eff} t_{ep}^3} \tag{3.8}$$

Substituting for $b_{eff} = 0.9 m_{ep1}$:

$$F_{ep} = \frac{\Delta_{ep}}{T} = \frac{m_{ep2}^3}{0.675 E m_{ep1} t_{ep}^3} \tag{3.9}$$

where :

$$m_{ep1} = \frac{G}{2} - \frac{t_{bw}}{2} - 0.8 L_w, \leq m_{ep2},$$

$$m_{ep2} = E_{1t} - t_{bf} - 0.8 L_f,$$

t_{bw} - Beam web thickness

t_{bf} - Beam flange thickness

E_{1t} - Vertical distance between the centre-line of the top row of bolts and the outer most surface of the top flange of the beam

L_w - Leg length of the web weld

L_f - Leg length of the flange weld.

Total flexibility

The total flexibility can be attained by substituting equations 3.7 and 3.9 into equation 3.1:

$$F_{bc} = \frac{\gamma}{0.675 E} \left[\frac{m_{cf}^2}{t_{cf}^3} + \frac{m_{ep2}^3}{m_{ep1} t_{ep}^3} \right] \tag{3.10}$$

For convenience, the value for the Modulus of elasticity. 'E'. was taken as 0.2 MN/mm^2, thus enabling the corresponding units for flexibility to be directly calculated in radians/kNm when all the lengths and thicknesses are entered into the formula in mm units.

The flexibility was assumed to be enhanced by a factor of 1.4 due to the influence of the other component parts.

Therefore substituting for E and γ in equation 3.10:

$$F_{bc} = \frac{1.4}{0.135}\left[\frac{m_{cf}^2}{t_{cf}^3} + \frac{m_{ep2}^3}{m_{ep1}t_{ep}^3}\right] \tag{3.11}$$

This therefore represents the linear flexibility associated with the action of one bolt with a tensile force T (see Figure 3.1).

The rotational stiffness of a steel connection

The rotational stiffness of a steel connection with one row of tension bolts can be represented by Figure 3.9 and expressed mathematically by equation 3.12.

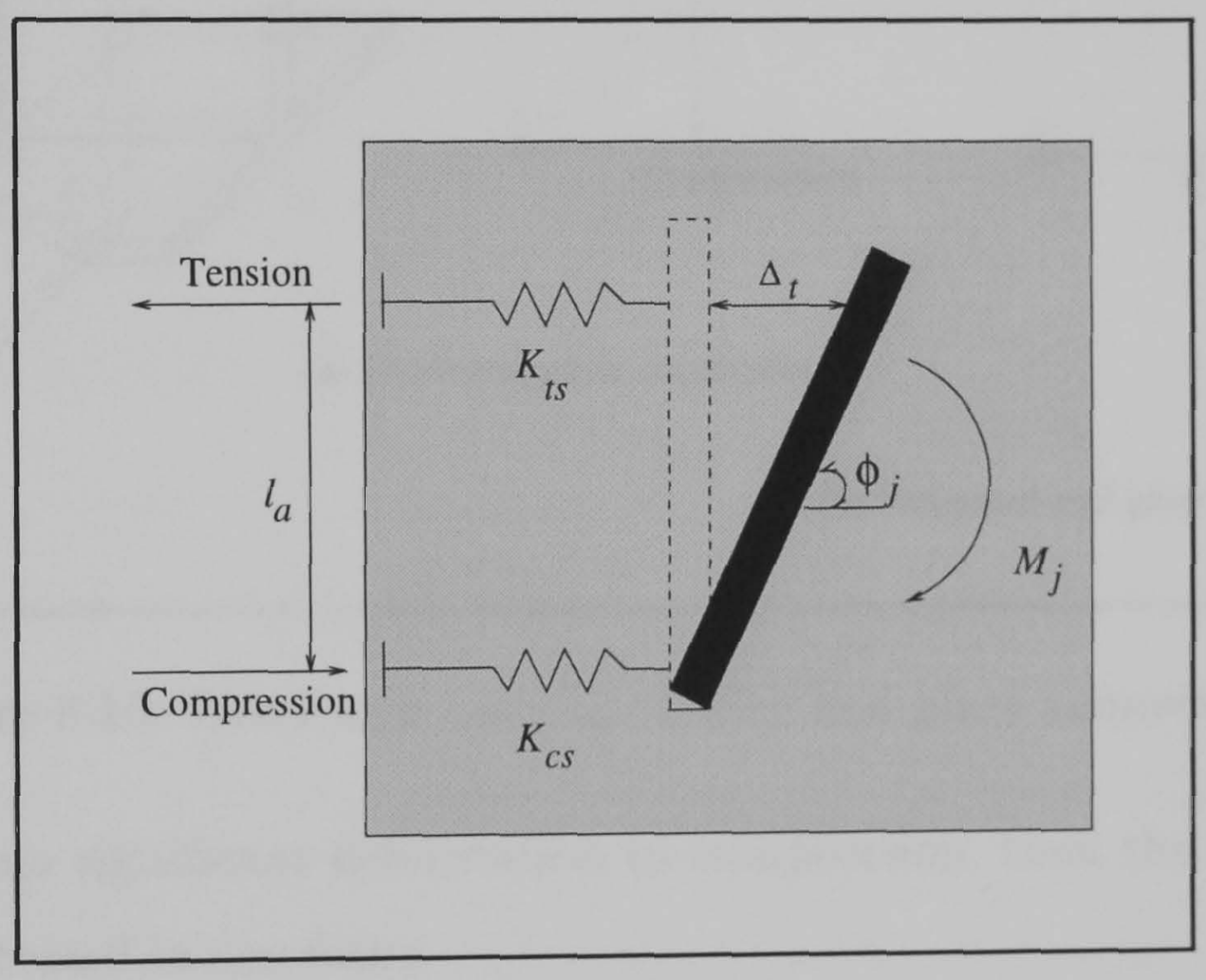

Figure 3.9: Rotational stiffness model

$$K_j = \frac{M_j}{\phi_j} = \frac{2Tl_a}{\phi_j} \tag{3.12}$$

where :

M_j - Applied moment

ϕ_j - Corresponding rotation

l_a - Connection lever arm (see figure 3.10(a)).

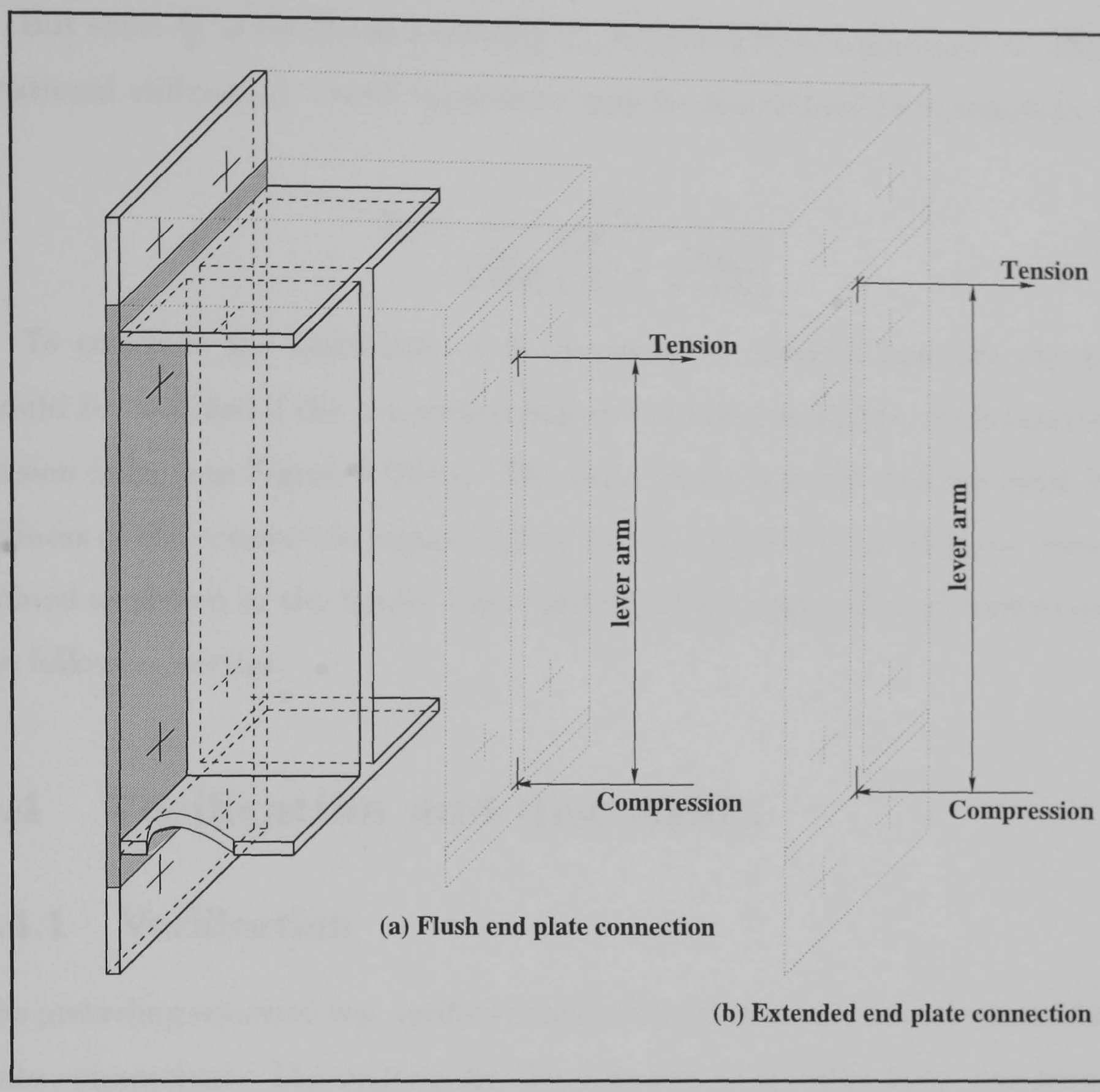

(a) Flush end plate connection

(b) Extended end plate connection

Figure 3.10: Lever arm associated with end plate connections

Assuming no significant deformation in compression, then the joint rotation ϕ_j can be expressed in the form:

$$\phi_j = \frac{\Delta_t}{l_a} \tag{3.13}$$

where :

Δ_t = extension of the tension spring of stiffness K_{ts} (see Figure 3.9), thus representing the lateral displacement of the tensile force.

Substituting equation 3.13 into 3.12:

$$K_j = \frac{2Tl_a^2}{\Delta_t} \tag{3.14}$$

But since $\frac{\Delta_t}{T}$ is the linear flexibility F_c, it follows from equation 3.11. that the rotational stiffness of a steel connection may be determined from equation 3.15:

$$K_j = \frac{1}{\frac{0.7}{0.135 l_a^2}\left[\frac{m_{cf}^2}{t_{cf}^3} + \frac{m_{ep2}^3}{m_{ep1} t_{ep}^3}\right]} \tag{3.15}$$

To conclude the derivation, it is necessary to consider how the expression should be modified if the connection has an extended end plate, with two rows of tension bolts (see Figure 3.10(b)). The assumption is made that the total initial stiffness of the connection remains given by equation 3.15 but with the lever arm defined as shown in the figure. The validity of this approach is demonstrated in the following section.

3.4 Verification and discussion

3.4.1 Verification

The preceding equation was verified empirically using experimental results for end plate connections. The criteria for the selection of suitable tests was based on the detailing of the connection, required to resemble that of the proposed ductile connections under consideration. In particular, the end plate thickness was not greater than 16mm. Summaries of the tests which were considered suitable, indicating the connection configurations, are shown in Table 3.1 for flush end plates and Table 3.2 for extended end plates. The moment-rotation curves are available from references [9, 22, 45], or other sources quoted in these references, in addition to the authors experimental programme itself (see Chapter 6). The figures referred to during the following paragraphs can be found in numerical order at the end of this chapter. Moreover, since there is a common key applicable to all the moment-rotation characteristics illustrated in the subsequent figures, the key is only reproduced once at the start of the sequence and is illustrated in Figure 3.13.

Table 3.1: Flush end plate connection configurations

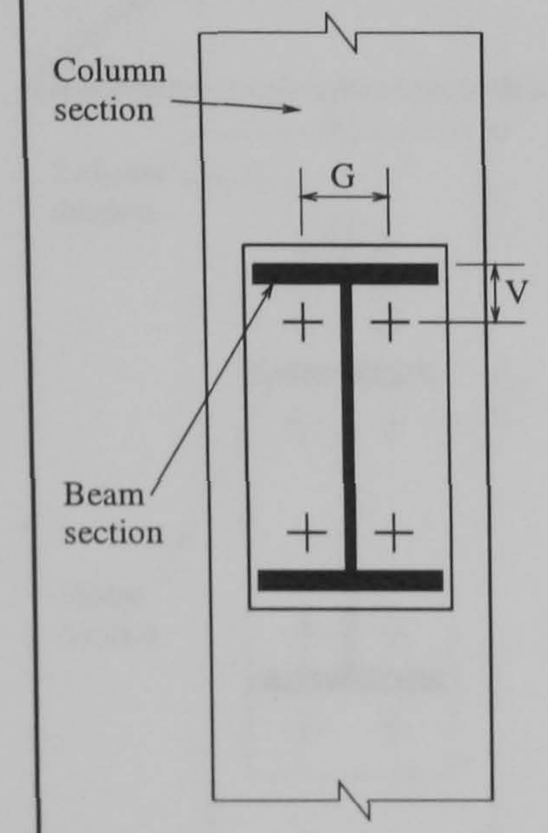

	Test reference	Beam section	Column section	End plate size (mm)	G (mm)	V (mm)	Bolt size/grade	Pretension force (kN)	Initial stiffness prediction equations (kNm/mrad) Proposed Equation (3.15)	Initial stiffness prediction equations (kNm/mrad) Annex J revised (jj)#
Flush end plate details with one bolt row in tension										
Brown										
	1	457x152x52	203x203x52	500x200x15	90	50	M20/8.8	N/A	36	75
Najafi										
	9	305x165x40	203x203x52	352x200x15	86	50	M20/8.8	N/A	15	31
Ostrander										
	13	W12x27	W8x40	330x190x15.8	101.5	63.5	19/A325	189	10	22
	23	W12x27	W8x48	330x190x15.8	101.5	63.5	19/A325	189	13	26
Zoetemeijer										
	17	HE300A	HE450M	290x230x16	120	55	M22/8.8	40	36	24
	19	HE300A	HE450M	290x230x16	120	75	M24/8.8	36	11	26
	34	IPE400	HE450M	400x180x16	100	55	M24/8.8	70	66	50
Bose										
	1*	406x178x60	254x254x89	450x200x15	90	60	M24/8.8	N/A	33	53
	2*	686x254x125	254x254x89	720x250x15	90	60	M24/8.8	N/A	123	173
	9*	406x178x60	254x254x89	450x200x12	90	60	M20/8.8	N/A	19	44

Note : * - Test follows standard detail 1 and denotes the tests which were not originally available to calibrate the proposed equation
- See Chapter 2, equation 2.3

Table 3.2: External end plate connection configurations

	Test reference	Beam section	Column section	End plate size (mm)	G (mm)	V (mm)	Bolt size/grade	Pretension force (kN)	Initial stiffness prediction equations (kNm/mrad) Proposed Equation (3.15)	Initial stiffness prediction equations (kNm/mrad) Annex J revised (jj)#
	Extended end plate details with two bolts in tension									
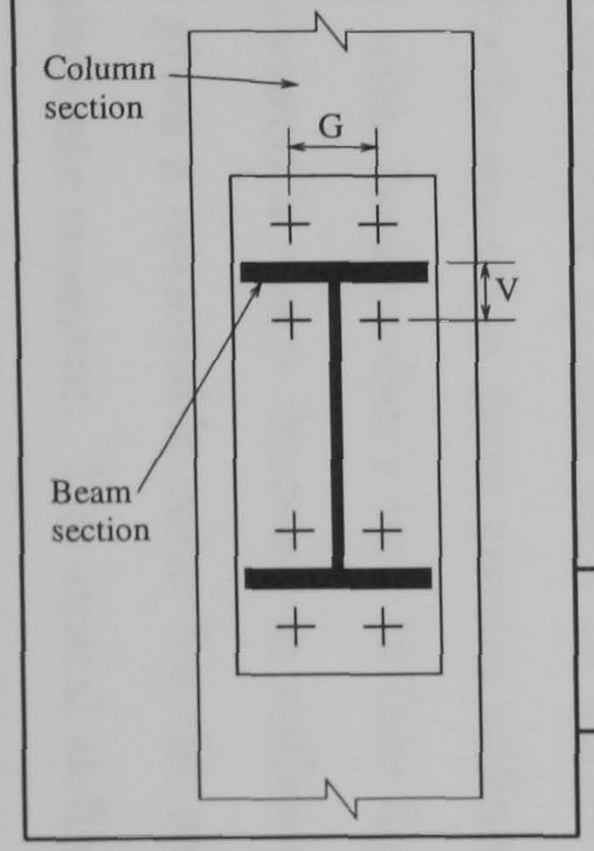	**Bose**									
	4*	**457x191x74**	**254x254x89**	**640x200x15**	**90**	**60**	**M24/8.8**	**N/A**	**62**	**128**
	5*	**762x267x147**	**254x254x89**	**930x250x15**	**90**	**60**	**M24/8.8**	**N/A**	**196**	**368**
	6*	**457x191x74**	**254x254x73**	**640x200x15**	**90**	**60**	**M24/8.8**	**N/A**	**50**	**104**
	7*	**457x191x74**	**254x254x132**	**640x200x15**	**90**	**60**	**M24/8.8**	**N/A**	**77**	**183**
	8*	**762x267x147**	**254x254x132**	**930x250x15**	**90**	**60**	**M24/8.8**	**N/A**	**253**	**529**
	10*	**457x191x74**	**254x254x89**	**640x200x15**	**90**	**60**	**M20/8.8**	**N/A**	**62**	**123**

Note : * - Test follows standard detail 4 and denotes the tests which were not originally available to calibrate the proposed equation

\# - See Chapter 2, equation 2.3

The comparisons for the flush end plates are shown in Figures 3.14 to 3.28. The experiments by the author and Najafi (see Figures 3.14 to 3.17) concerned bare steel connections tested for comparison with composite joints. Each figure shows comparisons with the initial and unloading stiffnesses. The predicted initial values applicable to the author's equation were then halved, in accordance with the recommendations of Annex J[18] to obtain a secant stiffness applicable for global analysis. The complete moment-rotation characteristic is also shown, to provide a convenient overall picture of the connection's response. It can be seen that the proposed equation provides very close correlation with the unloading stiffness in all cases, whereas Annex J consistently over estimates this value. Unfortunately, the unloading stiffnesses were not available for the remaining tests, therefore the comparisons were undertaken by studying what was considered to be the initial part of the moment-rotation characteristic.

The comparisons with Ostrander's tests (see Figure 3.18 and 3.19) lead to similar conclusions to those just made, despite both of these tests using pre-loaded bolts. The presence of such a pre-load, which is not the intention for the standardised connections, would have the effect of increasing the initial slope of the moment-rotation characteristic. Consequently, the assessment of this experimental programme was undertaken with an appreciation of this effect.

Zoetemeijer's test 17 (see Figure 3.20) employed a wide gauge distance between the bolts, coupled with positioning close to the underside of the tension flange (see Table 3.1). This weakens the validity of the assumptions made concerning the proportions of the cantilever models used to derive the author's equation. For this test therefore, the equation gives greater stiffnesses than the test and Annex J. Comparisons with Zoetemeijer's test 19 (see figure 3.21) are made difficult because the test showed a sharp decrease in stiffness at 15 kNm. However, the author's equation gives a reasonable value for the secant stiffness at two-thirds of the predicted ultimate moment. The initial stiffness predicted by Annex J is substantially stiffer than the test value at this level of moment.

Finally in this series of tests, the equation gives a good prediction for the initial stiffness value for Zoetemeijer's test 34 (see Figure 3.22).

For Bose's first test (see Figures 3.23 and 3.24), the equation gives very close agreement with the initial stiffness for the more flexible connection (see Figure 3.24). The same conclusion applies to both joints in Test 9 (see Figures 3.27 and 3.28) and to one joint in Test 2 (see Figure 3.26). Neither prediction method gave good agreement with Figure 3.25, in which a virtually linear response was obtained from the test to beyond the predicted ultimate resistance.

For prediction of the behaviour of flush end plate standardised connections, it was concluded that the author's equation generally provided good agreement with the initial and unloading stiffnesses. Furthermore, following the modification necessary to represent the connections characteristic, it can be seen that the author's equation produces a bi-linear characteristic that lies completely beneath the actual characteristic in all cases except for Zoetemeijer's test 17 (see Figure 3.20). It is also important to remember the purpose of this work, which was to examine the suitability of Wind-Moment frames using the standardised (and flexible) end plate connections. Any underestimate of stiffness will therefore be conservative with regard to second-order effects and the overall stability of the frame.

For the extended end plate connections, significant differences appear between tests on nominally identical left-hand and right-hand joints. In several instances though, the author's equation provides a good estimate of the initial stiffness (see Figures 3.32 and 3.34 to 3.38), whereas, Annex J provides significant overestimates of the initial stiffness in several cases (see Figures 3.32 to 3.36 and 3.38 to 3.40). The conclusions are therefore similar to those already stated for the flush end plate connections, namely, that the use of the author's proposed equation to predict the connection's response during frame analysis can be expected to result in conservative assessments of frame stability at Ultimate Limit State and good

estimates of sway deflections under service loading. In contrast. Annex J would generally lead to the bare frame deflections being underestimated. resulting in unconservative assessments for frame stability and sway.

3.5 Shear flexibility in the column web panel

The flexibility of a connection can be influenced by the effects of web shear induced by a differential between the applied bending moments on each side of a column. This differential will always exist for an external column. However. depending upon the type of structure, the corresponding effect for an internal column may or may not need to be considered. For a braced frame of equal bays, where the effects of pattern loading can be neglected[50], the corresponding bending moments on either side of the column would cancel out, and therefore the connection stiffness would not be further reduced. However, the same simplification does not apply to unbraced frame design, since the effects of web shear need to be considered for each load combination as a consequence of the frame itself resisting the applied horizontal forces.

In the absence of any test results that induced web shear and could be considered representative of the proposed standard connections, the development of a corresponding empirical coefficient was prevented. However, an elastic stiffness coefficient which compensates for this effect is given by clause 3.3.3(2) of Annex J:

$$k_1 = \frac{0.38 A_{vc}}{\beta z} \tag{3.16}$$

where :

A_{vc} = The shear area for the column web

β = The bending moment distribution coefficient, which compensates for the variation between the bending moments either side of the column

z = The depth of the shear zone, taken as equivalent to the lever arm 'l_a' for the connection.

This term can be incorporated within equation 3.15, as explained below.

The shear forces generated in the column web panel, Q, due to an unbalanced moment, M_j, are assumed to induce a uniform shear stress, τ, on the shear area of the column web, A_{vc} (see Figure 3.11).

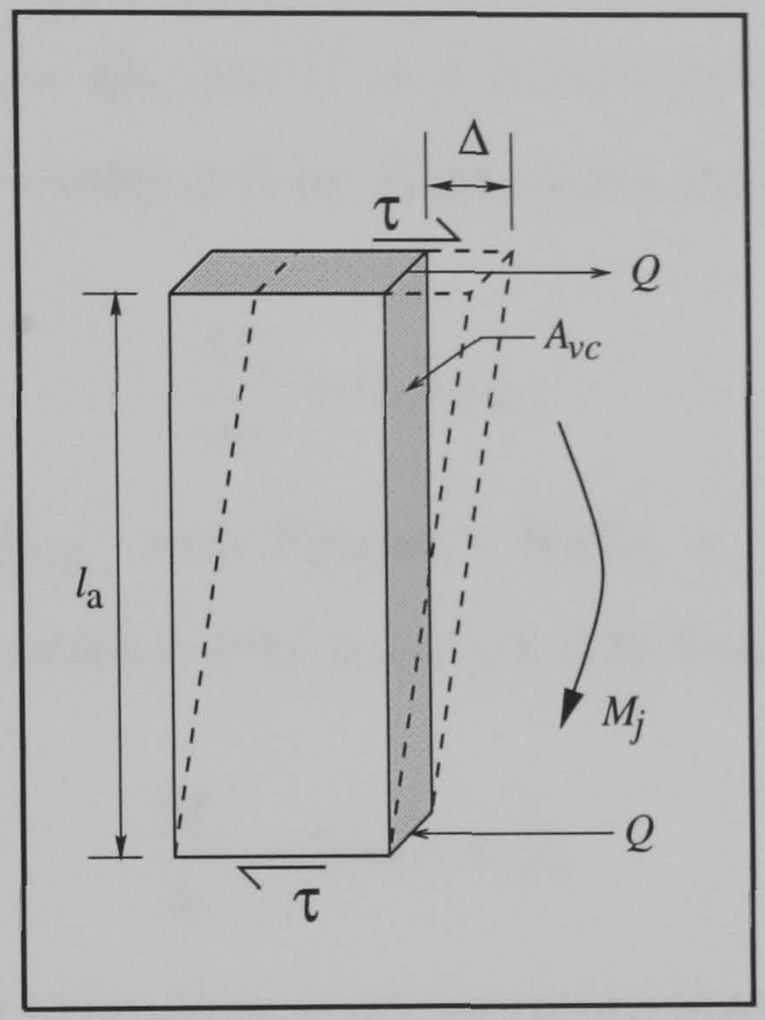

Figure 3.11: Column web panel in shear

Thus since

$$\tau = \frac{Q}{A_{vc}} = G\tau_\epsilon \tag{3.17}$$

where:

G - The shear modulus

τ_ϵ - The shear strain,

and:

$$\tau_\epsilon = \frac{\Delta}{l_a} \tag{3.18}$$

then substituting equation 3.18 into 3.17:

$$\frac{Q}{A_{vc}} = \frac{G\Delta}{l_a} \tag{3.19}$$

This may then be rearranged to obtain a linear stiffness in the form shown in equation 3.20

$$\frac{Q}{\Delta} = \frac{GA_{vc}}{l_a} \tag{3.20}$$

Furthermore, since $M_j = Ql_a$ and $\phi_j = \frac{\Delta}{l_a}$ then an equation representing the rotational stiffness can be configured by substitution into equation 3.20:

$$\frac{M_j}{\phi_j} = GA_{vc}l_a \tag{3.21}$$

Substituting $G = \frac{E}{[2(1+\nu)]}$, with Poisson's Ratio, ν, taken as 0.3, produces equation 3.22 which is consistent with equation 3.16 from Annex J.

$$\frac{M_j}{\phi_j} = 0.38EA_{vc}l_a \tag{3.22}$$

If A_{vc} and l_a are in mm units, then it can be shown that for the stiffness to be in kNm/radian, the Modulus of Elasticity should again be entered as 0.2MN/mm^2. Thus the rotational flexibility due to shear deformation of the column web panel is:

$$F_{cw} = \frac{1}{0.2\left[0.38A_{vc}l_a\right]} \tag{3.23}$$

It will be noticed however, that the common factor to the flexibility terms in equation 3.15 ($\frac{0.7}{0.138}$) is approximately $\frac{1}{0.2}$. Thus for convenience in calculation, the total flexibility can be expressed as:

$$F_{bc} = \frac{0.7}{0.135l_a^2}\left[\frac{m_{cf}^2}{t_{cf}^3} + \frac{m_{ep2}^3}{m_{ep1}t_{ep}^3} + \frac{\beta l_a}{0.38A_{vc}}\right] \tag{3.24}$$

where the bending moment distribution factor 'β' is included as in Annex J (see equation 3.16).

The total stiffness follows from:

$$K_{bc} = \frac{1}{F_{bc}} \tag{3.25}$$

The prediction equation is now complicated by the inclusion of the allowance for web shear flexibility, since the parameter β must first be determined. As already stated, this parameter is a function of the bending moment distribution, which in turn is influenced by the type and intensity of the load being applied. An exhaustive treatment of this would thus involve an iterative procedure, considering each connection in turn to ensure that equilibrium is maintained throughout the frame. This procedure in itself would not be beyond the scope of a computer simulation; however when one considers that the computer simulation at present already contains two iterative processes (see Chapter 4), adding a third would render convergence at a particular load level almost impossible to achieve without the program being completely re-structured. Due to the time available, such re-structuring was considered not to be a viable option therefore an alternative method for establishing the corresponding bending moment distribution was sought.

To help in this instance, guidance rules have been given in table J.4 of the revised annex J, whereby for standard cases, approximate values for β have been tabulated (see Figure 3.12). For the forthcoming frame study the author made use of this table, to ascertain the suitable bending moment distribution coefficients for both external and internal column locations. To explain the approaches adopted, the two cases will be considered separately below.

External column

For this particular location, the shear induced into the web would be the result of the applied connection moment on only one side of the column. Therefore the action of the moment is able to be resisted by the whole depth of the column web panel and the value of coefficient 'β', would equal unity.

Column location	Load diagram	Bending moment diagram	Bending moment distribution Coefficient 'β'
External	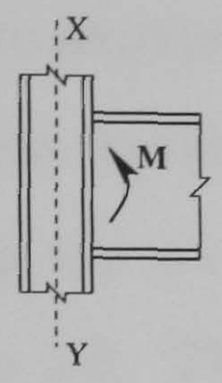	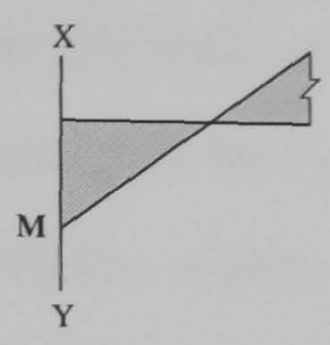	**1.0**
Internal	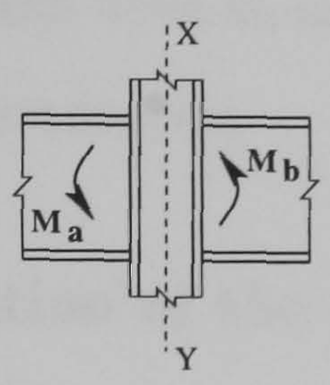	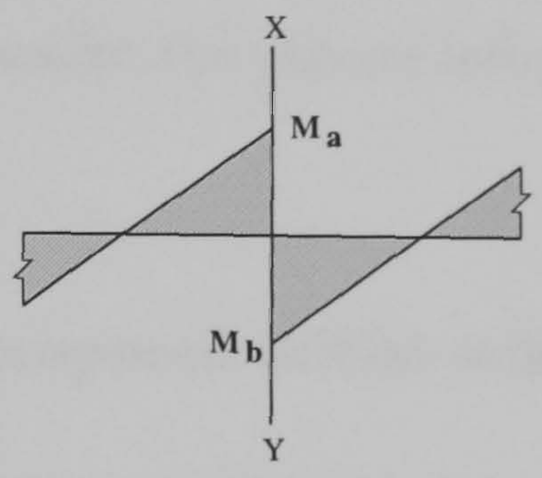	**2.0**
	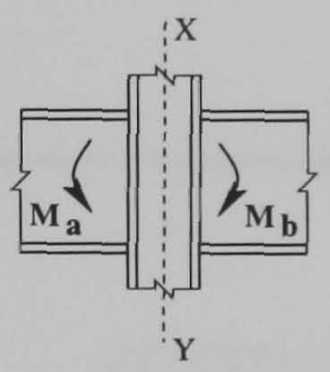	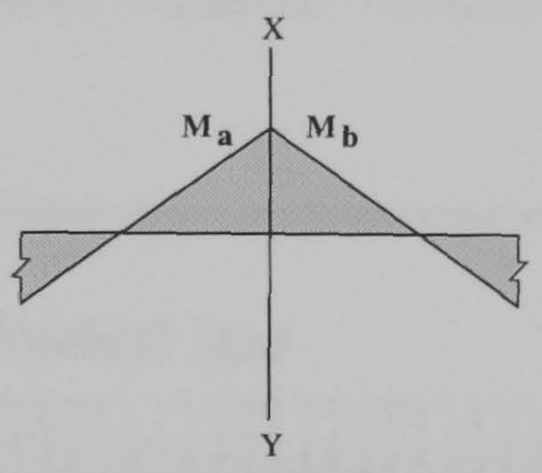	**0.0**

Figure 3.12: Values for the bending moment distribution coefficient

Internal column

The determination of a suitable value for the bending moment distribution coefficient for this situation, is far more complicated than its equivalent outlined above for the external column. The added complication is the result of having connection moments on either side of a column in this location. The relative magnitudes of these moments depend upon the bending moment distribution throughout the frame and consequently, the value for the coefficient β would vary between 0 and 2.0. The lower limit of 0 would be applicable in the situation where there is no bending moment variation between the two connections and the effects of web shear flexibility can therefore be neglected. The upper value of 2.0 is the result of evenly proportioning the influence of the web shear flexibility between two elastic springs when the beam end moments are of equal magnitude and their

effect on the web shear is cumulative. In the studies in Chapter 4, each frame was therefore analysed twice. On the first occasion, no account was taken of the influence of shear forces existing within the web panel and consequently, β, was set to zero. The web was therefore assumed to be infinitely stiff. This was subsequently rectified during the second analysis, which was undertaken by adopting a β coefficient equal to 2.0. This enabled both extremes of this influence to be considered, without the need to consider the precise influence based on the values of moment in each connection.

Graphical verification of the proposed initial stiffness equation

The key for the subsequent moment-rotation characteristics is illustrated in Figure 3.13.

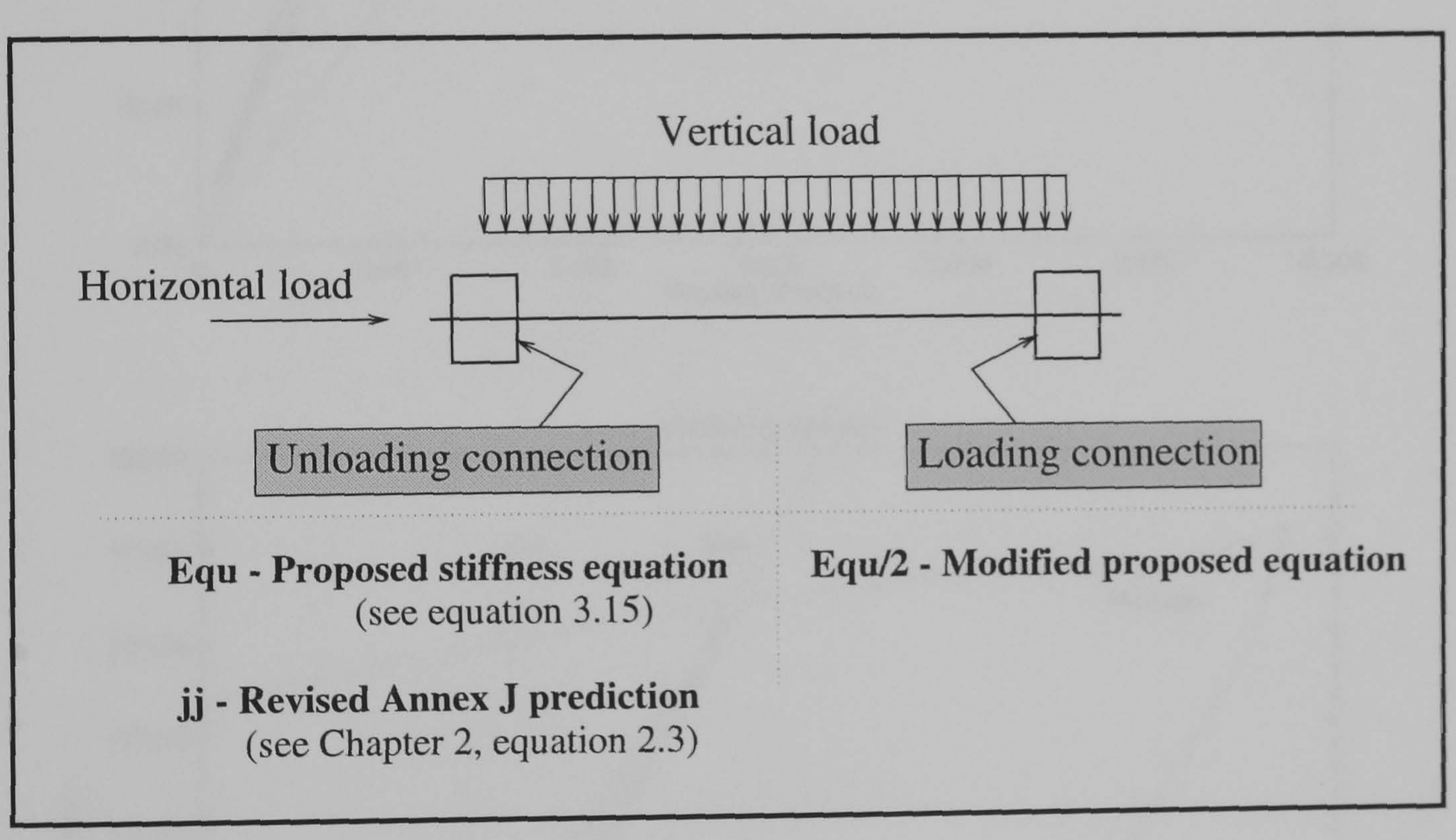

Figure 3.13: Key for the moment-rotation graphs

Brown's test 1 - Right hand connection

Figure 3.14:

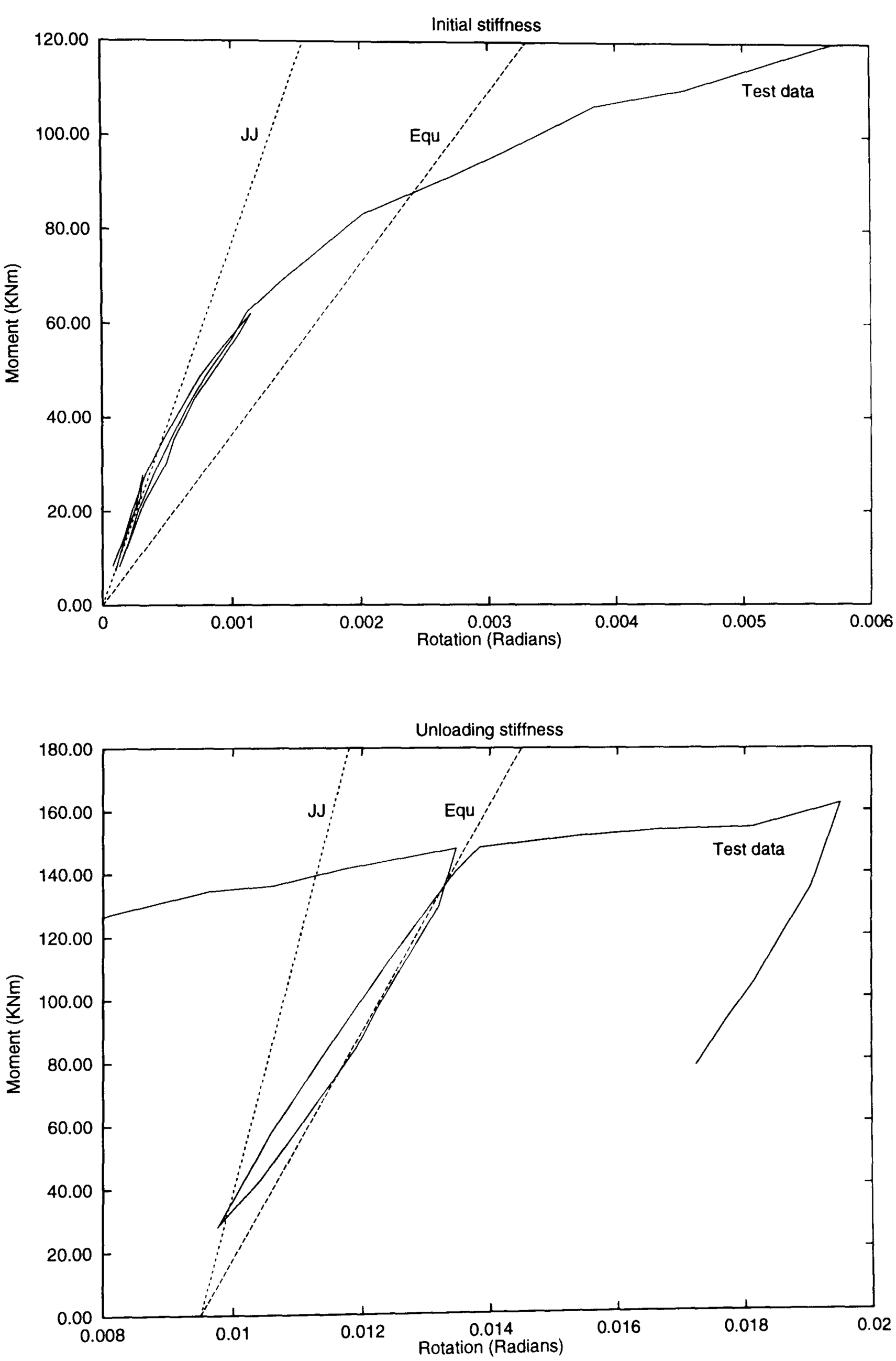

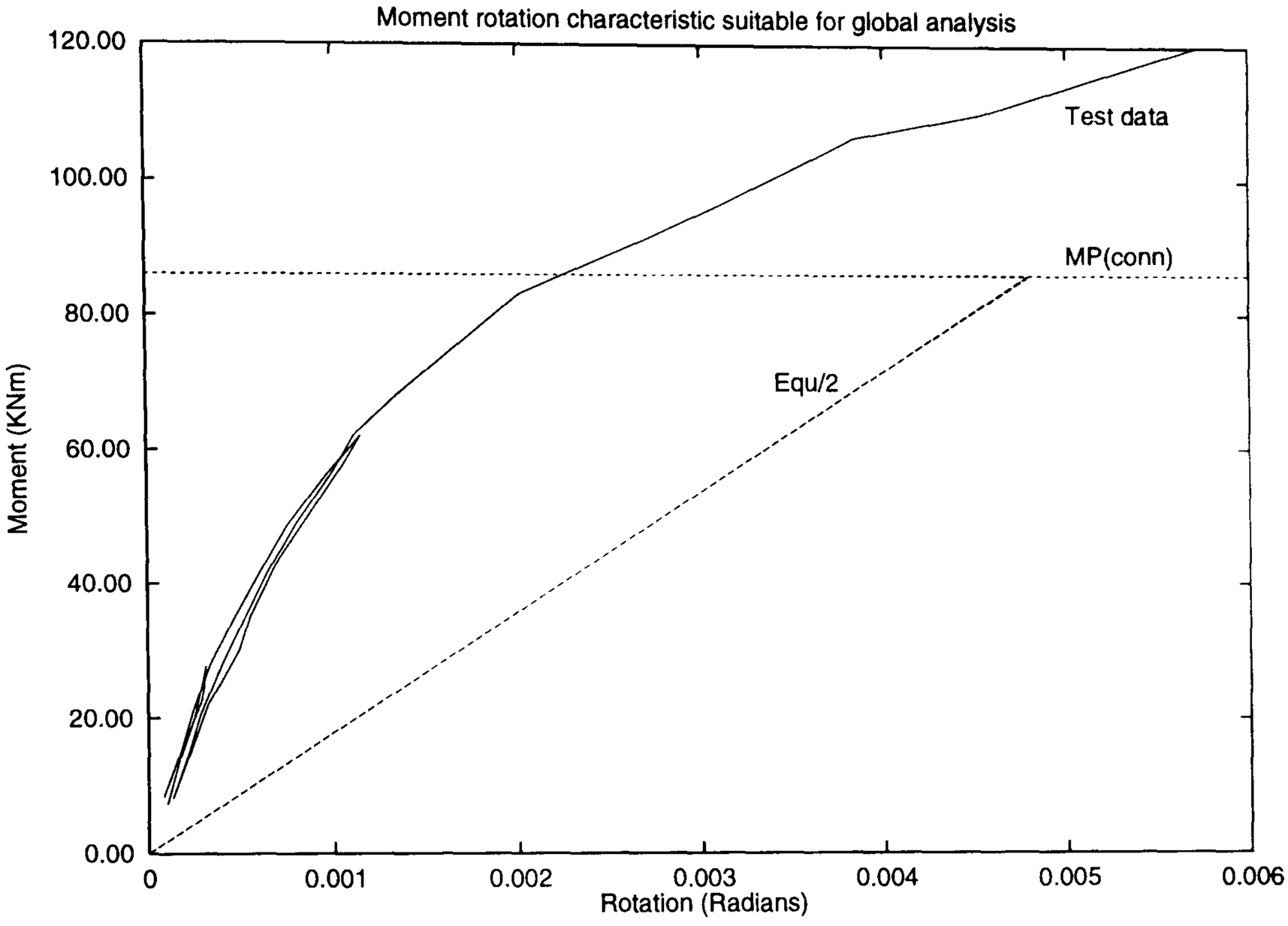
Moment rotation characteristic suitable for global analysis
120.00
100.00
80.00
60.00
40.00
20.00
0.00
Moment (KNm)
Test data
MP(conn)
Equ/2
0
0.001
0.002
0.003
0.004
0.005
0.006
Rotation (Radians)

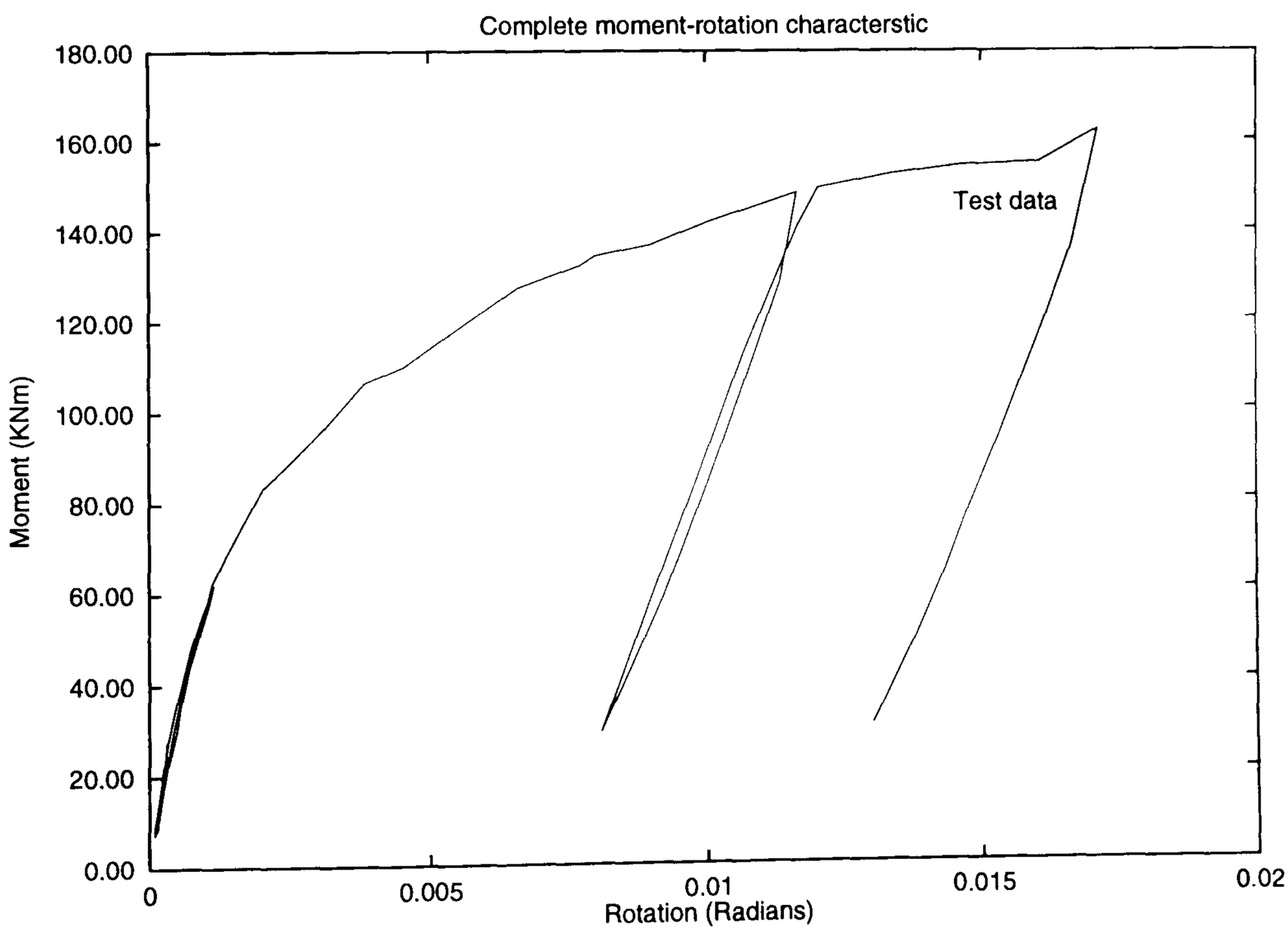
Complete moment-rotation characterstic
180.00
160.00
140.00
120.00
100.00
80.00
60.00
40.00
20.00
0.00
Moment (KNm)
Test data
0
0.005
0.01
0.015
0.02
Rotation (Radians)

Brown's test 1 - Left hand connection

Figure 3.15:

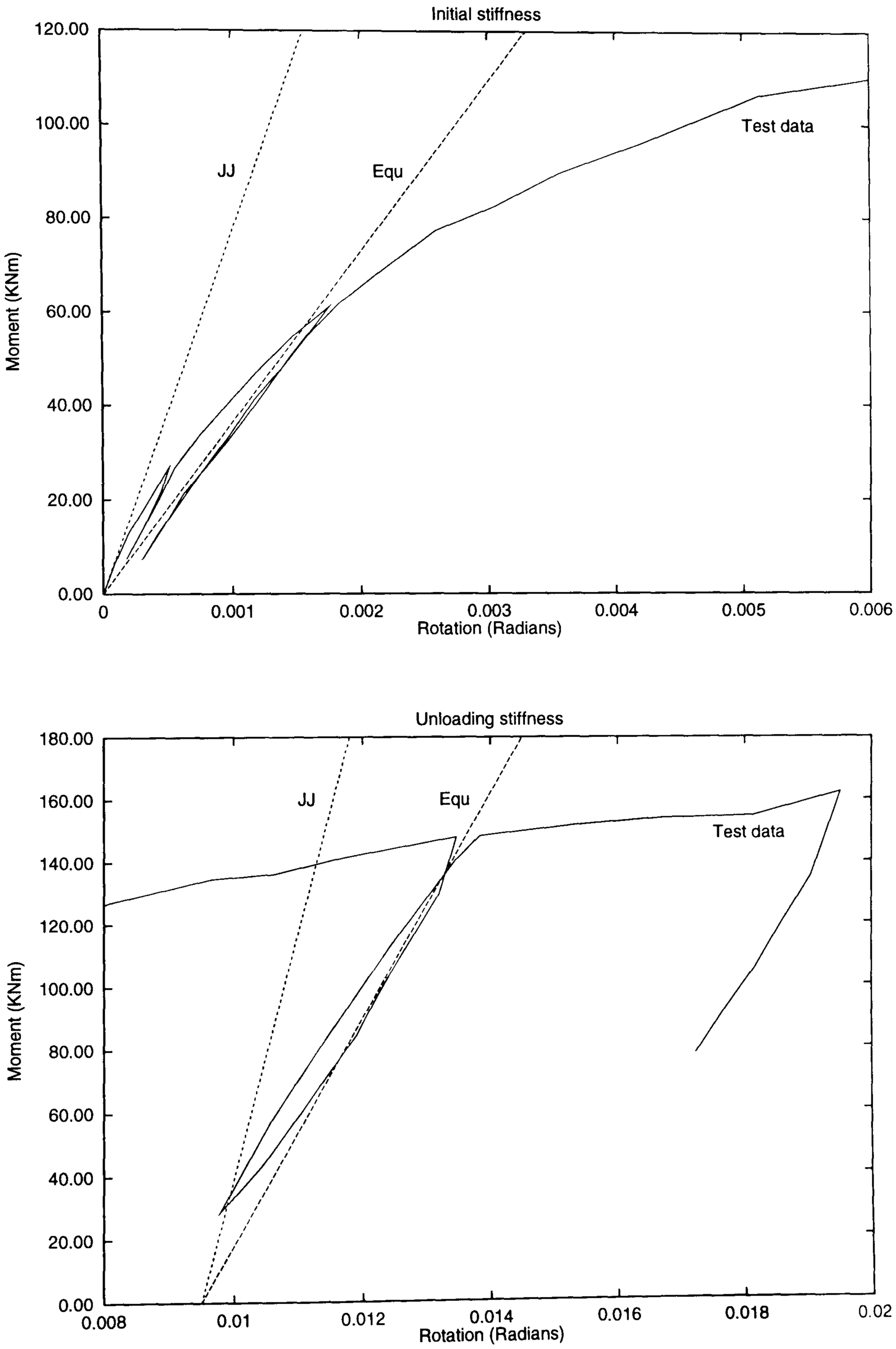

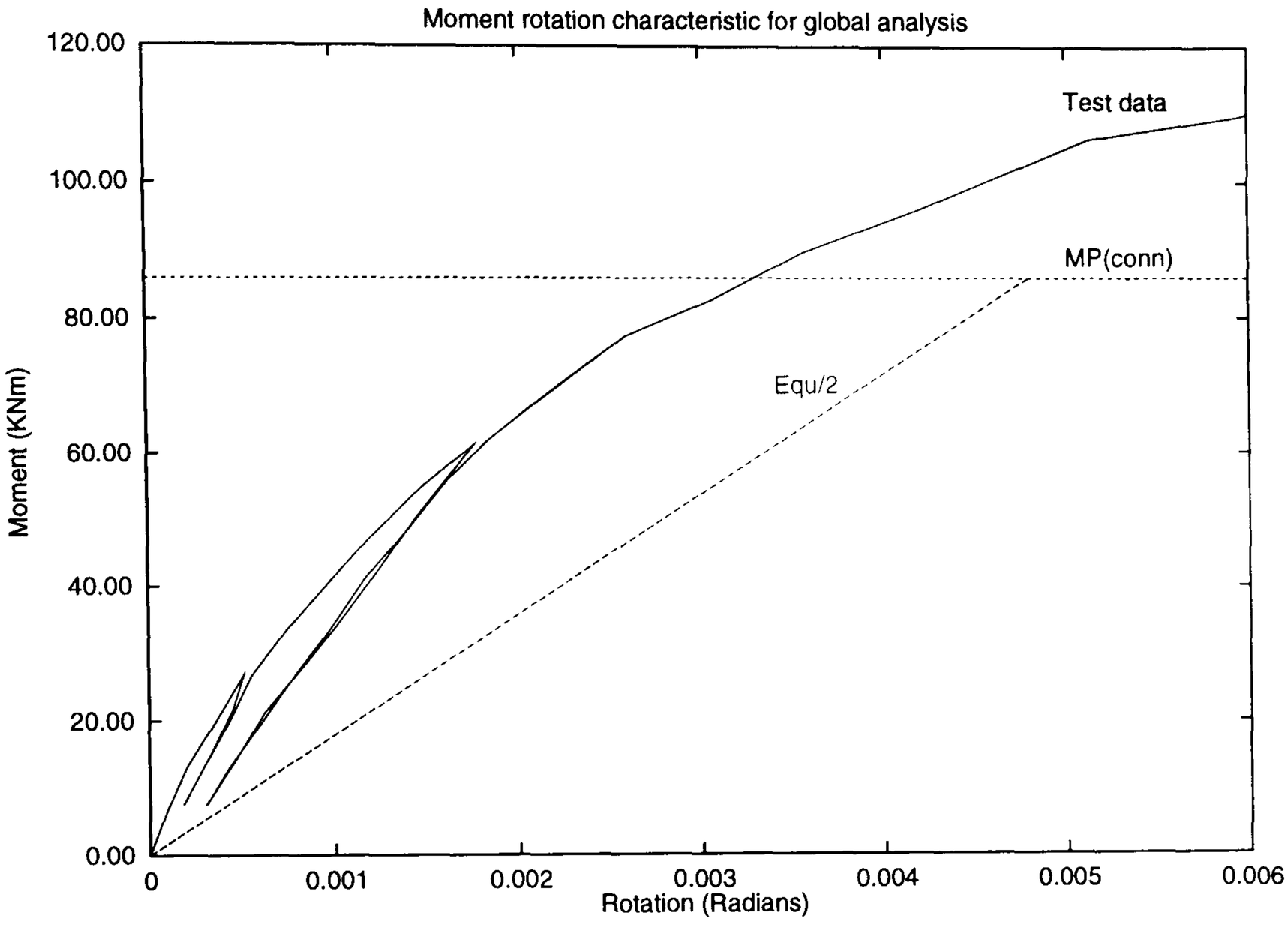
Moment rotation characteristic for global analysis
Test data
MP(conn)
Equ/2
Moment (KNm)
120.00
100.00
80.00
60.00
40.00
20.00
0.00
0
0.001
0.002
0.003
0.004
0.005
0.006
Rotation (Radians)

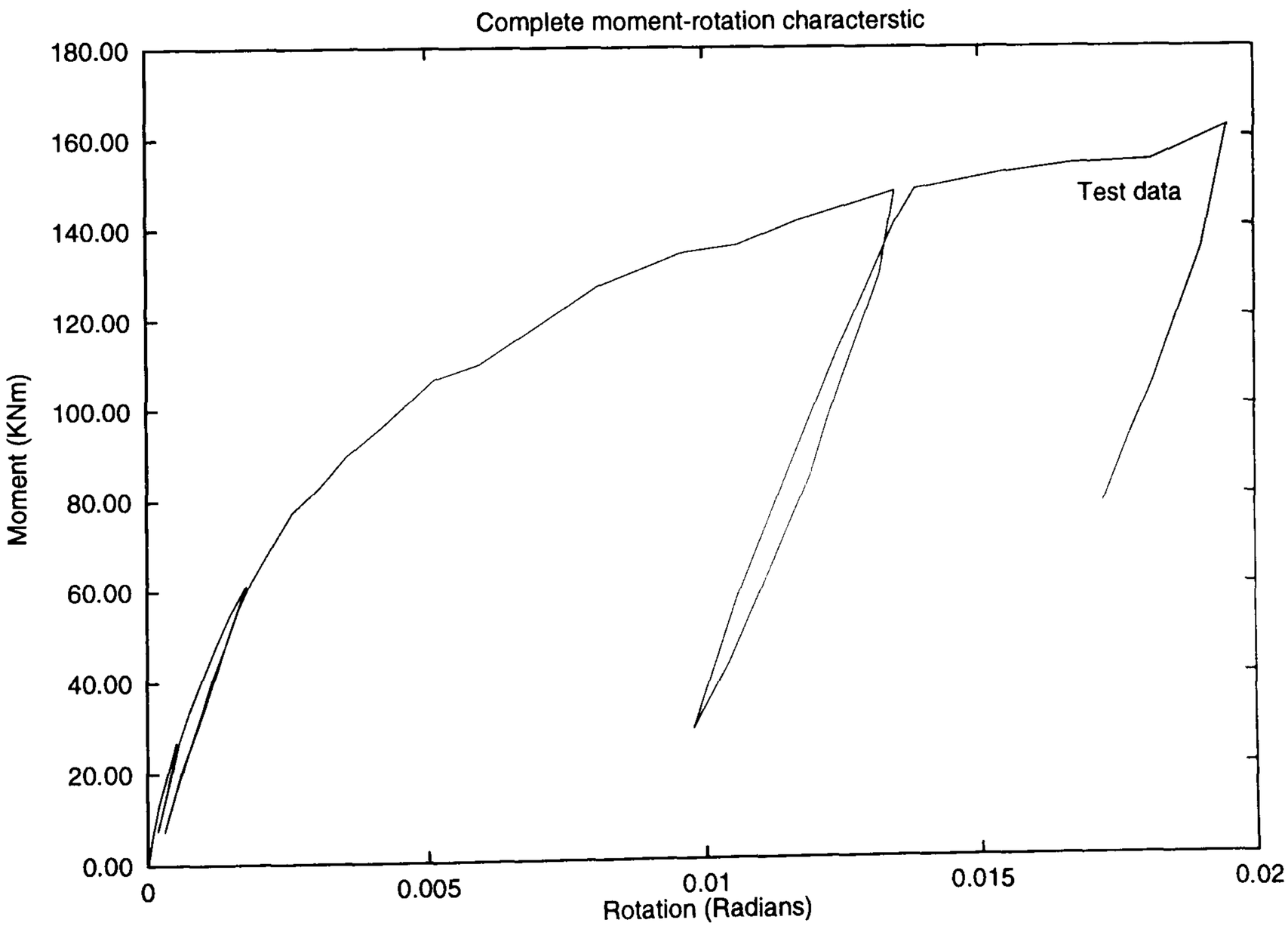
Complete moment-rotation characterstic
Test data
Moment (KNm)
180.00
160.00
140.00
120.00
100.00
80.00
60.00
40.00
20.00
0.00
0
0.005
0.01
0.015
0.02
Rotation (Radians)

Najafi's test 9 - Right hand connection

Figure 3.16:

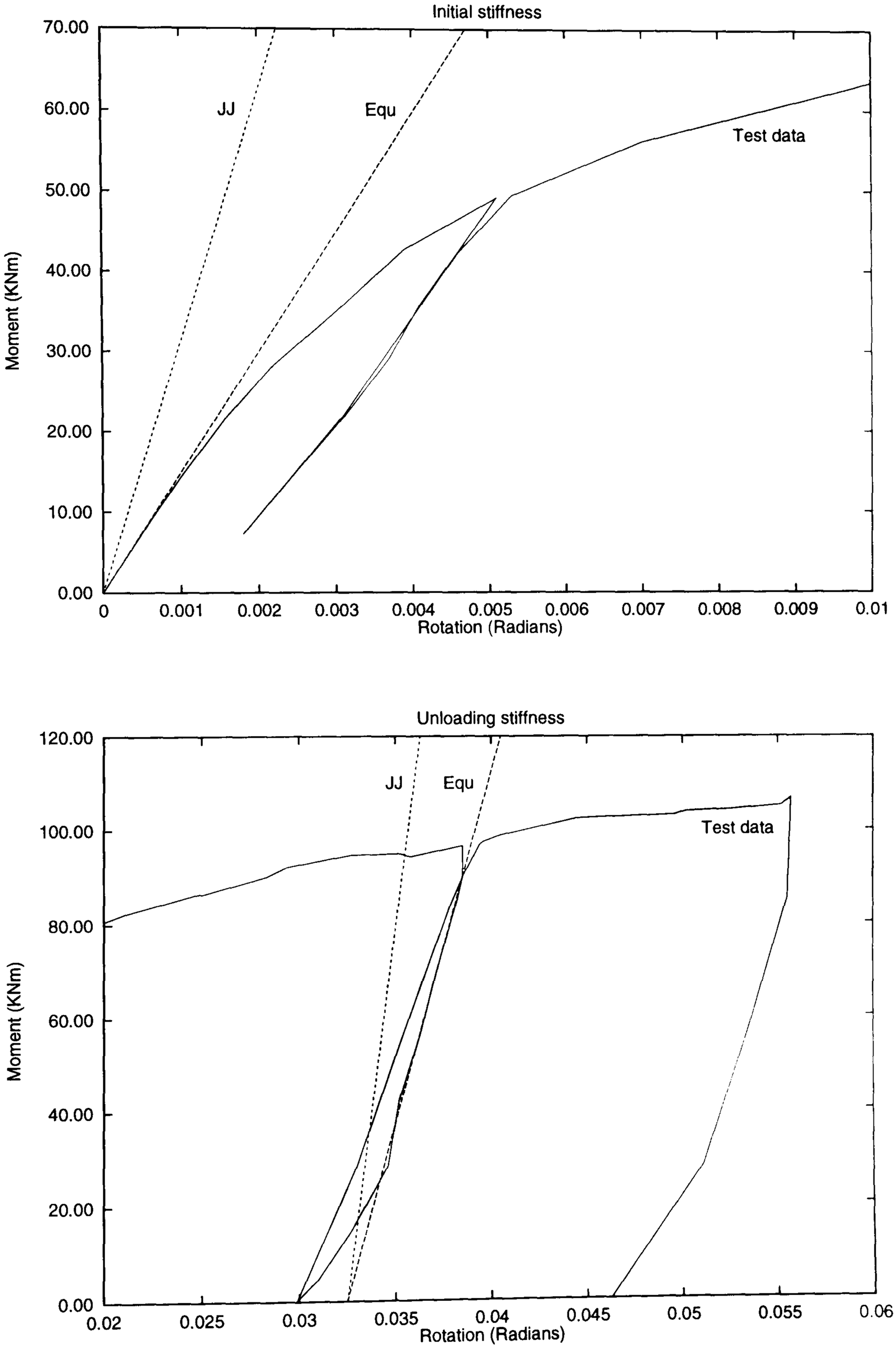

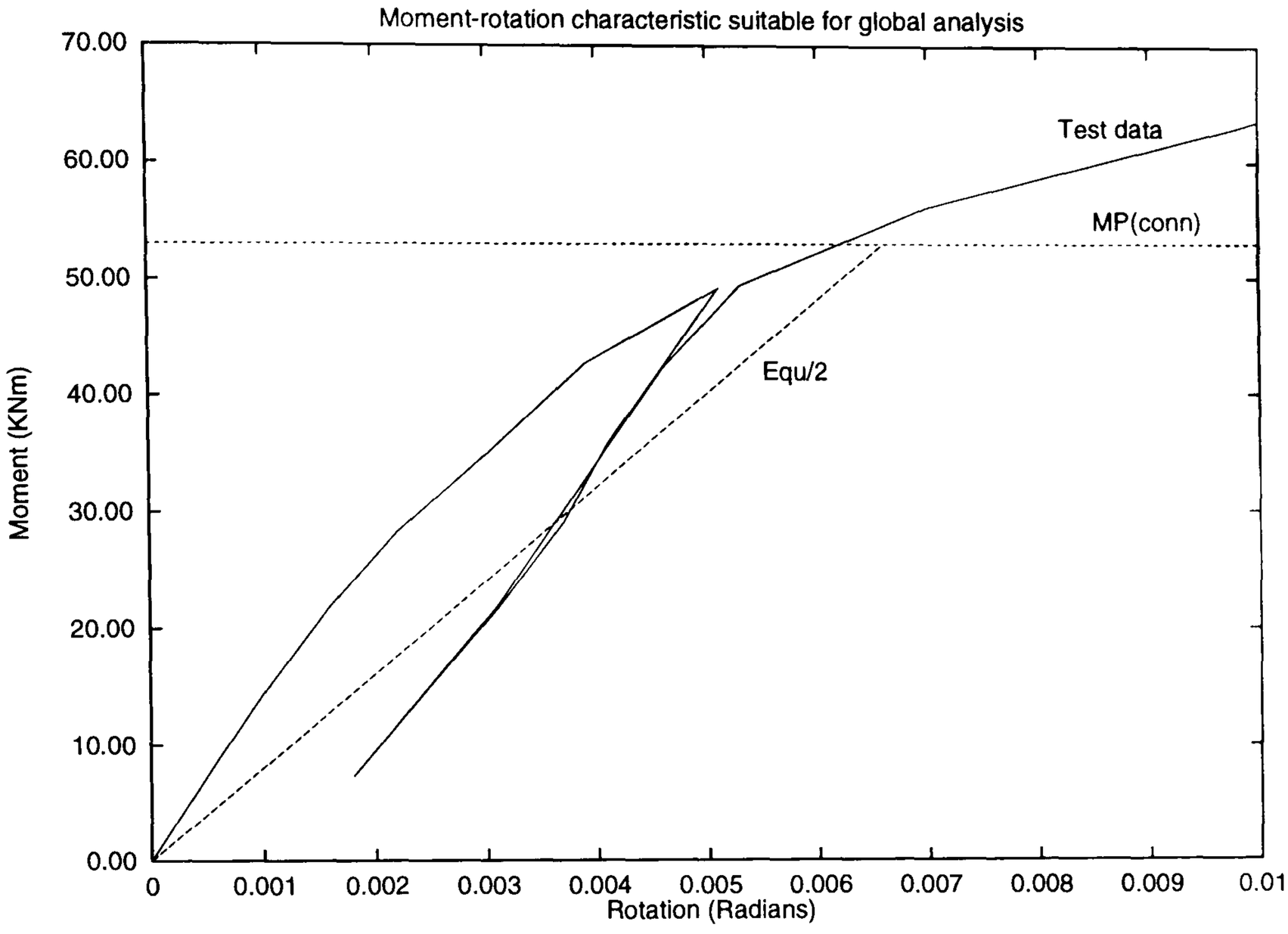
Moment-rotation characteristic suitable for global analysis
Test data
MP(conn)
Equ/2
Moment (KNm)
Rotation (Radians)
70.00
60.00
50.00
40.00
30.00
20.00
10.00
0.00
0
0.001
0.002
0.003
0.004
0.005
0.006
0.007
0.008
0.009
0.01

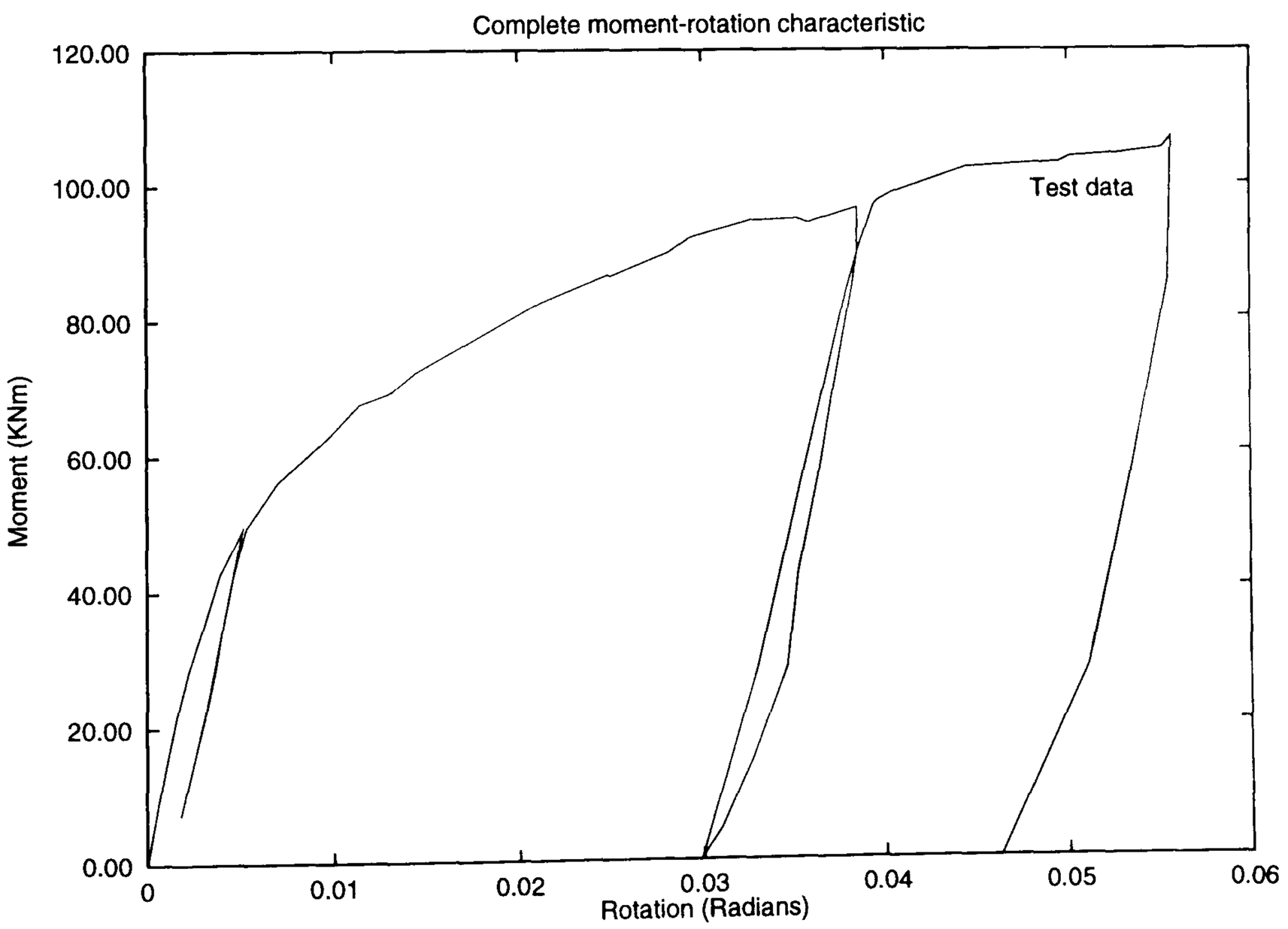
Complete moment-rotation characteristic
Test data
Moment (KNm)
Rotation (Radians)
120.00
100.00
80.00
60.00
40.00
20.00
0.00
0
0.01
0.02
0.03
0.04
0.05
0.06

Najafi's test 9 - Left hand connection

Figure 3.17:

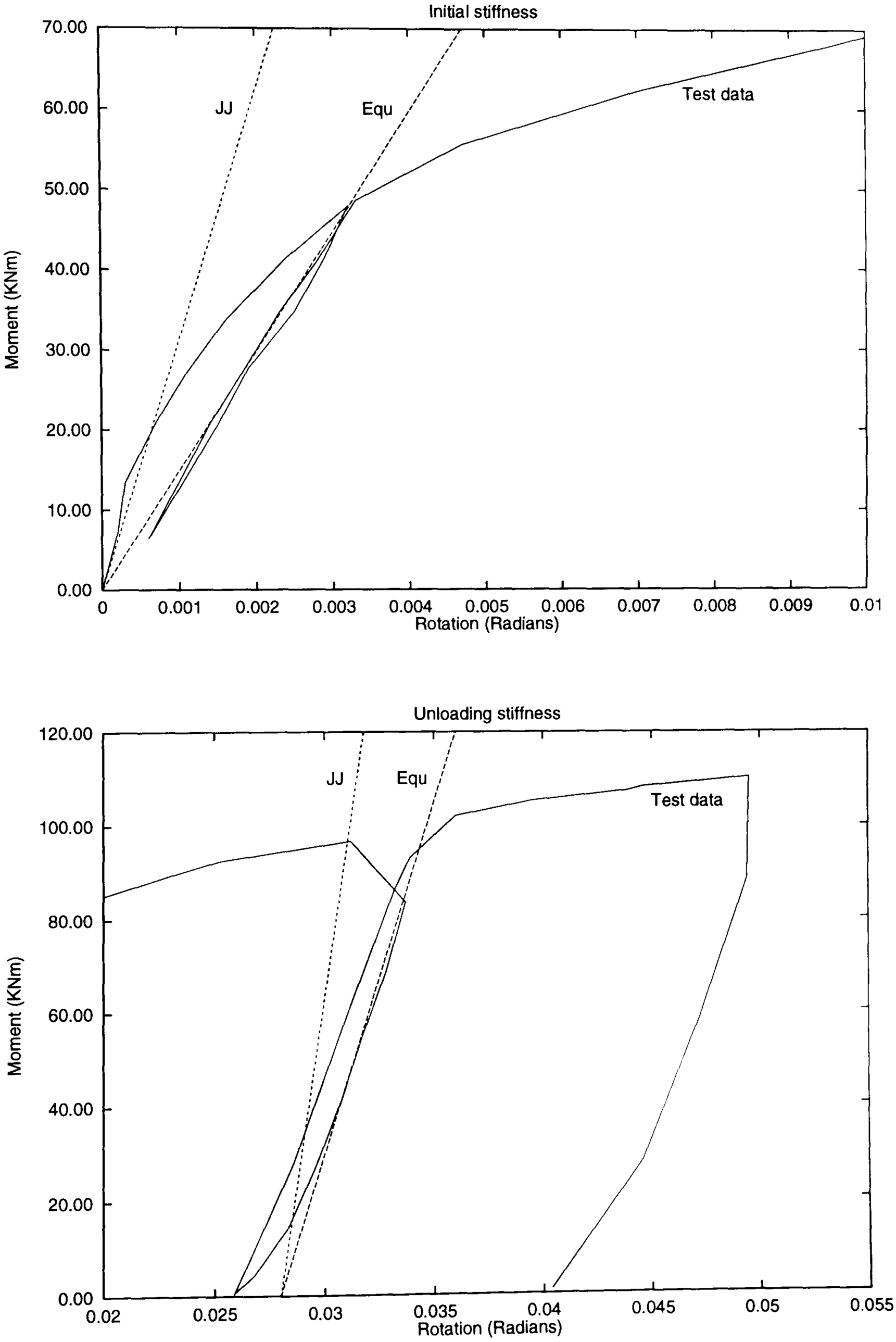

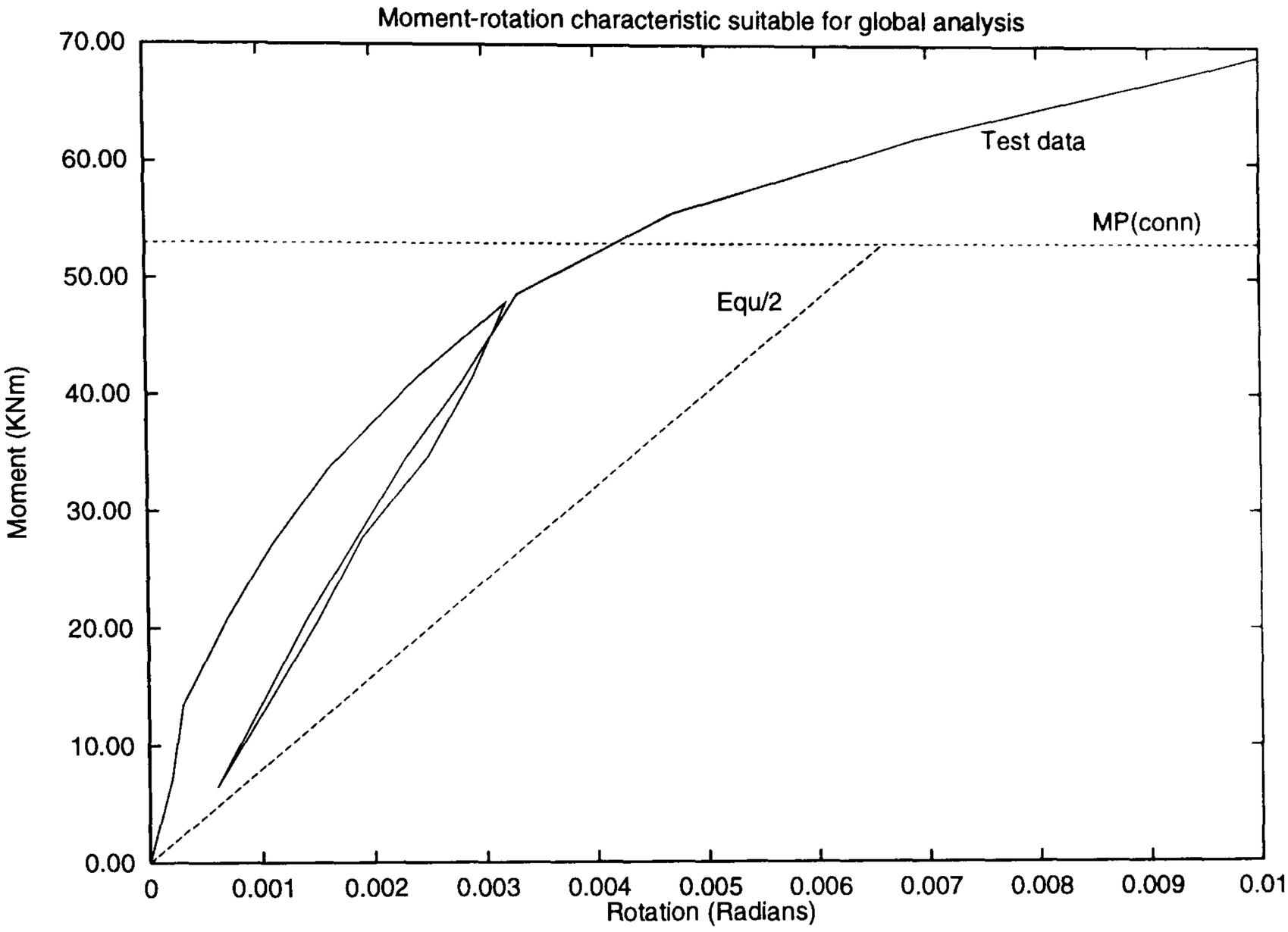
Moment-rotation characteristic suitable for global analysis
70.00
60.00
50.00
40.00
30.00
20.00
10.00
0.00
Moment (KNm)
Test data
MP(conn)
Equ/2
0
0.001
0.002
0.003
0.004
0.005
0.006
0.007
0.008
0.009
0.01
Rotation (Radians)

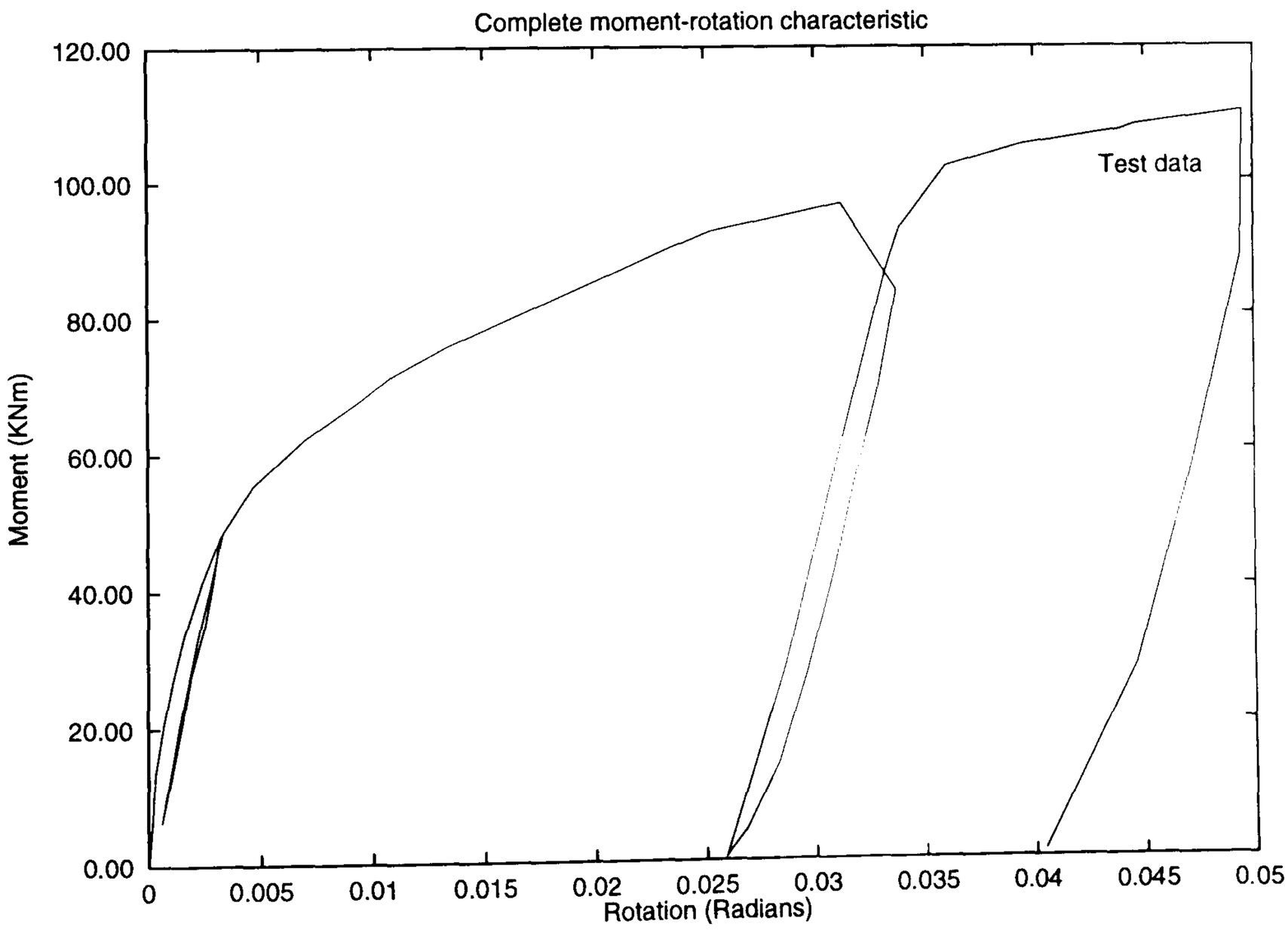
Complete moment-rotation characteristic
120.00
100.00
80.00
60.00
40.00
20.00
0.00
Moment (KNm)
Test data
0
0.005
0.01
0.015
0.02
0.025
0.03
0.035
0.04
0.045
0.05
Rotation (Radians)

Ostrander's test 13

Figure 3.18:

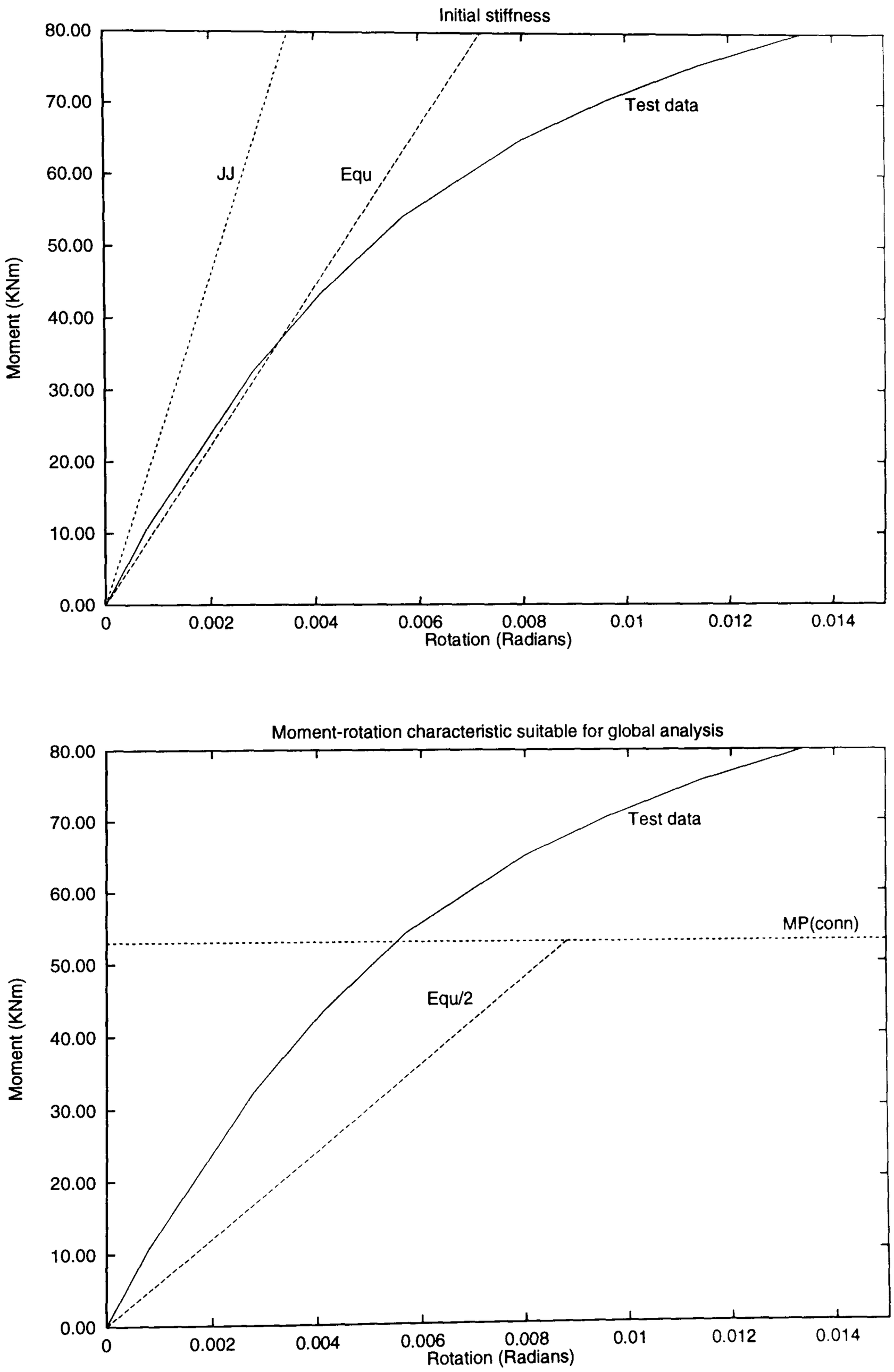

Ostrander's test 23

Figure 3.19:

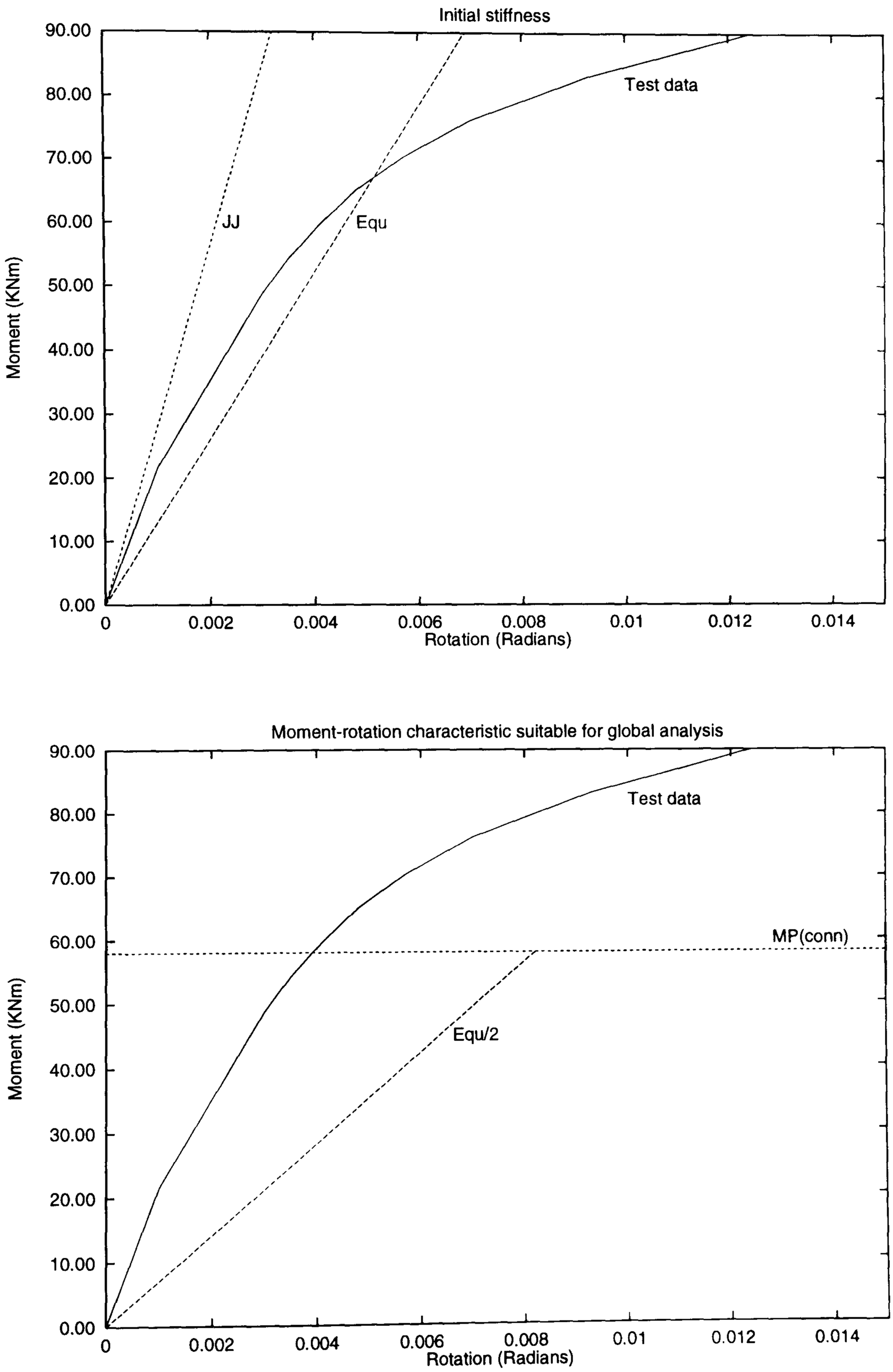

Zoetemeijer's test 17

Figure 3.20:

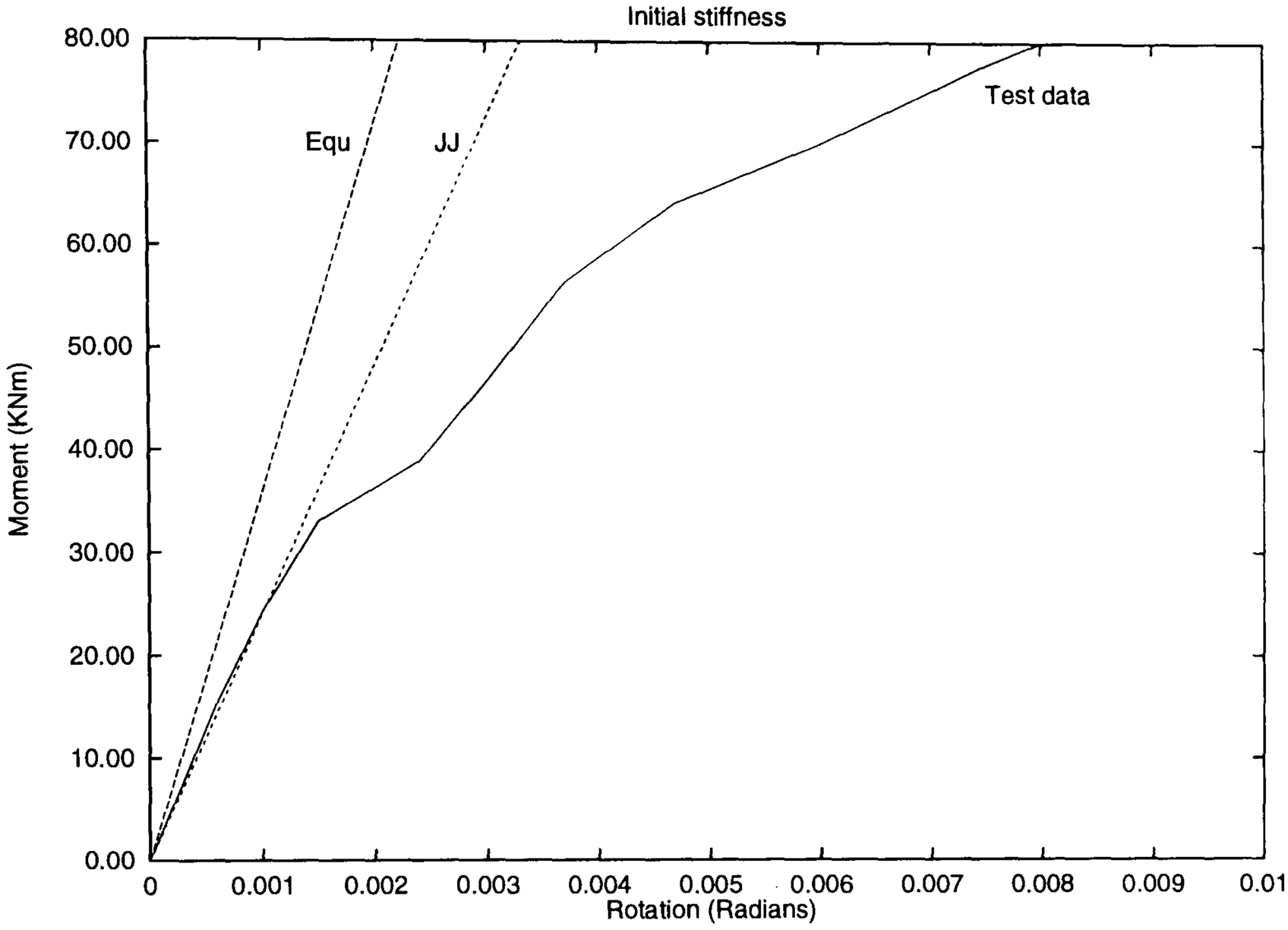

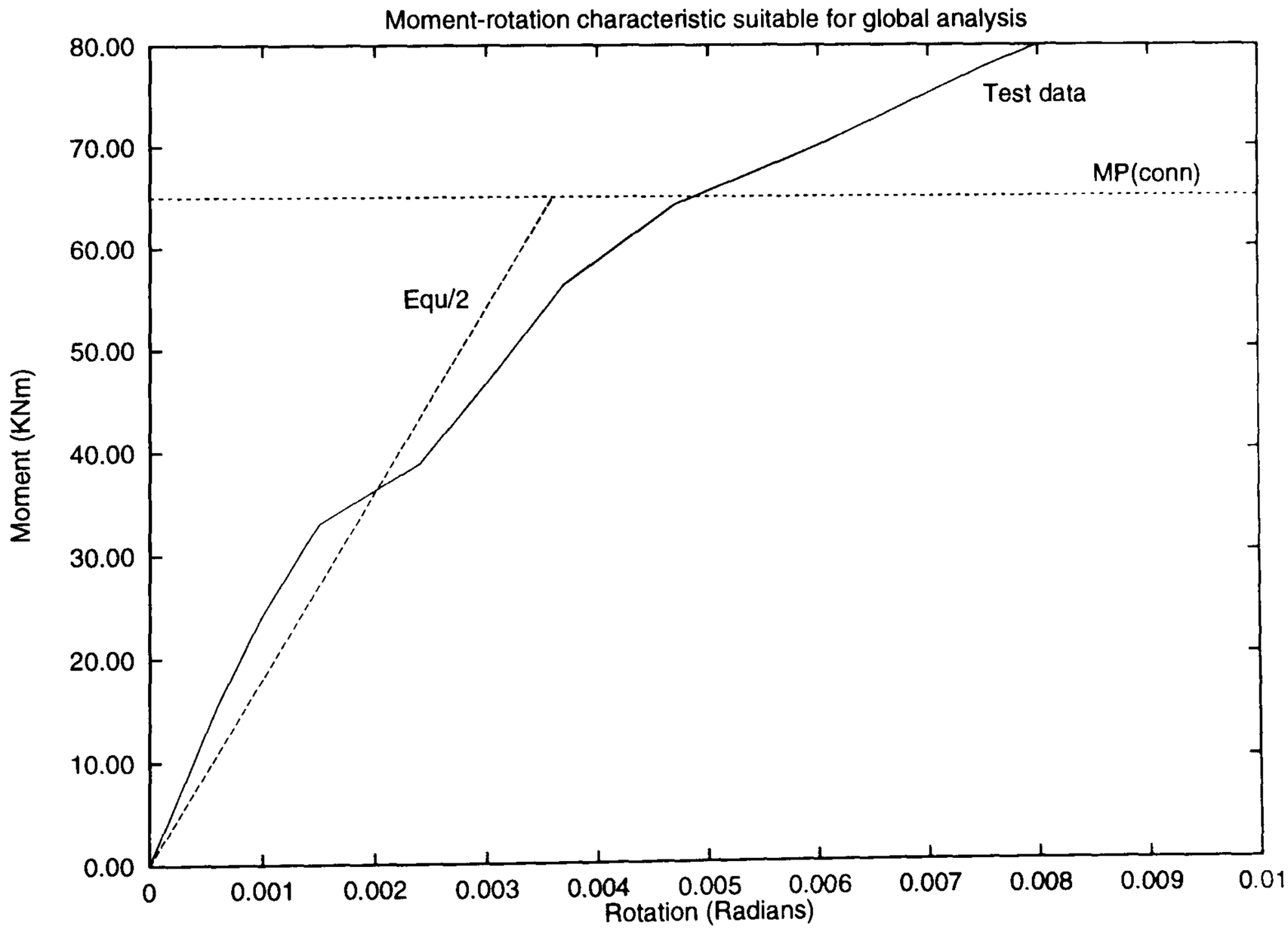

Zoetemeijer's test 19

Figure 3.21:

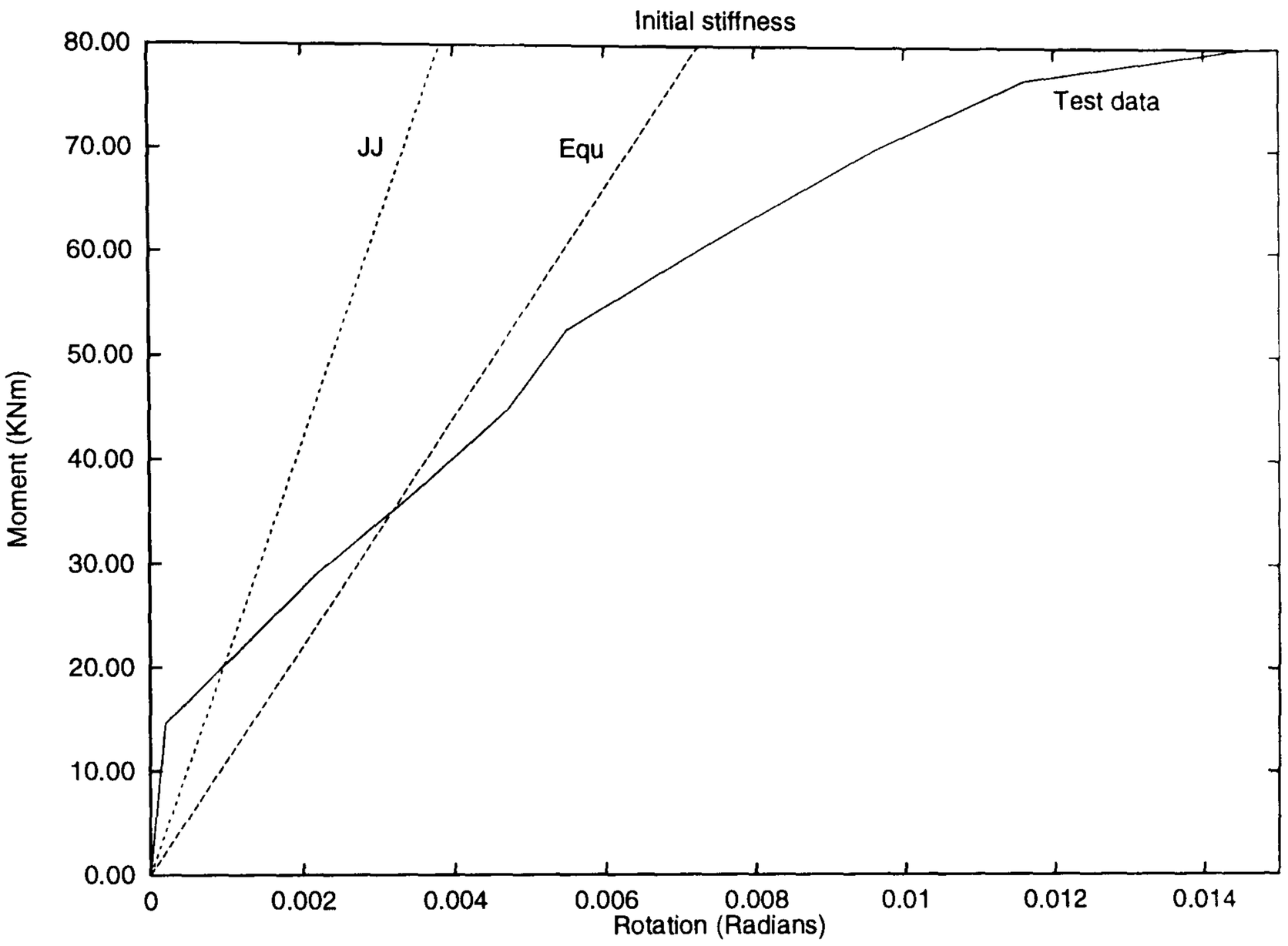

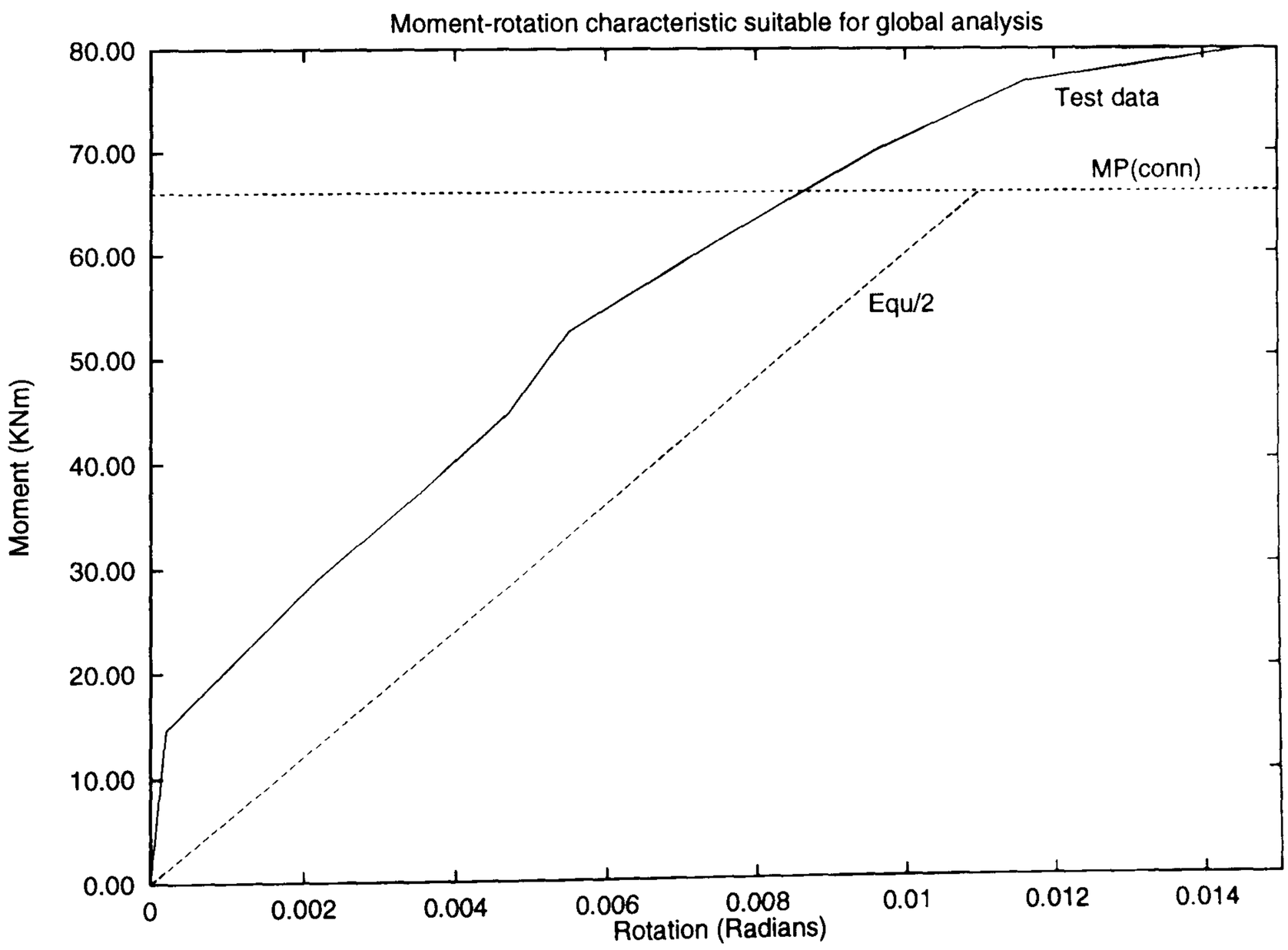

Zoetemeijer's test 34

Figure 3.22:

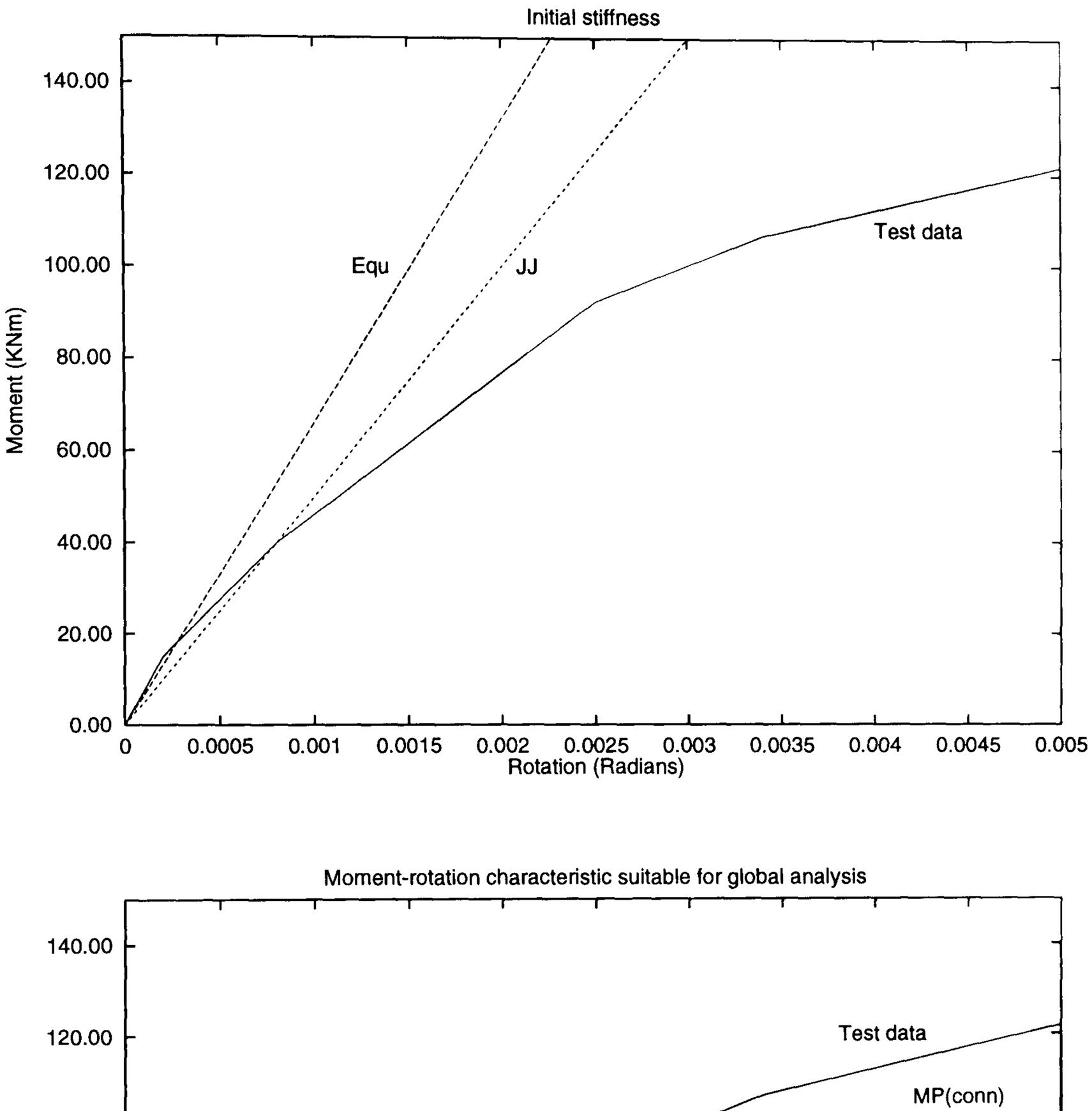

Bose's test 1 - Right hand connection

Figure 3.23:

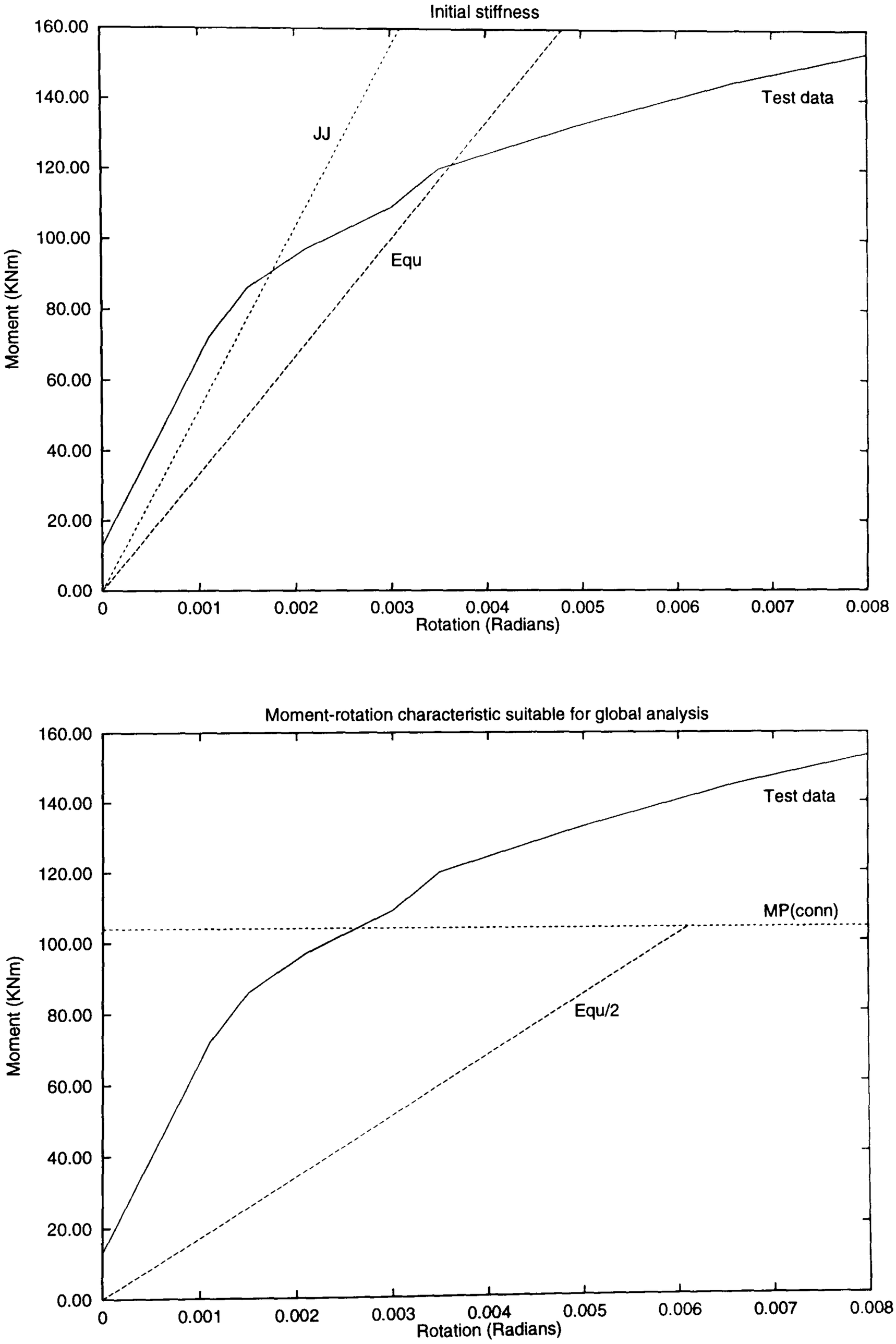

Bose's test 1 - Left hand connection

Figure 3.24:

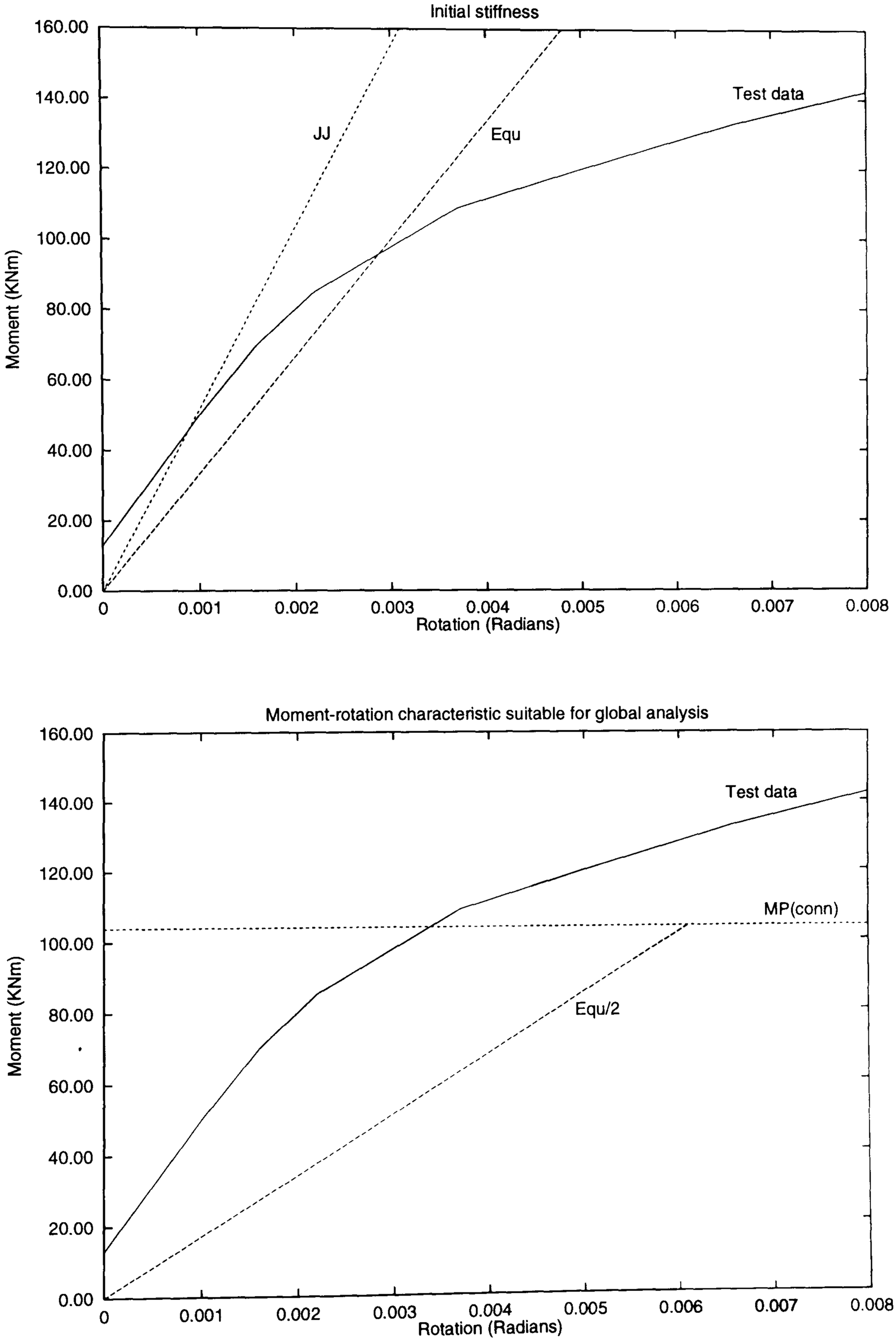

Bose's test 2 - Right hand connection

Figure 3.25:

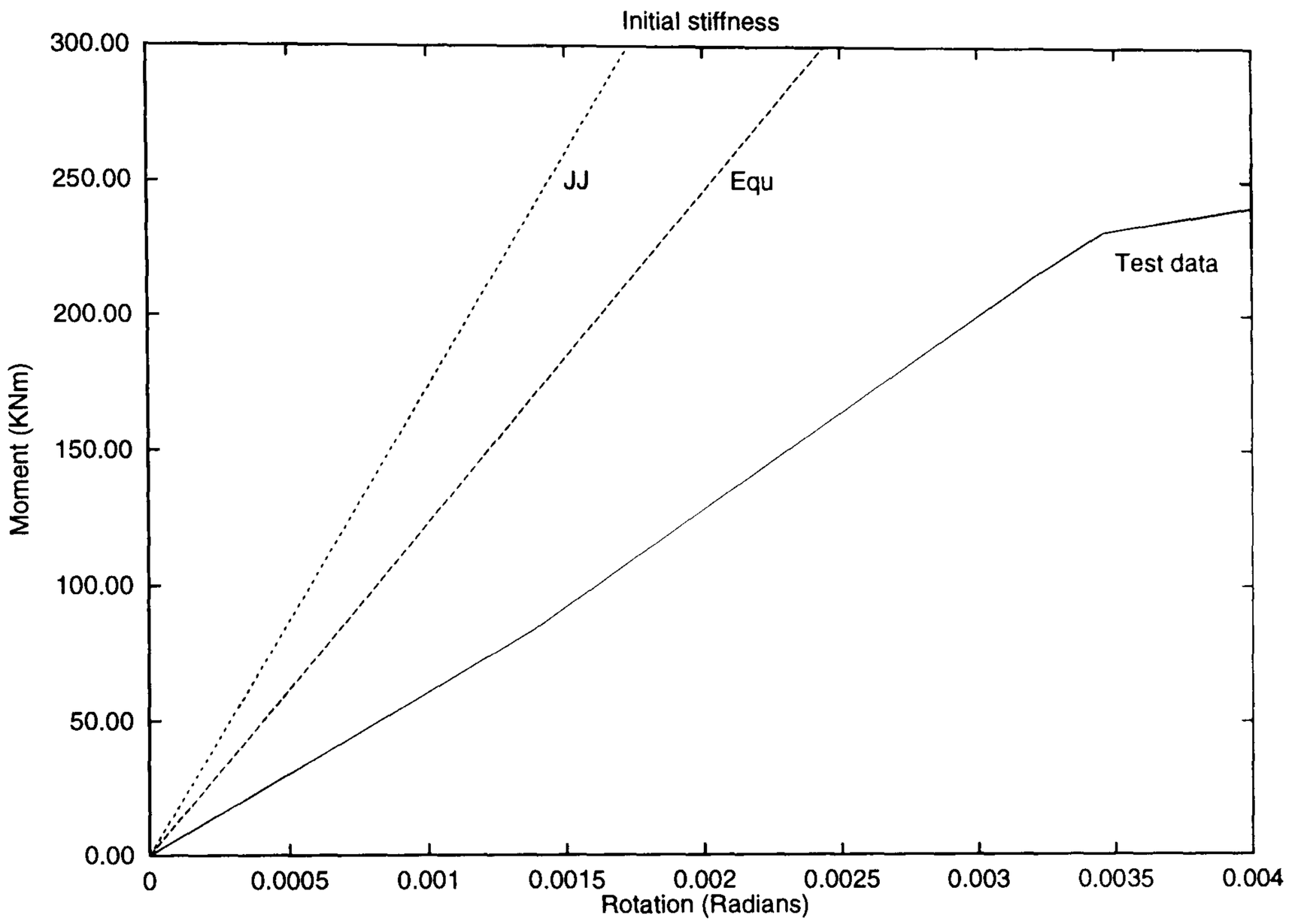

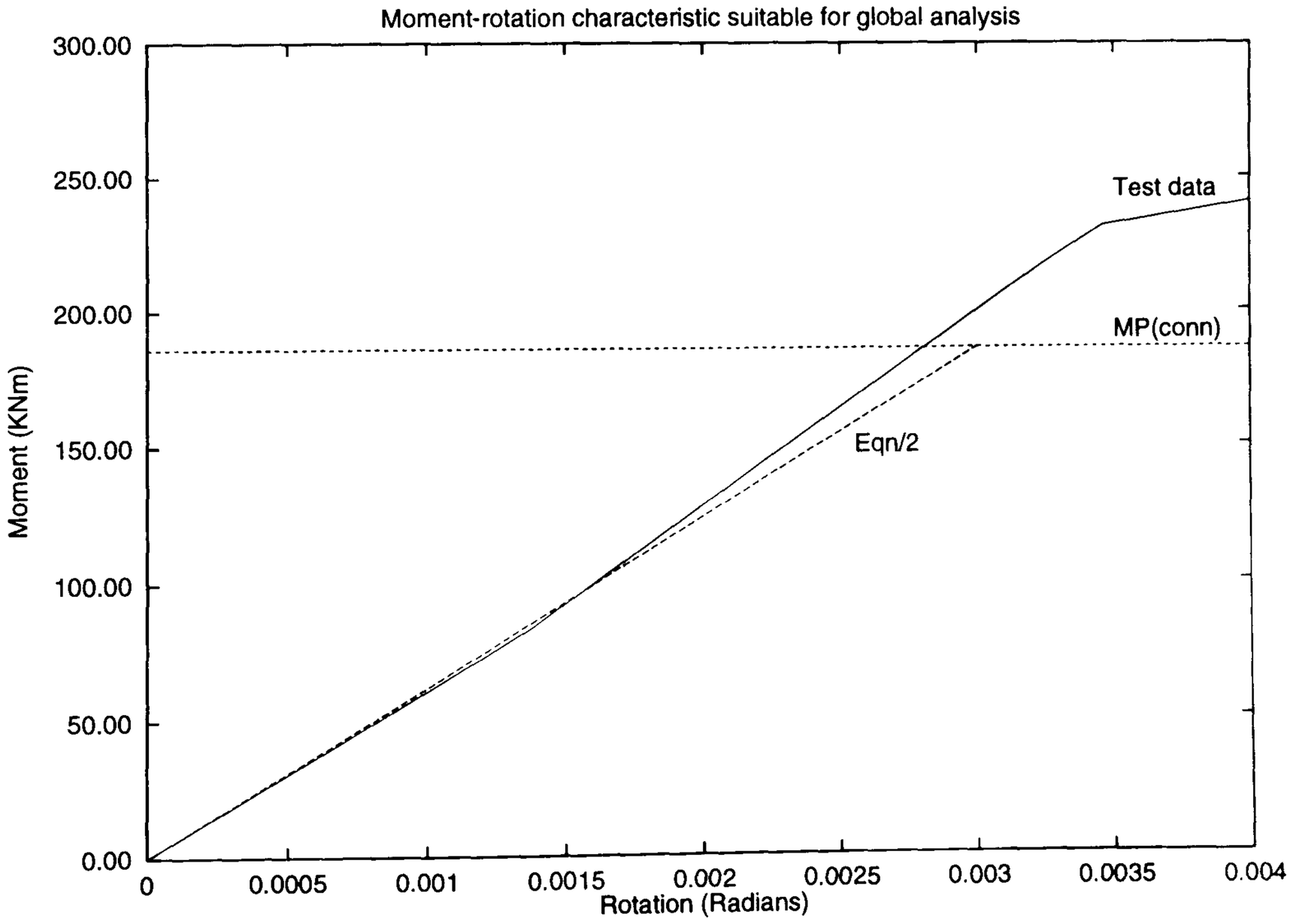

Bose's test 2 - Left hand connection

Figure 3.26:

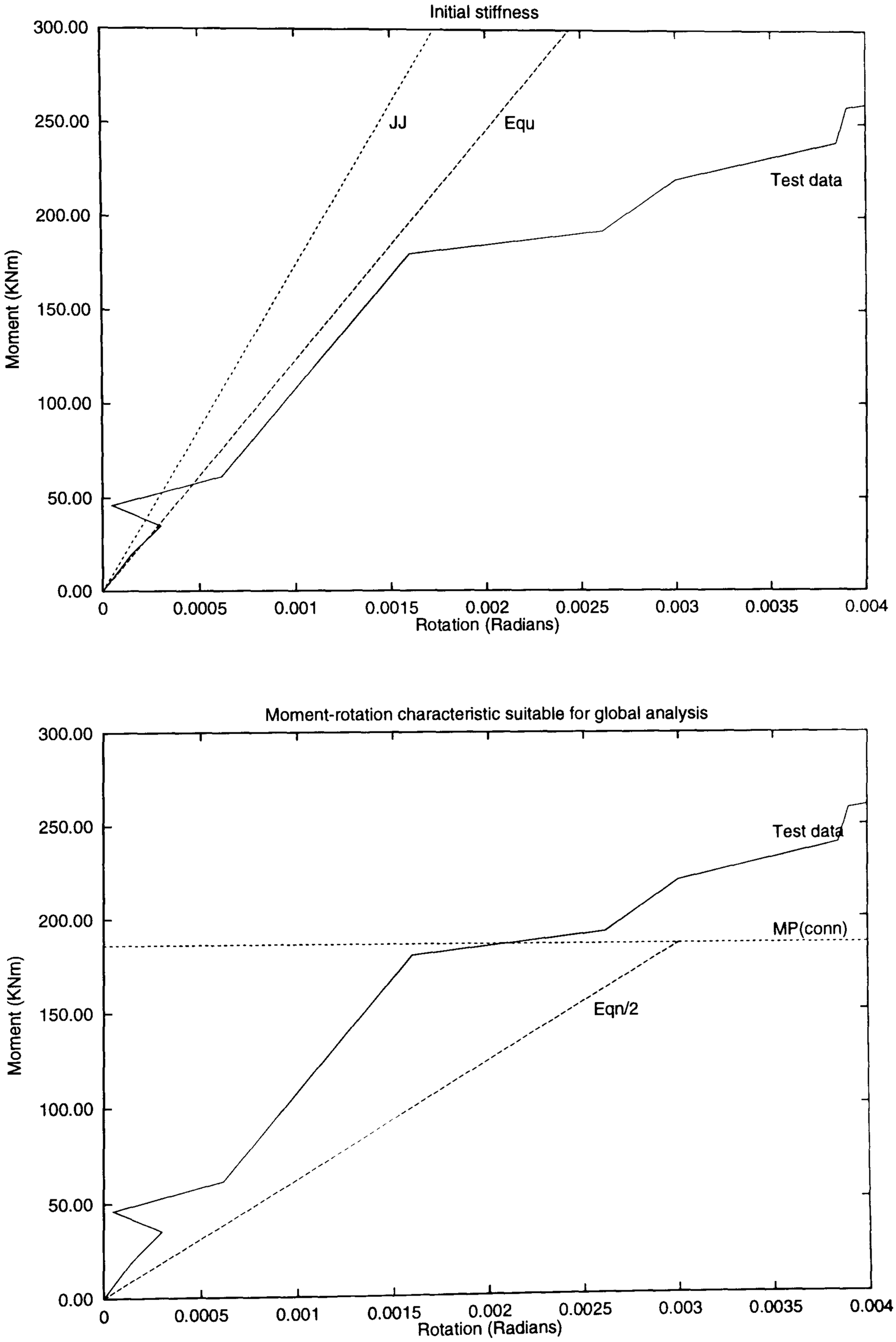

Bose's test 9 - Right hand connection

Figure 3.27:

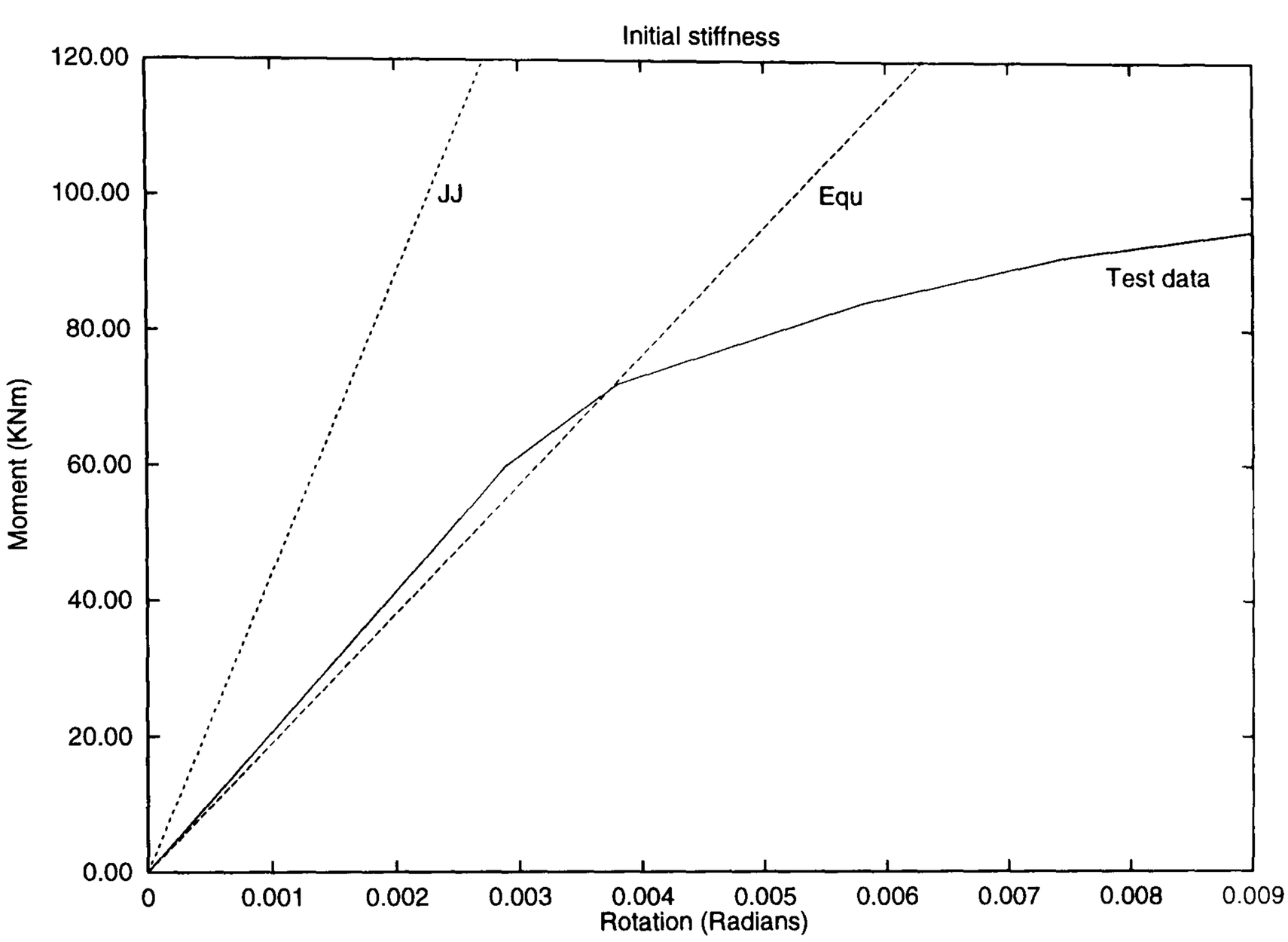

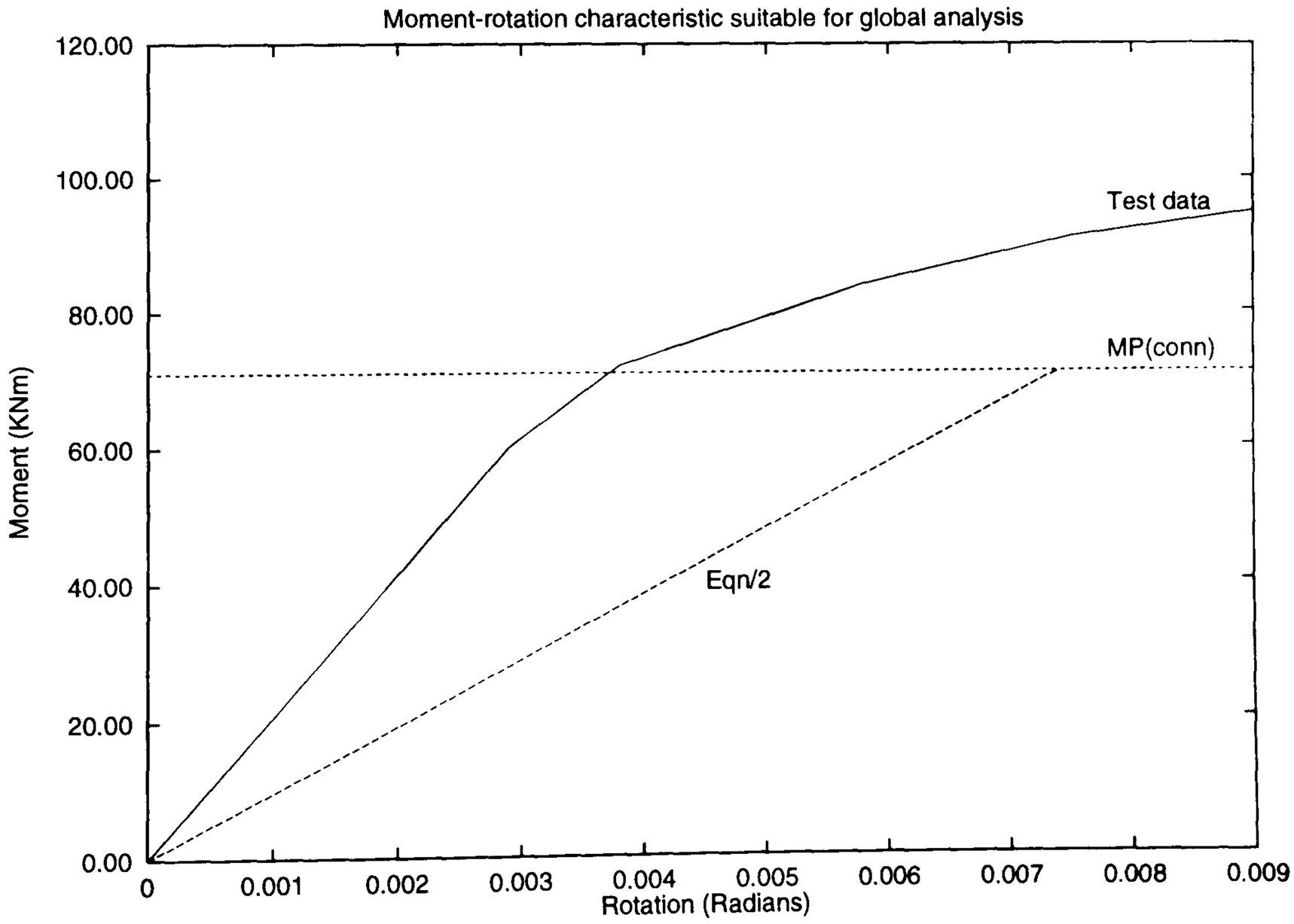

Bose's test 9 - Left hand connection

Figure 3.28:

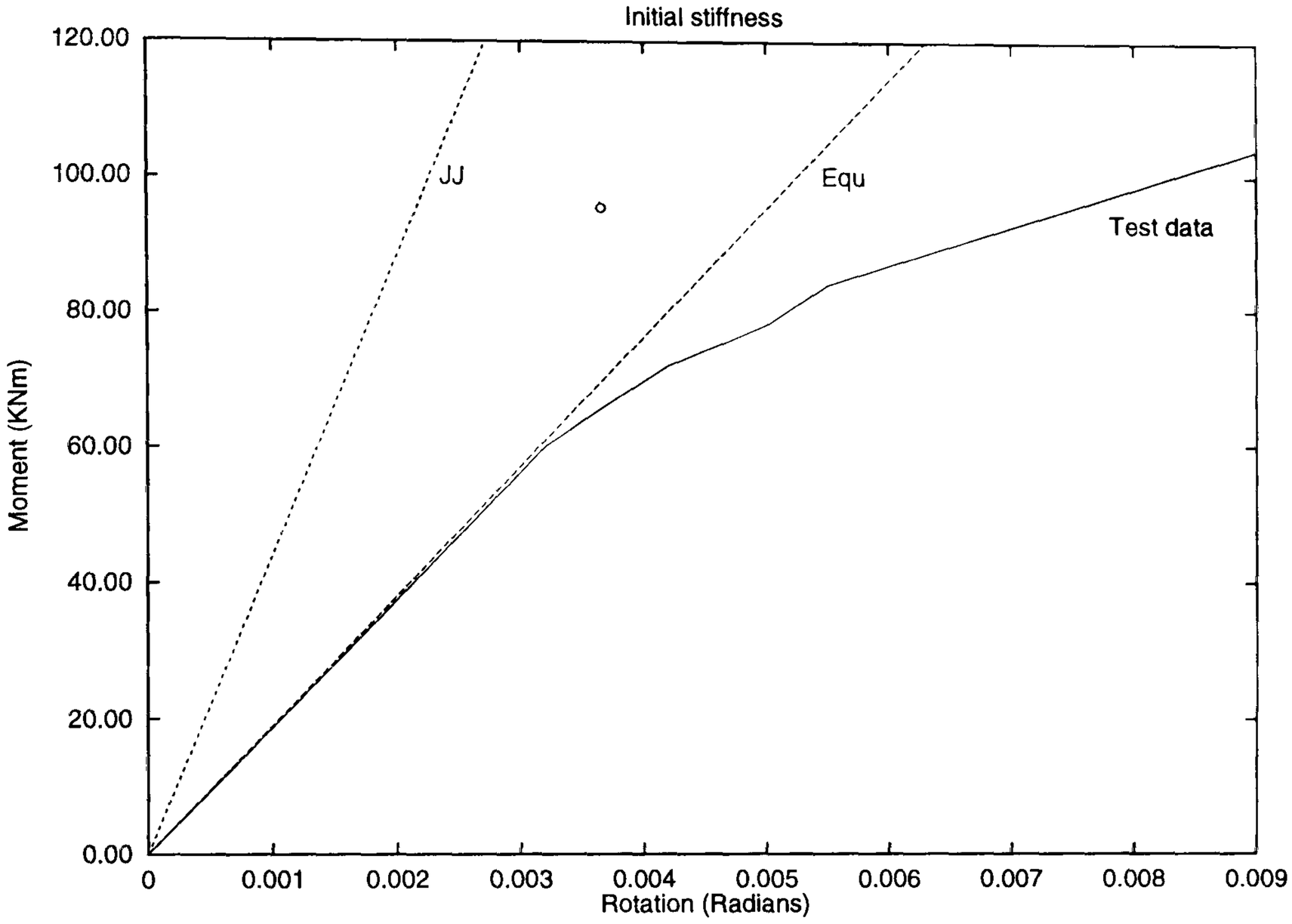

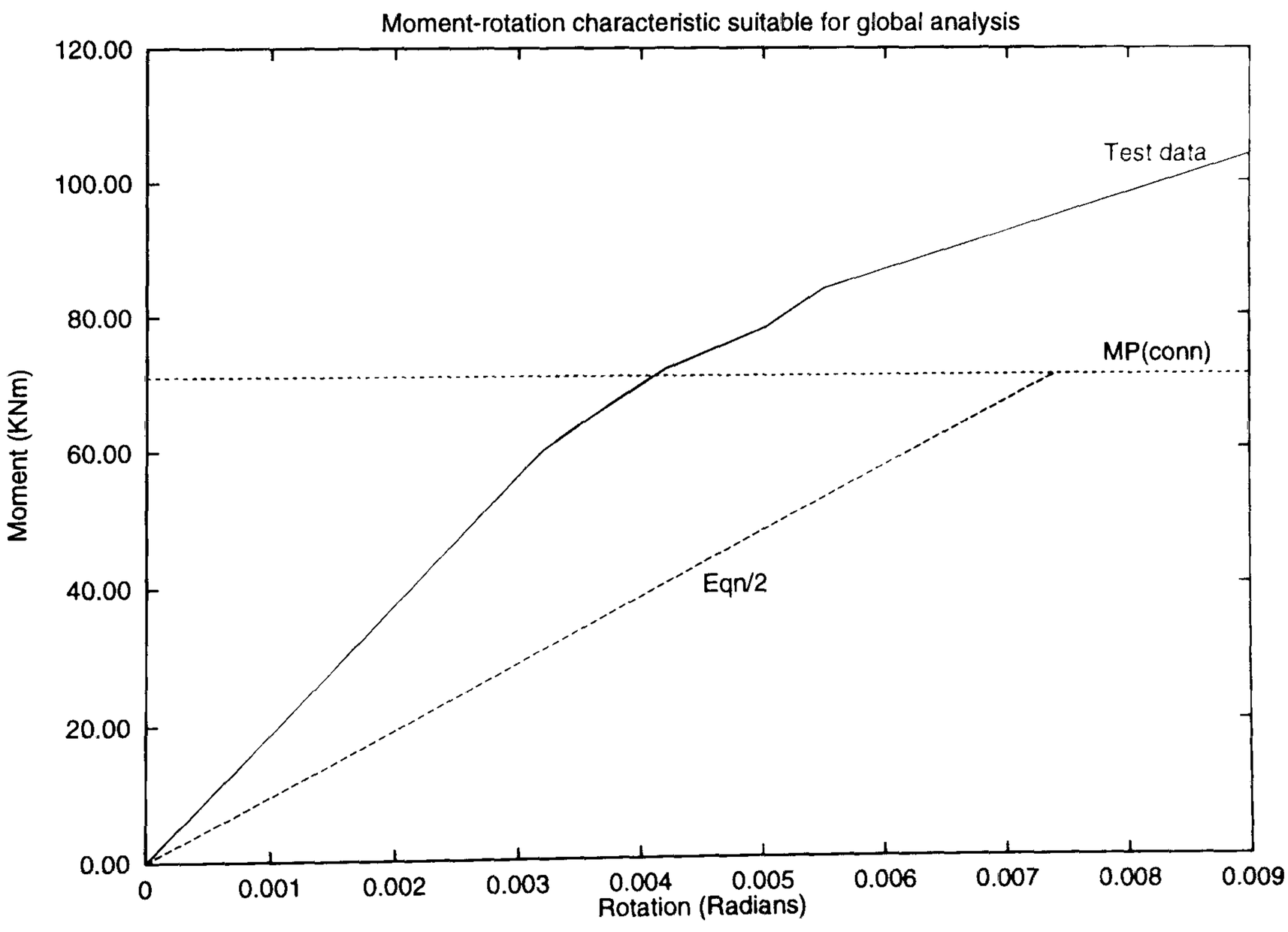

Bose's test 4 - Right hand connection

Figure 3.29:

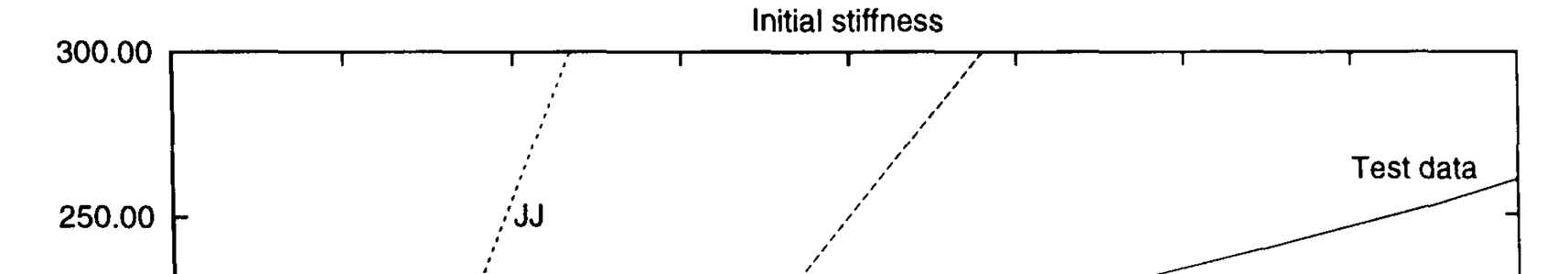

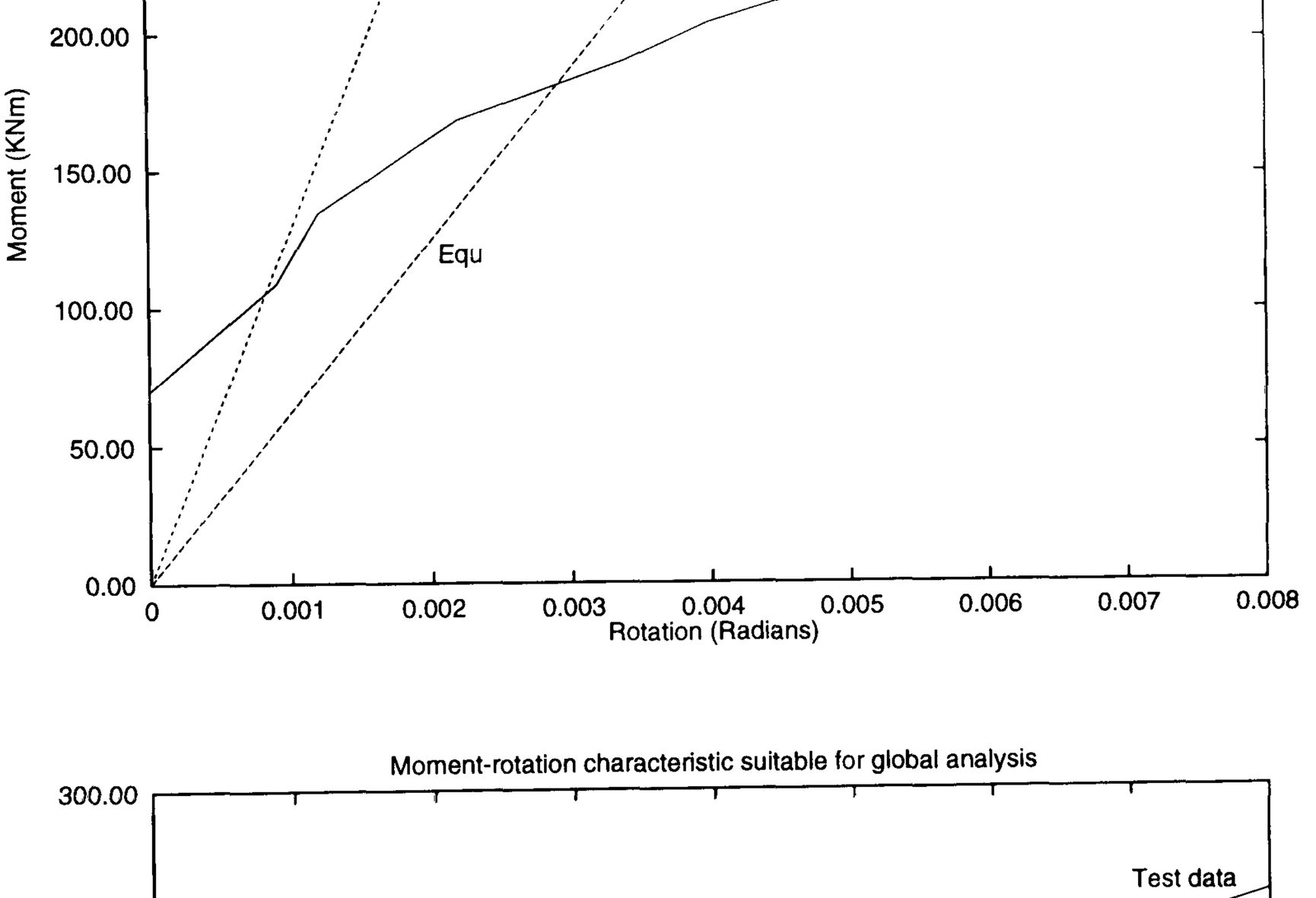

Bose's test 4 - Left hand connection

Figure 3.30:

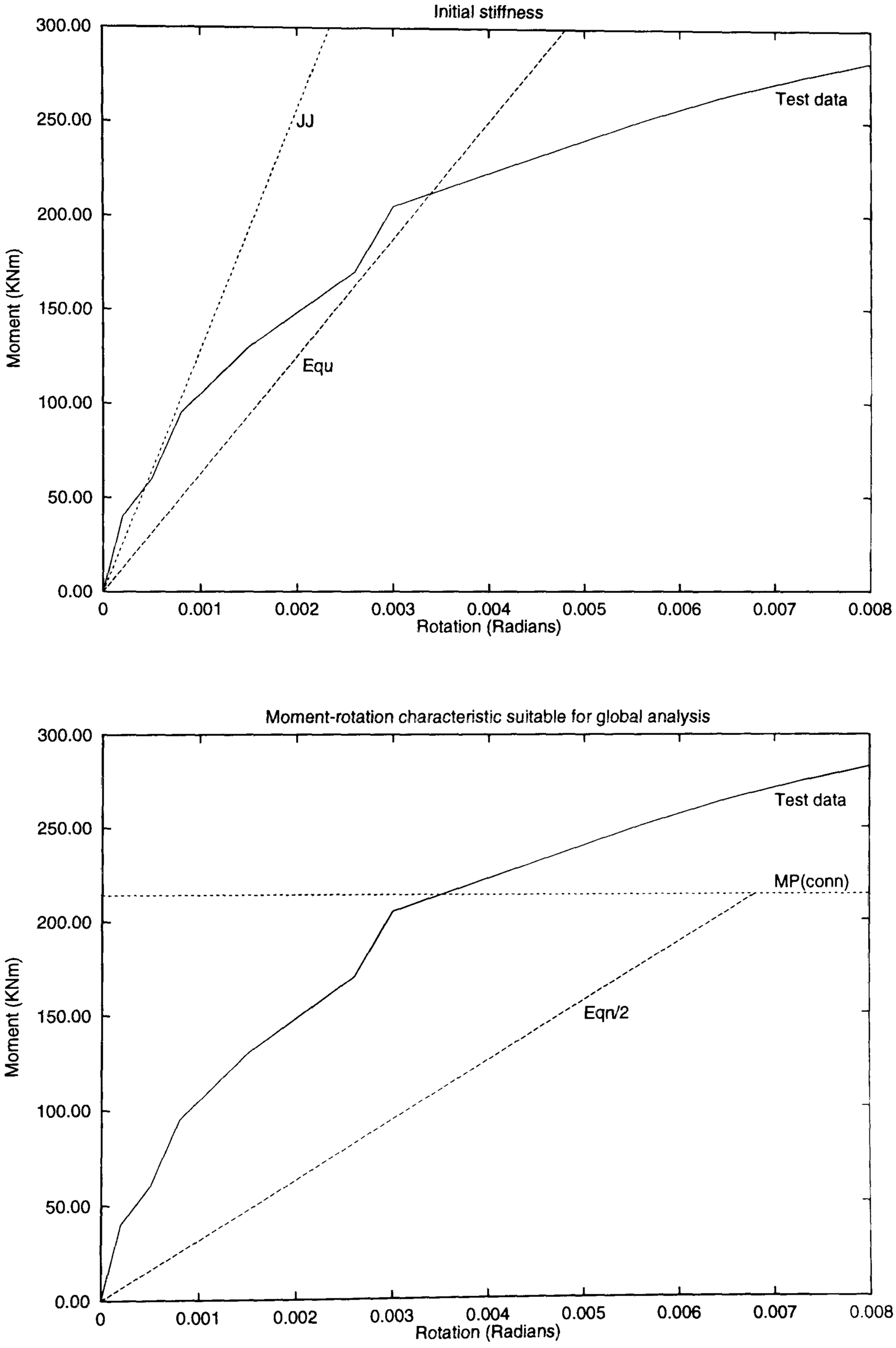

Bose's test 5 - Right hand connection

Figure 3.31:

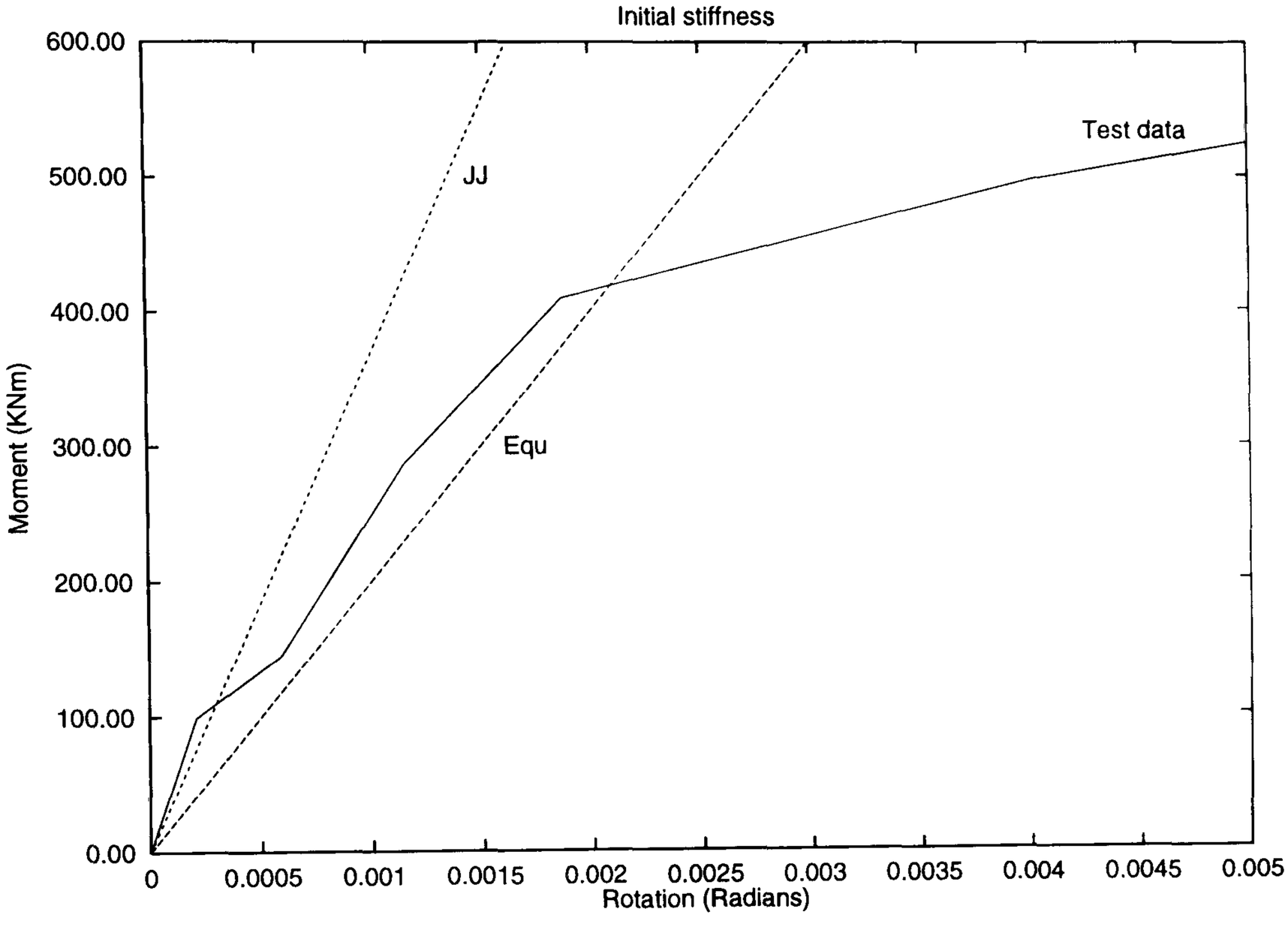

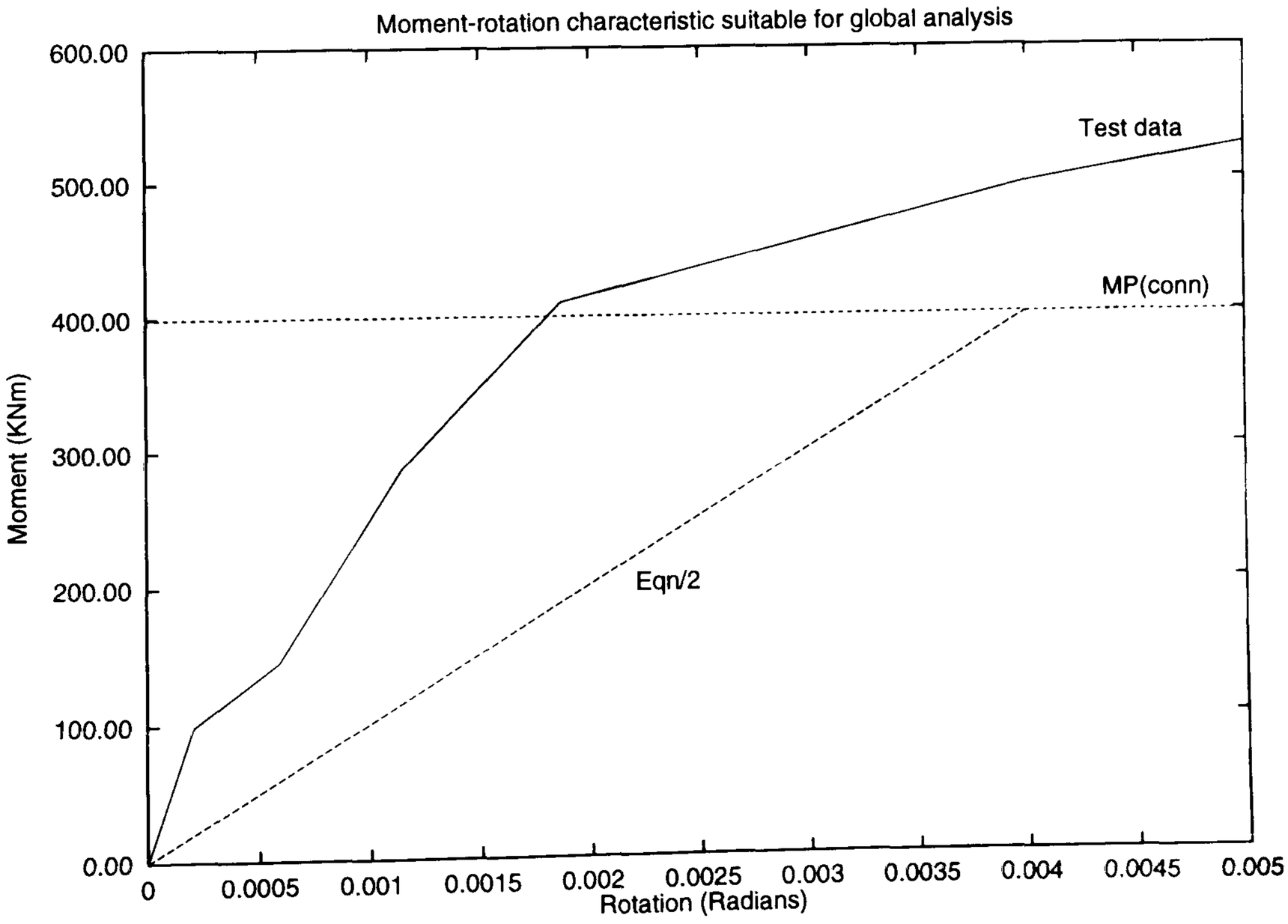

Bose's test 5 - Left hand connection

Figure 3.32:

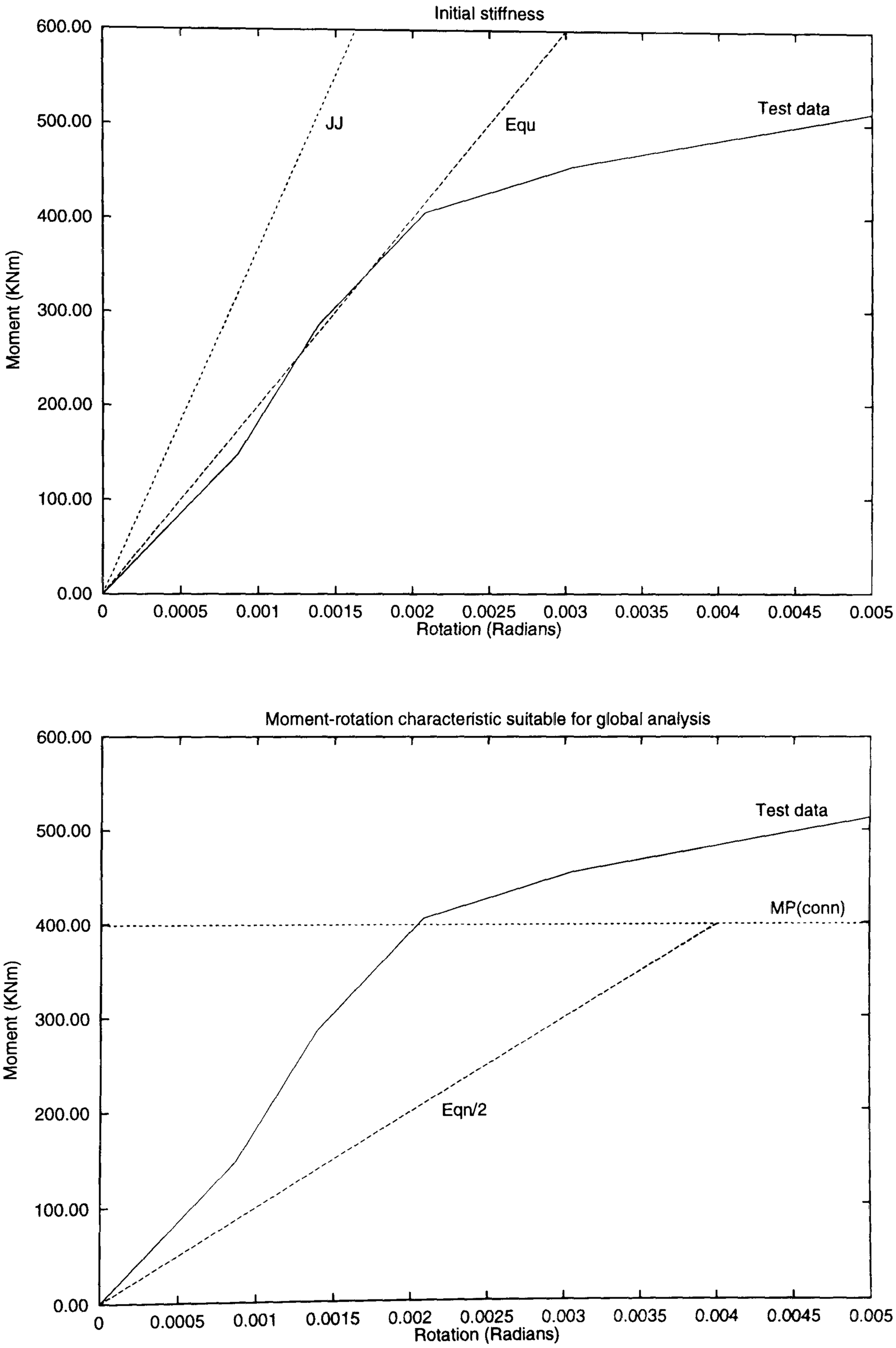

Bose's test 6 - Right hand connection

Figure 3.33:

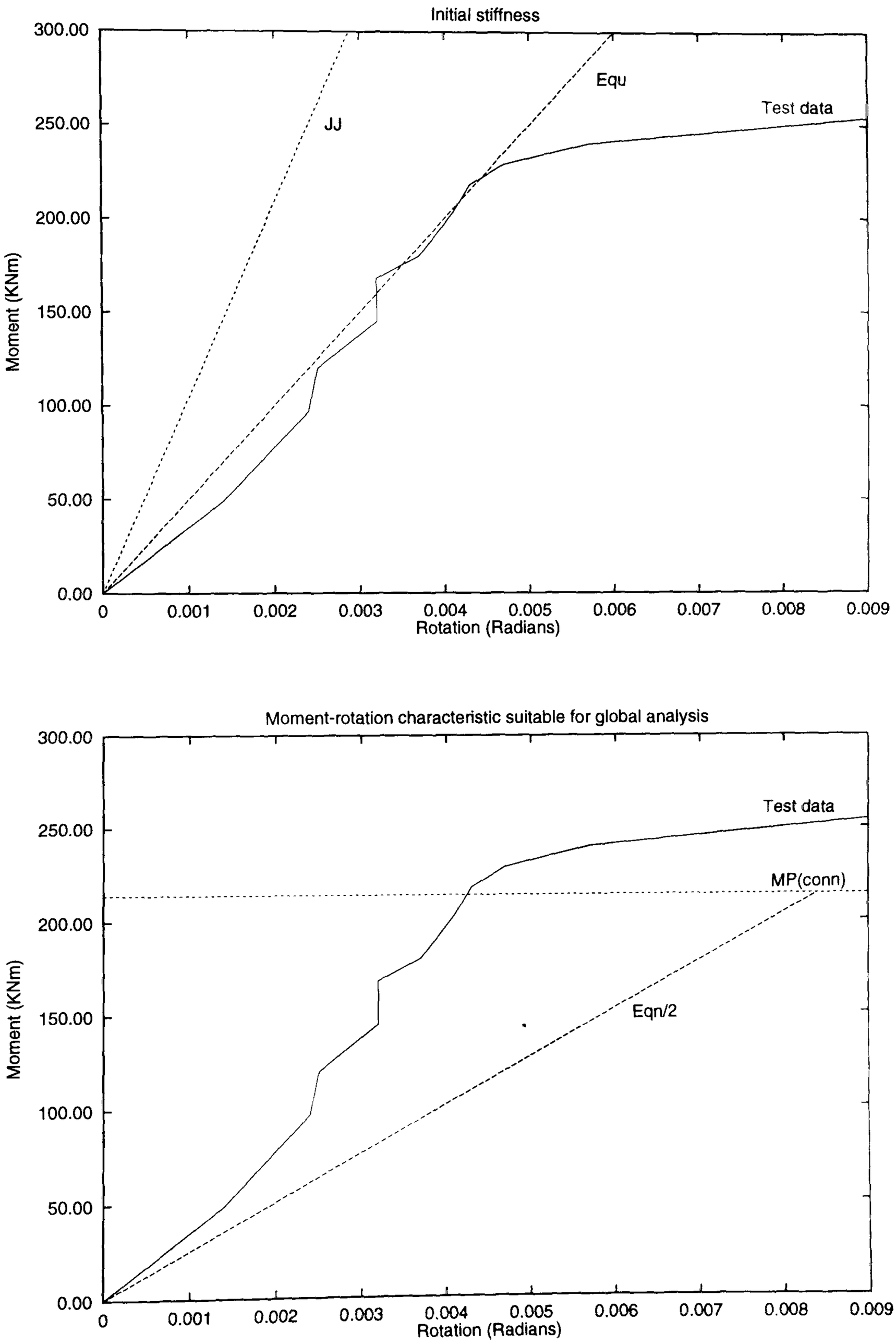

Bose's test 6 - Left hand connection

Figure 3.34:

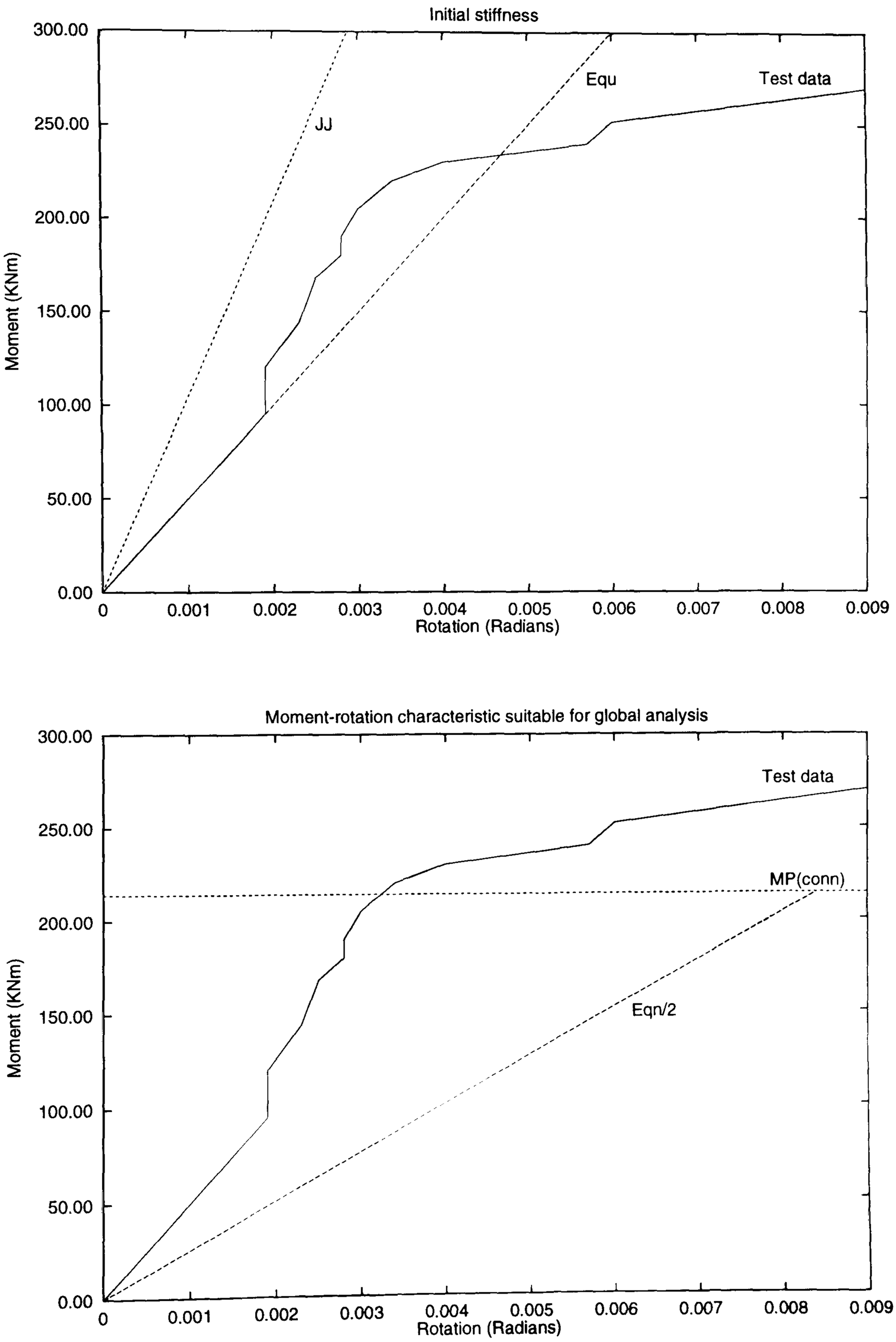

Bose's test 7 - Right hand connection

Figure 3.35:

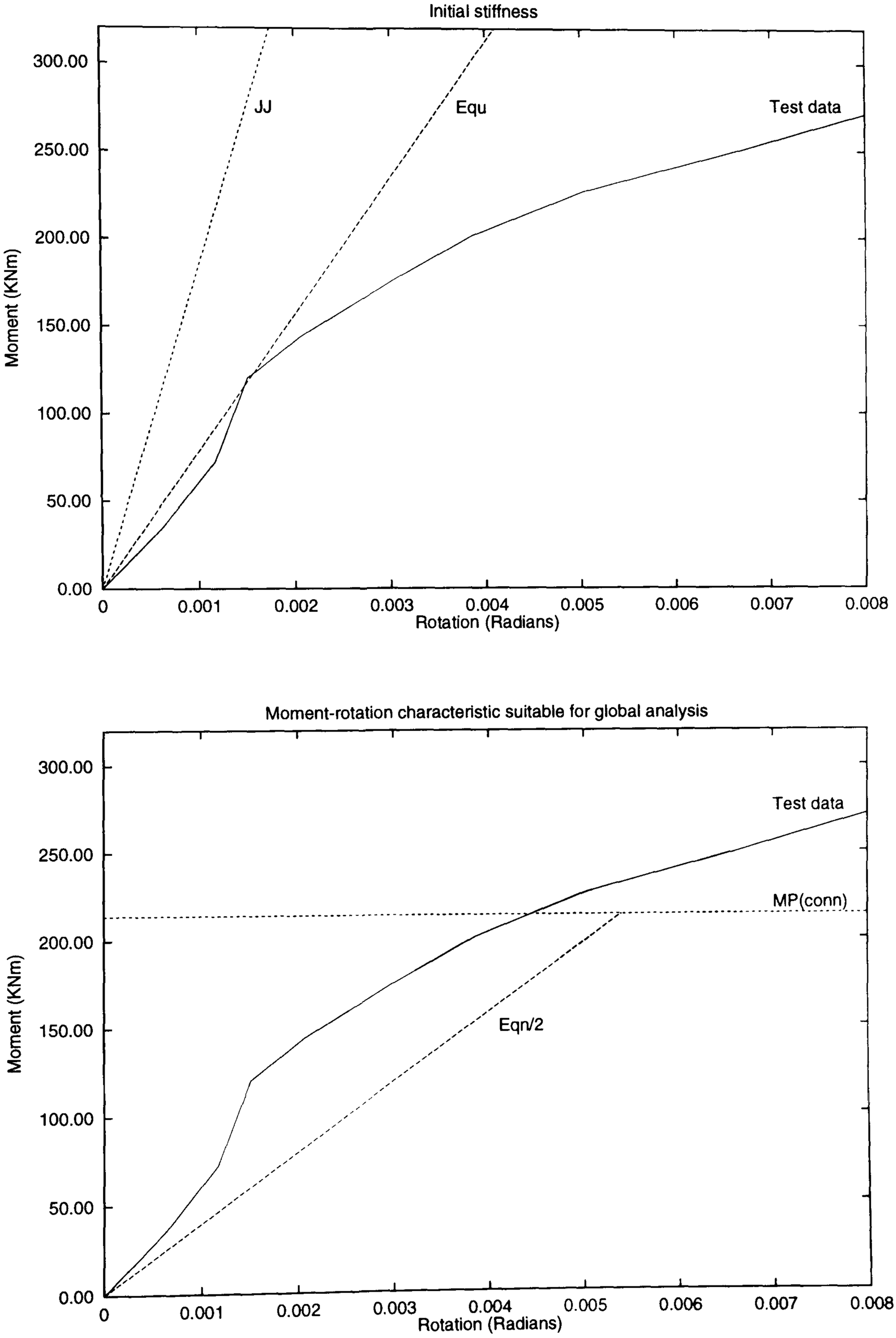

Bose's test 7 - Left hand connection

Figure 3.36:

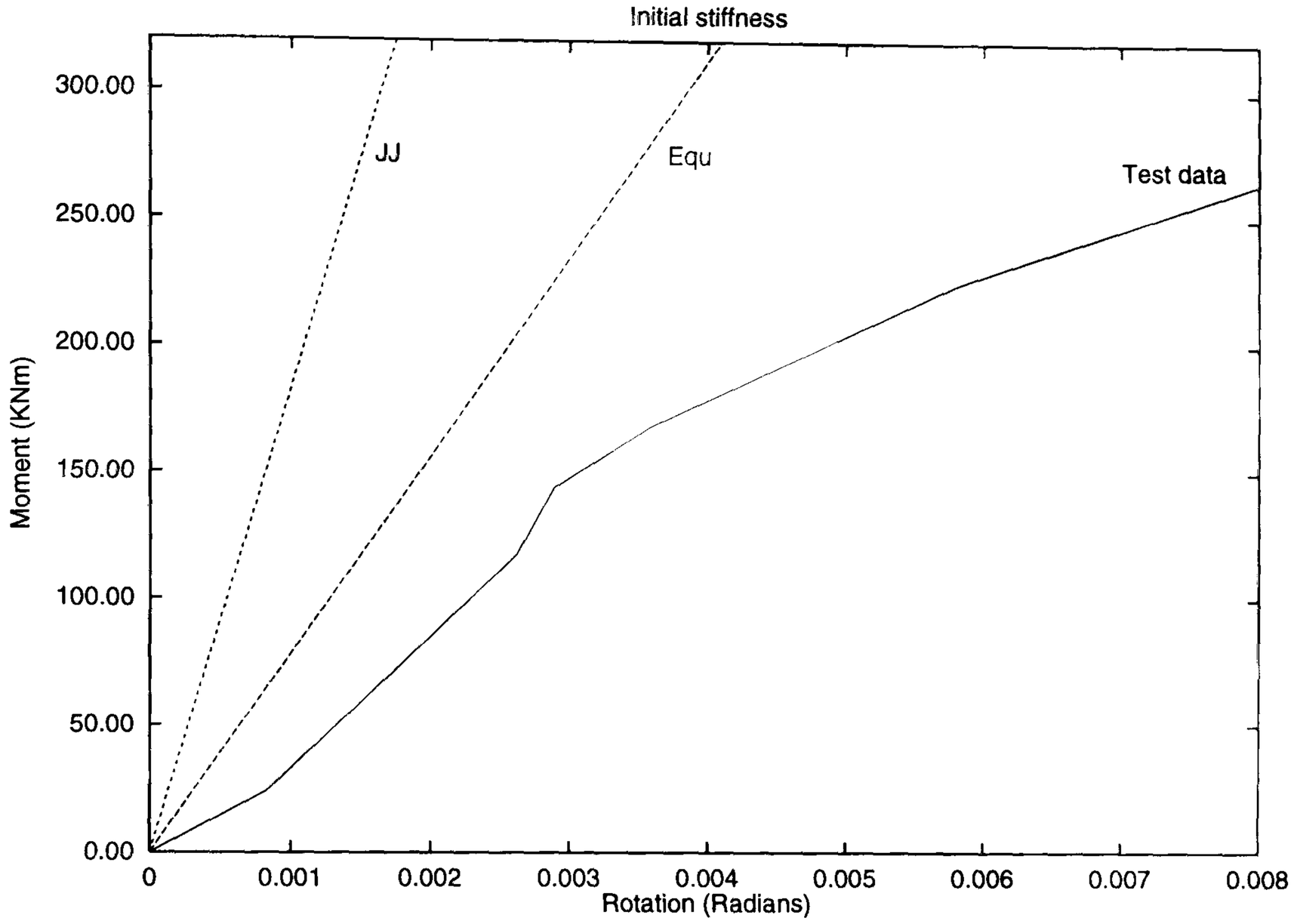

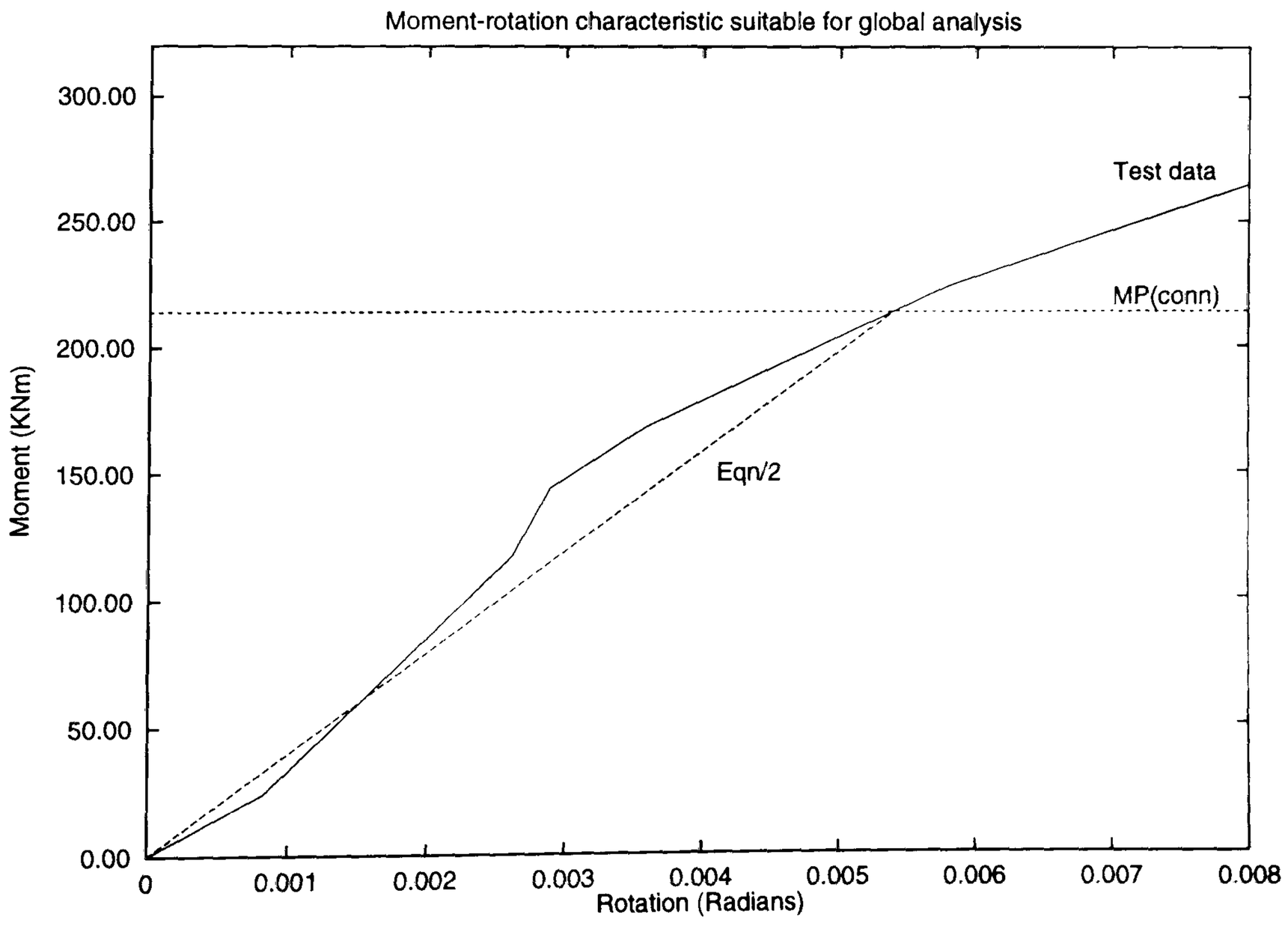

Bose's test 8 - Right hand connection

Figure 3.37:

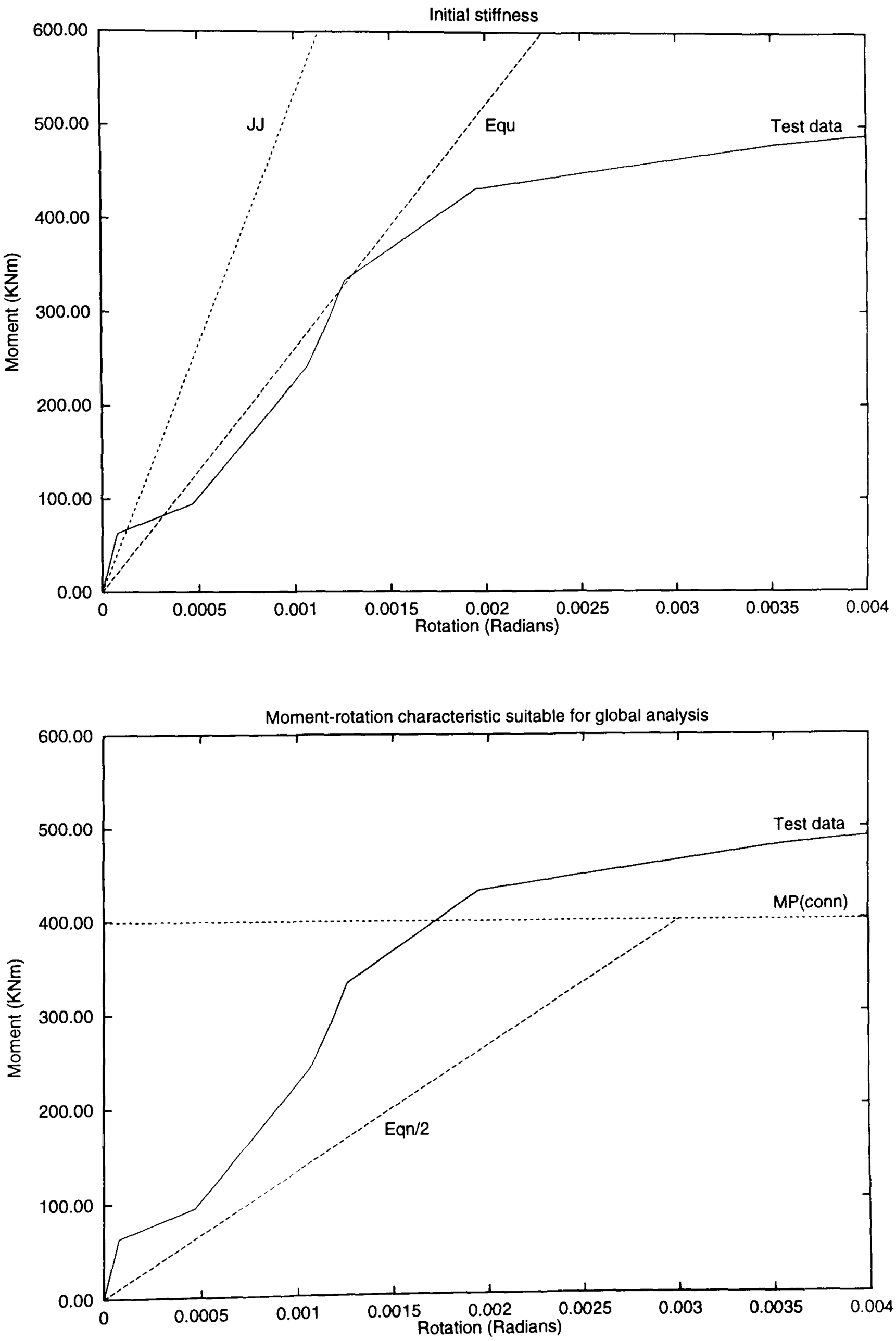

Bose's test 8 - Left hand connection

Figure 3.38:

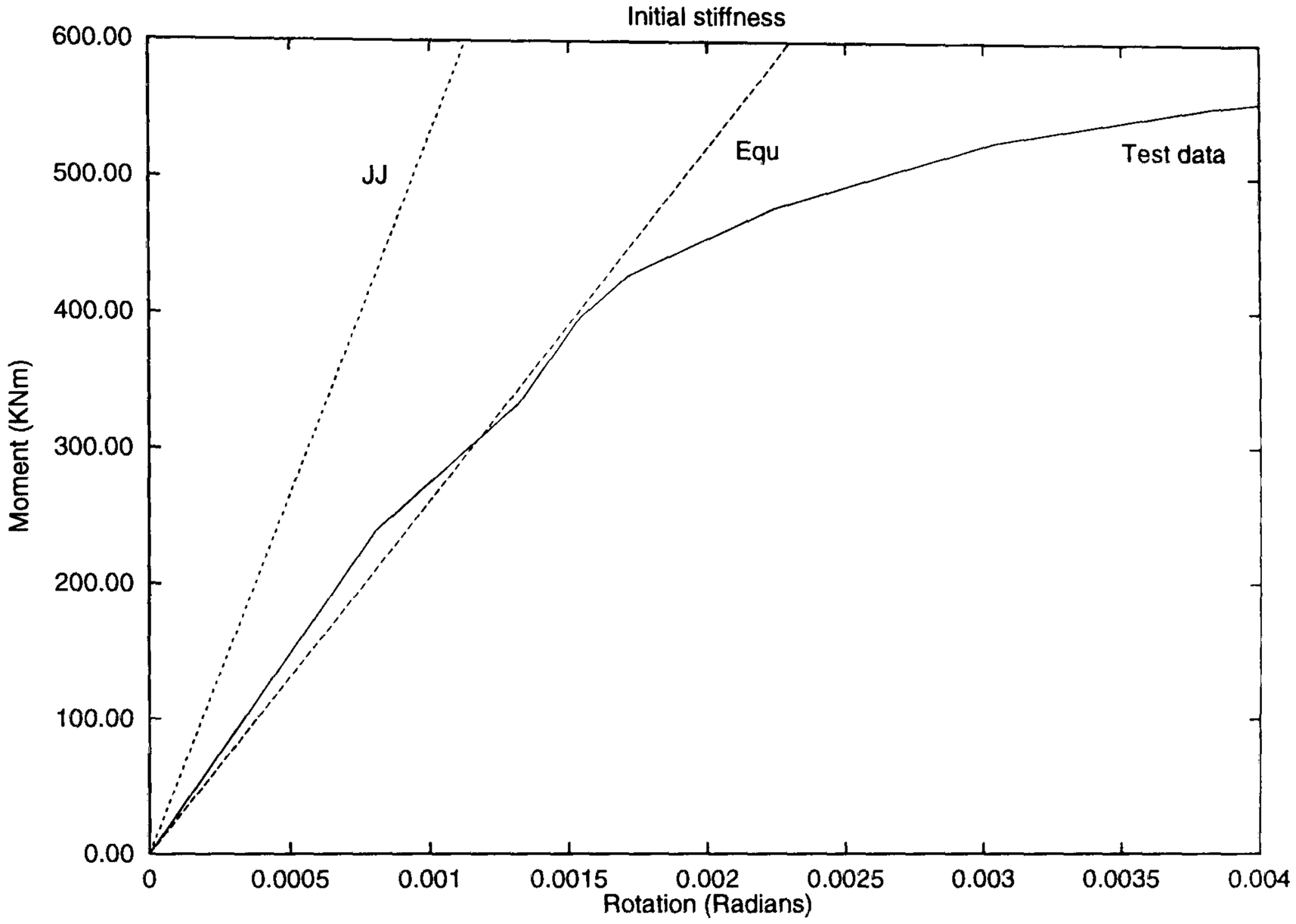

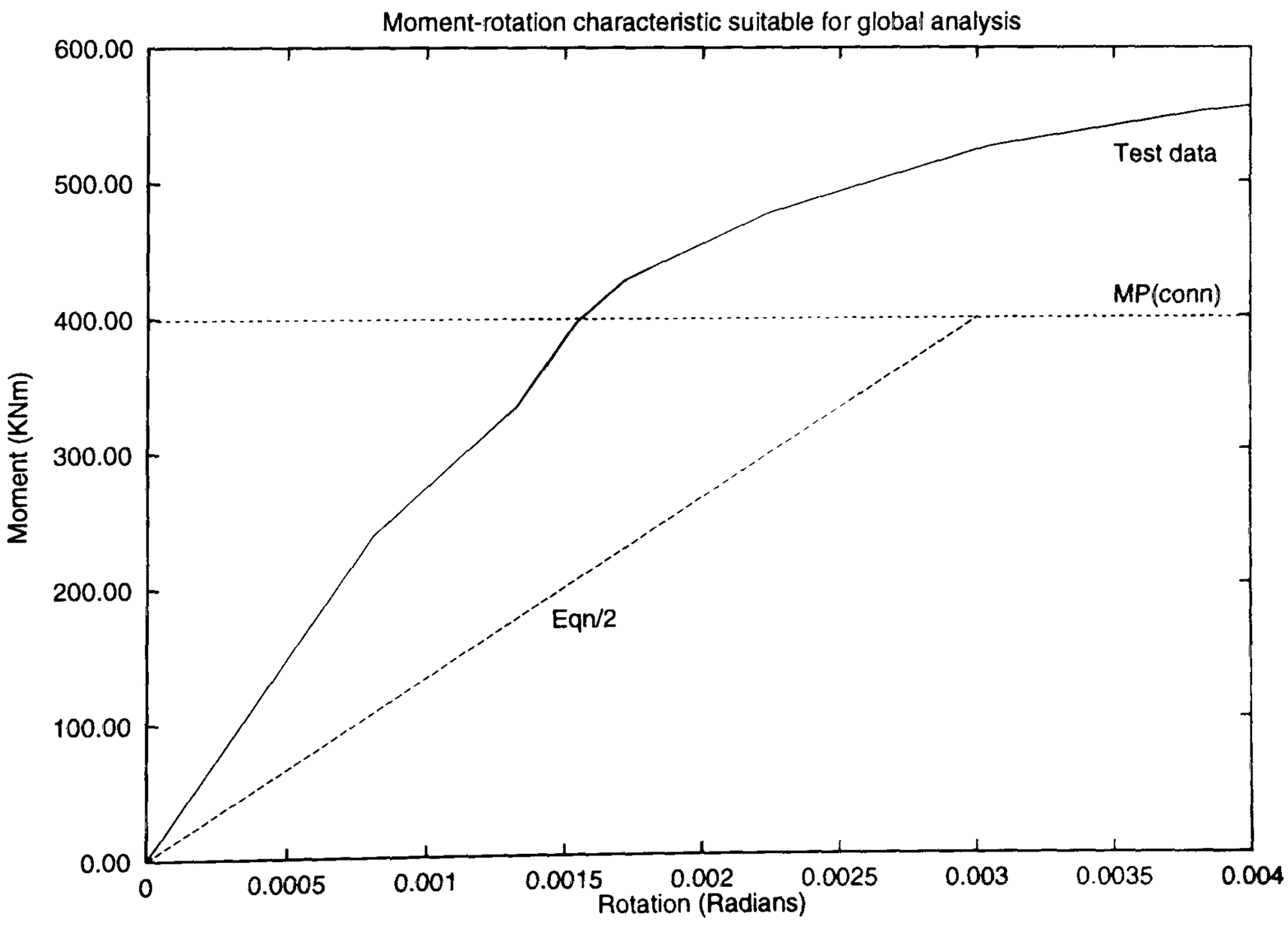

Bose's test 10 - Right hand connection

Figure 3.39:

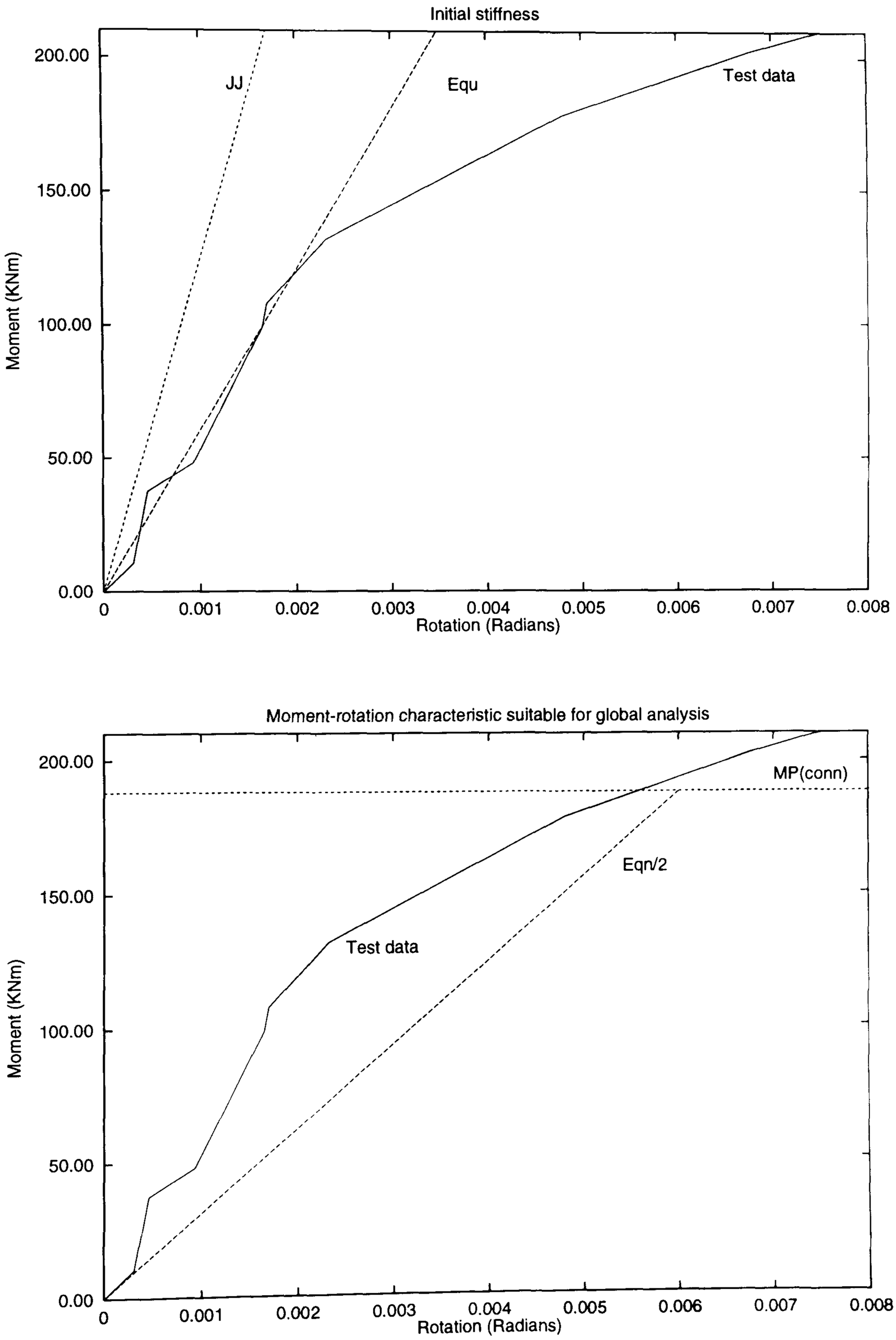

Bose's test 10 - Left hand connection

Figure 3.40:

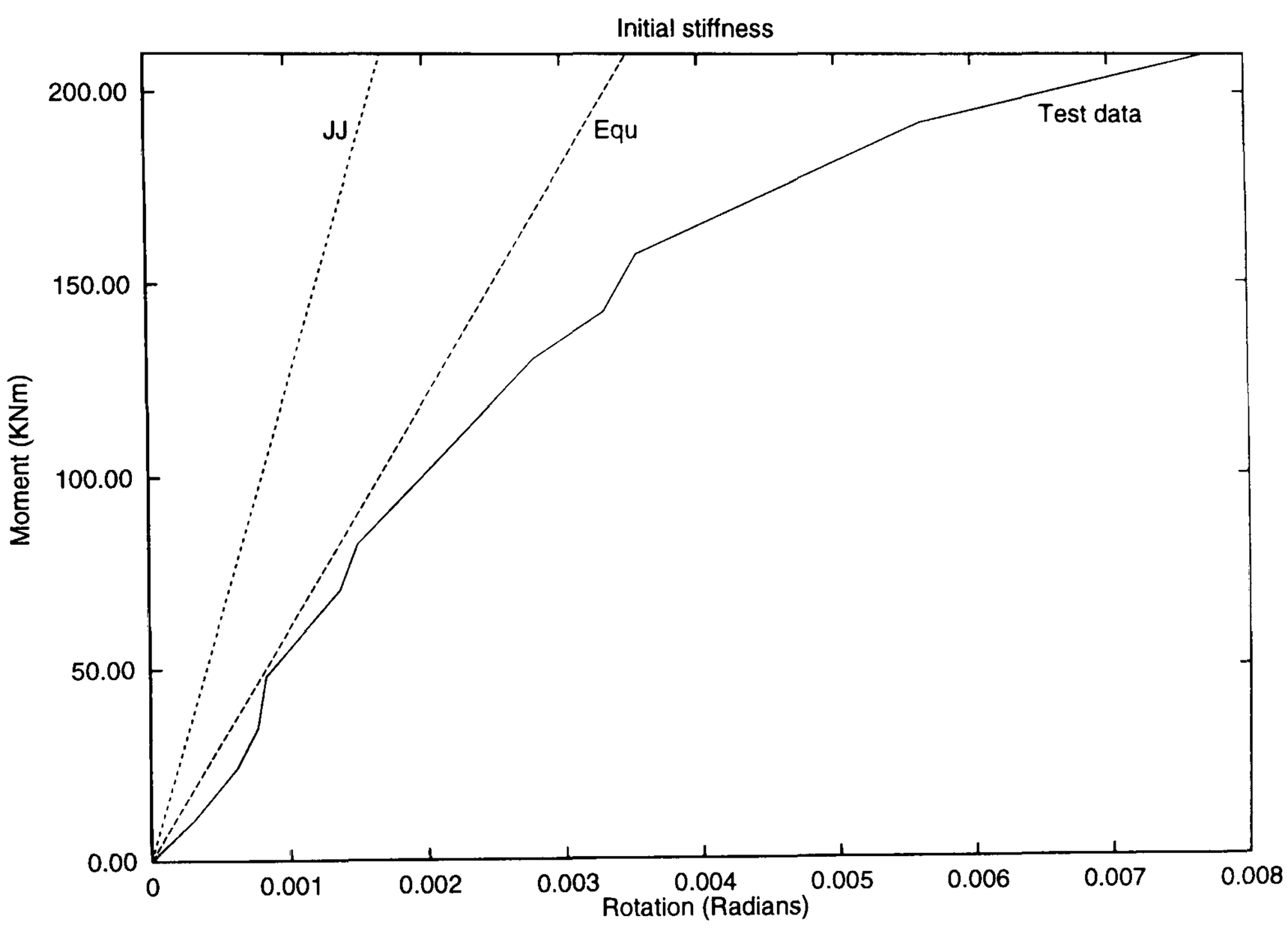

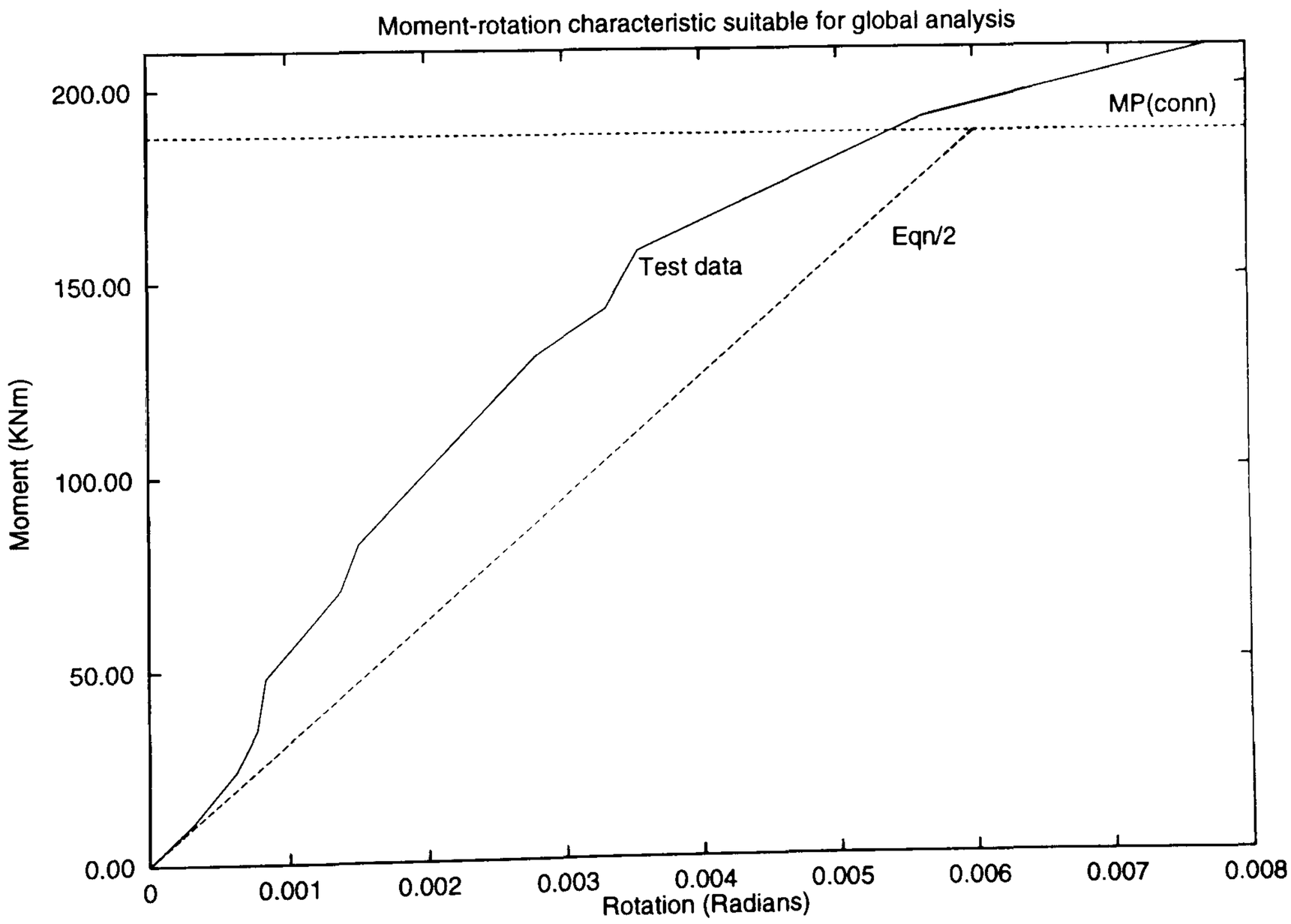

Chapter 4

Aspects of sway frame design

4.1 General

The aspects of sway frame design which are considered within this chapter are concerned with the following: (i) Frame stability under the actions of ultimate loads. This included the stability of individual column members, in addition to the overall frame response. (ii) Sway deflections under service loads.

The methodology used previously to verify the design rules for Wind-Moment frames designed to BS5950[12, 8] has been used as the basis of the study now described. The frames considered were within the ranges given in Table 1 of SCI Publication 082[1], which has been reproduced as Table 1.1 in Chapter 1.

The emphasis in the study, which uses the standard ductile connections described in Chapter 1, was on frame configurations up to four storeys in height, as the most usual application of the Wind-Moment method is considered to be in this range. However, a selection of eight storey structures were also considered, since these would constitute the tallest frame configurations that could be designed by the method. The frame configurations considered were therefore: (i) Two storey single and two bay frames. (ii) Four storey two and four bay frames. (iii) Eight storey two bay frame.

4.2 Design of Wind-Moment frames

The Wind-Moment design itself was undertaken by using the computer software written by Reading[8] for the original verification. No modifications were therefore necessary, with the exception that the effective length used to assess minor axis column buckling, which was set at 0.85, was increased to 1.0 to reflect the design guidance that was subsequently written[1]. To enable the programme to be executed, it was necessary to create a representative data file. This file reflected not only the frame geometry and applied gravity loads, but also the basic wind speed and ground roughness factor to enable the wind pressures and forces to be calculated and also the member yield stresses, to facilitate member design.

4.2.1 Range of loading

The Wind-Moment frames were designed by adopting the following ranges of loads:

1. Maximum gravity load in conjunction with minimum wind load.

2. Minimum gravity load in conjunction with maximum wind load.

These ranges were achieved by choosing appropriate load values, bay widths and column lengths from Table 1.1. Furthermore, in addition to the extremes of loading indicated above, a 6.0m bay width was also included to enable a medium range of frame configurations to be studied.

This study did however depart from the earlier one in an important respect related to connection resistance.

A restriction on the method has always been that the wind load should not be such that it controls the design of the beam[1]. This rule was introduced at the onset of Reading's original verification[8], since it was felt that if this was the case, then the frame should be designed as rigid-jointed as the serviceability limit on sway would almost certainly be exceeded by a semi-rigid Wind-Moment frame.

Consequently, beam sections were determined as before by only considering the applied gravity loading. However, under the actions of minimum wind loading, it was usually found that even with the weakest standard connection for that beam, the connection's moment of resistance was significantly greater than would be strictly required. A random degree of over-strength would therefore have been provided in the connections. This clearly would have had a pronounced influence on the corresponding frame stiffness and strength and consequently, have the potential to affect the conclusions drawn from the study. Therefore to minimise this influence, after designing the frames for the minimum wind load, the basic wind speed was increased until the wind-moments caused at least one connection in the frame to experience a moment close to its moment of resistance. During this process, a careful check was maintained to ensure that the frame members originally specified with the lower basic wind speed, were not altered in the quest to achieve a full demand on connection performance. The increased wind speed then became the reference load for that frame during its subsequent analysis. This procedure was not adopted for frames analysed under the actions of maximum wind load, because to increase the wind speed any further would exceed the range of loading previously agreed for the method[1], and in any case, such frames had already achieved a high degree of mobilisation of the connection's moment of resistance under the maximum wind speed of 52m/s.

4.2.2 Beam and column members

All the beam and column members were designed in Grade 50 steel. This steel strength was adopted to obtain the smallest member sizes for a given frame geometry. The frame design was approached in this manner, since it was thought that not only would the second-order effects be amplified by the less stiff sections resulting from Grade 50, but more importantly, adopting a minimum beam size would result in the incorporation of more flexible connections, than would otherwise be specified from a design utilising Grade 43 material. Consequently, the

results concerning the overall frame stability and sway deflections under service loads, would therefore be expected to be conservative when applied to frames of the lower grade.

No sections were excluded on grounds of classification for local buckling. To have done so would have introduced a further random source of over-strength, in addition to that which would occur as a result of the finite number of rolled sections that were available. A further justification for not restricting the choice of section classification used for the study results from one of the aims of the revalidation itself; namely, to investigate the positions of plastic hinges in Wind-Moment frames, to see whether or not the existing restrictions to Class 1 sections could be removed.

As a result of practical considerations, the column sections were made continuous over a height of two storeys; the corresponding splice connection being assumed to be located immediately above the corresponding floor level where the change in column section occurred.

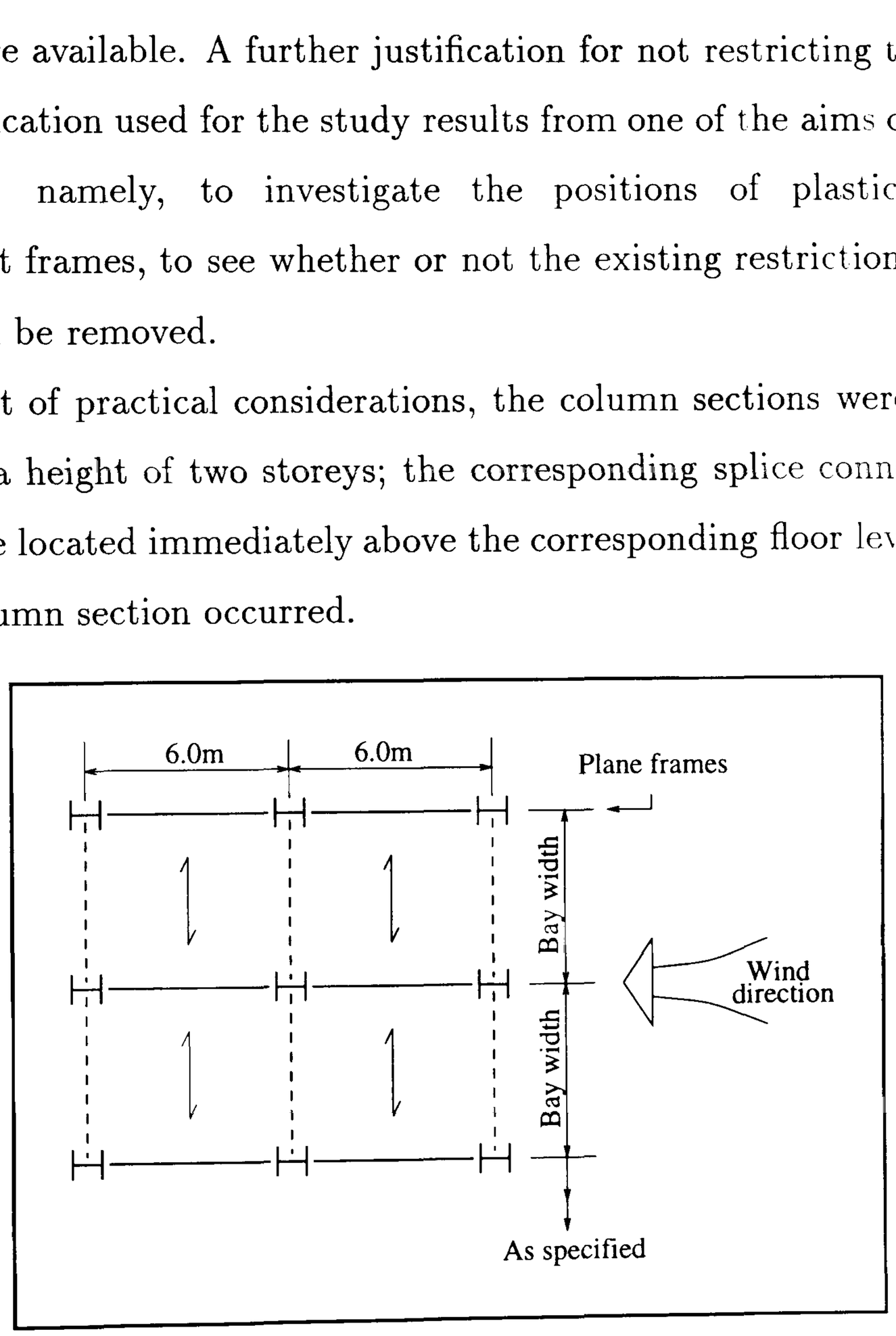

Figure 4.1: Building plan area

In addition, it was assumed that the floor units spanned horizontally a distance of 6.0m between adjacent plane frames (see Figure 4.1).

4.2.3 Connections

The standard ductile connections and the capacity tables used in the Wind-Moment designs are shown in Appendix A of this thesis.

Notation

The notation adopted for the standard connections is illustrated in Figure 4.2.

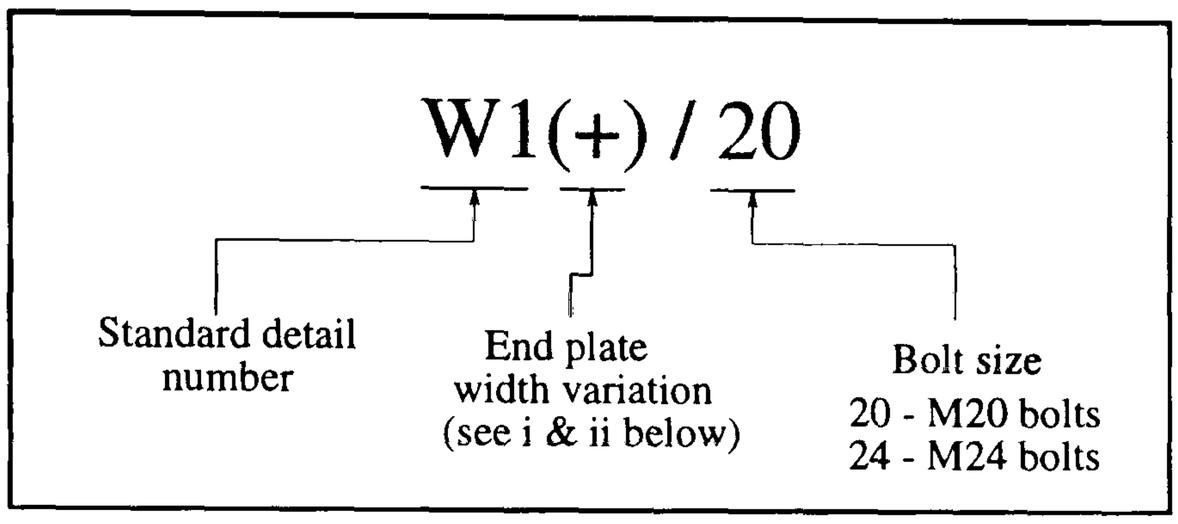

Figure 4.2: Notation adopted for the standard connections

The following two end plate widths are available for each standard connection: (i) 200mm and (ii) 250mm. The later variation is indicated by a '+' sign positioned immediately following the standard detail number (see Figure 4.2) . The choice of which end plate width to use rests with the beam and column section sizes that are specified by the Wind-Moment method, coupled with engineering judgement. Clearly, as the frame height or gravity load increases, the column section sizes and hence the corresponding flange width, must also increase. Under these circumstances, the designer may consider it appropriate to increase the plate width, such that the overall connection detail would appear to be more suited to the column to which it is attached. This wide variation could however, only be adopted if the beam section specified is large enough to enable this choice to be available. The option of adopting a wider end plate for the larger serial size beams is available for all the standard details, even though it would appear at first sight, from looking at the capacity tables, that this was not the case for standard detail number one. This particular detail is however unique in one crucial aspect concerning the calculation of its moment

capacity; namely, that unlike the other details, the moment capacity for this detail is independent of the width of the end plate. This arises because the smallest effective length of the yield line pattern that governs the connections design is always a function of the horizontal distance between the bolt position and the adjacent web of the welded beam member. The same is not true for the remaining details, where the smallest effective length of the yield line pattern that governs the design would always be a function of the end plate width.

Understanding the column limitation tables

To understand the column limitation tables, the following symbols were defined as follows: the presence of a tick next to an associated limitation would indicate that the limitation would not influence the connection's performance and could therefore be ignored. In contrast, a black square associated with the limitations of web buckling, crushing or tension, would indicate that the column would have to be reinforced to prevent these modes predominating. If however, the black square is surrounded by brackets, examples of which can been seen in the crushing limitation applicable to the larger standard details (see Chapter 1. Figure 1.5 or Appendix A), this would indicate that this limitation may be satisfied if the bearing length applicable to the actual beam member specified was used as the basis for determining the actual crushing resistance of the column web. A special case arises however, if a black square indicates that flange bending would be limiting. As an alternative to reinforcing the flange to alleviate this limitation, it is permitted to calculate a lower bolt force to satisfy the flange requirements, and then re-calculate a lower connection capacity. To aid this, a formula has been provided at the top of each capacity table. This formula contains two parts: namely, a bolt force and its respective lever arm. This basic equation has been reproduced for as many bolt rows as there are in the connection detail being considered. Consequently, performing a simple addition sum would be all that is necessary to calculate the adjusted moment capacity for a detail with more

than one bolt row in tension. The bolt force(s) used in the calculation would be determined by adopting the following procedure:

1. If the connection detail has only a single tensile bolt row, then the new bolt force would be directly substituted into the equation.

2. If the connection detail contains more than one tensile bolt row, then the force acting through the lowest bolt row would be sacrificed, whilst maintaining the force(s) at the higher bolt row level(s).

It is acceptable for this particular limitation to restrict the connection's capacity to that of the column's flange in bending, since flange bending by definition would promote ductility from the connection throughout its working life.

The final column limitation is associated with web shear. The tick indicates that the shear resistance of the column web would be greater than twice the maximum bolt force which could be applied by the connection. A tick would therefore be needed to satisfy the requirements at internal column locations.

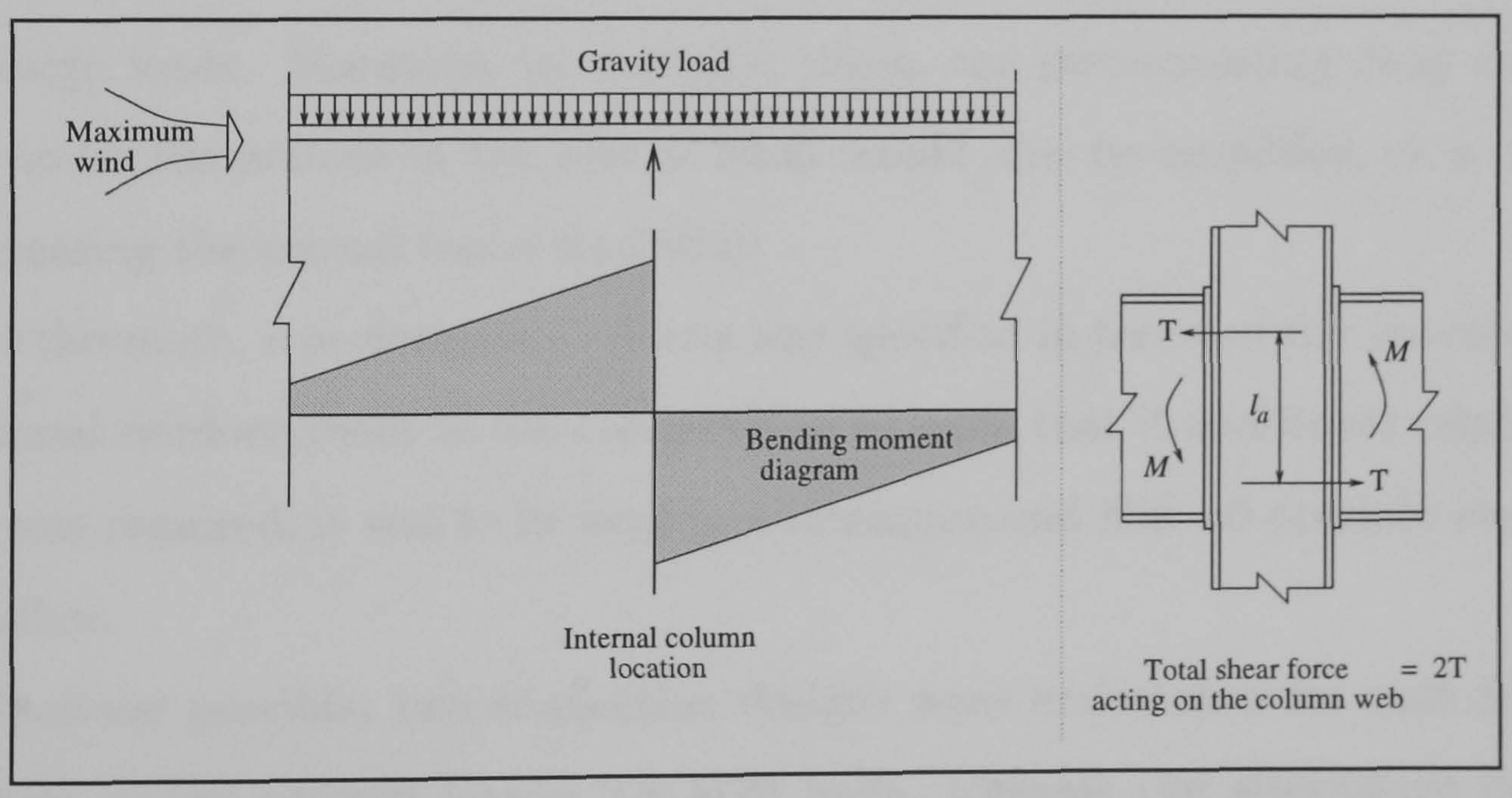

Figure 4.3: Accumulative influence of wind moments

This necessity results from considering the consequences of a bending moment distribution of the type indicated by Figure 4.3, which could occur as an extreme case in a Wind-Moment frame. If the tick has been replaced by a number printed

in the box, then this indicates that there may be problems associated with any internal columns, since the shear resistance of the web would no longer be able to withstand twice the bolt force; however, there would be no problems associated with the external columns. The third and final variation which is applicable to the shear limitation is indicated by the number being printed together with a superscript asterisk. Under these circumstances the resistance of the column's web would be insufficient to withstand the bolt force from either an external or internal connection.

Connection selection process

The primary objective of the selection process undertaken to obtain suitable connections between the frame members was to ensure that the connections specified represented the most flexible and weakest available, that could withstand the applied moments and forces calculated by the Wind-Moment method. This approach was adopted to exacerbate the potential for stability problems to occur within the frame, which may lead to its subsequent collapse prior to experiencing the design loads. Moreover, by a similar token, the corresponding sway deflections under the actions of the service loads would also be amplified, as a result of increasing the overall frame flexibility.

Furthermore, a performance criteria was specified in terms of the provision of additional reinforcement to the connections; namely, that if additional reinforcement was required, it was to be kept to a minimum and if at all possible avoided altogether.

Wherever possible, two connection designs were undertaken for each frame. The first design utilised Grade 8.8 M20 bolts, whereas the alternative design adopted Grade 8.8 M24 bolts. No frame had a mixture of M20 and M24 bolted connections, since this combination was thought to be unacceptable on the grounds of the obvious problems which could ensue during the construction phase of such a frame. Furthermore, the M20 option was judged unavailable if either of the

following two situations arose:

1. The vertical shear dictated the choice of the connection.

2. The moment of resistance applicable to the largest standard detail was not capable of resisting the applied connection moments.

To illustrate the design procedure adopted to select the most suitable connections for a frame, a worked example has been included in Appendix B, section B.3, of this thesis. The following description will therefore use this example as a convenient reference frame, to further aid the explanation of the design procedures adopted by the author when choosing the appropriate connections.

A four storey two bay frame is shown, which has been designed to withstand the load case requiring that the minimum gravity load is combined with the maximum wind load. The results from the Wind-Moment design are given in the figure. In particular, the connection requirements are specified.

To initiate the design sequence, the M20 option would be considered in the context of assessing its suitability in comparison with items 1 and 2 above. To facilitate this comparison, the first floor moments and shears would be considered, to see whether or not a suitable connection could be chosen from the standard details available. For this particular frame however, the bending moment at the first floor level was in excess of the maximum connection capacity for all the connection details, and therefore this option was not available. Consequently, this frame could only be designed with M24 bolts.

Connection design adopting the M24 option

To enable the connections to be specified, each horizontal level of the frame was systematically considered in turn. To this end, the roof was considered first.

Roof level

Starting with standard detail number one, the connection's moment capacity was directly obtained from the relevant capacity tables, since the size of the beam member was known (see Appendix A, detail reference W1/24). This was then compared to the connection requirements and if, the connection's moment capacity was greater than the applied moment, as was the case for this example, then the first stage of the design would be complete. A similar comparison would then be used to assess the shear resistance of the connection, to establish whether or not an extra row of bolts would be required. For the example chosen the extra row of bolts would not be necessary.

The connection design would then be completed by considering the effects, if any, that the external and internal column members would have on the chosen connection detail. This process would again be facilitated by knowing the column size, since any associated limitations could be immediately identified from the column limitation tables. For the example chosen, there were no column limitations concerned with the external members; however, possible problems with shear were indicated for an internal column. To overcome the limitation of web shear on this occasion, and any others which arose during the study, it was assumed that appropriate web reinforcement would be provided. Furthermore, since the influence of the web panel under the action of shearing forces has been bounded in the manner described in Chapter 3, section 3.5 (i.e. initially infinitely stiff and then at its most flexible) nothing would be gained by increasing the shear area of the web when determining the connection's initial stiffness for the second analysis. Consequently, it was acceptable to simply assume that the necessary reinforcement would be provided, and not explicitly take it into account by amending the shear area term, A_{vc}, in the stiffness prediction equation (see Chapter 3, equation 3.24).

Consequently, standard detail number one was considered suitable to provide the necessary structural performance at the roof level.

Third floor level

The third floor was considered next. The moment capacity of all the standard details, together with the associated column limitations have been reproduced on the second page of the worked example, Appendix B3. It can be seen that all the standard details, with the exception of number one, would possess the necessary moment capacity to fulfill the structural requirements of the connection. However, it is also evident from the associated column limitations that adopting any other detail for the connections to the external columns, other than number four, would necessitate the provision of additional reinforcement. Consequently, the author considered that the slight increase in capacity that would result by adopting this connection would be acceptable on grounds of cost implications. To maintain consistency, the same standard detail was also adopted for the internal connections.

Second floor level

The design sequence undertaken to propose appropriate connections for the second floor level was similar to that described above. However, since the column section size had now been increased, the subsequent column limitations were significantly reduced. This would have enabled standard detail number three to be used for the connection to the external columns without any reinforcement, and thereby promote the main objective of the study of adopting minimum connections. This connection type was not adopted, since it was felt by the author that to do so, the fabrication of the frame components would be further complicated. This would probably increase the overall fabrication cost, when compared with a frame which adopts essentially the same connection configurations throughout. Consequently, standard detail number four was adopted for this level, since there were again no problems associated with column limitations for either the external or internal locations.

First floor level

The final connections to design were at the first floor level. From the final page of the worked example, it can be seen that the only suitable standard detail which could be adopted was number five. Unfortunately, this particular detail had significant limitations associated with the external column sizes specified by the Wind-Moment method. Consequently, it was thought by the author, that to reinforce the detail adequately, would result in a connection detail more suited to a rigidly jointed frame, rather than as part of a semi-rigid Wind-Moment frame. Therefore, since one of the main objectives of the standard details was to simplify fabrication by reducing the need for costly reinforcement, the column size was increased to the next heaviest section whilst maintaining the serial designation. As a result, no column limitations would then apply and the problem of costly reinforcement would be avoided, albeit with a slight increase in the cost of the member itself. No such problems were forthcoming as far as the internal columns were concerned and consequently, standard detail number five was adopted at this level.

Final design

The final frame configuration is illustrated at the bottom of the final page of the worked example.

4.2.4 Summary of Wind-Moment designs

Appendix B of this thesis contains all the relevant design information obtained by implementing the Wind-Moment method, for the frame configurations considered. The tables referred to in the subsequent section may therefore be found in Appendix B, section B.2.

The design details of the frames that were subjected to minimum wind load and maximum gravity load are given in Tables B.1 and B.2. The corresponding connection designs, together with details of the extent by which the wind load

was increased to more-fully utilise the connection's moment capacity. are given in Tables B.3 to B.5. A Wind-Moment design was not undertaken for the eight storey two bay frame, when the bay widths were only 4.5m, since this frame configuration was judged impractical.

The design details of the frames that were subjected to maximum wind load and minimum gravity load are given in Table B.6. The corresponding connection designs are given in Tables B.7 to B.9. Under this load case, no eight storey two bay frames were designed, because either the wind moments were such that they controlled the designs of the beams, or none of the standard connections provided sufficient moment resistance.

For the particular tables that relate to the connection designs, the 'standard detail number' may be related to Appendix A via Figure 4.2.

Connection design under minimum wind load

It can be seen from Tables B.3 to B.5, that generally all the connection details specified were flush end plates. The exception was the connections to the first floor beams in the eight storey two bay frames, which were extended end plates. It can also be seen in several instances that the connections moment capacity was limited by the resistance of the column flange in bending. Under such circumstances, an adjusted moment capacity was calculated in accordance with the procedure described earlier.

Furthermore, these tables show that using the minimum basic wind speed of 37m/sec results in none of the connections being used to their full potential. However, by increasing the wind speed to the values shown in later columns of the tables, the mobilisation of moment capacity by the design wind moments is increased, such that in at least one level of each frame there is no significant over-capacity.

Finally, the tables give the predicted values for connection stiffness calculated by the method proposed in Chapter 3. When considering the connec-

tions to external columns account always has to be taken of shear flexibility. However, for internal columns, the initial stiffness was first calculated neglecting shear flexibility, and then including it; in the latter case the parameter β (see equation 3.24) would be set to 2.0, for the reasons explained in Chapter 3. section 3.5.

Connection design under maximum wind load

Tables B.7 to B.9 give details of the chosen connection designs under maximum wind load. Where the shear resistance of a column web panel limits the moment capacity of the connections, it was assumed that the web would be reinforced. When the flange bending limitation governed the connection's resistance, an adjusted moment capacity was again calculated.

For these frames, it was inappropriate to further increase the wind speed to eliminate over-strength in the connections, for the reason already explained. The final columns of these tables again give the predicted values for connection stiffness that were subsequently used during the analysis.

4.3 Analysis of Wind-Moment frames

The analyses on the Wind-Moment designs were performed by a computer program which takes account of semi-rigid and partial-strength connections[6]. Each analysis traces the load-deflection behaviour of the frame up the point of collapse. allowing for in-plane second-order effects, commonly referred to as '$P-\Delta$ effects' (see Chapter 2, Figure 2.7), and the development of plastic hinges. The connection behaviour is represented by a piece-wise linear moment-rotation characteristic (see Chapter 2, Figure 2.5). Once the design moment of resistance has been reached, the semi-rigid connection is replaced by a plastic hinge whose moment capacity is set equal to the connection's design moment resistance.

The matrix displacement method is used to solve predefined equations thereby

calculating the internal moments, forces and joint displacements. The piece-wise linear moment-rotation characteristic is used to obtain successive estimates of the secant stiffness, thus allowing for the natural reduction in connection stiffness as the moment increases (see Chapter 2). The overall effects of axial load in the frame are accounted for by stability functions and where appropriate, the presence of axial load within a member was also accounted for by reducing the member's plastic capacity by the method proposed by Horne and Morris[15]. The solution produces iterations about axial force and secant stiffness, with convergence occurring when the difference between two successive iterations is within a preset limit. The program is terminated if the determinant of the stiffness matrix is negative, or convergence within the iteration loops could not be reached.

The verification of the program was achieved by comparison with results from other independent computer programs from various research centres across Europe[51]. This work was undertaken as part of another research programme[6].

To enable the computer program to be executed, a further data file containing the following information must be created.

(i) Frame geometry - This would be specified in terms of member lengths. The beams and columns would be differentiated by specifying their orientation relative to the horizontal. Furthermore, each member together with its respective joints would be given identification reference numbers.

(ii) Section properties - These would include second moment of area, Young's modulus, yield strength of steel, cross-sectional area and the plastic section modulus, together with the associated parameters to calculate subsequent reductions in member capacity[52].

(iii) Type of connection at each numbered joint - The available choices were pinned, fully fixed and semi-rigid. If the latter type was specified then a number of points on the moment-rotation curve were given to represent the approximate behaviour. Semi-rigid connections were adopted for the study.

(iv) Applied loading at each joint - This can be specified independently as

either a concentrated vertical or horizontal load, or an applied moment. Any combination of these forces and moments could also be applied at a joint location. For the frame study, the gravity loading was applied in a series of point loads acting at the member ends and centrally. It was recognised that a uniformly distributed load could be more accurately represented by increasing the number of point loads, but in view of the approximations inherent in the modelling of the joints by a bi-linear characteristic, there would seem no justification in going to further refinement to represent the gravity load. Furthermore, the verification of the program against other researchers' results based on distributed load showed little difference in overall frame behaviour[51]

During the operation of the computer program, convergence problems were encountered for all but the most robust frame configurations considered. This problem has been identified before with frames which have very flexible connections[6]. These problems were eased by specifying load increments such that generally the plastification within the frame was very gradual. In particular, the number of connections that plastified during any one increment was kept to a minimum and preferably each connection would plastify individually. Consequently, the load was applied in 0.0025kN increments. This therefore is the reason why in some instances the load levels quoted in Appendix C, section C.4, are identified with five significant figures. Moreover, the author changed the source code of the program to allow the computations to be undertaken in double precision, rather than single precision which was formly used. Fortunately, this did not alter the general structure of the program and consequently, the lengthy validation procedures were not required. This also overcame the convergence problems that had been suffered by Reading[8].

To enable a continuous check to be undertaken during the analysis procedure, the author modified the program to enable a graph representing the load deflection response of the frame to be simultaneously produced. This drew immediate attention to any unusual behaviour, which could either signify the formation of

a plastic hinge mechanism within the frame, or that there was a numerical conditioning problem with the analysis. Problems of this nature were not frequently encountered. However, when they did occur, they were the result of a beam type mechanism occurring somewhere in the frame (see Figure 4.4(a)) under the actions of load case one (see section 4.3.1). In these situations, the mechanism was identified by the load deflection response of the frame indicating that the deflections were reducing as the load was increasing (i.e. the members were deflecting in the opposite direction of the applied loads, see Figure 4.4(b)). Furthermore, the graphs substantiated the point at which the frames lost their stiffness completely. The graphical representation produced for a typical frame configuration is illustrated in Appendix C, section C.3.

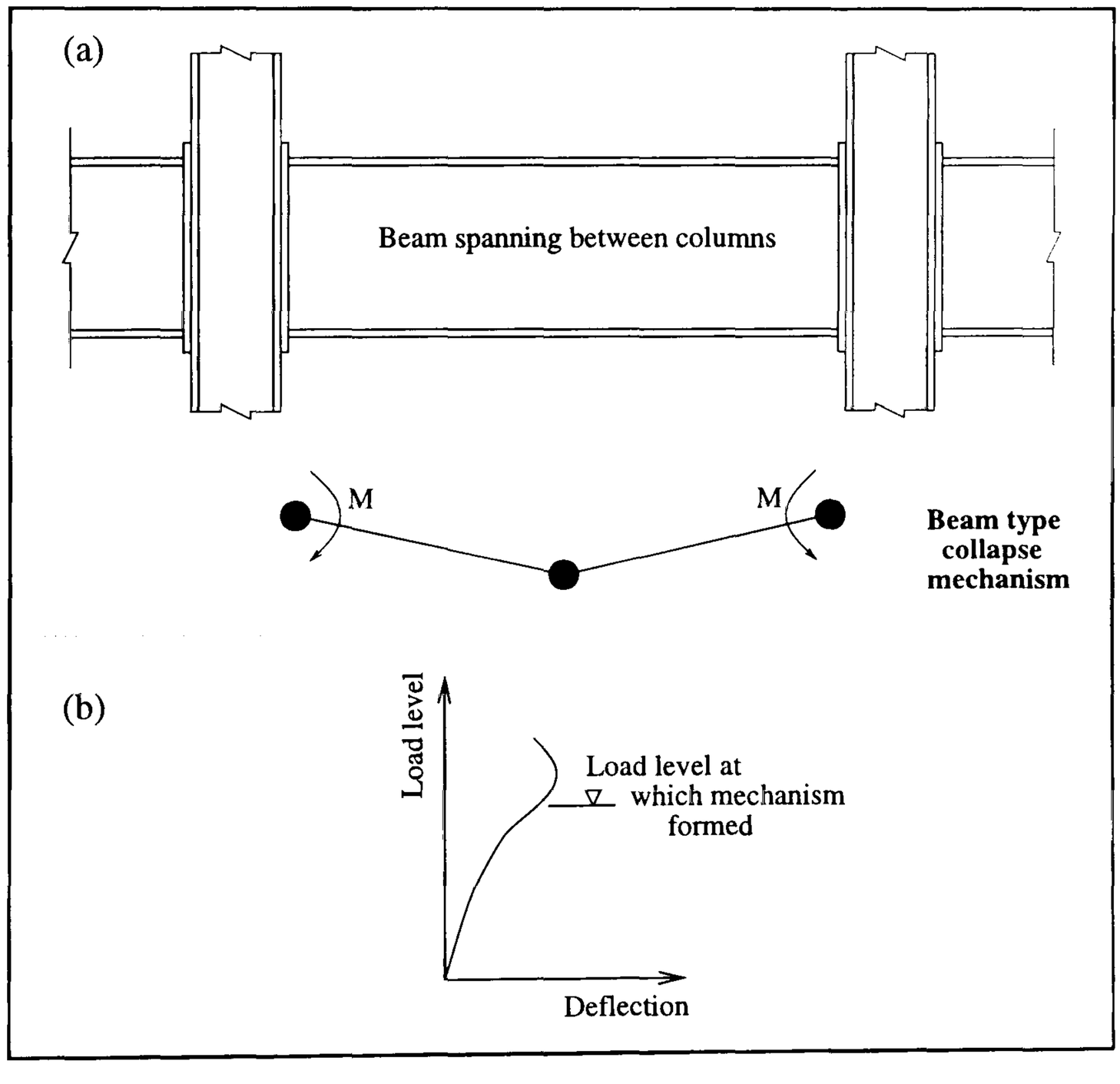

Figure 4.4: Beam type failure mechanism

In addition to the frames being analysed with semi-rigid connections, an additional analysis was undertaken to obtain an upper bound on the connections performance, by assuming that the connections were rigid and full strength.

4.3.1 Load combinations

Ultimate limit state

For ultimate limit state, the load combinations given in SCI Publication 082[1] were applied, namely:

(LC1) - 1.4(Dead load) + 1.6(Imposed load) + Notional horizontal forces;

(LC2) - 1.2(Dead load + Imposed load + Wind load);

(LC3) - 1.4(Dead load + Wind load).

The notional horizontal forces were calculated in accordance with BS5950.

Serviceability limit state

For deflections under service load, the load combination considered was :

1.0(Dead load) + 0.8(Imposed load + Wind load).

This was chosen because a service load combination which included no imposed load was judged to be unrealistic. It was also desired to investigate the influence of second-order effects under service conditions; in order to maximise these, the imposed load must be included. The 0.8 factor arises from the recommendations of BS5950.

4.4 Assessment of results - ultimate limit state

The most important results concern the stability of the frames at the design load level, and the avoidance of brittle failure in the connections. These results are given in Appendix C, section C.2 of this thesis.

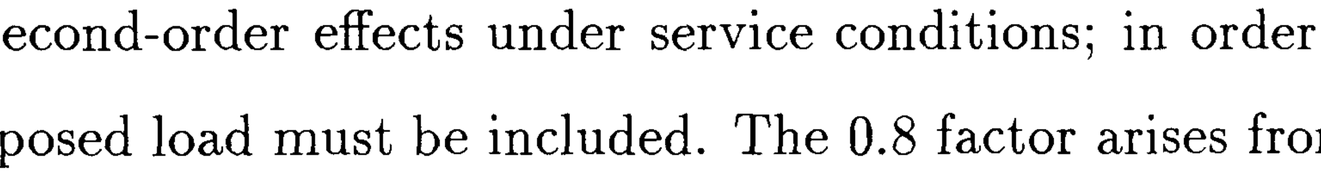

Figure 4.5: Notation adopted to identify the frames considered

For ease of recognition, each frame has been identified with a unique alphanumeric reference number (see Figure 4.5). Furthermore, adopting this

approach enables the corresponding frame configurations, together with details of the sequence in which their plastic hinges formed, to be established by cross-referencing to Appendix B, section B.2 and Appendix C, section C.4 respectively.

The load cases to which the results apply are identified by a number, together with the prefix 'LC', which relates back to section 4.3.1.

4.4.1 Overall in-plane stability

The overall in-plane stability of the frames was assessed by examining the load factor at which the frame collapsed, where for each load case, a load level of unity corresponds to the ultimate design loads for that combination.

Load case	2 Storey 1 bay	2 Storey 4 bay	4 Storey 2 bay	4 Storey 4 bay	8 Storey 2 bay
	Plastic collapse load factors				
LC1	**1.16 - 1.72**	**1.15 - 1.88**	**1.11 - 1.36**	**1.11 - 1.34**	**1.06 - 1.20**
LC2	**1.40 - 1.69**	**1.40 - 1.63**	**1.20 - 1.50**	**1.23 - 1.53**	**1.01 - 1.27**
LC3	**1.41 - 2.04**	**1.68 - 2.21**	**1.26 - 1.92**	**1.24 - 1.95**	**1.19 - 1.58**

Table 4.1: Range of plastic collapse load factors

It can be seen from Table 4.1 that for all the frames considered, the plastic collapse load factors were all in excess of unity. Consequently, it can be concluded that Wind-Moment designs, even when flexible end plate connections are incorporated, continue to demonstrate adequate overall stability. It can also be seen from Table 4.1, that the lowest plastic collapse factor equalled 1.01, and was applicable to frame 'f35b24' (see Appendix C, section C.2). This particular frame configuration was eight stories high and two bays wide. The corresponding bay width was 6.0m and was therefore relatively narrow in comparison to its height, which in turn would lead to high second-order effects. In addition, Table B2 (see Appendix B, section B.2) shows that after the wind speed was increased to 39m/s, which then provided the basis for the analysis, the connections at three

consecutive floor levels were loaded to over 90% of their respective capacities by the wind moments. A much more robust frame was obtained when the bay width was increased to 9.0m, 'f34b24', which had a plastic collapse load factor of 1.2 (see Appendix C, section C.2).

4.4.2 Lateral-stability of columns

It is assumed in this study that the frames are braced against out-of-plane sway at roof level and each floor level. The internal forces and moments given by the analysis enable checks to be made on the lateral-stability of columns over each storey height. This was done using the simplified overall buckling check of BS5950, as described for Reading's original verification[8] (see Chapter 1, section 1.2.2).

Load case	2 Storey 1 bay	2 Storey 4 bay	4 Storey 2 bay	4 Storey 4 bay	8 Storey 2 bay
	Stability factors				
LC1	**0.22 - 0.55**	**0.55 - 1.00**	**0.97 - 0.92**	**0.71 - 0.93**	**0.91 - 1.01**
LC2	**0.49 - 0.65**	**0.70 - 0.90**	**0.73 - 0.85**	**0.75 - 0.97**	**0.76 - 0.93**
LC3	**0.39 - 0.59**	**0.49 - 0.70**	**0.49 - 0.62**	**0.48 - 0.76**	**0.50 - 0.62**

Table 4.2: Range of column stability factors

The right hand side of equation 1.3 is termed the *stability factor*, which was calculated for all the column members of the frames considered. A summary of the results obtained from Appendix C, section C.2, is shown in Table 4.2

It can be seen from this table, that maximum values of 1.00 and 1.01 were obtained for the frames with four storeys or less, and the eight storeys respectively. Values in excess of unity are unsafe. It can therefore be concluded, that for all but the eight storey frames, lateral-stability would not manifest itself as a problem. In defence of the suggestion that the eight storey frames would also produce safe designs, it must be remembered that these maxima occurred in

ground floor columns in which rigid bases were assumed. The assumption of a point of contraflexure at the mid-height of such members is less accurate than elsewhere in the frame, because the base fixity attracts a greater moment to the lower end of the column. In practice, a value for the stability factor of less than unity would be expected because the inevitable flexibility of a practical 'fixed base' would cause some redistribution of moment to the less heavily-loaded upper end. Furthermore, it has to be remembered that the effective length used to calculate the lateral-torsional buckling resistance moment was based on an effective length of $1.0H_t$, this would be conservative under the rules for such effective lengths in BS5950[12].

This of course would have implications as far as the overall frame stability is concerned. If one accepts the argument above; namely, that the stability factor in an '*actual*' frame would be less than 1.0 due to base flexibility, then to what extent would the frame's corresponding plastic collapse load factor be reduced? An exact answer to this question was not available, since the study did not embrace the possibility of column base flexibility. However, it must be emphasised that the results obtained can only be considered in the context of representing an approximate measure of the frame's performance. Consequently, since the numbers involved are extremely close to those that would indicate a safe design as of right, the author found no justification to suggest sweeping modifications, such as the exclusion of all eight storey frame geometries. The approximate nature of 'simple' design methods in comparison with their vindication utilising sophisticated software has also been discussed by Gibbons *et al*[53], who undertook a computer based investigation to establish the influence of steelwork connections on the behaviour of simple three dimensional braced steel frames. They found that the variation in the column failure load was dependent on the direction of the initial column deformations assumed for the analysis. This lead them to suggest that *it was unreasonable to expect that any 'simple' design method could cater for such inherent variability.* This logic can be extended to the present

investigation with respect to representing the base flexibility, such that again it could be considered unreasonable to expect this design method, which was based on the 'simple' design philosophy, to rigorously take account of all eventualities.

For the multi-bay frames, the highest stability factors were always applicable to the internal columns, and generally associated with the ground floor length. However, in several instances in frames which were greater than two storeys high, the lower length of an upper storey section proved critical (see Appendix C, section C.2). On these occasions, the maximum stability factor for each frame concerned was within the range indicated in Table 4.2. Consequently, it should be borne in mind that just considering the base column lengths in the frames would not always reflect the worst case, which therefore implies a need to systematically consider the lower section of each two storey column length in turn.

4.4.3 Beam-to-column connection rotations

Table 4.3 shows a summary of the range of rotations developed at the beam-to-column connections due to the design load levels for ultimate limit state. For the full set of results, reference should be made to Appendix C, section C.2.

Load case	2 Storey 1 bay	2 Storey 4 bay	4 Storey 2 bay	4 Storey 4 bay	8 Storey 2 bay
	Rotations (mrads)				
LC1	**5.69 - 10.2**	**9.09 - 17.7**	**9.39 - 17.0**	**9.34 - 19.7**	**16.7 - 21.0**
LC2	**8.43 - 16.1**	**9.31 - 16.3**	**11.7 - 21.8**	**11.0 - 24.1**	**14.3 - 23.6**
LC3	**7.24 - 15.8**	**6.47 - 15.29**	**7.26 - 15.1**	**6.94 - 16.3**	**6.82 - 11.3**

Table 4.3: Range of connection rotations

It can be seen from Table 4.3, that the maximum connection rotation was of the order of 24mradians and corresponds to a four storey four bay frame: namely 'f31b20'. It can therefore be concluded, that since the rotations quoted are well within the experimentally-observed rotation capacities for the standard

connections[22], they would not be susceptible to brittle fracture.

Furthermore, the rotations quoted in Table 4.3 are, as expected, applicable to the connections positioned on the leeward side of the frame.

4.4.4 Frame plasticity

Details showing the development of plasticity within the frames considered, have been included in Appendix C, section C.4. A summary of the salient results are shown in Table 4.4.

	Beam member		Column member		Column base	
	S - R	Rigid	S - R	Rigid	S - R	Rigid
	Load factors					
2 storey 1 bay	**1.14** (LC1)	**1.27** (LC2)	**N/A**	**1.52** (LC1)	**1.40** (LC2)	**1.56** (LC2)
2 storey 4 bay	**1.13** (LC1)	**1.49** (LC2)	**N/A**	**1.74** (LC2)	**1.47** (LC2)	**1.77** (LC2)
4 storey 2 bay	**1.11** (LC1)	**1.31** (LC2)	**1.28** (LC3)	**1.46** (LC1)	**1.16** (LC2)	**1.44** (LC1)
4 storey 4 bay	**1.09** (LC1)	**1.21** (LC2)	**N/A**	**1.48** (LC2)	**1.13** (LC2)	**1.41** (LC2)
8 storey 2bay	**1.06** (LC1)	**N/A**	**1.06** (LC1)	**1.14** (LC1)	**1.06** (LC1)	**1.25** (LC1)

Table 4.4: Minimum load factors at member plastification

The load factors within the table above represent the lowest load level in which a plastic hinge formed in any of the beam and column members. To aid clarity, the column base has been considered independently from the remaining column member.

The 'S-R ' designation represents the frame that contained the standard connections, whereas the 'Rigid ' designation, refers to an identical frame with rigid full strength connections.

It can be seen from Table 4.4, that plasticity did not develop sufficiently to produce a plastic hinge within any of the framed members prior to the attainment of the design load at ultimate limit state. This is indicated by the load factors

quoted all being in excess of unity. The significance of unity in this context has been explained in section 4.4.1.

To re-iterate, the objective for including such comprehensive design information was to investigate the possibility of lifting the Class 1 restriction imposed on the structural members designed by the Wind-Moment method. This restriction was incorporated because the frame had to allow for the possibility of plastic hinges forming in the members prior to the design loads being applied. It can be seen from the results obtained, that relaxing this classification to include Class 2 sections would not be unreasonable; since this type of section would still have the ability to reach its plastic capacity.

4.5 Assessment of results - serviceability limit state

First order and second order sway deflections for the frames considered are given in Tables C.6 to C.8, which can be found in Appendix C, section C.5 of this thesis. The subsequent discussion therefore will refer to the contents of this appendix section unless otherwise stated. Furthermore, the sway deflections quoted were calculated based on the horizontal drift of the top left hand corner of the frame. The frames again are identified using the same alphanumeric referencing system to that used previously (see Figure 4.5), thereby enabling the corresponding frame configurations and other associated results to be cross-referenced, in a similar manner to that described in section 4.4.

It can be seen from these tables that in many instances, the frames' sway deflection exceeds BS5950's limit for horizontal deflection of height/300. Under these circumstances, the frame configurations concerned would have to be stiffened accordingly, such that this criteria can be met. This of course would also have the benefit of further increasing the overall stability of the structures and, if the stiffening measures involved boosting the column section sizes, then

this would also produce dividends as far as the lateral-stability of the individual column lengths were concerned. Strengthening the connections however, by for example adopting a thicker end plate, would not be recommended by the author unless a rigid design was considered appropriate. The reason is that carrying out strengthening measures other than those required to overcome any associated column limitations[20] could destroy the vital ductility component that makes the standard connections acceptable for use in a Wind-Moment frame.

The rigid design multiplier of 1.5, which is the approach recommended at present[1] to establish a Wind-Moment frame's sway under the service load, still generally stands good for the results obtained, provided the comparison is associated with the first order results which neglect the influence of web shear. The only exceptions are frames 'f12b20 ' and 'f12b24 ' (see Table C.6). These particular frame configurations had the smallest bay width, namely 4.5m, and consequently, small beams would have been specified (see Table B.1,Appendix B, section B.2). This would influence connection performance since by definition the smaller the beam, the more flexible the connection. This is substantiated in comparison to the equivalent 6.0m bay frames' namely 'f11b20 ' and 'f11b24 ', which meet the criterion of height/300 (see Table C.6), despite similar levels of capacity mobilisation being experienced by the connections (see Tables B.4 and B.5, Appendix B, section B.2).

If one now considers the influence of the second-order effects, it can be shown that the corresponding sway could be increased by a further 4% over and above that calculated by the first order analysis. However, even under these circumstance it can be seen from the tables that the 1.5 multiplier would generally still produce conservative results for the frames which incorporate bay widths of 6.0m or greater. A more severe case arises for bay widths equal to 4.5m for the reasons explained above, whereupon it can be seen that the multiplier should be increased to 2.0.

The area where the 1.5 multiplier is generally inadequate is when the influence

of web shear at the internal columns is considered with the β coefficient equal to 2.0 (see Chapter 3, section 3.5). Under these circumstances it can be shown from Table C.7, frame 'f31b24 ' that the shear flexibility will increase the frames deflection by either 19% or 22% depending on whether the first-order or second order analyses are compared with the equivalent analyses undertaken ignoring shear flexibility in the internal columns. To reflect this increase, if one increases the rigid multiplier to 1.6 and 1.7 for first-order or second order analyses respectively, it can be seen that this would generally be sufficient to compensate for the unconservatism of the previous proposal. The exceptions to this rule are the frames in which the bay width was set at 4.5m, which would require a multiplyer of 2.1. These results were however severe, since following the examination of the computer output, although web shear was found to be present in the majority of cases, it was not sufficient to necessitate the β coefficient being set equal to 2.0.

In comparable frames, such as frames f17b20 and f17b24 in Table C.6, it can be seen that the sway deflection can be reduced by adopting M24 bolted connections in preference to the M20 option. Consequently, the author has no reservations in suggesting that M24 details should be recommended in the first instance, and only if there are circumstances that could potentially ease problems associated with limitations to the column, should the M20 option be considered as an alternative. If this reasoning is implemented, it can be seen from Table C.8, that the sway problems within frame f35b20 would no longer be encountered. The author believes that this would be acceptable on the grounds that with a building of that height, the preferred design solution would almost certainly involve adopting the most robust connection configurations that possessed the necessary structural performance, which by their very nature would involve M24 bolts.

The results presented neglect the stiffening effect on the building due to the influence of the cladding system. Consequently, it would be reasonable to expect that the true semi-rigid deflections would be somewhat lower than those calcu-

lated during the study. It is customary to neglect this influence on the grounds that the cladding does not constitute a permanent feature to the building, since it could be expected to be replaced on one or more occasions during the working life of the structure.

Approximate methods of estimating multi-storey, multi-bay, frame deflections, have not been considered as part of this study. Such methods include the model proposed by Macleod[54], which effectively represents a multi-bay frame by a single bay equivalent. This particular aspect of structural behaviour is at present being undertaken as an integral part of another research project[55].

4.6 Conclusions

4.6.1 Ultimate limit state

A systematic frame study has been undertaken to investigate the structural performance of Wind-Moment designs that incorporate flexible end plate connections. At no stage did the author find any justification for modifying the design method. Consequently, the proposed standard connections may be used with confidence in a Wind-Moment frame.

Furthermore, the member classification can be relaxed to embrace Class 2 structural beams and columns.

4.6.2 Serviceability limit state

An estimate of the maximum sway applicable to a Wind-Moment frame, may be calculated by undertaking a rigid analysis and multiplying the corresponding deflections by the factors shown in Table 4.5. These convert a first-order rigid analysis into a first-order semi-rigid one, and similarly for the second-order analyses.

Furthermore, whenever possible, the M24 option should be used in preference to the M20 option.

	Bay width	Type of analysis: First-order	Type of analysis: Second-order
		Multiplying factor	
4 storeys and less	⩾ 6.0m	**1.6**	**1.7**
	< 6.0m	**2.1**	**2.1**
Greater than 4 stories	⩾ 6.0m	**2.2**	**2.5**

Note :
These vaules include allowances for web shear at internal column locations of multi-bay frames

Table 4.5: Rigid frame multipliers for serviceability calculations

Part II

Ductility of composite end plate connections

Chapter 5

Introduction to composite beams and connections

5.1 Composite beams

In structural engineering, the term 'composite beam' is generally used to refer to a system of two materials, steel and concrete, that are connected such that both materials work together to give an improved performance in flexure. The system is formed with a concrete floor slab, usually cast these days on profiled steel sheeting, containing mesh reinforcement and possibly high-tensile reinforcing bars. The slab is connected to parallel steel beams which span beneath it. Once connected, these components interact to produce a load supporting system that exhibits a higher strength and stiffness than its bare steel equivalent. This in turn, results in a more economic structure in terms of construction depth and weight savings, since shallower beams are needed to carry a specific load. The economic advantage of this type of construction has been known for many years and consequently, composite beams have been used extensively in the commercial building sector within the United Kingdom[56, 57].

The connection between the slab and the beams is achieved by shear connectors that are secured, usually by welding, to the top flange of the beam. These are

subsequently embedded within the slab following the placement of the concrete. The composite system works by transferring the load applied to the slab through to the steel beams by longitudinal shear at the interface. The connectors also act to control the relative slip between the two respective surfaces. The most common shear connector is the headed stud which, in addition to giving identical properties in all directions, provides minimal disruption to the slab reinforcement, and is easily and quickly welded to a beam. The presence of steel decking does not inhibit the welding process, provided that the decking is not coated in plastic, or the stud position does not coincide with decking overlaps or stiffening ribs.

5.2 Composite connections

A composite frame generally consists of a system of composite beams, connected to columns which are usually arranged in a grid formation. Consequently, the beam-to-column connections can exist in many forms depending upon their position within the frame as a whole. The following section concentrates on primary connections, which may be identified as those which connect adjoining primary members of the frame together. These include predominately perimeter and internal connections.

The traditional design approach for the treatment of connections in composite building structures has, like all design concepts, been gradually changing over the years. Originally, the connections to composite beams were assumed only to possess the characteristics of a hinge, and consequently, the beam design followed as though simply supported. However, with the need to produce ever increasing economy in design, studies were initiated during the early 1970s[58] and again in the early 1980s[59] to investigate this assumption. The resulting conclusions from these studies confirmed that adopting a semi-rigid approach to the treatment of composite connections could potentially produce economic benefits. In particular,

it was suggested that the economic benefits are most likely to be realised in braced frame construction, as a consequence of the trend for larger spans. If simple framing, where the connections are treated as hinges, was adopted for buildings of this nature, serviceability considerations would invariably govern the design of the beams. Therefore, incorporating the naturally occurring joint stiffness into the design procedures could be seen as a cost effective method of reducing beam deflections, and thus enabling a more effective use of the material strength to be achieved.

For the purpose of this thesis, a composite connection refers to the definition contained within Eurocode 4[60]; namely, *a connection between a composite member and any other member in which reinforcement is intended to contribute to the resistance of the connection.*

The early researchers concentrated on investigating a composite connection's response under monotonically increasing loads. The specimens were configured in either a cantilever or cruciform arrangement, which were deemed to represent perimeter and internal primary connections respectively.

The following section of this thesis provides a general overview of research on composite connections undertaken to date, to enable the current state of knowledge to be described. Although composite connections are considered in general below, the test results given at the end of the chapter are restricted to major axis end plate connections. This is in recognition of the author's experimental programme which was confined to this type of connection.

A review of early work on composite connections was prepared by Zandonini[61], who provides comprehensive details of the experimental programmes undertaken up to 1987. These are summarised below. Experimentally-based programmes of research undertaken since 1987 are subsequently considered in more detail, and the results are summarised in section 5.2.1.

Tests undertaken pre 1970

Johnson *et al.*[62], and later Climenhaga and Johnson[63] investigated the behaviour of continuous composite beams. The beams were fully welded to the adjoining columns, which were additionally stiffened between the flanges at the compression level. The resulting connection was therefore assumed to be rigid and thus possessed full slope continuity. From this work, the first indications were forthcoming with regard to the severe limitations that would have to be imposed on the slenderness ratios of the web and compression flanges, if a composite beam was to possess an adequate rotation capacity to develop the full plastic moment at mid span. This is due in part to the shift in the position of the plastic neutral axis, which moves upwards as a consequence of the slab reinforcement. The movement of the axis has the effect of increasing the depth of the web which would be subjected to compression, and consequently increases its susceptibility to buckling. It was further concluded, that since the moment of resistance of the connection would be considerably lower than the plastic moment of resistance at mid span, a greater connection rotation would be demanded from the system in order to redistribute sufficient bending moment to enable the simple plastic collapse condition to be developed.

Tests undertaken between 1970 and 1980

Semi-rigid connections were first tested by Barnard[64] as a possible alternative to the rigid approach. It was suggested that this type of connection could be used to provide a significant degree of continuity, while reducing the problems associated with local buckling. In particular, the susceptibility of the web to buckling was thought to be practically eliminated as a consequence of the manner in which semi-rigid action is developed. In addition, it was thought that the flange buckling could be controlled by careful detailing of the reinforcement contained within the slab.

These conclusions and ideas were investigated by Johnson and Hope-Gill[58].

The connection consisted of an arrangement of bottom cleats secured above and below the lower flange of the connected beams. A reinforced concrete slab was also included to provide the composite action. This type of connection was chosen primarily to provide simplicity in detailing and a capability of stablising the compression flange of the connected beams. The testing programme consisted of a series of 5 specimens, all of which were subjected to symmetrical loading in a cruciform arrangement. The emphasis was directed towards investigating the slenderness ratio of the steel section's web and the influence of a force ratio, defined as the ratio between the axial yield strengths of the reinforcing bars and the overall steel section. This approach resulted from rigid tests undertaken previously [63] which suggested that for a given slenderness ratio, the web's susceptibility to buckling increased as the force ratio increased. From the experimental programme they concluded that with the type of connection detail tested, good returns in terms of stiffness, strength and rotation capacity could be achieved. In addition, the presence of the stiffening influence of the cleats proved successful in limiting the development of flange buckling.

As an alternative to internal connections, primary perimeter connections have also been studied. Ansourian and Roderick[65] conducted a series of tests to investigate the feasibility of developing semi-rigid action at connections with perimeter columns. The columns themselves were encased and particular attention was paid to the detailing of the reinforcement. The steel part of the connection consisted of a single bottom cleat secured to the underside of the beams only. To provide a benchmark to enable the performance of the composite arrangement to be compared, the experimental programme included three tests without the concrete element. The main findings were as follows: (i) The moment resistance of the composite arrangement was of the order of twice that of the steel sections acting alone. (ii) The composite connections were found to produce a satisfactory performance when subjected to working loads; however, collapse of the slab as a result of anchorage failure followed shortly afterwards.

To further complement the investigation into perimeter connections, Ansourian[66] undertook an additional six tests, which represented internal composite connections. The steel detail remained unaltered from the previous test programme, however, an axial load equal to 20% of the squash load was applied to the columns. Symmetrical and asymmetrical load arrangements were considered, in addition to variations in the connected beams to cover a range of flange width to thickness ratios. During the programme, it was established that the extent of yielding before the onset of buckling increased as the ratio of the flange width to thickness reduced. The tests were terminated as a result of local buckling occurring to the compression flanges.

Tests undertaken between 1980 and 1990

Another five specimens were tested by Ansourian and Sase[67]. Three represented perimeter connections, with the other two representing internal connections. Flush end plate connections were adopted for the steel detail in the first test and again in the third, although on this occasion backing plates were also included in the tension region. The remaining tests incorporated flange cleats secured to both the tension and compression flanges of the connected beams. Where an internal connection was considered, encasement was provided to the column. It was demonstrated from this experimental programme that larger deflections would be induced into the steelwork as a result of providing a top flange cleat to the steel detail. In addition, problems were encountered with the perimeter connections which failed by a brittle collapse of the slab, prior to the attainment of the plastic moment. However, this was not the case for the internal connections which attained the plastic moment easily and failed as a result of local buckling induced into the compression flange of the connected beams. Improvements in connection performance, in terms of both strength and stiffness, were also obtained by encasing the columns in concrete, compared with their uncased counterpart.

Owens and Echeta[59] devised a experimental test programme to investigate a novel plastic design approach for dealing with semi-rigid composite frames. To satisfy this design approach, the connections between the composite members must possess the following characteristics: (i) Cheap to fabricate and straight forward to erect on site. (ii) Able to act as simple supports during the construction phase. (iii) Following the development of composite action, the connections should behave rigidly up to a predetermined moment. For internal connections this level was set at 75% of the plastic moment of the steel beam, whereas for the external connections the level was reduced to 60%. (iv) The connections should possess the capability to rotate at the predetermined level of moment enabling the redistribution of moments to proceed uninhibited. (v) The rotation of the connection should not effect the transfer of shear force from the beams into the columns.

One internal and four external connection tests were undertaken. The steel detail adopted to secure the beams to the columns for the internal connections consisted of bottom flange cleats and web cleats positioned in the tension region of the beam. For the external connections, the initial test adopted the same steel detail as before. This detail was later modified by excluding the web cleat and substituting plate stiffeners bolted through the lower flange and bottom cleat. As an alternative, one of the external tests dispensed with cleats altogether and produced the connection via a partial depth end plate located in the compression region of the beam. The amount of reinforcement specified within the slab was deliberately kept low as a consequence of the relatively small moment of resistance that was required. Ratios of reinforcement to slab cross-sectional area were varied between 0.38% and 0.51%. The external connections were loaded in the traditional cantilever arrangement; however, careful attention was given to the cruciform loading arrangement for the internal connection test. The method adopted is illustrated in Figure 5.1. Loading in this manner enabled the moment at the face of the column to be kept constant whilst the moment/shear ratio could

be varied by increasing the shear force, 'V'. This arrangement was designed to simulate the moment redistribution process from the connections. after plasticity has been attained. No adverse interaction was found as a consequence of varying the moment/shear ratio. In addition, it was concluded that there would be sufficient rotation capacity at the connections to allow a high degree of moment redistribution without problems associated with buckling to the flanges and/or web of the connected beams. It was further concluded that if premature slip occurred at the bottom cleat, then the corresponding connection stiffness would reduce and crack widths in the concrete slab would increase.

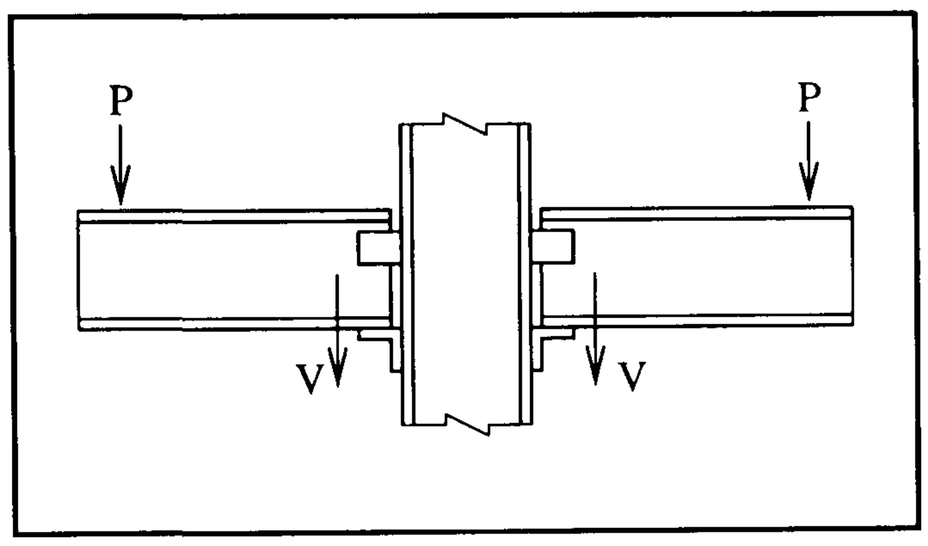

Figure 5.1: Load arrangement adopted to enable the moment/shear ratio at the column face to be varied

A further series of 6 flush end plate connections was undertaken at the University of Warwick by Johnson and Law[68]. The programme was divided into three groups, with each group consisting of two cruciform specimens. The composite beams framed into the major axis of the column for the first group of tests and then switched to the minor axis for the second group. In addition, for each of these four specimens a different degree of shear connection was provided on either side of the column, thereby enabling full and partial shear interaction to be investigated. The third group of tests were similar to the first with the sole exception that the depth of the concrete slab was increased. Other variable parameters included column encasement and the presence of an axial load within the column. Pattern loading conditions were simulated by adopting an asymmetrical loading sequence, which was implemented in the following manner. Initially, the load on

one side of the specimen only was increased until the plastic moment resistance of the connection had been reached. This load was then kept constant while the other side of the specimen was loaded to a similar level. The test was completed by incrementing the loads on either side symmetrically until failure occurred. The following conclusions were drawn from the expermental programme. (i) The degree of shear interaction at the slab/beam interface was found to influence the connections behaviour throughout its operating range for both major and minor column orientations. (ii) This influence became more pronounced as the test proceeded, whereupon it became apparent that the connection with partial shear interaction was capable of developing a higher rotation capacity. (iii) The stiffening effect of the column encasement was sufficient to allow the connection to be assumed as rigid up to half of its ultimate strength, provided a full shear connection is provided.

The experimental programme conducted by Van Dalen and Godoy[69] consisted of a total eight connection tests adopting the cruciform arrangement with a symmetrical load arrangement. Five of the eight were composite tests configured to represent typical connections from across the range, from simple, through semi-rigid to rigid. The simple steel detail was constructed from top and bottom flange cleats; removal of the top cleat with the tension flange of the beam then being welded to the column flange constituted a semi-rigid connection, and with the addition of a welded plate in the tension zone, a rigid connection was configured. The other three tests were undertaken without the concrete element, thereby providing a control from which the effects of composite action could be assessed. The main parameter which was investigated was the reinforcement ratio, which was varied between 0.46% and 0.80%. This range was considered to bound the range of practical interest. It was concluded that as the reinforcement ratio increased, so did the moment resistance of the connection. This was accompanied by an increase in connection stiffness. As a consequence of slippage occurring in the cleated arrangements, it was suggested that this should be elim-

inated by either welding the cleats to the flanges of the beams, or providing an alternative type of connection, such as an end plate. The results also showed that there was a greater potential for increasing the moment resistance of a simple connection by increasing the reinforcement ratio. This was highlighted by the comparisons with the control specimens, where it was found that the moment resistance for the simple connections showed an increase of six times that of the control specimen, whereas, only an increase of 1.5 times was forthcoming for the rigid connections. The final conclusion from the work reiterated findings from previous investigations[58] concerning the beneficial stabilising effects of connections that incorporated a lower flange cleat.

The experimental programme undertaken by Redwood *et al* [70] consisted of two rigidly connected, composite, cruciform specimens. The beams were fully welded to the column flanges which were additionally stiffened in both the tension and compression regions of the connection. Diagonal stiffeners between the horizontal stiffeners were also present. The objective of the tests was to study their cyclic behaviour under load reversal conditions. The two specimens were identical in every respect, with the variation coming from the method adopted to apply the loads (see Figure5.2).

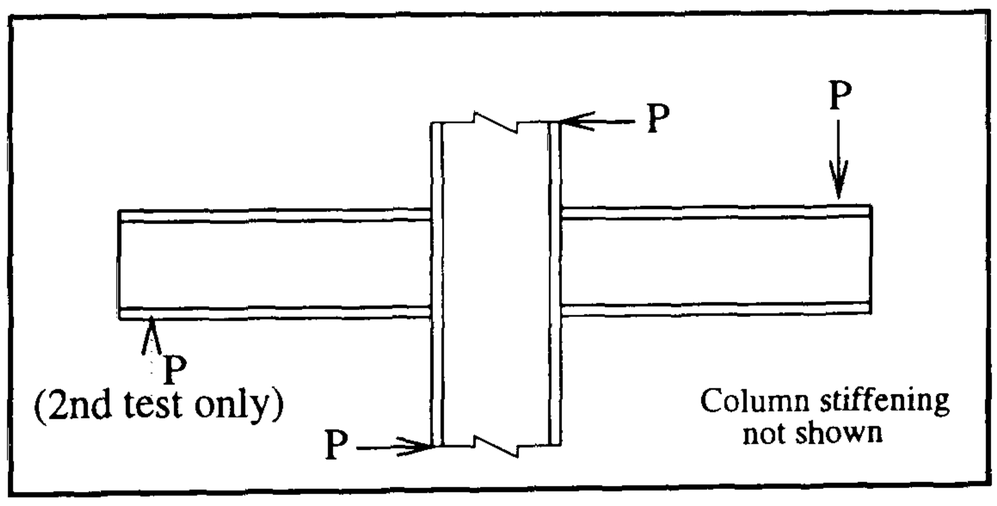

Figure 5.2: Load arrangement adopted to simultaneously induce positive and negative bending moments at the column face

Under these loading arrangements, positive and negative bending moment are developed at the column face simultaneously. The effect of these moments create shear forces within the column web, which would not be present under symmetrical monotonic loading. The first test demonstrated that it was possible

to exceed the moment of resistance of a similar connection detail under monotonic loading. However, an overall similarity between the moment-rotation envelopes obtained from cyclic and monotonic loading sequences was reported. The second test highlighted the stability and high energy absorbing capability of the column web over the depth of the connection. In both cases, the moment of resistance of the connections were not governed by the column despite the concrete crushing at the column face during the second test. The tests were terminated due to lateral buckling; however, this was not before considerable rotation at the connections had been achieved. This lateral buckling was accompanied by local buckling occurring to the lower beam flange on one side of the connection, during the first test.

A two phase experimental investigation was undertaken principally by Leon[71, 72, 73] to assess the suitability of semi-rigid composite connections in providing the necessary stiffness to an unbraced composite frame. The first phase of the investigation consisted of three connection tests all having a cruciform arrangement. The first two were composite and the third provided a control by omitting the composite element. The steel details chosen varied slightly between the composite tests. For the first test, top and bottom cleat arrangements were provided on one side of the column and bottom cleats only were adopted for the other side. The second test, however, incorporated the same steel detail either side of the column, whereupon the connection was via bottom cleats only. The same combination of steel details that was utilised for the first test was adopted for the third test. In addition to the flange cleats, web cleats were provided on the centre line of the connecting beam in all the steel details. The loading arrangements also differed between the tests. Monotonic loading was adopted for tests 1 and 3, whereas cyclic loading was adopted for test 2. The cyclic response was achieved by applying a horizontal load to the base of the column, rather than at the beam ends. Following comparisons with the control, it was established that the presence of the reinforcement in the absence of a top cleat produced a similar

performance to the non-composite connection which included this cleat. However, although the connection characteristics showed similarities in performance, the initial linear portion of the characteristic was extended for the reinforced connection when compared to the non-composite equivalent. Consequently, it was thought that the initial linear portion could be further extended by increasing the reinforcement ratio. In addition, it was concluded that problems associated with the column web crippling may not be as severe for semi-rigid connections as is expected when the connections are rigid. This phase of the experimental programme was further complemented by a full scale test on a two-bay frame, which confirmed the findings of the earlier studies. The second phase of this work was undertaken during 1990 and consequently will be described subsequently.

A series of end plate connections were investigated by Benussi *et al* [74, 75]. The first phase of the project consisted of four symmetrically loaded cruciform specimens. Two of them had full depth end plates, which were deemed to represent semi-rigid connections, whereas header plates welded in the compression region were adopted for the remaining two specimens to represent simple connections. For each of the different connection types, reinforcement ratios of 0.7% and 1.2% were adopted, to enable the strength of the reinforcement to be established and the influence of changing the connection detail to be assessed. They concluded that despite the considerable difference in terms of strength and stiffness between the specimens, certain similarities existed which could be used to define key elements of the moment-rotation characteristic (see Figure 5.3).

It was further suggested that to improve the performance of a composite connection, emphasis should be directed towards increasing the reinforcement within the slab rather than opting for a more complicated steel detail.

The second phase of the project concerned the following investigations: firstly the influence of the shear connection, secondly the interaction between the concrete slab and the column and finally, the effect of unbalanced moments. This phase consisted of a series of a further six connection tests in a cruciform arrange-

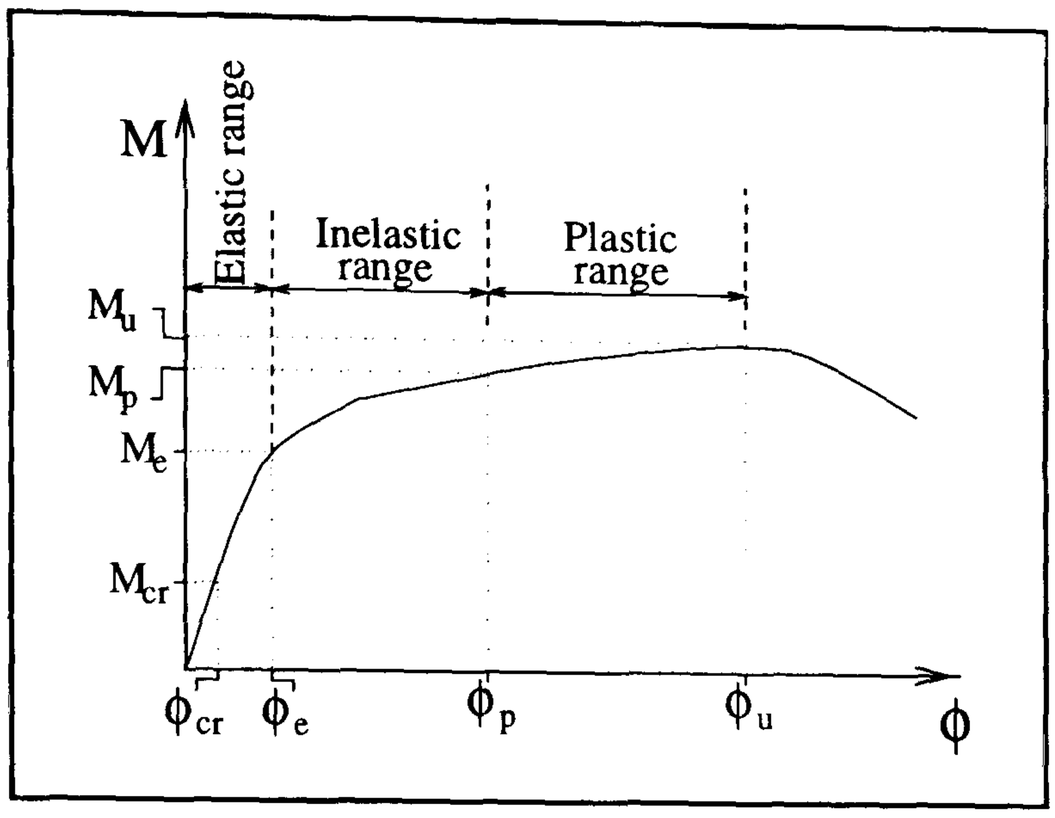

Figure 5.3: Key elements of the moment-rotation characteristic

ment. The same steel detail was adopted for five out of the six tests, and was identical to the header plate detail utilised during phase 1. For the sixth test, the beam was fully welded to an unstiffened column. The shear connection was provided by various sized welded studs, or mechanically fastened connectors. To study the interaction between the concrete slab and the column, a gap between the slab and the left hand side of the column flanges was introduced in four of the tests. It was concluded that the moment resisted by the connection increased during the inelastic range of the characteristic as a result of strain hardening within the reinforcement. In addition, substantially more uplift was observed at the steel/concrete interface when the shear connection was provided through mechanically fastened connectors. In the absence of the concrete bearing on the column, the left hand connection showed a marked difference in performance, when compared to its right hand counterpart. It was further concluded that substituting a welded detail for the header plate would lead to a limited increase in the moment resistance of the connection. However, this increased strength was also accompanied with a reduction in the rotation capacity.

A research project consisting of a total of 11 connection tests has been undertaken by Lam[76]. Six represented internal composite connections and were tested in a cruciform configuration. The remaining five were external connections and consequently a cantilever configuration was adopted. The steel detail

chosen was kept constant throughout and consisted of a bottom cleat in conjunction with web cleats positioned centrally on the beam. The variable parameters were column orientation, reinforcement ratio, and since the slab was cast on steel decking, the decking direction was also varied. During the cruciform tests, the load was applied to the top of the column, with the cantilever arms reacting against the test rig. The decking orientation was found to influence the stiffness of the uncracked slab, which increased when the ribs were parallel with the beam. The rotation capacity and moment resistance of the composite connection were improved by providing a higher reinforcement ratio. In contrast, when the slab only contained a nominal amount of reinforcement, its performance was severely diminished in every respect.

Tests undertaken between 1990 and 1995

A further four cruciform composite tests were undertaken by Leon[77], to complete the research project originally started in the late 1980s. The steel detail was again the cleated arrangement described above; however the thickness of the bottom cleat was varied. The loading sequence adopted represented either monotonic or cyclic actions. During the early stages of each test, slippage was observed at the interface between the cleats and the beam flanges. Under cyclic loading it was found that the hysteresis exhibited by the connection was reduced by increasing the thickness of the bottom cleat. It was finally concluded that, in areas of low to moderate seismicity or where moderate to high wind loads exist, a semi-rigid composite system could be advantageous.

A comprehensive research programme consisting of 38 composite cleated connections was tested by Altman *et al*[78]. The tests were all cruciform in arrangement and subjected to symmetrical monotonic loading. The steel detail adopted took the form of top and bottom flange cleats in conjunction with centrally positioned web cleats. However, for certain tests, the top cleat was removed. Three different beam depths were considered, which were combined with reinforcing

ratios equivalent to 0.67%, 1.3% and 2.1%. The flexibility of the connection was found to be increased as a consequence of slip occurring between the cleated angles and the beam flanges. However, it was found that the reinforcement ratio was the single most important parameter which governed the connections' overall behaviour. As this ratio increased, both the strength and stiffness were improved. Details concerning the rotation capacity of the connections were unfortunately not reported.

Nine composite and two steel end plate connections have been tested by Anderson and Najafi[9]. The experimental programme was based on a programme undertaken by Lawson *et al* [79], which investigated similar connection details under fire conditions. For Lawson's work, the steel details were selected to represent a range which could be considered as being typical of those used in practice. The details therefore included extended and flush end plates as well as web cleat connections. The latter group were not considered by Anderson and Najafi, since the aim of their experimental programme was to concentrate on end plate details. The connections were configured to represent primary internal joints and framed into both the major and minor axis of the column. Symmetrical and asymmetrical loading sequences were adopted for the major axis and minor axis tests respectively. Periodically throughout each test, an unloading sequence was initiated to enable the connections' unloading stiffness to be established. The reinforcement ratio was generally varied between 0.5% to 1.5%; however, one of the minor axis tests incorporated mesh reinforcement only. The provision of such a small amount of reinforcement represented the minimum required for composite action to be developed, and is subsequently referred to as the nominal provision. The majority of the tests incorporated a full shear connection, although a partial connection was provided on two occasions. As an additional variable. the beam depth was increased for the final major axis test. The steel-only details were incorporated to provide a control by which the composite performance could be

judged. Following the assessment of the results the following were concluded : (i) The amount of reinforcement increases the moment resistance of the connection, thus making it possible to provide a full strength composite connection. (ii) The rotation capacity of a connection is influenced by the amount of reinforcement provided, with a satisfactory performance being achieved when the reinforcement ratio is of the order of 1%. (iii) The amount of reinforcement does not influence the initial stiffness of composite connections. (iv) The type and sequence of loading influences the connection's response. In particular, during the asymmetrical sequence, the point at which the unloading phase is initiated has a pronounced effect of the connection's unloading stiffness. (v) The extended end plate detail increases the moment resistance of both the steel and composite connections in comparison to a similar flush end plate detail. In addition, the extended end plate detail also reduces the column flange deformation and consequently reduces the need for stiffening in the tension region of major axis connections. (vi) The column orientation influences the stiffness response of the attached connections. The minor axis connections produced a stiffer response than their equivalent major axis counterpart. (vii) An increase in the connection's moment of resistance can be achieved by increasing the beam depth; however, the rotation capacity is severely restricted.

A series of fourteen composite connection tests have been undertaken by Aribert *et al* [80, 81] . The test programme was divided into four phases, with each phase concentrating on a different aspect of connection design. All the tests represented major axis connections and were configured in a symmetrical cruciform arrangement. The first phase combined a flush end plate detail with a slab containing a constant reinforcement ratio. A total of four tests were carried out. with the variables being the beam and column depth. To enable the composite action to be assessed, the first test in this phase was conducted on the bare steel end plate detail without the concrete slab. The second phase of the project was designed to investigate the effect of changing the reinforcing ratio when the slab

is combined with an extended end plate detail. A benchmark test consisting of the steel detail only was again undertaken during this phase. For phase three of the project, the same steel detail that was utilised during phase one was adopted. The purpose of this set of three tests was to investigate the influence of using a different type of decking and to assess the effect of changing the degree of shear interaction. The first test in this phase had a full shear connection, whereas 75% and 50% shear connection was provided for the second and third tests respectively. The final phase of the project adopted a cleated arrangement to form the steel detail. Flange cleats were provided in conjunction with centrally positioned web cleats. The variable parameters to be studied during this phase were the reinforcement ratio and the degree of shear interaction. To achieve this objective, 100%, 75% and 50% shear connection was provided for the second, third and fourth tests respectively. The first test in this phase consisted of the steel detail only, to provide the control from which the composite action could be compared. Aribert and Lachal drew the following conclusions from their experimental programme. (i) The more flexible the steel detail, the greater the influence in terms of stiffness and strength for a given reinforcement ratio. (ii) A decrease in the depth of the connected beam leads to a reduction in both the stiffness and moment resistance of the connection; however, the rotation capacity is improved. (iii) A partial shear connection reduces the rotation capacity of a composite end plate connection, since the failure is now associated with the fracture of the shear connectors themselves. It was suggested that a partial shear connection, even as low as 50%, could remain feasible provided the risk of connector failure can be controlled. (iv) Slip between the beam elements and the cleats have a pronounced influence in increasing the connection's flexibility during the early stages of the loading sequences.

Following a preliminary pilot study undertaken by Davison *et al*[82] at the University of Sheffield, a comprehensive experimental programme was undertaken by Xiao *et al*[83]. The project considered a wide variety of steel details

which included bottom cleat arrangements, flush end plate, partial depth end plate and finplate connections. All the steel details, with the exception of the first to provide a control, were combined with various reinforcing details to form a composite arrangement. For the end plate connections, various forms of stiffening were incorporated to strengthen the column web. The type of stiffening provided included plate stiffeners welded between the flanges of the column in the compression region, or stub beams framing into the minor axis of the column and bolted in position. In addition, backing plates to the column flanges were also included for the last test on this type of connection. These plates were located in the compression region of the connection, with the objective being to reduce the flange deformation in this area. For the tests that adopted partial depth end plates, one of the variable parameters was the position of the plate in relation to the depth of the beam. Three positions were considered, namely at the top, middle and at the bottom of the connected beam. The beam depth and decking orientation were taken as the variable parameters for the finplate connection tests. The connection test comprising the deeper beam was configured to match previous tests undertaken on bare steel finplate connections[84], thus enabling the influence of the composite slab to be assessed. The reinforcement ratio varied between nominal and 1.2%, and was applicable to all the connection tests undertaken. Internal and external primary connections were considered and arranged in cruciform and cantilever configurations respectively. For the external connections, partial depth end plates were considered and positioned either at the top or bottom of the connecting beam. In an attempt to improve the anchorage provided to the reinforcement, the longitudinal bars were bent into the slab and extra transverse bars were added to both the top and bottom of the slab at the back of the column. In addition, trim bars bent to 45^0 were placed around the back of the column in an attempt to control the diagonal cracking. The columns were orientated such that the beams framed into the major axis for all the tests except for two occasions, where they spanned into the minor axis. The minor

axis tests incorporated partial depth end plate details. A symmetrical loading sequence was adopted throughout the programme with periodic unloading phases to monitor the connections' unloading stiffness. The emphasis of the experimental work was directed towards assessing the moment of resistance, rotational stiffness and rotation capacity of commonly available composite connections with varying reinforcing details.

For cleated connections, the initial rotational stiffness was influenced by horizontal slip between the connecting elements. However, this type of detail does possess some degree of moment resistance and rotational stiffness in its bare steel state. Composite action though has the effect of further increasing the connection's initial stiffness and moment of resistance over its bare steel equivalent. However, when only a nominal amount of reinforcement is provided, the rotation capacity is restricted. In addition, providing composite action through a suitable reinforcing detail has the effect of reducing the horizontal slip. Consequently, the rate at which stiffness is lost by the connection is reduced during the early stages of loading. Increasing the reinforcement ratio above that denoted nominal, produces a further increase in the moment of resistance and a considerable improvement in the connection's rotation capacity.

The end plate connections produced the highest initial stiffness of all the connection types considered, for a given reinforcing detail. The moment of resistance and rotational stiffness were enhanced by the presence of stiffening to the column web, since web buckling was precluded from the possible modes of failure. As the reinforcement ratio increased, the rotation capacity of the connection also improved. This beneficial effect was the result of the mode of failure of the connection being changed from brittle to ductile and thus associated with deformation within the components of the steelwork detail. The backing plate located in the compression region of the connection prevented excessive deformation to the column flange, therefore eliminating the need for costly welded stiffeners.

The position of the partial depth end plate significantly influenced the con-

nection behaviour and eventual failure mode. The weakest position, in terms of producing the most flexible response, was when the plate was secured at the top of the beam. Improvements in both the moment resistance and stiffness of the connection were achieved by lowering the position of the plate. The rotation capacity was also influenced by the location of the plate, with the best performance coming from the central position. The lowest rotation capacity was achieved when the plate was secured at the bottom of the beam. This was the result of the failure mode being associated with the column web buckling rather than the beam web, which governed the failure when the plate was located in the other positions. Following the completion of the minor axis tests, it was again concluded that the positioning of the plate is crucial to the achievement of high stiffness and moment resistance. The low position of the plate again proved to outperform higher plate positions; however, increased strength and stiffness was achieved at the expense of the rotation capacity.

Following the completion of the finplate tests the following conclusions were drawn: (i) The finplate connection produced a more flexible response than its cleated counterpart in comparable tests. (ii) An increase in moment resistance is forthcoming as the reinforcement ratio is increased. However, when the reinforcing detail is restricted to the mesh only, the rotation capacity of the connection is restricted. (iii) The moment resistance of this type of connection was governed by the tensile resistance of the reinforcement and/or bearing in the beam web or finplate. (vi) The decking may be regarded as equivalent reinforcement when it is positioned to run parallel with the beam direction. However, an increase in the connection's initial flexibility would also result.

For the external details, the connection failure was always associated with loss of anchorage to the reinforcement. This mode of failure was very sudden and brittle and consequently clearly undesirable. The connection flexibility and rotation capacity were increased when the partial depth end plate was positioned at the top of the beams. However, this was accompanied by a reduction in the

moment resistance of the connection.

A series of six composite flush end plate connection tests has been undertaken by Li[85] at the University of Nottingham. The primary objective of the experimental programme was to study the effects of varying the shear/moment ratio at the column/beam interface. Consequently, the steel detail adopted and reinforcement arrangement were kept constant throughout. with the shear/moment ratio being varied by adjusting the load positions and intensities thereof. relative to the column position (see Table 5.4). The connections were configured in a cruciform arrangement and framed into the major axis of the column. In addition, the same end plate detail was tested in isolation from the slab to enable the effects of the composite action to be assessed. The main findings of the programme were as follows: (i) The moment resistance of the connections were not significantly influenced by the presence of the shear force, except when a high level of shear coexists with a relatively weak beam web. (ii) The effect of asymmetrical loading on the connection's moment of resistance is influenced by the column web shear resistance or the concrete strength. (iii) The moment resistance of a steel end plate detail can by increased by composite action. (iv) The failures of the connections were generally associated with deformation within the steel detail, and consequently the rotation capacity was not restricted by a non-ductile type of failure.

A two-phase experimental programme has been undertaken by Ren and Crisinel[86]. The first phase was concerned with bare steel connections only, to enable the composite performance to be assessed when the steel details are combined with a concrete slab. Two types of steel detail were considered, namely, web cleat arrangements and flush end plate connections. The main variable parameter for the composite tests was the reinforcement ratio. The tests were configured to represent primary internal connections, with the beams spanning into the major axis of the column. A symmetrical loading sequence was adopted and the shear connection was designed to provide full interaction. Fol-

lowing the completion of the programme, the following conclusions were drawn: (i) The flush end plate connection exhibits a high moment of resistance and very poor rotational capacity. (ii) The rotation capacity is improved by adopting cleated arrangements; however, the improved ductility is accompanied by a reduction in the moment resistance of the connection. (iii) When a nominal percentage of reinforcement is provided with a flexible steel detail (web cleats), the moment resistance and rotational capacity are significantly reduced.

5.2.1 Experimental results for end plate connections

The following section provides detailed experimental results which are applicable to the major axis end plate connections that have been discussed previously. Consequently, the work undertaken by the following authors has been included.

1. Anderson and Najafi[87] - The connection configurations are shown in Table 5.1 and the moment-rotation characteristics are given in Figures 5.4 and 5.5.

2. Xiao *et al*[83] - The connection configurations are shown in Table 5.2 and the moment-rotation characteristics are given in Figures 5.6 and 5.7.

3. Aribert *et al*[81] - The connection configurations are shown in Table 5.3 and typical moment-rotation characteristics are given in Figure 5.8.

4. Li *et al*[85] - The connection configurations are shown in Table 5.4 and the moment-rotation characteristics are given in Figure 5.9.

5. Johnson and Law[88] - The connection configurations are shown in Table 5.5 and the moment-rotation characteristics are given in Figure 5.10.

6. Benussi *et al*[74] - The connection configurations are shown in Table 5.5 and the moment-rotation characteristics are given in Figure 5.11.

7. Ren and Crisinel[86] - The connection configurations are shown in Table 5.5 and the moment-rotation characteristics are given in Figure 5.12.

5.3 The need for further experimentation

It can be seen from the tables referenced in section 5.2.1, that the majority of end-plate connections which have been tested to date, have incorporated beams of relatively shallow serial size (less than 400mm). Composite beams of this depth could be reasonably expected to span between columns which are up to 9m apart. To further increase their capability however, would necessitate a larger serial size beam being adopted to form the composite arrangement. This has been recognised by amongst others Anderson and Najafi[87], who included a single test on a composite connection that included a 457 serial size beam. The results from this particular test showed an improvement in the connection's moment of resistance over its smaller beam equivalent, however, this was accompanied with a dramatic decrease in ductility. For this type of beam to be considered acceptable for general use in plastically designed continuous composite construction, the problem of the lack of ductility of a connection must be addressed. Consequently, the author's experimental programme (see Chapters 6 - 8 inclusive) was primarily designed to investigate the ductility of composite flush end plate connections, that incorporate 457 serial size beams; however, a single test on a 533 serial size beam was also undertaken. Composite beams that include beams of these sizes, would be expected to span between columns which are up to 14m and 16m apart, respectively (see Chapter 8, section 8.2.2). In addition, other variable parameters investigated by the author were end plate thickness and horizontal spacing of the reinforcement. Furthermore, the tests also enabled further checks to be made on existing methods proposed for calculating the moment of resistance of such connections.

Table 5.1: Experimental programme undertaken by Anderson and Najafi

Author	Test reference	Type of connection	Beam section	Column section	Web reinforced	Concrete slab Breadth (mm)	Concrete slab Depth (mm)	Reinforcement : type provided Mesh	Re-bars Number & diameter	Re-bars Total steel area (mm^2)	Re-bars % reinforcement	Shear connection	Type of decking	Position of re-bars above top beam flange (mm)
Anderson &Najafi	**S4F**	**Flush**	**305x165x40UB**	**203x203x52UC**	**At compression level**	**1100**	**120**	**A142**	**4T12**	**452**	**0.55**	**19mm studs x 100mm long before welding**	**PMF-CF46 0.9mm thick**	**90**
	S8F	**Flush**	**305x165x40UB**	**203x203x52UC**		**1100**	**120**	**A142**	**8T12**	**905**	**1.1**			**90**
	S12F	**Flush**	**305x165x40UB**	**203x203x52UC**		**1100**	**120**	**A142**	**12T12**	**1357**	**1.65**			**90**
	S8E	**Extended**	**305x165x40UB**	**203x203x52UC**		**1100**	**120**	**A142**	**8T12**	**905**	**1.1**			**90**
	S8FD	**Flush**	**457x152x52UB**	**203x203x52UC**		**1100**	**120**	**A142**	**8T12**	**905**	**1.1**			**90**
	SBF	**Flush**	**305x165x40UB**	**203x203x52UC**		**Control test : steel connection only**								

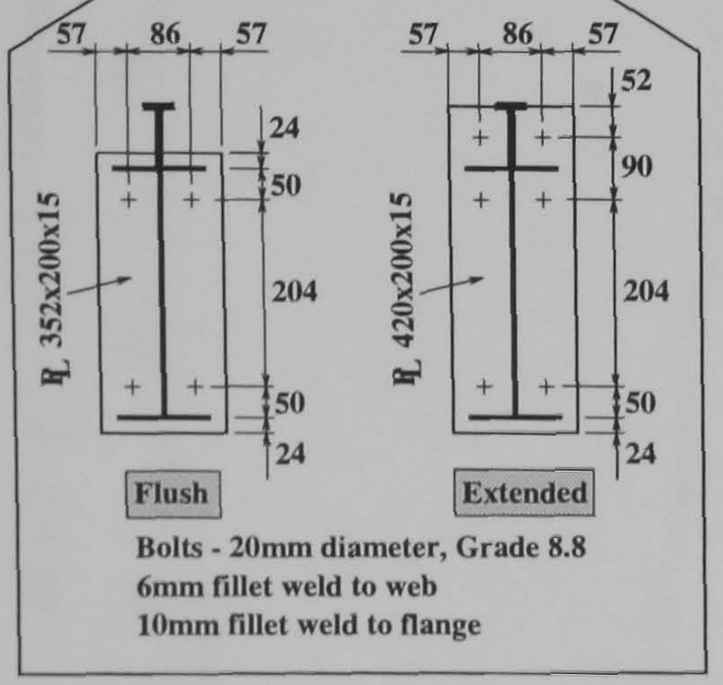

Test reference	Failure mode	Material properties: Steel members Yield strength (N/mm^2) Column web	Column flange	Beam web	Beam flange	Reinforcement Yield strength (N/mm^2) mesh	re-bars	Ductility % elongation at fracture re-bars	Moment capacity of the connection M_c (kNm)	Rotation at maximum moment ϕ_u (mrads)	Rotation at connection failure ϕ_{ult}
S4F	**Fracture of mesh & rebars**	**296**	**284**	**295**	**272**	**668**	**486**	**17**	**179**	**15.7**	**26.6**
S8F	**Fracture of mesh & rebars**	**296**	**284**	**293**	**271**	**668**	**486**	**17**	**262**	**28.0**	**35.8**
S12F	**Local buckling of the bottom beam flange**	**296**	**284**	**302**	**272**	**668**	**486**	**17**	**302**	**22.7**	**55.7**
S8E	**Local buckling of the bottom beam flange**	**296**	**284**	**297**	**273**	**668**	**486**	**17**	**291**	**20.0**	**40.0**
S8FD	**Fracture of mesh & rebars**	**296**	**284**	**330**	**310**	**668**	**486**	**17**	**416**	**14.0**	**14.0**
SBF	**Deformation of the column flange**	**296**	**284**	**302**	**272**	**N/A**	**N/A**	**N/A**	**105**	**55.8**	**55.8**

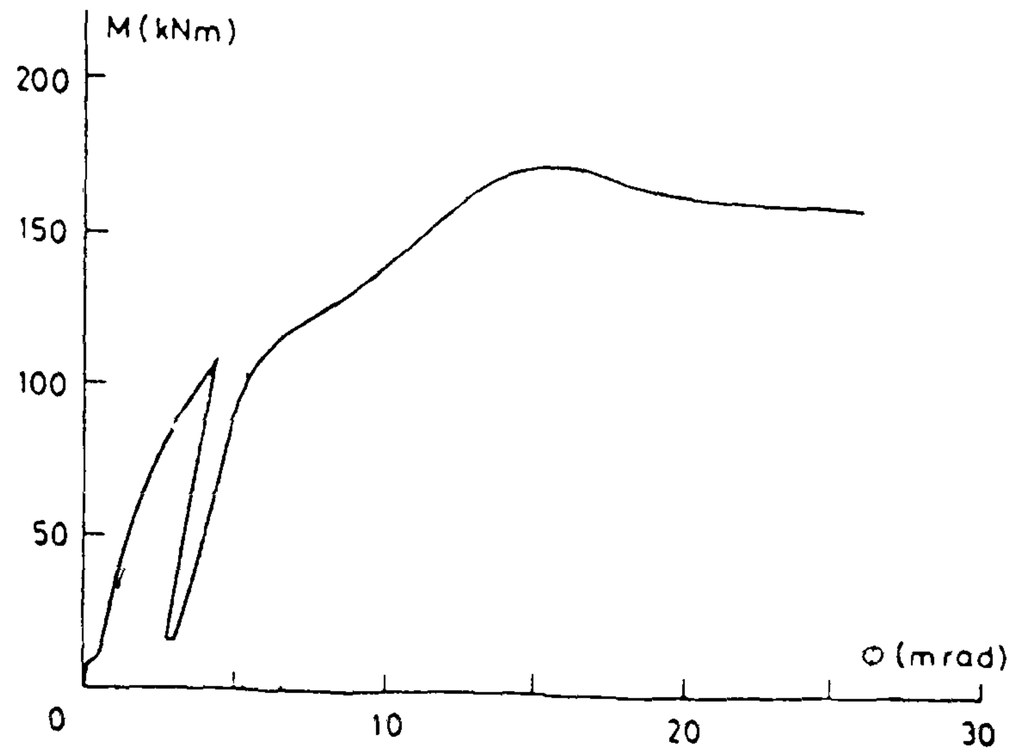

Moment–rotation curve of S4F

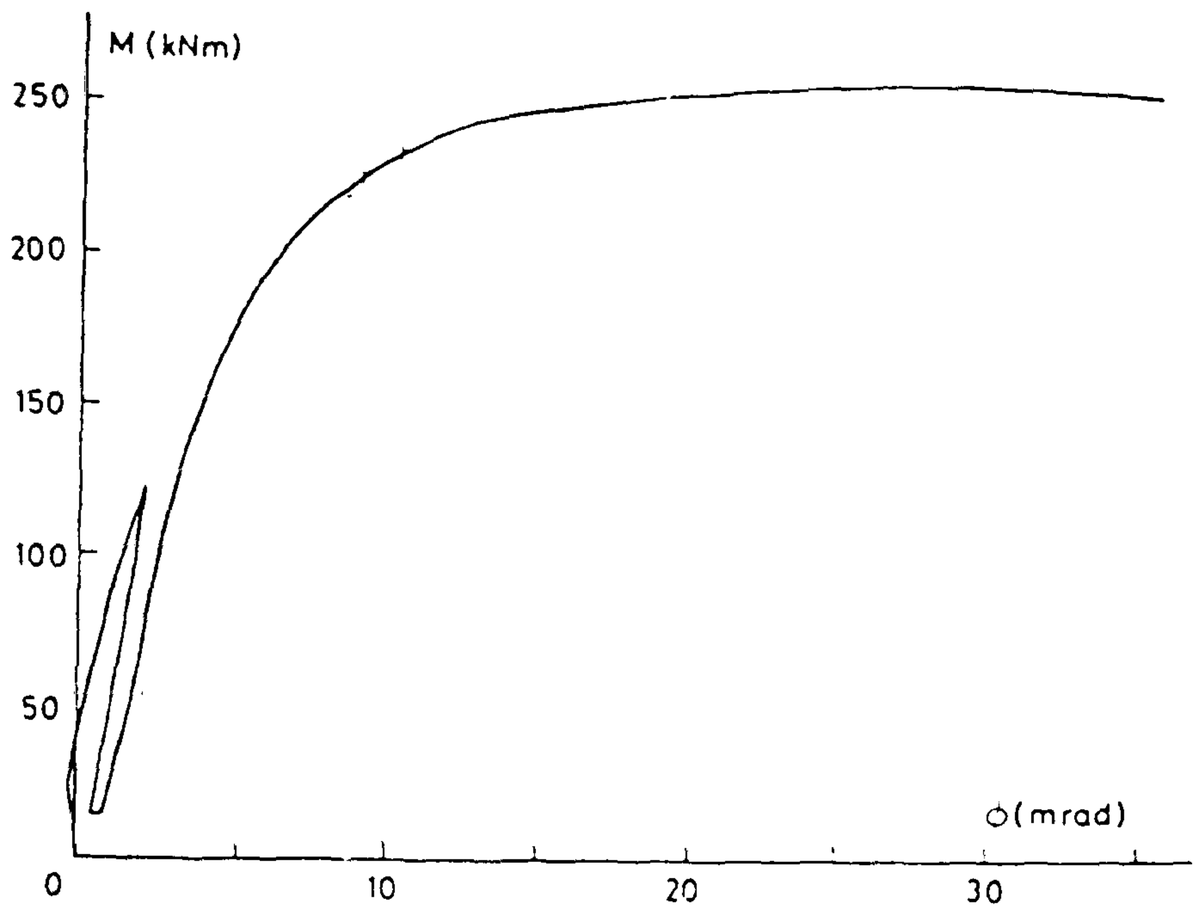

Moment–rotation curve of S8F.

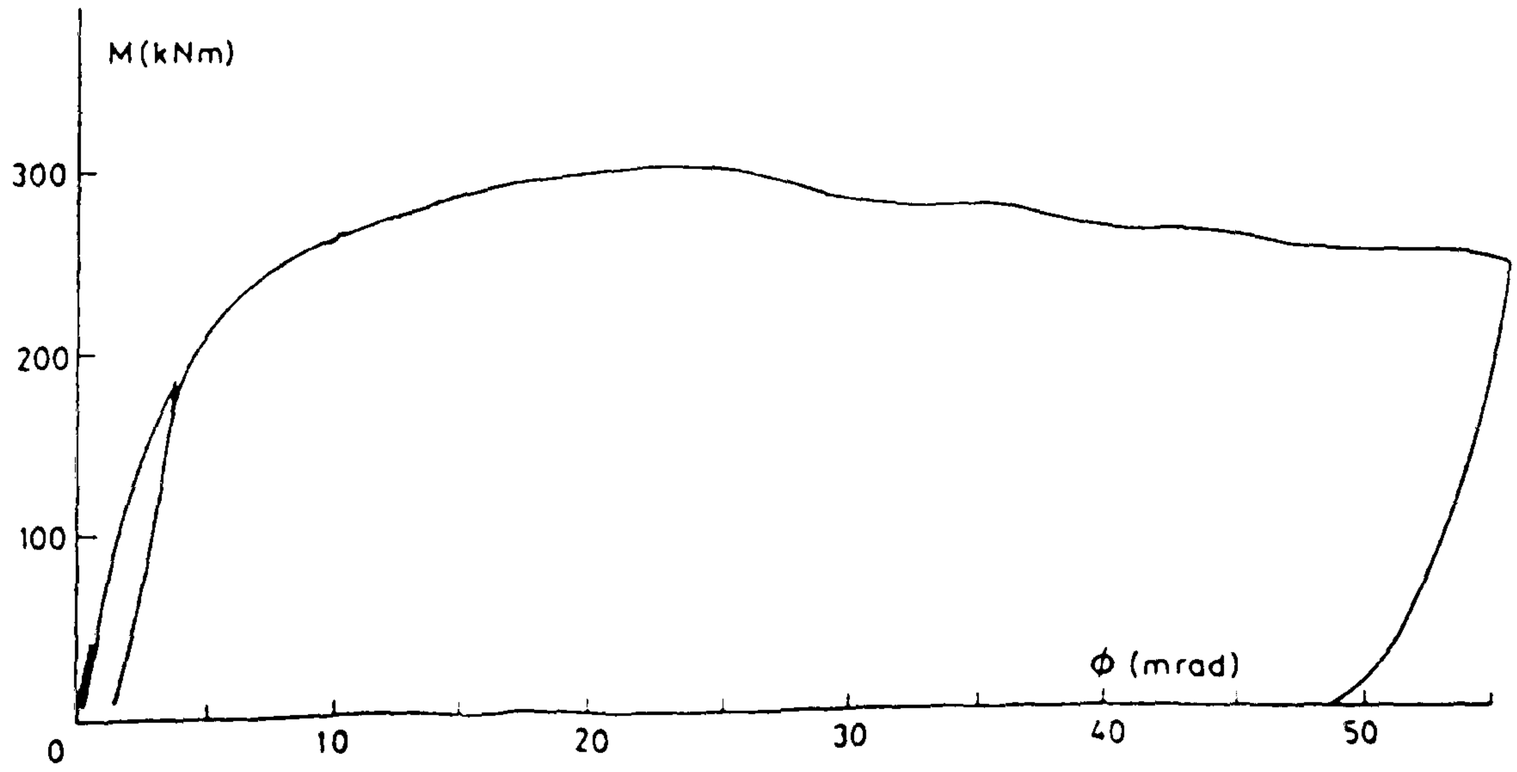

Moment–rotation curve of S12F.

Figure 5.4: Moment-rotation characteristics from the programme undertaken by Anderson and Najafi

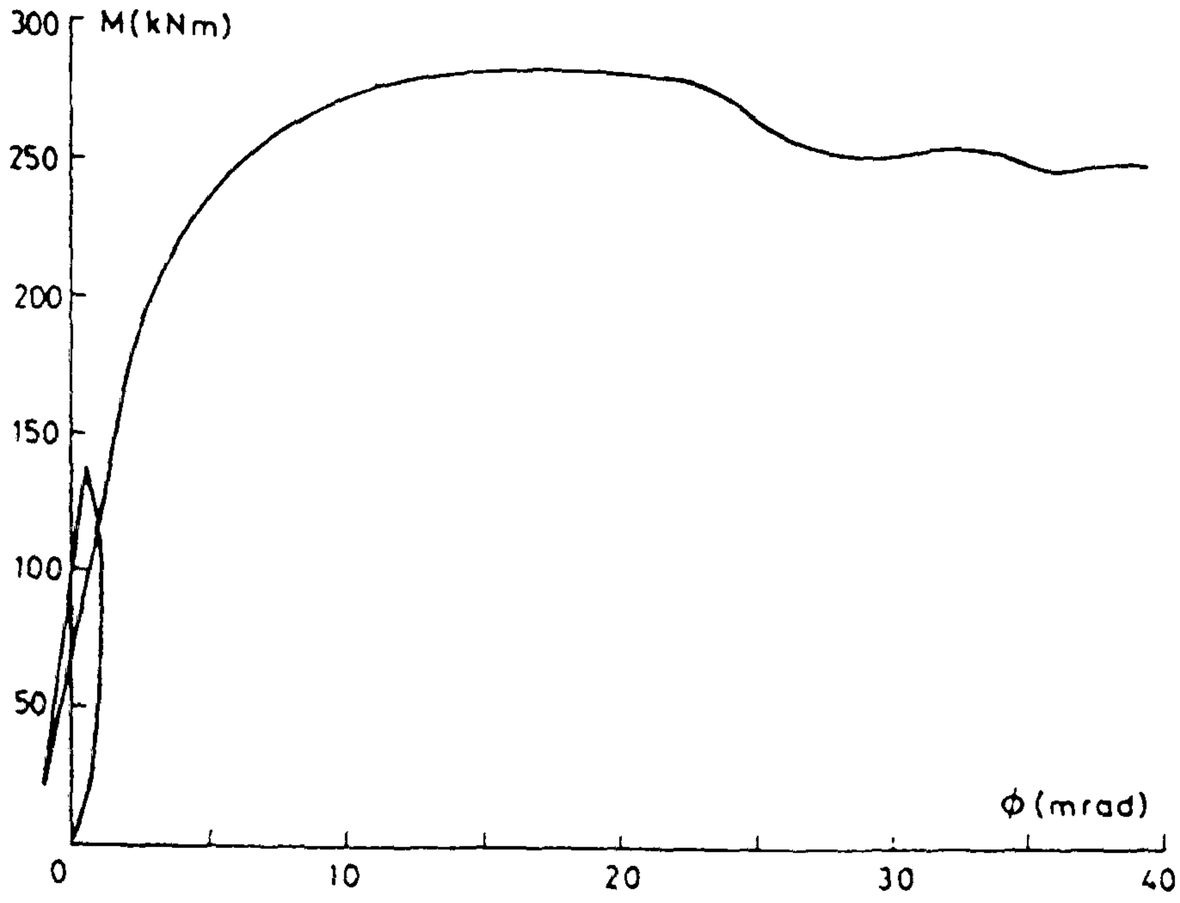

Moment–rotation curve of S8E.

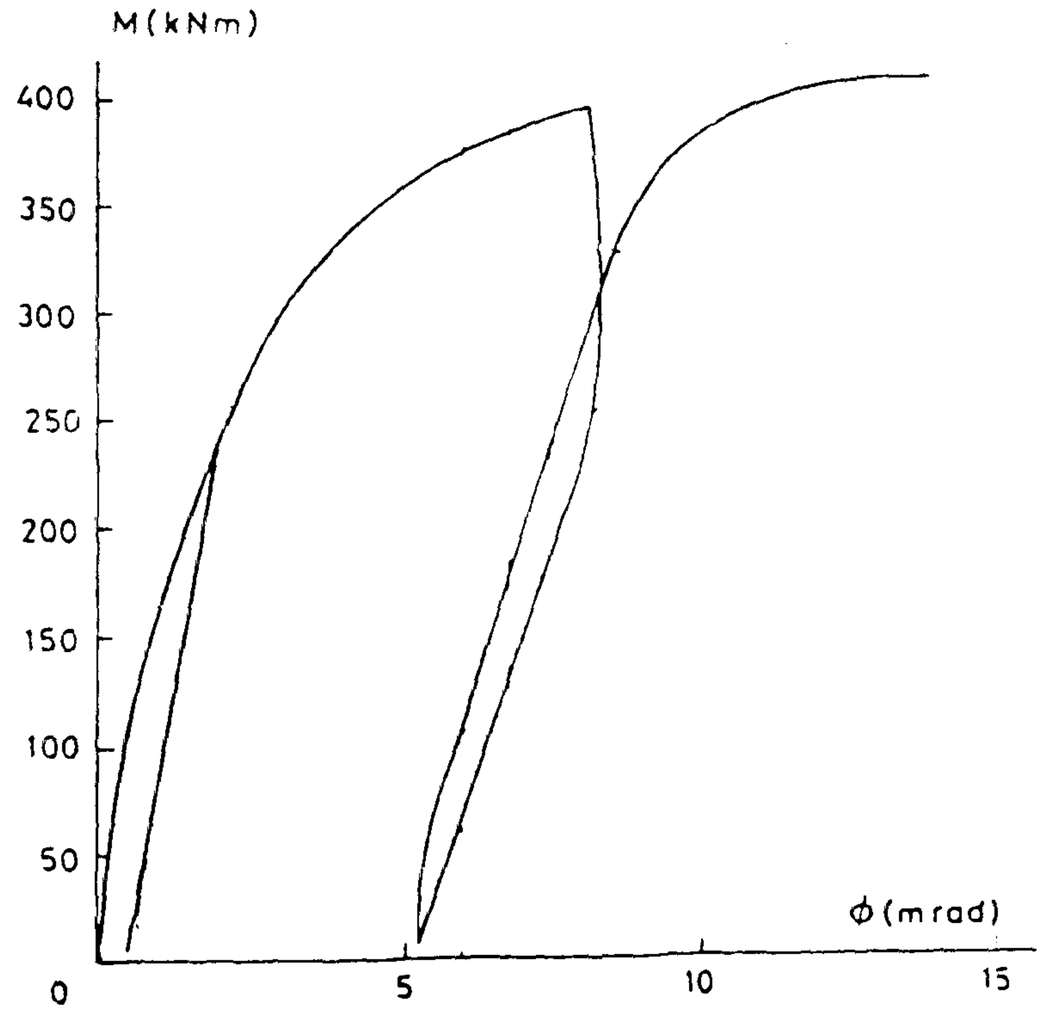

Moment–rotation curve of S8FD.

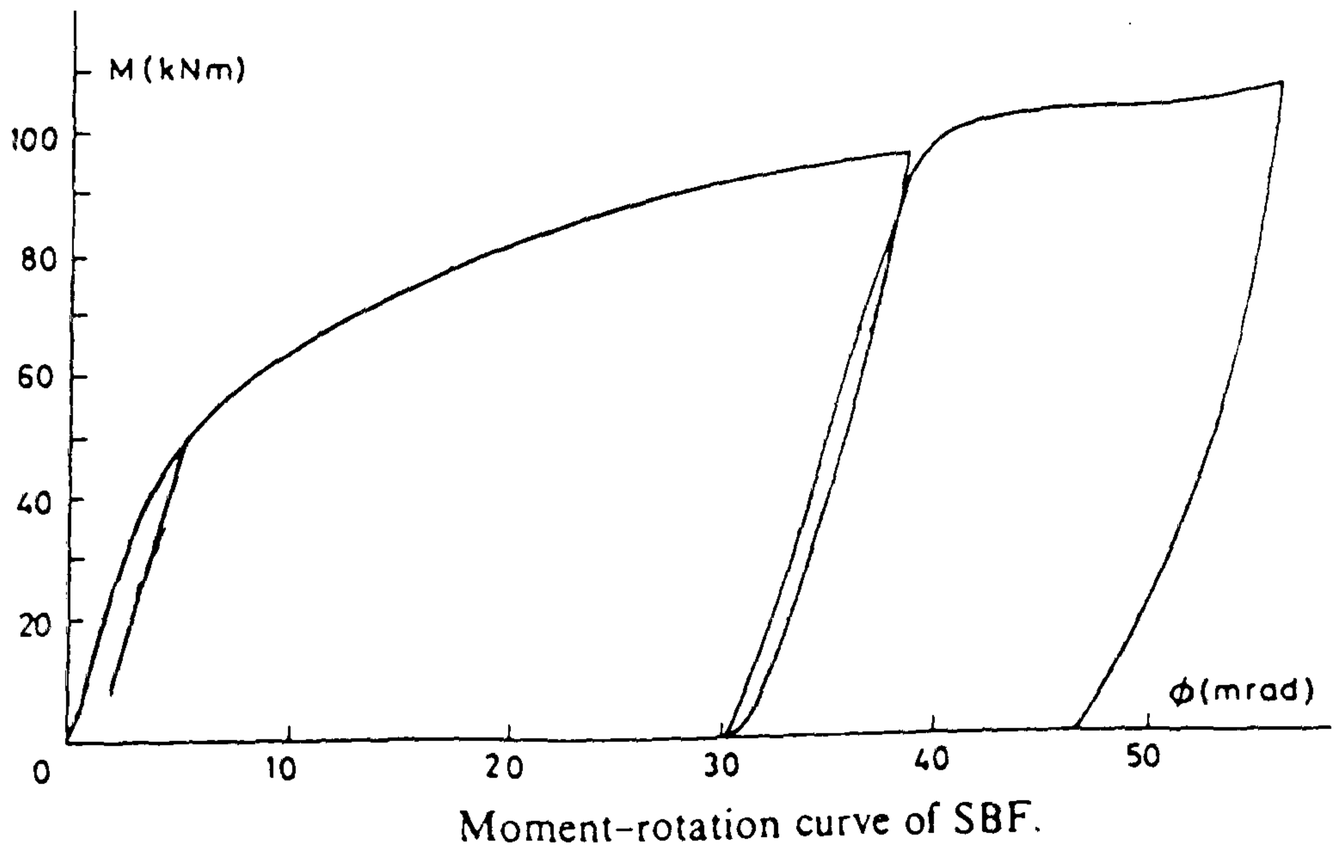

Moment–rotation curve of SBF.

Figure 5.5: Moment-rotation characteristics from the programme undertaken by Anderson and Najafi

Table 5.2: Experimental programme undertaken by Xiao *et al*

Author	Test reference	Type & size of connection (mm)	Beam section	Column section	Web reinforced	Concrete slab Breadth (mm)	Concrete slab Depth (mm)	Reinforcement : type provided Mesh	Re-bars Number & diameter	Re-bars Total steel area (mm^2)	Re-bars % reinforcement	Shear connection	Type of decking
Xiao, Nethercot & Choo	**SCJ 3**	**Flush 150x285x10**	**305x165x40UB**	**203x203x60UC**	**None**	**1200**	**120**	**A142**	**N/A**	**N/A**	**0.2**	**19mm studs x 100mm long before welding**	**PMF-CF46 0.9mm thick**
	SCJ 4	**Flush 150x285x10**	**305x165x40UB**	**203x203x60UC**	**None**	**1200**	**120**	**N/A**	**10T12**	**905**	**1.0**		
	SCJ 5	**Flush 150x285x10**	**305x165x40UB**	**203x203x60UC**	**Compression level**	**1200**	**120**	**N/A**	**10T12**	**905**	**1.0**		
	SCJ 6	**Flush 150x285x10**	**305x165x40UB**	**203x203x60UC**	**None**	**1200**	**120**	**A142**	**8T12**	**905**	**1.0**		
	SCJ 7	**Flush 150x285x10**	**305x165x40UB**	**203x203x52UC**	**Bolted beam stub**	**1200**	**120**	**A142**	**10T12**	**1358**	**1.2**		
	SCJ 15	**Flush 140x254x10**	**305x165x40UB**	**203x203x52UC**		**1200**	**120**	**A142**	**8T12**	**905**	**1.0**		

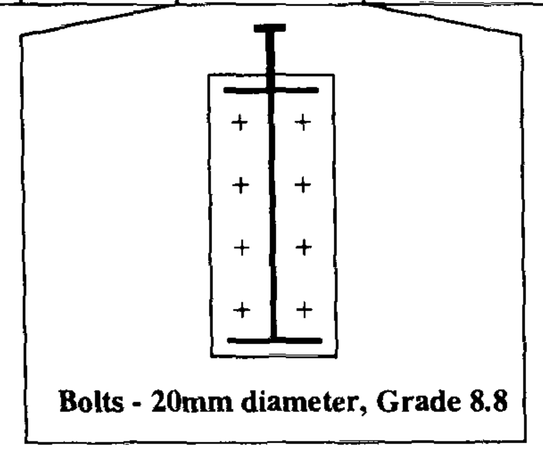

Bolts - 20mm diameter, Grade 8.8

Test reference	Failure mode	Material properties: Steel members Yield strength (N/mm^2) Column web	Column flange	Beam web	Beam flange	Reinforcement Yield strength (N/mm^2) mesh	re-bars	Moment capacity of the connection M_c (kNm)	Rotation at maximum moment ϕ_u (mrads)	Rotation at connection failure ϕ_{ult}
SCJ 3	**Fracture of mesh**	-	-	-	-	571	**N/A**	**85.7**	**7.2**	**26.6**
SCJ 4	**Excessive column flange deformation and buckling of the column web**	-	-	-	-	N/A	**570**	**202.9**	**23.4**	**41.1**
SCJ 5	**Shear stud failure and buckling of beam flange**	-	-	-	-	N/A	**570**	**240.8**	**26.0**	**35.0**
SCJ 6	**Excessive column flange deformation and buckling of the column web**	-	-	**326**	-	**571**	**570**	**157.6**	**11.5**	**23.0**
SCJ 7	**Shear stud failure and buckling of column web**	**318**	**290**	**342**	295	**571**	**570**	**204.5**	**26.5**	**46.9**
SCJ 15	**Excessive deflection of the beams**	317	**290**	**377**	**314**	571	**570**	**185.5**	**23.2**	**27.7**

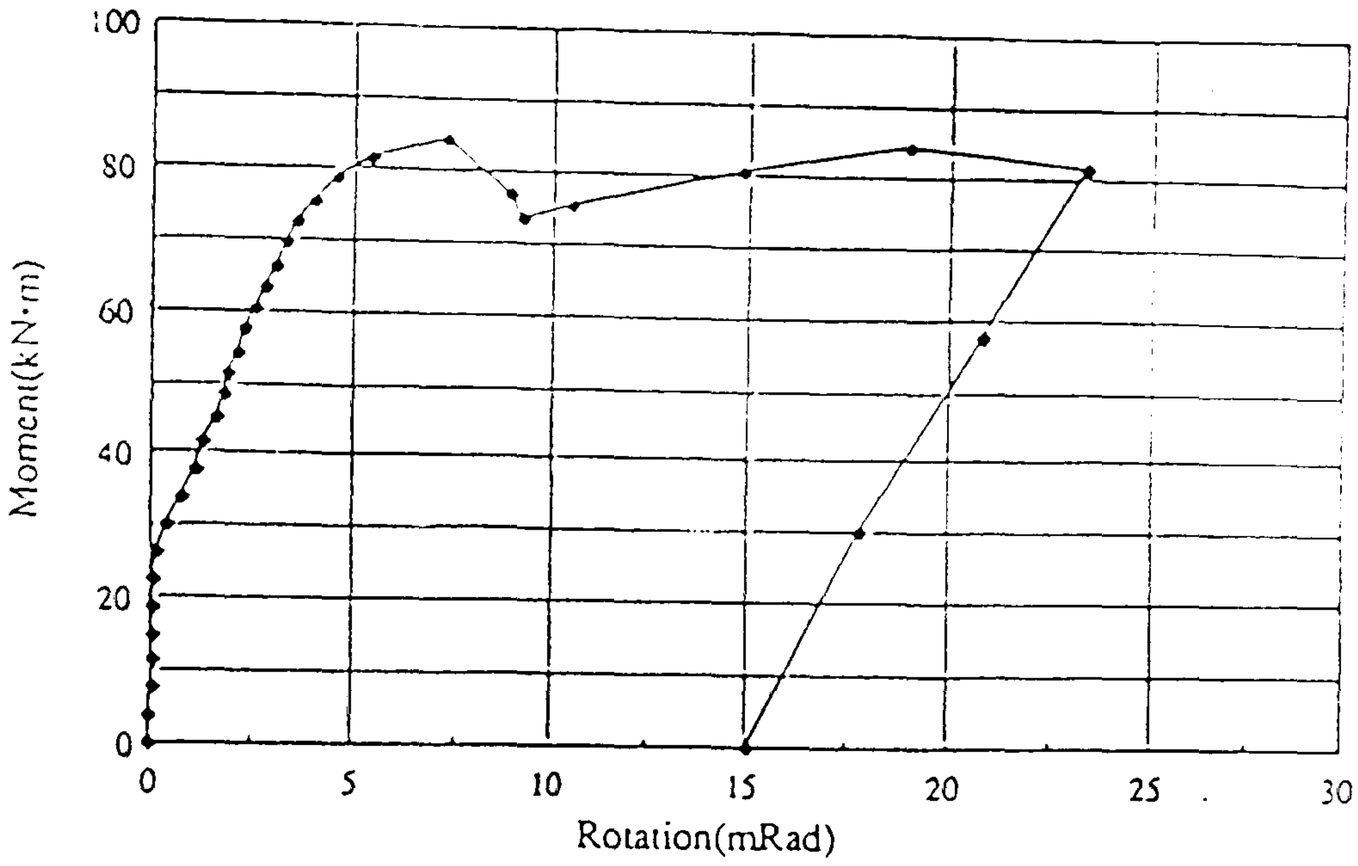

SCJ3 moment-rotation relation

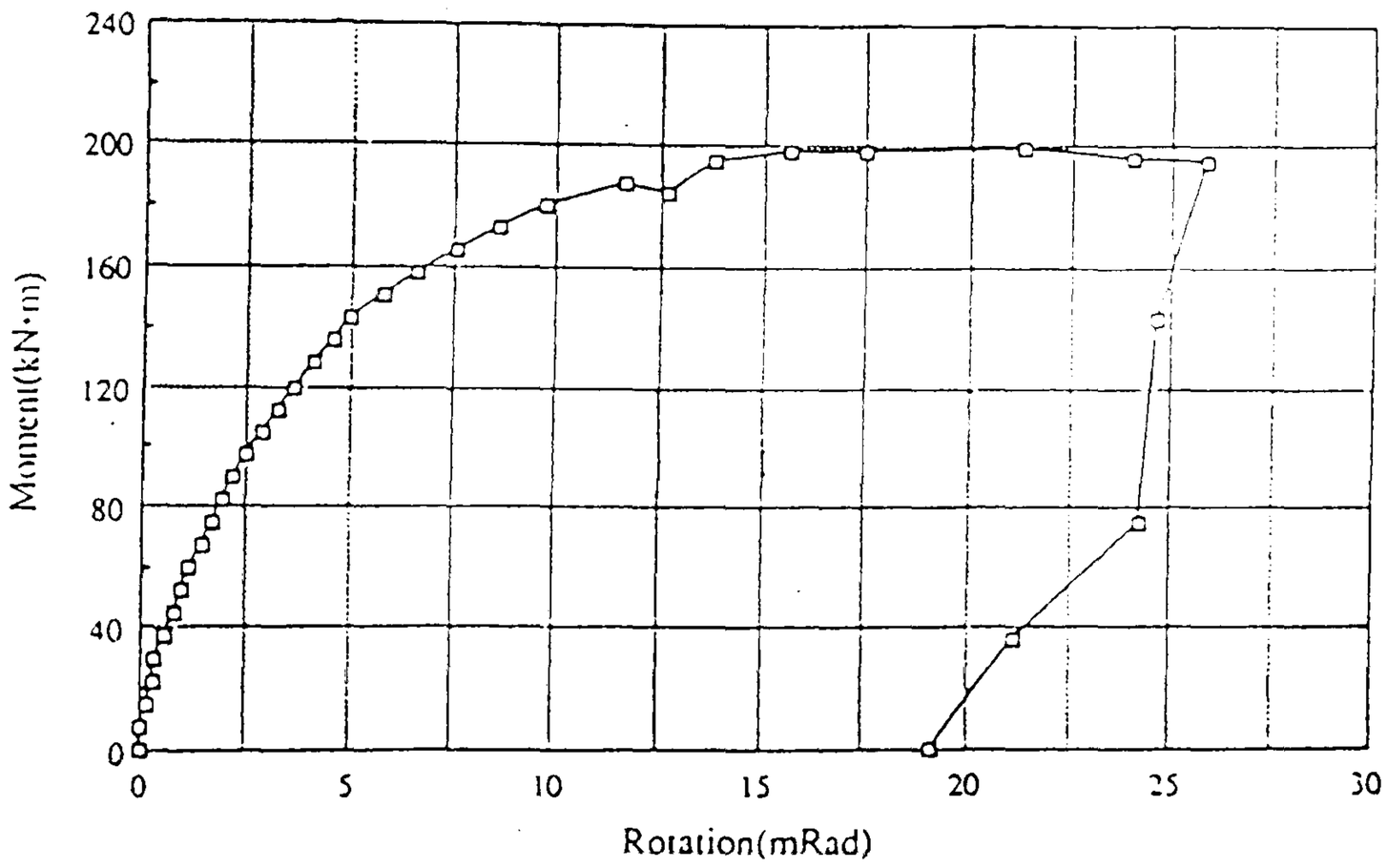

SCJ4 Moment-rotation relation

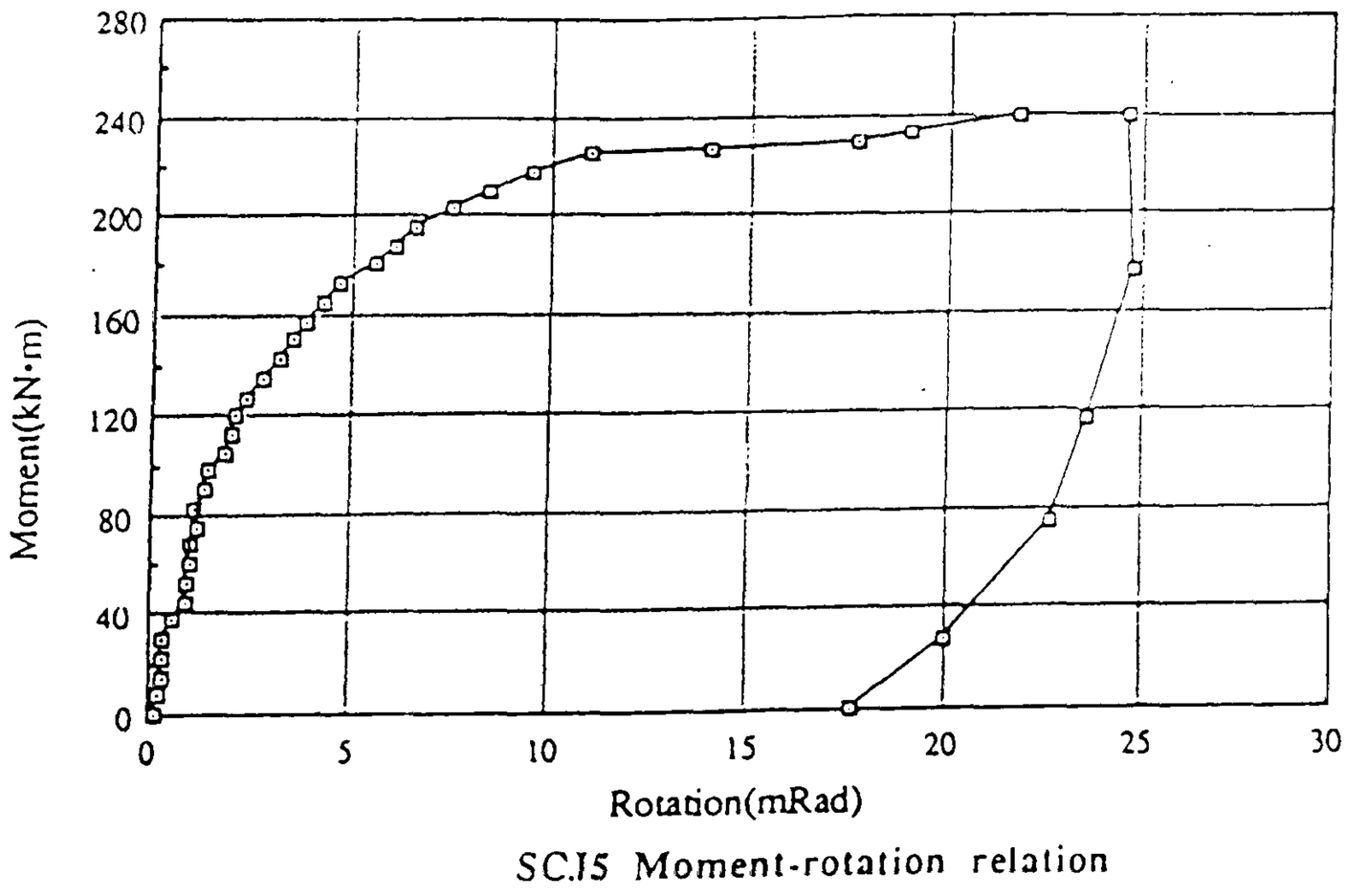

SCJ5 Moment-rotation relation

Figure 5.6: Moment-rotation characteristics from the programme undertaken by Xiao *et al*

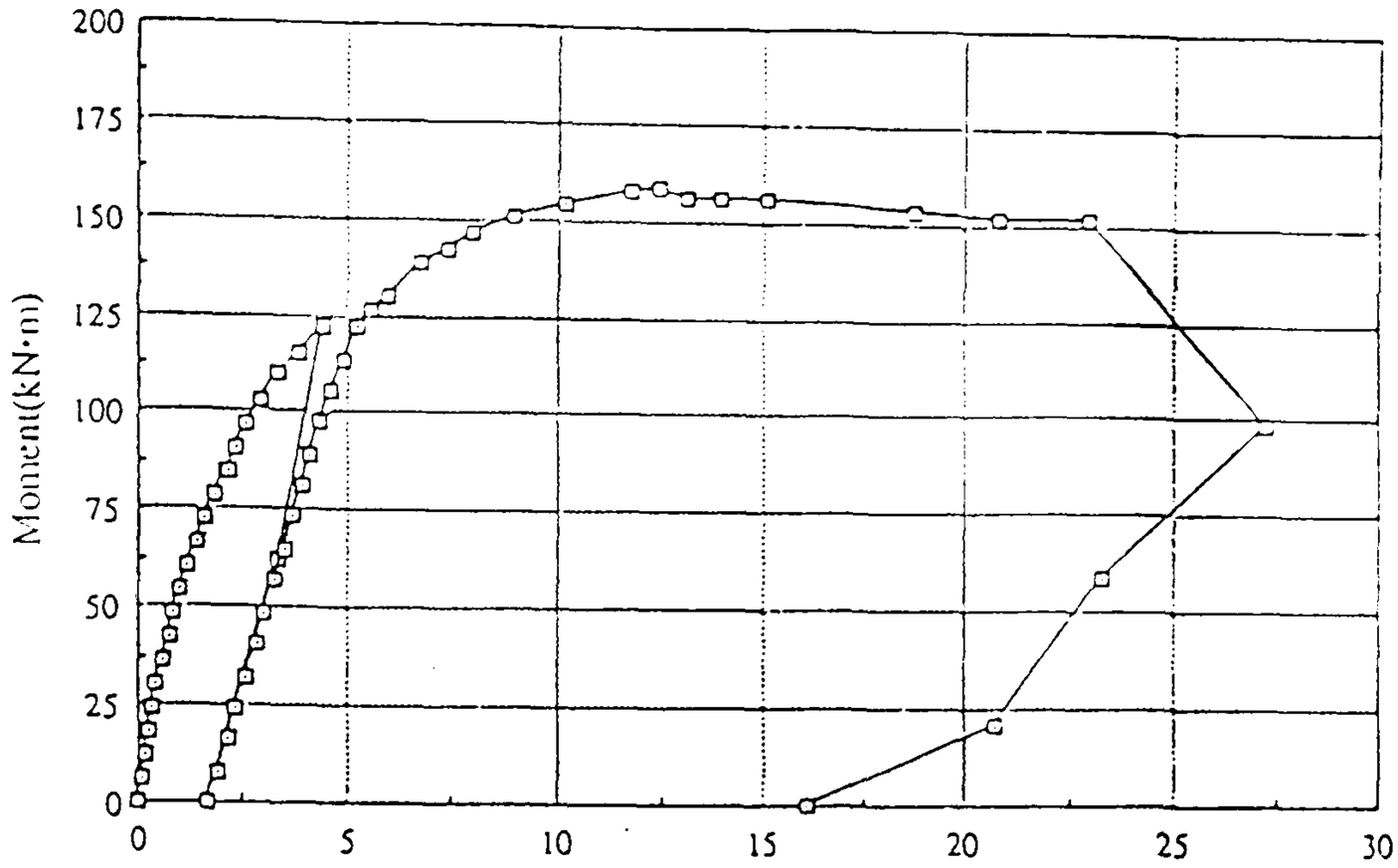

SCJ6 Moment-rotation relation

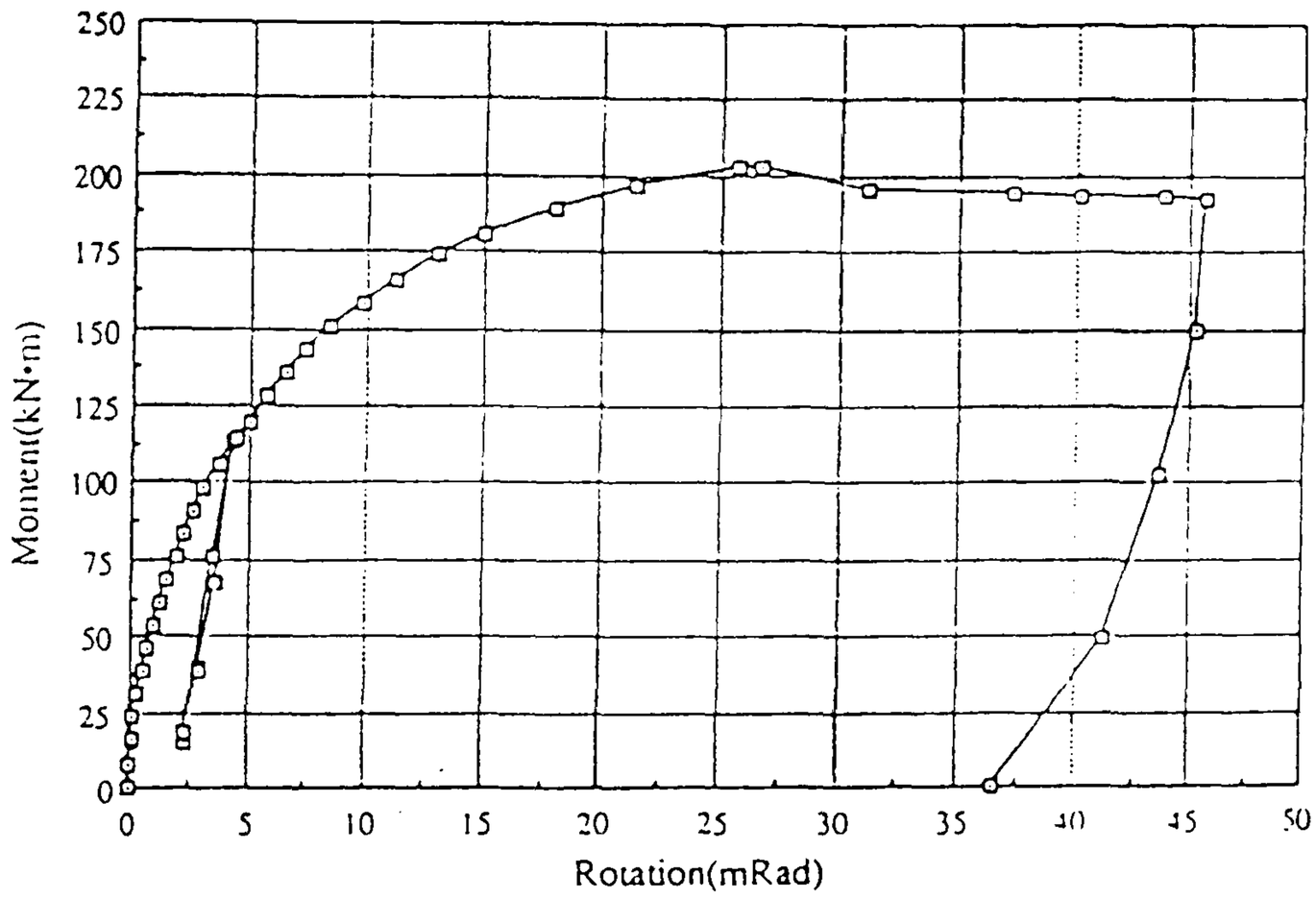

SCJ7 Moment-rotation relation

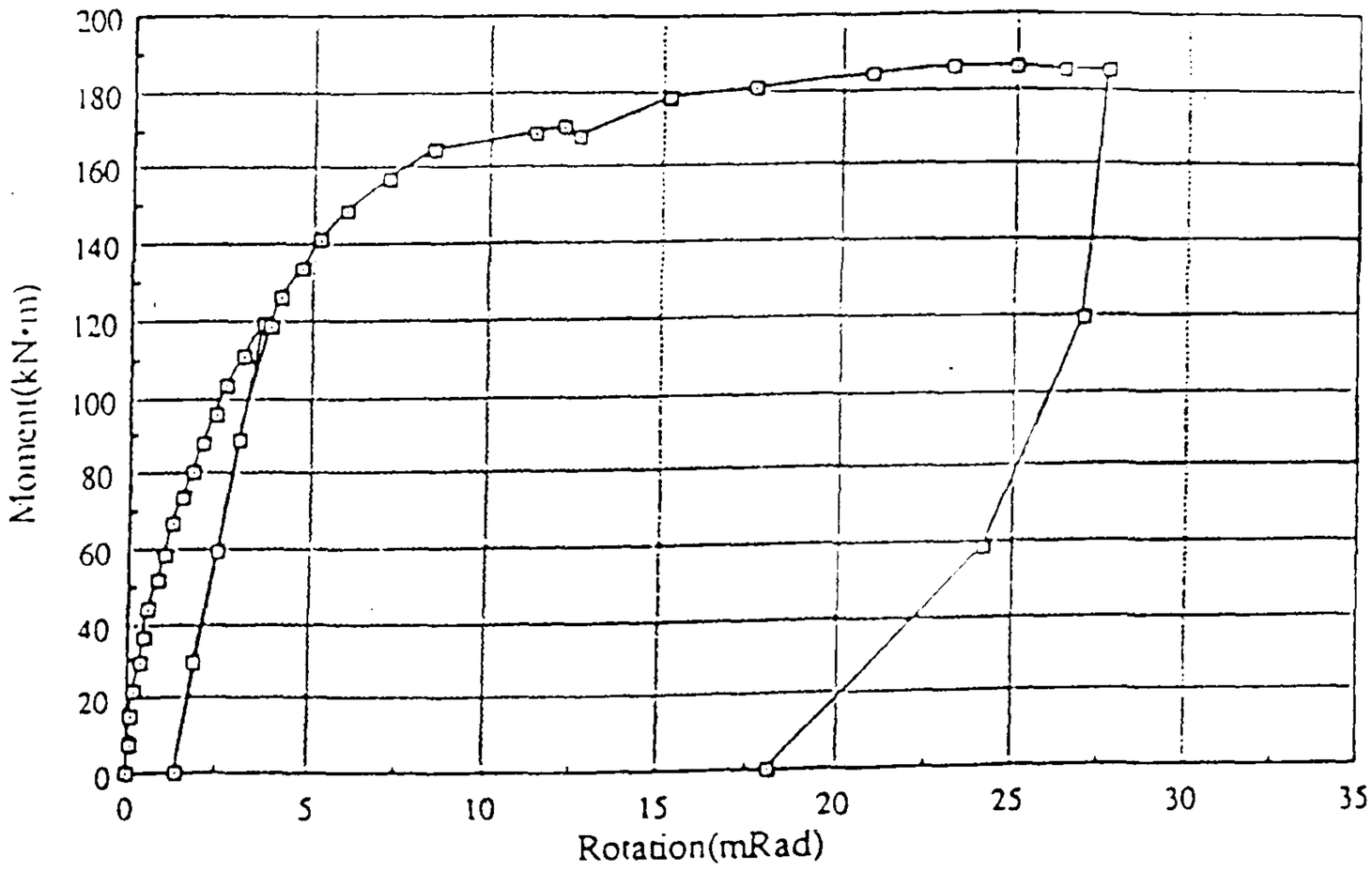

SCJ15 Moment-rotation relation

Figure 5.7: Moment-rotation characteristics from the programme undertaken by Xiao *et al*

Table 5.3: Experimental programme undertaken by Aribert *et al*

Author	Test reference	Type & size of connection (mm)	Beam section	Column section	Web reinforced	Concrete slab Depth (mm)	Reinforcement provided Re-bars Number & diameter	Reinforcement provided Re-bars Total steel area (mm^2)	Shear connection	Type of decking
Aribert & Lachal	**A1**	**Flush 400x200x15**	**IPE360**	**HEB200**	**At compression level**	**Control test : steel connection only**				
	A2	**Flush 400x200x15**	**IPE360**	**HEB200**		**120**	**10T8**	**503**	**19mm studs x 100mm long before welding**	**HI-BOND 55 1.2mm thick**
	A3	**Flush 230x200x15**	**HEA200**	**HEB200**		**120**	**10T8**	**503**		
	A4	**Flush 400x200x18**	**IPE360**	**HEA360**		**120**	**10T8**	**503**		
	B1	**Extended 453x200x15**	**IPE360**	**HEB200**		**Control test : steel connection only**				
	B2	**Extended 453x200x15**	**IPE360**	**HEB200**		**120**	**10T8**	**503**	**19mm studs x 100mm long before welding**	**HI-BOND 55 1.2mm thick**
	B3	**Extended 453x200x15**	**IPE360**	**HEB200**		**120**	**10T8**	**503**		
	C1	**Flush 400x200x15**	**IPE360**	**HEB200**		**120**	**14T8**	**704**	**Cold formed angles 80x60x24.3**	**COFRASTRA 40 0.8mm thick**
	C2	**Flush 400x200x15**	**IPE360**	**HEB200**		**120**	**14T8**	**704**		
	C3	**Flush 400x200x15**	**IPE360**	**HEB200**		**120**	**14T8**	**704**		

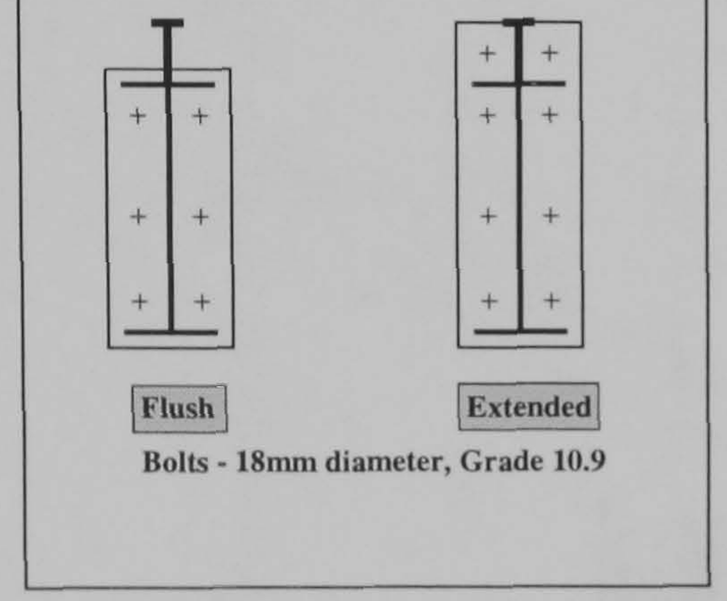

Test reference	Failure mode	Moment capacity of the connection M_c (kNm)	Rotation at connection failure ϕ_{ult} (mrads)
A1	**Fracture of tension bolts with plastic mechanism in the end plate**	**168**	**23**
A2	**Fracture of reinforcing bars followed by fracture of tension with a plastic mechanism in the end plate**	**296**	**31**
A3		**152**	**36**
A4		**297**	**39**
B1	**Fracture of tension bolts with significant deformation in the column flange and end plate**	**274**	**35**
B2	**Fracture of reinforcing bars simultaneously with two tension end bolts**	**376**	**38**
B3	**Fracture of four tension bolts (extended and end bolts) followed by fracture in the reinforcement**	**392**	**40**
C1	**Fracture of the tension bolts**	**344**	**28**
C2	**Fracture of the shear connectors**	**326**	**29**
C3		**288**	**21**

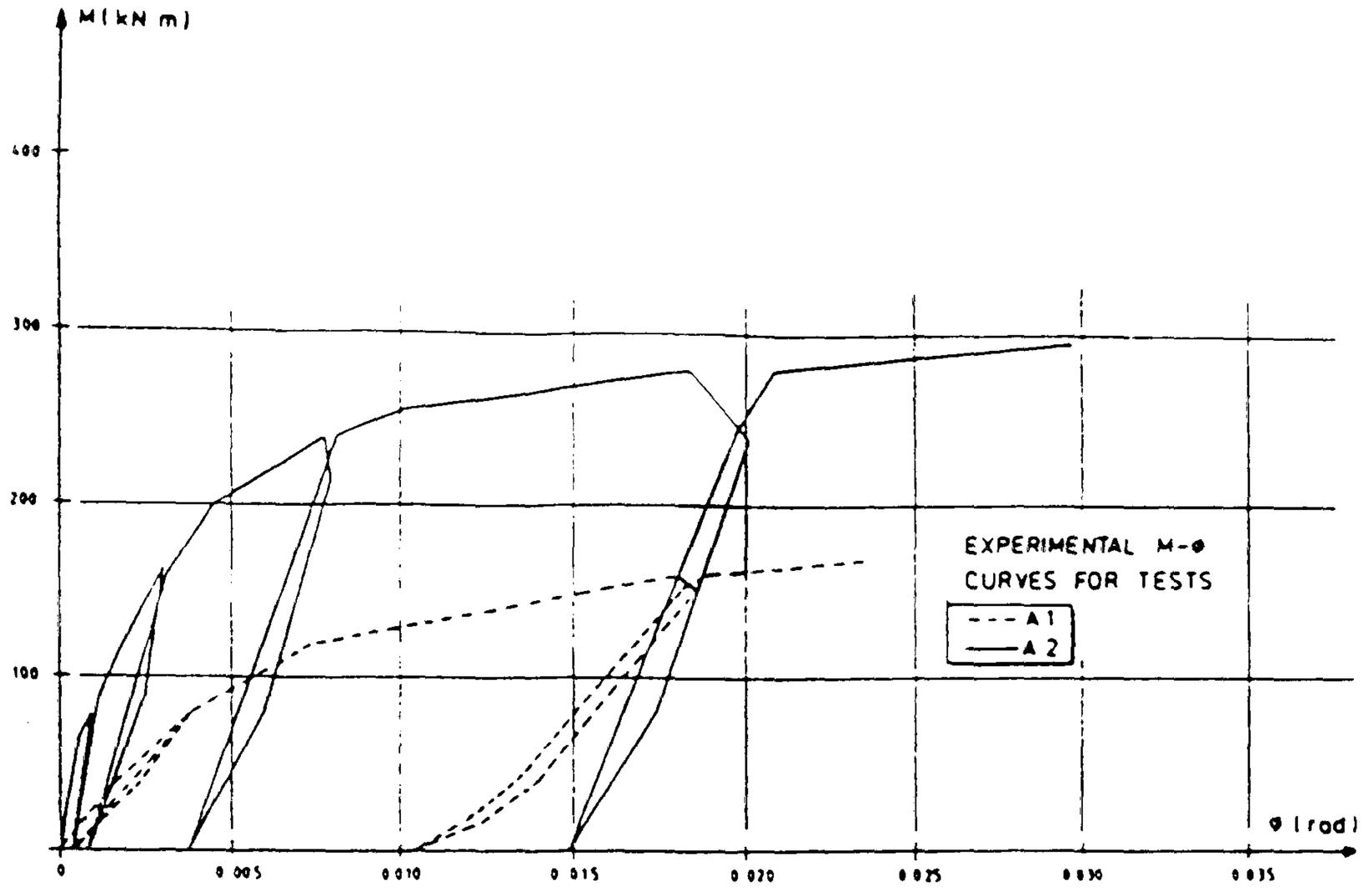

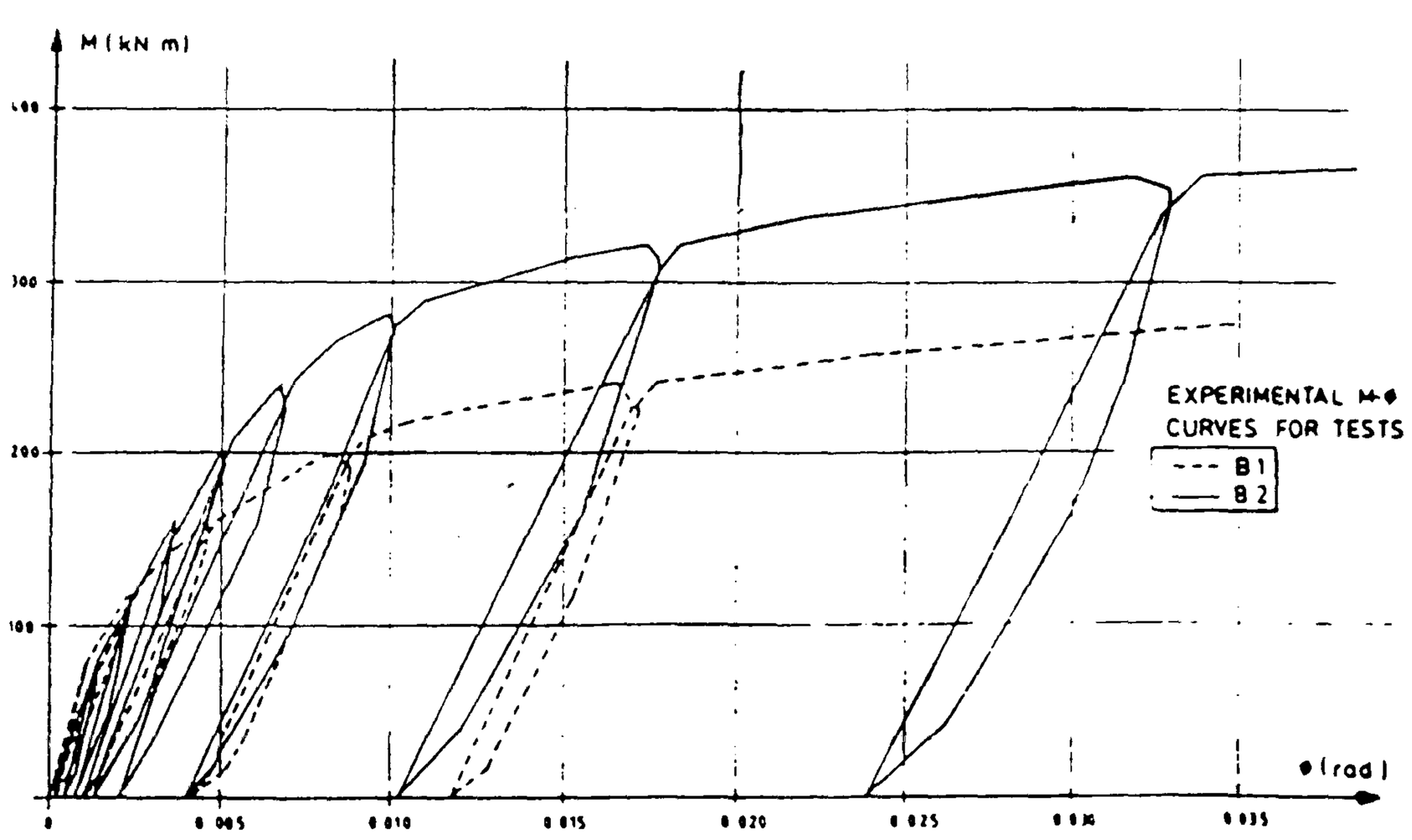

Figure 5.8: Moment-rotation characteristics from the programme undertaken by Aribert *et al*

Table 5.4: Experimental programme undertaken by Li *et al*

Author	Test reference	Type of connection	Beam section	Column section	Web reinforced	Concrete slab Breadth (mm)	Concrete slab Depth (mm)	Reinforcement : type provided — Number & diameter	Re-bars Total steel area (mm^2)	Re-bars % reinforcement	Shear connection	Type of decking	Test variables
Li, Nethercot & Choo	**SJS 1**	**Flush**	**254x102x25UB**	**203x203x46UC**	**Control test : Steel connection only**								
	CJS 1	**Flush**	**254x102x25UB**	**203x203x46UC**									
	CJS 2	**Flush**	**254x102x25UB**	**203x203x46UC**									
	CJS 3	**Flush**	**254x102x25UB**	**203x203x46UC**	**Bolted beam stub**	**1000**	**110**	**4T12 + 4T10**	**767**	**1.2**	**19mm studs x 100mm long before welding**	**PMF-CF46 0.9mm thick**	
	CJS 4	**Flush**	**254x102x25UB**	**203x203x46UC**									
	CJS 5	**Flush**	**254x102x25UB**	**203x203x46UC**									
	CJS 6	**Flush**	**254x102x25UB**	**203x203x46UC**									

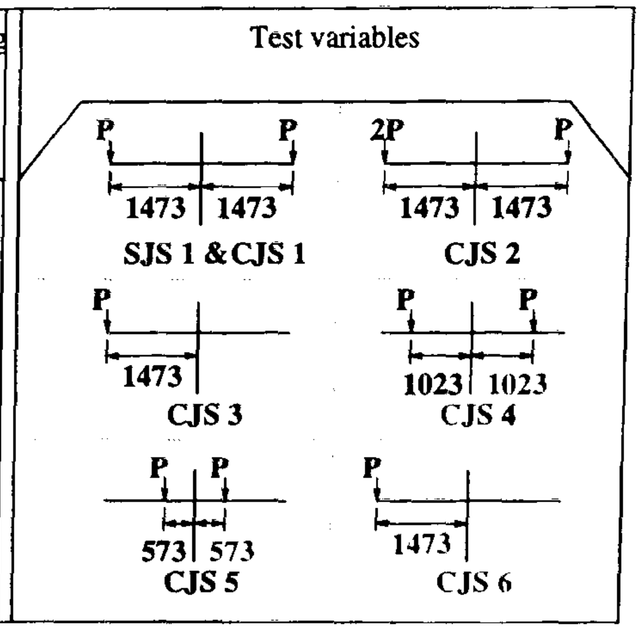

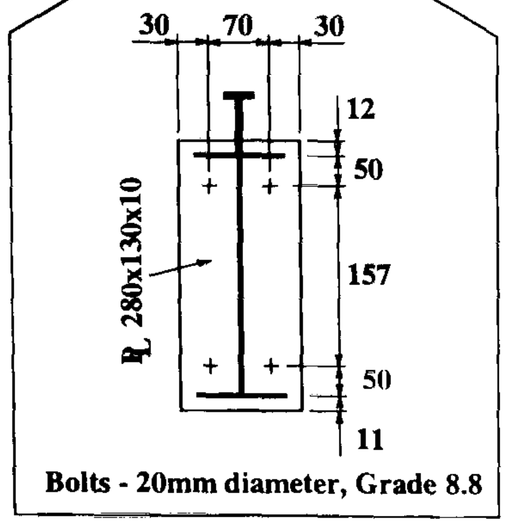

Test reference	Failure mode	Material properties — Steel members Yield strength (N/mm^2) Column web	Column flange	Beam web	Beam flange	Reinforcement Yield strength (N/mm^2) re-bars T10, T12	Moment capacity of the connection M_c (kNm)	Rotation at connection failure ϕ_{ult} (mrads)
SJS 1		**354**	**333**	**435**	**413**	**471, 488**	**63**	**57**
CJS 1		**354**	**333**	**435**	**413**	**471, 488**	**181**	**54**
CJS 2	Buckling of **beam flange and web**	**354**	**333**	**435**	**413**	**471, 488**	**173**	**63**
CJS 3		**354**	**333**	**435**	**413**	**471, 488**	**149**	**78**
CJS 4		**354**	**333**	**435**	**413**	**471, 488**	**160**	**60**
CJS 5	**Failure of the slab in shear**	**354**	**333**	**435**	**413**	**471, 488**	**195**	**51**
CJS 6	Buckling of **beam flange and web**	**354**	**333**	**435**	**413**	**471, 488**	**174**	**84**

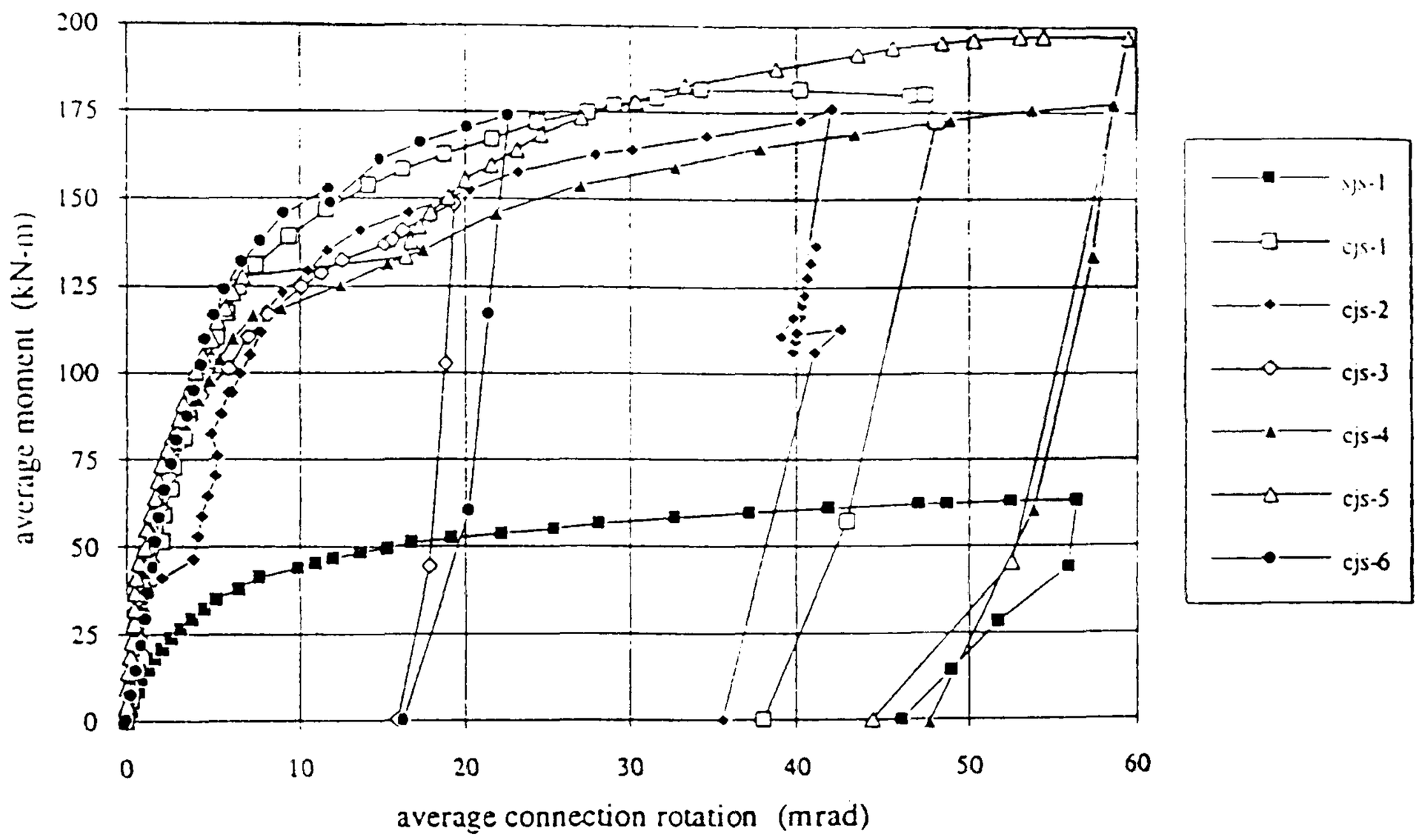

Figure 5.9: Moment-rotation characteristics from the programme undertaken by Li *et al*

Table 5.5: Experimental programme undertaken by Johnson and Law, Benussi *et al* and Ren and Crisinel

Author	Test reference	Type of connection	Beam section	Column section	Web reinforced	Concrete slab Breadth (mm)	Concrete slab Depth (mm)	Reinforcement : type provided — Mesh	Re-bars Number & diameter	Re-bars Total steel area (mm^2)	Re-bars % reinforcement	Shear connection	Type of decking
Johnson & Law	**JX 1**	**Flush**	**457x191x67UB**	**203x203x46UC**	**N/A**	**1400**	**125**	**Y10 @ top + Y12&Y8 @ bottom**	**8T10**	**628**	**1.0**	**19mm studs x 100mm long before welding**	**N/A**
	JX 2	**Flush**	**457x191x67UB**	**203x203x46UC**	**Encased**	**1400**	**125**		**8T10**	**628**	**1.0**		**N/A**
	JC 1	**Flush**	**457x191x67UB**	**203x203x46UC**	**Encased**	**1400**	**125**		**8T10**	**628**	**1.0**		**N/A**
	JC 2	**Flush**	**457x191x67UB**	**203x203x46UC**	**Encased**	**1400**	**200**		**8T10**	**628**	**0.6**		**N/A**
Benussi & Zandonini	**SJB 10**	**Flush**	**IPE300**	**HEB260**	**At compression level**	**1000**	**120**	**8T6 +T6 stirrups @ 150 centres**	**8T10**	**628**	**0.7**	**20mm studs x 100mm long before welding**	**N/A**
	SJB 14	**Flush**	**IPE300**	**HEB260**		**1000**	**120**		**8T14**	**1232**	**1.02**		**N/A**
Ren & Crisinel	**CP 01**	**Flush**	**IPE330**	**HEB240**	**N/A**	**-**	**120**	**K188**	**4T12**	**452**	**-**	**-**	**N/A**
	SP 11	**Flush**	**IPE330**	**HEB240**	**N/A**	**Control test : Steel connection only**							

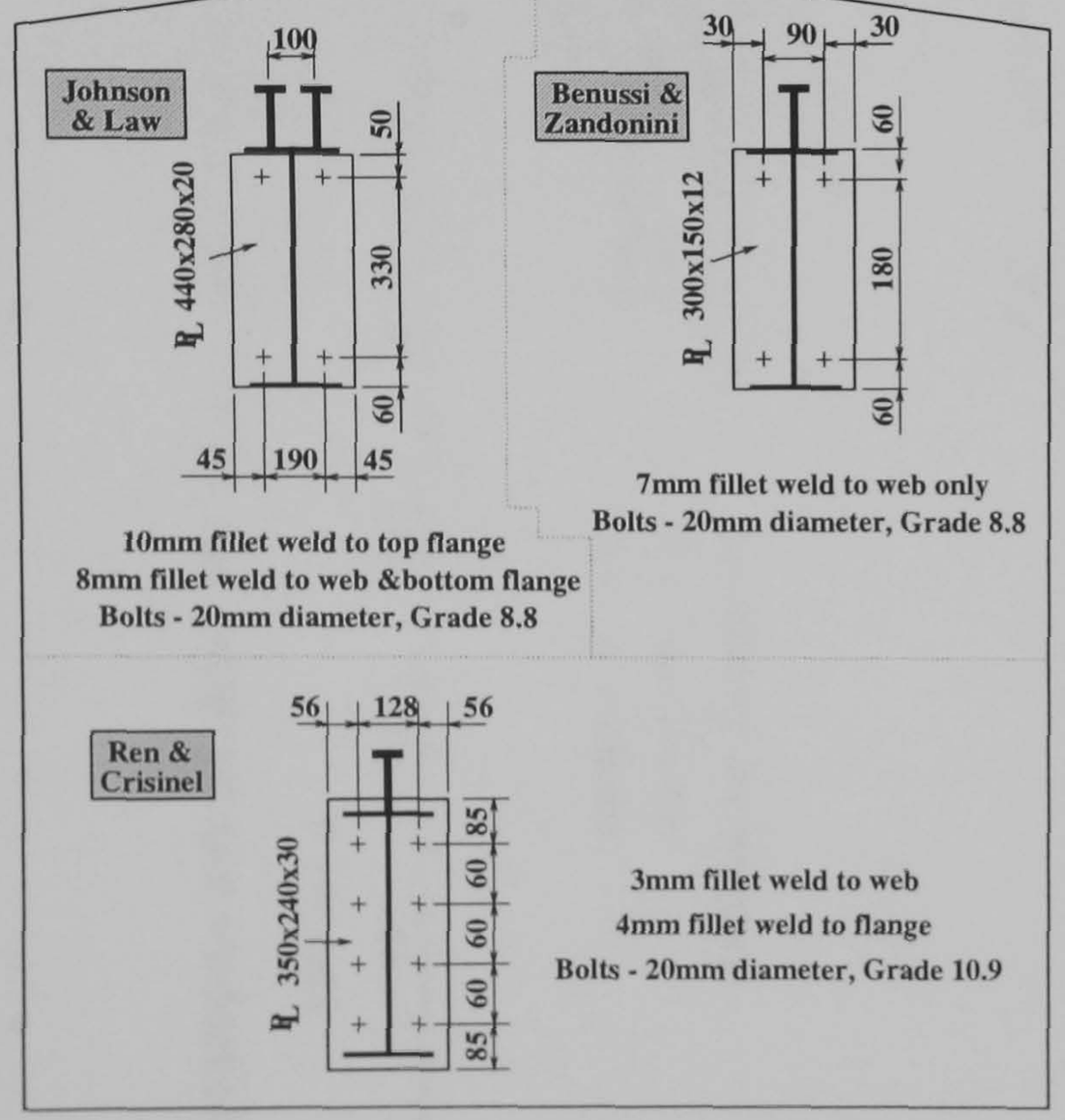

Test reference	Failure mode	Material properties — Steel members Yield strength (N/mm^2) Column web	Column flange	Beam web	Beam flange	Reinforcement Yield strength (N/mm^2) re-bars	Moment capacity of the connection M_c (kNm)	Rotation at connection failure ϕ_{ult} (mrads)
JX 1	**Excessive joint deformation**	**-**	**246**	**251.2**	**278.1**	**461**	**354**	**24**
JX 2	**Excessive joint deformation**	**-**	**-**	**251.2**	**278.1**	**461**	**370**	**35**
JC 1	**Fracture of slab reinforcement**	**-**	**251.3**	**262.4**	**279.3**	**461**	**449**	**19**
JC 2	**Fracture of slab reinforcement**	**-**	**251.3**	**262.4**	**279.3**	**461**	**530**	**18**
SJB 10	**Excessive joint deformation**	**-**	**-**	**-**	**-**	**495**	**208**	**>22**
SJB 14	**Local buckling of beam flange/web**	**-**	**-**	**-**	**-**	**413**	**261**	**24**
CP 01	**Concrete slab failure**	**357**	**310**	**315**	**291**	**634**	**250**	**11**
SP 11	**Local buckling of column web**	**357**	**310**	**315**	**291**	**634**	**155**	**62**

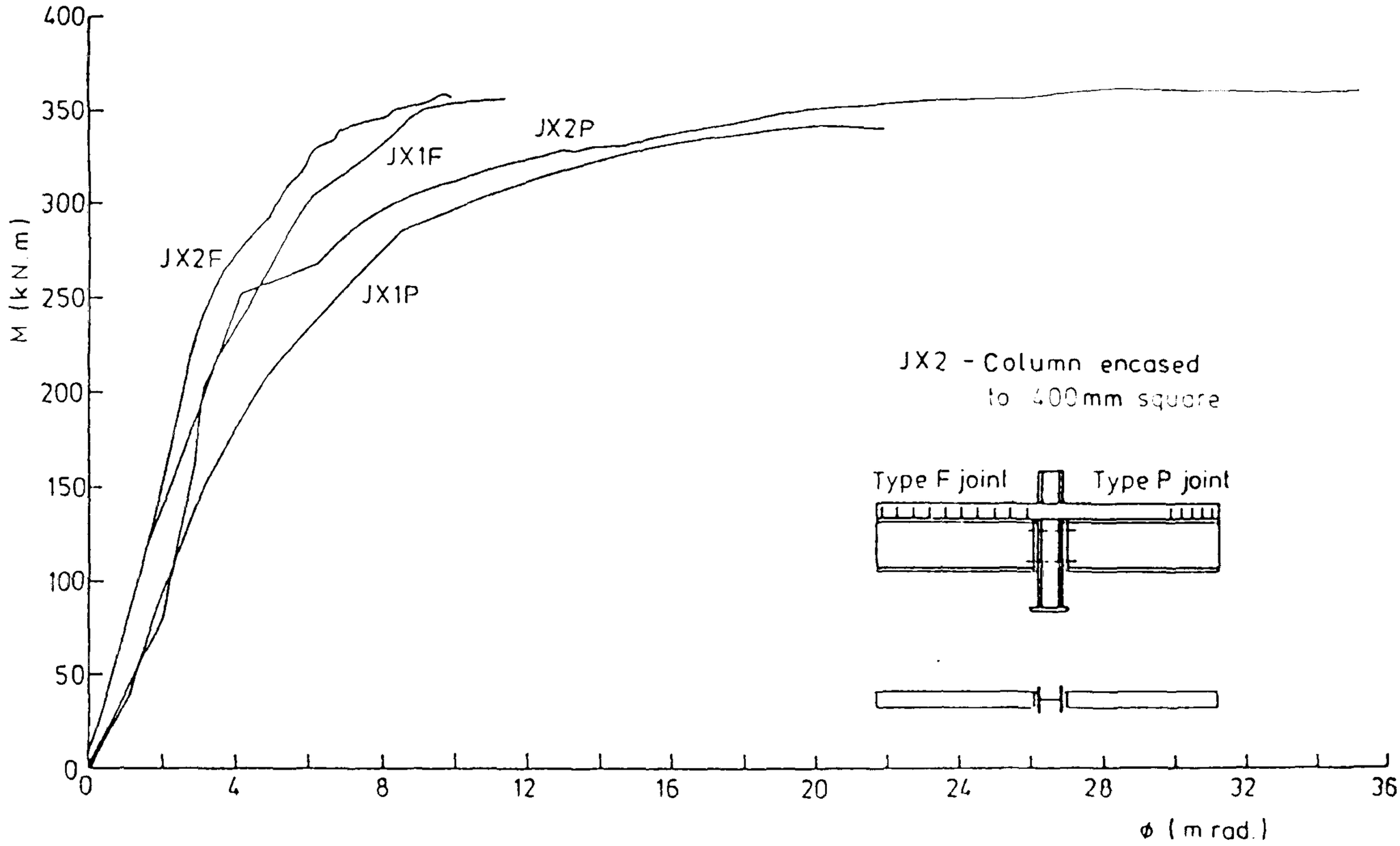

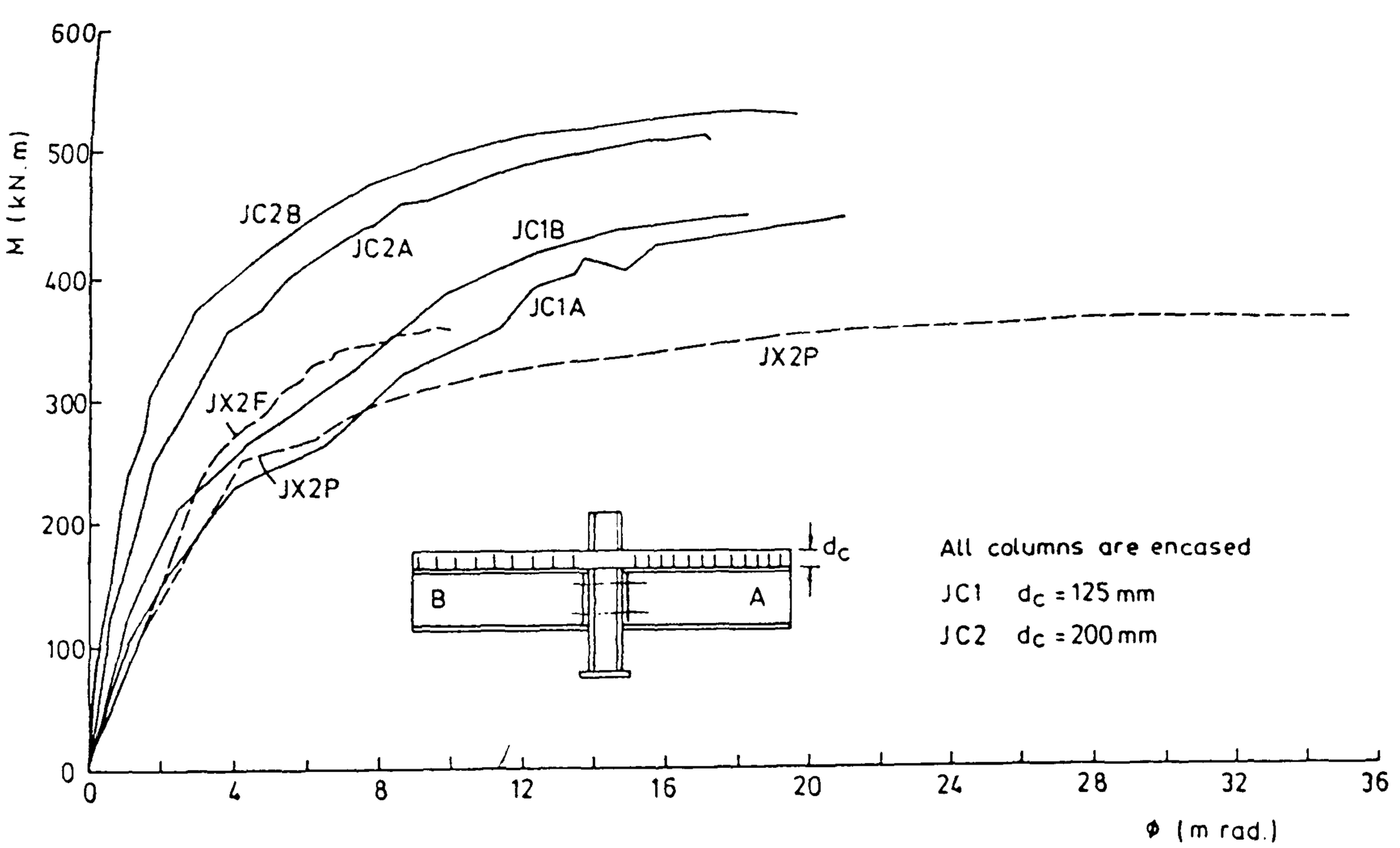

Figure 5.10: Moment-rotation characteristics from the programme undertaken by Johnson and Law

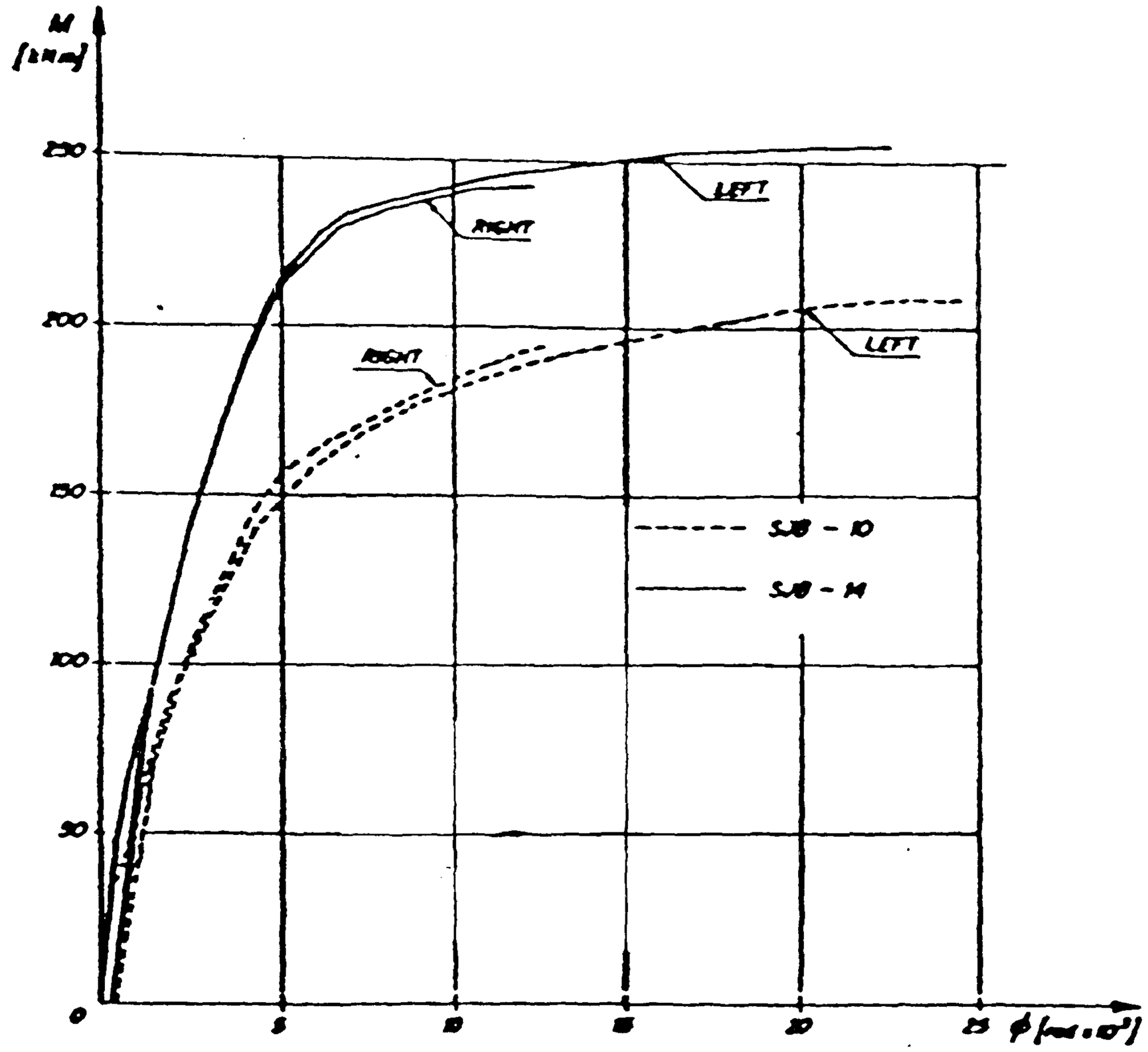

Figure 5.11: Moment-rotation characteristics from the programme undertaken Benussi *et al*

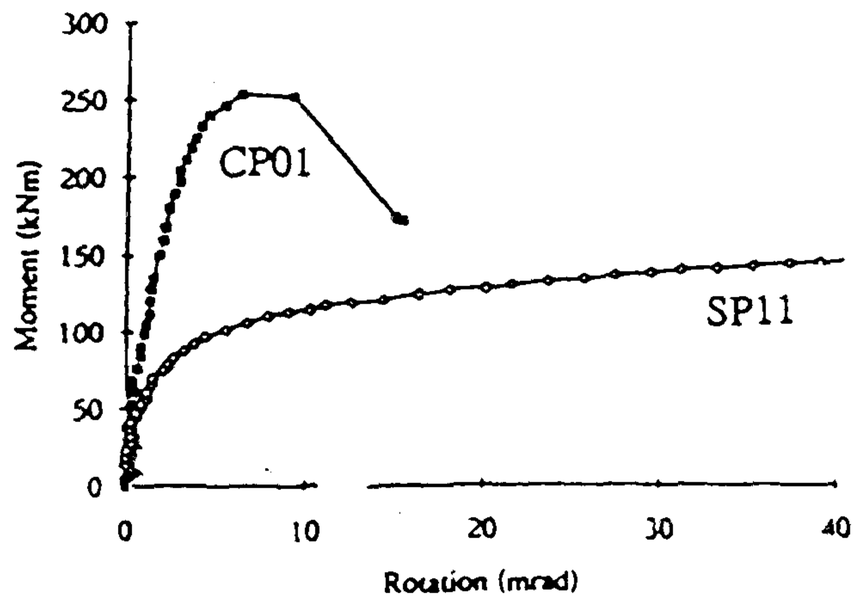

Figure 5.12: Moment-rotation characteristics from the programme undertaken and Ren and Crisinel

Chapter 6

Test configurations and instrumentation

According to Eurocode 4[60], for a connection to be considered in the context of providing composite action, it should be reinforced in such a manner that the reinforcement would contribute to its overall moment of resistance. Connection configurations which meet this criteria have been discussed in Chapter 5, where it has been established that to achieve this enhanced performance, the slab reinforcement would generally take the form of high tensile steel bars which run continuously past the column in a symmetrical formation.

To enable plastic methods of structural analysis to be applied to a braced composite structure, the internal connections must be capable of redistributing bending moments to the midspan region whilst maintaining their enhanced moment resistance. To enable this to happen, the connection detail must be capable of deforming in a ductile manner, with sufficient rotation capacity for the assumed redistribution to occur.

Five connection tests were commissioned by the Building Research Establishment and carried out by the author. All the tests represented major axis, internal beam-to-column connections and were thus configured in a cruciform arrangement.

The end plate connections were designed in accordance with European codes of practice[17, 60]. The shear resistance for each connection was provided by two rows of bolts positioned in the compression region of the connection. This accords with everyday practice, which assumes that shear is only resisted by the bolts adjacent to the lower flange. Consequently, this allows the full tensile capacity of the bolts positioned just beneath the top flange to be utilised when calculating the moment of resistance of the connection.

6.1 Experimental programme

Unless otherwise stated, the common parameters between the composite tests are indicated in Figure 6.1

Decking	**PMF46** - orientated transversely with respect to the beam direction
Effective breadth	**1100mm**
Overall slab depth	**120mm**
Full shear connection	**7 no. 19mm diameter studs on each beam**
Main longitudinal reinforcement	**4 no. T16 bars**
Secondary reinforcement	**A142 mesh** - arranged symmetrically about the centre lines of the column
Cover to reinforcement	**25mm**
Concrete compressive strength	**Nominally 30 N/mm^2** - cube strength
Lever arm for the applied moment	**1410mm**
Steel section	**457x152x52 Universal beam**
Column section	**203x203x52 Universal column**
End plate thickness	**15mm**
Structural grade for the steel	**Grade 43 (S275)**
Bolt specification	**M20, structural grade 8.8**

Figure 6.1: Common parameters between the composite connection tests

Test 1 : Steel only (non-composite) comprising two 457x152x52 universal beams connected to a 203x203x52 universal column. This test was designed to provide a control for the following 3 composite tests, by enabling the behaviour of the steel sections to be studied in isolation. This would allow the change in the connection behaviour due to the beams acting compositely with a reinforced concrete slab to be compared. The steelwork fabrication drawings for this and the subsequent composite tests are illustrated by Figure 6.2.

Test 2 : This was the first of the series of composite connection tests. The primary slab reinforcement consisted of four 16mm bars grouped closely together on either side of the column. Details for the reinforcing arrangements for this and the subsequent tests may be obtained from the general arrangement drawing (see Figure 6.3). The reinforcement arrangement adopted differs from that used in previous tests[9], in which the bars were uniformly spaced over the width of the slab. Where the secondary mesh reinforcement had to be cut to accommodate the column section, continuity was restored in the longitudinal direction by securing additional reinforcement. This additional reinforcement was created by separating the mesh into individual lengths sufficient to enable an overlap of at least 150mm. The mesh was non-continuous in the transverse direction for all the composite tests.

Test 3 : For this composite connection the primary reinforcement was the same as for test 2, except that the transverse spacing between the bars was increased to the maximum allowed by current codes of practice[89]. The secondary reinforcement consisted of A142 mesh; however for this and for the subsequent tests, no attempt was made to restore continuity in the longitudinal direction.

Test 4 : The primary and secondary reinforcement for this composite test were identical with that adopted for test 3. The difference in this test was the end plate thickness being reduced from 15mm to 10mm. It was anticipated that the deformation of the column flange in the tension region would reduce significantly as a result of this change of thickness. Consequently the rotational deformation

of the connection should be primarily associated with the deformation characteristics of the end plate. The intention of this test was to determine the influence of the end plate thickness on the resistance and rotation capacity of the composite connection. In addition for this test and the final test, the bolt size was increased from M20 to M24. However, the structural grade of the bolts was maintained. The justification for increasing the bolt size for the final two tests was the necessity to lower the risk of the mode of failure being bolt fracture occurring in the tension region of the connection. This failure mode was considered unacceptable, on the grounds that the experimental programme was being conducted in an open laboratory.

Test 5 : The final composite test comprised of much larger beam and column sections. A 533x210x82 universal beam was connected to a 254x254x73 universal column. The end plate thickness was restored to 15mm, and the main and secondary reinforcements were similar to tests 3 and 4. The difference in the reinforcing arrangement was the result of having to increase the horizontal spacing between the internal rebars to accommodate the larger column section. The purpose of this test was to provide evidence on the behaviour of a beam that is towards the upper end of the range of universal beams, likely to be incorporated into a composite building frame.

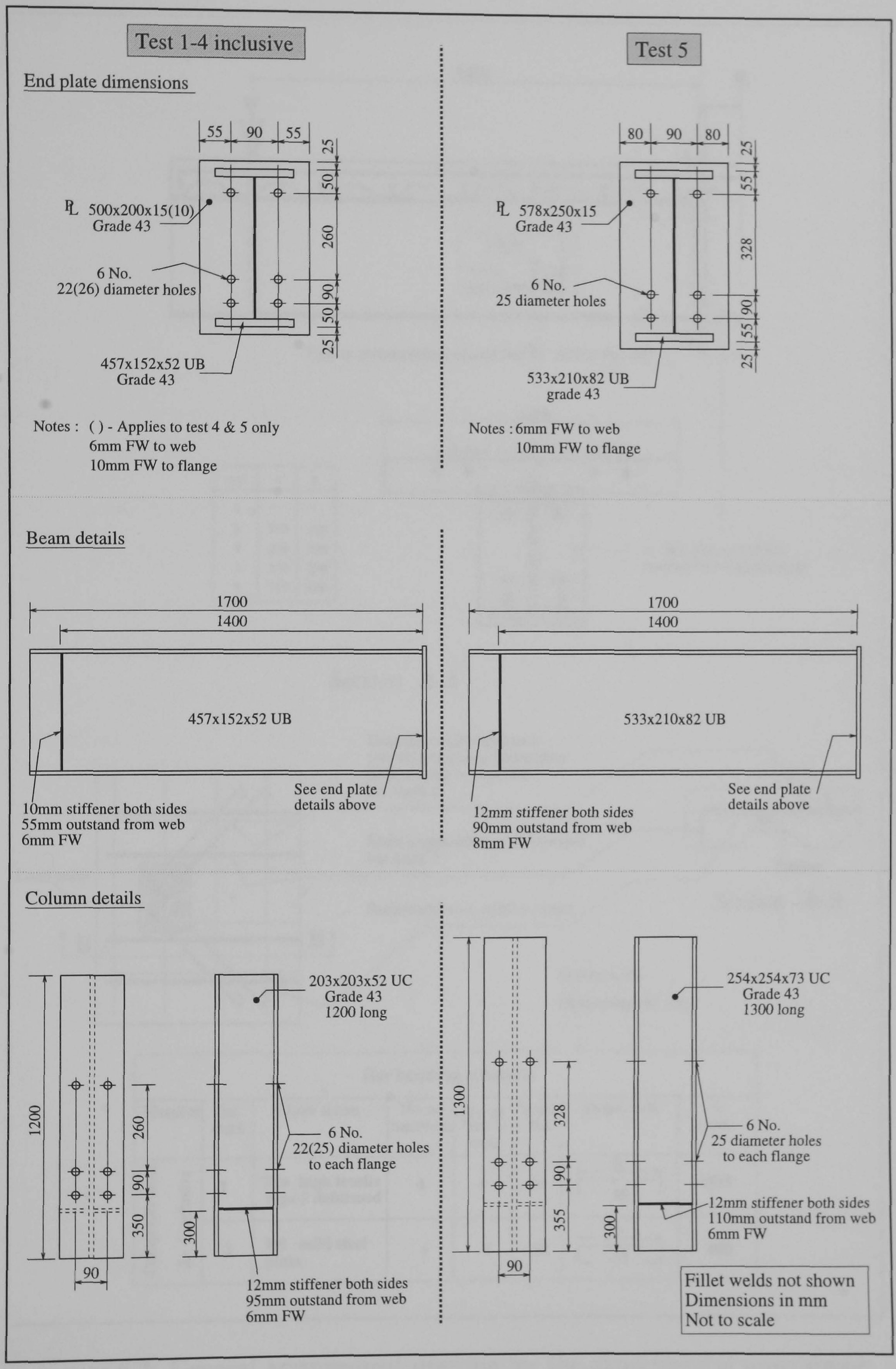

Figure 6.2: Steelwork fabrication drawings

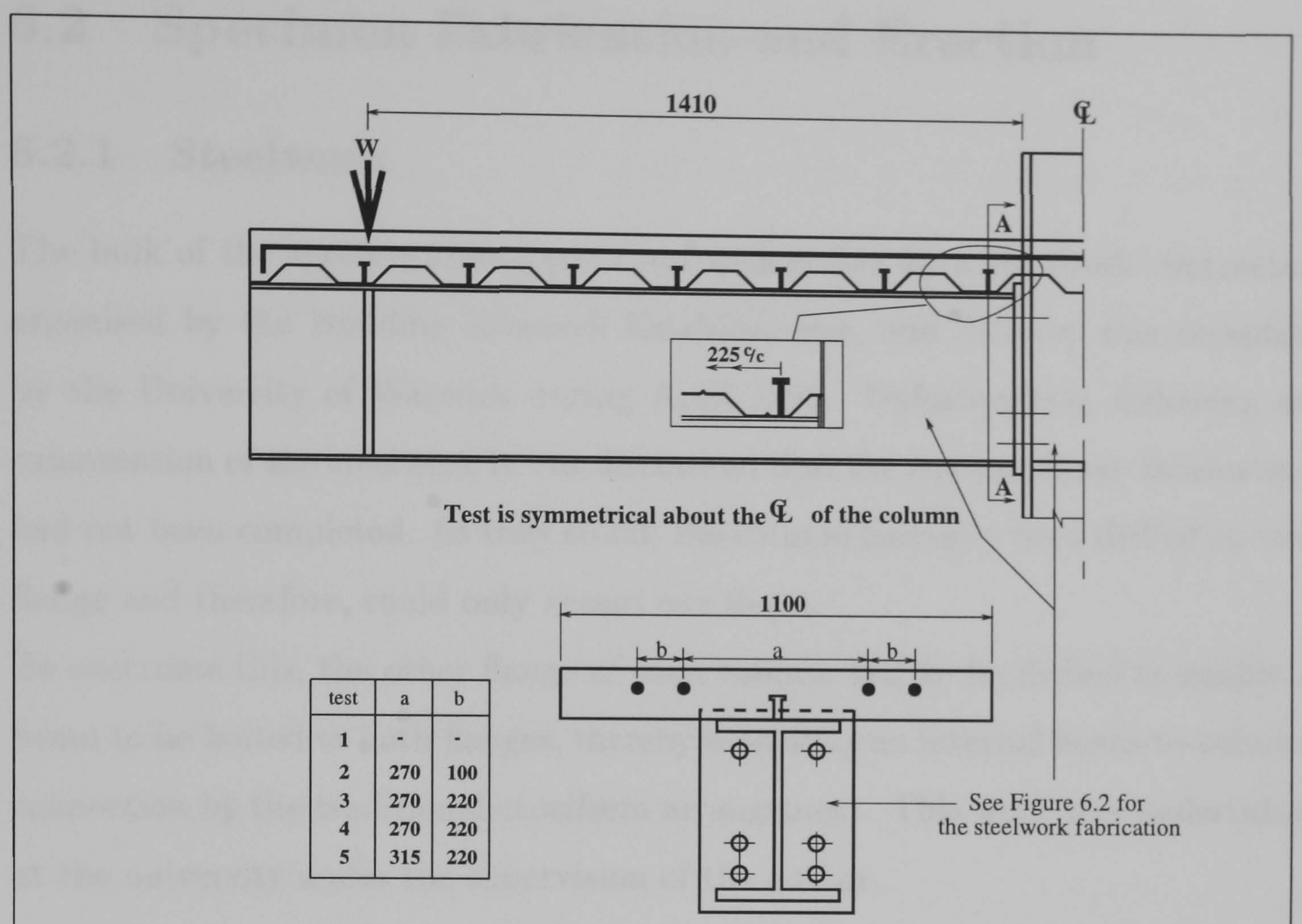

test	a	b
1	-	-
2	270	100
3	270	220
4	270	220
5	315	220

Section A-A

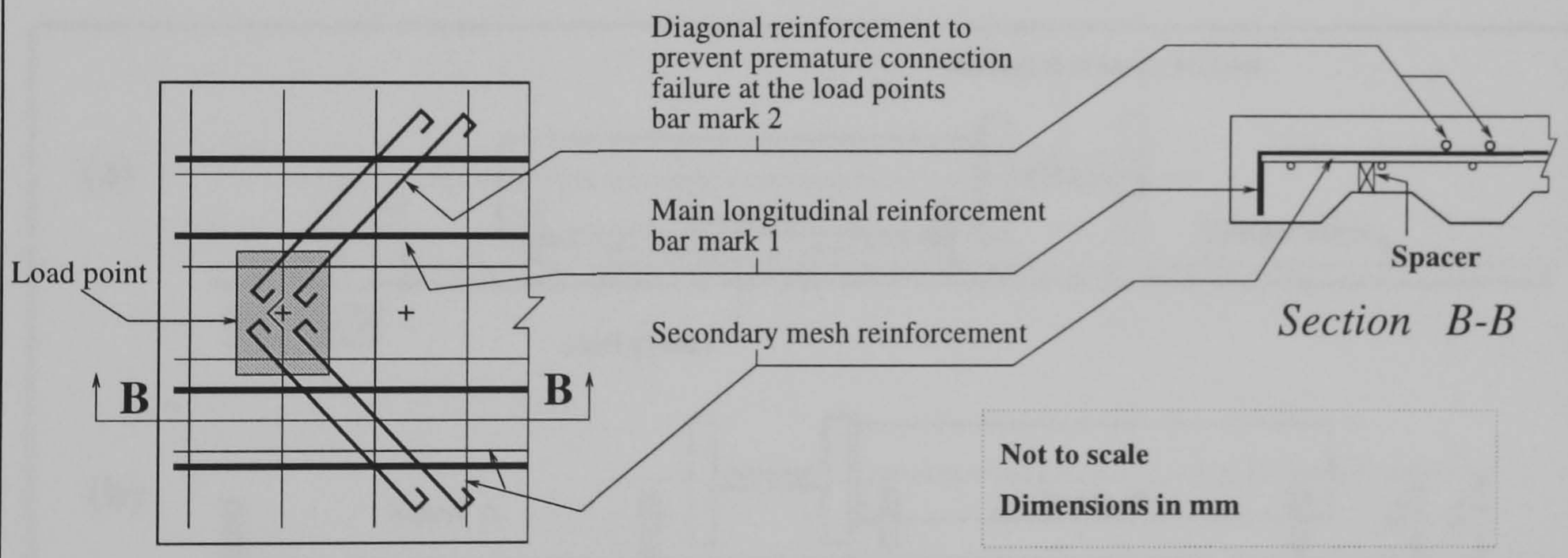

Section B-B

Not to scale

Dimensions in mm

Bar bending schedule

Member	Bar mark	Type &size	No. of members	No. of bars in each	Total No.	Shape code	A (mm)
Composite tests 2 - 4 inclusive	1	T16 high tensile type 2 deformed	4	4	16	A 35	3585
	2	R8 mild steel plain	4	8	32	A 33	600

Figure 6.3: General arrangement drawing for the experimental programme

6.2 Specimen Fabrication and Erection

6.2.1 Steelwork

The bulk of the specimen fabrication was undertaken by a steelwork contractor organised by the Building Research Establishment, and delivery was accepted by the University of Warwick during April 1993. Unfortunately, following an examination of the steelwork it was discovered that the column flange fabrication had not been completed. As they stood, the column had only been drilled on one flange and therefore, could only accept one beam.
To overcome this, the other flange of each column had to be drilled to enable a beam to be bolted to both flanges, thereby modelling an internal beam-to-column connection by the traditional cruciform arrangement. This work was undertaken at the university under the supervision of the author.

To enable the drilling operation to be completed, the column flanges were initially marked out and the beams aligned by adopting the following procedures.

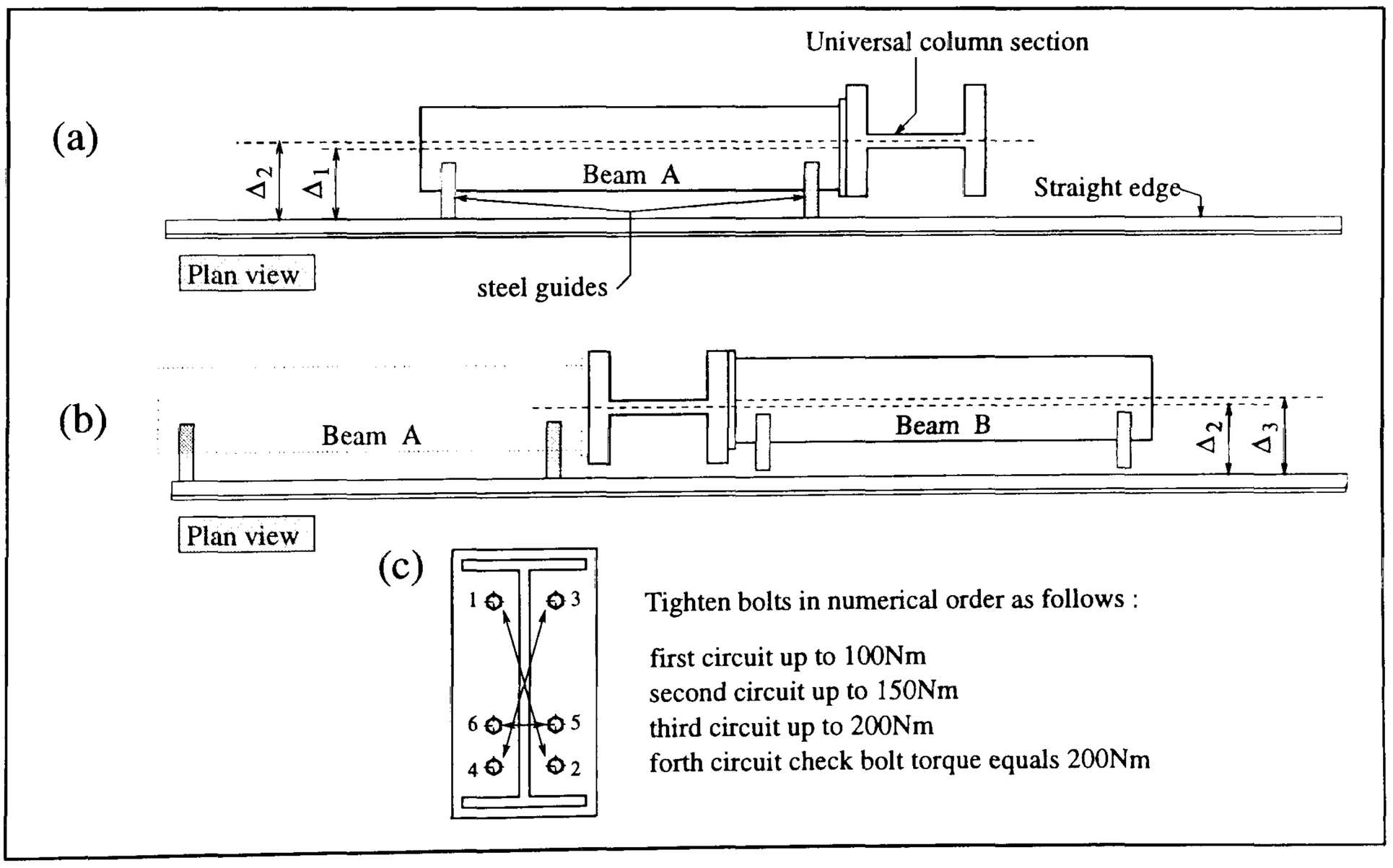

Figure 6.4: Steelwork errection

1. An elevated horizontal surface consisting of two separately levelled and aligned tables, to support the beams, were set out in the laboratory with a 300mm gap between them to accept the column. Alignment of the members was achieved by using a long straight edge, which was checked for its straightness using the diagonal length of a surface table. The level of each table surface was adjusted by placing metal shims beneath the table legs where necessary and checked using a spirit level. The first beam, denoted A in Figure 6.4(a), was then positioned on one of the tables, such that its top flange was horizontal in both the perpendicular and parallel directions in relation to the length of the beam. This was achieved by tapping small wooden wedges beneath the bottom flange.

2. The column was then positioned between the tables and loosely bolted to the beam. A spirit level was used to ensure column verticality prior to tightening the bolts to prevent further movement.

   Two steel guides were then secured to the top flange of the beam. The straight edge was then offered up to the guides and measurements between the edge and the beam's centre line (denoted Δ_1) and the edge and the column's centre line (denoted Δ_2) were recorded (see Figure 6.4(a)). The column was then moved horizontally such that the difference between the two measurements tended to zero.

   The first misalignment imperfection φ_1 could then be described mathematically in accordance with equation 6.1.

$$\varphi_1 = \Delta_2 - \Delta_1 \tag{6.1}$$

3. Beam B was then positioned flush against the insitu column, such that the bolt holes in the pre-drilled end plate were equidistant either side of the column web, ensuring that the beam's top flange was horizontal by the method described previously. The assembly was then clamped in position.

The centre of the bolt holes to be drilled were marked on the column flange by punching through the pre-drilled end plate, using a 22mm diameter centre-punch. Identifying marks were then painted on to the beams together with their respective column flanges, to enable re-assembly at a later date.

4. The remainder of the steelwork for each test was then erected by repeating the majority of the above procedure; however this time the second beam was bolted in position rather than being clamped. The erection was then completed by adopting the following procedure.

5. Two further steel guides were secured to beam B (see Figure 6.4(b)), in a similar manner to that described previously. The straight edge was offered up to the guides and measurements between the edge and the column's centre line (denoted Δ_2) and the edge and the beam's centre line (denoted Δ_3) were recorded. The second misalignment imperfection φ_2 could then be expressed mathematically by equation 6.2.

$$\varphi_2 = \Delta_2 - \Delta_3 \tag{6.2}$$

Taking the column centre line as the datum, a total misalignment imperfection 'φ' , was established. Beam B was positioned such that the conditions described by equation 6.3 were approached. This centering procedure was carried out to minimise the influence of an out-of-plane turning moment about the connection during the loading sequences (see Table 6.1).

$$\varphi \rightarrow min \begin{cases} \varphi_1 \geq 0 \ \text{ and } \ \varphi_2 \leq 0 \\ \qquad \text{OR} \\ \varphi_1 \leq 0 \ \text{ and } \ \varphi_2 \geq 0 \end{cases} \tag{6.3}$$

6. The bolts were then gradually tightened to a torque of 200 Nm by the procedure shown by figure 6.4(c). A predetermined value of torque was

adopted to maintain consistency between all of the test specimens.

Misalignment imperfections (mm)	Test				
	1	2	3	4	5
ϑ_1	**+7.0**	**+6.5**	**+8.0**	**+9.5**	**-1.0**
ϑ_2	**+7.5**	**+6.5**	**+7.5**	**+15.0**	**-1.0**

Table 6.1: Specimen misalignment imperfections

Further details of the geometrical imperfections within the structural members may be obtained from Appendix D.

6.2.2 Composite arrangement

Two casting bays were constructed and secured to the laboratory floor. Each bay consisted of a centrally positioned column support, a continuous edge support running the full length and breadth of the cruciform connection arrangement and adjustable supports for the lower beam flanges to rest upon (see Figure 6.5).

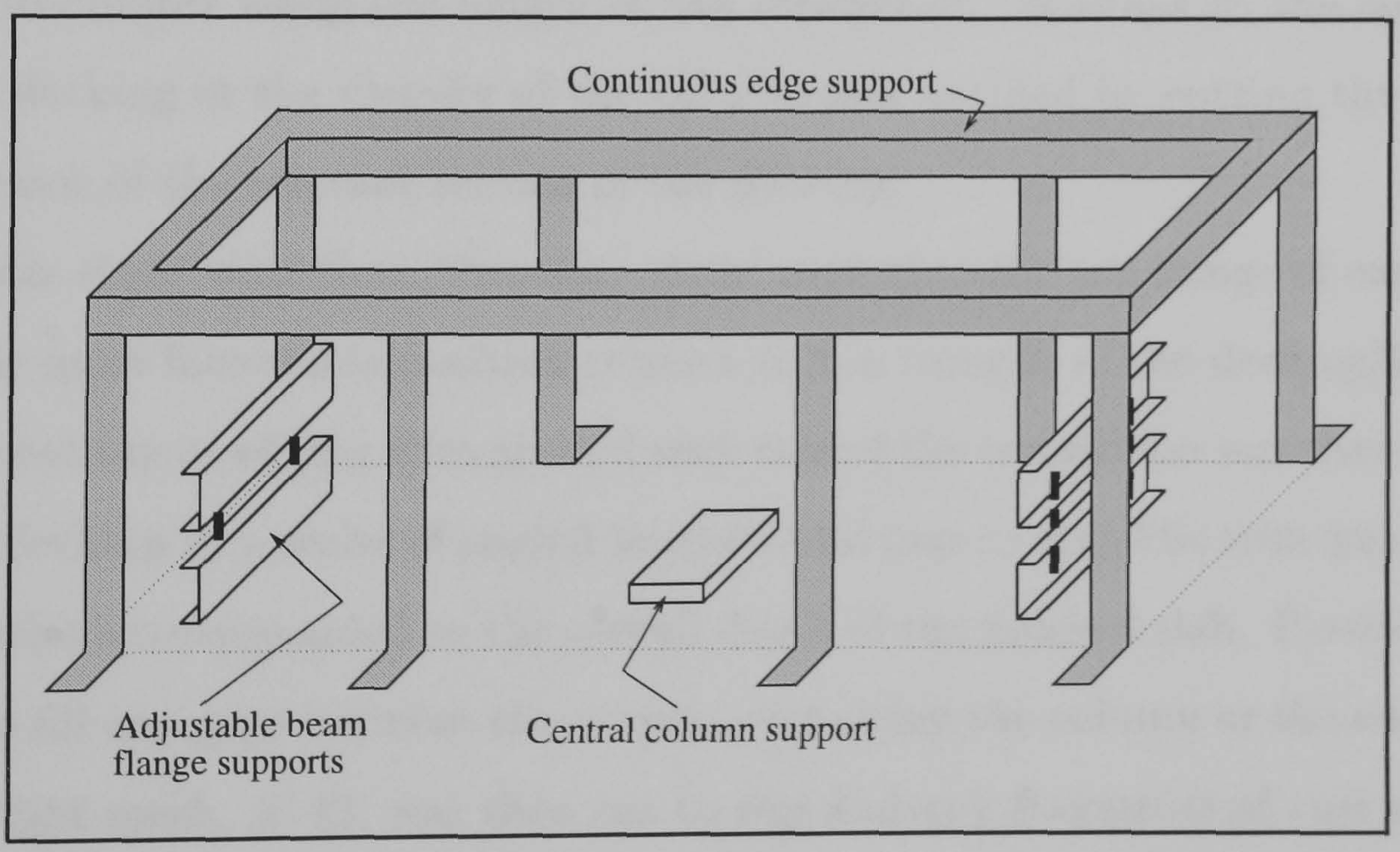

Figure 6.5: General arrangement of the casting bay

The continuous edge supports were constructed first and levelled. Their height above the laboratory floor was sufficient for the connection to be positioned in the

bay, such that initially the beam's top flanges were lower than the edge supports. The adjustable beam supports were then assembled and positioned near each end of the bay. These supports consisted of two small channel sections bolted together with a threaded bar, with a gap left between the sections to allow for adjustment. The column support was then positioned centrally in the bay.

The connection assembly was then lifted into the bay, and the column lowered on to its support. The beam supports were adjusted such that the top flanges were horizontal in both the perpendicular and parallel directions in relation to the length of the beams. The column was then raised using metal packing until. following the levelling operation, the top flanges were exactly the same height as the continuous edge supports. The lower flanges were then clamped to the beam supports to stabilise the connection in the bay.

Steel sheet decking, code CF46 - 0.9mm, manufactured by Precision Metal Forming Limited[90] was then placed around the connection to provide permanent formwork. The decking was orientated such that the ribs spanned transversely across the beams. The decking consisted of 1100mm by 990mm sections which were overlapped along the length of the connection. A break in the continuity of the decking in the vicinity of the column was avoided by cutting the column profile out of the relevant section of the decking.

Shear studs were then 'through - deck' welded to the top flange of each beam in their most favourable position relative to the troughs in the decking[57].

A continuous edging trim around each side of the connection was then secured to the decking by a series of angled brackets and pop-rivets. The trim was 120mm deep, which corresponded to the overall depth of the finished slab. Plasticine was used to fill any gaps between the decking and either the column or the edge trim.

A light mesh, A142, was then cut to size and any fragments of rust removed using wire wool. The mesh was lowered over the column to rest on 25mm spacer blocks positioned on top of the decking and tied in place using the angled brackets supporting the edging trim as suitable anchorage points. The spacer blocks were

positioned randomly over the decking to provide uniform support for the mesh.

Premature connection failure has been reported previously for cruciform test arrangements[9]. The failure took the form of the main longitudinal reinforcement being effectively pulled out of the concrete slab in the vicinity of load points, thus destroying the structural integrity of the specimen. This type of failure has been likened to a punching shear failure created by the concentrated load over a small area. To prevent this from occurring, diagonal reinforcement was specified and positioned in the vicinity of both the load points (see Figure 6.3).

The primary reinforcement and diagonal reinforcement were prepared in accordance with the bar bending schedule shown in Figure 6.3. The primary reinforcement constituted 16mm diameter high tensile steel bars which ran longitudinally over the full length of the slab. The diagonal reinforcement constituted 8mm diameter mild steel bars. The reinforcement was then secured in the slab by utilising the mesh as a suitable anchorage system.

The concrete was manufactured at the University of Warwick. The cement type used throughout the composite tests was Ordinary Portland Cement[91]. The coarse and fine aggregates used were uncrushed and taken from natural sources. Prior to the concrete mix being designed, the aggregates were graded[92] with the following results being established. The coarse aggregate was classified as a 20mm to 5mm graded aggregate, whereas the fine aggregate was classified as a medium concreting sand.

The concrete was designed in accordance with the Department of the Environment's method of mix design [93]. The characteristic strength of the concrete at 28 days was designed to be 30 N/mm^2 with a corresponding workability equal to a slump of 75mm. The maximum free water/cement ratio, maximum cement content and the minimum cement content were not specified. The proportions for the cement, water, fine and course aggregates were 345kg, 180kg, 595kg and 1260kg respectively. Verification for the concrete design was achieved through a series of trial mixes undertaken prior to the first slab being cast, whereupon

the fresh concrete was mixed and sampled in accordance with BS1881[94]. The maximum volume which could be prepared in any one mix was approximately $0.066m^3$; therefore seven mixes were required for each slab. While one mix was being placed the next was being manufactured, thereby enabling a continuous process to be achieved. Standard cubes and cylinders were taken from each mix in accordance with BS1881 [95] and [96] respectively, following the procedure shown in Table 6.2 and compacted using a vibrating table.

Mix number	Number taken from each mix	
	150mm standard cube mould	100mm x 200mm standard cylinder mould
1	1	None
2	2	1
3	2	1
4	1	1
5	2	1
6	2	1
7	2	1

Table 6.2: Procedure for taking standard cubes and cylinders for each test

The concrete was transported to the slab in the mixer drum using a specially equipped trolley, and placed using shovels. Vibrating pokers were used to initially compact the concrete. Following the placement of the final mix, a vibrating beam resting on the edge trim was guided along the full length of the connection. This completed the concrete's compaction and allowed the excess concrete to flow towards, and finally over, the edges of the slab to achieve a uniform thickness. The slab was then float finished to provide a smooth surface.

The slab, cubes and cylinders were cured in an identical manner using continually moistened hessian. The hessian was removed after 7 days, leaving the concrete exposed to the air in the laboratory. During the initial curing period, evaporation was minimised by wrapping the slab, cubes and cylinders in polythene sheeting.

6.3 Material testing

Reinforcement and structural steel members

To enable the true material properties of the connection components to be established, standard samples were prepared in accordance with the procedures listed below. Following their preparation, standard tensile tests[97] were carried out to determine specifically, the yield and ultimate stresses and in the case of the mesh and reinforcement, their ductility characteristics. The results from these tests are reported in Appendix D.

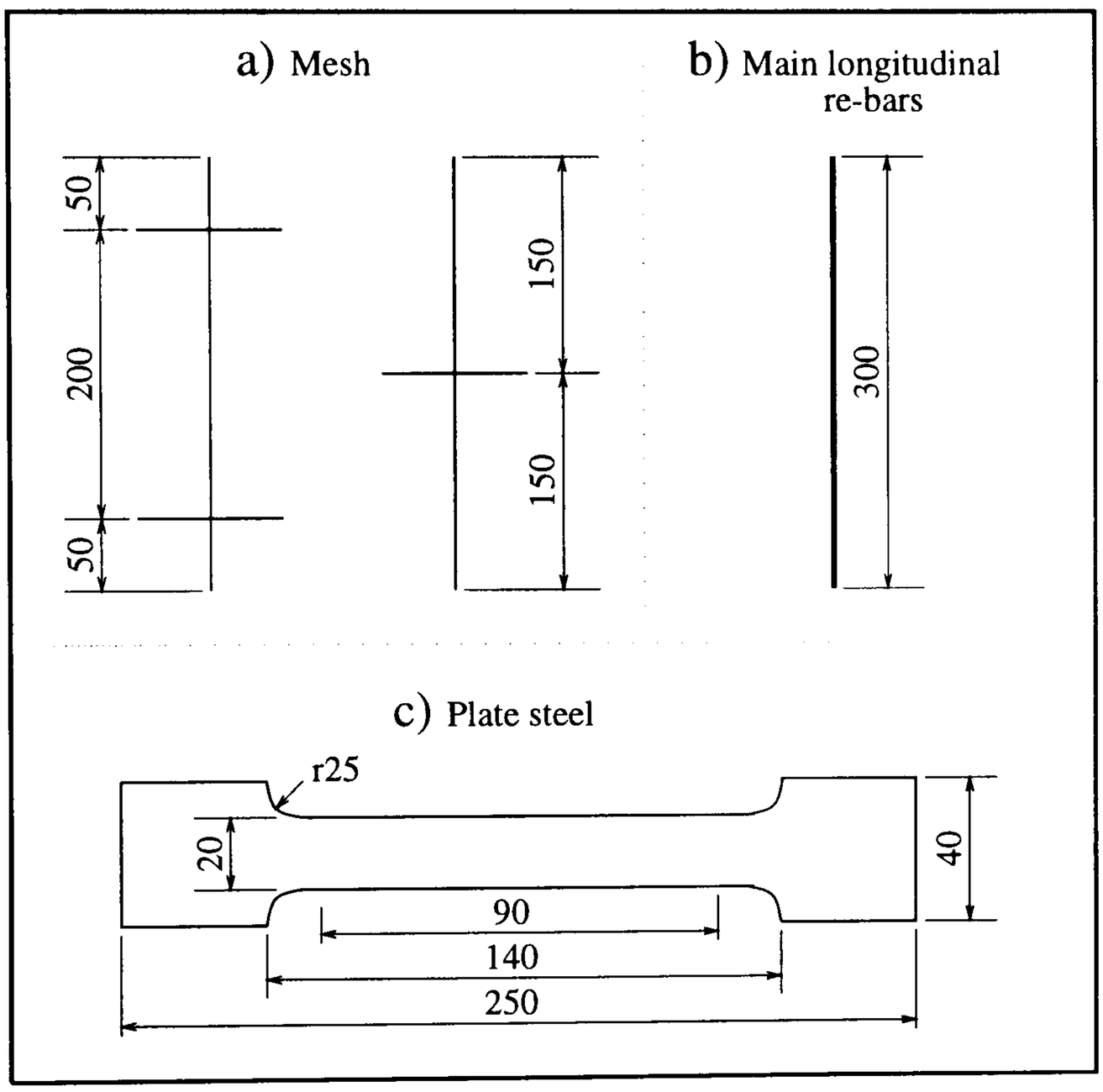

Figure 6.6: Form of the tensile samples

1. Mesh reinforcement - The two configurations shown in Figure 6.6(a) were adopted as representative samples. Each configuration includes at least one welded transverse member, since it was known from the experimental programme itself, that the mesh was susceptible to fracture within this vicinity. A total of eight samples were cut in a random manner from the bulk of the unused mesh.

2. Main longitudinal reinforcement - Two 300mm samples (see Figure 6.6(b)) were cut for each longitudinal bar used during the experimental programme. A total of 24 samples were therefore prepared. Each sample was cut from a random position along the available spare material, ensuring that the samples obtained were not always directly adjacent to one another.

3. Structural members - Coupon samples were initially flame cut and then machined to the dimensions shown in Figure 6.6(c), from the positions shown in Figure 6.7. The samples were obtained from the tension and compression regions of the connections, in addition to each end plate. During the flame cutting process, care was taken to avoid unnecessary heat concentrations in the vicinity of the finished form of the samples.

Concrete

The properties of the hardened concrete were determined in accordance with BS1881[98, 99], which are applicable to the determination of the compressive and tensile strength respectively.

The compressive strength was determined at 7 and then 28 days, by testing two cubes and averaging the results. The remainder of the cubes were saved to enable the compressive strength to be determined on the day the specimen itself was tested. The tensile strength was determined from the cylindrical samples on the day the specimen itself was tested. The average properties of the hardened concrete are reported in Appendix D.

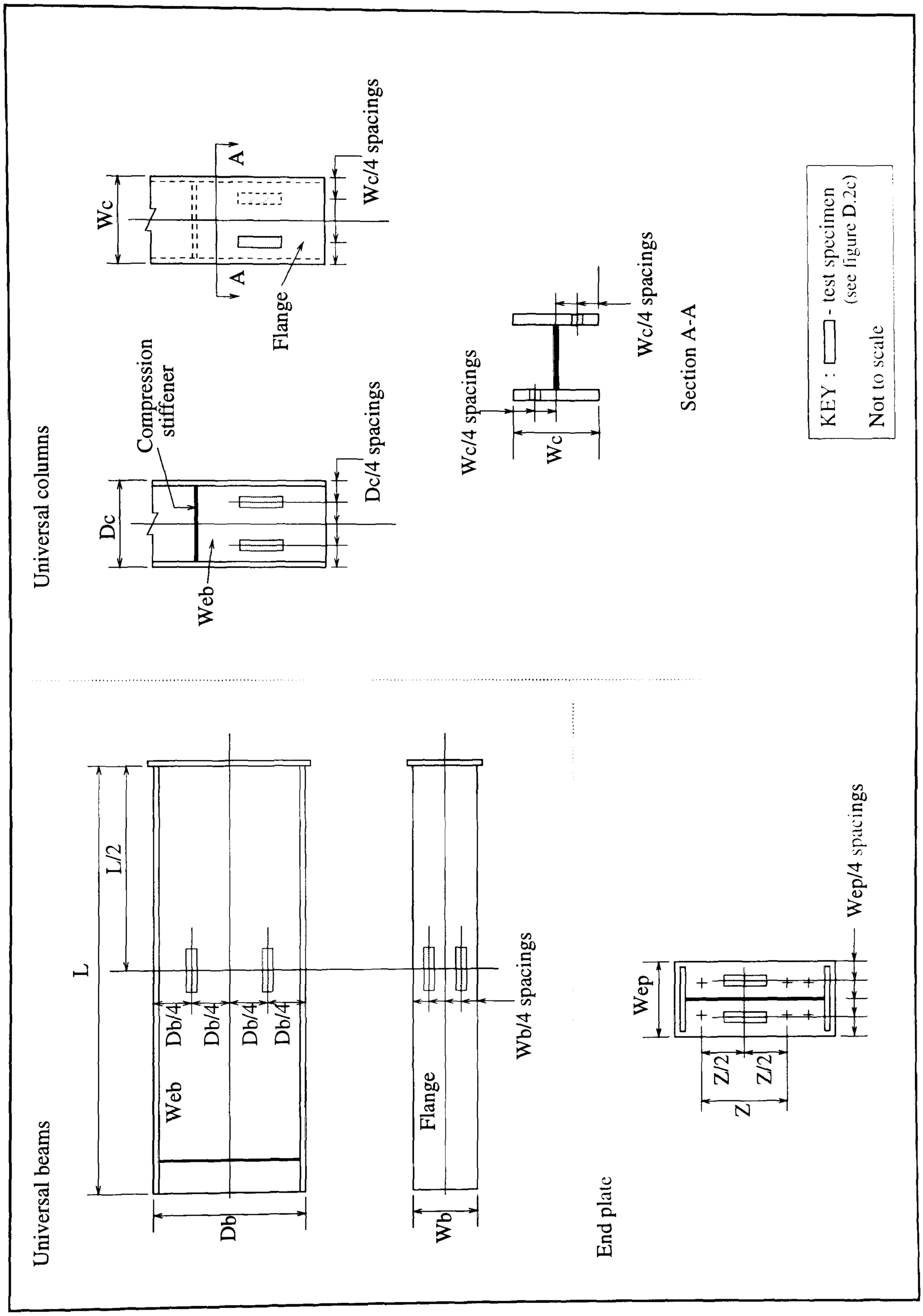

Figure 6.7: Positions of the tensile coupon samples taken from the beams, column and end plates

6.4 Testing apparatus

6.4.1 General

A purpose-built test rig was designed by the author and constructed to enable the experimental programme to be undertaken. It consisted of channel sections bolted together to form loading frames, which were subsequently secured to the laboratory strong floor. Furthermore, in addition to the design of the loading rig, particular attention was directed towards the loading arrangement and the support conditions at the base of the column.

6.4.2 Loading arrangement

The loading arrangement was built up using a uni-directional rocker on to which a uni-directional roller system was attached (see Figure 6.8).

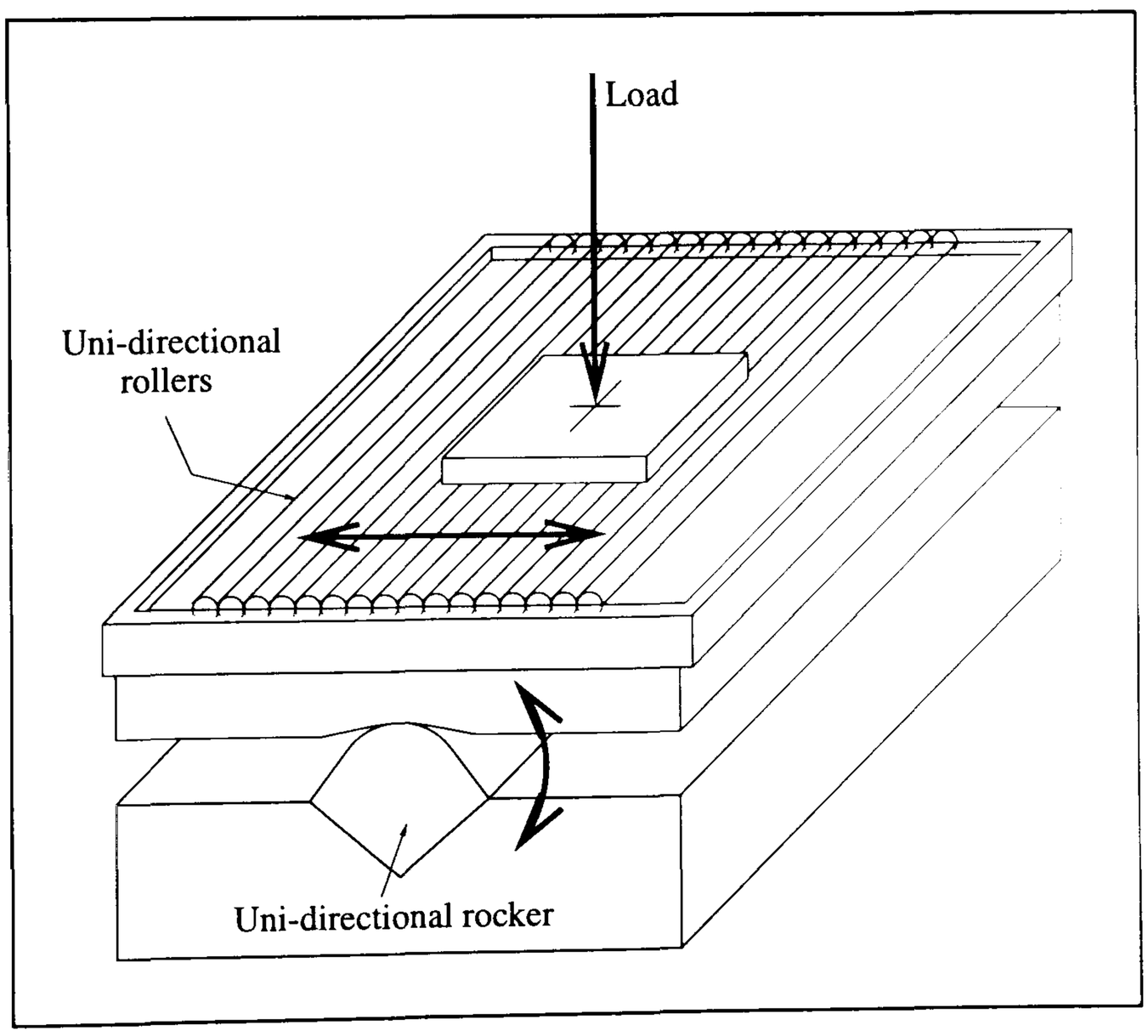

Figure 6.8: Loading arrangement adopted for the experimental programme

The purpose for adopting this arrangement was to ensure that the lever applied to the connection was kept constant throughout the duration of the test.

The position of the loading arrangement was carefully chosen, since it should create a situation whereby the connection experiences a similar ratio of the moment to the vertical shear, representative of general practice. To achieve this in a continuous beam, the distance between the connection and the load point should be approximately equal to the corresponding distance from an internal support to the adjoining point of contraflexture. However, the location of the point of contraflexture depends upon many factors, including the degree of plasticity within the beam, and the amount of moment redistribution that has taken place. The distance adopted for the experimental programme was applicable to the situation where a plastic mechanism had been reached in the beam.

6.4.3 Column support

Two types of column support were adopted during the experimental programme. The first type consisted of a ball joint, which effectively held the column in position, but left it free to rotate in any direction. This type of support was used for the first and second tests. However, following the premature termination of the second test, as a result of the out-of-plane rotation of the column becoming excessive, steps were taken to re-design the column support to prevent this from happening in the future tests. A number of options were considered for the re-design, including providing full fixity to the base of the column, or keeping the ball joint and providing a suitable bracing system to restrain the top of the column. However, the solution adopted was a simple exchange, whereby the ball joint was replaced with a uni-directional rocker similar to that already being used as part of the loading arrangement. The uni-directional rocker was considered to be the most appropriate solution, since it permitted the magnitude of the moments experienced by the connections to be equalised during each loading stage, while at the same time achieving the desired objective of preventing any out-of-plane rotation of the column member.

6.5 Instrumentation

6.5.1 General

The instrumentation system adopted for the experimental programme was designed to capture all the necessary measurements that would be required to enable the behavioural characteristics of the connections to be determined. The general arrangement of the instrumentation system is illustrated by Figure 6.9

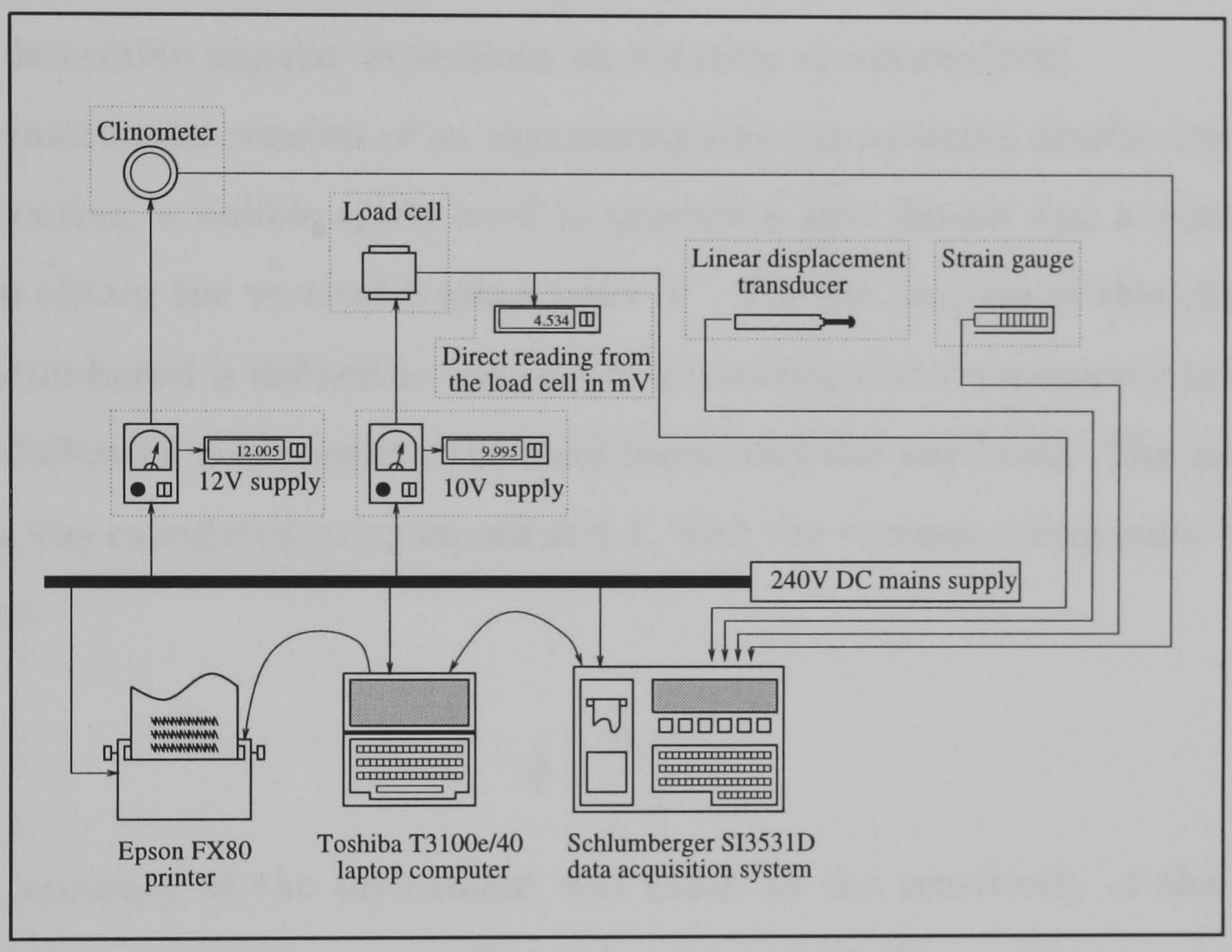

Figure 6.9: Circuit diagram for the instrumentation system adopted for the experimental programme

With the exception of a steel rule and a straight edge, the remainder of the instrumentation incorporated either analogue or digital output devices, which were monitored through a data acquisition system, which in turn was controlled through a laptop computer. All the data was recorded directly on to the computer's internal disk drive, with a hard copy being provided by the attached dot matrix printer.

The instrumentation adopted may be broadly split up into categories which configured to measure rotations, linear displacements, surface strains or applied loads.

6.5.2 Rotational measurement

Mayes Inclinometer

This instrument was originally developed by the Cement and Concrete Association to determine angular deflections on concrete structures[100].

The instrument consists of an engineering sine bar mounted upside down using 3 inch centres, a bubble spirit level to provide a zero datum and a micrometer barrel to obtain the vertical displacement 'V'. For the purpose of this chapter, a micrometer barrel is defined as the part of a traditional micrometer containing all but the following components; the steel frame and the anvil end. The measured rotation was calculated using equation 6.4, with the corresponding units being in mradians.

$$\phi = \frac{0.1V}{3} \tag{6.4}$$

The accuracy of the instrument was taken as the sensitivity of the bubble spirit level, resulting in an overall angular error of ± 0.29 mradians.

The base of the instrument stands on three small ball bearings secured and positioned in a triangular arrangement. These locate on three metal footings which are cemented to the structure at the measurement points to be checked. The footings provide a total of six directional restraints (see Figure 6.10). which enable accurate repositioning of the inclinometer, such that the vertical height measured over foot 'C' is unaffected by any relative changes in the positions of the footings due to the influence of surface stresses.

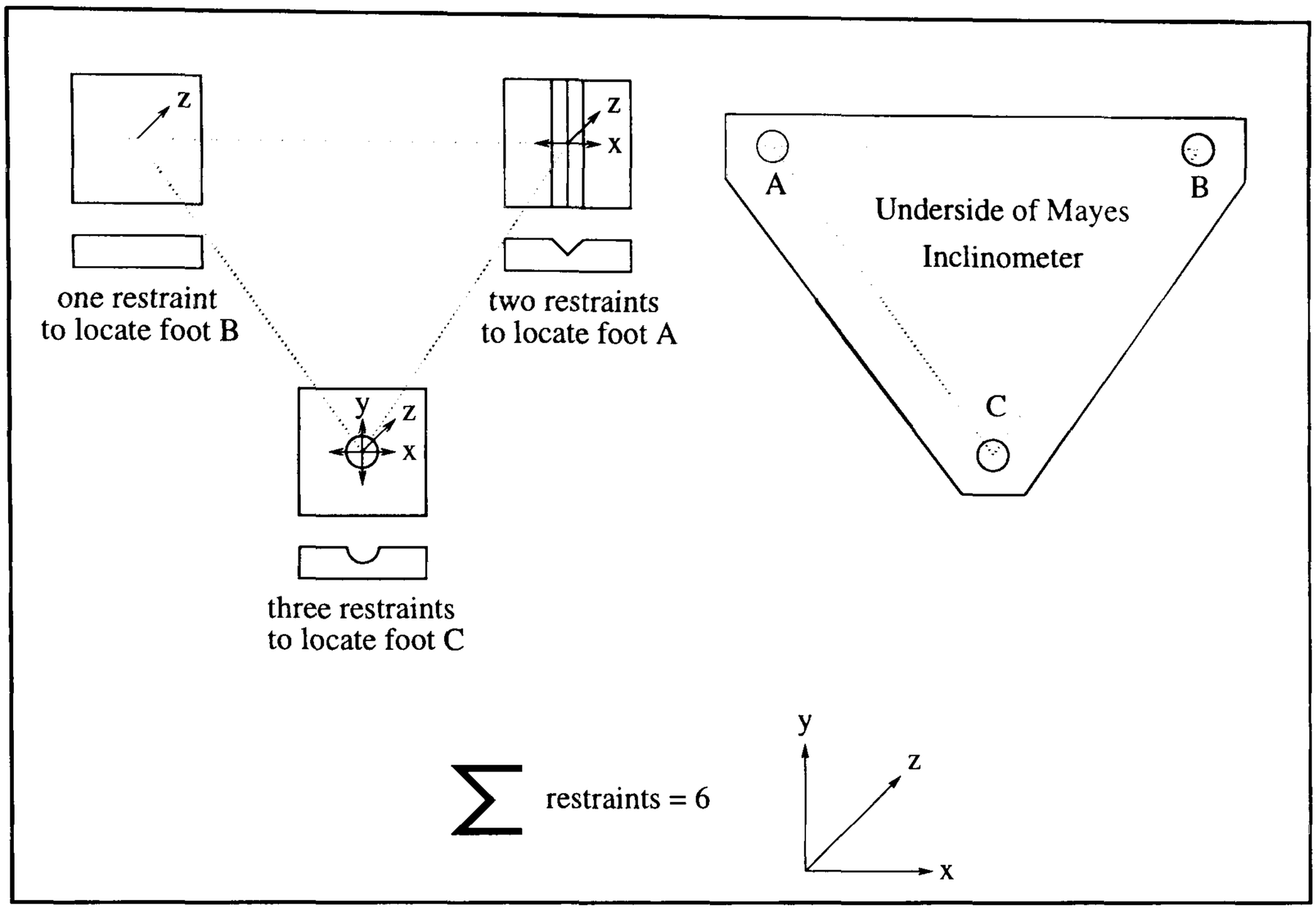

Figure 6.10: The directional restraints required to locate the Mayes Inclinometer

Accustar Electric Clinometer

This small instrument consists of an all-metal gravity sensor, which does not contain any moving parts. It is powered by CMOS (Complementary metal oxide semi-conductor) electronics which are encased in a rugged housing. This housing can be easily secured in any position required.

The principle upon which the clinometer is based is that, when rotated about its sensitive axis, the sensor provides a linear variation in capacitance. This is then electronically converted into an analogue DC voltage output, corresponding to the magnitude and direction of the angular displacement. Following the calibration of the output voltage (see section 6.5.6) the actual angular displacement can be calculated.

The full performance specifications may be obtained elsewhere[101], from which the following have been extracted.

Threshold and resolution : 17.45μradians

Linearity - null to 0.174 radians : $\pm$1.74mradians

Angular measurement using linear displacement transducers

Angular measurement may be obtained using linear displacement transducers by following the procedure described below.

A measuring arm, consisting of a 30x30x3 by 500mm long rolled steel angle section, was welded to the top beam flange. Two linear displacement transducers were then secured to the centre line of the connected column a distance of 450mm apart, such that half of the available linear displacement had been taken up (see Figure 6.11).

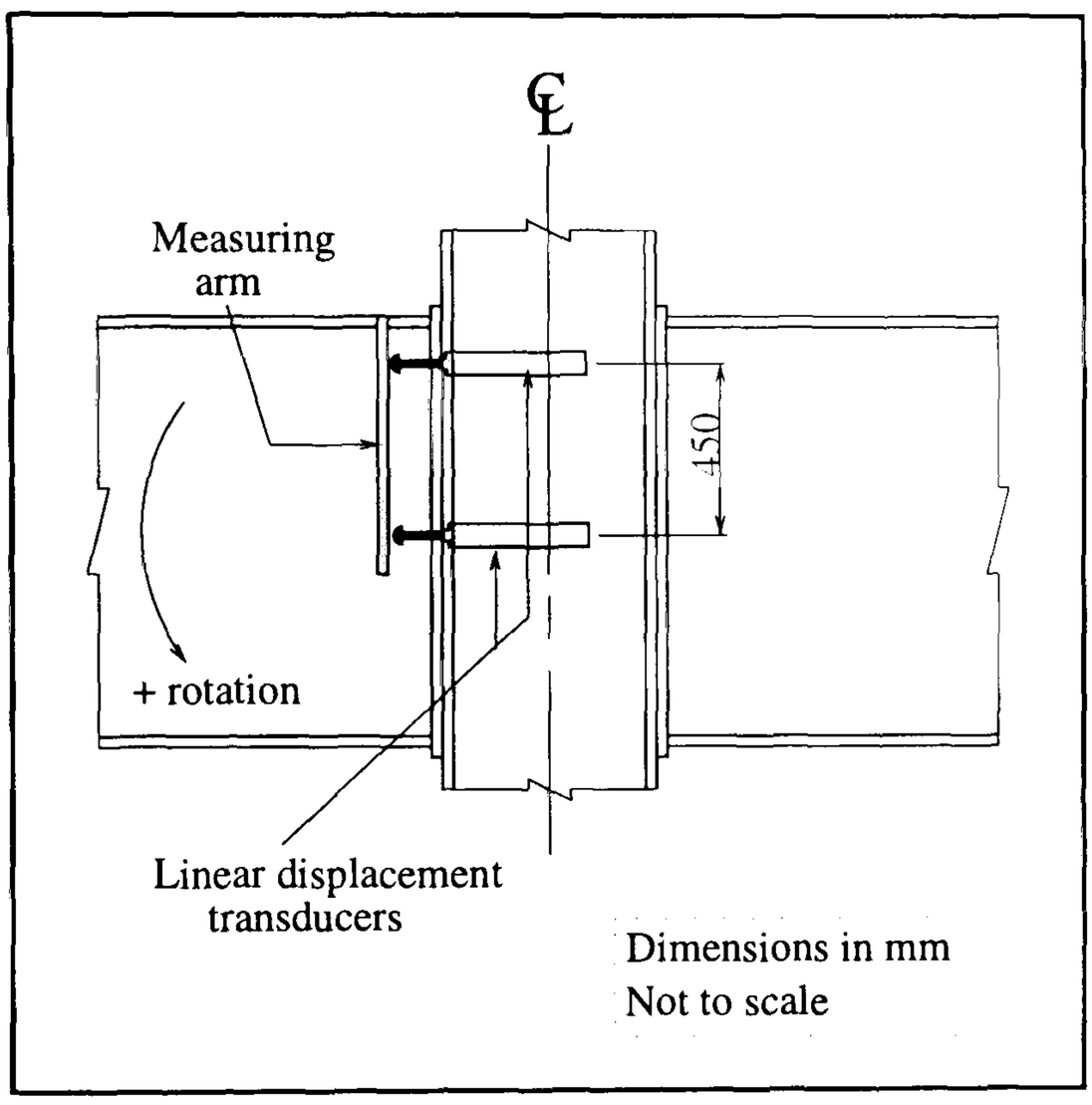

Figure 6.11: Rotational measurement using linear displacement transducers

When the connection rotates in a positive direction, linear displacements within the transducers will occur. Therefore, if we let the change in linear displacement of the top and bottom transducers equal δ_1 and δ_2 mm respectively and assuming that the angle arm is infinitely stiff, then the rotation ϕ relative to the top beam flange may be calculated from equation 6.5.

$$\phi = \frac{\delta_1 - \delta_2}{450} \tag{6.5}$$

One advantage in favour for this method of rotational measurement is that

the column rotation is automatically compensated for as a consequence of using the centre line of the connected column as the datum for the measurement system. However, this system was dropped following the completion of the first test, since an alternative method became available which eradicated the risk of disturbing the delicate instrumentation set up as the test progressed. The performance specifications applicable to this type of linear displacement transducers are detailed in section 6.5.3.

It has already been established (see Chapter 2) that the most significant property of a beam-to-column connection that influences frame behaviour is that concerned with rotational deformation only. It is assumed that the same can be said for composite connections, since their use is similar. Consequently, as the connection's rotation is of fundamental importance, for each connection test undertaken there were at least two independent methods for establishing the rotation. A separate check on this parameter was therefore continuously incorporated, thus enabling gross errors, should they occur, to be identified immediately.

For all the connection tests carried out, a set of electrical inclinometers were adopted, in conjunction with the Mayes inclinometer. In addition, test 1 (steel only) incorporated an angular measurement system adopting linear displacement transducers. For tests 2 to 5 inclusive, a second set of electrical inclinometers, were incorporated as a replacement for the displacement transducers.

6.5.3 Linear displacement measurement

Linear displacements were measured using strain gauge displacement transducers. They operate on the strain gauge principle, whereby a linear displacement is converted into a corresponding change of resistance. This change can then be measured by a wheatstone bridge configuration within the data acquisition system, in a similar manner to that described in section 6.5.4. To convert the bridge output signal into a corresponding linear displacement, the calibration procedure described in section 6.5.6 was implemented.

The full specification for the types of displacement transducers used may be found elsewhere[102], from which the following have been reproduced.

Type HS25 : Non-linearity 0.1%Full scale reading (FS) with infinite resolution

Type HS50 : Non-linearity 0.1%FS with infinite resolution

Type HS100 : Non-linearity 0.2%FS with infinite resolution

The type HS25 transducers were used to measure small displacements, such as vertical slips at the connection interface, or horizontal slips of the concrete slab relative to the structurally connected beams. The type HS100 transducers were used to measure the large vertical deflections which occurred at the ends of each beam. The type HS50 transducers were only used during test 1, to provide an alternative method for determining the connection's rotation.

6.5.4 Strain measurement

Surface strains were measured using adhesively bonded electrical resistance strain gauges. These gauges consist of a fragile metal foil gauge, which was formed by photoetching and then bonded to a suitable carrier material for protection.

Following the application of the load, the subsequent surface strains developed in the component are detected by the foil gauge. This results in a change in the gauge's resistance as a consequence of its elongation.

The gauge signal is fed into a wheatstone bridge circuit within the data acquisition system, which is balanced such that at the start of a test the strain readings can be taken as zero. All subsequent readings of strain are relative to the initial setting and therefore give strain differences.

The full specification for the types of strain gauges used may be found elsewhere[103], from which the following have been reproduced.

Yield gauges :

PRS-10 - 2% strain limit

PL-10 - 2% strain limit

Post yield gauges :

YL-10 - 10→20% strain limit

The yield gauges were used throughout the experimental programme and were located in the compression region of the connections. The post yield gauges were used from test 3 onwards, to measure the strains being resisted by the reinforcement within the concrete slab.

6.5.5 Applied load measurement

The applied load was measured in terms of unit strain, by using electrical resistance strain gauge load cells.

The load cell consists of a central cylinder and sensing bridge, all of which are housed in a robust outer casing which is hermetically sealed to make it completely waterproof. The sensing bridge comprises four strain gauges bonded to the inner wall of a central cylinder. The gauges are orientated such that two will measure strains in the axial direction and the other two in the transverse direction. A wheatstone bridge is thus configured within the cell, with the transverse and axial gauges being in opposite arms. When a load P is subsequently applied, a compressive stress is induced. This in turn produces axial and transverse strains, ϵ_a and ϵ_t respectively, which can be related to the following load expressions :

$$-\epsilon_a = \frac{P}{AE} \tag{6.6}$$

$$\epsilon_t = \frac{\nu P}{AE} \tag{6.7}$$

where :

A - cross sectional area

E - Youngs modulus

ν - possions ratio for steel.

It can be shown that for the wheatstone bridge configuration above[104], that

the output circuit voltage from the bridge, E_{Th}, may be given by equation 6.8.

$$E_{Th} \approx \frac{V_s}{2}(1+\nu)\frac{S_g P}{AE} \tag{6.8}$$

where :

S_g - Gauge factor or calibration constant for the gauge

V_s - Supply voltage.

The output voltage was then calibrated to obtain the corresponding applied load (see Section 6.5.6).

The full specification for the load cells used may be found elsewhere[105]. from which it is found that the accuracy of the load cells are better than 0.25% of the applied load.

Throughout the duration of the experimental programme, the output voltage was continuously monitored via an external digital voltmeter. The purpose for this was to enable a secondary check to be established to guard against possible errors which otherwise may go unnoticed.

6.5.6 Calibration

The success of an instrumentation system does not only involve using the right type of instrument for the task in hand, but fundamentally, the data received from any type of instrument must be in a form that may be subsequently processed to obtain meaningful measurements. To enable this objective to be achieved, the instrumentation was calibrated by adopting the following procedures :

Linear displacement transducers

The linear displacement transducers were calibrated individually using a purpose built calibration rig. The rig consisted of a base, on to which at the far end a micrometer barrel was secured, but free to rotate. Each transducer was secured in the rig by way of an adjustable mount, therefore enabling various transducer

diameters to be accommodated. Following the transducer being secured in position and connected to the data acquisition system. the micrometer barrel was adjusted until a detectable change in the instrument's response could be measured. This position was then assumed to be the datum from which all the other measurements could be related. A linear displacement was then gradually built up using slip gauges. The increments adopted were as follows; up to and including 10mm, 1mm increments were adopted; however displacements in excess of 10mm were achieved in 5mm increments up to the maximum permitted by the respective transducer. When two or more gauges were used together, they were ringed, to ensure that the summation of the individual gauge thickness could be used reliably to represent the total thickness. Following the attainment of the maximum linear displacement, the procedure was reversed observing the same incremental changes as the displacement decreased. This cycle was repeated three times and the results averaged.

Rotational clinometers

The clinometers were again calibrated using a purpose-built calibration rig. The rig consisted of a base, on to which a metal plinth was secured by a pivot at the far end. A pre-determined horizontal length (600mm) was marked out on the base, measuring down from the pivot. The clinometers were then secured to the plinth and connected to the data acquisition system. The plinth was then displaced through a vertical distance V, which in turn would have the effect of inducing a rotation within the clinometers. For small angles this rotation ϕ may be represented by equation 6.9 and has corresponding units of radians.

$$\phi = \frac{V}{600} \tag{6.9}$$

The vertical distance was controlled using slip gauges in various combinations to achieve the desired increment. The increment was set at 1mm, up to a maximum distance of 30mm, which corresponds to a rotation of 0.05 radians. When

two or more gauges were used together, they were again ringed. Each clinometer was raised and lowered three times with the voltage response at each increment being recorded and subsequently averaged.

Calibration rigs

The purpose-built calibration rigs described above were already available at the University.

Load cells

The load cells were calibrated using the the Denison compression machine, number T91080 and the Monsanto tensometer type E machine, number N120-79.

The load cells were first positioned in the Denison and connected to a digital voltmeter. Load was applied in 100 kN intervals up to 500 kN, recording the voltage response from the cell at each increment. Following the attainment of the maximum load, the cell was unloaded in similar increments. This procedure was repeated three times and the results averaged. To increase the accuracy of the calibration within the range $0 \leq$ applied load ≤ 100 kN, the Monsanto tensometer was additionally used. The loading and unloading cycles were identical to that adopted earlier, with the exception that the interval was reduced to 20 kN. Three cycles were undertaken and the results averaged. Where the two calibrations overlapped, i.e. at 0 kN and 100 kN, the voltage response from the cell was again averaged.

Interpretation of the calibration results

The results from the various calibrations were interpretated using linear regression analysis techniques. A line that best fits was then calculated for each measurement instrument, producing an equation of the general form given by

equation 6.10.

$$y = mx + c \tag{6.10}$$

Furthermore, the linear regression analysis produced the following correlation coefficients :

Linear displacement transducers - 0.999991

Rotational clinometers - 0.9998

Load cells - 0.999993

Adopting the procedure outlined above enabled direct readings from the instrumentation to be fed from the data acquisition system into the computer. Consequently an on-line process was established, whereby following manipulation according to the linear equations, the connection's behaviour could be monitored continuously.

6.5.7 Instrumentation locations

The instrumentation positions adopted for the experimental programme are shown in Figure 6.12.

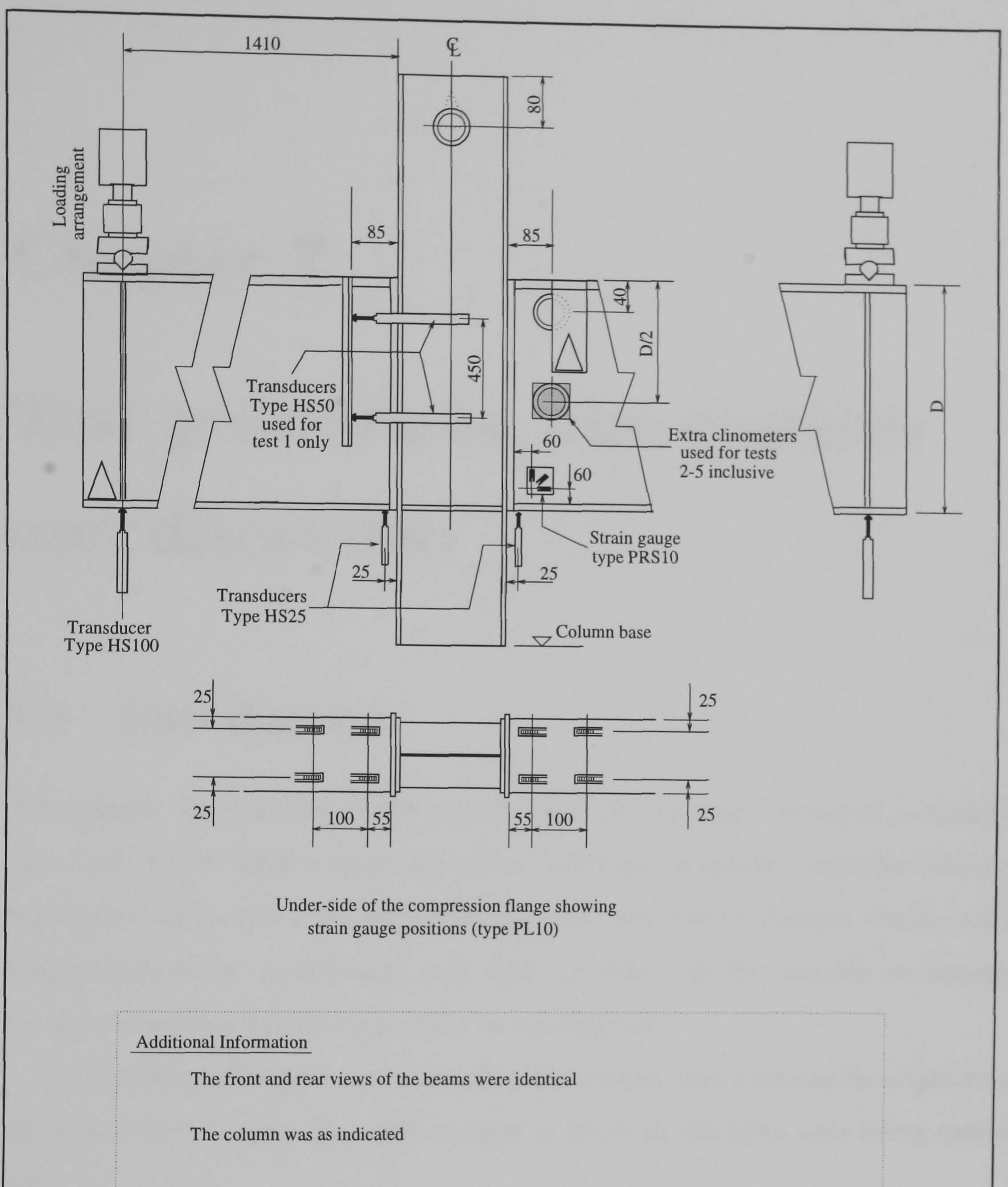

Under-side of the compression flange showing
strain gauge positions (type PL10)

Additional Information

The front and rear views of the beams were identical

The column was as indicated

Electric climometers

Mechanical inclinometers

Composite tests :

The instrumentation for the composite tests were identical to that shown, with the addition of two type HS25 transducers positioned centrally on the slab at the beam ends, to measure the horizontal slip relative to the connected beam (not shown).

For tests 3-5 inclusive, the reinforcement was strain gauged using type YL10 gauges.
8 No. were used per test, 2 per bar, located on the top and outside of each bar.
The gauges were positioned in line with the column flange on one side of the connection only.

Figure 6.12: Instrumentation positions adopted for the experimental programme

Chapter 7

Test procedures, observations and discussion

7.1 Introduction

Throughout the duration of the experimental programme, the set of procedures discussed in this chapter were adopted to facilitate consistency between the loading aspects of the tests. In doing this, the resulting standardisation would enable comparisons to be undertaken, such that the effects of the variable parameters on the connection's behaviour could be ascertained.

In addition to the procedural details, this chapter also contains descriptions of the visual observations that were evident at the time the tests were being carried out.

The chapter is concluded by a pictorial representation of the experimental programme. This takes the form of a sequence of photographic plates, starting with some of the more important aspects of the test arrangements (see Plates 7.1 - 7.7), before moving on to the tests themselves (see Plates 7.8 - 7.32). The purpose of the latter is to show the extent of the plastic deformation that each specimen sustained following the completion of the applicable test.

7.2 Test procedures

The test procedure was based on an incremental approach and consisted of four phases. To prevent excessive in-plane rotation of the column, each increment was applied to the specimen in such a manner as to keep the beam's deflections on either side of the column reasonably similar to one another.

Initial phase

With the test specimen located in the rig, it was necessary to stabilise the column prior to the removal of the supporting restraints. This was achieved by imparting a small amount of load, in the order of 0.5kN, into each beam via the hydraulic jacking system. The external restraints were then removed and this stabilised position was assumed to be the datum to which all the subsequent measurements were related.

A check on the instrumentation was then initiated by loading the specimen up to 20kN (28kNm), and then unloading back down to 5kN (7kNm). The load increment adopted for this cycle was 5kN.

Comparisons between the various methods for determining the connection's moment and rotation were then undertaken to establish their correlation. If the correlation fell within the bounds of the accuracy of the types of instruments compared, then the instrumentation was assumed to be operating satisfactorily and the test was commenced. If, however, problems were identified, they were isolated, corrected and then re-checked before proceeding.

Second phase

The specimen was loaded up to two-thirds of its calculated moment of resistance (see Section 7.3). For each test the load increment was specified as follows.

Test 1 : 5kN increments were adopted

Tests 2 - 4 : 10kN increments were adopted, as the composite tests would be considerably stronger due to the influence of the reinforcement.

Test 5: 20kN increments were adopted, as for this final test a further increase in resistance would be expected due to the influence of the greater beam depth.

Following the completion of the loading cycle, the specimen was unloaded back down to 10kN (14kNm), in increments equal to twice the magnitude adopted for the loading cycle. This was undertaken to enable the connections unloading stiffness to be monitored as the test progressed.

Third phase

Initially, the loading cycle described for the second phase was repeated: however, the load level for this phase was not restricted to two-thirds of the calculated moment of resistance of the connection. Consequently, the load increments were continually applied above this level until the moment-rotation characteristic showed signs of becoming asymptotic to the horizontal, upon which, this phase was brought to a close.

Fourth phase

As the connection stiffness reduced appreciably, the incremental approach was adjusted accordingly to reflect the impending situation when the actual moment of resistance of the connection would be reached. To achieve this a pre-determined angular rotation was imposed on the connection, as the connection moved into its plastic range. An angular rotation of 0.5mradian was adopted as a suitable increment. This phase was continued until the specimen had reached its ultimate condition, or until any other circumstances arose which required the test to be brought to a conclusion. The ultimate condition was deemed to have been reached when one of the following situations arose.

1. A significant and sudden reduction in the applied load occurred as a result of a non-ductile failure mode being attained.

2. Local buckling inducing excessive steelwork deformation in the vicinity of a connection. The failure criteria under these circumstances was deemed to have been achieved when the loss in moment capacity, indicated by a downward trend to the moment-rotation characteristic, coincided with the predicted moment capacity applicable to the connection being tested.

Application of increments

During the initial phase of the test procedure, the loading and unloading increments were applied at one minute intervals.

During the loading cycles applicable from phase 2 onwards, the data from the instrumentation was immediately recorded following the application of each increment and a stopwatch started. After a time delay of one minute and then ten minutes, further sets of instrumentation data were obtained. The purpose of the one minute delay was to obtain standardised data to enable the moment-rotation characteristic for the connections to be plotted as the test progressed. This would eliminate peaks in the calculated connection moment that would otherwise have arisen if the load value used was based on the instantaneous value applicable to when the increment level was first achieved. This results from the connection rotation being induced by a deflection control, whereby the beam deflections are held constant following the attainment of the desired increment. This prevents further movement, such that during connection plastification, the load level tends to reduce for a specific rotation. The further nine minute delay was incorporated into the procedure for the following two reasons. Firstly, to enable the specimen to be inspected at regular intervals throughout the test and secondly, when undertaking the composite tests, to allow sufficient time to enable the crack pattern on the concrete slab to be traced as it developed. Consequently, the frequency at which each increment was applied was unaffected by the collection of all the applicable data on the connection's behaviour.

During the unloading cycles, which were applicable from phase 2 onwards, a similar procedure to that outlined above was adopted, with the following modification. The second time interval was reduced from ten minutes down to two minutes, as a reflection that the connection's response would be ostensibly linear-elastic under reverse loading conditions.

Special cases to maintain test continuity

During unavoidable periods where the time delay between successive incre-

ments was in excess of ten minutes, further rotational movement of the connections was prevented by applying the external vertical restraints to the beams.

At the end of each evening, if the test had not been completed. the specimen was unloaded in even increments of load. This was continued until the load level had been reduced to between 5kN and 15kN (7kNm - 21kNm). For the first test (steel only), the unloading increment was set at 20kN, whereas for the composite tests, the increment was specified as 50kN. A small amount of load was left on the specimen to enable continuity to be maintained the following day. All the external restraints were then carefully applied to the specimen to prevent further movement. The following day began by the re-establishment of the final position attained previously and was achieved by using identical load increments as those used to unload the specimen. A shorter total time delay between successive increments, equal to two minutes rather than ten, was adopted until appreciable stiffness was again lost within the connection, upon which the ten minute delay was reinstated. Following the attainment of the previous connection response, the test was continued as though no interruption had occurred.

Should anything occur during the application of an increment which required special consideration, the increment was stopped prematurely to allow for suitable records to be taken and the instrumentation data to be recorded. The test would then proceed by applying the remaining magnitude of the interrupted increment, before returning to applying the full increments as before. If, however, a reduction in the applied load occurred within an increment, such as that resulting from the mesh reinforcement fracturing in the composite tests, the test would again be temporarily suspended to permit data collection. The following increment applied to the specimen restored the load level to the magnitude which would have been obtained, had the interruption not occurred. The test then progressed by applying full increments as before. During these periods of discontinuity. the time constraints between successive increments, or part thereof. were still applicable.

7.3 Method for calculating the connection's moment of resistance

7.3.1 General

The moment of resistance of the bare steelwork connection was predicted using Annex J of Eurocode 3[18], with the assumption that there was only one bolt row resisting the induced tensile force. When the steel connection formed part of a composite arrangement, the contribution of the reinforcement was additionally included (see equation 7.1).

$$Mp_{conn} = Mp_{steel} + Mp_{rein} \tag{7.1}$$

where :

Mp_{steel} : Moment of resistance of the bare steel connection

Mp_{rein} : Moment of resistance of the reinforcement.

and

$$Mp_{rein} = A_s f_{yr} L_r \tag{7.2}$$

where :

A_s - Total area of the rebars (4T16s)

f_{yr} - Yield stress applicable to the reinforcement

L_r - Lever arm to the reinforcement.

Characteristic material properties were used throughout the predictions, since the actual properties could not be established until the experimental programme had been completed. The lever arm applicable to both the bare steel connection and the reinforcement was calculated on the assumption that the centre of the compression flange was the point of rotation for the connection.

7.4 Test observations and discussion

7.4.1 General

No visual deformations were apparent during the initial phase of the test procedure during any of the experiments. This was to be expected, since this phase was designed solely to provide a method of checking the instrumentation prior to the commencement of the test. The observations and discussions below are therefore applicable from phase two onwards.

Throughout the duration of the experimental programme, there was no evidence to suggest that any vertical slip had occurred at the interface between the end plate and column flange. This was despite the presence of clearance holes, which were provided for ease of connection assembly. The lack of slip could be attributed to the available clearance within the connections being utilised during the alignment of the specimens (see Chapter 6, section 6.2.1).

During the unloading cycles, the connection stiffness recovered in an ostensibly linear-elastic fashion. This unloading stiffness compared favourably to the connections' corresponding initial stiffnesses, and was independent of when the unloading cycles were implemented. Consequently, it may be concluded that the unloading stiffnesses of the connections tested were constant throughout their working range and equivalent in magnitude to their initial stiffness.

Throughout the following sections, the load level at which an observation occurred will be identified by its corresponding connection moment. Where not specifically referred to, this moment will appear as a bracketed value located within the applicable sentence. Any reference to a connection rotation is applicable to that of connection A. Connection B was not referred to specifically, with the exception of the discussions applicable to Test 1, since for the composite tests the rotation induced in to connection A was found to consistently govern the eventual failure mode. This can be explained in part by probability: however, from test three onwards the predominance of connection A was attributable

to the presence of the strain gauges secured to the reinforcement (see section 7.4.4). The moment of resistance and the available rotation capacity for each specimen, refers to the connection which has progressed the furthest along the moment-rotation characteristic.

In addition, certain keywords will also be referred to and in the context of this thesis are defined as follows :

Specimen : Cruciform test arrangement, consisting of both connections A and B.

Front : Front of the specimen, with connection A on the right hand side of the column and connection B on the left.

Back : Opposite side of the specimen, with the connection positions reversed with respect to the column.

Rebar : 16mm diameter longitudinal reinforcement

Plate : The word 'Plate', followed by a specific reference number, identifies that a photograph is available to illustrate the particular point of discussion. The reader is referred to section 7.7, where the photographs are presented in numerical order.

7.4.2 Test 1 - steel only

For details of the connection configuration refer to Chapter 6, Figure 6.2.

The first visible deformation within the steelwork was restricted to the tension region of the connection, and took the form of the tip of the end plate moving away from its mating position against the column flange (48kNm). This deformation appeared to be symmetrical between the front and back of the specimen and was probably caused by the column flange deforming in the region closest to the upper most bolt row. However, no collaborating deformation could be detected within the column flange at this stage.

The first detectable signs of the column flange deforming occurred following the attainment of two-thirds of the connection's predicted moment of

resistance (57kNm). In addition, it became apparent at this load level that the separation of the tips of the end plates were visibly different between the front and back of the specimen (see Figure 7.1(a)). This was the result of the column beginning to rotate about its out-of-plane axis (see Figure 7.1(b)). This was accompanied by lateral displacements occurring to the compression flanges, which were monitored at the beam ends. However, since the lateral movements were small, measured as 2.0mm for connection A and 1.0mm for connection B, no attempt at this stage was made to prevent further movement.

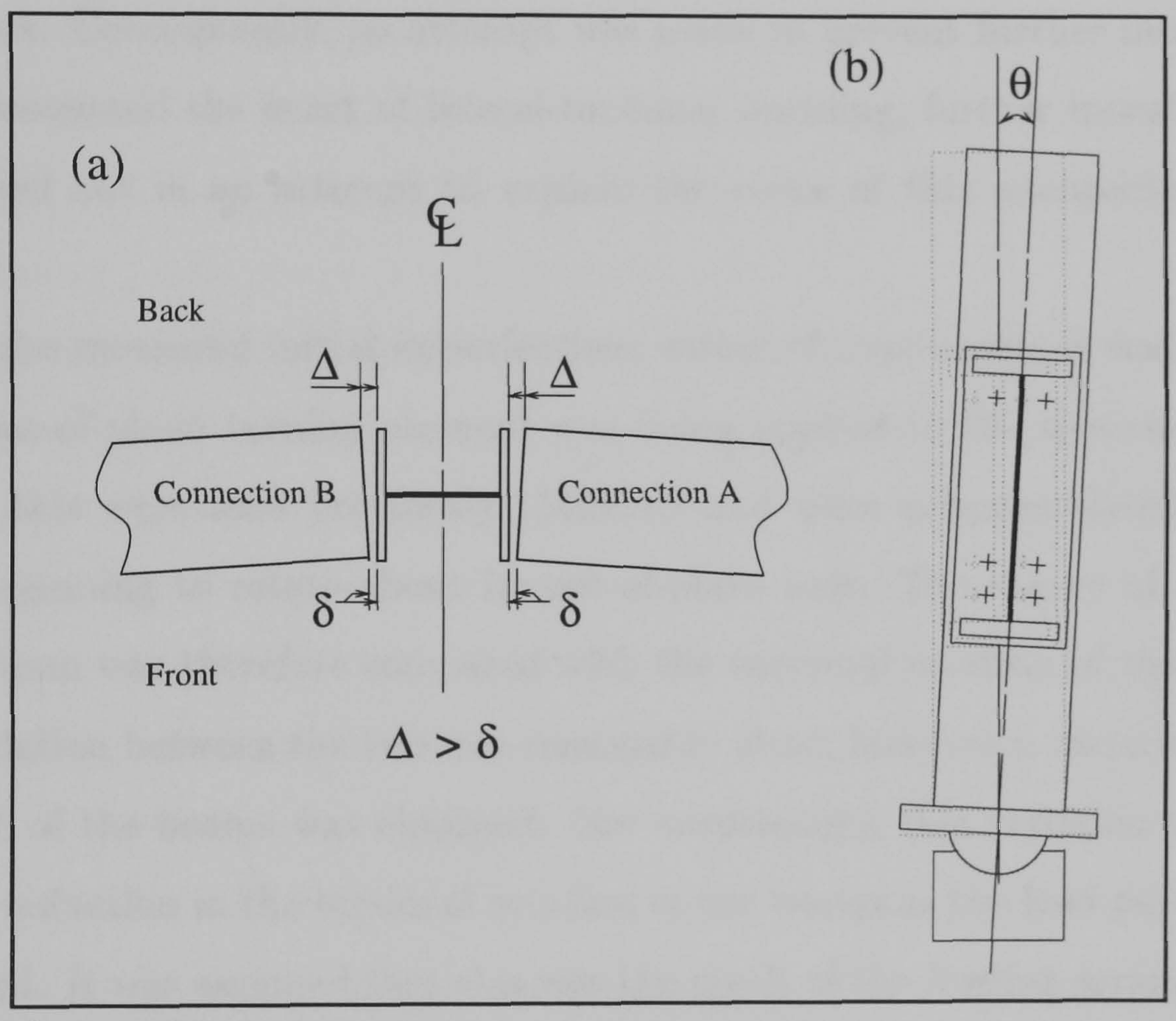

Figure 7.1: Out-of-plain column rotation

Following the completion of the first unloading cycle (7kNm), the deformation within the steelwork recovered slightly, although not completely. This would tend to indicate that, although the connection had only been loaded to two-thirds of its moment of resistance, plastic deformations were already present. No recovery was forthcoming as far as the out-of-plane rotation of the column was concerned and consequently the lateral displacements of the compression flanges showed little change.

Phase three was now implemented. Following the attainment of a connection moment equal to 63kNm, it became evident that the unevenness observed at the tips of the end plates was being reciprocated in the column flange deformation. In addition, the lateral displacements of the compression flanges had increased significantly. The movement at connection A was now 7.0mm and 5.0mm was evident at connection B. The possibility of lateral-torsional buckling was considered at this stage. However, there was no evidence to suggest that the torsional rotation of the beams were in any way influencing the behavioural characteristic of the connections. Consequently, no attempt was made to prevent further movement. Having discounted the onset of lateral-torsional buckling, further investigations were carried out in an attempt to explain the cause of this unexpected beam behaviour.

From the measured initial imperfections within the specimen, it was evident that an out-of-plane turning moment was being applied to the specimen. The effects of this were seen previously (57kNm) and were accommodated by the column beginning to rotate about its out-of-plane axis. The degree of rotation of the column was therefore compared with the torsional rotation of the beams. The correlation between the two was reasonably close; however a variation along the length of the beams was obtained. Not surprisingly, this variation took the form of a reduction in the torsional rotation of the beams as the load points were approached. It was assumed that this was the result of the loading arrangements and the presence of the web stiffeners providing a degree of torsional stiffness to the ends of the beams. Therefore, the most plausible explanation to the cause of the lateral displacements was the out-of-plane rotation of the column. Having established this explanation, it was decided not to apply any lateral restraints to the compression flanges unless the twisting effect began to destabilise the loading arrangements or influence the connection behaviour.

The incremental approach was changed from even intervals of load, to rotational increments when a connection moment of 140kNm had been achieved.

As the connection moved into its plastic range, a clear gap below the top bolt row began to open up between the end plate and the column flange. The depth to which this gap extended was restricted to where the upper bolt row, assumed in the design to resist the applied vertical shear, was located. This could possibly indicate that the end plate was bending about the centre line of this bolt row, as plasticity in the column flange increased (see Figure 7.2). This gap opened at a faster rate for connection B than A, and thus could be in part the explanation of why, at a given period of time, the measured rotation of connection B was always in excess of that measured for connection A. In addition, at this stage during all the tests, vigilance was exercised in monitoring possible bolt elongation and/or thread stripping. However, no evidence of either of these two events happening was forthcoming throughout the remainder of this test.

The lateral displacements of the compression flanges stabilised shortly after rotational increments were adopted, whereupon maximum displacements of 11.0mm and 9.0mm were measured at connections A and B respectively.

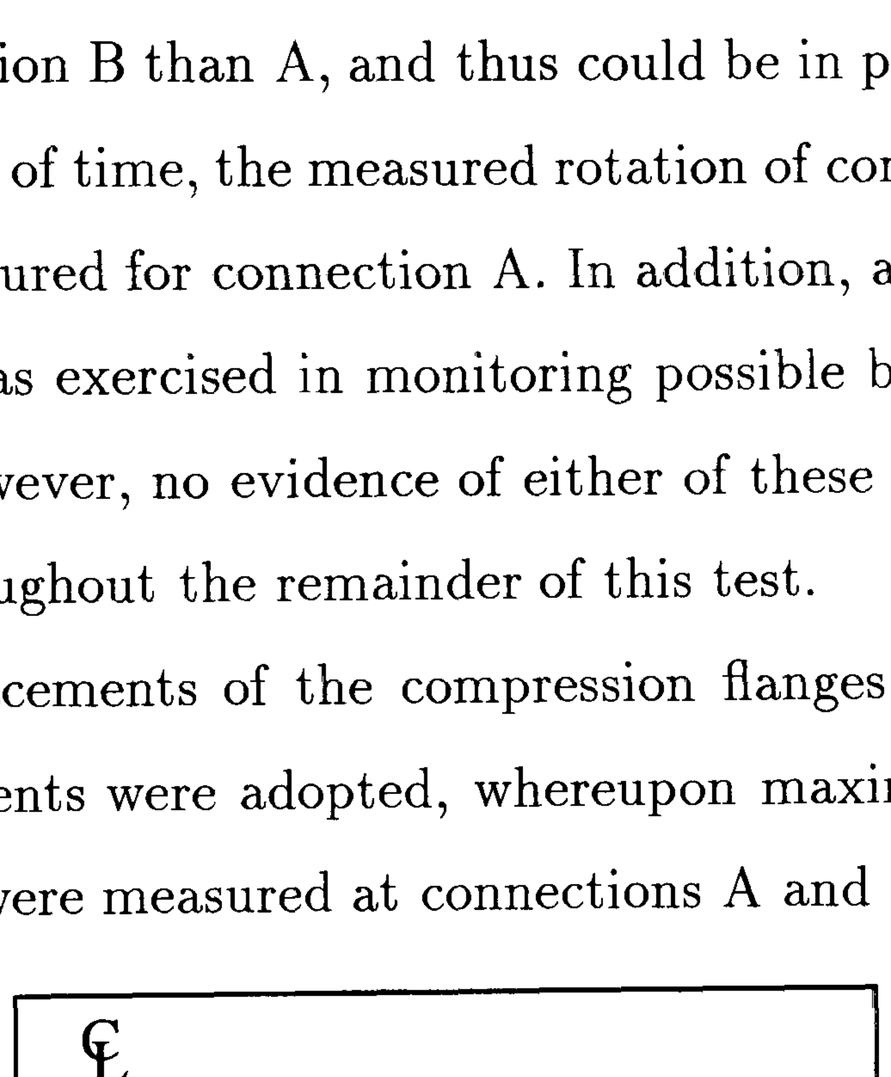

Figure 7.2: Possible hinge position within the end plate

As the connection rotation increased, the vertical load continued to increase.

This created concerns about the force that the tension bolts were resisting to the point where the test was stopped for fear of the bolts fracturing. The experimental programme was conducted in an open laboratory. Therefore, the potentially hazardous situation that may have been created, should the bolts have fractured, had to be avoided. Consequently, no specific mode of ultimate failure could be identified for this test.

At this point in the test proceedings, a bolt force of 200kN was calculated on the assumption that plane sections remain plane. Experimental work undertaken by Godley and Needham[106], who carried out comparative tests between Grade 8.8 and HSFG bolts in tension and shear, suggests that the maximum tensile resistance of a Grade 8.8, M20 bolt before fracture would be 225kN. It can be seen that in the author's test this level of force was being approached, which considering that the assumption of plane sections remaining plane also neglects the influence of prying forces, justified ending the test.

The moment-rotation characteristic determined by this test is shown by Figure 7.8 (see Section 7.5), from which the following can be identified.

The moment of resistance of the connection : at least 162kNm

Available rotation capacity : > 19mradians

The permanent plastic deformation induced into the steelwork is illustrated by Plates 7.8 and 7.9. There was no evidence of any local buckling having occurred to the compression flanges of the beams. However, assuming that the behaviour of mild steel in compression is very similar to its behaviour in tension, particularly in the elastic range[107], it could be concluded that material yielding was beginning to occur following the attainment of a connection moment of 127kNm. The onset of material yielding was assumed to be when a compressive strain of 0.1% had been attained. The strains measured in the beam webs were all considerably lower than those corresponding to the flanges. There was negligible strain in the vertical arms of the strain gauge rosettes, which measured a tensile strain of 0.01%. However, higher strains were measured in the corresponding horizontal

and diagonal arms, which were approaching the assumed yield point by the end of the test (0.09%).

When the connection was dismantled it was alarming to discover that the tension bolts were very loose and easily removable by hand. However, this was not the case for the shear bolts, which required the use of spanners and considerable effort. The explanation as to why the tension bolts were so loose can be seen by examining plate 7.10. Deep impressions of the bolt heads were left indelibly on the insides of the column flanges. Consequently, the small pre-tension force which was induced into the bolts when they were originally tightened was released by the formation of these impressions. This does imply however, that there was no plastic deformation of the bolts themselves. If plastic deformation had been induced into the bolts, it would have been detected by the end plate and column flange separating in this region. However, from the observations reported above, no evidence of this happening was detected and therefore the assumption that the bolts were behaving elastically seems reasonable. Similar impressions, but to a much reduced depth, can also be seen in the two lower bolt rows located in the compression region of the connection (see Plate 7.11).

Having established that the bolts were behaving elastically at the end of the test, raises the question as to whether the test should have been curtailed before a clear mode of ultimate failure could be identified. In defence of this action, it has to be remembered that bolt fracture would occur relatively quickly following the onset of plasticity[108]. Furthermore, the purpose of undertaking this particular test was to establish the response of the steelwork part of the subsequent composite tests. This had been ostensibly achieved, since we know from other experimental programmes[9], that the rotation of a steel-only connection would simply continue until fracture of one of the component parts occurs.

7.4.3 Test 2 - composite (4T16 rebars closely spaced)

For details of the connection configuration refer to Chapter 6, section 6.2

The first signs of the induced moment that the connection was experiencing came in the form of small cracks appearing on the concrete surface (42kNm), propagating from the column flange tips in a transversely orientated direction. The formation was reasonably symmetrical between the front and back of connection A. However, although there was a similar crack at the front of connection B, the back of the connection remained intact. This began to crack when the next load increment was applied (56kNm), although by now the shorter cracks on connection A had formed a complete transverse crack across the breadth of the slab. A duplicate transverse crack applicable to connection B was achieved when a connection moment of 112kNm had been obtained. As the test progressed, several new independent transverse cracks appeared on both connections A and B. Their positions approximated the positions where the transverse bars of the mesh reinforcement were located within the slab. All such cracks had formed by the time the connection characteristic was indicating that the moment of resistance of the connection had been attained. By the end of the test, the furthest transverse cracks were located 1200mm away from the column flanges for both connections.

When the connection moment had reached 197kNm, the first longitudinal cracks appeared in the vicinity of the connection, above the positions where the inner-most rebars were located. These were joined by similar longitudinal cracks appearing above the outer-most rebars soon after (211kNm). This alternating pattern was a characteristic which continued throughout the duration of the test, as the cracking progressed towards the loading points. The likely explanation as to why the longitudinal cracks appear above the inner-most rebars first, could be attributed to the fact that the rebars located in this position carry a greater proportion of the load, than the equivalent outer-most rebars. This was substantiated from Test 3 onwards, where the strain within the rebars was measured.

However, following the completion of the test, the extent of the cracking had evened itself out above all the rebars, and extended in a symmetrical fashion to a distance 800mm from the column flange. The widths of these cracks were at their greatest where they intersected with the column centre line between the flanges.

There are two possible explanations to why longitudinal cracking occurs. Firstly, as the connection rotates, the rebars are forced into single curvature and consequently tensile strains are generated. These strains are identified by the appearance of the transverse cracking. By their very nature, the rebars would try to straighten as much as possible to enable the strain within them to be dissipated. However, this process is restricted due to the presence of the concrete slab which accommodates the reinforcement's requirements by inducing transverse curvature across the breadth of the specimen. Consequently, tensile forces are generated on the slab surface and concentrated above the positions where the rebars were located (see Figure 7.3).

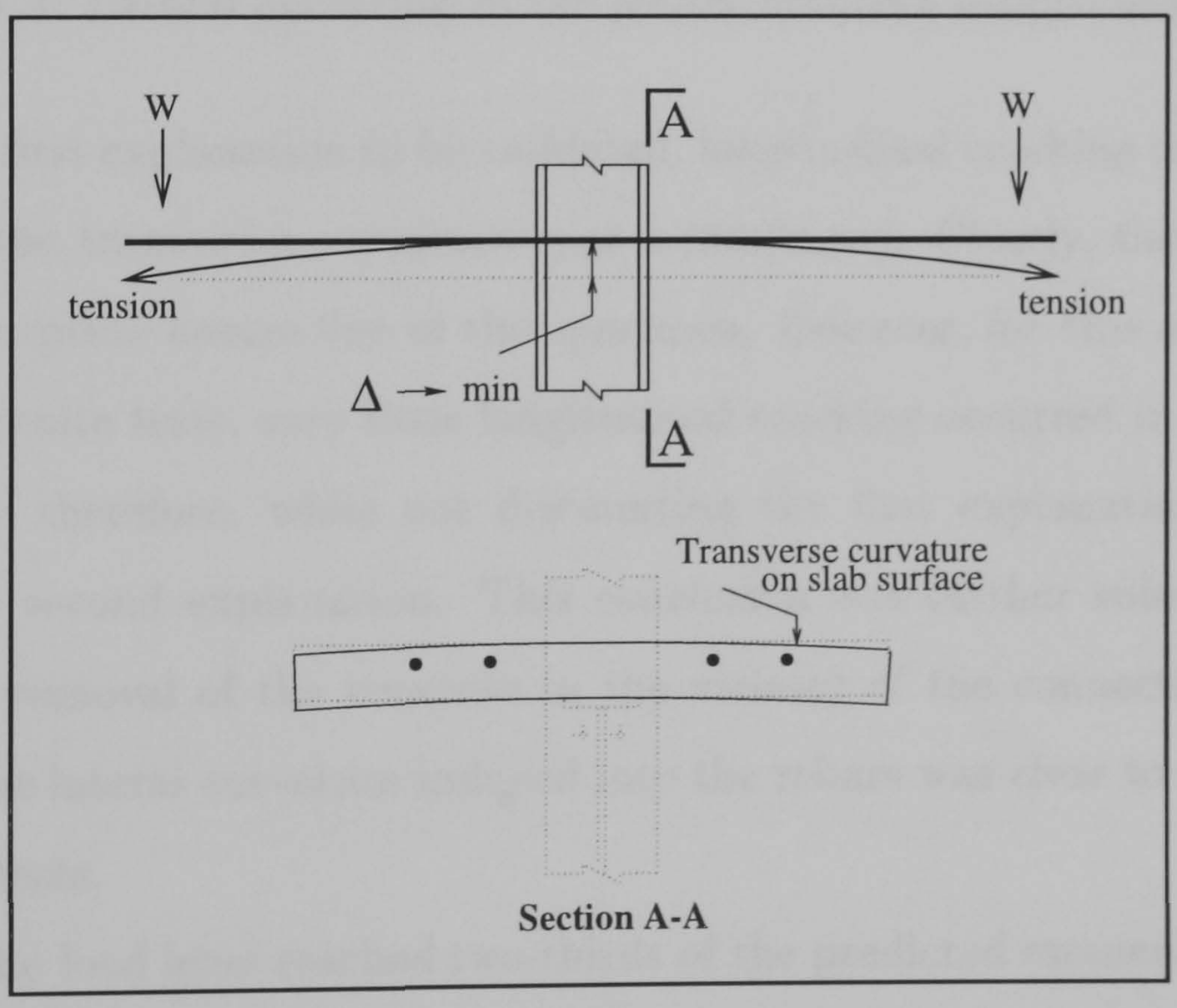

Figure 7.3: Transverse bending of the concrete slab inducing longitudinal cracking

Alternatively, the tensile force within the rebars must be balanced by an equal and opposite force within the shear studs. This creates a couple, with the lever

arm equal to the distance from the centre line of the shear studs to the centre line of the applicable rebar under consideration. Under the action of this moment, lateral curvature would be induced into the rebars. The influence of this lateral curvature would again tend to generate tensile forces in the concrete above the positions of the reinforcement (see Figure 7.4).

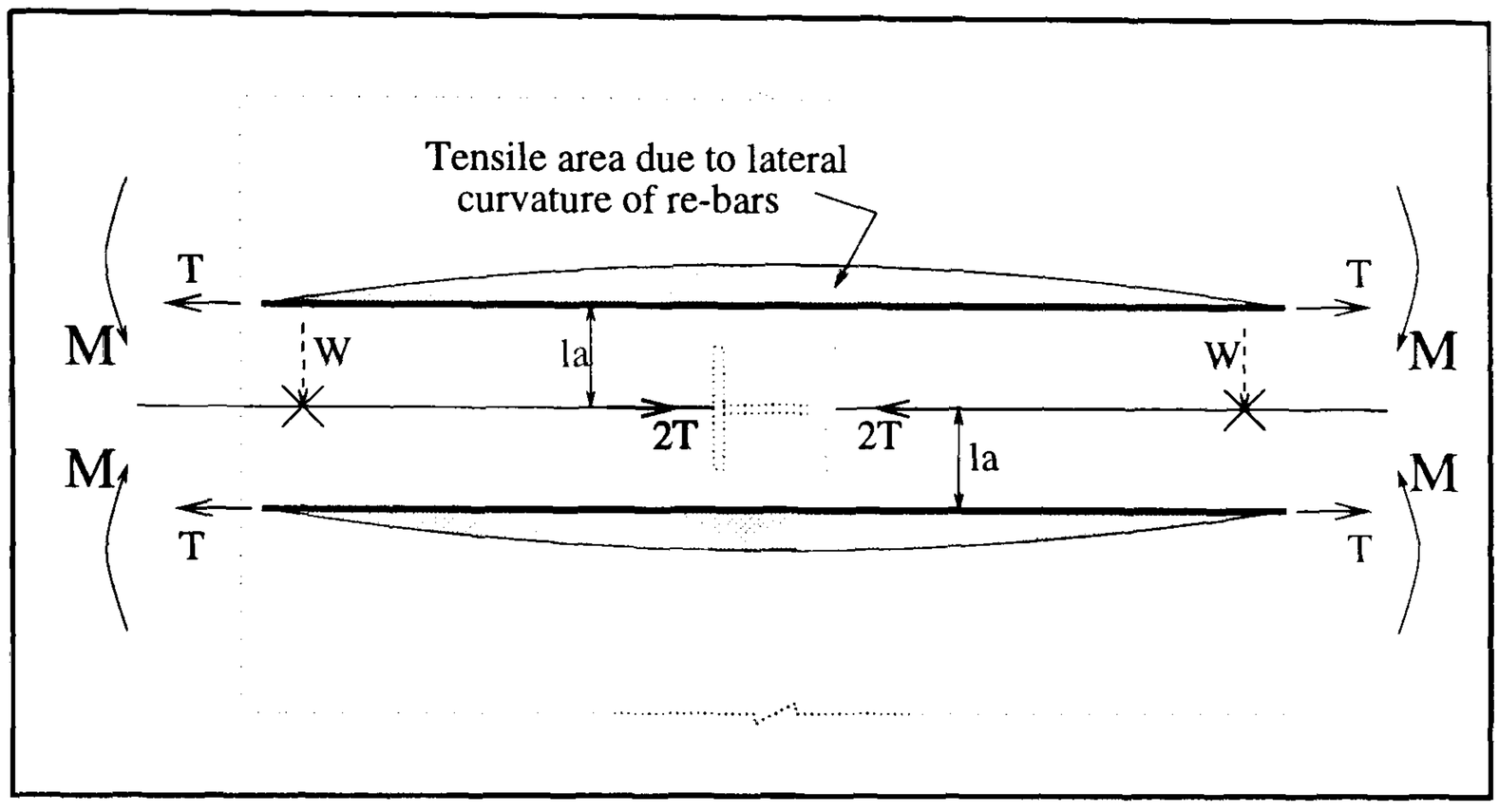

Figure 7.4: Lateral curvature of the rebars inducing longitudinal cracking

For the first explanation to be validated, longitudinal cracking must be apparent where the transverse curvature is at a maximum. Clearly, this would occur along the in-plane centre line of the specimen. However, for this and the subsequent composite tests, very little longitudinal cracking occurred in this position. The author therefore, while not discounting the first explanation completely, favours the second explanation. This conclusion was further substantiated following the removal of the concrete in the vicinity of the connection, since the extent of the lateral curvature induced into the rebars was clear to see for all the composite tests.

When the load level reached two-thirds of the predicted moment of resistance of the connection (237kNm), there were signs that the end plate and column flange were beginning to deform. However, it became apparent at this load level that the original transverse cracks propagating from the column flange tips were not opening symmetrically on connection A. The crack located on the back of

the specimen had opened slightly further than its reciprocal crack on the front. These observations were not mirrored on connection B. where the crack width for both the front and the back of the specimen appeared to be of similar magnitude. This unexpected crack pattern development was accompanied by the column beginning to rotate about its out-of-plane axis. Consequently, lateral displacements of the compression flanges were again evident at the respective beam ends. Since the lateral displacements were small and did not effect the performance of the connections in the first test, no attempt was made initially to prevent further movement.

The connection was then unloaded to monitor its unloading stiffness. Following its reloading, a drop in the applied moment of the order of 3% occurred when a connection moment of 340kNm was achieved. This was accompanied by an audible muffled bang, which sounded as though it had come from within the concrete slab. Following the subsequent examination of the slab, it was apparent that the initial transverse crack on the back of the specimen applicable to connection A, had opened appreciably in the region closest to the edge of the slab. Therefore, it was deduced that the longitudinal members of the mesh reinforcement located in this position had fractured. A further bang was heard when a connection rotation of 11mradians had been induced. This had the effect of enlarging this back crack sufficiently to expose the fractured ends of the mesh reinforcement and consequently substantiating the former deduction. The next increment restored the load level to that achieved prior to the reduction, upon which the test proceeded by applying rotational increments.

As the test progressed into its plastic range, the progression of the deformation associated with the steel part of the connection followed a similar pattern to that observed for the first test; in particular, the re-occurrence of the gap that opened up between the column flange and the end plate as a result of the column flange deformation. However, differences came to light between the tests following the attainment of a connection rotation of 10.5mradians when local buckling

became apparent in the back compression flange of the specimen. Similar local buckles became apparent on the front of the specimen after a further 3mradians of rotation had been induced. It was thought that the local buckles occurred in this test, as a direct consequence of the increased compressive force arising from the influence of the steel reinforcement within the slab.

Unfortunately however, as plasticity continued, the out-of-plane rotation of the column, which was exacerbated by the onset of local buckling, was beginning to take precedence in terms of controlling the destiny of the test. Moreover, as the plastic plateau was approached, the author had expected the out-of-plane rotation of the column, and consequently the lateral displacements of the compression flanges, to stabilise in a similar manner to that seen during the first test. However, this was not the case due to the influence of local buckling occurring in the vicinity of the connections. Attempts were made at this stage to restrict further out-of-plain rotation, by applying lateral restraints to the beam ends (see Plate 7.2). However, although further lateral displacement of the compression flanges was prevented, the restraints did nothing to prevent the continuation of the column rotating about its out-of-plane axis. With the test rig set up as it was, no external restraints could be applied directly to the column. Consequently, the test was abandoned following the attainment of the theoretical rotation required to allow plastic analysis to be vindicated for this type of connection[9]. A clear mode of ultimate failure could not therefore be established for this test.

The moment-rotation characteristic determined for this test is shown by Figure 7.9 (see Section 7.5), from which the following can be identified.

The moment of resistance of the connection : at least 380kNm

Available rotation capacity : $>$ 32.8mradians

The level of strain induced into the lower compression flanges of connection B indicated the onset of material yield when a connection moment of 226kNm had been obtained. The compressive strain applicable to connection A was 25% lower. This difference was not so pronounced for the corresponding web strains, where

the horizontal and diagonal arms of the rosette measured 0.08% and 0.07%, for connection B and A respectively. The vertical strain within the beams was very small at 0.02%. Connection A reached the onset of material yield soon afterwards (282kNm), whereupon the corresponding strain within connection B had risen to 0.13%. The web strains were also approaching material yield at this load level and 0.1% was surpassed following the attainment of the next increment (310kNm).

The general deformation induced into the steelwork is shown for the front of the specimen by Plate 7.12 and for the back of the specimen by Plate 7.13.

The general form of the concrete crack pattern, showing the extent of the uneven crack enlargement applicable to connection A, is illustrated by Plate 7.14.

Following the completion of this and all subsequent composite tests, all the concrete in the vicinity of the connection was broken out by the author. This not only revealed the deformed and fractured reinforcement in the slab, but also the deformation (if any) of the shear studs nearest the column.

Throughout the composite tests, no deformation was apparent within the shear stud connectors positioned closest to the column.

The out-of-plane rotation of the column can be see in Plate 7.15. In addition, the lateral curvature of the main rebars located in the back of the specimen can also be seen. Similar curvature to the front rebars also occurred, however to a much lesser extent. Another observation which was unexpected concerns the direction of the corresponding curvature. The author would have expected the directions of the lateral curvatures of the rebars to have been approximately equal and opposite between the front and the back of the specimen. However, from the exposed reinforcement this was found not to be the case. In reality, the curvatures were in the same direction. The smallest curvature occurred to the outer-most rebar which was located in the front of the specimen, and increased over the breadth of the slab with the greatest curvature apparent in the back

outer-most rebar. This unexpected result was thought to be as a consequence of the out-of-plane rotation of the column altering the balance of the tensile forces within the rebars. Further confirmation that the balance of the tensile forces within the rebars was not symmetrical between the front and back of the specimen, can be seen in Plates 7.16 and 7.17. Plate 7.16 shows only part of the mesh reinforcement located in the front of the specimen to have fractured, with the corresponding distance between the fractured ends being small. In contrast, the mesh reinforcement located in the back of the specimen (see Plate 7.17), has been completely fractured across the slab, with a significant distance between the fractured ends.

As already stated, the cause of the out-of-plane rotation of the column was attributed to the imperfections within the connections inducing an out-of-plane turning moment. The column could not be rotationally restrained to resist this applied moment, because its base was being supported on a ball joint (see Plate 7.4) and was consequently free to rotate in any direction should the need arise. In reality, the column would not be able to behave in this manner, due to the geometrical constraints of the building as a whole. Therefore, to prevent a further repetition of this uncharacteristic behaviour, the column support was re-designed. Restraint in the out-of-plane direction was achieved by replacing the ball joint with an uni-directional rocker (see Plate 7.5).

When the specimen was dismantled, similar impressions of the bolt nuts were left on the insides of the column flanges in the tension region, as were described in Test 1. However, much lighter impressions could be seen on the column flanges in the compression region of the connection. It is thought that shallower impressions were obtained due to the neutral axis being displaced upwards with the influence of the reinforcement. Consequently, the tensile force being resisted by these bolts would be reduced. Similar observations could be made for all the subsequent composite tests as far as the compression region was concerned. However, differences were apparent in the corresponding depths of the impressions left in the

tension region for all the tests, which appeared to be a function of the amount of rotation induced into the connection.

Following a close examination of the test prior to the removal of the load, an unexpected form of deformation had occurred within the depth of the end plate (see Figure 7.5).

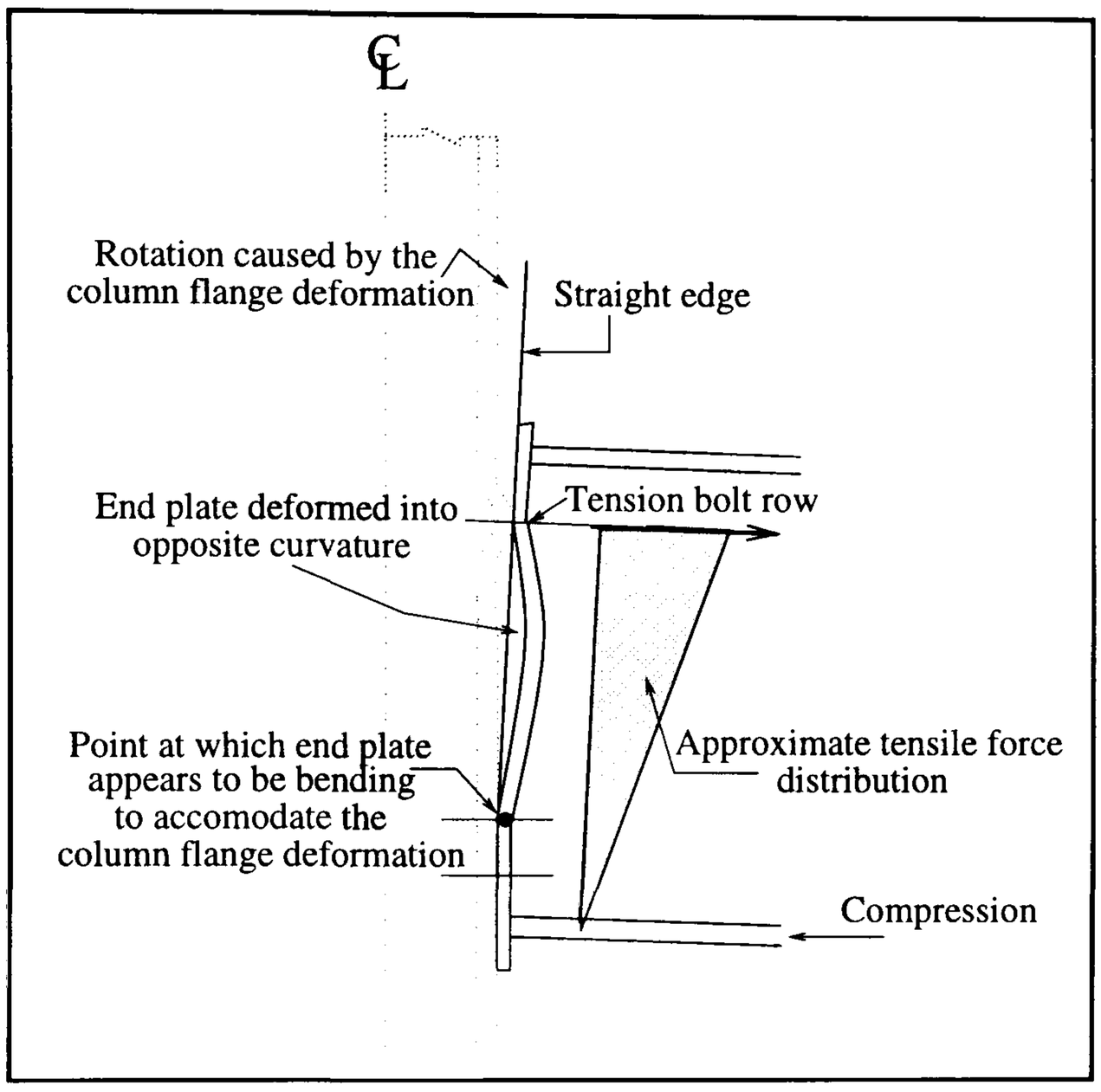

Figure 7.5: Curvature of the end plate between the bolt rows

From this figure, it can be seen that the curvature of the end plate was in the opposite direction to that which the author would have expected. However, following due consideration to the actions of the forces involved, a possible explanation for this occurrence was apparent.

The end plate would be restrained at both positions where the bolt rows were located. Consequently, if we then superimpose the tensile forces acting on the end plate, due to the action of the induced bending throughout the depth of the beam, a deflected form of the type shown would be produced. The justification for extending the tensile force distribution down to the lower beam flange, was as a result of tensile action being indicated at the lower two bolt rows by the

formation of impressions of the nuts, which were left on the column flanges in this region of the connection.

Continuing along this line of thinking, it would also be reasonable to expect the maximum displacement to occur towards the position of the tension bolt row. Although this was indicated from the measurements taken, the position could not be established with certainty, because the displacements were very small, i.e. < 1.5mm for a 15mm plate thickness and approximately 2.5mm for a 10mm end plate.

7.4.4 Test 3 - composite (4T16 rebars widely spaced)

The connection configuration for this test was identical to Test 2 above, except that the spacing of the rebars was increased to the maximum permitted by present-day codes of practice (see Chapter 6, section 6.1). In addition, to enable the performance of these rebars to be monitored as the test progressed, strain gauges were secured on the rebars in the vicinity of the connection (see Plate 7.7).

Initially the test progressed in exactly the same fashion as Test 2. Transversely orientated cracks appeared propagating from the column flange tips on the back of the specimen for both connections (56kNm). These were joined by a similar crack on the front of the specimen applicable to connection B, to produce the first complete transverse crack across the breadth of the slab (70kNm). This was duplicated on connection A shortly afterwards (113kNm). The pattern of transverse cracking observed during this test was similar to that established during Test 2. However, the primary difference between the two patterns was that the dominant crack (connection A), opened in a relatively symmetrical manner between the front and the back of the specimen as a consequence of the column now being restrained from deflecting out-of-plane. This was in contrast to Test 2, where the corresponding crack on the back of the specimen was considerably wider than the crack on the front. Following the test completion, the

furthest cracks were measured to be 1200mm from the column face. The width of the cracks varied considerably along the length of the connections. with the initial cracks being by far the largest, with the others being at least one order of magnitude smaller.

The first longitudinal cracks became apparent above the inner-most rebars when a connection moment of 197kNm had been obtained. This was exactly the same load level that produced the initial longitudinal cracks in Test 2, and was to be expected since the positions of these rebars relative to the column had not altered. However, similar cracks did not appear over the outer-most rebars until a connection moment of 268kNm had been achieved. Consequently, one of the effects of increasing the spacing of the rebars was to increase the applied connection moment by 27% prior to longitudinal cracking occurring above the outer rebars. By the end of the test however, there was a similar degree of longitudinal cracking over both the inner and outer rebars. The length of these cracks extended a distance of 800mm from the face of the column, for both connections A and B.

The observations for this test began to differ from those made during the previous test as the mid point of phase 2 was approached (211kNm). The apparent difference was that now there was no out-of-plane rotation occurring to the column, and consequently, the lateral displacements of the compression flanges were reduced significantly. They were not however eliminated completely. It is thought that the small lateral displacements were again caused by the out-of-plane turning moment. However for this and the subsequent tests, this moment could now be resisted by the torsional stiffness of the beams which had not been mobilised to its full potential when the column was being supported on a ball joint.

The first signs of deformation within the column flange and end plate came as two-thirds of the predicted moment of resistance of the connection was attained (237kNm).

Following the attainment of a connection moment of 325kNm, the applied

load dropped by 3% and simultaneously, a muffled bang was heard. Following this occurrence, the initial transverse crack on connection A opened slightly in the direction towards the column, but was unaltered at the outermost edges. Therefore it was concluded that the longitudinal members of the mesh located in the middle of the slab had fractured and the external members were still intact. This could not be verified visually, since the crack width was not sufficient to expose the fractured ends. The next increment restored the load level and the test progressed in rotational increments. When a connection rotation of 15mradians had been induced, a similar bang was heard. This again was accompanied by a 4% decrease in the applied load. It was concluded that this second bang was the outer longitudinal rebars of the mesh reinforcement fracturing in the vicinity of the connection. This second fracture had the effect of re-establishing a reasonably uniform crack width across the breadth of the slab on connection A. The width of the corresponding transverse crack applicable to connection B was considerably smaller throughout the duration of the test. The crack width on connection A was always dominant, because the diameter of the rebars in the vicinity of the connection had been reduced to enable the strain gauges to be secured. This process was necessary as a consequence of the deformed pattern being present on the surface of the rebars. For a given load in the rebar therefore, the corresponding elongation would be greatest in this locality by virtue of its reduced area. Furthermore, this would also explain why, for a given point in the test procedure, the connection rotation for connection A was always in excess of that applicable to connection B.

As plasticity continued to develop, the deformation within the column flange increased, thus producing the familiar gap between the flange and the end plate.

The onset of local buckling and its development throughout the test was similar to that observed for Test 2, with the exception that the buckles developed on the front of the specimen before the back. By the end of the test however, another difference became apparent. The magnitude of the local buckles were

larger in this test than their equivalent in the previous test. It is thought that this difference was a function of the induced rotation, since the moment resistances of the connections, and hence the compressive force within the lower flanges, were not significantly different.

This test was brought to a dramatic conclusion by fracture occurring to the rebars themselves. This was indicated by a significant reduction in the applied load, of 36%. In addition, following the examination of the specimen it became apparent that thread stripping to either the nut or bolt had also occurred to the back tension bolt of connection B. When the connection was dismantled, it was found that the threads had stripped on the nut rather than the bolt itself.

The moment-rotation characteristic determined for this test is shown in Figure 7.10 (see Section 7.5), from which the following can be identified.

The moment of resistance of the connection : 390kNm

Available rotation capacity : 47.7mradians

The strain reached 0.1% within the inner rebars when a connection moment of 112kNm had been obtained. During the earlier stages of loading, the strains measured in the rebars showed slight variation between the force resisted by the inner rebars and that resisted by the outer rebars and is typical of elastic shear lag[109]. Generally, the strains in the inner-most rebars were of the order of 8% higher than the corresponding strains in the outer-most rebars. When a strain of 0.1% was exceeded however, the variation increased, such that when two-thirds of the connections moment of resistance had been obtained (237kNm), the difference was in the order of 20%. It is thought that the increase in the variation between the rebars was the result of the inner rebars beginning to yield, whereas elastic conditions were still applicable to the outer bars. The strain in the inner-most rebars was approaching 0.2% at this load level, with 0.15% applicable to the outer-most rebars. Unfortunately, no further reliable data could be obtained from these strain gauges due to inconsistences within the measured values being obtained at higher load levels. The strain levels applicable to the lower compression flanges

and webs were of the same order as those ascertained from Test 2, at a comparable load level. Therefore, it can be concluded that the horizontal spacing of the rebars has a negligible effect on the compressive strains within the lower flanges of the beams. This statement is only valid up to the onset of material yield, since the materials characteristics in compression were not known beyond the approximate elastic limit corresponding to a strain of 0.1%.

The deformation characteristics applicable to the tension region of the steel part of the connection were very similar between the front and the back of the specimen. However, this was not reflected in the development of the local buckles within the compression flanges, where the buckles in the front of the specimen were larger than those applicable to the back. This can be clearly seen by Plates 7.18 and 7.19, which show the general deformation induced into the steelwork for the front and back of the specimen respectively.

Plate 7.20 shows the back bolt of connection B, where thread stripping to the nut had occurred. It was thought that this situation was created as a result of the force being carried by the fractured rebar being redistributed between the other components of the connection when it actually fractured. The explosive manner in which this load transfer occurred would have the effect of applying what would amount to an impact load to the connection. This was accommodated by necking being induced into the inner rebar located at the back of the specimen, and the nut at the back of the specimen (connection B) having its threads stripped. Clearly, the possibility of bolt failure is undesirable, since had the threads not stripped, then fracture of the bolt may have been the result. Consequently, to prevent this from occurring in the future tests, the bolts were increased to M24 diameter for the subsequent specimens. This solution was implemented, since the author believed that this would limit the behavioural differences that would inevitably occur, as a result of altering the tension resistance of the connection.

The general form of the concrete crack pattern for this test, showing a more uniform crack formation on connection A, is illustrated by Plate 7.21.

Following the removal of the concrete in the vicinity of the connection, the lateral curvatures of the rebars were found to be approximately equal in magnitude and opposite in direction (see Plate 7.22). This was a feature of all the composite tests where the column was supported on an uni-directional rocker. Plate 7.23 shows clearly that the fracture occurred to the outer rebar located on the back of the connection, in addition to necking being induced into the corresponding inner rebar. It can also be seen, although not as clearly, that the fracture of the mesh reinforcement had occurred across the complete breadth of connection A. The corresponding distances between the fractured ends were found to be relatively constant, therefore it could be assumed that the strain distribution across the breadth of the slab could be considered to be uniform at the completion of the test. The fractures within the mesh were duplicated on connection B; however, the distances between their respective fractured ends were significantly less than those measured for connection A. An explanation as to why the outer rebar fractured in preference to the inner rebar, could be in part attributed to the area of the rebars being reduced to enable the strain gauges to be secured in position. The extent to which the area was reduced was not specifically controlled; however, no more surface metal was removed than was considered necessary. Inevitably therefore, a variation in the area of the rebars would be present across the breadth of the slab, thereby influencing which rebar would eventually fracture.

Following a comparison between the moment-rotation characteristics applicable to all the composite tests, close correlation was achieved. Therefore it can be concluded that the effect of increasing the horizontal spacing of the rebars does not significantly effect the resistance and stiffness of the connections. No comment could be made as far as the rotation capacity of the connection was concerned, because a mode of failure for the previous composite test was not established.

7.4.5 Test 4 - composite (thin end plate)

This test was very similar in configuration to those that were undertaken previously, the difference being that the end plate thickness was reduced. The reinforcement arrangement was identical to Test 3 (see Chapter 6. Section 6.2).

The sequence in which the initial transverse cracks propagated from the column flange tips was similar to that observed for the previous composite tests. The cracks located on the back of the specimen appeared first (42kNm). with the front cracks following soon afterwards (56kNm). In addition, at this load level. the crack located at the back of the specimen on connection A progressed to the edge of the slab. Complete transverse cracks were evident on both connections following the attainment of a connection moment of 70kNm. However, a difference in the formation of the crack pattern located on the front of the specimen applicable to connection A, was also observed at this connection moment. The standard pattern which had occurred in all of the previous composite tests, and indeed for three of the four initial transverse cracks in this test, was that the progression of the cracks from the flange tips occurred generally in a perpendicular direction (see Figure 7.6a).

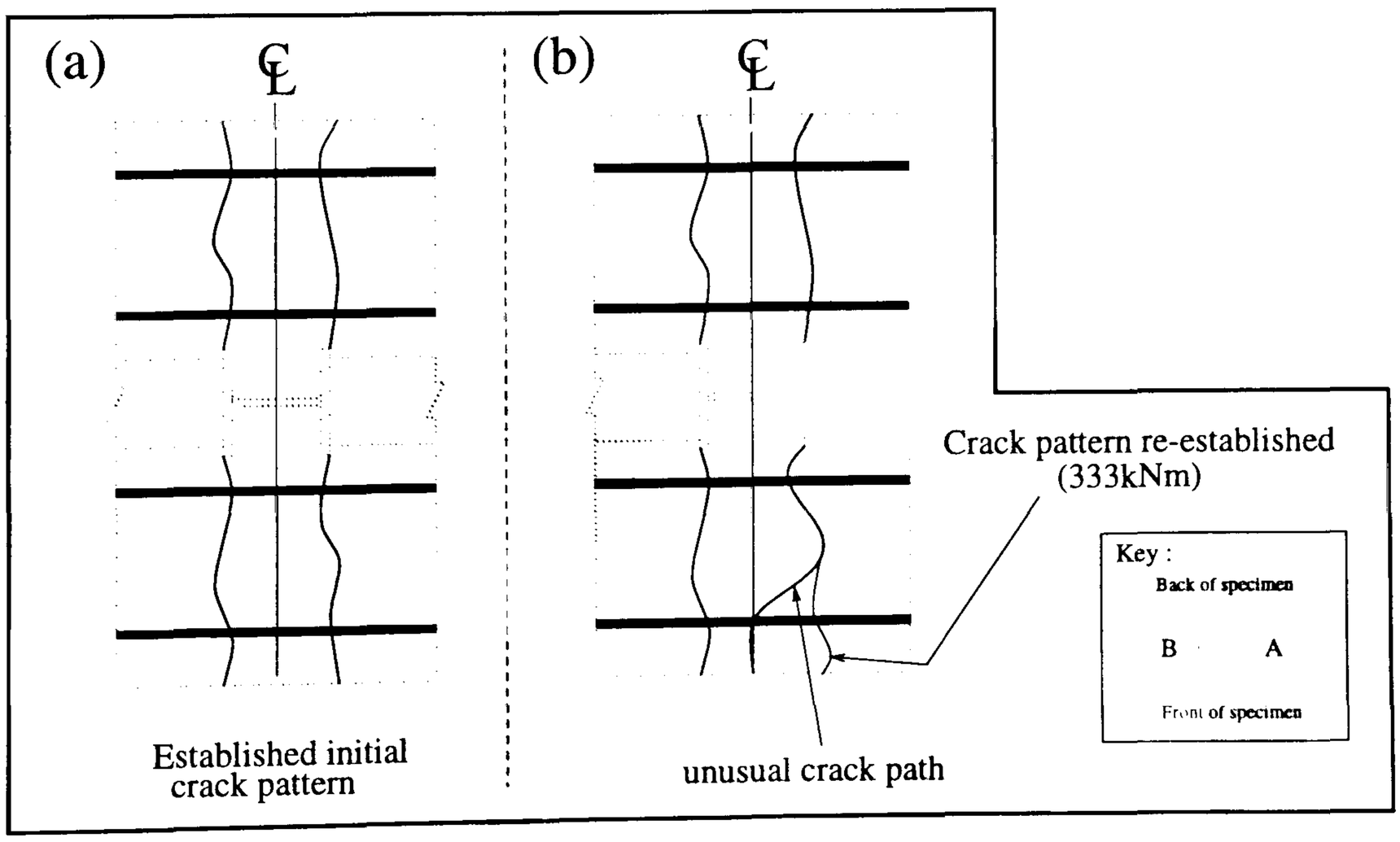

Figure 7.6: Unusual concrete crack pattern

However, for the front crack on connection A, although initially its progression followed the established pattern, on reaching midway between the inner-most and outer-most rebars, its path changed. The change took the form of the crack progressing diagonally to meet the centre line of the column between the flanges. before finally progressing perpendicularly to the slab edge (see Figure 7.6b). The diagonal length of this crack intersected the column's centre line approximately in the position where it also intersected the external rebar.

As the test continued, these established cracks opened reasonably symmetrically between the front and back of the specimen. However, the width of the crack applicable to connection A was always larger than that observed for connection B. When a connection moment of 333kNm had been obtained, a new transverse crack appeared on the front of the specimen, applicable to connection A. It propagated from the position where the path of the initial transverse crack described above was diverted diagonally. The new crack extended perpendicularly to the slab edge. Consequently, uniformity of the crack pattern between the composite tests in the vicinity of the connections was re-established. As loading continued, the width of the diagonal crack remained unchanged, with the extension of the new crack accommodating the connection rotation.

The development of the longitudinal crack pattern was identical to that seen in the previous composite tests. Longitudinal cracking above the inner rebars was initiated first (141kNm). However, these were not duplicated on the outer rebars until the connection moment had risen to 282kNm. By the end of the test, the extent of the longitudinal cracking above all the rebars was similar on both sides of the specimen, and was also reasonably symmetrical between the connections. These cracks progressed to approximately 800mm in length when measured from the column flanges.

It had become apparent at connection moment of 65kNm that the connection stiffness had been reduced as a result of the change in end plate thickness.

Steel deformation became apparent in the end plate when the connection

moment was 155kNm. This deformation took the form of the end plate peeling away from its mating position against the column flange. There was no evidence at this stage to suggest that the column flange was deforming (see Figure 7.7).

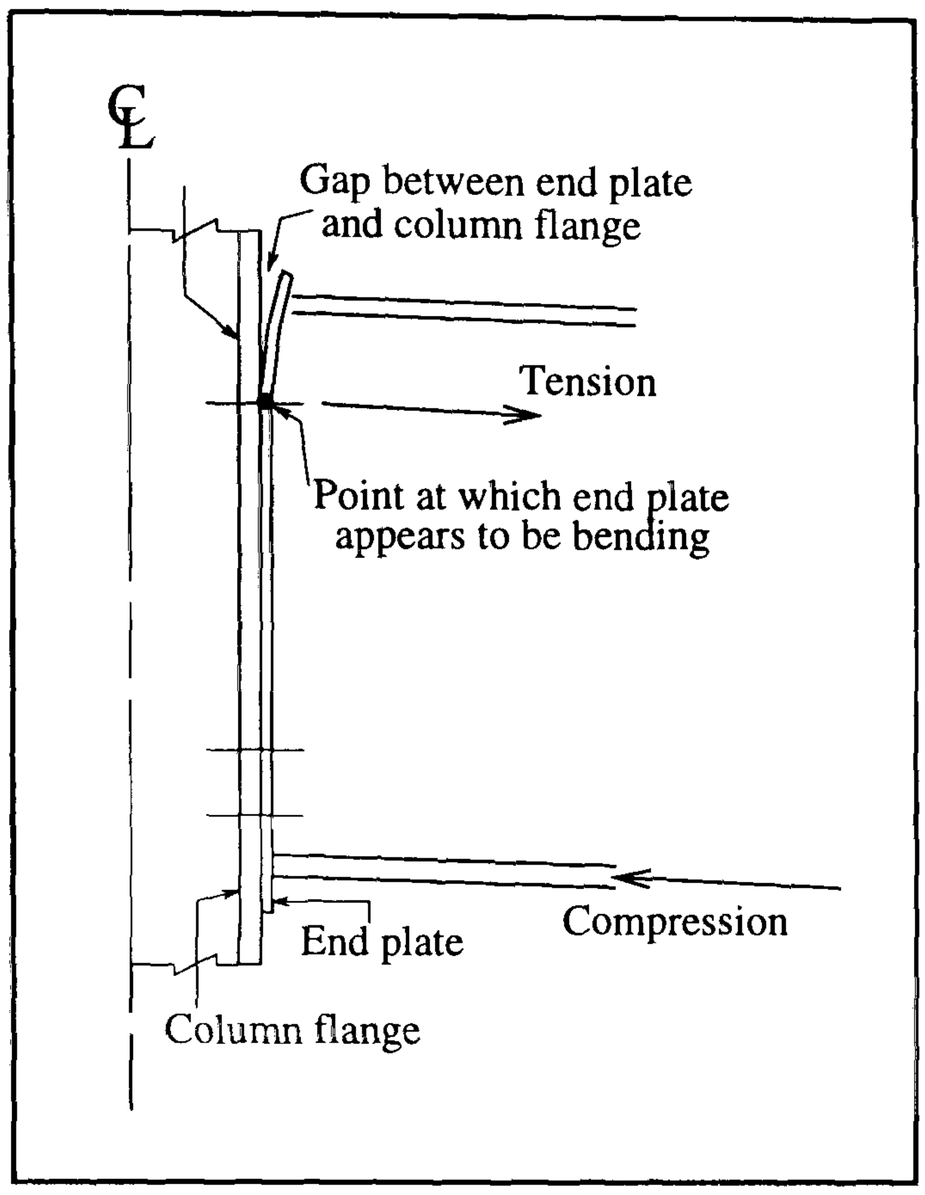

Figure 7.7: End plate deformation within the tension region of the connection

Following the attainment of two-thirds of the calculated moment of resistance of the connection (200kNm), the end plate deformation had increased appreciably in comparison to the previous tests. At this stage it looked as though this deformation was the result of the end plate bending about the centre line of the tension bolt row. This was in contrast to the previous tests, where at this load level no visible steelwork deformation had occurred. It was therefore thought that the increase in connection flexibility could be attributed to the end plate deformation in the tension region initially influencing the connection's rotation.

At this load stage, the strain measured in the inner rebars had reached 0.18%, whereas the corresponding strain applicable to the outer rebars was 28.5% lower. Following a comparison between the corresponding strains in the rebars between this test and Test 3, it was established that the level of strain measured in the rebars were slightly higher than their corresponding values established previously.

In addition, the variation in the strain distribution between the inner and outer rebars had increased. The strain in the inner-most rebars reached 0.1% when a connection moment of 112kNm had been obtained. However, the corresponding strain in the external rebars was 25% lower. This difference gradually increased. such that by the time the strain measured 0.2% (219kNm). the difference had risen to 30%. In addition, the strains in the compression zone were symmetrical between the front and back of the specimen, with a compressive strain in the lower flanges equal to 0.06%. This was approximately matched by the horizontal and diagonal arms of the rosettes which measured 0.055%. The corresponding strain within the vertical arms of the rosettes was equal to 0.023%.

The first signs of deformation within the column flanges became evident when the connection moment had reached 254kNm. This was only slightly higher than the load level that induced similar deformation during Tests 2 and 3. Therefore, it can be concluded that the end plate thickness does not have a substantial influence on the deformation characteristics of the column flange.

Rotational increments were adopted above a connection moment of 300kNm.

As the plastic plateau of the moment-rotation characteristic was approached, and a connection rotation of 8mradians had been achieved, the applied load dropped by 6% as the mesh fractured in the vicinity of connection A. This was accompanied by the initial transverse crack applicable to connection A opening in a symmetrical manner between the front and back of the specimen.

As plasticity continued the column flange deformation increased. However, the deformation within the end plate located in the tension region appeared to stabilise. Consequently, the column flange deformation was accommodated by the end plate bending at the centre line of the upper bolt row assumed to resist shear. This had the effect of opening a gap between the column flange and the end plate in an identical manner to that observed during the previous tests.

Local buckling within the compression flanges close to the column. applicable to the back of the specimen, was observed when a connection rotation of 15mra-

dians had been induced. This was not duplicated on the front of the specimen until a rotation of 17mradians had occurred. However, unlike the previous tests, as the connection rotation increased the magnitude of the buckles appeared to increase at a slower rate. It is thought that a possible explanation for this could be attributed to the lower moment of resistance of the connection not being able to overcome the strain hardening effect, due to plastic deformation, as effectively as was seen in the previous tests. This could have a pronounced effect on the strain level within the reinforcement. Clearly, if the rotation of the connection is not, in part, associated with buckling of the lower flange, then it must be a result of deformation within the tension region. This deformation would be coming from the column flange and the end plate, which would in turn subject the rebars to a greater strain for a given rotation. Consequently, the author believes that the above explanation is the reason why a considerably lower connection rotation was achieved for this test, in comparison with that achieved for Test 3, where the connection rotation was 34% higher (see Table 7.1).

When a connection rotation of 22mradians had been induced, the specimen was unloaded completely to enable the loading jack applicable to connection A to be re-set. The problem was associated with the loading arrangement (see Plate 7.3). The rocker/roller configuration permits a certain maximum horizontal displacement of the rollers relative to the rocker, before the arrangement becomes inherently unstable. This limit was approached during the test. Following the re-positioning of the loading arrangement, the specimen was loaded to failure.

The mode of failure for this specimen was fracture of the rebars within the concrete slab.

The moment-rotation characteristic determined for this test is shown by Figure 7.11 (see Section 7.5), from which the following can be identified.

The moment of resistance of the connection : 370kNm

Available rotation capacity : 35.5mradians

The plastic deformation induced into the steelwork is shown by Plates 7.24 and 7.25, which are applicable to the front and the back of the specimen respectively.

The deformed and fractured reinforcement can be seen by Plate 7.26. From this photograph, it can be seen that the connection failure was clearly the result of an outer-most rebar located on the front of the specimen fracturing. It can also be seen that the mesh reinforcement had fractured across the breadth of the slab. However, the distance between the fractured ends tend to indicate that the front of the specimen was resisting a greater strain than the back. This, however, was not indicated in the crack pattern until fracture had occurred. The deformed and fractured reinforcement applicable to the front of the specimen is shown in more detail by Plate 7.27. In addition, the lack of deformation induced into the shear stud connectors is apparent.

7.4.6 Test 5 - composite (deeper beams/larger column)

The reinforcement arrangement for this test remained unaltered form the previous test and the end plate thickness was restored to 15mm (see Chapter 6, section 6.2).

The crack pattern was initiated again by transverse cracks propagating from the column flange tips. The front and back cracks for both connections opened when the connection moment was 42kNm. Subsequently, they reached the edges of the slab to form complete transverse cracks when the connection moment was 98kNm and 127kNm for connections A and B respectively. The initial cracks opened up in a symmetrical fashion between the front and back of the specimen.

At a connection moment of 127kNm, a transverse crack propagating from midway between the inner and outer rebars, appeared on the centre line of the column between the flanges. This crack was symmetrical between the front and back of the specimen. The crack extended to the slab edges first (183kNm), followed by the column (268kNm). As the connection rotation increased, the width of this crack was unaffected and remained only just visible by the conclusion of the test.

The formation of the longitudinal cracks again followed the same pattern that has been discussed previously. The cracks formed above the inner rebars first (183kNm), and were subsequently mirrored on the outer rebars (240kNm). These cracks formed in a symmetrical fashion between the front and back of the specimen. By the end of the test, the extent of the cracking had evened out between the internal and external rebars. The longitudinal cracks extended approximately 800mm from the column flanges on both connections A and B.

As the load level increased to two-thirds of the predicted connection resistance (340kNm), deformation was just detectable within the tension region of the column flange.

When a connection moment of 437kNm had been obtained, there was an audible bang which was accompanied by a reduction of the applied load by 5%. This was again coincident with the width of the initial transverse crack applicable to connection A increasing. It was therefore assumed that the longitudinal rebars of the mesh reinforcement located in the vicinity of the column had fractured.

As the connection rotation increased, the deformation within the column flange increased and a gap was duly created between the flange and the end plate, as before. There was no evidence to suggest that the end plate itself was bending about the centre line of the tension bolt row.

Prior to the completion of the test, when a connection rotation of 18mradians had been achieved, it became apparent that the bolts were beginning to elongate. This was indicated by the end plate and column flange separating at the position where the tension bolts were located. To avoid concerns about the bolts fracturing, the specimen was unloaded to enable remedial strengthening measures to be undertaken. These took the form of welding as much as was practicable of the bolt head and the nut to the end plate and column flange respectively (see Plate 7.30). In doing this, bolt fracture was not prevented; however, should it occur then the bolt parts would be held in position. When the specimen was re-loaded, the loading path was very similar to that which was obtained dur-

ing the earlier stages of the test procedure. Therefore, it was concluded that the remedial measures undertaken to protect against bolt fracture would have a negligible effect on the connection's performance.

The test was then resumed until the connection failed by the rebar fracturing. This was indicated by the applied load dropping by 17%.

The moment-rotation characteristic determined for this test is shown by Figure 7.12 (see Section 7.5), from which the following can be identified.

The moment of resistance of the connection : 493kNm

Available rotation capacity : 20.1mradians

The plastic deformation induced into the steelwork is shown by Plates 7.28 and 7.29, which are applicable to the front and back of the specimen respectively.

There was no visible evidence to suggest that local buckling was occurring to the compression flanges of the beams in the vicinity of the connections. However, the compressive strains in the lower beam flanges were sufficient to indicate the onset of material yielding when the connection moment had reached 340kNm. By the end of the test, the compressive strain had reached 0.17%. The compressive strains applicable to the horizontal and diagonal arms of the rosettes secured to the beam webs were of a similar order as those obtained from the flanges.

The low rotation capacity for this particular connection configuration was again assumed to be associated with virtually no deformation occurring within the compression region. Consequently, the deformation within the tension region accommodated the connection rotation in a similar manner to that described for Test 4.

The strain in the inner rebars reached 0.1% when a connection moment of 125kNm had been obtained. However, the corresponding strain in the outer rebars was 18% lower. This difference gradually increased, such that by the time the strain measured 0.2% within the inner rebars (266kNm), the difference had risen to 25%.

Following a comparison between strain levels for this and Test 3, which were identical with the exception of the beam and column sizes, it was established that

for any level of applied moment, the level of strain within the rebars would be reduced as a consequence of the member section designations increasing. This can be explained by the increase in the column flange thickness, which reduces the flange deformation for a given moment. However, this comparison was restricted to the onset of material yield ($0 \leq$ strain $\leq 0.2\%$). Although post-yield strain gauges were adopted to measure the rebars performance from Test 3 onwards, no reliable data could be collected following the attainment of material yield, because inconsistencies in the measured values were obtained at higher load levels. These inconsistencies were symptomatic of the sort of variable measurements which could be caused by the failure of the securing bond. Furthermore, the influence of the change in beam depth must also be significant, since the connection's rotation capacity was servely reduced when the connection's ultimate condition was reached (see section 7.6, Table 7.1).

The concrete crack pattern is shown by Plate 7.31. In addition, the symmetrical nature of this pattern can be seen together with the uniform width of the largest transverse crack applicable to connection A.

The deformed and fractured reinforcement is shown in Plate 7.32. It can be seen that the outer rebar located at the front of the specimen caused the connection failure. In addition, it is evident that the mesh reinforcement had fractured across the breadth of the slab.

7.5 Moment-rotation characteristics determined from the experimental programme

The moment-rotation characteristics presented in Figures 7.8 - 7.12 inclusive, represent the connection's behaviour following a ten minute time delay from the initial attainment of the appropriate increment. Moreover, the rotations of the connections were based on the measurements obtained from the electrical clinometers, which were positioned at the height of the tension bolt row.

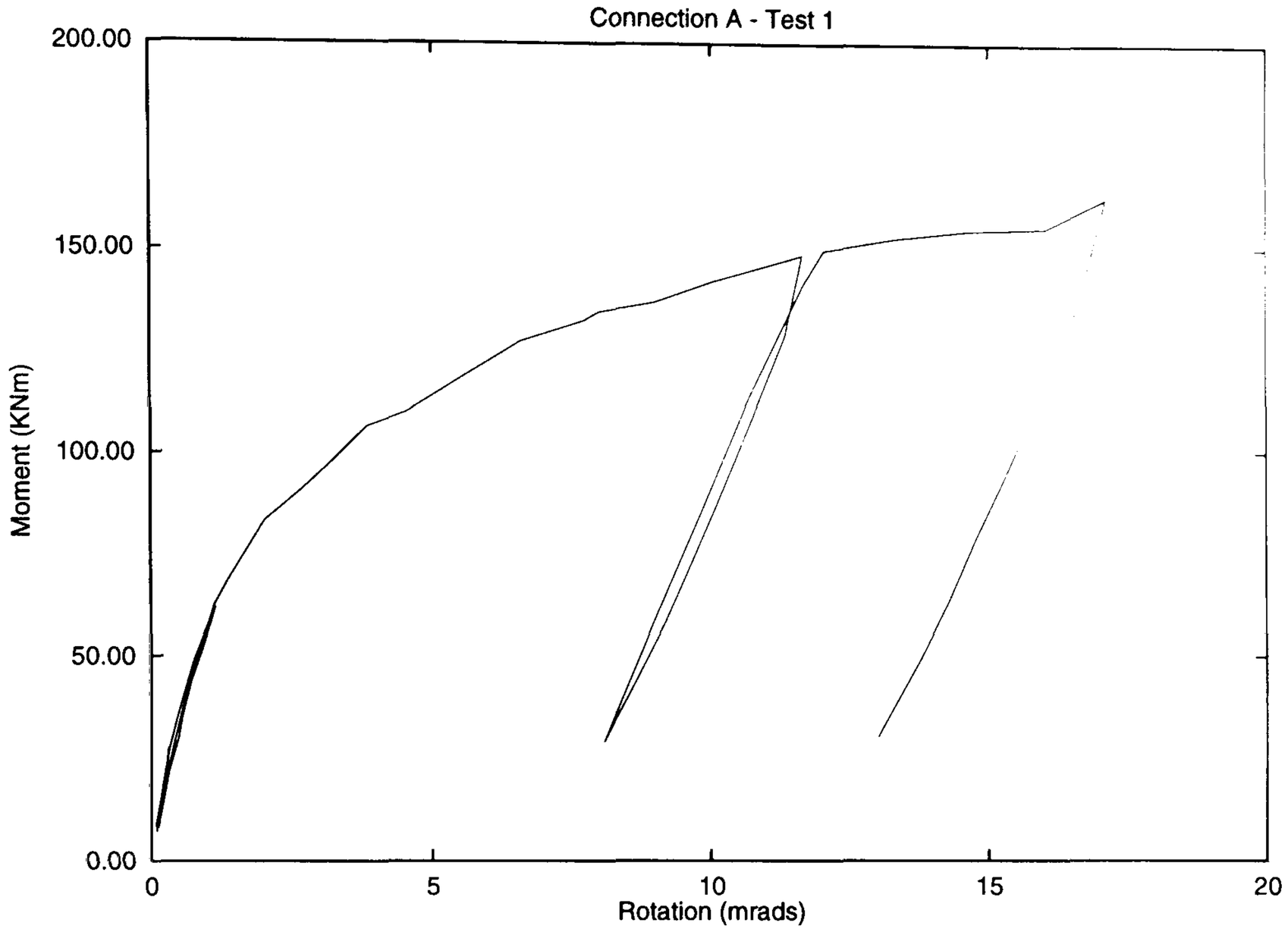

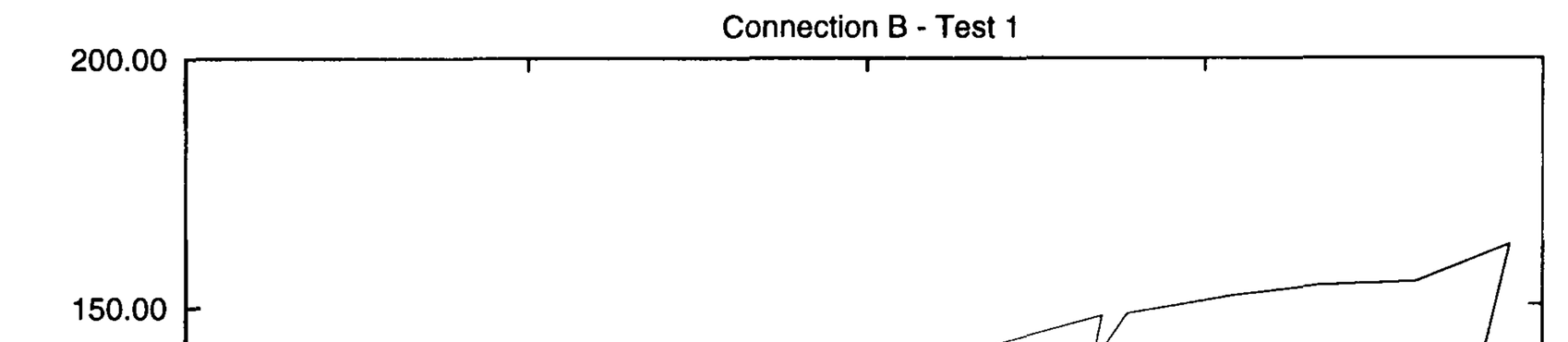

Figure 7.8: Moment-rotation characteristics for Test 1

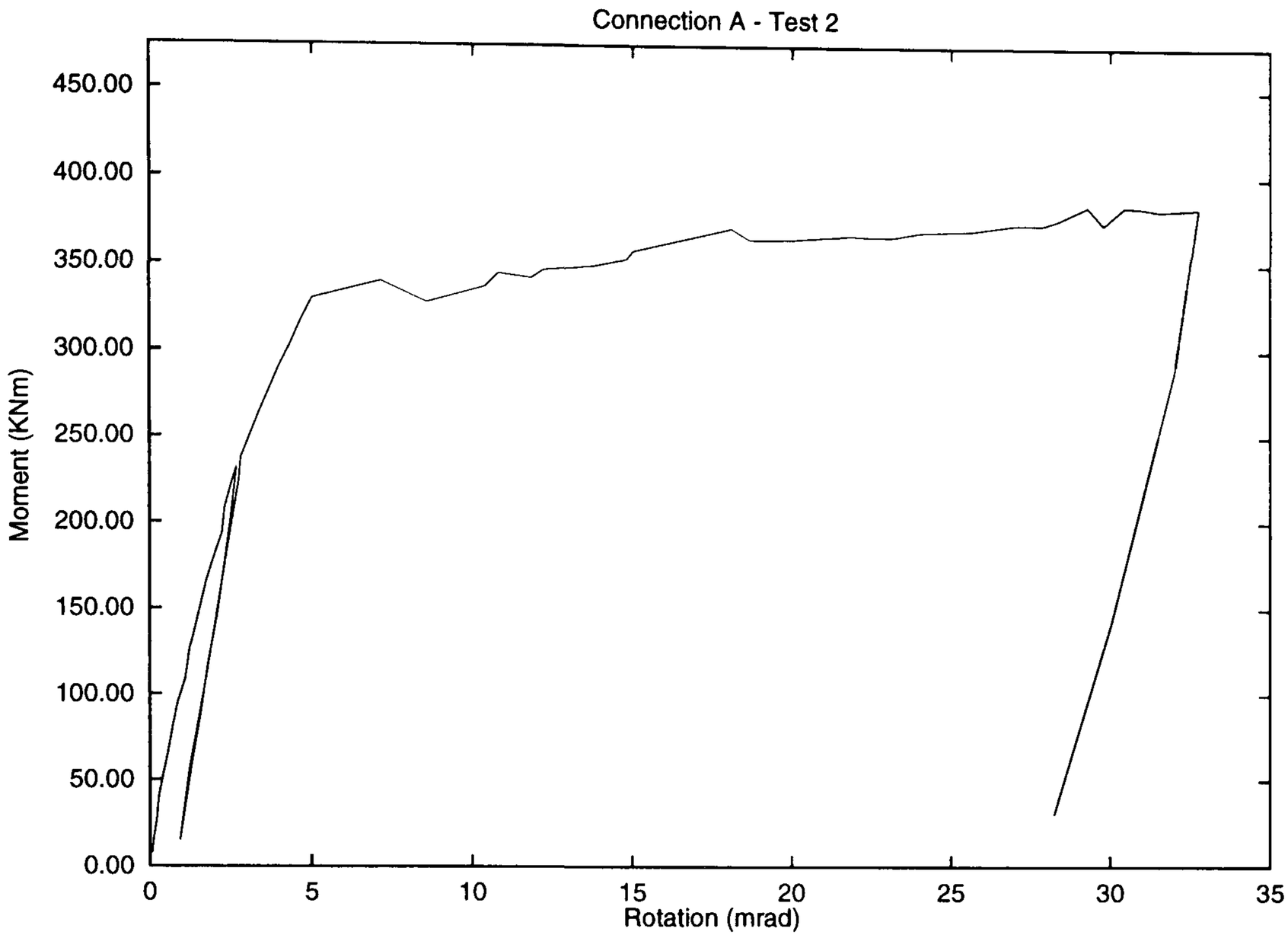

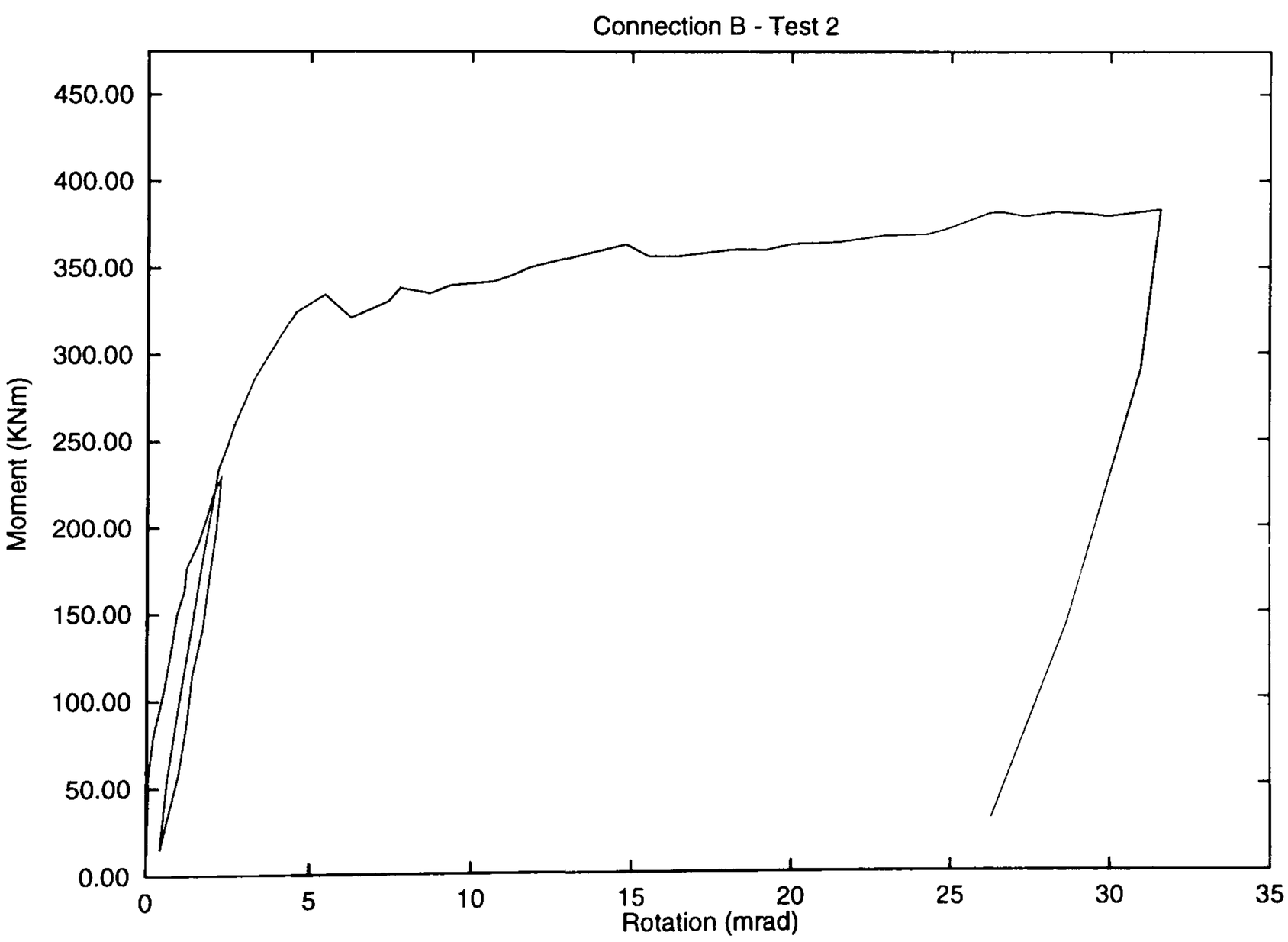

Figure 7.9: Moment-rotation characteristics for Test 2

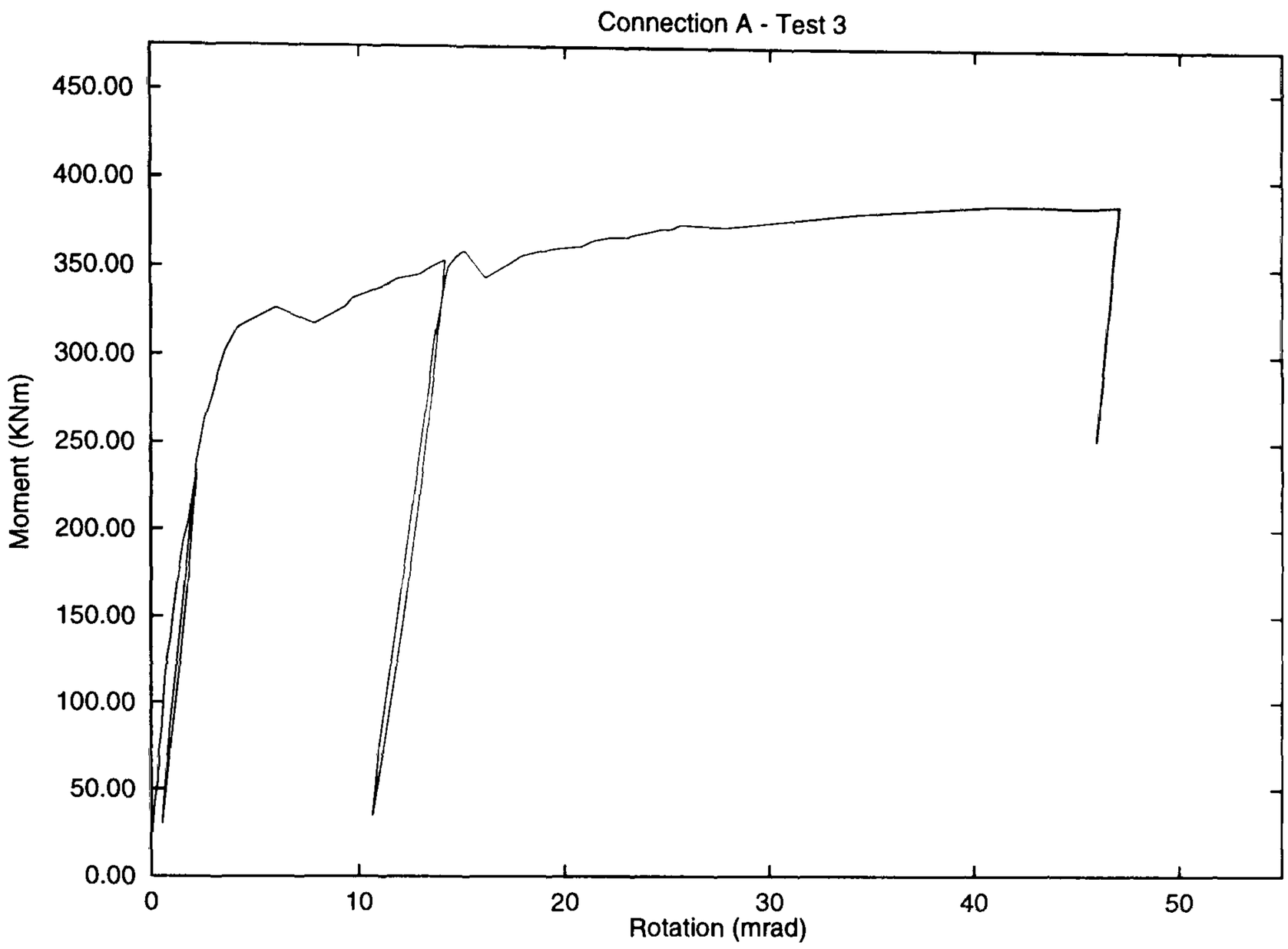

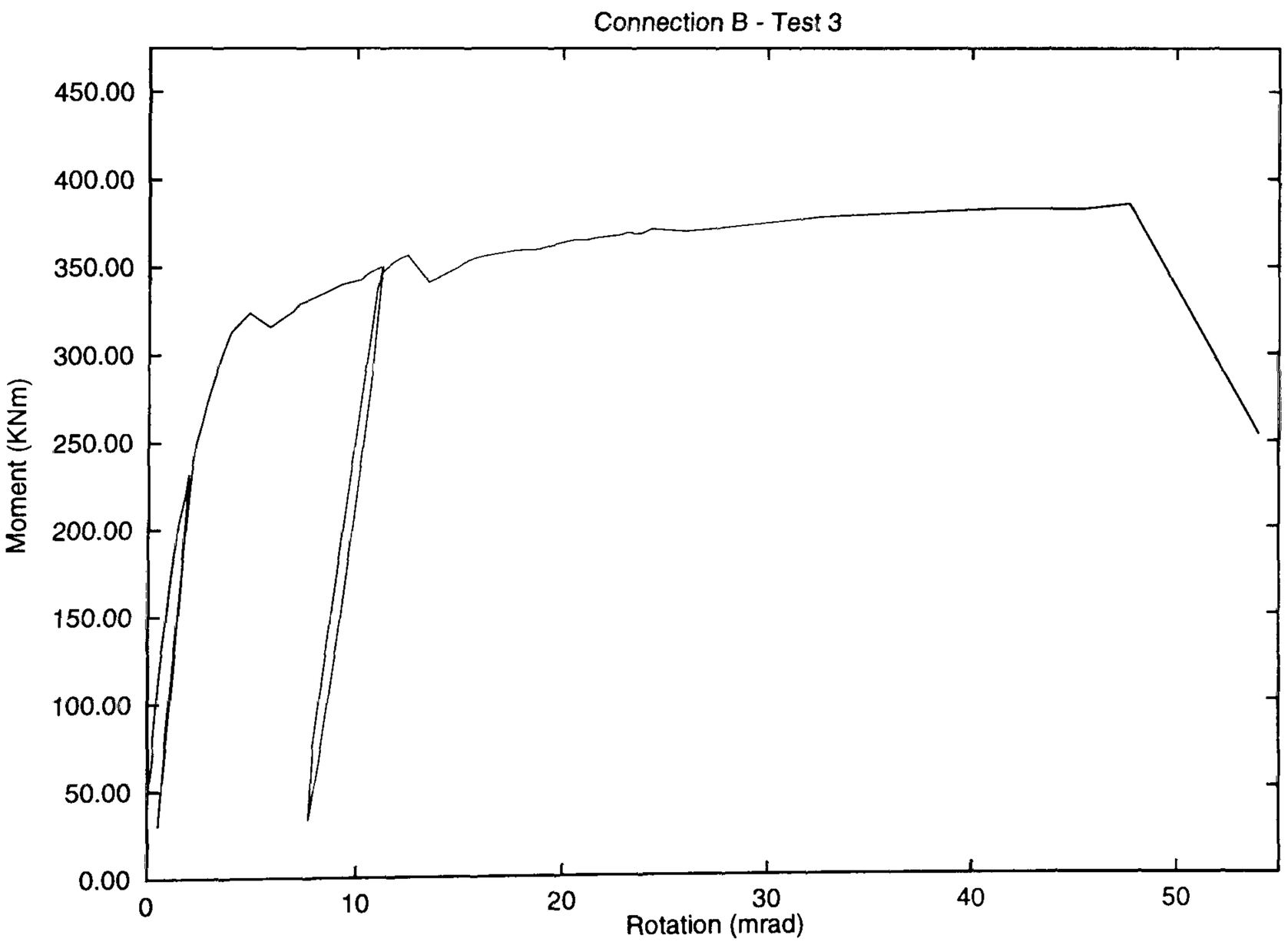

Figure 7.10: Moment-rotation characteristics for Test 3

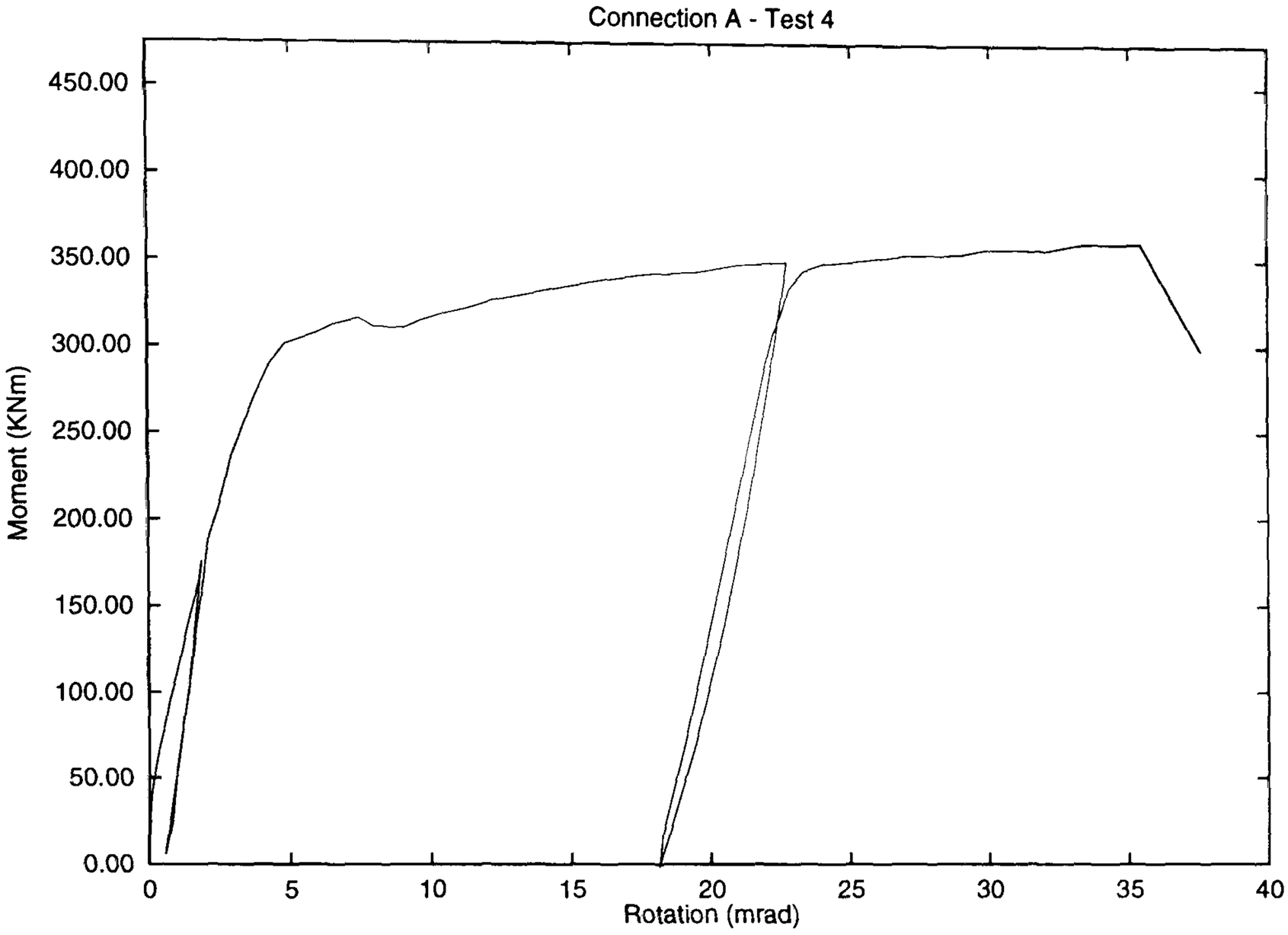

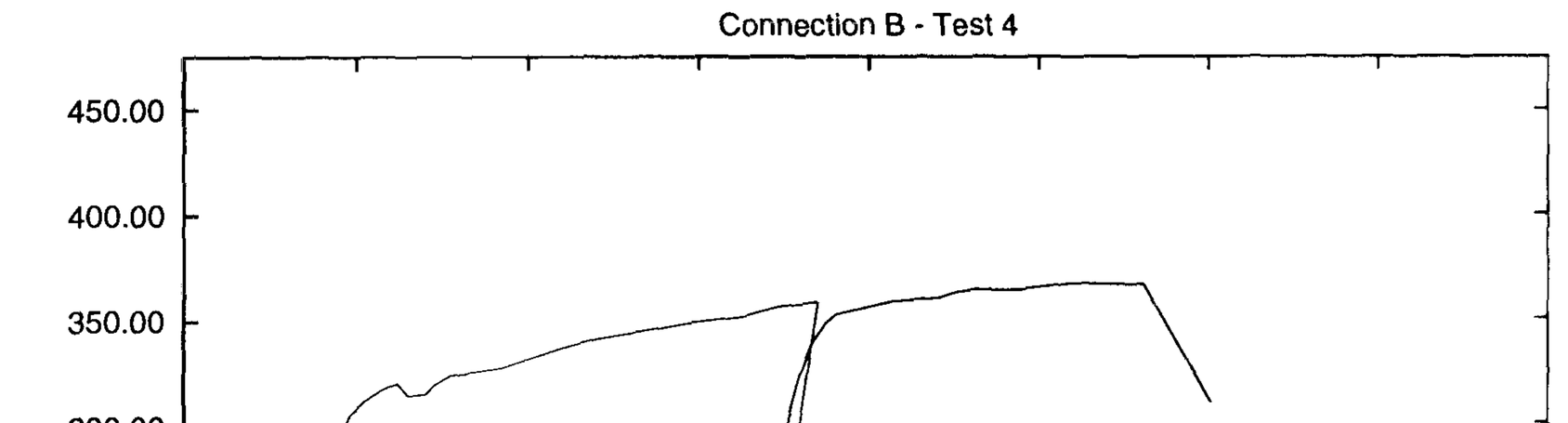

Figure 7.11: Moment-rotation characteristics for Test 4

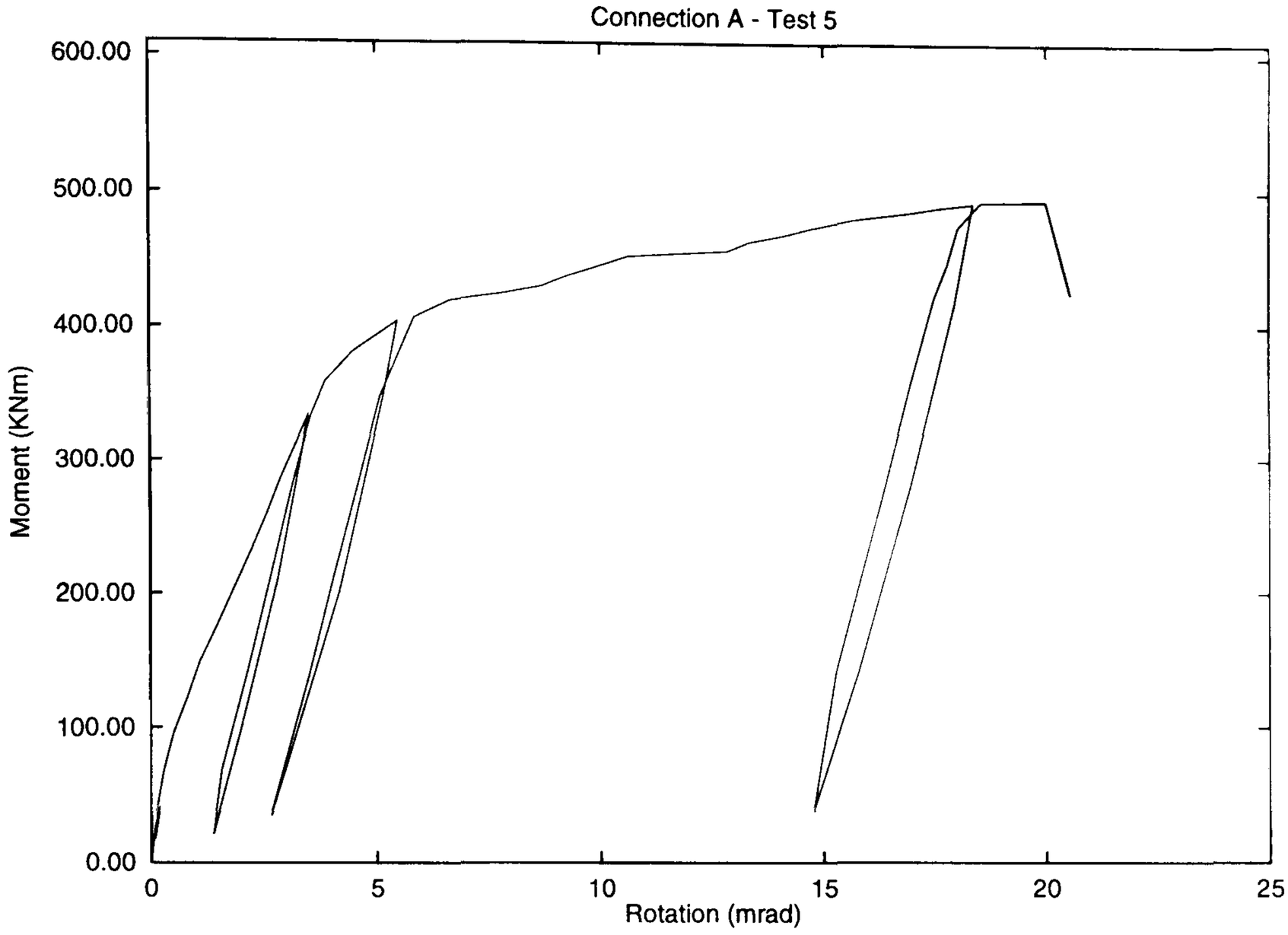

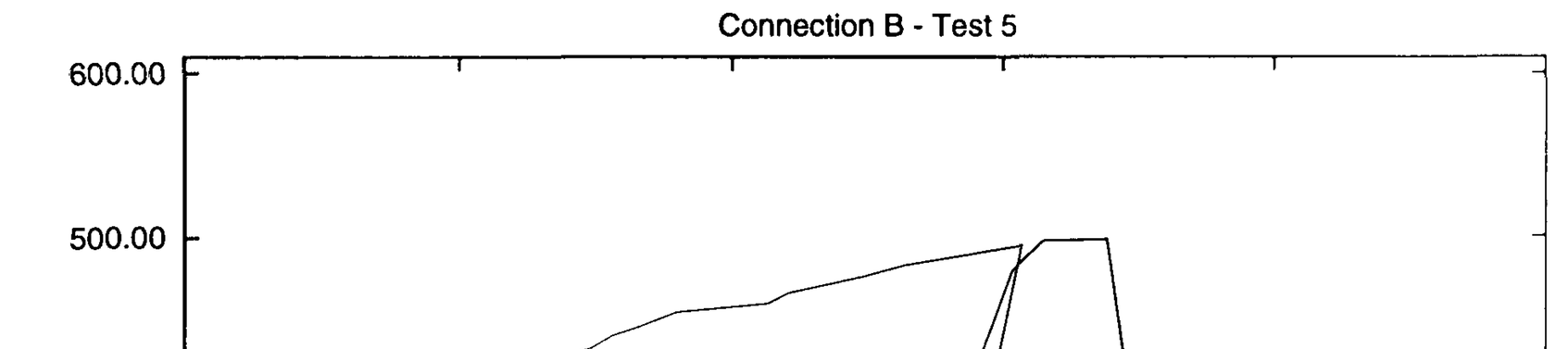

Figure 7.12: Moment-rotation characteristics for Test 5

7.6 Summary of experimental results

Connection performance

It can be seen from the moment-rotation characteristics illustrated in section 7.5, that for the connections tested, each unloading stiffness was constant throughout the working range and approximately equivalent in magnitude to the corresponding initial stiffness.

To facilitate the comparison between the tests performed, the connections performances are summarised in Table 7.1, from which the following can be concluded.

	Moment capacity (kNm) $M_{(ult)}$	Rotation capacity (mrads) $\phi_{(ult)}$	Mode of failure
Test 1#	**162**	**> 19.0**	N/A
Test 2#	**380**	**> 32.8**	
Test 3	**390**	**47.7**	**External re-bar fracture**
Test 4	**370**	**35.5**	
Test 5	**493**	**20.1**	

Note :
- Ultimate condition not reached

Table 7.1: Connection performance

1. The moment resistance of the bare steel connection, indicated by Test 1. can be increased when it acts compositely with a reinforced composite slab. This increase would be in the order of 135% if 4T16 longitudinal rebars were adopted as continuous reinforcement within the slab.

2. From a comparison between Tests 2 and 3, it can be seen that increasing the horizontal spacing of the rebars does not significantly affect the performance of a composite connection.

3. The effect of reducing the end plate thickness can be established by comparing Tests 3 and 4. It can be shown that the moment resistance of the composite connection was reduced by 5% and the rotation capacity by 26%.

4. From a comparison between Tests 3 and 5, it can be seen that increasing the serial sizes of the connected members increases the moment resistance of the composite connection by 26%. However, this was accompanied by a reduction in the available rotation capacity of 58%.

5. When the ultimate condition was reached, all the applicable tests failed as a result of the external re-bar fracturing.

An overall comparison between the behavioural characteristics of the connections tested is shown by Figure 7.13. In addition, Figure 7.14 has been included to enable comparisons to be undertaken between the corresponding connection stiffnesses, when the connection rotation is relatively low (< 5mrads).

From these figures, the following can be concluded :

1. The bare steel connection has by far the lowest moment of resistance and overall stiffness.

2. A considerable increase in strength and stiffness results from the effects of composite action (Tests 2 - 4).

3. A further increase in strength occurs when the serial sizes of the connected members are increased (Test 5). However, there is not a corresponding increase in connection stiffness.

4. The behavioural characteristics for the composite 457 serial size beams (Tests 2 - 4) were very similar.

5. For a given reinforcement detail, the available rotation capacity of the connections is influenced by the end plate thickness and the serial size of the connected members.

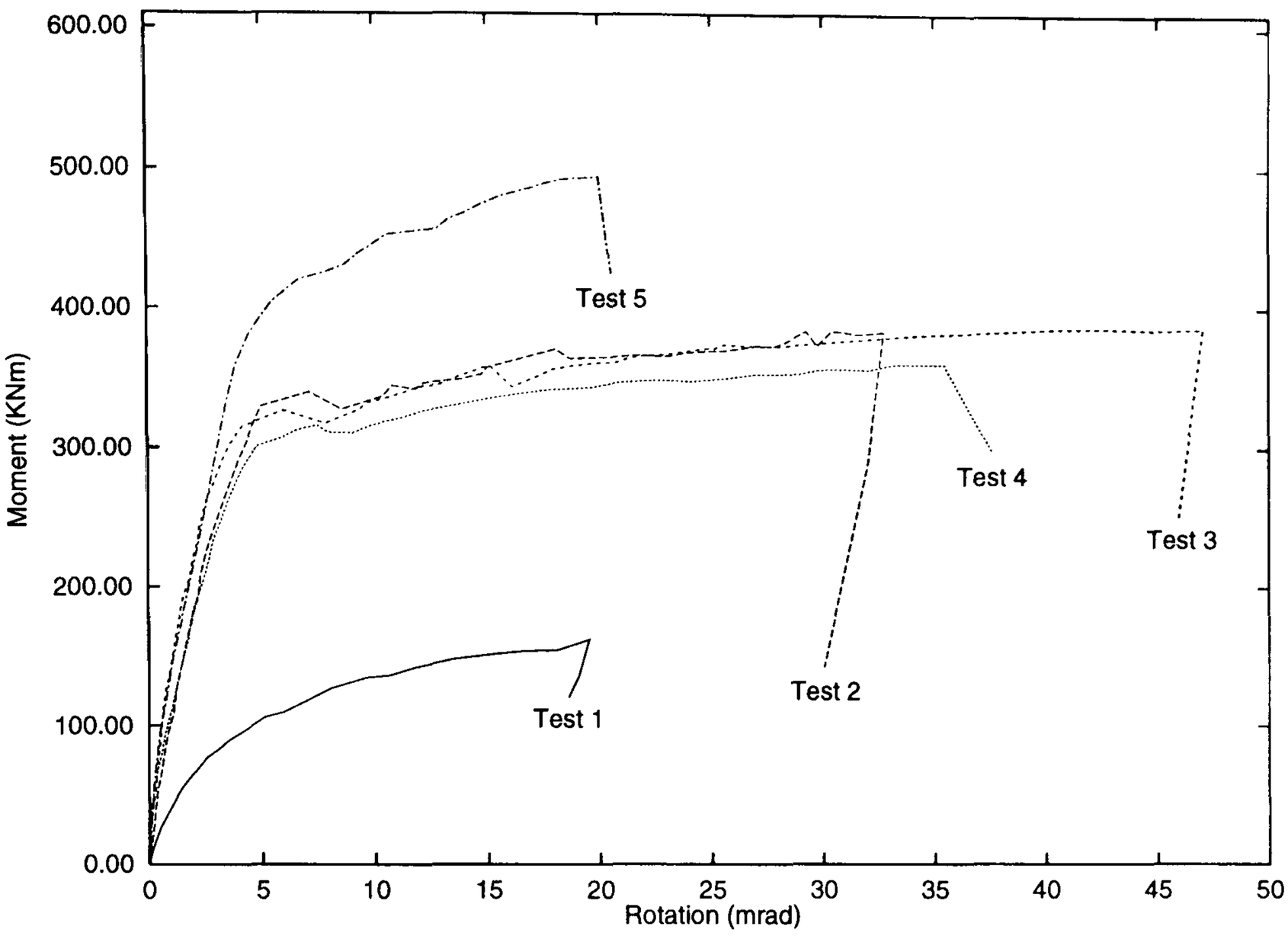

Figure 7.13: Comparison between the moment-rotation characteristics for the connection configurations considered

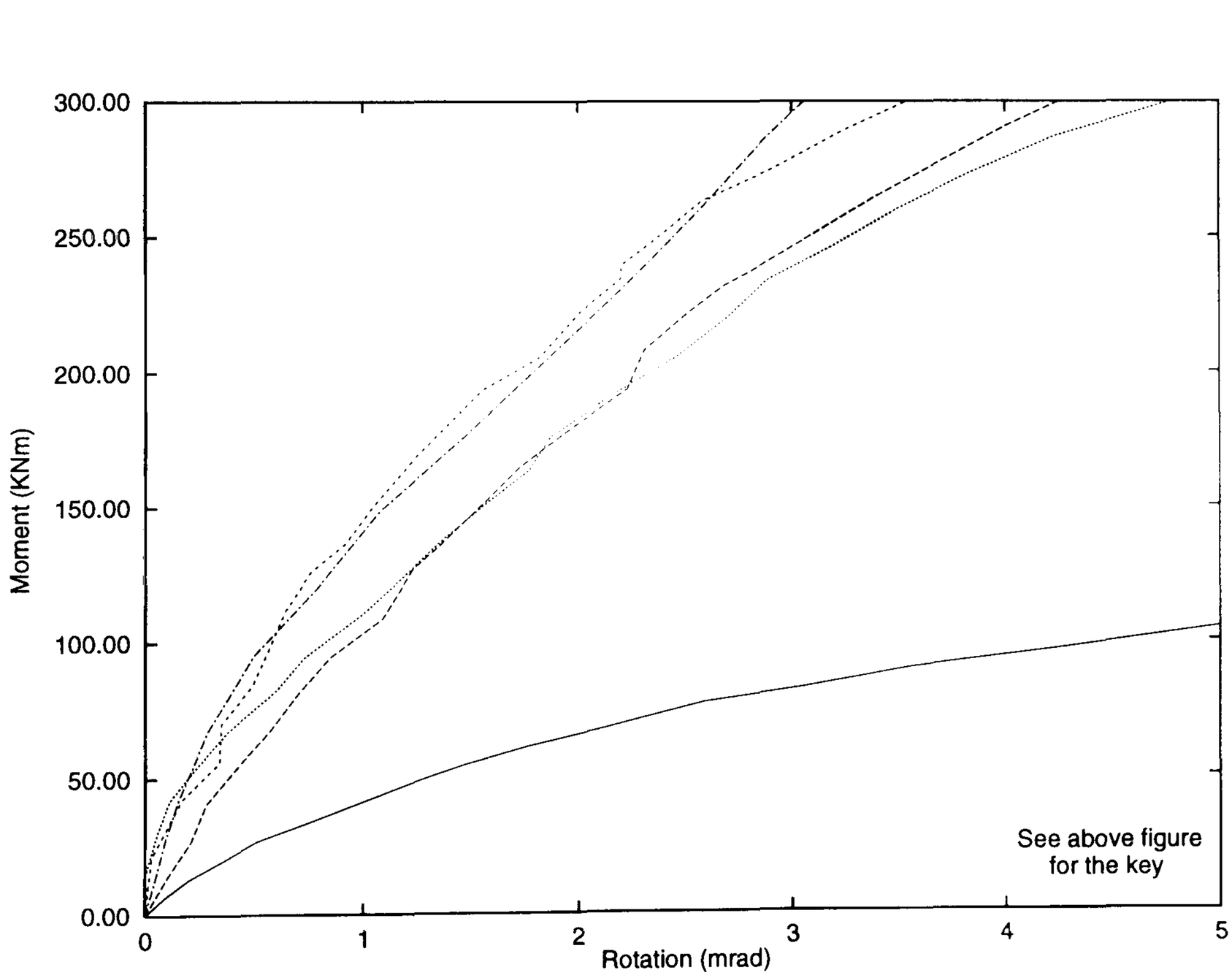

Figure 7.14: Comparison between the connections initial stiffnesses for the connection configurations considered

Deformation characteristics within the steelwork

For all the tests that incorporated a 15mm thick end plate and 457 serial size beams (Tests 1 - 3), the early rotation of the connections was the result of the column flange deforming in the tension zone. As the connection rotation increased, the deformation within the column flange was accommodated by the end plate bending about the centre line of the upper bolt row assumed in the connection design, to resist the vertical shear. In addition, with the exception of Test 1, compression buckling occurred to the lower flanges of the beams in the vicinity of the connections, prior to the ultimate condition being reached.

For the composite test that incorporated a 15mm thick end plate but had larger serial size members (Test 5), the deformation characteristics were similar to those described above. However, there was no evidence to suggest that compression buckling was occurring in the vicinity of the connections prior to the connection failure.

For the composite test that incorporated a thinner end plate in conjunction with a 457 serial size beam (Test 4), the deformation characteristics within the tension zone changed initially. The change took the form of the end plate bending about the centre line of the tension bolt row. This occurred from an early stage in the proceedings and continued until the deformation within the column flange developed. At this point, the deformation within the end plate located in the tension zone appeared to stabilise, with the increasing flange deformation being accommodated as before. The load level at which the column flange started to deform was not influenced significantly by the change in the end plate thickness.

7.7 Photographic plates for the experimental programme

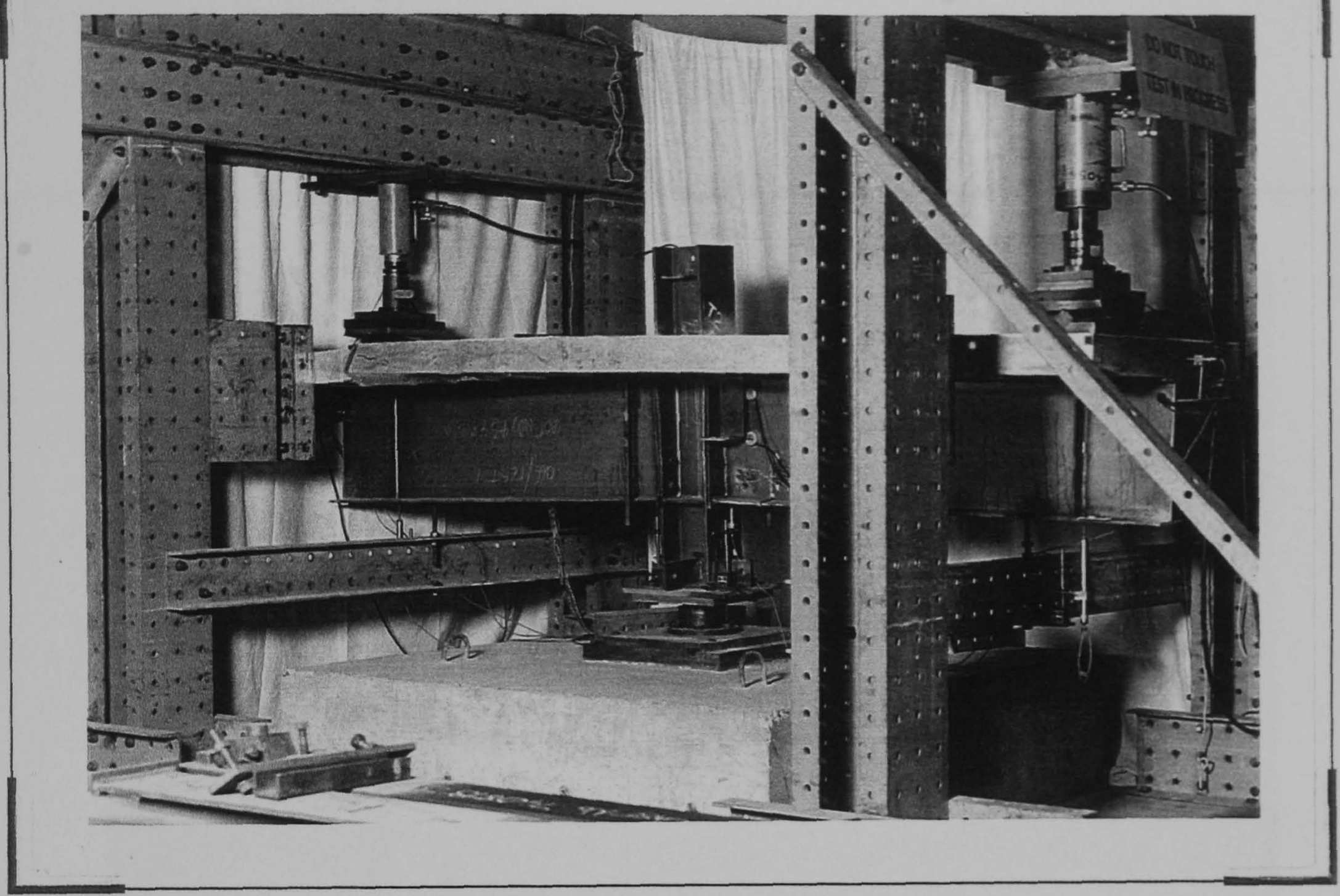

Plate 7.1 - Purpose built test rig

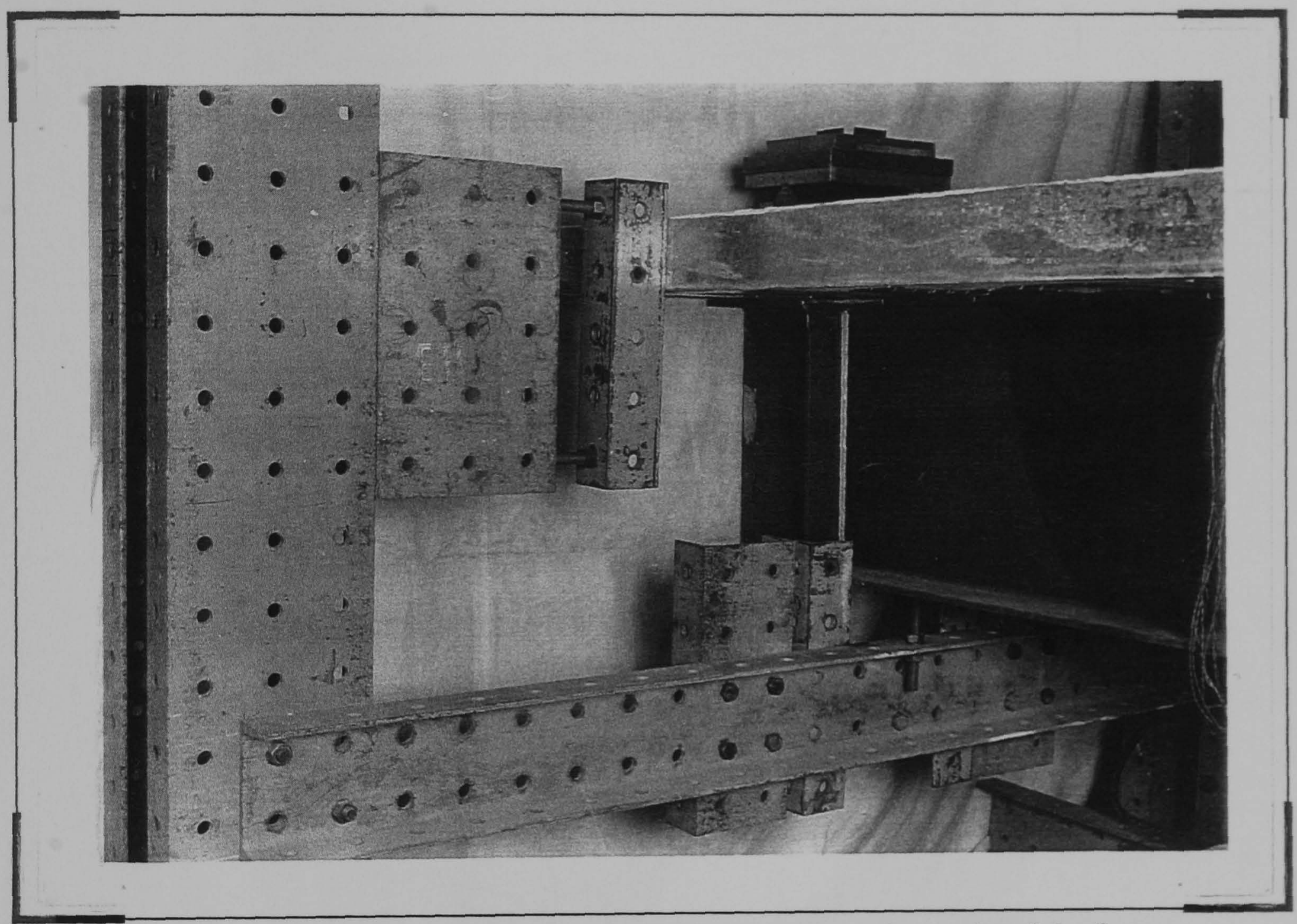

Plate 7.2 - Methods to prevent lateral movement at the ends of the beams

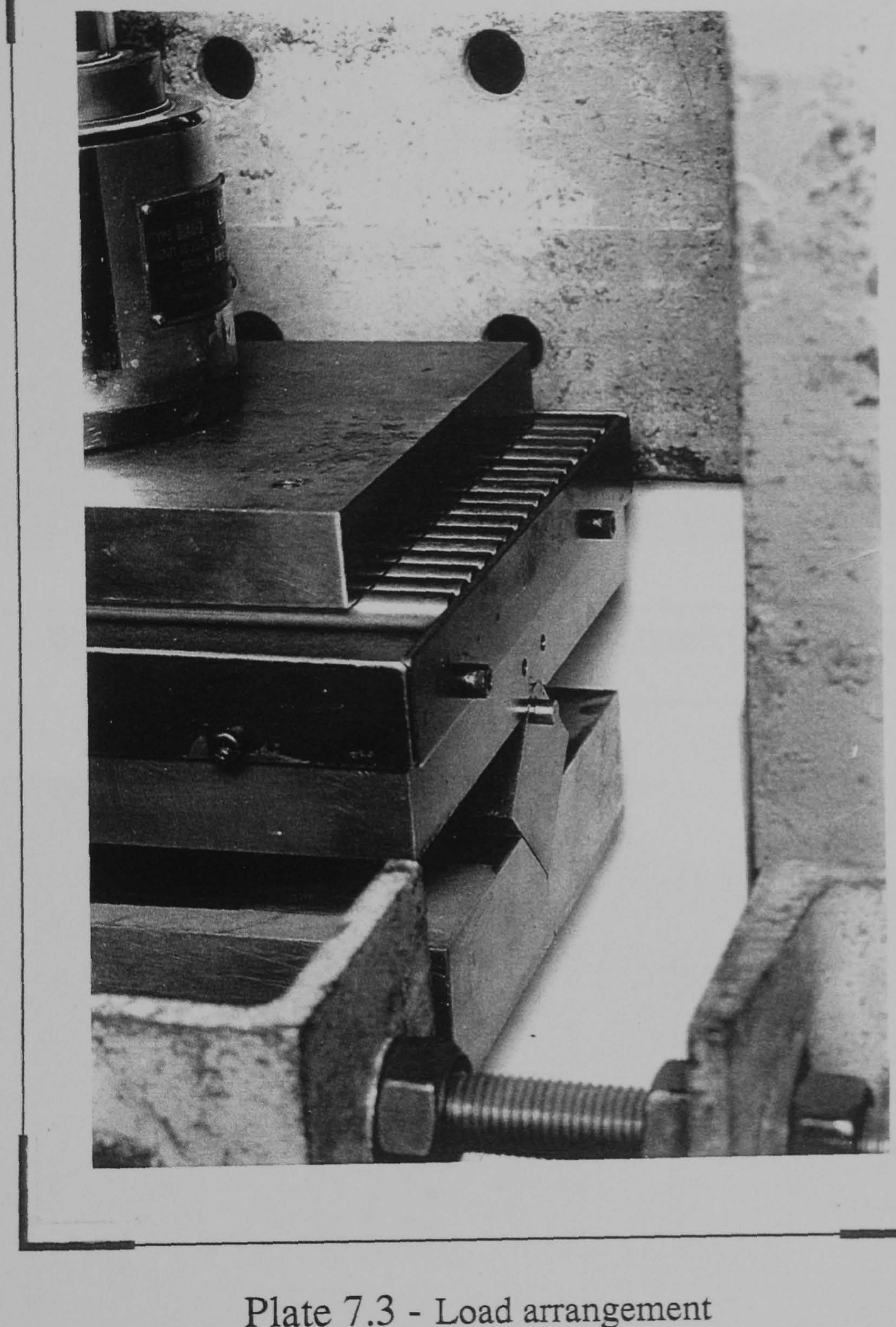

Plate 7.3 - Load arrangement

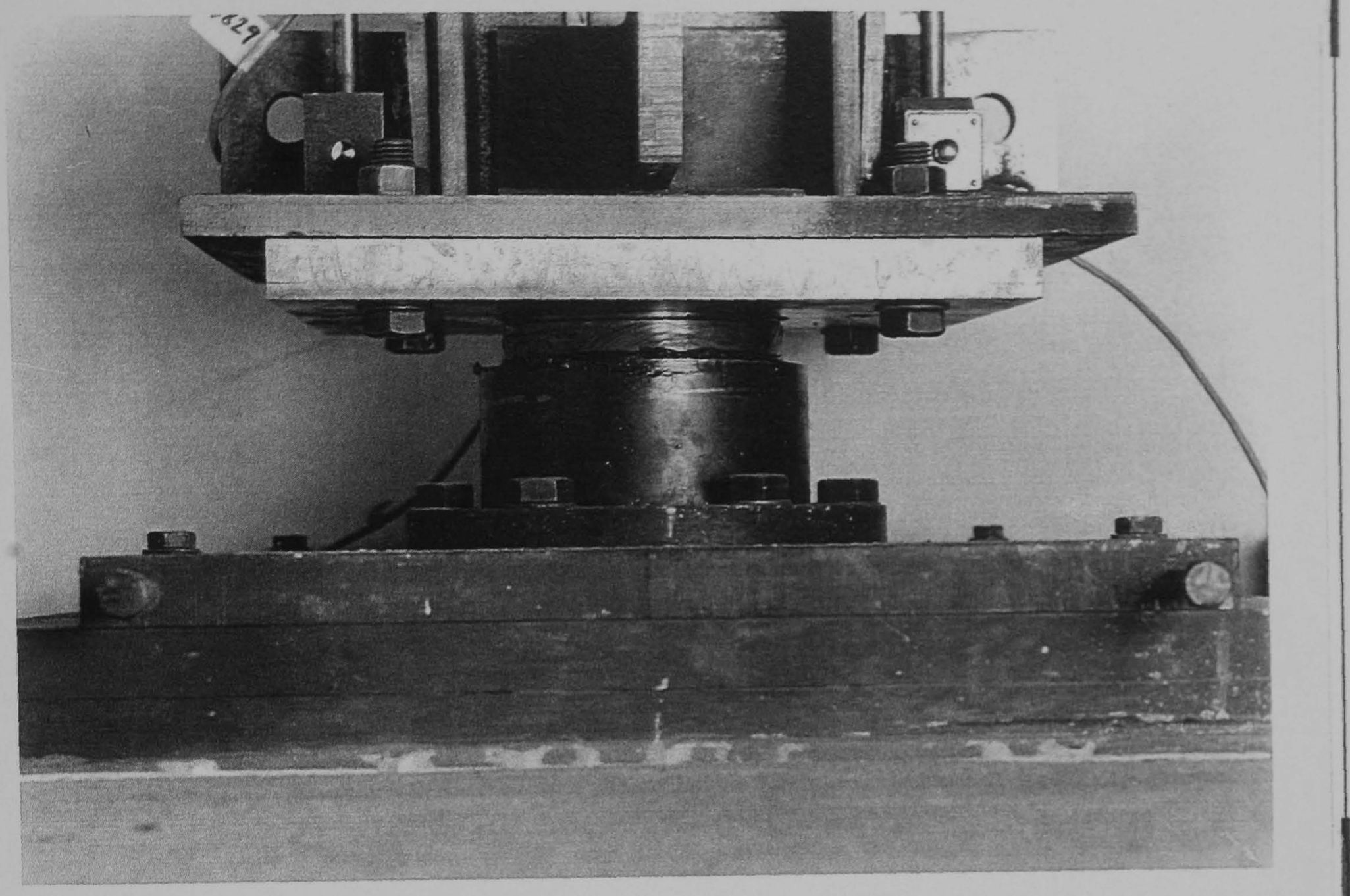

Plate 7.4 - Ball joint column support used for tests 1 and 2

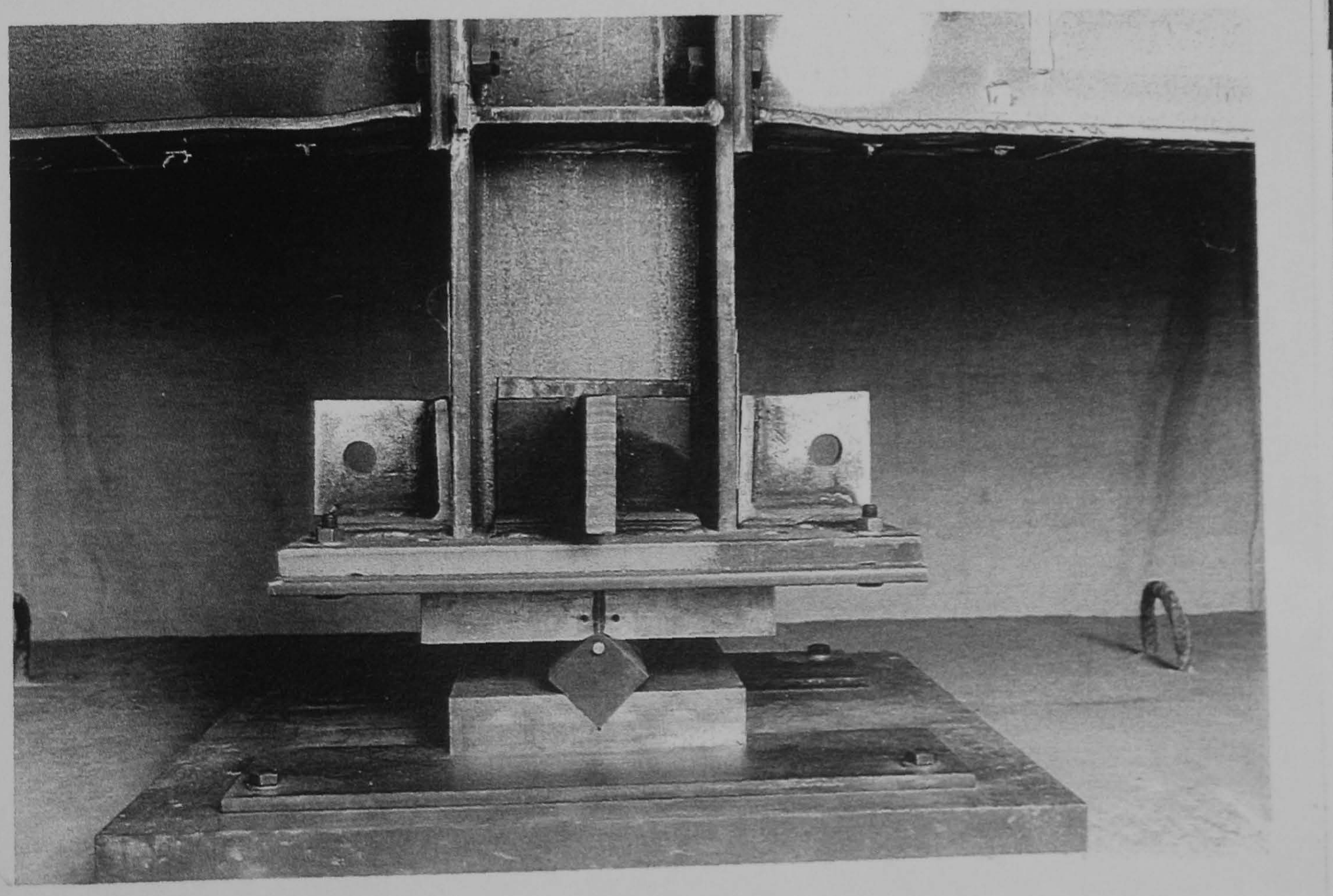

Plate 7.5 - Uni-directional rocker column support used for tests 2, 3 and 5

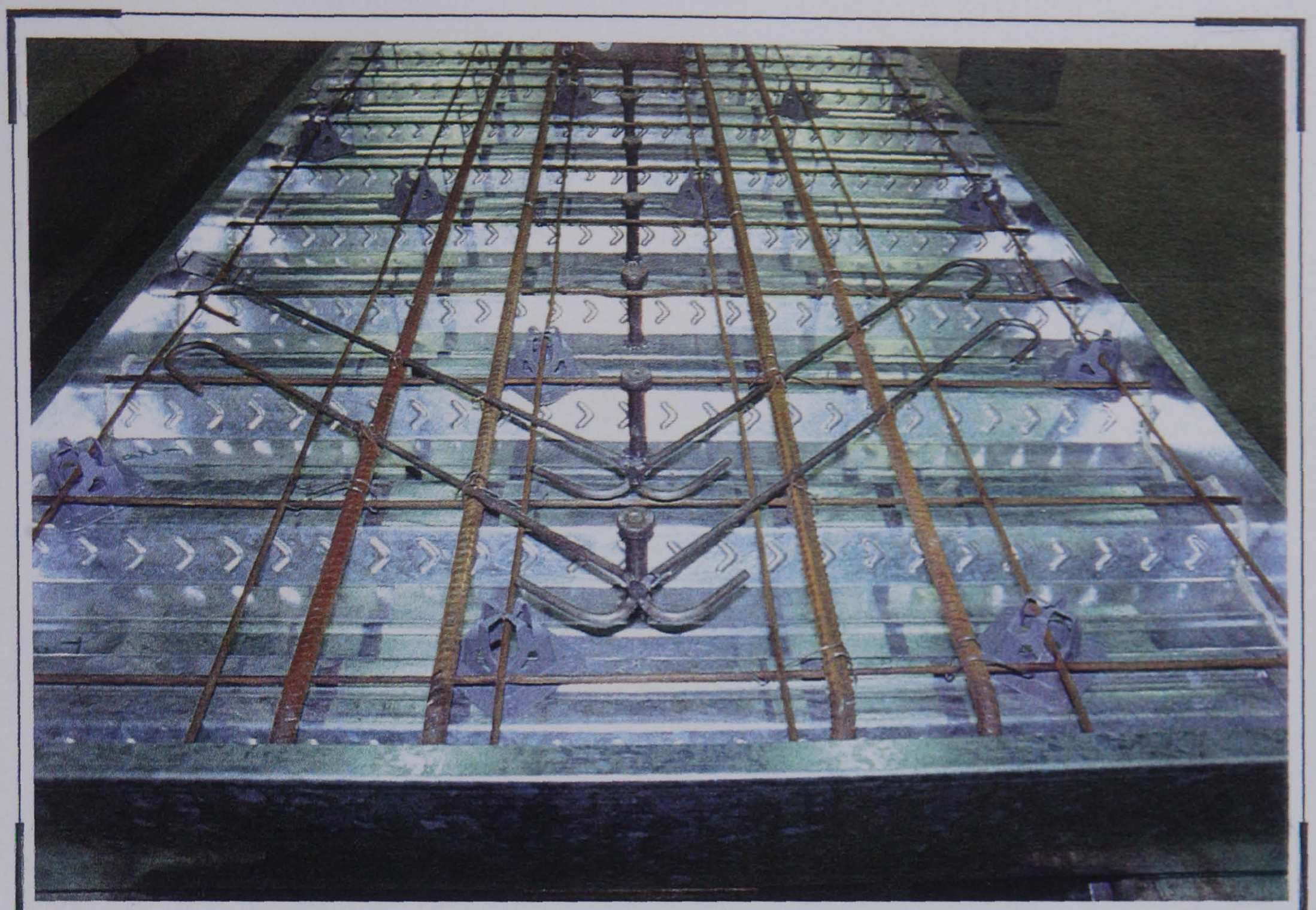

Plate 7.6 - Reinforcement arrangement adopted for the tests

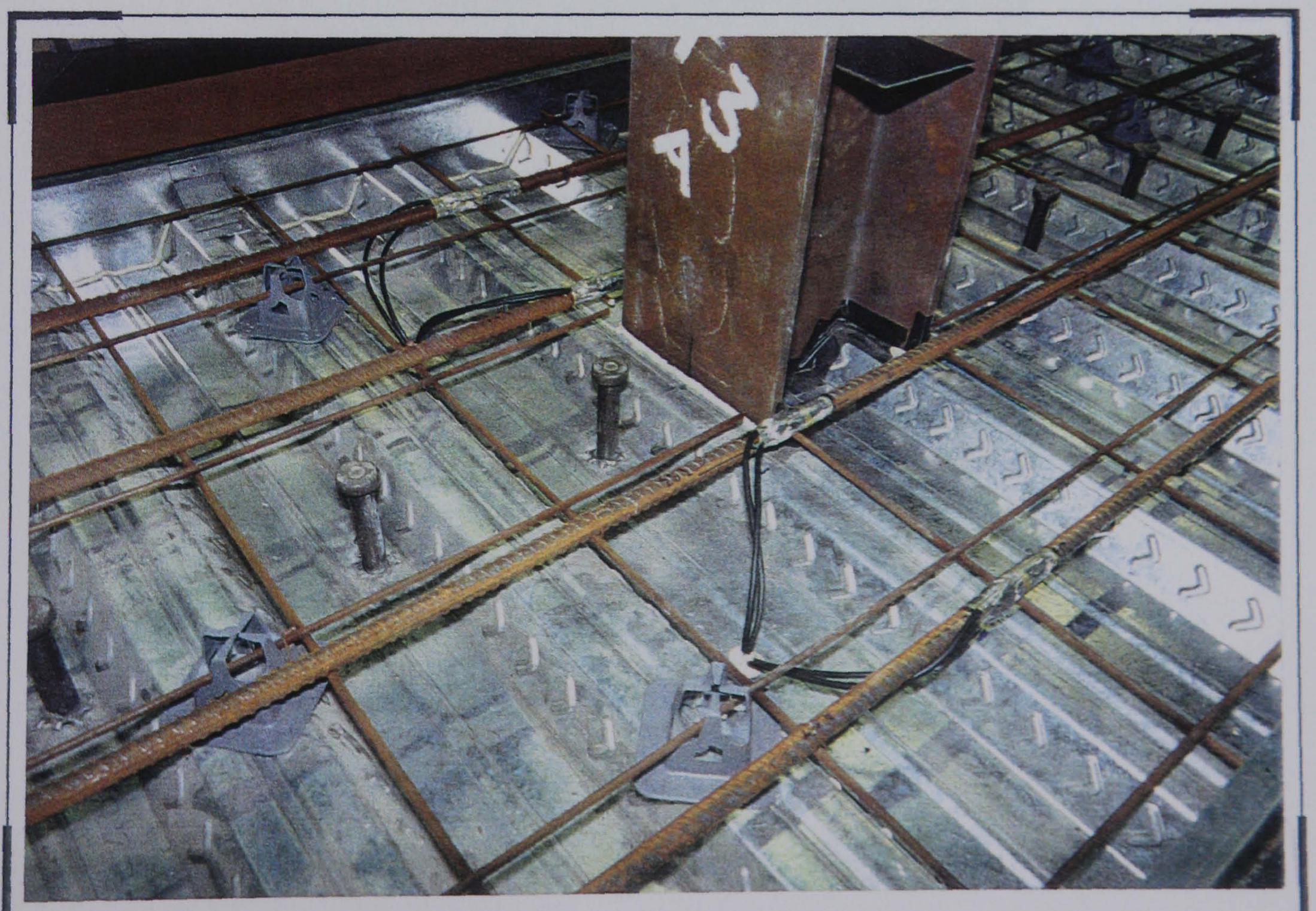

Plate 7.7 - Strain gauge and shear stud positions within the concrete slab

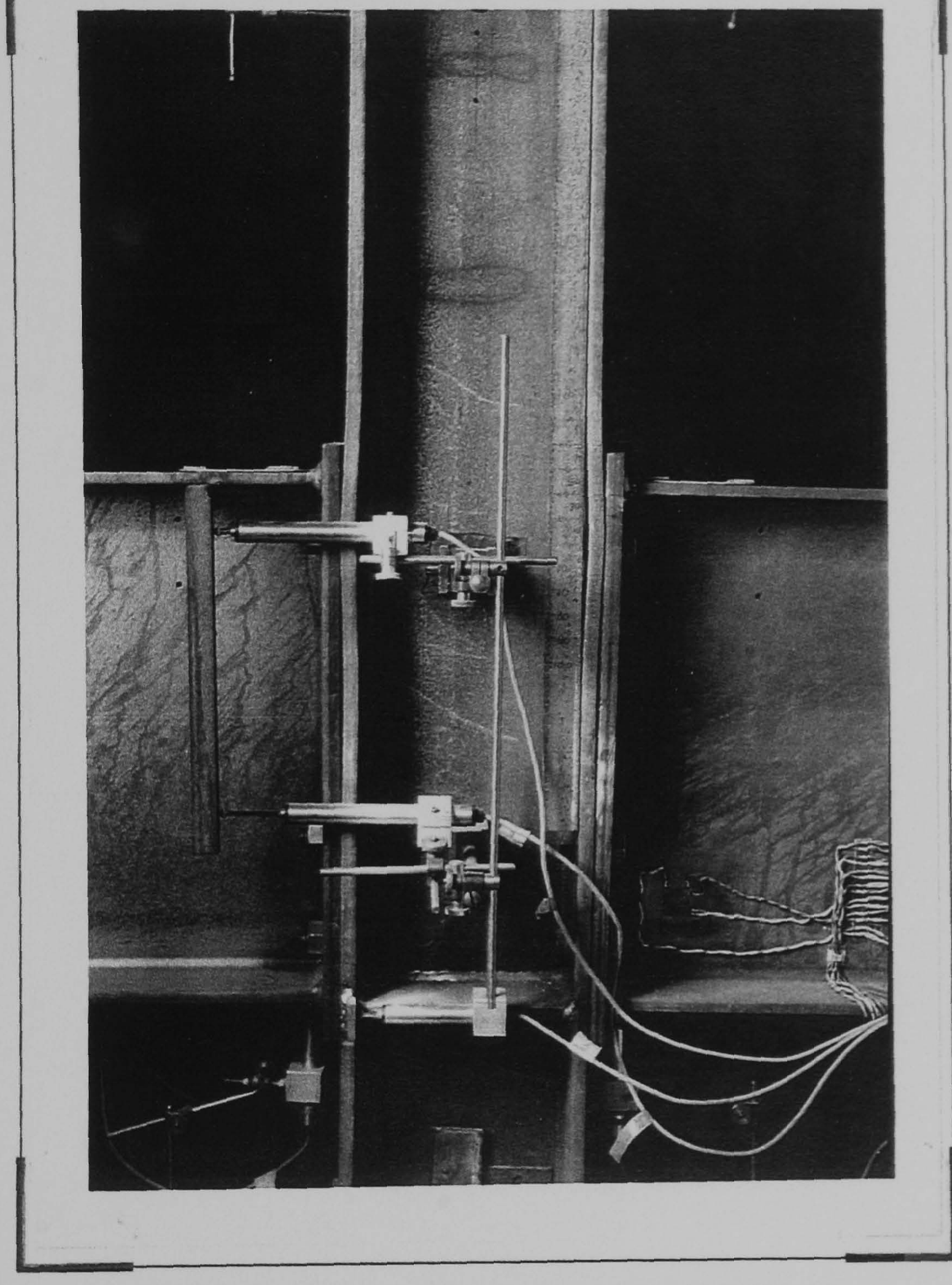

Plate 7.8 - Test 1: steelwork deformation (front)

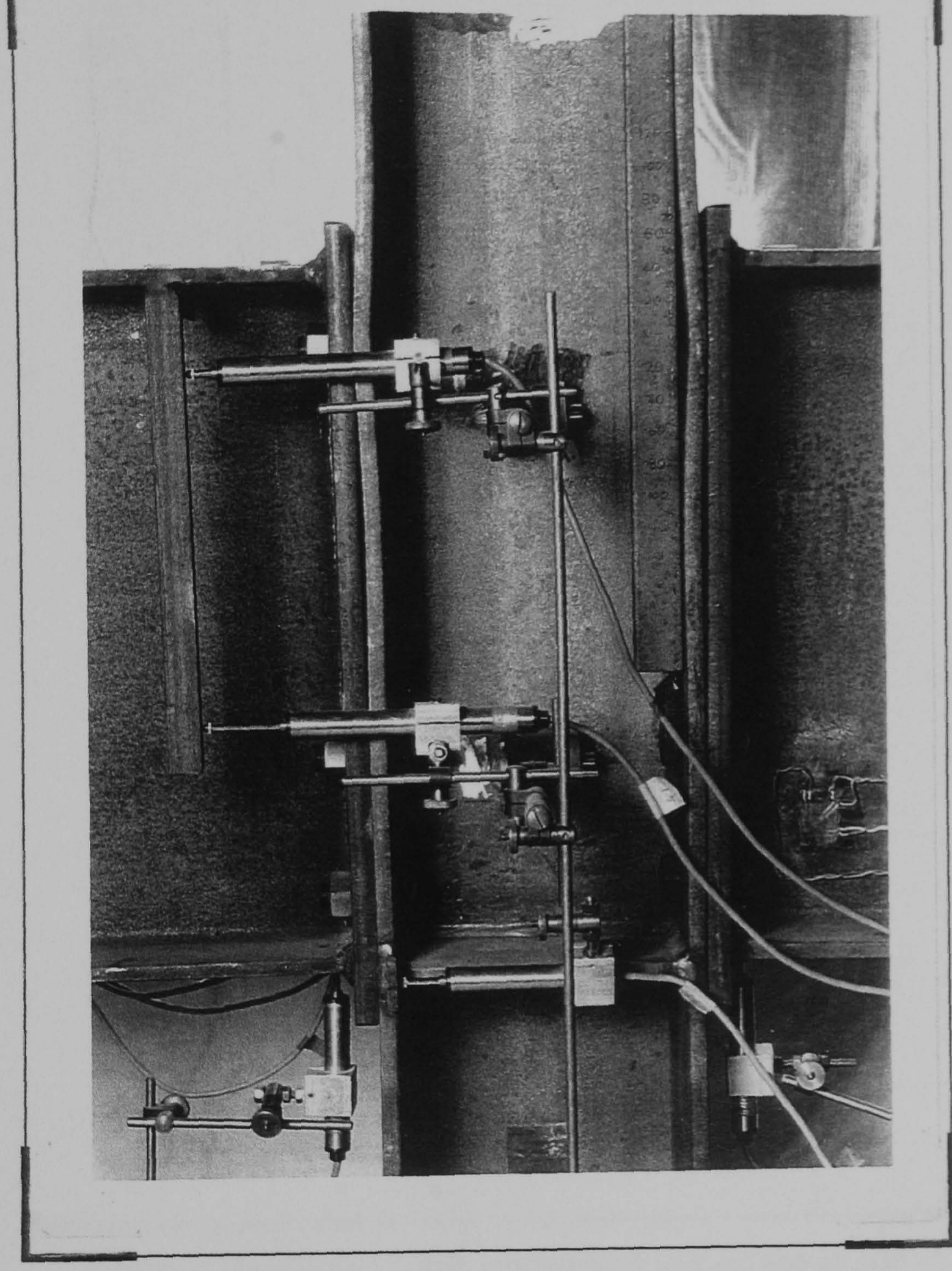

Plate 7.9 - Test 1: steelwork deformation (back)

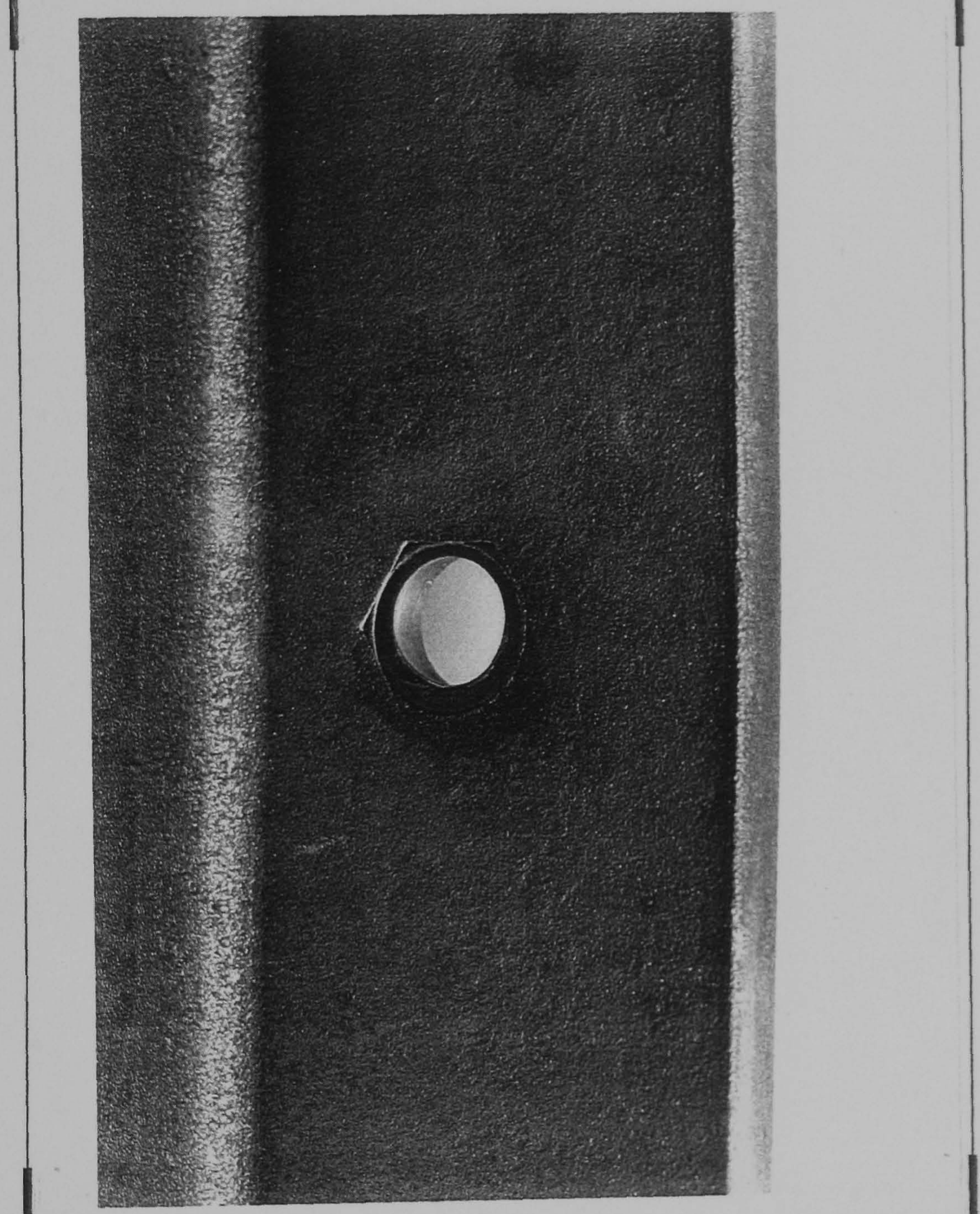

Plate 7.10 - Test 1: Bolt impression left on the inside of the column flange in the tension region

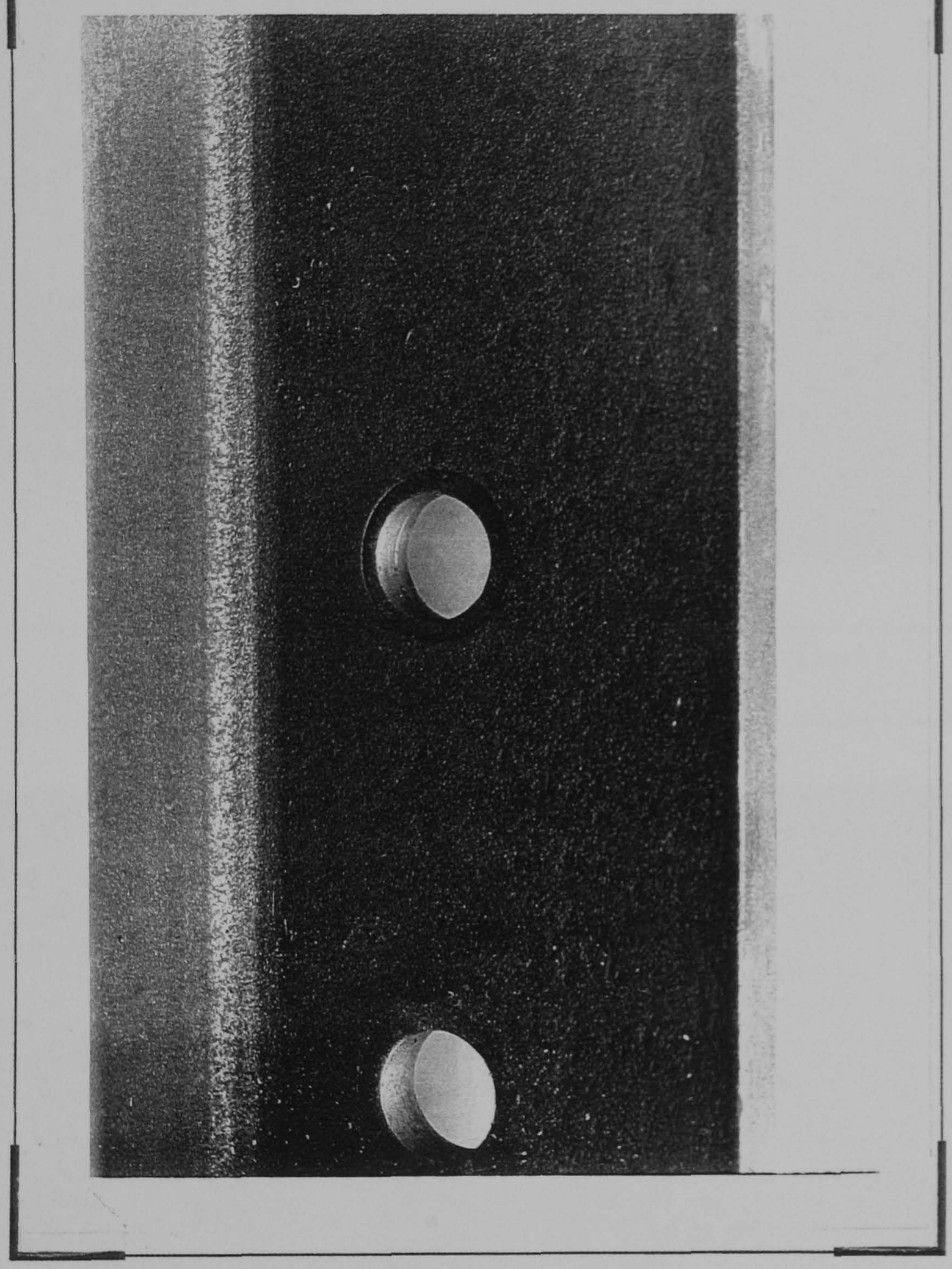

Plate 7.11 - Test 1: Bolt impression left on the inside of the column flange in the compression region

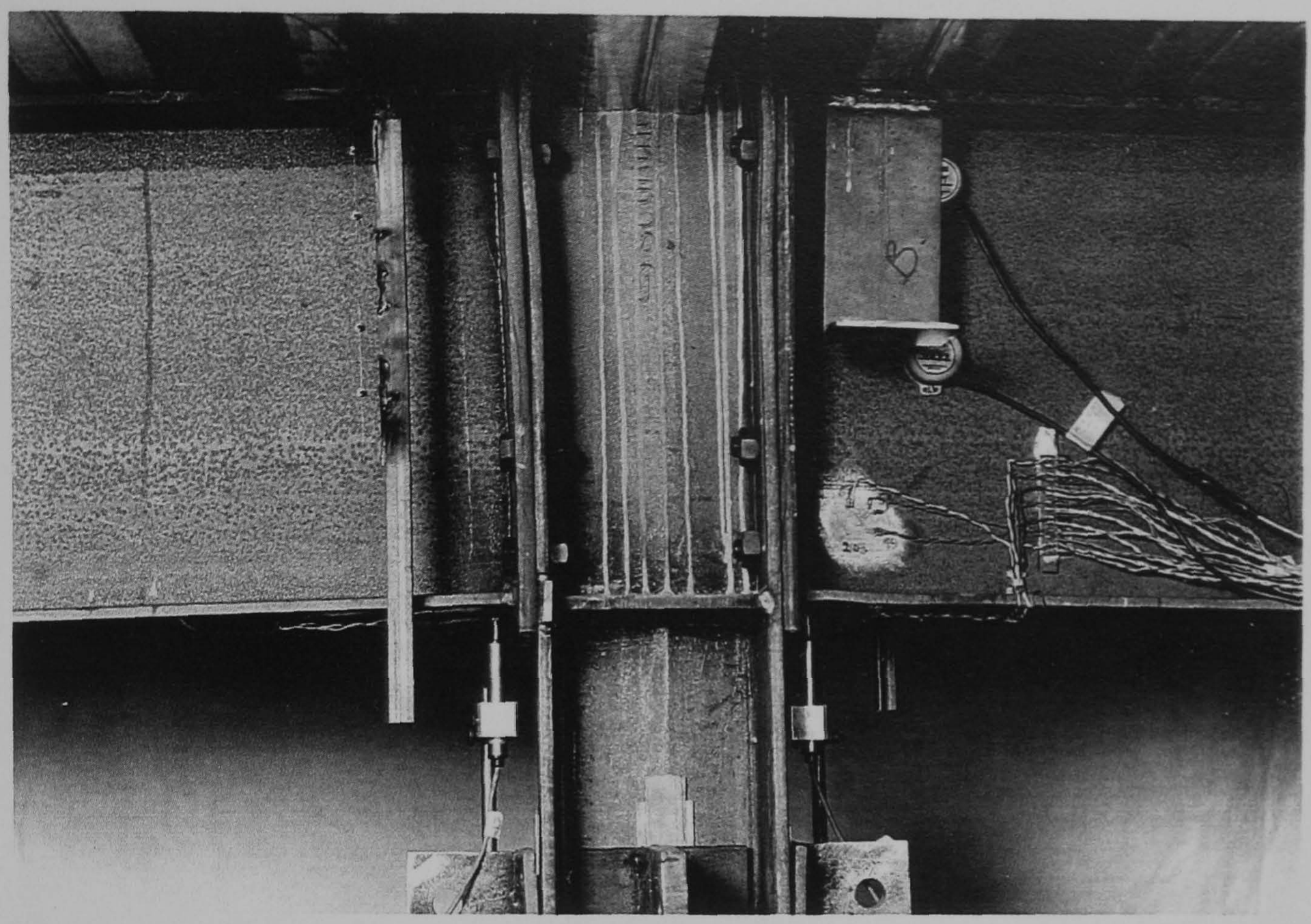

Plate 7.12 - Test 2 : steelwork deformation (front)

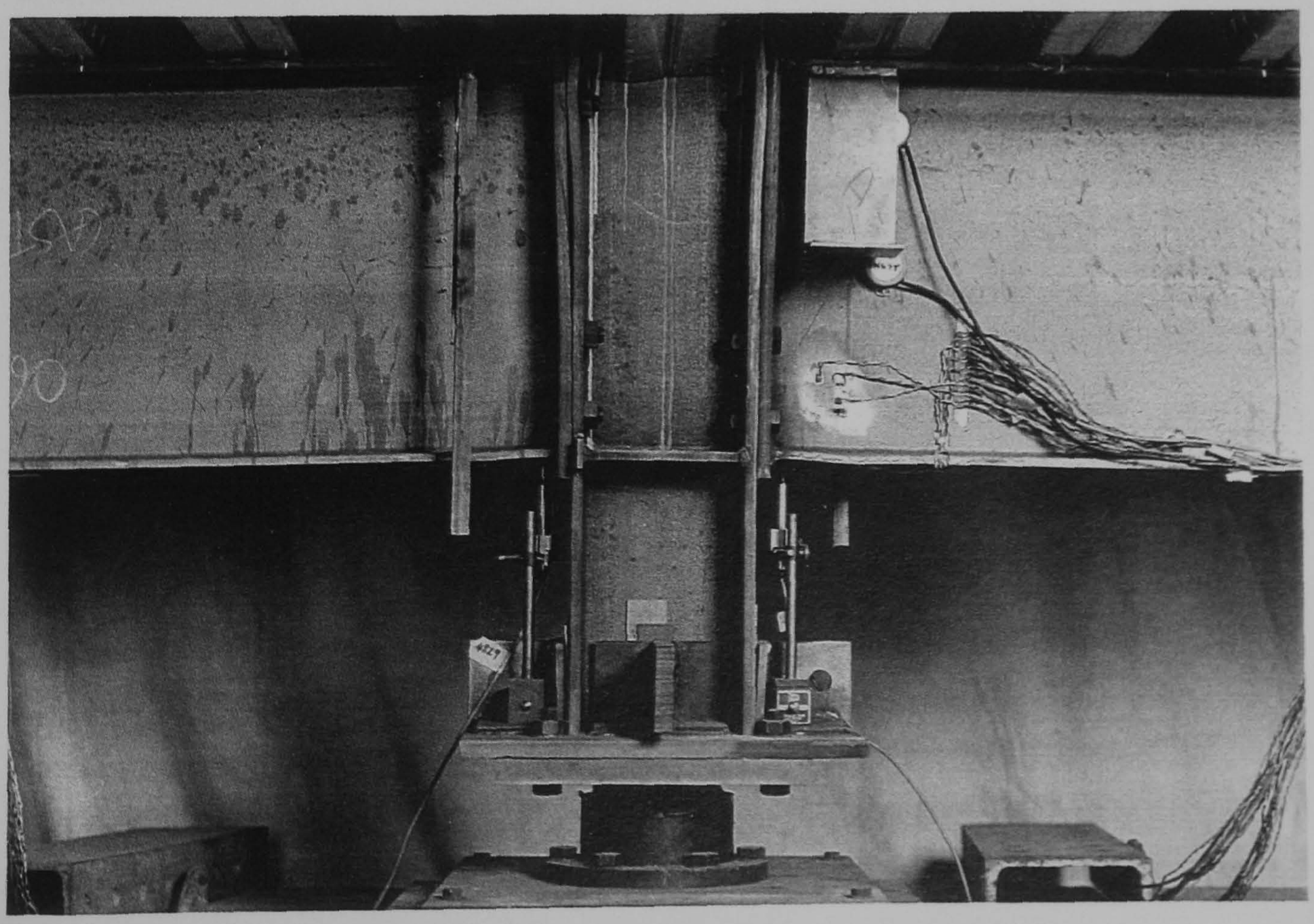

Plate 7.13 - Test 2 : steelwork deformation (back)

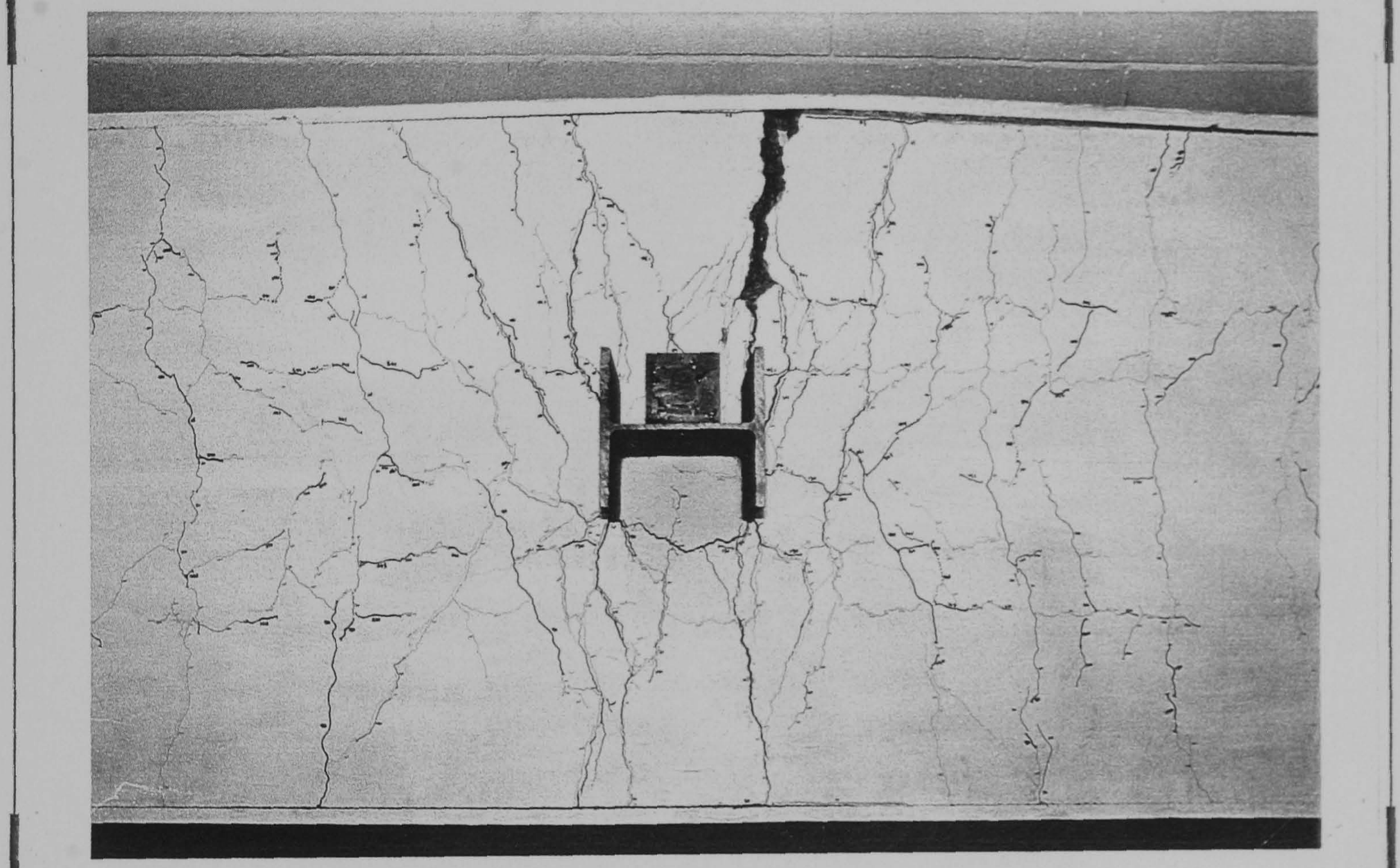

Plate 7.14 - Test 2 : concrete slab crack pattern

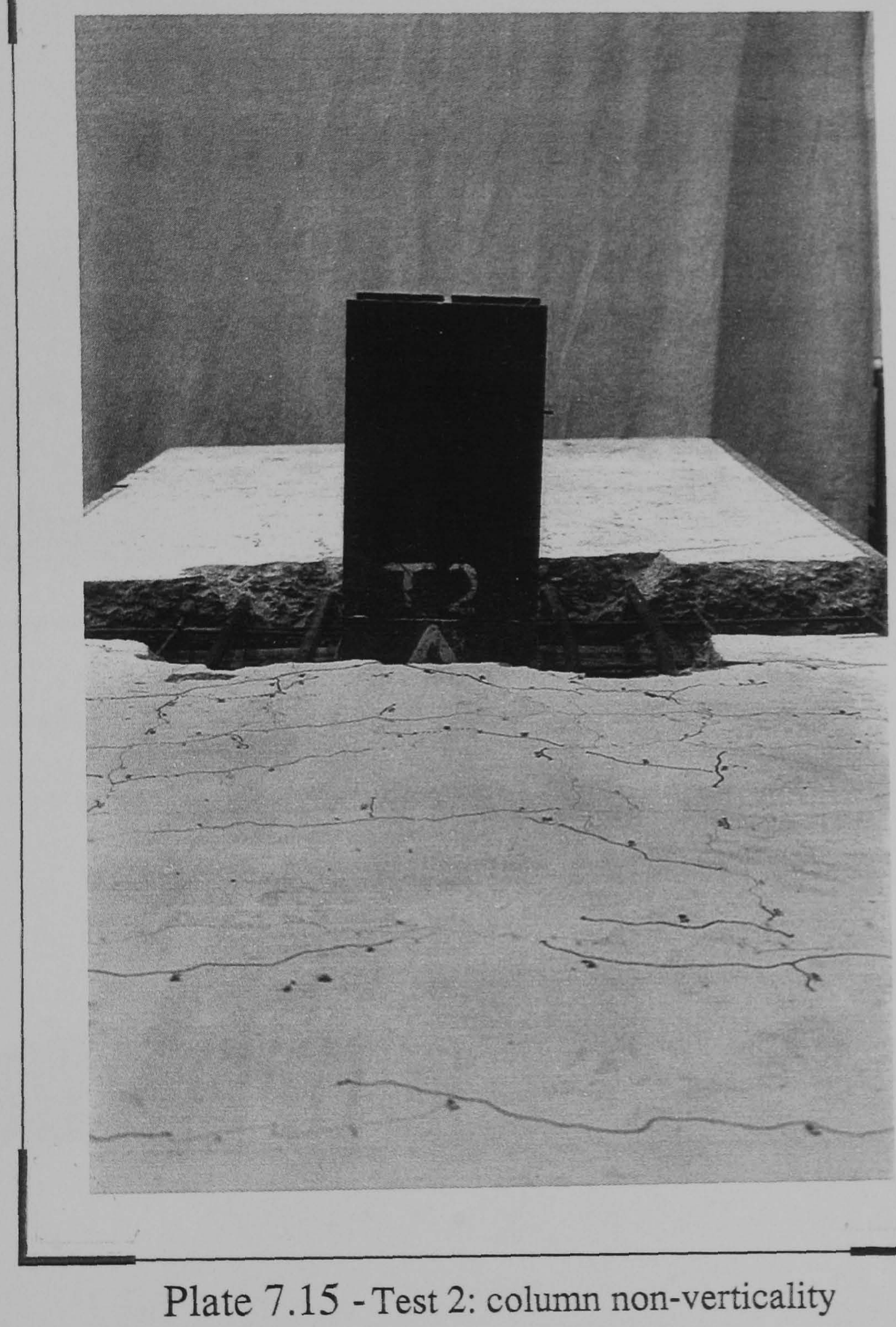

Plate 7.15 - Test 2: column non-verticality
inconjunction with lateral deformation of the reinforcement

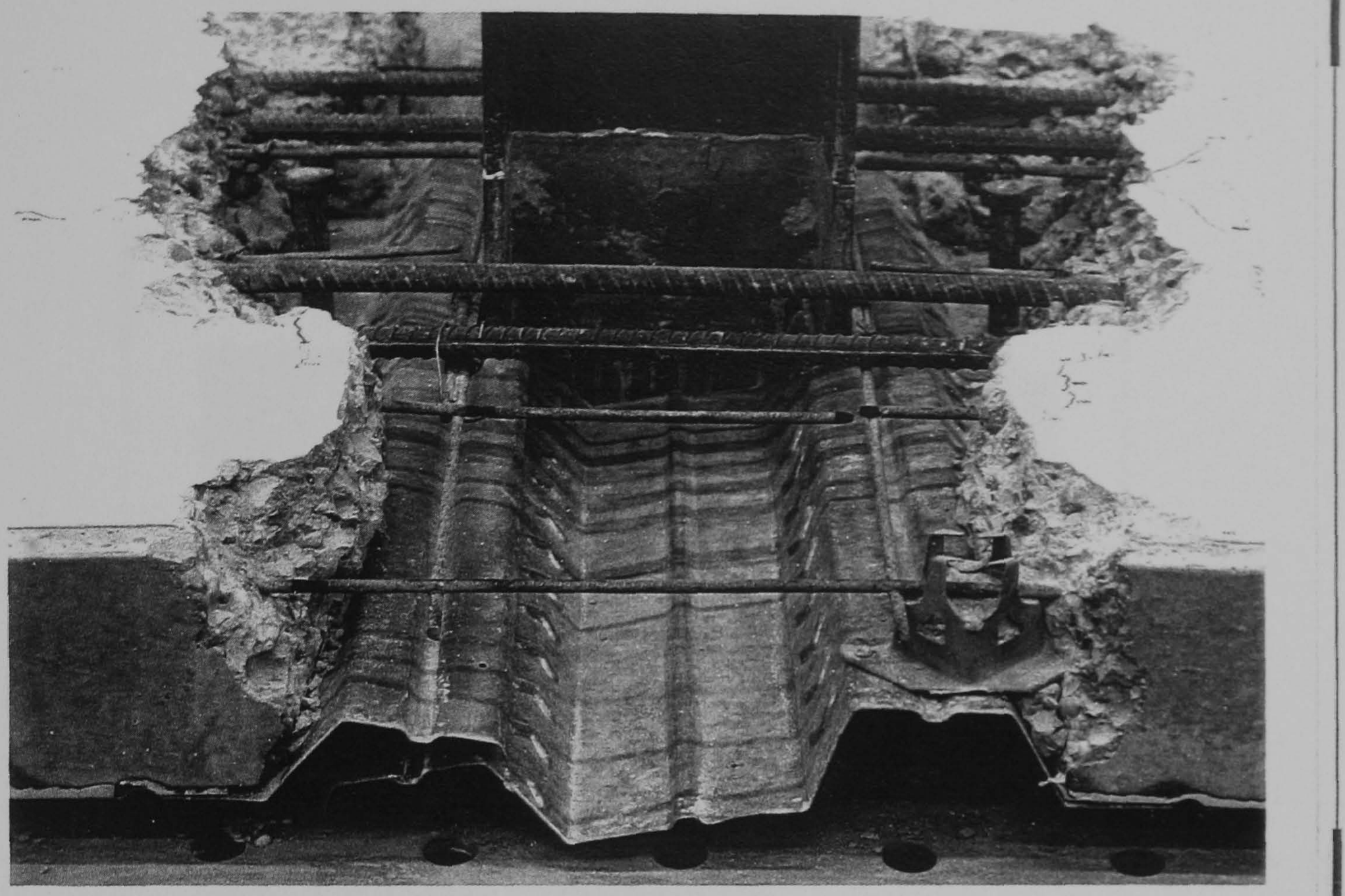

Plate 7.16 - Test 2: exposed reinforcement (front)

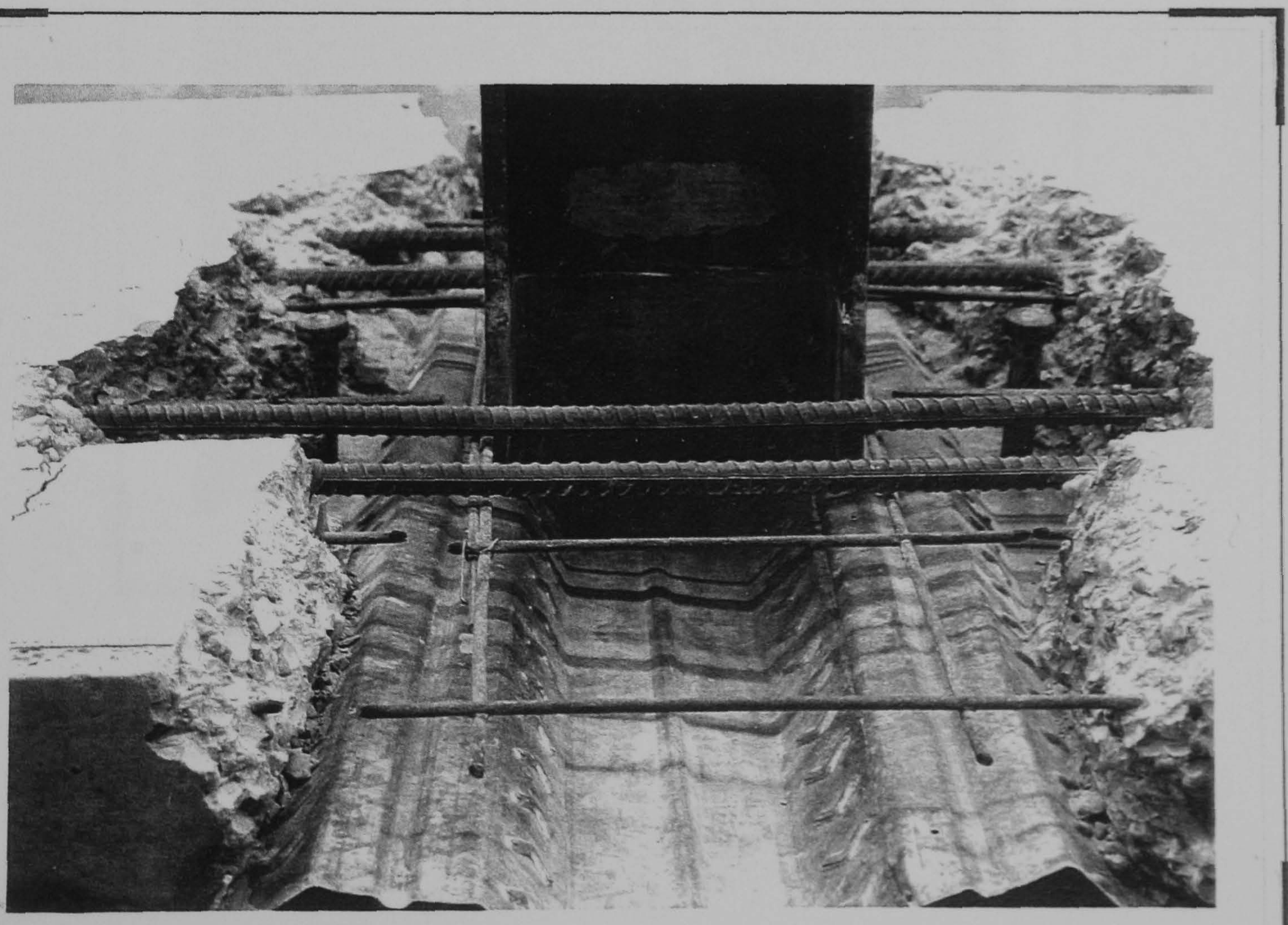

Plate 7.17 - Test 2: exposed reinforcement (back)

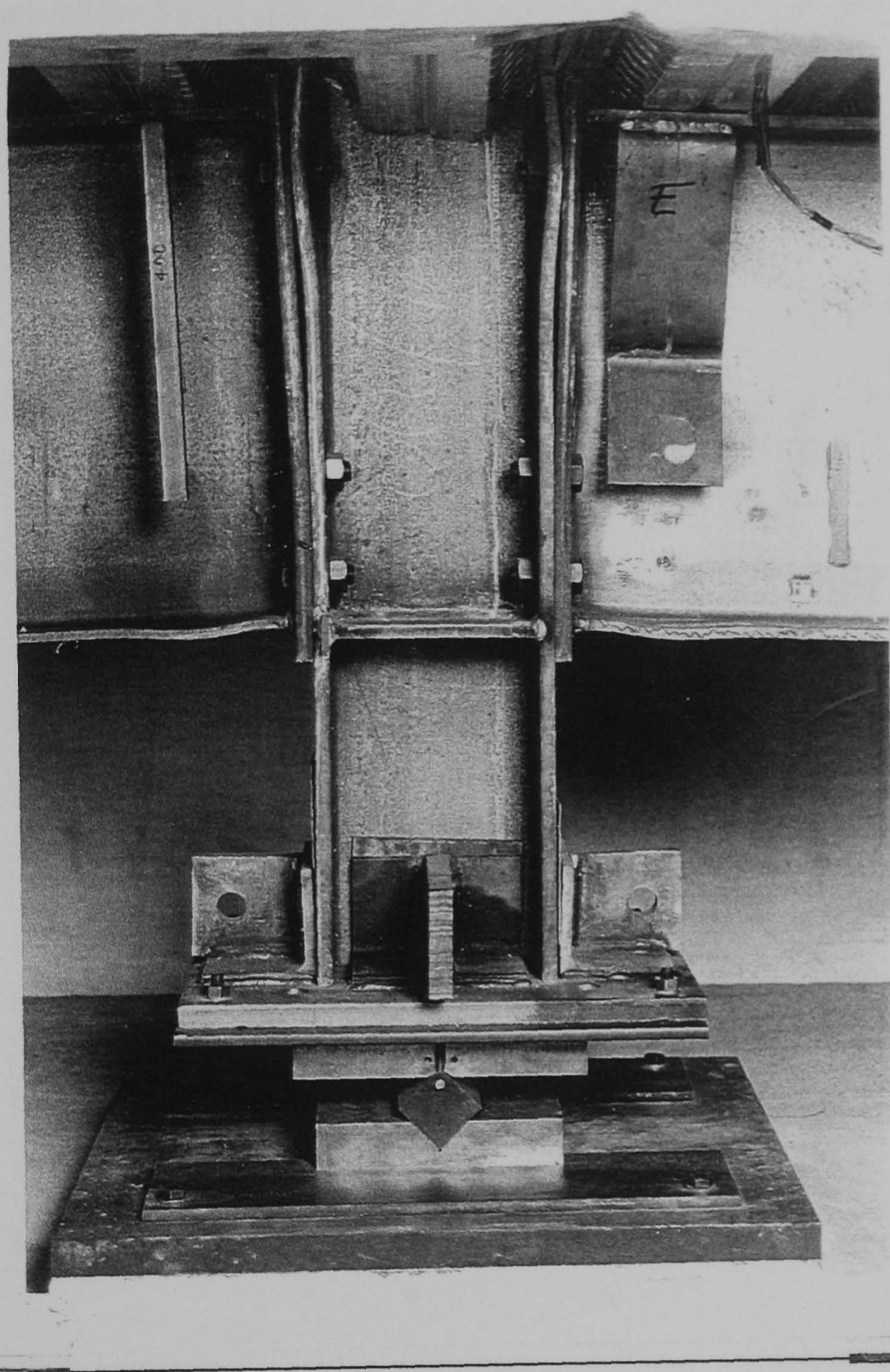

Plate 7.18 - Test 3: steelwork deformation (front)

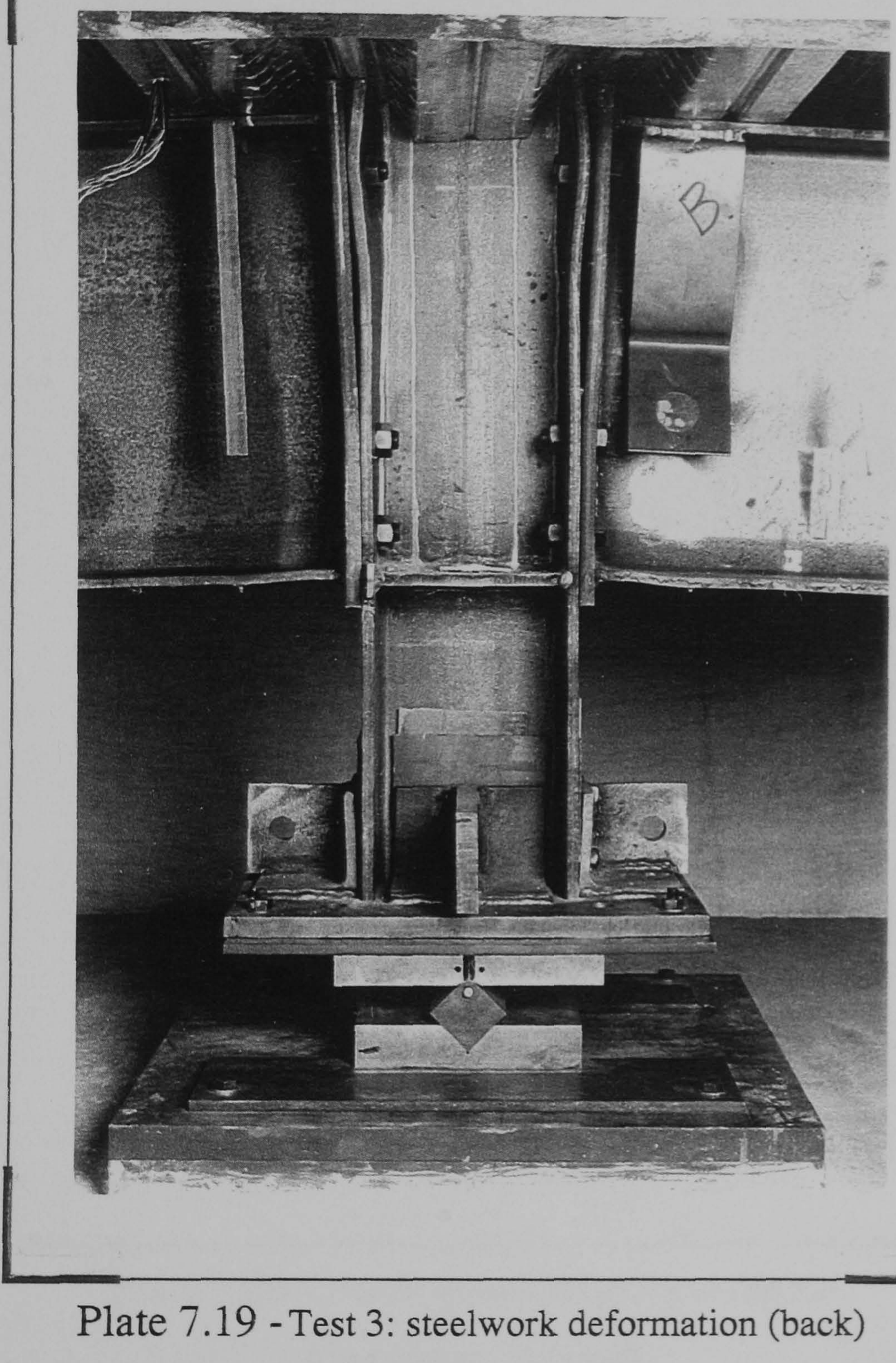

Plate 7.19 - Test 3: steelwork deformation (back)

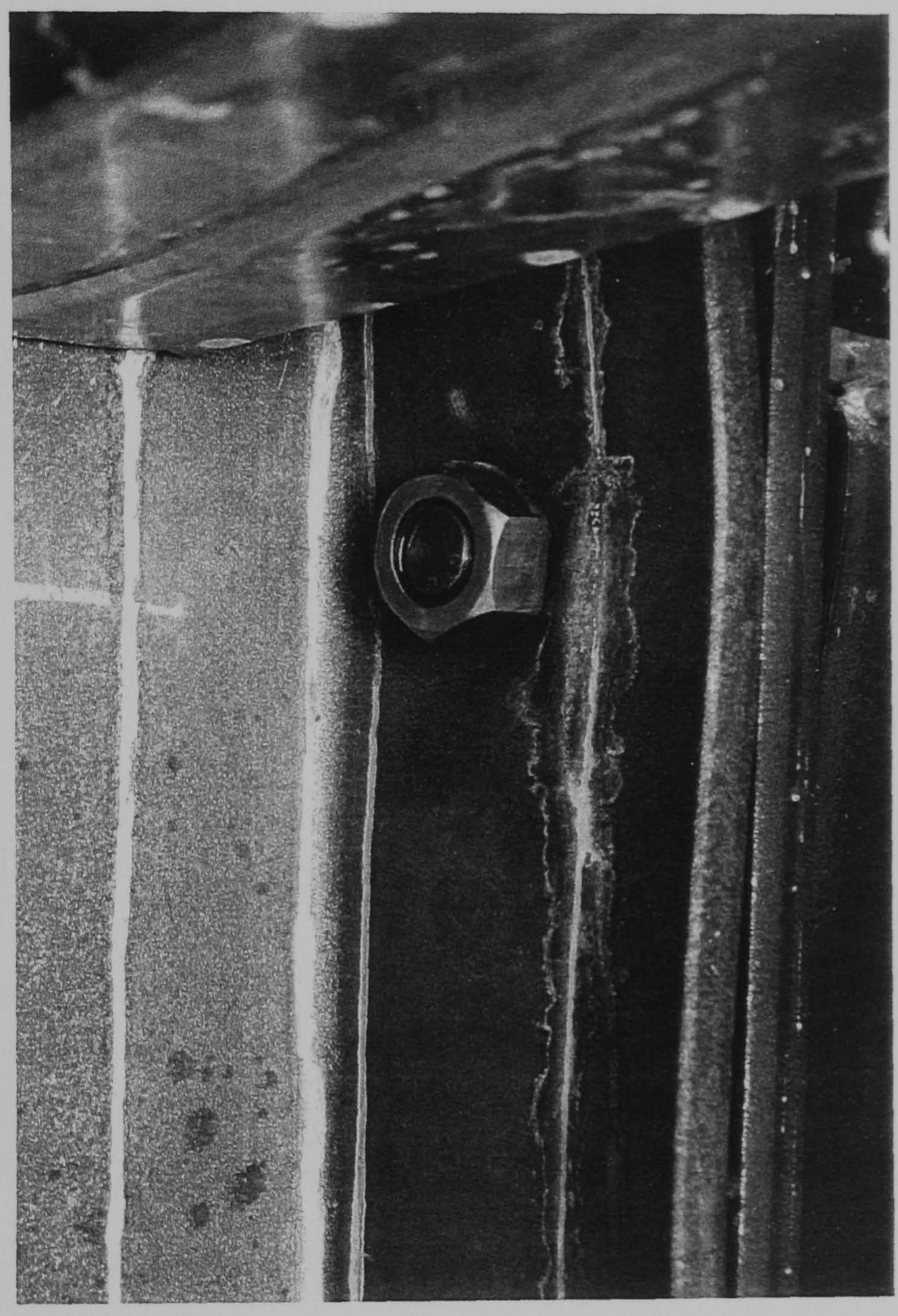

Plate 7.20 - Test 3: thread stripping to the nut

Connection 'B' (back)

Plate 7.21 - Test 3: crack pattern in the vicinity of the column

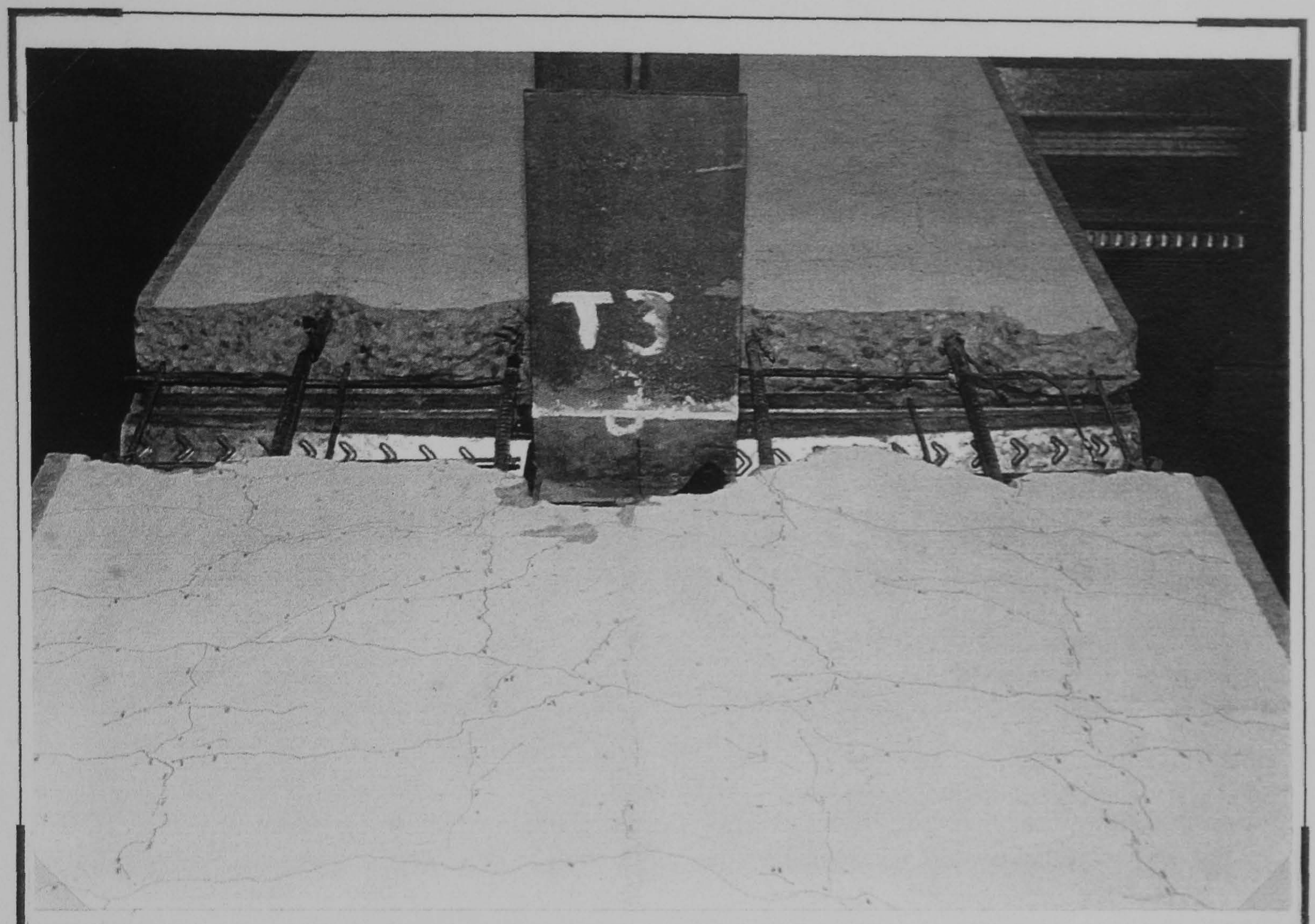

Plate 7.22 - Test 3: lateral deformation of the reinforcement

Plate 7.23 - Test 3: exposed reinforcement showing external rebar fracture (back)

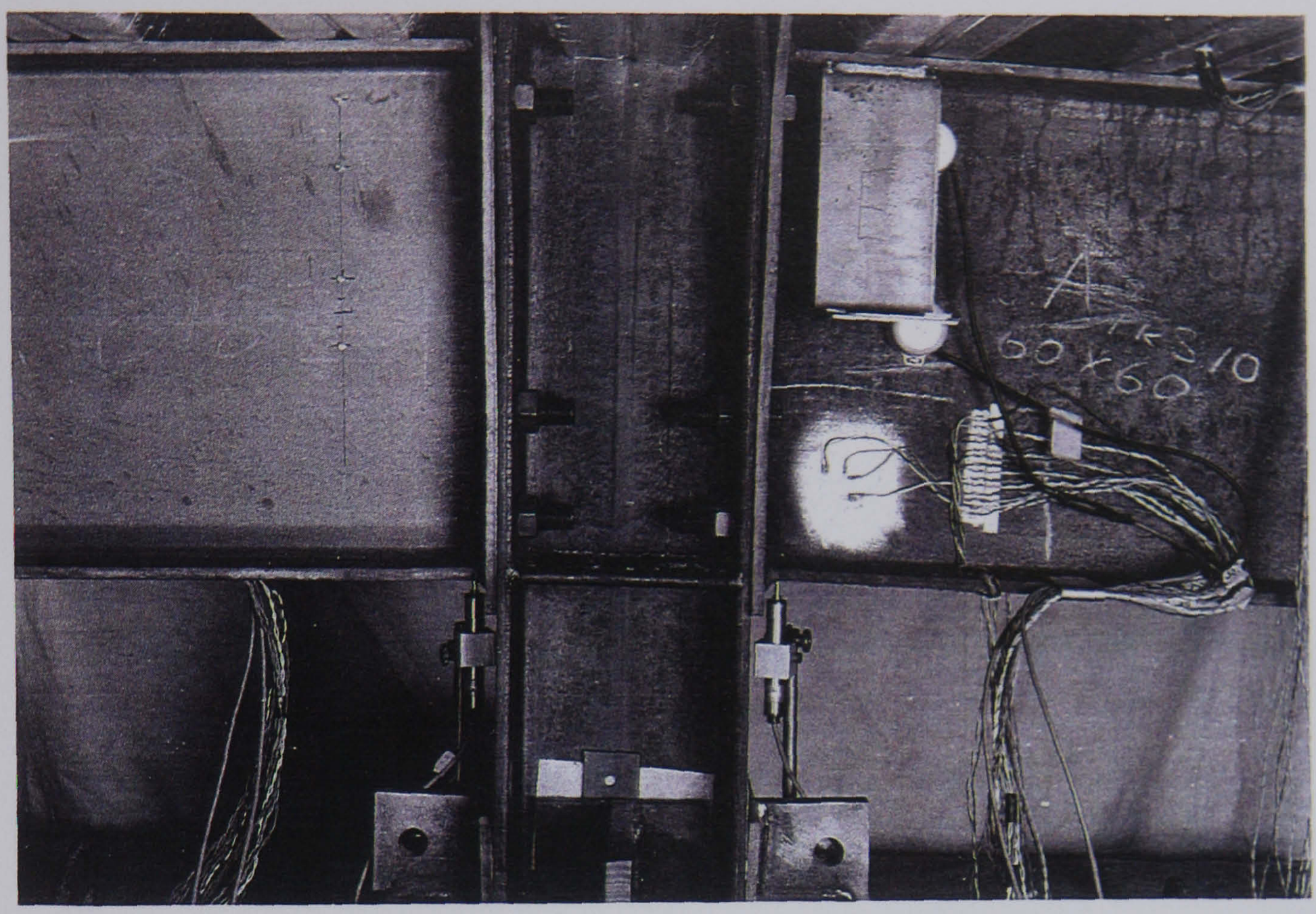

Plate 7.24 - Test 4: steelwork deformation (front)

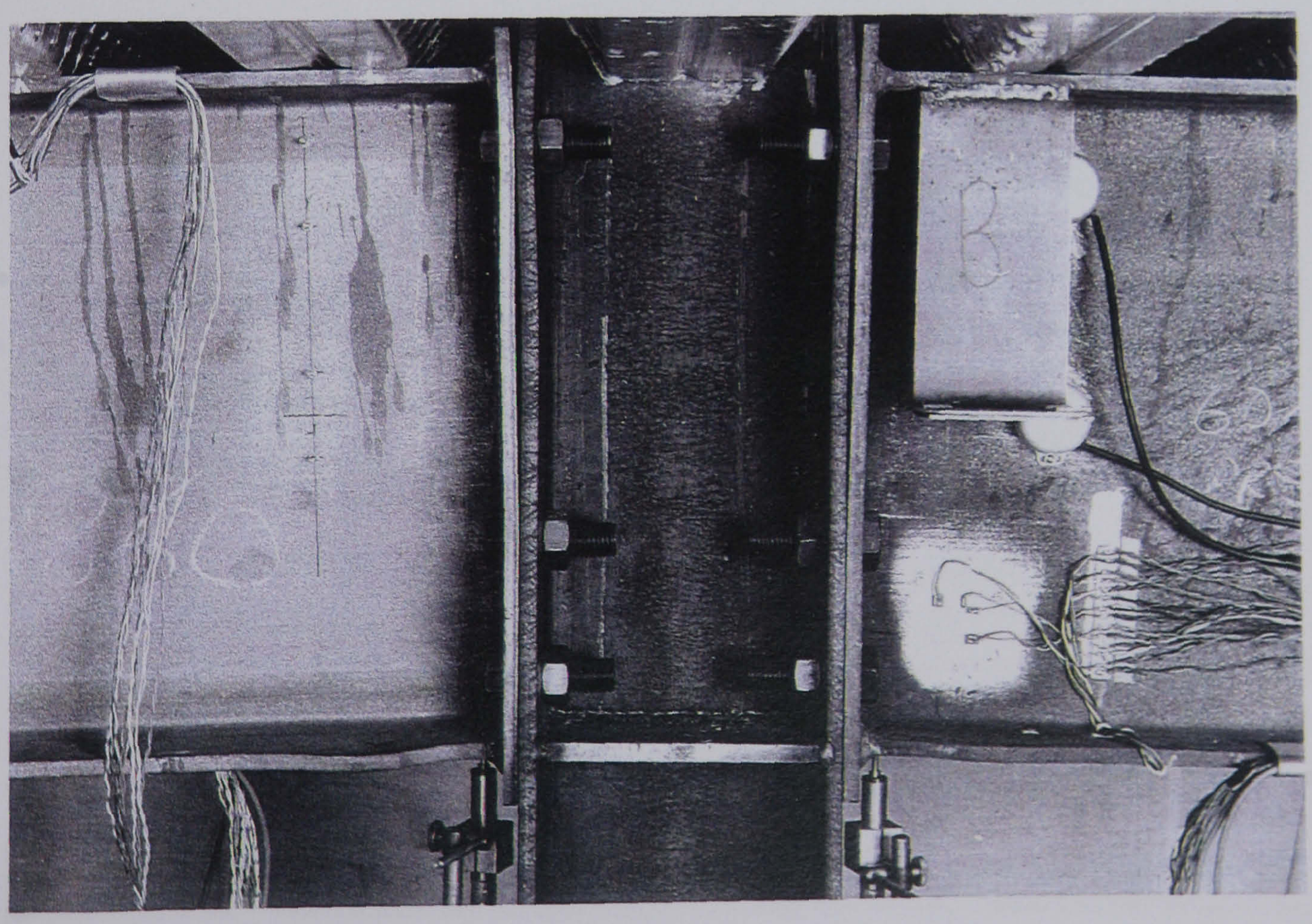

Plate 7.25 - Test 4: steelwork deformation (back)

Plate 7.26 - Test 4: exposed reinforcement

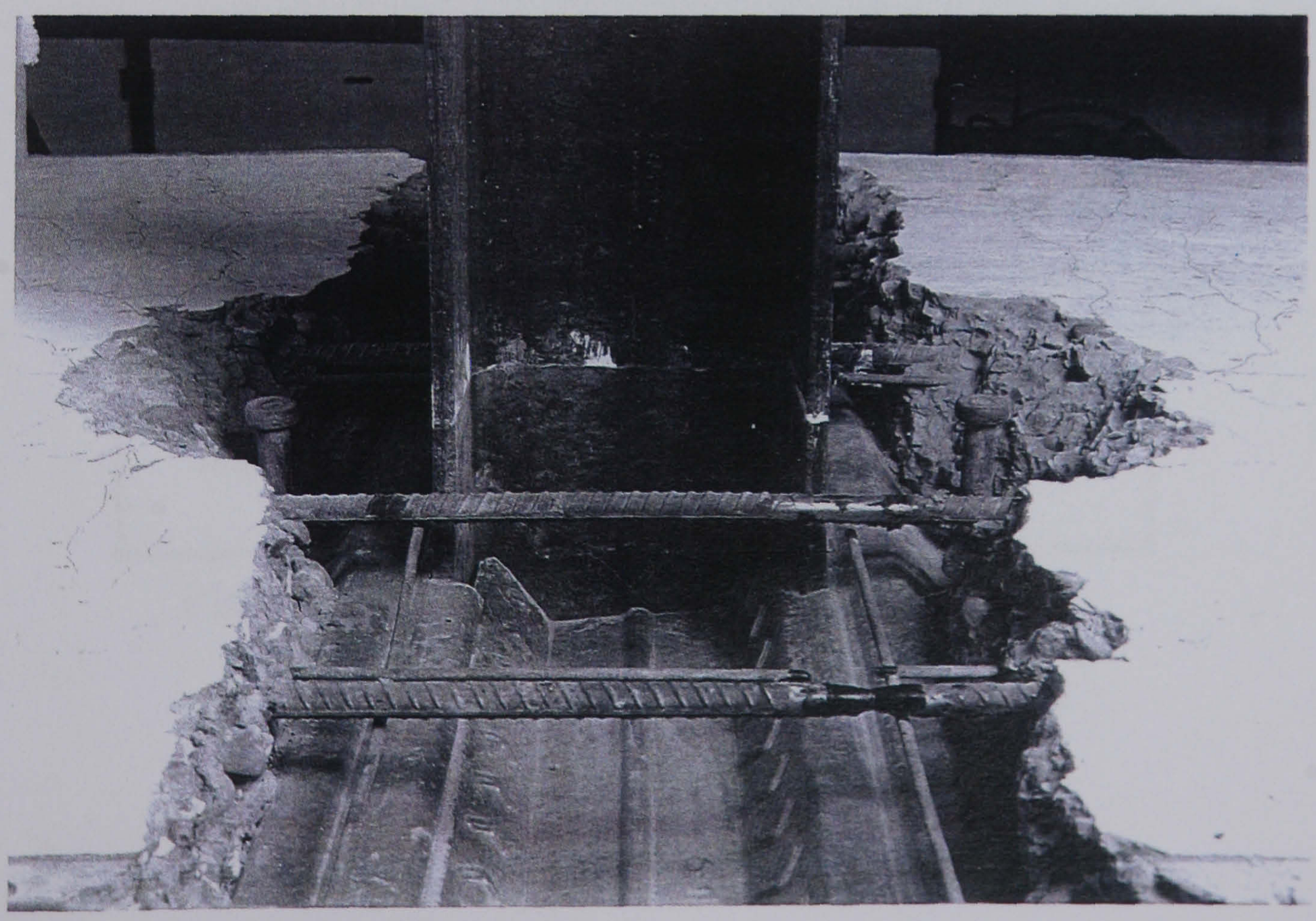

Plate 7.27 - Test 4: fracture of rebar (front)

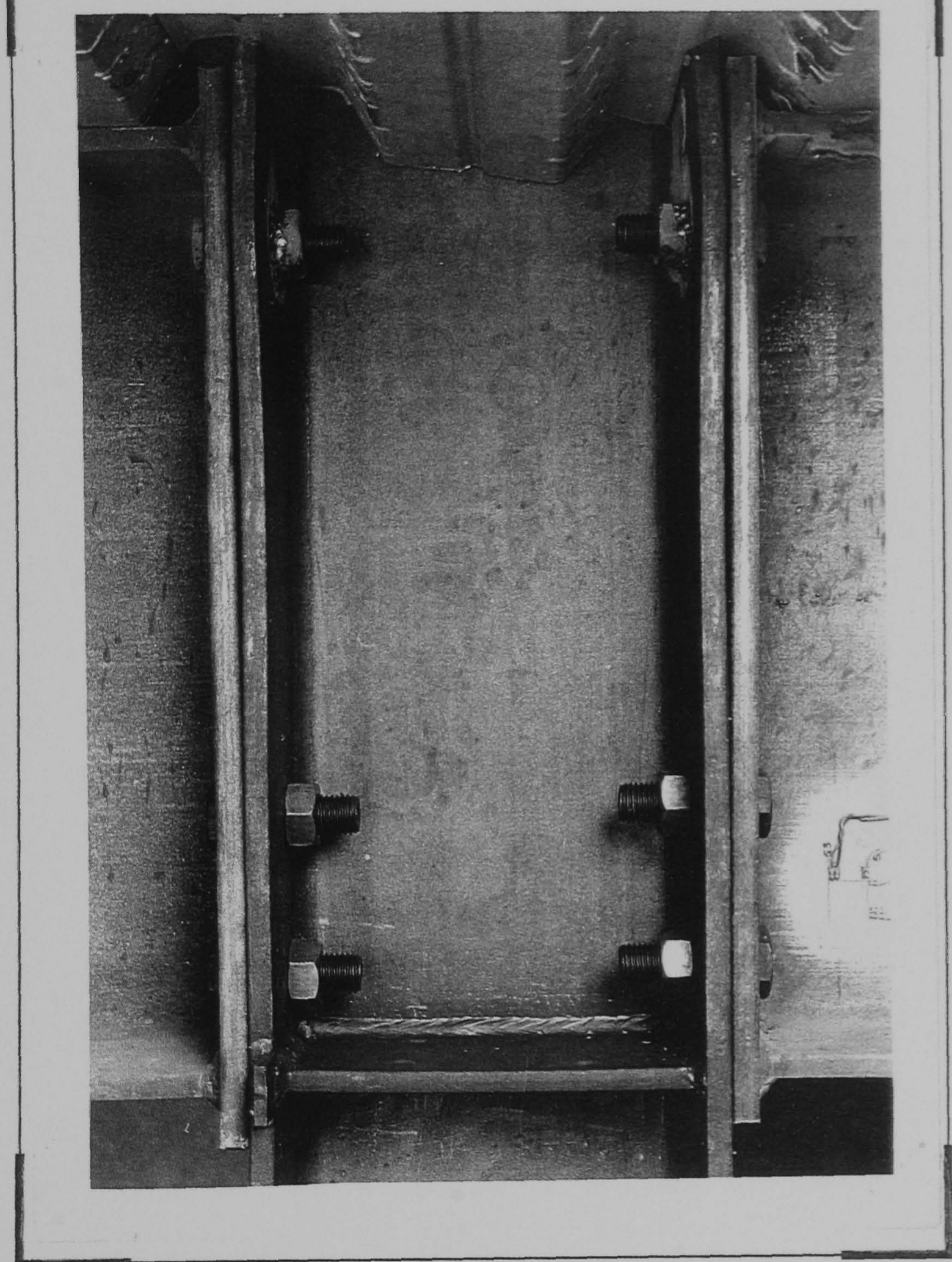

Plate 7.28 - Test 5: steelwork deformation (front)

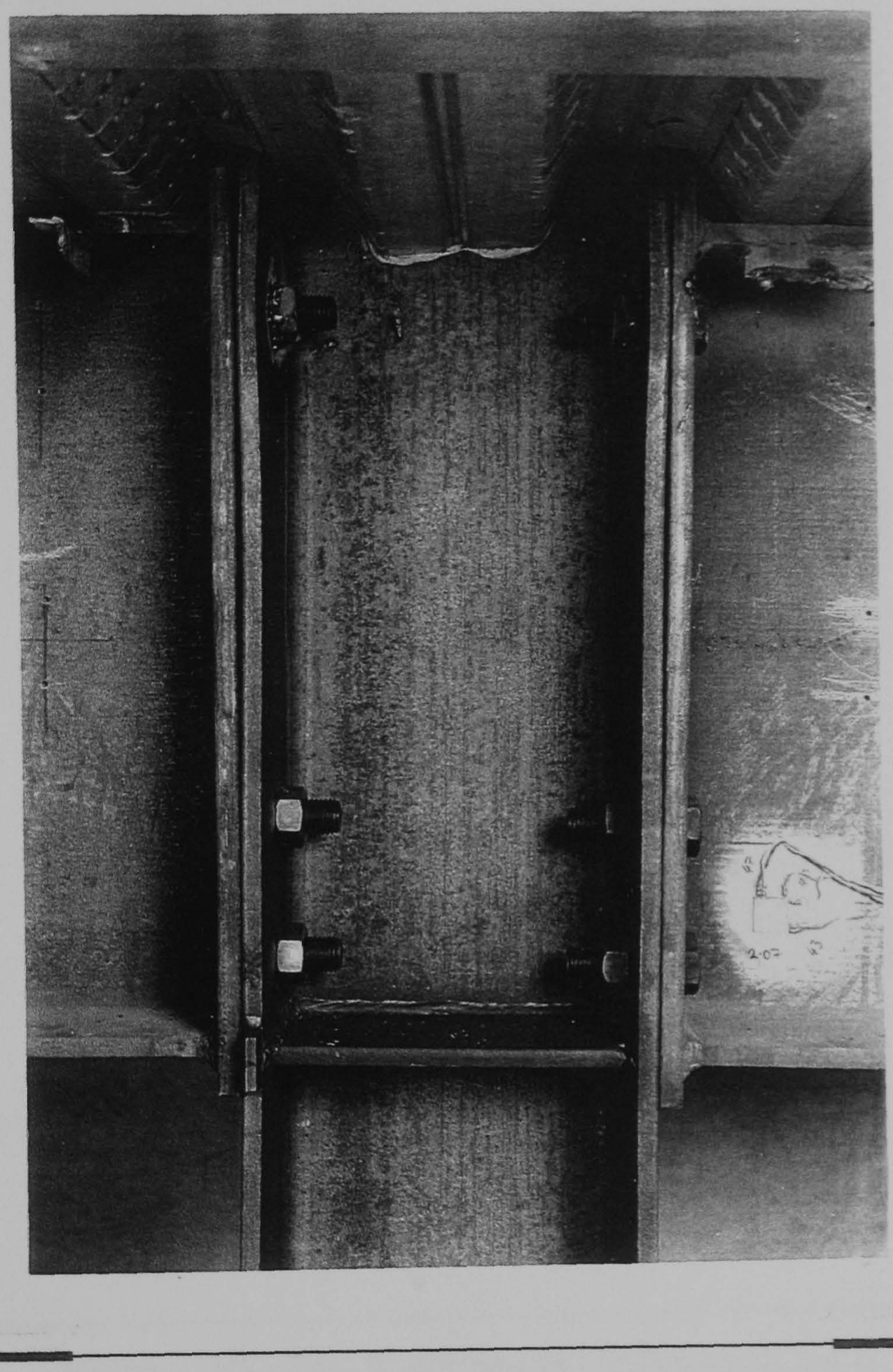

Plate 7.29 - Test 5: steelwork deformation (back)

Plate 7.30 - Test 5: nut welded to flange to guard against bolt fracture

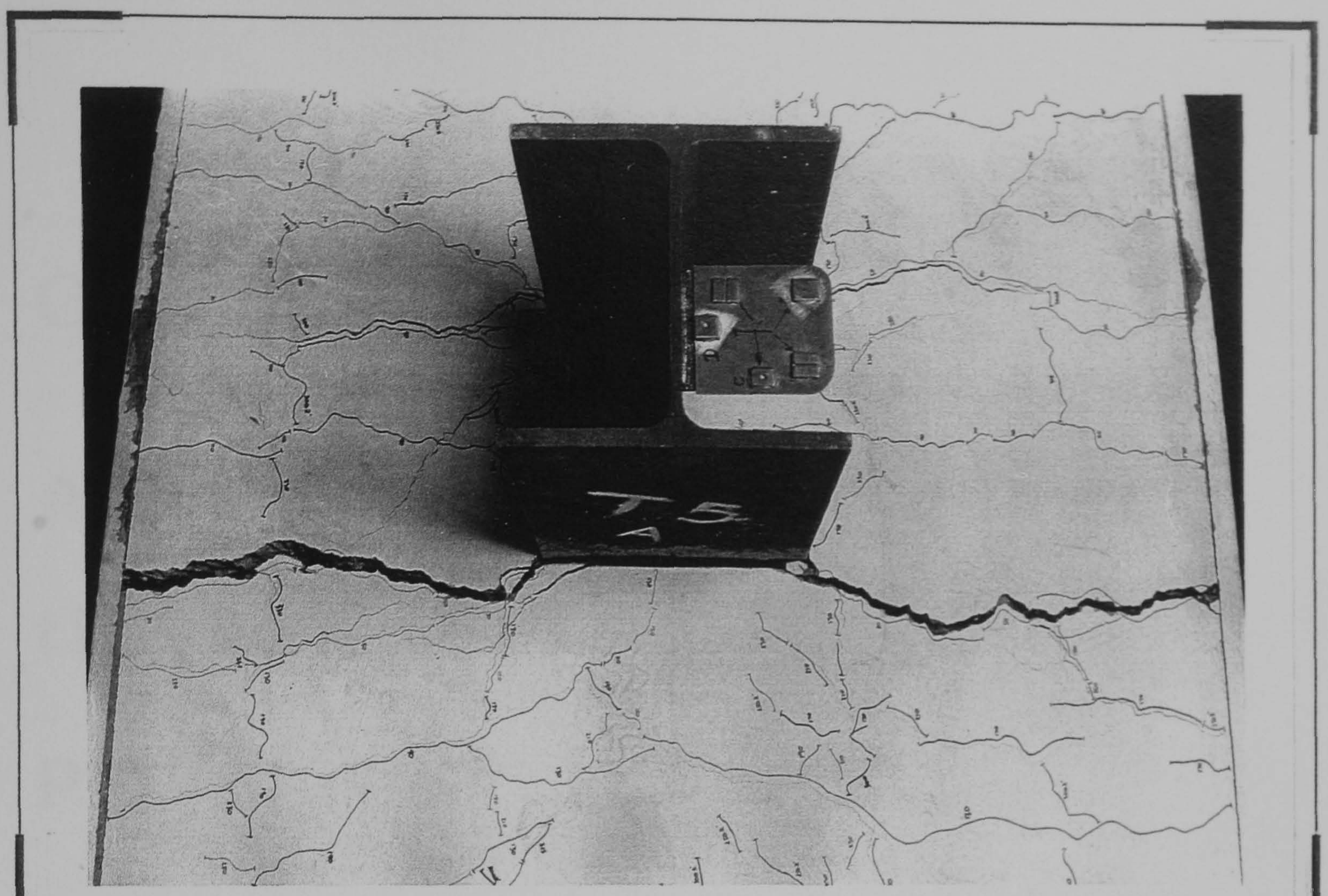

Plate 7.31 - Test 5: slab crack pattern

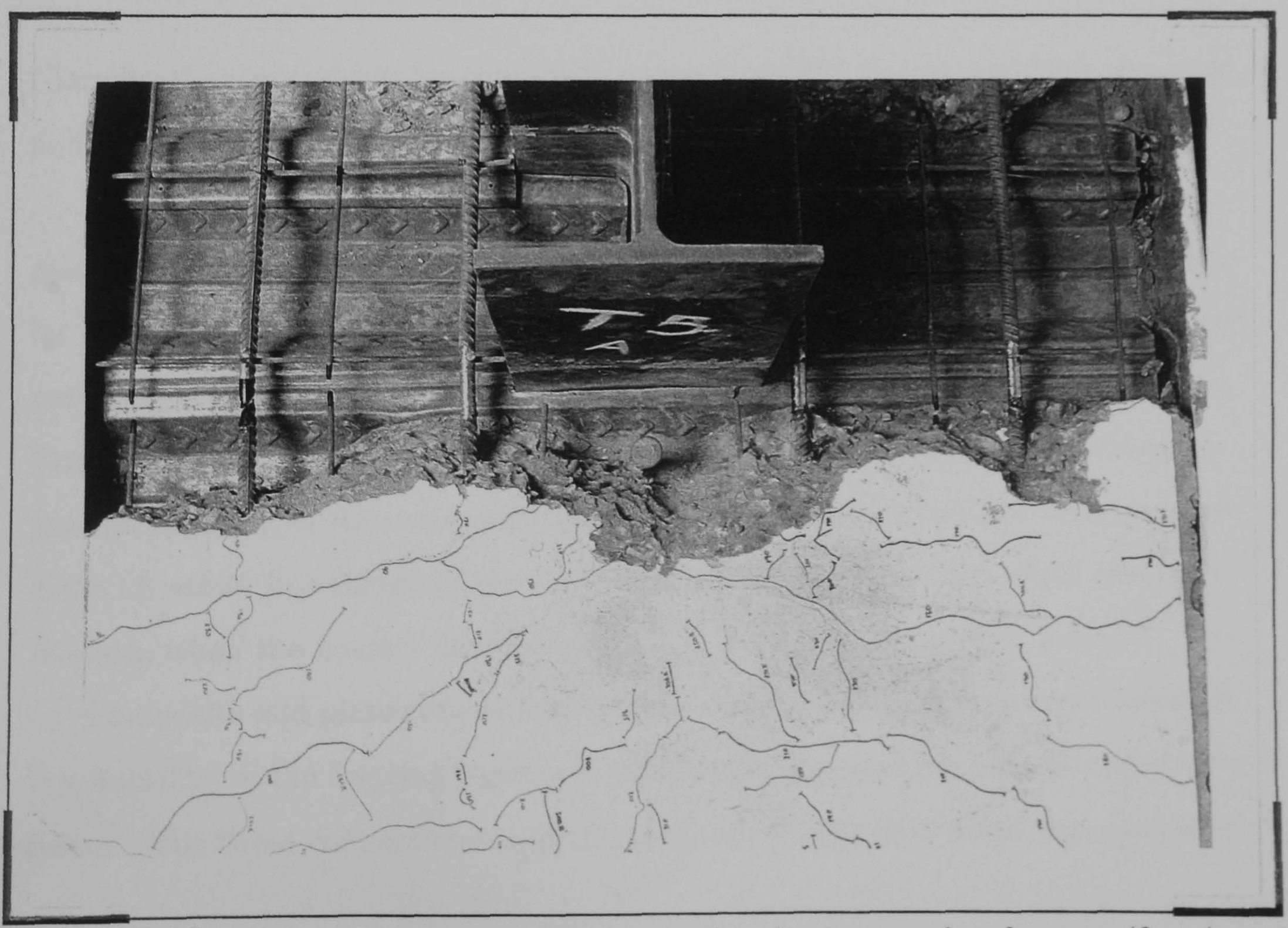

Plate 7.32 - Test 5: exposed reinforcement showing outer rebar fracture (front)

Chapter 8

Analysis of the test results in the context of connection performance

8.1 Introduction

Classification procedures for composite connections[60], in terms of both strength and rotational stiffness, are applied to the author's experimental results.

Incumbent within the procedures for the strength classification, is the requirement to predict the connection's moment of resistance. Consequently, particular emphasis will be given to the suitability of modern prediction methods to perform this calculation satisfactorily. Furthermore, the approach adopted by Eurocode 4[60] to classify the connection by its rotational stiffness, considers the flexural stiffness of the composite beam either to be in its cracked or uncracked state. A study has therefore been undertaken to investigate the effect on classification, when the beam's flexural stiffness is varied between these limits.

Composite end plate connections are also considered in the context of providing ductility in the hogging regions of plastically designed continuous composite beams. For these connections to perform satisfactorily, they must be capable of

redistributing bending moments from the support regions to the mid span region. It is shown that the ductility requirements cannot be expressed solely in terms of simple rules concerning material properties for reinforcing steel. To this end, existing ductility models are assessed prior to deriving an alternative semi-empirical method that considers the behaviour of the joint as a whole.

8.2 Classification of bolted composite beam-to-column connections

The classification procedures for bolted beam-to-column connections in accordance with Eurocode 3 have been described in Chapter 2. Eurocode 4 adapts these rules to classify similar composite connections, although the following restrictions are imposed: (i) The connections must incorporate slab reinforcement to enhance their tensile resistance. (ii) Although recognising the existence of semi-rigid connections, they are at present outside the scope of the code, and (iii) Eurocode 4 will only classify connections in frames that satisfy the requirements applicable to a braced frame (see clause 4.9.4.3 of the code).

Classification limits have been proposed in terms of both strength and rotational stiffness for composite connections. However, no detailed rules have been provided for calculating the key elements which can describe the moment-rotation characteristic. These elements include the connection's moment of resistance, its rotational stiffness and rotational capacity. This omission was a result of the code drafting panel concluding; *that the available prediction methods to determine these properties, were not yet sufficiently well established to justify their inclusion in Eurocode 4*[110].

8.2.1 Classification by strength

The classification limits for strength have been non-dimensionalised by comparing

the properties of the connection with that of the beam (see equation 8.1).

$$\bar{M} = \frac{Mp_{conn}}{M_{pl.Rd}} \begin{cases} \text{when } \bar{\text{M}} \geq 1.0 \rightarrow \text{Connection is Full strength} \\ \text{or} \\ \text{when } \bar{\text{M}} < 1.0 \rightarrow \text{Connection is Partial strength} \end{cases} \quad (8.1)$$

where :

Mp_{conn} - Connection moment of resistance

$M_{pl.Rd}$ - Negative moment of resistance of the composite beam.

Connection moment of resistance

An adaptation of the rules for steel connections can be used to calculate the moment of resistance of composite connections, provided that yielding of the slab reinforcement is included. To this end, it has been suggested[110] that adopting the following prediction model[87] (see Figure 8.1), would provide a suitable approach to this calculation.

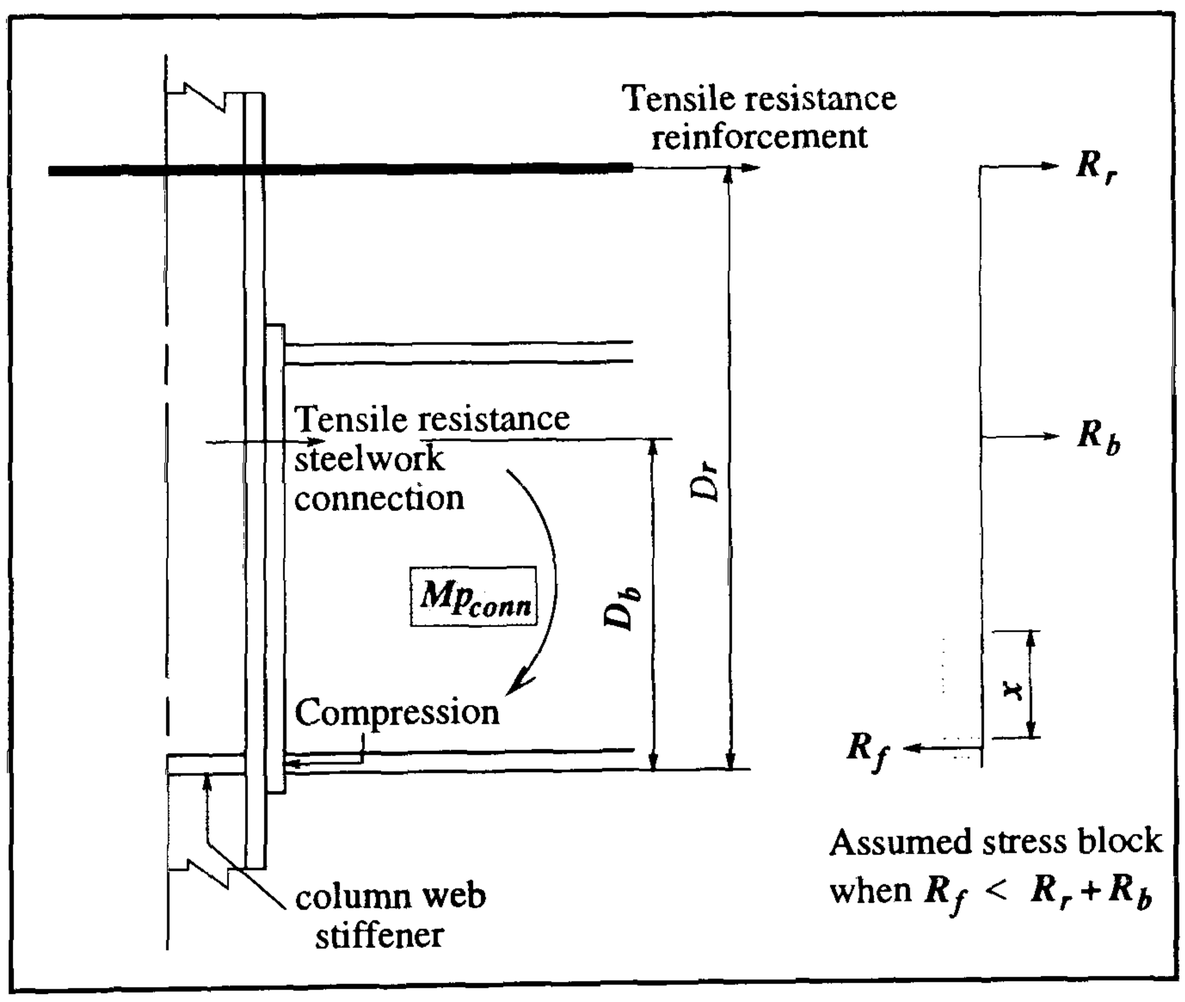

Figure 8.1: Prediction model for determining the moment resistance of a composite end plate connection

It would therefore follow that the moment of resistance could be evaluated by

equation 8.2.

$$Mp_{conn} = R_r \left[D_r - \frac{t_{bf}}{2}\right] + R_b \left[D_b - \frac{t_{bf}}{2}\right] - (R_r + R_b - R_f)\left[\frac{x}{2} + \frac{t_{bf}}{2}\right] \quad (8.2)$$

where :

R_r - Tensile resistance of the reinforcement = $f_{yr} A_s$

D_r - Lever arm between the centre line of the reinforcement and the bottom of the connected beam

R_b - Effective tensile resistance of the steelwork connection at the level of the tension bolts, in accordance with Annex J of Eurocode 3[18]

D_b - Lever arm between the centre line of the tension bolts and the bottom of the connected beam

R_f - Compressive resistance of the lower beam flange = $B_{bf} t_{bf} f_{ybf}$

f_{yr} - Yield stress applicable to the reinforcement

A_s - Total reinforcement area

B_{bf} - Width of the lower beam flange

t_{bf} - Thickness of the lower beam flange

f_{ybf} - Yield stress applicable to the beams flange

x - Depth of beam web in compression (see equation 8.3).

$$\left.\begin{array}{c} \text{When } R_f < (R_r + R_b), \quad x = \frac{(R_r + R_b - R_f)}{t_{bw} f_{ybw}} \\ \text{or alternatively} \\ \text{When } R_f > (R_r + R_b), \quad \text{the third term drops out of the calculation} \end{array}\right\} \quad (8.3)$$

where :

t_{bw} - Thickness of the beams web

f_{ybw} - Yield stress applicable to the beam web.

It can be seen from equation 8.2 that the prediction model was based on

the tensile resistance of the reinforcement and the steelwork connection acting together, about the centre of the lower compression flange of the beam. The equation is then further modified in recognition that the resistance R_f, at the compression level, may influence the development of the connection's moment of resistance. This situation would occur if the total tensile resistance $R_r + R_b$ exceeds the compressive resistance of the lower beam flange R_f. To ensure that equilibrium of horizontal forces are maintained under these circumstances, part of the depth of the web, denoted 'x' in Figure 8.1, is assumed to have yielded. The familiar rectangular stress block distribution also shown in the figure, is adopted to determined 'x'. The increased web thickness in the region of the curved fillet in rolled sections is ignored.

The above model also precludes the possibility of the failure being associated with the column web buckling. Consequently, where appropriate, strengthening measures should be provided to ensure that this requirement is satisfied. Furthermore the model is restricted to Class 1 'plastic' or Class 2 'compact' steel sections.

Beam's negative plastic moment of resistance

To complete the classification by strength, the composite beam's plastic moment of resistance with respect to negative bending, $M_{pl.Rd}$, must be determined. The derivation of the necessary design formulae, together with a comprehensive explanation of their implementation, may be found elsewhere[57] and are therefore not reproduced here. However, in essence they are based on establishing the position of the plastic neutral axis within the cross-section, and subsequently determining the moment of resistance by taking moments.

Assessment of the results

The results are shown in Table 8.1 and were based on the measured material properties and measured section dimensions (see Appendix D, sections D.2

and D.3 respectively).

Test	Test moment (M)	Connection moment of resistance Mp_{conn} kNm	Composite beam negative moment of resistance ($M_{pl.Rd}$)	Ratio $\frac{\text{test moment}}{\text{predicted moment}}$	Strength classification $\overline{m} = \frac{M}{M_{pl.Rd}}$	Member classification
1#	162	87 (Annex J)	357 (Steel beam)	1.86	0.45 - partial	Class 1 'plastic'
2	380	295 [371]	458	1.29	0.83 - partial	Class 2 'compact'
3	390	295 [371]	450	1.32	0.87 - partial	Class 2 'compact'
4	370	296	458	1.25	0.81 - partial	Class 2 'compact'
5	493	393	885	1.25	0.56 - partial	Class 2 'compact'

Notes

- Steel only test

[] - Prediction incorporating the steelwork test moment of 162kNm

Table 8.1: Classification by strength

It can be seen from Table 8.1 that the lowest strength classification was applicable to the steel-only test (Test 1). This results as a consequence of the flush end plate steel detail, in which the tension bolt row is incorporated within the depth of the connected beam, producing the lowest moment of resistance of all the connections tested. A similar classification, although slightly higher, was obtained for the final composite test (Test 5). This results as a consequence of adopting a deeper beam, which inevitably leads to a much higher negative moment of resistance for the beam section at the supports. This could not be approached by adopting the same reinforcing detail that was used for the previous composite tests, despite the increase in the lever arm to both the bolt row and the reinforcement. The remainder of the tests (Tests 2,3 and 4) all had a strength classification of at least 80% of the beam's negative plastic moment of resistance. Consequently, it would seem reasonable to assume that a full strength composite connection could be provided. However, the desirability of providing full strength connections is a subject of debate. A composite beam's susceptibility to lateral-distortional buckling would be reduced by providing partial strength connections

at internal supports of continuous beams. This beneficial effect is the result of restricting the moment transmitted at the support to less than the full negative moment resistance of the beam member. Consequently, the length of the hogging moment region would be reduced, which in turn would ensure that a more stable performance from the beam would be obtained.

Alternatively, the strength classification could be based on the predicted connection moment of resistance rather than the test moment discussed above. Under these circumstances, the classification would decrease such that for tests 2-3 inclusive, 64% of the beam's negative plastic moment of resistance would be expected. However, despite the partial strength nature of the connections involved for these three tests, an ultimate rotation capacity in excess of 30mradians was achieved. This encourages the view that the ductility needed by a composite system is not impaired if the connection resistance is lower than that of the connected beam. Unfortunately, in comparison with Test 5 a similar conclusion cannot be drawn. The partial strength nature of the connection does limit the available ductility, since only 20mradians was obtained prior to rebar fracture. This change in behaviour can in part be explained by a further drop in the strength classification of between 30 and 35%. This would result in the resistance of the connection dropping below half the strength of the connected beam, if the classification was based on the predicted value for the connection.

These results tend to suggest that an adequate ductile performance would be achieved, by providing a connection whose predicted resistance was at least 65% of that of the connected beam. However, it will be shown in Section 8.3, that the problem of connection ductility is very complicated and cannot be assessed by simply comparing the relative strengths of the component parts that make up the composite connection.

The prediction method described previously to determine a composite connection's moment of resistance produces, at first sight, a poor approximation to the true test moment achieved. However, if one compares the predictions which

incorporate the experimentally determined steelwork moment, see Tests 2 and 3, it can be seen that very close correlation was achieved. Consequently, it can be concluded that the method proposed to enhance a steelwork connection's moment of resistance, when part of a composite arrangement, may be used as a basis for predicting the moment of resistance of composite bolted flush end plate connections. This further underlines the conclusions of previous experimental work, from which a preliminary design guide has been published[111].

The explanation to the failure of the method in the first instance, can be attributed to the poor prediction of the steelwork component of the composite arrangement. It can be seen from Table 8.1 that the steel-only connection's moment of resistance was under predicted by 86%. However it has to be remembered, that the moment of resistance of the steelwork connection was undertaken in accordance with the revised Annex J of Eurocode 3[18], which seeks to predict the moment at the 'Knee' of the moment-rotation characteristic. The 'Knee' is defined in the context of a connections behaviour, by the moment at which the connection exhibits a significant loss in stiffness.

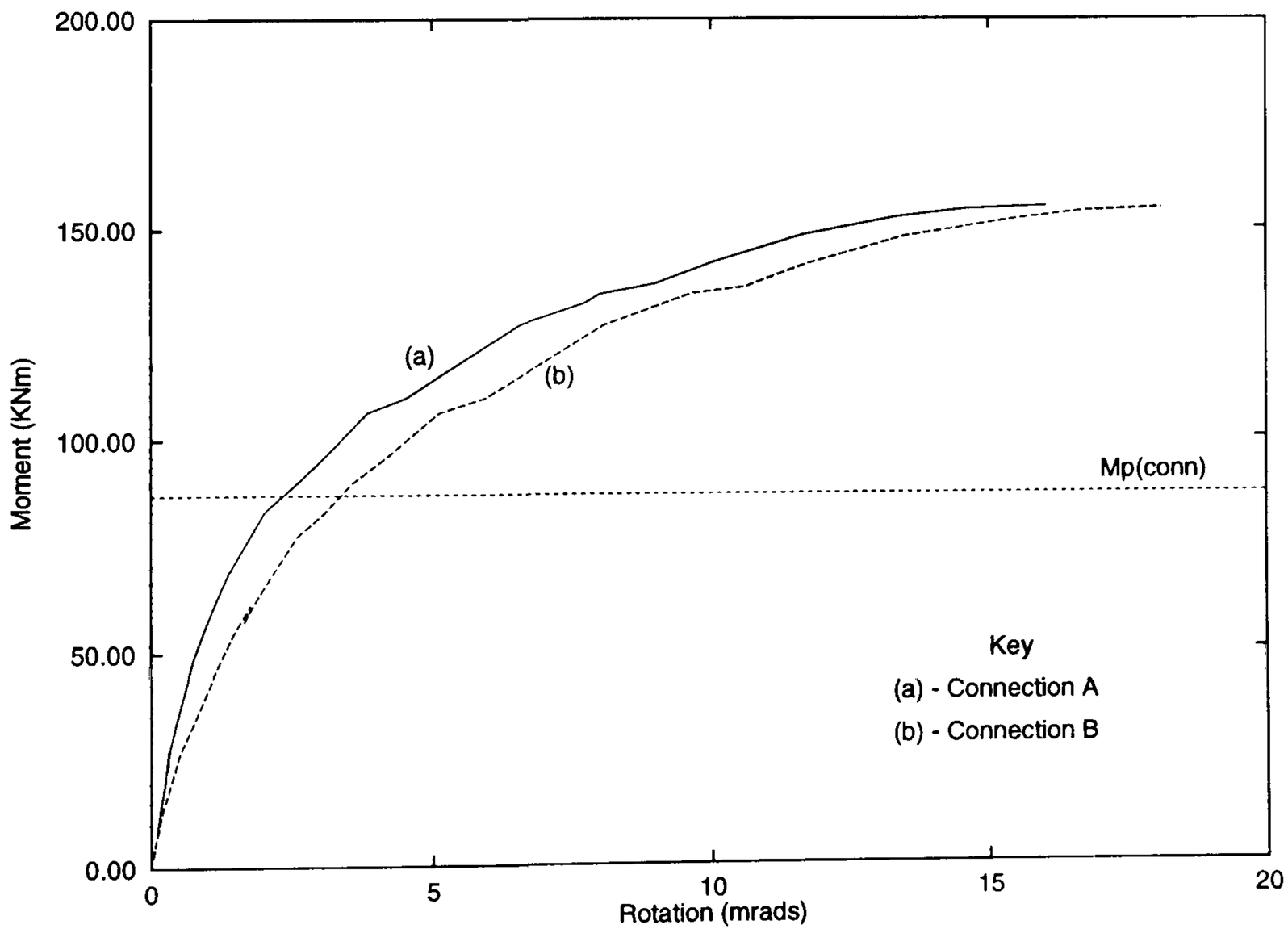

Figure 8.2: Revised Annex J's prediction for the steel-only test (Test 1)

It can be seen from Figure 8.2, which illustrates the moment-rotation characteristic for Test 1, that Mp(conn) does represent a good prediction for the 'Knee' of the moment-rotation characteristic for this particular test.

Following the substitution of the characteristic material properties and partial safety factors, further conservatism within the method would be realised. In a design situation therefore, there would be a tendency for the ratio of the test moment to the predicted moment to increase slightly. This can be proved for the author's experimental programme, where the increase varied between 5 and 13%.

In terms of structural performance, conservative predictions with regard to the connection's moment of resistance would be acceptable on the grounds that it would generally translate into improvements in the overall behavioural response from the frame. However, it must also be appreciated that problems may arise if the mode of failure of the connection changes to one which had not been previously considered, as a direct result of the underestimation of the connection's strength.

8.2.2 Classification by rotational stiffness

The revised Annex J for Eurocode 3[18] provides the following boundary for classification by stiffness for steel connections within a braced frame. This is undertaken by comparing the connection's initial stiffness, with a boundary criteria indicated by Figure 8.3. From this figure, it can be seen that if the connection's initial stiffness is greater than this boundary, then its corresponding behaviour can be considered as rigid. Likewise, if the boundary criteria is not satisfied, then the connection behaviour should be considered as semi-rigid.

As indicated from the introduction, Eurocode 4 assumes that the flexural stiffness of a composite beam EI_b, would be based on either its cracked or uncracked state. The choice being consistent with the assumptions adopted for the global analysis of the frame.

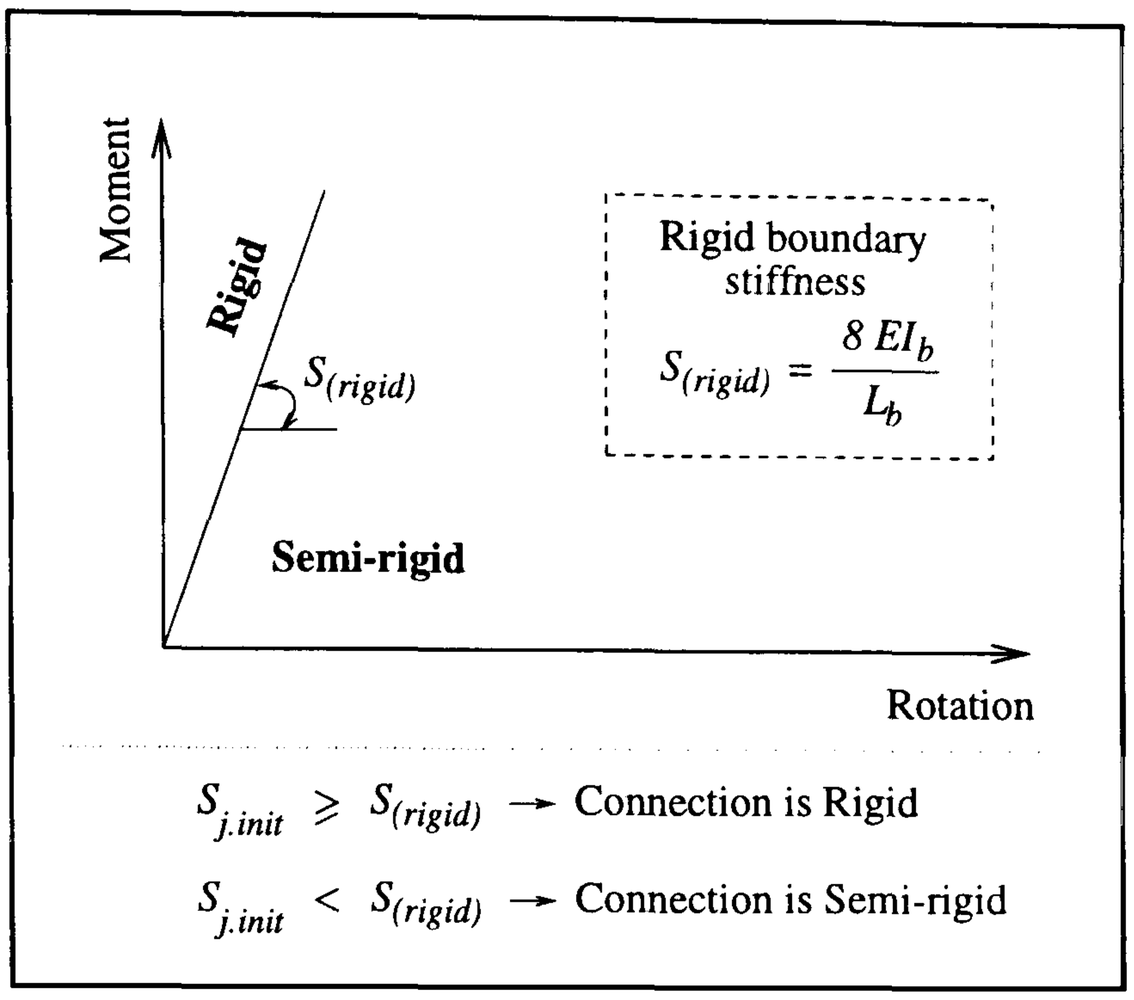

Figure 8.3: Classification by rotational stiffness

In Figure 8.3: EI_b - Flexural rigidity of the beam

S_b - Length of the beam

$S_{j.init}$ - Connection's initial stiffness.

Clearly, if the beam is assumed to be cracked, the corresponding classification would move in favour of the connection being considered as rigid. This would result from a decrease in the stiffness of the rigid boundary, as a consequence of utilising the second moment of area applicable to a cracked composite beam. For internal connections of continuous composite beams, the 'cracked' approach has traditionally been considered to be the more accurate model. This stems from a comparison with reality, where it can be seen that as a result of hogging bending, strictly the cracked section properties would be applicable. However, although cracking within this region occurs, it certainly does not extend over the full length of the beam. Consequently, a more realistic approach to the calculation of the classification boundary, would be to base the classification on an effective beam section applicable to the entire beam span; hence the beam properties would be somewhere in between the cracked and uncracked extremes. To this end, slope deflection equations were utilised to develop an algebraic equation to determine an equivalent second moment of area applicable to this non-uniform situation.

Algebraic solution to a non-uniform composite beam

For an internal span of a continuous beam resisting uniformly distributed loads, the bending moment distribution is shown by Figure 8.4.

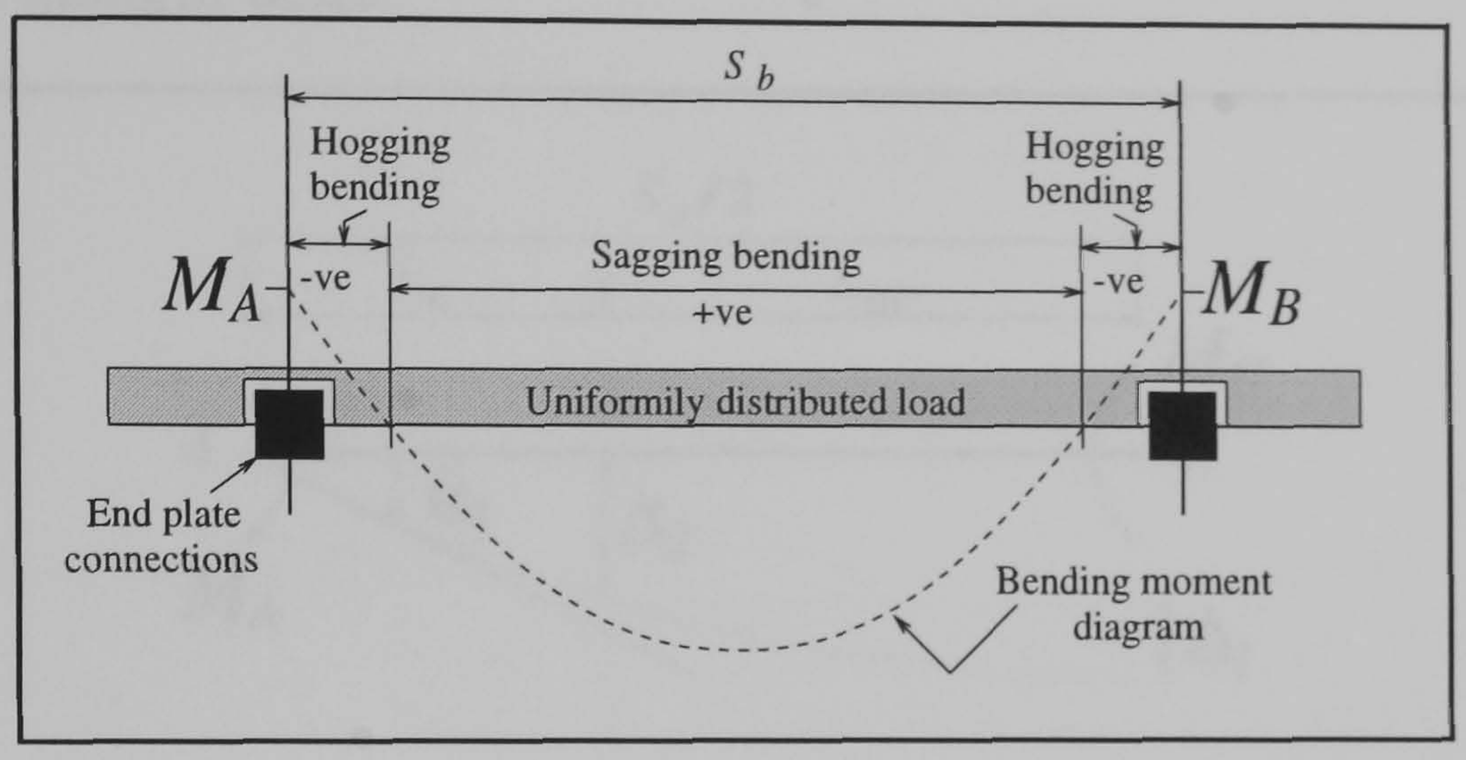

Figure 8.4: Bending distribution for a internal span of a continuous beam

If this beam was constructed from a bare steel rolled section, then the second moment of area for the section would be uniform throughout its length. Consequently, for the situation shown in Figure 8.5, it can be shown using slope deflection relationships that equation 8.4, which is subsequently used as a measure of rotational stiffness, represents the beam stiffness at the supports.

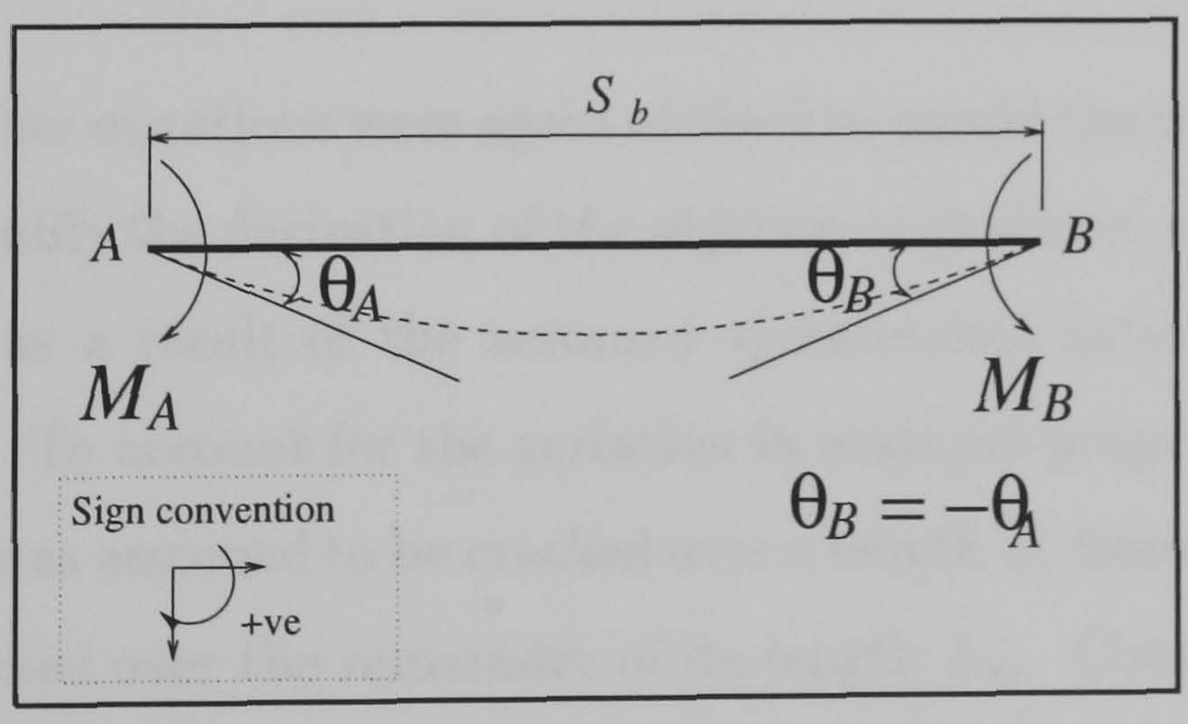

Figure 8.5: Uniform steel beam

$$\frac{M_A}{\theta_A} = \frac{2EI_b}{S_b} \tag{8.4}$$

where EI_b has been defined previously in Figure 8.3.

However, if this beam was constructed as a composite member, the second moment of area for the section would be influenced by the bending moment distribution throughout its length. This situation will be subsequently referred to as a non-uniform beam.

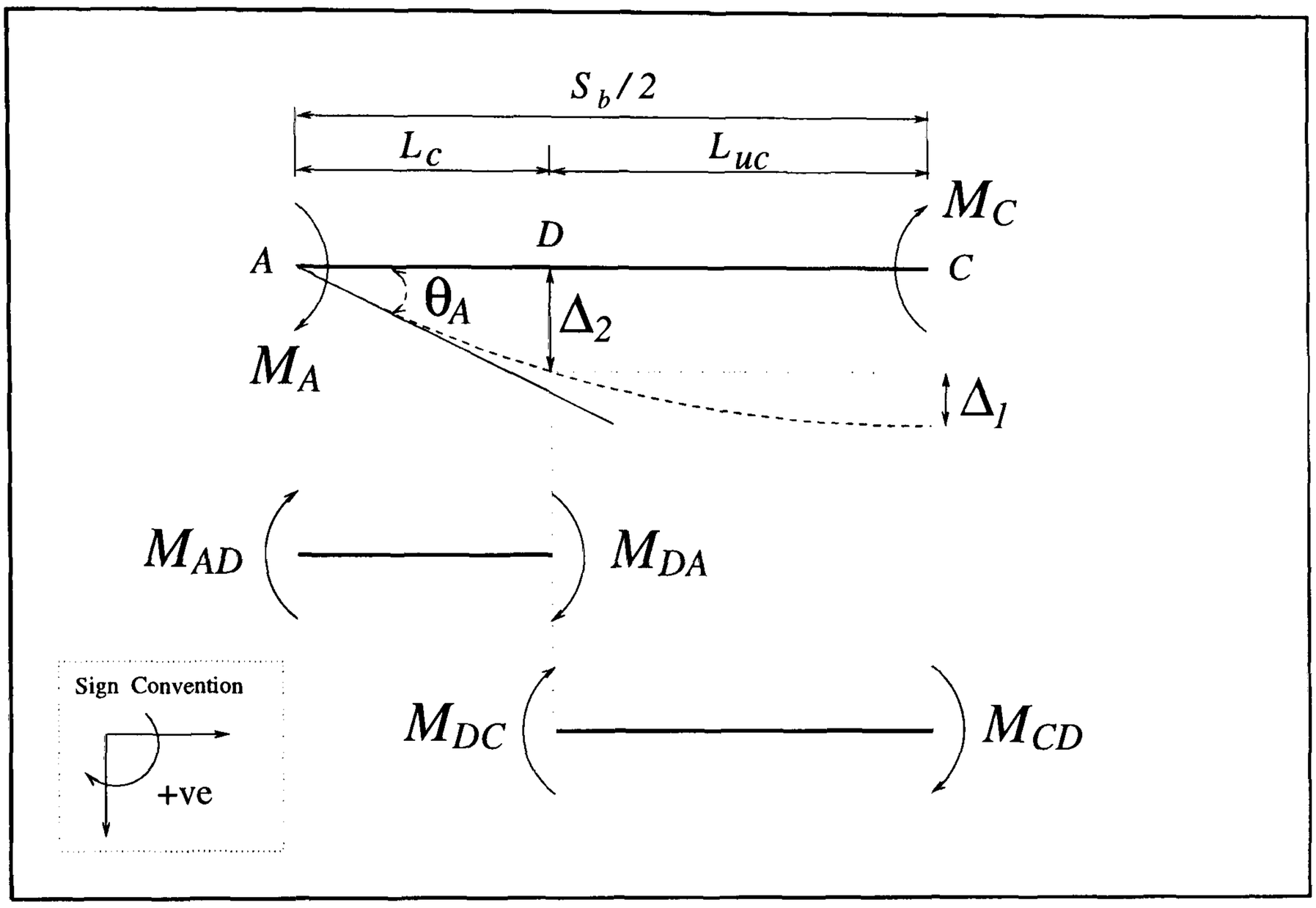

Figure 8.6: Non-uniform composite beam

Slope deflection equations were again utilised to model the non-uniform beam. However, to simplify the derivation of the algebraic equations, only half the beam was considered as a result of the assumed symmetrical nature of the problem (see Figure 8.6). To account for the variation in material properties over half the span, the beam was assumed to be cracked over a length L_c from the adjacent support and uncracked over the remainder of its length L_{uc}. Consequently, cracked and uncracked material properties, EI_c and EI_{uc} respectively, were adopted for these lengths.

Consider the cracked span AD :

$$M_A = \frac{2EI_c}{L_c}\left(2\theta_A + \theta_D - \frac{3\Delta_2}{L_c}\right) \tag{8.5}$$

and

$$M_{DA} = \frac{2EI_c}{L_c}\left(\theta_A + 2\theta_D - \frac{3\Delta_2}{L_c}\right) \tag{8.6}$$

Consider the uncracked span DC :

$$M_{DC} = \frac{2EI_{uc}}{L_{uc}}\left(2\theta_D + \theta_C - \frac{3\Delta_1}{L_{uc}}\right) \tag{8.7}$$

and

$$M_{CD} = \frac{2EI_{uc}}{L_{uc}}\left(\theta_D + 2\theta_C - \frac{3\Delta_1}{L_{uc}}\right) \tag{8.8}$$

From joint equilibrium :

$M_{DA} + M_{DC} = 0$

$M_A =$ applied moment

$\theta_c = 0$

Sway equations :

Since the beam is loaded with constant moment M, the beam shear $= 0$.

$M_A + M_{DA} = 0$

$M_{DC} + M_{CD} = 0$

We wish to eliminate θ_D, Δ_1 and Δ_2, to obtain an equivalent expression, $\frac{M_A}{\theta_A}$, which would represent the rotational stiffness of the non-uniform beam.

To simplify the algebra, the following variable substitutions were adopted :

Let $Y = \frac{2EI_c}{L_c}$ and

Let $Z = \frac{2EI_{uc}}{L_{uc}}$.

Re-writing equations 8.5 - 8.8 and incorporating $\theta_c = 0$:

$$M_A = 2Y\theta_A + Y\theta_D - \frac{3Y\Delta_2}{L_c} \tag{8.9}$$

$$M_{DA} = Y\theta_A + 2Y\theta_D - \frac{3Y\Delta_2}{L_c} \tag{8.10}$$

$$M_{DC} = 2Z\theta_D - \frac{3Z\Delta_1}{L_{uc}} \tag{8.11}$$

$$M_{CD} = Z\theta_D - \frac{3Z\Delta_1}{L_{uc}} \tag{8.12}$$

Using $M_A + M_{DA} = 0$ and simplifying

$$3Y\theta_A + 3Y\theta_D - \frac{6Y\Delta_2}{L_c} = 0 \tag{8.13}$$

Using $M_{DC} + M_{CD} = 0$ and simplifying

$$3Z\theta_D - \frac{6Z\Delta_1}{L_{uc}} = 0 \tag{8.14}$$

Using $M_{DA} + M_{DC} = 0$ and simplifying

$$Y\theta_A + \theta_D\left(2Y + 2Z\right) - \frac{3Y\Delta_2}{L_c} - \frac{3Z\Delta_1}{L_{uc}} = 0 \tag{8.15}$$

Eliminating $\frac{\Delta_2}{L_c}$ from equation 8.15 by using equation 8.13

$$-Y\theta_A + \theta_D\left(Y + 4Z\right) - \frac{6Z\Delta_1}{L_{uc}} = 0 \tag{8.16}$$

Eliminating $\frac{\Delta_1}{L_{uc}}$ from equations 8.16 by using equation 8.14

$$-Y\theta_A + \theta_D\left(Y + Z\right) = 0 \tag{8.17}$$

Re-arranging equation 8.17 to obtain θ_D in terms of θ_A

$$\theta_D = \frac{Y\theta_A}{(Y + Z)} \tag{8.18}$$

Substituting equation 8.18 into equation 8.13 to obtain $\frac{-3Y\Delta_2}{L_c}$ in terms of θ_A

$$\frac{-3Y\Delta_2}{L_c} = \frac{-\theta_A}{2}\left(3Y + \frac{3Y^2}{(Y + Z)}\right) \tag{8.19}$$

Substituting for $\frac{-3Y\Delta_2}{L_c}$ in equation 8.9, dividing through by θ_A and simplifying, gives

$$\frac{M_A}{\theta_A} = \frac{Y}{2} - \frac{Y^2}{2(Y+Z)} \tag{8.20}$$

Re-introducing the actual variables for Y and Z and simplifying

$$\frac{M_A}{\theta_A} = \frac{EI_c}{L_c} - \frac{\left(\frac{2EI_c}{L_c}\right)^2}{4E\left(\frac{I_c}{L_c} + \frac{I_{uc}}{L_{uc}}\right)} \tag{8.21}$$

By equating equations 8.21 and 8.4, an equivalent second moment of area representative of the non-uniform situation may be established.

$$I_b = \frac{S_b}{2}\left(\frac{I_c}{L_c} - \frac{\left(\frac{I_c}{L_c}\right)^2}{\left(\frac{I_c}{L_c} + \frac{I_{uc}}{L_{uc}}\right)}\right) \tag{8.22}$$

A comparison with the author's experimental programme was undertaken to assess the influence of incorporating the equivalent second moment of area derived above, as a basis to determine the classification by rotational stiffness of a composite connection.

The spans chosen for the comparison were based on limiting span to depth ratios for continuous composite beams. These have been published elsewhere[112] and were based on limiting values which should avoid serviceability controlling the design. For an end span of a continuous composite beam, this ratio ranges between 22 and 25, whereas for an internal span the ratio is increased to between 25 and 30.

It can be seen from Table 8.2, that the smaller the beam span considered, the stiffer the rigid boundary becomes. Consequently, a span to depth ratio range applicable to an end span was adopted to determine suitable spans for the study. Approaching the comparison in this manner would therefore increase the possibility of the connection falling outside the rigid classification.

The length over which the beam was assumed to be cracked was expressed as

a percentage of the complete span of the beam and varied between 5 and 20%. This range was set to bound the true cracked lengths of the composite beams measured during the author's experimental programme.

The numerical results are shown in Table 8.2, together with the uniform uncracked and cracked alternatives, to aid the comparison.

		457x152x52UB			533x210x82UB		
		12m	13m	14m	15m	16m	
		Stiffness for Rigid boundary classification (kNm/mrad)					
Uncracked		**77**	**73**	**69**	**124**	**118**	**113**
Non-uniform beam proportion cracked	5%	**70**	**66**	**62**	**113**	**107**	**102**
	10%	**64**	**60**	**56**	**104**	**99**	**94**
	15%	**59**	**55**	**51**	**97**	**91**	**86**
	20%	**55**	**51**	**48**	**90**	**85**	**80**
Cracked		**38**	**35**	**33**	**64**	**59**	**56**

Table 8.2: Composite beams flexural stiffness applicable to support regions

Discussion of the results

As expected, the greater the proportion of the beam that is assumed to be cracked, the less severe the rigid classification boundary becomes. This is further exemplified by comparison with the moment-rotation characteristics obtained from the experimental programme. Figure 8.7 shows the comparison for Tests 2,3 and 4, since they all incorporated 457 serial size beams, whereas the final test, Test 5, adopted a 533 serial size beam and therefore the comparison is shown independently in Figure 8.8.

For the flush end plate connection configuration adopted for the 457 serial size beams, it can be seen from Figure 8.7 that the corresponding classification would be rigid. Furthermore, the classification would be independent of the cracked state or otherwise assumed for the beam. However, the rotational classification for the 533 serial size beam, shown in Figure 8.8, can not be so clearly defined by direct reference to the initial loading line of the moment-rotation characteristic.

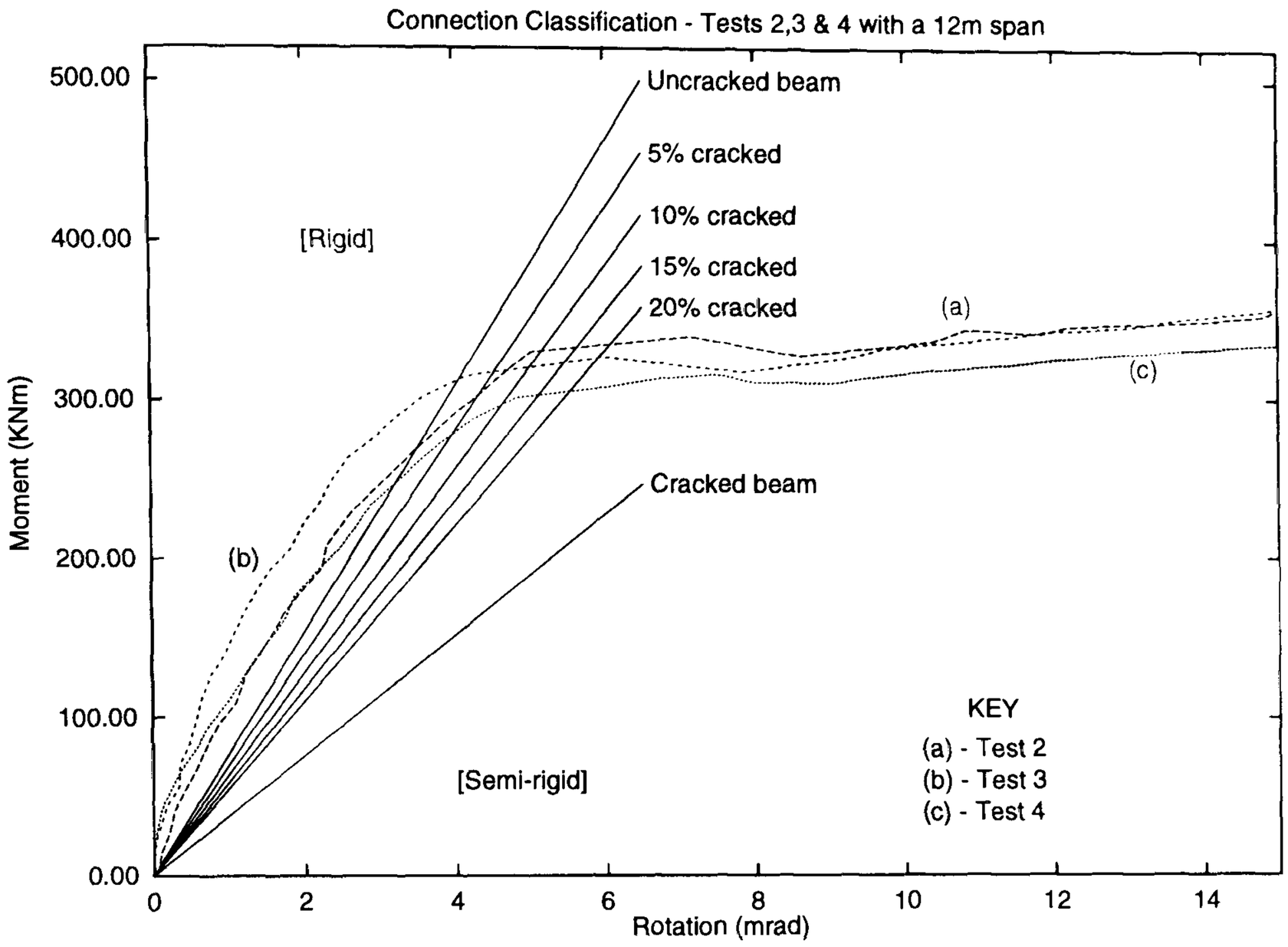

Figure 8.7: Connection classification - Tests 2,3 and 4

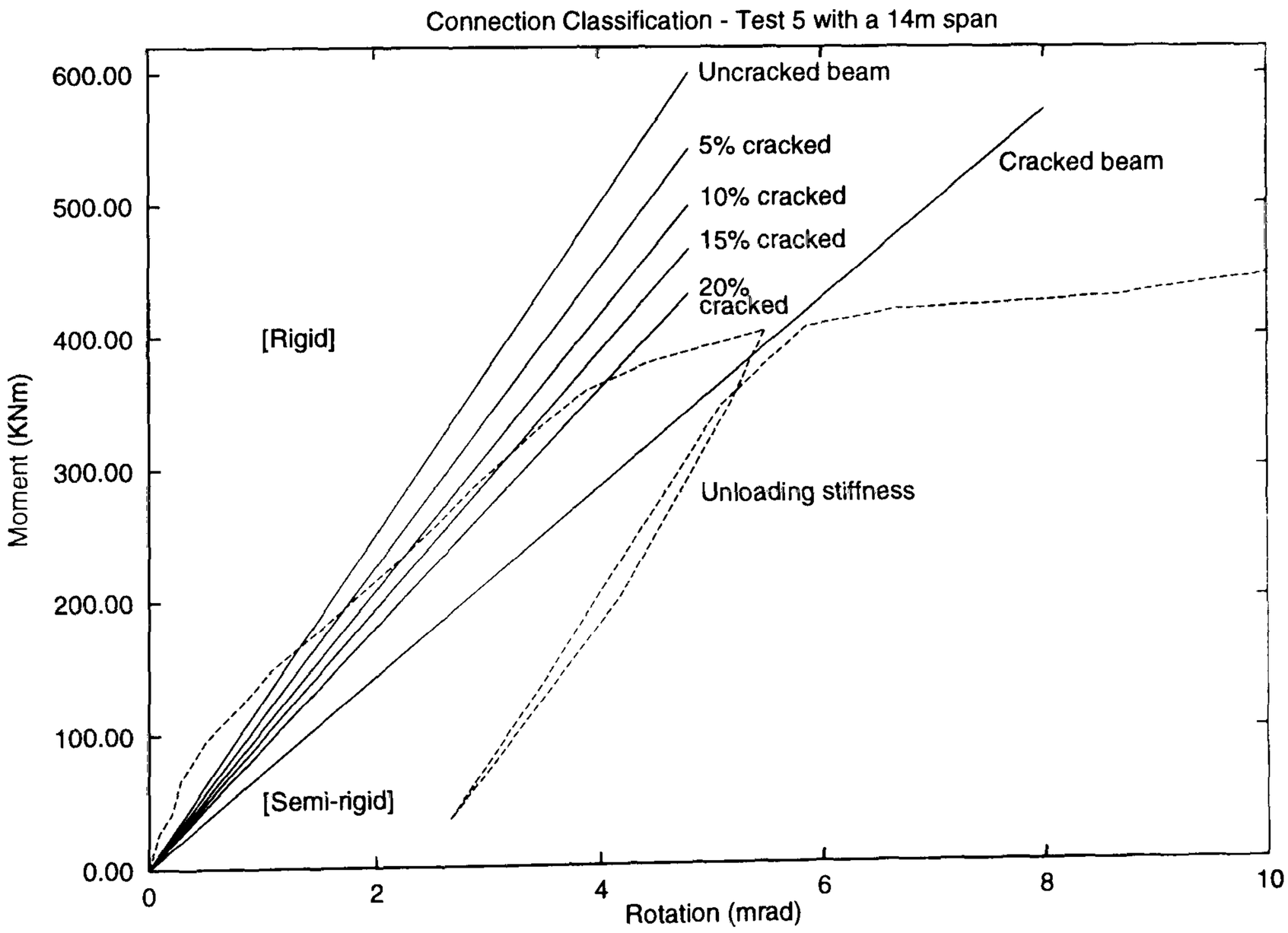

Figure 8.8: Connection classification - Test 5

It has been established in Chapter 2, that for non-composite steel connections. the problem of representing the corresponding initial stiffness has been resolved by assuming that an acceptable parallel could be drawn with its unloading stiffness. Moreover, from Chapter 7 it was concluded that this parallel would also be acceptable for estimating the initial stiffness of composite connections, thereby avoiding the difficulties associated with the variation in stiffness shown by the initial loading line of the moment-rotation characteristic. To this end, the unloading stiffness determined experimentally during Test 5 has been additionally illustrated in Figure 8.8.

If the equivalent initial stiffness is now positioned such that it passes through the origin of the moment-rotation characteristic, it could be shown that the classification would again be rigid, and independent of the cracked state assumed for the beam.

It therefore follows that the connection configurations adopted for the author's experimental programme may be regarded as rigid and consequently acceptable for general use in continuous composite beams designed in accordance with Eurocode 4.

The question still arises however, as to which would be the appropriate beam stiffness to apply for this classification procedure? Clearly as far as the author's experimental programme is concerned it is irrelevant, since the rigid classification is not influenced by the extent of cracking assumed for the beam. The aim of the classification procedure in the revised Annex J of Eurocode 3 is to avoid significant loss of restraint given by a beam to a column because of semi-rigid action of the connections[113]. It is therefore appropriate to adopt the uncracked stiffness of the composite beam when calculating its corresponding second moment of area. This stems from the consideration of the column at failure, when second order effects generate an opposing bending moment at the beam level[114]. This would have the effect of inducing sagging bending at the connections. A further argument in favour of the uncracked approach concerns the value of the

connection stiffness to be classified. Following the revised Annex J of Eurocode 3, which is concerned with the connection's initial value, it is clear that under these circumstances the beam would be operating in its initial state. Consequently, the uncracked properties would be applicable.

It is apparent therefore that if the classification system adopted in the revised Annex J of Eurocode 3 is also used for composite joints, it will no longer be possible to employ the beam's cracked stiffness. Although the resulting classification limit is therefore severe, it has already been shown by the author's tests that it is still possible to provide examples of rigid behaviour. This is despite the use of relatively thin flush end plates for the steelwork part of the connection, and only one row of tension bolts. Thus with this form of steelwork connection, it will not prove difficult to ensure rigid behaviour of the overall composite connection.

8.3 Ductility - how can it be assured ?

Ductility in continuous composite construction is needed when adopting plastic methods of structural analysis. This is the result of assuming that the frame is capable of allowing the formation of sufficient plastic hinges to form a collapse mechanism. Consequently, the positions of these hinges are of importance, since they must possess the behavioural characteristics consistent with the method of global analysis employed for the frame.

At internal supports, hinges may form either in the beam or in the connection depending upon which is weaker. Following the formation of the hinge, the redistribution of bending moments from the support region to mid span must be able to proceed without this process being brought to an end by premature local failure in the vicinity of the support.

8.3.1 Understanding connection ductility

The development of composite action at the connections involves the provision of high tensile steel bars running continuously past the internal column. This reinforcement is additional to the standard mesh reinforcement, which is usually placed in the slab to resist shrinkage and to improve fire resistance. As part of the design process therefore, it is incumbent upon the designer to ensure that the connections located in hogging moment regions of plastically designed continuous composite beams are capable of achieving adequate ductility.

From a design point of view, there are two avenues that need satisfactory investigation before a designer can be confident that the connections will behave in accordance with the design assumptions. Firstly, what connection rotation would theoretically be required to produce the collapse mechanism? Secondly, what rotation would be produced by the full scale connection when it has been incorporated within the structural frame as a whole? Clearly, if the answer to the second question is greater than the first, then plastic analysis techniques would

be valid.

With these objectives in mind, the first question has been investigated by several researchers[9, 111, 85], who have undertaken theoretical studies, based on computer simulations, to establish the rotation required by a connection to fulfill the requirements implied by plastic methods of design. With partial strength connections, the requirements depend partly on the ratio of the connection moment of resistance to the midspan moment of resistance of the composite beam. Clearly, the lower the ratio becomes, the higher the ductility demand required from the connections.

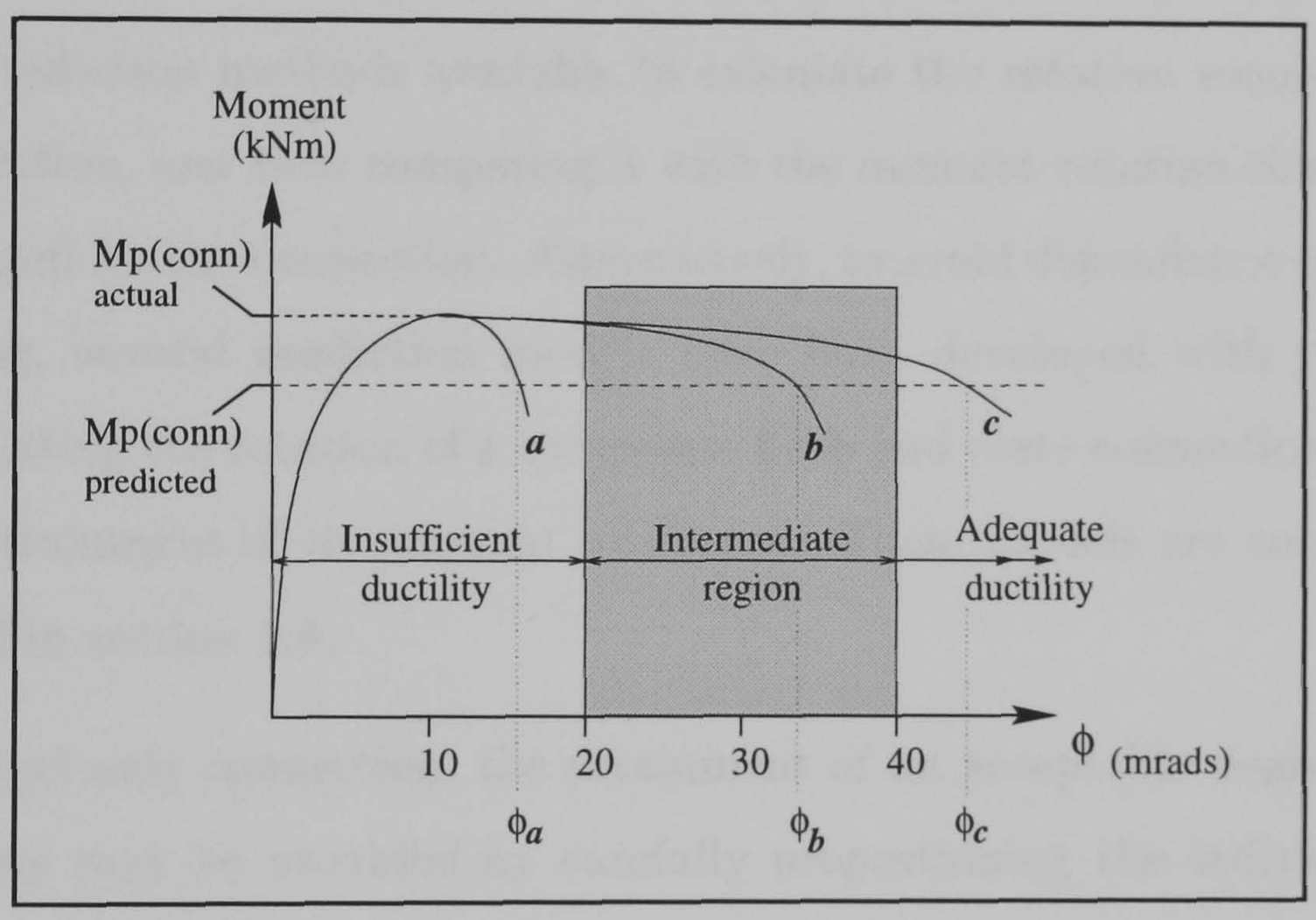

Figure 8.9: Ductility demand required from composite connections

The results of the investigations indicate that a connection rotation of between 20 - 40mradians would be sufficient to cover even the most demanding situations encountered in practice. Figure 8.9 illustrates the above requirements diagrammatically, from which the following can be concluded:-

1. If the composite connection exhibited characteristics similar to '*a*' in the figure, then insufficient ductility would be available, and consequently this type of connection would be incompatible with requirements for plastic analysis.

2. In contrast, if the composite connection exhibited characteristics similar to '*c*', then the connection would be compatible with the assumptions adopted for plastic analysis, since the characteristic demonstrates that ductility would be available in abundance.

3. However, there are intermediate cases whereby the designer has to make an informed decision as to whether or not the connection detail would be acceptable. Such cases are within the range $(20 < \phi_b < 40)$mradians and are exemplified by a composite connection that exhibits a characteristic similar to '*b*'. The informed decision may be assisted by utilising one of the prediction methods available to calculate the rotation required by the connection, and then comparing it with the moment-rotation characteristic obtained for the connection. Alternatively, to avoid dependence of full scale testing, several prediction models have been developed with the aim of calculating the rotation of a composite flush end plate connection following the attainment of its moment resistance. These models are considered in detail in section 8.4.

For a steel-only connection, the attainment of an acceptable degree of rotation capacity may be provided by carefully proportioning the individual components that make up the connection, to ensure that a Mode 1 type of failure is achieved[18]. In doing this though, the ductility is achieved at the expense of the connection's moment of resistance. The criteria for Mode 1 are deemed to be satisfied if the failure of the connection is only associated with deformation within the end plate and/or the column flange. Alternatively, the plastic hinge can be forced to form in one of the adjacent members by providing the so-called '120% connection'. For this type of connection, the designer should seek to achieve a moment of resistance at least 1.2 times greater than that of the connected members. Under these circumstances, provided that the connected members are classified as 'Class 1', in accordance with the provisions specified in Eurocode 3[17], then sufficient rotation capacity is assured. However, in com-

posite construction, the above provisions for achieving ductility require further consideration, since the reinforcement becomes an integral part of the connection's ability to resist the applied bending moments. The 120% rule has been assumed by Eurocode 4[60] to remain valid for composite connections, provided again that the adjacent members where the hinges are assumed to form are classified as 'Class 1'. For composite connections, the classification must be undertaken in accordance with Eurocode 4[60]. The 120% connection in this instance is required to attain a minimum moment of resistance 20% greater than the moment resistance of the connected composite beam with respect to negative bending. If, however, the 120% connections are not provided, then the burden of the ductility requirement would be dependent on the reinforcement contained within the concrete slab. Tests have shown however, that relying on the reinforcement alone to provide the necessary connection ductility can lead to unacceptable connection performance[87]. For continuous composite beams, Eurocode 4 assumes that adequate ductility will be ensured if reinforcement of '*high ductility steel*' is provided. For composite connections consideration must therefore be directed towards establishing whether or not there is a definable relationship between the material properties of the reinforcement and the connection performance.

8.3.2 Properties of the reinforcement

A pilot study was undertaken to ascertain the material properties applicable to typical diameters of reinforcing bars in isolation from a composite arrangement. The study took the form of establishing the stress-strain characteristics[97] for a total of 42 specimens of varying diameters. The results shown in Figure 8.10(a) refer to the average material properties obtained from the study and conform to the notation illustrated in Figure 8.10(b)[115].

It is customary in the United Kingdom to express the ductility of a steel bar as the percentage elongation at fracture, with the calculation being based on a standardised gauge length equal to 5 times the nominal bar diameter. The

a)

Bar diameter (mm)		Yield stress f_y N/mm²	Ultimate stress f_t	f_t / f_y	Ulitmate strain ε_u (%)	% elongation at fracture
6 (A142 mesh)		**602**	**633**	**1.05**	**1.30**	**12**
Structural reinforcement	8	**503**	**686**	**1.36**	**9.90**	**24**
	10	**537**	**627**	**1.16**	**9.70**	**24**
	12	**512**	**604**	**1.17**	**10.90**	**22**
	16	**504**	**611**	**1.21**	**12.80**	**26**
	20	**538**	**669**	**1.24**	**N/A**	**25**

Note :
The yield stress measured based on a proof strain equal to 0.2%

b)

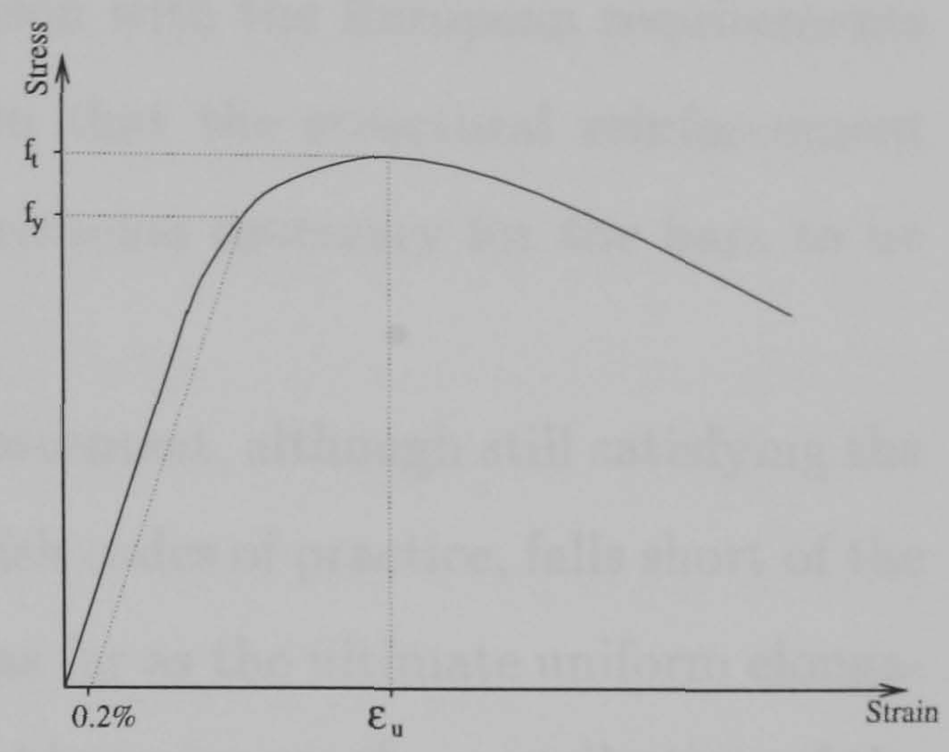

Figure 8.10: Material properties for commonly available reinforcing bars

minimum requirement for high tensile steels having a characteristic yield strength of 460N/mm^2 is specified as 12%[116]. This limit is set such that a satisfactory compromise between strength and ductility may be achieved economically from the manufacturing process[117].

An alternative approach has been adopted by Eurocode 4[60], which makes use of the design guidance applicable to the ductility of reinforcing bars specified within the provisions of Eurocode 2[89]. The European approach is to identify two types of reinforcing steel, namely *'Normal Ductile Steel'* and *'High Ductile Steel'*. These types are characterised by means of the ultimate uniform elongation ϵ_u and the ratio of the ultimate strength and the yielding stress f_t/f_y (see Figures 8.10(b) and Table8.3).

Properties	Normal Ductility Steel	High Ductility Steel
ε_u	$\geqslant$ **2.50%**	$\geqslant$ **5.00%**
f_t / f_y	$\geqslant$ **1.05%**	$\geqslant$ **1.08%**

Table 8.3: Steel property definitions specified in Eurocode 2

From Figure 8.10(a), it can be seen that all the structural reinforcement tested conformed with comparative ease to the minimum requirements specified by the British codes of practice and consequently could be considered as suitable for

general use in plastically designed continuous composite beams. This conclusion is further substantiated following a comparison with the European requirements shown in Table 8.3. It can be clearly seen that the structural reinforcement does in fact conform to the property requirements necessary for the bars to be identified as possessing high ductility.

In contrast to the rebars, the mesh reinforcement, although still satisfying the minimum requirements specified by the British codes of practice, falls short of the requirements for the 'Normal Ductile Steel' as far as the ultimate uniform elongation is concerned. Consequently, it is advisable to ignore the contribution of the mesh reinforcement to the overall moment resistance of the connection, thereby rendering its ductility classification superfluous. This conclusion may be justified on the grounds that since the mesh fractures at a very low rotation, the full tensile resistance of the main longitudinal reinforcement would not have been fully mobilised. This can be seen following examination of the moment-rotation characteristics applicable to the author's experimental programme (see Chapter 7). It has been established within this chapter, that although a slight reduction in the moment being resisted at the connection occurred when the mesh fractured, the connection recovered easily to produce an eventual failure moment in excess of that achieved prior to the mesh fracturing. Furthermore, this approach to the treatment of the mesh reinforcement has been generally advocated, since it has been included within a recent design guide covering composite end plate connections[118].

It has been suggested[115] that for materials manufactured to present British regulations, only reinforcing bars of diameter in excess of 16mm will comply with the high ductility requirements specified by Eurocode 2. However, from the pilot study outlined above, the results tend to indicate that the ductility of the structural reinforcement cannot be directly related to the consideration of the bar diameter only.

8.3.3 Performance of the connections

Although it has been established from the previous section that the commonly available structural steel bars can be classified as being of high ductility, the translation into the connection performance is somewhat variable. The mere fact that high ductility reinforcing steels are provided is insufficient to ensure that ductility requirements of the connection as a whole would be automatically satisfied[87]. The structural demand levelled at the reinforcement must be considered along side the deformation characteristics of the steelwork connection.

End plate joints, with the tensile action taking place within the steelwork connection, result in significant local deformation of the column flange and/or the end plate. This causes a wide crack to form in the slab at the face of the column, which leads to the fracture of the brittle mesh, followed by an even wider crack and therefore high local deformation in the reinforcing bars.

In composite connections, fracture of the reinforcement can be avoided if local buckling of the beam's lower steel flange provides the necessary ductility. However, although some loss of peak moment resistance occurs, this would not be as substantial as that due to rebar fracture, and it occurs in a gradual manner[87]. Local buckling in this manner can be achieved by providing sufficient reinforcing bars, such that the moment resistance of the connection is high enough to produce the benign local failure in the compression flange of the connected beams in the vicinity of the joints[9, 85]. In doing this, the performance of the connection could be guaranteed, since the failure is no longer associated with the connection itself, but with a ductile failure mode within the attached beam member.

Problems which need to be addressed before compliant design rules can be formulated to guarantee connection performance

There are many problems which need to be considered and overcome, prior to acceptable design rules being produced. The main points which the author considers important are summarised in the subsequent paragraphs.

How many reinforcing bars would be required to induce the ductile mode of failure advocated above?

The susceptibility of the lower flange to compression buckling must be a function of the total tensile force induced from the reinforcement and the bolts acting together. This relationship is further complicated by the influence of compression deformation within the beam's web, which has been reported[119] to occur simultaneously with the flange deformation. Existing design codes[17, 60, 12] give simple rules based only on the classification of the section dimensions and material properties; however, these have been calibrated to avoid local buckling, rather than to guarantee it.

How will the shear connection be influenced by providing a reinforcing detail that complies with the initial question?

If the connection design requires the provision of an increasing number of reinforcing bars, as inferred above, then the shear connection must be capable of transmitting the higher tensile force generated at the level of the reinforcement into the beam member. For a solid slab, the extra shear connectors that may be necessary for compliance could be positioned evenly along the length of the hogging moment region of the beam. However, if the beam incorporates profiled steel decking, which would be generally the case in the United Kingdom, difficulties arise if the decking is orientated to span transversely across the beam members. Under these circumstances both the number and position of the shear connectors would be limited to the positions where the troughs cross the beam. Therefore, it may not be possible to provide a full shear connection to transmit the required tensile force from the reinforcement. One possible solution to this situation would be to increase the tensile contribution of the bolts. This may be achieved by providing an extended end plate connection, or by increasing the number of bolt rows resisting tension within the depth of a flush end plate connection. In doing this, the tensile demand levelled at the reinforcement would be reduced and hence a lower demand would be placed on the shear connection.

thus enabling it to be designed with full interaction. whilst maintaining a satisfactory ductile performance. The first of these solutions has been investigated during Najafi's programme (test S8E[87]) with encouraging results. The failure mode was reported to be local buckling of the bottom beam flange, with a corresponding ultimate connection rotation of 40mradians. The alternative solution of including a greater number of bolts within the depth of a flush end plate connections has also proved generally successful; although for a given number of rebars, a slightly poorer ductile performance has been generally reported[81, 120] (see Chapter 5, Tables 5.1 to 5.3).

Another factor which concerns the shear connection is the acceptability of allowing slip to develop at the beam/slab interface. It is generally acknowledged that should it occur, then provided the connection's structural integrity is not lost by the failure of the shear connection, then a small amount of slip may be desirable in a ductile composite connection. In addition, the presence of slip at the interface may also have the added advantage that it could provide a means of safe-guarding the connection's performance against other factors which inherently distroy ductility, such as over-strength factors which are subsequently discussed below.

Is there a need to consider over-strength factors?

The over-strength factors which may be of concern include such effects as: (i) variations in the stress level required to initiate the onset of yielding within the cross-section of the attached beam, and (ii) strain hardening as compression deformation takes place. Both of these occurrences, which are traditionally neglected in calculations for resistance, have to be considered when ductility of the connection is being sought. The combined effect of these factors will tend to increase the compressive resistance of the lower flange which may for the worst scenario, prevent the local buckles forming prior to the reinforcement fracturing. This consideration stems from the fact that for almost identical tests, the ductility of the connections may vary considerably. Ultimate rotations of 14.0mradi-

ans and 47.7mradians were achieved for Najafi's test S8FD[87] and the author's Test 3, respectively, despite these tests being almost identical. This large difference may be explained in part by the difference in the diameter of the reinforcing bars used within the slabs. Najafi's test incorporated 12mm diameter bars, whereas the author's had 16mm diameter bars. According to United Kingdom codes of practice[97], the elongation at fracture is calculated based on a standardised gauge length equal to five times the bar's nominal diameter. Consequently, it can be shown that the bars adopted in the Najafi's test, would only be able to sustain half of the elongation available to the bars adopted for the authors test. This would translate into a poorer performance in terms of connection ductility which was evident from the test results. However, this explanation would be insufficient as the sole reason for the considerable difference that was obtained. Consequently, it is thought that the remaining difference between the ductility of the two independent tests could be attributed to over-strength factors being present in sufficient magnitude in Najafi's test, to influence the formation of the local buckles. This can be further substantiated by comparison between the respective yield stresses applicable to the beam flanges for these two tests. A yield stress of 293 N/mm^2 was determined for the author's test 3, whereas a yield stress equal to 310 N/mm^2 was reported for Najafi's test. Consequently, the beams used within the author's experimental programme were more susceptible to local buckling, than in Najafi's test. Furthermore, Najafi also reported[9] that for his particular test, no local compression deformation occurred in the lower flanges of the connected beams prior to the fracture of the reinforcement. This is in distinct contrast to the observations made by the author during the execution of test 3.

In the absence of design rules which would guarantee local buckling, research has being undertaken to produce prediction methods which enable the ductility of composite end plate connections to be calculated when failure occurs by rebar fracture. Proposals based on the rotation at maximum moment are already

available[120], but the prediction of the total rotation capacity at the design resistance has until now not been considered.

8.4 Suitability of existing prediction methods

If the ductility of a composite connection cannot be guaranteed, it becomes incumbent on the designer to assess the suitability of the connection's performance. This may be achieved by utilising a suitable prediction model which reflects the connection configuration under consideration.

8.4.1 SCI model

Ductility achieved through tension zone deformation

This model was based on the very simple concept, namely, that the rotation of the connection may be determined by considering the elongation of the reinforcement alone [111] (see Figure 8.11).

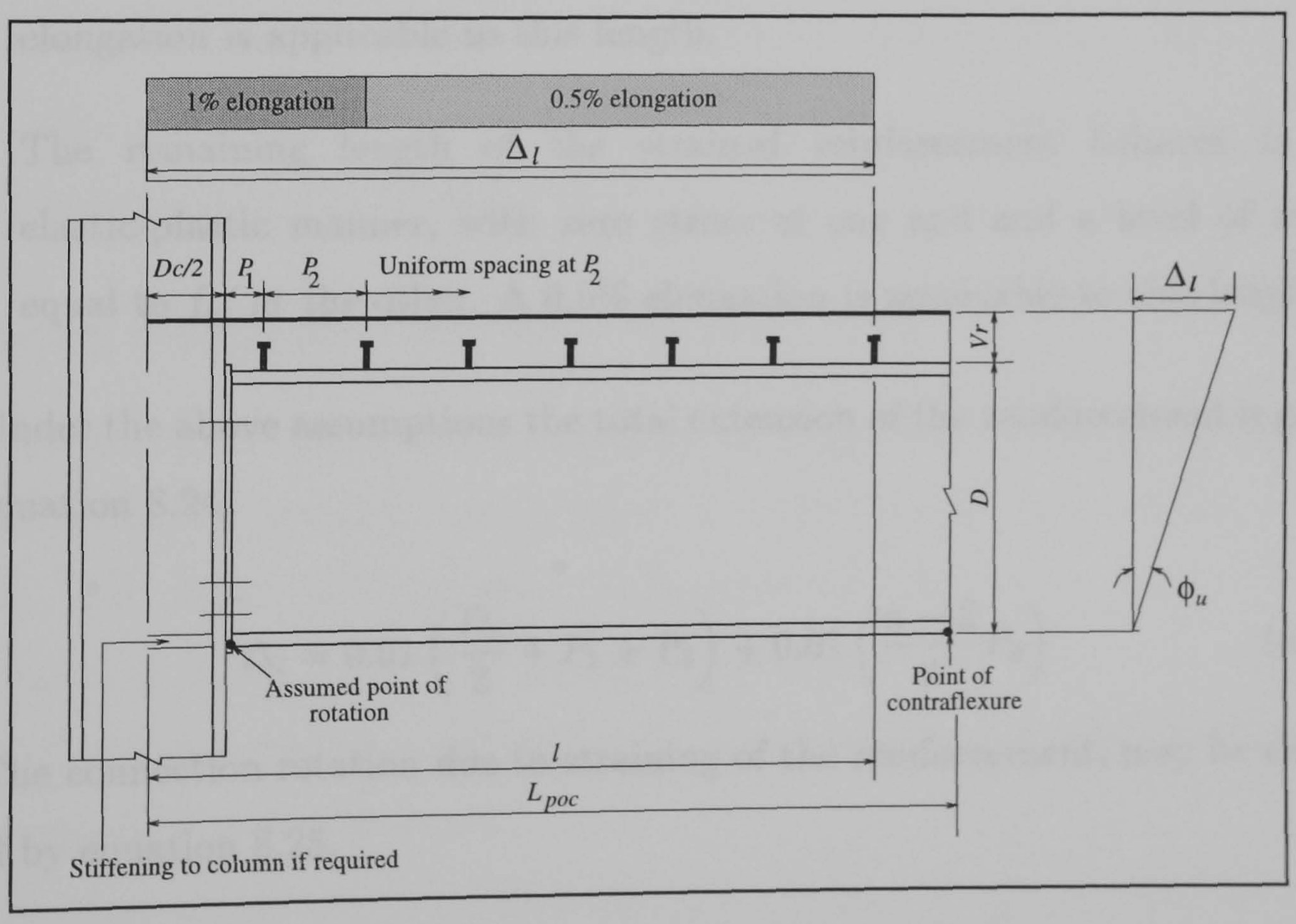

Figure 8.11: Connection parameters assumed by the SCI model

The model assumes the following :

1. The length of reinforcement effectively contributing to the connection's rotation is equal to the distance from the column centre line to the shear stud located closest to the adjacent point of contraflexure (see equation 8.23).

$$l = \frac{D_c}{2} + P_1 + (n-1)\,P_2 \tag{8.23}$$

where :

D_c - Depth of the column

P_1 - Distance to the first shear stud

P_2 - Pitch of the shear studs

n - The number of shear studs provided in the hogging moment region.

2. The length of reinforcement between the column centre line and the second shear stud along the beam is fully strained and deforms plastically. A 1% elongation is applicable to this length.

3. The remaining length of the strained reinforcement behaves in an elastic-plastic manner, with zero stress at one end and a level of stress equal to f_{yr} at the other. A 0.5% elongation is applicable to this length.

Under the above assumptions the total extension of the reinforcement is given by equation 8.24.

$$\Delta_l = 0.01\left(\frac{D_c}{2} + P_1 + P_2\right) + 0.01\left(\frac{n-2}{2}P_2\right) \tag{8.24}$$

The connection rotation due to straining of the reinforcement, may be calculated by equation 8.25.

$$\phi_u = \frac{\Delta_l}{D + V_r} \quad \text{for} \quad f_{yr}\,A_s < f_{ybf}\,B_{bf}\,t_{bf} \tag{8.25}$$

where :

D - Depth of the beam

V_r - Distance from top of beam to the reinforcement.

In the condition for equation 8.25 to be applicable, the tensile resistance of the steelwork connection is neglected.

This model is consistent with an increase in reinforcement leading to a corresponding increase in connection ductility, as observed by Najafi[9]. This results from an increase in reinforcement leading to transfer of the longitudinal force via an increased number of shear studs, and hence a longer length of strained reinforcement becomes available in the calculation. However, it was recognised by the proposer of the method, that the real behaviour of a composite connection differs from that assumed for the model, since the majority of the longitudinal force is resisted by the first two or three studs along the beam. Under these circumstances, the resulting plastic deformation induced into these studs would contribute to the overall ductility of the connection. It was argued therefore that although this would have the effect of reducing the strained length of the reinforcement that would be suitable for the calculation model, the method proposed was a valid simplification on the grounds that any plastic deformation within the studs themselves had been neglected.

Including compression zone deformation

To allow for the beneficial effects arising from compression deformation, the connection's centre of rotation was modified. The modification took the form of reducing the depth of the beam component of the lever arm by 30% (see equation 8.26). The deformation within the tension zone is assumed to be unaltered; therefore the calculation to determine the elongation of the reinforcement Δ_l remains the same.

$$\phi_u = \frac{\Delta_l}{0.7D + V_r} \quad \text{for} \quad f_{yr} A_s \geq f_{ybf} B_{bf} t_{bf} \tag{8.26}$$

8.4.2 Nottingham model

An alternative model to that adopted by SCI, was developed at the University of Nottingham[120] (see Figure 8.12). The objective was to create an acceptably accurate model, with the emphasis being directed towards a standardised approach between the ductility calculation and the corresponding moment resistance calculation. The effect of adopting a standardised approach results in the prediction of the connection rotation being calculated at the maximum moment, rather than the design resistance.

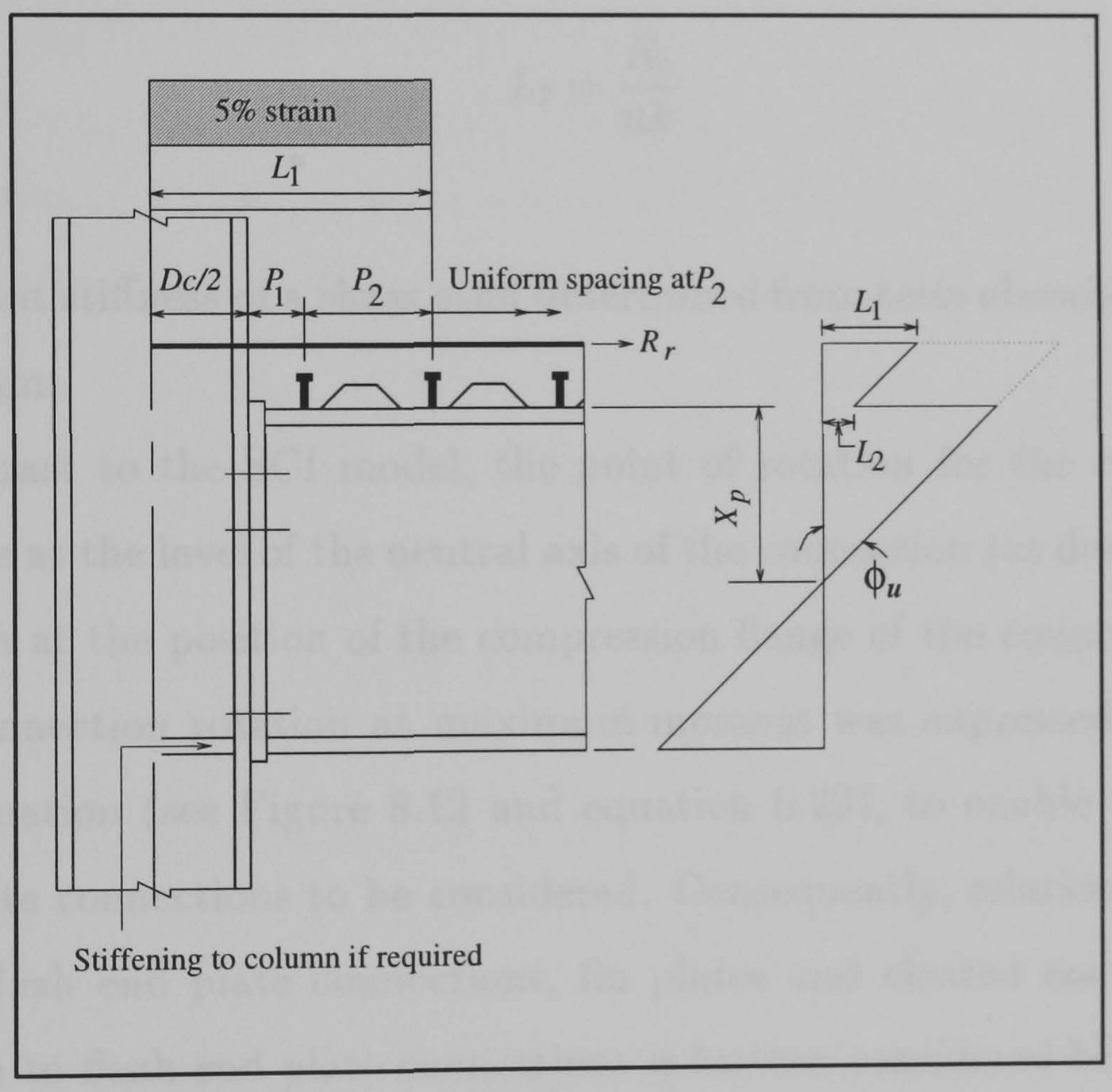

Figure 8.12: Connection parameters assumed by the Nottingham model

A length of reinforcement L_1 was again considered, although on this occasion a constant level of strain was assumed over a much shorter length (see equation 8.27).

$$L_1 = \epsilon\left(P_1 + P_2 + \frac{D_c}{2}\right) \tag{8.27}$$

where :

ϵ - Level of strain taken as 5%.

As a consequence of adopting a shorter length of reinforcement, albeit strained to a much higher level, the influence on the connection ductility as a result of the shear stud deformation was incorporated.

The slip 'L_2' of the beam end adjacent to the composite connection was expressed in terms of a ratio between the tensile force within the reinforcement R_r to the number of shear studs n (see equation 8.28).

$$L_2 = \frac{R_r}{nk} \tag{8.28}$$

where :

k - Secant stiffness of a shear stud determined from tests elsewhere[121], taken as 30kN/mm.

In contrast to the SCI model, the point of rotation for the connection was assumed be at the level of the neutral axis of the connection (as described below), rather than at the position of the compression flange of the connecting beams.

The connection rotation at maximum moment was expressed in terms of a general equation (see Figure 8.12 and equation 8.29), to enable different types of composite connections to be considered. Consequently, relationships were derived for flush end plate connections, fin plates and cleated connections. The application to flush end plate connections is further considered below.

$$\phi_u \approx tg\phi = \frac{L_1}{d_c + X_p} + \frac{L_2}{X_p} \tag{8.29}$$

where :

d_c - The effective depth of the concrete slab measured to the centre of the rebars

X_p - The depth of the plastic neutral axis below the upper beam flange.

Composite flush end plate connection

From the position of the neutral axis, it can be seen that compression deformation is assumed to occur and consequently is automatically included in the calculation procedure. This assumption was based on the observations made during the Nottingham test programme, where compression deformation was reported to have been substantial.

The depth of the neutral axis X_p, depends on the configuration of the connection, in particular the percentage reinforcement provided in the slab. To reflect this variability, the following four positions were considered. The equations presented are consistent with BSI codes of practice[12][122]; however similar equations in accordance with European codes of practice[17][60] are also available[120].

Case 1- Neutral axis in the concrete section : $F_s > F_b$

$$\phi_u \approx tg\phi = \frac{L_1}{X_p} \tag{8.30}$$

where :

F_s - Tensile force of concrete floor $= 0.87 f_{yr} A_s$, neglecting the contribution of the decking

F_b - Compressive resistance of the end of the beam $= f_{yb} A_b$

X_p - Depth of the concrete not in compression $= \frac{F_s - F_b}{0.45 b_c f_{cu}}$

b_c - Effective width of slab[122]

f_{cu} - Concrete compressive strength

f_{yb} - average yield stress applicable to the steel member

A_b - Beam section area.

Case 2- Neutral axis in the upper beam flange : $F_s < F_b$ and $F_b - F_s \leq f_{ybf} B_{bf} t_{bf}$

$$\phi_u \approx tg\phi = \frac{L_1}{d_c + X_p} + \frac{L_2}{X_p} \tag{8.31}$$

where :

X_p - Depth of the beam flange not in compression $= \frac{F_s - F_b}{f_{ybf} B_{bf}}$

Case 3- Neutral axis is in the beam web but not beyond the first row of bolts : $F_b - F_s > f_{ybf} B_{bf} t_{bf}$ and $F_b - F_s - f_{ybf} B_{bf} t_{bf} \leq f_{ybw} (S1 - t_{bf}) t_{bw}$

$$\phi_u \approx tg\phi = \frac{L_1}{d_c + t_{bf} + X_p} + \frac{L_2}{t_{bf} + X_p} \tag{8.32}$$

where :

S_1 - The depth from the upper flange of the beam to the centre of the first row of bolts

X_p - The depth of the beam web not in compression = $\frac{F_b - F_s - f_{ybf} B_{bf} t_{bf}}{t_{bw} f_{ybw}}$

t_{bw} - The thickness of the beam web

f_{ybw} - Yield stress applicable to the beams web.

Case 4- Neutral axis is below the first row of bolts : $X_p > S_1$

$$\phi_u \approx tg\phi = \frac{L_1}{d_c + S_1 + iP_b + \frac{2}{3}P_b} + \frac{L_2}{S_1 + iP_b + \frac{2}{3}P_b} \tag{8.33}$$

where :

P_b - The pitch of the bolts

i - Number of tension bolt rows which have yielded =

$$\frac{f_{ybf} B_{bf} t_{bf} - F_s + f_{ybw} t_{bw} \left(D - S_1 - t_{bf} + \frac{1}{3} P_b \right)}{2F_t + f_{ybw} t_{bw} P_b}$$

D - Depth of beam member

F_t - Tensile resistance of the bolts calculated in accordance with BS5950[12].

8.4.3 Prediction assessment and the need for further development

The ductility models described previously have been configured to predict the rotation of a composite flush end plate connection following the attainment of its moment resistance. Validation of these approaches has been undertaken elsewhere[120], by comparing the calculated predictions with the results obtained from full scale experimental investigations into the behaviour of such connections.

Unfortunately, these values remain unsubstantiated and therefore corresponding comparisons with the author's experimental programme have not been included. Subsequently, it was found that the Nottingham model produced the closest correlation with the available test results, since the SCI model produced unconservative predictions for all the connections that did not fail as a result of local buckling occurring within the compression regions of the attached beams.

However, it has been established from section 8.3.1 that for plastic analysis to be acceptable, the designer needs to be able to predict the ductility of the composite connection when it eventually fails. This point on the moment-rotation characteristic does not necessarily coincide with the attainment of the connection's maximum moment resistance (see Figure 8.9). Consequently, the connection may therefore be unfairly considered inappropriate for the task in hand, when in reality problems would not be encountered. To illustrate this point more clearly, the test programme undertaken by Anderson and Najafi will be used as a convenient example (see Chapter 5, Table 5.1).

By comparing the last two columns of Table 5.1, the extent to which the ductility is underestimated by only considering the rotation at maximum moment can be clearly demonstrated for the majority of test results. Furthermore, it is interesting to note that the corresponding rotation at maximum moment for several connections falls close to or below the minimum capacity of 20mradians (see Figure 8.9); below this a connection may be regarded as disqualified from being deemed suitable for inclusion within a plastically designed beam. This is in distinct contrast to the ductile performance that was obtained for the majority of experimental tests undertaken. In the author's opinion, this omission constitutes a practical drawback to the Nottingham model which would unnecessarily influence the eventual choice of the composite connection. In addition, a potentially more serious oversight can also be identified from this series of tests. It can be seen that a brittle failure mode existed in all the connections tested that produced an ultimate rotation of less than 40mradians. This mode of fail-

ure occurred as a result of the reinforcement fracturing, which leads to a sudden and significant reduction in the moment at the connection. For a connection to behave in a ductile manner, it is imperative that all the brittle modes of failure are eliminated until well beyond the theoretically required rotation capacity. However, neither of the two prediction models described above have the capability of predicting when this catastrophic failure would occur. Consequently, an alternative prediction method has been developed by the author, that attempts overcome these problems by predicting the full length of the plastic region of the connection's moment-rotation characteristic, based on failure of the connection being associated with the reinforcement fracturing.

8.5 Empirical ductility model for an end plate composite connection

The objective of the proposed ductility model is to predict the rotation capacity of a composite end plate connection, whose eventual failure mode is controlled by the elongation within the main longitudinal reinforcement. In order to achieve this objective, following assumptions are made:

1. The deformation within the steelwork components of the composite connection may be simplified to consideration of the column flange and the end plate only.

2. The deformations mentioned in 1 above could be calculated by adopting the principles of elastic bending theory. The contradiction in principles between this assumption and the need to calculate plastic deformations is resolved by calibrating the resultant elastic deflections to approximate the plastic deformations measured during the experimental programme.

3. The rotation of the connection would be about the upper most bolt row assumed in the connection design to resist the applied vertical shear. The

accompanying horizontal displacement of the end plate, which would occur at the level of the tension bolt row, would be a function of the column flange deformation.

Test reference	Depth to assumed point of rotation h (mm)	Ultimate connection rotation (rads)	δ_{cf} required (mm)	δ_{cf} measured (mm)
3	**260**	**0.0477**	**12.4**	**11.95**
4	**260**	**0.0355**	**9.2**	**8.85**
5	**328**	**0.0201**	**6.6**	**6.35**

Table 8.4: Verification of the assumptions regarding the connections ultimate rotation

The justification for this approach was made initially by observation as each test progressed. This was further substantiated following the connection failure, whereby the actual column flange deformation was measured prior to the conclusion of each test (see Table 8.4 and Figure 8.13). The measurements were taken on the outermost edges of the flange outstands and averaged for each connection. The measurements contained within Table 8.4 are applicable to the connection that caused the failure of the specimen. In all cases therefore, the quoted values refer to connection A. It can be therefore be shown that the measured values are all within 4% of the required values and consequently, the ultimate rotation of the connection may in essence be represented by equation 8.34.

$$\phi_{ul} = \frac{\delta_{cf}}{h} \tag{8.31}$$

where :

δ_{cf} - Column flange deformation

h - Depth below the tension bolt row to the assumed point of rotation.

4. The extension of the reinforcement as a result of the column flange deformation, is further influenced by the following :

   (a) Variations in its position relative to the centre line of the tension bolt row.

   (b) The depth of the beam, since this has the effect of changing the depth of the assumed point of rotation for the connection.

   (c) The compression deformation associated with the lower beam flanges.

5. The extension of the reinforcement as a result of the induced deformation within the column flange and end plate, may be based on linear extrapolation from the point of maximum deformation of the steelwork component up to the level of the reinforcement.

6. The failure of the connection would be as a result of the main longitudinal reinforcement fracturing within the concrete slab. Consequently, the failure criteria was reached when the extension in the reinforcement had attained its maximum value. This could be determined from remote material property tests[97], carried out to assess the ductility of the reinforcing bar in isolation from the concrete slab.

7. The influence of the shear connection between the steel beams and the concrete slab was neglected. This accords with the author's experimental programme, whereby the shear connection did not show any signs of slip as a result of plastic deformation.

8. The elongation of the bolts would be small enough not to significantly influence the strain within the reinforcement and consequently could be neglected.

8.5.1 Limitations

Owing to the complex nature of composite connections and the variety of possible configurations, a single ductility model that encompasses every possible situation would be very difficult to develop. The approach adopted by the author was therefore subject to the following limitations :

1. The prediction model may only be applied to major axis flush end plate composite connections.

2. The model was configured around the hypothesis that the failure mode for the composite connection would be as a result of the main longitudinal reinforcement fracturing. Consequently, failure by any other means must be prevented in order to validate the proposed technique.

3. The rotation of the connection was derived primarily from the deformation characteristics of the column flange, induced by the action of a single bolt row in tension. Consequently, multi-bolt rows acting in tension are excluded at present. It is the author's opinion that a similar expression to that described below could be derived to cover this omission. However, a clear understanding of how the ductility of this type of connection can be achieved, based on the observed deformation characteristics within the steel part of the connection, would be a clear pre-requisite to its development. Unfortunately, this particular question has not been addressed in sufficient detail by other researchers who have included multi-bolt row end plate composite connections as part of their experimental programmes.

8.5.2 Mathamatical derivation

The following derivation reintroduces the concept of enabling the ductility of a connection to be established based on limitations associated with the permissible elongations within the reinforcement. However, the proposed model moves

forward from current thinking because it takes into account deformations to key components of the steelwork connection, which have previously been ignored.

Elongation of the reinforcement

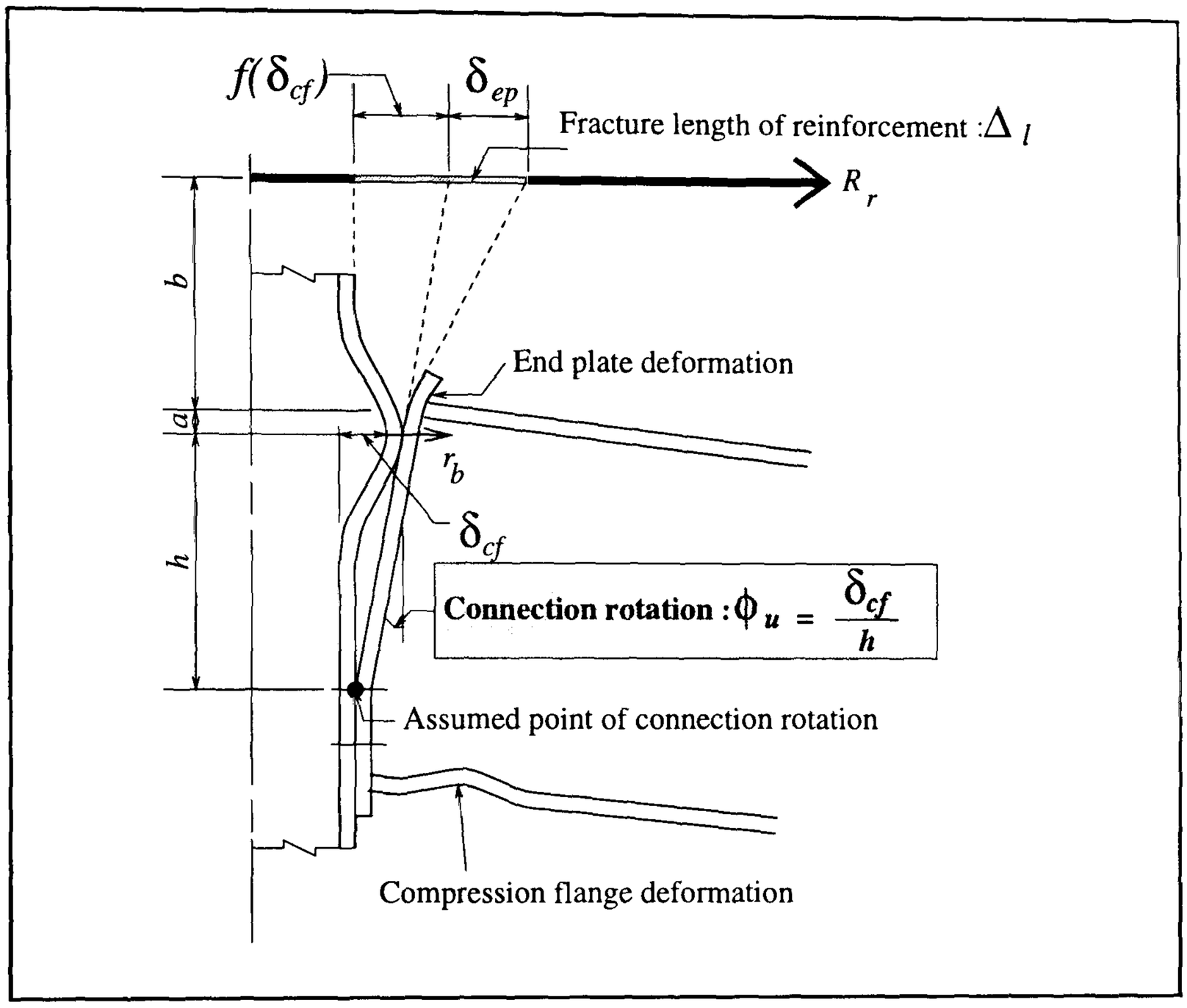

Figure 8.13: General arrangement of the proposed ductility model

The total elongation of the reinforcement may be represented by the summation of the respective elongations due to the deformations in the column flange and end plate (see Figure 8.13 and equation 8.35).

$$\Delta_l = f(\delta_{cf}) + \delta_{ep} \tag{8.35}$$

where :

$f(\delta_{cf})$ - Elongation due to the column flange deformation

$f()$ - Denotes a variable function which has been configured to allow for the influence of compression deformation associated with the lower beam flanges, and

to permit variations in the position of the reinforcement in relation to the beam depth to be evaluated.

δ_{ep} - Elongation due to the end plate deformation

Column flange deformation

The deformation within the column flange is idealised as a fixed ended beam of length L, with a central point load. The point load in this instance was assumed to be equal in magnitude to that which could be induced by a single bolt force r_b, acting through the column flange. Under these circumstances, the elastic central deflection may be calculated by utilising the standard case equation applicable to this situation (see equation 8.36).

$$\delta_{cf} = \frac{r_b L^3}{192 E I_{cf}} \tag{8.36}$$

where :

E - Young's modulus for steel

I_{cf} - Second moment of area applicable to a single column flange outstand (see equation 8.37).

$$I_{cf} = \frac{d\,(t_{cf})^3}{12} \tag{8.37}$$

where :

$d = \frac{B_{cf}}{2} - \frac{t_{cw}}{2} - r_k$

B_{cf} - Width of the column section

t_{cw} - Width of the column web

r_k - Root radius of the column.

In order to calibrate the elastic deflection with the corresponding plastic deflection, the length of the fixed ended beam was assumed to be equivalent to the length over which the deformed shape actually occurred. The subsequent measurements following the completion of each test established this length at

approximately 300mm. This value did not appear to vary significantly from test to test, nor did it appear to be influenced by the change in column section during the final test. Consequently it was assumed to be constant for the purposes of the model. Furthermore, since the restraining effect of the column web has not been included within the simple elastic model, the calculated performance will provide a more flexible response to the applied bolt force, than would otherwise be the case, as long as the components remain elastic.

Quantifying the relationship between the column flange deformation and the subsequent elongation of the reinforcement

The relationship between the column flange deformation induced at the position of the tension bolt row and the subsequent elongation of the reinforcement was assumed to be represented by a function comprising of two coefficients (see equation 8.38).

$$f(\delta_{cf}) = \frac{\beta \delta_{cf}}{\eta} \tag{8.38}$$

where :

η - Force ratio coefficient to allow for the influence of compression deformation associated with the lower beam flanges.

β - Empirical coefficient to allow for variations in the position of the reinforcement and the beam depth.

To enable these coefficients to be evaluated and correlated to the authors test results, the following combinations of η and β were considered.

Case 1 - When the distance between the tension bolt row and the centre of the reinforcement coincides with the distance between the tension bolt row and the point assumed for the connection rotation. Furthermore, the magnitude of the compressive force acting through the beams lower flange would not be sufficient to exceed its compressive resistance and therefore precludes the possibility of

local buckling forming.

This case is illustrated in figure 8.14(a). Under these circumstances, the elongation in the reinforcement was assumed to be a direct extrapolation of δ_{cf} up to the level of the reinforcement. Consequently, η and β were set to unity to enable the corresponding elongation to be calculated by equation 8.39.

$$\delta_r^i = f(\delta_{cf}) = \frac{(h + a + b)\,\delta_{cf}}{h} \tag{8.39}$$

where :

a - Vertical distance between the centre line of the top bolt row and the centre line of the top beam flange

b - Vertical distance between the centre line of the top beam flange and the centre line of the rebar.

Case 2 - By keeping the same connection geometry that was described for case 1 above, such that β would remain at unity, the force ratio can be incorporated into the model for the case when the magnitude of the compressive force acting through the beam's lower flange, would exceed the compressive resistance of the flange, therefore inducing local buckling.

This case is illustrated in figure 8.14(b) and has been included since it has been established from experimental results that the rotational capability of a composite connection is significantly improved when local buckling is associated with the lower beam flanges. It subsequently follows therefore, that for a given rotation, if local buckling occurs the level of strain within the reinforcement must be smaller when compared to an equivalent connection in the absence of such buckles. To take account of this in the model, equation 8.39 was modified by introducing the force ratio coefficient η to the denominator (see equation 8.40).

$$\delta_r^{ii} = f(\delta_{cf}) = \frac{(h + a + b)\,\delta_{cf}}{\eta h} \tag{8.40}$$

The definition of η is given later.

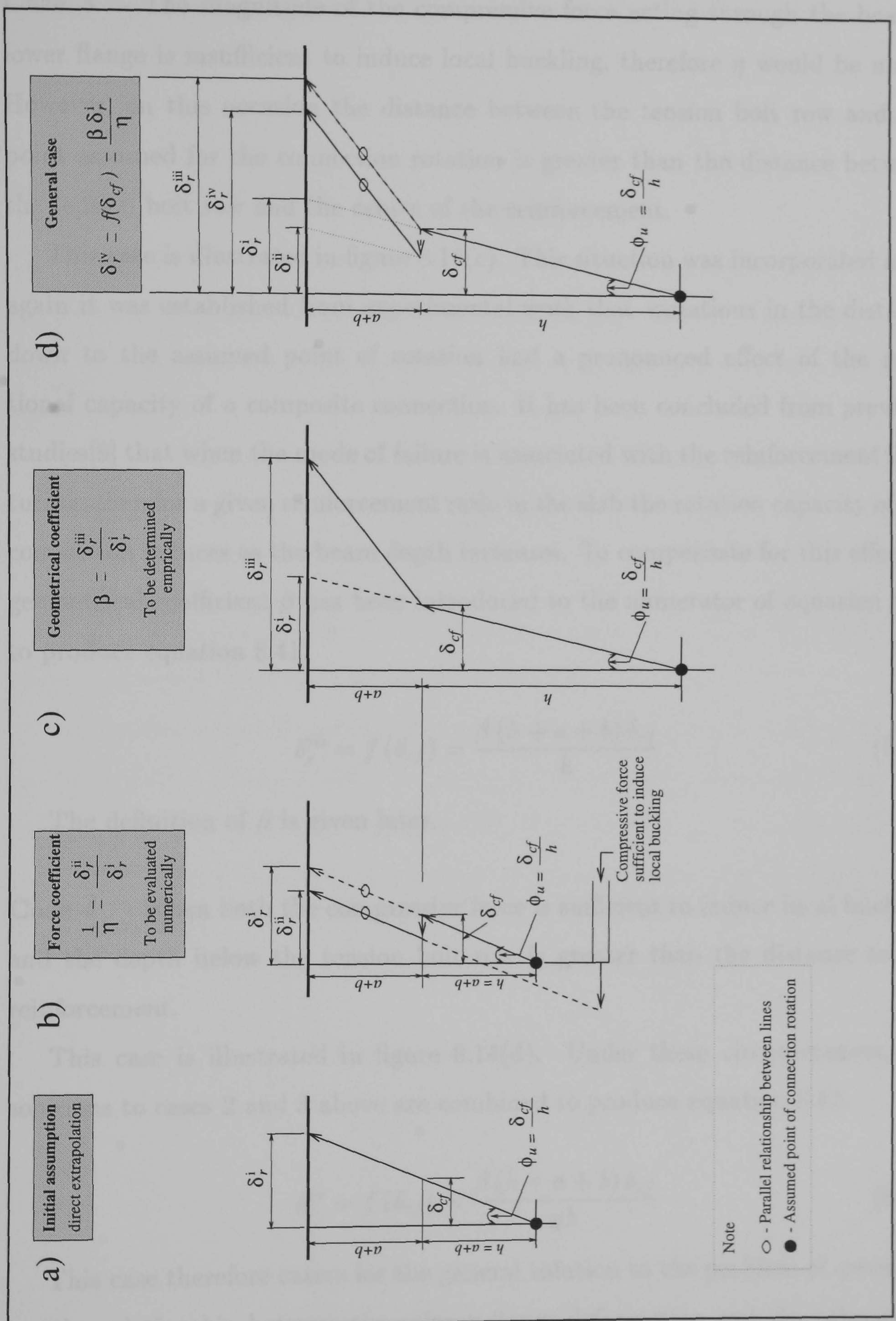

Figure 8.14: Influence of connection geometry and compression deformation on the elongation of the reinforcement

Case 3 - The magnitude of the compressive force acting through the beam's lower flange is insufficient to induce local buckling, therefore η would be unity. However, on this occasion the distance between the tension bolt row and the point assumed for the connection rotation is greater than the distance between the tension bolt row and the centre of the reinforcement.

This case is illustrated in figure 8.14(c). This situation was incorporated after again it was established from experimental work that variations in the distance down to the assumed point of rotation had a pronounced effect of the rotational capacity of a composite connection. It has been concluded from previous studies[9] that when the mode of failure is associated with the reinforcement fracturing, then for a given reinforcement ratio in the slab the rotation capacity of the connection reduces as the beam depth increases. To compensate for this effect, a geometrical coefficient β has been introduced to the numerator of equation 8.39 to produce equation 8.41.

$$\delta_r^{iii} = f(\delta_{cf}) = \frac{\beta(h+a+b)\,\delta_{cf}}{h} \tag{8.41}$$

The definition of β is given later.

Case 4 - When both the compressive force is sufficient to induce local buckling and the depth below the tension bolt row is greater than the distance to the reinforcement.

This case is illustrated in figure 8.14(d). Under these circumstances, the solutions to cases 2 and 3 above are combined to produce equation 8.42.

$$\delta_r^{iv} = f(\delta_{cf}) = \frac{\beta(h+a+b)\,\delta_{cf}}{\eta h} \tag{8.42}$$

This case therefore caters for the general solution to the problem of quantifying the relationship between the column flange deformation and the subsequent elongation of the reinforcement. An expression for δ_{cf}, in terms of the ultimate

connection rotation ϕ_{ult}, may be obtained by re-arranging equation 8.34. such that

$$f(\delta_{cf}) = \frac{\beta(h+a+b)\phi_{ult}}{\eta} \tag{8.43}$$

Force ratio coefficient 'η'

The force ratio coefficient aims to compensate for the compressive force C_{bf} acting through the centre line of the lower beam flange when the connections moment of resistance has been attained. The ratio can therefore be defined by equation 8.44.

$$\eta = \frac{C_{bf}}{R_f} \geq 1.0 \tag{8.44}$$

where :

R_f - Resistance of the beam flange, subject to Class 1 'plastic' or Class 2 'compact' steel sections (see section 8.2.1).

To establish a method for calculating the compressive force C_{bf} acting through the beam flange, a model which incorporated the moment resistance of the connection was considered (see Figure 8.15). The underlying assumption for this approach was that the moment resistance of the connection could be represented by equation 8.45.

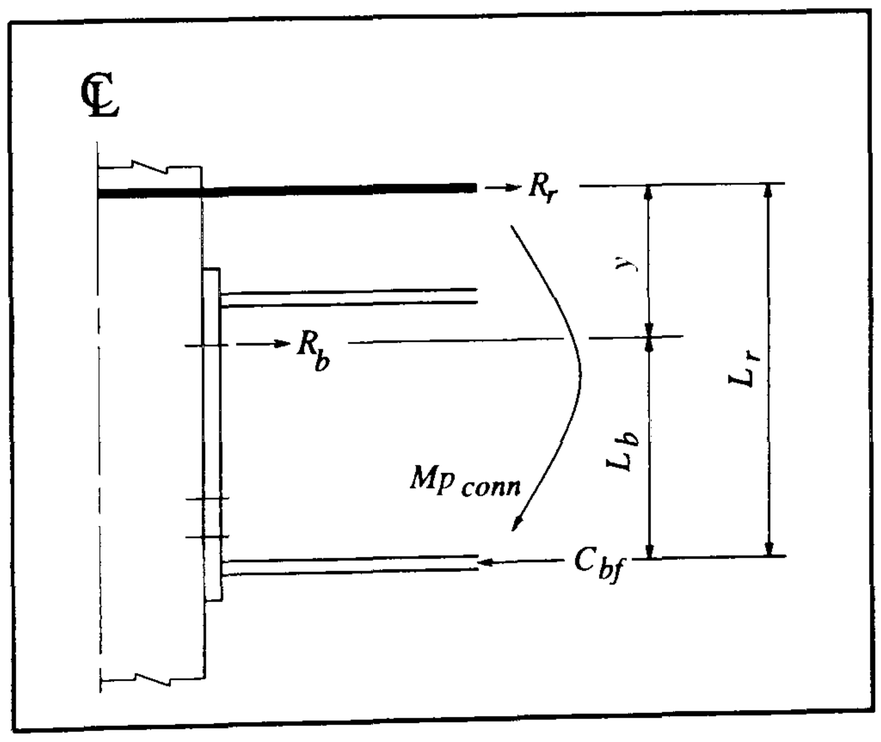

Figure 8.15: Model adopted to calculate the compressive force C_{bf}

$$Mp_{conn} = R_b L_b + R_r L_r \tag{8.45}$$

where :

R_b and R_r - Resistances of the tensile region of the steelwork connection and reinforcement respectively (see section 8.2.1)

L_b - Lever arm to the centre line of the bolt row in tension, measured from the centre line of the compression flange of the beam

L_r - Lever arm to the centre line of the reinforcement measured from the centre line of the compression flange of the beam.

This approach generally accords with the proposed model for determining the connection's moment of resistance described in section 8.2.1. However, to enable C_{bf} to be calculated directly, it was assumed that no consideration of a possible plastic stress block in the web was necessary.

From equilibrium, the total tensile force must be equal and opposite to the compressive force C_{bf} (see equation 8.46).

$$C_{bf} = R_b + R_r \tag{8.46}$$

Consequently, R_b can be written in terms of C_{bf} and R_r, which in turn can be substituted into equation 8.45 (see equation 8.47).

$$Mp_{conn} = (C_{bf} - R_r) L_b + R_r L_r \tag{8.47}$$

Substituting for $L_b = L_r - y$ into equation 8.47 and simplifying

$$Mp_{conn} = C_{bf} (L_r - y) + R_r y \tag{8.48}$$

Finally, rearranging equation 8.48 and making a substitution for $L_r - y$, an expression for C_{bf} may be obtained (see equation 8.49).

$$C_{bf} = \frac{Mp_{conn} - R_r y}{L_b} \tag{8.49}$$

It has be shown that for the purposes of deriving an expression for C_{bf}, no attempt need be made in establishing the total bolt force applicable to the tension bolt row, since this has been expressed in terms of the total force in the reinforcement and C_{bf} itself. Consequently, all that would be required for the justification of the underlying assumption is the acceptance that the moment resistance of the connection could be represented by equation 8.45.

Geometrical Coefficient 'β'

The coefficient β, was incorporated to reflect the probable influence of the connection geometry, with respect to the relative positions of the assumed point of rotation, tension bolt row and the main longitudinal reinforcement (see Figure 8.16(a) and Case 3 described previously above).

To obtain the greatest enhancement to the moment resistance of the connection, it would be reasonable to assume that the reinforcement would be positioned as close to the slab surface as durability and fire resistance permit. Consequently, the variation in its height, denoted b in Figure 8.16, would be small. A similar conclusion could also be arrived at as far as the position of the tension bolt row is concerned, whereby through the use of standard details to improve connection economy the height below the centre line of the tension flange, denoted a in Figure 8.16, would be fixed. However, the depth of the assumed point of rotation could vary significantly, since it is a function of the serial size of the beam that comprises the steelwork part of the composite connection. It was the author's opinion therefore, that a simple empirical relationship could be developed to account for the influence of altering the connection geometry in this manner.

This parameter was derived last by rearranging the final equation (see equation 8.56) to establish the coefficient required to obtain an exact correlation with the rotation achieved by the author's connection tests when the re-

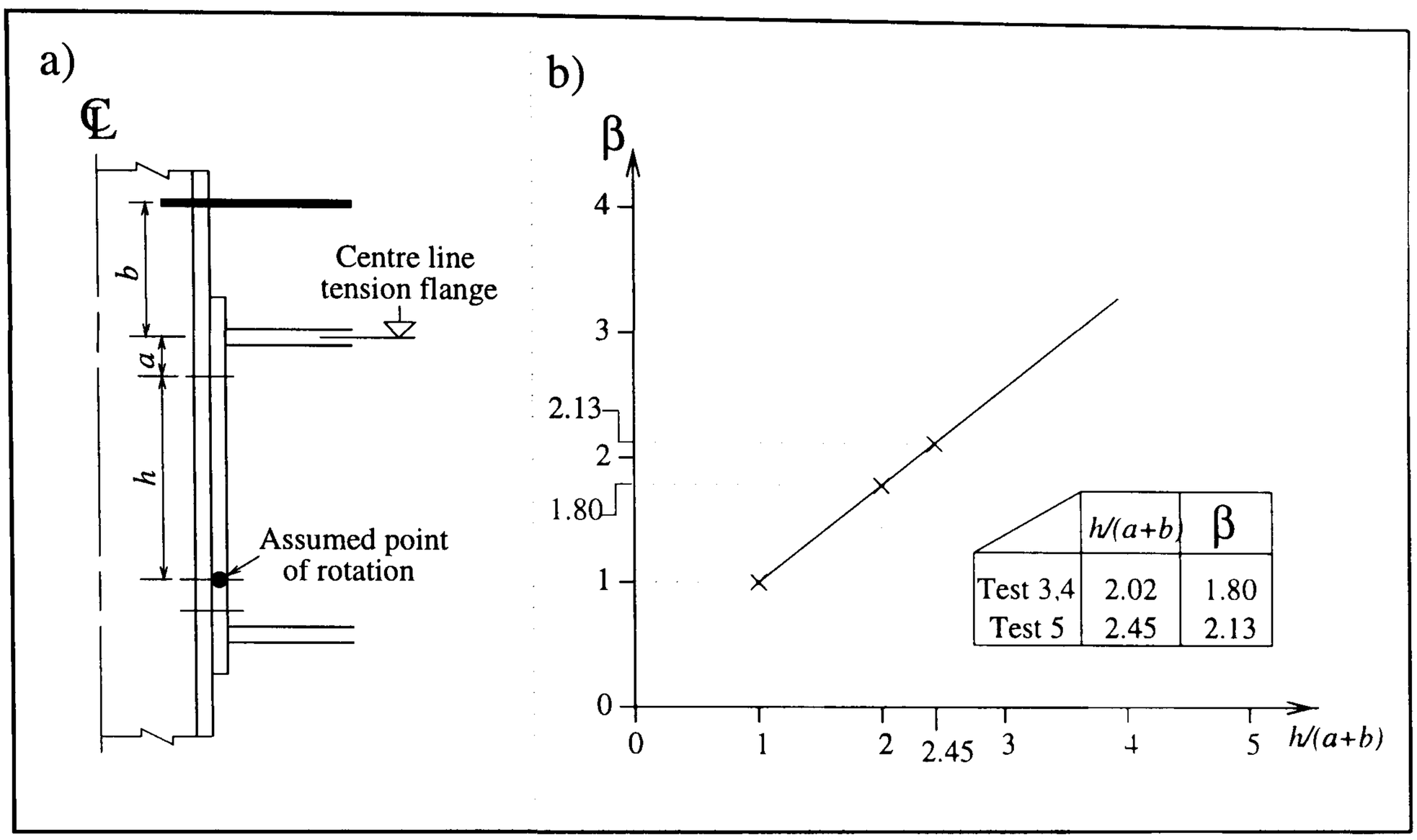

Figure 8.16: Empirical approach adopted to the determination of the geometrical coefficient β

inforcement fractured. The results were plotted graphically (see Figure 8.16(b)) and a linear regression analysis performed to produce a relationship of the form shown in equation 8.50. Furthermore, a correlation coefficient equal to 0.999987 was obtained directly from the analysis of the data, thereby in part justifying the linear approximation adopted.

$$\beta = 0.78\left(\frac{h}{a+b}\right) + 0.22 \tag{8.50}$$

Elongation due to the end plate deformation

The deformation within the end plate was again compared to a standard case situation. The approach adopted was to assume a fixed ended cantilever beam subject to a point load, r_b, part way along its length (see Figure 8.17). The length of the representative cantilever was controlled by the distance between the level of the reinforcement and the level of the tension bolt row. It was assumed that the action of the bolts would provide the clamping force necessary to provide

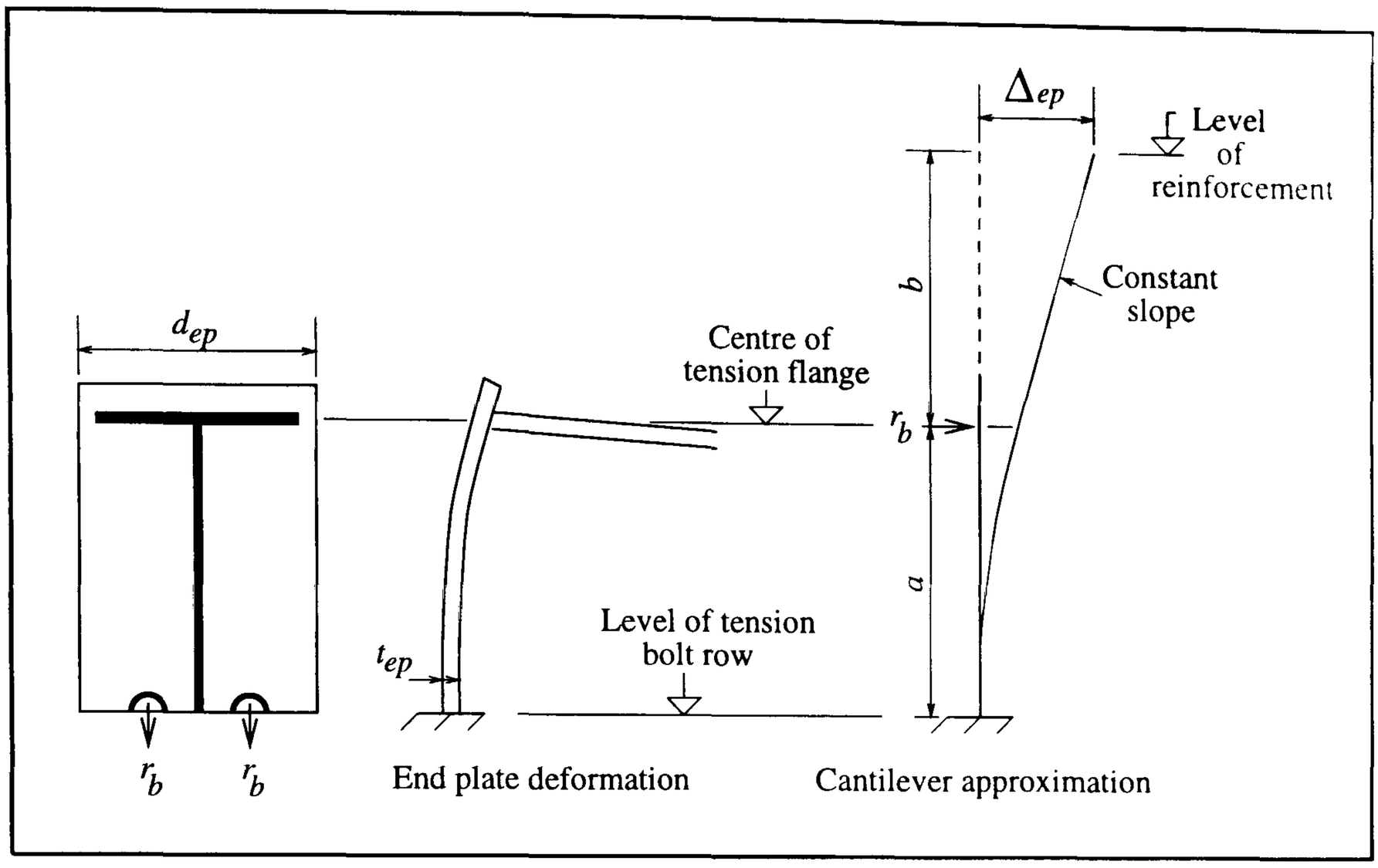

Figure 8.17: Simplified approach to model the end plate deformation

fixity at that level.

The elongation of the reinforcement due to the end plate deformation can therefore be estimated by equation 8.51.

$$\delta_{ep} = \frac{r_b a^3}{3EI_{ep}}\left(1 + \frac{3b}{2a}\right) \tag{8.51}$$

where:

I_{ep} - Second moment of area applicable to end plate (see equation 8.52)

$$I_{ep} = \frac{d_{ep}\,(t_{ep})^3}{12} \tag{8.52}$$

where :

d_{ep} - Breadth of the end plate

t_{ep} - Thickness of the end plate.

The magnitude of the point load assumed to induce the deformation cannot be easily assessed, since the stiffening effect on the cantilevered end plate as a result of welding to the beam cross section cannot be accounted for directly. The estimation of this load was further complicated, since the actual deflection of

the end plate, which was measured during the individual tests. was very small and therefore hard to establish with any degree of certainty. The error in the measurement was further influenced by the congested and cramped conditions that existed in the vicinity of the connection. Consequently, it was thought appropriate to a adopt the load r_b assumed to be responsible for the column flange deformation. Effectively this assumes that only half the force at the level of the tension bolts causes deformation of the cantilever model whose breadth is the full width of the end plate.

Therefore rearranging equation 8.36 and substituting for δ_{cf} with equation 8.34, an expression for the bolt force r_b can be configured in terms of the ultimate connection rotation ϕ_u (see equation 8.53).

$$r_b = \frac{192EI_{cf}\phi_u h}{300^3} \tag{8.53}$$

(all dimensions in mm)

Substituting for r_b in equation 8.51 and simplifying :

$$\delta_{ep} = \frac{64I_{cf}h\phi_u a^3}{I_{ep}300^3}\left(1+\frac{3b}{2a}\right) \tag{8.54}$$

To obtain an expression for the elongation of the reinforcement in terms of the ultimate connection rotation ϕ_u, substitute for δ_{cf} and δ_{ep} in equation 8.35 by equations 8.43 and 8.54 respectively.

$$\Delta_l = \frac{\beta(h+a+b)\phi_u}{\eta} + \frac{64I_{cf}h\phi_u a^3}{I_{ep}300^3}\left(1+\frac{3b}{2a}\right) \tag{8.55}$$

Finally, equation 8.55 can be rearranged to obtain the ultimate connection rotation for a given elongation within the reinforcement (see equation 8.56)

$$\phi_u = \Delta_l\left[\frac{\beta(h+a+b)}{\eta} + \frac{64I_{cf}ha^3}{I_{ep}300^3}\left(1+\frac{3b}{2a}\right)\right]^{-1} \tag{8.56}$$

To calculate the maximum connection rotation corresponding to the point where the reinforcement fractures, let Δ_l equal the value applicable to the elongation at fracture determined from material property tests (see equation 8.57).

$$\Delta_l = \%\text{ elongation at fracture } \times 5\text{bar diameters} \tag{8.57}$$

8.5.3 Verification and discussion

A comparative approach between known test results and equation 8.56, was adopted to verify the proposed model (see Table 8.5). Unfortunately, the number of flush end plate connections whose failure mode was associated with the fracture of the longitudinal reinforcement was limited. However, from the list contained within Chapter 5, section 5.2.1, the following two programmes were deemed suitable.

1. The author's experimental programme

2. Anderson and Najafi's experimental programme.

	Reference	Model Assumption #	Ultimate connection rotations (mrads)	
			Predicted Equ (8.56)	Attained
Author's tests	Test 3	Case 4	**46.3**	**47.7**
	Test 4	Case 4	**35.3**	**35.5**
	Test 5	Case 3	**20.2**	**20.1**
Najafi's tests	Test 1 (or S8F)	Case 4	**33.4**	**35.8**
	Test 3 (or S4F)	Case 4	**25.4**	**26.6**
	Test 10 (or S8FD)	Case 4	**15.1**	**14.0**
Note: # - See pages 313 - 317 inclusive & Figure 3.14				

Table 8.5: Validation of the proposed ductility model

From Table 8.5, it can be seen that good correlation between the predicted value and the actual value for the ultimate connection rotation was achieved in

all cases. However as far as the author's programme was concerned, the equation was configured to predict the performance of these tests. However, the point which should be emphasised is the correlation obtained for test 4. For this test the difference was associated solely with the end plate thickness. Consequently, all the other empirical parameters required by equation 8.56 would remain unaltered from those calculated for the previous test (Test 3). It can reasonably be assumed therefore, that this result provides some reassurance that the proposed method adopted to assess the influence of the end plate on the extension of the reinforcement, could be considered a satisfactory simplification.

The overall suitability of the proposed model can only be properly assessed when the comparison involves totally independent test results, such as those from Najafi. From this comparison, which was undertaken using the measured material properties, it can be seen that the proposed model again produces a very close and acceptably accurate prediction for the connection's ultimate rotation, for all of the connections considered.

In considering the above comparison, one must also consider the suitability of the model within a design situation. Under these circumstances, the designer would rely on a predicted value for the moment resistance of the connection, and be bound to the characteristic value applicable to the ductility of high yield reinforcing bar. Incorporating these two requirements into equation 8.56, would significantly reduce the predicted value of the ultimate connection rotation. In particular, the change in the calculated elongation of the reinforcement at fracture, from a minimum value of 26% for the authors programme and 17% for Najafi's programme, down to its characteristic value of 12%, would have the most pronounced influence on the calculated ductility performance of the connections. It can be shown that by substituting the characteristic value of 12% into the model, would result in an average reduction in the connection rotation at failure of 54% and 29% for the author's and Najafi's experimental programmes respectively. This reduction is clearly undesirable, but unfortunately in design

reliance can only be placed on specified material properties. A solution to this difficulty would be the specification of a class of reinforcement having a limit on ductility, closer to the values obtained in practice.

Although there are only a few results available to assess the performance of the proposed equation, it must be born in mind that in these six connection tests alone there was considerable variation in many of the key components that make up practical composite connections. These variations can be summarised as follows :

1. Column section - 203 and 254 serial size universal columns.

2. Beam section - 305, 457 and 533 serial size universal beams.

3. Total area of reinforcement - 4T12, 8T12 and 4T16 high yield bars

4. The position and arrangement of the reinforcing bars within the depth of the slab. In particular, the horizontal spacing was varied from the minimum to the maximum permitted by modern codes of practice.

5. End plate thickness - 15mm and 12mm thicknesses.

6. Bolt diameters - M24 and M20, grade 8.8 bolts.

7. Variations in the measured material properties. In particular :

   (a) The reinforcement's percentage elongation at fracture.

   (b) The yield stress applicable to the reinforcement and the compression flange of the attached beams.

Consequently, it is the author's opinion that although one may criticise the empirical nature of the model, its physical nature provides a foundation to enable a greater understanding of connection ductility to be developed in the future.

8.5.4 Concluding remarks

Composite flush end plate connections have been considered in the context of providing ductility in the hogging regions of plastically designed continuous composite beams. It has been shown that the ductility requirements of the connection cannot be expressed solely in terms of simple rules concerning material properties for reinforcing steel. The behaviour of the joint as a whole needs to be considered. It has also been suggested that local buckling of the beam's steel section provides a benign form of failure, for which appropriate design rules should be established, thus simplifying composite connection design considerably. However, in the absence of such rules, a ductility model has been proposed which for the first time enables the total rotation capacity to be assessed, when the failure occurs by fracture of the reinforcing bars.

Chapter 9

Conclusions and suggestions for further work

The research work presented within this thesis has been undertaken by the author during the period from January 1992 - December 1995. The work covered a variety of aspects of interest in structural enginnering, which can be broadly subdivided into to the following sections :

1. The design of steelwork sway frames in accordance with limit state principals in conjunction with the Wind-Moment Method[1]. This aspect of the work has been described in Part I of the thesis, which encompasses Chapters 1 to 4 inclusive.

2. An experimental investigation into the ductility of composite flush end plate connections incorporating 457 and 533 serial size Universal Beams. This aspect of the work has been described in Part II of the thesis, which encompasses Chapters 5 to 8 inclusive.

The conclusions and suggestions for further work have been separated along identical lines to those indicated above. Consequently, the first and second sections of the work will be subsequently referred to as Part I and Part II respectively.

9.1 Part I - Aspects of sway frame design

9.1.1 Conclusions

An in-depth investigation has been undertaken to assess the suitability of incorporating standardised ductile end plate connections[20] within low to medium rise structural steel sway frames. The investigation was computer-based and utilised an existing second order elastic-plastic computer program for plane frames.

The standardised ductile end plate connections (see Chapter 1) were found to exhibit very flexible characteristics. Consequently, the computer program had to be modified to ease the convergence problems which had been previously encountered when analysing semi-rigid frames which incorporate very flexible connections[6]. In addition, the investigation necessitated the development of a method for predicting the initial response of the standardised connections. This was a requirement of the computer program, whereby the connections' responses under the actions of the applied forces were simulated by a bi-linear representation of the moment-rotation characteristics (see Chapter 2). A simple equation was therefore proposed (see Chapter 3), based on the consideration of the deformations within the column flange and end plate only. This equation was successfully validated against test results, mainly from the literature. Its suitability was further substantiated following a comparison with the more general equation proposed within the revised Annex J to Eurocode 3[18]. From this comparison, it was concluded that closer predictions to the test results were achieved by adopting the proposed equation.

In addition to the above and following the completion of the frame study (see Chapter 4), further conclusions were obtained. These are listed below under the limit states to which they apply.

Analysis for ultimate limit states

1. Incorporating the standard connections within the design of a Wind-Moment

frame would result in a structural frame capable of withstanding the applied design loads, without stability problems being encountered. Consequently, adopting effective length factors of 1.0 and 1.5 for the major and minor axes respectively, resistance to column buckling remain satisfactory.

2. The standard connections performed satisfactorily and were not susceptible to brittle fracture.

3. The connection types utilised within the investigation were all partial strength with respect to the beams and were also classified as semi-rigid in accordance with Eurocode 3[17].

4. Due to the partial strength nature of the standard connections, the Class 1 'plastic' requirement placed on the structural members can be relaxed to include Class 2 'compact' rolled steel sections.

5. The effect of including the influence of web shear in the analysis reduces the stiffness of the connections considerably and consequently decreases the overall stiffness of the frame. In addition, the connection rotation at the design load showed a slight increase; however, the stability factors applicable to the columns and the overall second-order elastic-plastic collapse load factor of the frame, were not significantly affected.

Analysis for serviceability limit states

An estimate of the maximum sway applicable to a Wind-Moment frame, may be calculated by undertaking a rigid analysis and multiplying the corresponding deflections by the factors shown in Table 4.5. These convert a first-order rigid analysis into a first-order semi-rigid one, and similarly for the second-order analyses.

Two bolt sizes are available for use with the standard connections: namely M20 and M24 Grade 8.8 bolts. The author has concluded however that the M24 option should be specified in preference to the M20 option.

	Bay width	Type of analysis	
		First-order	Second-order
		Multiplying factor	
4 storeys and less	⩾ 6.0m	**1.6**	**1.7**
	< 6.0m	**2.1**	**2.1**
Greater than 4 stories	⩾ 6.0m	**2.2**	**2.5**

Note :
These vaules include allowances for web shear at internal column locations of multi-bay frames

Table 9.1: Rigid frame multipliers for serviceability calculations

9.1.2 Suggestions for further work

The following represents several suggestions whereby the work undertaken by the author could be extended to further improve existing knowledge and to provide additional design guidance

1. The author's investigation was based on the premise that full fixity existed at the foundation level. However, it has been found[123, 124], in a similar fashion to that for connections in general, that this particular assumption does not necessarily always exist in engineering practice. Therefore it is suggested that the existing computer program could be modified to enable the stiffness of the foundations to be varied. Following this modification, a selection of the more flexible frames could be re-examined with the objective of establishing the degree foundation stiffness that would be required for the frame to withstand the applied design loads. An experimental study could then follow to obtain test data applicable to various foundation configurations. However, should an experimental investigation be undertaken careful consideration would have to be given to how, if appropriate, the

layers of subsoil beneath the founding level should could be represented. Design rules could then be derived to provide minimum foundation requirements in conjunction with their actual behavioural characteristics.

2. The development of a simple but acceptably accurate method of calculating the sway deflections under the actions of the Serviceability limit state for frames incorporating the standardised end plate connections. This would be preferred to the multiplier proposed above, since by its very nature it would result in an over estimation of the sway deflections for many practical frame configurations.

3. Another aspect that has been often neglected in the studies of unbraced sway frames is the beneficial effect that the cladding to the building will have on reducing the subsequent horizontal deflections. It is necessary to adopt a conservative approach with respect to the enhancement of the overall stiffness of frames, because at present there only exists a limited guidance covering this area[125, 126]. An opportunity therefore exists for further research into this area, to increase the overall economy of semi-rigid design of unbraced steel frames.

4. In Wind-Moment designs with partial-strength connections it has been often found that only very limited plasticity develops in the members below the design load level for ultimate limit state. Furthermore as Wind-Moment designs are characterised by constant beam sections up the frame, it may be expected that connections will develop plastic hinges first in the lowest part of the frame and progress upwards. Knowledge of the order of formation and location of such hinges could lead to simplified second-order analysis, based on the calculation of a 'deteriorated critical load'[127]. For this reason full details of the formation of plastic hinges in the Wind-Moment frames are included in Appendix C, section C.4 of this thesis.

9.2 Part II - Ductility of composite flush end plate connections

9.2.1 Conclusions

As a consequence of the experimental work undertaken by the author (see Chapter 7), which dealt with composite flush end plate connections, the following conclusions were drawn:

1. The strength and stiffness of a bare steel connection can be increased when its acts compositely with a reinforced composite slab.

2. The horizontal spacing of the rebars contained within the effective breadth of a composite slab does not significantly effect the performance of the connection as a whole.

3. Reducing the end plate thickness has the effect of reducing both the moment capacity and rotation capacity of a composite connection that incorporates a nominally identical reinforcing detail.

4. Increasing the beam depth has the effect of increasing the connections moment capacity; however, this is at considerable expense to the available rotation capacity when a nominally identical reinforcing detail is considered.

5. End plate connections of the type considered by the author are susceptible to a brittle failure mode associated with rebar fracture.

6. When a composite connection incorporates 4T16 rebars as the main longitudinal reinforcement, in conjunction with 457 series universal beams the rotation capacity of such an arrangement would be sufficient to allow plastic methods of design to be adopted. In contrast however, if a larger 533 serial size beam is substituted, plastic design would not be permitted on

the grounds that the available rotation capacity at the connections would not be sufficient to meet the necessary requirements for plastic design.

7. The deformation within the steelwork detail is influenced by the connection configuration adopted.

Following the experimental programme the results were analysed in the context of connection performance, from which the following conclusions were obtained:

1. The composite connections tested by the author were all partial strength when compared to the strength of the beam member in negative bending.

2. The composite connections tested by the author were all classified as rigid and consequently, are acceptable for general use in continuous composite beams.

3. All diameters of reinforcement between 8mm and 20mm conform to the property requirements necessary for them to be identified as possessing 'high ductility' in accordance with Eurocode2[89]; and comply with the minimum requirements specified by British codes of practice[116]. Consequently, bars of these diameters are suitable for general use in plastically designed continuous composite beams. However, the corresponding ductility requirements applicable to a composite connection cannot be expressed solely in terms of simple rules concerning material properties for reinforcing steel.

4. If mesh reinforcement is provided, it should not be included as part of the total area of steel reinforcement when calculating the enchanced moment of resistance applicable to a composite flush end plate connection.

5. The ductility model proposed in Chapter 8 provides a satisfactory estimate of the total rotation capacity of a composite flush end plate connection with a single bolt row in tension, when the failure occurs as a result of the rebars fracturing.

9.2.2 Suggestions for further work

A single test has been undertaken by the author on a composite connection that incorporates a 533 serial size beam. The results from this test indicate that the reinforcement detail adopted was unsuitable in as far as the rotation capacity was considerably reduced when compared with the tests undertaken with the shallower 457 serial size beams. It is therefore suggested that further tests should be undertaken on this particular size of connection in an attempt to find a more suitable reinforcing arrangement to overcome the problem of the lack of ductility.

A ductility model has been proposed which enables the total rotation capacity of a composite flush end plate connection to be calculated, when the failure occurs as a result of the rebars fracturing. Refinements to this model could take the form of adopting a more theoretical approach to the representation of the plastic deformations within the column flange and the end plate. Furthermore, additional studies are also required to investigate the influence of beam depth on a composite connection's rotation capacity that incorporates a nominally identical reinforcement arrangement. The ductility model could also usefully be extended to include end plate connections that incorporate more than a single bolt row in tension.

It has also been suggested in Chapter 8, that local buckling of the beam's steel section provides a benign form of failure, which could be utilised to guarantee a connection's ductility. However, many problems need to be addressed before design rules can be formulated to guarantee connection performance. These have been summarised in section 8.3.3. The author therefore suggests that future experimental and theoretical investigations should be directed towards the formulation of appropriate design rules, since it is the author's opinion that if such rules were forthcoming then a major simplification to the process of composite connection design would have been achieved.

References

[1] Anderson D. Reading S.J. and Kavianpour K. *Wind-Moment Design for Unbraced Frames*, 1991. The Steel Construction Institute. SCI-082.

[2] Gray C. Kent L.E. Mitchell W.A. and Godfrey G.B., editors. *Steel Designers Manual.* Crosby Lockwood Staples, 4th edition, 1972.

[3] Sivakumaran K.S. Lateral load response of unbraced steel building frames. *Canadian Journal of Civil Eng.*, Vol 17, No 6:p974, 1990.

[4] Nethercot D.A. Joint action and the design of steel frames. *The Structural Engineer*, Vol 63A, No. 12:p371, 1985.

[5] Gerstle K.H. *Flexibly connected steel frames.* In Steel framed structures Stability and strength. Edited by Narayanan R, Elsevier Science, 1985. p205.

[6] Kavianpour K. *Design and analysis of unbraced steel frames.* Ph.D Thesis, University of Warwick, 1990.

[7] Ackroyd M. Design of flexibly connected unbraced steel building frames. *Journal of Construction Steelwork Research*, Vol 8:p261, 1987.

[8] Reading S.J. *Investigation of the wind connection method.* MSc Thesis, University of Warwick, 1989.

[9] Najafi A.A. *End plate connections and their influence on steel and composite structures.* Ph.D Thesis, University of Warwick, 1992.

[10] Neal B.G. *The Plastic Methods of Structural Analysis.* 3rd edition, Chapman and Hall, 1977.

[11] Lay M.G. Effective lengths with wind-connection method. *Steel Construction, AISC (Australia)*, Vol 7, No. 2:p2.

[12] BS 5950. *Structural use of steelwork in buildings, Part 1: Code of practice for design of simple and continuous beams*, 1990. British Standards Institution, London.

[13] CP3. *Code of Basic Data for the Design of Buildings, Chapter V. Loading Part 2, Wind Loads*, 1972. British Standards Institution. London.

[14] Pask J.W. *Manual on connections for beam and column construction.* 1982. British Constructional Steelwork Association.

[15] Horne M.R. and Morris L.J. *Plastic design of low rise frames.* Granada Publishing, 1981.

[16] Anderson D. and Kavianpour K. Analysis of steel frames with semi-rigid connections. *Structural Engineering Review*, Vol 3:p79. 1991.

[17] ENV 1993 1-1. *Eurocode 3: Design of steel structures, part 1.1: General rules and rules for buildings.* CEN Brussels. 1992.

[18] Eurocode 3. *Design of Steel Structures Part 1.1 : General Rules and Rules for Buildings, Revised Annex J : Joints in Building Frames.* CEN Brussels. (To be published).

[19] MD Tahir M. Ph.D Thesis, University of Warwick (To be submitted).

[20] BCSA/SCI. *Joints in steel construction - moment connections.* 1995. Joint Publication between Steel Construction Institute and The British Constructional Steelwork Association, Publication No. 207/95.

[21] Moore D.B. *The design of end plate connections.* 1989. In Slabs and Structures, Edited by Armer G.S.T. and Moore D.B.. Butterworths. London. p75.

[22] Bose B. and Hughes A.F. Verifying the performance of standard connections for semi-continuous frames. *Proceedings of the Institution of Civil Engineers*, (To be published).

[23] Bose B. *Tests to verify the performance of standard ductile connections*, 1993. Dundee Institute of Technology Consultancy Report No. DIT/CESB/HSRG/C1/93.

[24] Bose B. *Additional tests on standardized ductile connections.* 1994. Dundee Institute of Technology Consultancy Report No. UAD/CESB/SRG/C1/94.

[25] Girardier E.V. Fewster S.M.C. and Owens G.W. *Economic design and the importance of standardised connections.* In Constructional Steel Design - World Developments, Edited by Dowling P.J., Harding J.E., Bjorhovde R. and Martinez-Romero E., Elsevier Applied Science, 1992. p541.

[26] BS 449. *Specification for the use of structural steel in buildings*, 1969. British Standards Institution, London.

[27] Chen W.F. and Lui E.M. *Stability design of steel frames.* CRC Press Inc.. 1991. p235.

[28] Nethercot D.A. *Steel beam to column connections - A review of test data and their application to the evaluation of joint behaviour on the performance of steel frames.* CIRIA Report, RP 338, 1985.

[29] Davison J.B. and Nethercot D.A. *Overview of connection behaviour.* In Structural connections - Stability and strength. Elsevier Science. 1989. Edited by Narayanan R. p1.

[30] Anderson D. Bijlaard F. Nethercot D.A. and Zandonini R. *Analysis and design of steel frames with semi-rigid connections.* IABSE Survey S-39/87. 1987.

[31] Bijlaard F. Snijder H.H. *Influence of semi-rigid and partial strength joints on the behaviour of frames.* In Connections in steel structures - Behaviour, strength and design. Edited by Bjorhovde R. Brozzetti J. and Colson A., Elsevier Science, 1988. p280.

[32] Chen W.F., editor. *Joint flexibility in steel frames.* Journal of Construction Steelwork Research, 1987. Special issue.

[33] Gerstle K.H. and Cook N.V. *Practical Analysis of Flexibly Connected Building Frames: Materials and Member Behaviour*, 1987. Proceedings of the Session at Structures Congress 87 : Related to Materials and Member Behaviour, ASCE, Structural Division, p122.

[34] Nethercot D.A. and Zandonini R. *Methods of Prediction of Joint Behaviour: Beam-to-Column Connections.* In Structural connections - Stability and strength. Edited by Narayanan R., Elsevier Science. 1989. p23.

[35] Rathbun J. Elastic properties of rivited connections. *Transactions, ASCE.* Vol 101:p524, 1936.

[36] Baker J.F., 1934. Second Report, Steel Research Committee, Department of Scientific and Industrial Research. HMSO, London.

[37] Romstad K.M. and Subramanian C.V. Analysis of frames with partial connection rigidity. *Journal of the Structural Division, ASCE.* Vol 96(ST11):p2283, 1970.

[38] Lionberger S.R. and Weaver W. Dynamic response of frames with non-rigid connections. *Journal Engineering Mechanical Division, ASCE.* Vol 95(EM1):p95, 1969.

[39] Poggi C. and Zandonini R. *Behaviour and Strength of Steel Frames with Semi-Rigid Connections.* In Connection flexibility and steel frame behaviour. Edited by Chen W.F., ASCE, 1985. p57.

[40] Lui E.M. and Chen W.F. Analysis and the behaviour of flexibly jointed frames. *Engineering Structures*, Vol 8(2):p107, 1986.

[41] Ang K.M. and Morris G.A. Analysis of three dimensional frames with flexible beam-to-column connections. *Canadian Journal of Civil Engineering*, Vol 11:p245, 1984.

[42] Kennedy D.J.L. Moment-rotation characteristics of shear connections. *Engineering Journal, AISC*, page p105, 1969.

[43] Frye M.J. and Morris G.A. Analysis of flexibility connected steel frames. *Canadian Journal of Civil Engineers*, Vol 2:p280, 1975.

[44] Sommer W.H. *Behaviour of Welded Header Plate Connections*, 1969. MSc Thesis, University of Toronto, Ontario, Canada.

[45] Benterkia Z. *End Plate Connections and Analysis of Semi-Rigid Steel Frames.* Ph.D Thesis, University of Warwick, 1991.

[46] Jones S.W. Kirby P.A. and Nethercot D.A. *Modelling of Semi-Rigid Connection Behaviour and its Influence on Steel Column Behaviour.* In Joints in Structural Steelwork. Edited by Howlett J.H. Jenkins W.M. and Stainsby R., Pentech Press, 1981. p5.73.

[47] Richard R.M. and Abbott B.J. Versatile elastic-plastic stress-strain formulea. *Journal of the Engineering Mechanical Division, ASCE*, Vol 101(EM4):p511, 1975.

[48] Kukreti A.R. Murray T.M. and Abolmaali A. End-plate connection moment-rotation relationship. *Journal of Constructional Steelwork Research*, Vol 8:p137, 1987.

[49] Tschemmernegg F. *On the non-linear behaviour of joints in steel frames.* In Connections in steel structures - Behaviour, strength and design. Edited by Bjorhovde R. Brozzetti J. and Colson A. Elsevier Science. 1988. p15.

[50] Anderson D. and MD Tahir M. *Economic comparisons between simple and partial strength design of braced steel frames*, May 1995. Preliminary Proceedings to the Third International Workshop on Connections in Steel Structures. University of Trento. (Unpublished).

[51] ECCS Technical Committee 8 Working group 8.1/8.2 Skeletal Structures. *Analysis and design of steel frames with semi-rigid joints.* European Convention for Constructural Steelwork, 1st edition. 1992. No 67. p57.

[52] Steel Construction Insitute. *Steelwork design guide to BS 5950: Part 1: 1990 - Volume 1, Section properties, Member capacities*, 3rd edition, 1991. SCI-202.

[53] Gibbons C. Wang Y.C. and Nethercot D.A. The influence of steelwork connections on the behaviour of simple 3-dimensional steel frames. *Steel Structures, Journal of Singapore Structural Steel Society.* Vol 1. No 1:p17. 1990.

[54] Macleod I.A. Simplified equations for deflection of multi-storey frames. *Building Society*, Vol 6, No 25-31:p25, 1971.

[55] Saim A.A. Ph.D Thesis, University of Warwick (To be submitted 1997).

[56] Lawson M. *Design of composite slabs and beams with steel decking.* Steel Construction Insitute, 1989. SCI-055.

[57] Lawson M. *Commentary on BS 5950: Part 3: Section 3.1: Composite beams.* Steel Construction Insitute, 1991. SCI-078.

[58] Johnson R.P. and Hope-Gill M.C. *Semi-rigid joints in composite frames.* 1972. IABSE, Ninth Congress, Preliminary Report. Amsterdam. p133.

[59] Owens G.W. and Echeta C.B. *A semi-rigid connection for composite frames - Initial test results.* In Joints in Structural Steelwork. Edited by Howlett J.H. Jenkins W.M. and Stainsby R., Pentech Press, 1981. p3.20.

[60] ENV 1994 1-1. *Eurocode 4: Design of composite steel and concrete structures, part 1.1: General rules and rules for buildings.* CEN Brussels, 1992.

[61] Zandonini R. *Semi-rigid composite joints.* In Structural Connections - Stability and Strength. Edited by Narayanan R.. Elsevier Applied Science, 1989. p63.

[62] Johnson R.P. Van Dalen K. and Kemp A.R. *Ultimate strength of continuous composite beams*, 1966. British Constructional Steelwork Association - Conference on Structural Steel, p27.

[63] Climenhaga J.J. and Johnson R.P. Local buckling in continuous composite beams. *The Structural Engineer*, Vol 50 No.9:p180, 1972.

[64] Barnard P.R. *Innovations in composite floor systems*, 1970. Canadian Structural Engineering Conference, Canadian Steel Industries Construction Council, p13.

[65] Ansourian P. and Roderick J.W. Composite connections to external columns. *Journal of the Structural Division, ASCE*, Vol 102, No.ST8:p1609, 1976.

[66] Ansourian P. *Composite connections to external columns*, 1977. Research Report No.R311, School of Civil Engineering, University of Sidney.

[67] Ansourian P. and Sase T. *Bolted connections in composite structures*, 1981. Research Report No.R382, School of Civil Engineering, University of Sidney.

[68] Johnson R.P. and Law C.L.C. *Semi-rigid joints for composite frames.* In Joints in Structural Steelwork. Edited by Howlett J.H. Jenkins W.M. and Stainsby R., Pentech Press, 1981. p3.20.

[69] Van Dalen K. and Godoy H. Strength and rotational behaviour of composite beam-to-column connections. *Canadian Journal of Civil Engineering*, Vol 9:p313, 1982.

[70] Redwood R.G. Mitchell D. and Dunberry M. *Cyclic load tests on composite beam-to-column connections*, 1985. Research Report, Department of Civil Engineering and Applied Mechanics, McGill University, Montreal, Canada.

[71] Ammerman D. and Leon R.T. Behaviour of semi-rigid composite connections. *Engineering Journal, AISC*, Vol 42(June), No 2:p53. 1987.

[72] Leon R.T. *Behaviour of semi-rigid composite frames.* In Composite Steel Structures - Advances, Design and Construction. Edited by Narayanan R., Elsevier Applied Science, 1987. p145.

[73] Leon R.T. and Ammerman D. *Seismic Performance of composite semi-rigid subassemblages*, 1986. Proceedings of the 8th Lisbon Conference ECEE. Vol 4, p25.

[74] Benussi F. Puhali R. and Zandonini R. *Experimental analysis of semi-rigid connections in composite frames*, 1986. Proceedings of the International Conference on Steel Structures - Recent Advances and their Applications to Design, Budva, Yugoslavia.

[75] Benussi F. Puhali R. and Zandonini R. *Composite braced frames with semi-rigid joints*, 1987. Proceedings of the International Symposium on Composite Steel Concrete Structures, Bratislava.

[76] Lam D. *Influence of composite flooring on steel beam-column connections.* 1989. MSc Thesis, University of Sheffield.

[77] Leon R.T. Semi-rigid composite construction. *Journal of Constructional Steelwork Research*, Vol 15:p99, 1990.

[78] Altman R. Maquoi R. and Jaspart J.P. *Experimental study of the non-linear behaviour of beam-to-column composite joints*. October 1992. Proceedings of the Strasbourg Workshop COST C1 : Semi-rigid behaviour, p132.

[79] Lawson R.M. Behaviour of steel beam-to-column connections in fire. *The Structural Engineer*, Vol 68 No.14:p261, 1990.

[80] Aribert J.M. and Lachal A. *Experimental investigation of composite connection and global interpretation*, October 1992. Proceedings of the Strasbourg Workshop COST C1 : Semi-rigid behaviour, p158.

[81] Aribert J.M. Lachal A. Muzeau J.P. and Racher P. *Recent tests on steel and composite connections in France*, October 1994. Proceedings of the Prague Workshop COST C1 : Semi-rigid behaviour, p61.

[82] Davison J.B. Lam D. and Nethercot D.A. Semi-rigid action of composite joints. *The Structural Engineer*, Vol 68 No.24:p489, 1990.

[83] Xiao Y. Choo B.S. and Nethercot D.A. Composite connections in steel and concrete i - experimental behaviour of composite beam-column connections. *Journal of Constructional Steelwork Research*, Vol 31:p3, 1994.

[84] Owens G.W. and Moore D.B. Steelwork connections. *The Structural Engineer*, Vol 70 No.3/4:p37, 1992.

[85] Li T. *The Analysis and Ductility Requirements of Semi-Rigid Composite Frames*. Ph.D Thesis, University of Nottingham. UK., 1994.

[86] Ren P. and Crisinel M. *Effect of reinforced concrete slab on the moment-rotation behaviour of standard steel beam-to-column joints*. October 1994. Proceedings of the Prague Workshop COST C1 : Semi-rigid behaviour, p175.

[87] Anderson D. and Najafi A.A. Performance of composite connections - major axis end plate joints. *Journal of Construction Steelwork Research*, Vol 31:p31, 1994.

[88] Law C.L.C. *Planar no-sway frames with semi-rigid beam-to-column joints.* Ph.D Thesis, University of Warwick, 1983.

[89] ENV 1993 1-1. *Eurocode 2, part 1.1: Design of concrete structures.* CEN Brussels. 1992.

[90] Precision Metal Forming Ltd, Swindon Rd, Cheltenham, Gloucestershire. *Composite floor decking*, 1991. Technical specification: CF46.

[91] BS 12. *Specification for ordinary and rapid-harding Portland cement*, 1991. British Standards Institution, London.

[92] BS 882. *Specification for aggregates from natural sources for concrete*, 1983. British Standards Institution, London.

[93] Teychenne D.C. *et al. Design of normal concrete mixes.* Department of the Environment, 2nd edition, 1988.

[94] BS 1881. *Testing concrete, Part 125: Methods for mixing and sampling fresh concrete in the laboratory*, 1986. British Standards Institution, London.

[95] BS 1881. *Testing concrete, Part 108: Methods for making test cubes from fresh concrete*, 1983. British Standards Institution, London.

[96] BS 1881. *Testing concrete, Part 110: Methods for making test cylinders from fresh concrete*, 1983. British Standards Institution, London.

[97] BS 18. *Tensile testing of metals (including aerospace materials)*, 1991. British Standards Institution, London.

[98] BS 1881. *Testing concrete, Part 116: Method for determination of compressive strength of concrete cubes*, 1983. British Standards Institution, London.

[99] BS 1881. *Testing concrete, Part 117: Method for determination of tensile splitting strength*, 1983. British Standards Institution, London.

[100] W.H.Mays and Sons (Windsor) Ltd, Arthur Rd, Windsor, Berkshire. *High accuracy measurement of angular deflections on structures - Inclinometer.* Technical specification: MP103.

[101] Sensing Systems Inc., 14th Avenue, Phoenix AZ 85027-2839. *Accustar electronic clinometer.* Technical specification.

[102] Welwyn Strain Measurement, Armstrong Rd, Basingstoke. *Strain gauge displacement transducers.* Technical specification: HS/HLS.

[103] Tokyo Sokki Kenkyujo Co. Ltd, Alcester Rd, Studley, Warwickshire. *TML strain gauges.* Technical specification: TML pam E-101.

[104] Bentley J.P. *Principles of measurement systems.* Longman Scientific and Technical, 3rd edition, 1995. p178.

[105] W.H.Mays and Sons (Windsor) Ltd, Arthur Rd, Windsor, Berkshire. *Compression load cell.* Technical specification: MP105.

[106] Godley M.H.R. and Needham F.H. Comparative tests on 8.8 and hsfg bolts in tension and shear. *The Structural Engineer*, Vol 60A, No 3:p94, 1982.

[107] Megson T.H.G. *Strength of Materials for Civil Engineers*, 1987. Edward Arnold Ltd, 2nd edition, p49.

[108] Owens G.W. and Cheal B.D. *Structural steelwork connections.* 1989. Butterworths, London. p52.

[109] Johnson R.P. *Composite structures of steel and concrete, Vol 1: Beams, Slabs, Columns and Frames for buildings*, 1994. Blackwell Scientific Publications, 2nd Edition, p44.

[110] Johnson R.P. and Anderson D. *Designers' Handbook to Eurocode 4 part 1.1: Design of Composite Steel and Concrete Structures.* Thomas Telford Services Ltd, 1st edition, 1995.

[111] Gibbons C. and Lawson M. *Partial Strength Moment Resisting Connections in Composite Frames.* Steel Construction Insitute, 1993. SCI-RT-257.

[112] Owens G.W. and Knowles P.R., editors. *Steel Designers Manual.* Blackwell Scientific Publications, 5th edition, 1994. p595.

[113] Tschemmernegg F. and Huter M. *Classification of beam-to-column joints*, Liege, June 1993. COST C1 : Working Group meeting, C1/WD2/93-3.

[114] Snijder H.H. Bijlaard F.S.K. and Stark J.W.B. *Use of the Elastic Effective Length for Stability Checks of Columns and Consequences for Checks on Beams in Braced Frames*, 1983. Proceedings of the Michael R. Horne Conference : Instability and Plastic Collapse of Steel Structures. p152.

[115] Beeby A.W. Narayanan R.S. *Designers' Handbook to Eurocode 2: part 1.1: Design of Concrete Structures.* Thomas Telford Services Ltd, 1st edition, 1995. p47.

[116] BS 4449. *Carbon steel bars for the reinforcement of concrete*, 1988. British Standards Institution, London.

[117] Llewellyn D.T. *Steels - Metallurgy and Applications.* Butterworth-Heinemann Ltd, 2nd edition, 1994. p65.

[118] Lawson M. Gibbons C. *Design of Composite Connections in Composite Frames - Interim Guidance for End Plate Type Connections.* Steel Construction Insitute and Ove Arup and Partners, Rev 3, 1994. SCI-RT-330.

[119] Nethercot D.A. *Local Buckling Effects in Composite Connections*, September 1995. Preliminary Report of the International Colloquium: Stability of Steel Structures, Edited by Ivanyi M. and Veroci B., Technical University of Budapest, Hungry, p231.

[120] Xiao Y. *Behaviour of Composite Connections in Steel and Concrete.* Ph.D Thesis, University of Nottingham, UK., 1994.

[121] Wright H.D. Evans H.R. and Harding P.W. The use of profiled steel sheeting on floor construction. *Journal of Construction Steelwork Research*, Vol 7:p279, 1987.

[122] BS 5950. *Structural use of steelwork in buildings, Part 3 : Design in composite construction, Section 3.1 : Code of practice for design of simple and continuous composite beams*, 1990. British Standards Institution, London.

[123] Wald F. Simek I. Sokol J. Seifert J. *The column-base stiffness tests*, October 1994. Proceedings of the Prague Workshop COST C1 : Semi-rigid behaviour, p281.

[124] Nakashima S. *Steel column bases in Japan : Experimental research and design practice*, October 1994. Proceedings of the Prague Workshop COST C1 : Semi-rigid behaviour, p247.

[125] Wood R.H. Roberts E.H. A graphical method of predicting side-sway in the design of multistorey buildings. *Proc. ICE*, vol 59, Part 2:p353, 1975.

[126] Cunningham R. Some aspects of semi-rigid connections in structural steelwork. *The Structural Engineer*, Vol 68, No. 5:p85, 1990.

[127] Wood R.H. *The stability of tall buildings.* 1989. In Slabs and Structures, Edited by Armer G.S.T. and Moore D.B., Butterworths, London. p225.

List of Publications

1. Anderson D. and Brown N.D. *Steel Frames with Partial-Strength Connections.* Conference to commemorate the 60th birthday of Professor Vogal, University of Karlsruhe, Germany, p207, 1993.

2. Brown N.D. and Anderson D. *Ductility in Continuous Composite Construction.* International Colloquium - Stability of Steel Structures, Technical University of Bubapest, Hungary. Edited by Ivanyi M. and Veroci B., 1995

Aspects of Sway Frame Design and Ductility of Composite End Plate Connections

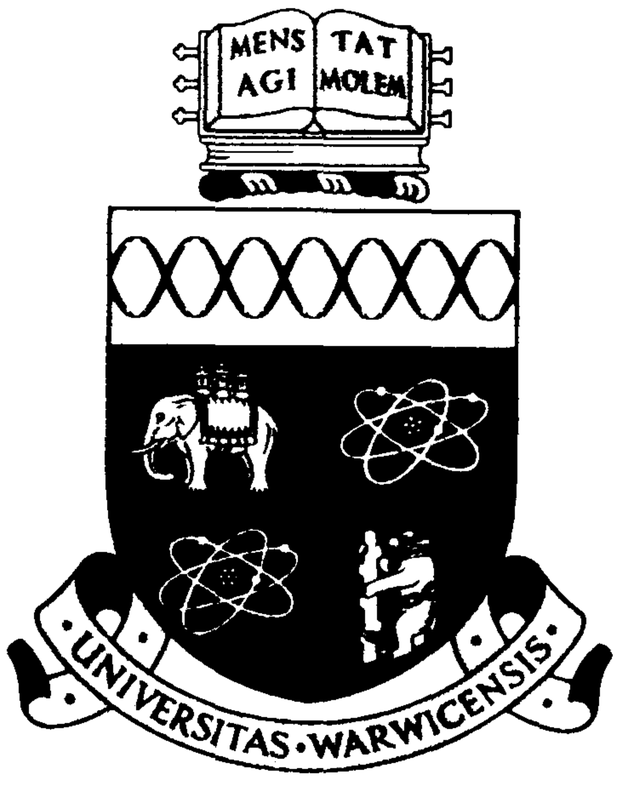

Nigel D Brown BEng(Hons)

Department of Engineering

University of Warwick

Thesis submitted to the University of Warwick for the degree of

Doctor of Philosophy

December 1995

Appendices - Volume II

Appendices - Volume II

Appendix A

Design tables applicable to ductile end plate connections

A.1 Scope

Tables of standard dimensions, moment resistance values, column limitations and shear resistances are presented in this appendix for the ductile end plate connections described in chapter 1.

A.2 Dimension tables

Flush Details

Dimensions for detailing (mm)

Serial Size Mass per Metre	a_2	a_3	a_4	a_5	c	d
762 x 267						820
197	60	150	620	710	25	
173	60	150	612	702	29	
147	60	150	604	694	33	
686 x 254						750
170	60	150	543	633	29	
152	60	150	538	628	31	
140	60	150	534	624	33	
125	60	150	528	618	36	
610 x 229						670
140	60	150	467	557	27	
125	60	150	462	552	29	
113	60	150	457	547	31	
101	60	150	452	542	34	
533 x 210						600
122	60	150	395	485	28	
109	60	150	390	480	30	
101	60	150	387	477	32	
92	60	150	383	473	33	
82	60	150	378	468	36	
457 x 191						520
98	60	150	317	407	26	
89	60	150	314	404	28	
82	60	150	310	400	30	
74	60	150	307	397	31	
67	60	150	304	394	33	
457 x 152						520
82	60	150	315	405	27	
74	60	150	311	401	29	
67	60	150	307	397	31	
60	60	150	305	395	33	
52	60	150	300	390	35	
406 x 178						470
74	60	150	263	353	29	
67	60	150	259	349	30	
60	60	150	256	346	32	
54	60	150	253	343	34	
406 x 140						460
46	60	150	252	342	29	
39	60	150	247	337	31	
356 x 171						420
67	60	N/A	N/A	304	28	
57	60	N/A	N/A	299	31	
51	60	N/A	N/A	296	32	
45	60	N/A	N/A	292	34	
356 x 127						410
39	60	N/A	N/A	293	29	
33	60	N/A	N/A	289	31	
305 x 165						370
54	60	N/A	N/A	251	30	
46	60	N/A	N/A	247	31	
40	60	N/A	N/A	244	33	
305 x 127						370
48	60	N/A	N/A	250	30	
42	60	N/A	N/A	247	32	
37	60	N/A	N/A	244	33	
305 x 102						370
33	60	N/A	N/A	253	29	
28	60	N/A	N/A	249	31	
25	60	N/A	N/A	245	33	
254 x 146						310
43	60	N/A	N/A	200	25	
37	60	N/A	N/A	196	27	
31	60	N/A	N/A	192	29	
254 x 102						310
28	60	N/A	N/A	200	25	
25	60	N/A	N/A	197	27	
22	60	N/A	N/A	194	28	

3

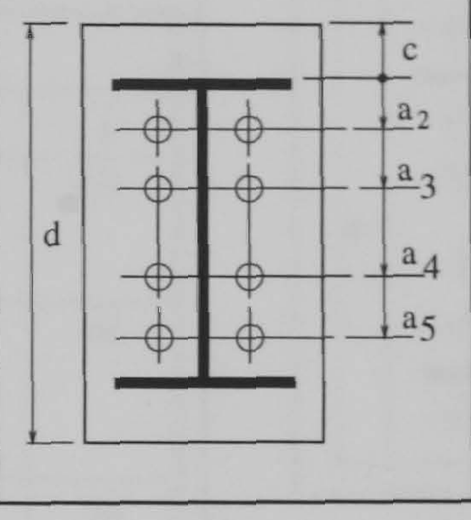

1

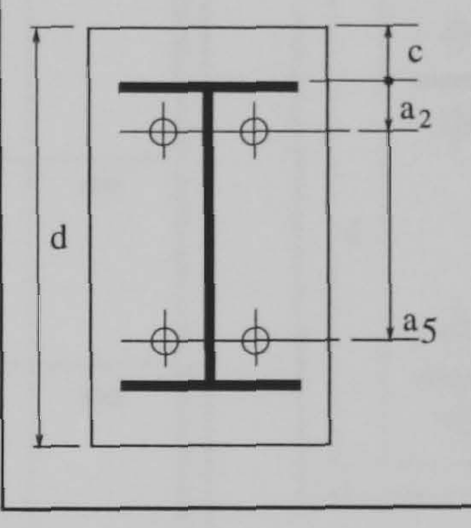

Note : see individual details for remaining dimensions

Extended Details

Dimensions for detailing (mm)

Serial Size Mass per Metre	a_1	a_2	a_3	a_4	a_5	a_6	c	d
762 x 267								950
197	40	60	150	620	710	810	90	
173	40	60	150	612	702	802	94	
147	40	60	150	604	694	794	98	
686 x 254								870
170	40	60	150	543	633	733	89	
152	40	60	150	538	628	728	91	
140	40	60	150	534	624	724	93	
125	40	60	150	528	618	718	96	
610 x 229								780
140	40	60	150	467	557	657	82	
125	40	60	150	462	552	652	84	
113	40	60	150	457	547	647	86	
101	40	60	150	452	542	642	89	
533 x 210								720
122	40	60	150	395	485	585	88	
109	40	60	150	390	480	580	90	
101	40	60	150	387	477	577	92	
92	40	60	150	383	473	573	93	
82	40	60	150	378	468	568	96	
457 x 191								650
98	40	60	150	317	407	507	91	
89	40	60	150	314	404	504	93	
82	40	60	150	310	400	500	95	
74	40	60	150	307	397	497	96	
67	40	60	150	304	394	494	98	
457 x 152								650
82	40	60	150	315	405	505	92	
74	40	60	150	311	401	501	94	
67	40	60	150	307	397	497	96	
60	40	60	150	305	395	495	98	
52	40	60	150	300	390	490	100	
406 x 178								590
74	40	60	150	263	353	453	89	
67	40	60	150	259	349	449	90	
60	40	60	150	256	346	446	92	
54	40	60	150	253	343	443	94	
406 x 140								580
46	40	60	150	252	342	442	89	
39	40	60	150	247	337	437	91	
356 x 171								540
67	40	60	N/A	N/A	304	404	88	
57	40	60	N/A	N/A	299	399	91	
51	40	60	N/A	N/A	296	396	92	
45	40	60	N/A	N/A	292	392	94	
356 x 127								540
39	40	60	N/A	N/A	293	393	94	
33	40	60	N/A	N/A	289	389	96	
305 x 165								490
54	40	60	N/A	N/A	251	351	90	
46	40	60	N/A	N/A	247	347	91	
40	40	60	N/A	N/A	244	344	93	
305 x 127								490
48	40	60	N/A	N/A	250	350	90	
42	40	60	N/A	N/A	247	347	92	
37	40	60	N/A	N/A	244	344	93	
305 x 102								490
33	40	60	N/A	N/A	253	353	89	
28	40	60	N/A	N/A	249	349	91	
25	40	60	N/A	N/A	245	345	93	
254 x 146								440
43	40	60	N/A	N/A	200	300	90	
37	40	60	N/A	N/A	196	296	92	
31	40	60	N/A	N/A	192	292	94	
254 x 102								440
28	40	60	N/A	N/A	200	300	90	
25	40	60	N/A	N/A	197	297	92	
22	40	60	N/A	N/A	194	294	93	

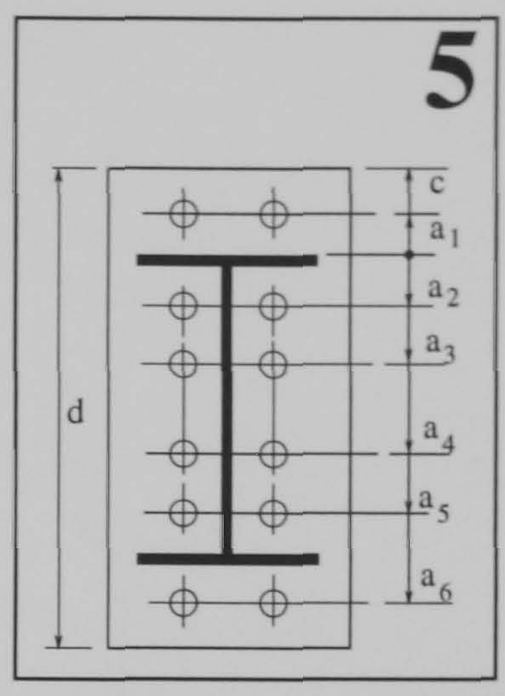

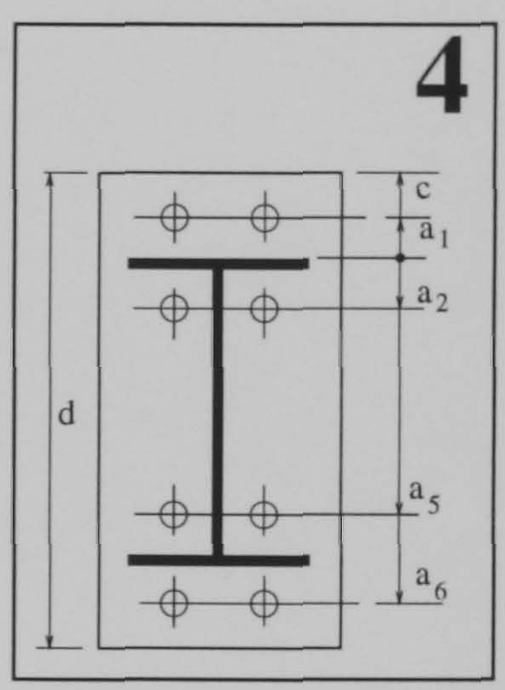

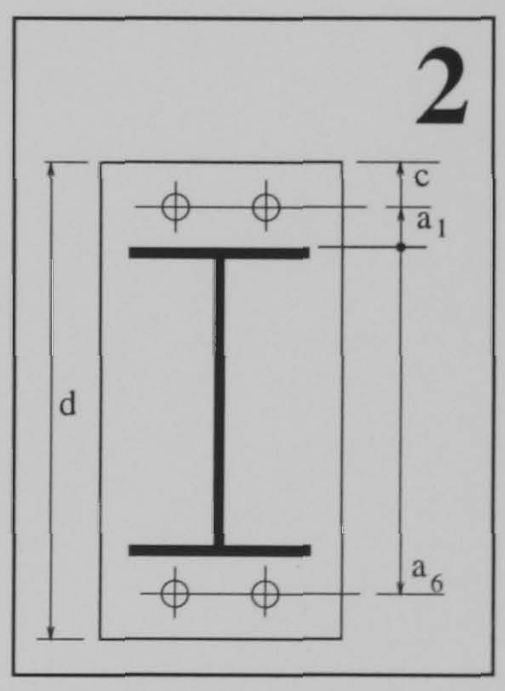

Note : see individual details for remaining dimensions

A.3 Design tables

W1/20

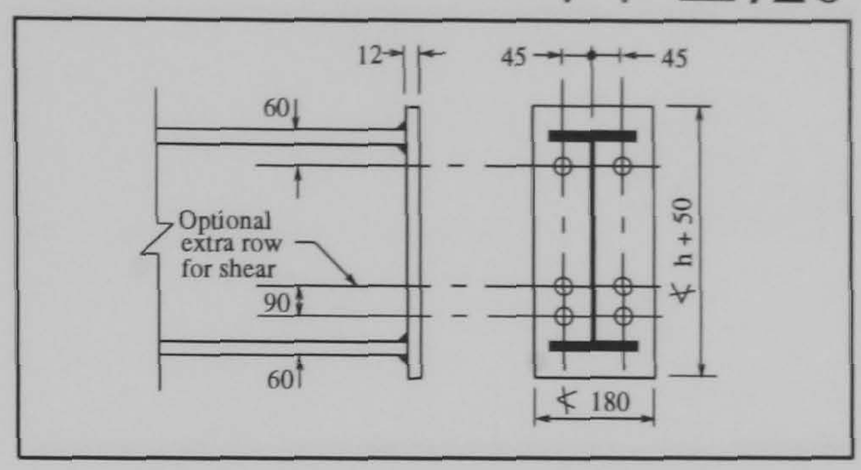

Box 1

Moment Resistance

M.R. (in Nm) = 208 (h - 0.5 t_f - 60)

t_f (mm)	h (mm)	Serial Size Mass per metre	Moment Resistance kNm
		762 x 267	
25.4	769.6	197 b	145
21.6	762.0	173 b	143
17.5	753.9	147	142
		686 x 254	
23.7	692.9	170 b	129
21.0	687.6	152 b	128
19.0	683.5	140 b	127
16.2	677.9	125	127
		610 x 229	
22.1	617.0	140 b	113
19.6	611.9	125 b	112
17.3	607.3	113	112
14.8	602.2	101	111
		533 x 210	
21.3	544.6	122 b	98
18.8	539.5	109 b	98
17.4	536.7	101	97
15.6	533.1	92	97
13.2	528.3	82	96
		457 x 191	
19.6	467.4	98 b	83
17.7	463.6	89 bw	82
16.0	460.2	82	81
14.5	457.2	74	81
12.7	453.6	67	80
		457 x 152	
18.9	465.1	82 b	82
17.0	461.3	74	82
15.0	457.2	67	81
13.3	454.7	60	81
10.9	449.8	52	80
		406 x 178	
16.0	412.8	74	72
14.3	409.4	67	71
12.8	406.4	60	71
10.9	402.6	54	70
		406 x 140	
11.2	402.3	46	70
8.6	397.3	39	69
		356 x 171	
15.7	364.0	67	61
13.0	358.6	57	61
11.5	355.6	51	60
9.7	352.0	45	60
		356 x 127	
10.7	352.8	39	60
8.5	348.5	33	59
		305 x 165	
13.7	310.9	54	51
11.8	307.1	46	50
10.2	303.8	40	50
		305 x 127	
14.0	310.4	48	51
12.1	306.6	42	50
10.7	303.8	37	49
		305 x 102	
10.8	312.7	33	51
8.9	308.9	28	51
6.8	304.8	25	50
		254 x 146	
12.7	259.6	43	40
10.9	256.0	37	40
8.6	251.5	31	39
		254 x 102	
10.0	260.4	28	41
8.4	257.0	25	40
6.8	254.0	22	40

b - Where $t_f > 18$ use a butt weld to the flange

bw- If the beam is S275 use a butt weld to the flange

Box 2

Column Limitations

$\Sigma F_b \geq 208$ kN

See Note 2

S275					Grade	S355				
v	iv	iii	ii	i	Zone	i	ii	iii	iv	v
Web Tension	Web Crushing	Web Buckling	Web Shear	Flange Bending	**Serial Size** Mass per metre	Flange Bending	Web Shear	Web Buckling	Web Crushing	Web Tension
					356 x 368					
✓	✓	✓	✓	✓	202	✓	✓	✓	✓	✓
✓	✓	✓	✓	✓	177	✓	✓	✓	✓	✓
✓	✓	✓	✓	✓	153	✓	✓	✓	✓	✓
✓	✓	✓	✓	✓	129	✓	✓	✓	✓	✓
					305 x 305					
✓	✓	✓	✓	✓	283	✓	✓	✓	✓	✓
✓	✓	✓	✓	✓	240	✓	✓	✓	✓	✓
✓	✓	✓	✓	✓	198	✓	✓	✓	✓	✓
✓	✓	✓	✓	✓	158	✓	✓	✓	✓	✓
✓	✓	✓	✓	✓	137	✓	✓	✓	✓	✓
✓	✓	✓	✓	✓	118	✓	✓	✓	✓	✓
✓	✓	✓	✓	✓	97	✓	✓	✓	✓	✓
					254 x 254					
✓	✓	✓	✓	✓	167	✓	✓	✓	✓	✓
✓	✓	✓	✓	✓	132	✓	✓	✓	✓	✓
✓	✓	✓	✓	✓	107	✓	✓	✓	✓	✓
✓	✓	✓	✓	✓	89	✓	✓	✓	✓	✓
✓	✓	✓	406	✓	73	✓	✓	✓	✓	✓
					203 x 203					
✓	✓	✓	✓	✓	86	✓	✓	✓	✓	✓
✓	✓	✓	395	✓	71	✓	✓	✓	✓	✓
✓	✓	✓	349	✓	60	✓	✓	✓	✓	✓
✓	✓	✓	300	✓	52	✓	387	✓	✓	✓
✓	✓	✓	273	■	46	✓	353	✓	✓	✓

* - Less than ΣF_b

▒ - Sections are not designated class 1

Box 3

Shear Resistance

See Note 4

236 kN

(optional extra row adds 184 kN)

W1/24

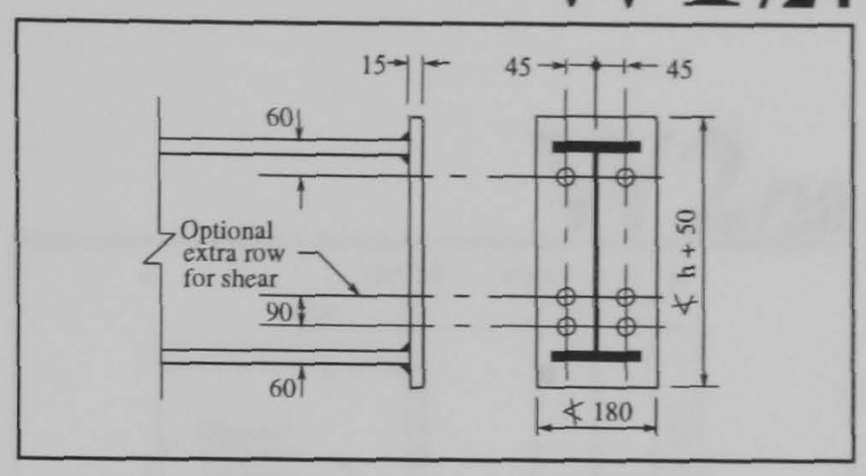

Box 1

Moment Resistance

M.R. (in Nm) = 305 (h - 0.5 t_f - 60)

t_f (mm)	h (mm)	Serial Size Mass per metre	Moment Resistance kNm
		762 x 267	
25.4	769.6	197 b	213
21.6	762.0	173 b	211
17.5	753.9	147	209
		686 x 254	
23.7	692.9	170 b	190
21.0	687.6	152 b	188
19.0	683.5	140 b	187
16.2	677.9	125	186
		610 x 229	
22.1	617.0	140 b	167
19.6	611.9	125 b	165
17.3	607.3	113	164
14.8	602.2	101	163
		533 x 210	
21.3	544.6	122 b	145
18.8	539.5	109 b	144
17.4	536.7	101	143
15.6	533.1	92	142
13.2	528.3	82	141
		457 x 191	
19.6	467.4	98 b	121
17.7	463.6	89 bw	121
16.0	460.2	82	120
14.5	457.2	74	119
12.7	453.6	67	118
		457 x 152	
18.9	465.1	82 b	121
17.0	461.3	74	120
15.0	457.2	67	119
13.3	454.7	60	118
10.9	449.8	52	117
		406 x 178	
16.0	412.8	74	105
14.3	409.4	67	104
12.8	406.4	60	104
10.9	402.6	54	103
		406 x 140	
11.2	402.3	46	103
8.6	397.3	39	102
		356 x 171	
15.7	364.0	67	90
13.0	358.6	57	89
11.5	355.6	51	88
9.7	352.0	45	88
		356 x 127	
10.7	352.8	39	88
8.5	348.5	33	87
		305 x 165	
13.7	310.9	54	75
11.8	307.1	46	74
10.2	303.8	40	73
		305 x 127	
14.0	310.4	48	74
12.1	306.6	42	73
10.7	303.8	37	73
		305 x 102	
10.8	312.7	33	75
8.9	308.9	28	75
6.8	304.8	25	74
		254 x 146	
12.7	259.6	43	59
10.9	256.0	37	58
8.6	251.5	31	57
		254 x 102	
10.0	260.4	28	60
8.4	257.0	25	59
6.8	254.0	22	58

b - Where t_f > 18 use a butt weld to the flange

bw - If the beam is S275 use a butt weld to the flange

Box 2

Column Limitations

$\Sigma F_b \geq 305$ kN

See Note 2

S275					Grade	S355				
v	iv	iii	ii	i	Zone	i	ii	iii	iv	v
Web Tension	Web Crushing	Web Buckling	Web Shear	Flange Bending	**Serial Size** Mass per metre	Flange Bending	Web Shear	Web Buckling	Web Crushing	Web Tension
					356 x 368					
✓	✓	✓	✓	✓	202	✓	✓	✓	✓	✓
✓	✓	✓	✓	✓	177	✓	✓	✓	✓	✓
✓	✓	✓	✓	✓	153	✓	✓	✓	✓	✓
✓	✓	✓	✓	✓	129	✓	✓	✓	✓	✓
					305 x 305					
✓	✓	✓	✓	✓	283	✓	✓	✓	✓	✓
✓	✓	✓	✓	✓	240	✓	✓	✓	✓	✓
✓	✓	✓	✓	✓	198	✓	✓	✓	✓	✓
✓	✓	✓	✓	✓	158	✓	✓	✓	✓	✓
✓	✓	✓	✓	✓	137	✓	✓	✓	✓	✓
✓	✓	✓	✓	✓	118	✓	✓	✓	✓	✓
✓	✓	✓	565	✓	97	✓	✓	✓	✓	✓
					254 x 254					
✓	✓	✓	✓	✓	167	✓	✓	✓	✓	✓
✓	✓	✓	✓	✓	132	✓	✓	✓	✓	✓
✓	✓	✓	✓	✓	107	✓	✓	✓	✓	✓
✓	✓	✓	497	✓	89	✓	✓	✓	✓	✓
✓	✓	✓	406	■	73	✓	525	✓	✓	✓
					203 x 203					
✓	✓	✓	497	✓	86	✓	✓	✓	✓	✓
✓	✓	✓	395	✓	71	✓	510	✓	✓	✓
✓	✓	✓	349	■	60	✓	451	✓	✓	✓
✓	✓	✓	300*	■	52	■	387	✓	✓	✓
✓	✓	✓	273*	■	46	■	353	✓	✓	✓

* - Less than ΣF_b

▒ - Sections are not designated class 1

Box 3

Shear Resistance

See Note 4

340 kN

(optional extra row adds 265 kN)

W2/20

Box 1

Moment Resistance

M.R. (in Nm) = 193 (h - 0.5 t_f + 40)

t_f (mm)	h (mm)	Serial Size Mass per metre	Moment Resistance kNm
		533 x 210	
21.3	544.6	122 b	111
18.8	539.5	109 b	110
17.4	536.7	101	110
15.6	533.1	92	109
13.2	528.3	82	109
		457 x 191	
19.6	467.4	98 b	96
17.7	463.6	89 bw	96
16.0	460.2	82	95
14.5	457.2	74	95
12.7	453.6	67	94
		457 x 152	
18.9	465.1	82 b	96
17.0	461.3	74	95
15.0	457.2	67	95
13.3	454.7	60	94
10.9	449.8	52	94
		406 x 178	
16.0	412.8	74	86
14.3	409.4	67	86
12.8	406.4	60	85
10.9	402.6	54	85
		406 x 140	
11.2	402.3	46	84
8.6	397.3	39	84
		356 x 171	
15.7	364.0	67	77
13.0	358.6	57	76
11.5	355.6	51	75
9.7	352.0	45	75
		356 x 127	
10.7	352.8	39	75
8.5	348.5	33	74
		305 x 165	
13.7	310.9	54	67
11.8	307.1	46	66
10.2	303.8	40	65
		305 x 127	
14.0	310.4	48	66
12.1	306.6	42	66
10.7	303.8	37	65
		305 x 102	
10.8	312.7	33	67
8.9	308.9	28	67
6.8	304.8	25	66
		254 x 146	
12.7	259.6	43	57
10.9	256.0	37	56
8.6	251.5	31	56
		254 x 102	
10.0	260.4	28	57
8.4	257.0	25	57
6.8	254.0	22	56

b - Where t_f > 18 use a butt weld to the flange

bw - If the beam is S275 use a butt weld to the flange

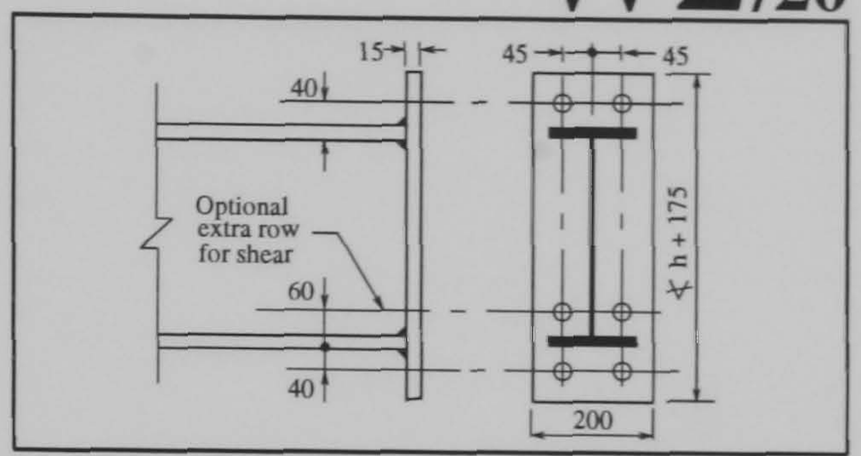

Box 2

Column Limitations

$\Sigma F_b \geq$ 197 kN

See Note 2

S275					Grade	S355				
v	iv	iii	ii	i	Zone	i	ii	iii	iv	v
Web Tension	Web Crushing	Web Buckling	Web Shear	Flange Bending	**Serial Size** Mass per metre	Flange Bending	Web Shear	Web Buckling	Web Crushing	Web Tension
					356 x 368					
✓	✓	✓	✓	✓	202	✓	✓	✓	✓	✓
✓	✓	✓	✓	✓	177	✓	✓	✓	✓	✓
✓	✓	✓	✓	✓	153	✓	✓	✓	✓	✓
✓	✓	✓	✓	✓	129	✓	✓	✓	✓	✓
					305 x 305					
✓	✓	✓	✓	✓	283	✓	✓	✓	✓	✓
✓	✓	✓	✓	✓	240	✓	✓	✓	✓	✓
✓	✓	✓	✓	✓	198	✓	✓	✓	✓	✓
✓	✓	✓	✓	✓	158	✓	✓	✓	✓	✓
✓	✓	✓	✓	✓	137	✓	✓	✓	✓	✓
✓	✓	✓	✓	✓	118	✓	✓	✓	✓	✓
✓	✓	✓	✓	✓	97	✓	✓	✓	✓	✓
					254 x 254					
✓	✓	✓	✓	✓	167	✓	✓	✓	✓	✓
✓	✓	✓	✓	✓	132	✓	✓	✓	✓	✓
✓	✓	✓	✓	✓	107	✓	✓	✓	✓	✓
✓	✓	✓	✓	✓	89	✓	✓	✓	✓	✓
✓	✓	✓	✓	✓	73	✓	✓	✓	✓	✓
					203 x 203					
✓	✓	✓	✓	✓	86	✓	✓	✓	✓	✓
✓	✓	✓	✓	✓	71	✓	✓	✓	✓	✓
✓	✓	✓	349	✓	60	✓	✓	✓	✓	✓
✓	✓	✓	300	✓	52	✓	387	✓	✓	✓
✓	✓	✓	273	✓	46	✓	353	✓	✓	✓

* - Less than ΣF_b

- Sections are not designated class 1

Box 3

Shear Resistance

See Note 4

236 kN

(optional extra row adds 184 kN)

W2/24

Box 1

Moment Resistance

M.R. (in Nm) = 295 (h - 0.5 t_f + 40)

t_f (mm)	h (mm)	Serial Size Mass per metre	Moment Resistance kNm
		533 x 210	
21.3	544.6	122 b	169
18.8	539.5	109 b	168
17.4	536.7	101	168
15.6	533.1	92	167
13.2	528.3	82	166
		457 x 191	
19.6	467.4	98 b	147
17.7	463.6	89 bw	146
16.0	460.2	82	145
14.5	457.2	74	145
12.7	453.6	67	144
		457 x 152	
18.9	465.1	82 b	146
17.0	461.3	74	146
15.0	457.2	67	145
13.3	454.7	60	144
10.9	449.8	52	143
		406 x 178	
16.0	412.8	74	131
14.3	409.4	67	131
12.8	406.4	60	130
10.9	402.6	54	129
		406 x 140	
11.2	402.3	46	129
8.6	397.3	39	128
		356 x 171	
15.7	364.0	67	117
13.0	358.6	57	116
11.5	355.6	51	115
9.7	352.0	45	114
		356 x 127	
10.7	352.8	39	114
8.5	348.5	33	113
		305 x 165	
13.7	310.9	54	102
11.8	307.1	46	101
10.2	303.8	40	100
		305 x 127	
14.0	310.4	48	101
12.1	306.6	42	101
10.7	303.8	37	100
		305 x 102	
10.8	312.7	33	103
8.9	308.9	28	102
6.8	304.8	25	101
		254 x 146	
12.7	259.6	43	87
10.9	256.0	37	86
8.6	251.5	31	85
		254 x 102	
10.0	260.4	28	87
8.4	257.0	25	86
6.8	254.0	22	86

b - Where t_f > 18 use a butt weld to the flange

bw - If the beam is S275 use a butt weld to the flange

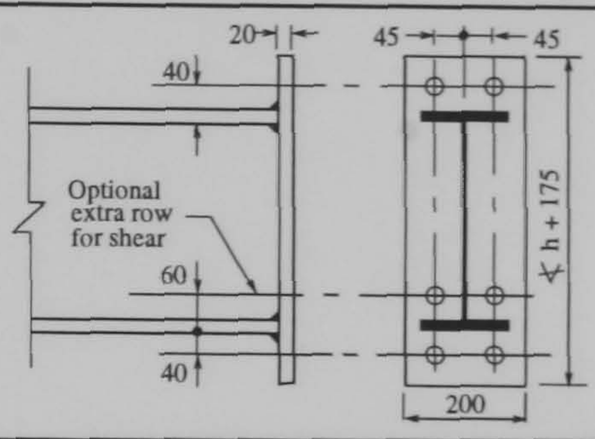

Box 2

Column Limitations

$\Sigma F_b \geq 299$ kN

See Note 2

S275					Grade	S355				
v	iv	iii	ii	i	Zone	i	ii	iii	iv	v
Web Tension	Web Crushing	Web Buckling	Web Shear	Flange Bending	**Serial Size** Mass per metre	Flange Bending	Web Shear	Web Buckling	Web Crushing	Web Tension
					356 x 368					
✓	✓	✓	✓	✓	202	✓	✓	✓	✓	✓
✓	✓	✓	✓	✓	177	✓	✓	✓	✓	✓
✓	✓	✓	✓	✓	153	✓	✓	✓	✓	✓
✓	✓	✓	✓	✓	129	✓	✓	✓	✓	✓
					305 x 305					
✓	✓	✓	✓	✓	283	✓	✓	✓	✓	✓
✓	✓	✓	✓	✓	240	✓	✓	✓	✓	✓
✓	✓	✓	✓	✓	198	✓	✓	✓	✓	✓
✓	✓	✓	✓	✓	158	✓	✓	✓	✓	✓
✓	✓	✓	✓	✓	137	✓	✓	✓	✓	✓
✓	✓	✓	✓	✓	118	✓	✓	✓	✓	✓
✓	✓	✓	565	✓	97	✓	✓	✓	✓	✓
					254 x 254					
✓	✓	✓	✓	✓	167	✓	✓	✓	✓	✓
✓	✓	✓	✓	✓	132	✓	✓	✓	✓	✓
✓	✓	✓	✓	✓	107	✓	✓	✓	✓	✓
✓	✓	✓	497	✓	89	✓	✓	✓	✓	✓
✓	✓	✓	406	■	73	✓	525	✓	✓	✓
					203 x 203					
✓	✓	✓	497	✓	86	✓	✓	✓	✓	✓
✓	✓	✓	395	✓	71	✓	510	✓	✓	✓
✓	✓	✓	349	■	60	✓	451	✓	✓	✓
✓	✓	✓	300	■	52	■	387	✓	✓	✓
✓	✓	✓	273*	■	46	■	353	✓	✓	✓

* - Less than ΣF_b

▒ - Sections are not designated class 1

Box 3

Shear Resistance

See Note 4

340 kN

(optional extra row adds 265 kN)

W2+ /20

Box 1

Moment Resistance

M.R. (in Nm) = 206 (h - 0.5 t_f + 40)

t_f (mm)	h (mm)	Serial Size Mass per metre	Moment Resistance kNm
		762 x 267	
25.4	769.6	197 b	164
21.6	762.0	173 b	163
17.5	753.9	147	162
		686 x 254	
23.7	692.9	170 b	148
21.0	687.6	152 b	148
19.0	683.5	140 b	147
16.2	677.9	125	146
		610 x 229	
22.1	617.0	140 b	133
19.6	611.9	125 b	132
17.3	607.3	113	132
14.8	602.2	101	131
		533 x 210	
21.3	544.6	122 b	118
18.8	539.5	109 b	117
17.4	536.7	101	117
15.6	533.1	92	116
13.2	528.3	82	116
		457 x 191	
19.6	467.4	98 b	102
17.7	463.6	89 bw	102
16.0	460.2	82	101
14.5	457.2	74	101
12.7	453.6	67	100

b - Where t_f > 18 use a butt weld to the flange

bw - If the beam is S275 use a butt weld to the flange

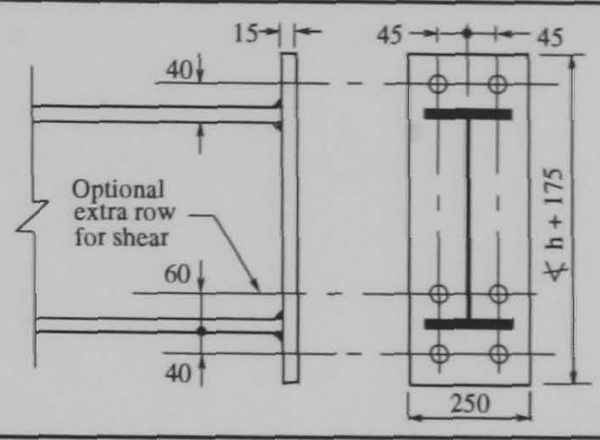

Box 2

Column Limitations

$\Sigma F_b \geq 209$ kN

See Note 2

S275					Grade	S355				
v	iv	iii	ii	i	Zone	i	ii	iii	iv	v
Web Tension	Web Crushing	Web Buckling	Web Shear	Flange Bending	**Serial Size** Mass per metre	Flange Bending	Web Shear	Web Buckling	Web Crushing	Web Tension
					356 x 368					
✓	✓	✓	✓	✓	202	✓	✓	✓	✓	✓
✓	✓	✓	✓	✓	177	✓	✓	✓	✓	✓
✓	✓	✓	✓	✓	153	✓	✓	✓	✓	✓
✓	✓	✓	✓	✓	129	✓	✓	✓	✓	✓
					305 x 305					
✓	✓	✓	✓	✓	283	✓	✓	✓	✓	✓
✓	✓	✓	✓	✓	240	✓	✓	✓	✓	✓
✓	✓	✓	✓	✓	198	✓	✓	✓	✓	✓
✓	✓	✓	✓	✓	158	✓	✓	✓	✓	✓
✓	✓	✓	✓	✓	137	✓	✓	✓	✓	✓
✓	✓	✓	✓	✓	118	✓	✓	✓	✓	✓
✓	✓	✓	✓	✓	97	✓	✓	✓	✓	✓
					254 x 254					
✓	✓	✓	✓	✓	167	✓	✓	✓	✓	✓
✓	✓	✓	✓	✓	132	✓	✓	✓	✓	✓
✓	✓	✓	✓	✓	107	✓	✓	✓	✓	✓
✓	✓	✓	✓	✓	89	✓	✓	✓	✓	✓
✓	✓	✓	406	✓	73	✓	✓	✓	✓	✓
					203 x 203					
✓	✓	✓	✓	✓	86	✓	✓	✓	✓	✓
✓	✓	✓	395	✓	71	✓	✓	✓	✓	✓
✓	✓	✓	349	✓	60	✓	✓	✓	✓	✓
✓	✓	✓	300	✓	52	✓	387	✓	✓	✓
✓	✓	✓	273	*	46	✓	353	✓	✓	✓

* - Less than ΣF_b

▒ - Sections are not designated class 1

Box 3

Shear Resistance

See Note 4

236 kN

(optional extra row adds 184 kN)

W2+/24

Box 1

Moment Resistance

M.R. (in Nm) = 314 (h - 0.5 t_f + 40)

t_f (mm)	h (mm)	Serial Size Mass per metre	Moment Resistance kNm
		762 x 267	
25.4	769.6	197 b	251
21.6	762.0	173 b	249
17.5	753.9	147	247
		686 x 254	
23.7	692.9	170 b	227
21.0	687.6	152 b	225
19.0	683.5	140 b	224
16.2	677.9	125	223
		610 x 229	
22.1	617.0	140 b	203
19.6	611.9	125 b	202
17.3	607.3	113	201
14.8	602.2	101	200
		533 x 210	
21.3	544.6	122 b	180
18.8	539.5	109 b	179
17.4	536.7	101	179
15.6	533.1	92	178
13.2	528.3	82	177
		457 x 191	
19.6	467.4	98 b	156
17.7	463.6	89 bw	156
16.0	460.2	82	155
14.5	457.2	74	154
12.7	453.6	67	153

b - Where t_f > 18 use a butt weld to the flange

bw - If the beam is S275 use a butt weld to the flange

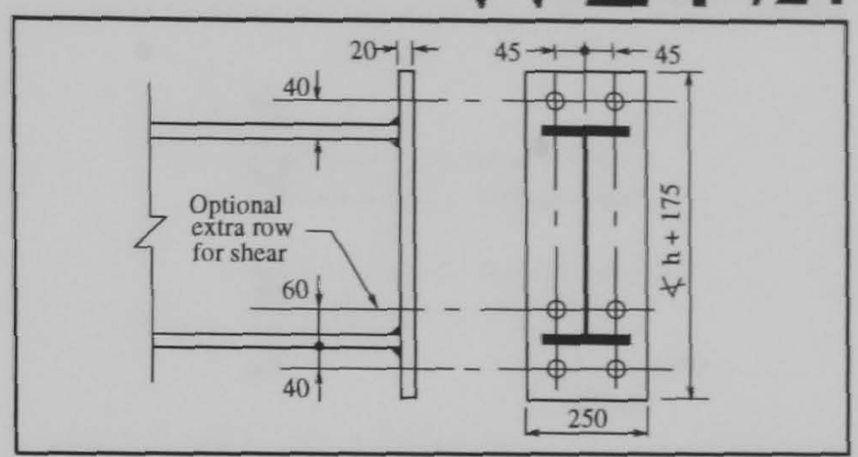

Box 2

Column Limitations

$\Sigma F_b \geq 319$ kN

See Note 2

S275					Grade	S355				
v	iv	iii	ii	i	Zone	i	ii	iii	iv	v
Web Tension	Web Crushing	Web Buckling	Web Shear	Flange Bending	**Serial Size** Mass per metre	Flange Bending	Web Shear	Web Buckling	Web Crushing	Web Tension
					356 x 368					
✓	✓	✓	✓	✓	202	✓	✓	✓	✓	✓
✓	✓	✓	✓	✓	177	✓	✓	✓	✓	✓
✓	✓	✓	✓	✓	153	✓	✓	✓	✓	✓
✓	✓	✓	✓	✓	129	✓	✓	✓	✓	✓
					305 x 305					
✓	✓	✓	✓	✓	283	✓	✓	✓	✓	✓
✓	✓	✓	✓	✓	240	✓	✓	✓	✓	✓
✓	✓	✓	✓	✓	198	✓	✓	✓	✓	✓
✓	✓	✓	✓	✓	158	✓	✓	✓	✓	✓
✓	✓	✓	✓	✓	137	✓	✓	✓	✓	✓
✓	✓	✓	✓	✓	118	✓	✓	✓	✓	✓
✓	✓	✓	565	■	97	✓	✓	✓	✓	✓
					254 x 254					
✓	✓	✓	✓	✓	167	✓	✓	✓	✓	✓
✓	✓	✓	✓	✓	132	✓	✓	✓	✓	✓
✓	✓	✓	613	✓	107	✓	✓	✓	✓	✓
✓	✓	✓	497	✓	89	✓	✓	✓	✓	✓
✓	✓	✓	406	■	73	■	525	✓	✓	✓
					203 x 203					
✓	✓	✓	497	✓	86	✓	✓	✓	✓	✓
✓	✓	✓	395	✓	71	✓	510	✓	✓	✓
✓	✓	✓	349	■	60	■	451	✓	✓	✓
✓	✓	✓	300*	■	52	■	387	✓	✓	✓
✓	✓	✓	273*	■	46	■	353	✓	✓	✓

* - Less than ΣF_b

▒ - Sections are not designated class 1

Box 3

Shear Resistance

See Note 4

340 kN

(optional extra row adds 265 kN)

W3 /20

Box 1

Moment Resistance

M.R. (in Nm) = 208 (h - 0.5 t_f - 60)
190 (h - 0.5 t_f - 150)

t_f (mm)	h (mm)	**Serial Size** Mass per metre	Moment Resistance kNm
		533 x 210	
21.3	544.6	122 b	171
18.8	539.5	109 b	170
17.4	536.7	101	169
15.6	533.1	92	168
13.2	528.3	82	166
		457 x 191	
19.6	467.4	98 b	141
17.7	463.6	89 bw	140
16.0	460.2	82	139
14.5	457.2	74	138
12.7	453.6	67	137
		457 x 152	
18.9	465.1	82 b	140
17.0	461.3	74	139
15.0	457.2	67	138
13.3	454.7	60	137
10.9	449.8	52	136
		406 x 178	
16.0	412.8	74	120
14.3	409.4	67	119
12.8	406.4	60	118
10.9	402.6	54	117
		406 x 140	
11.2	402.3	46	117
8.6	397.3	39	115

b - Where t_f > 18 use a butt weld to the flange
bw- If the beam is S275 use a butt weld to the flange

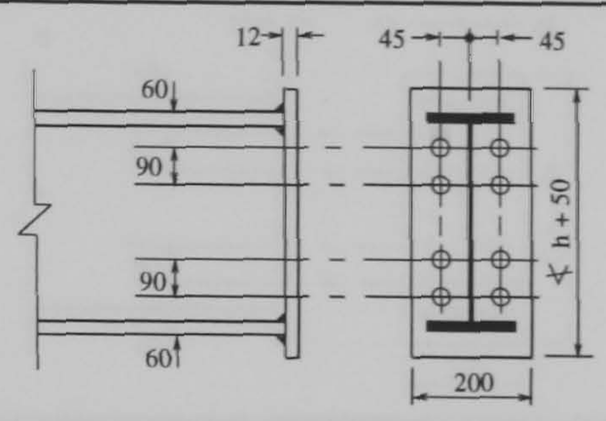

Box 2

Column Limitations

$\Sigma F_b \geq 399$ kN

See Note 2

S275					Grade	S355				
v	iv	iii	ii	i	Zone	i	ii	iii	iv	v
Web Tension	Web Crushing	Web Buckling	Web Shear	Flange Bending	**Serial Size** Mass per metre	Flange Bending	Web Shear	Web Buckling	Web Crushing	Web Tension
					356 x 368					
✓	✓	✓	✓	✓	202	✓	✓	✓	✓	✓
✓	✓	✓	✓	✓	177	✓	✓	✓	✓	✓
✓	✓	✓	✓	✓	153	✓	✓	✓	✓	✓
✓	✓	✓	691	✓	129	✓	✓	✓	✓	✓
					305 x 305					
✓	✓	✓	✓	✓	283	✓	✓	✓	✓	✓
✓	✓	✓	✓	✓	240	✓	✓	✓	✓	✓
✓	✓	✓	✓	✓	198	✓	✓	✓	✓	✓
✓	✓	✓	✓	✓	158	✓	✓	✓	✓	✓
✓	✓	✓	791	✓	137	✓	✓	✓	✓	✓
✓	✓	✓	681	✓	118	✓	✓	✓	✓	✓
✓	✓	✓	565	✓	97	✓	730	✓	✓	✓
					254 x 254					
✓	✓	✓	✓	✓	167	✓	✓	✓	✓	✓
✓	✓	✓	746	✓	132	✓	✓	✓	✓	✓
✓	✓	✓	613	✓	107	✓	791	✓	✓	✓
✓	✓	✓	497	✓	89	✓	642	✓	✓	✓
✓	✓	✓	406	✓	73	✓	525	✓	✓	✓
					203 x 203					
✓	✓	✓	497	✓	86	✓	642	✓	✓	✓
✓	✓	✓	395*	✓	71	✓	510	✓	✓	✓
✓	✓	✓	349*	✓	60	✓	451	✓	✓	✓
✓	■	■	300*	■	52	✓	387*	✓	✓	✓
✓	■	■	273*	■	46	■	353*	■	✓	✓

* - Less than ΣF_b

▒ - Sections are not designated class 1

Box 3

Shear Resistance

See Note 4

236 kN

(optional extra row adds 184 kN)

W3/24

Box 1

Moment Resistance

M.R. (in Nm) = 305 (h - 0.5 t_f - 60)

277 (h - 0.5 t_f - 150)

t_f (mm)	h (mm)	Serial Size Mass per metre	Moment Resistance kNm
		533 x 210	
21.3	544.6	122 b	251
18.8	539.5	109 b	249
17.4	536.7	101	248
15.6	533.1	92	246
13.2	528.3	82	244
		457 x 191	
19.6	467.4	98 b	207
17.7	463.6	89 bw	205
16.0	460.2	82	203
14.5	457.2	74	202
12.7	453.6	67	201
		457 x 152	
18.9	465.1	82 b	206
17.0	461.3	74	204
15.0	457.2	67	202
13.3	454.7	60	201
10.9	449.8	52	199
		406 x 178	
16.0	412.8	74	176
14.3	409.4	67	174
12.8	406.4	60	173
10.9	402.6	54	171
		406 x 140	
11.2	402.3	46	171
8.6	397.3	39	169

b - Where t_f > 18 use a butt weld to the flange

bw- If the beam is S275 use a butt weld to the flange

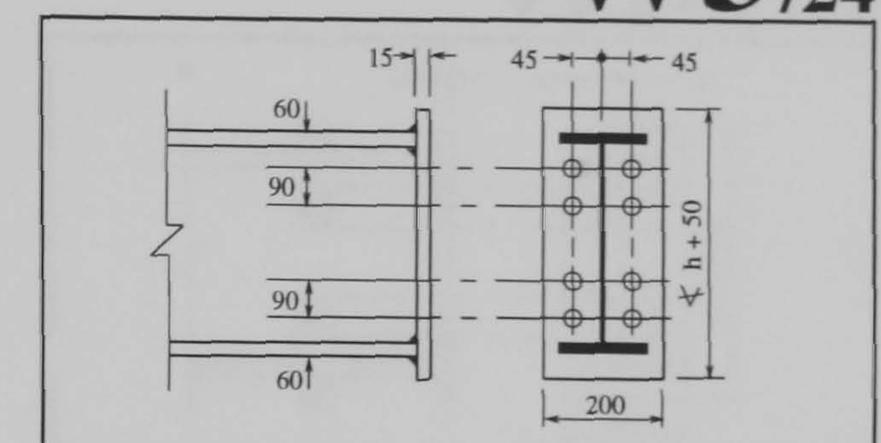

Box 2

Column Limitations

$\Sigma F_b \geq 586$ kN

See Note 2

S275					Grade	S355				
v	iv	iii	ii	i	Zone	i	ii	iii	iv	v
Web Tension	Web Crushing	Web Buckling	Web Shear	Flange Bending	**Serial Size** Mass per metre	Flange Bending	Web Shear	Web Buckling	Web Crushing	Web Tension
					356 x 368					
✓	✓	✓	1089	✓	202	✓	✓	✓	✓	✓
✓	✓	✓	940	✓	177	✓	✓	✓	✓	✓
✓	✓	✓	814	✓	153	✓	1051	✓	✓	✓
✓	✓	✓	691	✓	129	✓	892	✓	✓	✓
					305 x 305					
✓	✓	✓	✓	✓	283	✓	✓	✓	✓	✓
✓	✓	✓	✓	✓	240	✓	✓	✓	✓	✓
✓	✓	✓	1124	✓	198	✓	✓	✓	✓	✓
✓	✓	✓	905	✓	158	✓	1168	✓	✓	✓
✓	✓	✓	791	✓	137	✓	1021	✓	✓	✓
✓	✓	✓	681	✓	118	✓	879	✓	✓	✓
✓	(■)	✓	565*	✓	97	✓	730	✓	✓	✓
					254 x 254					
✓	✓	✓	935	✓	167	✓	✓	✓	✓	✓
✓	✓	✓	746	✓	132	✓	963	✓	✓	✓
✓	✓	✓	613	✓	107	✓	791	✓	✓	✓
✓	✓	✓	497*	✓	89	✓	642	✓	✓	✓
✓	■	■	406*	■	73	✓	525*	■	✓	✓
					203 x 203					
✓	✓	✓	497*	✓	86	✓	642	✓	✓	✓
✓	(■)	■	395*	✓	71	✓	510*	✓	✓	✓
✓	■	■	349*	■	60	■	451*	✓	✓	✓
✓	■	■	300*	■	52	■	387*	■	■	✓
■	■	■	273*	■	46	■	353*	■	■	✓

* - Less than ΣF_b

(■) - Re - calculate

▒ - Sections are not designated class 1

Box 3

Shear Resistance

See Note 4

340 kN

(optional extra row adds 265 kN)

W3+/20

Box 1

Moment Resistance

M.R. (in Nm) = 208 (h - 0.5 t_f - 60)
194 (h - 0.5 t_f - 150)

t_f (mm)	h (mm)	Serial Size Mass per metre	Moment Resistance kNm
		762 x 267	
25.4	769.6	197 b	262
21.6	762.0	173 b	260
17.5	753.9	147	258
		686 x 254	
23.7	692.9	170 b	232
21.0	687.6	152 b	230
19.0	683.5	140 b	229
16.2	677.9	125	227
		610 x 229	
22.1	617.0	140 b	202
19.6	611.9	125 b	200
17.3	607.3	113	199
14.8	602.2	101	197
		533 x 210	
21.3	544.6	122 b	173
18.8	539.5	109 b	171
17.4	536.7	101	171
15.6	533.1	92	169
13.2	528.3	82	168
		457 x 191	
19.6	467.4	98 b	142
17.7	463.6	89 bw	141
16.0	460.2	82	140
14.5	457.2	74	139
12.7	453.6	67	138

b - Where t_f > 18 use a butt weld to the flange

bw - If the beam is S275 use a butt weld to the flange

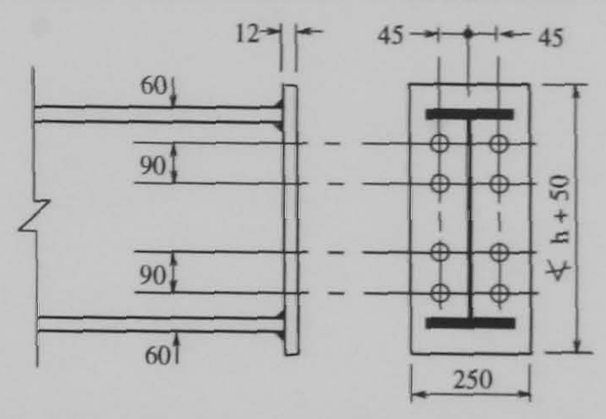

Box 2

Column Limitations

$\Sigma F_b \geq 404$ kN

See Note 2

S275					Grade	S355				
v	iv	iii	ii	i	Zone	i	ii	iii	iv	v
Web Tension	Web Crushing	Web Buckling	Web Shear	Flange Bending	**Serial Size** Mass per metre	Flange Bending	Web Shear	Web Buckling	Web Crushing	Web Tension
					356 x 368					
✓	✓	✓	✓	✓	202	✓	✓	✓	✓	✓
✓	✓	✓	✓	✓	177	✓	✓	✓	✓	✓
✓	✓	✓	✓	✓	153	✓	✓	✓	✓	✓
✓	✓	✓	691	✓	129	✓	✓	✓	✓	✓
					305 x 305					
✓	✓	✓	✓	✓	283	✓	✓	✓	✓	✓
✓	✓	✓	✓	✓	240	✓	✓	✓	✓	✓
✓	✓	✓	✓	✓	198	✓	✓	✓	✓	✓
✓	✓	✓	✓	✓	158	✓	✓	✓	✓	✓
✓	✓	✓	791	✓	137	✓	✓	✓	✓	✓
✓	✓	✓	681	✓	118	✓	✓	✓	✓	✓
✓	✓	✓	565	✓	97	✓	730	✓	✓	✓
					254 x 254					
✓	✓	✓	✓	✓	167	✓	✓	✓	✓	✓
✓	✓	✓	746	✓	132	✓	✓	✓	✓	✓
✓	✓	✓	613	✓	107	✓	791	✓	✓	✓
✓	✓	✓	497	✓	89	✓	642	✓	✓	✓
✓	✓	✓	406	✓	73	✓	525	✓	✓	✓
					203 x 203					
✓	✓	✓	497	✓	86	✓	642	✓	✓	✓
✓	✓	✓	395*	✓	71	✓	510	✓	✓	✓
✓	✓	✓	349*	✓	60	✓	451	✓	✓	✓
✓	■	■	300*	■	52	✓	387*	✓	✓	✓
✓	■	■	273*	■	46	■	353*	■	✓	✓

* - Less than ΣF_b

▒ - Sections are not designated class 1

Box 3

Shear Resistance

See Note 4

236 kN

(optional extra row adds 184 kN)

W3+/24

Box 1

Moment Resistance

M.R. (in Nm) = 305 (h - 0.5 t_f - 60)
284 (h - 0.5 t_f - 150)

t_f (mm)	h (mm)	Serial Size Mass per metre	Moment Resistance kNm
		762 x 267	
25.4	769.6	197 b	385
21.6	762.0	173 b	382
17.5	753.9	147	378
		686 x 254	
23.7	692.9	170 b	341
21.0	687.6	152 b	338
19.0	683.5	140 b	336
16.2	677.9	125	334
		610 x 229	
22.1	617.0	140 b	296
19.6	611.9	125 b	294
17.3	607.3	113	292
14.8	602.2	101	290
		533 x 210	
21.3	544.6	122 b	254
18.8	539.5	109 b	252
17.4	536.7	101	250
15.6	533.1	92	249
13.2	528.3	82	247
		457 x 191	
19.6	467.4	98 b	209
17.7	463.6	89 bw	207
16.0	460.2	82	206
14.5	457.2	74	204
12.7	453.6	67	203

b - Where t_f > 18 use a butt weld to the flange

bw - If the beam is S275 use a butt weld to the flange

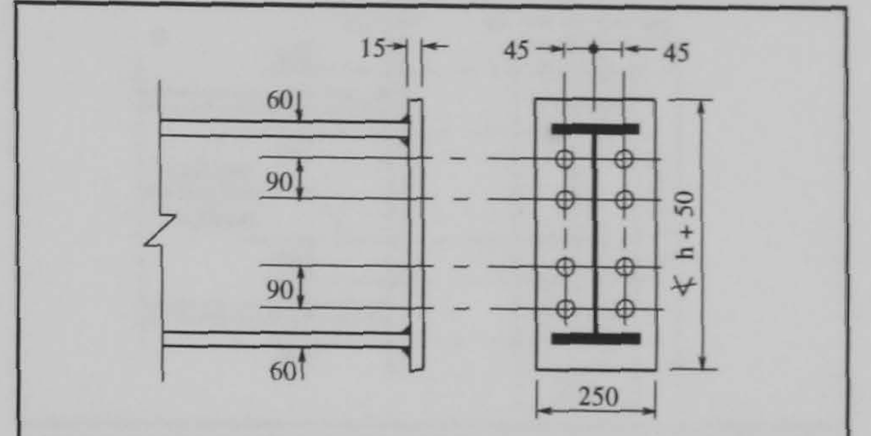

Box 2

Column Limitations

$\Sigma F_b \geq 594$ kN

See Note 2

S275					Grade	S355				
v	iv	iii	ii	i	Zone	i	ii	iii	iv	v
Web Tension	Web Crushing	Web Buckling	Web Shear	Flange Bending	**Serial Size** Mass per metre	Flange Bending	Web Shear	Web Buckling	Web Crushing	Web Tension
					356 x 368					
✓	✓	✓	**1089**	✓	202	✓	✓	✓	✓	✓
✓	✓	✓	**940**	✓	177	✓	✓	✓	✓	✓
✓	✓	✓	**814**	✓	153	✓	**1051**	✓	✓	✓
✓	✓	✓	**691**	✓	129	✓	**892**	✓	✓	✓
					305 x 305					
✓	✓	✓	✓	✓	283	✓	✓	✓	✓	✓
✓	✓	✓	✓	✓	240	✓	✓	✓	✓	✓
✓	✓	✓	**1124**	✓	198	✓	✓	✓	✓	✓
✓	✓	✓	**905**	✓	158	✓	**1168**	✓	✓	✓
✓	✓	✓	**791**	✓	137	✓	**1021**	✓	✓	✓
✓	✓	✓	**681**	✓	118	✓	**879**	✓	✓	✓
✓	(■)	✓	**565***	✓	97	✓	**730**	✓	✓	✓
					254 x 254					
✓	✓	✓	**935**	✓	167	✓	✓	✓	✓	✓
✓	✓	✓	**746**	✓	132	✓	**963**	✓	✓	✓
✓	✓	✓	**613**	✓	107	✓	**791**	✓	✓	✓
✓	✓	✓	**497***	✓	89	✓	**642**	✓	✓	✓
✓	■	■	**406***	■	73	✓	**525***	■	✓	✓
					203 x 203					
✓	✓	✓	**497***	✓	86	✓	**642**	✓	✓	✓
✓	(■)	■	**395***	✓	71	✓	**510***	✓	✓	✓
✓	■	■	**349***	■	60	■	**451***	■	✓	✓
■	■	■	**300***	■	52	■	**387***	■	■	✓
■	■	■	**273***	■	46	■	**353***	■	■	✓

* - Less than ΣF_b

(■) - Re - calculate

▒ - Sections are not designated class 1

Box 3

Shear Resistance

See Note 4

340 kN

(optional extra row adds 265 kN)

W4/20

Box 1

Moment Resistance

M.R. (in Nm) = $124 (h - 0.5\ t_f + 40)$

$208 (h - 0.5\ t_f - 60)$

t_f (mm)	h (mm)	**Serial Size** Mass per metre	Moment Resistance kNm
		533 x 210	
21.3	544.6	122 b	169
18.8	539.5	109 b	168
17.4	536.7	101	167
15.6	533.1	92	167
13.2	528.3	82	165
		457 x 191	
19.6	467.4	98 b	144
17.7	463.6	89 bw	143
16.0	460.2	82	142
14.5	457.2	74	142
12.7	453.6	67	141
		457 x 152	
18.9	465.1	82 b	143
17.0	461.3	74	142
15.0	457.2	67	141
13.3	454.7	60	141
10.9	449.8	52	140
		406 x 178	
16.0	412.8	74	127
14.3	409.4	67	126
12.8	406.4	60	125
10.9	402.6	54	124
		406 x 140	
11.2	402.3	46	124
8.6	397.3	39	123
		356 x 171	
15.7	364.0	67	110
13.0	358.6	57	109
11.5	355.6	51	108
9.7	352.0	45	107
		356 x 127	
10.7	352.8	39	108
8.5	348.5	33	107
		305 x 165	
13.7	310.9	54	93
11.8	307.1	46	92
10.2	303.8	40	91
		305 x 127	
14.0	310.4	48	93
12.1	306.6	42	92
10.7	303.8	37	91
		305 x 102	
10.8	312.7	33	94
8.9	308.9	28	93
6.8	304.8	25	92
		254 x 146	
12.7	259.6	43	76
10.9	256.0	37	75
8.6	251.5	31	74
		254 x 102	
10.0	260.4	28	77
8.4	257.0	25	76
6.8	254.0	22	76

b - Where $t_f > 18$ use a butt weld to the flange

bw- If the beam is S275 use a butt weld to the flange

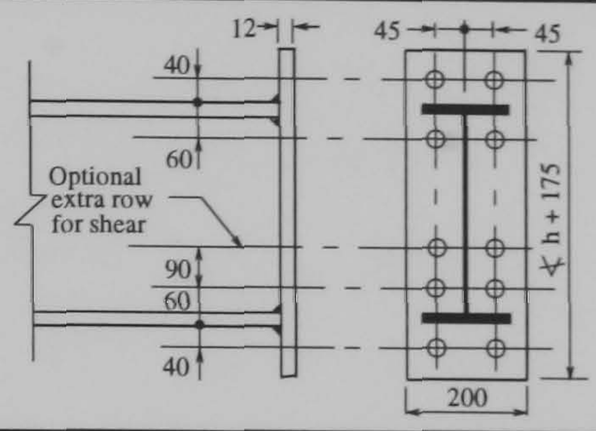

Box 2

Column Limitations

$\Sigma F_b \geq 338$ kN

See Note 2

S275					Grade	S355				
v	iv	iii	ii	i	Zone	i	ii	iii	iv	v
Web Tension	Web Crushing	Web Buckling	Web Shear	Flange Bending	**Serial Size** Mass per metre	Flange Bending	Web Shear	Web Buckling	Web Crushing	Web Tension
					356 x 368					
✓	✓	✓	✓	✓	202	✓	✓	✓	✓	✓
✓	✓	✓	✓	✓	177	✓	✓	✓	✓	✓
✓	✓	✓	✓	✓	153	✓	✓	✓	✓	✓
✓	✓	✓	✓	✓	129	✓	✓	✓	✓	✓
					305 x 305					
✓	✓	✓	✓	✓	283	✓	✓	✓	✓	✓
✓	✓	✓	✓	✓	240	✓	✓	✓	✓	✓
✓	✓	✓	✓	✓	198	✓	✓	✓	✓	✓
✓	✓	✓	✓	✓	158	✓	✓	✓	✓	✓
✓	✓	✓	✓	✓	137	✓	✓	✓	✓	✓
✓	✓	✓	✓	✓	118	✓	✓	✓	✓	✓
✓	✓	✓	565	✓	97	✓	✓	✓	✓	✓
					254 x 254					
✓	✓	✓	✓	✓	167	✓	✓	✓	✓	✓
✓	✓	✓	✓	✓	132	✓	✓	✓	✓	✓
✓	✓	✓	613	✓	107	✓	✓	✓	✓	✓
✓	✓	✓	497	✓	89	✓	642	✓	✓	✓
✓	✓	✓	406	✓	73	✓	525	✓	✓	✓
					203 x 203					
✓	✓	✓	497	✓	86	✓	642	✓	✓	✓
✓	✓	✓	395	✓	71	✓	510	✓	✓	✓
✓	✓	✓	349	✓	60	✓	451	✓	✓	✓
✓	✓	✓	300*	✓	52	✓	387	✓	✓	✓
✓	(■)	■	273*	■	46	✓	353	✓	✓	✓

* - Less than ΣF_b

(■)- Re - calculate

- Sections are not designated class 1

Box 3

Shear Resistance

See Note 4

236 kN

(optional extra row adds 184 kN)

W4/24

Box 1

Moment Resistance

M.R. (in Nm) = 193 (h - 0.5 t_f + 40)

305 (h - 0.5 t_f - 60)

t_f (mm)	h (mm)	Serial Size Mass per metre	Moment Resistance kNm
		533 x 210	
21.3	544.6	122 b	256
18.8	539.5	109 b	254
17.4	536.7	101	253
15.6	533.1	92	251
13.2	528.3	82	250
		457 x 191	
19.6	467.4	98 b	218
17.7	463.6	89 bw	216
16.0	460.2	82	215
14.5	457.2	74	214
12.7	453.6	67	212
		457 x 152	
18.9	465.1	82 b	217
17.0	461.3	74	215
15.0	457.2	67	214
13.3	454.7	60	213
10.9	449.8	52	211
		406 x 178	
16.0	412.8	74	191
14.3	409.4	67	190
12.8	406.4	60	189
10.9	402.6	54	187
		406 x 140	
11.2	402.3	46	187
8.6	397.3	39	185
		356 x 171	
15.7	364.0	67	167
13.0	358.6	57	165
11.5	355.6	51	164
9.7	352.0	45	163
		356 x 127	
10.7	352.8	39	163
8.5	348.5	33	161
		305 x 165	
13.7	310.9	54	141
11.8	307.1	46	140
10.2	303.8	40	138
		305 x 127	
14.0	310.4	48	141
12.1	306.6	42	139
10.7	303.8	37	138
		305 x 102	
10.8	312.7	33	143
8.9	308.9	28	141
6.8	304.8	25	140
		254 x 146	
12.7	259.6	43	116
10.9	256.0	37	114
8.6	251.5	31	113
		254 x 102	
10.0	260.4	28	117
8.4	257.0	25	115
6.8	254.0	22	114

b - Where t_f > 18 use a butt weld to the flange

bw- If the beam is S275 use a butt weld to the flange

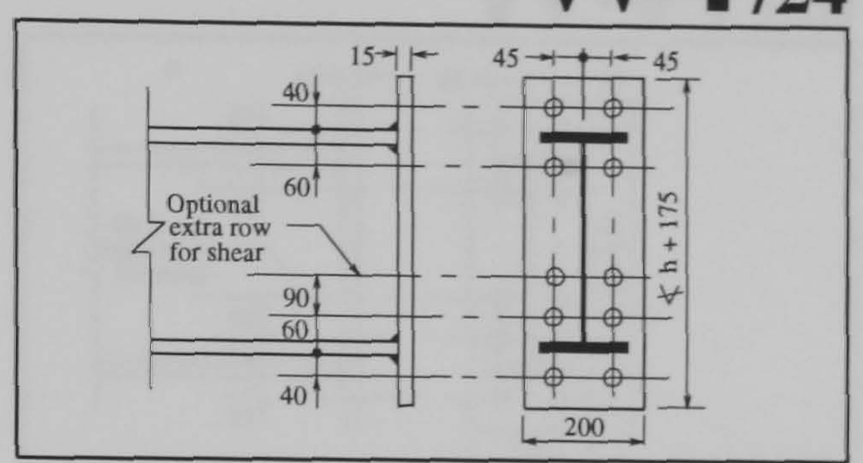

Box 2

Column Limitations

$\Sigma F_b \geq 509$ kN

See Note 2

S275					Grade	S355				
v	iv	iii	ii	i	Zone	i	ii	iii	iv	v
Web Tension	Web Crushing	Web Buckling	Web Shear	Flange Bending	**Serial Size** Mass per metre	Flange Bending	Web Shear	Web Buckling	Web Crushing	Web Tension
					356 x 368					
✓	✓	✓	✓	✓	202	✓	✓	✓	✓	✓
✓	✓	✓	940	✓	177	✓	✓	✓	✓	✓
✓	✓	✓	814	✓	153	✓	✓	✓	✓	✓
✓	✓	✓	691	✓	129	✓	892	✓	✓	✓
					305 x 305					
✓	✓	✓	✓	✓	283	✓	✓	✓	✓	✓
✓	✓	✓	✓	✓	240	✓	✓	✓	✓	✓
✓	✓	✓	✓	✓	198	✓	✓	✓	✓	✓
✓	✓	✓	905	✓	158	✓	✓	✓	✓	✓
✓	✓	✓	791	✓	137	✓	✓	✓	✓	✓
✓	✓	✓	681	✓	118	✓	879	✓	✓	✓
✓	✓	✓	565	✓	97	✓	730	✓	✓	✓
					254 x 254					
✓	✓	✓	935	✓	167	✓	✓	✓	✓	✓
✓	✓	✓	746	✓	132	✓	963	✓	✓	✓
✓	✓	✓	613	✓	107	✓	791	✓	✓	✓
✓	✓	✓	497*	✓	89	✓	642	✓	✓	✓
✓	■	■	406*	■	73	✓	525	✓	✓	✓
					203 x 203					
✓	✓	✓	497*	✓	86	✓	642	✓	✓	✓
✓	✓	✓	395*	✓	71	✓	510	✓	✓	✓
✓	■	■	349*	■	60	✓	451*	✓	✓	✓
✓	■	■	300*	■	52	■	387*	■	(■)	✓
✓	■	■	273*	■	46	■	353*	■	■	✓

* - Less than ΣF_b

(■) - Re - calculate

▒ - Sections are not designated class 1

Box 3

Shear Resistance

See Note 4

340 kN

(optional extra row adds 265 kN)

W4+/20

Box 1

Moment Resistance

M.R. (in Nm) = $155 (h - 0.5\, t_f + 40)$

$208 (h - 0.5\, t_f - 60)$

t_f (mm)	h (mm)	Serial Size Mass per metre	Moment Resistance kNm
		762 x 267	
25.4	769.6	197 b	268
21.6	762.0	173 b	266
17.5	753.9	147	264
		686 x 254	
23.7	692.9	170 b	240
21.0	687.6	152 b	239
19.0	683.5	140 b	238
16.2	677.9	125	236
		610 x 229	
22.1	617.0	140 b	213
19.6	611.9	125 b	212
17.3	607.3	113	211
14.8	602.2	101	209
		533 x 210	
21.3	544.6	122 b	187
18.8	539.5	109 b	186
17.4	536.7	101	185
15.6	533.1	92	184
13.2	528.3	82	183
		457 x 191	
19.6	467.4	98 b	159
17.7	463.6	89 bw	158
16.0	460.2	82	158
14.5	457.2	74	157
12.7	453.6	67	156

b - Where $t_f > 18$ use a butt weld to the flange

bw - If the beam is S275 use a butt weld to the flange

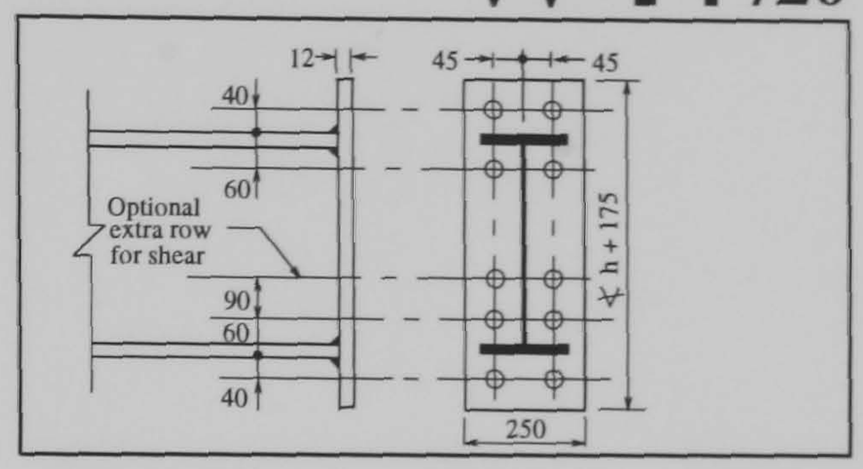

Box 2

Column Limitations

$\Sigma F_b \geq 370$ kN

See Note 2

S275					Grade	S355				
v	iv	iii	ii	i	Zone	i	ii	iii	iv	v
Web Tension	Web Crushing	Web Buckling	Web Shear	Flange Bending	**Serial Size** Mass per metre	Flange Bending	Web Shear	Web Buckling	Web Crushing	Web Tension
					356 x 368					
✓	✓	✓	✓	✓	202	✓	✓	✓	✓	✓
✓	✓	✓	✓	✓	177	✓	✓	✓	✓	✓
✓	✓	✓	✓	✓	153	✓	✓	✓	✓	✓
✓	✓	✓	691	✓	129	✓	✓	✓	✓	✓
					305 x 305					
✓	✓	✓	✓	✓	283	✓	✓	✓	✓	✓
✓	✓	✓	✓	✓	240	✓	✓	✓	✓	✓
✓	✓	✓	✓	✓	198	✓	✓	✓	✓	✓
✓	✓	✓	✓	✓	158	✓	✓	✓	✓	✓
✓	✓	✓	✓	✓	137	✓	✓	✓	✓	✓
✓	✓	✓	681	✓	118	✓	✓	✓	✓	✓
✓	✓	✓	565	✓	97	✓	730	✓	✓	✓
					254 x 254					
✓	✓	✓	✓	✓	167	✓	✓	✓	✓	✓
✓	✓	✓	✓	✓	132	✓	✓	✓	✓	✓
✓	✓	✓	613	✓	107	✓	✓	✓	✓	✓
✓	✓	✓	497	✓	89	✓	642	✓	✓	✓
✓	✓	✓	406	✓	73	✓	525	✓	✓	✓
					203 x 203					
✓	✓	✓	497	✓	86	✓	642	✓	✓	✓
✓	✓	✓	395	✓	71	✓	510	✓	✓	✓
✓	✓	✓	349*	✓	60	✓	451	✓	✓	✓
✓	✓	✓	300*	✓	52	✓	387	✓	✓	✓
✓	■	■	273*	■	46	✓	353*	✓	✓	✓

* - Less than ΣF_b

▒ - Sections are not designated class 1

Box 3

Shear Resistance

See Note 4

236 kN

(optional extra row adds 184 kN)

W4+/24

Box 1

Moment Resistance

M.R. (in Nm) = $242 (h - 0.5\, t_f + 40)$

$305 (h - 0.5\, t_f - 60)$

t_f (mm)	h (mm)	Serial Size Mass per metre	Moment Resistance kNm
		762 x 267	
25.4	769.6	197 b	405
21.6	762.0	173 b	402
17.5	753.9	147	399
		686 x 254	
23.7	692.9	170 b	364
21.0	687.6	152 b	362
19.0	683.5	140 b	360
16.2	677.9	125	358
		610 x 229	
22.1	617.0	140 b	323
19.6	611.9	125 b	321
17.3	607.3	113	319
14.8	602.2	101	317
		533 x 210	
21.3	544.6	122 b	283
18.8	539.5	109 b	281
17.4	536.7	101	280
15.6	533.1	92	279
13.2	528.3	82	277
		457 x 191	
19.6	467.4	98 b	242
17.7	463.6	89 bw	240
16.0	460.2	82	239
14.5	457.2	74	237
12.7	453.6	67	236

b - Where $t_f > 18$ use a butt weld to the flange

bw - If the beam is S275 use a butt weld to the flange

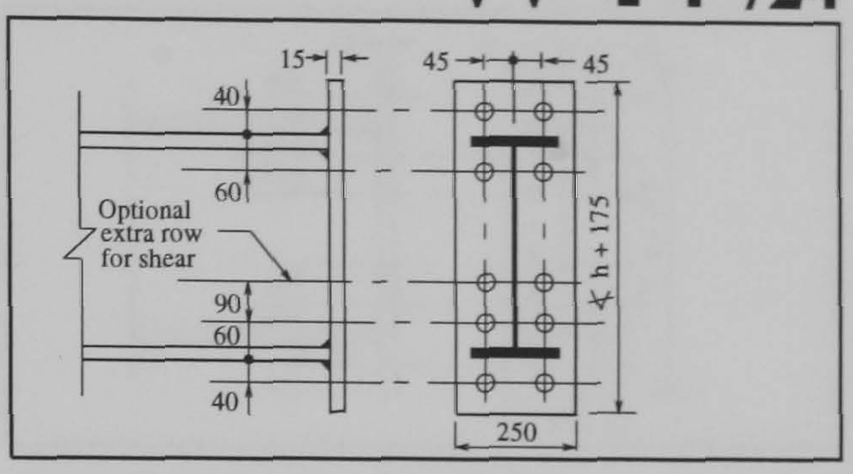

Box 2

Column Limitations

$\Sigma F_b \geq 560$ kN

See Note 2

S275					Grade	S355				
v	iv	iii	ii	i	Zone	i	ii	iii	iv	v
Web Tension	Web Crushing	Web Buckling	Web Shear	Flange Bending	**Serial Size** Mass per metre	Flange Bending	Web Shear	Web Buckling	Web Crushing	Web Tension
					356 x 368					
✓	✓	✓	1089	✓	202	✓	✓	✓	✓	✓
✓	✓	✓	940	✓	177	✓	✓	✓	✓	✓
✓	✓	✓	814	✓	153	✓	1051	✓	✓	✓
✓	✓	✓	691	✓	129	✓	892	✓	✓	✓
					305 x 305					
✓	✓	✓	✓	✓	283	✓	✓	✓	✓	✓
✓	✓	✓	✓	✓	240	✓	✓	✓	✓	✓
✓	✓	✓	✓	✓	198	✓	✓	✓	✓	✓
✓	✓	✓	905	✓	158	✓	✓	✓	✓	✓
✓	✓	✓	791	✓	137	✓	1021	✓	✓	✓
✓	✓	✓	681	✓	118	✓	879	✓	✓	✓
✓	✓	✓	565	✓	97	✓	730	✓	✓	✓
					254 x 254					
✓	✓	✓	935	✓	167	✓	✓	✓	✓	✓
✓	✓	✓	746	✓	132	✓	963	✓	✓	✓
✓	✓	✓	613	✓	107	✓	791	✓	✓	✓
✓	✓	✓	497*	✓	89	✓	642	✓	✓	✓
✓	■	■	406*	■	73	✓	525*	■	✓	✓
					203 x 203					
✓	✓	✓	497*	✓	86	✓	642	✓	✓	✓
✓	✓	■	395*	✓	71	✓	510*	✓	✓	✓
✓	■	■	349*	■	60	✓	451*	✓	✓	✓
✓	■	■	300*	■	52	■	387*	■	■	✓
✓	■	■	273*	■	46	■	353*	■	■	✓

* - Less than ΣF_b

▒ - Sections are not designated class 1

Box 3

Shear Resistance

See Note 4

340 kN

(optional extra row adds 265 kN)

W5 /20

Box 1

Moment Resistance

M.R. (in Nm) = 124 (h - 0.5 t_f + 40)

208 (h - 0.5 t_f - 60)

190 (h - 0.5 t_f - 150)

t_f (mm)	h (mm)	**Serial Size** Mass per metre	Moment Resistance kNm
		533 x 210	
21.3	544.6	122 b	242
18.8	539.5	109 b	240
17.4	536.7	101	239
15.6	533.1	92	238
13.2	528.3	82	236
		457 x 191	
19.6	467.4	98 b	202
17.7	463.6	89 bw	201
16.0	460.2	82	200
14.5	457.2	74	198
12.7	453.6	67	197
		457 x 152	
18.9	465.1	82 b	201
17.0	461.3	74	200
15.0	457.2	67	198
13.3	454.7	60	197
10.9	449.8	52	195
		406 x 178	
16.0	412.8	74	175
14.3	409.4	67	174
12.8	406.4	60	172
10.9	402.6	54	171
		406 x 140	
11.2	402.3	46	171
8.6	397.3	39	169

b - Where t_f > 18 use a butt weld to the flange

bw- If the beam is S275 use a butt weld to the flange

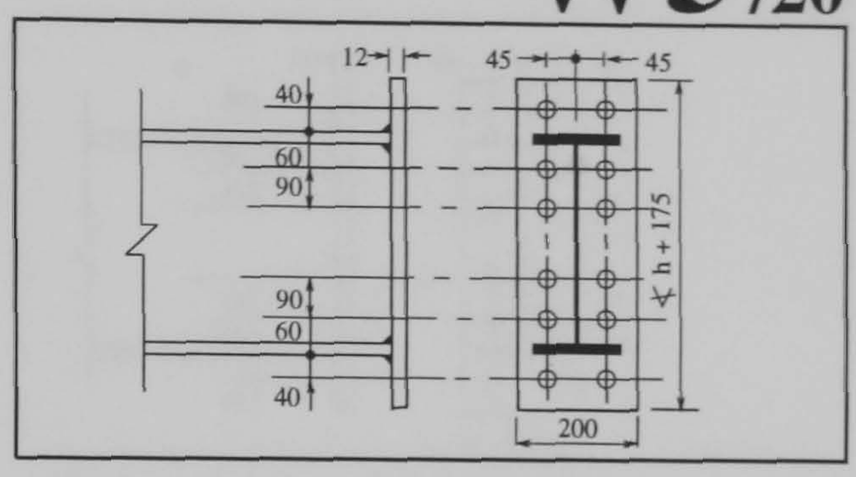

Box 2

Column Limitations

ΣF_b ⩾ 529 kN

See Note 2

S275					Grade	S355				
v	iv	iii	ii	i	Zone	i	ii	iii	iv	v
Web Tension	Web Crushing	Web Buckling	Web Shear	Flange Bending	**Serial Size** Mass per metre	Flange Bending	Web Shear	Web Buckling	Web Crushing	Web Tension
					356 x 368					
✓	✓	✓	✓	✓	202	✓	✓	✓	✓	✓
✓	✓	✓	940	✓	177	✓	✓	✓	✓	✓
✓	✓	✓	814	✓	153	✓	1051	✓	✓	✓
✓	✓	✓	691	✓	129	✓	892	✓	✓	✓
					305 x 305					
✓	✓	✓	✓	✓	283	✓	✓	✓	✓	✓
✓	✓	✓	✓	✓	240	✓	✓	✓	✓	✓
✓	✓	✓	✓	✓	198	✓	✓	✓	✓	✓
✓	✓	✓	905	✓	158	✓	✓	✓	✓	✓
✓	✓	✓	791	✓	137	✓	1021	✓	✓	✓
✓	✓	✓	681	✓	118	✓	879	✓	✓	✓
✓	✓	✓	565	✓	97	✓	730	✓	✓	✓
					254 x 254					
✓	✓	✓	935	✓	167	✓	✓	✓	✓	✓
✓	✓	✓	746	✓	132	✓	963	✓	✓	✓
✓	✓	✓	613	✓	107	✓	791	✓	✓	✓
✓	✓	✓	497*	✓	89	✓	642	✓	✓	✓
✓	■	■	406*	■	73	✓	525*	✓	✓	✓
					203 x 203					
✓	✓	✓	497*	✓	86	✓	642	✓	✓	✓
✓	✓	✓	395*	✓	71	✓	510*	✓	✓	✓
✓	■	■	349*	■	60	■	451*	✓	✓	✓
✓	■	■	300*	■	52	■	387*	■	■	✓
✓	■	■	273*	■	46	■	353*	■	■	✓

* - Less than ΣF_b

▒ - Sections are not designated class 1

Box 3

Shear Resistance

See Note 4

236 kN

(optional extra row adds 184 kN)

W5 /24

Box 1

Moment Resistance

M.R. (in Nm) = 193 (h - 0.5 t_f + 40)

305 (h - 0.5 t_f - 60)

277 (h - 0.5 t_f - 150)

t_f (mm)	h (mm)	**Serial Size** Mass per metre	Moment Resistance kNm
		533 x 210	
21.3	544.6	122 b	362
18.8	539.5	109 b	359
17.4	536.7	101	357
15.6	533.1	92	355
13.2	528.3	82	353
		457 x 191	
19.6	467.4	98 b	303
17.7	463.6	89 bw	301
16.0	460.2	82	299
14.5	457.2	74	297
12.7	453.6	67	295
		457 x 152	
18.9	465.1	82 b	301
17.0	461.3	74	299
15.0	457.2	67	297
13.3	454.7	60	295
10.9	449.8	52	293
		406 x 178	
16.0	412.8	74	262
14.3	409.4	67	260
12.8	406.4	60	258
10.9	402.6	54	256
		406 x 140	
11.2	402.3	46	256
8.6	397.3	39	253

b - Where t_f > 18 use a butt weld to the flange

bw - If the beam is S275 use a butt weld to the flange

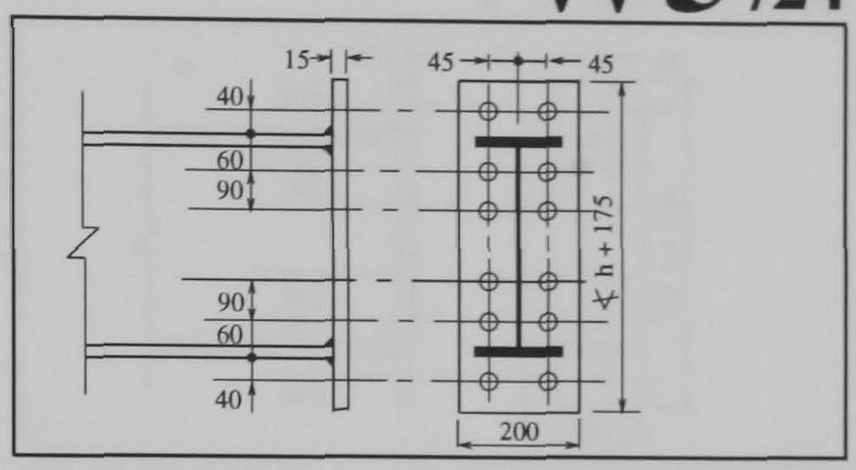

Box 2

Column Limitations

ΣF_b ⩾ 789 kN

See Note 2

S275					Grade	S355				
v	iv	iii	ii	i	Zone	i	ii	iii	iv	v
Web Tension	Web Crushing	Web Buckling	Web Shear	Flange Bending	**Serial Size** Mass per metre	Flange Bending	Web Shear	Web Buckling	Web Crushing	Web Tension
					356 x 368					
✓	✓	✓	1089	✓	202	✓	1406	✓	✓	✓
✓	✓	✓	940	✓	177	✓	1213	✓	✓	✓
✓	✓	✓	814	✓	153	✓	1051	✓	✓	✓
✓	■	■	691*	✓	129	✓	892	✓	✓	✓
					305 x 305					
✓	✓	✓	1502	✓	283	✓	✓	✓	✓	✓
✓	✓	✓	1364	✓	240	✓	✓	✓	✓	✓
✓	✓	✓	1124	✓	198	✓	1451	✓	✓	✓
✓	✓	✓	905	✓	158	✓	1168	✓	✓	✓
✓	✓	✓	791	✓	137	✓	1021	✓	✓	✓
✓	■	✓	681*	✓	118	✓	879	✓	✓	✓
✓	■	■	565*	■	97	■	730*	■	■	✓
					254 x 254					
✓	✓	✓	935	✓	167	✓	1207	✓	✓	✓
✓	✓	✓	746*	✓	132	✓	963	✓	✓	✓
✓	✓	✓	613*	✓	107	✓	791	✓	✓	✓
✓	■	■	497*	■	89	✓	642*	■	(■)	✓
✓	■	■	406*	■	73	■	525*	■	■	✓
					203 x 203					
✓	(■)	■	497*	✓	86	✓	642*	✓	✓	✓
✓	■	■	395*	■	71	■	510*	■	■	✓
✓	■	■	349*	■	60	■	451*	■	■	✓
✓	■	■	300*	■	52	■	387*	■	■	✓
■	■	■	273*	■	46	■	353*	■	■	✓

* - Less than ΣF_b

(■) - Re - calculate

▒ - Sections are not designated class 1

Box 3

Shear Resistance

See Note 4

340 kN

(optional extra row adds 265 kN)

W5+/20

Box 1

Moment Resistance

M.R. (in Nm) = 155 (h - 0.5 t_f + 40)

208 (h - 0.5 t_f - 60)

194 (h - 0.5 t_f - 150)

t_f (mm)	h (mm)	**Serial Size** Mass per metre	Moment Resistance kNm
		762 x 267	
25.4	769.6	197 b	386
21.6	762.0	173 b	383
17.5	753.9	147	379
		686 x 254	
23.7	692.9	170 b	344
21.0	687.6	152 b	341
19.0	683.5	140 b	340
16.2	677.9	125	337
		610 x 229	
22.1	617.0	140 b	302
19.6	611.9	125 b	300
17.3	607.3	113	298
14.8	602.2	101	296
		533 x 210	
21.3	544.6	122 b	262
18.8	539.5	109 b	260
17.4	536.7	101	258
15.6	533.1	92	257
13.2	528.3	82	255
		457 x 191	
19.6	467.4	98 b	219
17.7	463.6	89 bw	218
16.0	460.2	82	216
14.5	457.2	74	215
12.7	453.6	67	213

b - Where t_f > 18 use a butt weld to the flange

bw - If the beam is S275 use a butt weld to the flange

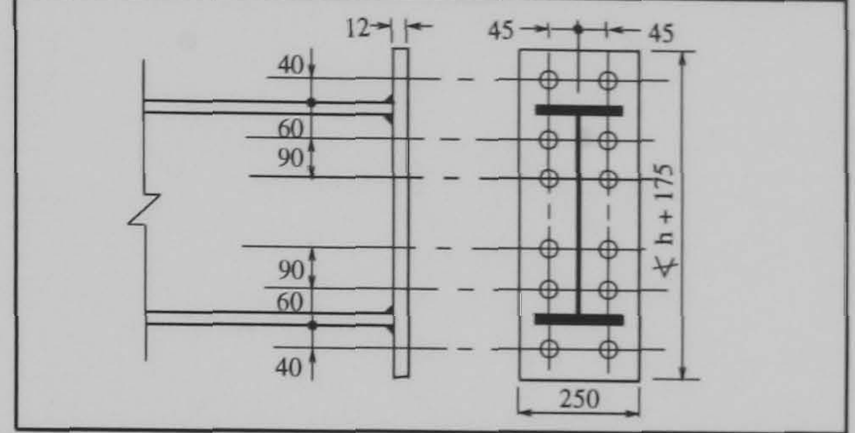

Box 2

Column Limitations

$\Sigma F_b \geq 567$ kN

See Note 2

S275					Grade	S355				
v	iv	iii	ii	i	Zone	i	ii	iii	iv	v
Web Tension	Web Crushing	Web Buckling	Web Shear	Flange Bending	**Serial Size** Mass per metre	Flange Bending	Web Shear	Web Buckling	Web Crushing	Web Tension
					356 x 368					
✓	✓	✓	**1089**	✓	202	✓	✓	✓	✓	✓
✓	✓	✓	**940**	✓	177	✓	✓	✓	✓	✓
✓	✓	✓	**814**	✓	153	✓	**1051**	✓	✓	✓
✓	✓	✓	**691**	✓	129	✓	**892**	✓	✓	✓
					305 x 305					
✓	✓	✓	✓	✓	283	✓	✓	✓	✓	✓
✓	✓	✓	✓	✓	240	✓	✓	✓	✓	✓
✓	✓	✓	**1124**	✓	198	✓	✓	✓	✓	✓
✓	✓	✓	**905**	✓	158	✓	✓	✓	✓	✓
✓	✓	✓	**791**	✓	137	✓	**1021**	✓	✓	✓
✓	✓	✓	**681**	✓	118	✓	**879**	✓	✓	✓
✓	✓	✓	**565***	✓	97	✓	**730**	✓	✓	✓
					254 x 254					
✓	✓	✓	**935**	✓	167	✓	✓	✓	✓	✓
✓	✓	✓	**746**	✓	132	✓	**963**	✓	✓	✓
✓	✓	✓	**613**	✓	107	✓	**791**	✓	✓	✓
✓	✓	✓	**497***	✓	89	✓	**642**	✓	✓	✓
✓	■	■	**406***	■	73	✓	**525***	■	✓	✓
					203 x 203					
✓	✓	✓	**497***	✓	86	✓	**642**	✓	✓	✓
✓	(■)	■	**395***	✓	71	✓	**510***	✓	✓	✓
✓	■	■	**349***	■	60	■	**451***	✓	✓	✓
✓	■	■	**300***	■	52	■	**387***	■	■	✓
✓	■	■	**273***	■	46	■	**353***	■	■	✓

* - Less than ΣF_b

(■) - Re - calculate

▒ - Sections are not designated class 1

Box 3

Shear Resistance

See Note 4

236 kN

(optional extra row adds 184 kN)

W5+/24

Box 1

Moment Resistance

M.R. (in Nm) = 242 (h - 0.5 t_f + 40)

305 (h - 0.5 t_f - 60)

284 (h - 0.5 t_f - 150)

t_f (mm)	h (mm)	Serial Size Mass per metre	Moment Resistance kNm
		762 x 267	
25.4	769.6	197 b	578
21.6	762.0	173 b	573
17.5	753.9	147	568
		686 x 254	
23.7	692.9	170 b	515
21.0	687.6	152 b	512
19.0	683.5	140 b	509
16.2	677.9	125	506
		610 x 229	
22.1	617.0	140 b	452
19.6	611.9	125 b	449
17.3	607.3	113	446
14.8	602.2	101	443
		533 x 210	
21.3	544.6	122 b	393
18.8	539.5	109 b	389
17.4	536.7	101	388
15.6	533.1	92	385
13.2	528.3	82	382
		457 x 191	
19.6	467.4	98 b	329
17.7	463.6	89 bw	327
16.0	460.2	82	325
14.5	457.2	74	323
12.7	453.6	67	321

b - Where t_f > 18 use a butt weld to the flange

bw - If the beam is S275 use a butt weld to the flange

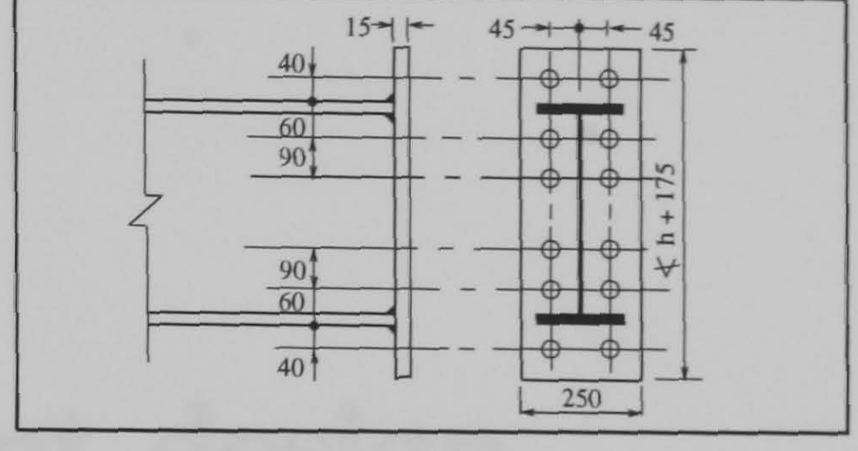

Box 2

Column Limitations

ΣF_b ⩾ 849 kN

See Note 2

S275					Grade	S355				
v	iv	iii	ii	i	Zone	i	ii	iii	iv	v
Web Tension	Web Crushing	Web Buckling	Web Shear	Flange Bending	**Serial Size** Mass per metre	Flange Bending	Web Shear	Web Buckling	Web Crushing	Web Tension
					356 x 368					
✓	✓	✓	1089	✓	202	✓	1406	✓	✓	✓
✓	✓	✓	940	✓	177	✓	1213	✓	✓	✓
✓	(■)	✓	814*	✓	153	✓	1051	✓	✓	✓
✓	■	■	691*	✓	129	✓	892	✓	✓	✓
					305 x 305					
✓	✓	✓	1502	✓	283	✓	✓	✓	✓	✓
✓	✓	✓	1364	✓	240	✓	✓	✓	✓	✓
✓	✓	✓	1124	✓	198	✓	1451	✓	✓	✓
✓	✓	✓	905	✓	158	✓	1168	✓	✓	✓
✓	✓	✓	791*	✓	137	✓	1021	✓	✓	✓
✓	■	■	681*	✓	118	✓	879	✓	✓	✓
✓	■	■	565*	■	97	■	730*	■	■	✓
					254 x 254					
✓	✓	✓	935	✓	167	✓	1207	✓	✓	✓
✓	✓	✓	746*	✓	132	✓	963	✓	✓	✓
✓	(■)	✓	613*	✓	107	✓	791*	✓	✓	✓
✓	■	■	497*	■	89	✓	642*	■	■	✓
✓	■	■	406*	■	73	■	525*	■	■	✓
					203 x 203					
✓	■	■	497*	✓	86	✓	642*	✓	✓	✓
✓	■	■	395*	■	71	■	510*	■	■	✓
✓	■	■	349*	■	60	■	451*	■	■	✓
■	■	■	300*	■	52	■	387*	■	■	✓
■	■	■	273*	■	46	■	353*	■	■	✓

* - Less than ΣF_b

(■) - Re - calculate

▒ - Sections are not designated class 1

Box 3

Shear Resistance

See Note 4

340 kN

(optional extra row adds 265 kN)

Appendix B

Wind-Moment design incorporating ductile end plate connections

B.1 Scope

Details for all the frame configurations considered are presented in conjunction with a worked example, to illustrate the design proceedure adopted to choose appropriate connections between the structural members of a typical Wind-Moment frame.

B.2 Frame configurations considered and their design

Table B.1: Wind-Moment design (Min wind + Max gravity)

Basic Frame Type	Frame Identification	Width of Bay (m)	Height of Columns: Ground (m)	Height of Columns: Elevated (m)	No. of Longitudinal Bays	Width of Longitudinal Bays (m)	Gravity Load (kN/m^2): Floor DL	Gravity Load (kN/m^2): Floor LL	Gravity Load (kN/m^2): Roof DL	Gravity Load (kN/m^2): Roof LL	Basic Wind Speed (m/s)	Ground Roughness Factor	Section Designation: Universal Beams Floor	Section Designation: Universal Beams Roof		Section Designation: Universal Columns External	Section Designation: Universal Columns Internal	Connection Requirements: Bending Moment (kNm) Floor	Connection Requirements: Bending Moment (kNm) Roof	Connection Requirements: Shear Force (kN) Floor	Connection Requirements: Shear Force (kN) Roof
2 Storey 1 Bay	**f10 b24**	9.0											**686x254x125**	**457x191x67**	Upto 2nd Storey	**203x203x71**	**N/A**	**125**	**48**	**515**	**207**
2 Storey 4 Bay	**f16 b24**												**686x254x125**	**457x191x67**	Upto 2nd Storey	**203x203x71**	**203x203x71**	**125**	**48**	**515**	**207**
4 Storey 2 Bay	**f22 b24**												**686x254x125**	**457x191x67**	Upto 2nd Storey	**254x254x89**	**305x305x118**	1st - **146** 2nd - **133** 3rd - **124**	**48**	1st - **520** 2nd - **517** 3rd - **515**	**207**
															2nd - 4th Storey	**203x203x60**	**203x203x60**				
4 Storey 4 Bay	**f28 b24**												**686x254x125**	**457x191x67**	Upto 2nd Storey	**254x254x89**	**305x305x118**	1st - **146** 2nd - **133** 3rd - **124**	**48**	1st - **520** 2nd - **517** 3rd - **515**	**207**
															2nd - 4th Storey	**203x203x60**	**203x203x60**				
2 Storey 1 Bay	**f11 b20** **f11 b24**	6.0											**457x191x67**	**406x140x39**	Upto 2nd Storey	**203x203x46**	**N/A**	**60**	**22**	**344**	**138**
2 Storey 4 Bay	**f17 b20** **f17 b24**												**457x191x67**	**406x140x39**	Upto 2nd Storey	**203x203x46**	**203x203x46**	**58**	**22**	**344**	**138**
4 Storey 2 Bay	**f23 b20** **f23 b24**												**457x191x67**	**406x140x39**	Upto 2nd Storey	**203x203x71**	**254x254x89**	1st - **72** 2nd - **63** 3rd - **57**	**22**	1st - **349** 2nd - **346** 3rd - **344**	**138**
															2nd - 4th Storey	**203x203x46**	**203x203x46**				
4 Storey 4 Bay	**f29 b20** **f29 b24**												**457x191x67**	**406x140x39**	Upto 2nd Storey	**203x203x71**	**254x254x89**	1st - **72** 2nd - **63** 3rd - **57**	**22**	1st - **349** 2nd - **346** 3rd - **344**	**138**
															2nd - 4th Storey	**203x203x46**	**203x203x46**				
2 Storey 1 Bay	**f12 b20** **f12 b24**	4.5											**406x140x46**	**305x120x25**	Upto 2nd Storey	**203x203x46**	**N/A**	**42**	**15**	**259**	**104**
2 Storey 4 Bay	**f18 b20** **f18 b24**												**406x140x46**	**305x120x25**	Upto 2nd Storey	**203x203x46**	**203x203x46**	**34**	**13**	**259**	**104**
4 Storey 2 Bay	**f24 b20** **f24 b24**												**406x140x46**	**305x120x25**	Upto 2nd Storey	**203x203x52**	**254x254x73**	1st - **54** 2nd - **43** 3rd - **35**	**14**	1st - **263** 2nd - **260** 3rd - **258**	**104**
															2nd - 4th Storey	**203x203x46**	**203x203x46**				
4 Storey 4 Bay	**f30 b20** **f30 b24**												**406x140x46**	**305x120x25**	Upto 2nd Storey	**203x203x52**	**254x254x73**	1st - **44** 2nd - **37** 3rd - **33**	**13**	1st - **263** 2nd - **260** 3rd - **258**	**104**
															2nd - 4th Storey	**203x203x46**	**203x203x46**				

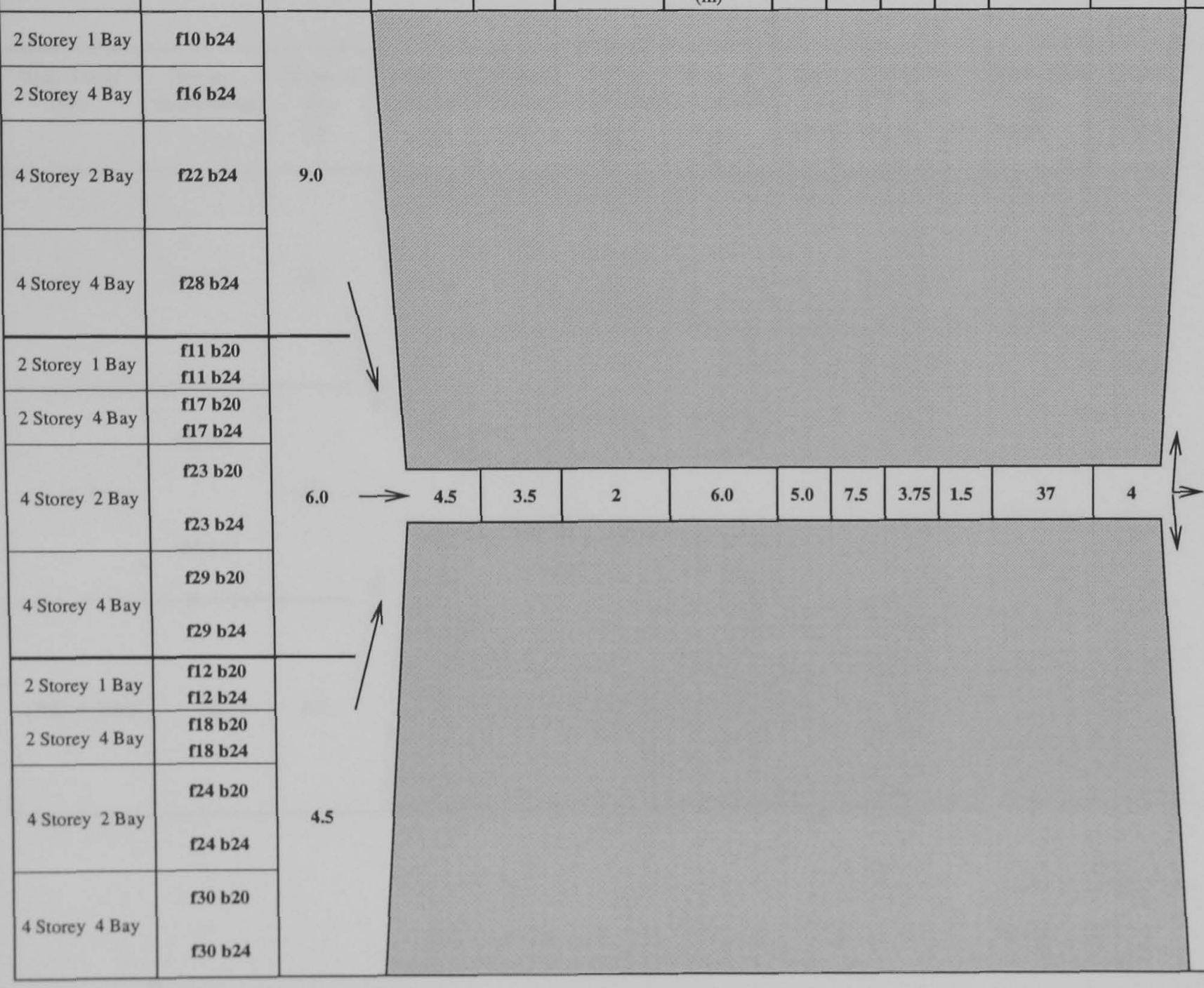

Table B.2: Wind-Moment design (Min wind + Max gravity)

Basic Frame Type	Frame Identification	Width of Bay (m)	Height of Columns: Ground (m)	Height of Columns: Elevated (m)	No. of Longitudinal Bays	Width of Longitudinal Bays (m)	Gravity Load (kN/m^2): Floor DL	Gravity Load (kN/m^2): Floor LL	Gravity Load (kN/m^2): Roof DL	Gravity Load (kN/m^2): Roof LL	Basic Wind Speed (m/s)	Ground Roughness Factor	Section Designation: Universal Beams Floor	Section Designation: Universal Beams Roof	Section Designation: Universal Columns	Universal Columns External	Universal Columns Internal	Connection Requirements: Bending Moment (kNm) Floor	Bending Moment (kNm) Roof	Shear Force (kN) Floor	Shear Force (kN) Roof
8 Storey 2 Bay	**f34 b24**	**9.0**											**686x254x125**	**457x191x67**	Upto 2nd Storey	**356x368x129**	**356x368x202**	1st - **187**		1st - **529**	
															2nd - 4th Storey	**305x305x97**	**356x368x129**	2nd - **168** 3rd - **159**		2nd - **525** 3rd - **523**	
															4th - 6th Storey	**254x254x73**	**305x305x97**	4th - **150** 5th - **142**	**48**	4th - **521** 5th - **519**	**207**
															6th - 8th Storey	**203x203x60**	**203x203x60**	6th - **133** 7th - **124**		6th - **517** 7th - **515**	
8 Storey 2 Bay	**f35 b20** **f35 b24**	**6.0**	**4.5**	**3.5**	**2**	**6.0**	**5.0**	**7.5**	**3.75**	**1.5**	**37**	**4**	**457x191x67**	**406x140x39**	Upto 2nd Storey	**305x305x97**	**356x368x129**	1st - **126**		1st - **358**	
															2nd - 4th Storey	**203x203x71**	**305x305x97**	2nd - **108** 3rd - **101**		2nd - **354** 3rd - **352**	
															4th - 6th Storey	**203x203x60**	**254x254x73**	4th - **92** 5th - **83**	**23**	4th - **350** 5th - **348**	**138**
															6th - 8th Storey	**203x203x46**	**203x203x46**	6th - **72** 7th - **60**		6th - **346** 7th - **344**	
8 Storey 2 Bay	**f36**	**4.5**											**N/A**	**N/A**	Upto 2nd Storey	**N/A**	**N/A**	**N/A**	**N/A**	**N/A**	**N/A**
															2nd - 4th Storey						
															4th - 6th Storey						
															6th - 8th Storey						

Table B.3: Connection design for frames with 9.0m bay width(s)

Basic Frame Type	Frame Identification	Location	Standard Detail Number	Moment of Resistance (kNm)	Column Limitations		Reduced Moment of Resistance (kNm)		% Mobilisation of Resistance		Basic Wind Speed (m/s)	Ground Roughness Factor	Connection Requirements		% Mobilisation of Resistance		Initial Stiffness Prediction (kNm/mrad)		
					External	Internal	External	Internal	External	Internal			Bending Moments (kNm)	Shear Force (kN)	External	Internal	External Columns	Internal Columns No Shear	Internal Columns Including Shear
2 Storey 1 Bay	**f10 b24**	Roof	**W1/24**	**118**	**None**	**None**	**N/A**	**N/A**	**41**	**N/A**	**49**	**1**	**64**	**207**	**54**	**N/A**	**25.65**	**N/A**	**N/A**
		Floor	**W1/24**	**186**	**None**	None	N/A	**N/A**	67	**N/A**			**183**	**515**	**98**	**N/A**	**56.21**	**N/A**	**N/A**
2 Storey 4 Bay	**f16 b24**	Roof	**W1/24**	**118**	**None**	**None**	**N/A**	**N/A**	**41**	**41**	**52**	**1**	**48**	**207**	**41**	**41**	**25.65**	**40.30**	**18.81**
		Floor	**W1/24**	**186**	**None**	None	N/A	**N/A**	**67**	**67**			**125**	**515**	**67**	**67**	**56.21**	**114.00**	**37.33**
4 Storey 2 Bay	**f22 b24**	Roof	**W1/24**	**118**	**None**	**None**	**N/A**	**N/A**	**41**	**41**	**45**	**1**	**50**	**207**	**42**	**42**	**21.42**	**32.66**	**15.94**
		3rd floor	**W1/24**	**186**	**None**	**None**	**N/A**	**N/A**	**67**	**67**			**127**	**515**	**68**	**68**	**46.88**	**89.83**	**31.70**
		2nd floor	**W1/24**	**186**	**None**	**None**	**N/A**	**N/A**	**72**	**72**			**149**	**517**	**80**	**80**	**64.48**	**131.11**	**55.57**
		1st floor	**W1/24**	**186**	None	**None**	**N/A**	**N/A**	**78**	**78**			**183**	**520**	**98**	**98**	64.48	**131.11**	**55.57**
4 Storey 4 Bay	**f28 b24**	Roof	**W1/24**	**118**	None	**None**	**N/A**	**N/A**	**41**	**41**	**52**	**1**	**48**	**207**	**41**	**41**	**21.42**	32.66	**15.94**
		3rd floor	**W1/24**	**186**	None	None	**N/A**	**N/A**	**67**	**67**			**124**	**515**	**67**	**67**	**46.88**	89.83	31.70
		2nd floor	**W1/24**	**186**	**None**	**None**	**N/A**	**N/A**	**72**	**72**			133	**517**	**72**	**72**	**64.48**	**131.11**	**55.57**
		1st floor	**W1/24**	**186**	**None**	None	**N/A**	**N/A**	**78**	**78**			155	**520**	**83**	83	64.48	131.11	55.57
8 Storey 2 Bay	f34 b24	**Roof**	**W1/24**	**118**	**None**	None	**N/A**	**N/A**	**41**	**41**	**43**	**4**	**48**	**207**	**41**	**41**	21.42	32.66	15.94
		7th floor	**W1/24**	**186**	None	**None**	**N/A**	**N/A**	**67**	**67**			**124**	**515**	67	67	46.88	89.83	31.70
		6th floor	**W1/24**	**186**	None	**None**	**N/A**	**N/A**	**72**	**72**			133	517	**72**	**72**	**51.62**	**110.00**	**46.04**
		5th floor	**W1/24**	**186**	None	**None**	**N/A**	**N/A**	**76**	**76**			**148**	519	80	**80**	51.62	**110.00**	**46.04**
		4th floor	**W1/24**	**186**	**None**	**None**	**N/A**	**N/A**	81	81			161	**521**	**87**	**87**	**64.99**	**124.20**	**54.38**
		3rd floor	**W1/24**	**186**	**None**	None	**N/A**	**N/A**	85	85			173	**523**	93	93	**64.99**	**124.20**	**54.38**
		2nd floor	**W1/24**	186	None	**None**	**N/A**	N/A	90	90			183	**525**	**98**	**98**	**75.64**	153.65	76.71
		1st floor	**W4+/24**	**358**	None	None	**N/A**	**N/A**	**52**	**52**			**207**	529	**58**	**58**	87.87	185.37	**88.21**

Table B.4: Connection design for frames with 6.0m bay width(s)

Basic Frame Type	Frame Identification	Location	Standard Detail Number	Moment of Resistance (kNm)	Column Limitations		Reduced Moment of Resistance (kNm)		% Mobilisation of Resistance		Basic Wind Speed (m/s)	Ground Roughness Factor	Connection Requirements		% Mobilisation of Resistance		Initial Stiffness Prediction (kNm/mrad)	
					External	Internal	External	Internal	External	Internal			Bending Moments (kNm)	Shear Force (kN)	External	Internal	External Columns	Internal Columns No Shear	Including Shear
2 Storey 1 Bay	fI1 b20	Roof	W1/20	69	None	N/A	N/A	N/A	32	32	52	4	28	138	41	N/A	8.45	N/A	N/A
		Floor	W1/20	80	None	N/A	N/A	N/A	75	N/A			79	344	99	N/A	11.83	N/A	N/A
	fI1 b24	Roof	W1/24	102	Flange Bending	N/A	88	N/A	25	N/A	42	1	33	138	38	N/A	10.97	N/A	N/A
		Floor	W1/24	118	Flange Bending	N/A	101	N/A	59	N/A			99	344	98	N/A	14.87	N/A	N/A
2 Storey 4 Bay	fI7 b20	Roof	W1/20	69	None	None	N/A	N/A	32	32	52	1	24	138	35	35	8.45	10.59	7.03
		Floor	W1/20	80	None	None	N/A	N/A	73	73			65	344	81	81	11.83	15.63	9.52
	fI7 b24	Roof	W1/24	102	Flange Bending	Flange Bending	88	88	25	25	52	1	24	138	27	27	10.97	14.87	8.69
		Floor	W1/24	118	Flange Bending	Flange Bending	101	101	57	57			65	344	64	64	14.87	21.41	11.39
4 Storey 2 Bay	fZ3 b20	Roof	W1/20	69	None	None	N/A	N/A	32	32	43	4	22	138	32	32	8.45	10.59	7.03
		3rd floor	W1/20	80	None	None	N/A	N/A	71	71			57	344	71	71	11.83	15.63	9.52
		2nd floor	W1/20	80	None	None	N/A	N/A	79	79			65	346	81	81	17.78	24.27	15.76
		1st floor	W1/20	80	None	None	N/A	N/A	90	90			78	349	98	98	17.78	24.27	15.76
	fZ3 b24	Roof	W1/24	102	Flange Bending	Flange Bending	88	88	25	25	41	1	27	138	31	31	10.97	14.87	8.69
		3rd floor	W1/24	118	Flange Bending	Flange Bending	101	101	56	56			70	244	69	69	14.87	21.41	11.39
		2nd floor	W1/24	118	None	None	N/A	N/A	53	53			89	346	75	75	25.65	41.75	21.60
		1st floor	W1/24	118	None	None	N/A	N/A	61	61			116	349	98	98	25.65	41.75	21.60
4 Storey 4 Bay	fZ9 b20	Roof	W1/20	69	None	None	N/A	N/A	32	32	40	1	22	138	32	32	8.45	10.59	7.03
		3rd floor	W1/20	80	None	None	N/A	N/A	71	71			57	344	71	71	11.83	15.63	9.52
		2nd floor	W1/20	80	None	None	N/A	N/A	79	79			65	346	81	81	17.78	24.27	15.76
		1st floor	W1/20	80	None	None	N/A	N/A	90	90			79	349	99	99	17.78	24.27	15.76
	fZ9 b24	Roof	W1/24	102	Flange Bending	Flange Bending	88	88	25	25	52	1	25	138	28	28	10.97	14.87	8.69
		3rd floor	W1/24	118	Flange Bending	Flange Bending	101	101	56	56			66	344	65	65	14.87	21.41	11.39
		2nd floor	W1/24	118	None	None	N/A	N/A	53	53			81	346	69	69	25.65	41.75	21.60
		1st floor	W1/24	118	None	None	N/A	N/A	61	61			105	349	89	89	25.65	41.75	21.60
8 Storey 2 Bay	fZ5 b20	Roof	W1/20	69	None	None	N/A	N/A	32	32	40	4	24	138	35	35	8.45	10.59	7.03
		7th floor	W1/20	80	None	None	N/A	N/A	75	75			63	344	79	79	11.83	15.63	9.52
		6th floor	W1/20	80	None	None	N/A	N/A	90	90			77	346	96	96	15.64	21.45	13.49
		5th floor	W4/20	141	None	None	N/A	N/A	59	59			90	348	64	64	20.08	28.61	17.00
		4th floor	W4/20	141	None	None	N/A	N/A	65	65			101	350	72	72	22.82	31.22	20.28
		3rd floor	W4/20	141	None	None	N/A	N/A	72	72			111	352	79	79	22.82	31.22	20.28
		2nd floor	W4/20	141	None	None	N/A	N/A	77	77			120	354	85	85	24.59	33.15	22.60
		1st floor	W4/20	141	None	None	N/A	N/A	89	89			141	358	100	100	24.59	33.15	22.60
	fZ5 b24	Roof	W1/24	102	Flange Bending	Flange Bending	88	88	26	26	39	4	24	138	27	27	10.97	14.87	8.69
		7th floor	W1/24	118	Flange Bending	Flange Bending	101	101	59	59			62	344	61	61	14.87	21.40	11.39
		6th floor	W1/24	118	None	None	N/A	N/A	61	61			75	346	64	64	21.42	34.05	17.57
		5th floor	W1/24	118	None	None	N/A	N/A	70	70			87	348	74	74	21.42	34.05	17.57
		4th floor	W1/24	118	None	None	N/A	N/A	78	78			98	350	83	83	25.65	39.27	22.02
		3rd floor	W1/24	118	None	None	N/A	N/A	86	86			108	352	92	92	25.65	39.27	22.02
		2nd floor	W1/24	118	None	None	N/A	N/A	92	92			116	354	98	98	28.22	43.51	25.47
		1st floor	W4/24	212	None	None	N/A	N/A	59	59			136	358	94	94	36.07	58.05	31.93

Table B.5: Connection design for frames with 4.5m bay width(s)

Basic Frame Type	Frame Identification	Location	Standard Detail Number	Moment of Resistance (kNm)	Column Limitations		Reduced Moment of Resistance (kNm)		% Mobilisation of Resistance		Basic Wind Speed (m/s)	Ground Roughness Factor	Connection Requirements		% Mobilisation of Resistance		Initial Stiffness Prediction (kNm/mrad)		
					External	Internal	External	Internal	External	Internal			Bending Moments (kNm)	Shear Force (kN)	External	Internal	External Columns	Internal Columns No Shear	Internal Columns Including Shear
2 Storey 1 Bay	f12 b20	Roof	W1/20	50	None	N/A	N/A	N/A	30	N/A	37	1	23	104	46	N/A	4.17	N/A	N/A
		Floor	W1/20	70	None	N/A	N/A	N/A	60	N/A			68	259	97	N/A	8.88	N/A	N/A
	f12 b24	Roof	W1/24	74	Flange Bending	N/A	64	N/A	23	N/A	44	1	29	104	45	N/A	5.72	N/A	N/A
		Floor	W1/24	103	Flange Bending	N/A	88	N/A	48	N/A			87	259	99	N/A	11.41	N/A	N/A
2 Storey 4 Bay	f18 b20	Roof	W1/20	50	None	None	N/A	N/A	26	26	52	1	16	104	32	32	4.17	4.83	3.67
		Floor	W1/20	70	None	None	N/A	N/A	49	49			46	259	66	66	8.88	11.24	7.34
	f18 b24	Roof	W1/24	74	Flange Bending	Flange Bending	64	64	20	20	52	1	16	104	25	25	5.72	7.05	4.81
		Floor	W1/24	103	Flange Bending	Flange Bending	88	88	39	39			46	259	52	52	11.41	15.60	8.98
4 Storey 2 Bay	f24 b20	Roof	W1/20	50	None	None	N/A	N/A	28	28	45	4	16	104	32	32	4.17	4.83	3.67
		3rd floor	W1/20	70	None	None	N/A	N/A	50	50			41	258	59	59	8.88	11.24	7.34
		2nd floor	W1/20	70	None	None	N/A	N/A	61	61			52	260	74	74	10.23	15.14	10.23
		1st floor	W1/20	70	None	None	N/A	N/A	77	77			69	263	99	99	10.23	15.14	10.23
	f24 b24	Roof	W1/24	74	Flange Bending	Flange Bending	64	64	22	22	37	1	18	104	28	28	5.72	7.05	4.81
		3rd floor	W1/24	103	Flange Bending	Flange Bending	88	88	40	40			49	258	56	56	11.41	15.60	8.98
		2nd floor	W1/24	103	Flange Bending	None	100	N/A	43	42			66	260	66	64	13.74	24.34	13.74
		1st floor	W1/24	103	Flange Bending	None	100	N/A	54	52			91	263	91	88	13.74	24.34	13.74
4 Storey 4 Bay	f30 b20	Roof	W1/20	50	None	None	N/A	N/A	26	26	45	1	15	104	30	30	4.17	4.83	3.67
		3rd floor	W1/20	70	None	None	N/A	N/A	47	47			41	258	59	59	8.88	11.24	7.34
		2nd floor	W1/20	70	None	None	N/A	N/A	53	53			52	260	74	74	10.23	15.14	10.23
		1st floor	W1/20	70	None	None	N/A	N/A	63	63			69	263	99	99	10.23	15.14	10.23
	f30 b24	Roof	W1/24	74	Flange Bending	Flange Bending	64	64	20	20	52	1	17	104	27	27	5.72	7.05	4.81
		3rd floor	W1/24	103	Flange Bending	Flange Bending	88	88	38	38			47	258	53	53	11.41	15.60	8.98
		2nd floor	W1/24	103	Flange Bending	None	100	N/A	37	36			62	260	62	60	13.74	24.34	13.74
		1st floor	W1/24	103	Flange Bending	None	100	N/A	33	32			84	263	84	82	13.74	24.34	13.74
8 Storey 2 Bay	f36	N/A	N/A	N/A	N/A	N/A	N/A	N/A	N/A	N/A	N/A	N/A	N/A	N/A	N/A	N/A	N/A	N/A	N/A

Table B.6: Wind-Moment design (Max wind + Min gravity)

Basic Frame Type	Frame Identification	Width of Bay (m)	Height of Columns Ground (m)	Height of Columns Elevated (m)	No. of Longitudinal Bays	Width of Longitudinal Bays (m)	Gravity Load (kN/m^2) Floor DL	Gravity Load (kN/m^2) Floor LL	Gravity Load (kN/m^2) Roof DL	Gravity Load (kN/m^2) Roof LL	Basic Wind Speed (m/s)	Ground Roughness Factor	Section Designation Universal Beams Floor	Universal Beams Roof		Universal Columns External	Universal Columns Internal	Connection Requirements Bending Moment (kNm) Floor	Bending Moment (kNm) Roof	Shear Force (kN) Floor	Shear Force (kN) Roof
2 Storey 1 Bay	f13 b24	9.0	6.0	5.0	2	6.0	3.5	4.0	3.75	1.5	52	1	533x210x82	457x191x67	Upto 2nd Storey	254x254x73	N/A	243	93	307	207
2 Storey 4 Bay	f19 b20 f19 b24												533x210x82	457x191x67	Upto 2nd Storey	203x203x71	254x254x73	103	52	307	207
4 Storey 2 Bay	f25 b24 #												533x210x82	457x191x67	Upto 2nd Storey	305x305x118*	356x368x129	1st - 348 2nd - 237 3rd - 158	71	1st - 311 2nd - 309 3rd - 307	207
															2nd - 4th Storey	203x203x71	254x254x73				
4 Storey 4 Bay	f31 b20 f31 b24												533x210x82	457x191x67	Upto 2nd Storey	254x254x89	305x305x97	1st - 198 2nd - 148 3rd - 109	55	1st - 311 2nd - 309 3rd - 307	207
															2nd - 4th Storey	203x203x52	203x203x71				
2 Storey 1 Bay	f14 b24												406x140x46	406x140x39	Upto 2nd Storey	254x254x107*	N/A	215	72	220	138
2 Storey 4 Bay	f20 b20 f20 b24												406x140x46	406x140x39	Upto 2nd Storey	203x203x46	203x203x71	72	31	206	138
4 Storey 2 Bay	f26	6.0											N/A	N/A	Upto 2nd Storey	N/A	N/A	N/A	N/A	N/A	N/A
															2nd - 4th Storey						
4 Storey 4 Bay	f32 b24												406x140x46	406x140x39	Upto 2nd Storey	254x254x73	305x305x97	1st - 180 2nd - 122 3rd - 78	34	1st - 210 2nd - 207 3rd - 205	138
															2nd - 4th Storey	203x203x46	203x203x52				
2 Storey 1 Bay	f15 b24	4.5											406x140x39	305x102x25	Upto 2nd Storey	203x203x86*	N/A	209	65	198	107
2 Storey 4 Bay	f21 b20 f21 b24												356x127x33	305x102x25	Upto 2nd Storey	203x203x46	203x203x52	61	23	155	104
4 Storey 2 Bay	f28												N/A	N/A	Upto 2nd Storey	N/A	N/A	N/A	N/A	N/A	N/A
															2nd - 4th Storey						
4 Storey 4 Bay	f33												N/A	N/A	Upto 2nd Storey	N/A	N/A	N/A	N/A	N/A	N/A
															2nd - 4th Storey						

NOTES
- See the following worked example in section B.3
* - Section increased due to limitations associated with the original column designation

Table B.7: Connection design for frames with 9.0m bay width(s)

Basic Frame Type	Frame Identification	Location	Standard Detail Number	Moment of Resistance (kNm)	Column Limitations		Reduced Moment of Resistance (kNm)		% Mobilisation of Resistance		Initial Stiffness Prediction (kNm/mrad)		
					External	Internal	External	Internal	External	Internal	External Columns	Internal No Shear	Columns Including Shear
2 Storey 1 Bay	**f13 b24**	Roof	**W1/24**	**118**	**None**	**N/A**	**N/A**	**N/A**	**79**	**N/A**	**23.18**	**N/A**	**N/A**
		Floor	**W4/24**	**250**	**None**	**N/A**	**N/A**	**N/A**	**97**	**N/A**	**42.50**	**N/A**	**N/A**
2 Storey 4 Bay	**f19 b20**	Roof	**W1/20**	**80**	**None**	None	**N/A**	**N/A**	**65**	**65**	**17.78**	**21.45**	**13.49**
		Floor	**W4/20**	**165**	**None**	None	**N/A**	N/A	**62**	**62**	**30.06**	**39.59**	**21.88**
	f19 b24	Roof	**W1/24**	**118**	**None**	**None**	**N/A**	**N/A**	**44**	**44**	**25.65**	**34.05**	**17.57**
		Floor	**W1/24**	**141**	**None**	**None**	**N/A**	**N/A**	**73**	**73**	**34.41**	**49.07**	**23.00**
4 Storey 2 Bay	**f25 b24 #**	Roof	**W1/24**	**118**	**None**	**None**	**N/A**	**N/A**	**60**	**60**	**25.65**	**34.05**	**21.53**
		3rd floor	**W4/24**	**250**	**None**	**None**	**N/A**	**N/A**	**63**	**63**	**41.72**	**62.66**	**35.00**
		2nd floor	**W4/24**	**250**	**None**	**None**	**N/A**	**N/A**	**95**	**95**	**55.80**	**80.38**	**40.80**
		1st floor	**W5/24**	**353**	**None**	**Web Shear**	**N/A**	**Reinforce**	**99**	**99**	**55.80**	**80.38**	**40.80**
4 Storey 4 Bay	**f31 b20**	Roof	**W1/20**	**80**	**None**	**None**	**N/A**	N/A	**69**	**69**	13.70	23.77	14.20
		3rd floor	**W4/20**	**165**	**None**	**None**	**N/A**	N/A	**66**	**66**	**23.07**	**43.97**	**22.84**
		2nd floor	**W4/20**	**165**	**None**	**None**	N/A	N/A	**90**	**90**	**32.75**	**43.28**	**26.38**
		1st floor	**W5/20**	**236**	**None**	**None**	N/A	N/A	**84**	**84**	32.75	**43.28**	**26.38**
	f31 b24	Roof	W1/24	**118**	**Flange Bending**	**None**	**114**	**N/A**	**48**	**47**	17.93	**40.31**	18.81
		3rd floor	**W1/24**	**141**	**Flange Bending**	**None**	136	**N/A**	**80**	**77**	**24.12**	**58.24**	**24.42**
		2nd floor	**W4/24**	**250**	**None**	**None**	N/A	N/A	**59**	**59**	**47.09**	**72.41**	**29.12**
		1st floor	**W4/24**	**250**	**None**	None	**N/A**	**N/A**	**79**	79	**47.09**	**72.41**	29.12
8 Storey 2 Bay	**f37**	**N/A**	**N/A**	**N/A**	**N/A**	**N/A**	**N/A**	**N/A**	**N/A**	N/A	**N/A**	**N/A**	N/A

NOTES
- See the following worked example in section B.3

Table B.8: Connection design for frames with 6.0m bay width(s)

Basic Frame Type	Frame Identification	Location	Standard Detail Number	Moment of Resistance (kNm)	Column Limitations		Reduced Moment of Resistance (kNm)		% Mobilisation of Resistance		Initial Stiffness Prediction (kNm/mrad)		
					External	Internal	External	Internal	External	Internal	External Columns	Internal Columns No Shear	Internal Columns Including Shear
2 Storey 1 Bay	f14 b24	Roof	W1/24	102	None	N/A	N/A	N/A	71	N/A	23.03	N/A	N/A
		Floor	W5/24	256	None	N/A	N/A	N/A	84	N/A	32.51	N/A	N/A
2 Storey 4 Bay	f20 b20	Roof	W1/20	69	None	None	N/A	N/A	45	45	8.45	15.43	10.23
		Floor	W4/20	124	None	None	N/A	N/A	58	58	11.88	23.13	14.11
	f20 b24	Roof	W1/24	102	Flange Bending	None	88	N/A	35	30	10.97	26.59	14.17
		Floor	W1/24	103	Flange Bending	None	88	N/A	82	70	11.41	28.53	14.78
4 Storey 2 Bay	f26	N/A	N/A	N/A	N/A	N/A	N/A	N/A	N/A	N/A	N/A	N/A	N/A
4 Storey 4 Bay	f32 b24	Roof	W1/24	102	Flange Bending	Flange Bending	88	99	39	34	10.97	18.39	10.25
		3rd floor	W1/24	103	Flange Bending	Flange Bending Web Shear	88	99 Reinforce	89	79	11.41	19.44	10.62
		2nd floor	W4/24	187	None	None	N/A	N/A	65	65	23.24	38.64	22.05
		1st floor	W4/24	187	None	Web Shear	N/A	Reinforce	96	96	23.24	38.64	22.05
8 Storey 2 Bay	f38	N/A	N/A	N/A	N/A	N/A	N/A	N/A	N/A	N/A	N/A	N/A	N/A

Table B.9: Connection design for frames with 4.5m bay width(s)

Basic Frame Type	Frame Identification	Location	Standard Detail Number	Moment of Resistance (kNm)	Column Limitations		Reduced Moment of Resistance (kNm)		% Mobilisation of Resistance		Initial Stiffness Prediction (kNm/mrad)		
					External	Internal	External	Internal	External	Internal	External Columns	Internal Columns No Shear	Internal Columns Including Shear
2 Storey 1 Bay	**f15 b24**	Roof	**W1/24**	**74**	**None**	N/A	**N/A**	**N/A**	**88**	**N/A**	**10.43**	**N/A**	**N/A**
		Floor	**W5/24**	**253**	**Web Shear**	N/A	**220**	**N/A**	**95**	**N/A**	**23.04**	N/A	N/A
2 Storey 4 Bay	**f21 b20**	Roof	**W1/20**	**50**	**None**	**None**	N/A	N/A	**46**	**46**	**4.17**	**5.48**	**4.13**
		Floor	**W4/20**	**107**	**None**	**None**	N/A	N/A	**57**	**57**	**8.49**	**12.10**	**8.04**
	f21 b24	Roof	**W1/24**	**74**	**Flange Bending**	**Flange Bending**	**64**	**71**	**36**	**32**	**5.72**	**8.52**	**5.65**
		Floor	**W1/24**	**87**	**Flange Bending**	**Flange Bending**	**75**	**84**	**81**	**73**	**8.00**	**12.60**	**7.70**
4 Storey 2 Bay	**f28**	**N/A**	**N/A**	**N/A**	**N/A**	**N/A**	**N/A**	**N/A**	**N/A**	**N/A**	**N/A**	**N/A**	**N/A**
4 Storey 4 Bay	**f33**	**N/A**	**N/A**	**N/A**	**N/A**	**N/A**	**N/A**	**N/A**	**N/A**	**N/A**	**N/A**	**N/A**	**N/A**
8 Storey 4 Bay	**f39**	**N/A**	**N/A**	**N/A**	**N/A**	**N/A**	**N/A**	**N/A**	**N/A**	**N/A**	**N/A**	**N/A**	**N/A**

B.3 A worked example using the design tables

The following worked example applies to frame f25b24.

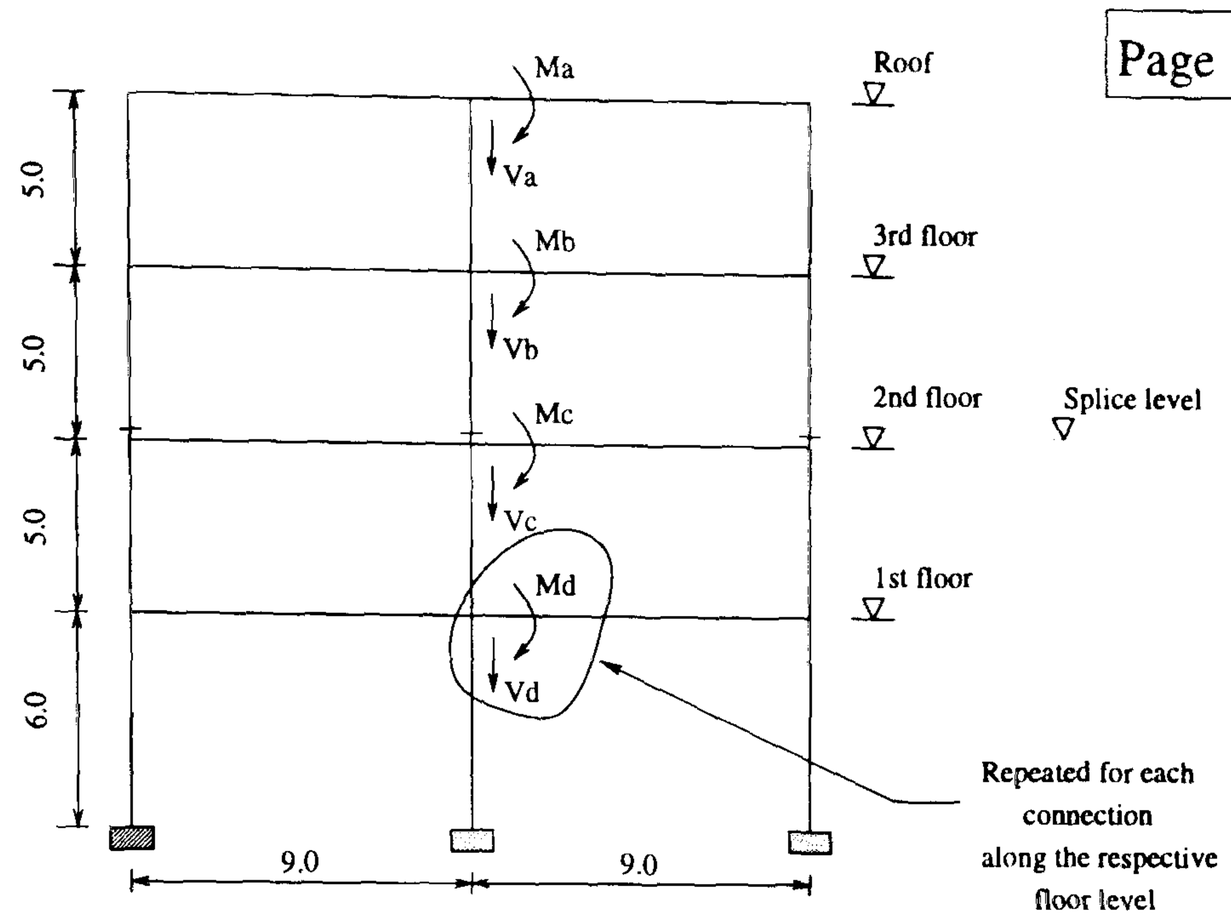

4 Storey 2 Bay

Original section designation designed by the Wind-Moment Method					Connection Requirements			
Universal Beams			Universal Columns		Bending Moment		Shear Force	
Floor	Roof		External	Internal	Floor	Roof	Floor	Roof
533x210x82	**457x191x67**	Upto 2nd Storey	**305x305x97**	**356x368x129**	Mb - **158**	Ma- **71**	Vb - **307**	Va- **207**
		2nd - 4th Storey	**203x203x71**	**254x254x73**	Mc - **237**		Vc - **309**	
					Md - **348**		Vd - **311**	

For the roof & 3rd floor, the shear is governed by load case 1 and the moment is governed by load case 2

For the 2nd & 1st floors, the shear is governed by load case 1 and the moment is governed by load case 3

where : Load case 1 = 1.4DL+1.6LL+Notional horizontal force

Load case 2 = 1.2(DL+LL+Wind)

Load case 3 = 1.4(DL+Wind)

Connection design using M24 bolts

Roof

Beam : 457x191x67UB

Detail 1 M_{Rd} - **118kNm** > 71kNm

V_{Rd} - **340kN** > 207kN

Column :

External : 203x203x71UC **No limitations**

Internal : 254x254x73UC **No limitations (ignoring the effect of web shear)**

Therefore Detail 1 is satisfactory

Worked Example : **f25b24**

3rd Floor

Beam : 533x210x82UB

Detail 1	M_{Rd} -	**141kNm** < 158kNm	fail
Detail 3	M_{Rd} -	**244kNm** > 158kNm	pass
Detail 3W	M_{Rd} -	**247kNm** > 158kNm	pass
Detail 4	M_{Rd} -	**250kNm** > 158kNm	pass
Detail 4W	M_{Rd} -	**277kNm** > 158kNm	pass
Detail 5	M_{Rd} -	**353kNm** > 158kNm	pass
Detail 5W	M_{Rd} -	**382kNm** > 158kNm	pass

Column :

External : 203x203x71UC	**Detail 3**	**Web shear**
	Detail 3W	**Web shear**
	Detail 4	**No limitations**
	Detail 4W	**Web shear**
	Detail 5	**Flange bending, web buckling, web crushing, web shear**
	Detail 5W	**Flange bending, web buckling, web crushing, web shear**
Internal : 254x254x73UC	**Detail 4**	**No limitations (ignoring the effect of web shear)**

Detail 4 M_{Rd} - **250kNm** > 158kNm

V_{Rd} - **640kN** > 307kN

Therefore Detail 4 is satisfactory

Note : Detail 3, although giving a lower M_{Rd}, would probably not be chosen since reinforcement in the way of supplementary web plates would be required to satisfy the web shear check for an external column.

2nd Floor

Beam : 533x210x82UB

Detail 4 M_{Rd} - **250kNm** > 237kNm

V_{Rd} - **640kN** > 309kN

Column :

External : 305x305x97UC	**Detail 4**	**No limitations**
Internal : 356x368x129UC	**Detail 4**	**No limitations**

Therefore Detail 4 is satisfactory

Worked Example : **f25b24**

1st Floor

Beam : 533x210x82UB

Detail 1	M_{Rd} -	**141kNm** <	348kNm	fail
Detail 3	M_{Rd} -	**244kNm** <	348kNm	fail
Detail 3W	M_{Rd} -	**247kNm** <	348kNm	fail
Detail 4	M_{Rd} -	**250kNm** <	348kNm	fail
Detail 4W	M_{Rd} -	**277kNm** <	348kNm	fail
Detail 5	M_{Rd} -	**353kNm** >	348kNm	pass
Detail 5W	M_{Rd} -	**382kNm** >	348kNm	pass

Column :

External : 305x305x97UC **Detail 5** **Flange bending, web buckling, web crushing, web shear**

Detail 5W **Flange bending, web buckling, web crushing, web shear**

Note : To provide sufficient reinforcement to enable detail 5 to be adopted would render the connection similar to one in a rigidly jointed frame. Since the main objective of these proposed standard details was to simplify fabrication by reducing the need for costly reinforcement, an increase in the column mass per metre would eradicate this problem. **Therefore increase the column to 305x305x118UC**

Internal : 356x368x129UC **Detail 5** **No limitations (ignoring the effect of web shear)**

Detail 5 M_{Rd} - **353kNm** > 348kNm

V_{Rd} - **1020kN** > 311kN

Therefore Detail 5 is satisfactory

Note : The increased external column designation will extend upto the level of the splice. Therefore by inspection the connection design already specified for the 2nd floor level will be unaffected.

Proposed section designation designed by the Wind-Moment Method					Connection design		
Universal Beams			Universal Columns		Location	Standard Detail Number	Moment of Resistance (kNm)
Floor	Roof		External	Internal			
533x210x82	457x191x67	Upto 2nd Storey	**305x305x118**	356x368x129	Roof	**one**	**118**
					3rd floor	**four**	**250**
		2nd - 4th Storey	203x203x71	254x254x73	2nd floor	**four**	**250**
					1st floor	**five**	**353**

Worked Example : **f25b24**

Appendix C

Computer simulation results, for the structural frames analysed in accordance with limit state procedures

C.1 Scope

The structural responses of the frames, induced by either ultimate or serviceability loads are detailed in this appendix. In particular, connection rotations, column stability factors, plastic collapse load factors, a graphical representation for the load-deflection behaviour for a typical Wind-Moment frame, the sequence of hinge formations and sway deflections are reported in the following sections.

C.2 Connection rotations, column stability factors and plastic collapse load factors

With the exception of the plastic collapse load factors, all the other data is applicable to the frame's response under the design load.

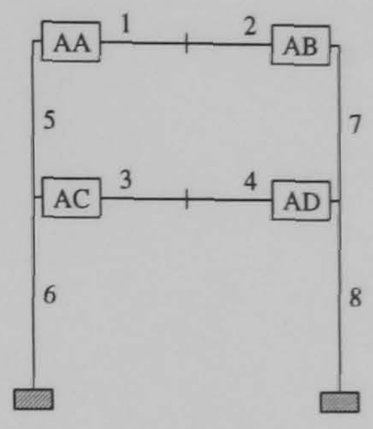

2 Storey 1 Bay

Member	Semi - Rigid Hinge Reference	Rotation (mrad)		
		LC1	LC2	LC3
1	AA	**3.93**	**1.92**	**1.19**
2	AB	**-7.98**	**-8.43**	**-7.24**
3	AC	**2.53**	**0.31**	**-0.88**
4	AD	**-5.71**	**-8.19**	**-5.38**

Member	Stability Factors		
	LC1	LC2	LC3
5	**0.281**	**0.168**	**0.127**
6	**0.539**	**0.483**	**0.367**
7	**0.288**	**0.279**	**0.238**
8	**0.547**	**0.570**	**0.425**

Load Case	Frames Plastic Collapse Load Factor
LC1	**1.337**
LC2	**1.550**
LC3	**1.837**

Frame Identification : **f10 b24**

Member	Semi - Rigid Hinge Reference	Rotation (mrad)		
		LC1	LC2	LC3
1	AA	**3.71**	**1.24**	**0.38**
2	AB	**-8.68**	**-9.63**	**-8.43**
3	AC	**4.54**	**0.87**	**-1.58**
4	AD	**-10.21**	**-11.82**	**-8.60**

Member	Stability Factors		
	LC1	LC2	LC3
5	**0.212**	**0.136**	**0.078**
6	**0.548**	**0.504**	**0.364**
7	**0.220**	**0.212**	**0.183**
8	**0.543**	**0.560**	**0.406**

Load Case	Frames Plastic Collapse Load Factor
LC1	**1.162**
LC2	**1.415**
LC3	**2.045**

Frame Identification : **f11 b20**

Member	Semi - Rigid Hinge Reference	Rotation (mrad)		
		LC1	LC2	LC3
1	AA	**3.25**	**0.54**	**-0.31**
2	AB	**-7.50**	**-9.23**	**-8.32**
3	AC	**4.15**	**-0.21**	**-2.55**
4	AD	**-9.18**	**-12.27**	**-9.56**

Member	Stability Factors		
	LC1	LC2	LC3
5	**0.228**	**0.133**	**0.077**
6	**0.552**	**0.545**	**0.420**
7	**0.234**	**0.245**	**0.216**
8	**0.549**	**0.630**	**0.483**

Load Case	Frames Plastic Collapse Load Factor
LC1	**1.205**
LC2	**1.460**
LC3	**1.960**

Frame Identification : **f11 b24**

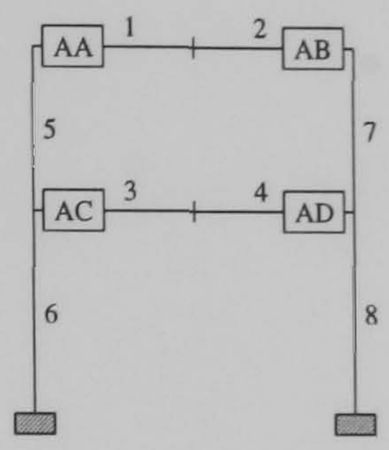

2 Storey 1 Bay

Member	Semi - Rigid Hinge Reference	Rotation (mrad)		
		LC1	LC2	LC3
1	AA	**5.06**	**0.34**	**-0.94**
2	AB	**-10.65**	**-13.97**	**-12.96**
3	AC	**3.68**	**-1.51**	**-3.87**
4	AD	**-8.58**	**-12.76**	**-10.47**

Member	Stability Factors		
	LC1	LC2	LC3
5	**0.142**	**0.065**	**0.082**
6	**0.409**	**0.443**	**0.346**
7	**0.155**	**0.157**	**0.140**
8	**0.404**	**0.491**	**0.396**

Load Case	Frames Plastic Collapse Load Factor
LC1	**1.332**
LC2	**1.482**
LC3	**1.862**

Frame Identification : **f12 b20**

Member	Semi - Rigid Hinge Reference	Rotation (mrad)		
		LC1	LC2	LC3
1	AA	**4.30**	**-0.49**	**-1.72**
2	AB	**-9.11**	**-13.29**	**-12.61**
3	AC	**3.33**	**-2.42**	**-4.67**
4	AD	**-7.66**	**-13.21**	**-11.39**

Member	Stability Factors		
	LC1	LC2	LC3
5	**0.153**	**0.067**	**0.092**
6	**0.410**	**0.481**	**0.392**
7	**0.165**	**0.186**	**0.170**
8	**0.405**	**0.559**	**0.464**

Load Case	Frames Plastic Collapse Load Factor
LC1	**1.395**
LC2	**1.507**
LC3	**1.722**

Frame Identification : **f12 b24**

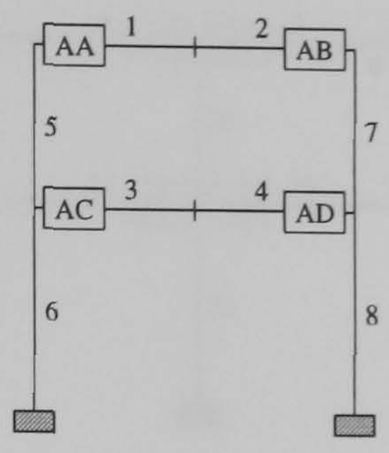

2 Storey 1 Bay

Member	Semi - Rigid Hinge Reference	Rotation (mrad) LC1	LC2	LC3
1	AA	**4.14**	**-0.13**	**-0.93**
2	AB	**-8.74**	**-16.16**	**-13.24**
3	AC	**3.38**	**-1.62**	**-3.22**
4	AD	**-7.38**	**-14.28**	**-10.90**

Member	Stability Factors LC1	LC2	LC3
5	**0.265**	**0.100**	**0.108**
6	**0.442**	**0.543**	**0.493**
7	**0.276**	**0.288**	**0.274**
8	**0.436**	**0.659**	**0.592**

Load Case	Frames Plastic Collapse Load Factor
LC1	**1.367**
LC2	**1.405**
LC3	**1.440**

Frame Identification : **f13 b24**

Member	Semi - Rigid Hinge Reference	Rotation (mrad) LC1	LC2	LC3
1	AA	**2.45**	**-1.08**	**-1.92**
2	AB	**-5.24**	**-10.30**	**-10.12**
3	AC	**2.83**	**-1.59**	**-3.25**
4	AD	**-5.69**	**-10.86**	**-9.91**

Member	Stability Factors LC1	LC2	LC3
5	**0.165**	**0.102**	**0.109**
6	**0.304**	**0.494**	**0.477**
7	**0.173**	**0.236**	**0.227**
8	**0.280**	**0.578**	**0.570**

Load Case	Frames Plastic Collapse Load Factor
LC1	**1.720**
LC2	**1.692**
LC3	**1.787**

Frame Identification : **f14 b24**

Member	Semi - Rigid Hinge Reference	Rotation (mrad) LC1	LC2	LC3
1	AA	**3.12**	**-3.17**	**-4.54**
2	AB	**-6.34**	**-14.58**	**-15.88**
3	AC	**1.65**	**-5.32**	**-7.01**
4	AD	**-3.94**	**-13.66**	**-14.06**

Member	Stability Factors LC1	LC2	LC3
5	**0.144**	**0.097**	**0.117**
6	**0.221**	**0.388**	**0.378**
7	**0.115**	**0.183**	**0.176**
8	**0.218**	**0.524**	**0.522**

Load Case	Frames Plastic Collapse Load Factor
LC1	**1.427**
LC2	**1.482**
LC3	**1.410**

Frame Identification : **f15 b24**

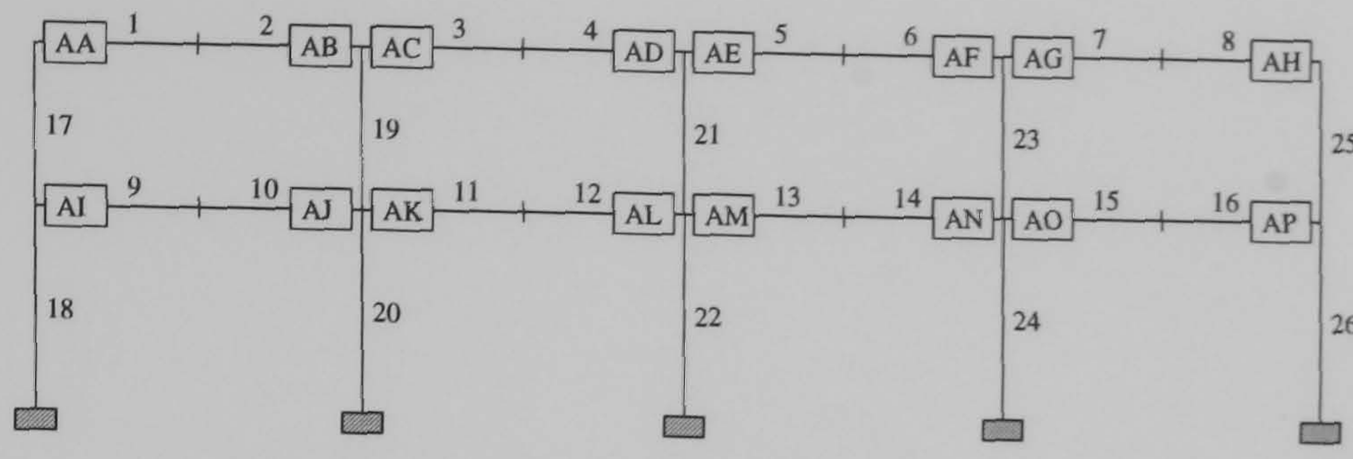

2 Storey 4 Bay

Member	Semi - Rigid Hinge Reference	Rotation (mrad)					
		No Shear at Internal Columns			Including Shear at Internal Columns		
		LC1	LC2	LC3	LC1	LC2	LC3
1	AA	**3.32**	**2.21**	**1.91**	**3.55**	**2.59**	**1.93**
2	AB	**-12.74**	**-10.39**	**-6.47**	**-12.23**	**-10.57**	**-8.98**
3	AC	**5.08**	**2.61**	**2.44**	**6.02**	**4.64**	**3.80**
4	AD	**-12.02**	**-9.27**	**-5.63**	**-12.02**	**-10.34**	**-8.71**
5	AE	**5.22**	**2.63**	**2.40**	**6.03**	**4.65**	**3.79**
6	AF	**-11.87**	**-9.34**	**-5.80**	**-11.95**	**-10.27**	**-8.70**
7	AG	**5.35**	**2.73**	**2.67**	**6.03**	**4.64**	**3.83**
8	AH	**-8.57**	**-7.36**	**-5.06**	**-8.31**	**-7.25**	**-5.80**
9	AI	**1.98**	**0.99**	**0.27**	**2.18**	**1.28**	**0.23**
10	AJ	**-11.37**	**-9.63**	**-2.74**	**-10.25**	**-8.60**	**-4.63**
11	AK	**3.43**	**1.37**	**0.84**	**4.61**	**3.22**	**1.00**
12	AL	**-11.06**	**-9.13**	**-2.56**	**-10.08**	**-8.47**	**-4.57**
13	AM	**3.47**	**1.38**	**0.79**	**4.64**	**3.23**	**1.02**
14	AN	**-11.01**	**-9.06**	**-2.62**	**-9.98**	**-8.41**	**-4.49**
15	AO	**3.36**	**1.39**	**0.88**	**4.62**	**3.18**	**0.95**
16	AP	**-6.45**	**-5.83**	**-3.11**	**-6.18**	**-5.61**	**-3.60**

Member	Stability Factors					
	No Shear at Internal Columns			Including Shear at Internal Columns		
	LC1	LC2	LC3	LC1	LC2	LC3
17	**0.251**	**0.181**	**0.153**	**0.263**	**0.200**	**0.156**
18	**0.527**	**0.428**	**0.260**	**0.530**	**0.423**	**0.277**
19	**0.211**	**0.191**	**0.188**	**0.211**	**0.194**	**0.174**
20	**0.942**	**0.798**	**0.518**	**0.929**	**0.786**	**0.511**
21	**0.211**	**0.187**	**0.177**	**0.208**	**0.188**	**0.169**
22	**0.934**	**0.787**	**0.505**	**0.925**	**0.781**	**0.508**
23	**0.214**	**0.181**	**0.171**	**0.208**	**0.188**	**0.169**
24	**0.936**	**0.791**	**0.515**	**0.926**	**0.783**	**0.509**
25	**0.302**	**0.252**	**0.183**	**0.295**	**0.250**	**0.202**
26	**0.569**	**0.487**	**0.295**	**0.563**	**0.483**	**0.314**

Load Case	Frames Plastic Collapse Load Factor	
	No Shear at Internal Columns	Including Shear at Internal Columns
LC1	**1.292**	**1.320**
LC2	**1.630**	**1.630**
LC3	**1.965**	**1.967**

Frame Identification : **f16 b24**

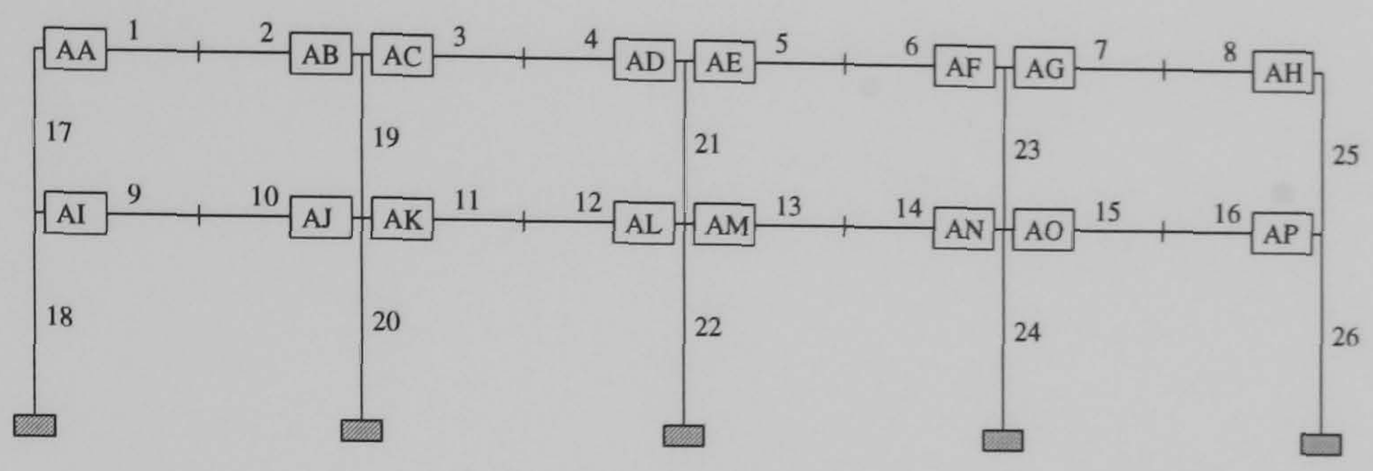

2 Storey 4 Bay

Member	Semi - Rigid Hinge Reference	Rotation (mrad)					
		No Shear at Internal Columns			Including Shear at Internal Columns		
		LC1	LC2	LC3	LC1	LC2	LC3
1	AA	**3.26**	**1.66**	**1.03**	**3.45**	**1.53**	**0.77**
2	AB	**-9.52**	**-8.96**	**-7.76**	**-10.87**	**-10.63**	**-9.34**
3	AC	**4.04**	**2.53**	**1.94**	**4.76**	**2.69**	**1.95**
4	AD	**-9.36**	**-8.82**	**-7.58**	**-10.97**	**-10.64**	**-9.26**
5	AE	**4.03**	**2.53**	**1.93**	**4.80**	**2.72**	**1.96**
6	AF	**-9.36**	**-8.81**	**-7.61**	**-10.87**	**-10.54**	**-9.20**
7	AG	**4.08**	**2.58**	**2.02**	**4.63**	**2.55**	**1.86**
8	AH	**-9.01**	**-8.74**	**-7.15**	**-9.28**	**-9.37**	**-7.88**
9	AI	**3.87**	**1.17**	**-0.92**	**4.06**	**1.02**	**-1.22**
10	AJ	**-13.26**	**-11.94**	**-6.68**	**-13.44**	**-13.21**	**-8.29**
11	AK	**4.74**	**2.47**	**0.10**	**5.92**	**2.57**	**-0.57**
12	AL	**-13.07**	**-11.74**	**-6.63**	**-13.54**	**-13.21**	**-8.27**
13	AM	**4.76**	**2.50**	**0.11**	**5.95**	**2.59**	**-0.55**
14	AN	**-13.01**	**-11.70**	**-6.60**	**-13.47**	**-13.13**	**-8.20**
15	AO	**4.76**	**2.51**	**0.11**	**5.77**	**2.40**	**-0.71**
16	AP	**-10.99**	**-11.25**	**-7.59**	**-11.15**	**-11.83**	**-8.25**

Member	Stability Factors					
	No Shear at Internal Columns			Including Shear at Internal Columns		
	LC1	LC2	LC3	LC1	LC2	LC3
17	**0.204**	**0.151**	**0.095**	**0.208**	**0.147**	**0.089**
18	**0.546**	**0.500**	**0.349**	**0.552**	**0.513**	**0.365**
19	**0.244**	**0.238**	**0.208**	**0.228**	**0.230**	**0.204**
20	**1.005**	**0.902**	**0.612**	**0.997**	**0.902**	**0.615**
21	**0.240**	**0.234**	**0.204**	**0.228**	**0.229**	**0.202**
22	**0.998**	**0.895**	**0.607**	**0.995**	**0.899**	**0.612**
23	**0.240**	**0.234**	**0.203**	**0.230**	**0.231**	**0.203**
24	**1.002**	**0.900**	**0.611**	**0.994**	**0.898**	**0.611**
25	**0.218**	**0.198**	**0.164**	**0.223**	**0.208**	**0.174**
26	**0.571**	**0.553**	**0.385**	**0.573**	**0.565**	**0.401**

Load Case	Frames Plastic Collapse Load Factor	
	No Shear at Internal Columns	Including Shear at Internal Columns
LC1	**1.162**	**1.152**
LC2	**1.407**	**1.422**
LC3	**2.107**	**2.092**

Frame Identification : **f17 b20**

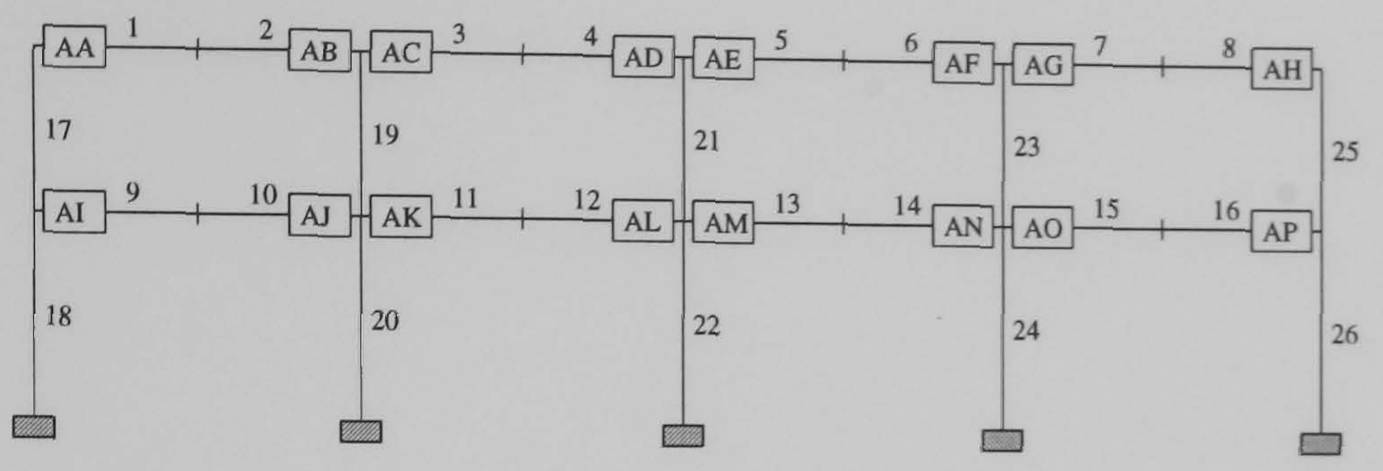

2 Storey 4 Bay

Member	Semi - Rigid Hinge Reference	Rotation (mrad)					
		No Shear at Internal Columns			Including Shear at Internal Columns		
		LC1	LC2	LC3	LC1	LC2	LC3
1	AA	**2.87**	**1.64**	**1.02**	**3.02**	**1.49**	**0.82**
2	AB	**-8.06**	**-7.43**	**-6.46**	**-9.97**	**-9.58**	**-8.39**
3	AC	**3.50**	**2.35**	**1.83**	**4.47**	**2.73**	**2.05**
4	AD	**-7.83**	**-7.23**	**-6.22**	**-10.03**	**-9.55**	**-8.27**
5	AE	**3.47**	**2.33**	**1.80**	**4.51**	**2.76**	**2.05**
6	AF	**-7.86**	**-7.25**	**-6.28**	**-9.93**	**-9.45**	**-8.22**
7	AG	**3.59**	**2.44**	**1.93**	**4.36**	**2.60**	**1.97**
8	AH	**-7.55**	**-7.15**	**-5.88**	**-8.01**	**-7.95**	**-6.63**
9	AI	**3.55**	**1.31**	**-0.60**	**3.71**	**1.14**	**-0.85**
10	AJ	**-11.83**	**-10.05**	**-5.68**	**-12.74**	**-12.29**	**-7.57**
11	AK	**4.37**	**2.63**	**0.40**	**5.78**	**2.80**	**-0.17**
12	AL	**-11.42**	**-9.65**	**-5.58**	**-12.81**	**-12.26**	**-7.53**
13	AM	**4.39**	**2.65**	**0.41**	**5.80**	**2.82**	**-0.15**
14	AN	**-11.45**	**-9.70**	**-5.56**	**-12.73**	**-12.17**	**-7.45**
15	AO	**4.47**	**2.76**	**0.44**	**5.64**	**2.63**	**-0.32**
16	AP	**-9.62**	**-9.65**	**-6.58**	**-10.03**	**-10.50**	**-7.27**

Member	Stability Factors					
	No Shear at Internal Columns			Including Shear at Internal Columns		
	LC1	LC2	LC3	LC1	LC2	LC3
17	**0.217**	**0.162**	**0.102**	**0.222**	**0.157**	**0.096**
18	**0.540**	**0.482**	**0.339**	**0.552**	**0.503**	**0.356**
19	**0.244**	**0.237**	**0.210**	**0.228**	**0.229**	**0.202**
20	**1.001**	**0.897**	**0.609**	**0.993**	**0.897**	**0.610**
21	**0.238**	**0.232**	**0.203**	**0.228**	**0.227**	**0.200**
22	**0.990**	**0.888**	**0.602**	**0.991**	**0.893**	**0.607**
23	**0.238**	**0.229**	**0.201**	**0.230**	**0.229**	**0.201**
24	**0.999**	**0.895**	**0.607**	**0.990**	**0.892**	**0.605**
25	**0.228**	**0.205**	**0.170**	**0.238**	**0.221**	**0.184**
26	**0.565**	**0.542**	**0.380**	**0.575**	**0.564**	**0.399**

Load Case	Frames Plastic Collapse Load Factor	
	No Shear at Internal Columns	Including Shear at Internal Columns
LC1	**1.202**	**1.172**
LC2	**1.455**	**1.477**
LC3	**2.210**	**2.197**

Frame Identification : **f17 b24**

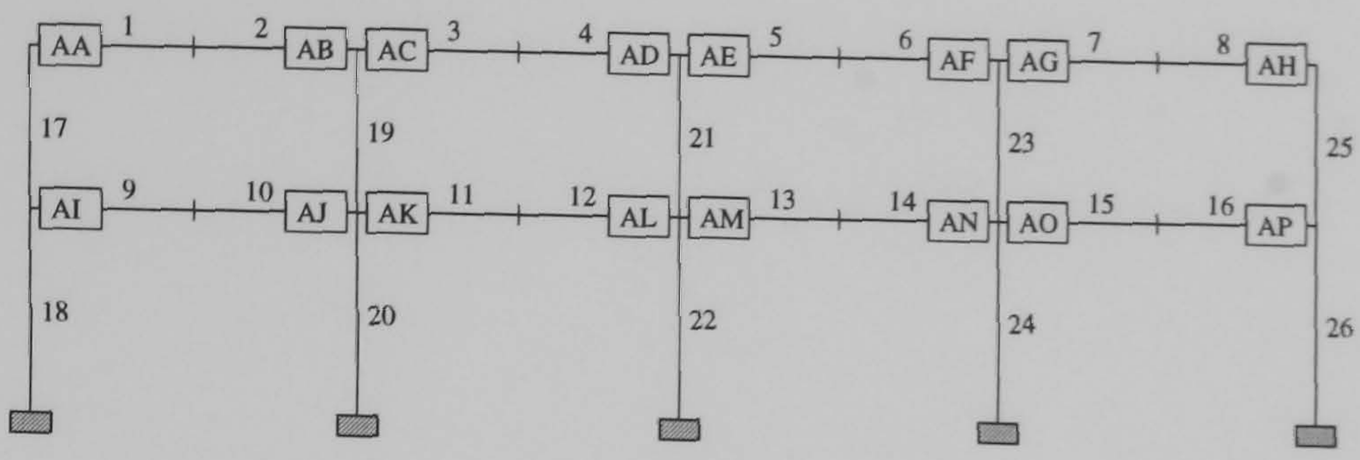

2 Storey 4 Bay

Member	Semi - Rigid Hinge Reference	Rotation (mrad) No Shear at Internal Columns			Rotation (mrad) Including Shear at Internal Columns		
		LC1	LC2	LC3	LC1	LC2	LC3
1	AA	**4.85**	**2.11**	**1.11**	**4.85**	**1.79**	**0.75**
2	AB	**-11.13**	**-11.45**	**-10.22**	**-12.25**	**-13.03**	**-11.71**
3	AC	**5.11**	**2.57**	**1.70**	**5.68**	**2.54**	**1.54**
4	AD	**-11.11**	**-11.41**	**-10.12**	**-12.44**	**-13.08**	**-11.66**
5	AE	**5.13**	**2.59**	**1.71**	**5.72**	**2.57**	**1.56**
6	AF	**-11.07**	**-11.38**	**-10.11**	**-12.37**	**-13.01**	**-11.61**
7	AG	**5.14**	**2.62**	**1.77**	**5.51**	**2.36**	**1.42**
8	AH	**-10.83**	**-11.41**	**-9.92**	**-11.33**	**-12.26**	**-10.73**
9	AI	**3.34**	**0.12**	**-1.88**	**3.34**	**-0.16**	**-2.23**
10	AJ	**-9.48**	**-9.96**	**-6.61**	**-10.59**	**-11.73**	**-8.13**
11	AK	**3.98**	**1.22**	**-0.98**	**4.44**	**0.79**	**-1.80**
12	AL	**-9.43**	**-9.91**	**-6.61**	**-10.74**	**-11.77**	**-8.11**
13	AM	**3.98**	**1.23**	**-0.96**	**4.47**	**0.81**	**-1.78**
14	AN	**-9.42**	**-9.89**	**-6.58**	**-10.68**	**-11.69**	**-8.05**
15	AO	**4.00**	**1.24**	**-0.98**	**4.27**	**0.60**	**-1.96**
16	AP	**-8.94**	**-10.47**	**-7.79**	**-9.39**	**-11.21**	**-8.42**

Member	Stability Factors No Shear at Internal Columns			Stability Factors Including Shear at Internal Columns		
	LC1	LC2	LC3	LC1	LC2	LC3
17	**0.139**	**0.094**	**0.066**	**0.139**	**0.088**	**0.067**
18	**0.407**	**0.402**	**0.296**	**0.416**	**0.418**	**0.311**
19	**0.171**	**0.181**	**0.167**	**0.168**	**0.175**	**0.161**
20	**0.750**	**0.706**	**0.494**	**0.751**	**0.709**	**0.499**
21	**0.169**	**0.179**	**0.166**	**0.168**	**0.174**	**0.160**
22	**0.746**	**0.702**	**0.492**	**0.750**	**0.707**	**0.497**
23	**0.169**	**0.179**	**0.166**	**0.169**	**0.176**	**0.161**
24	**0.750**	**0.705**	**0.494**	**0.749**	**0.705**	**0.495**
25	**0.152**	**0.138**	**0.118**	**0.157**	**0.145**	**0.124**
26	**0.415**	**0.438**	**0.325**	**0.424**	**0.454**	**0.341**

Load Case	Frames Plastic Collapse Load Factor No Shear at Internal Columns	Frames Plastic Collapse Load Factor Including Shear at Internal Columns
LC1	**1.277**	**1.307**
LC2	**1.537**	**1.515**
LC3	**2.012**	**1.977**

Frame Identification : **f18 b20**

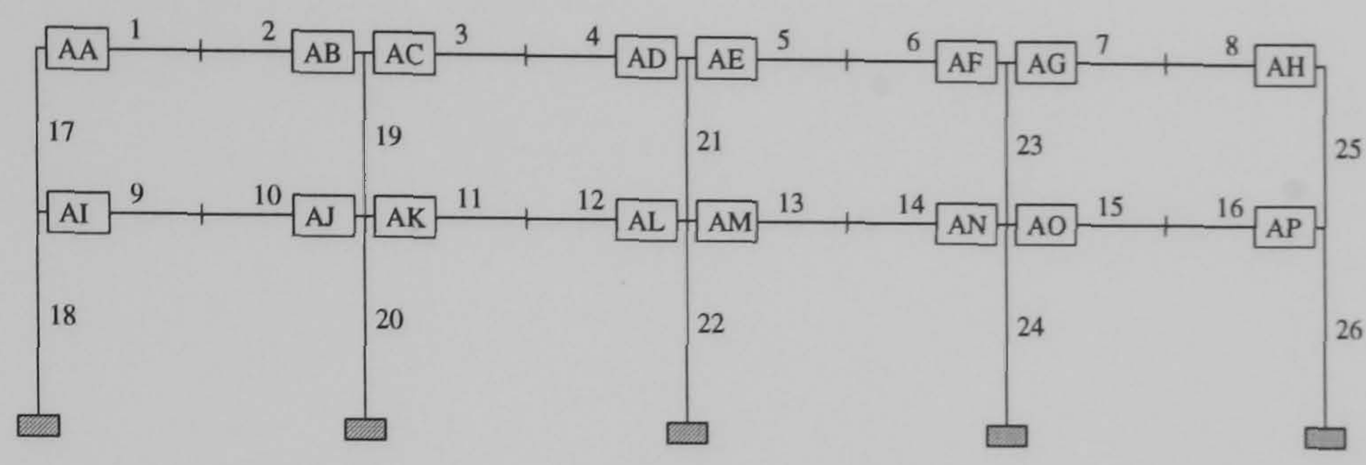

2 Storey 4 Bay

Member	Semi - Rigid Hinge Reference	Rotation (mrad) No Shear at Internal Columns			Rotation (mrad) Including Shear at Internal Columns		
		LC1	LC2	LC3	LC1	LC2	LC3
1	AA	4.09	2.02	1.18	4.13	1.78	0.91
2	AB	-9.32	-9.30	-8.25	-10.94	-11.33	-10.14
3	AC	4.24	2.41	1.71	5.13	2.63	1.76
4	AD	-9.19	-9.18	-8.09	-11.09	-11.35	-10.06
5	AE	4.25	2.42	1.71	5.17	2.66	1.77
6	AF	-9.17	-9.16	-8.10	-11.01	-11.27	-10.01
7	AG	4.34	2.51	1.82	4.97	2.46	1.64
8	AH	-9.06	-9.31	-8.01	-9.68	-10.22	-8.86
9	AI	3.02	0.41	-1.31	3.05	0.17	-1.62
10	AJ	-8.37	-8.48	-5.45	-9.91	-10.66	-7.22
11	AK	3.59	1.46	-0.43	4.31	1.20	-1.22
12	AL	-8.23	-8.36	-5.41	-10.04	-10.67	-7.18
13	AM	3.58	1.46	-0.42	4.34	1.22	-1.20
14	AN	-8.25	-8.36	-5.38	-9.97	-10.59	-7.11
15	AO	3.66	1.51	-0.42	4.15	1.00	-1.38
16	AP	-7.81	-8.97	-6.60	-8.38	-9.78	-7.26

Member	Stability Factors No Shear at Internal Columns			Stability Factors Including Shear at Internal Columns		
	LC1	LC2	LC3	LC1	LC2	LC3
17	0.149	0.104	0.071	0.150	0.098	0.070
18	0.403	0.387	0.283	0.415	0.406	0.299
19	0.172	0.181	0.167	0.166	0.175	0.159
20	0.747	0.701	0.489	0.747	0.702	0.493
21	0.168	0.178	0.164	0.166	0.174	0.157
22	0.740	0.695	0.486	0.746	0.700	0.490
23	0.167	0.177	0.164	0.168	0.176	0.159
24	0.747	0.699	0.488	0.745	0.698	0.488
25	0.160	0.147	0.125	0.168	0.156	0.133
26	0.412	0.432	0.319	0.426	0.451	0.335

Load Case	Frames Plastic Collapse Load Factor No Shear at Internal Columns	Frames Plastic Collapse Load Factor Including Shear at Internal Columns
LC1	1.320	1.375
LC2	1.637	1.587
LC3	2.167	2.165

Frame Identification : **f18 b24**

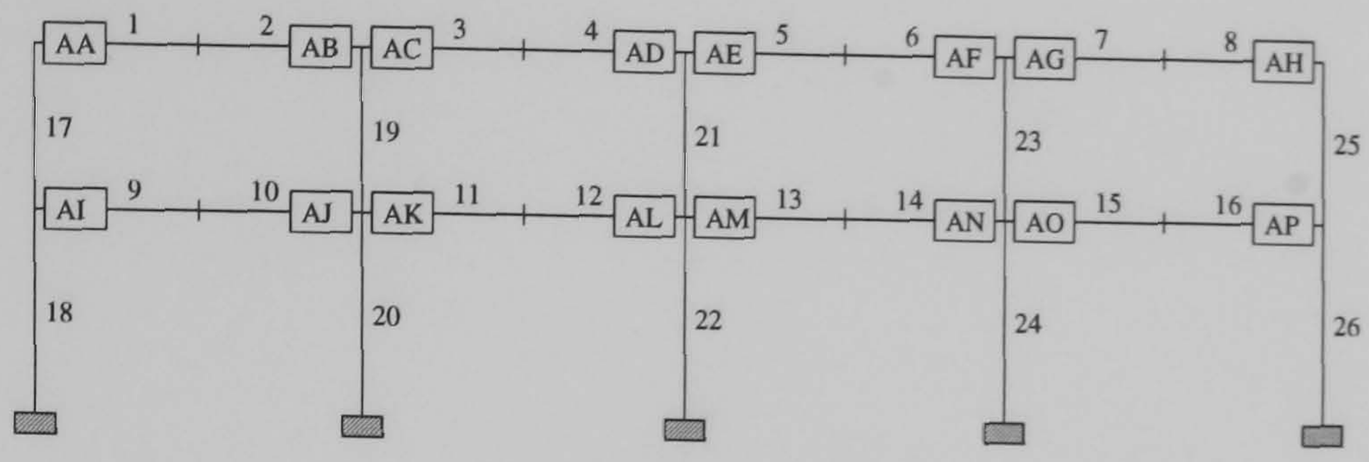

2 Storey 4 Bay

Member	Semi - Rigid Hinge Reference	Rotation (mrad)					
		No Shear at Internal Columns			Including Shear at Internal Columns		
		LC1	LC2	LC3	LC1	LC2	LC3
1	AA	**3.37**	**1.76**	**1.36**	**3.67**	**1.94**	**1.28**
2	AB	**-17.75**	**-16.34**	**-12.29**	**-16.92**	**-15.37**	**-11.85**
3	AC	**5.37**	**2.61**	**2.36**	**6.08**	**3.78**	**3.24**
4	AD	**-17.43**	**-15.87**	**-11.70**	**-16.69**	**-15.07**	**-11.56**
5	AE	**5.43**	**2.62**	**2.39**	**6.17**	**3.81**	**3.22**
6	AF	**-17.32**	**-15.73**	**-11.64**	**-16.63**	**-14.97**	**-11.55**
7	AG	**5.31**	**2.58**	**2.43**	**6.00**	**3.74**	**3.21**
8	AH	**-13.48**	**-12.22**	**-8.03**	**-12.60**	**-11.85**	**-8.32**
9	AI	**2.78**	**0.71**	**-0.47**	**3.11**	**0.88**	**-0.51**
10	AJ	**-14.16**	**-12.96**	**-6.73**	**-13.56**	**-13.42**	**-9.08**
11	AK	**3.82**	**1.91**	**0.50**	**5.79**	**2.72**	**0.15**
12	AL	**-13.30**	**-12.25**	**-6.51**	**-13.33**	**-13.17**	**-8.94**
13	AM	**3.82**	**1.92**	**0.46**	**5.76**	**2.70**	**0.15**
14	AN	**-13.35**	**-12.27**	**-6.56**	**-13.32**	**-13.13**	**-8.87**
15	AO	**3.88**	**1.95**	**0.55**	**5.73**	**2.60**	**0.02**
16	AP	**-9.40**	**-9.91**	**-6.99**	**-9.25**	**-9.94**	**-7.44**

Member	Stability Factors					
	No Shear at Internal Columns			Including Shear at Internal Columns		
	LC1	LC2	LC3	LC1	LC2	LC3
17	**0.273**	**0.185**	**0.149**	**0.284**	**0.192**	**0.146**
18	**0.563**	**0.497**	**0.370**	**0.567**	**0.499**	**0.385**
19	**0.251**	**0.241**	**0.221**	**0.256**	**0.236**	**0.214**
20	**0.761**	**0.724**	**0.560**	**0.747**	**0.721**	**0.561**
21	**0.249**	**0.239**	**0.217**	**0.252**	**0.233**	**0.211**
22	**0.754**	**0.718**	**0.553**	**0.743**	**0.716**	**0.558**
23	**0.246**	**0.238**	**0.215**	**0.252**	**0.234**	**0.211**
24	**0.757**	**0.719**	**0.555**	**0.744**	**0.716**	**0.558**
25	**0.336**	**0.292**	**0.251**	**0.333**	**0.290**	**0.258**
26	**0.582**	**0.572**	**0.427**	**0.581**	**0.577**	**0.445**

Load Case	Frames Plastic Collapse Load Factor	
	No Shear at Internal Columns	Including Shear at Internal Columns
LC1	**1.265**	**1.267**
LC2	**1.482**	**1.480**
LC3	**1.817**	**1.812**

Frame Identification : **f19 b20**

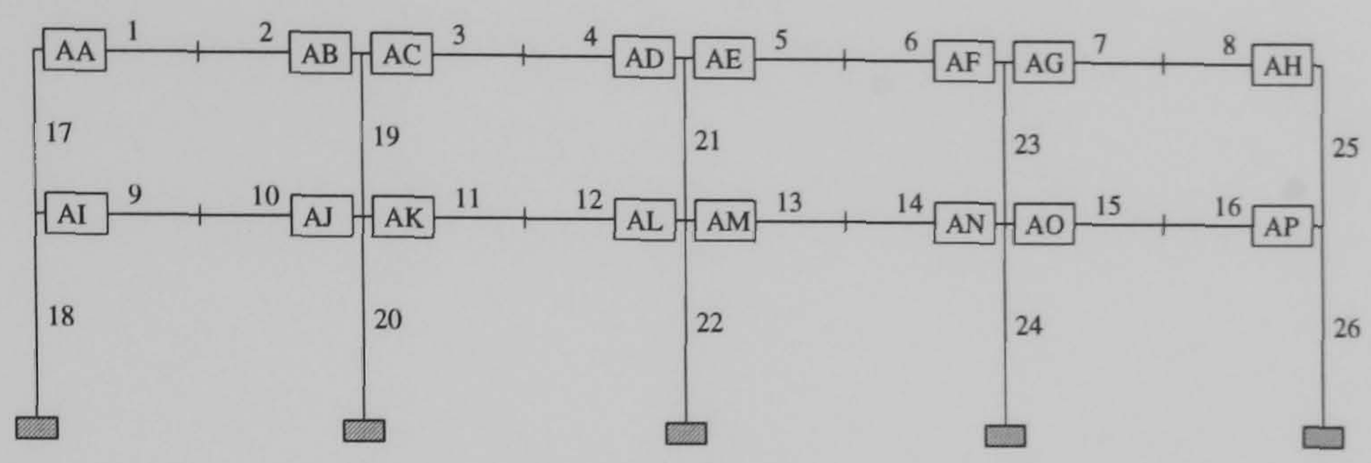

2 Storey 4 Bay

Member	Semi - Rigid Hinge Reference	Rotation (mrad)					
		No Shear at Internal Columns			Including Shear at Internal Columns		
		LC1	LC2	LC3	LC1	LC2	LC3
1	AA	**2.38**	**1.32**	**1.18**	**1.04**	**1.60**	**1.26**
2	AB	**-15.23**	**-12.44**	**-8.05**	**-10.46**	**-12.13**	**-8.81**
3	AC	**3.29**	**2.35**	**2.25**	**3.11**	**3.97**	**7.37**
4	AD	**-14.12**	**-11.40**	**-6.94**	**-10.11**	**-11.80**	**-10.49**
5	AE	**3.30**	**2.36**	**2.27**	**3.07**	**3.93**	**3.36**
6	AF	**-14.08**	**-11.48**	**-7.26**	**-10.13**	**-11.79**	**-9.85**
7	AG	**3.32**	**2.42**	**2.50**	**3.08**	**3.93**	**3.26**
8	AH	**-8.43**	**-7.74**	**-5.61**	**-6.42**	**-7.58**	**-6.18**
9	AI	**2.49**	**0.71**	**-0.19**	**-0.34**	**0.97**	**-0.24**
10	AJ	**-15.96**	**-14.71**	**-5.76**	**-8.71**	**-13.50**	**-8.77**
11	AK	**3.37**	**1.38**	**0.61**	**0.30**	**2.69**	**0.23**
12	AL	**-15.26**	**-14.13**	**-5.50**	**-8.56**	**-13.15**	**-8.46**
13	AM	**3.40**	**1.39**	**0.57**	**0.31**	**2.71**	**0.42**
14	AN	**-15.22**	**-14.02**	**-5.54**	**-8.47**	**-13.07**	**-8.31**
15	AO	**3.25**	**1.37**	**0.71**	**0.15**	**2.66**	**0.28**
16	AP	**-10.84**	**-11.34**	**-6.03**	**-6.80**	**-10.59**	**-6..64**

Member	Stability Factors					
	No Shear at Internal Columns			Including Shear at Internal Columns		
	LC1	LC2	LC3	LC1	LC2	LC3
17	**0.272**	**0.194**	**0.159**	**0.154**	**0.208**	**0.166**
18	**0.566**	**0.507**	**0.362**	**0.381**	**0.498**	**0.384**
19	**0.239**	**0.248**	**0.222**	**0.217**	**0.247**	**0.256**
20	**0.777**	**0.730**	**0.557**	**0.559**	**0.722**	**0.550**
21	**0.235**	**0.244**	**0.218**	**0.211**	**0.242**	**0.212**
22	**0.769**	**0.723**	**0.548**	**0.555**	**0.717**	**0.559**
23	**0.236**	**0.242**	**0.209**	**0.212**	**0.242**	**0.203**
24	**0.770**	**0.726**	**0.554**	**0.555**	**0.719**	**0.555**
25	**0.372**	**0.329**	**0.250**	**0.274**	**0.326**	**0.268**
26	**0.587**	**0.576**	**0.419**	**0.445**	**0.570**	**0.443**

Load Case	Frames Plastic Collapse Load Factor	
	No Shear at Internal Columns	Including Shear at Internal Columns
LC1	**1.267**	**1.885**
LC2	**1.492**	**1.465**
LC3	**1.887**	**1.865**

Frame Identification : **f19 b24**

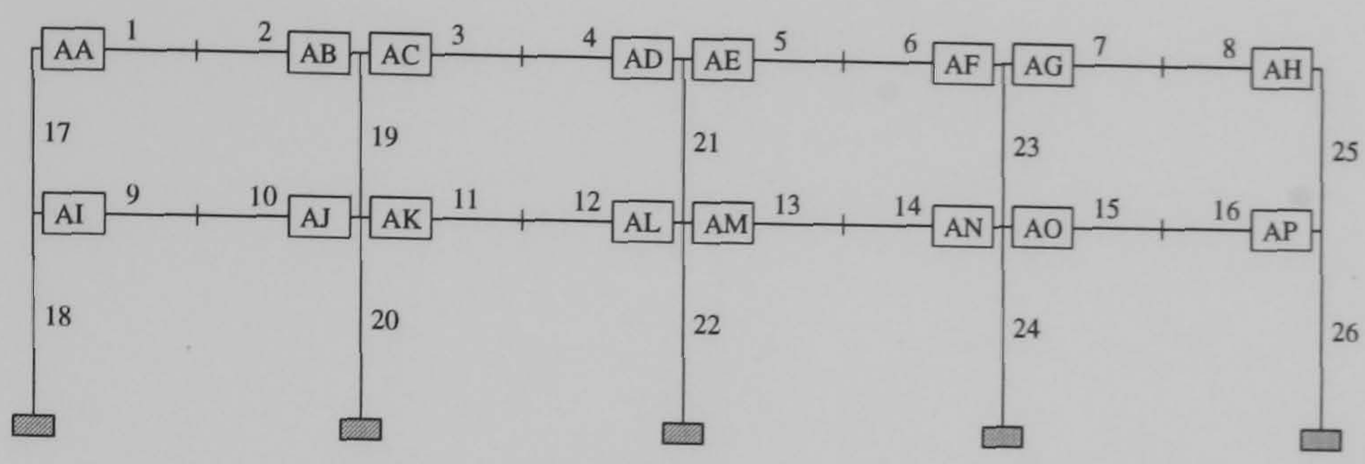

2 Storey 4 Bay

Member	Semi - Rigid Hinge Reference	Rotation (mrad)					
		No Shear at Internal Columns			Including Shear at Internal Columns		
		LC1	LC2	LC3	LC1	LC2	LC3
1	AA	**2.97**	**0.55**	**-0.25**	**2.95**	**0.17**	**-0.65**
2	AB	**-8.23**	**-8.63**	**-7.77**	**-9.86**	**-10.86**	**-9.88**
3	AC	**3.46**	**1.54**	**0.89**	**4.11**	**1.38**	**0.57**
4	AD	**-7.71**	**-8.29**	**-7.49**	**-9.51**	**-10.60**	**-9.66**
5	AE	**3.40**	**1.49**	**0.83**	**4.08**	**1.36**	**0.53**
6	AF	**-7.84**	**-8.42**	**-7.64**	**-9.56**	**-10.65**	**-9.72**
7	AG	**3.76**	**1.84**	**1.15**	**4.29**	**1.55**	**0.71**
8	AH	**-7.41**	**-8.79**	**-7.92**	**-8.05**	**-9.86**	**-8.93**
9	AI	**3.29**	**-0.70**	**-2.49**	**3.35**	**-0.97**	**-2.84**
10	AJ	**-8.96**	**-10.21**	**-7.57**	**-11.21**	**-13.50**	**-10.32**
11	AK	**3.65**	**0.78**	**-0.98**	**4.64**	**0.39**	**-1.95**
12	AL	**-8.31**	**-9.84**	**-7.47**	**-10.77**	**-13.21**	**-10.22**
13	AM	**3.55**	**0.72**	**-0.99**	**4.60**	**0.37**	**-1.95**
14	AN	**-8.51**	**-10.01**	**-7.56**	**-10.85**	**-13.26**	**-10.22**
15	AO	**4.00**	**1.15**	**-0.71**	**4.85**	**0.57**	**-1.85**
16	AP	**-8.46**	**-11.74**	**-9.82**	**-9.18**	**-12.84**	**-10.75**

Member	Stability Factors					
	No Shear at Internal Columns			Including Shear at Internal Columns		
	LC1	LC2	LC3	LC1	LC2	LC3
17	**0.253**	**0.175**	**0.120**	**0.256**	**0.171**	**0.126**
18	**0.554**	**0.565**	**0.471**	**0.571**	**0.591**	**0.492**
19	**0.227**	**0.256**	**0.235**	**0.221**	**0.253**	**0.231**
20	**0.687**	**0.729**	**0.586**	**0.687**	**0.733**	**0.592**
21	**0.217**	**0.250**	**0.230**	**0.216**	**0.249**	**0.228**
22	**0.672**	**0.718**	**0.581**	**0.679**	**0.727**	**0.588**
23	**0.213**	**0.245**	**0.226**	**0.214**	**0.247**	**0.227**
24	**0.687**	**0.729**	**0.589**	**0.686**	**0.731**	**0.592**
25	**0.270**	**0.269**	**0.235**	**0.283**	**0.289**	**0.254**
26	**0.570**	**0.666**	**0.552**	**0.591**	**0.696**	**0.577**

Load Case	Frames Plastic Collapse Load Factor	
	No Shear at Internal Columns	Including Shear at Internal Columns
LC1	**1.417**	**1.387**
LC2	**1.535**	**1.532**
LC3	**1.945**	**1.930**

Frame Identification : **f20 b20**

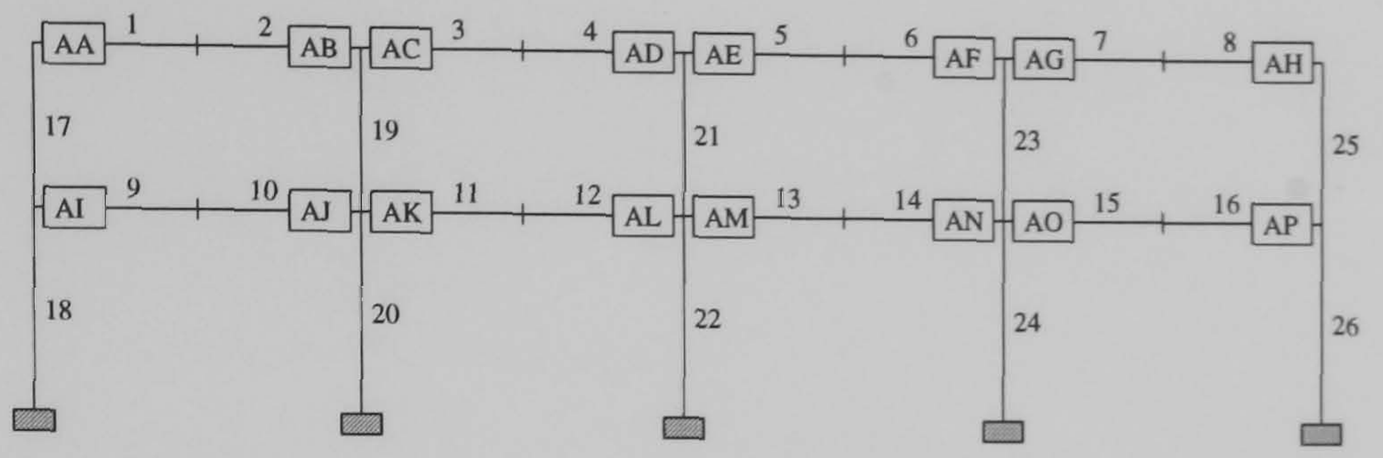

2 Storey 4 Bay

Member	Semi - Rigid Hinge Reference	Rotation (mrad)					
		No Shear at Internal Columns			Including Shear at Internal Columns		
		LC1	LC2	LC3	LC1	LC2	LC3
1	AA	**2.37**	**0.35**	**-0.05**	**2.42**	**0.26**	**-0.41**
2	AB	**-6.04**	**-6.20**	**-5.44**	**-8.54**	**-9.14**	**-8.26**
3	AC	**2.51**	**1.27**	**0.88**	**3.57**	**1.48**	**0.80**
4	AD	**-5.48**	**-5.97**	**-5.10**	**-8.09**	**-8.81**	**-7.97**
5	AE	**2.38**	**1.17**	**0.80**	**3.51**	**1.43**	**0.75**
6	AF	**-5.70**	**-6.02**	**-5.31**	**-8.20**	**-8.91**	**-8.08**
7	AG	**2.77**	**1.52**	**1.13**	**3.78**	**1.66**	**0.96**
8	AH	**-5.96**	**-7.30**	**-6.17**	**-6.66**	**-8.07**	**-7.29**
9	AI	**3.44**	**-0.66**	**-2.35**	**3.51**	**-0.85**	**-2.76**
10	AJ	**-9.09**	**-12.02**	**-6.45**	**-10.99**	**-13.09**	**-9.94**
11	AK	**3.05**	**0.46**	**-0.67**	**4.54**	**0.51**	**-1.76**
12	AL	**-7.63**	**-11.40**	**-6.35**	**-10.52**	**-12.80**	**-9.85**
13	AM	**3.08**	**0.48**	**-0.67**	**4.49**	**0.48**	**-1.75**
14	AN	**-8.01**	**-11.56**	**-6.46**	**-10.60**	**-12.86**	**-9.86**
15	AO	**3.50**	**0.75**	**-0.35**	**4.79**	**0.74**	**-1.61**
16	AP	**-8.46**	**-12.28**	**-9.56**	**-9.30**	**-12.91**	**-10.78**

Member	Stability Factors					
	No Shear at Internal Columns			Including Shear at Internal Columns		
	LC1	LC2	LC3	LC1	LC2	LC3
17	**0.252**	**0.181**	**0.125**	**0.258**	**0.177**	**0.127**
18	**0.542**	**0.568**	**0.458**	**0.565**	**0.586**	**0.488**
19	**0.234**	**0.269**	**0.241**	**0.226**	**0.258**	**0.237**
20	**0.683**	**0.726**	**0.581**	**0.688**	**0.733**	**0.592**
21	**0.219**	**0.258**	**0.232**	**0.218**	**0.253**	**0.232**
22	**0.667**	**0.716**	**0.573**	**0.678**	**0.725**	**0.587**
23	**0.218**	**0.253**	**0.226**	**0.217**	**0.250**	**0.230**
24	**0.686**	**0.728**	**0.586**	**0.687**	**0.732**	**0.592**
25	**0.270**	**0.276**	**0.234**	**0.292**	**0.299**	**0.262**
26	**0.557**	**0.668**	**0.534**	**0.585**	**0.688**	**0.571**

Load Case	Frames Plastic Collapse Load Factor	
	No Shear at Internal Columns	Including Shear at Internal Columns
LC1	**1.342**	**1.335**
LC2	**1.497**	**1.452**
LC3	**1.882**	**1.880**

Frame Identification : **f20 b24**

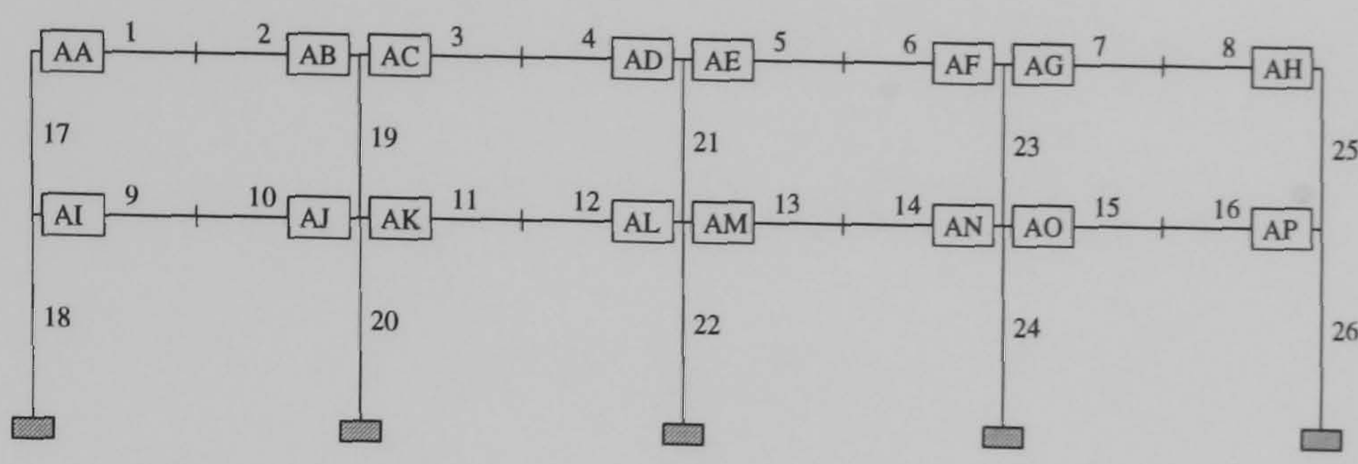

2 Storey 4 Bay

Member	Semi - Rigid Hinge Reference	Rotation (mrad)					
		No Shear at Internal Columns			Including Shear at Internal Columns		
		LC1	LC2	LC3	LC1	LC2	LC3
1	AA	4.31	-0.54	-1.80	4.27	-1.23	-2.54
2	AB	-10.87	-13.63	-12.79	-12.16	-16.14	-15.29
3	AC	4.69	0.52	-0.56	5.25	-0.14	-1.43
4	AD	-10.65	-13.51	-12.67	-12.13	-16.04	-15.14
5	AE	4.68	0.51	-0.57	5.26	-0.14	-1.44
6	AF	-10.66	-13.53	-12.71	-12.10	-16.01	-15.13
7	AG	4.85	0.69	-0.39	5.22	-0.23	-1.50
8	AH	-10.32	-14.19	-13.35	-10.91	-15.61	-14.75
9	AI	2.74	-3.17	-5.05	2.75	-3.66	-5.61
10	AJ	-8.34	-12.12	-10.04	-9.91	-15.46	-13.14
11	AK	3.18	-1.25	-3.09	3.76	-2.46	-4.78
12	AL	-8.08	-11.94	-9.99	-9.85	-15.25	-12.96
13	AM	3.15	-1.27	-3.09	3.76	-2.47	-4.79
14	AN	-8.14	-11.98	-9.99	-9.83	-15.19	-12.89
15	AO	3.32	-1.12	-3.02	3.72	-2.63	-4.98
16	AP	-8.13	-14.34	-12.92	-8.67	-15.52	-14.00

Member	Stability Factors					
	No Shear at Internal Columns			Including Shear at Internal Columns		
	LC1	LC2	LC3	LC1	LC2	LC3
17	0.183	0.113	0.099	0.184	0.115	0.111
18	0.428	0.532	0.466	0.440	0.559	0.488
19	0.232	0.283	0.265	0.228	0.280	0.262
20	0.718	0.831	0.692	0.719	0.840	0.702
21	0.228	0.280	0.263	0.226	0.279	0.261
22	0.710	0.825	0.688	0.716	0.834	0.697
23	0.226	0.279	0.262	0.227	0.280	0.261
24	0.718	0.830	0.691	0.717	0.833	0.695
25	0.198	0.214	0.192	0.205	0.227	0.205
26	0.444	0.630	0.556	0.457	0.658	0.581

Load Case	Frames Plastic Collapse Load Factor	
	No Shear at Internal Columns	Including Shear at Internal Columns
LC1	1.447	1.435
LC2	1.482	1.522
LC3	1.730	1.710

Frame Identification : **f21 b20**

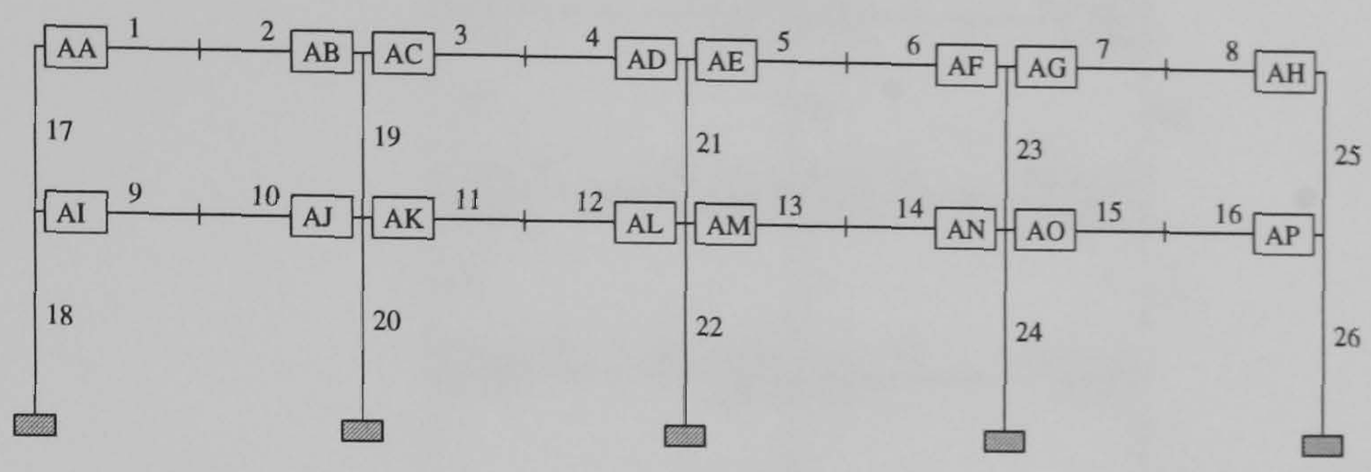

2 Storey 4 Bay

Member	Semi - Rigid Hinge Reference	Rotation (mrad)					
		No Shear at Internal Columns			Including Shear at Internal Columns		
		LC1	LC2	LC3	LC1	LC2	LC3
1	AA	**3.47**	**-0.23**	**-1.23**	**3.47**	**-0.84**	**-1.88**
2	AB	**-8.82**	**-10.61**	**-9.88**	**-10.69**	**-13.78**	**-12.98**
3	AC	**3.72**	**0.84**	**0.03**	**4.59**	**0.36**	**-0.70**
4	AD	**-8.46**	**-10.38**	**-9.67**	**-10.56**	**-13.58**	**-12.74**
5	AE	**3.68**	**0.81**	**0.00**	**4.58**	**0.34**	**-0.72**
6	AF	**-8.54**	**-10.45**	**-9.76**	**-10.56**	**-13.56**	**-12.74**
7	AG	**3.92**	**1.06**	**0.23**	**4.60**	**0.29**	**-0.75**
8	AH	**-8.42**	**-11.44**	**-10.74**	**-9.11**	**-12.94**	**-12.20**
9	AI	**2.95**	**-3.03**	**-4.98**	**2.97**	**-3.62**	**-5.65**
10	AJ	**-8.14**	**-11.67**	**-9.61**	**-10.03**	**-15.64**	**-13.27**
11	AK	**3.17**	**-1.08**	**-2.89**	**3.88**	**-2.48**	**-4.87**
12	AL	**-7.86**	**-11.50**	**-9.59**	**-9.99**	**-15.46**	**-13.12**
13	AM	**3.14**	**-1.09**	**-2.87**	**3.89**	**-2.48**	**-4.86**
14	AN	**-7.92**	**-11.55**	**-9.60**	**-9.96**	**-15.40**	**-13.05**
15	AO	**3.35**	**-0.88**	**-2.75**	**3.85**	**-2.64**	**-5.04**
16	AP	**-8.25**	**-14.39**	**-12.93**	**-8.93**	**-15.84**	**-14.24**

Member	Stability Factors					
	No Shear at Internal Columns			Including Shear at Internal Columns		
	LC1	LC2	LC3	LC1	LC2	LC3
17	**0.189**	**0.125**	**0.103**	**0.191**	**0.122**	**0.112**
18	**0.422**	**0.527**	**0.463**	**0.437**	**0.560**	**0.489**
19	**0.232**	**0.294**	**0.276**	**0.227**	**0.290**	**0.273**
20	**0.719**	**0.830**	**0.690**	**0.719**	**0.840**	**0.702**
21	**0.225**	**0.289**	**0.272**	**0.224**	**0.287**	**0.269**
22	**0.709**	**0.823**	**0.686**	**0.716**	**0.834**	**0.697**
23	**0.224**	**0.287**	**0.270**	**0.225**	**0.288**	**0.270**
24	**0.719**	**0.831**	**0.692**	**0.718**	**0.834**	**0.695**
25	**0.206**	**0.225**	**0.209**	**0.216**	**0.244**	**0.222**
26	**0.438**	**0.623**	**0.549**	**0.454**	**0.656**	**0.580**

Load Case	Frames Plastic Collapse Load Factor	
	No Shear at Internal Columns	Including Shear at Internal Columns
LC1	**1.512**	**1.530**
LC2	**1.520**	**1.517**
LC3	**1.700**	**1.682**

Frame Identification : **f21 b24**

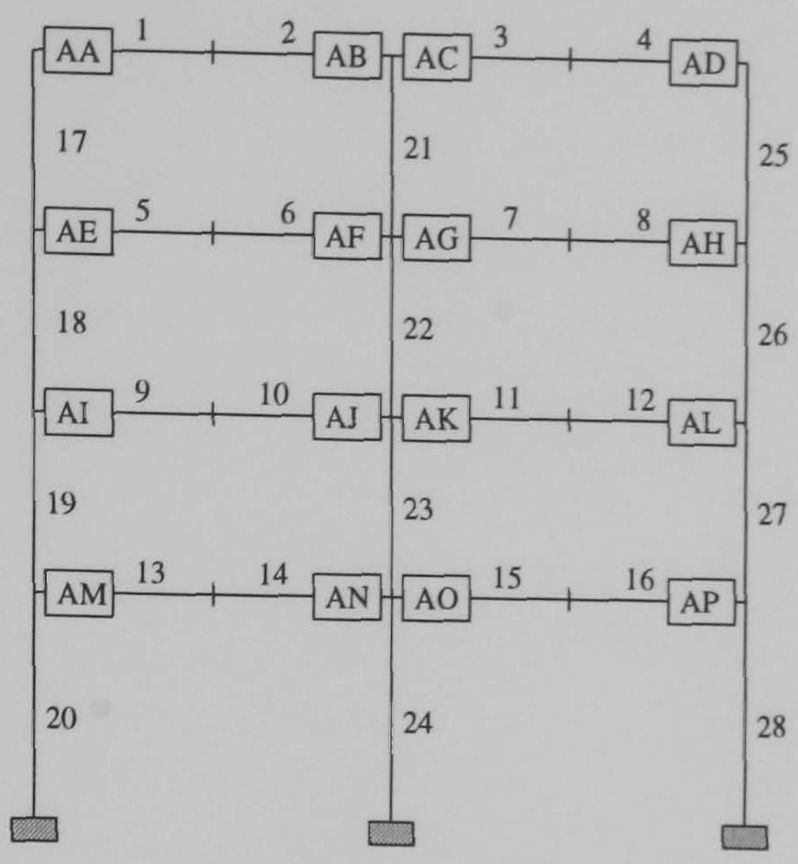

4 Storey 2 Bay

Member	Semi - Rigid Hinge Reference	Rotation (mrad)					
		No Shear at Internal Columns			Including Shear at Internal Columns		
		LC1	LC2	LC3	LC1	LC2	LC3
1	AA	**3.56**	**2.22**	**1.63**	**3.87**	**2.49**	**1.72**
2	AB	**-12.30**	**-10.58**	**-7.45**	**-12.84**	**-11.56**	**-10.00**
3	AC	**5.51**	**3.07**	**2.85**	**6.42**	**4.60**	**3.74**
4	AD	**-8.90**	**-8.03**	**-6.07**	**-8.78**	**-8.22**	**-6.73**
5	AE	**2.08**	**0.83**	**-0.04**	**2.48**	**1.02**	**-0.08**
6	AF	**-11.98**	**-9.62**	**-3.39**	**-10.42**	**-9.44**	**-5.25**
7	AG	**2.25**	**1.43**	**0.74**	**4.53**	**2.58**	**0.38**
8	AH	**-7.74**	**-7.30**	**-4.35**	**-7.41**	**-7.31**	**-4.82**
9	AI	**1.25**	**0.25**	**-0.33**	**1.81**	**0.39**	**-0.40**
10	AJ	**-14.35**	**-11.63**	**-3.98**	**-12.23**	**-11.16**	**-5.08**
11	AK	**0.32**	**0.50**	**0.24**	**2.67**	**1.04**	**0.04**
12	AL	**-11.82**	**-10.42**	**-4.15**	**-10.38**	**-10.09**	**-4.47**
13	AM	**1.33**	**0.17**	**-0.52**	**1.82**	**0.27**	**-0.58**
14	AN	**-13.84**	**-12.09**	**-4.80**	**-12.21**	**-11.73**	**-5.60**
15	AO	**0.97**	**0.39**	**-0.03**	**2.78**	**0.81**	**-0.32**
16	AP	**-11.03**	**-10.47**	**-4.58**	**-9.95**	**-10.23**	**-4.80**

Member	Stability Factors					
	No Shear at Internal Columns			Including Shear at Internal Columns		
	LC1	LC2	LC3	LC1	LC2	LC3
17	**0.285**	**0.199**	**0.155**	**0.301**	**0.214**	**0.163**
18	**0.460**	**0.318**	**0.220**	**0.487**	**0.323**	**0.230**
19	**0.415**	**0.299**	**0.166**	**0.447**	**0.309**	**0.172**
20	**0.694**	**0.587**	**0.364**	**0.685**	**0.587**	**0.376**
21	**0.275**	**0.242**	**0.241**	**0.247**	**0.242**	**0.222**
22	**0.841**	**0.748**	**0.518**	**0.844**	**0.746**	**0.489**
23	**0.543**	**0.480**	**0.327**	**0.542**	**0.479**	**0.313**
24	**0.915**	**0.796**	**0.525**	**0.883**	**0.786**	**0.517**
25	**0.328**	**0.287**	**0.223**	**0.326**	**0.293**	**0.241**
26	**0.600**	**0.523**	**0.309**	**0.587**	**0.526**	**0.326**
27	**0.516**	**0.429**	**0.270**	**0.513**	**0.432**	**0.282**
28	**0.701**	**0.636**	**0.424**	**0.694**	**0.638**	**0.436**

Load Case	Frames Plastic Collapse Load Factor	
	No Shear at Internal Columns	Including Shear at Internal Columns
LC1	**1.247**	**1.295**
LC2	**1.505**	**1.492**
LC3	**1.917**	**1.927**

Frame Identification : **f22 b24**

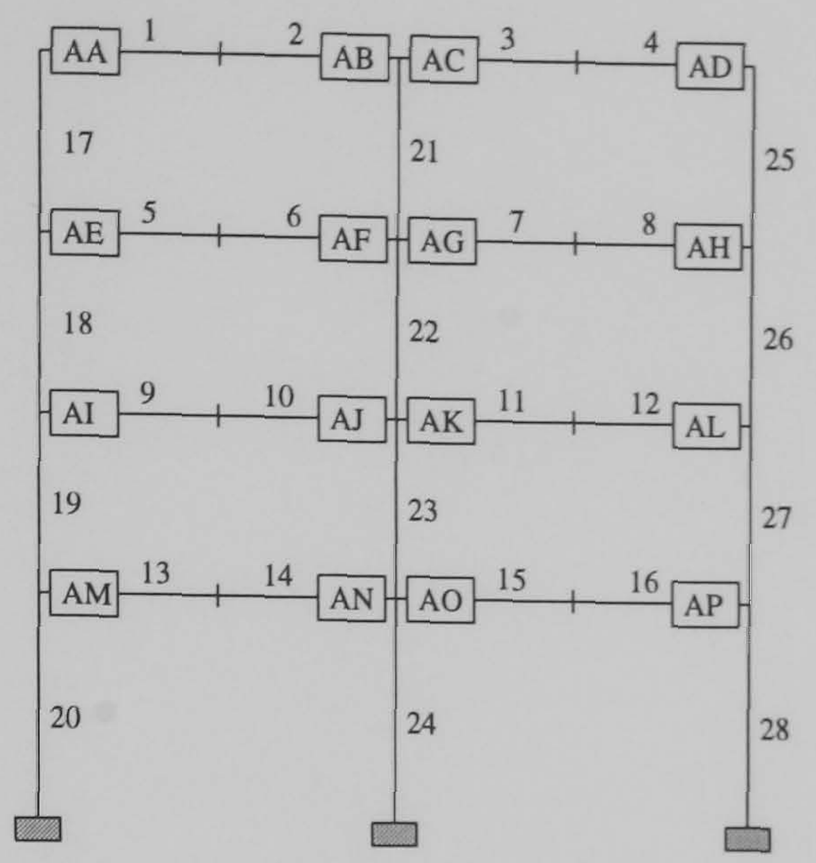

4 Storey 2 Bay

Member	Semi - Rigid Hinge Reference	Rotation (mrad)					
		No Shear at Internal Columns			Including Shear at Internal Columns		
		LC1	LC2	LC3	LC1	LC2	LC3
1	AA	**3.16**	**1.97**	**1.43**	**3.35**	**1.95**	**1.35**
2	AB	**-9.50**	**-8.52**	**-7.26**	**-10.77**	**-9.87**	**-8.46**
3	AC	**3.75**	**2.60**	**2.22**	**4.20**	**2.71**	**2.28**
4	AD	**-9.36**	**-8.51**	**-6.77**	**-9.60**	**-8.96**	**-7.22**
5	AE	**3.50**	**1.77**	**0.05**	**3.74**	**1.77**	**-0.13**
6	AF	**-13.91**	**-11.23**	**-5.88**	**-13.97**	**-12.48**	**-7.09**
7	AG	**3.81**	**2.51**	**0.46**	**4.67**	**2.46**	**-0.05**
8	AH	**-12.97**	**-11.54**	**-6.89**	**-13.01**	**-11.93**	**-7.37**
9	AI	**1.76**	**0.54**	**-0.48**	**2.03**	**0.55**	**-0.67**
10	AJ	**-17.09**	**-14.07**	**-5.83**	**-16.41**	**-13.93**	**-7.11**
11	AK	**1.77**	**0.74**	**0.03**	**2.51**	**0.98**	**-0.47**
12	AL	**-16.52**	**-13.71**	**-6.32**	**-16.00**	**-13.73**	**-6.82**
13	AM	**1.74**	**0.46**	**-0.64**	**1.99**	**0.52**	**-0.78**
14	AN	**-17.02**	**-14.27**	**-6.18**	**-16.36**	**-14.11**	**-7.46**
15	AO	**1.95**	**0.76**	**-0.15**	**2.71**	**1.00**	**-0.66**
16	AP	**-15.51**	**-13.20**	**-6.45**	**-15.07**	**-13.10**	**-6.87**

Member	Stability Factors					
	No Shear at Internal Columns			Including Shear at Internal Columns		
	LC1	LC2	LC3	LC1	LC2	LC3
17	**0.207**	**0.153**	**0.105**	**0.209**	**0.153**	**0.104**
18	**0.392**	**0.295**	**0.185**	**0.398**	**0.292**	**0.192**
19	**0.375**	**0.282**	**0.162**	**0.385**	**0.287**	**0.168**
20	**0.725**	**0.599**	**0.369**	**0.722**	**0.601**	**0.381**
21	**0.257**	**0.230**	**0.193**	**0.242**	**0.221**	**0.187**
22	**0.770**	**0.656**	**0.419**	**0.761**	**0.641**	**0.408**
23	**0.534**	**0.448**	**0.291**	**0.532**	**0.446**	**0.282**
24	**0.927**	**0.782**	**0.498**	**0.914**	**0.775**	**0.501**
25	**0.224**	**0.196**	**0.159**	**0.229**	**0.203**	**0.166**
26	**0.493**	**0.413**	**0.245**	**0.492**	**0.417**	**0.252**
27	**0.465**	**0.388**	**0.237**	**0.466**	**0.390**	**0.245**
28	**0.746**	**0.641**	**0.415**	**0.743**	**0.643**	**0.425**

Load Case	Frames Plastic Collapse Load Factor	
	No Shear at Internal Columns	Including Shear at Internal Columns
LC1	**1.117**	**1.115**
LC2	**1.342**	**1.342**
LC3	**1.925**	**1.910**

Frame Identification : **f23 b20**

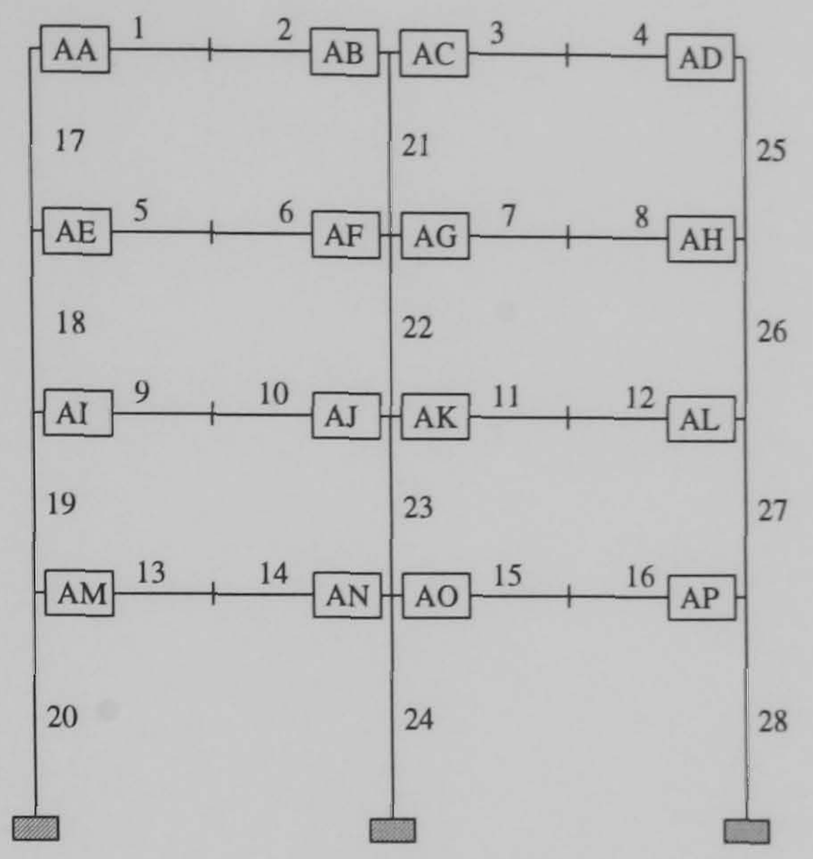

4 Storey 2 Bay

Member	Semi - Rigid Hinge Reference	Rotation (mrad)					
		No Shear at Internal Columns			Including Shear at Internal Columns		
		LC1	LC2	LC3	LC1	LC2	LC3
1	AA	**2.91**	**1.15**	**0.59**	**3.09**	**1.11**	**0.45**
2	AB	**-7.93**	**-7.82**	**-6.85**	**-9.57**	**-9.84**	**-8.74**
3	AC	**3.42**	**1.96**	**1.56**	**4.16**	**1.99**	**1.46**
4	AD	**-7.66**	**-8.08**	**-6.70**	**-8.02**	**-8.69**	**-7.33**
5	AE	**3.80**	**0.63**	**-1.04**	**4.20**	**0.55**	**-1.37**
6	AF	**-11.58**	**-11.37**	**-6.25**	**-12.46**	**-13.24**	**-8.31**
7	AG	**4.12**	**1.64**	**-0.21**	**5.20**	**1.31**	**-1.28**
8	AH	**-10.97**	**-11.90**	**-7.82**	**-11.11**	**-12.49**	**-8.59**
9	AI	**2.30**	**-0.56**	**-1.49**	**2.78**	**-0.68**	**-1.78**
10	AJ	**-12.76**	**-14.07**	**-5.48**	**-11.07**	**-14.32**	**-8.13**
11	AK	**1.96**	**-0.05**	**-0.45**	**3.90**	**-0.18**	**-1.65**
12	AL	**-10.48**	**-13.64**	**-6.84**	**-9.43**	**-14.00**	**-7.63**
13	AM	**2.19**	**-0.90**	**-1.86**	**2.67**	**-0.98**	**-2.13**
14	AN	**-12.95**	**-15.19**	**-6.91**	**-11.37**	**-15.49**	**-9.00**
15	AO	**2.00**	**-0.34**	**-0.94**	**3.90**	**-0.67**	**-2.24**
16	AP	**-9.95**	**-14.23**	**-7.51**	**-9.07**	**-14.36**	**-8.11**

Member	Stability Factors					
	No Shear at Internal Columns			Including Shear at Internal Columns		
	LC1	LC2	LC3	LC1	LC2	LC3
17	**0.213**	**0.148**	**0.086**	**0.215**	**0.147**	**0.083**
18	**0.411**	**0.303**	**0.217**	**0.424**	**0.307**	**0.231**
19	**0.410**	**0.281**	**0.180**	**0.435**	**0.286**	**0.193**
20	**0.691**	**0.636**	**0.409**	**0.687**	**0.642**	**0.430**
21	**0.247**	**0.265**	**0.232**	**0.232**	**0.252**	**0.223**
22	**0.750**	**0.712**	**0.485**	**0.729**	**0.693**	**0.465**
23	**0.519**	**0.495**	**0.347**	**0.520**	**0.492**	**0.328**
24	**0.893**	**0.850**	**0.581**	**0.863**	**0.848**	**0.580**
25	**0.231**	**0.222**	**0.184**	**0.239**	**0.234**	**0.197**
26	**0.490**	**0.463**	**0.291**	**0.490**	**0.471**	**0.305**
27	**0.498**	**0.429**	**0.275**	**0.497**	**0.430**	**0.292**
28	**0.723**	**0.719**	**0.504**	**0.720**	**0.726**	**0.521**

Load Case	Frames Plastic Collapse Load Factor	
	No Shear at Internal Columns	Including Shear at Internal Columns
LC1	**1.182**	**1.185**
LC2	**1.317**	**1.312**
LC3	**1.567**	**1.545**

Frame Identification : **f23 b24**

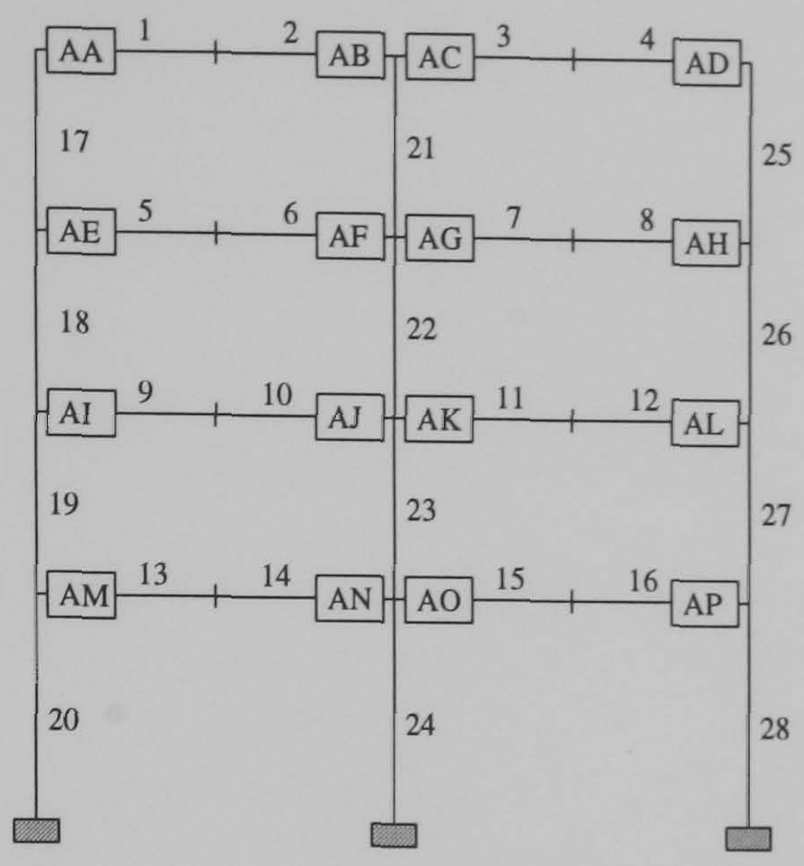

4 Storey 2 Bay

Member	Semi - Rigid Hinge Reference	Rotation (mrad)					
		No Shear at Internal Columns			Including Shear at Internal Columns		
		LC1	LC2	LC3	LC1	LC2	LC3
1	AA	**4.77**	**1.99**	**1.09**	**4.77**	**1.80**	**0.85**
2	AB	**-11.13**	**-11.49**	**-10.18**	**-12.30**	**-12.98**	**-11.60**
3	AC	**4.73**	**2.25**	**1.60**	**5.11**	**2.06**	**1.31**
4	AD	**-11.29**	**-11.89**	**-10.20**	**-11.77**	**-12.56**	**-10.86**
5	AE	**3.30**	**0.01**	**-1.82**	**3.25**	**-0.22**	**-2.22**
6	AF	**-9.63**	**-10.18**	**-6.65**	**-10.83**	**-11.90**	**-8.16**
7	AG	**3.36**	**0.64**	**-1.29**	**3.45**	**-0.05**	**-2.30**
8	AH	**-10.29**	**-11.57**	**-8.17**	**-10.76**	**-12.20**	**-8.83**
9	AI	**2.41**	**-1.14**	**-2.73**	**2.35**	**-1.40**	**-3.18**
10	AJ	**-10.01**	**-12.05**	**-7.44**	**-11.09**	**-12.86**	**-9.17**
11	AK	**2.57**	**-0.65**	**-1.97**	**2.67**	**-1.14**	**-3.10**
12	AL	**-10.30**	**-12.45**	**-8.67**	**-10.76**	**-12.87**	**-9.42**
13	AM	**2.09**	**-1.53**	**-3.10**	**2.07**	**-1.71**	**-3.44**
14	AN	**-10.41**	**-12.94**	**-8.09**	**-11.32**	**-13.44**	**-9.82**
15	AO	**2.57**	**-1.00**	**-2.38**	**2.74**	**-1.43**	**-3.53**
16	AP	**-9.91**	**-12.52**	**-9.01**	**-10.29**	**-12.74**	**-9.64**

Member	Stability Factors					
	No Shear at Internal Columns			Including Shear at Internal Columns		
	LC1	LC2	LC3	LC1	LC2	LC3
17	**0.138**	**0.091**	**0.067**	**0.138**	**0.089**	**0.066**
18	**0.294**	**0.228**	**0.165**	**0.296**	**0.232**	**0.174**
19	**0.393**	**0.293**	**0.193**	**0.396**	**0.298**	**0.202**
20	**0.693**	**0.629**	**0.422**	**0.706**	**0.637**	**0.438**
21	**0.173**	**0.182**	**0.166**	**0.169**	**0.178**	**0.157**
22	**0.564**	**0.523**	**0.356**	**0.555**	**0.509**	**0.345**
23	**0.481**	**0.436**	**0.296**	**0.473**	**0.430**	**0.286**
24	**0.806**	**0.760**	**0.529**	**0.801**	**0.761**	**0.539**
25	**0.150**	**0.142**	**0.120**	**0.154**	**0.147**	**0.125**
26	**0.340**	**0.319**	**0.205**	**0.347**	**0.325**	**0.213**
27	**0.455**	**0.411**	**0.262**	**0.465**	**0.417**	**0.271**
28	**0.730**	**0.721**	**0.514**	**0.743**	**0.729**	**0.530**

Load Case	Frames Plastic Collapse Load Factor	
	No Shear at Internal Columns	Including Shear at Internal Columns
LC1	**1.252**	**1.252**
LC2	**1.377**	**1.385**
LC3	**1.545**	**1.552**

Frame Identification : **f24 b20**

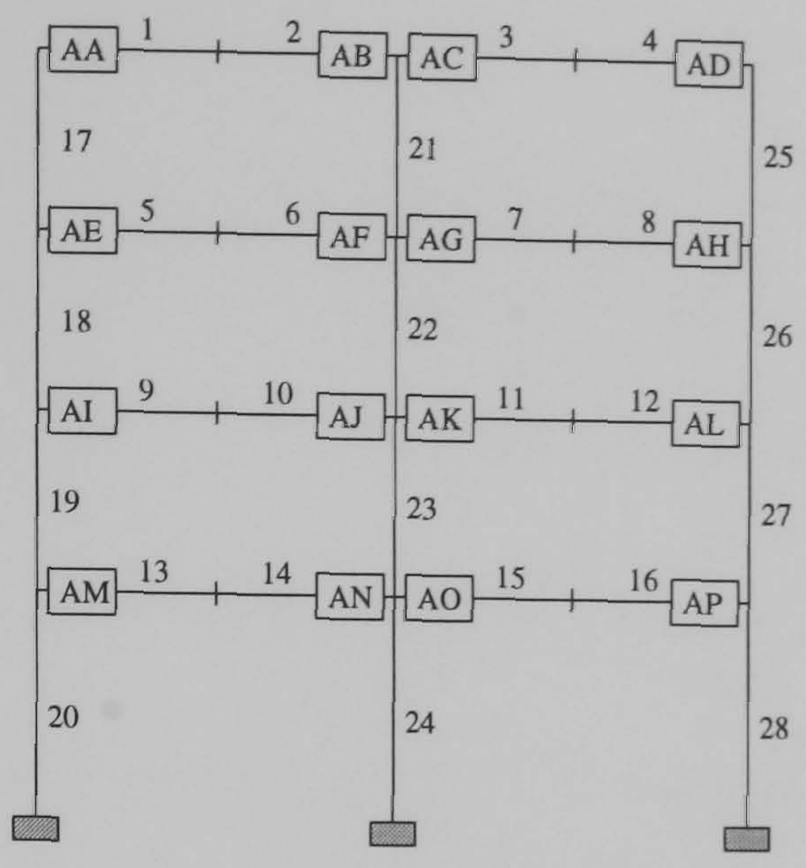

4 Storey 2 Bay

Member	Semi - Rigid Hinge Reference	Rotation (mrad) No Shear at Internal Columns			Rotation (mrad) Including Shear at Internal Columns		
		LC1	LC2	LC3	LC1	LC2	LC3
1	AA	**4.13**	**1.38**	**0.50**	**4.16**	**1.16**	**0.24**
2	AB	**-9.19**	**-9.99**	**-9.04**	**-10.73**	**-12.05**	**-10.99**
3	AC	**4.09**	**1.77**	**1.15**	**4.68**	**1.56**	**0.79**
4	AD	**-9.39**	**-10.57**	**-9.27**	**-9.91**	**-11.38**	**-10.05**
5	AE	**3.24**	**-0.36**	**-2.14**	**3.21**	**-0.69**	**-2.62**
6	AF	**-8.29**	**-9.40**	**-6.37**	**-9.86**	**-11.90**	**-8.54**
7	AG	**3.25**	**0.46**	**-1.36**	**3.56**	**-0.49**	**-2.76**
8	AH	**-8.86**	**-11.04**	**-8.23**	**-9.46**	**-11.94**	**-9.09**
9	AI	**2.40**	**-1.65**	**-3.19**	**2.35**	**-2.03**	**-3.76**
10	AJ	**-7.57**	**-10.58**	**-6.78**	**-9.63**	**-12.72**	**-9.59**
11	AK	**2.52**	**-0.64**	**-1.85**	**2.81**	**-1.66**	**-3.60**
12	AL	**-8.36**	**-11.88**	**-8.83**	**-9.13**	**-12.71**	**-9.90**
13	AM	**2.04**	**-2.32**	**-3.85**	**2.03**	**-2.64**	**-4.30**
14	AN	**-7.86**	**-12.34**	**-7.76**	**-9.93**	**-13.82**	**-10.76**
15	AO	**2.53**	**-1.30**	**-2.47**	**2.82**	**-2.35**	**-4.42**
16	AP	**-8.00**	**-12.50**	**-9.66**	**-8.71**	**-13.06**	**-10.58**

Member	Stability Factors No Shear at Internal Columns			Stability Factors Including Shear at Internal Columns		
	LC1	LC2	LC3	LC1	LC2	LC3
17	**0.148**	**0.091**	**0.061**	**0.150**	**0.089**	**0.060**
18	**0.301**	**0.235**	**0.183**	**0.306**	**0.246**	**0.197**
19	**0.404**	**0.299**	**0.204**	**0.410**	**0.311**	**0.221**
20	**0.672**	**0.644**	**0.444**	**0.697**	**0.662**	**0.471**
21	**0.172**	**0.200**	**0.185**	**0.168**	**0.194**	**0.177**
22	**0.561**	**0.558**	**0.395**	**0.550**	**0.538**	**0.380**
23	**0.484**	**0.476**	**0.338**	**0.472**	**0.463**	**0.323**
24	**0.799**	**0.808**	**0.589**	**0.790**	**0.813**	**0.599**
25	**0.159**	**0.159**	**0.137**	**0.165**	**0.167**	**0.145**
26	**0.342**	**0.345**	**0.233**	**0.354**	**0.359**	**0.246**
27	**0.454**	**0.442**	**0.292**	**0.473**	**0.454**	**0.309**
28	**0.713**	**0.782**	**0.581**	**0.738**	**0.799**	**0.606**

Load Case	Frames Plastic Collapse Load Factor No Shear at Internal Columns	Including Shear at Internal Columns
LC1	**1.347**	**1.332**
LC2	**1.365**	**1.370**
LC3	**1.525**	**1.520**

Frame Identification : **f24 b24**

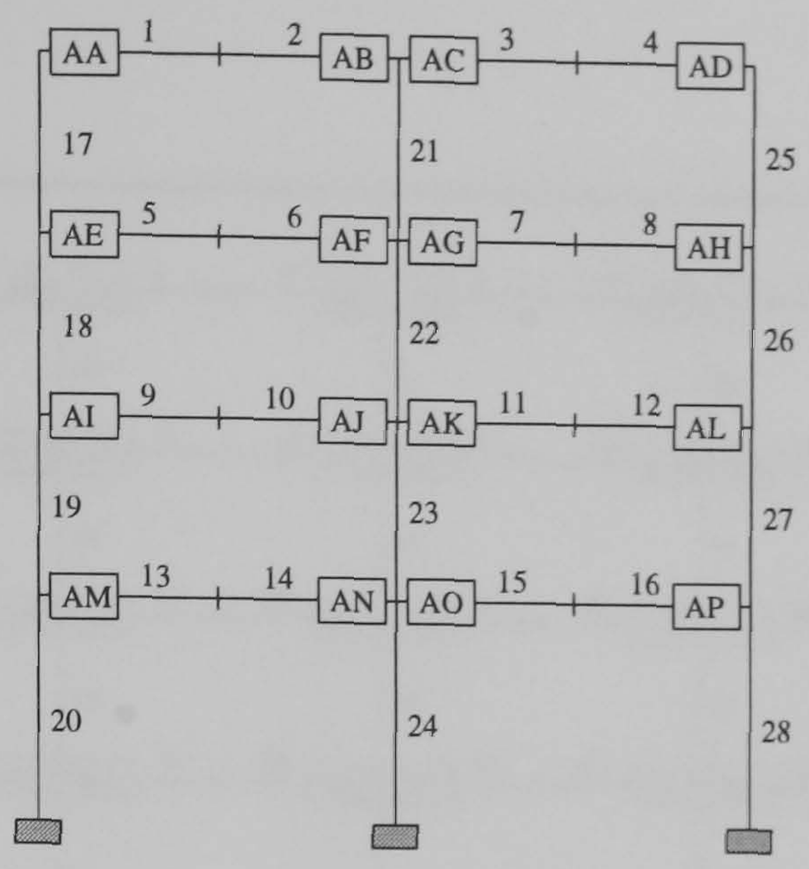

4 Storey 2 Bay

Member	Semi - Rigid Hinge Reference	Rotation (mrad)					
		No Shear at Internal Columns			Including Shear at Internal Columns		
		LC1	LC2	LC3	LC1	LC2	LC3
1	AA	**3.13**	**0.67**	**0.07**	**3.12**	**0.71**	**-0.04**
2	AB	**-12.18**	**-14.66**	**-11.80**	**-12.20**	**-14.20**	**-11.66**
3	AC	**5.47**	**1.50**	**1.15**	**5.54**	**2.17**	**1.57**
4	AD	**-7.41**	**-9.74**	**-7.91**	**-7.54**	**-9.75**	**-8.22**
5	AE	**2.74**	**-1.15**	**-2.26**	**2.91**	**-1.17**	**-2.40**
6	AF	**-8.47**	**-13.55**	**-7.24**	**-10.72**	**-13.91**	**-10.45**
7	AG	**3.59**	**0.12**	**-0.82**	**4.77**	**0.06**	**-2.10**
8	AH	**-7.32**	**-11.58**	**-9.10**	**-7.76**	**-11.67**	**-9.64**
9	AI	**2.71**	**-2.18**	**-3.22**	**2.85**	**-2.37**	**-3.67**
10	AJ	**-8.57**	**-20.44**	**-12.64**	**-9.97**	**-21.38**	**-14.53**
11	AK	**2.70**	**-1.50**	**-2.29**	**4.04**	**-2.66**	**-4.18**
12	AL	**-7.31**	**-21.37**	**-13.51**	**-7.81**	**-21.88**	**-15.14**
13	AM	**2.77**	**-2.44**	**-3.77**	**3.04**	**-2.59**	**-3.91**
14	AN	**-6.99**	**-15.81**	**-9.36**	**-9.77**	**-16.92**	**-13.78**
15	AO	**2.93**	**-1.44**	**-2.36**	**4.16**	**-2.53**	**-4.66**
16	AP	**-7.15**	**-15.22**	**-11.10**	**-7.74**	**-15.63**	**-11.75**

Member	Stability Factors					
	No Shear at Internal Columns			Including Shear at Internal Columns		
	LC1	LC2	LC3	LC1	LC2	LC3
17	**0.313**	**0.171**	**0.100**	**0.312**	**0.175**	**0.100**
18	**0.435**	**0.410**	**0.358**	**0.448**	**0.417**	**0.375**
19	**0.291**	**0.215**	**0.170**	**0.299**	**0.222**	**0.184**
20	**0.388**	**0.518**	**0.423**	**0.405**	**0.528**	**0.451**
21	**0.243**	**0.296**	**0.285**	**0.235**	**0.303**	**0.293**
22	**0.584**	**0.735**	**0.626**	**0.573**	**0.736**	**0.609**
23	**0.373**	**0.441**	**0.358**	**0.362**	**0.437**	**0.342**
24	**0.566**	**0.724**	**0.600**	**0.560**	**0.735**	**0.620**
25	**0.344**	**0.371**	**0.316**	**0.347**	**0.371**	**0.325**
26	**0.493**	**0.617**	**0.473**	**0.510**	**0.624**	**0.493**
27	**0.318**	**0.354**	**0.268**	**0.330**	**0.357**	**0.280**
28	**0.387**	**0.610**	**0.524**	**0.402**	**0.619**	**0.551**

Load Case	Frames Plastic Collapse Load Factor	
	No Shear at Internal Columns	Including Shear at Internal Columns
LC1	**1.347**	**1.360**
LC2	**1.202**	**1.225**
LC3	**1.265**	**1.295**

Frame Identification : **f25 b24**

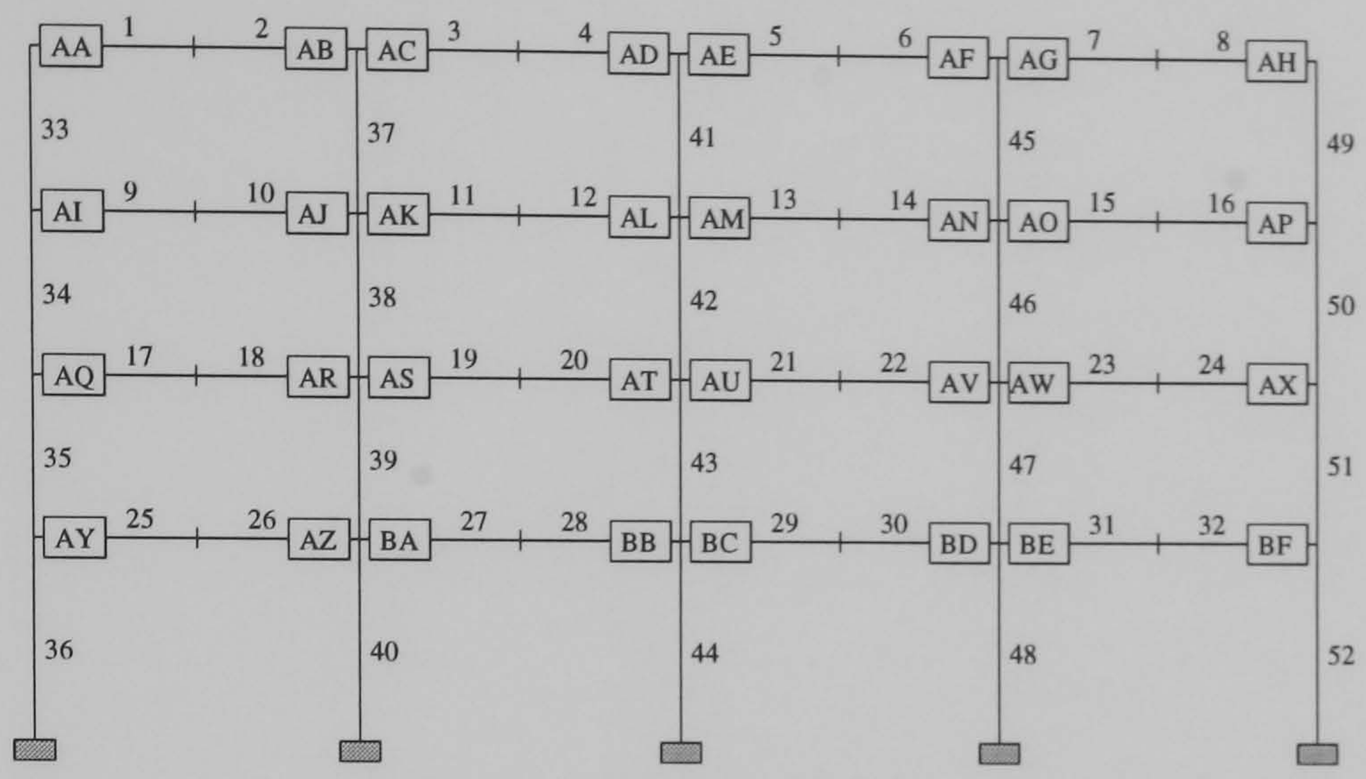

4 Storey 4 Bay

Member	Semi - Rigid Hinge Reference	Rotation (mrad)					
		No Shear at Internal Columns			Including Shear at Internal Columns		
		LC1	LC2	LC3	LC1	LC2	LC3
1	AA	**3.05**	**2.27**	**1.86**	**3.70**	**2.55**	**1.84**
2	AB	**-14.36**	**-10.25**	**-6.94**	**-13.21**	**-11.60**	**-9.91**
3	AC	**3.63**	**3.05**	**2.80**	**6.36**	**4.78**	**3.90**
4	AD	**-13.47**	**-9.33**	**-6.49**	**-13.15**	**-11.48**	**-9.70**
5	AE	**3.76**	**3.07**	**2.71**	**6.39**	**4.80**	**3.89**
6	AF	**-13.47**	**-9.49**	**-6.66**	**-13.07**	**-11.40**	**-9.67**
7	AG	**3.69**	**3.17**	**2.95**	**6.29**	**4.69**	**3.86**
8	AH	**-9.49**	**-7.84**	**-5.69**	**-8.95**	**-8.03**	**-6.49**
9	AI	**1.61**	**0.94**	**0.27**	**2.27**	**1.21**	**0.12**
10	AJ	**-13.03**	**-9.62**	**-3.19**	**-10.78**	**-9.32**	**-5.07**
11	AK	**1.92**	**1.53**	**0.85**	**4.59**	**2.98**	**0.77**
12	AL	**-12.92**	**-9.44**	**-3.12**	**-10.91**	**-9.40**	**-5.13**
13	AM	**1.93**	**1.54**	**0.85**	**4.63**	**3.02**	**0.80**
14	AN	**-12.64**	**-9.26**	**-3.11**	**-10.77**	**-9.26**	**-5.02**
15	AO	**1.85**	**1.51**	**0.88**	**4.41**	**2.82**	**0.65**
16	AP	**-9.03**	**-7.13**	**-3.84**	**-7.67**	**-7.04**	**-4.47**
17	AQ	**1.03**	**0.50**	**0.11**	**1.58**	**0.79**	**0.06**
18	AR	**-14.49**	**-11.14**	**-2.92**	**-12.86**	**-10.19**	**-4.60**
19	AS	**1.07**	**0.73**	**0.51**	**2.51**	**1.63**	**0.46**
20	AT	**-14.28**	**-10.95**	**-2.75**	**-12.86**	**-10.14**	**-4.57**
21	AU	**1.08**	**0.74**	**0.51**	**2.52**	**1.64**	**0.46**
22	AV	**-14.17**	**-10.85**	**-2.79**	**-12.77**	**-10.06**	**-4.55**
23	AW	**1.02**	**0.69**	**0.60**	**2.42**	**1.57**	**0.42**
24	AX	**-12.68**	**-9.58**	**-3.34**	**-11.09**	**-8.75**	**-3.94**
25	AY	**1.21**	**0.55**	**0.01**	**1.64**	**0.80**	**-0.12**
26	AZ	**-14.16**	**-11.21**	**-3.48**	**-12.70**	**-10.39**	**-4.90**
27	BA	**1.21**	**0.72**	**0.32**	**2.63**	**1.55**	**0.24**
28	BB	**-13.81**	**-10.97**	**-3.31**	**-12.59**	**-10.29**	**-4.86**
29	BC	**1.21**	**0.73**	**0.33**	**2.64**	**1.56**	**0.24**
30	BD	**-13.75**	**-10.92**	**-3.37**	**-12.55**	**-10.25**	**-4.85**
31	BE	**1.17**	**0.69**	**0.44**	**2.56**	**1.51**	**0.23**
32	BF	**-11.51**	**-9.13**	**-3.57**	**-10.44**	**-8.52**	**-4.07**

Member	Stability Factors					
	No Shear at Internal Columns			Including Shear at Internal Columns		
	LC1	LC2	LC3	LC1	LC2	LC3
33	**0.260**	**0.201**	**0.165**	**0.293**	**0.216**	**0.168**
34	**0.433**	**0.316**	**0.200**	**0.474**	**0.335**	**0.214**
35	**0.410**	**0.314**	**0.182**	**0.435**	**0.331**	**0.178**
36	**0.695**	**0.566**	**0.334**	**0.688**	**0.561**	**0.353**
37	**0.256**	**0.242**	**0.227**	**0.251**	**0.235**	**0.212**
38	**0.848**	**0.729**	**0.482**	**0.852**	**0.725**	**0.468**
39	**0.554**	**0.462**	**0.305**	**0.550**	**0.461**	**0.295**
40	**0.920**	**0.766**	**0.481**	**0.892**	**0.750**	**0.482**
41	**0.255**	**0.237**	**0.216**	**0.248**	**0.232**	**0.208**
42	**0.840**	**0.721**	**0.474**	**0.851**	**0.724**	**0.467**
43	**0.547**	**0.455**	**0.298**	**0.546**	**0.457**	**0.292**
44	**0.911**	**0.759**	**0.474**	**0.888**	**0.747**	**0.479**
45	**0.251**	**0.232**	**0.213**	**0.251**	**0.234**	**0.210**
46	**0.851**	**0.732**	**0.480**	**0.856**	**0.729**	**0.470**
47	**0.548**	**0.458**	**0.298**	**0.546**	**0.458**	**0.291**
48	**0.911**	**0.760**	**0.481**	**0.888**	**0.746**	**0.479**
49	**0.342**	**0.282**	**0.214**	**0.330**	**0.288**	**0.235**
50	**0.607**	**0.519**	**0.292**	**0.600**	**0.515**	**0.314**
51	**0.517**	**0.432**	**0.245**	**0.514**	**0.432**	**0.266**
52	**0.713**	**0.611**	**0.380**	**0.702**	**0.608**	**0.401**

Load Case	Frames Plastic Collapse Load	
	No Shear at Internal Columns	Including Shear at Internal Columns
LC1	**1.285**	**1.290**
LC2	**1.535**	**1.522**
LC3	**1.952**	**1.952**

Frame Identification : **f28 b24**

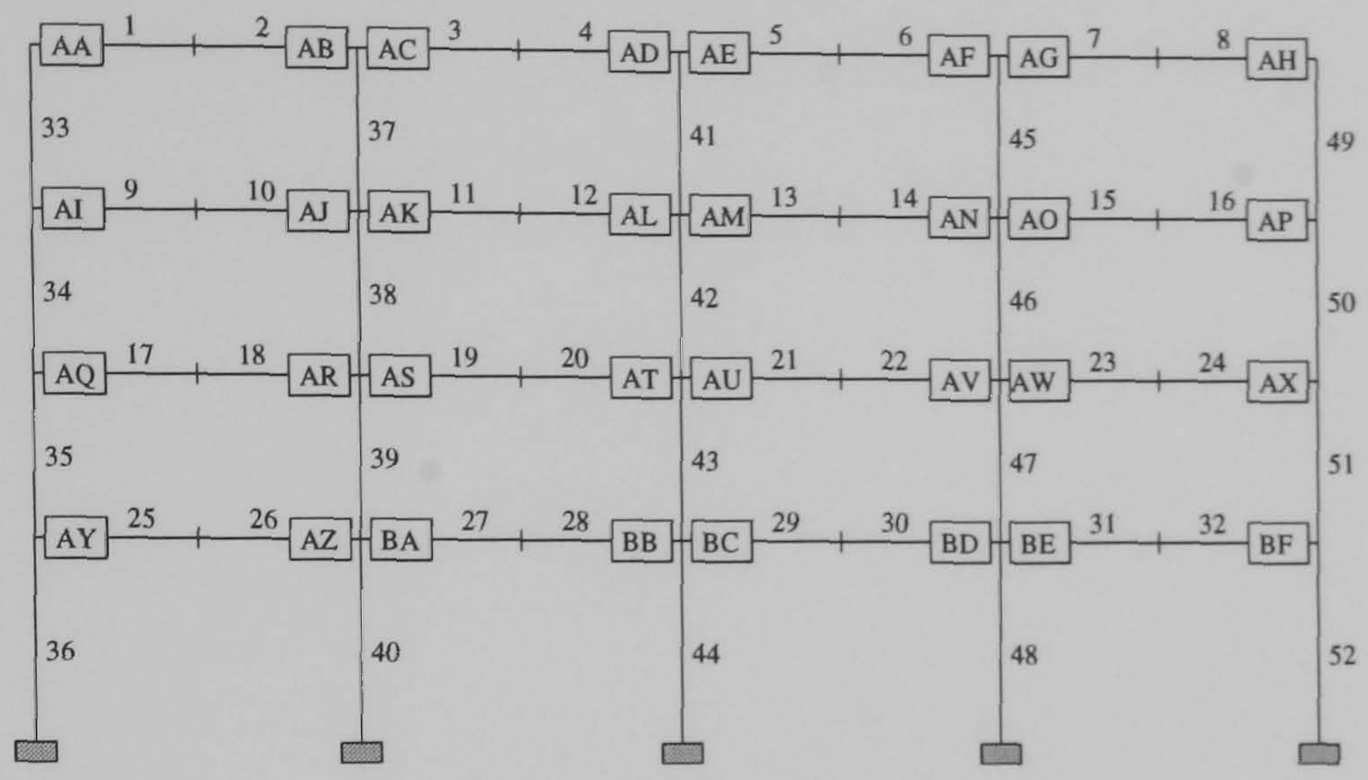

4 Storey 4 Bay

Member	Semi - Rigid Hinge Reference	Rotation (mrad)					
		No Shear at Internal Columns			Including Shear at Internal Columns		
		LC1	LC2	LC3	LC1	LC2	LC3
1	AA	3.03	1.98	1.48	3.25	1.86	1.27
2	AB	-9.65	-8.54	-7.20	-11.01	-10.09	-8.62
3	AC	3.76	2.67	2.25	4.46	2.92	2.37
4	AD	-9.71	-8.59	-7.15	-11.34	-10.32	-8.69
5	AE	3.79	2.70	2.25	4.52	2.97	2.40
6	AF	-9.67	-8.55	-7.14	-11.21	-10.19	-8.62
7	AG	3.70	2.65	2.27	4.18	2.69	2.25
8	AH	-9.52	-8.45	-6.66	-9.70	-9.05	-7.30
9	AI	3.14	1.61	0.06	3.57	1.54	-0.32
10	AJ	-14.64	-11.55	-5.92	-14.34	-12.86	-7.37
11	AK	3.73	2.49	0.54	4.91	2.60	0.02
12	AL	-14.91	-11.73	-6.04	-14.74	-13.16	-7.55
13	AM	3.74	2.50	0.58	4.97	2.64	0.05
14	AN	-14.72	-11.63	-5.98	-14.58	-13.04	-7.48
15	AO	3.48	2.38	0.50	4.56	2.28	-0.20
16	AP	-13.45	-11.73	-6.85	-13.25	-12.22	-7.59
17	AQ	1.34	0.29	-0.43	1.97	0.37	-0.83
18	AR	-17.96	-14.61	-5.76	-16.56	-14.33	-7.32
19	AS	1.56	0.65	0.05	2.66	0.94	-0.49
20	AT	-18.11	-14.75	-5.80	-16.82	-14.51	-7.37
21	AU	1.57	0.65	0.05	2.66	0.95	-0.48
22	AV	-18.03	-14.68	-5.80	-16.99	-14.53	-7.31
23	AW	1.41	0.53	0.08	2.33	0.75	-0.58
24	AX	-17.55	-14.31	-6.25	-16.18	-14.18	-7.02
25	AY	1.43	0.26	0.59	2.07	0.42	-0.92
26	AZ	-17.70	-14.72	-6.10	-16.24	-14.35	-7.63
27	BA	1.76	0.65	-0.18	2.93	0.99	-0.72
28	BB	-17.65	-14.73	-6.12	-16.31	-14.41	-7.66
29	BC	1.76	0.66	-0.18	2.94	0.99	-0.72
30	BD	-17.61	-14.69	-6.13	-15.58	-14.16	-7.78
31	BE	1.66	0.57	-0.09	4.74	1.51	-1.28
32	BF	-16.23	-13.66	-6.35	-15.45	-13.49	-6.93

Member	Stability Factors					
	No Shear at Internal Columns			Including Shear at Internal Columns		
	LC1	LC2	LC3	LC1	LC2	LC3
33	0.208	0.157	0.107	0.208	0.153	0.102
34	0.385	0.297	0.186	0.388	0.292	0.197
35	0.368	0.278	0.160	0.387	0.286	0.169
36	0.731	0.605	0.369	0.719	0.603	0.385
37	0.263	0.227	0.190	0.242	0.221	0.187
38	0.776	0.661	0.418	0.764	0.650	0.414
39	0.540	0.448	0.287	0.533	0.447	0.284
40	0.937	0.788	0.494	0.911	0.780	0.508
41	0.262	0.225	0.187	0.243	0.222	0.186
42	0.772	0.657	0.417	0.766	0.651	0.414
43	0.536	0.445	0.285	0.531	0.446	0.284
44	0.933	0.785	0.492	0.910	0.779	0.506
45	0.262	0.227	0.188	0.246	0.225	0.188
46	0.779	0.663	0.421	0.768	0.652	0.416
47	0.538	0.448	0.286	0.552	0.452	0.282
48	0.933	0.785	0.495	0.906	0.777	0.505
49	0.226	0.194	0.157	0.229	0.203	0.166
50	0.506	0.422	0.248	0.499	0.426	0.258
51	0.467	0.389	0.233	0.466	0.390	0.245
52	0.758	0.649	0.414	0.744	0.649	0.429

Load Case	Frames Plastic Collapse Load	
	No Shear at Internal Columns	Including Shear at Internal Columns
LC1	1.112	1.112
LC2	1.335	1.330
LC3	1.892	1.840

Frame Identification : **f29 b20**

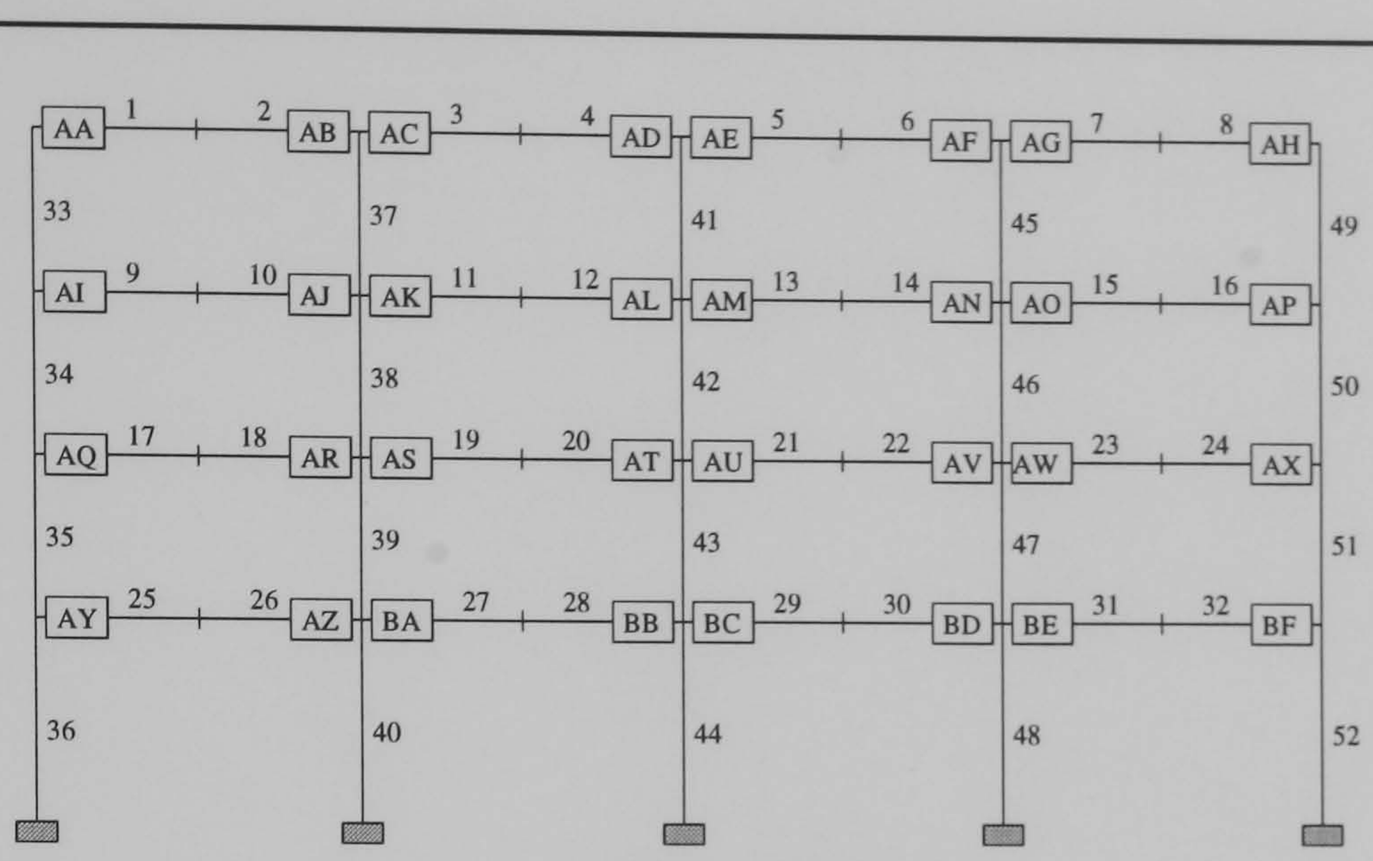

4 Storey 4 Bay

Member	Semi - Rigid Hinge Reference	Rotation (mrad)					
		No Shear at Internal Columns			Including Shear at Internal Columns		
		LC1	LC2	LC3	LC1	LC2	LC3
1	AA	**2.82**	**1.38**	**0.84**	**2.96**	**1.19**	**0.55**
2	AB	**-8.01**	**-7.59**	**-6.57**	**-9.89**	**-9.87**	**-8.69**
3	AC	**3.38**	**2.12**	**1.68**	**4.35**	**2.37**	**1.74**
4	AD	**-7.98**	**-7.55**	**-6.44**	**-10.17**	**-10.02**	**-8.68**
5	AE	**3.39**	**2.13**	**1.67**	**4.42**	**2.42**	**1.75**
6	AF	**-7.96**	**-7.53**	**-6.47**	**-10.03**	**-9.88**	**-8.61**
7	AG	**3.39**	**2.15**	**1.74**	**4.11**	**2.15**	**1.60**
8	AH	**-7.73**	**-7.66**	**-6.27**	**-8.16**	**-8.49**	**-7.12**
9	AI	**3.53**	**0.94**	**-0.65**	**3.93**	**0.74**	**-1.20**
10	AJ	**-12.14**	**-10.96**	**-5.90**	**-12.91**	**-13.14**	**-8.19**
11	AK	**3.99**	**1.97**	**0.09**	**5.36**	**1.89**	**-0.83**
12	AL	**-12.24**	**-11.02**	**-5.98**	**-13.32**	**-13.39**	**-8.32**
13	AM	**4.00**	**1.99**	**0.13**	**5.42**	**1.94**	**-0.79**
14	AN	**-12.11**	**-10.93**	**-5.92**	**-13.18**	**-13.25**	**-8.22**
15	AO	**3.89**	**1.93**	**0.09**	**4.99**	**1.55**	**-1.07**
16	AP	**-11.33**	**-11.44**	**-7.25**	**-11.43**	**-12.24**	**-8.33**
17	AQ	**1.96**	**-0.18**	**-0.96**	**2.54**	**-0.24**	**-1.48**
18	AR	**-13.60**	**-13.22**	**-4.99**	**-11.75**	**-13.22**	**-7.71**
19	AS	**2.02**	**0.35**	**-0.26**	**3.78**	**0.51**	**-1.16**
20	AT	**-13.41**	**-13.23**	**-4.98**	**-11.85**	**-13.26**	**-7.71**
21	AU	**2.03**	**0.35**	**-0.25**	**3.79**	**0.51**	**-1.16**
22	AV	**-13.28**	**-13.13**	**-5.01**	**-11.76**	**-13.20**	**-7.67**
23	AW	**1.92**	**0.27**	**-0.16**	**3.63**	**0.38**	**-1.31**
24	AX	**-11.60**	**-12.44**	**-6.05**	**-10.16**	**-12.69**	**-7.19**
25	AY	**1.91**	**-0.41**	**-1.28**	**2.48**	**0.39**	**-1.69**
26	AZ	**-13.64**	**-14.02**	**-5.52**	**-11.88**	**-13.99**	**-8.34**
27	BA	**2.06**	**0.09**	**-0.63**	**3.77**	**-0.15**	**-1.63**
28	BB	**-13.26**	**-13.97**	**-5.53**	**-11.83**	**-13.97**	**-8.33**
29	BC	**2.07**	**0.10**	**-0.62**	**3.78**	**0.15**	**-1.62**
30	BD	**-13.20**	**-13.93**	**-5.57**	**-11.78**	**-13.94**	**-8.31**
31	BE	**1.99**	**0.04**	**-0.46**	**3.67**	**0.07**	**-1.72**
32	BF	**-10.86**	**-12.62**	**-6.42**	**-9.47**	**-12.55**	**-7.43**

Member	Stability Factors					
	No Shear at Internal Columns			Including Shear at Internal Columns		
	LC1	LC2	LC3	LC1	LC2	LC3
33	**0.214**	**0.154**	**0.095**	**0.213**	**0.147**	**0.087**
34	**0.400**	**0.297**	**0.207**	**0.414**	**0.299**	**0.226**
35	**0.399**	**0.271**	**0.164**	**0.427**	**0.273**	**0.182**
36	**0.697**	**0.616**	**0.388**	**0.690**	**0.620**	**0.414**
37	**0.251**	**0.251**	**0.219**	**0.234**	**0.242**	**0.214**
38	**0.755**	**0.698**	**0.465**	**0.737**	**0.684**	**0.458**
39	**0.528**	**0.477**	**0.322**	**0.523**	**0.477**	**0.315**
40	**0.901**	**0.823**	**0.547**	**0.872**	**0.820**	**0.560**
41	**0.248**	**0.248**	**0.214**	**0.234**	**0.242**	**0.213**
42	**0.750**	**0.694**	**0.463**	**0.739**	**0.684**	**0.458**
43	**0.522**	**0.473**	**0.319**	**0.521**	**0.475**	**0.313**
44	**0.893**	**0.818**	**0.543**	**0.870**	**0.817**	**0.557**
45	**0.249**	**0.249**	**0.214**	**0.238**	**0.246**	**0.215**
46	**0.759**	**0.701**	**0.467**	**0.743**	**0.686**	**0.459**
47	**0.525**	**0.477**	**0.318**	**0.522**	**0.474**	**0.312**
48	**0.895**	**0.819**	**0.548**	**0.869**	**0.815**	**0.554**
49	**0.232**	**0.214**	**0.177**	**0.241**	**0.230**	**0.193**
50	**0.503**	**0.458**	**0.286**	**0.499**	**0.467**	**0.305**
51	**0.500**	**0.424**	**0.256**	**0.499**	**0.425**	**0.280**
52	**0.735**	**0.696**	**0.468**	**0.728**	**0.702**	**0.497**

Load Case	Frames Plastic Collapse Load	
	No Shear at Internal Columns	Including Shear at Internal Columns
LC1	**1.180**	**1.180**
LC2	**1.332**	**1.327**
LC3	**1.715**	**1.670**

Frame Identification : **f29 b24**

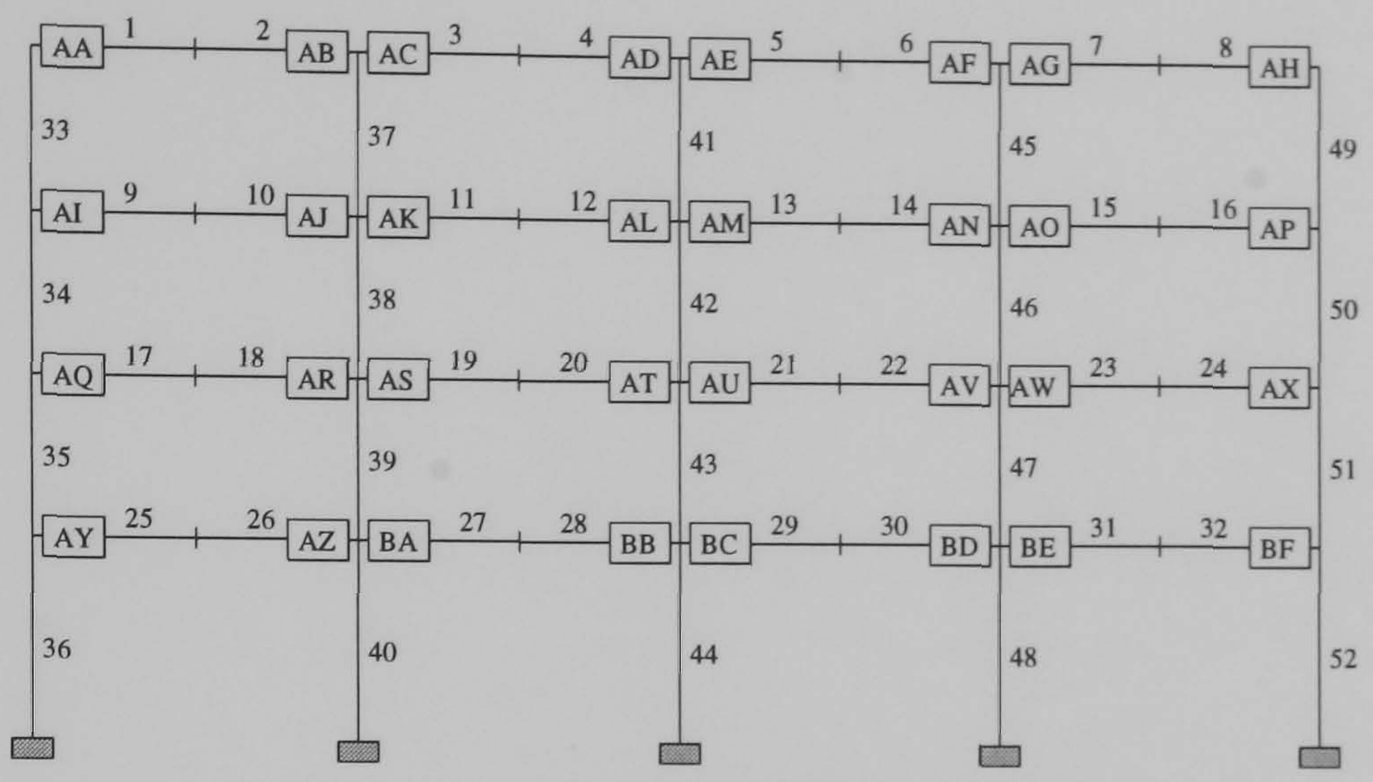

4 Storey 4 Bay

Member	Semi - Rigid Hinge Reference	Rotation (mrad)					
		No Shear at Internal Columns			Including Shear at Internal Columns		
		LC1	LC2	LC3	LC1	LC2	LC3
1	AA	**4.79**	**2.18**	**1.29**	**4.66**	**1.77**	**0.85**
2	AB	**-11.15**	**-11.31**	**-9.95**	**-12.36**	**-12.93**	**-11.50**
3	AC	**4.92**	**2.51**	**1.79**	**5.38**	**2.40**	**1.55**
4	AD	**-11.39**	**-11.51**	**-10.01**	**-12.79**	**-13.22**	**-11.62**
5	AE	**4.96**	**2.55**	**1.81**	**5.43**	**2.44**	**1.57**
6	AF	**-11.32**	**-11.45**	**-9.99**	**-12.71**	**-13.14**	**-11.56**
7	AG	**4.80**	**2.46**	**1.81**	**5.05**	**2.13**	**1.39**
8	AH	**-11.21**	**-11.56**	**-9.87**	**-11.81**	**-12.49**	**-10.77**
9	AI	**3.29**	**0.10**	**-1.67**	**3.11**	**-0.36**	**-2.31**
10	AJ	**-9.70**	**-10.15**	**-6.53**	**-11.11**	**-12.18**	**-8.34**
11	AK	**3.53**	**0.83**	**-1.09**	**3.74**	**0.17**	**-2.15**
12	AL	**-9.96**	**-10.37**	**-6.73**	**-11.58**	**-12.51**	**-8.53**
13	AM	**3.58**	**0.87**	**-1.06**	**3.78**	**0.21**	**-2.13**
14	AN	**-9.87**	**-10.32**	**-6.67**	**-11.48**	**-12.41**	**-8.46**
15	AO	**3.40**	**0.75**	**-1.14**	**3.35**	**-0.16**	**-2.37**
16	AP	**-10.27**	**-11.43**	**-7.94**	**-10.94**	**-12.36**	**-8.93**
17	AQ	**2.45**	**-1.07**	**-2.49**	**2.25**	**-1.48**	**-3.23**
18	AR	**-9.93**	**-11.93**	**-7.14**	**-11.24**	**-12.96**	**-9.21**
19	AS	**2.60**	**-0.53**	**-1.83**	**2.76**	**-1.07**	**-3.04**
20	AT	**-10.00**	**-12.21**	**-7.33**	**-11.43**	**-13.14**	**-9.35**
21	AU	**2.61**	**-0.53**	**-1.82**	**2.77**	**-1.06**	**-3.03**
22	AV	**-9.98**	**-12.18**	**-7.34**	**-11.39**	**-13.12**	**-9.34**
23	AW	**2.63**	**-0.57**	**-1.74**	**2.60**	**-1.19**	**-3.12**
24	AX	**-10.23**	**-12.35**	**-8.33**	**-10.91**	**-12.99**	**-9.49**
25	AY	**2.17**	**-1.42**	**-2.81**	**2.05**	**-1.67**	**-3.38**
26	AZ	**-10.23**	**-12.73**	**-7.74**	**-11.36**	**-13.40**	**-9.75**
27	BA	**2.54**	**-0.87**	**-2.27**	**2.77**	**-1.35**	**-3.45**
28	BB	**-10.10**	**-12.91**	**-7.92**	**-11.41**	**-13.50**	**-9.86**
29	BC	**2.55**	**-0.87**	**-2.26**	**2.77**	**-1.34**	**-3.43**
30	BD	**-10.12**	**-12.90**	**-7.94**	**-11.40**	**-13.49**	**-9.85**
31	BE	**2.67**	**-0.87**	**-2.11**	**2.72**	**-1.38**	**-3.46**
32	BF	**-9.77**	**-12.31**	**-8.60**	**-10.31**	**-12.67**	**-9.53**

Member	Stability Factors					
	No Shear at Internal Columns			Including Shear at Internal Columns		
	LC1	LC2	LC3	LC1	LC2	LC3
33	**0.138**	**0.096**	**0.069**	**0.137**	**0.091**	**0.064**
34	**0.292**	**0.230**	**0.165**	**0.291**	**0.237**	**0.178**
35	**0.394**	**0.290**	**0.186**	**0.394**	**0.293**	**0.198**
36	**0.691**	**0.627**	**0.417**	**0.705**	**0.635**	**0.437**
37	**0.169**	**0.176**	**0.159**	**0.168**	**0.176**	**0.156**
38	**0.561**	**0.523**	**0.353**	**0.557**	**0.515**	**0.351**
39	**0.477**	**0.431**	**0.287**	**0.474**	**0.428**	**0.284**
40	**0.798**	**0.754**	**0.517**	**0.802**	**0.761**	**0.538**
41	**0.169**	**0.177**	**0.159**	**0.170**	**0.177**	**0.156**
42	**0.561**	**0.523**	**0.354**	**0.560**	**0.516**	**0.351**
43	**0.474**	**0.429**	**0.288**	**0.473**	**0.428**	**0.284**
44	**0.793**	**0.752**	**0.518**	**0.801**	**0.760**	**0.538**
45	**0.172**	**0.178**	**0.160**	**0.173**	**0.180**	**0.157**
46	**0.565**	**0.526**	**0.356**	**0.562**	**0.517**	**0.352**
47	**0.475**	**0.431**	**0.288**	**0.473**	**0.427**	**0.283**
48	**0.799**	**0.754**	**0.521**	**0.800**	**0.758**	**0.536**
49	**0.149**	**0.139**	**0.118**	**0.154**	**0.146**	**0.124**
50	**0.341**	**0.322**	**0.206**	**0.351**	**0.331**	**0.218**
51	**0.453**	**0.407**	**0.253**	**0.465**	**0.416**	**0.267**
52	**0.727**	**0.715**	**0.503**	**0.744**	**0.728**	**0.528**

Load Case	Frames Plastic Collapse Load	
	No Shear at Internal Columns	Including Shear at Internal Columns
LC1	**1.250**	**1.250**
LC2	**1.387**	**1.377**
LC3	**1.565**	**1.552**

Frame Identification : **f30 b20**

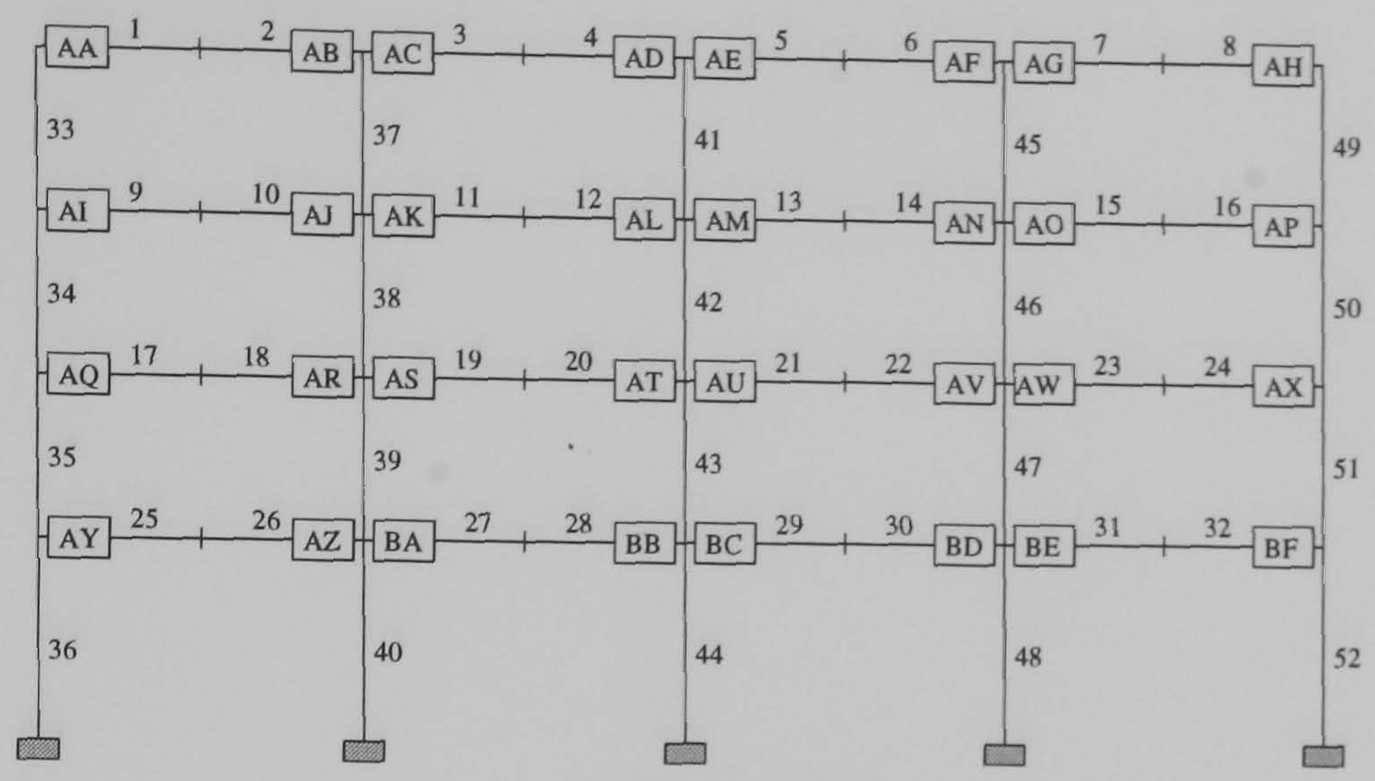

4 Storey 4 Bay

Member	Semi - Rigid Hinge Reference	Rotation (mrad) No Shear at Internal Columns			Rotation (mrad) Including Shear at Internal Columns		
		LC1	LC2	LC3	LC1	LC2	LC3
1	AA	4.13	1.71	0.84	4.06	1.27	0.39
2	AB	-9.21	-9.62	-8.64	-10.93	-11.97	-10.84
3	AC	4.18	2.07	1.38	4.95	2.01	1.15
4	AD	-9.34	-9.72	-8.61	-11.32	-12.20	-10.89
5	AE	4.22	2.11	1.39	5.00	2.05	1.18
6	AF	-9.28	-9.67	-8.61	-11.22	-12.11	-10.83
7	AG	4.15	2.09	1.45	4.65	1.74	0.99
8	AH	-9.31	-10.02	-8.72	-9.99	-11.15	-9.78
9	AI	3.25	0.07	-1.73	3.08	-0.58	-2.46
10	AJ	-8.34	-9.03	-6.00	-10.14	-11.87	-8.40
11	AK	3.36	0.82	-1.01	3.85	0.00	-2.33
12	AL	-8.52	-9.21	-6.17	-10.60	-12.15	-8.55
13	AM	3.42	0.87	-0.97	3.91	0.03	-2.30
14	AN	-8.43	-9.14	-6.10	-10.48	-12.04	-8.47
15	AO	3.31	0.81	-1.01	3.48	-0.34	-2.56
16	AP	-8.80	-10.40	-7.61	-9.63	-11.76	-8.83
17	AQ	2.49	-0.96	-2.47	2.27	-1.67	-3.33
18	AR	-7.45	-9.06	-6.01	-9.76	-12.21	-8.99
19	AS	2.44	-0.15	-1.49	2.86	-1.17	-3.07
20	AT	-7.35	-9.22	-6.19	-9.89	-12.36	-9.12
21	AU	2.44	-0.15	-1.48	2.88	-1.16	-3.07
22	AV	-7.37	-9.28	-6.22	-9.86	-12.33	-9.11
23	AW	2.59	0.01	-1.33	2.75	-1.26	-3.14
24	AX	-8.23	-10.72	-7.82	-9.24	-12.20	-9.31
25	AY	2.17	-1.48	-2.95	2.02	-2.04	-3.65
26	AZ	-7.68	-10.51	-6.77	-9.96	-12.99	-9.85
27	BA	2.37	-0.67	-2.05	2.82	-1.71	-3.73
28	BB	-7.45	-10.65	-6.98	-9.95	-13.07	-9.97
29	BC	2.35	-0.68	-2.03	2.82	-1.70	-3.71
30	BD	-7.51	-10.71	-7.03	-9.95	-13.07	-9.97
31	BE	2.61	-0.49	-1.79	2.81	-1.69	-3.71
32	BF	-7.81	-11.03	-8.34	-8.73	-12.16	-9.61

Member	Stability Factors No Shear at Internal Columns			Stability Factors Including Shear at Internal Columns		
	LC1	LC2	LC3	LC1	LC2	LC3
33	0.148	0.096	0.066	0.148	0.091	0.061
34	0.300	0.226	0.175	0.302	0.245	0.194
35	0.407	0.281	0.187	0.408	0.297	0.207
36	0.670	0.618	0.423	0.696	0.644	0.452
37	0.169	0.189	0.174	0.166	0.188	0.171
38	0.556	0.541	0.379	0.552	0.536	0.376
39	0.479	0.457	0.312	0.472	0.450	0.308
40	0.784	0.768	0.548	0.791	0.788	0.573
41	0.168	0.189	0.173	0.168	0.189	0.170
42	0.554	0.540	0.380	0.555	0.537	0.376
43	0.473	0.454	0.314	0.472	0.449	0.308
44	0.775	0.764	0.549	0.789	0.787	0.572
45	0.170	0.189	0.174	0.172	0.192	0.172
46	0.559	0.543	0.382	0.557	0.538	0.376
47	0.474	0.454	0.313	0.471	0.447	0.306
48	0.786	0.773	0.555	0.789	0.785	0.569
49	0.158	0.153	0.131	0.166	0.165	0.142
50	0.342	0.336	0.225	0.358	0.358	0.244
51	0.450	0.416	0.269	0.473	0.440	0.293
52	0.709	0.739	0.540	0.739	0.771	0.574

Load Case	Frames Plastic Collapse Load Factor No Shear at Internal Columns	Including Shear at Internal Columns
LC1	1.347	1.332
LC2	1.395	1.370
LC3	1.647	1.662

Frame Identification : **f30 b24**

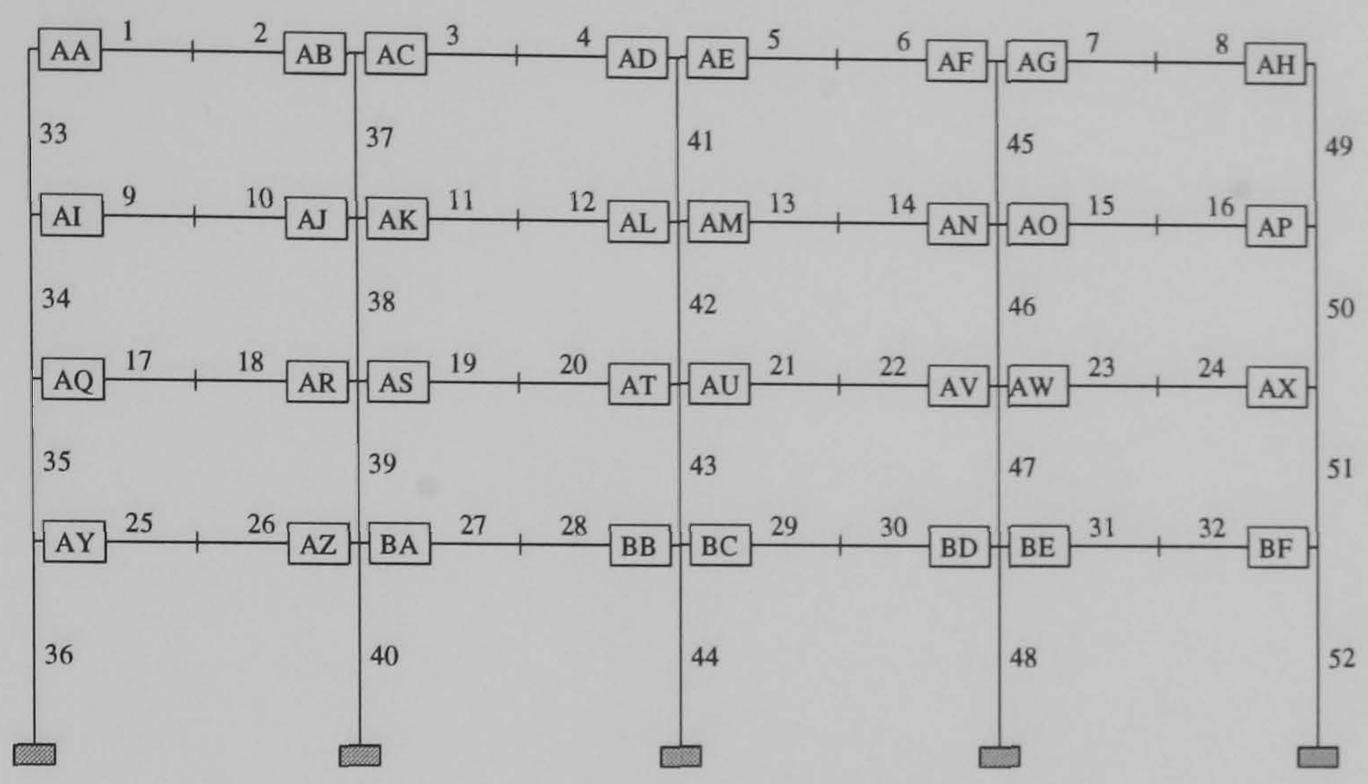

4 Storey 4 Bay

Member	Semi - Rigid Hinge Reference	Rotation (mrad)					
		No Shear at Internal Columns			Including Shear at Internal Columns		
		LC1	LC2	LC3	LC1	LC2	LC3
1	AA	**2.96**	**0.84**	**0.69**	**3.57**	**1.02**	**0.45**
2	AB	**-19.74**	**-18.24**	**-13.76**	**-17.70**	**-17.41**	**-13.53**
3	AC	**3.51**	**1.73**	**1.67**	**5.46**	**2.65**	**2.30**
4	AD	**-19.28**	**-17.96**	**-13.33**	**-17.50**	**-17.26**	**-13.18**
5	AE	**3.58**	**1.74**	**1.68**	**5.49**	**2.66**	**2.31**
6	AF	**-19.23**	**-17.76**	**-13.29**	**-17.27**	**-17.08**	**-13.18**
7	AG	**3.11**	**1.64**	**1.73**	**5.37**	**2.52**	**2.32**
8	AH	**-12.39**	**-13.29**	**-9.35**	**-11.14**	**-12.78**	**-9.89**
9	AI	**2.37**	**-1.25**	**-1.85**	**3.03**	**-1.22**	**-2.21**
10	AJ	**-15.82**	**-16.90**	**-7.18**	**-13.94**	**-16.75**	**-10.71**
11	AK	**2.96**	**0.34**	**-0.14**	**5.19**	**0.55**	**-1.25**
12	AL	**-15.21**	**-16.66**	**-7.07**	**-13.79**	**-16.55**	**-10.70**
13	AM	**2.96**	**0.34**	**-0.17**	**5.16**	**0.55**	**-1.25**
14	AN	**-15.17**	**-16.51**	**-7.16**	**-13.81**	**-16.43**	**-10.64**
15	AO	**2.93**	**0.25**	**-0.04**	**5.11**	**0.40**	**-1.35**
16	AP	**-12.26**	**-14.54**	**-9.86**	**-11.44**	**-14.48**	**-10.75**
17	AQ	**2.44**	**-2.33**	**-2.69**	**2.69**	**-2.59**	**-3.41**
18	AR	**-16.01**	**-22.39**	**-11.74**	**-14.85**	**-23.36**	**-13.74**
19	AS	**2.77**	**-1.64**	**-1.90**	**4.17**	**-2.58**	**-3.36**
20	AT	**-15.77**	**-22.64**	**-11.88**	**-14.91**	**-23.42**	**-13.60**
21	AU	**2.79**	**-1.64**	**-1.89**	**4.18**	**-2.58**	**-3.36**
22	AV	**-15.57**	**-22.55**	**-11.76**	**-14.79**	**-23.35**	**-13.58**
23	AW	**2.70**	**-1.73**	**-1.94**	**4.03**	**-2.72**	**-3.46**
24	AX	**-13.15**	**-23.45**	**-11.67**	**-12.70**	**-24.15**	**-14.13**
25	AY	**2.64**	**-2.69**	**-3.49**	**2.88**	**-2.96**	**-4.02**
26	AZ	**-11.27**	**-19.01**	**-10.40**	**-13.64**	**-19.87**	**-14.19**
27	BA	**3.45**	**-1.49**	**-2.29**	**4.44**	**-2.30**	**-3.94**
28	BB	**-10.77**	**-18.83**	**-10.34**	**-13.56**	**-19.50**	**-14.02**
29	BC	**3.42**	**-1.48**	**-2.29**	**4.44**	**-2.29**	**-3.94**
30	BD	**-10.87**	**-18.78**	**-10.38**	**-13.53**	**-19.45**	**-13.95**
31	BE	**3.65**	**-1.54**	**-2.17**	**4.31**	**-2.37**	**-4.17**
32	BF	**-10.59**	**-17.81**	**-11.71**	**-11.05**	**-18.46**	**-12.78**

Member	Stability Factors					
	No Shear at Internal Columns			Including Shear at Internal Columns		
	LC1	LC2	LC3	LC1	LC2	LC3
33	**0.333**	**0.219**	**0.167**	**0.361**	**0.230**	**0.156**
34	**0.539**	**0.517**	**0.395**	**0.563**	**0.526**	**0.423**
35	**0.404**	**0.304**	**0.222**	**0.405**	**0.314**	**0.243**
36	**0.613**	**0.660**	**0.496**	**0.624**	**0.669**	**0.526**
37	**0.331**	**0.333**	**0.313**	**0.332**	**0.338**	**0.307**
38	**0.783**	**0.822**	**0.641**	**0.785**	**0.827**	**0.633**
39	**0.586**	**0.579**	**0.433**	**0.562**	**0.580**	**0.437**
40	**0.894**	**0.961**	**0.747**	**0.897**	**0.971**	**0.765**
41	**0.327**	**0.330**	**0.309**	**0.328**	**0.336**	**0.304**
42	**0.774**	**0.816**	**0.635**	**0.778**	**0.823**	**0.629**
43	**0.578**	**0.576**	**0.429**	**0.557**	**0.577**	**0.433**
44	**0.884**	**0.955**	**0.742**	**0.892**	**0.965**	**0.759**
45	**0.327**	**0.344**	**0.306**	**0.327**	**0.340**	**0.305**
46	**0.779**	**0.820**	**0.638**	**0.782**	**0.826**	**0.633**
47	**0.573**	**0.577**	**0.433**	**0.559**	**0.578**	**0.435**
48	**0.888**	**0.955**	**0.745**	**0.893**	**0.965**	**0.758**
49	**0.459**	**0.426**	**0.346**	**0.447**	**0.427**	**0.358**
50	**0.711**	**0.733**	**0.511**	**0.697**	**0.739**	**0.540**
51	**0.487**	**0.458**	**0.336**	**0.487**	**0.461**	**0.340**
52	**0.642**	**0.762**	**0.596**	**0.657**	**0.769**	**0.629**

Load Case	Frames Plastic Collapse Load	
	No Shear at Internal Columns	Including Shear at Internal Columns
LC1	**1.220**	**1.230**
LC2	**1.177**	**1.160**
LC3	**1.247**	**1.287**

Frame Identification : **f31 b20**

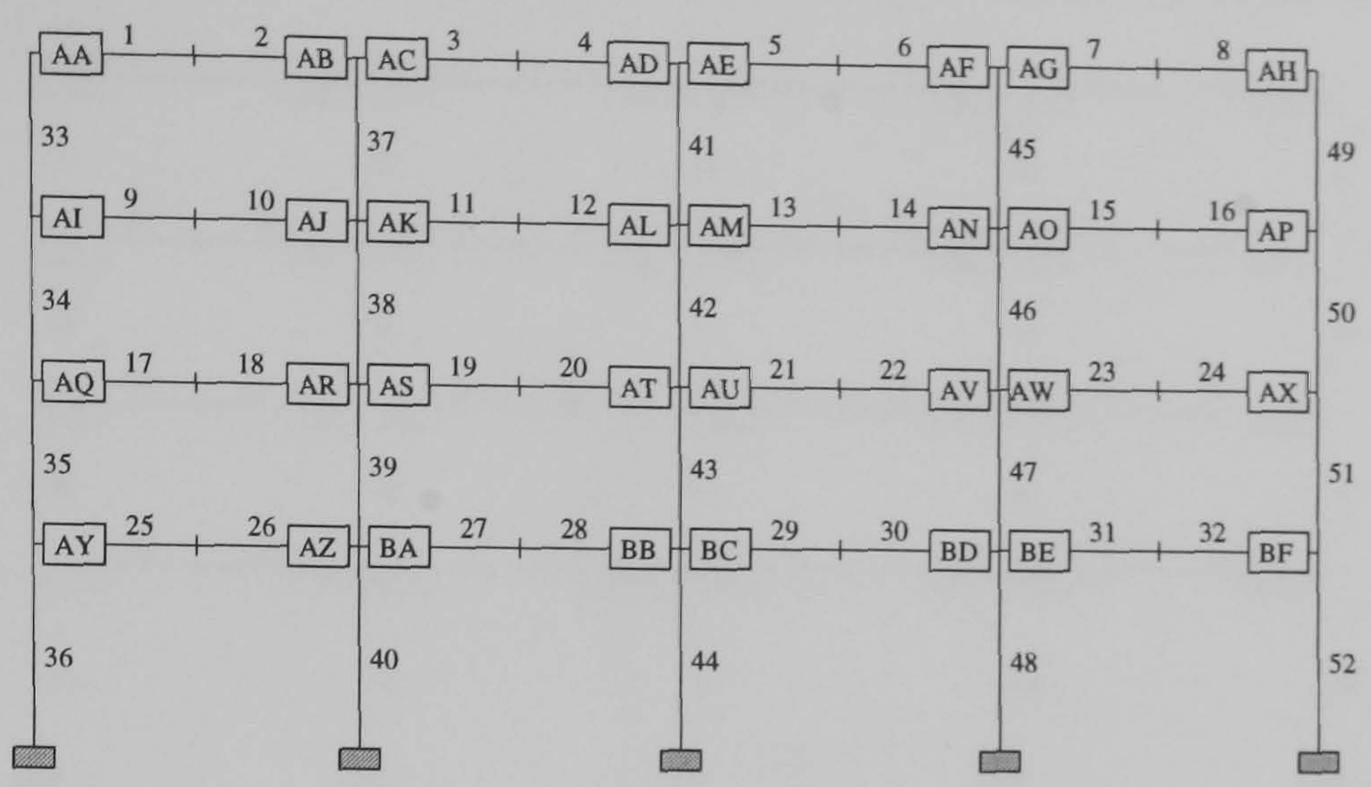

4 Storey 4 Bay

Member	Semi - Rigid Hinge Reference	Rotation (mrad)					
		No Shear at Internal Columns			Including Shear at Internal Columns		
		LC1	LC2	LC3	LC1	LC2	LC3
1	AA	**2.33**	**0.71**	**0.67**	**3.03**	**0.93**	**0.55**
2	AB	**-16.15**	**-13.99**	**-9.36**	**-13.21**	**-12.60**	**-10.78**
3	AC	**2.71**	**1.69**	**1.68**	**5.64**	**3.36**	**2.64**
4	AD	**-15.00**	**-13.05**	**-8.29**	**-12.52**	**-12.22**	**-10.43**
5	AE	**2.73**	**1.69**	**1.69**	**5.63**	**3.28**	**2.56**
6	AF	**-15.13**	**-13.26**	**-8.77**	**-12.66**	**-12.33**	**-10.54**
7	AG	**2.75**	**1.76**	**1.86**	**5.68**	**3.42**	**2.72**
8	AH	**-9.97**	**-9.50**	**-7.21**	**-8.82**	**-9.25**	**-7.81**
9	AI	**2.56**	**-0.59**	**-1.28**	**3.26**	**-0.53**	**-1.75**
10	AJ	**-17.60**	**-17.72**	**-7.59**	**-14.97**	**-17.50**	**-9.96**
11	AK	**2.18**	**0.31**	**-0.06**	**4.87**	**0.61**	**-0.85**
12	AL	**-17.12**	**-17.67**	**-7.51**	**-14.88**	**-17.49**	**-9.94**
13	AM	**2.18**	**0.31**	**-0.06**	**4.87**	**0.62**	**-0.83**
14	AN	**-16.85**	**-17.48**	**-7.47**	**-14.73**	**-17.35**	**-9.88**
15	AO	**2.12**	**0.26**	**0.02**	**4.74**	**0.53**	**-0.93**
16	AP	**-12.85**	**-17.09**	**-9.03**	**-11.05**	**-16.89**	**-10.11**
17	AQ	**2.11**	**-0.97**	**-1.57**	**2.33**	**-1.19**	**-2.25**
18	AR	**-10.15**	**-14.17**	**-6.26**	**-12.68**	**-16.01**	**-11.85**
19	AS	**2.53**	**0.00**	**-0.59**	**4.48**	**-0.46**	**-2.42**
20	AT	**-9.31**	**-13.80**	**-6.17**	**-12.72**	**-15.82**	**-11.67**
21	AU	**2.54**	**0.00**	**-0.60**	**4.51**	**-0.46**	**-2.43**
22	AV	**-9.38**	**-13.69**	**-6.21**	**-12.60**	**-15.72**	**-11.55**
23	AW	**2.65**	**-0.06**	**-0.48**	**4.19**	**-0.72**	**-2.82**
24	AX	**-8.22**	**-11.99**	**-7.43**	**-8.79**	**-13.31**	**-9.15**
25	AY	**2.39**	**-1.19**	**-2.14**	**2.52**	**-1.45**	**-2.75**
26	AZ	**-9.79**	**-15.44**	**-7.04**	**-12.55**	**-16.77**	**-12.95**
27	BA	**2.61**	**-0.33**	**-1.06**	**4.56**	**-0.97**	**-3.15**
28	BB	**-8.90**	**-15.13**	**-6.91**	**-12.56**	**-16.50**	**-12.67**
29	BC	**2.62**	**-0.32**	**-1.06**	**4.57**	**-0.98**	**-3.15**
30	BD	**-9.02**	**-15.06**	**-6.96**	**-12.48**	**-16.46**	**-12.56**
31	BE	**2.79**	**-0.36**	**-0.90**	**4.28**	**-1.13**	**-3.59**
32	BF	**-8.04**	**-14.09**	**-8.49**	**-8.85**	**-15.14**	**-10.15**

Member	Stability Factors					
	No Shear at Internal Columns			Including Shear at Internal Columns		
	LC1	LC2	LC3	LC1	LC2	LC3
33	**0.331**	**0.219**	**0.170**	**0.372**	**0.236**	**0.165**
34	**0.558**	**0.481**	**0.372**	**0.573**	**0.489**	**0.408**
35	**0.424**	**0.256**	**0.199**	**0.429**	**0.269**	**0.235**
36	**0.599**	**0.621**	**0.462**	**0.621**	**0.635**	**0.508**
37	**0.330**	**0.355**	**0.314**	**0.337**	**0.366**	**0.317**
38	**0.799**	**0.788**	**0.616**	**0.772**	**0.787**	**0.620**
39	**0.562**	**0.563**	**0.444**	**0.551**	**0.562**	**0.430**
40	**0.885**	**0.926**	**0.729**	**0.886**	**0.938**	**0.750**
41	**0.324**	**0.350**	**0.309**	**0.332**	**0.358**	**0.310**
42	**0.789**	**0.782**	**0.609**	**0.766**	**0.781**	**0.615**
43	**0.552**	**0.557**	**0.437**	**0.545**	**0.554**	**0.423**
44	**0.872**	**0.919**	**0.721**	**0.881**	**0.930**	**0.742**
45	**0.322**	**0.348**	**0.300**	**0.330**	**0.358**	**0.309**
46	**0.791**	**0.790**	**0.615**	**0.776**	**0.790**	**0.622**
47	**0.548**	**0.560**	**0.438**	**0.549**	**0.558**	**0.429**
48	**0.880**	**0.921**	**0.729**	**0.880**	**0.930**	**0.739**
49	**0.478**	**0.438**	**0.343**	**0.451**	**0.431**	**0.363**
50	**0.718**	**0.701**	**0.501**	**0.711**	**0.697**	**0.543**
51	**0.487**	**0.490**	**0.336**	**0.513**	**0.493**	**0.386**
52	**0.637**	**0.737**	**0.575**	**0.659**	**0.746**	**0.626**

Load Case	Frames Plastic Collapse Load Factor	
	No Shear at Internal Columns	Including Shear at Internal Columns
LC1	**1.245**	**1.235**
LC2	**1.260**	**1.230**
LC3	**1.447**	**1.377**

Frame Identification : **f31 b24**

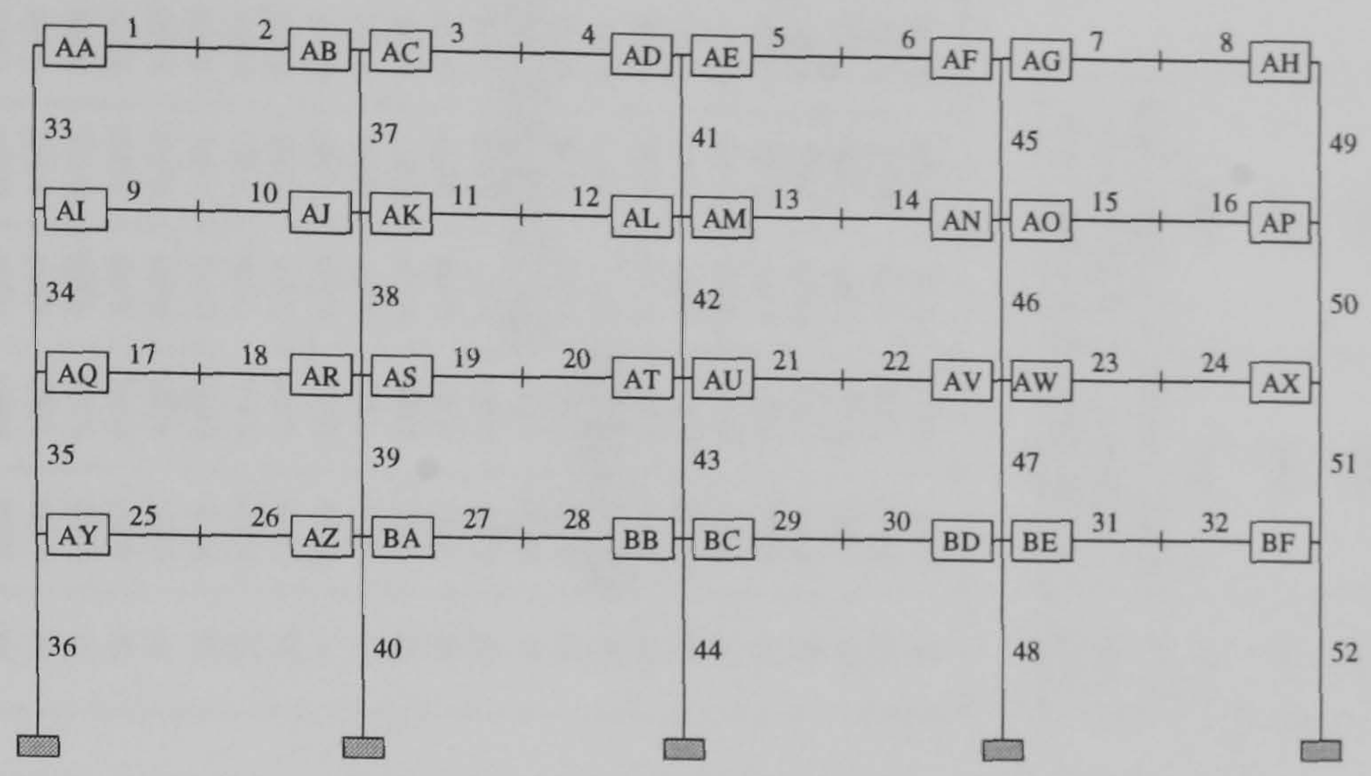

4 Storey 4 Bay

Member	Semi - Rigid Hinge Reference	Rotation (mrad)					
		No Shear at Internal Columns			Including Shear at Internal Columns		
		LC1	LC2	LC3	LC1	LC2	LC3
1	AA	**2.46**	**-0.59**	**-0.94**	**2.40**	**-0.95**	**-1.61**
2	AB	**-7.26**	**-8.28**	**-7.35**	**-9.59**	**-11.72**	**-10.74**
3	AC	**3.11**	**1.06**	**0.59**	**4.03**	**0.61**	**-0.14**
4	AD	**-7.02**	**-8.07**	**-7.18**	**-9.59**	**-11.67**	**-10.23**
5	AE	**3.07**	**1.01**	**0.55**	**4.04**	**0.61**	**-0.16**
6	AF	**-7.10**	**-8.20**	**-7.29**	**-9.54**	**-11.60**	**-10.62**
7	AG	**3.22**	**1.17**	**0.72**	**3.97**	**0.55**	**-0.21**
8	AH	**-6.55**	**-9.15**	**-8.04**	**-7.30**	**-10.07**	**-9.48**
9	AI	**3.69**	**-2.96**	**-4.58**	**3.59**	**-3.75**	**-5.75**
10	AJ	**-9.59**	**-16.46**	**-9.72**	**-12.57**	**-18.44**	**-14.83**
11	AK	**3.79**	**-1.08**	**-2.24**	**4.78**	**-2.36**	**-4.87**
12	AL	**-9.35**	**-16.56**	**-9.78**	**-12.69**	**-18.40**	**-14.80**
13	AM	**3.77**	**-1.08**	**-2.22**	**4.81**	**-2.36**	**-4.86**
14	AN	**-9.40**	**-16.48**	**-9.79**	**-12.62**	**-18.41**	**-14.72**
15	AO	**3.96**	**-1.04**	**-2.09**	**4.63**	**-2.38**	**-5.08**
16	AP	**-10.16**	**-18.92**	**-13.83**	**-11.34**	**-21.26**	**-16.37**
17	AQ	**2.15**	**-2.77**	**-3.85**	**2.08**	**-3.26**	**-4.65**
18	AR	**-6.70**	**-12.51**	**-8.48**	**-9.50**	**-15.87**	**-13.49**
19	AS	**2.26**	**-1.52**	**-2.52**	**3.09**	**-2.92**	**-4.76**
20	AT	**-6.43**	**-12.38**	**-8.55**	**-9.43**	**-15.68**	**-13.33**
21	AU	**2.24**	**-1.52**	**-2.52**	**3.10**	**-2.93**	**-4.77**
22	AV	**-6.47**	**-12.39**	**-8.75**	**-9.39**	**-15.61**	**-13.28**
23	AW	**2.44**	**-1.44**	**-2.34**	**3.02**	**-3.13**	**-4.99**
24	AX	**-6.90**	**-13.05**	**-10.68**	**-7.76**	**-14.09**	**-12.40**
25	AY	**2.29**	**-2.73**	**-4.12**	**2.30**	**-3.13**	**-4.70**
26	AZ	**-6.67**	**-13.63**	**-9.18**	**-9.30**	**-16.18**	**-14.09**
27	BA	**2.28**	**-1.83**	**-3.02**	**3.21**	**-3.21**	**-5.24**
28	BB	**-6.38**	**-13.79**	**-9.35**	**-9.22**	**-16.08**	**-14.02**
29	BC	**2.26**	**-1.83**	**-3.00**	**3.21**	**-3.20**	**-5.22**
30	BD	**-6.42**	**-13.78**	**-9.38**	**-9.21**	**-16.04**	**-13.98**
31	BE	**2.50**	**-1.75**	**-2.73**	**3.17**	**-3.35**	**-5.38**
32	BF	**-6.80**	**-13.30**	**-11.19**	**-7.57**	**-14.14**	**-12.59**

Member	Stability Factors					
	No Shear at Internal Columns			Including Shear at Internal Columns		
	LC1	LC2	LC3	LC1	LC2	LC3
33	**0.253**	**0.198**	**0.154**	**0.257**	**0.201**	**0.177**
34	**0.417**	**0.443**	**0.371**	**0.421**	**0.460**	**0.404**
35	**0.324**	**0.217**	**0.177**	**0.329**	**0.236**	**0.201**
36	**0.474**	**0.544**	**0.440**	**0.496**	**0.566**	**0.479**
37	**0.317**	**0.412**	**0.372**	**0.312**	**0.402**	**0.372**
38	**0.726**	**0.827**	**0.686**	**0.717**	**0.833**	**0.679**
39	**0.375**	**0.425**	**0.349**	**0.369**	**0.418**	**0.341**
40	**0.594**	**0.738**	**0.614**	**0.600**	**0.762**	**0.656**
41	**0.307**	**0.404**	**0.366**	**0.309**	**0.398**	**0.367**
42	**0.713**	**0.820**	**0.682**	**0.714**	**0.828**	**0.673**
43	**0.366**	**0.421**	**0.348**	**0.366**	**0.413**	**0.337**
44	**0.584**	**0.734**	**0.612**	**0.597**	**0.756**	**0.651**
45	**0.307**	**0.403**	**0.364**	**0.311**	**0.400**	**0.369**
46	**0.721**	**0.828**	**0.687**	**0.718**	**0.831**	**0.675**
47	**0.367**	**0.422**	**0.347**	**0.367**	**0.416**	**0.338**
48	**0.596**	**0.738**	**0.620**	**0.598**	**0.755**	**0.647**
49	**0.288**	**0.334**	**0.290**	**0.307**	**0.363**	**0.325**
50	**0.491**	**0.611**	**0.481**	**0.517**	**0.626**	**0.518**
51	**0.357**	**0.404**	**0.304**	**0.379**	**0.426**	**0.335**
52	**0.497**	**0.700**	**0.597**	**0.523**	**0.726**	**0.647**

Load Case	Frames Plastic Collapse Load Factor	
	No Shear at Internal Columns	Including Shear at Internal Columns
LC1	**1.327**	**1.302**
LC2	**1.295**	**1.272**
LC3	**1.330**	**1.320**

Frame Identification : **f32 b24**

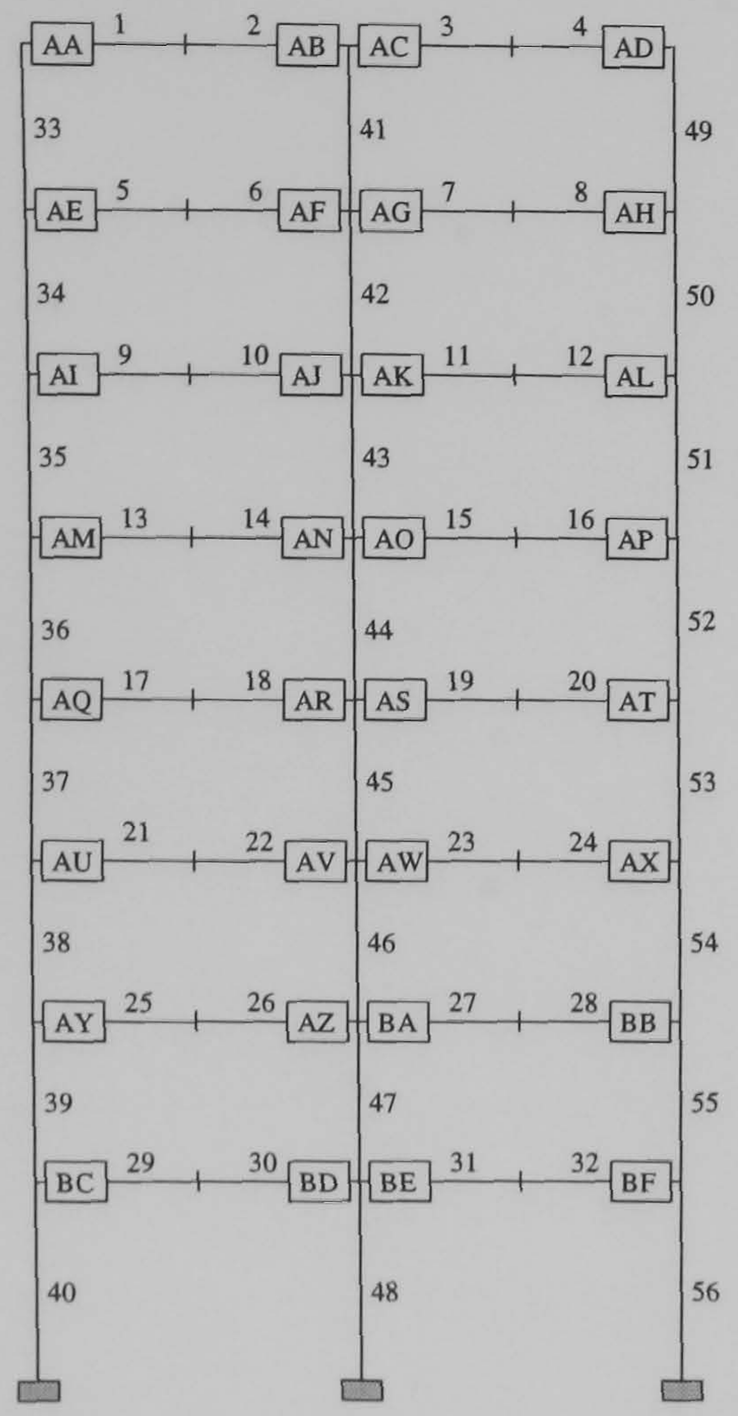

8 Storey 2 Bay

Member	Semi - Rigid Hinge Reference	Rotation (mrad)					
		No Shear at Internal Columns			Including Shear at Internal Columns		
		LC1	LC2	LC3	LC1	LC2	LC3
1	AA	3.41	2.39	1.81	3.70	2.62	1.89
2	AB	-11.57	-9.12	-6.82	-12.29	-10.76	-9.33
3	AC	4.87	3.18	2.88	6.09	4.58	3.84
4	AD	-8.39	-7.16	-5.42	-8.35	-7.44	-5.97
5	AE	2.32	1.40	0.42	2.65	1.58	0.37
6	AF	-11.18	-8.34	-2.91	-9.90	-8.52	-4.53
7	AG	1.96	1.53	0.74	4.18	2.69	0.58
8	AH	-8.05	-6.94	-4.01	-7.73	-7.02	-4.43
9	AI	1.52	0.79	0.05	1.88	0.93	-0.09
10	AJ	-13.20	-10.18	-3.09	-12.05	-9.59	-4.84
11	AK	1.17	0.76	0.47	2.44	1.52	0.13
12	AL	-11.91	-9.06	-4.08	-11.00	-8.71	-4.60
13	AM	0.95	0.28	-0.11	1.24	0.37	-0.30
14	AN	-14.80	-11.75	-3.73	-14.01	-11.53	-5.47
15	AO	0.67	0.24	0.17	1.47	0.51	-0.33
16	AP	-14.36	-11.45	-4.68	-13.69	-11.21	-5.23
17	AQ	0.27	-0.29	-0.32	0.41	-0.33	-0.49
18	AR	-16.48	-13.35	-4.43	-16.11	-13.47	-5.58
19	AS	0.16	-0.21	-0.09	0.45	-0.37	-0.54
20	AT	-16.67	-13.63	-4.81	-16.28	-13.64	-5.21
21	AU	0.06	-0.51	-0.46	0.19	-0.56	-0.63
22	AV	-17.16	-14.02	-4.92	-16.87	-14.20	-5.89
23	AW	0.02	-0.36	-0.23	0.20	-0.63	-0.72
24	AX	-17.37	-14.33	-5.23	-17.03	-14.36	-5.54
25	AY	0.64	0.00	-0.38	0.80	0.01	-0.57
26	AZ	-16.13	-13.20	-5.03	-15.71	-13.19	-5.50
27	BA	0.40	-0.01	-0.21	0.78	0.00	-0.49
28	BB	-16.19	-13.36	-4.93	-15.82	-13.32	-5.45
29	BC	1.09	0.35	-0.41	1.22	0.39	-0.40
30	BD	-10.72	-8.27	-3.03	-10.19	-8.13	-4.67
31	BE	0.96	0.54	0.09	1.77	0.94	-0.19
32	BF	8.95	-7.40	-4.10	-8.76	-7.41	-4.44

Member	Stability Factors					
	No Shear at Internal Columns			Including Shear at Internal Columns		
	LC1	LC2	LC3	LC1	LC2	LC3
33	0.301	0.224	0.176	0.319	0.239	0.183
34	0.482	0.352	0.193	0.505	0.366	0.205
35	0.499	0.382	0.208	0.519	0.394	0.208
36	0.592	0.471	0.284	0.605	0.479	0.299
37	0.478	0.382	0.239	0.484	0.388	0.251
38	0.609	0.492	0.301	0.613	0.499	0.314
39	0.548	0.431	0.249	0.553	0.435	0.254
40	0.744	0.600	0.370	0.741	0.600	0.388
41	0.271	0.233	0.222	0.245	0.229	0.206
42	0.837	0.721	0.486	0.846	0.715	0.463
43	0.669	0.566	0.373	0.673	0.566	0.354
44	0.891	0.750	0.492	0.889	0.746	0.470
45	0.754	0.632	0.431	0.749	0.626	0.415
46	0.924	0.768	0.510	0.919	0.764	0.500
47	0.735	0.608	0.388	0.736	0.609	0.376
48	0.928	0.769	0.504	0.916	0.763	0.504
49	0.345	0.290	0.227	0.345	0.300	0.244
50	0.606	0.510	0.293	0.601	0.513	0.310
51	0.604	0.516	0.298	0.610	0.521	0.318
52	0.727	0.618	0.389	0.734	0.626	0.406
53	0.587	0.496	0.341	0.592	0.500	0.353
54	0.696	0.587	0.398	0.700	0.592	0.406
55	0.673	0.558	0.336	0.674	0.562	0.347
56	0.773	0.656	0.430	0.769	0.657	0.448

Load Case	Frames Plastic Collapse Load Factor	
	No Shear at Internal Columns	Including Shear at Internal Columns
LC1	1.200	1.200
LC2	1.272	1.272
LC3	1.580	1.572

Frame Identification : **f34 b24**

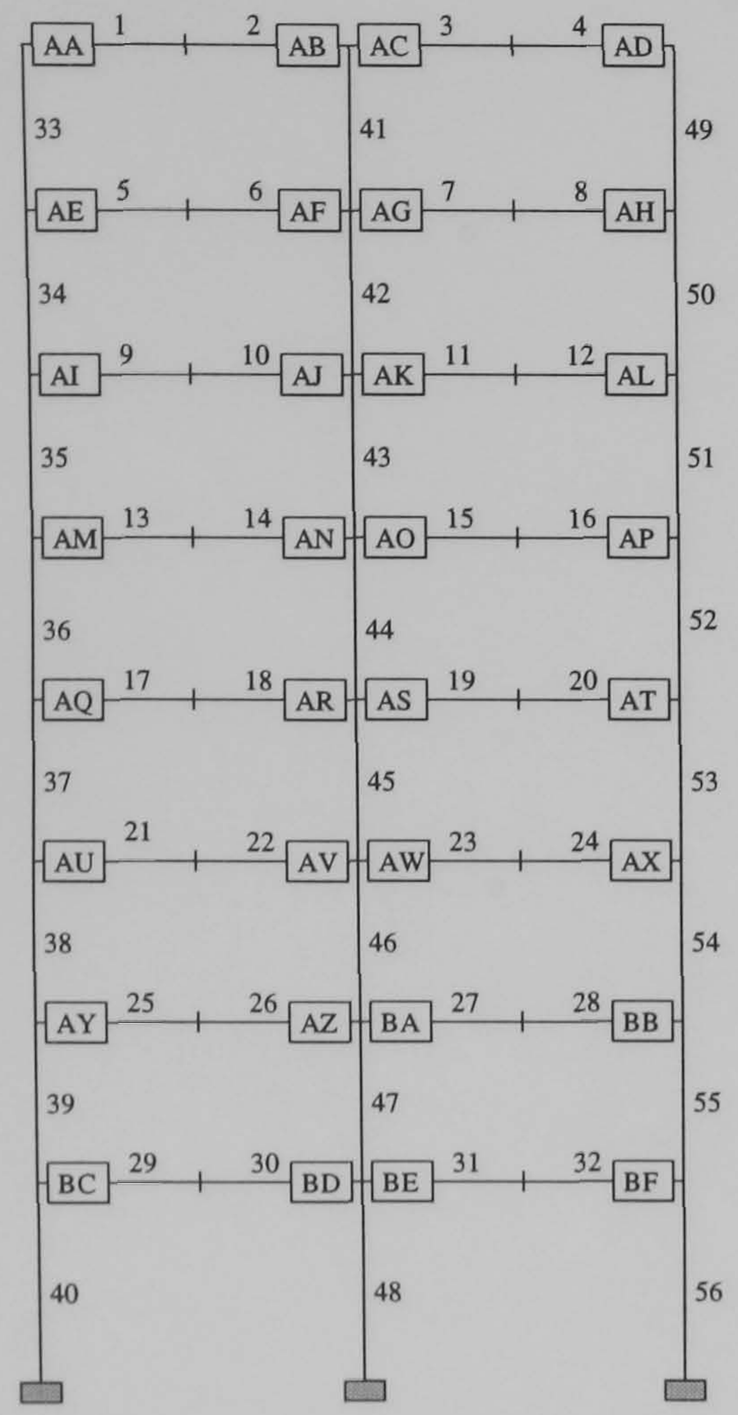

8 Storey 2 Bay

Member	Semi - Rigid Hinge Reference	Rotation (mrad)					
		No Shear at Internal Columns			Including Shear at Internal Columns		
		LC1	LC2	LC3	LC1	LC2	LC3
1	AA	3.68	1.80	1.14	3.74	1.63	0.95
2	AB	-8.66	-8.46	-7.41	-9.94	-10.06	-8.84
3	AC	3.29	1.81	1.56	3.64	1.58	1.38
4	AD	-9.90	-9.79	-7.85	-10.22	-10.37	-8.39
5	AE	4.22	1.12	-0.61	4.29	0.78	-1.00
6	AF	-12.35	-11.79	-6.36	-13.11	-13.41	-7.99
7	AG	3.55	1.20	-0.55	4.02	0.62	-1.49
8	AH	-13.43	-13.48	-8.58	-13.77	-14.58	-9.23
9	AI	2.65	-0.54	-1.57	2.66	-1.04	-2.07
10	AJ	-15.27	-15.91	-7.10	-15.01	-16.90	-9.12
11	AK	1.79	-0.91	-1.31	2.36	-1.66	-2.54
12	AL	-16.66	-18.06	-8.75	-16.73	-19.07	-9.60
13	AM	1.66	-1.48	-1.97	1.77	-2.00	-2.49
14	AN	-12.88	-14.29	-7.21	-13.95	-15.92	-9.74
15	AO	1.56	-1.20	-1.62	1.76	-2.31	-3.14
16	AP	-13.09	-14.67	-8.80	-13.25	-15.94	-9.74
17	AQ	0.98	-2.30	-2.44	1.01	-2.91	-2.99
18	AR	-14.98	-17.46	-7.95	-14.83	-19.06	-10.45
19	AS	0.71	-2.34	-2.15	0.98	-3.68	-3.69
20	AT	-14.75	-18.10	-9.13	-14.73	-19.51	-10.12
21	AU	0.30	-3.10	-2.89	0.37	-3.71	-3.43
22	AV	-16.81	-19.71	-8.74	-16.65	-21.36	-11.39
23	AW	0.10	-3.16	-2.62	0.23	-4.71	-4.30
24	AX	-16.25	-19.93	-9.70	-16.01	-21.25	-10.68
25	AY	0.56	-2.74	-2.89	0.66	-3.20	-3.33
26	AZ	-16.73	-19.15	-8.66	-16.49	-20.33	-10.75
27	BA	0.30	-2.65	-2.47	0.48	-3.76	-3.79
28	BB	-16.97	-19.83	-9.76	-16.72	-20.72	-10.56
29	BC	1.40	-1.58	-2.37	1.49	-1.88	-2.61
30	BD	-14.55	-16.02	-7.75	-14.28	-16.74	-9.52
31	BE	1.33	-1.26	-1.79	1.73	-1.86	-2.75
32	BF	-14.17	-16.18	-8.81	-14.05	-16.79	-9.38

Member	Stability Factors					
	No Shear at Internal Columns			Including Shear at Internal Columns		
	LC1	LC2	LC3	LC1	LC2	LC3
33	0.218	0.159	0.098	0.219	0.157	0.094
34	0.405	0.314	0.206	0.409	0.322	0.219
35	0.464	0.340	0.214	0.470	0.352	0.229
36	0.578	0.470	0.307	0.582	0.485	0.323
37	0.564	0.475	0.308	0.569	0.489	0.325
38	0.675	0.583	0.369	0.679	0.595	0.386
39	0.483	0.402	0.241	0.486	0.410	0.253
40	0.742	0.664	0.419	0.742	0.673	0.439
41	0.251	0.252	0.215	0.243	0.246	0.209
42	0.767	0.698	0.457	0.758	0.690	0.445
43	0.649	0.574	0.382	0.640	0.574	0.372
44	0.859	0.767	0.505	0.846	0.766	0.492
45	0.716	0.636	0.436	0.711	0.636	0.426
46	0.869	0.763	0.516	0.863	0.768	0.510
47	0.744	0.647	0.423	0.741	0.656	0.417
48	1.014	0.922	0.612	1.005	0.935	0.623
49	0.232	0.214	0.174	0.237	0.223	0.182
50	0.495	0.447	0.274	0.496	0.449	0.285
51	0.561	0.487	0.306	0.565	0.487	0.320
52	0.734	0.663	0.421	0.741	0.669	0.437
53	0.728	0.641	0.437	0.730	0.643	0.454
54	0.851	0.755	0.519	0.856	0.760	0.534
55	0.597	0.537	0.353	0.599	0.545	0.367
56	0.804	0.785	0.534	0.803	0.797	0.555

Load Case	Frames Plastic Collapse Load Factor	
	No Shear at Internal Columns	Including Shear at Internal Columns
LC1	1.095	1.092
LC2	1.065	1.067
LC3	1.235	1.255

Frame Identification : **f35 b20**

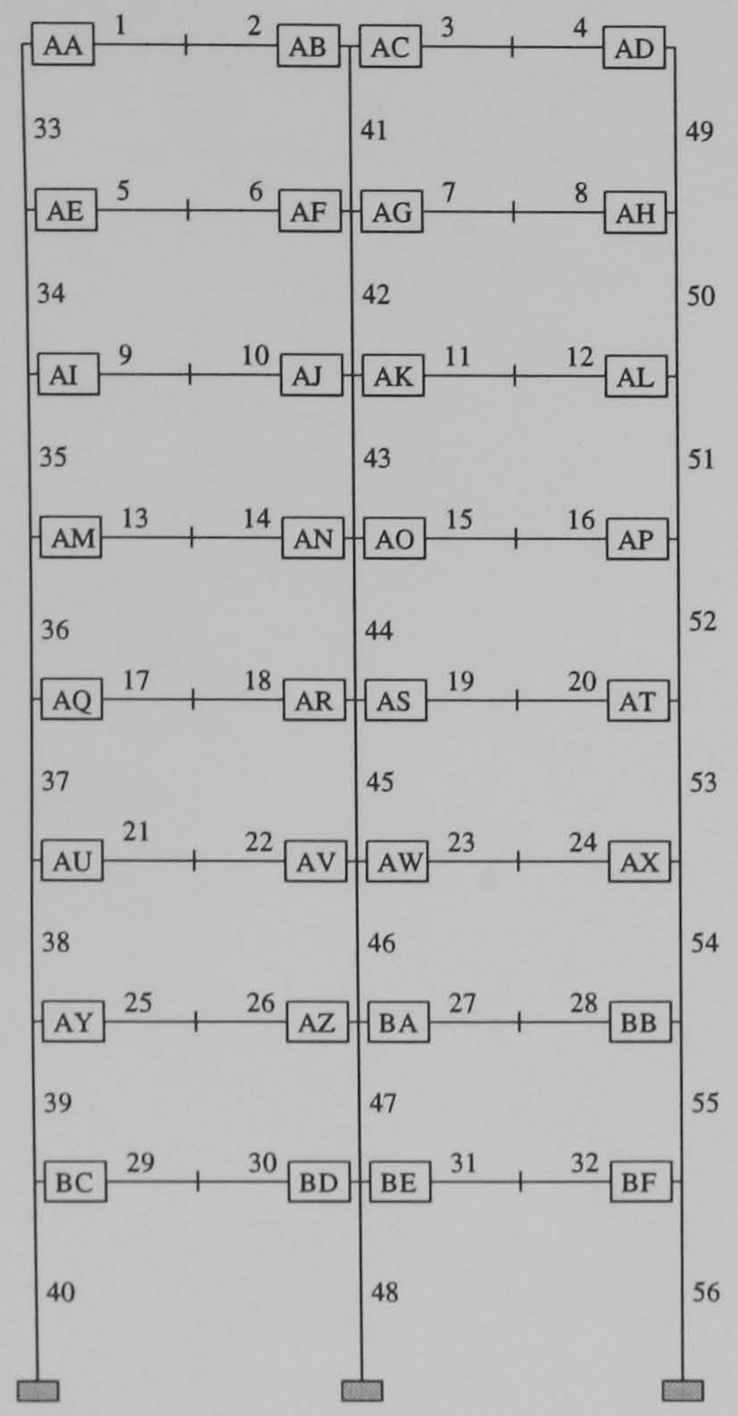

8 Storey 2 Bay

Member	Semi - Rigid Hinge Reference	Rotation (mrad)					
		No Shear at Internal Columns			Including Shear at Internal Columns		
		LC1	LC2	LC3	LC1	LC2	LC3
1	AA	3.34	1.89	1.20	3.38	1.81	1.09
2	AB	-7.23	-6.84	-6.07	-8.92	-8.68	-7.75
3	AC	2.98	1.91	1.62	3.56	1.97	1.65
4	AD	-8.17	-7.88	-6.41	-8.66	-8.51	-6.93
5	AE	4.39	1.92	-0.07	4.47	1.71	-0.38
6	AF	-10.14	-9.43	-5.31	-11.99	-11.71	-6.98
7	AG	3.94	2.02	-0.04	4.34	1.55	-0.83
8	AH	-11.84	-11.52	-7.36	-12.36	-12.29	-8.00
9	AI	2.52	0.21	-0.94	2.58	-0.17	-1.34
10	AJ	-12.24	-11.76	-5.55	-12.60	-13.11	-7.83
11	AK	1.98	0.21	-0.58	2.71	-0.27	-1.72
12	AL	-11.93	-12.13	-7.16	-12.21	-13.34	-7.97
13	AM	1.27	-1.29	-1.61	1.27	-1.89	-2.10
14	AN	-15.26	-15.48	-6.57	-15.15	-16.95	-9.29
15	AO	6.87	-1.22	-1.24	1.27	-2.39	-2.79
16	AP	-15.98	-16.74	-8.29	-15.96	-18.00	-9.26
17	AQ	-0.12	-2.59	-2.11	-0.24	-3.30	-2.60
18	AR	-18.96	-19.58	-7.64	-19.33	-21.57	-9.85
19	AS	-0.44	-2.56	-1.79	-0.72	-4.32	-3.26
20	AT	-19.54	-20.77	-8.66	-19.74	-22.38	-9.51
21	AU	-0.70	-3.17	-2.48	-0.89	-3.91	-2.98
22	AV	-20.51	-21.29	-8.91	-21.06	-23.34	-10.70
23	AW	-0.88	-3.11	-2.27	-1.40	-5.06	-3.79
24	AX	-20.75	-22.10	-9.28	-21.09	-23.67	-10.04
25	AY	0.42	-1.99	-2.26	0.26	-2.54	-2.75
26	AZ	-18.52	-19.01	-8.64	-18.92	-20.42	-9.88
27	BA	0.01	-1.98	-1.99	-0.14	-3.19	-3.11
28	BB	-19.00	-19.83	-9.03	-19.44	-21.01	-10.06
29	BC	0.90	-1.05	-1.73	0.94	-1.25	-1.86
30	BD	-11.31	-11.34	-5.89	-12.49	-12.92	-8.03
31	BE	1.09	-0.47	-1.05	1.28	-1.13	-1.99
32	BF	-11.25	-11.60	-7.21	-11.58	-12.12	-7.71

Member	Stability Factors					
	No Shear at Internal Columns			Including Shear at Internal Columns		
	LC1	LC2	LC3	LC1	LC2	LC3
33	0.225	0.164	0.108	0.227	0.164	0.106
34	0.436	0.308	0.194	0.441	0.309	0.208
35	0.484	0.361	0.209	0.493	0.369	0.226
36	0.574	0.493	0.303	0.584	0.514	0.319
37	0.555	0.484	0.305	0.566	0.504	0.320
38	0.710	0.603	0.371	0.718	0.620	0.385
39	0.510	0.419	0.246	0.511	0.427	0.254
40	0.726	0.623	0.400	0.736	0.637	0.420
41	0.243	0.244	0.211	0.237	0.235	0.203
42	0.762	0.680	0.450	0.741	0.662	0.436
43	0.667	0.594	0.384	0.660	0.592	0.371
44	0.884	0.778	0.503	0.882	0.777	0.485
45	0.728	0.636	0.433	0.722	0.633	0.420
46	0.894	0.775	0.510	0.890	0.781	0.507
47	0.789	0.681	0.424	0.784	0.688	0.419
48	0.997	0.877	0.588	0.997	0.891	0.599
49	0.240	0.219	0.179	0.250	0.231	0.190
50	0.500	0.444	0.273	0.510	0.458	0.285
51	0.591	0.515	0.309	0.594	0.519	0.327
52	0.725	0.639	0.414	0.734	0.649	0.431
53	0.709	0.617	0.433	0.717	0.624	0.448
54	0.843	0.747	0.514	0.849	0.757	0.523
55	0.635	0.571	0.355	0.643	0.586	0.366
56	0.790	0.740	0.510	0.801	0.757	0.530

Load Case	Frames Plastic Collapse Load Factor	
	No Shear at Internal Columns	Including Shear at Internal Columns
LC1	1.070	1.067
LC2	1.012	1.045
LC3	1.200	1.190

Frame Identification : **f35 b24**

C.3 Graphical representation for the load-deflection behaviour

The following section presents the load-lateral deflection response for a typical Wind-Moment frame that was considered during the study. The deflection plotted is applicable to that at the level of the roof.

A load factor equal to 1.0 indicates that the frame is able to withstand the design load for ultimate limit state.

The reference for the frame presented is f30b24.

FRAME : **f30b24**

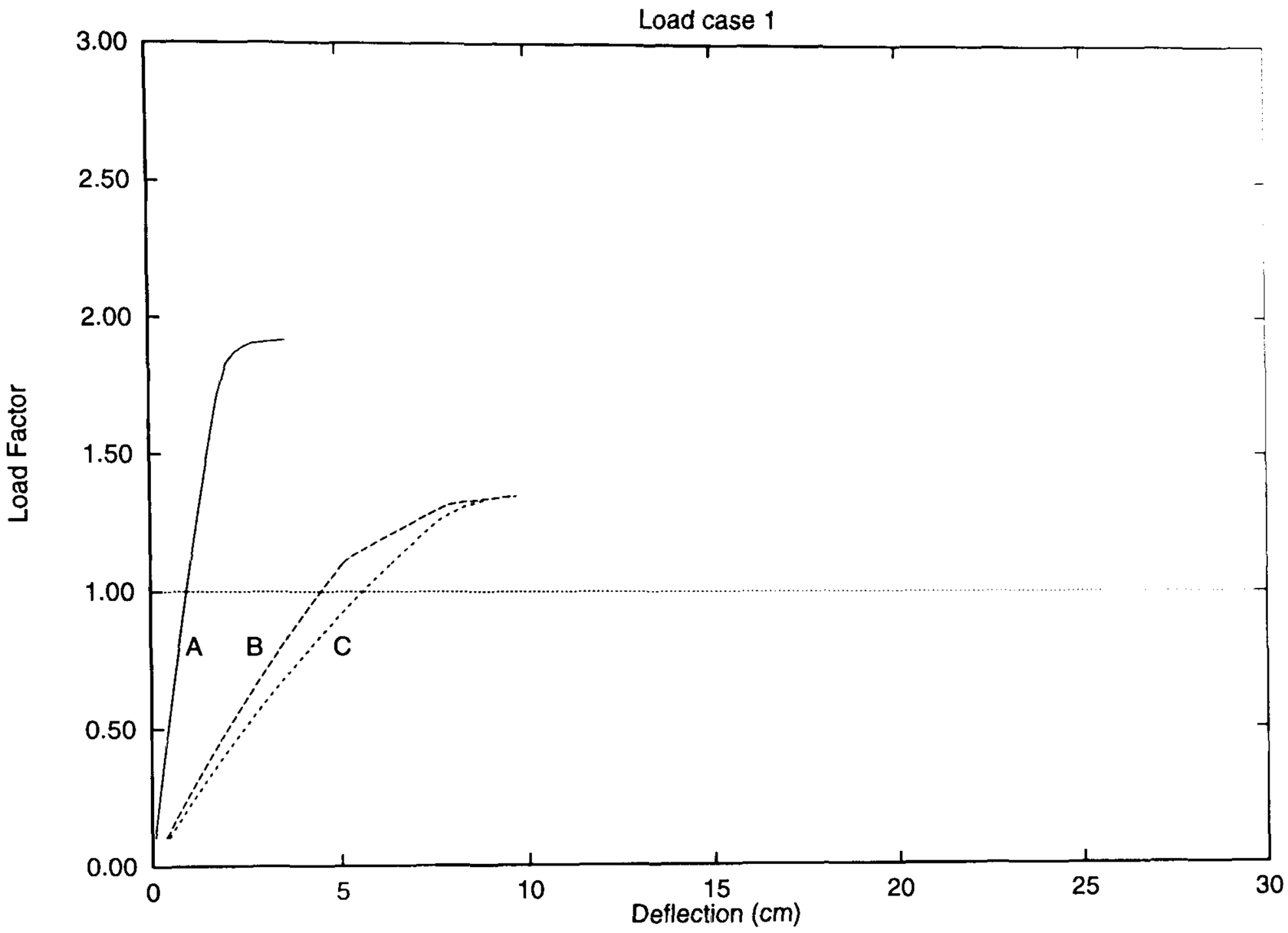

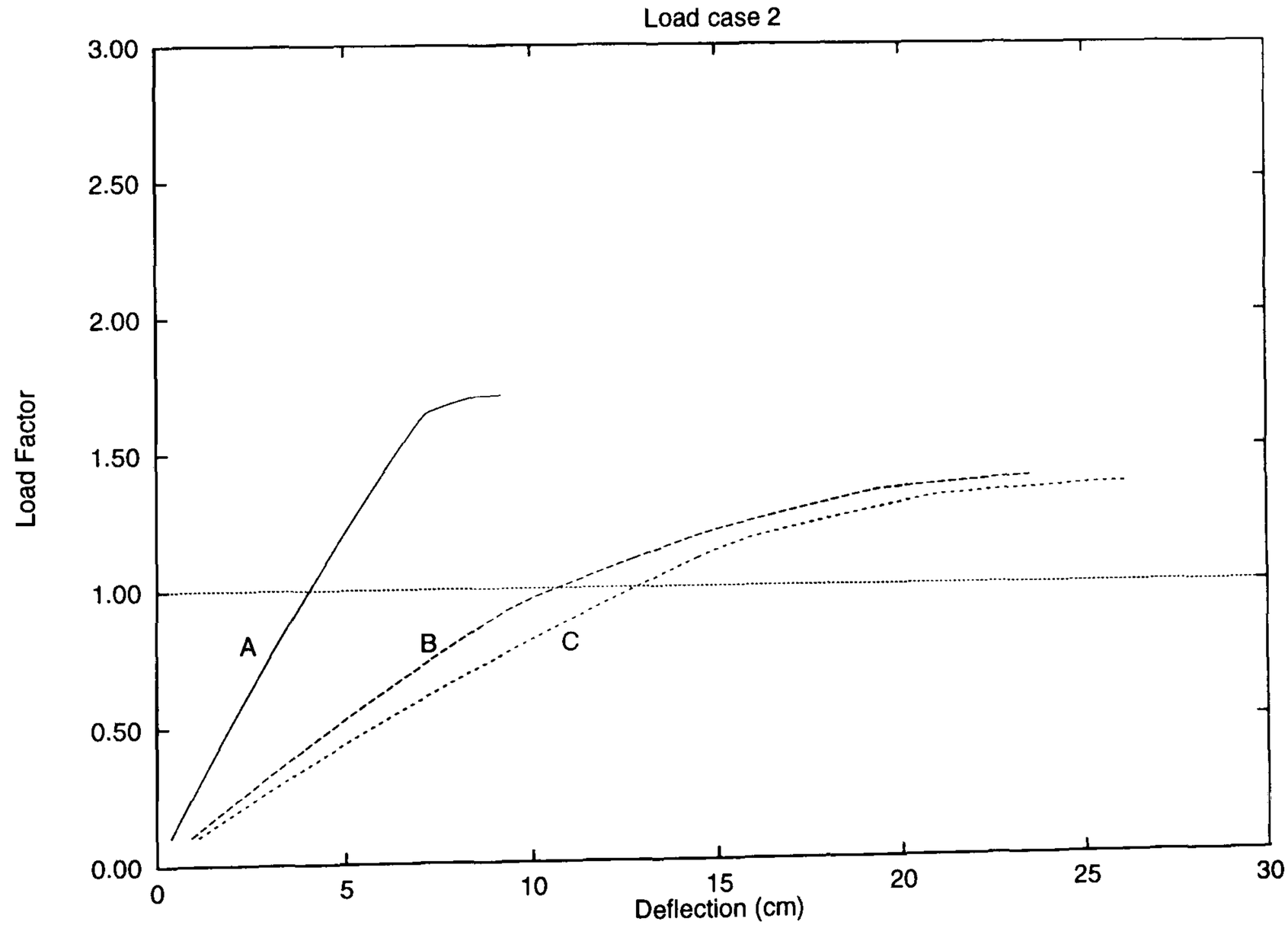

For the key please refer to the following page

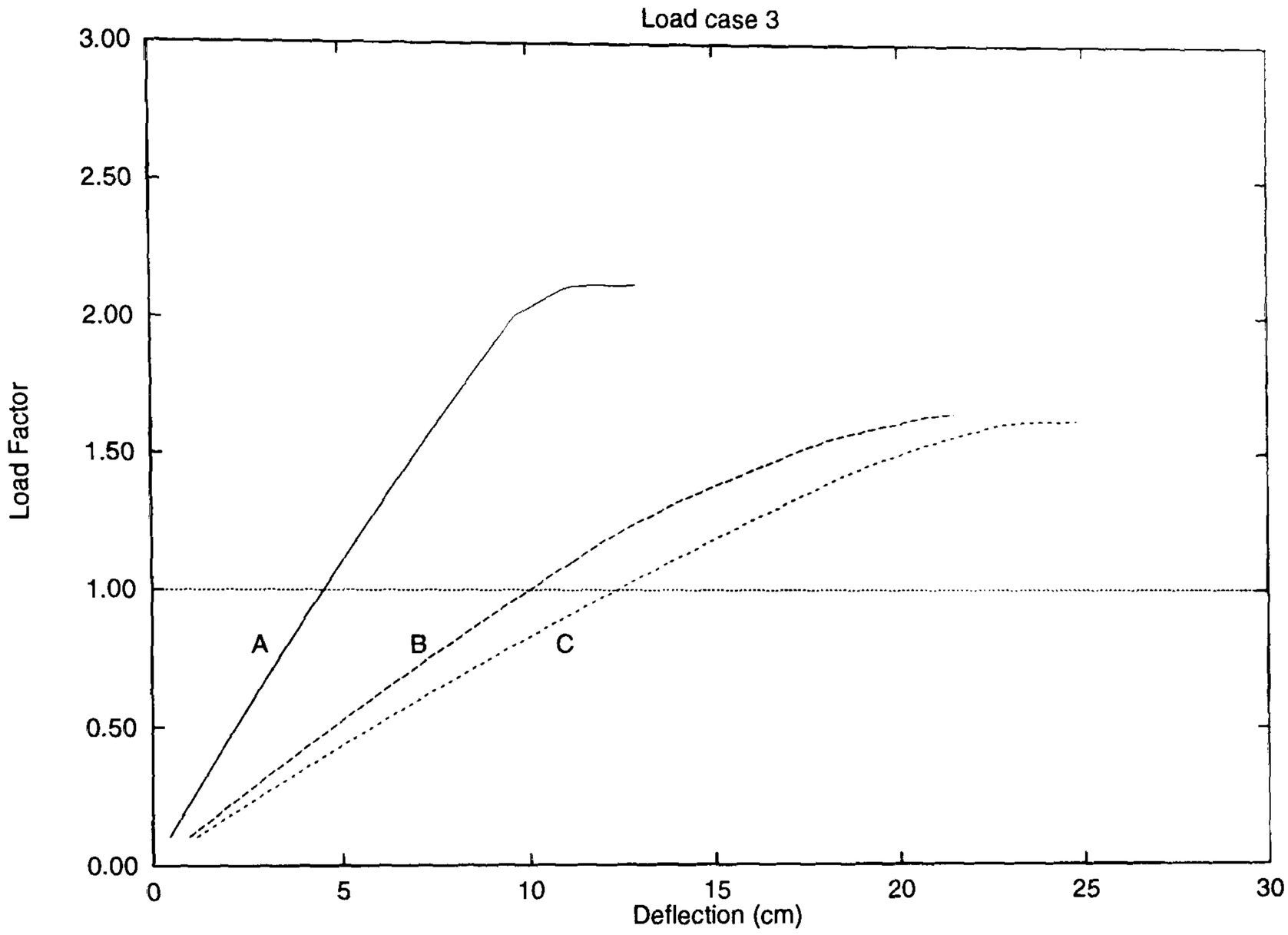

Key

A : Rigid frame

B : S-R(1) Negelecting web shear at the internal columns

C : S-R(2) Including web shear at the internal columns

C.4 Sequence of hinge formation

The following tables, C.1 to C.5, provide a summary of the plastification obtained in each Wind-Moment frame considered. The load factors within the tables represent the lowest load level in which a plastic hinge formed in any of the beam and column members. To aid clarity, the column end adjacent to the base base, has been considered independently from the remaining part of the column.

The 'S-R ' designation represents the frame employing the standard connections, whereas the 'Rigid ' designation refers to an identical frame with rigid full strength connections.

	Beam member		Column member		Column base	
	S - R	Rigid	S - R	Rigid	S - R	Rigid
	Load factors					
LC1	**1.14**	**1.37**	**N/A**	**1.52**	**N/A**	**N/A**
LC2	**1.38**	**1.27**	**N/A**	**1.58**	**1.40**	**1.56**
LC3	**1.68**	**1.42**	**N/A**	**1.76**	**1.43**	**1.68**

Table C.1: Load factor at member plastification (2 storey 1 bay frame)

	Beam member		Column member		Column base	
	S - R	Rigid	S - R	Rigid	S - R	Rigid
	Load factors					
LC1	**1.13**	**1.65**	**N/A**	**1.77**	**2.00**	**1.80**
LC2	**1.38**	**1.49**	**N/A**	**1.74**	**1.47**	**1.77**
LC3	**1.64**	**1.85**	**N/A**	**2.13**	**1.67**	**2.05**

Table C.2: Load factor at member plastification (2 storey 4 bay frame)

	Beam member		Column member		Column base	
	S - R	Rigid	S - R	Rigid	S - R	Rigid
	Load factors					
LC1	**1.11**	**1.57**	**N/A**	**1.46**	**1.24**	**1.44**
LC2	**1.30**	**1.31**	**1.49**	**1.51**	**1.16**	**1.45**
LC3	**1.87**	**1.60**	**1.28**	**1.70**	**1.23**	**1.52**

Table C.3: Load factor at member plastification (4 storey 2 bay frame)

	Beam member		Column member		Column base	
	S - R	Rigid	S - R	Rigid	S - R	Rigid
	Load factors					
LC1	**1.09**	**1.62**	**N/A**	**1.55**	**1.28**	**1.49**
LC2	**1.29**	**1.21**	**N/A**	**1.48**	**1.13**	**1.41**
LC3	**1.88**	**1.44**	**N/A**	**1.68**	**1.28**	**1.57**

Table C.4: Load factor at member plastification (4 storey 4 bay frame)

	Beam member		Column member		Column base	
	S - R	Rigid	S - R	Rigid	S - R	Rigid
	Load factors					
LC1	**1.06**	**N/A**	**1.06**	**1.14**	**1.06**	**1.25**
LC2	**N/A**	**N/A**	**1.23**	**1.32**	**1.06**	**1.35**
LC3	**N/A**	**N/A**	**N/A**	**1.90**	**N/A**	**1.83**

Table C.5: Load factor at member plastification (8 storey 2 bay frame)

S-R (1)

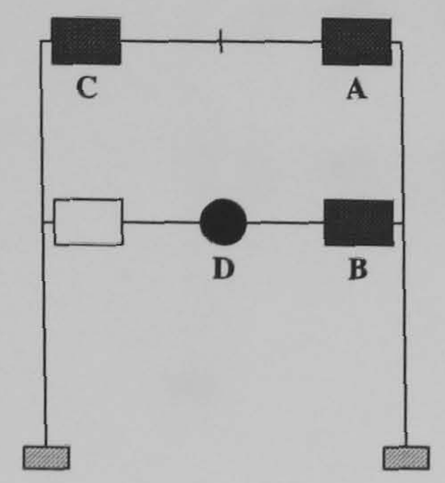

Rigid

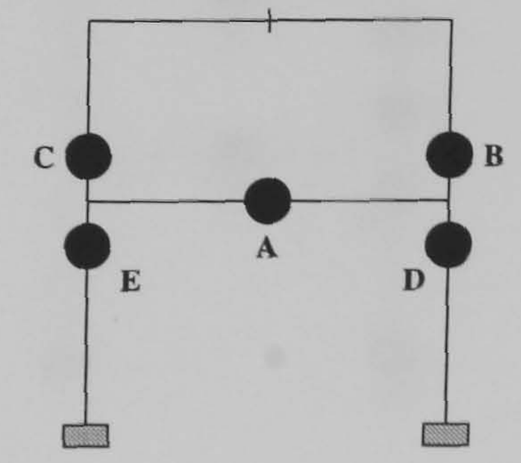

Key :

Plastification prior to ULS design load being attained

Semi-Rigid Connection

Plastification following the attainment of the design load

Member plastification

Hinge location	Load level at hinge formation	
	S-R(1)	Rigid
A	**1.145**	**1.487**
B	**1.15**	**1.525**
C	**1.24**	**1.537**
D	**1.325**	**1.57**
E	**N/A**	**1.585**

FRAME : **f10 b24**

Load Case 1

S-R (1)

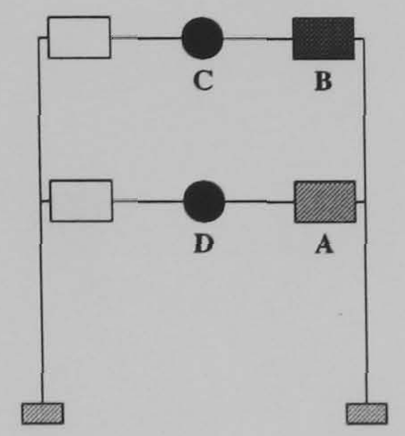

Rigid

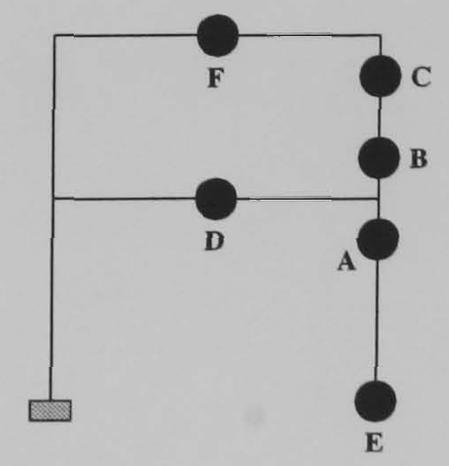

Key :

Plastification prior to ULS design load being attained

Semi-Rigid Connection

Plastification following the attainment of the design load

Member plastification

Hinge location	Load level at hinge formation	
	S-R(1)	Rigid
A	**0.935**	**1.587**
B	**1.075**	**1.67**
C	**1.535**	**1.707**
D	**1.55**	**1.815**
E	**N/A**	**1.82**
F	**N/A**	**1.837**

FRAME : **f10 b24**

Load Case 2

S-R (1)

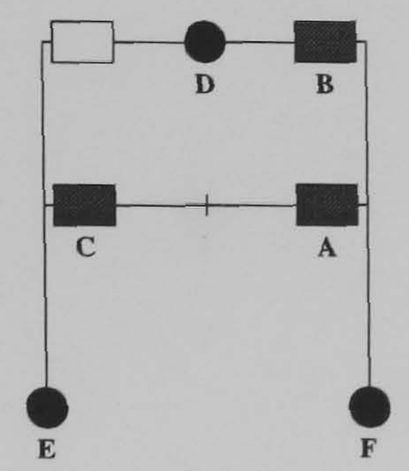

Rigid

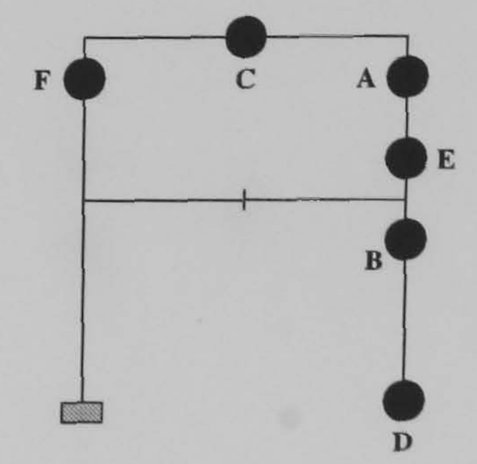

Key :

Semi-Rigid Connection

Plastification prior to ULS design load being attained

Plastification following the attainment of the design load

Member plastification

Hinge location	load level at hinge formation	
	S-R(1)	Rigid
A	**1.2125**	**2.042**
B	**1.255**	**2.107**
C	**1.8125**	**2.245**
D	**1.815**	**2.247**
E	**1.835**	**2.265**
F	**1.837**	**2.357**

FRAME : **f10 b24**
Load Case 3

S-R (1)

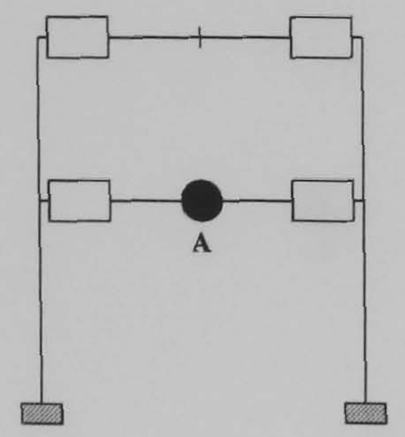

Rigid

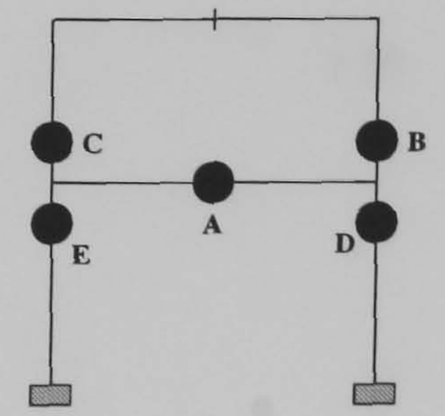

Key :

- Semi-Rigid Connection
- Plastification prior to ULS design load being attained
- Plastification following the attainment of the design load
- Member plastification

Hinge location	Load level at hinge formation	
	S-R(1)	Rigid
A	**1.14**	**1.37**
B	**N/A**	**1.56**
C	**N/A**	**1.577**
D	**N/A**	**1.59**
E	**N/A**	**1.61**

FRAME : **f11 b20**
Load Case 1

S-R (1)

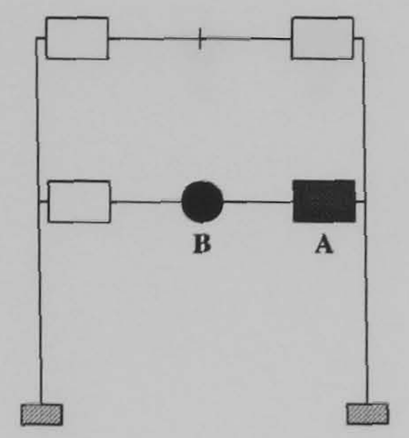

Rigid

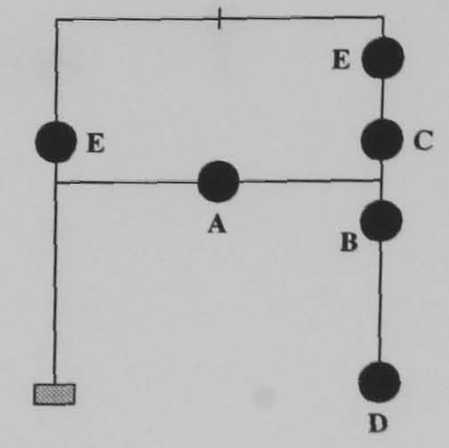

Key :

Semi-Rigid Connection

Plastification prior to ULS design load being attained

Plastification following the attainment of the design load

Member plastification

Hinge location	Load level at hinge formation	
	S-R(1)	Rigid
A	**1.1275**	**1.737**
B	**1.385**	**1.805**
C	**N/A**	**1.852**
D	**N/A**	**1.895**
E	**N/A**	**1.91**

FRAME : **f11 b20**
Load Case 2

S-R (1)

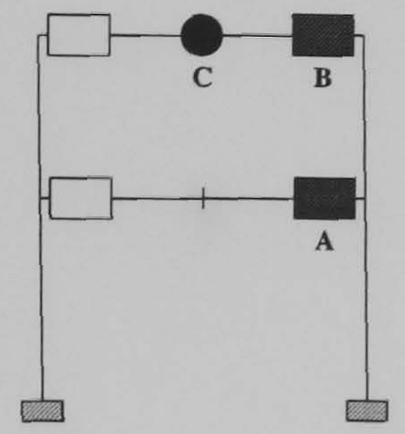

Rigid

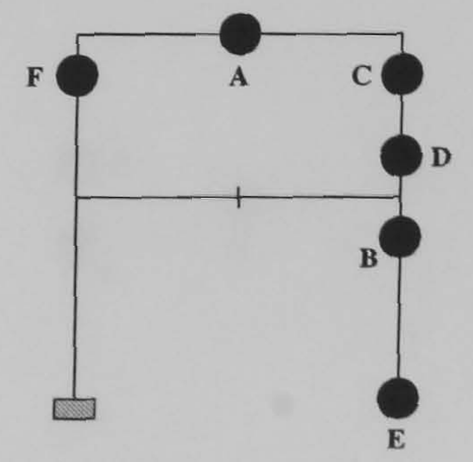

Key :

Semi-Rigid Connection

Plastification prior to ULS design load being attained

Plastification following the attainment of the design load

Member plastification

Hinge location	Load level at hinge formation	
	S-R(1)	Rigid
A	**1.5175**	**2.582**
B	**1.825**	**2.692**
C	**2.005**	**2.702**
D	**N/A**	**2.782**
E	**N/A**	**2.815**
F	**N/A**	**2.89**

FRAME : **f11 b20**
Load Case 3

S-R (1)

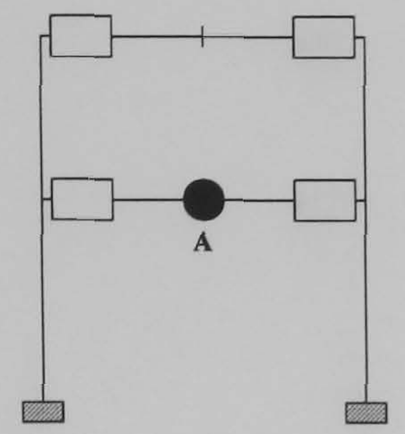

Rigid

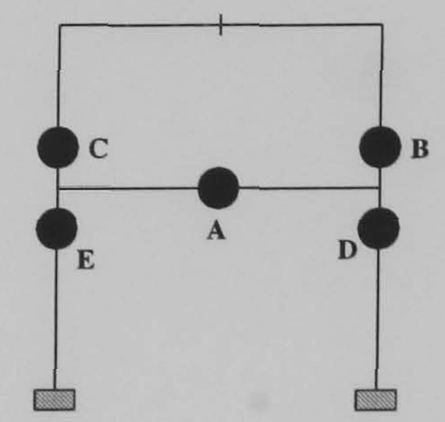

Key :

Semi-Rigid Connection

Plastification prior to ULS design load being attained

Plastification following the attainment of the design load

Member plastification

Hinge location	Load level hinge formation	
	S-R(1)	Rigid
A	**1.16**	**1.37**
B	**N/A**	**1.56**
C	**N/A**	**1.577**
D	**N/A**	**1.59**
E	**N/A**	**1.61**

FRAME : **f11 b24**
Load Case 1

S-R (1)

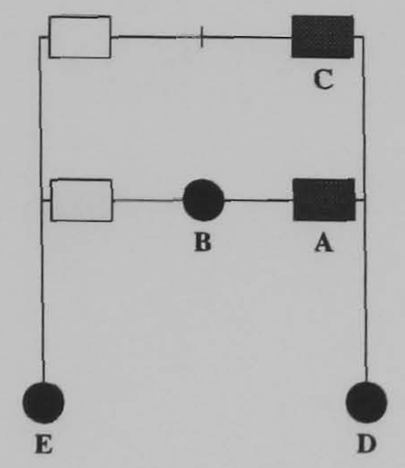

Rigid

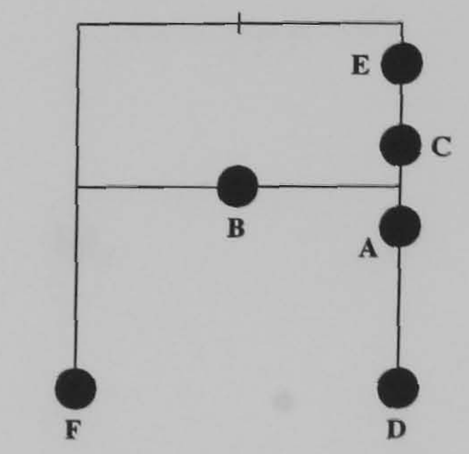

Key :

Semi-Rigid Connection

Plastification prior to ULS design load being attained

Plastification following the attainment of the design load

Member plastification

Hinge location	Load level at hinge formation	
	S-R(1)	Rigid
A	**1.0975**	**1.647**
B	**1.382**	**1.72**
C	**1.4175**	**1.777**
D	**1.445**	**1.785**
E	**1.46**	**1.817**
F	**N/A**	**1.827**

FRAME : **f11 b24**
Load Case 2

S-R (1)

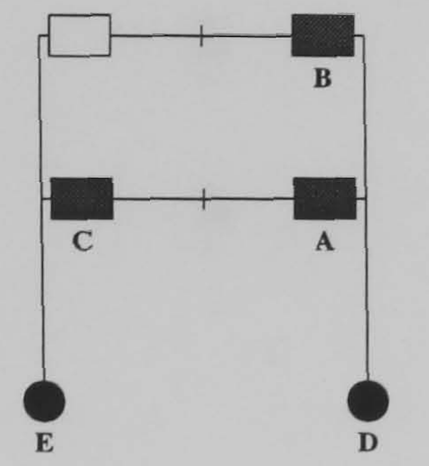

Rigid

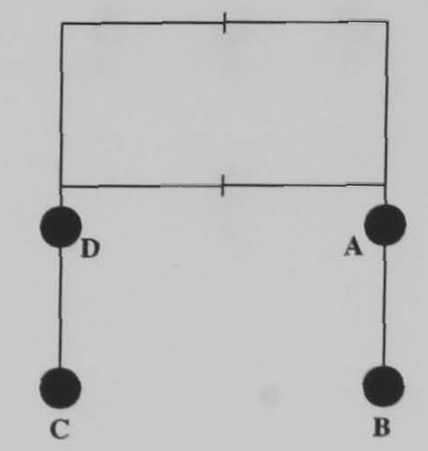

Key :

Semi-Rigid Connection

Plastification prior to ULS design load being attained

Plastification following the attainment of the design load

Member plastification

Hinge location	Load level at hinge formation	
	S-R(1)	Rigid
A	**1.3875**	**2.167**
B	**1.7875**	**2.245**
C	**1.8875**	**2.462**
D	**1.957**	**2.467**
E	**1.96**	**N/A**

FRAME : **f11 b24**
Load Case 3

S-R (1)

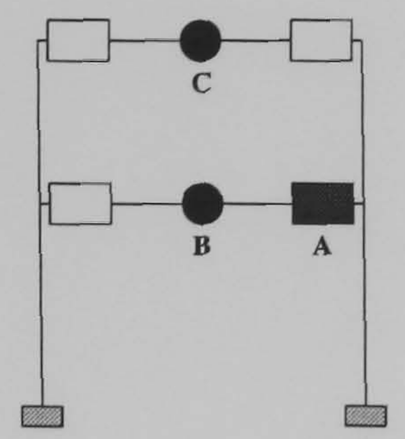

Rigid

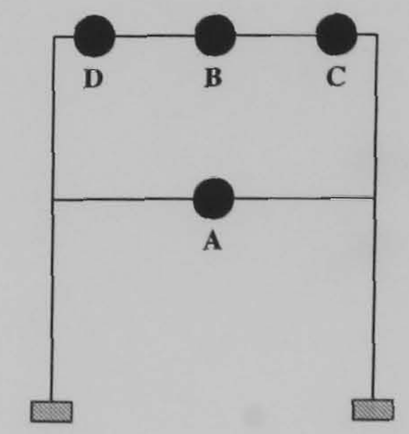

Key :

Semi-Rigid Connection

Plastification prior to ULS design load being attained

Plastification following the attainment of the design load

Member plastification

Hinge location	Load level at hinge formation	
	S-R(1)	Rigid
A	**1.32**	**1.562**
B	**1.24**	**1.795**
C	**1.262**	**2.015**
D	**N/A**	**2.03**

FRAME : **f12 b20**
Load Case 1

S-R (1)

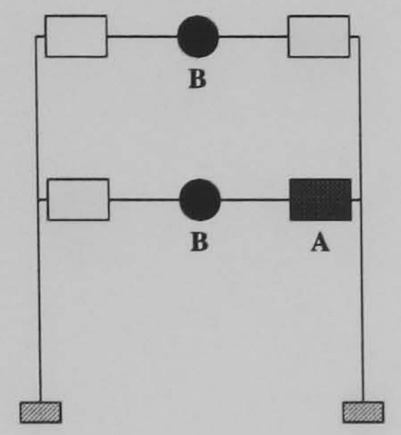

Rigid

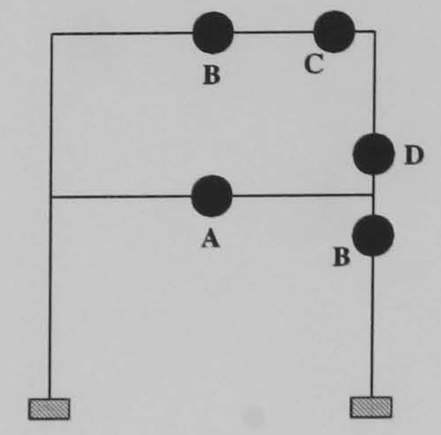

Key :

Semi-Rigid Connection

Plastification prior to ULS design load being attained

Plastification following the attainment of the design load

Member plastification

Hinge location	Load level at hinge formation	
	S-R(1)	Rigid
A	**1.215**	**1.982**
B	**1.465**	**2.130**
C	**N/A**	**2.172**
D	**N/A**	**2.235**

FRAME : **f12 b20**
Load Case 2

S-R (1)

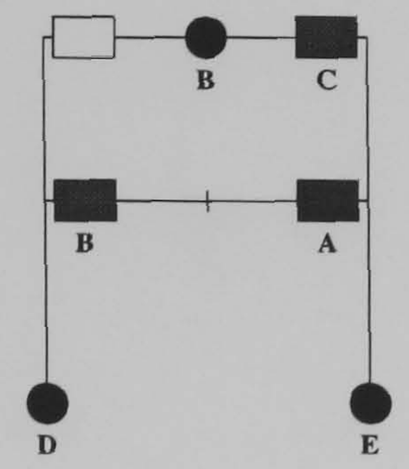

Rigid

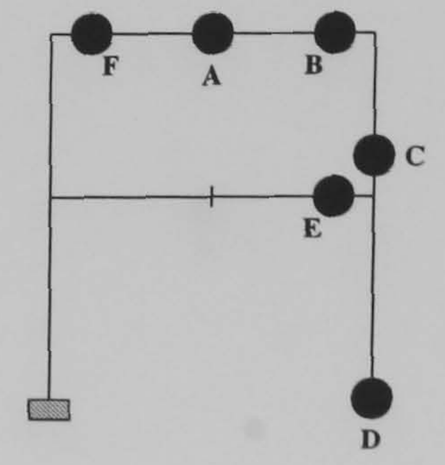

Key :

Semi-Rigid Connection

Plastification prior to ULS design load being attained

Plastification following the attainment of the design load

Member plastification

Hinge location	Load level hinge formation	
	S-R(1)	Rigid
A	**1.46**	**2.415**
B	**1.73**	**2.492**
C	**1.7325**	**2.847**
D	**1.857**	**2.87**
E	**1.862**	**2.885**
F	**N/A**	**2.892**

FRAME : **f12 b20**
Load Case 3

S-R (1)

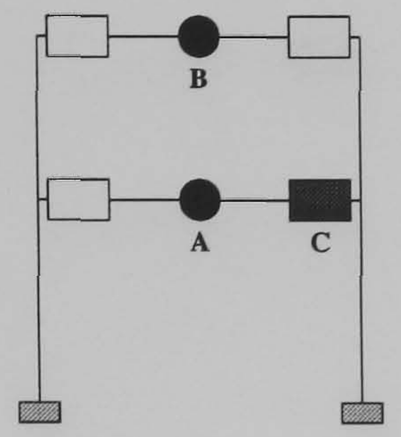

Rigid

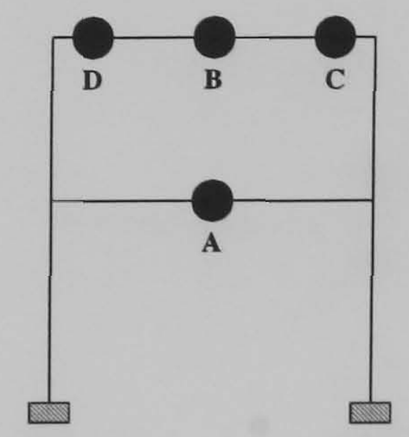

Key :

Semi-Rigid Connection

Plastification prior to ULS design load being attained

Plastification following the attainment of the design load

Member plastification

Hinge location	Load level at hinge formation	
	S-R(1)	Rigid
A	**1.267**	**1.562**
B	**1.315**	**1.795**
C	**1.3825**	**2.015**
D	N/A	**2.03**

FRAME : **f12 b24**
Load Case 1

S-R (1)

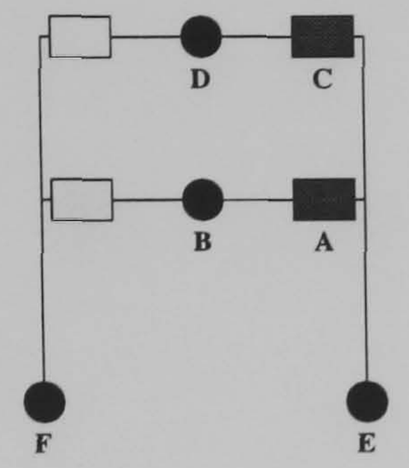

Rigid

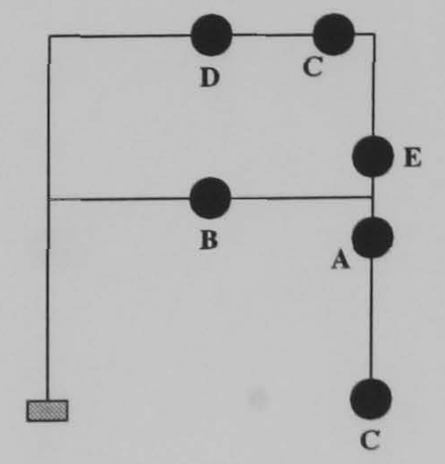

Key :

Semi-Rigid Connection

Plastification prior to ULS design load being attained

Plastification following the attainment of the design load

Member plastification

Hinge location	Load level at hinge formation	
	S-R(1)	Rigid
A	**1.15**	**1.93**
B	**1.45**	**1.97**
C	**1.4725**	**2.015**
D	**1.482**	**2.097**
E	**1.505**	**2.102**
F	**1.507**	N/A

FRAME : **f12 b24**
Load Case 2

S-R (1)

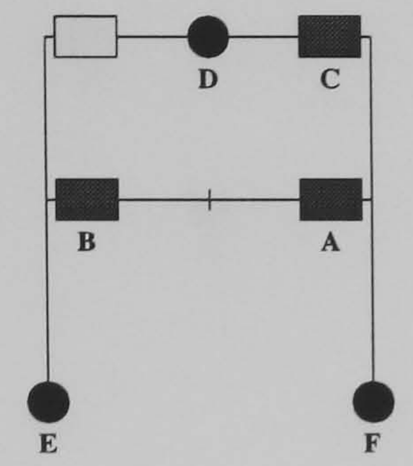

Rigid

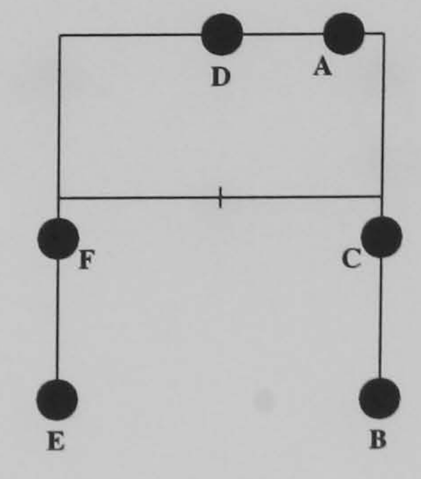

Key :

Semi-Rigid Connection

Plastification prior to ULS design load being attained

Plastification following the attainment of the design load

Member plastification

Hinge location	Load level at hinge formation	
	S-R(1)	Rigid
A	**1.3225**	**2.27**
B	**1.4925**	**2.285**
C	**1.6025**	**2.347**
D	**1.687**	**2.357**
E	**1.72**	**2.5**
F	**1.722**	**2.53**

FRAME : **f12 b24**
Load Case 3

S-R (1)

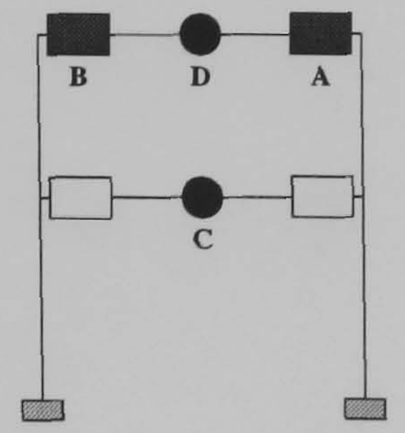

Rigid

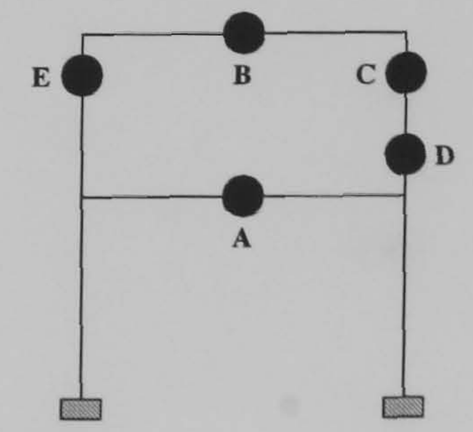

Key :

Plastification prior to ULS design load being attained

Semi-Rigid Connection

Plastification following the attainment of the design load

Member plastification

Hinge location	Load level hinge formation	
	S-R(1)	Rigid
A	**1.1575**	**1.595**
B	**1.27**	**1.677**
C	**1.355**	**1.812**
D	**1.367**	**1.817**
E	**N/A**	**1.822**

FRAME : **f13 b24**
Load Case 1

S-R (1)

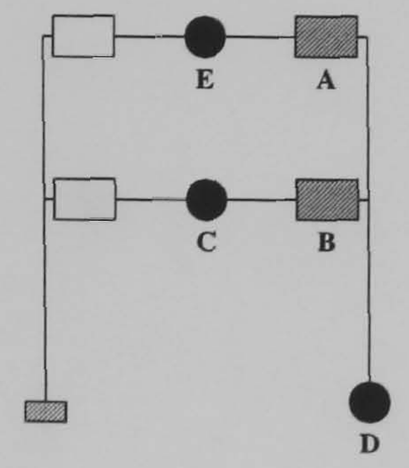

Rigid

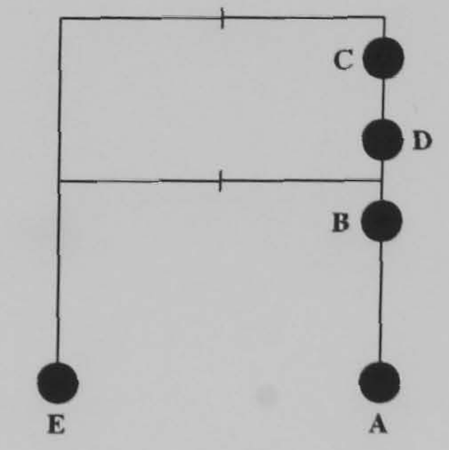

Key :

Semi-Rigid Connection

Plastification prior to ULS design load being attained

Plastification following the attainment of the design load

Member plastification

Hinge location	load level at hinge formation	
	S-R(1)	Rigid
A	**0.86**	**1.567**
B	**0.945**	**1.63**
C	**1.392**	**1.775**
D	**1.402**	**1.822**
E	**1.405**	**1.83**

FRAME : **f13 b24**
Load Case 2

S-R (1)

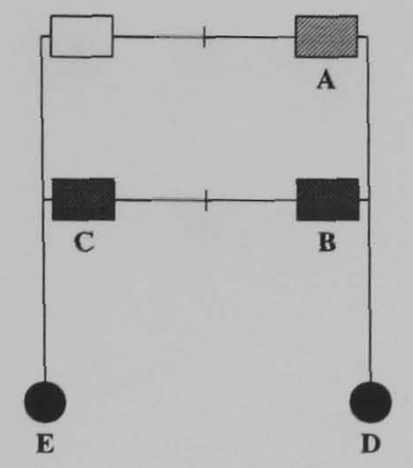

Rigid

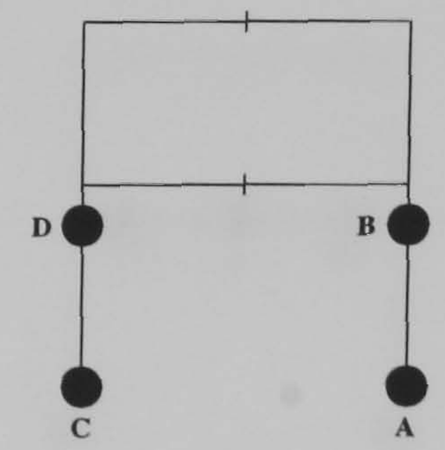

Key :

Semi-Rigid Connection

Plastification prior to ULS design load being attained

Plastification following the attainment of the design load

Member plastification

Hinge location	Load level at hinge formation	
	S-R(1)	Rigid
A	**0.915**	**1.687**
B	**1.06**	**1.765**
C	**1.365**	**1.847**
D	**1.435**	**1.88**
E	**1.44**	**N/A**

FRAME : **f13 b24**

Load Case 3

S-R (1)

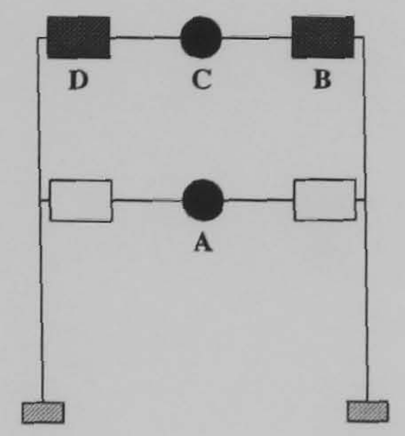

Rigid

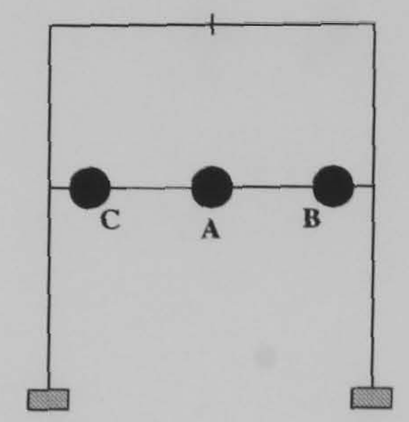

Key :

Semi-Rigid Connection

Plastification prior to ULS design load being attained

Plastification following the attainment of the design load

Member plastification

Hinge location	Load level at hinge formation	
	S-R(1)	Rigid
A	**1.475**	**1.81**
B	**1.6175**	**2.022**
C	**1.705**	**2.062**
D	**1.72**	**N/A**

FRAME : **f14 b24**
Load Case 1

S-R (1)

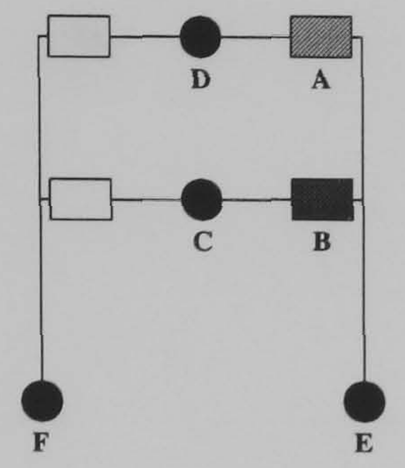

Rigid

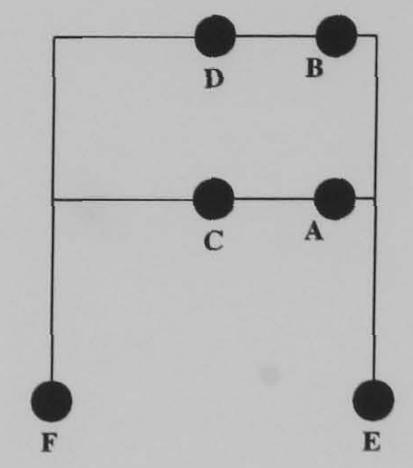

Key :

Semi-Rigid Connection

Plastification prior to ULS design load being attained

Plastification following the attainment of the design load

Member plastification

Hinge location	Load level at hinge formation	
	S-R(1)	Rigid
A	**0.9475**	**1.275**
B	**1.3725**	**1.692**
C	**1.567**	**1.765**
D	**1.58**	**1.93**
E	**1.68**	**1.95**
F	**1.692**	**1.967**

FRAME : **f14 b24**
Load Case 2

S-R (1)

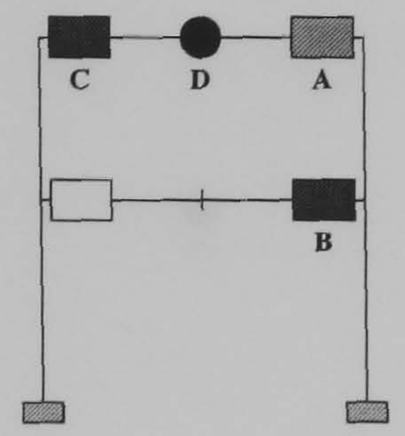

Rigid

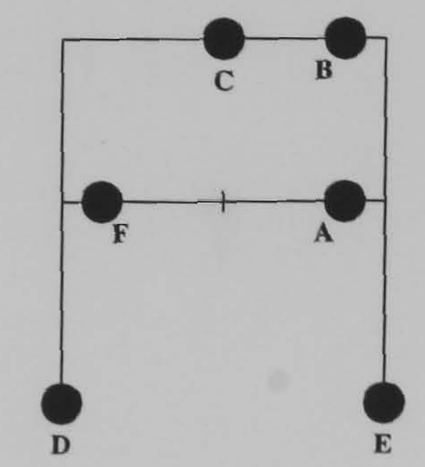

Key :

Plastification prior to ULS design load being attained

Semi-Rigid Connection

Plastification following the attainment of the design load

Member plastification

Hinge location	Load level at hinge formation	
	S-R(1)	Rigid
A	**0.9525**	**1.412**
B	**1.4825**	**1.78**
C	**1.6575**	**2.232**
D	**1.787**	**2.245**
E	**N/A**	**2.252**
F	**N/A**	**2.257**

FRAME : **f14 b24**
Load Case 3

S-R (1)

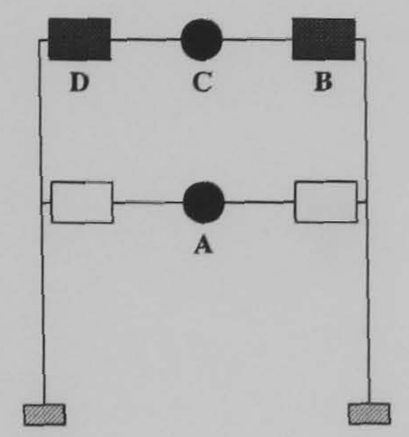

Rigid

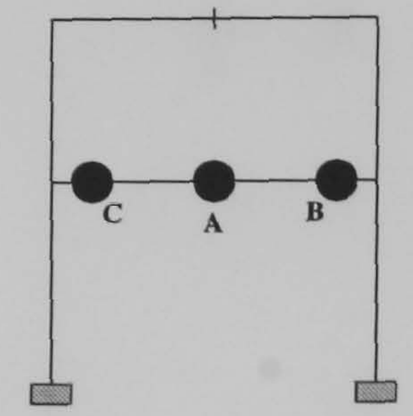

Key :

Plastification prior to ULS design load being attained

Semi-Rigid Connection

Plastification following the attainment of the design load

Member plastification

Hinge location	Load level at hinge formation	
	S-R(1)	Rigid
A	**1.475**	**1.81**
B	**1.6175**	**2.022**
C	**1.705**	**2.062**
D	**1.72**	**N/A**

FRAME : **f14 b24**
Load Case 1

S-R (1)

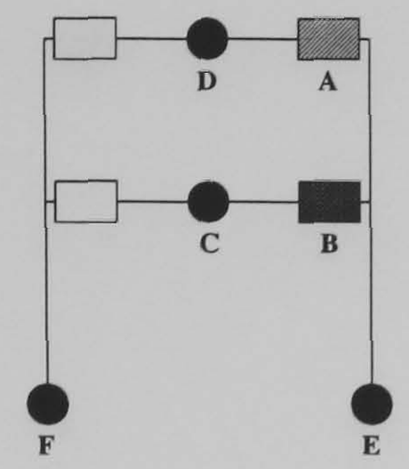

Rigid

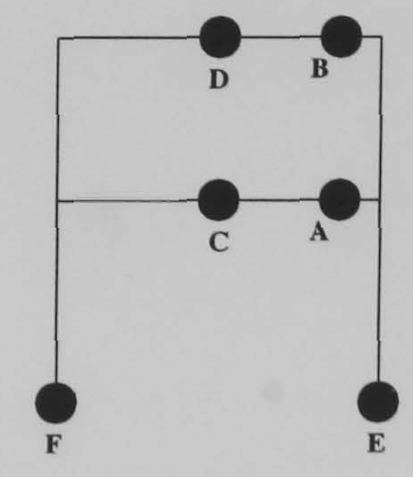

Key :

Semi-Rigid Connection

Plastification prior to ULS design load being attained

Plastification following the attainment of the design load

Member plastification

Hinge location	Load level at hinge formation	
	S-R(1)	Rigid
A	**0.9475**	**1.275**
B	**1.3725**	**1.692**
C	**1.567**	**1.765**
D	**1.58**	**1.93**
E	**1.68**	**1.95**
F	**1.692**	**1.967**

FRAME : **f14 b24**
Load Case 2

S-R (1)

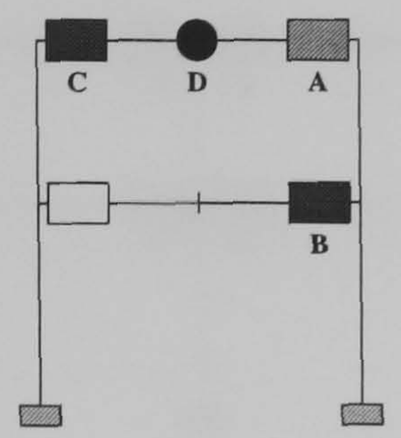

Rigid

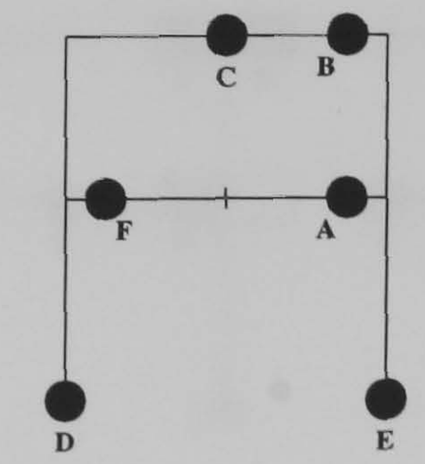

Key :

Plastification prior to ULS design load being attained

Semi-Rigid Connection

Plastification following the attainment of the design load

Member plastification

Hinge location	Load level at hinge formation	
	S-R(1)	Rigid
A	**0.9525**	**1.412**
B	**1.4825**	**1.78**
C	**1.6575**	**2.232**
D	**1.787**	**2.245**
E	**N/A**	**2.252**
F	**N/A**	**2.257**

FRAME : **f14 b24**
Load Case 3

S-R (1) Negelecting web shear at the internal columns

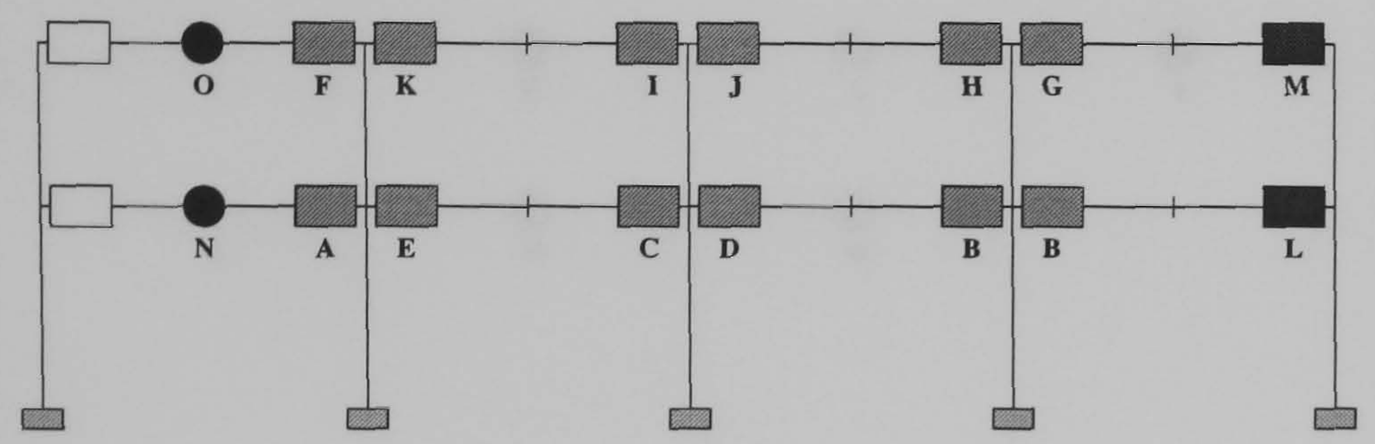

S-R (2) Including web shear at the internal columns

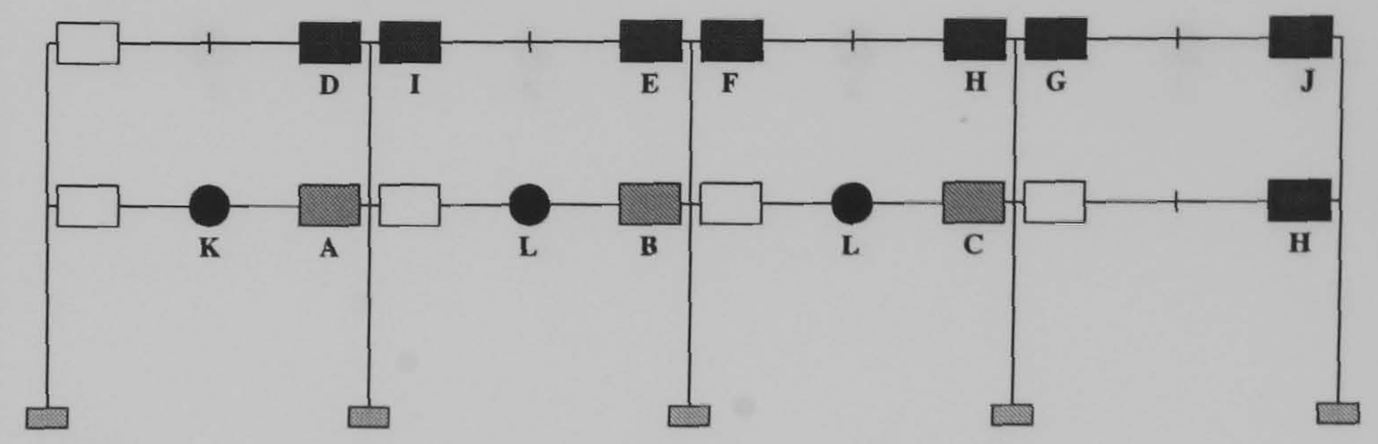

Rigid

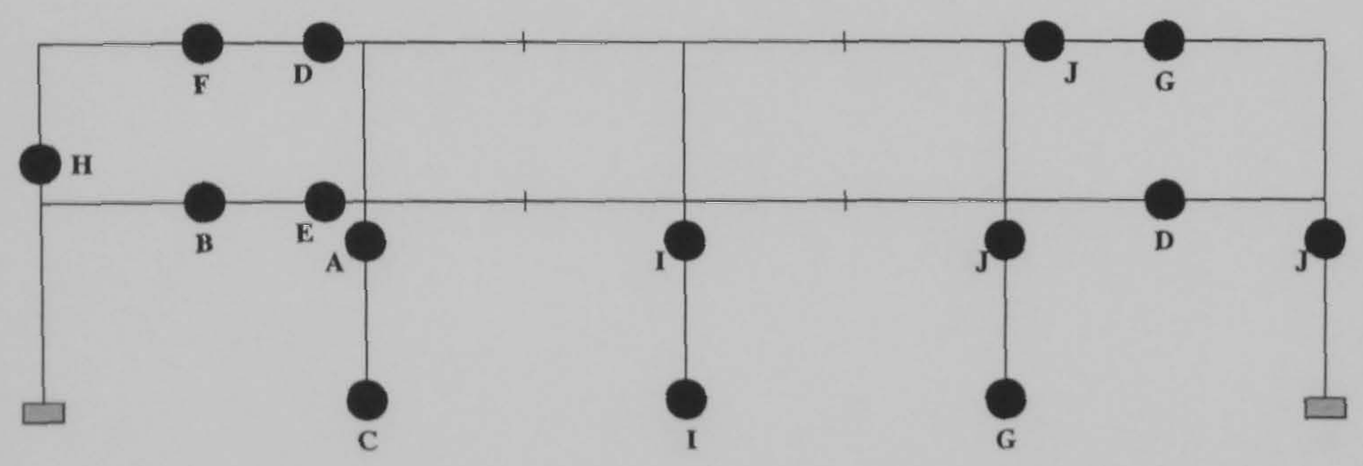

Hinge Location	Load Level at Hinge Formation S-R(1)	S-R(2)	Rigid
A	0.495	0.975	1.817
B	0.5125	0.9875	1.872
C	0.5325	0.9925	1.887
D	0.645	1.025	1.892
E	0.67	1.04	1.895
F	0.695	1.0425	1.91
G	0.7175	1.045	1.915
H	0.7275	1.0475	1.922
I	0.7425	1.07	1.927
J	0.8125	1.0775	1.93
K	0.825	1.305	N/A
L	1.1015	1.32	N/A
M	1.0525	N/A	N/A
N	1.285	N/A	N/A
O	1.292	N/A	N/A

Key :

Plastification prior to ULS design load being attained

Semi-Rigid Connection

Plastification following the attainment of the design load

Member plastification

FRAME : **f16 b24**
Load Case 1

S-R (1) Negelecting web shear at the internal columns

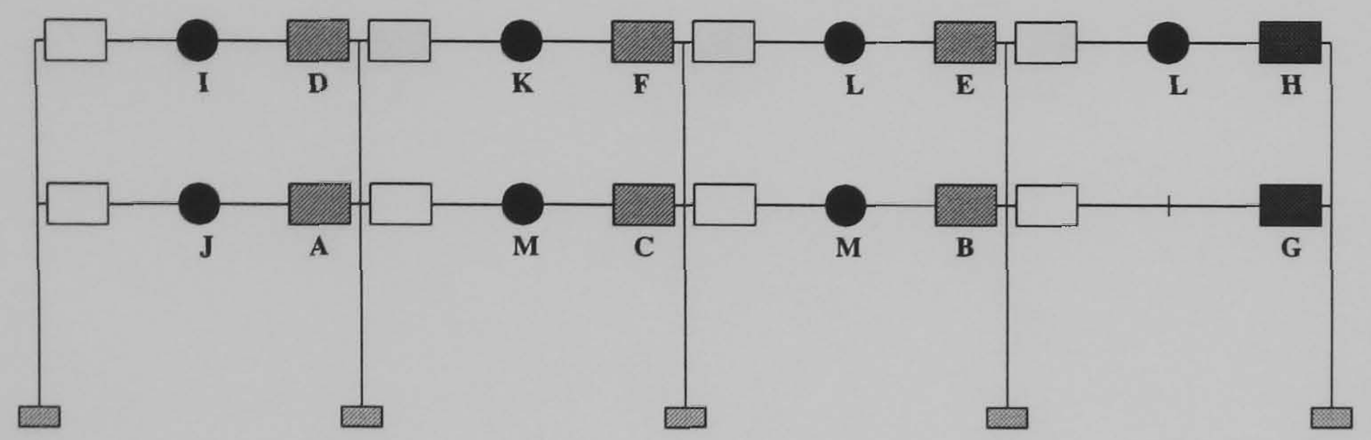

S-R (2) Including web shear at the internal columns

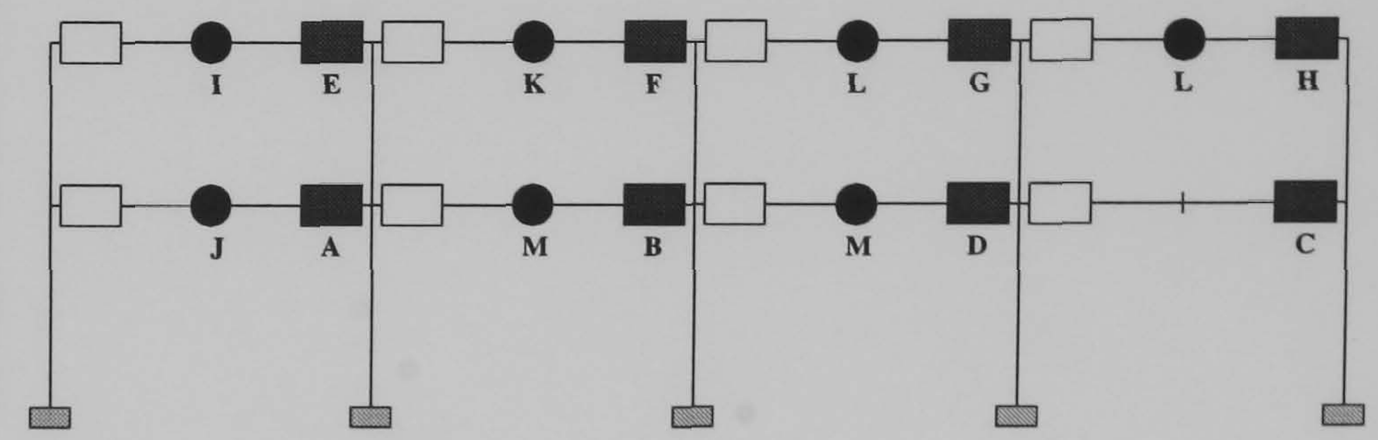

Rigid

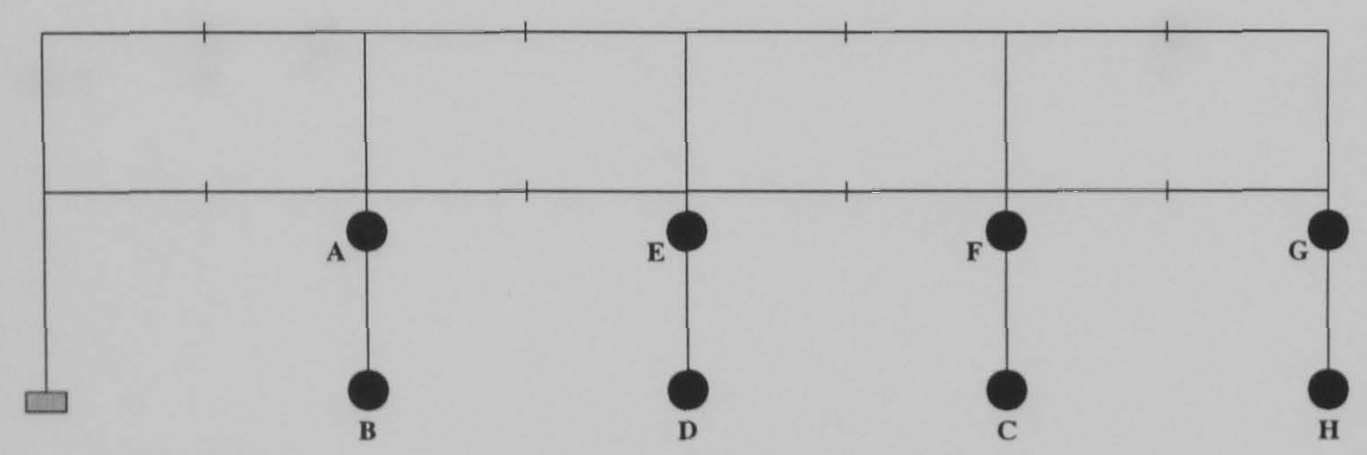

Hinge Location	Load Level at Hinge Formation S-R(1)	S-R(2)	Rigid
A	**0.5975**	**1.1425**	**1.952**
B	**0.62**	**1.1575**	**2.01**
C	**0.64**	**1.1625**	**2.067**
D	**0.81**	**1.1675**	**2.105**
E	**0.85**	**1.1825**	**2.117**
F	**0.865**	**1.2025**	**2.12**
G	**1.0875**	**1.21**	**2.142**
H	**1.165**	**1.24**	**2.155**
I	**1.577**	**1.595**	**N/A**
J	**1.6**	**1.615**	**N/A**
K	**1.622**	**1.62**	**N/A**
L	**1.625**	**1.622**	**N/A**
M	**1.63**	**1.63**	**N/A**

Key :

Semi-Rigid Connection

Plastification prior to ULS design load being attained

Plastification following the attainment of the design load

Member plastification

FRAME : **f16 b24**
Load Case 2

S-R (1) Negelecting web shear at the internal columns

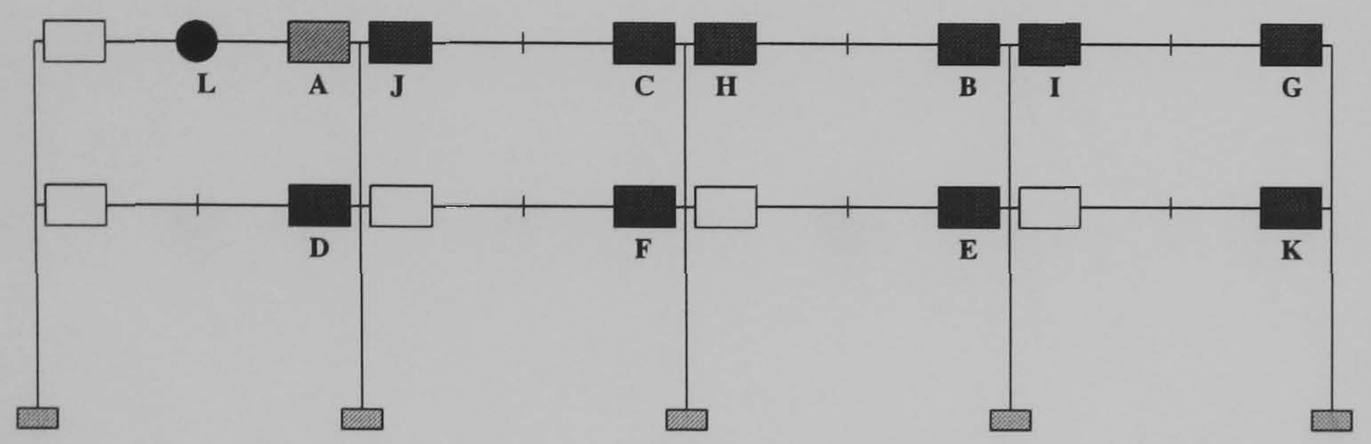

S-R (2) Including web shear at the internal columns

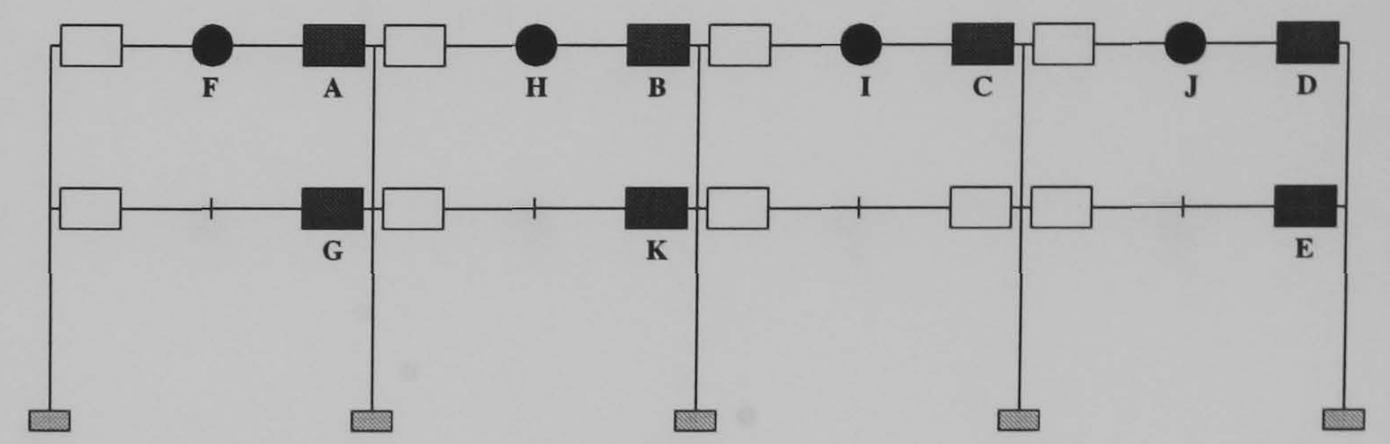

Rigid

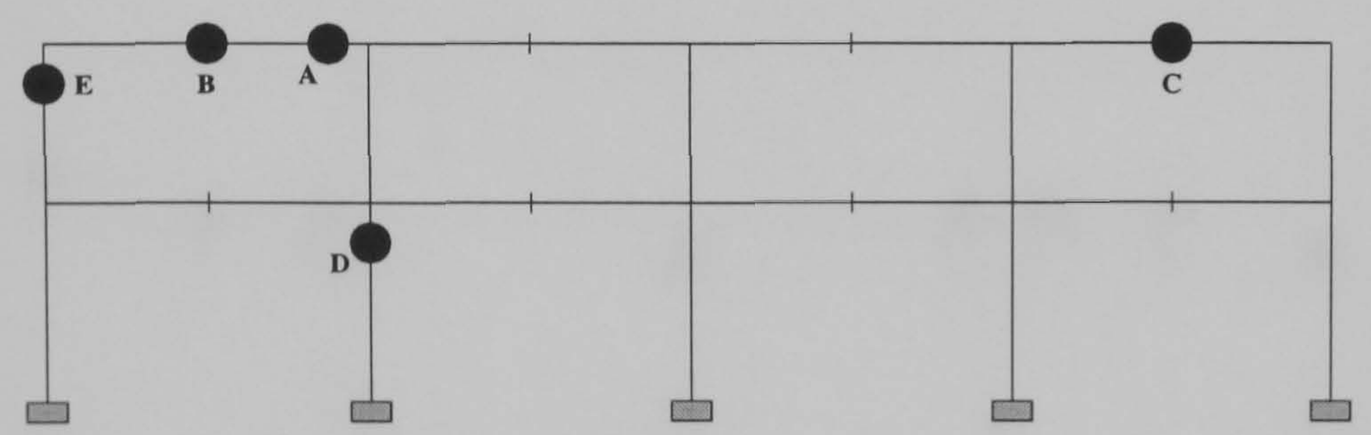

Hinge Location	Load Level at Hinge Formation S-R(1)	S-R(2)	Rigid
A	0.9625	1.39	2.612
B	1.0125	1.43	2.682
C	1.035	1.4325	2.765
D	1.1525	1.53	2.775
E	1.2	1.725	2.787
F	1.22	1.922	N/A
G	1.5025	1.955	N/A
H	1.5275	1.957	N/A
I	1.5575	1.96	N/A
J	1.625	1.962	N/A
K	1.6925	1.965	N/A
L	1.905	N/A	N/A

Key :

Semi-Rigid Connection

Plastification prior to ULS design load being attained

Plastification following the attainment of the design load

Member plastification

FRAME : **f16 b24**

Load Case 3

S-R (1) Negelecting web shear at the internal columns

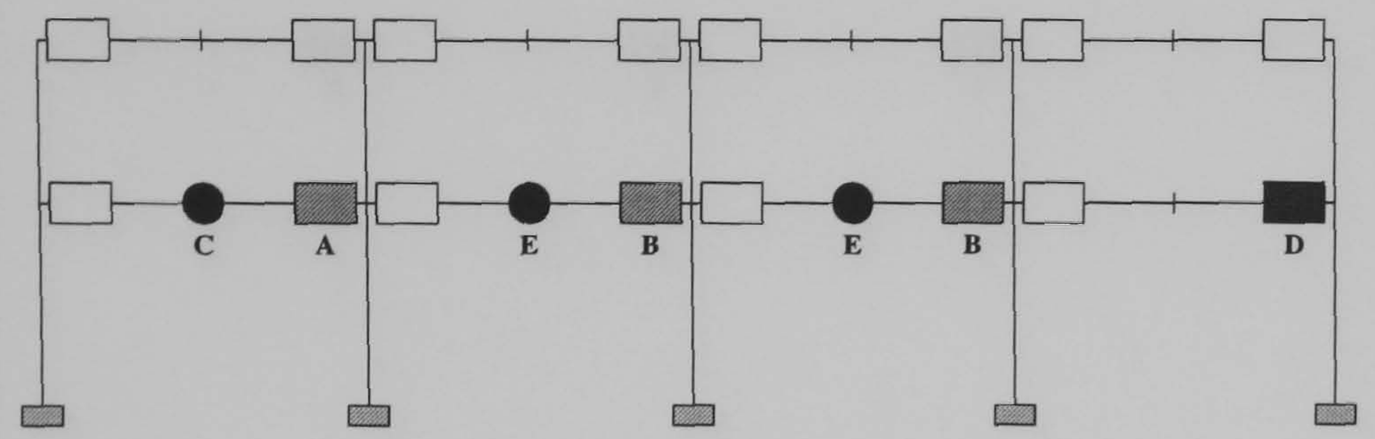

S-R (2) Including web shear at the internal columns

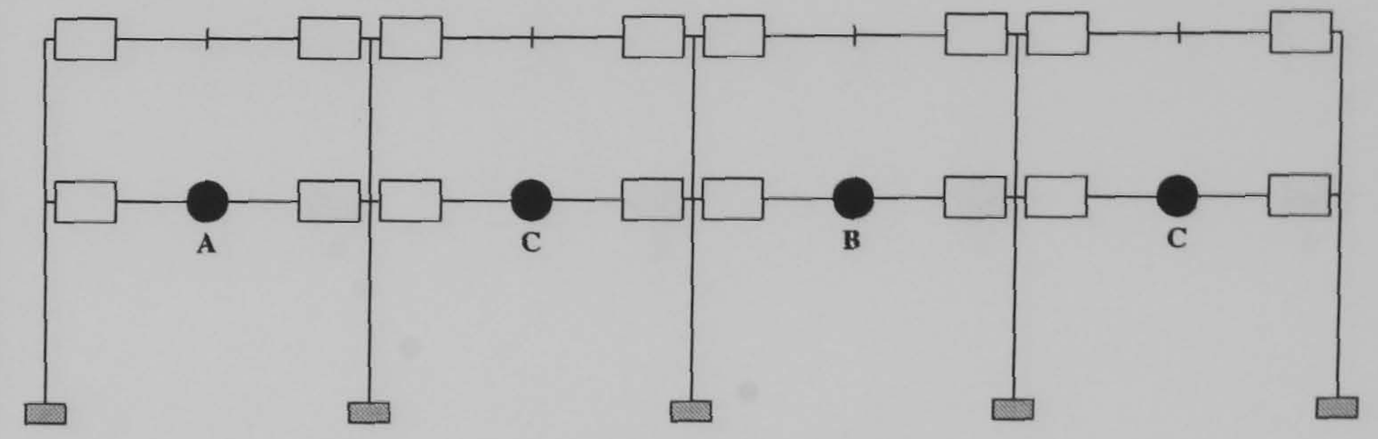

Rigid

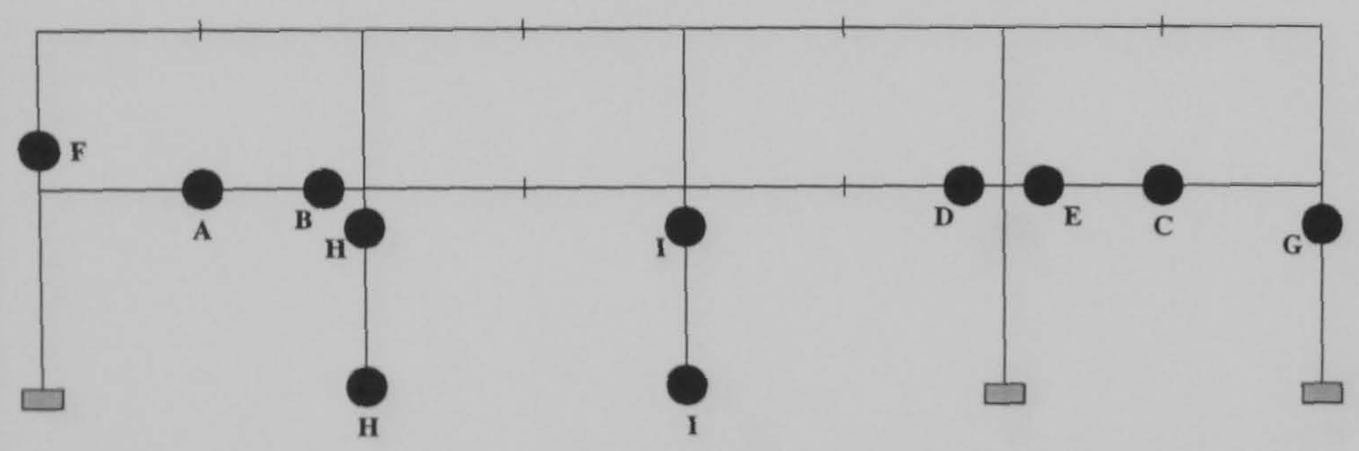

Hinge Location	Load Level at Hinge Formation S-R(1)	S-R(2)	Rigid
A	**0.86**	**1.137**	**1.66**
B	**0.8725**	**1.147**	**1.67**
C	**1.14**	**1.15**	**1.68**
D	**1.1525**	**N/A**	**1.73**
E	**1.162**	**N/A**	**1.742**
F	**N/A**	**N/A**	**1.777**
G	**N/A**	**N/A**	**1.8**
H	**N/A**	**N/A**	**1.802**
I	**N/A**	**N/A**	**1.81**

Key :

- Semi-Rigid Connection
- Plastification prior to ULS design load being attained
- Plastification following the attainment of the design load
- Member plastification

FRAME : **f17 b20**
Load Case 1

S-R (1) Negelecting web shear at the internal columns

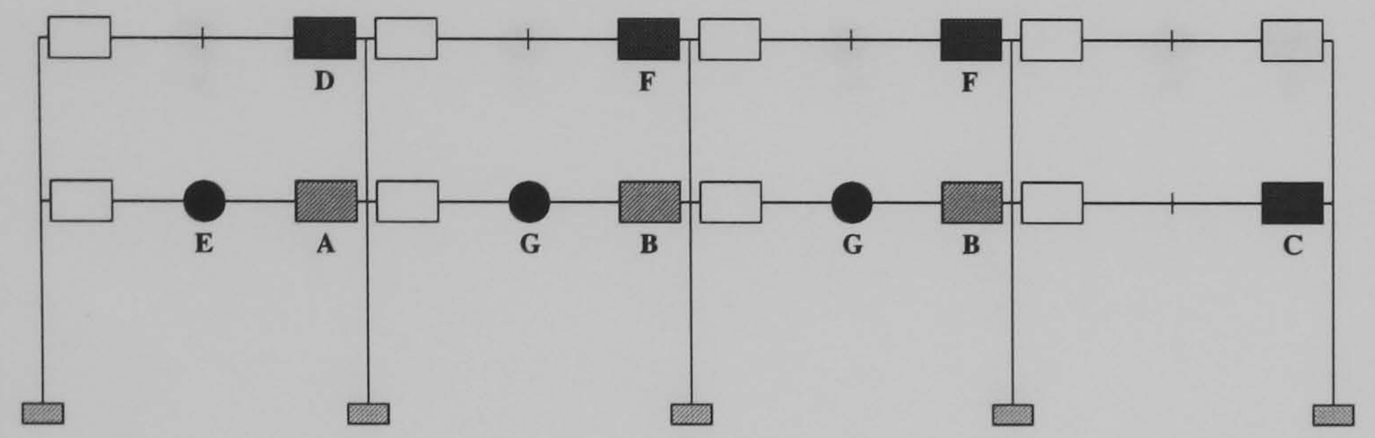

S-R (2) Including web shear at the internal columns

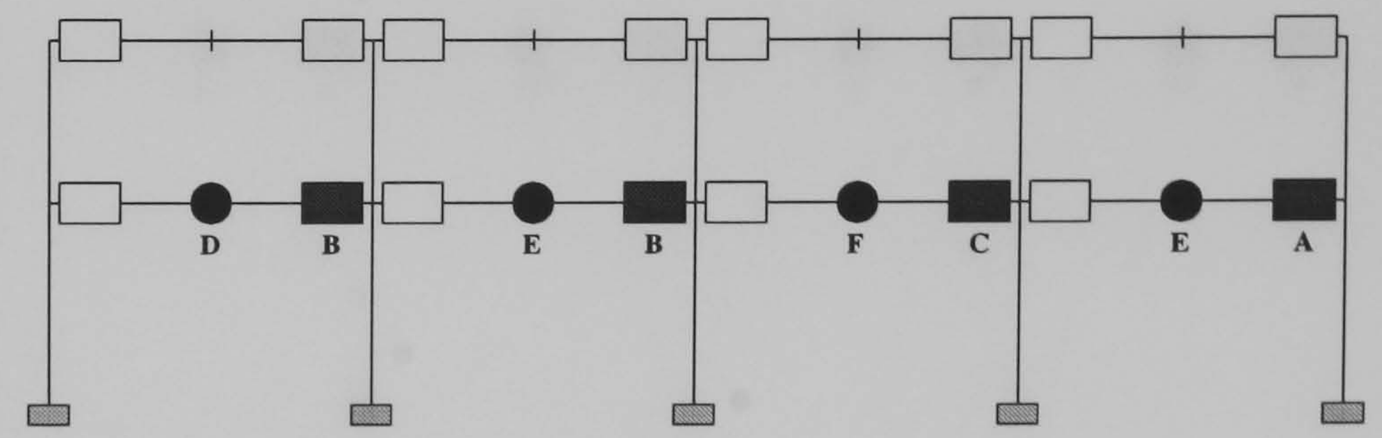

Rigid

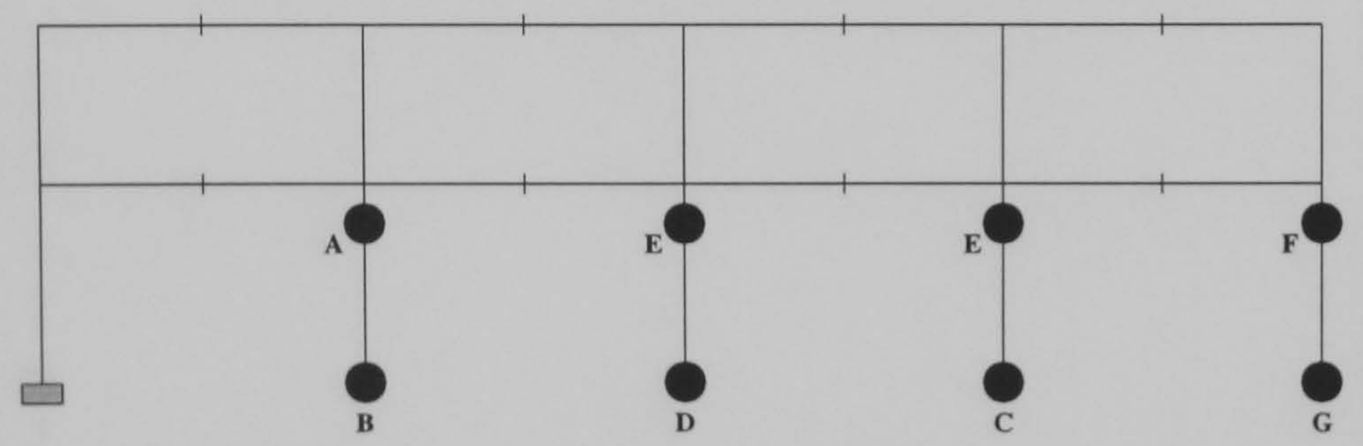

Hinge Location	Load Level at Hinge Formation S-R(1)	S-R(2)	Rigid
A	**0.915**	**1.125**	**1.755**
B	**0.9725**	**1.2375**	**1.775**
C	**1.1425**	**1.24**	**1.83**
D	**1.3675**	**1.387**	**1.852**
E	**1.387**	**1.402**	**1.87**
F	**1.39**	**1.405**	**1.89**
G	**1.407**	**N/A**	**1.897**

Key :

Semi-Rigid Connection

Plastification prior to ULS design load being attained

Plastification following the attainment of the design load

Member plastification

FRAME : **f17 b20**
Load Case 2

S-R (1) Negelecting web shear at the internal columns

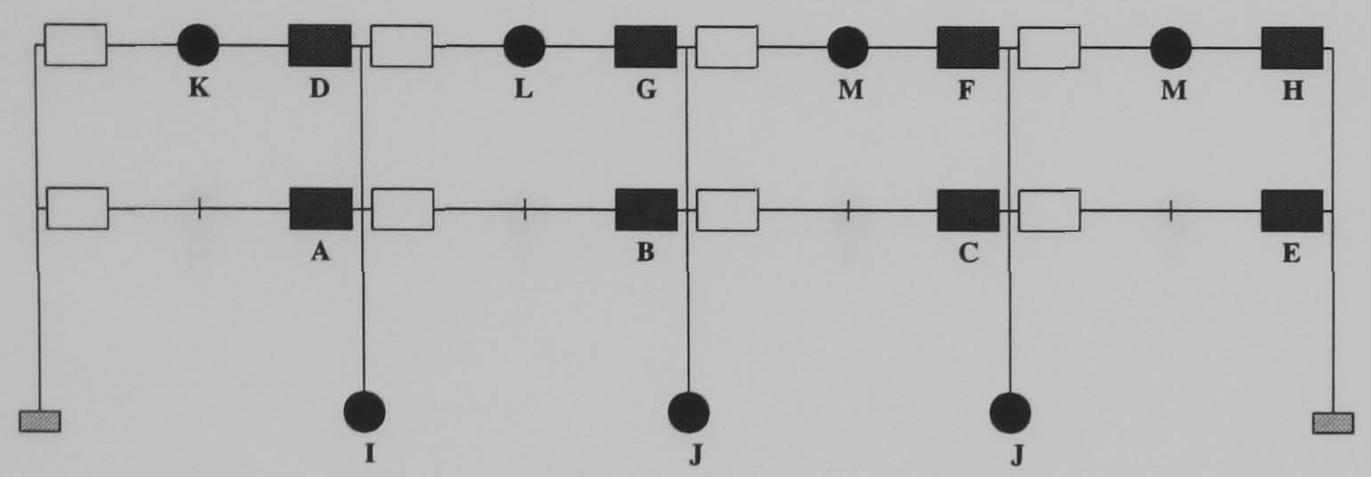

S-R (2) Including web shear at the internal columns

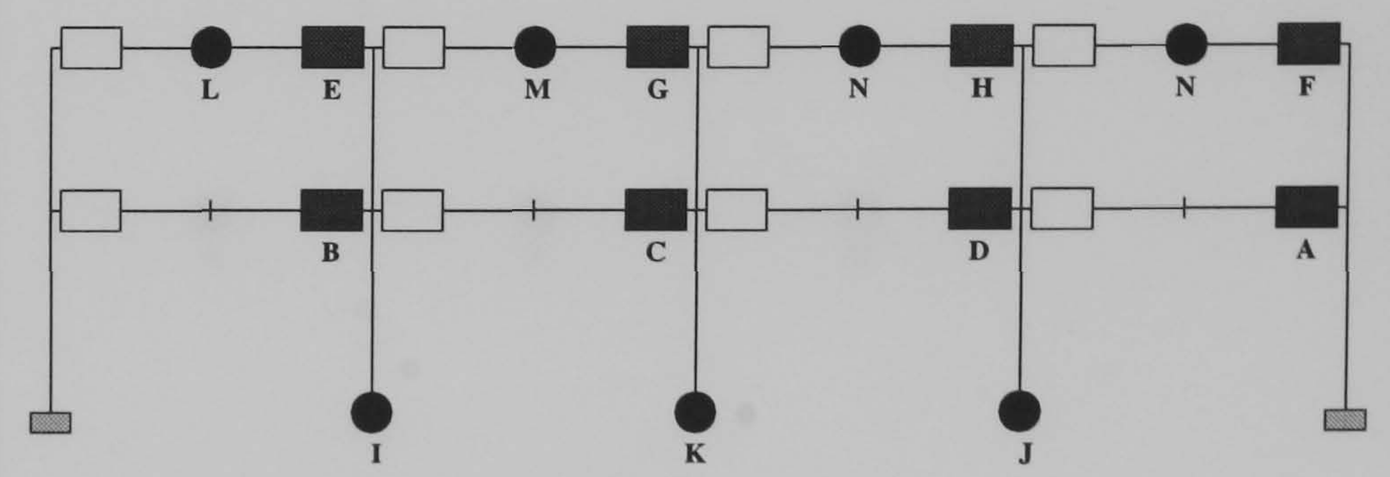

Rigid

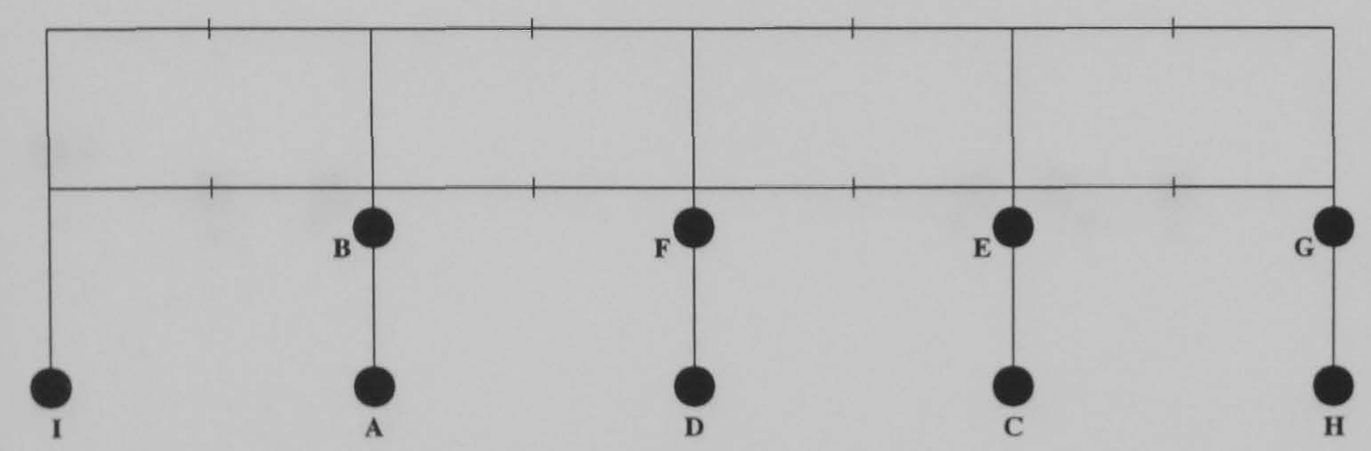

Hinge Location	Load Level at Hinge Formation		
	S-R(1)	S-R(2)	Rigid
A	1.4825	1.56	2.302
B	1.495	1.87	2.315
C	1.5	1.8775	2.36
D	1.63	1.885	2.385
E	1.6525	1.975	2.405
F	1.66	1.9825	2.42
G	1.665	1.9925	2.48
H	1.9925	2.0025	2.487
I	2.027	2.022	2.495
J	2.032	2.025	N/A
K	2.037	2.027	N/A
L	2.085	2.035	N/A
M	2.09	2.075	N/A
N	N/A	2.08	N/A

Key :

- Semi-Rigid Connection
- Plastification prior to ULS design load being attained
- Plastification following the attainment of the design load
- Member plastification

FRAME : **f17 b20**
Load Case 3

S-R (1) Negelecting web shear at the internal columns

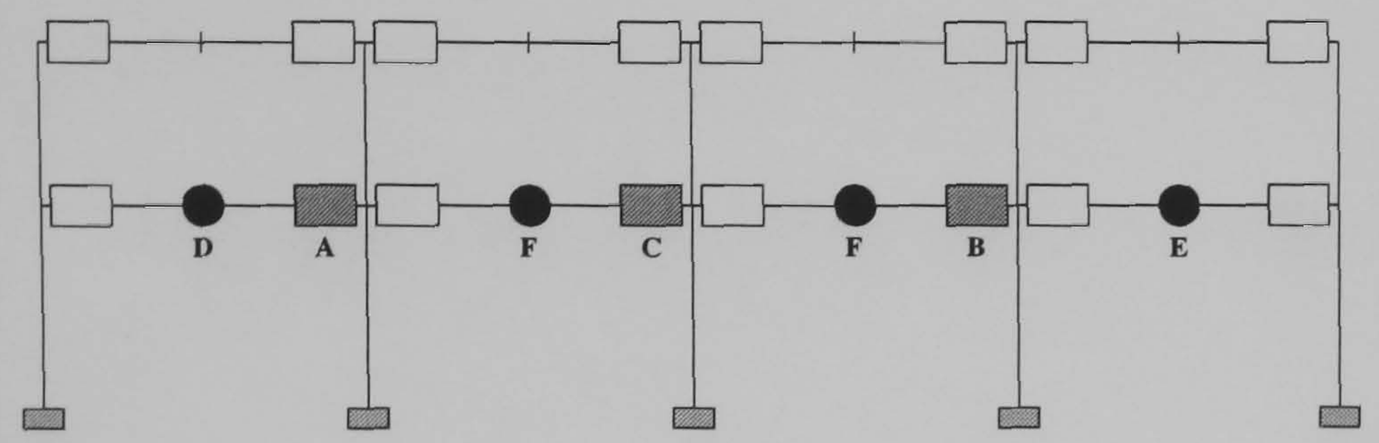

S-R (2) Including web shear at the internal columns

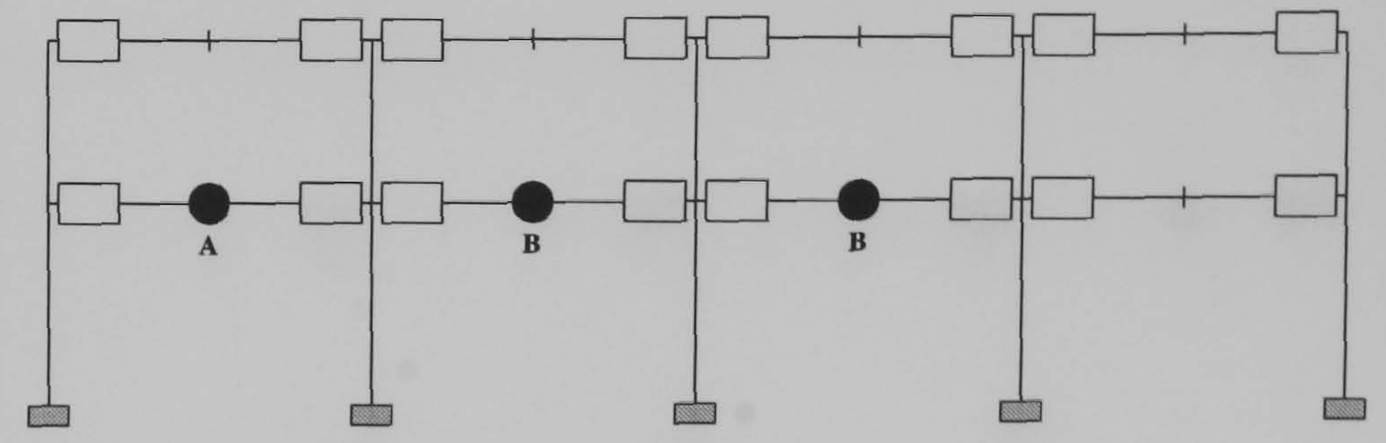

Rigid

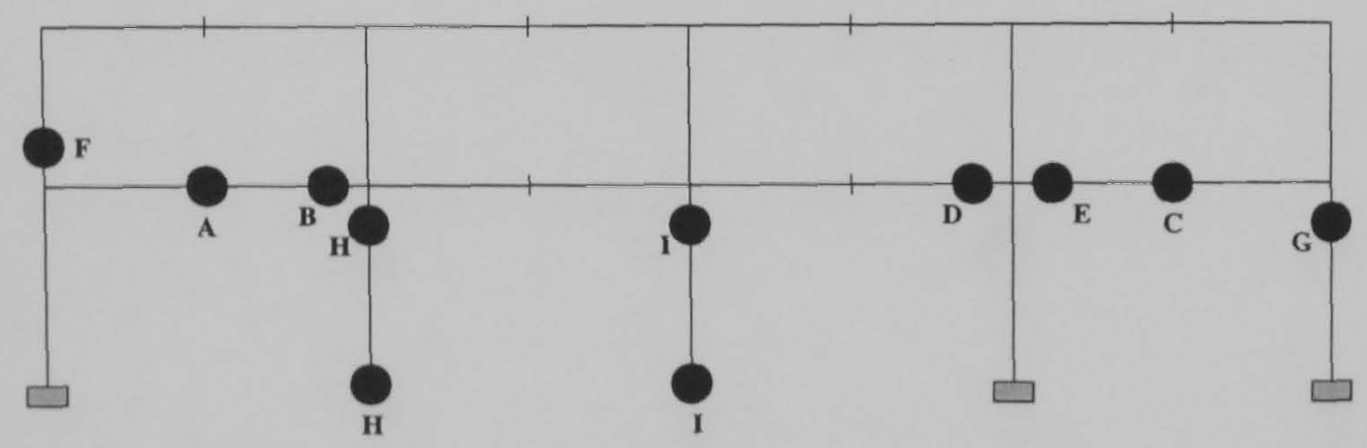

Hinge Location	Load Level at Hinge Formation S-R(1)	S-R(2)	Rigid
A	**0.885**	**1.157**	**1.66**
B	**0.905**	**1.172**	**1.67**
C	**0.91**	**N/A**	**1.68**
D	**1.167**	**N/A**	**1.73**
E	**1.195**	**N/A**	**1.742**
F	**1.202**	**N/A**	**1.777**
G	**N/A**	**N/A**	**1.8**
H	**N/A**	**N/A**	**1.802**
I	**N/A**	**N/A**	**1.81**

Key :

- Plastification prior to ULS design load being attained
- Semi-Rigid Connection
- Plastification following the attainment of the design load
- Member plastification

FRAME : **f17 b24**
Load Case 1

S-R (1) Negelecting web shear at the internal columns

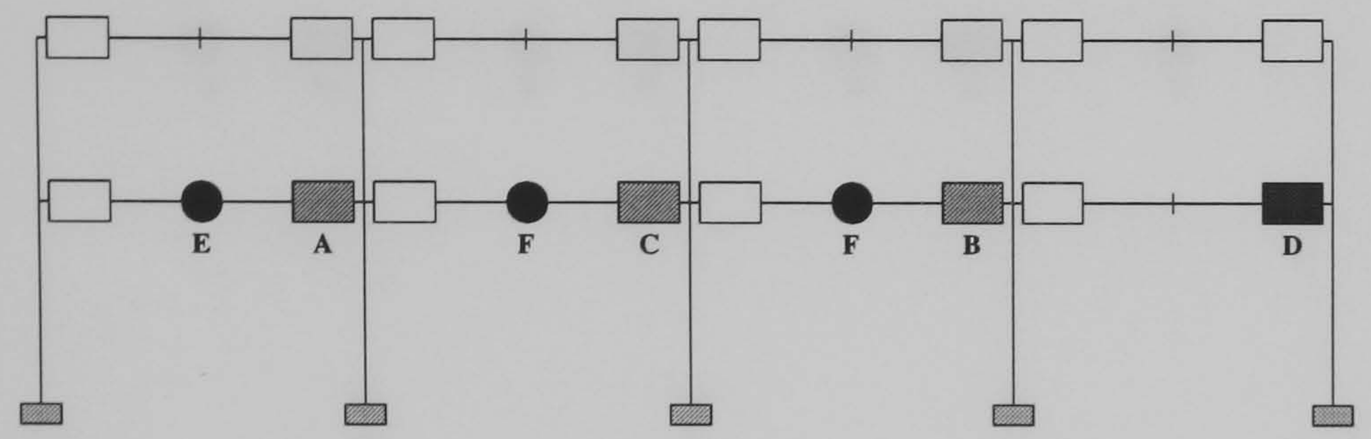

S-R (2) Including web shear at the internal columns

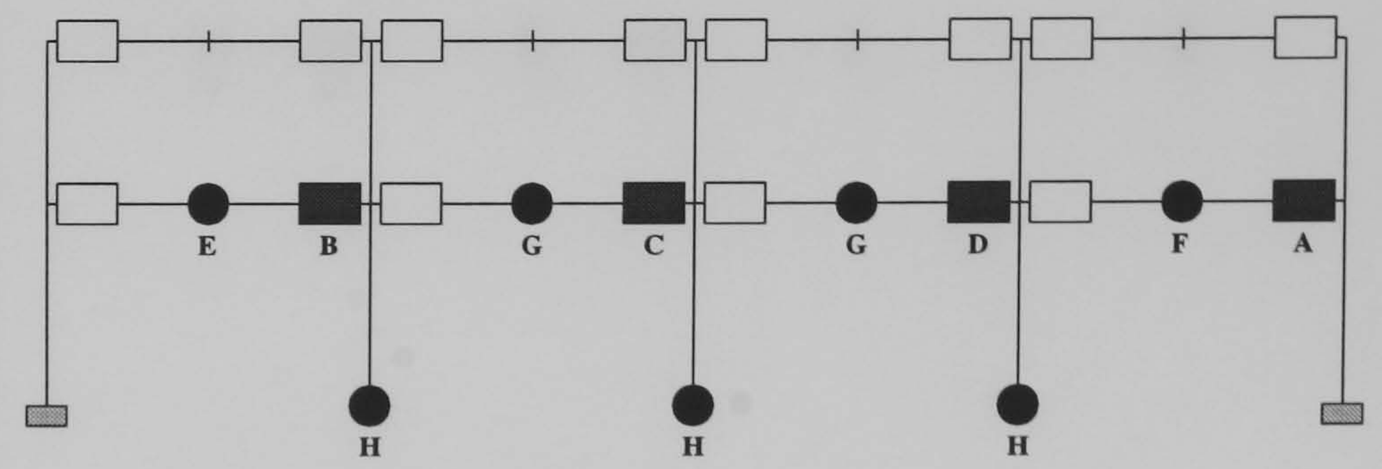

Rigid

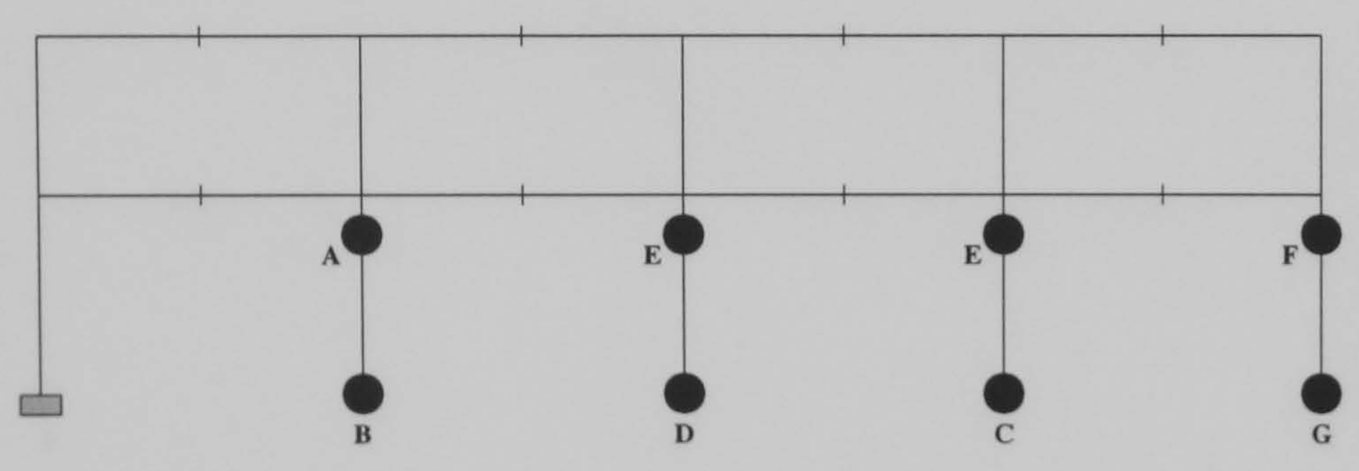

Hinge Location	Load Level at Hinge Formation S-R(1)	S-R(2)	Rigid
A	**0.9625**	**1.2625**	**1.755**
B	**0.9825**	**1.3875**	**1.775**
C	**0.985**	**1.3925**	**1.83**
D	**1.28**	**1.3975**	**1.852**
E	**1.422**	**1.427**	**1.87**
F	**1.455**	**1.447**	**1.89**
G	**N/A**	**1.45**	**1.897**
H	**N/A**	**1.472**	**N/A**

Key :

Semi-Rigid Connection

Plastification prior to ULS design load being attained

Plastification following the attainment of the design load

Member plastification

FRAME : **f17 b24**
Load Case 2

S-R (1) Negelecting web shear at the internal columns

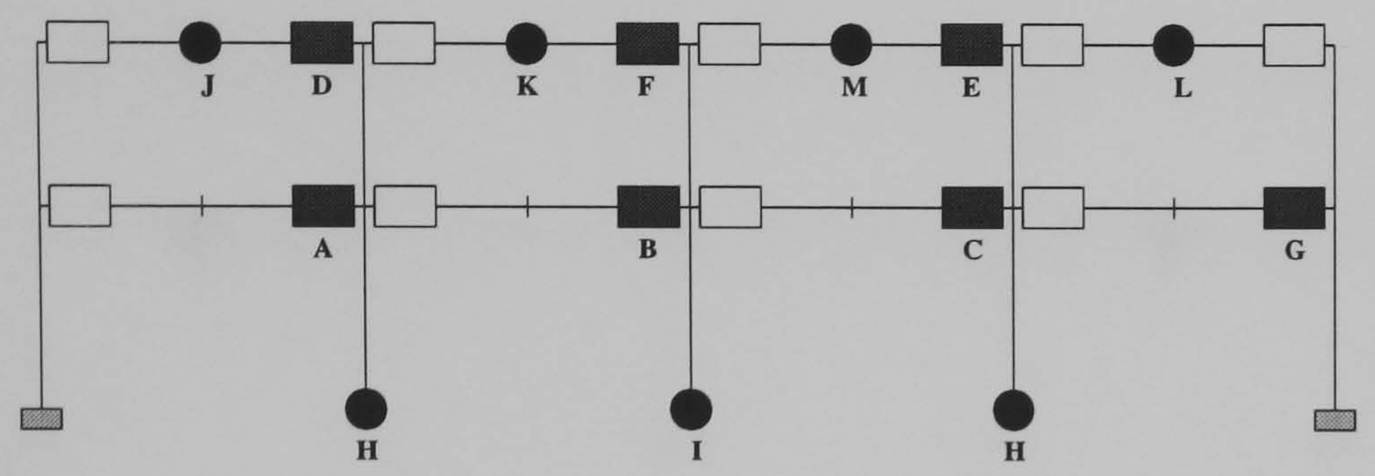

S-R (2) Including web shear at the internal columns

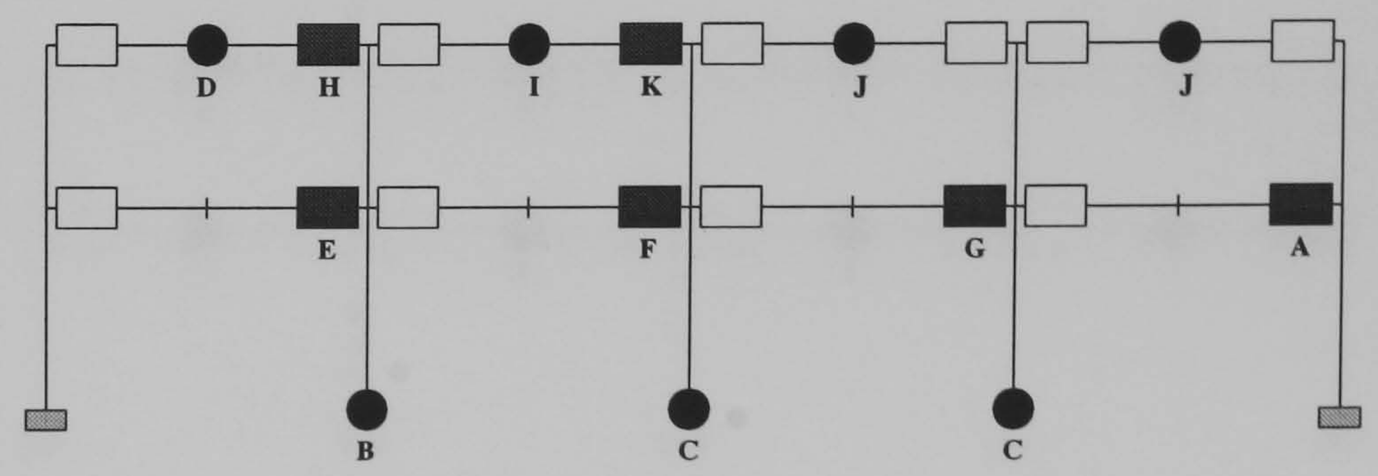

Rigid

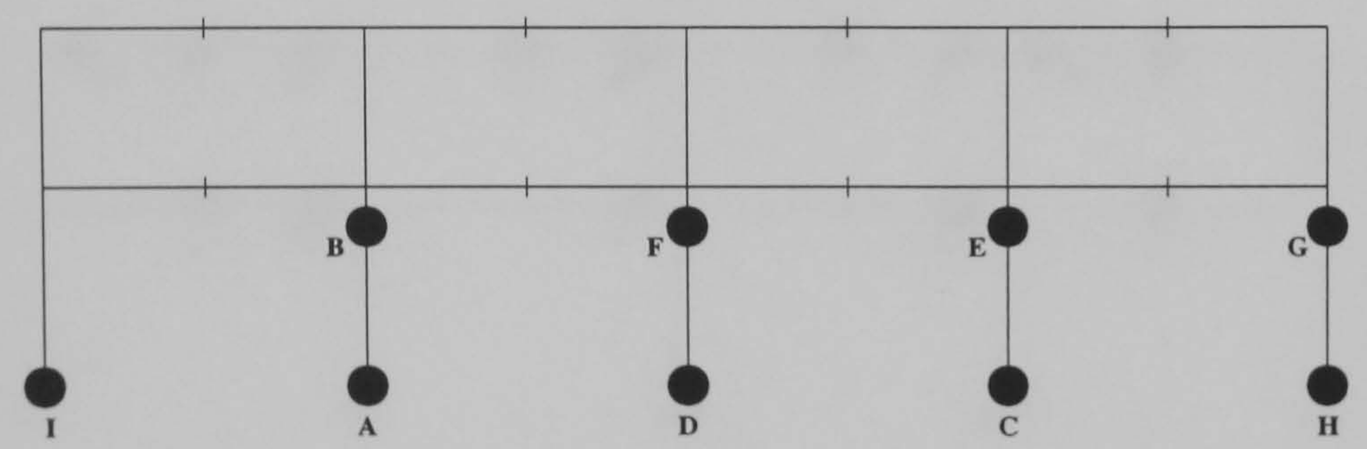

Hinge Location	Load Level at Hinge Formation S-R(1)	S-R(2)	Rigid
A	1.605	1.765	2.302
B	1.6325	2.082	2.315
C	1.6375	2.087	2.36
D	1.78	2.105	2.385
E	1.825	2.12	2.405
F	1.8375	2.13	2.42
G	1.87	2.1375	2.48
H	2.092	2.145	2.487
I	2.097	2.185	2.495
J	2.13	2.19	N/A
K	2.202	2.1925	N/A
L	2.205	N/A	N/A
M	2.207	N/A	N/A

Key :

- Semi-Rigid Connection
- Plastification prior to ULS design load being attained
- Plastification following the attainment of the design load
- Member plastification

FRAME : **f17 b24**
Load Case 3

S-R (1) Negelecting web shear at the internal columns

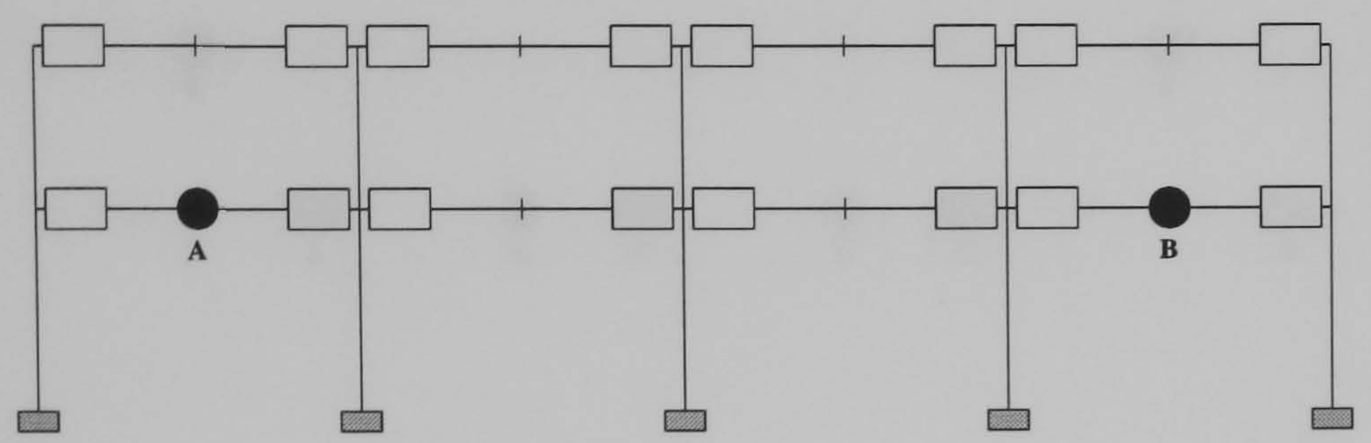

S-R (2) Including web shear at the internal columns

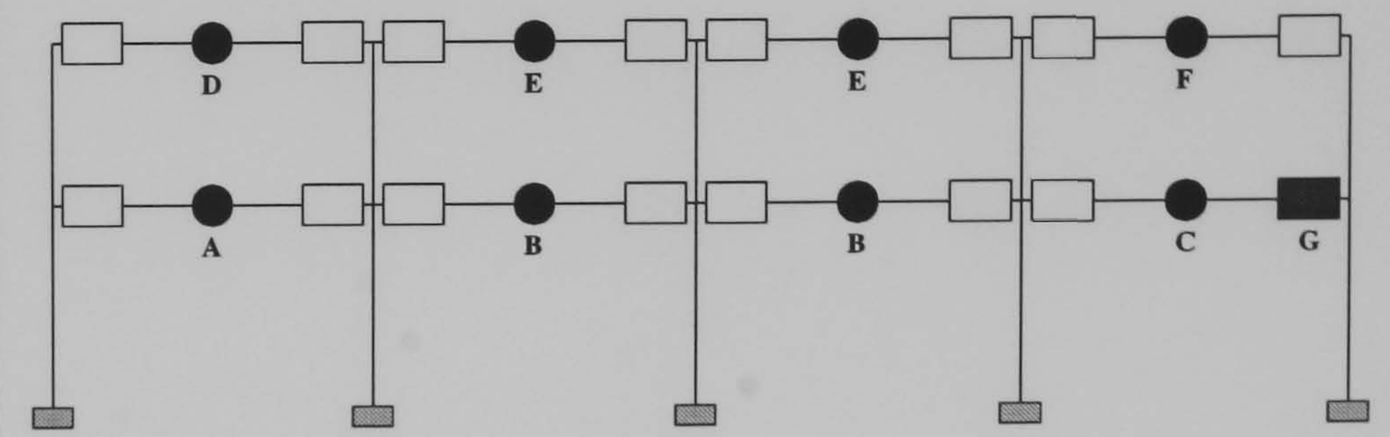

Rigid

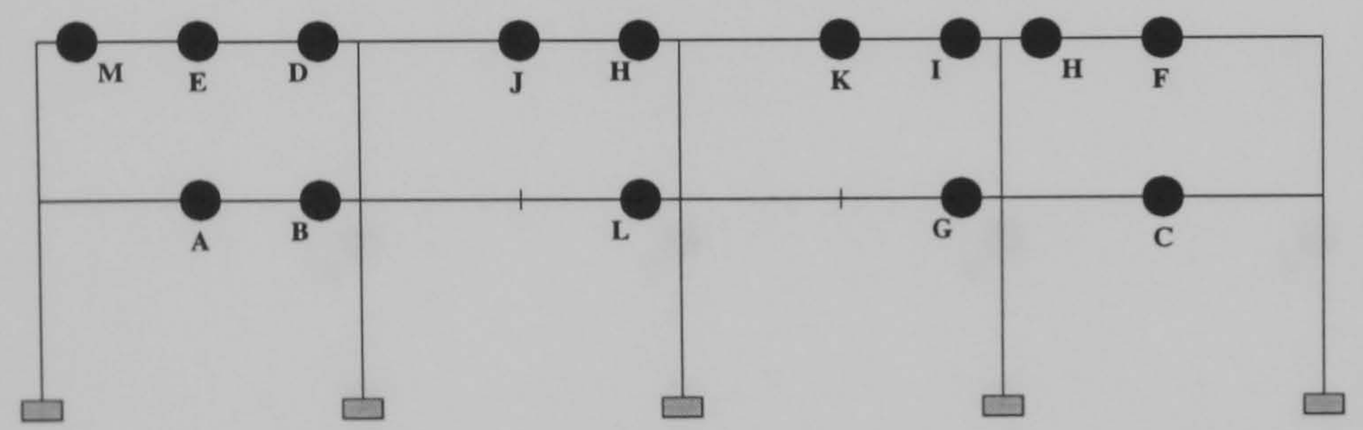

Hinge Location	Load Level at Hinge Formation S-R(1)	S-R(2)	Rigid
A	**1.27**	**1.232**	**1.832**
B	**1.275**	**1.242**	**1.837**
C	**N/A**	**1.245**	**1.855**
D	**N/A**	**1.255**	**1.857**
E	**N/A**	**1.262**	**1.875**
F	**N/A**	**1.265**	**1.877**
G	**N/A**	**1.305**	**1.907**
H	**N/A**	**N/A**	**1.932**
I	**N/A**	**N/A**	**1.935**
J	**N/A**	**N/A**	**1.98**
K	**N/A**	**N/A**	**1.985**
L	**N/A**	**N/A**	**2.0**
M	**N/A**	**N/A**	**2.025**

Key :

Semi-Rigid Connection

Plastification prior to ULS design load being attained

Plastification following the attainment of the design load

Member plastification

FRAME : **f18 b20**
Load Case 1

S-R (1) Negelecting web shear at the internal columns

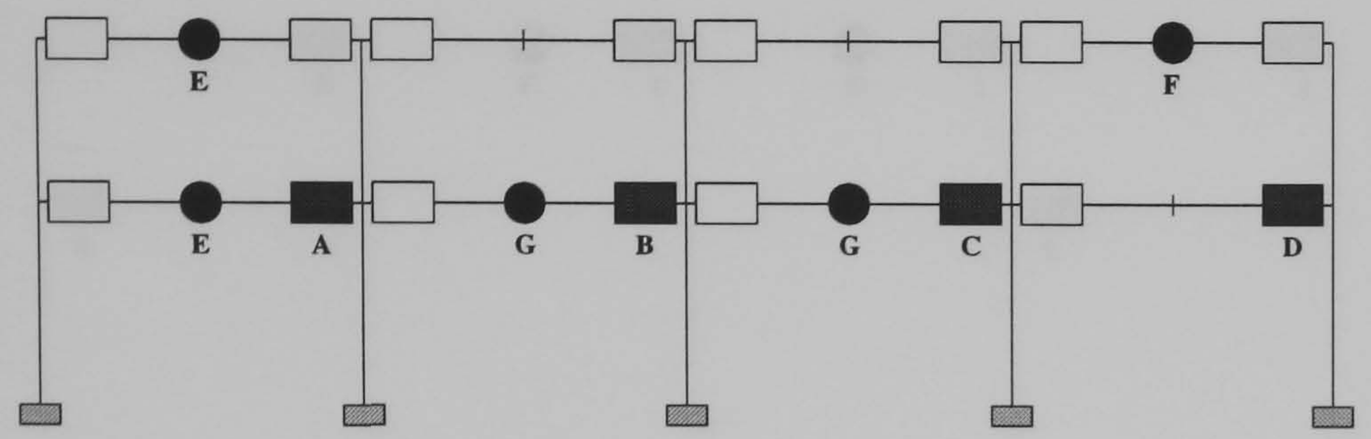

S-R (2) Including web shear at the internal columns

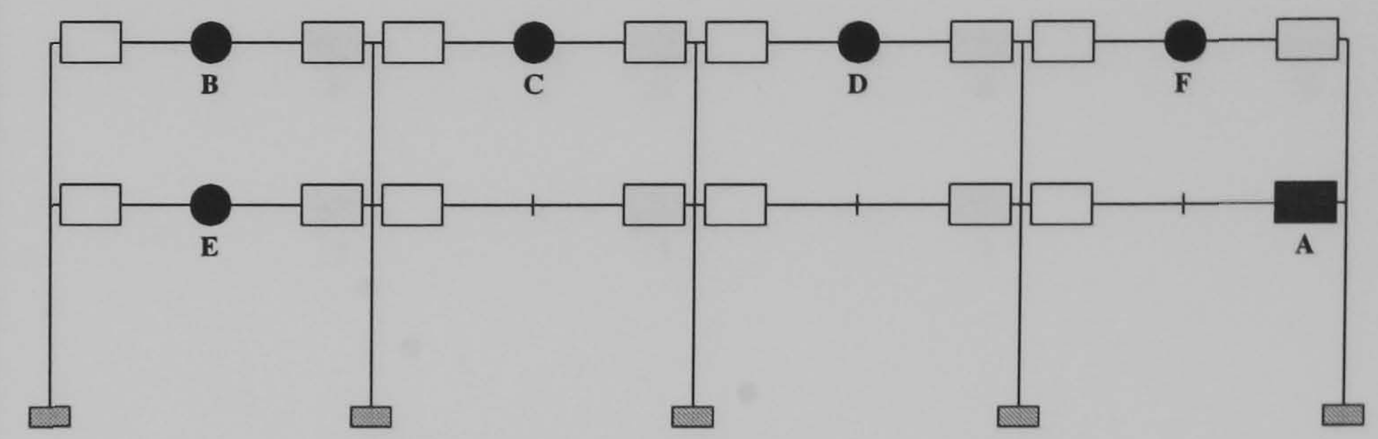

Rigid

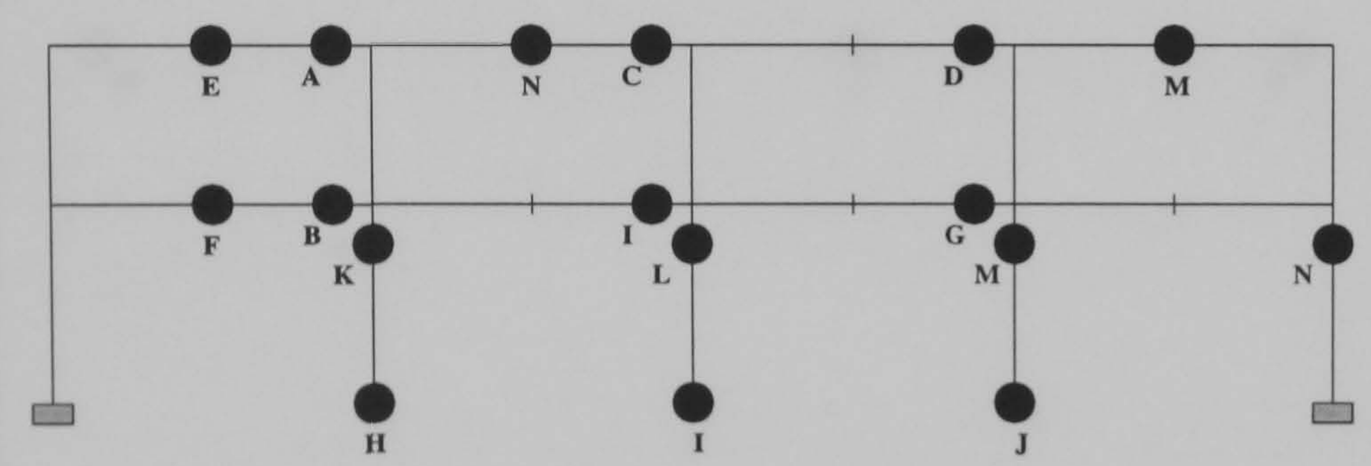

Hinge Location	Load Level at Hinge Formation S-R(1)	S-R(2)	Rigid
A	**1.2325**	**1.3575**	**1.992**
B	**1.2375**	**1.472**	**2.0**
C	**1.24**	**1.497**	**2.135**
D	**1.405**	**1.5**	**2.142**
E	**1.515**	**1.507**	**2.152**
F	**1.53**	**1.51**	**2.172**
G	**1.537**	**N/A**	**2.175**
H	**N/A**	**N/A**	**2.207**
I	**N/A**	**N/A**	**2.225**
J	**N/A**	**N/A**	**2.23**
K	**N/A**	**N/A**	**2.25**
L	**N/A**	**N/A**	**2.257**
M	**N/A**	**N/A**	**2.267**
N	**N/A**	**N/A**	**2.272**

Key :

Semi-Rigid Connection

Plastification prior to ULS design load being attained

Plastification following the attainment of the design load

Member plastification

FRAME : **f18 b20**

Load Case 2

S-R (1) Negelecting web shear at the internal columns

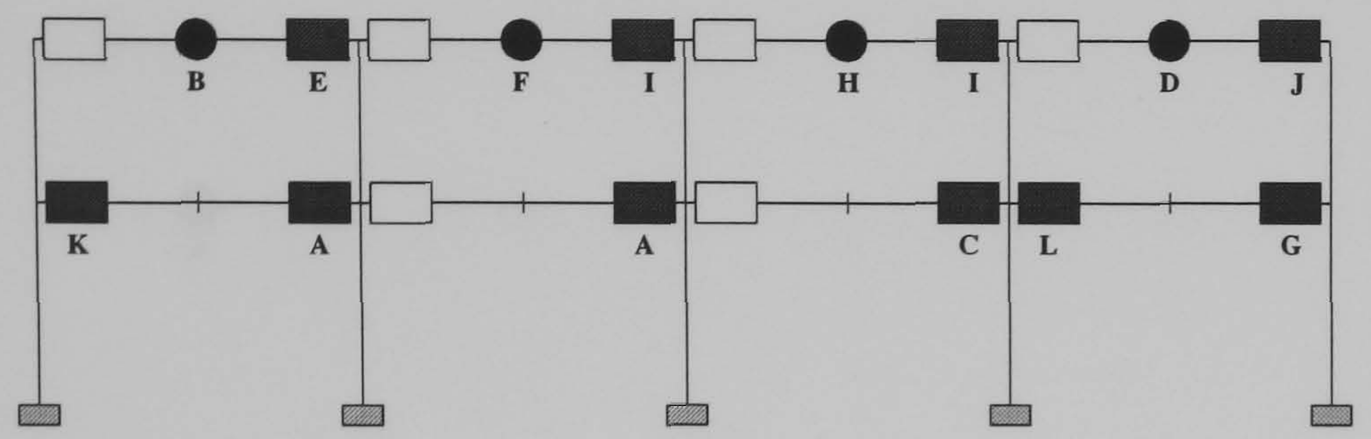

S-R (2) Including web shear at the internal columns

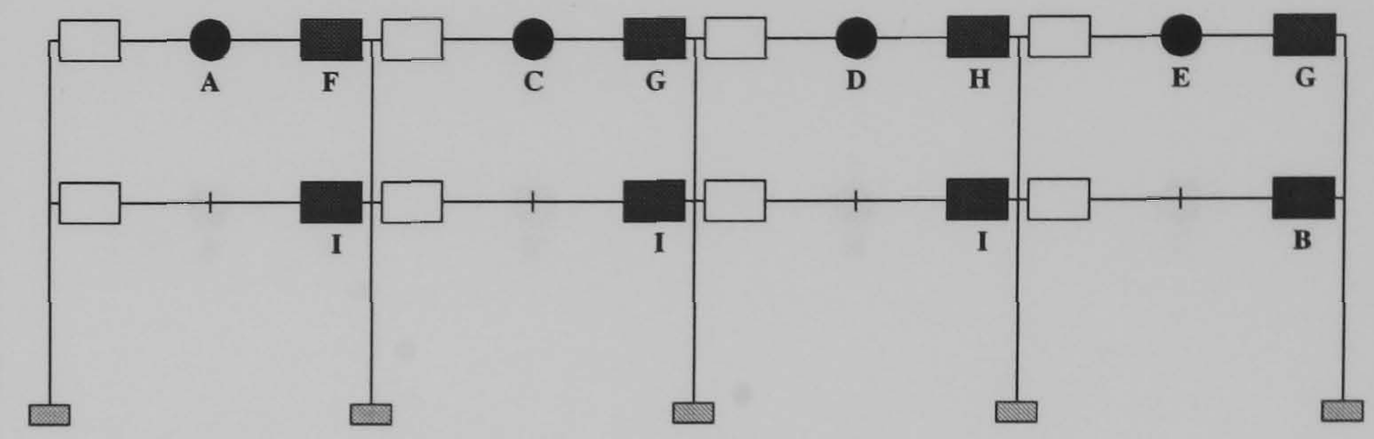

Rigid

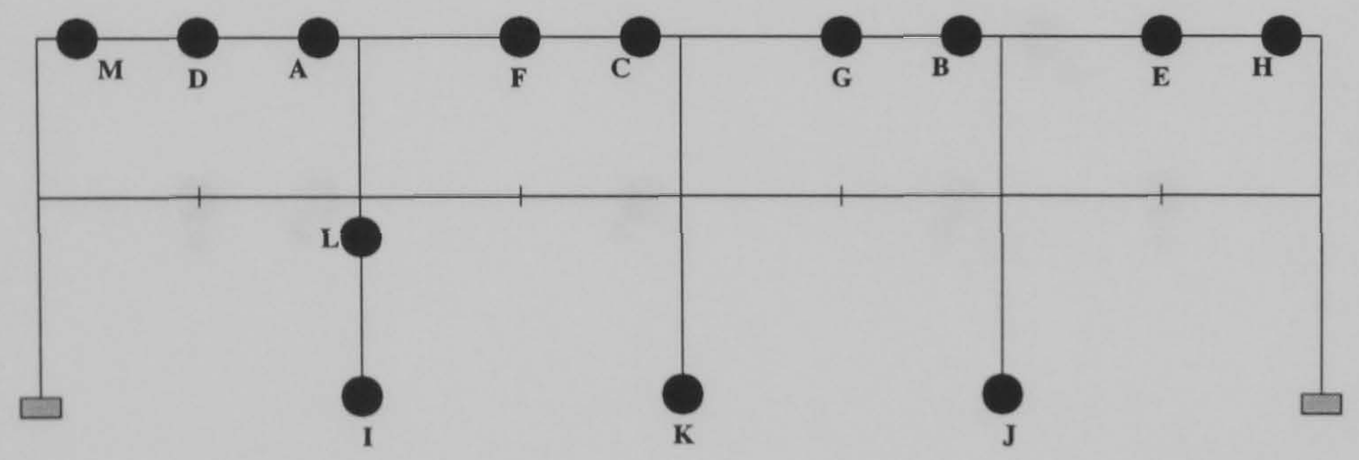

Hinge Location	Load Level at Hinge Formation S-R(1)	S-R(2)	Rigid
A	1.7975	1.742	2.237
B	1.805	1.76	2.43
C	1.8075	1.785	2.457
D	1.825	1.787	2.487
E	1.8475	1.802	2.665
F	1.862	1.86	2.685
G	1.8675	1.8875	2.707
H	1.87	1.8925	2.727
I	1.8825	1.95	2.745
J	1.9125	N/A	2.787
K	2.005	N/A	2.8
L	2.01	N/A	2.81
M	N/A	N/A	2.837

Key :

Semi-Rigid Connection

Plastification prior to ULS design load being attained

Plastification following the attainment of the design load

Member plastification

FRAME : **f18 b20**

Load Case 3

S-R (1) Negelecting web shear at the internal columns

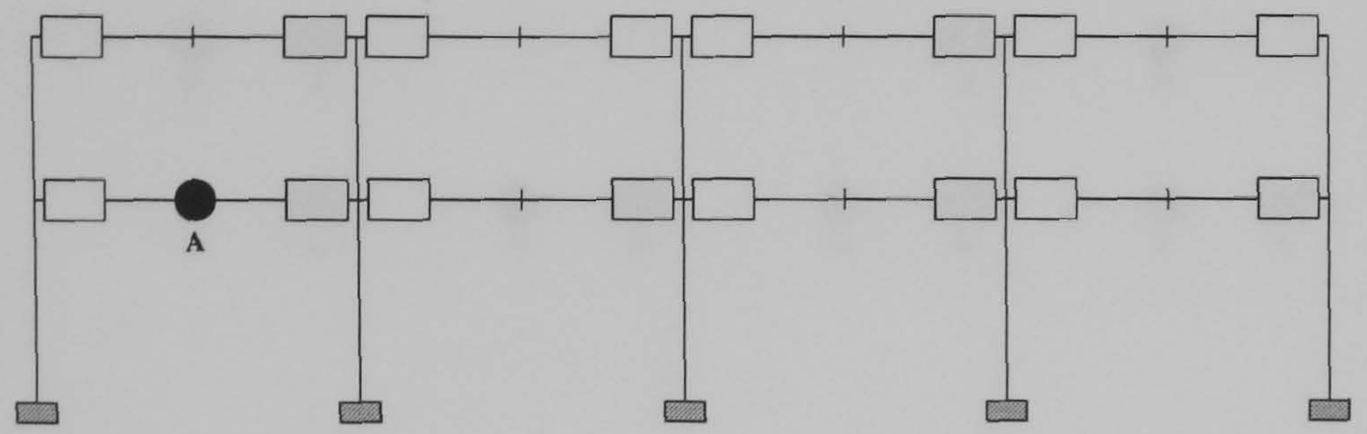

S-R (2) Including web shear at the internal columns

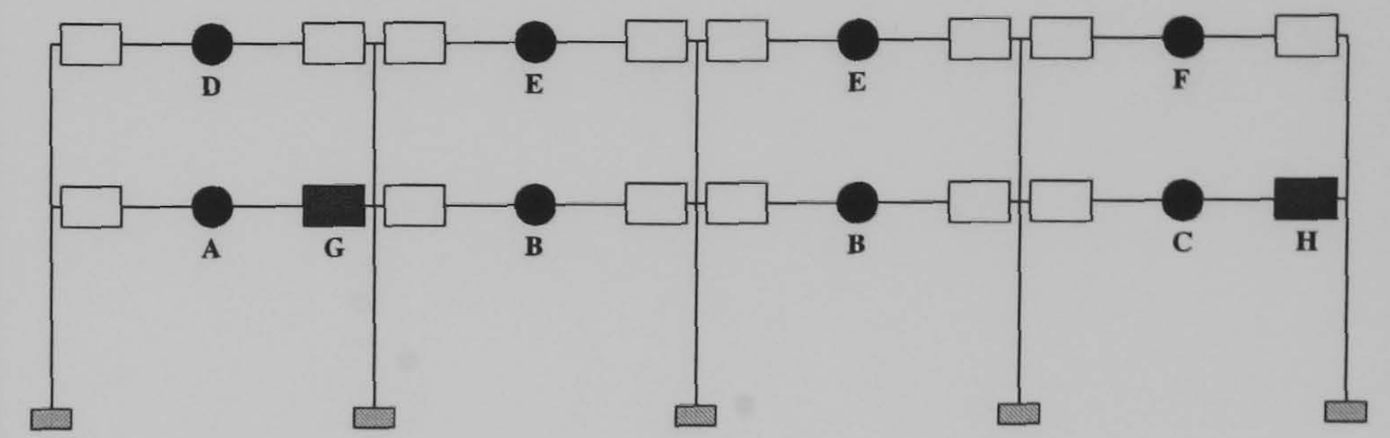

Rigid

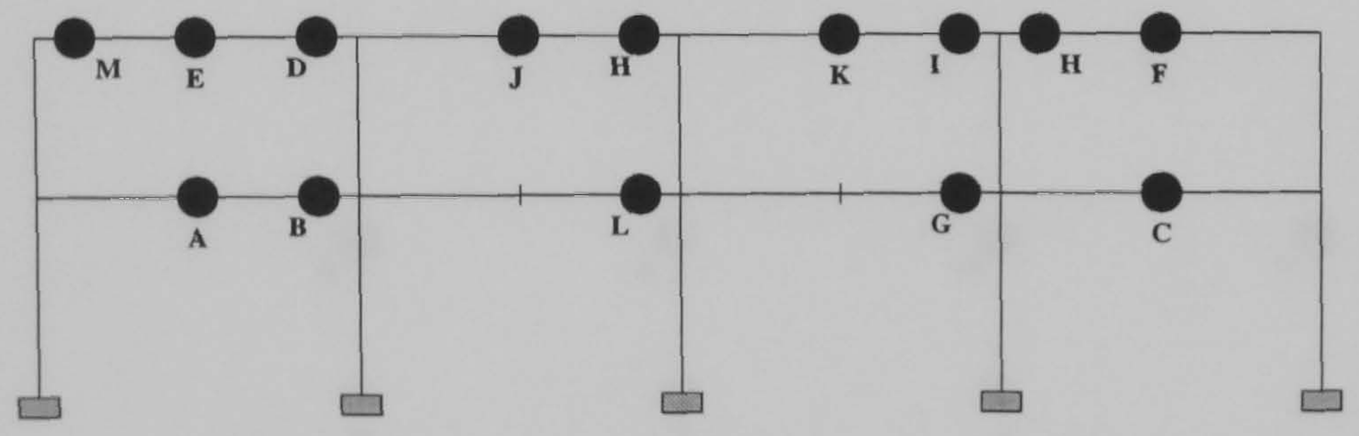

Hinge Location	Load Level at Hinge Formation S-R(1)	S-R(2)	Rigid
A	**1.315**	**1.26**	**1.832**
B	**N/A**	**1.272**	**1.837**
C	**N/A**	**1.277**	**1.855**
D	**N/A**	**1.307**	**1.857**
E	**N/A**	**1.312**	**1.875**
F	**N/A**	**1.32**	**1.877**
G	**N/A**	**1.365**	**1.907**
H	**N/A**	**1.3675**	**1.932**
I	**N/A**	**N/A**	**1.935**
J	**N/A**	**N/A**	**1.98**
K	**N/A**	**N/A**	**1.985**
L	**N/A**	**N/A**	**2.0**
M	**N/A**	**N/A**	**2.025**

Key :

Semi-Rigid Connection

Plastification prior to ULS design load being attained

Plastification following the attainment of the design load

Member plastification

FRAME : **f18 b24**

Load Case 1

S-R (1) Negelecting web shear at the internal columns

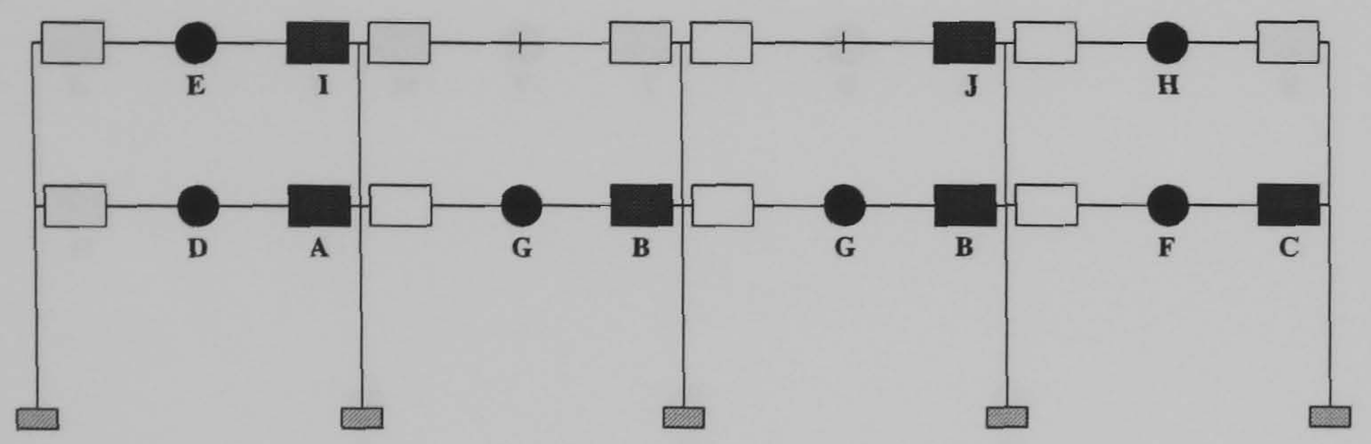

S-R (2) Including web shear at the internal columns

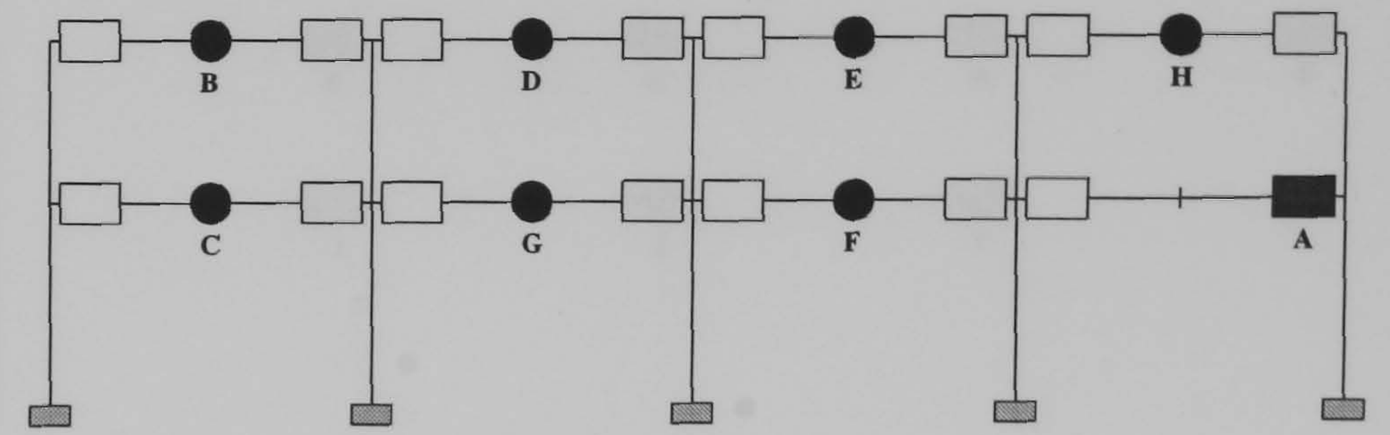

Rigid

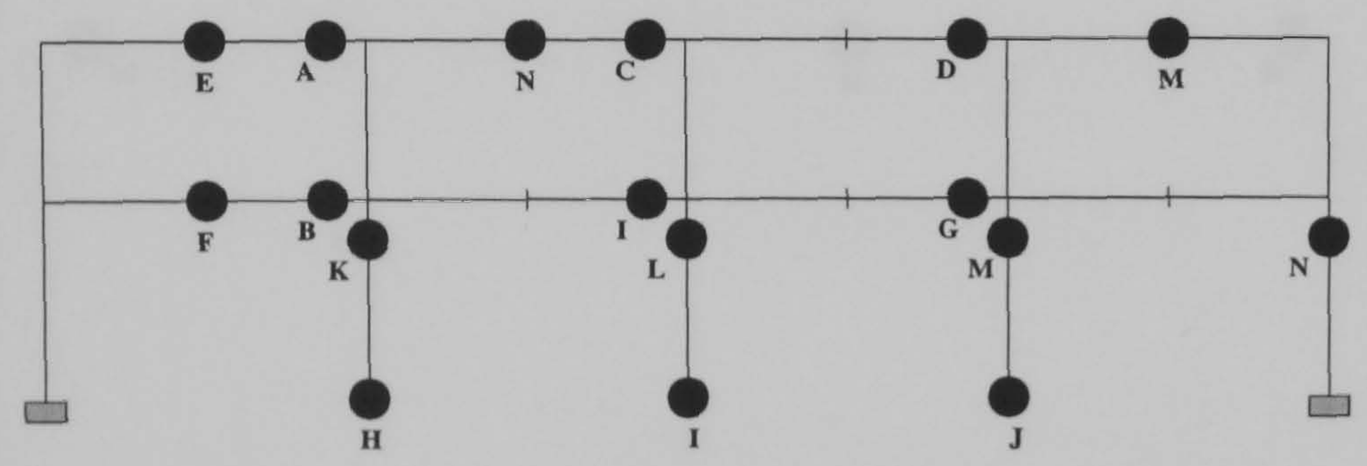

Hinge Location	Load Level at Hinge Formation S-R(1)	S-R(2)	Rigid
A	1.305	1.505	1.992
B	1.3225	1.53	2.0
C	1.5625	1.54	2.135
D	1.57	1.562	2.142
E	1.6	1.565	2.152
F	1.605	1.575	2.172
G	1.607	1.577	2.175
H	1.615	1.58	2.207
I	1.625	N/A	2.225
J	1.635	N/A	2.23
K	N/A	N/A	2.25
L	N/A	N/A	2.257
M	N/A	N/A	2.267
N	N/A	N/A	2.272

Key :

Semi-Rigid Connection

Plastification prior to ULS design load being attained

Plastification following the attainment of the design load

Member plastification

FRAME : **f18 b24**
Load Case 2

S-R (1) Negelecting web shear at the internal columns

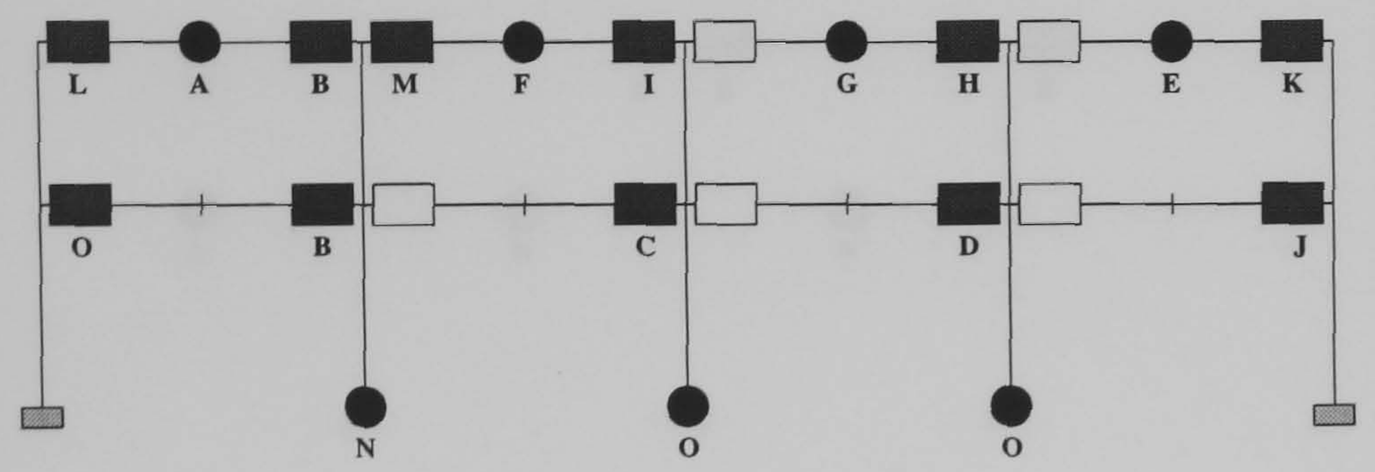

S-R (2) Including web shear at the internal columns

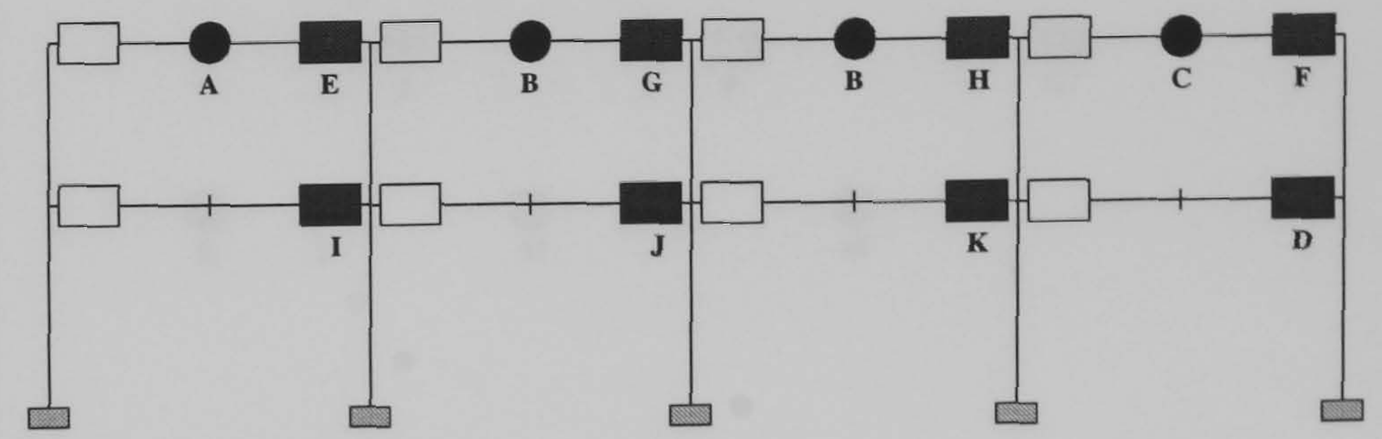

Rigid

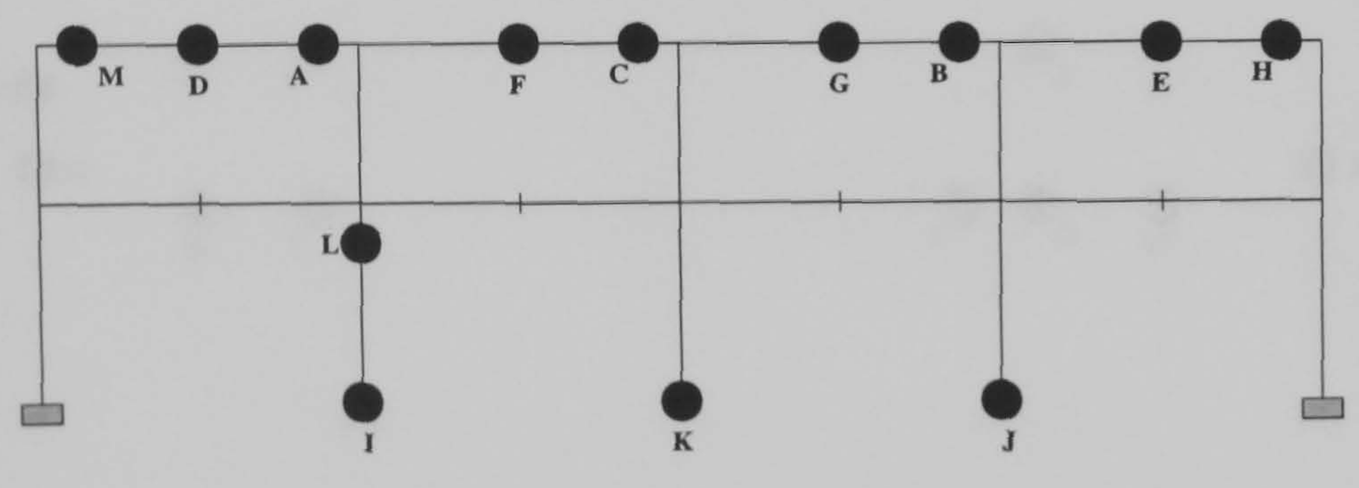

Hinge Location	Load Level at Hinge Formation S-R(1)	S-R(2)	Rigid
A	1.902	1.807	2.237
B	1.9625	1.865	2.43
C	1.9725	1.885	2.457
D	1.9875	1.95	2.487
E	1.922	1.99	2.665
F	1.99	2.0275	2.685
G	2.002	2.03	2.707
H	2.0175	2.035	2.727
I	2.02	2.1325	2.745
J	2.045	2.135	2.787
K	2.065	2.1375	2.8
L	2.1675	N/A	2.81
M	2.2	N/A	2.837
N	2.217	N/A	N/A
O	2.22	N/A	N/A

Key :

- Plastification prior to ULS design load being attained
- Semi-Rigid Connection
- Plastification following the attainment of the design load
- Member plastification

FRAME : **f18 b24**
Load Case 3

S-R (1) Negelecting web shear at the internal columns

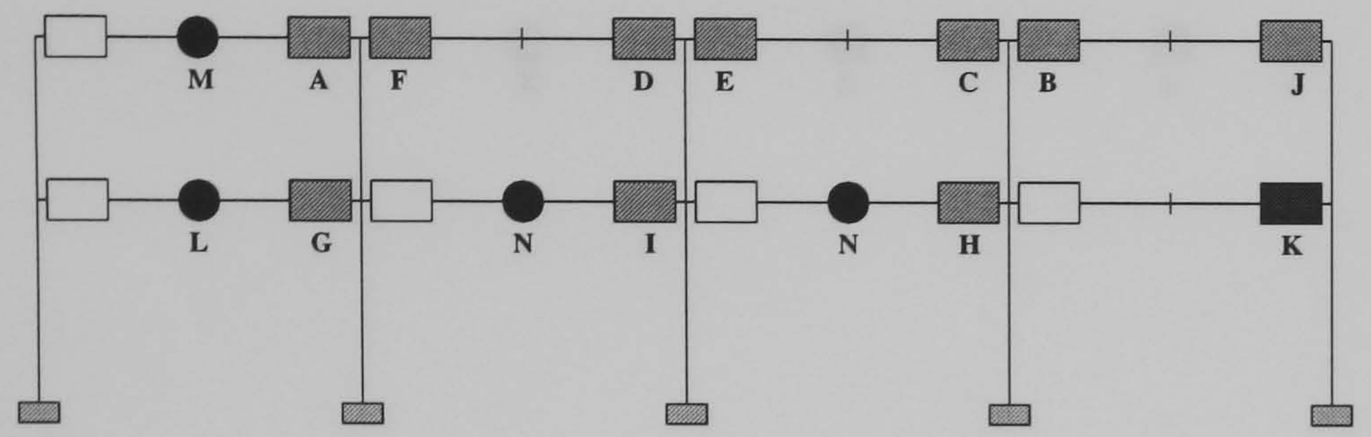

S-R (2) Including web shear at the internal columns

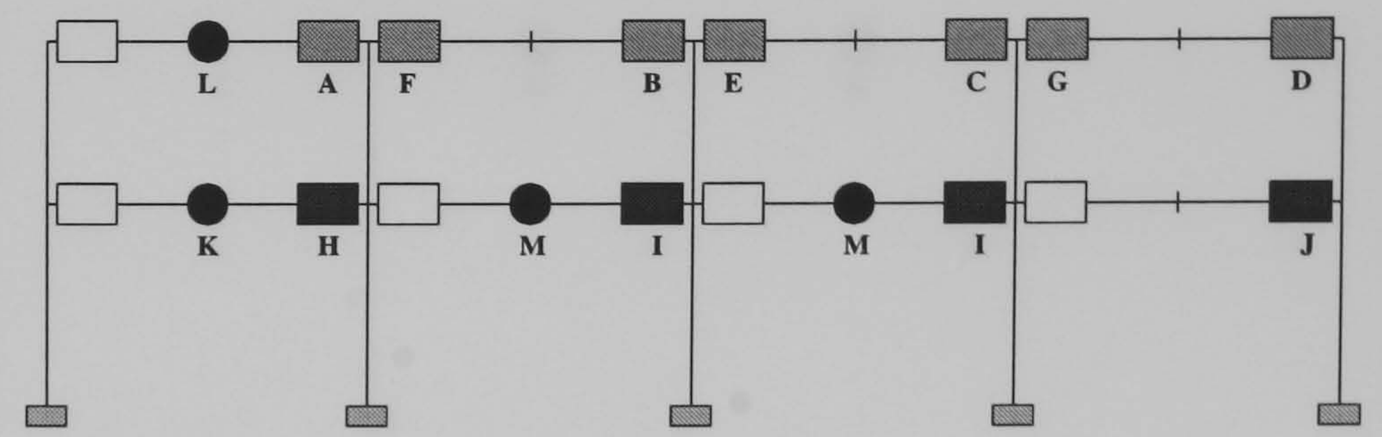

Rigid

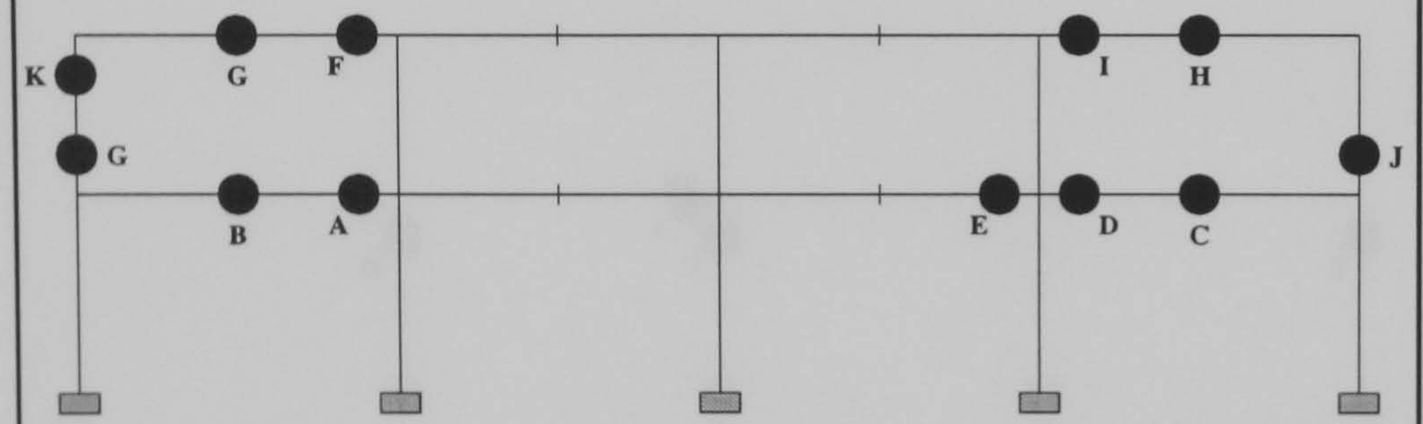

Hinge Location	Load Level at Hinge Formation S-R(1)	S-R(2)	Rigid
A	0.62	0.8225	1.73
B	0.64	0.8325	1.767
C	0.6425	0.835	1.792
D	0.6475	0.8875	1.827
E	0.7075	0.9325	1.845
F	0.7225	0.955	1.867
G	0.7975	0.97	1.892
H	0.8225	1.0975	1.895
I	0.835	1.1125	1.92
J	0.89	1.1525	1.925
K	1.1075	1.247	1.937
L	1.235	1.265	N/A
M	1.252	1.267	N/A
N	1.265	N/A	N/A

Key :

Semi-Rigid Connection

Plastification prior to ULS design load being attained

Plastification following the attainment of the design load

Member plastification

FRAME : **f19 b20**

Load Case 1

S-R (1) Negelecting web shear at the internal columns

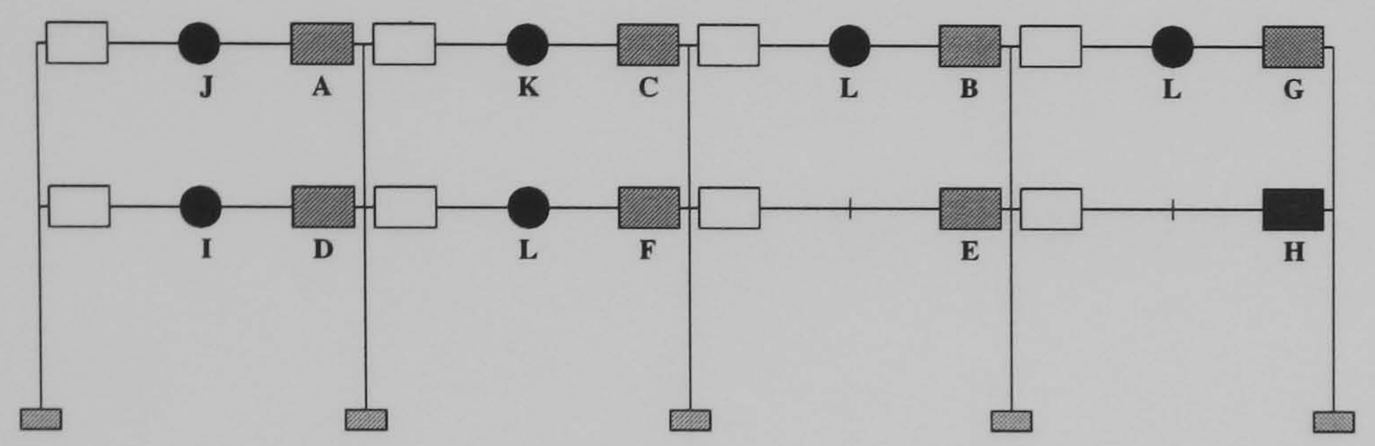

S-R (2) Including web shear at the internal columns

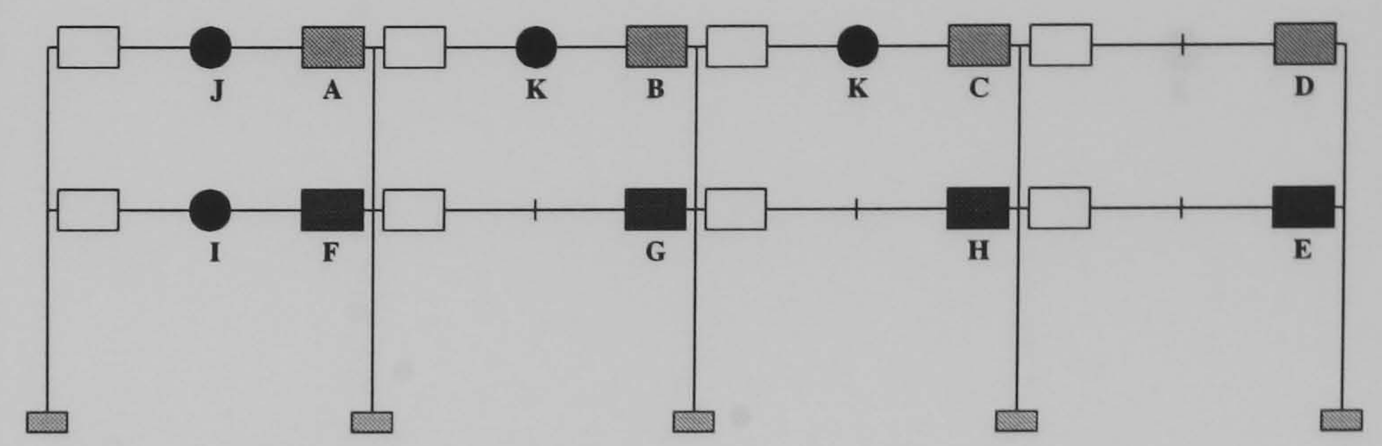

Rigid

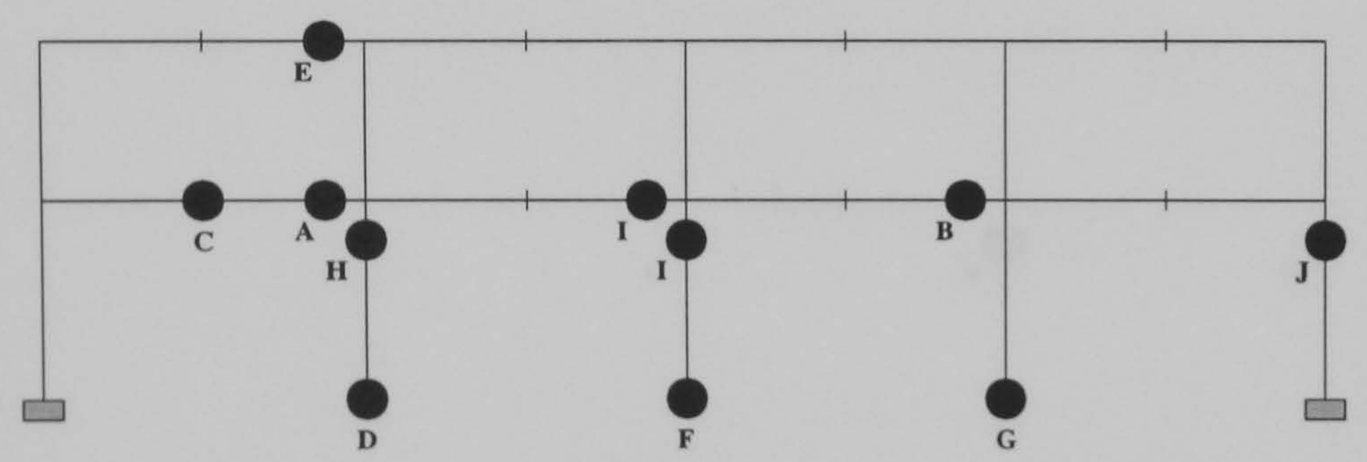

Hinge Location	Load Level at Hinge Formation		
	S-R(1)	S-R(2)	Rigid
A	0.6775	0.8725	1.907
B	0.7	0.885	2.077
C	0.705	0.89	2.11
D	0.8325	0.91	2.115
E	0.8575	1.0875	2.117
F	0.865	1.1	2.137
G	0.915	1.1175	2.142
H	1.0725	1.12	2.152
I	1.457	1.46	2.157
J	1.462	1.465	2.16
K	1.48	1.48	N/A
L	1.482	N/A	N/A

Key :

Semi-Rigid Connection

Plastification prior to ULS design load being attained

Plastification following the attainment of the design load

Member plastification

FRAME : **f19 b20**

Load Case 2

S-R (1) Negelecting web shear at the internal columns

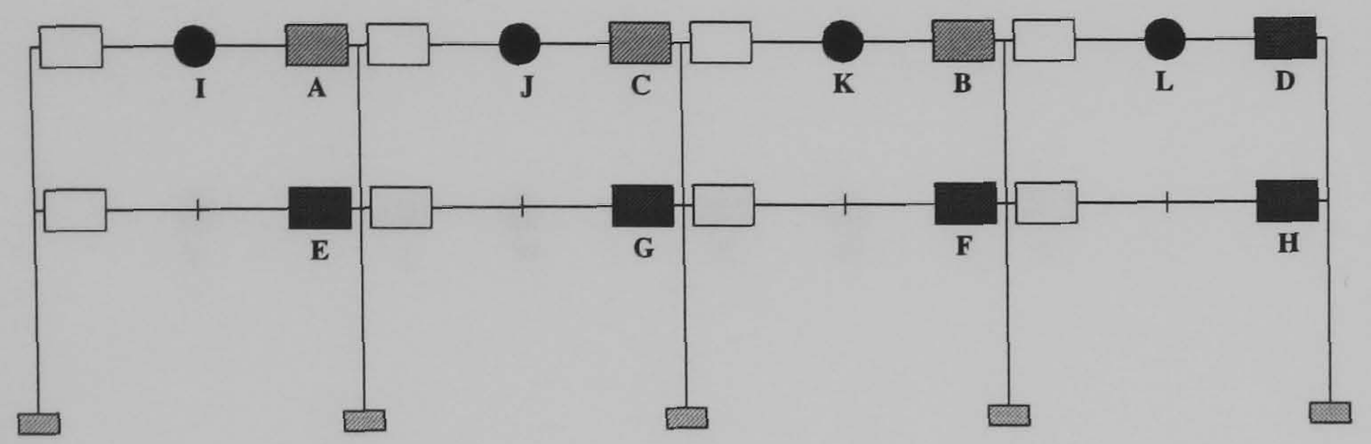

S-R (2) Including web shear at the internal columns

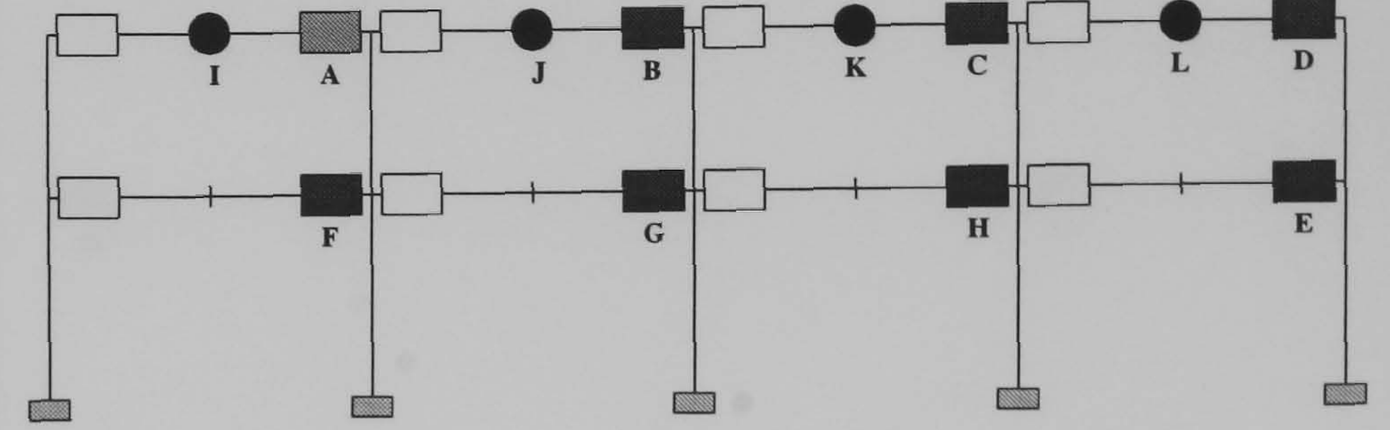

Rigid

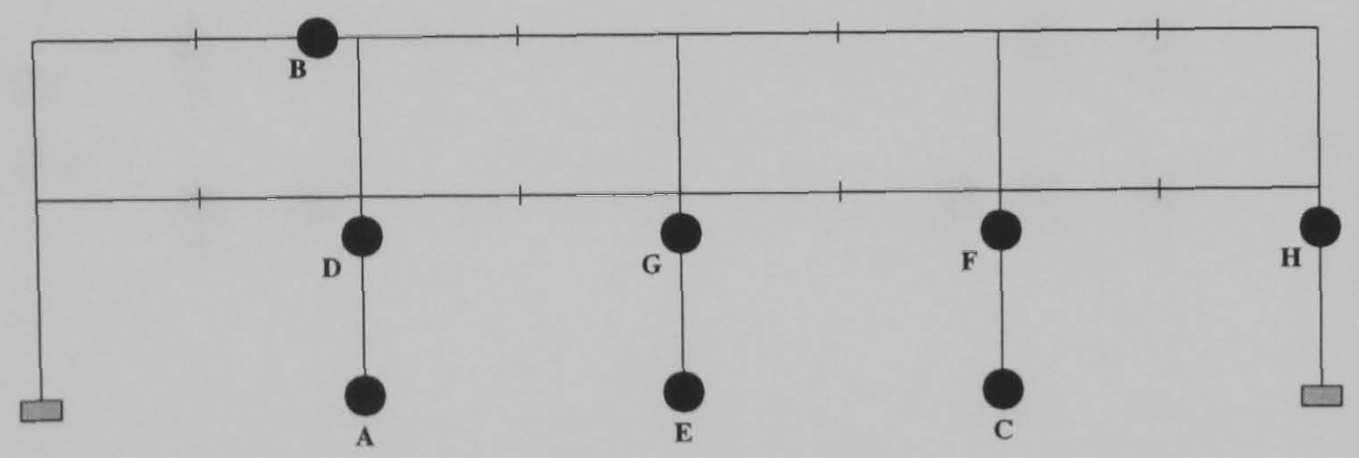

Hinge Location	Load Level at Hinge Formation S-R(1)	S-R(2)	Rigid
A	0.78	0.9925	2.395
B	0.805	1.015	2.445
C	0.8125	1.0175	2.452
D	1.0875	1.06	2.467
E	1.21	1.395	2.472
F	1.2375	1.515	2.52
G	1.2425	1.535	2.525
H	1.42	1.54	2.555
I	1.745	1.742	N/A
J	1.77	1.765	N/A
K	1.772	1.767	N/A
L	1.775	1.77	N/A

Key :

- Plastification prior to ULS design load being attained
- Semi-Rigid Connection
- Plastification following the attainment of the design load
- Member plastification

FRAME : **f19 b20**
Load Case 3

S-R (1) Negelecting web shear at the internal columns

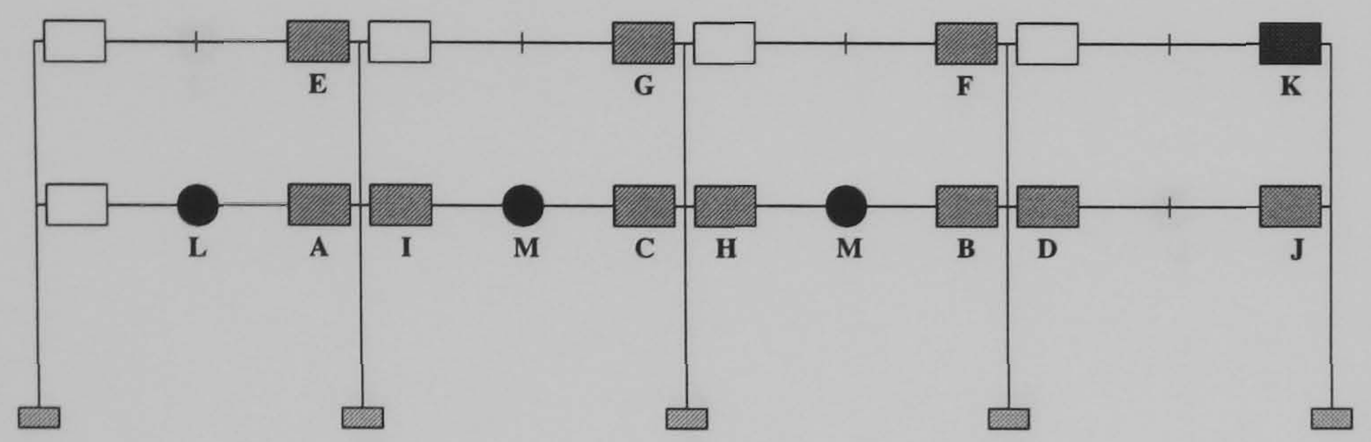

S-R (2) Including web shear at the internal columns

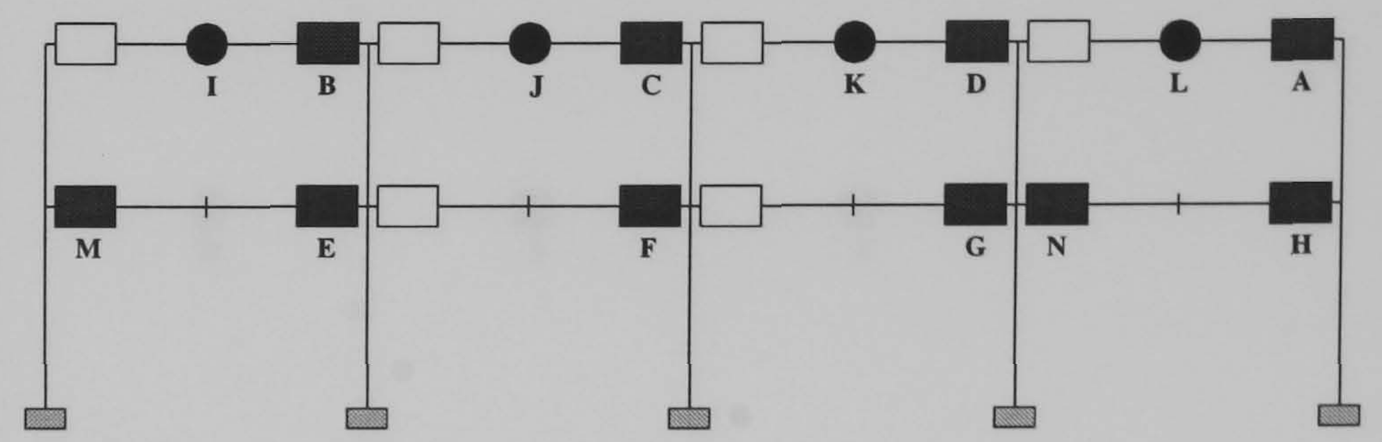

Rigid

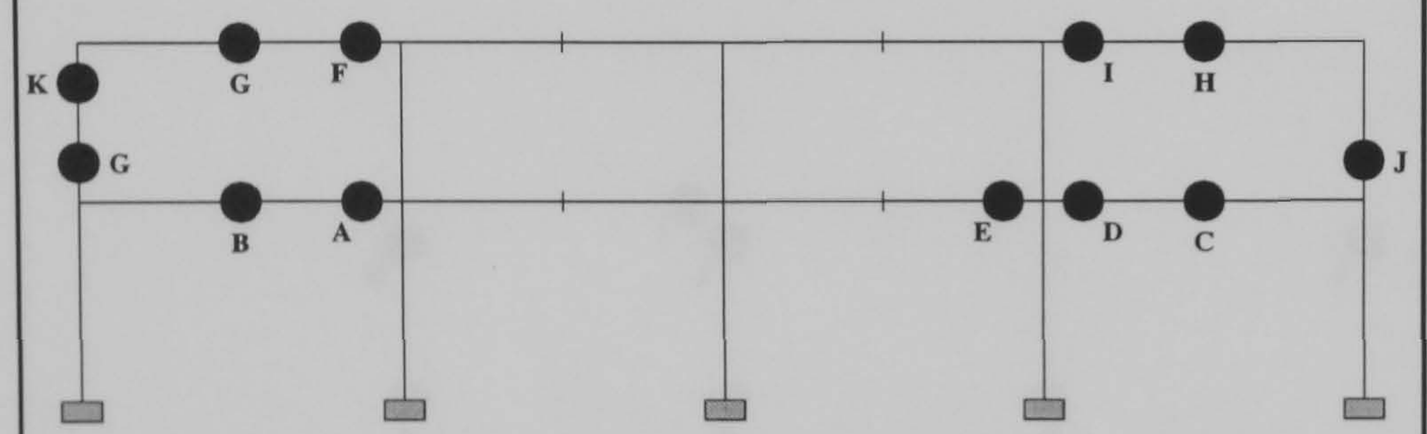

Hinge Location	Load Level at Hinge Formation S-R(1)	S-R(2)	Rigid
A	0.615	1.1875	1.73
B	0.6425	1.2625	1.767
C	0.655	1.2975	1.792
D	0.6575	1.3	1.827
E	0.7225	1.3475	1.845
F	0.755	1.365	1.867
G	0.77	1.37	1.892
H	0.8	1.39	1.895
I	0.8075	1.805	1.92
J	0.9275	1.847	1.925
K	1.0575	1.85	1.937
L	1.215	1.852	N/A
M	1.267	1.88	N/A
N	N/A	1.8825	N/A

Key :

Semi-Rigid Connection

Plastification prior to ULS design load being attained

Plastification following the attainment of the design load

Member plastification

FRAME : **f19 b24**
Load Case 1

S-R (1) Negelecting web shear at the internal columns

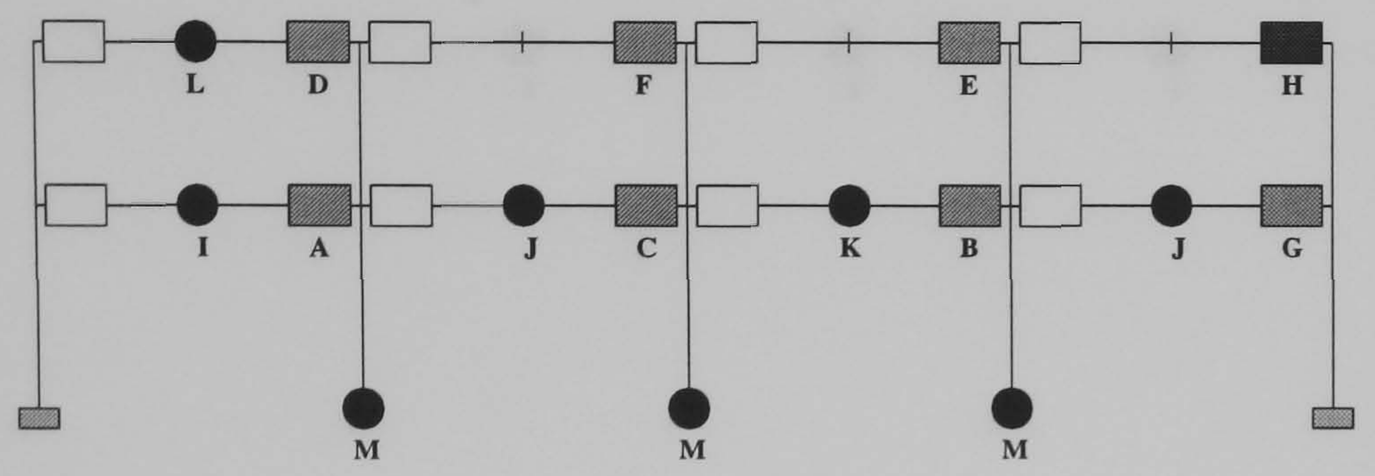

S-R (2) Including web shear at the internal columns

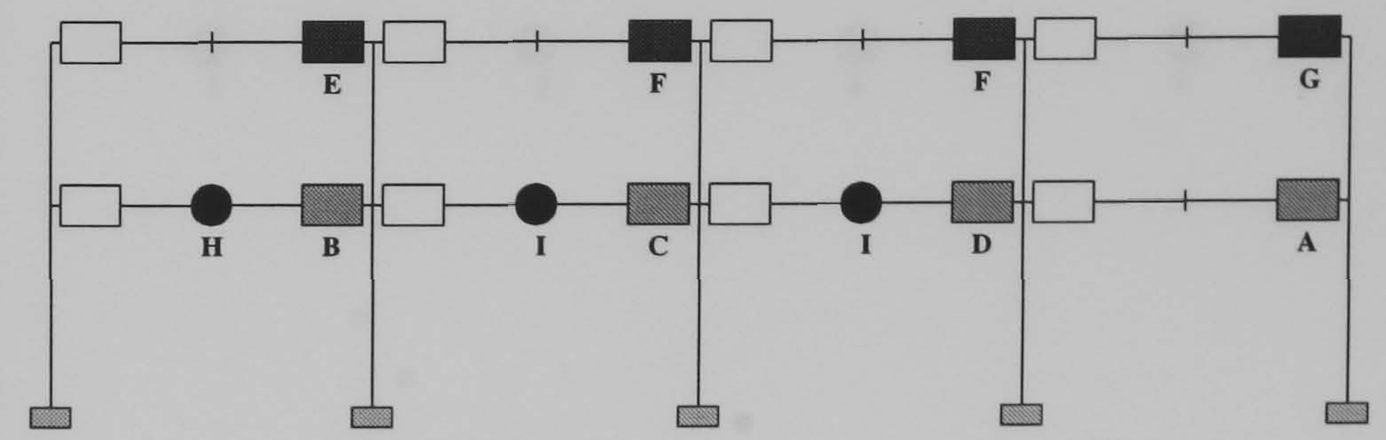

Rigid

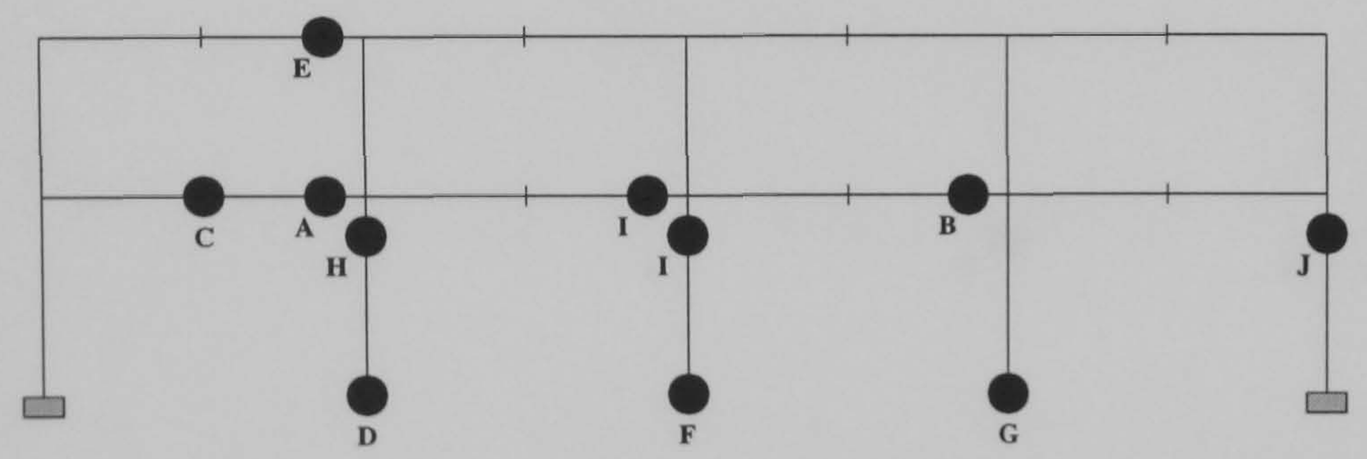

Hinge Location	Load Level at Hinge Formation		
	S-R(1)	S-R(2)	Rigid
A	**0.655**	**0.9125**	**1.907**
B	**0.6825**	**0.95**	**2.077**
C	**0.69**	**0.965**	**2.11**
D	**0.7975**	**0.9675**	**2.115**
E	**0.83**	**1.0825**	**2.117**
F	**0.845**	**1.1075**	**2.137**
G	**0.9125**	**1.16**	**2.142**
H	**1.125**	**1.445**	**2.152**
I	**1.44**	**1.465**	**2.157**
J	**1.462**	**N/A**	**2.16**
K	**1.465**	**N/A**	**N/A**
L	**1.487**	**N/A**	**N/A**
M	**1.492**	**N/A**	**N/A**

Key :

- Semi-Rigid Connection
- Plastification prior to ULS design load being attained
- Plastification following the attainment of the design load
- Member plastification

FRAME : **f19 b24**
Load Case 2

S-R (1) Negelecting web shear at the internal columns

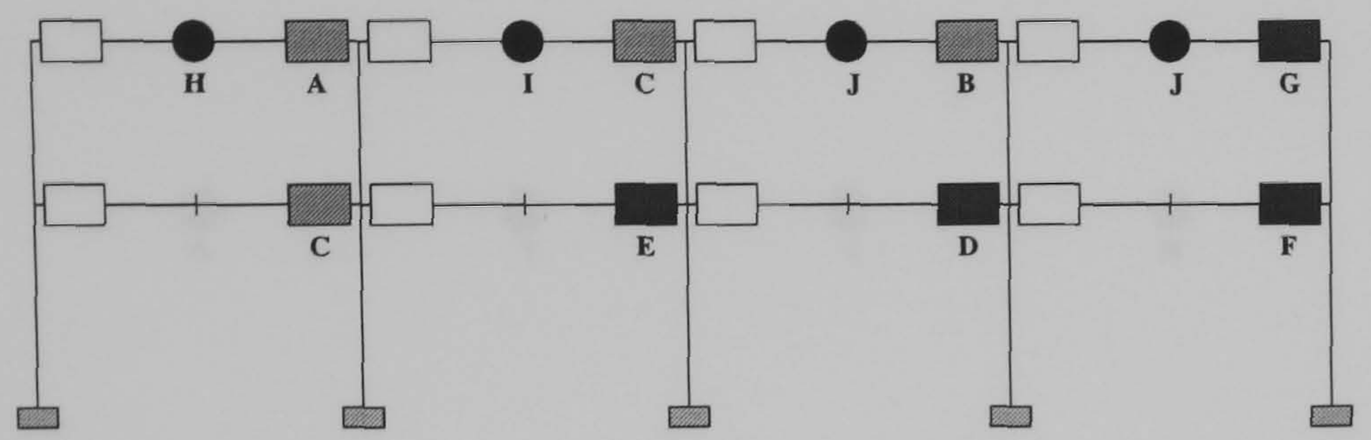

S-R (2) Including web shear at the internal columns

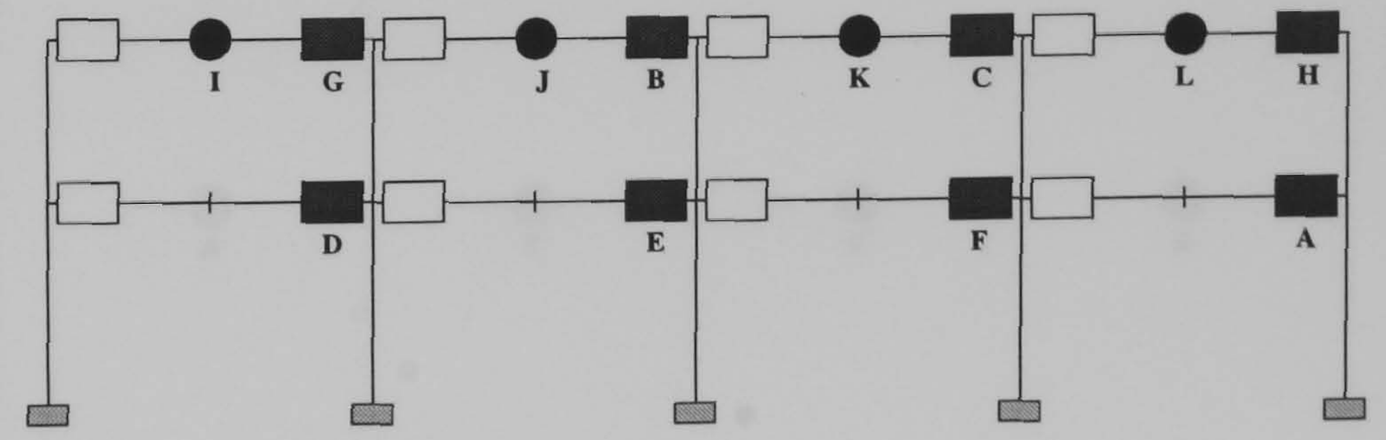

Rigid

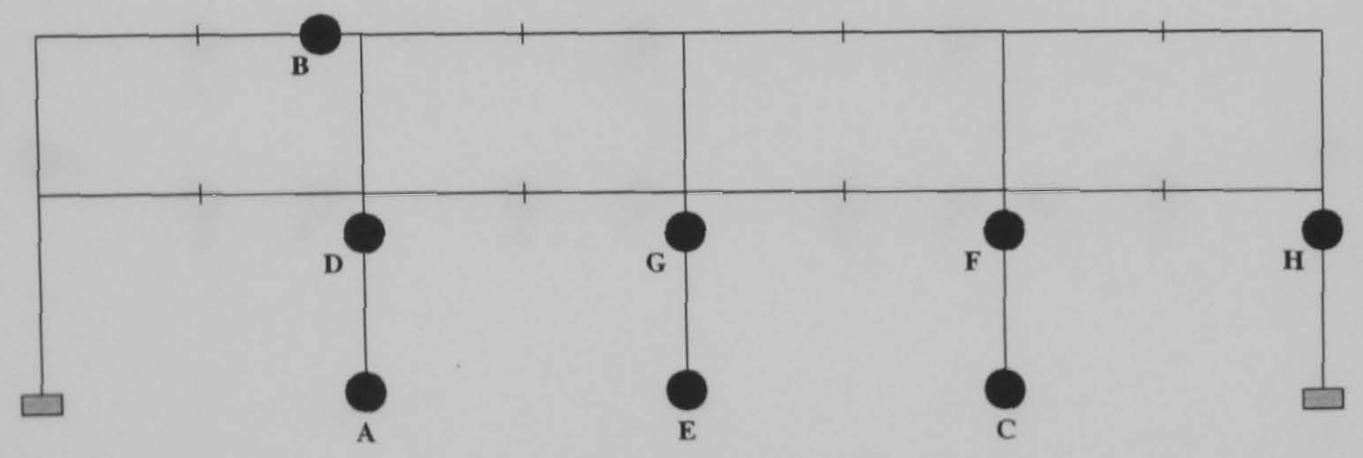

Hinge Location	Load Level at Hinge Formation S-R(1)	S-R(2)	Rigid
A	0.9325	1.2125	2.395
B	0.9725	1.2625	2.445
C	0.9925	1.3275	2.452
D	1.02	1.3425	2.467
E	1.025	1.385	2.472
F	1.2125	1.395	2.52
G	1.3675	1.4325	2.525
H	1.807	1.44	2.555
I	1.857	1.815	N/A
J	1.86	1.82	N/A
K	N/A	1.845	N/A
L	N/A	1.847	N/A

Key :

- Semi-Rigid Connection
- Plastification prior to ULS design load being attained
- Plastification following the attainment of the design load
- Member plastification

FRAME : **f19 b24**
Load Case 3

S-R (1) Negelecting web shear at the internal columns

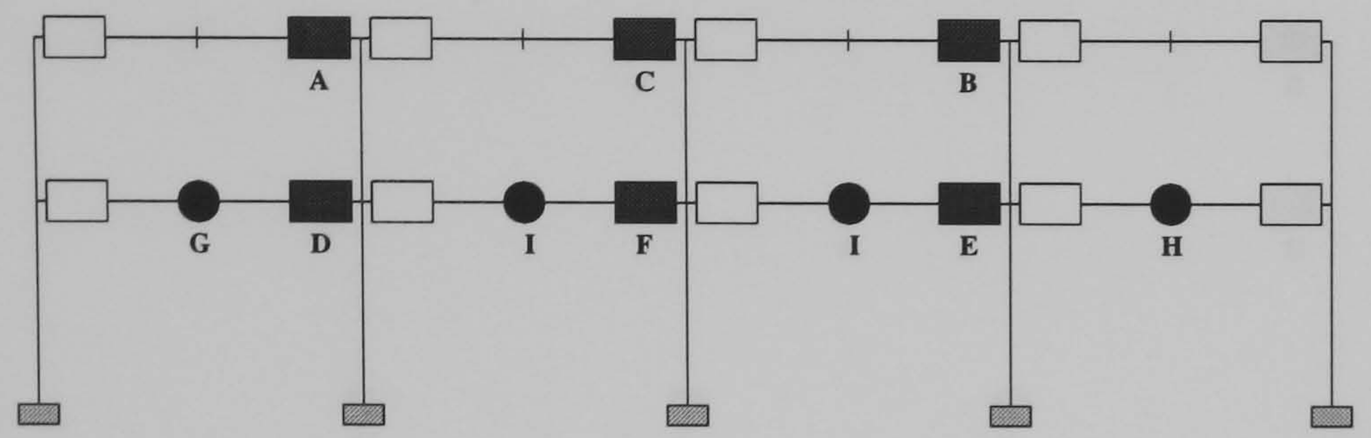

S-R (2) Including web shear at the internal columns

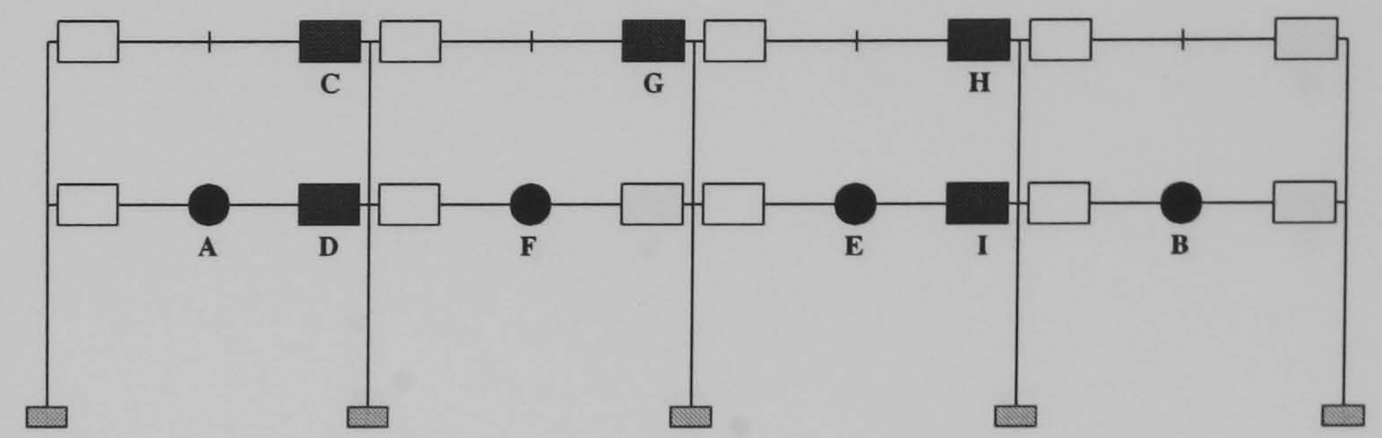

Rigid

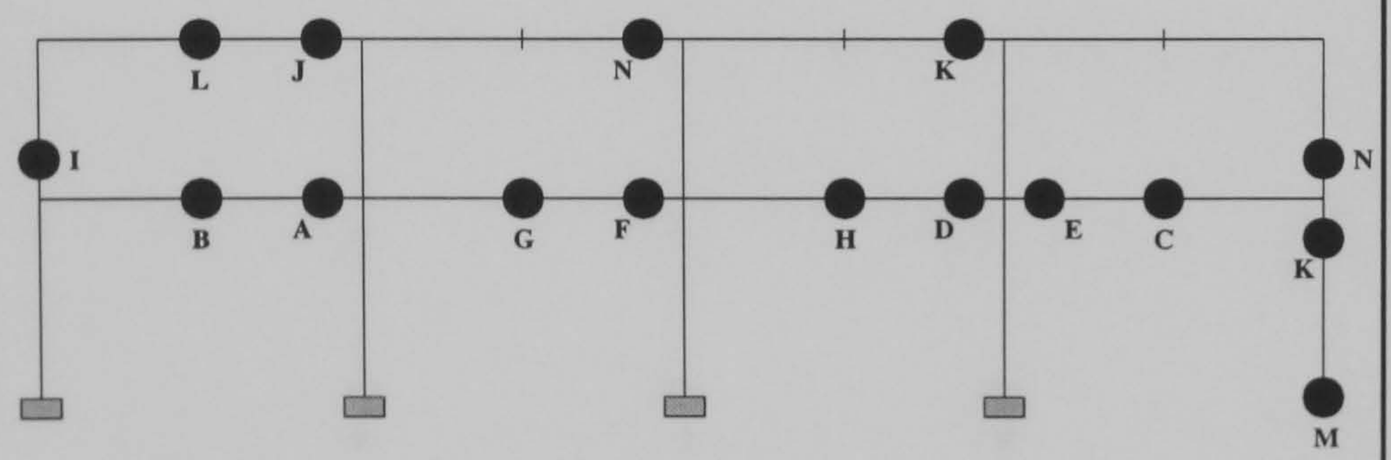

Hinge Location	Load Level at Hinge Formation S-R(1)	S-R(2)	Rigid
A	**1.085**	**1.277**	**1.655**
B	**1.135**	**1.29**	**1.722**
C	**1.15**	**1.335**	**1.76**
D	**1.19**	**1.34**	**1.78**
E	**1.24**	**1.342**	**1.817**
F	**1.26**	**1.345**	**1.872**
G	**1.31**	**1.3625**	**1.962**
H	**1.327**	**1.37**	**1.967**
I	**1.38**	**1.38**	**1.985**
J	**N/A**	**N/A**	**1.99**
K	**N/A**	**N/A**	**2.02**
L	**N/A**	**N/A**	**2.025**
M	**N/A**	**N/A**	**2.027**
N	**N/A**	**N/A**	**2.03**

Key :

Semi-Rigid Connection

Plastification prior to ULS design load being attained

Plastification following the attainment of the design load

Member plastification

FRAME : **f20 b20**

Load Case 1

S-R (1) Negelecting web shear at the internal columns

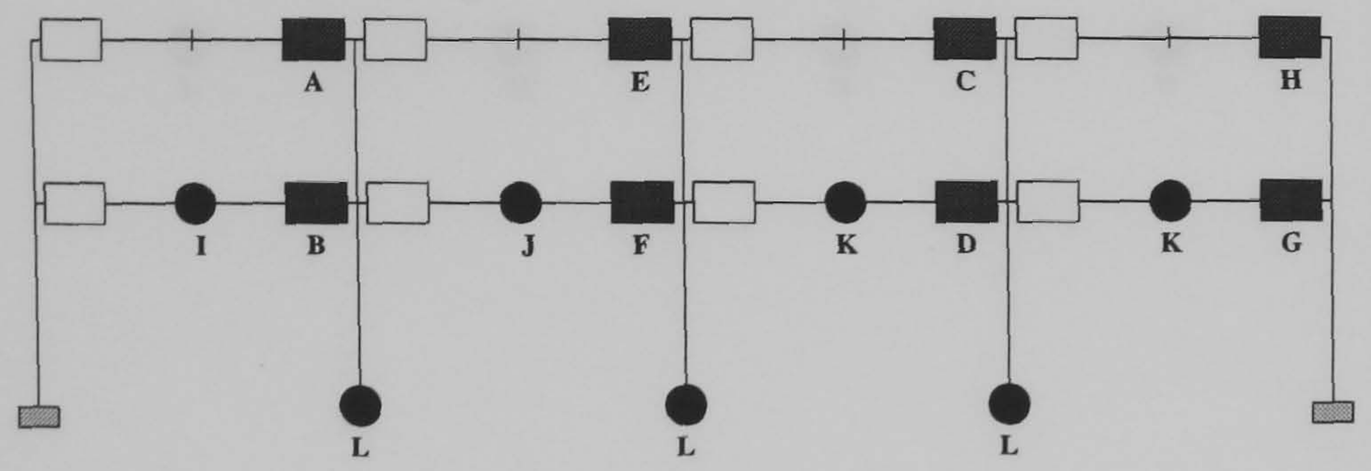

S-R (2) Including web shear at the internal columns

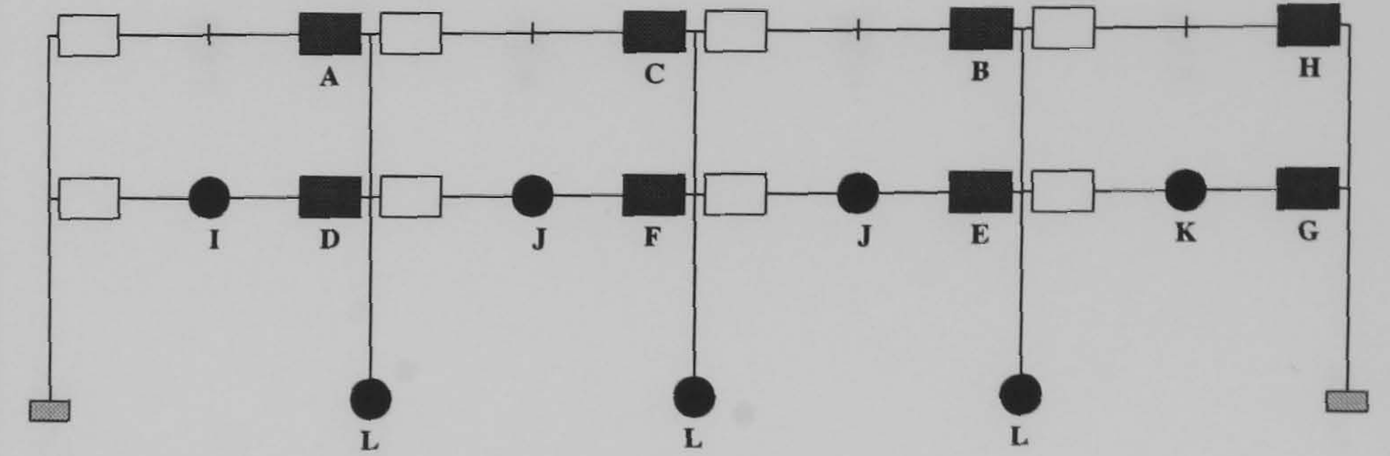

Rigid

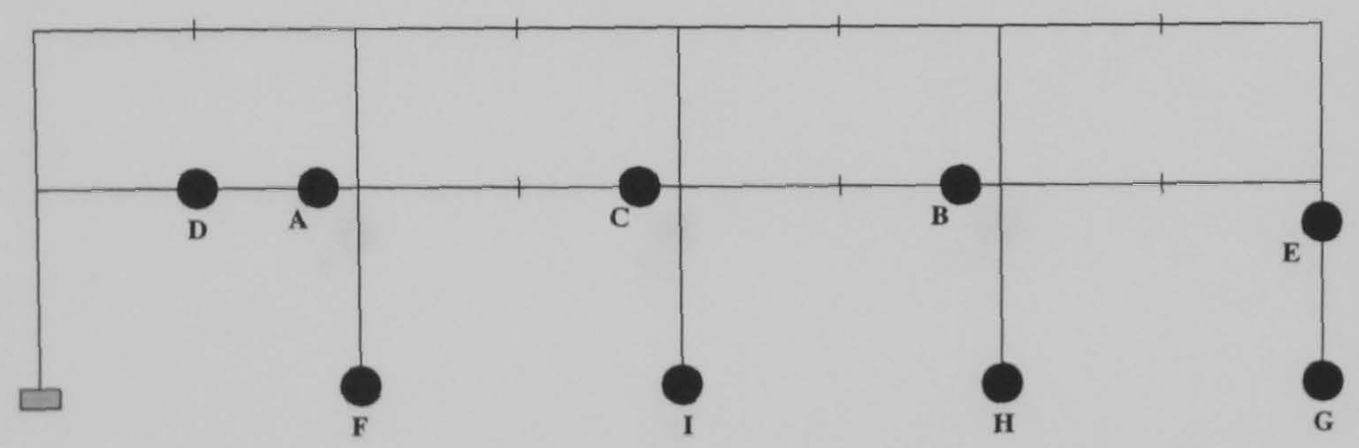

Hinge Location	Load Level at Hinge Formation S-R(1)	S-R(2)	Rigid
A	1.0375	1.2225	1.58
B	1.05	1.2425	1.712
C	1.06	1.2475	1.77
D	1.0675	1.265	1.927
E	1.0725	1.2825	1.977
F	1.08	1.2875	2.022
G	1.44	1.44	2.025
H	1.455	1.455	2.027
I	1.47	1.472	2.03
J	1.495	1.497	N/A
K	1.497	1.5	N/A
L	1.535	1.532	N/A

Key :

- Semi-Rigid Connection
- Plastification prior to ULS design load being attained
- Plastification following the attainment of the design load
- Member plastification

FRAME : **f20 b20**
Load Case 2

S-R (1) Negelecting web shear at the internal columns

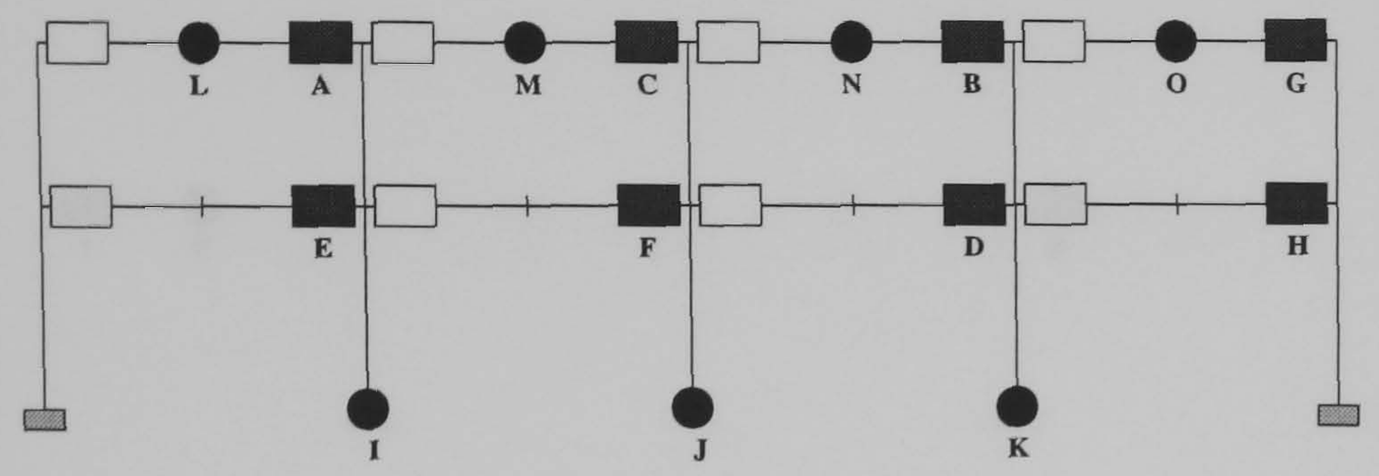

S-R (2) Including web shear at the internal columns

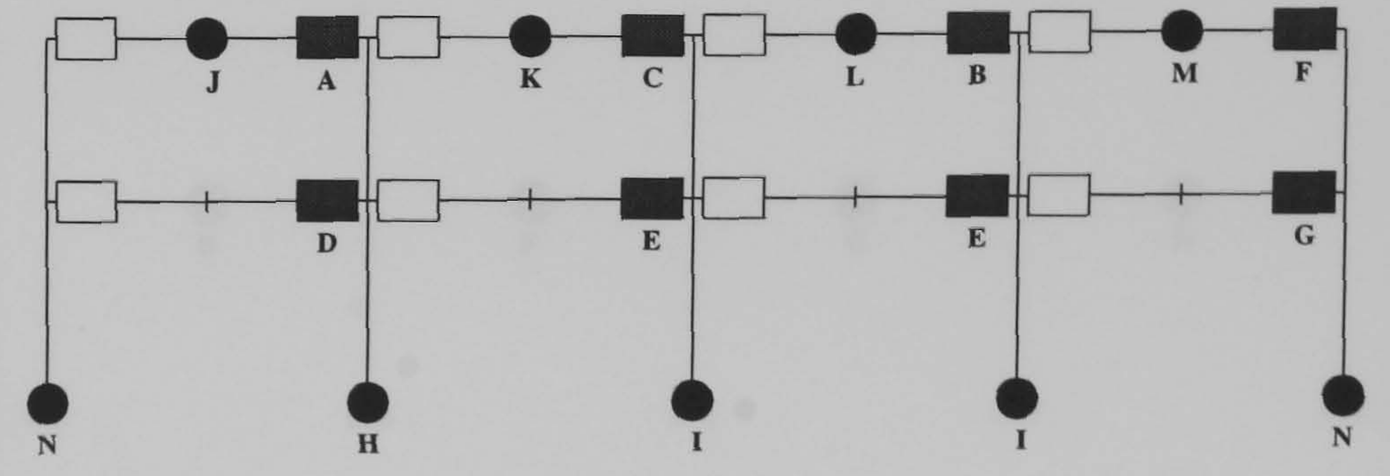

Rigid

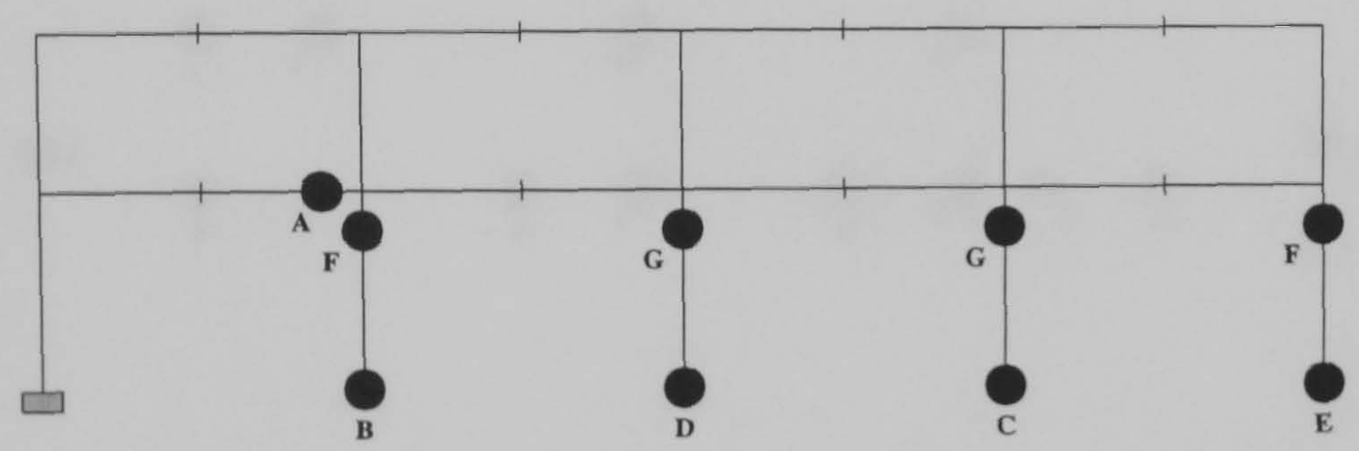

Hinge Location	Load Level at Hinge Formation S-R(1)	S-R(2)	Rigid
A	1.145	1.3375	2.225
B	1.165	1.3575	2.24
C	1.1825	1.3625	2.275
D	1.37	1.595	2.282
E	1.3725	1.6075	2.32
F	1.3825	1.645	2.337
G	1.67	1.7075	2.342
H	1.73	1.887	N/A
I	1.91	1.892	N/A
J	1.912	1.905	N/A
K	1.915	1.922	N/A
L	1.92	1.925	N/A
M	1.935	1.927	N/A
N	1.937	1.93	N/A
O	1.94	N/A	N/A

Key :

- Semi-Rigid Connection
- Plastification prior to ULS design load being attained
- Plastification following the attainment of the design load
- Member plastification

FRAME : **f20 b20**
Load Case 3

S-R (1) Negelecting web shear at the internal columns

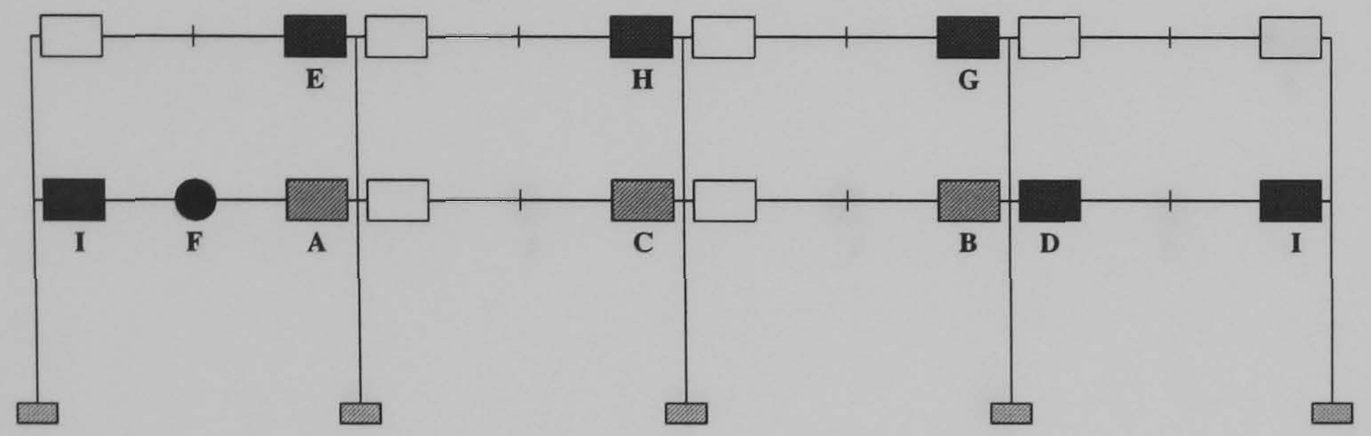

S-R (2) Including web shear at the internal columns

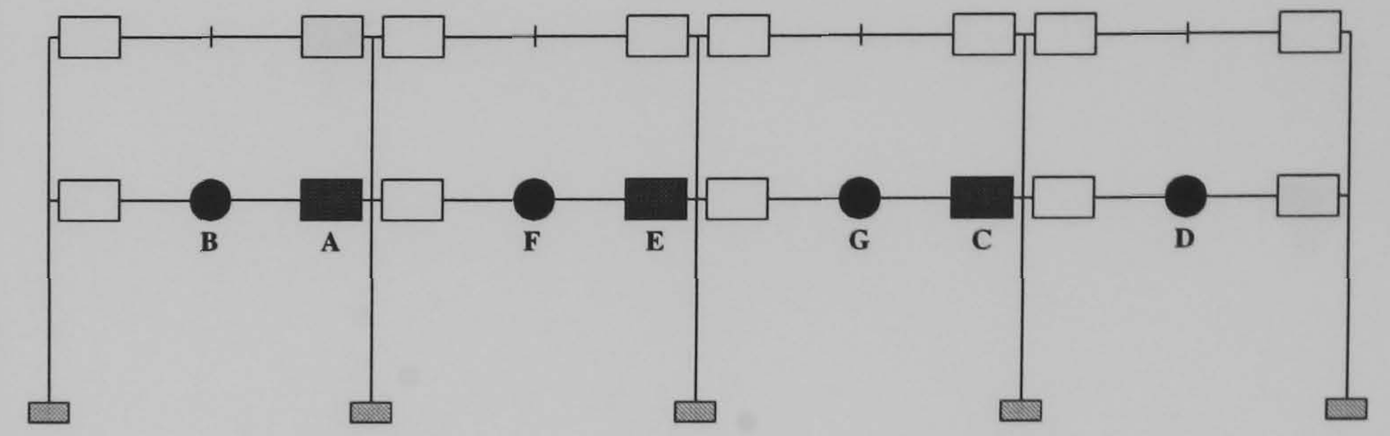

Rigid

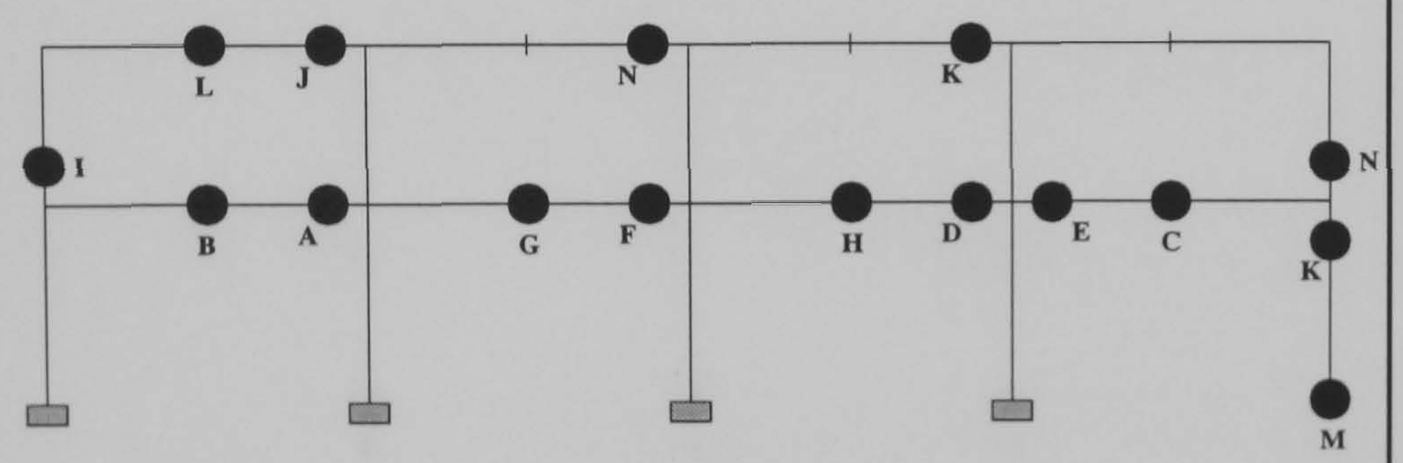

Hinge Location	Load Level at Hinge Formation S-R(1)	S-R(2)	Rigid
A	0.9075	1.255	1.655
B	0.96	1.28	1.722
C	0.98	1.29	1.76
D	1.2125	1.292	1.78
E	1.2225	1.295	1.817
F	1.272	1.327	1.872
G	1.2775	1.33	1.962
H	1.3	N/A	1.967
I	1.3425	N/A	1.985
J	N/A	N/A	1.99
K	N/A	N/A	2.02
L	N/A	N/A	2.025
M	N/A	N/A	2.027
N	N/A	N/A	2.03

Key :

Semi-Rigid Connection

Plastification prior to ULS design load being attained

Plastification following the attainment of the design load

Member plastification

FRAME : **f20 b24**
Load Case 1

S-R (1) Negelecting web shear at the internal columns

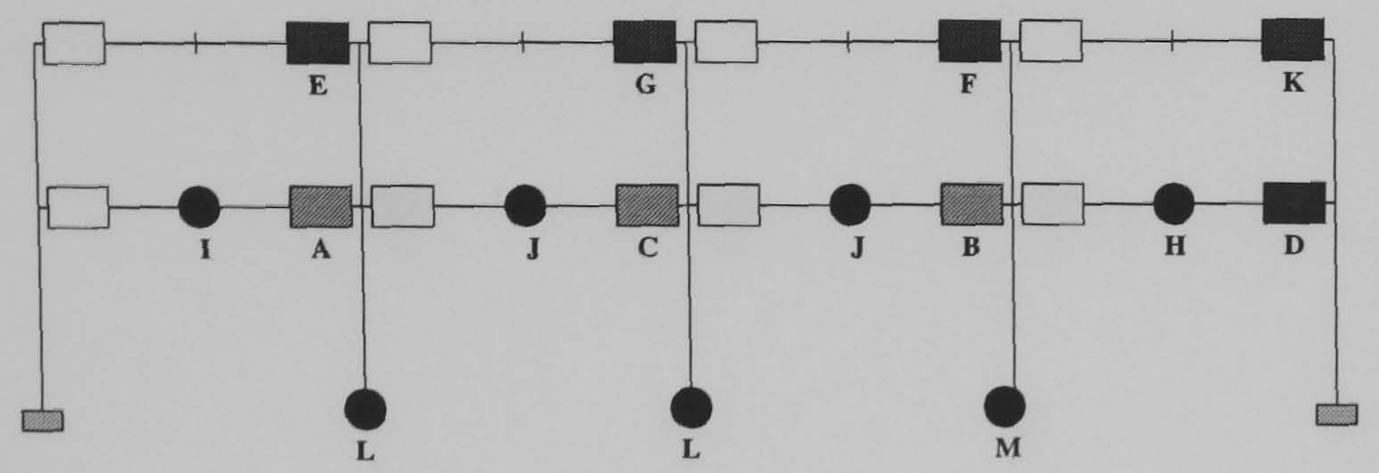

S-R (2) Including web shear at the internal columns

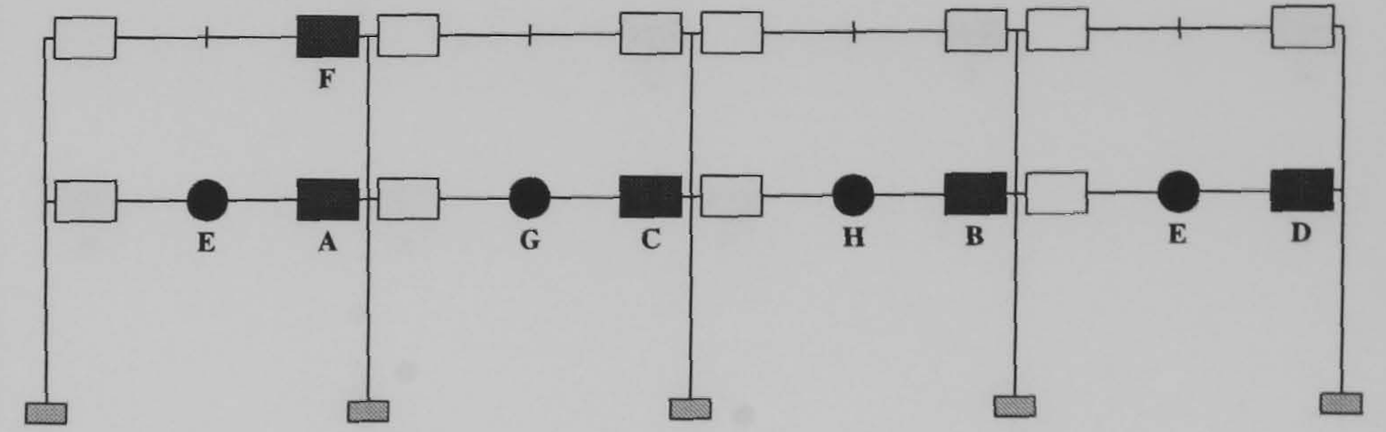

Rigid

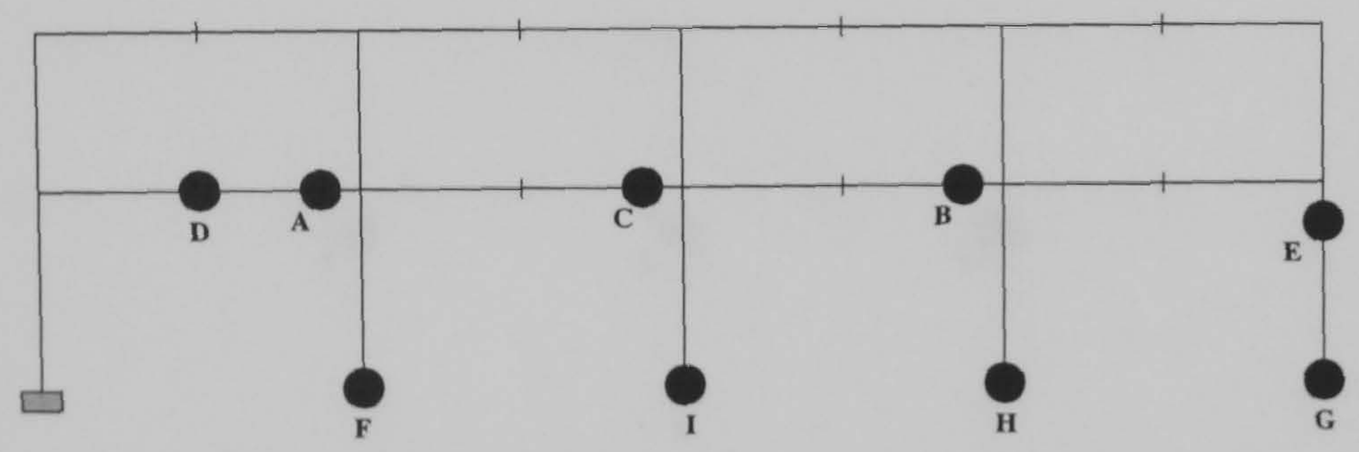

Hinge Location	Load Level at Hinge Formation S-R(1)	S-R(2)	Rigid
A	0.82	1.06	1.58
B	0.8375	1.0775	1.712
C	0.8525	1.08	1.77
D	1.1675	1.145	1.927
E	1.19	1.432	1.977
F	1.215	1.44	2.022
G	1.245	1.445	2.025
H	1.43	1.447	2.027
I	1.435	N/A	2.03
J	1.442	N/A	N/A
K	1.4775	N/A	N/A
L	1.495	N/A	N/A
M	1.497	N/A	N/A

Key :

Semi-Rigid Connection

Plastification prior to ULS design load being attained

Plastification following the attainment of the design load

Member plastification

FRAME : **f20 b24**
Load Case 2

S-R (1) Negelecting web shear at the internal columns

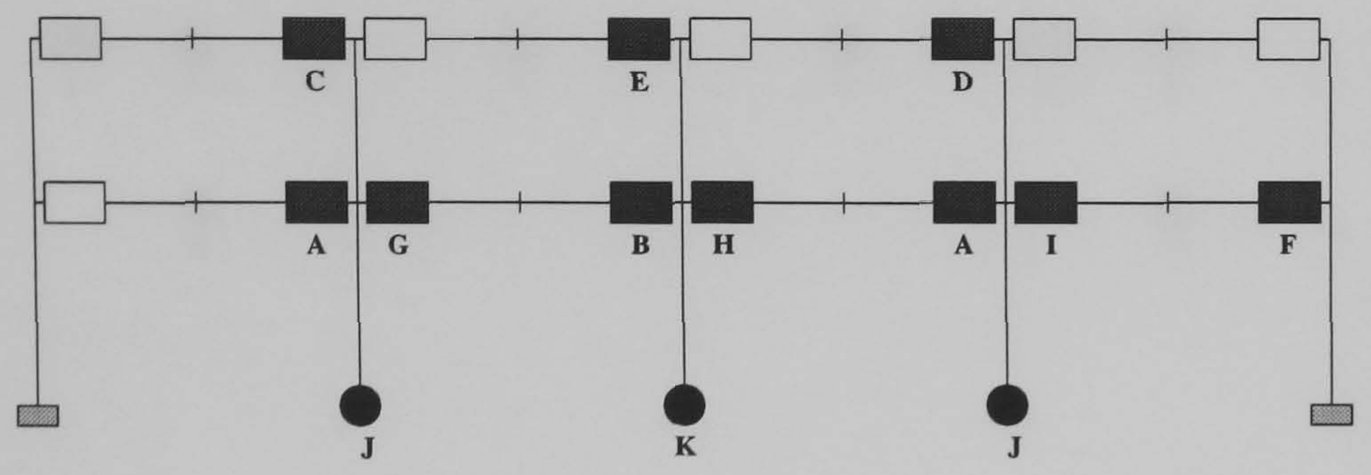

S-R (2) Including web shear at the internal columns

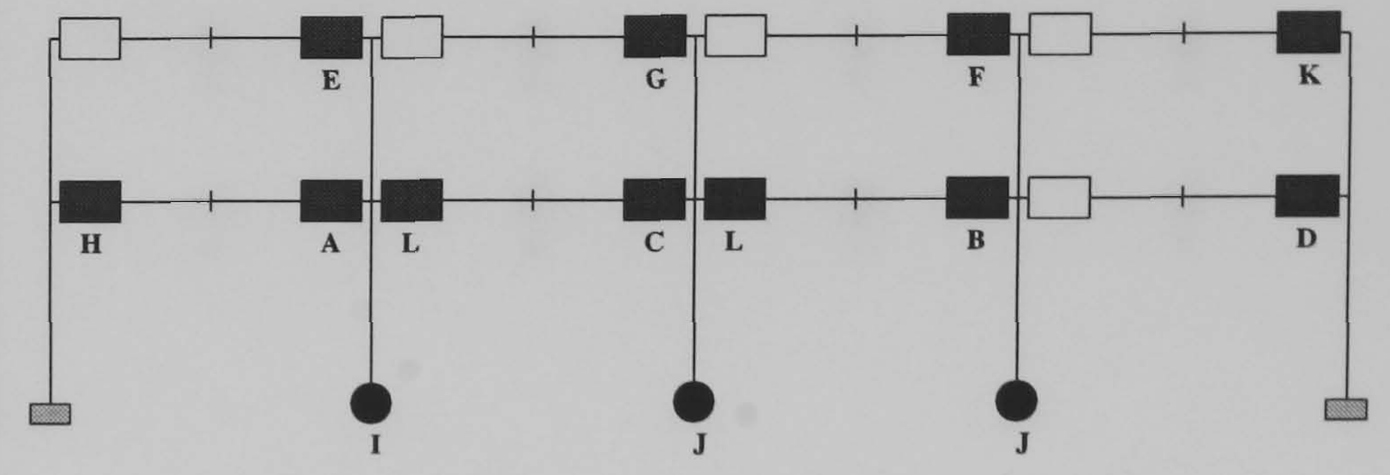

Rigid

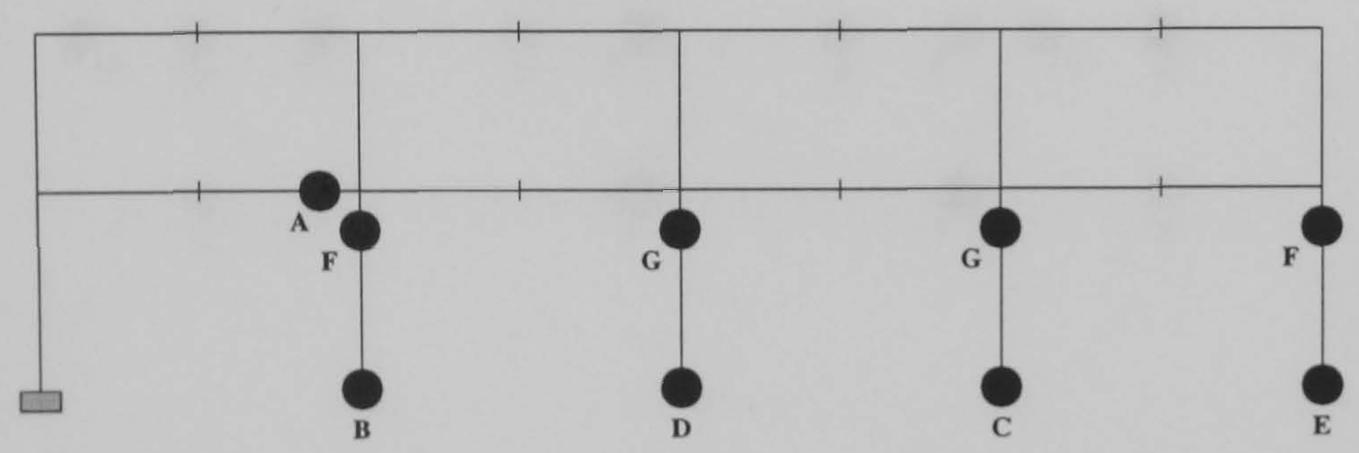

Hinge Location	Load Level at Hinge Formation S-R(1)	S-R(2)	Rigid
A	**1.1025**	**1.3625**	**2.225**
B	**1.1175**	**1.37**	**2.24**
C	**1.3525**	**1.3725**	**2.275**
D	**1.3775**	**1.375**	**2.282**
E	**1.415**	**1.63**	**2.32**
F	**1.4175**	**1.6575**	**2.337**
G	**1.84**	**1.67**	**2.342**
H	**1.8425**	**1.8525**	**N/A**
I	**1.8575**	**1.86**	**N/A**
J	**1.875**	**1.862**	**N/A**
K	**1.88**	**1.87**	**N/A**
L	**N/A**	**1.8775**	**N/A**

Key :

Semi-Rigid Connection

Plastification prior to ULS design load being attained

Plastification following the attainment of the design load

Member plastification

FRAME : **f20 b24**
Load Case 3

S-R (1) Negelecting web shear at the internal columns

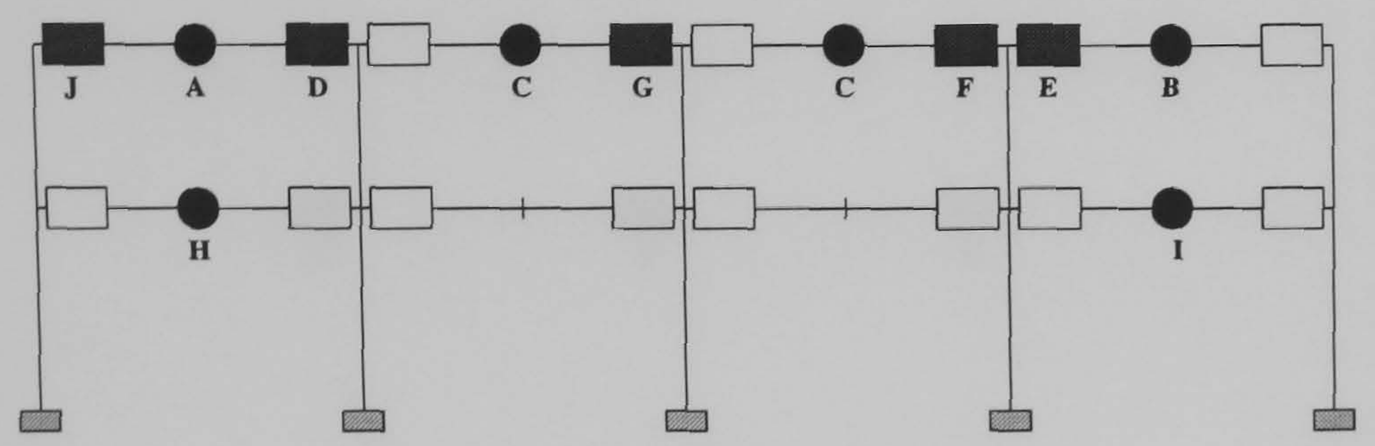

S-R (2) Including web shear at the internal columns

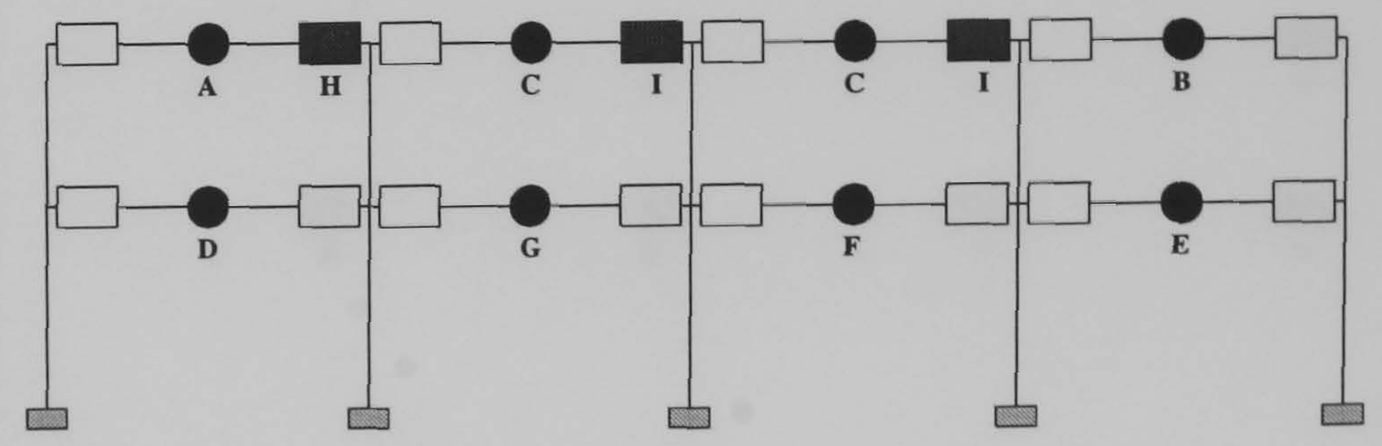

Rigid

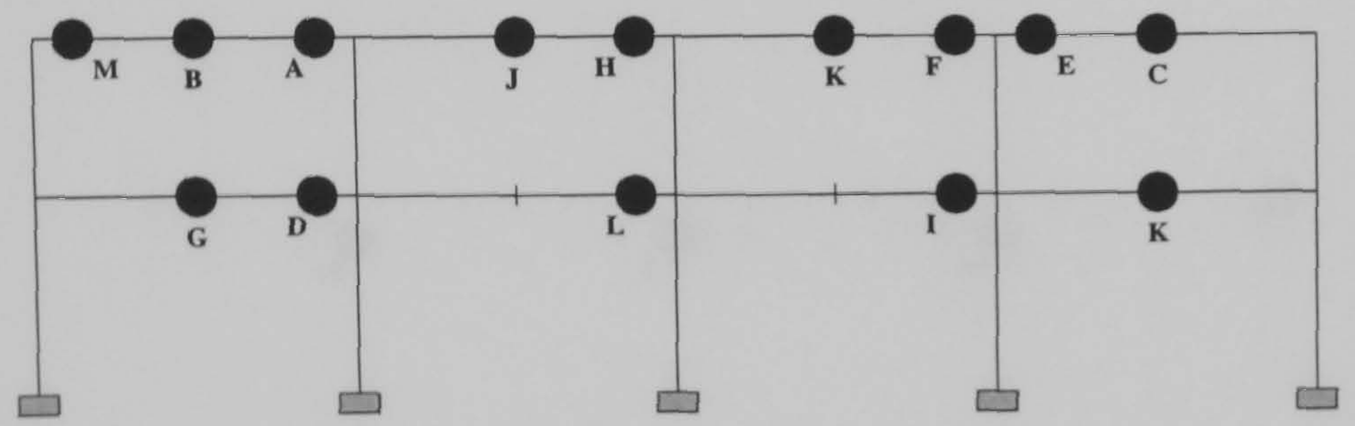

Hinge Location	Load Level at Hinge Formation S-R(1)	S-R(2)	Rigid
A	1.292	1.257	1.782
B	1.295	1.267	1.802
C	1.35	1.285	1.817
D	1.375	1.365	1.852
E	1.4	1.385	1.855
F	1.41	1.392	1.89
G	1.4175	1.395	1.932
H	1.422	1.3975	1.945
I	1.425	1.42	1.97
J	1.4475	N/A	1.992
K	N/A	N/A	1.995
L	N/A	N/A	2.0
M	N/A	N/A	2.03

Key :

Semi-Rigid Connection

Plastification prior to ULS design load being attained

Plastification following the attainment of the design load

Member plastification

FRAME : **f21 b20**
Load Case 1

S-R (1) Negelecting web shear at the internal columns

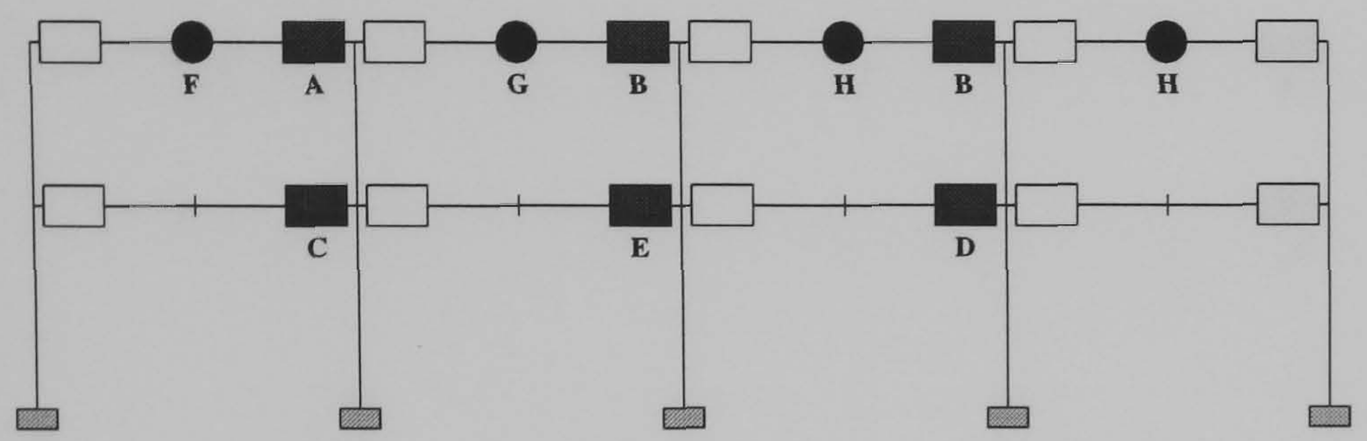

S-R (2) Including web shear at the internal columns

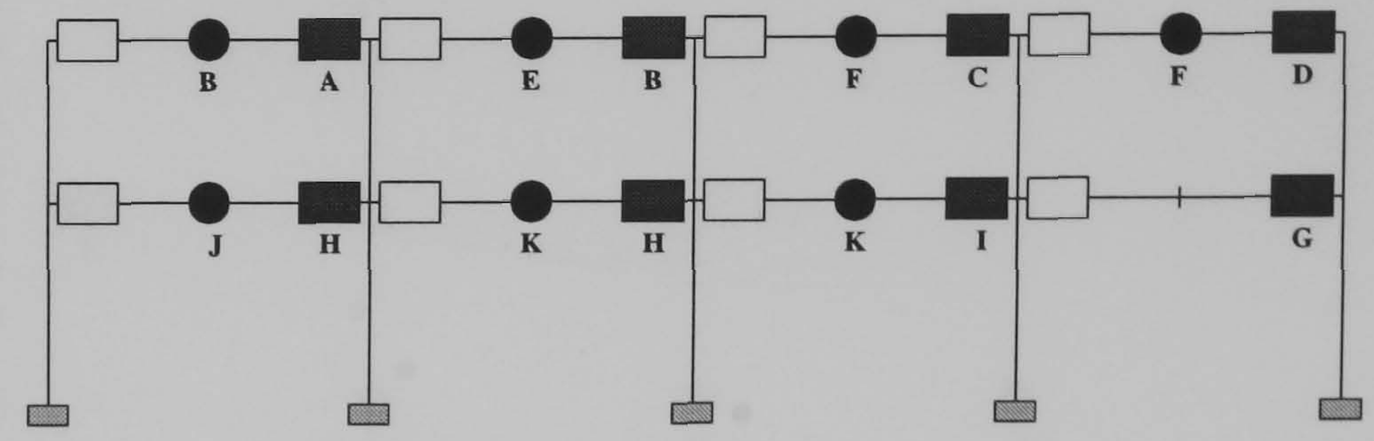

Rigid

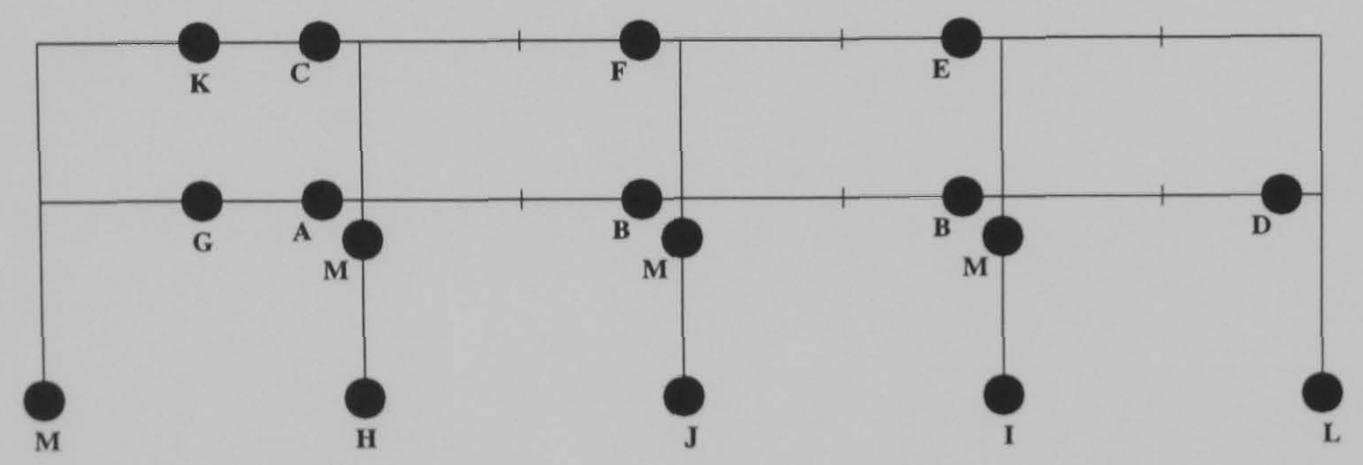

Hinge Location	Load Level at Hinge Formation S-R(1)	S-R(2)	Rigid
A	1.2975	1.4275	1.49
B	1.3075	1.4375	1.645
C	1.38	1.44	1.7
D	1.3925	1.4475	1.747
E	1.395	1.467	1.795
F	1.455	1.47	1.827
G	1.477	1.475	1.9
H	1.48	1.4975	1.905
I	N/A	1.5025	1.907
J	N/A	1.51	1.91
K	N/A	1.522	1.927
L	N/A	N/A	1.93
M	N/A	N/A	1.935

Key :

Semi-Rigid Connection

Plastification prior to ULS design load being attained

Plastification following the attainment of the design load

Member plastification

FRAME : **f21 b20**
Load Case 2

S-R (1) Negelecting web shear at the internal columns

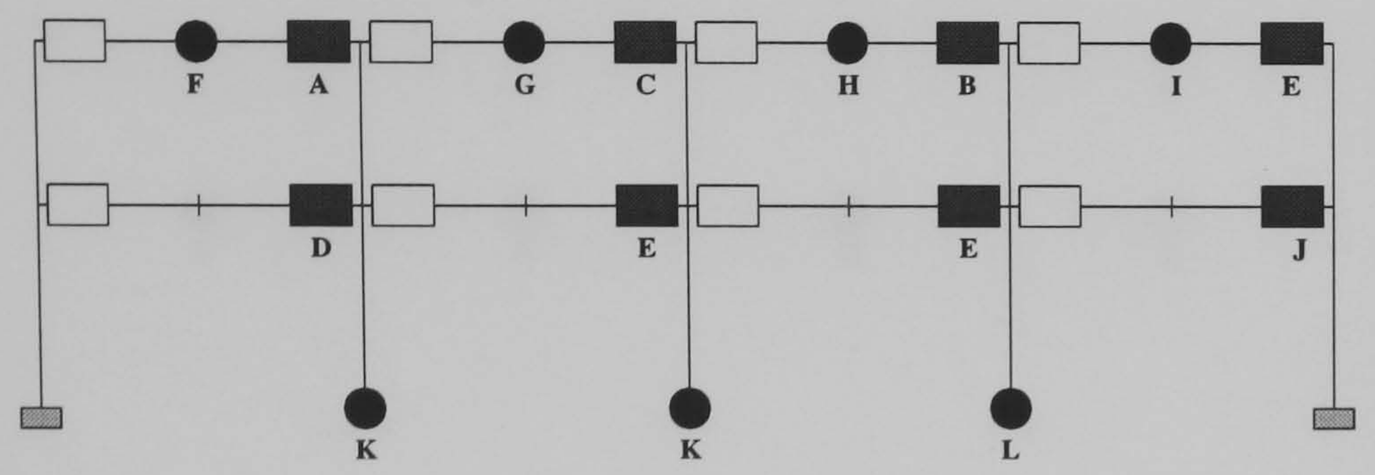

S-R (2) Including web shear at the internal columns

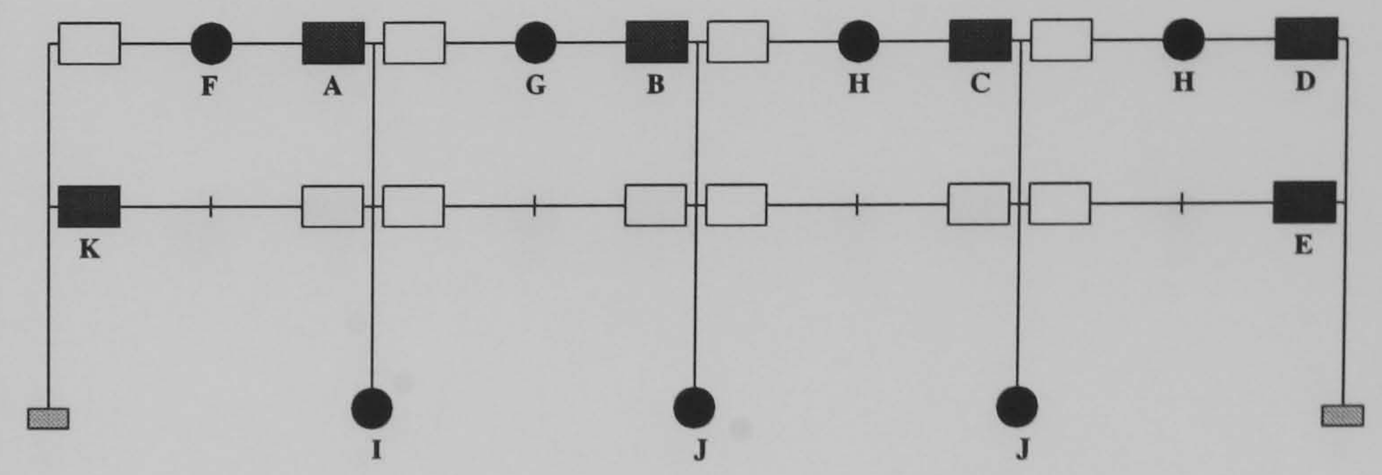

Rigid

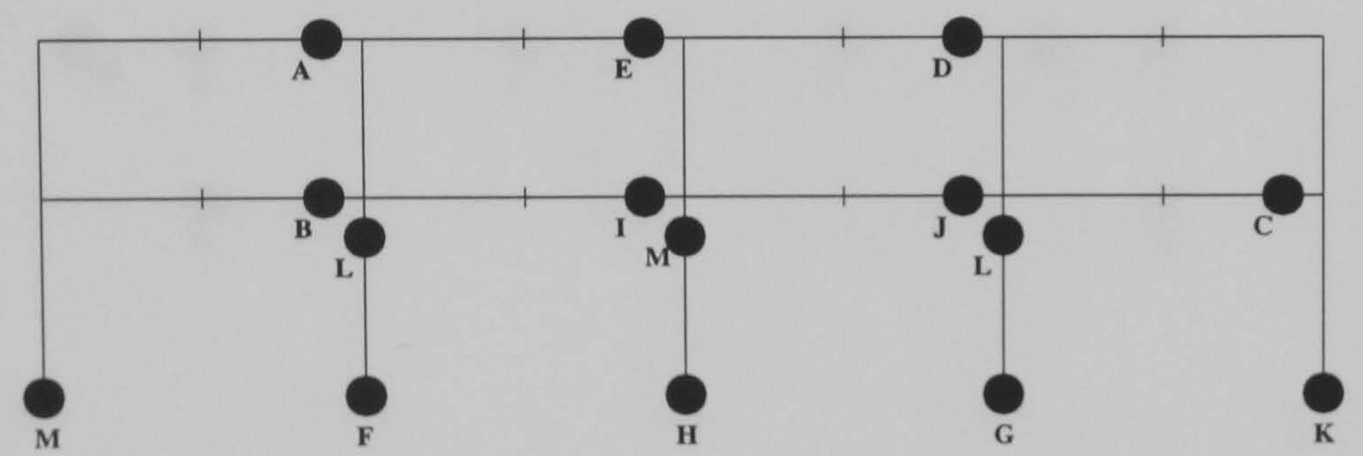

Hinge Location	Load Level at Hinge Formation		
	S-R(1)	S-R(2)	Rigid
A	**1.38**	**1.51**	**1.855**
B	**1.3875**	**1.5225**	**1.91**
C	**1.3925**	**1.525**	**1.992**
D	**1.62**	**1.5375**	**2.002**
E	**1.6275**	**1.64**	**2.042**
F	**1.67**	**1.642**	**2.05**
G	**1.69**	**1.675**	**2.06**
H	**1.695**	**1.68**	**2.065**
I	**1.697**	**1.702**	**2.067**
J	**1.6975**	**1.705**	**2.08**
K	**1.722**	**1.7075**	**2.122**
L	**1.725**	N/A	**2.137**
M	N/A	N/A	**2.142**

Key :

- Plastification prior to ULS design load being attained
- Semi-Rigid Connection
- Plastification following the attainment of the design load
- Member plastification

FRAME : **f21 b20**
Load Case 3

S-R (1) Negelecting web shear at the internal columns

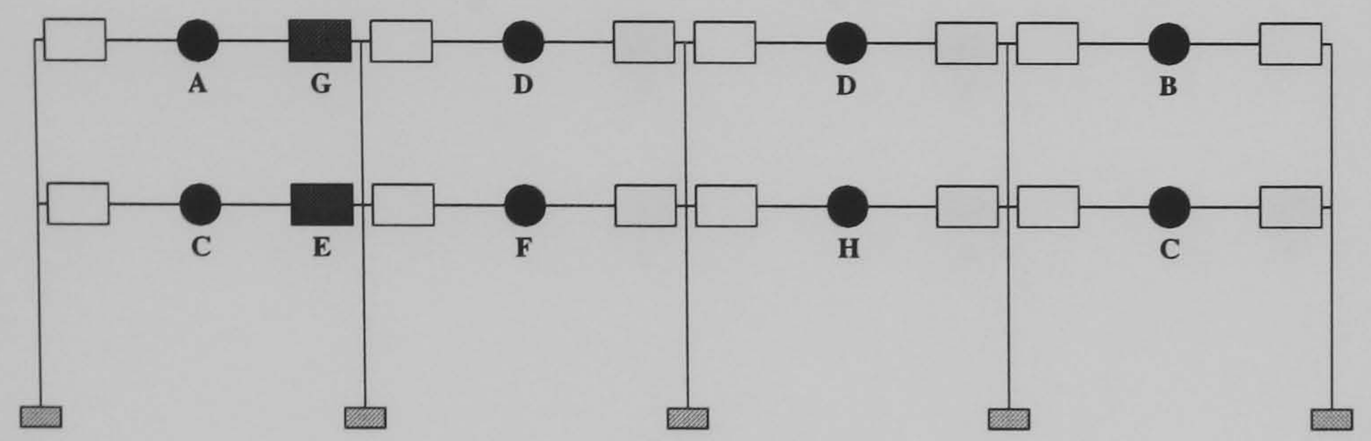

S-R (2) Including web shear at the internal columns

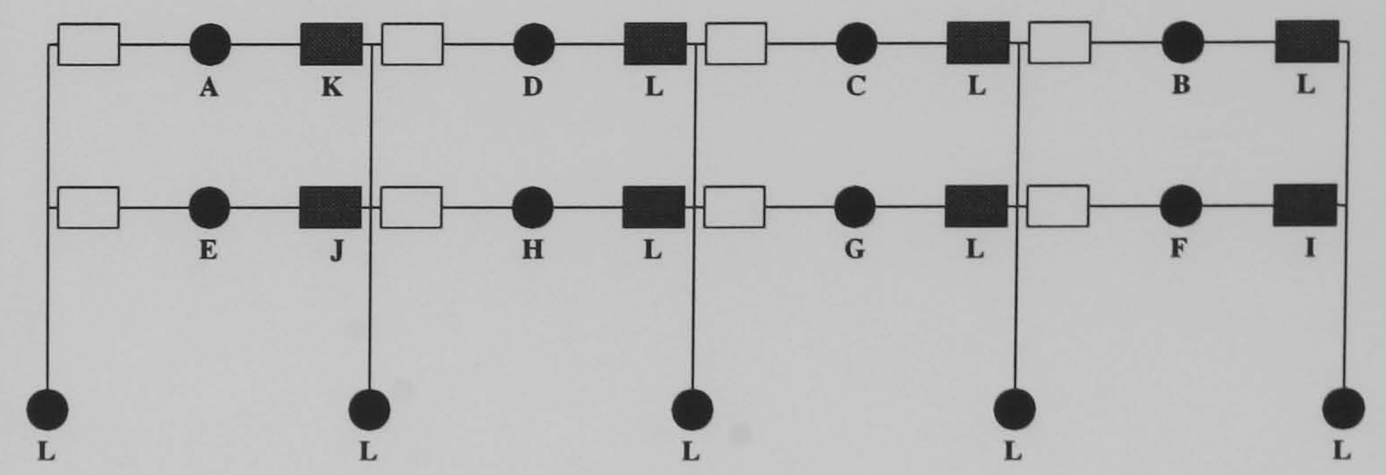

Rigid

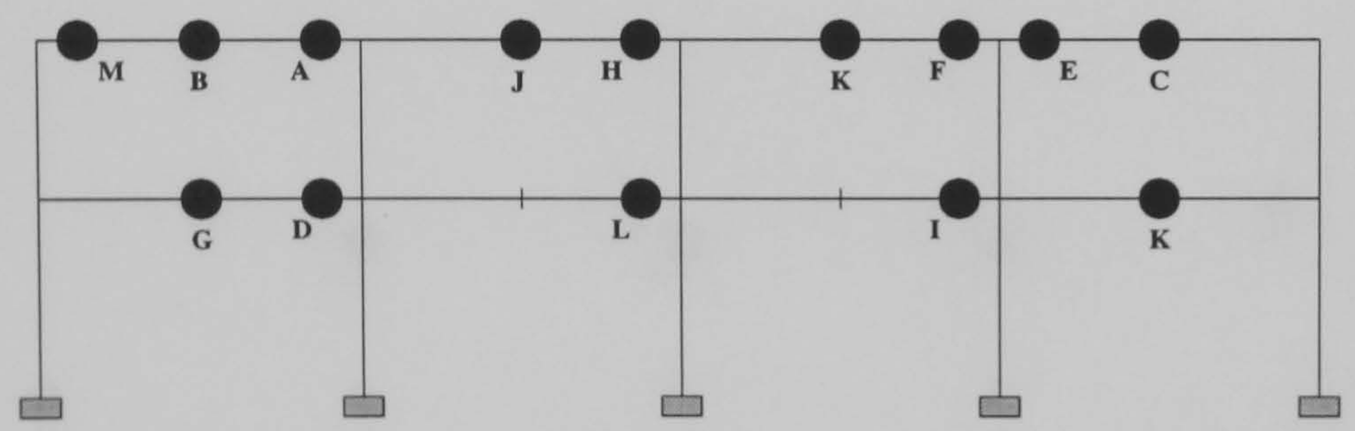

Hinge Location	Load Level at Hinge Formation S-R(1)	S-R(2)	Rigid
A	1.362	1.307	1.782
B	1.365	1.322	1.802
C	1.425	1.35	1.817
D	1.46	1.352	1.852
E	1.4675	1.357	1.855
F	1.497	1.372	1.89
G	1.5	1.382	1.932
H	1.507	1.385	1.945
I	N/A	1.51	1.97
J	N/A	1.5125	1.992
K	N/A	1.5275	1.995
L	N/A	1.53	2.0
M	N/A	N/A	2.03

Key :

- Semi-Rigid Connection
- Plastification prior to ULS design load being attained
- Plastification following the attainment of the design load
- Member plastification

FRAME : **f21 b24**
Load Case 1

S-R (1) Negelecting web shear at the internal columns

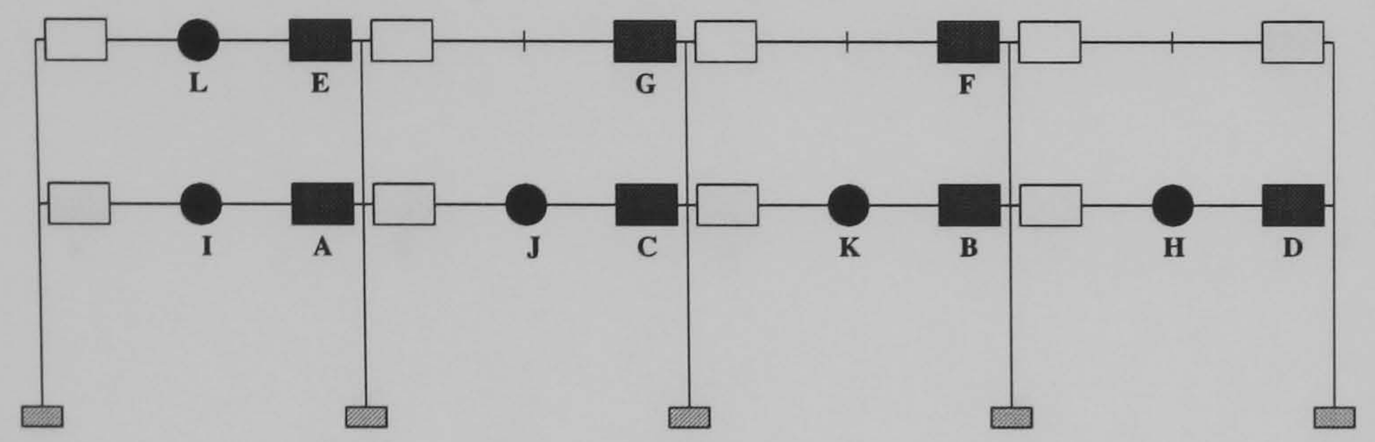

S-R (2) Including web shear at the internal columns

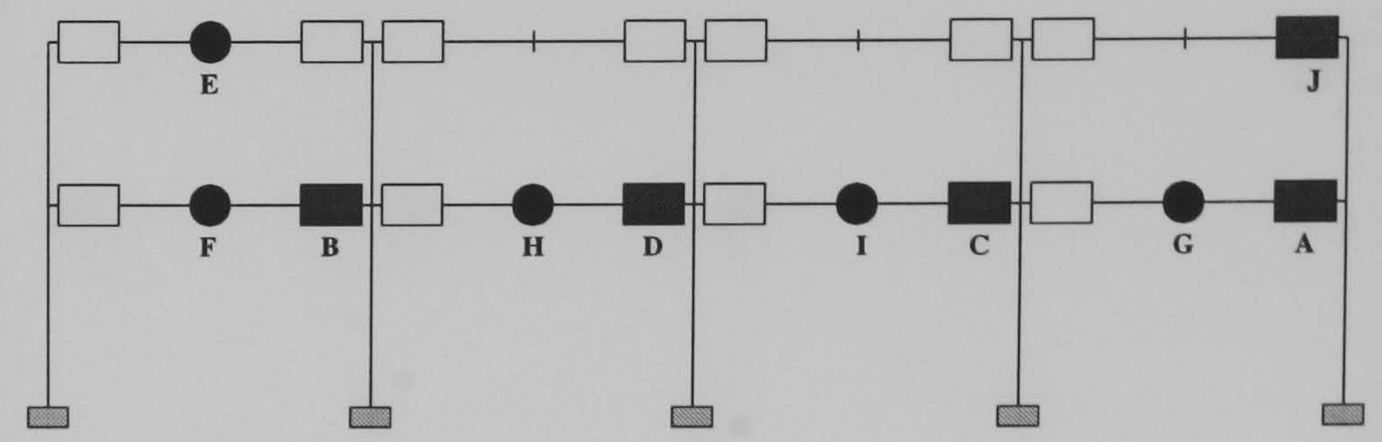

Rigid

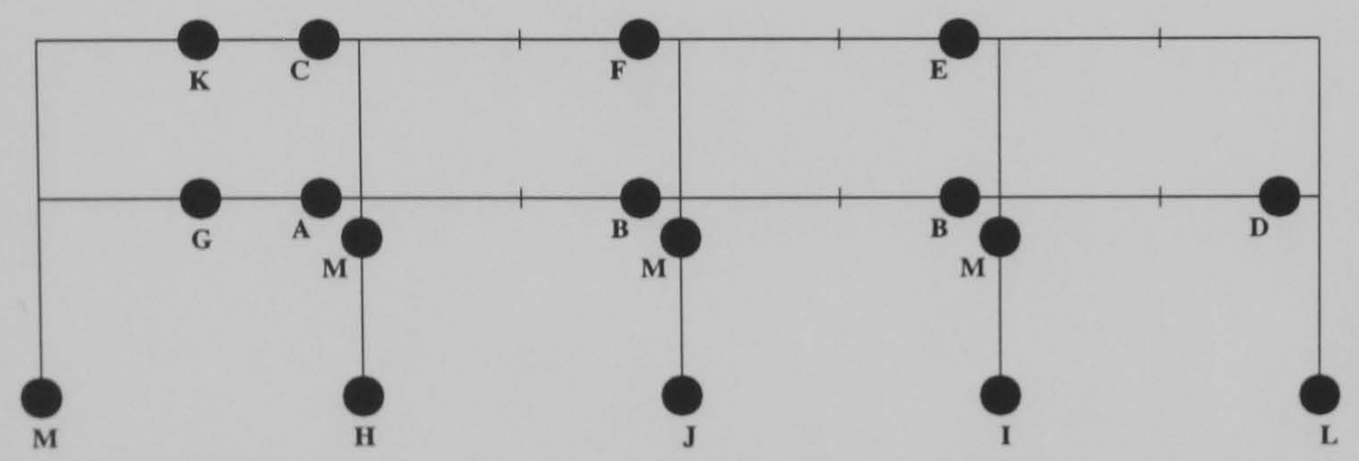

Hinge Location	Load Level at Hinge Formation S-R(1)	S-R(2)	Rigid
A	**1.12**	**1.155**	**1.49**
B	**1.13**	**1.325**	**1.645**
C	**1.135**	**1.335**	**1.7**
D	**1.2275**	**1.3375**	**1.747**
E	**1.445**	**1.48**	**1.795**
F	**1.46**	**1.482**	**1.827**
G	**1.4675**	**1.495**	**1.9**
H	**1.492**	**1.507**	**1.905**
I	**1.5**	**1.51**	**1.907**
J	**1.505**	**1.5125**	**1.91**
K	**1.507**	N/A	**1.927**
L	**1.515**	N/A	**1.93**
M	N/A	N/A	**1.935**

Key :

Semi-Rigid Connection

Plastification prior to ULS design load being attained

Plastification following the attainment of the design load

Member plastification

FRAME : **f21 b24**

Load Case 2

S-R (1) Negelecting web shear at the internal columns

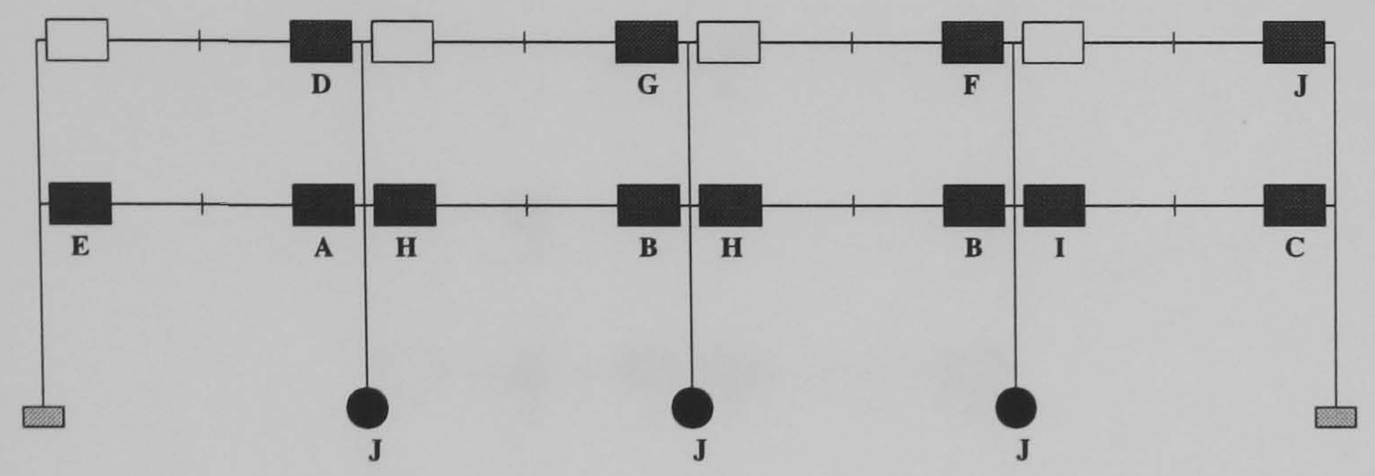

S-R (2) Including web shear at the internal columns

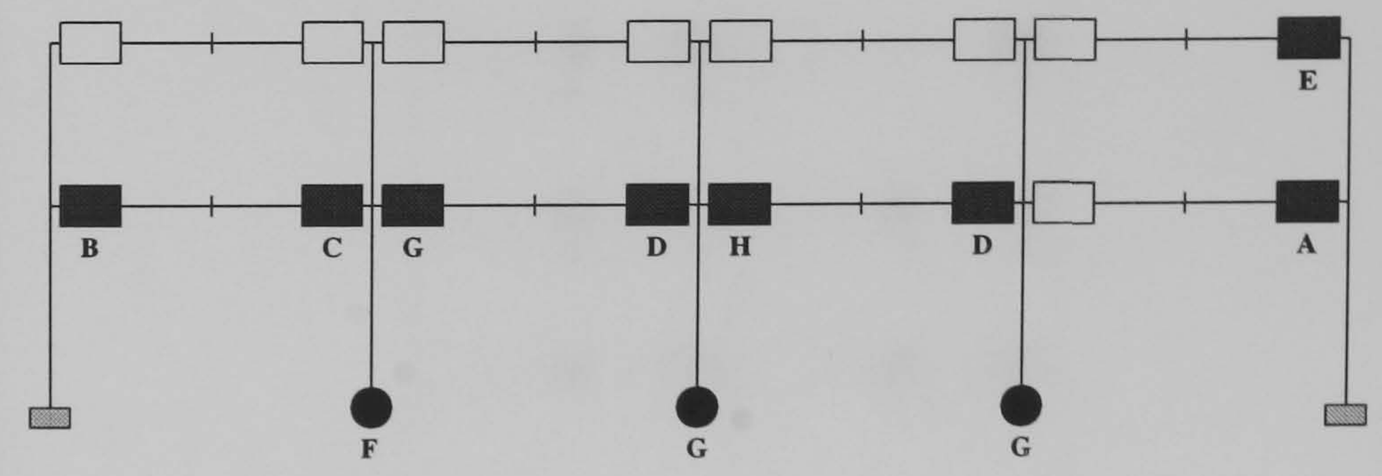

Rigid

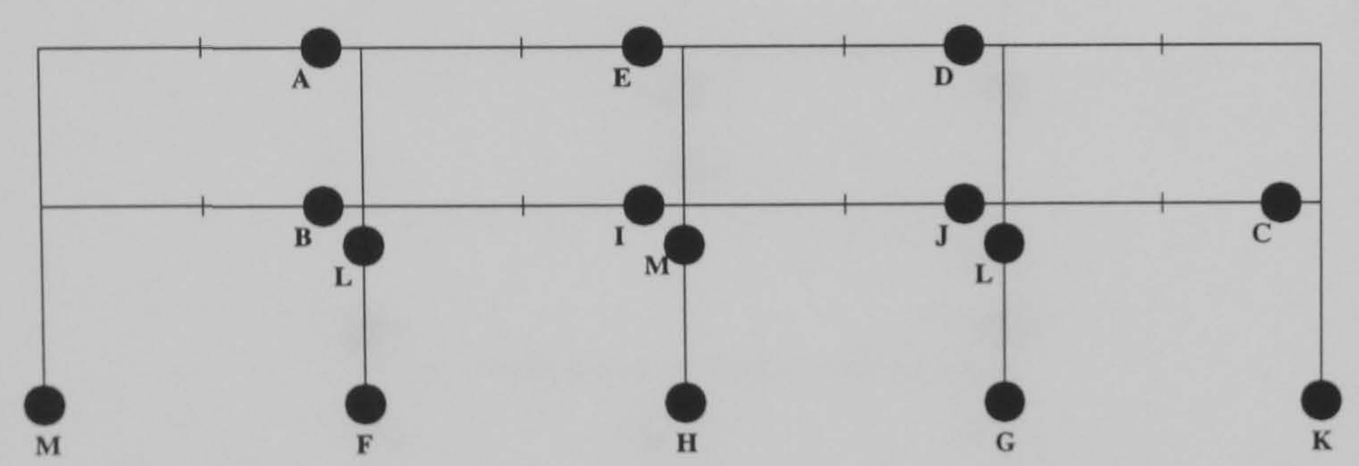

Hinge Location	Load Level at Hinge Formation		
	S-R(1)	S-R(2)	Rigid
A	1.335	1.2725	1.855
B	1.3375	1.4725	1.91
C	1.38	1.53	1.992
D	1.575	1.5375	2.002
E	1.585	1.655	2.042
F	1.59	1.675	2.05
G	1.6	1.6775	2.06
H	1.6425	1.68	2.065
I	1.65	N/A	2.067
J	1.69	N/A	2.08
K	N/A	N/A	2.122
L	N/A	N/A	2.137
M	N/A	N/A	2.142

Key :

Semi-Rigid Connection

Plastification prior to ULS design load being attained

Plastification following the attainment of the design load

Member plastification

FRAME : **f21 b24**

Load Case 3

S-R (1) Negelecting web shear at the internal columns

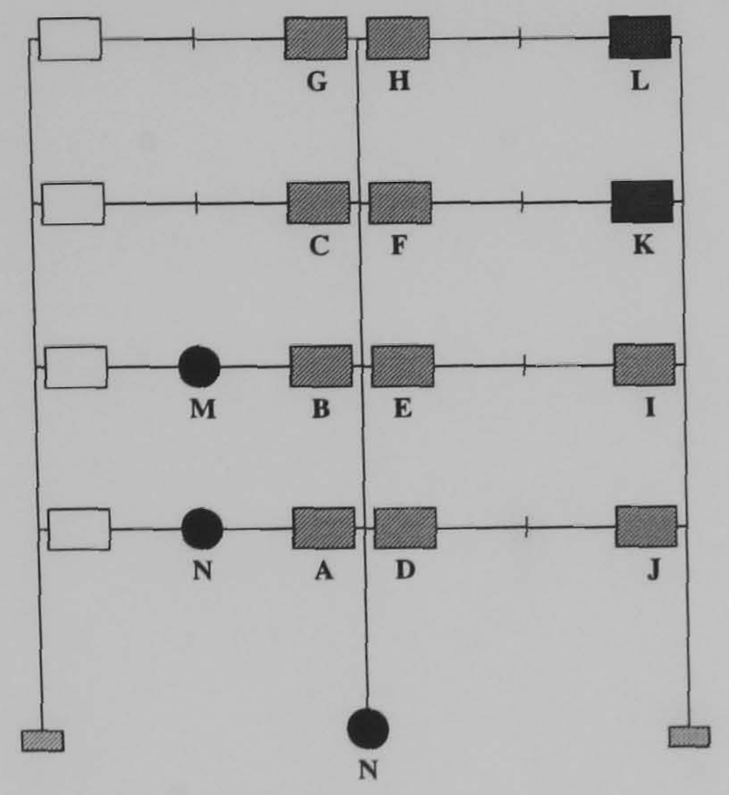

S-R (2) Including web shear at the internal columns

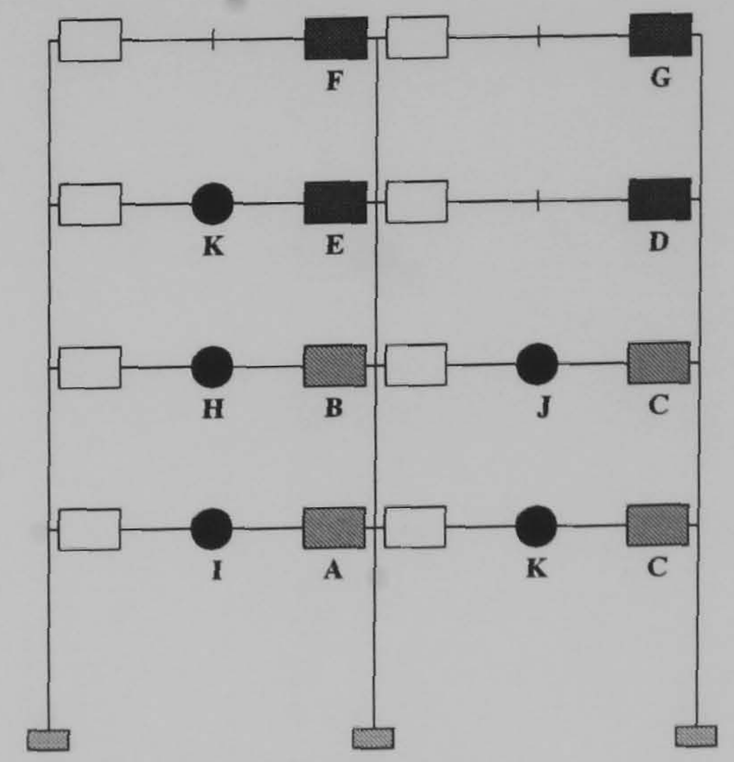

Rigid

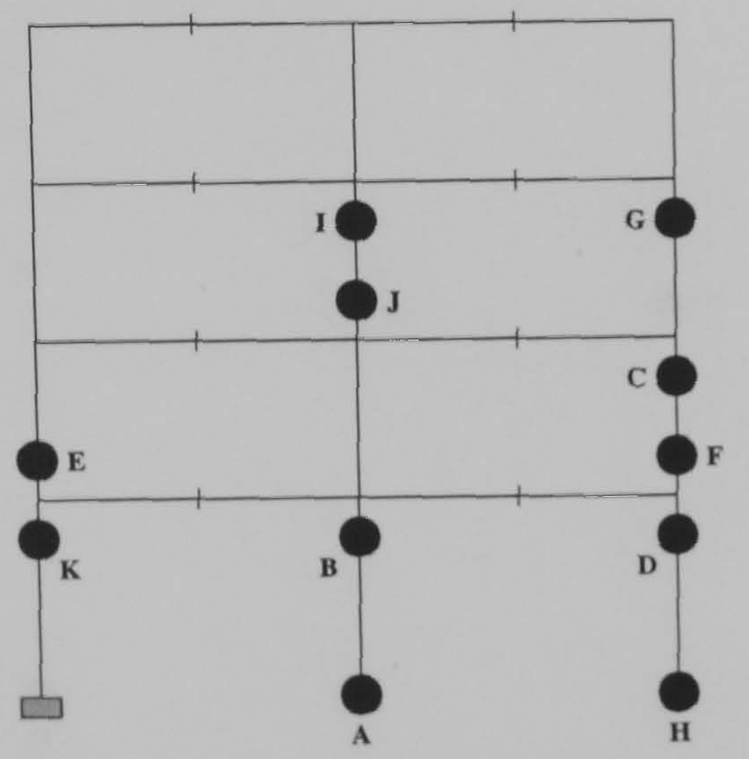

Hinge Location	Load Level at Hinge Formation S-R(1)	S-R(2)	Rigid
A	0.4425	0.73	1.445
B	0.45	0.7375	1.46
C	0.5675	0.8225	1.585
D	0.6325	1.0675	1.595
E	0.6775	1.1	1.645
F	0.723	1.1325	1.65
G	0.75	1.21	1.66
H	0.785	1.285	1.665
I	0.795	1.29	1.675
J	0.8	1.292	1.685
K	1.0325	1.295	1.69
L	1.155	N/A	N/A
M	1.245	N/A	N/A
N	1.247	N/A	N/A

Key :

- Plastification prior to ULS design load being attained
- Semi-Rigid Connection
- Plastification following the attainment of the design load
- Member plastification

FRAME : **f22 b24**
Load Case 1

S-R (1) Negelecting web shear at the internal columns

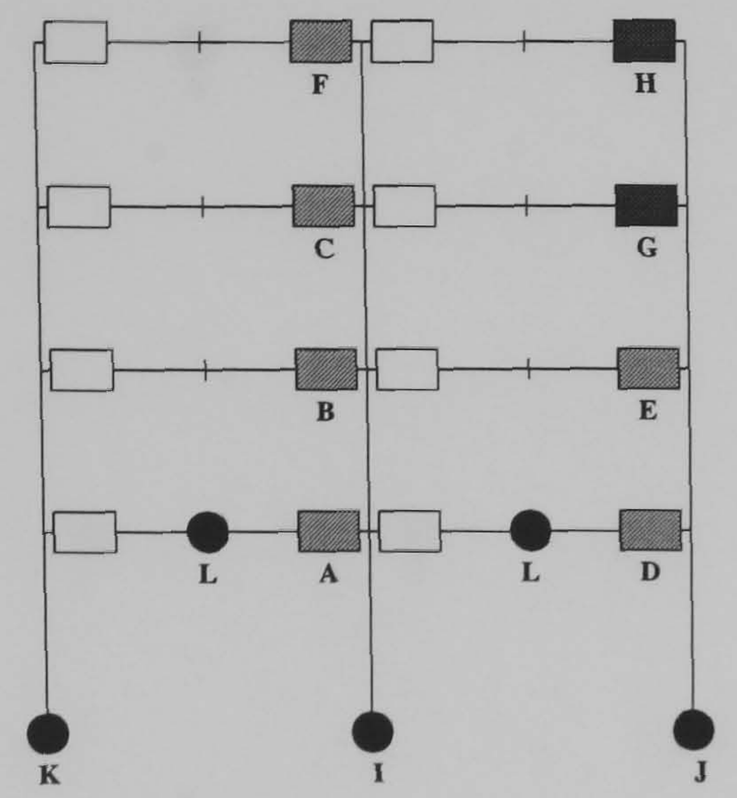

S-R (2) Including web shear at the internal columns

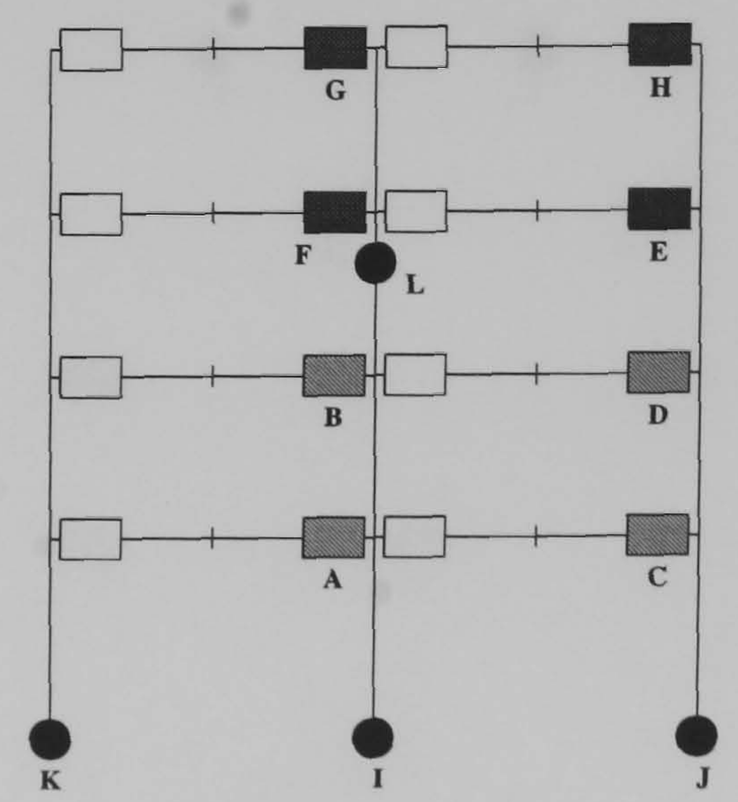

Rigid

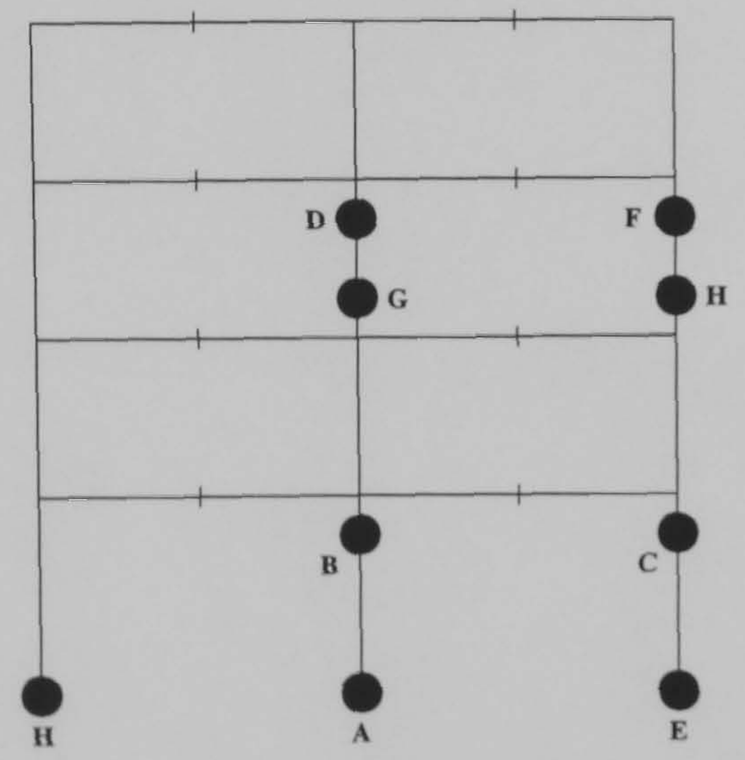

Hinge Location	Load Level at Hinge Formation S-R(1)	S-R(2)	Rigid
A	0.475	0.75	1.475
B	0.5	0.7825	1.52
C	0.655	0.81	1.635
D	0.795	0.833	1.68
E	0.815	1.08	1.685
F	0.8475	1.185	1.7
G	1.0675	1.24	1.705
H	1.2675	1.2975	1.735
I	1.307	1.307	N/A
J	1.47	1.462	N/A
K	1.497	1.485	N/A
L	1.505	1.49	N/A

Key :

Semi-Rigid Connection

Plastification prior to ULS design load being attained

Plastification following the attainment of the design load

Member plastification

FRAME : **f22 b24**

Load Case 2

S-R (1) Negelecting web shear at the internal columns

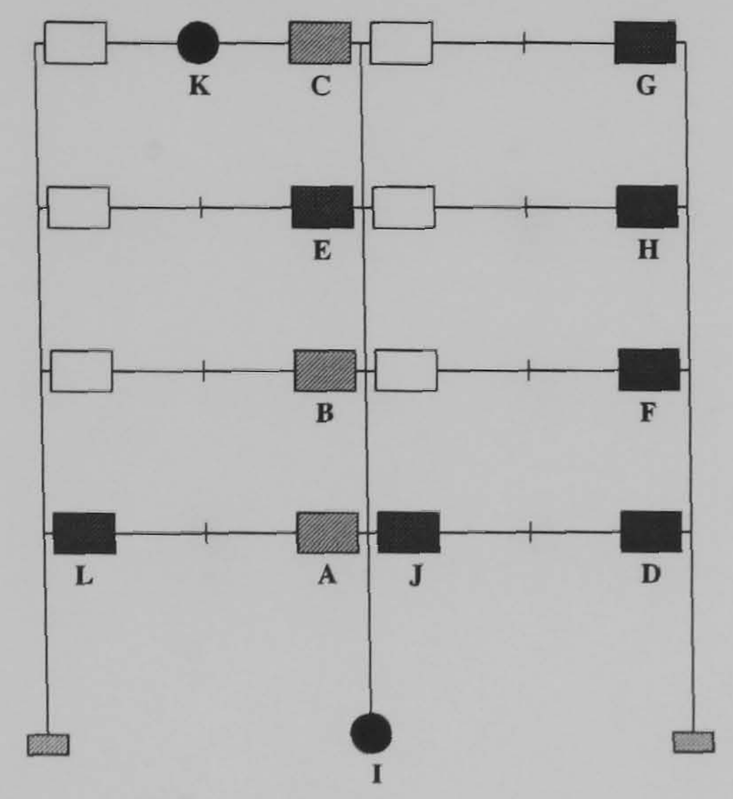

S-R (2) Including web shear at the internal columns

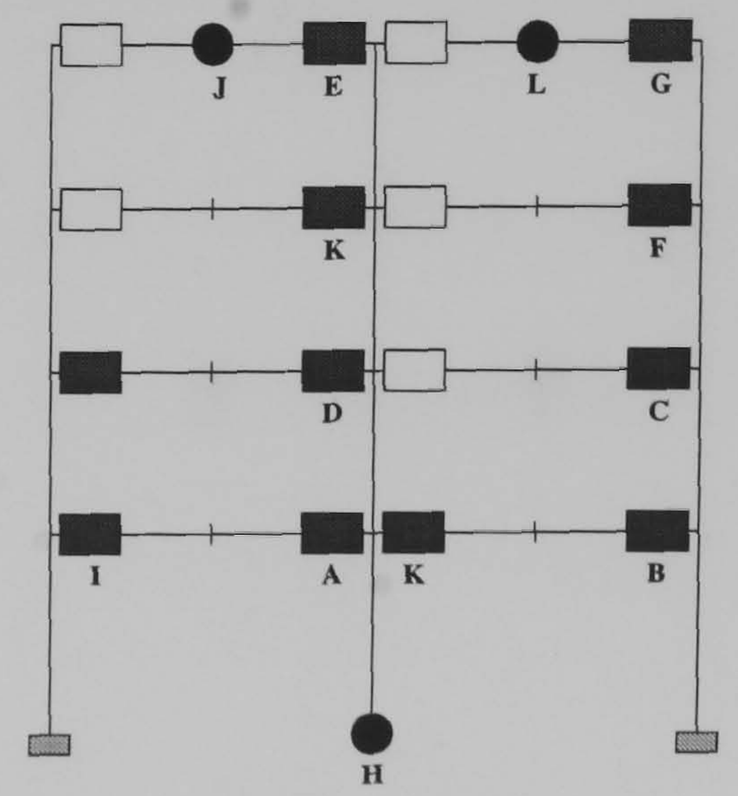

Rigid

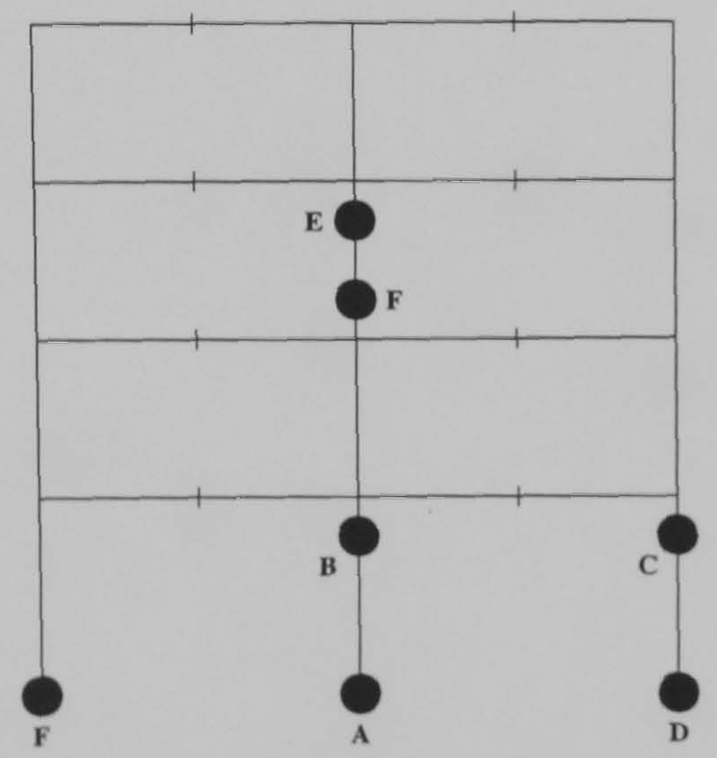

Hinge Location	Load Level at Hinge Formation S-R(1)	S-R(2)	Rigid
A	0.785	1.165	1.99
B	0.865	1.1875	2.08
C	0.985	1.265	2.24
D	1.195	1.2675	2.26
E	1.22	1.46	2.28
F	1.285	1.575	2.335
G	1.58	1.5775	N/A
H	1.6	1.757	N/A
I	1.77	1.865	N/A
J	1.8175	1.88	N/A
K	1.875	1.895	N/A
L	1.9	1.912	N/A

Key :

Semi-Rigid Connection

Plastification prior to ULS design load being attained

Plastification following the attainment of the design load

Member plastification

FRAME : **f22 b24**
Load Case 3

S-R (1) Negelecting web shear at the internal columns

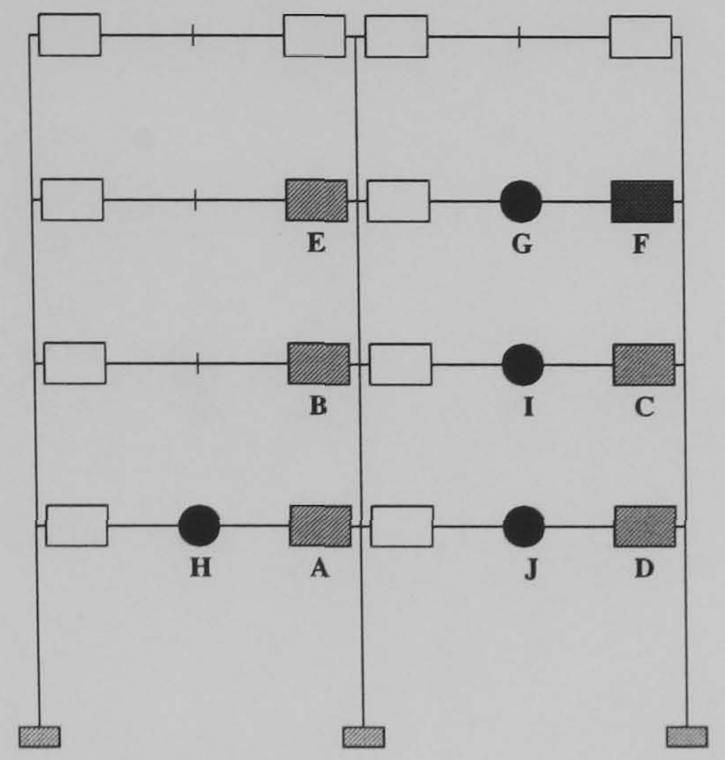

S-R (2) Including web shear at the internal columns

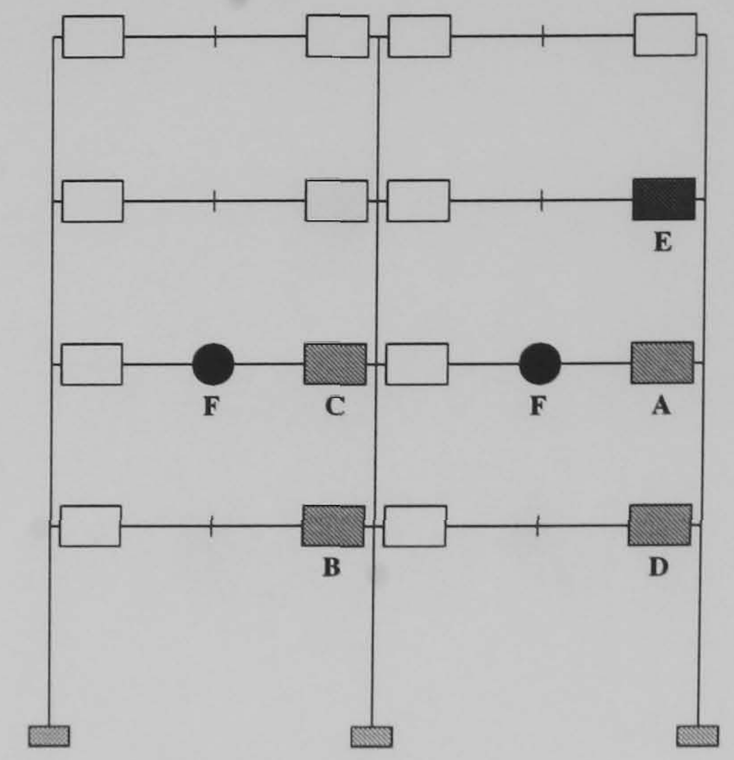

Rigid

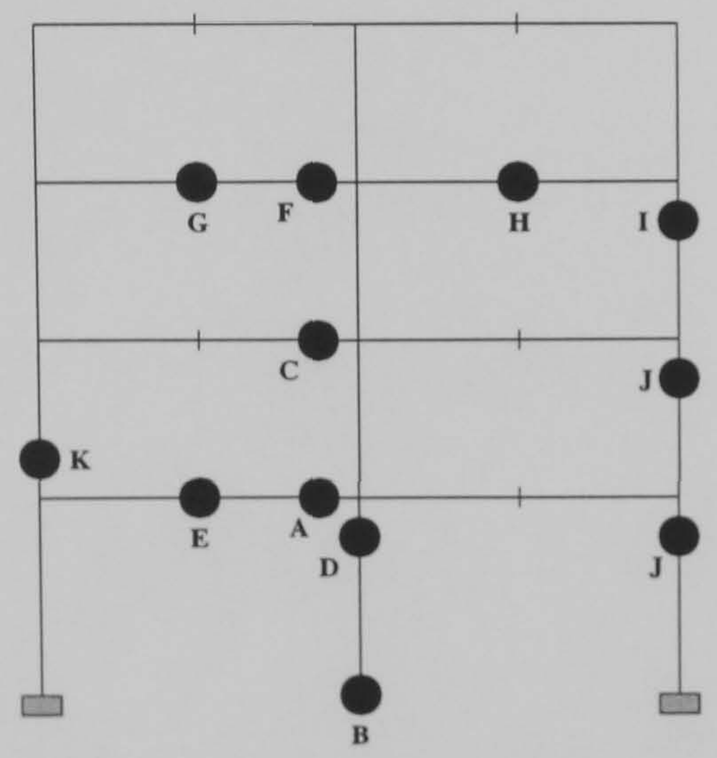

Hinge Location	Load Level at Hinge Formation S-R(1)	S-R(2)	Rigid
A	**0.6075**	**0.795**	**1.575**
B	**0.615**	**0.805**	**1.642**
C	**0.7875**	**0.81**	**1.68**
D	**0.8025**	**0.8175**	**1.69**
E	**0.8475**	**1.025**	**1.702**
F	**1.025**	**1.115**	**1.717**
G	**1.11**	**N/A**	**1.722**
H	**1.112**	**N/A**	**1.735**
I	**1.115**	**N/A**	**1.742**
J	**1.117**	**N/A**	**1.747**
K	**N/A**	**N/A**	**1.75**

Key :

- Semi-Rigid Connection
- Plastification prior to ULS design load being attained
- Plastification following the attainment of the design load
- Member plastification

FRAME : **f23 b20**
Load Case 1

S-R (1) Negelecting web shear at the internal columns

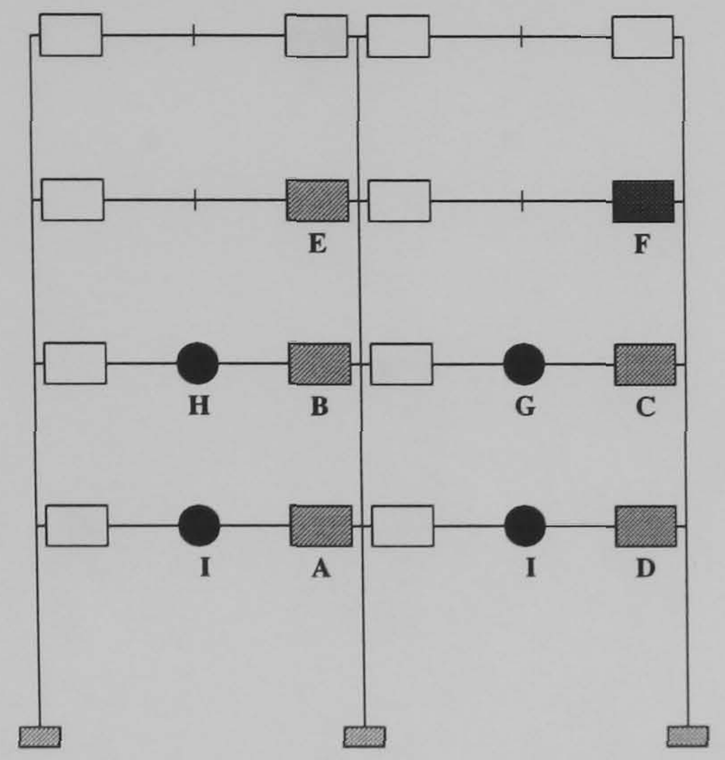

S-R (2) Including web shear at the internal columns

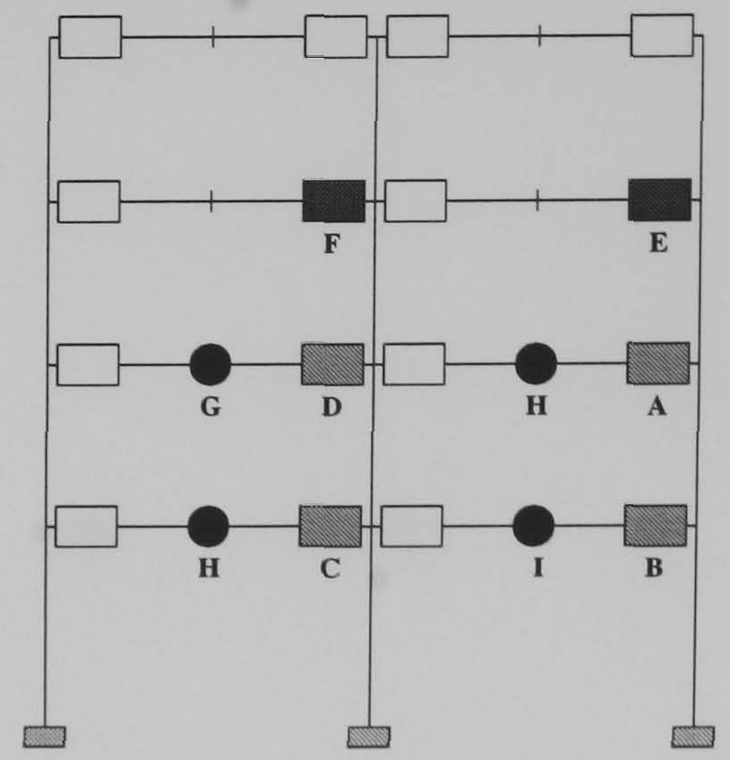

Rigid

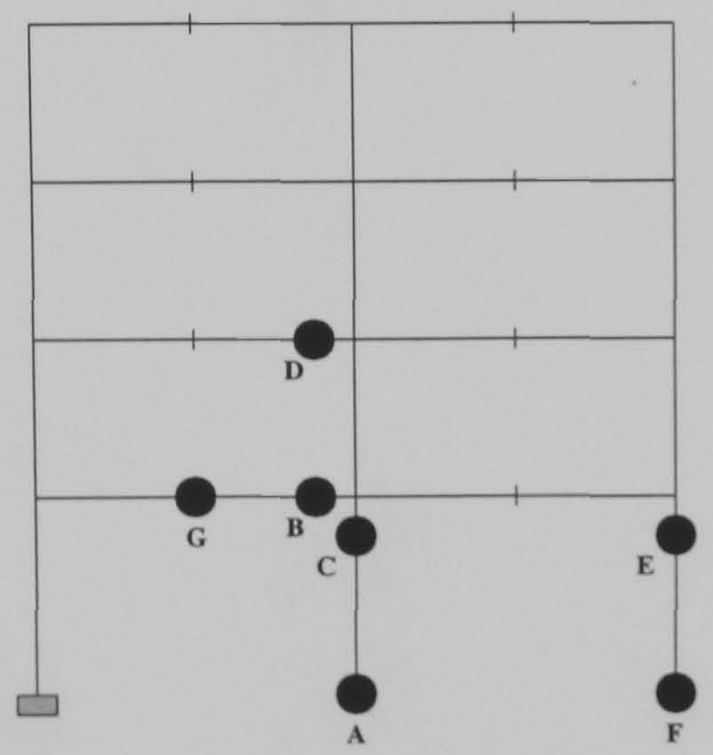

Hinge Location	Load Level at Hinge Formation S-R(1)	S-R(2)	Rigid
A	0.6675	0.8425	1.8
B	0.6825	0.86	1.825
C	0.845	0.8625	1.86
D	0.855	0.8725	1.977
E	0.95	1.0975	1.982
F	1.115	1.2325	2.012
G	1.337	1.337	2.02
H	1.34	1.34	N/A
I	1.342	1.342	N/A

Key :

Semi-Rigid Connection

Plastification prior to ULS design load being attained

Plastification following the attainment of the design load

Member plastification

FRAME : **f23 b20**
Load Case 2

S-R (1) Negelecting web shear at the internal columns

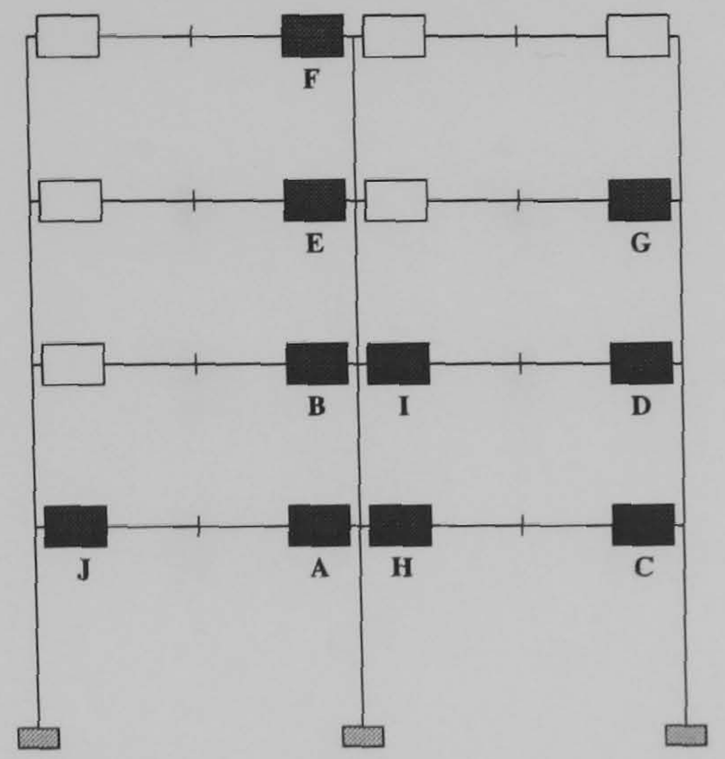

S-R (2) Including web shear at the internal columns

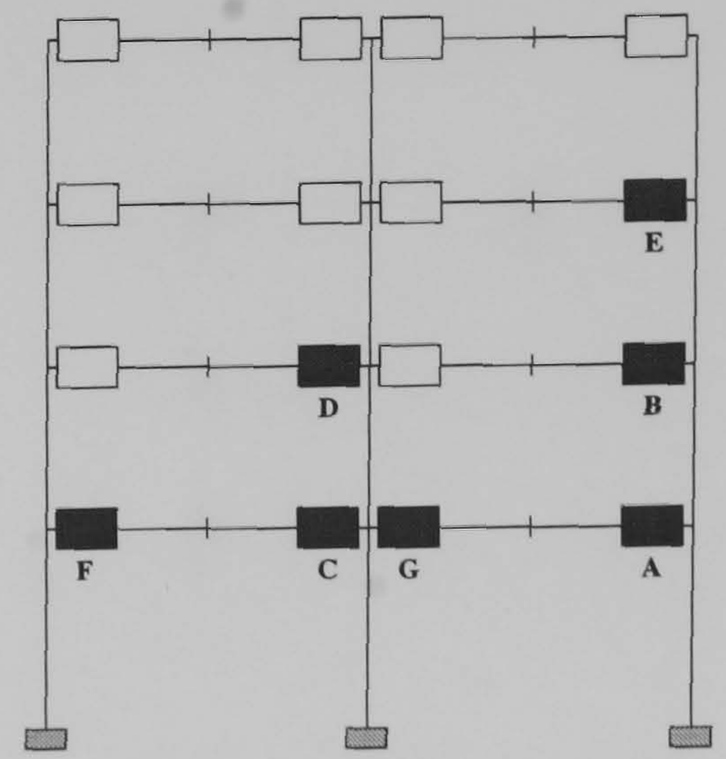

Rigid

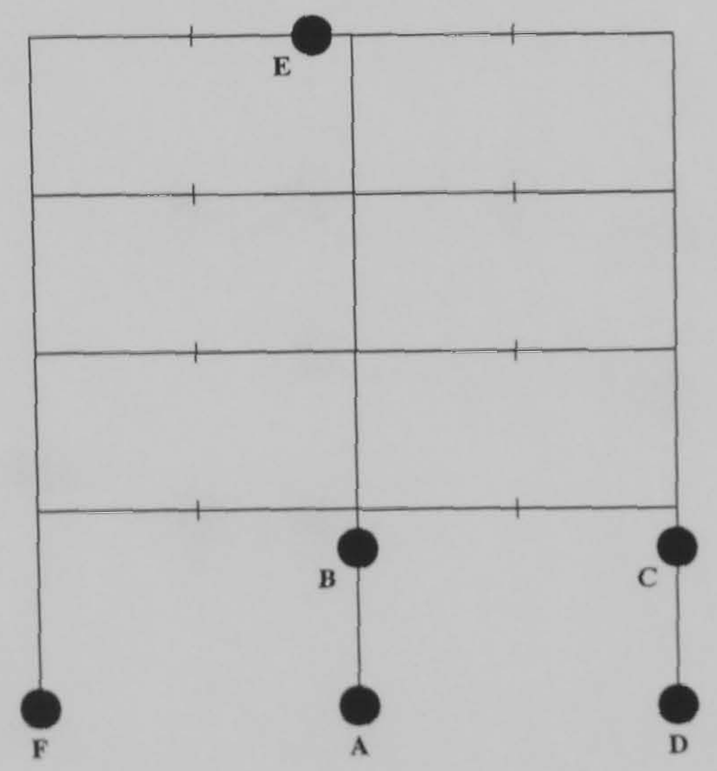

Hinge Location	Load Level at Hinge Formation S-R(1)	S-R(2)	Rigid
A	1.0575	1.27	2.485
B	1.115	1.2825	2.607
C	1.2925	1.315	2.81
D	1.315	1.3575	2.815
E	1.6075	1.6675	2.852
F	1.7225	1.8975	2.867
G	1.7375	1.9075	N/A
H	1.85	N/A	N/A
I	1.8875	N/A	N/A
J	1.9175	N/A	N/A

Key :

- Plastification prior to ULS design load being attained
- Semi-Rigid Connection
- Plastification following the attainment of the design load
- Member plastification

FRAME : **f23 b20**
Load Case 3

S-R (1) Negelecting web shear at the internal columns

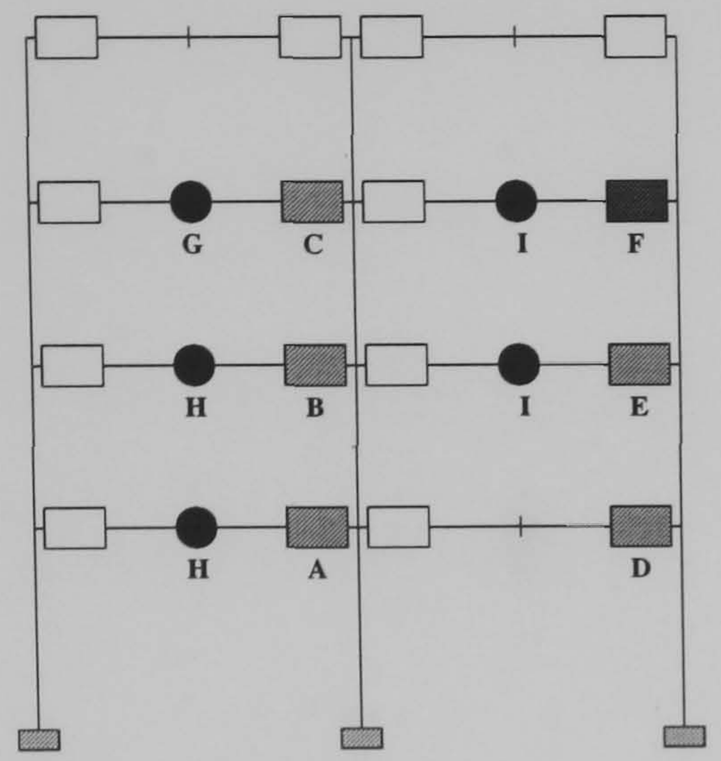

S-R (2) Including web shear at the internal columns

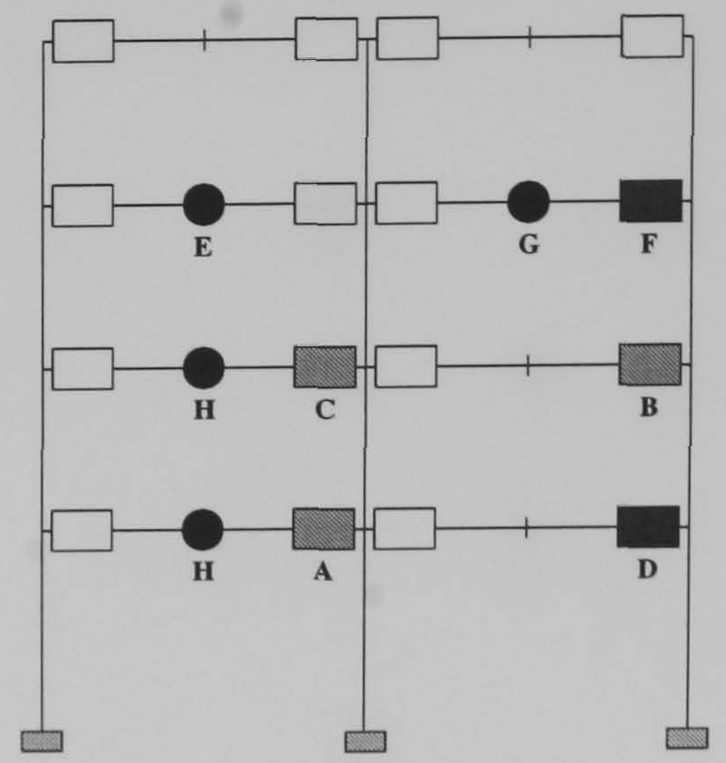

Rigid

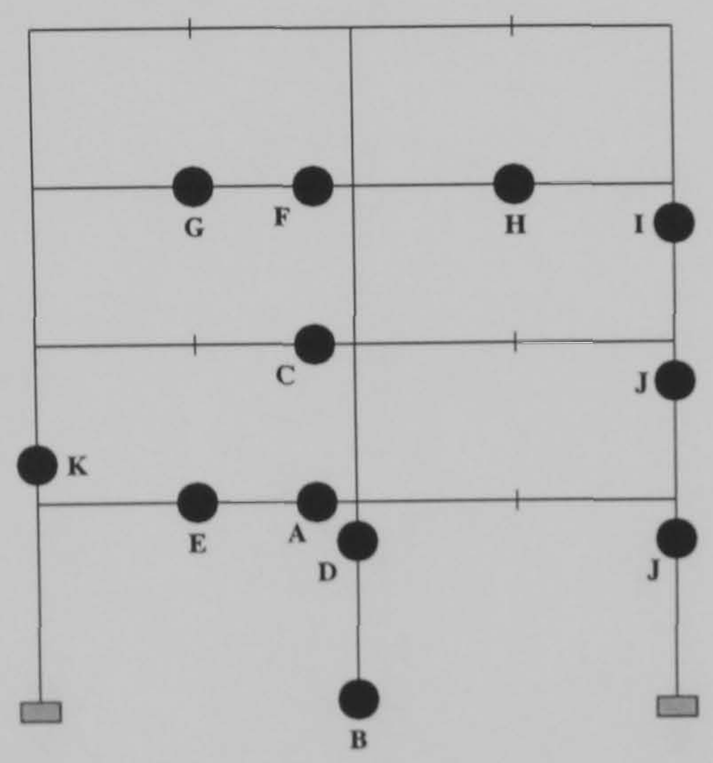

Hinge Location	Load Level at Hinge Formation S-R(1)	S-R(2)	Rigid
A	**0.62**	**0.98**	**1.575**
B	**0.6325**	**0.9875**	**1.642**
C	**0.905**	**0.995**	**1.68**
D	**0.975**	**1.0075**	**1.69**
E	**0.96**	**1.157**	**1.702**
F	**1.165**	**1.17**	**1.717**
G	**1.17**	**1.175**	**1.722**
H	**1.172**	**1.182**	**1.735**
I	**1.182**	**N/A**	**1.742**
J	**N/A**	**N/A**	**1.747**
K	**N/A**	**N/A**	**1.75**

Key :

Semi-Rigid Connection

Plastification prior to ULS design load being attained

Plastification following the attainment of the design load

Member plastification

FRAME : **f23 b24**

Load Case 1

S-R (1) Negelecting web shear at the internal columns

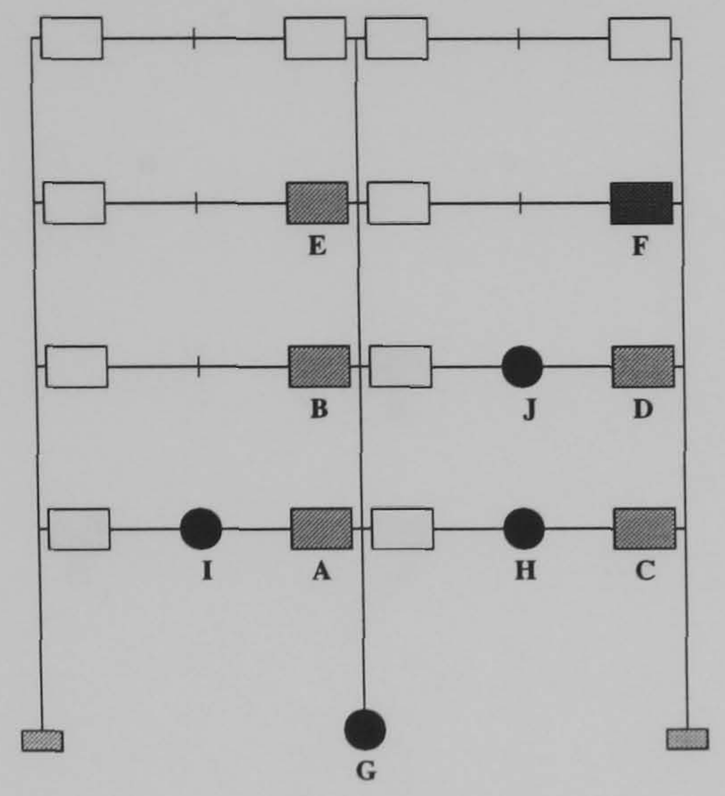

S-R (2) Including web shear at the internal columns

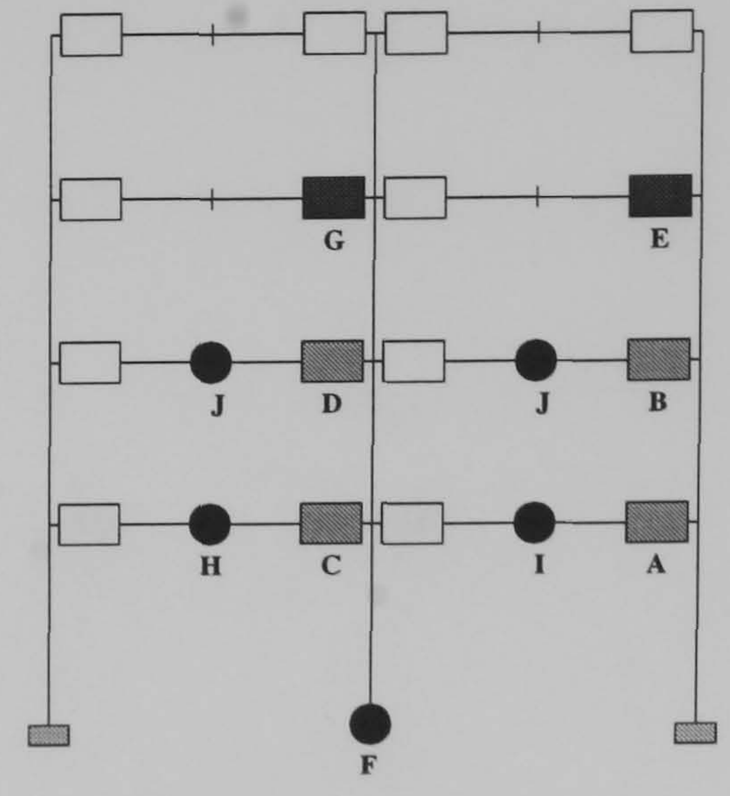

Rigid

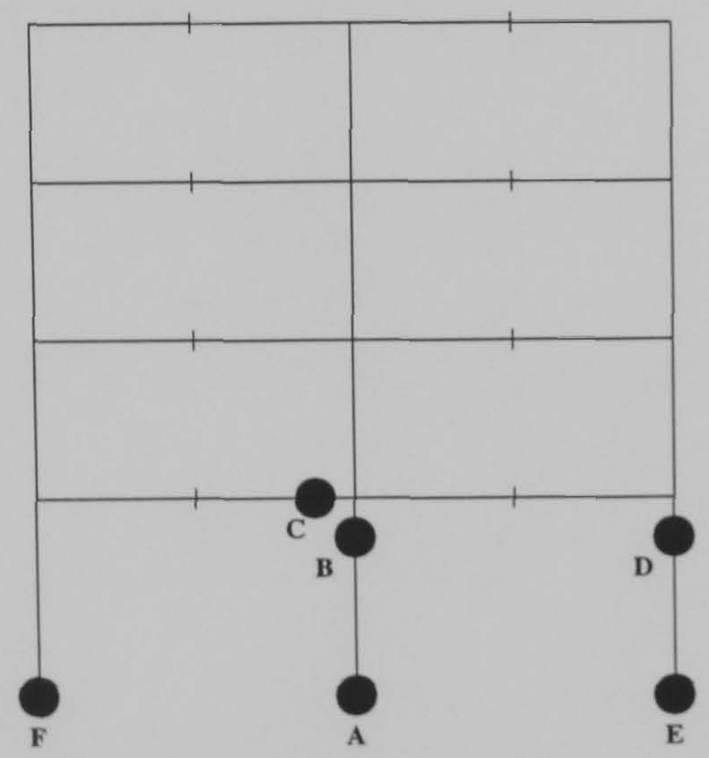

Hinge Location	Load Level at Hinge Formation		
	S-R(1)	S-R(2)	Rigid
A	0.585	0.85	1.482
B	0.6225	0.865	1.557
C	0.855	0.8675	1.605
D	0.8775	0.9025	1.657
E	0.92	1.0725	1.67
F	1.1025	1.222	1.707
G	1.232	1.235	N/A
H	1.305	1.302	N/A
I	1.312	1.31	N/A
J	1.315	1.312	N/A

Key :

Semi-Rigid Connection

Plastification prior to ULS design load being attained

Plastification following the attainment of the design load

Member plastification

FRAME : **f23 b24**

Load Case 2

S-R (1) Negelecting web shear at the internal columns

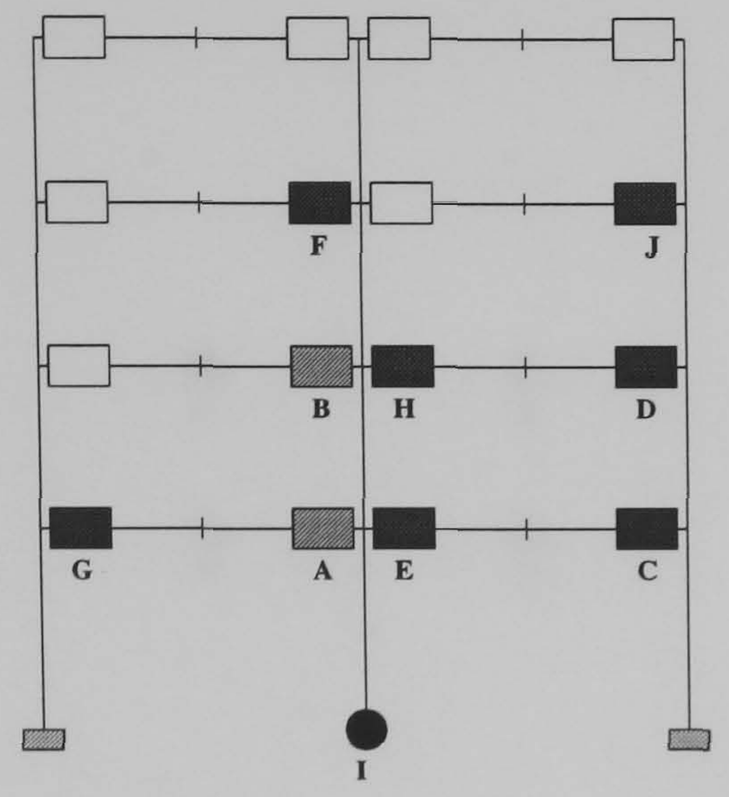

S-R (2) Including web shear at the internal columns

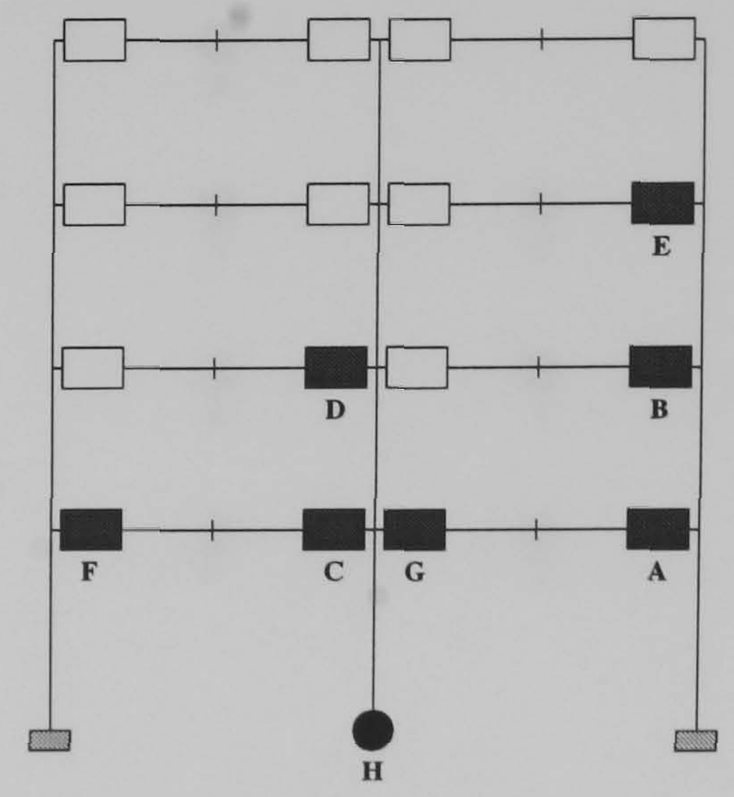

Rigid

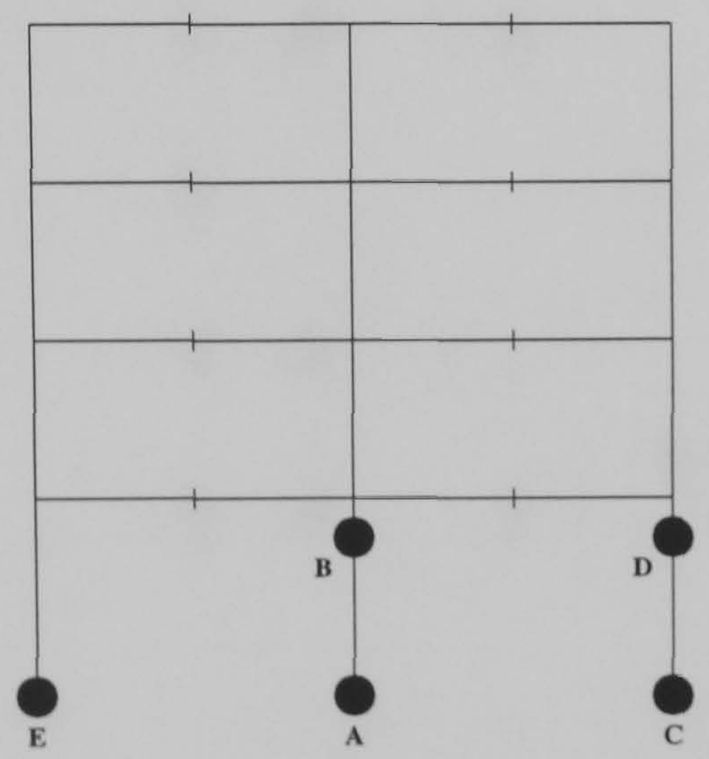

Hinge Location	Load Level at Hinge Formation		
	S-R(1)	S-R(2)	Rigid
A	0.8525	1.1175	1.862
B	0.9475	1.18	2.007
C	1.1575	1.185	2.107
D	1.235	1.27	2.135
E	1.4225	1.485	2.177
F	1.445	1.4925	N/A
G	1.5375	1.515	N/A
H	1.5475	1.532	N/A
I	1.553	N/A	N/A
J	1.56	N/A	N/A

Key :

- Semi-Rigid Connection
- Plastification prior to ULS design load being attained
- Plastification following the attainment of the design load
- Member plastification

FRAME : **f23 b24**
Load Case 3

S-R (1) Negelecting web shear at the internal columns

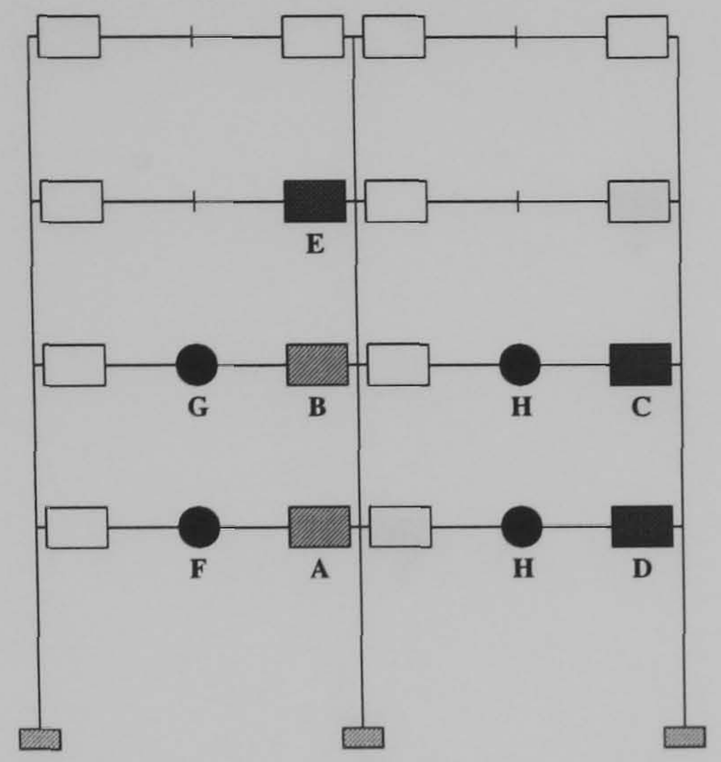

S-R (2) Including web shear at the internal columns

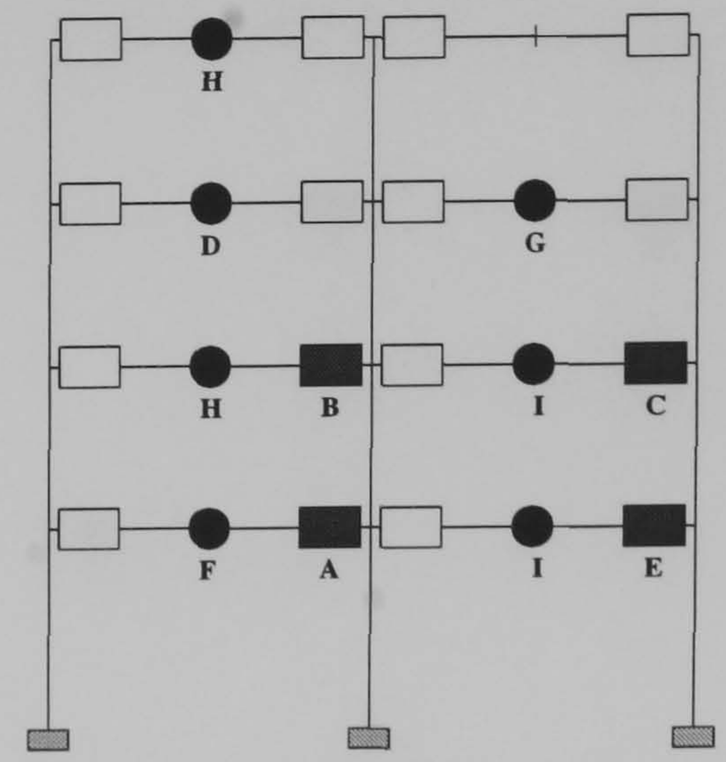

Rigid

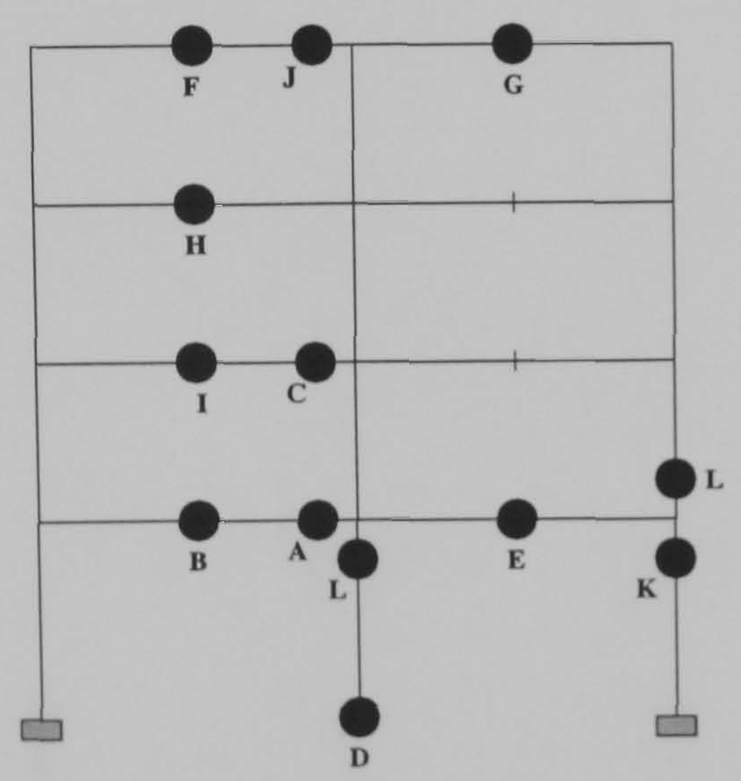

Hinge Location	Load Level at Hinge Formation		
	S-R(1)	S-R(2)	Rigid
A	0.935	1.1725	1.655
B	0.9575	1.195	1.82
C	1.2025	1.21	1.832
D	1.225	1.232	1.845
E	1.235	1.2375	1.857
F	1.242	1.242	1.862
G	1.247	1.245	1.865
H	1.252	1.25	1.885
I	N/A	1.252	1.897
J	N/A	N/A	1.9
K	N/A	N/A	1.902
L	N/A	N/A	1.905

Key :

- Plastification prior to ULS design load being attained
- Semi-Rigid Connection
- Plastification following the attainment of the design load
- Member plastification

FRAME : **f24 b20**
Load Case 1

S-R (1) Negelecting web shear at the internal columns

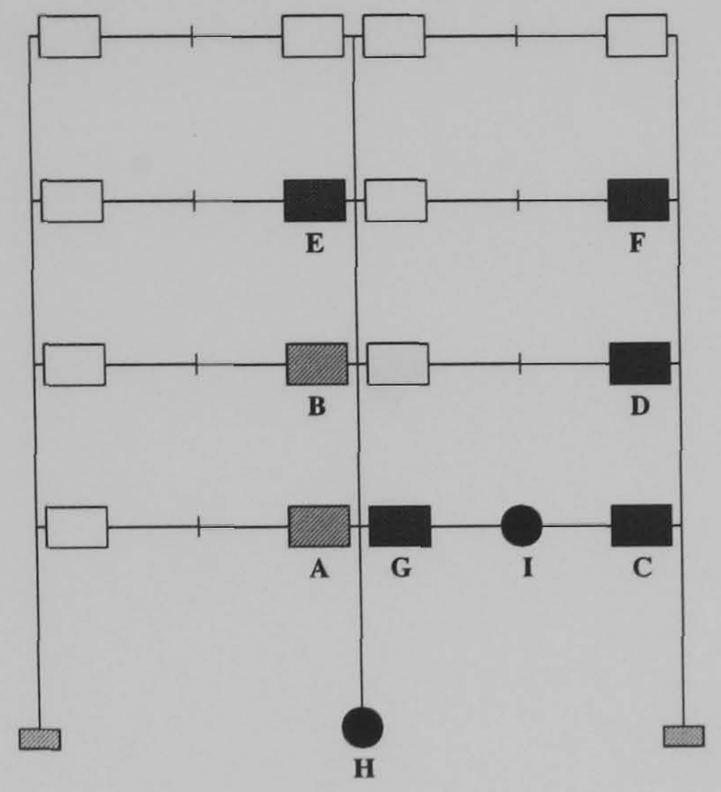

S-R (2) Including web shear at the internal columns

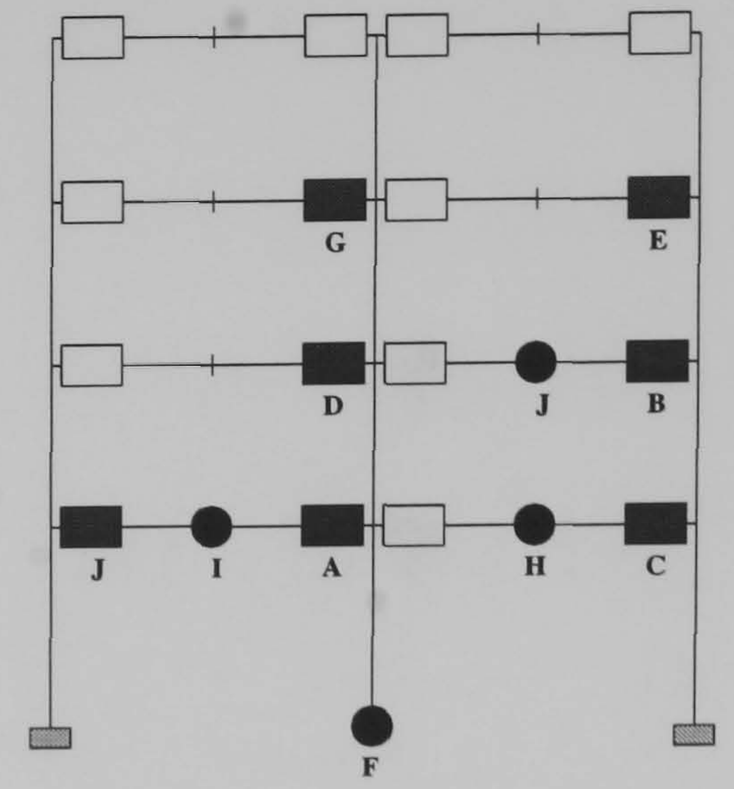

Rigid

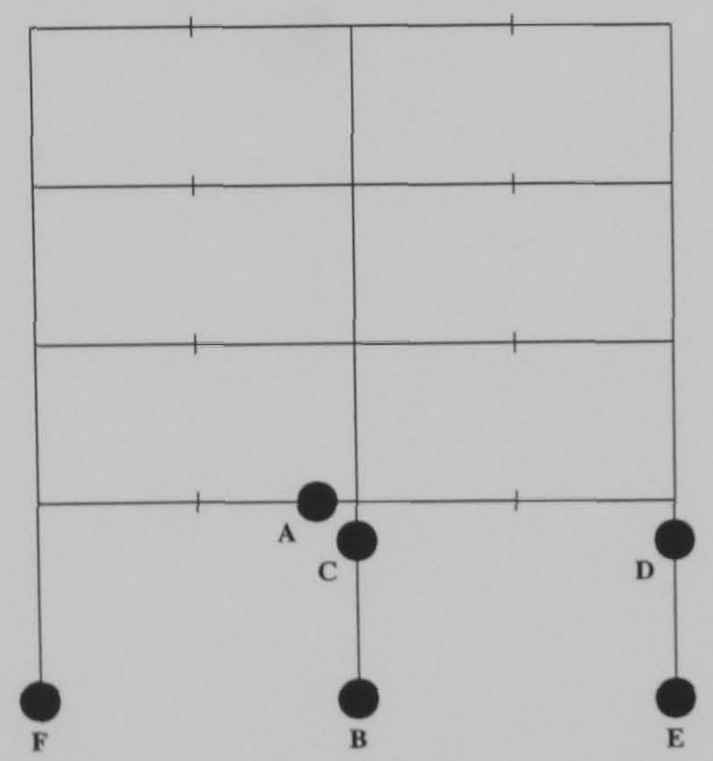

Hinge Location	Load Level at Hinge Formation S-R(1)	S-R(2)	Rigid
A	0.83	1.0125	1.675
B	0.8675	1.0425	1.762
C	1.055	1.0475	1.887
D	1.06	1.05	1.897
E	1.165	1.2075	1.91
F	1.2475	1.36	1.925
G	1.365	1.3625	N/A
H	1.375	1.38	N/A
I	1.377	1.382	N/A
J	N/A	1.385	N/A

Key :

- Semi-Rigid Connection
- Plastification prior to ULS design load being attained
- Plastification following the attainment of the design load
- Member plastification

FRAME : **f24 b20**
Load Case 2

S-R (1) Negelecting web shear at the internal columns

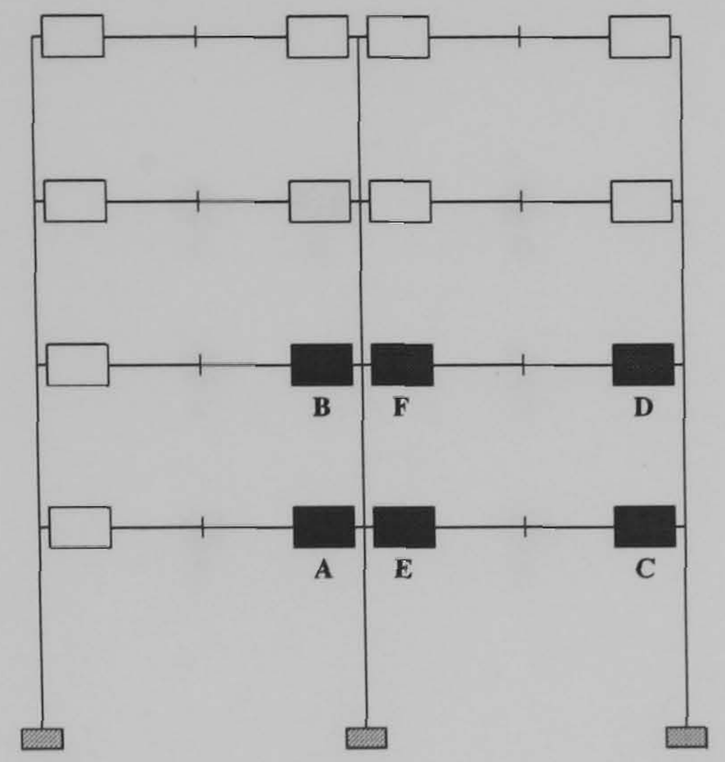

S-R (2) Including web shear at the internal columns

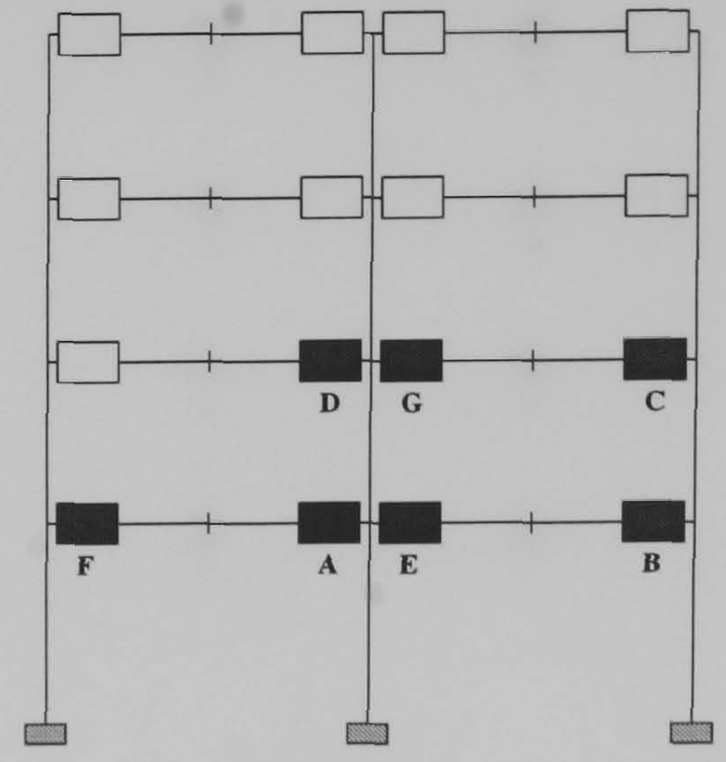

Rigid

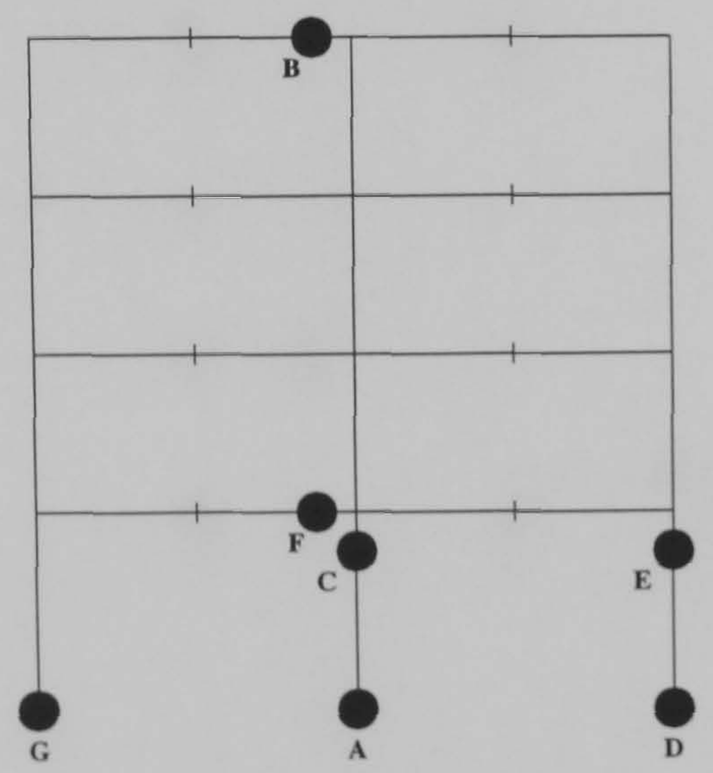

Hinge Location	Load Level at Hinge Formation S-R(1)	S-R(2)	Rigid
A	1.1175	1.33	2.255
B	1.2	1.34	2.337
C	1.37	1.3675	2.432
D	1.4175	1.4	2.472
E	1.43	1.495	2.492
F	1.51	1.5225	2.52
G	N/A	1.5475	2.53

Key :

- Plastification prior to ULS design load being attained
- Semi-Rigid Connection
- Plastification following the attainment of the design load
- Member plastification

FRAME : **f24 b20**
Load Case 3

S-R (1) Negelecting web shear at the internal columns

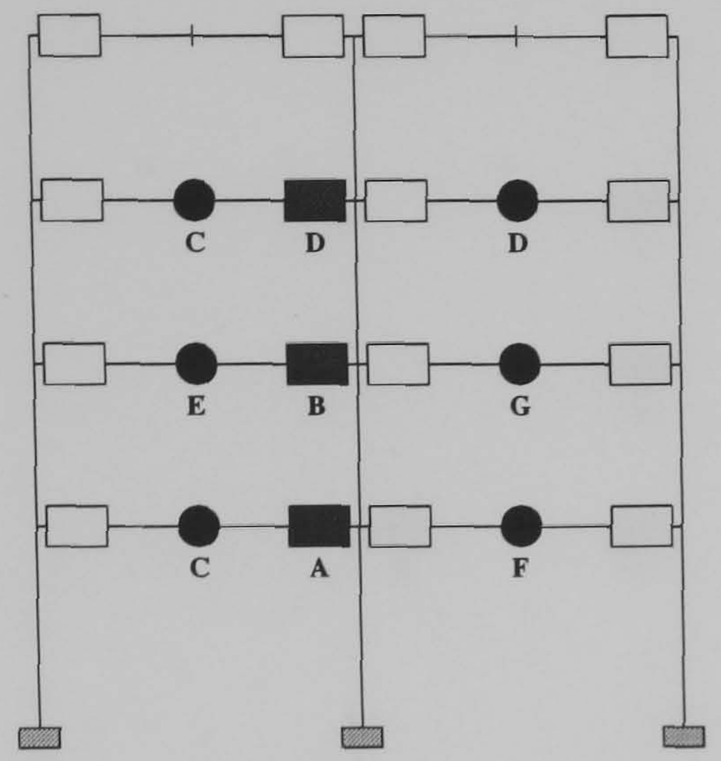

S-R (2) Including web shear at the internal columns

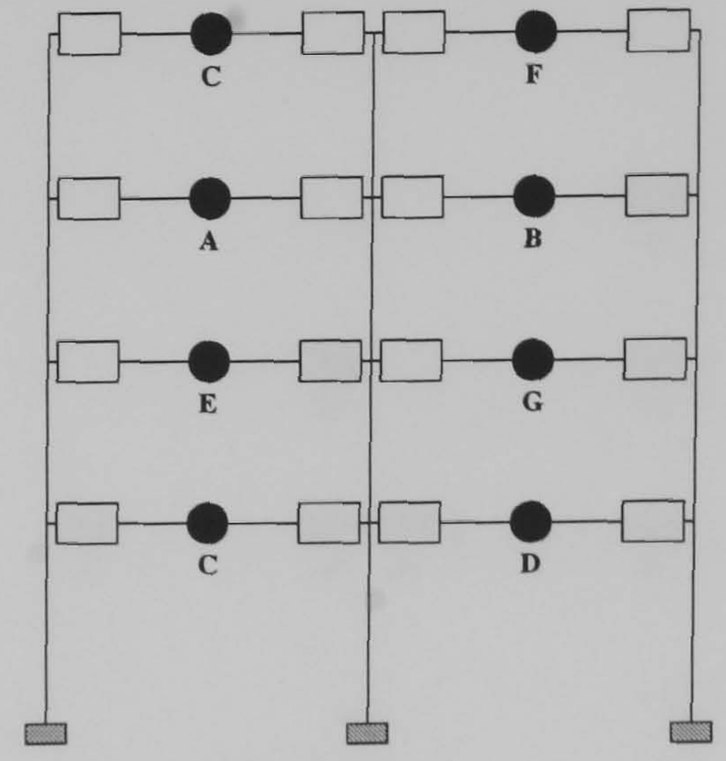

Rigid

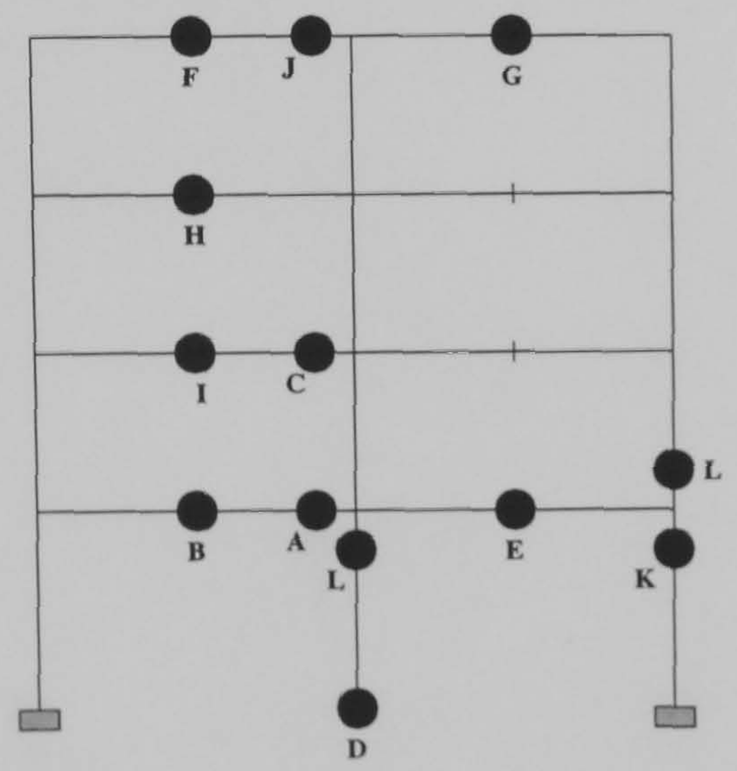

Hinge Location	Load Level at Hinge Formation		
	S-R(1)	S-R(2)	Rigid
A	1.0575	1.262	1.655
B	1.095	1.28	1.82
C	1.317	1.302	1.832
D	1.32	1.307	1.845
E	1.327	1.31	1.857
F	1.33	1.312	1.862
G	1.337	1.317	1.865
H	N/A	N/A	1.885
I	N/A	N/A	1.897
J	N/A	N/A	1.9
K	N/A	N/A	1.902
L	N/A	N/A	1.905

Key :

- Plastification prior to ULS design load being attained
- Semi-Rigid Connection
- Plastification following the attainment of the design load
- Member plastification

FRAME : **f24 b24**
Load Case 1

S-R (1) Negelecting web shear at the internal columns

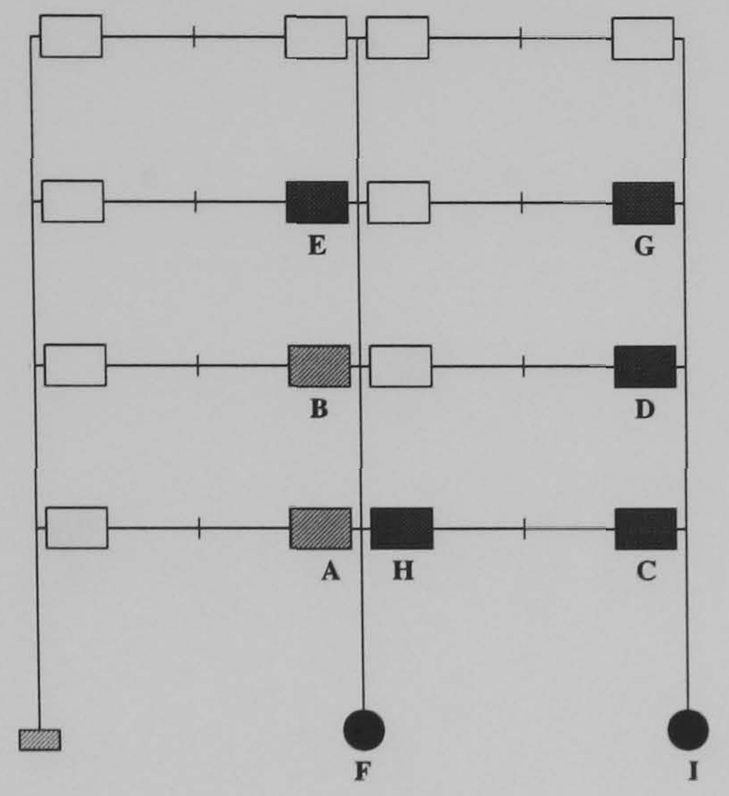

S-R (2) Including web shear at the internal columns

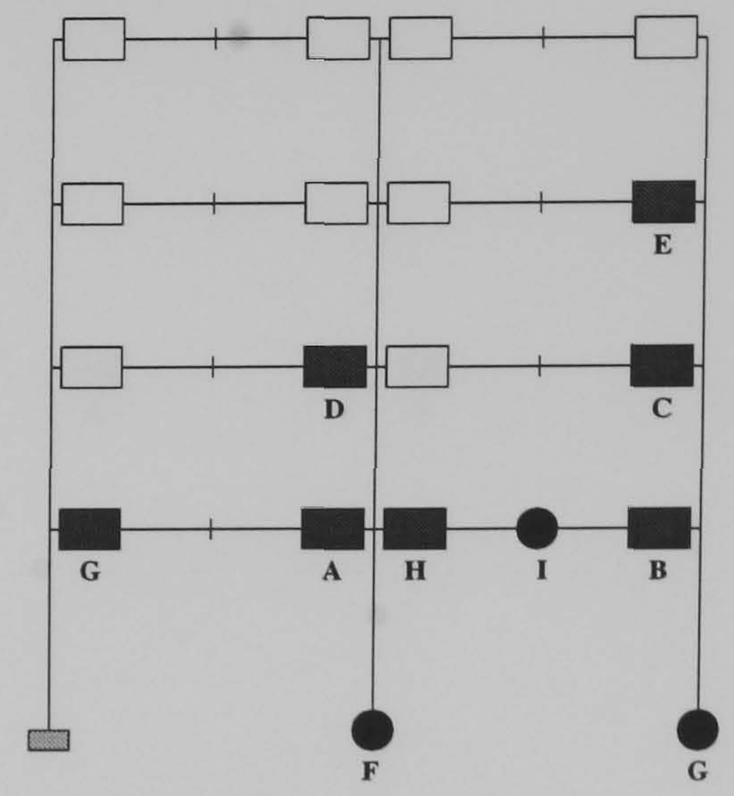

Rigid

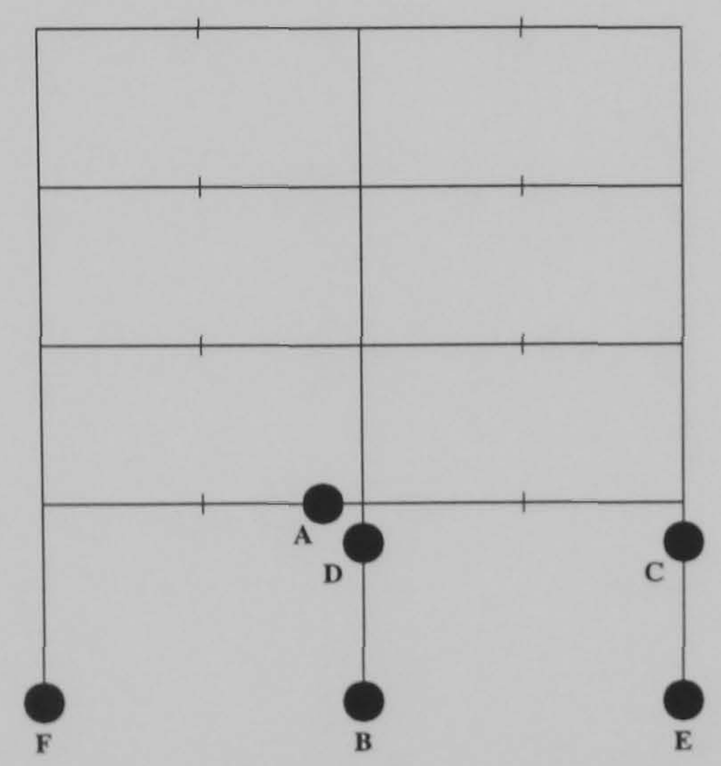

Hinge Location	Load Level at Hinge Formation S-R(1)	S-R(2)	Rigid
A	**0.8325**	**1.0675**	**1.485**
B	**0.9025**	**1.0925**	**1.525**
C	**1.1075**	**1.1175**	**1.655**
D	**1.1475**	**1.135**	**1.657**
E	**1.175**	**1.235**	**1.66**
F	**1.27**	**1.257**	**1.69**
G	**1.2875**	**1.345**	**N/A**
H	**1.3375**	**1.3475**	**N/A**
I	**1.36**	**1.37**	**N/A**

Key :

- Semi-Rigid Connection
- Plastification prior to ULS design load being attained
- Plastification following the attainment of the design load
- Member plastification

FRAME : **f24 b24**
Load Case 2

S-R (1) Negelecting web shear at the internal columns

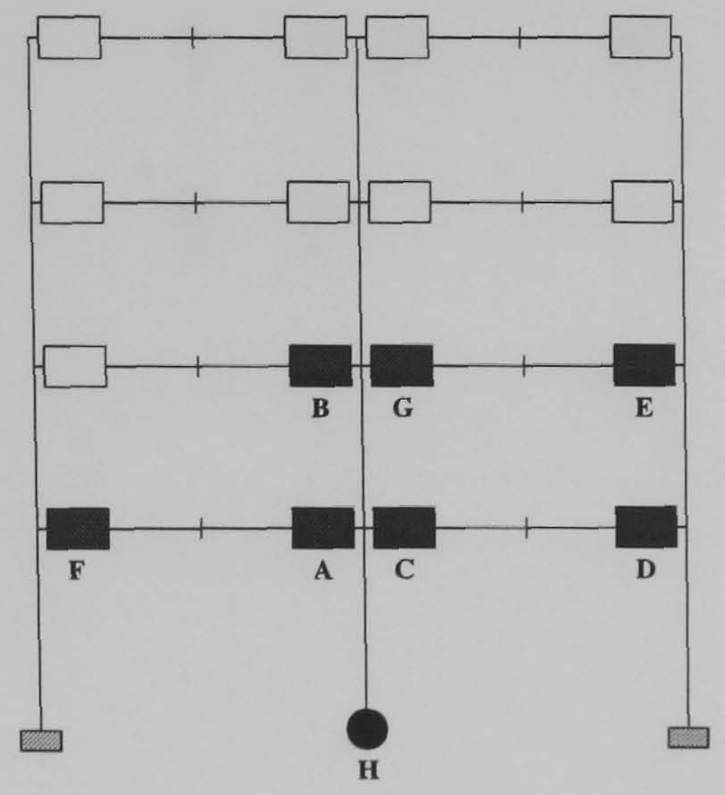

S-R (2) Including web shear at the internal columns

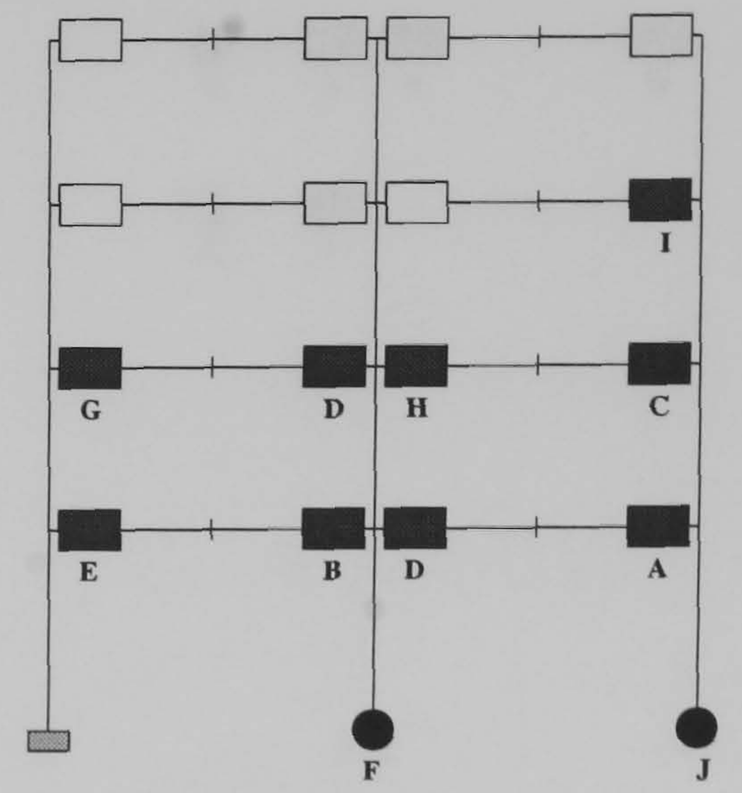

Rigid

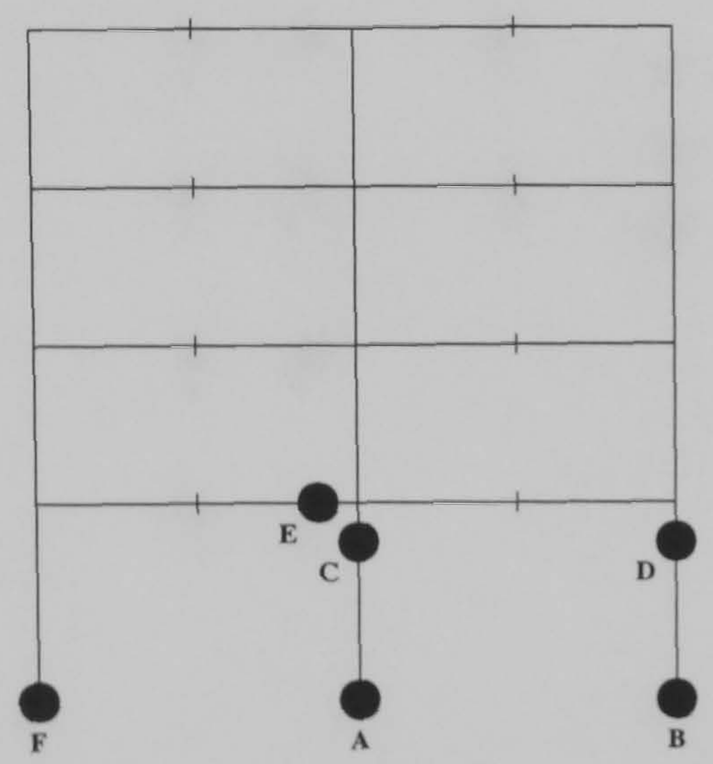

Hinge Location	Load Level at Hinge Formation S-R(1)	S-R(2)	Rigid
A	1.07	1.32	1.84
B	1.2025	1.3325	2.02
C	1.35	1.3975	2.022
D	1.365	1.4475	2.055
E	1.4475	1.46	2.072
F	1.495	1.49	2.087
G	1.4975	1.5075	N/A
H	1.505	1.5125	N/A
I	N/A	1.5175	N/A
J	N/A	1.52	N/A

Key :

- Semi-Rigid Connection
- Plastification prior to ULS design load being attained
- Plastification following the attainment of the design load
- Member plastification

FRAME : **f24 b24**
Load Case 3

S-R (1) Negelecting web shear at the internal columns

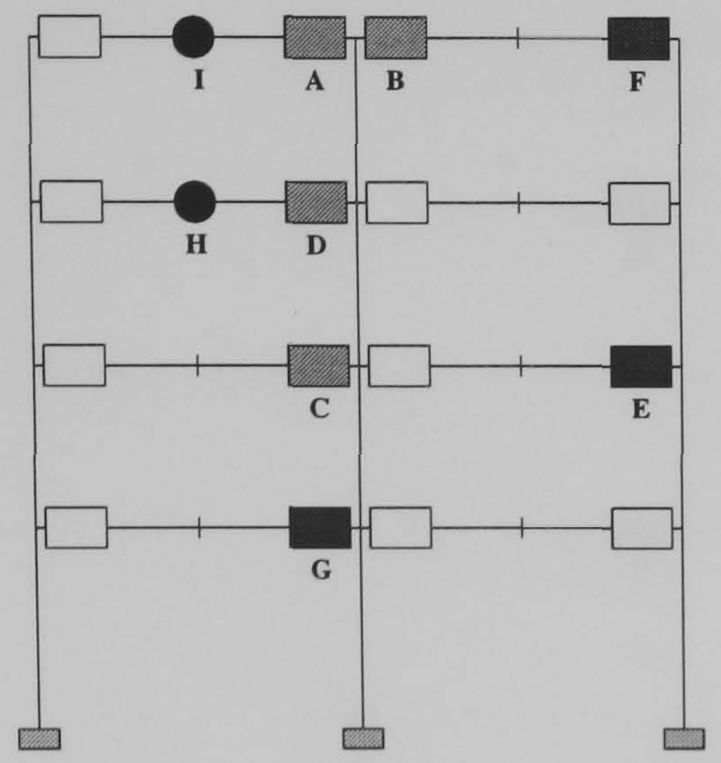

S-R (2) Including web shear at the internal columns

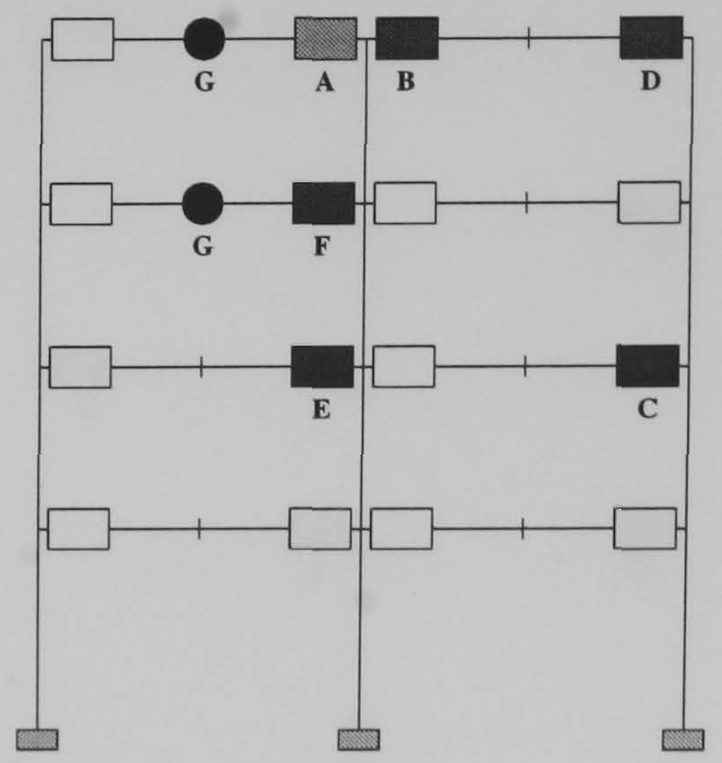

Rigid

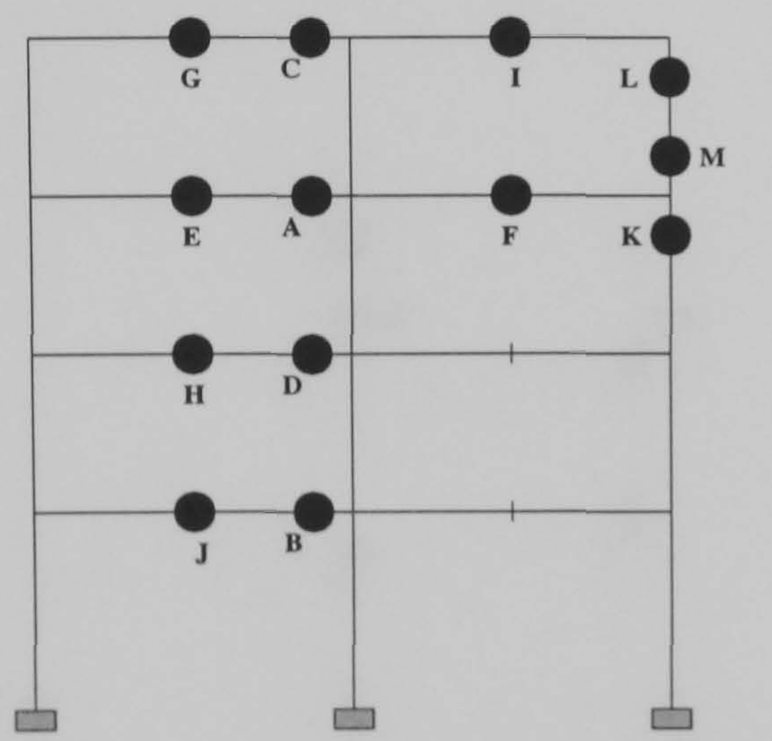

Hinge Location	Load Level at Hinge Formation		
	S-R(1)	S-R(2)	Rigid
A	**0.7425**	**0.9475**	**1.727**
B	**0.7925**	**1.015**	**1.787**
C	**0.885**	**1.1375**	**1.792**
D	**0.9775**	**1.18**	**1.802**
E	**1.16**	**1.1925**	**1.805**
F	**1.17**	**1.28**	**1.825**
G	**1.215**	**1.347**	**1.875**
H	**1.338**	N/A	**1.892**
I	**1.34**	N/A	**1.897**
J	N/A	N/A	**1.907**
K	N/A	N/A	**1.91**
L	N/A	N/A	**1.915**
M	N/A	N/A	**1.917**

Key :

- Semi-Rigid Connection
- Plastification prior to ULS design load being attained
- Plastification following the attainment of the design load
- Member plastification

FRAME : **f25 b24**
Load Case 1

S-R (1) Negelecting web shear at the internal columns

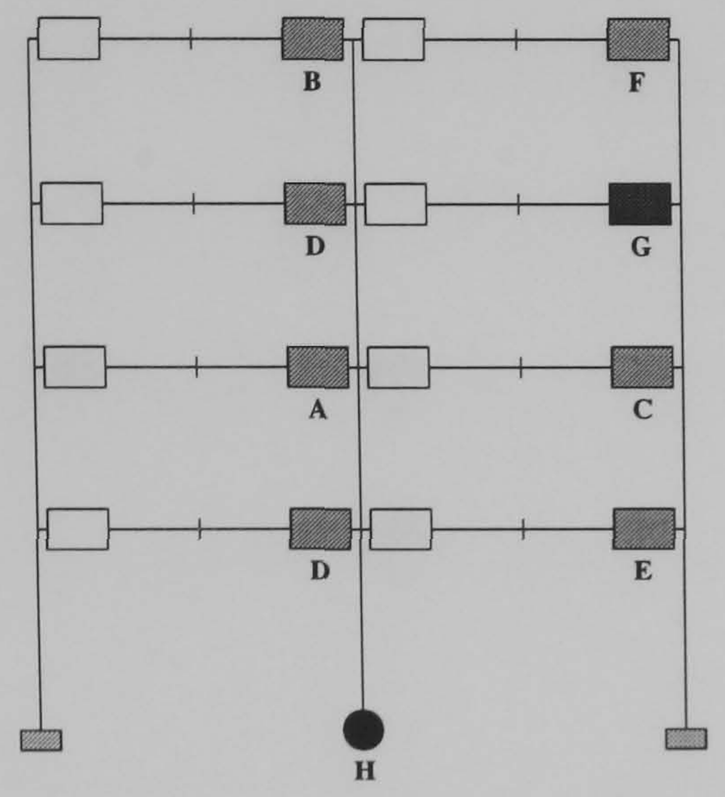

S-R (2) Including web shear at the internal columns

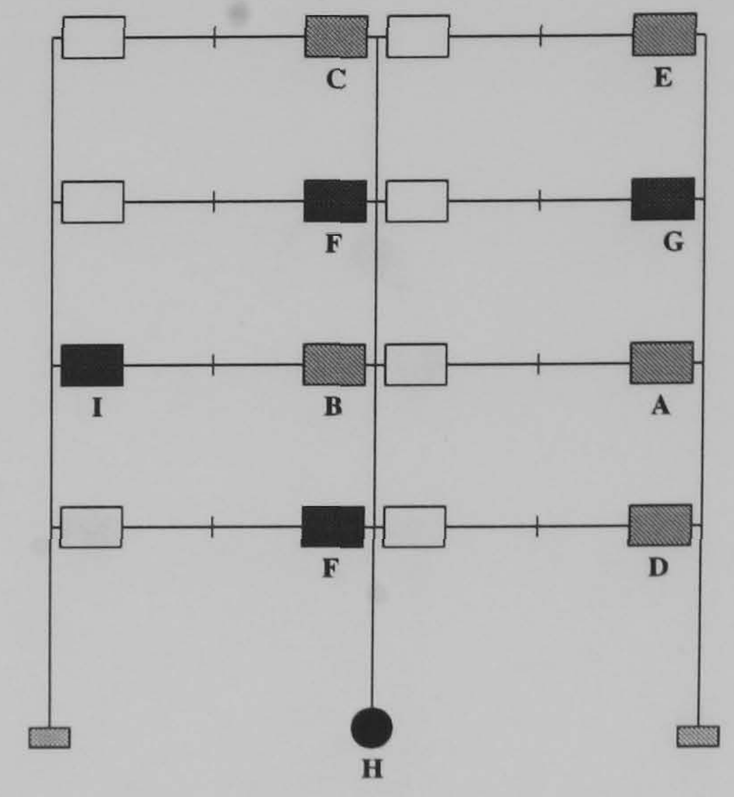

Rigid

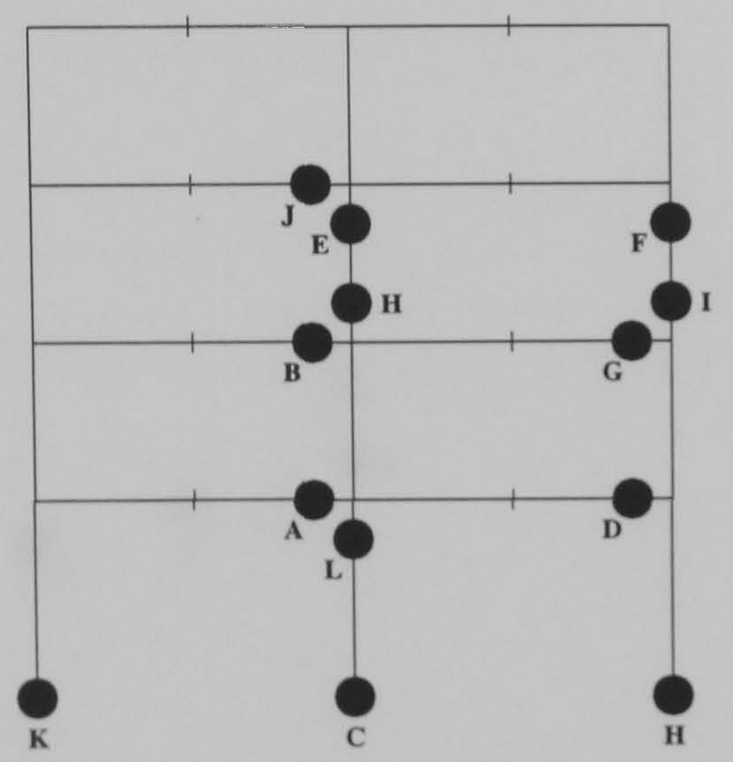

Hinge Location	Load Level at Hinge Formation		
	S-R(1)	S-R(2)	Rigid
A	**0.64**	**0.72**	**1.31**
B	**0.72**	**0.795**	**1.437**
C	**0.7625**	**0.885**	**1.452**
D	**0.83**	**0.9275**	**1.462**
E	**0.95**	**0.985**	**1.515**
F	**0.9875**	**1.0125**	**1.535**
G	**1.02**	**1.0175**	**1.592**
H	**1.175**	**1.162**	**1.602**
I	**N/A**	**1.2025**	**1.625**
J	**N/A**	**N/A**	**1.642**
K	**N/A**	**N/A**	**1.667**
L	**N/A**	**N/A**	**1.68**

Key :

Semi-Rigid Connection

Plastification prior to ULS design load being attained

Plastification following the attainment of the design load

Member plastification

FRAME : **f25 b24**
Load Case 2

S-R (1) Negelecting web shear at the internal columns

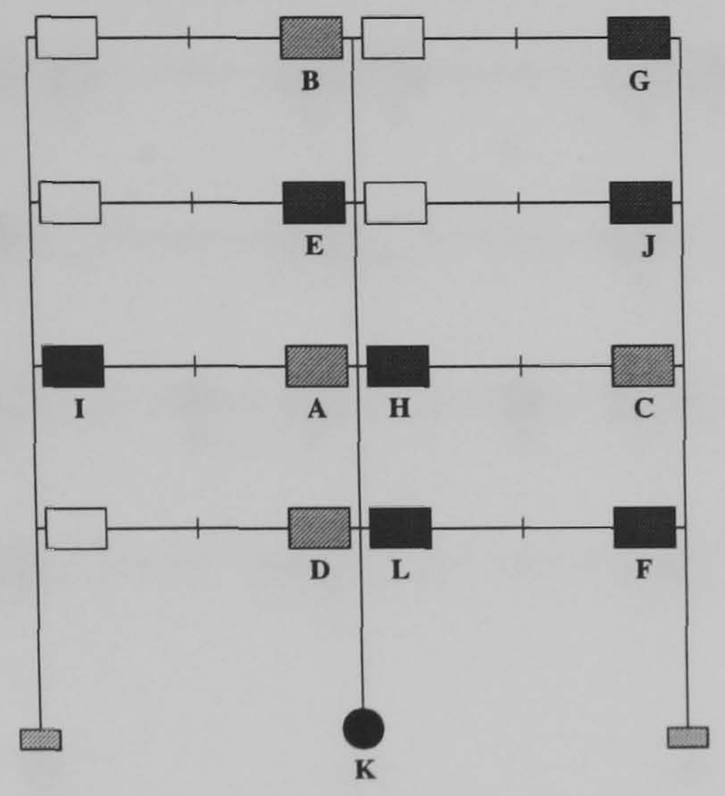

S-R (2) Including web shear at the internal columns

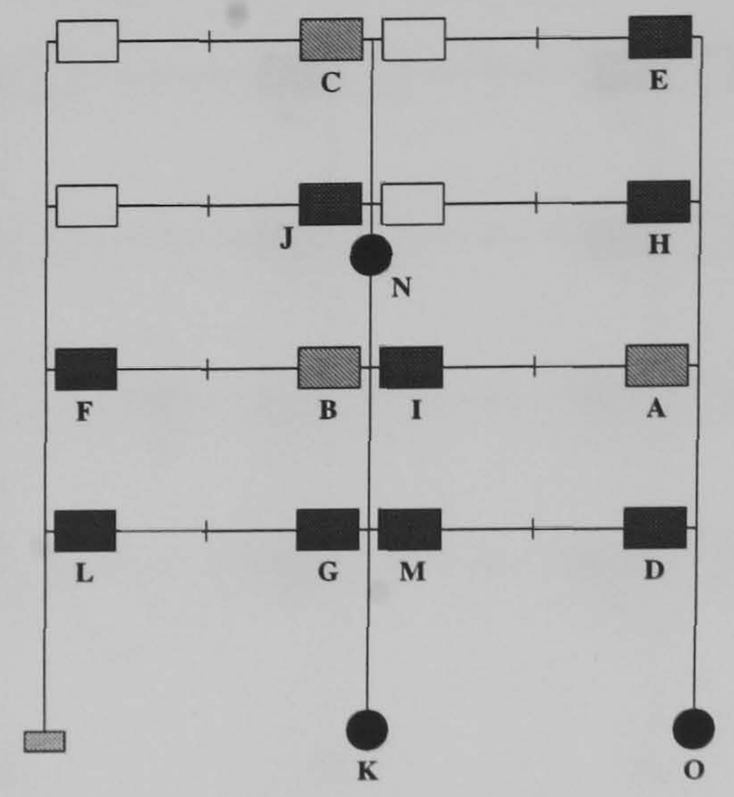

Rigid

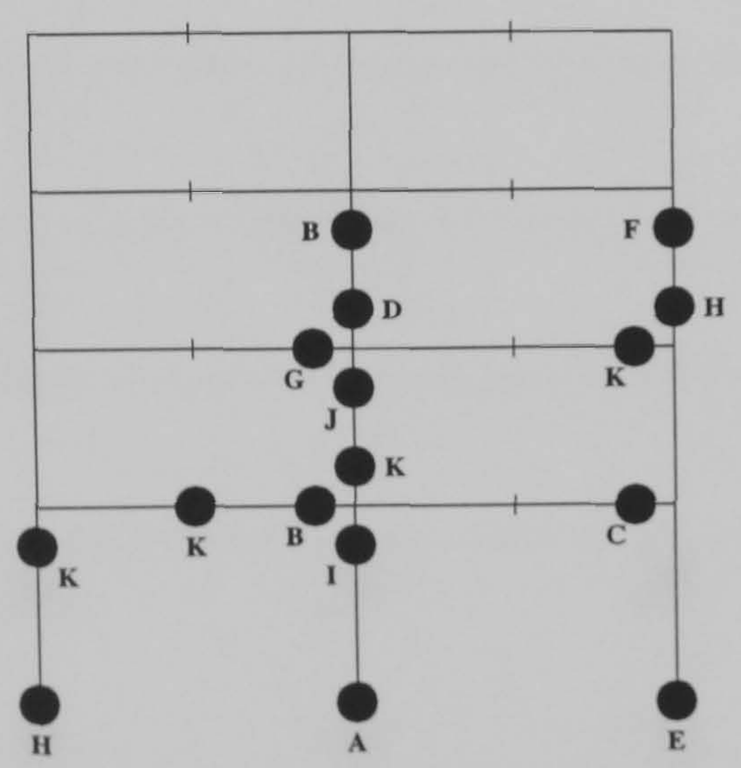

Hinge Location	Load Level at Hinge Formation S-R(1)	S-R(2)	Rigid
A	0.775	0.825	1.527
B	0.795	0.9325	1.602
C	0.88	0.97	1.667
D	0.98	1.055	1.707
E	1.0825	1.0875	1.725
F	1.0875	1.1275	1.737
G	1.1175	1.165	1.78
H	1.145	1.18	1.802
I	1.175	1.185	1.825
J	1.2	1.2275	1.832
K	1.245	1.235	1.835
L	1.2575	1.245	N/A
M	N/A	1.28	N/A
N	N/A	1.282	N/A
O	N/A	1.292	N/A

Key :

- Semi-Rigid Connection
- Plastification prior to ULS design load being attained
- Plastification following the attainment of the design load
- Member plastification

FRAME : **f25 b24**
Load Case 3

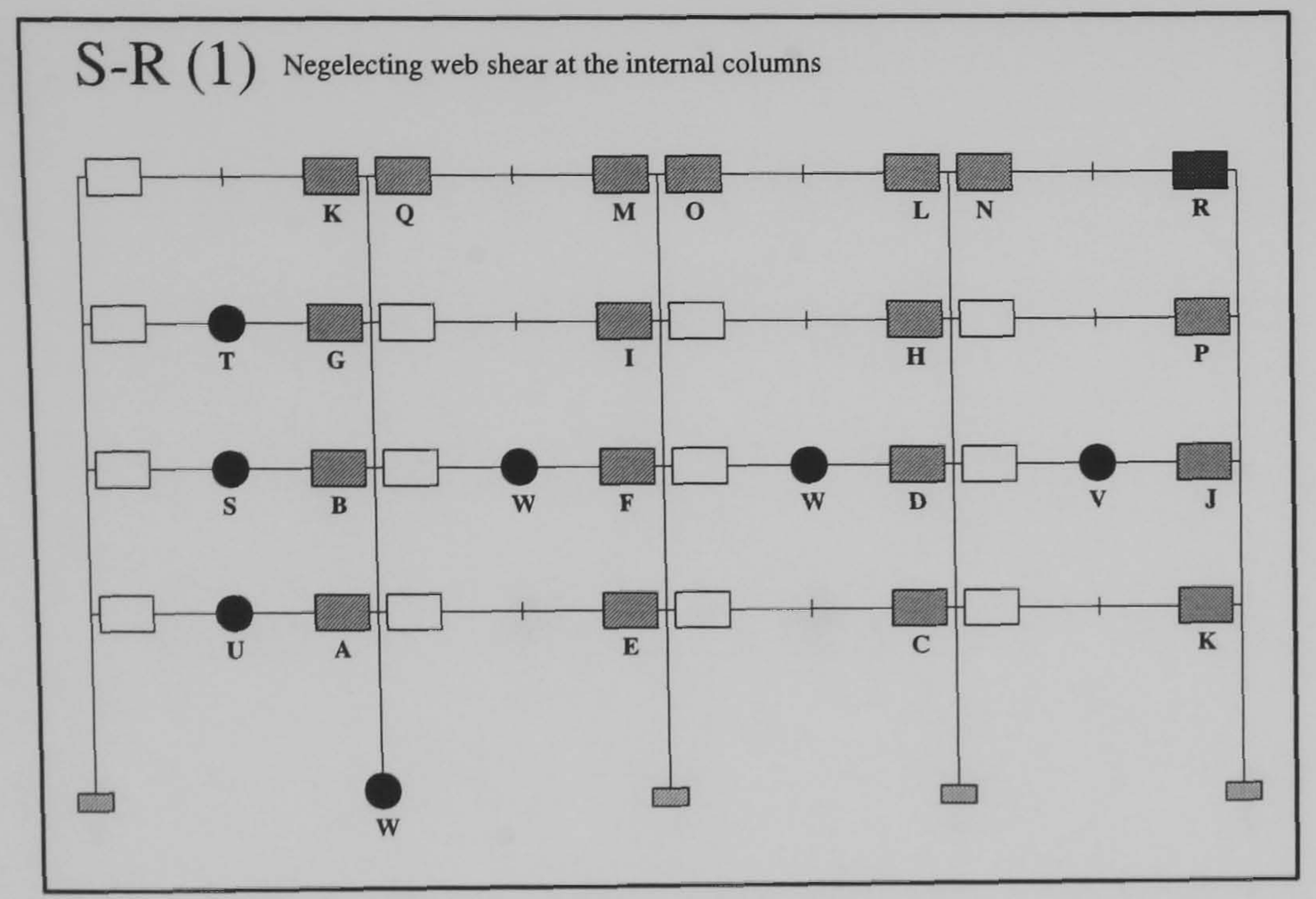

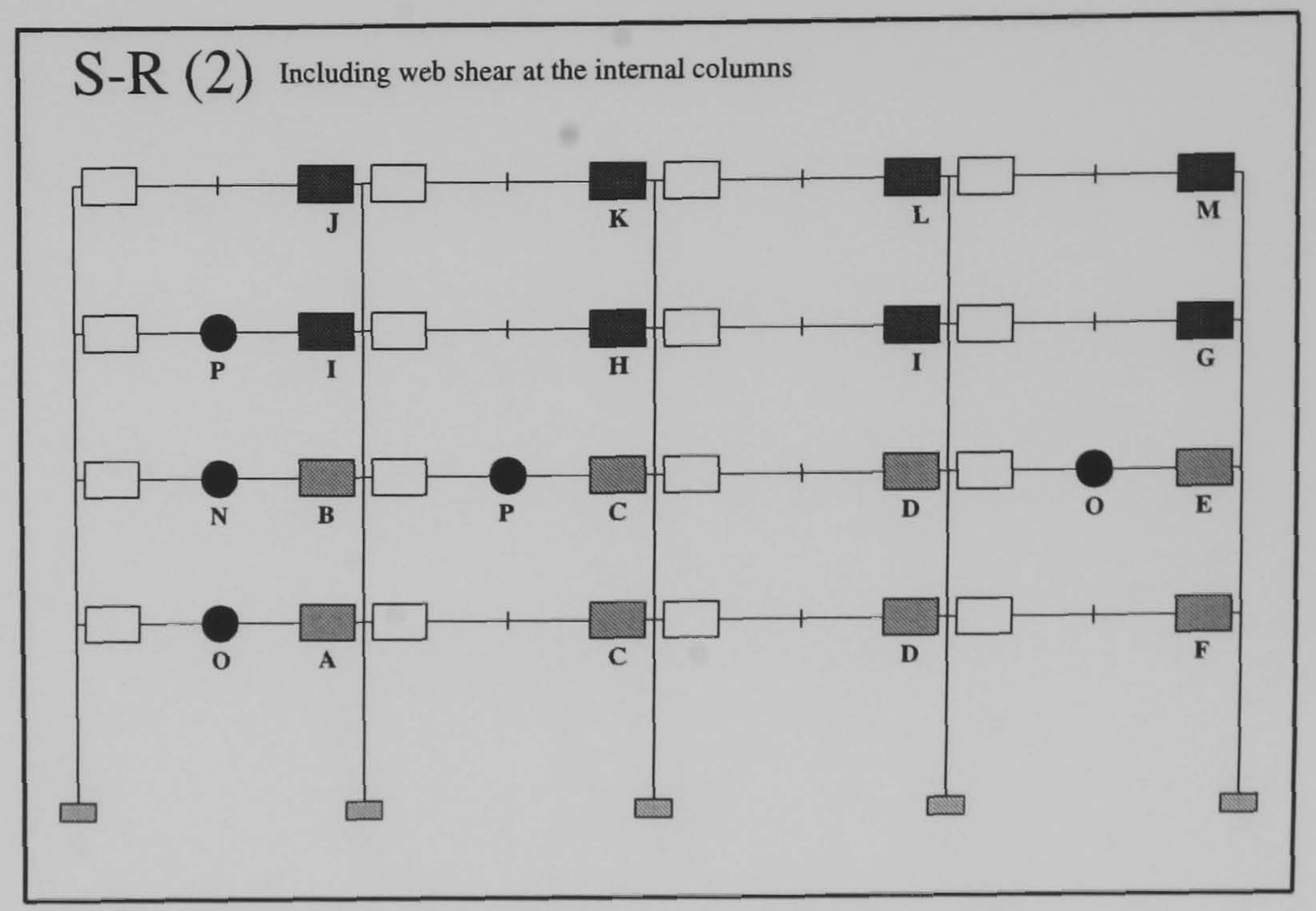

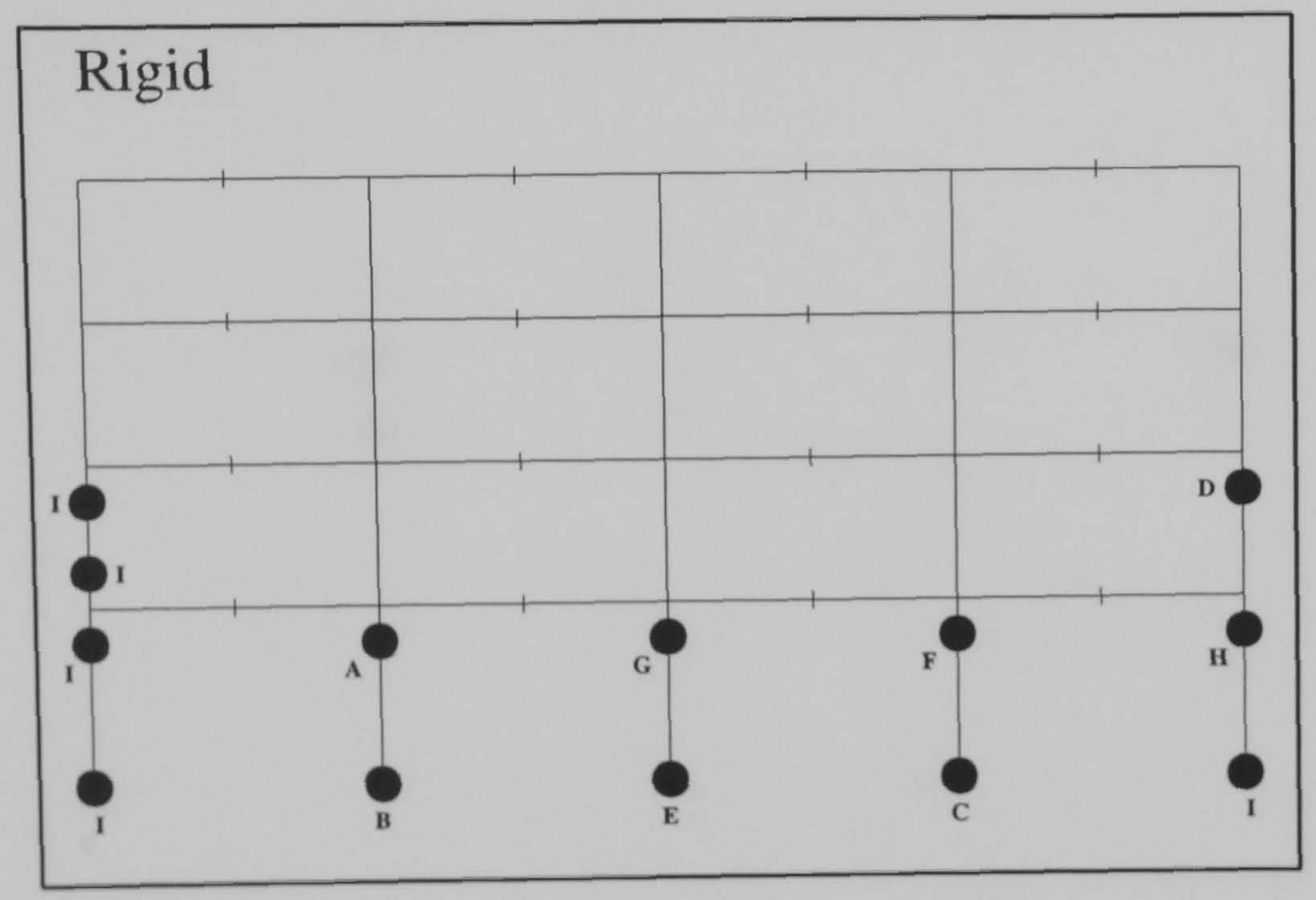

Hinge Location	Load Level at Hinge Formation S-R(1)	S-R(2)	Rigid
A	0.4525	0.72	1.475
B	0.46	0.7225	1.495
C	0.475	0.73	1.525
D	0.48	0.7325	1.552
E	0.4825	0.7975	1.562
F	0.485	0.8025	1.565
G	0.5725	1.035	1.572
H	0.585	1.06	1.582
I	0.5925	1.07	1.585
J	0.7475	1.1175	N/A
K	0.755	1.1225	N/A
L	0.78	1.1275	N/A
M	0.7925	1.19	N/A
N	0.875	1.227	N/A
O	0.9475	1.287	N/A
P	0.9625	1.29	N/A
Q	0.965	N/A	N/A
R	1.1175	N/A	N/A
S	1.265	N/A	N/A
T	1.275	N/A	N/A
U	1.277	N/A	N/A
V	1.282	N/A	N/A
W	1.285	N/A	N/A

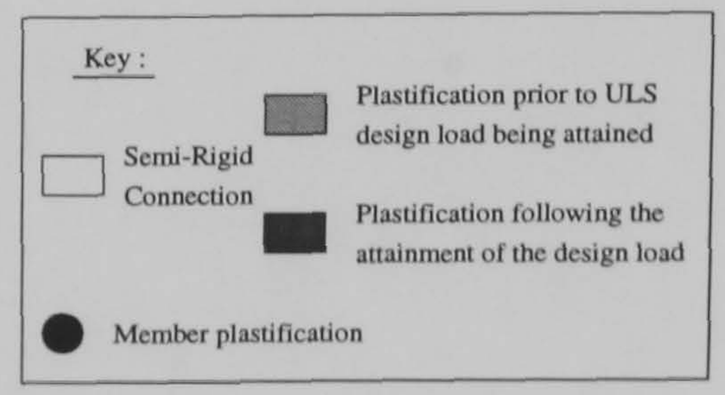

FRAME : **f28b24**
Load Case 1

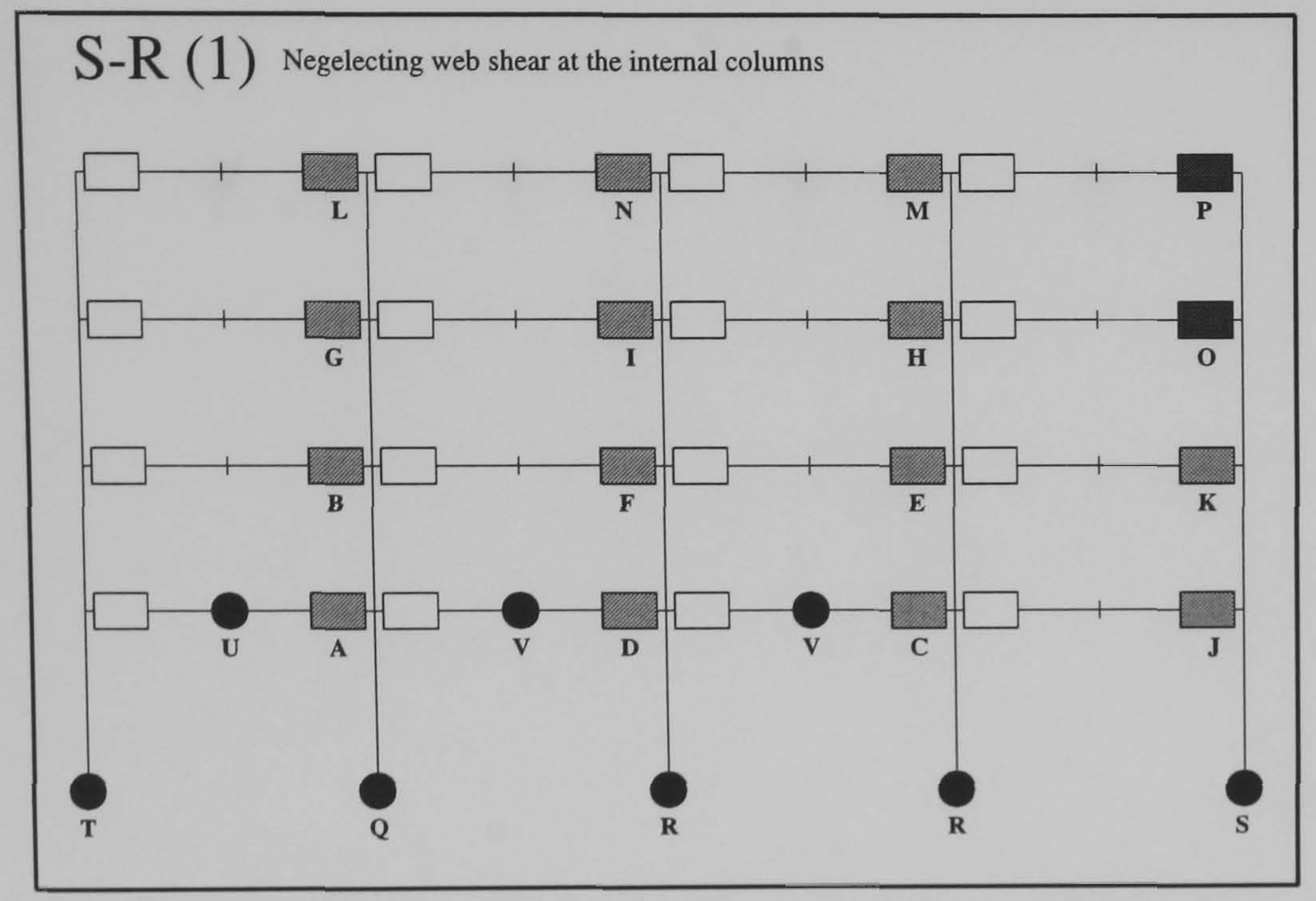

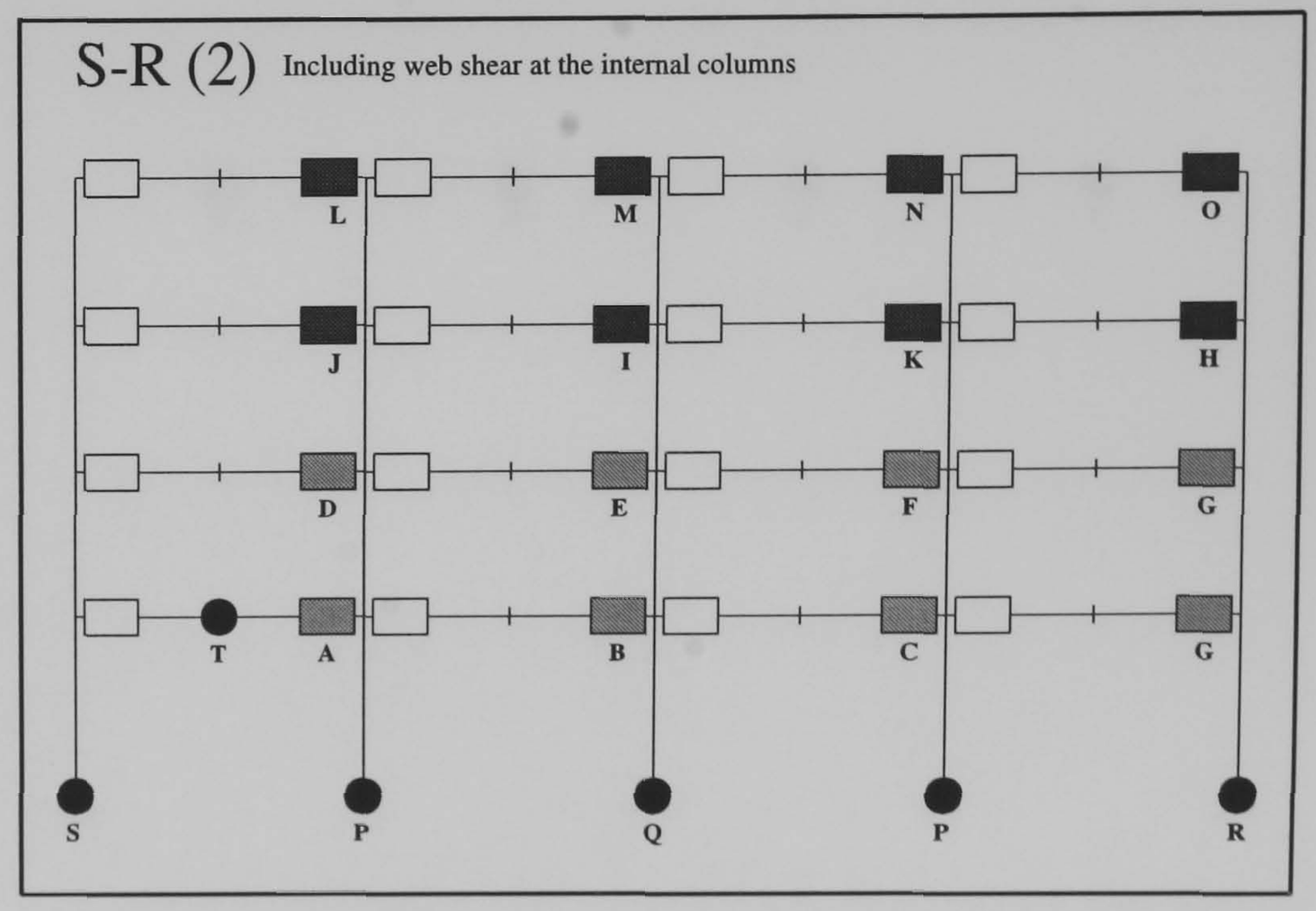

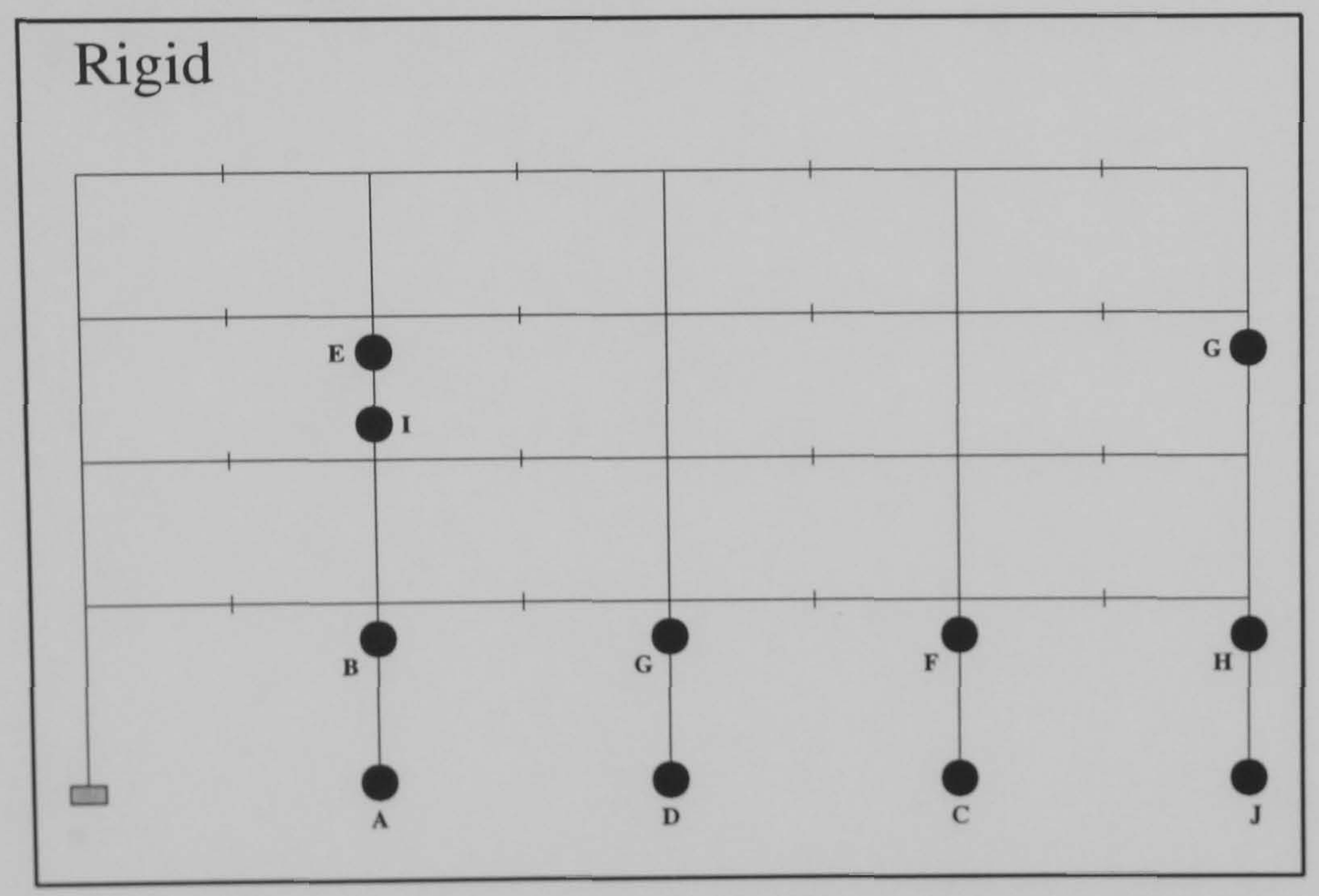

Hinge Location	Load Level at Hinge Formation S-R(1)	S-R(2)	Rigid
A	0.52	0.8	1.63
B	0.5375	0.81	1.64
C	0.54	0.8125	1.672
D	0.5475	0.8175	1.705
E	0.555	0.825	1.707
F	0.5625	0.8275	1.72
G	0.68	0.8725	1.727
H	0.695	1.115	1.74
I	0.7025	1.2075	1.745
J	0.8375	1.2125	1.747
K	0.84	1.2175	N/A
L	0.8725	1.2625	N/A
M	0.9025	1.275	N/A
N	0.9175	1.2825	N/A
O	1.08	1.3325	N/A
P	1.2675	1.415	N/A
Q	1.41	1.417	N/A
R	1.412	1.505	N/A
S	1.51	1.52	N/A
T	1.53	1.522	N/A
U	1.532	N/A	N/A
V	1.535	N/A	N/A

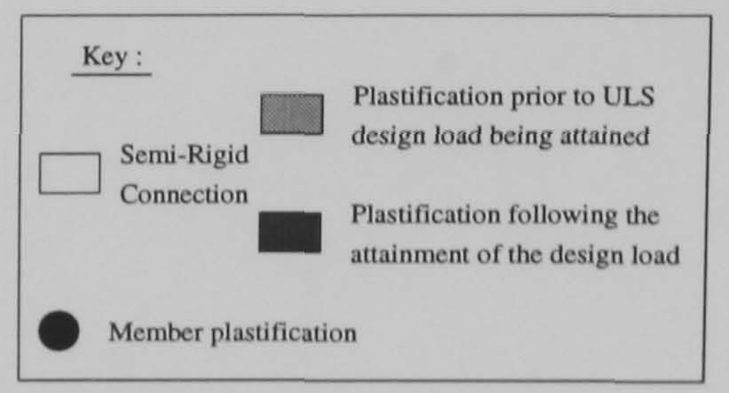

FRAME : **f28b24**
Load Case 2

S-R (1) Negelecting web shear at the internal columns

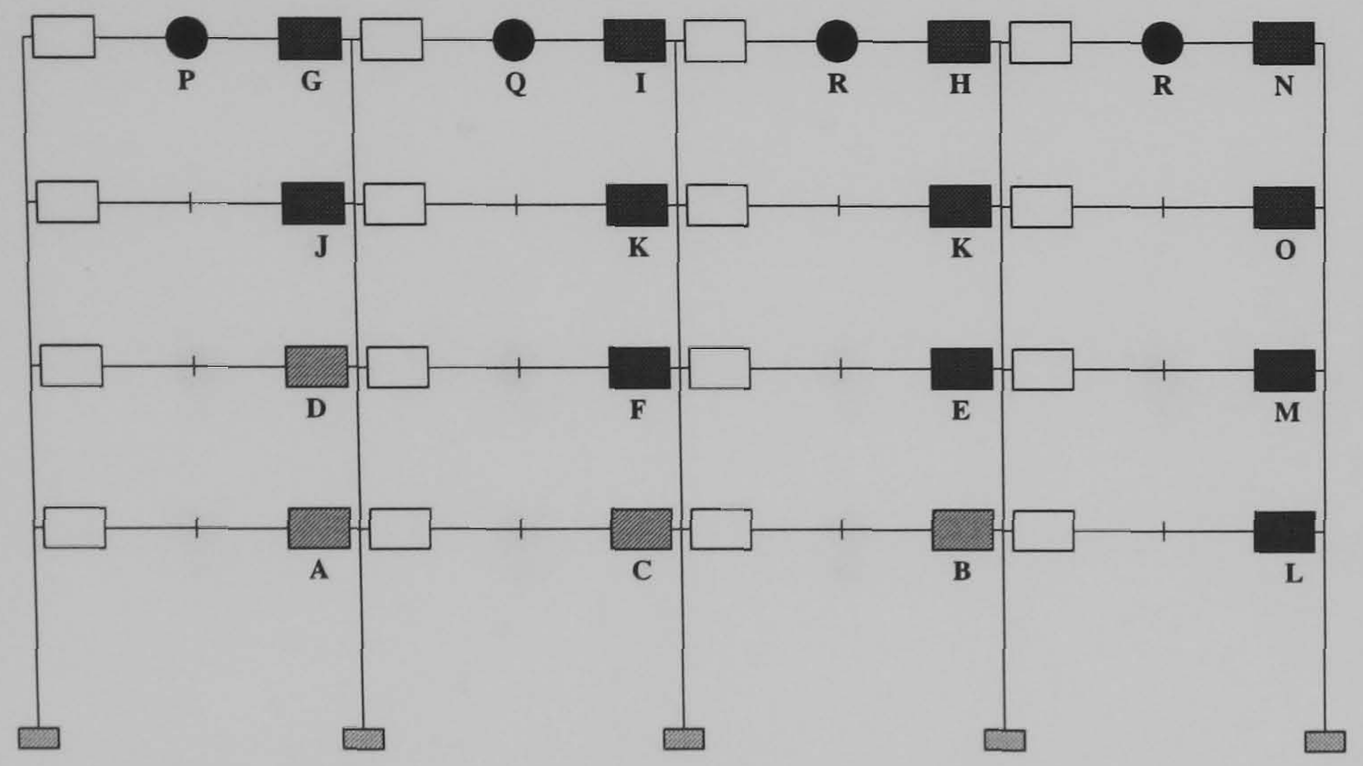

S-R (2) Including web shear at the internal columns

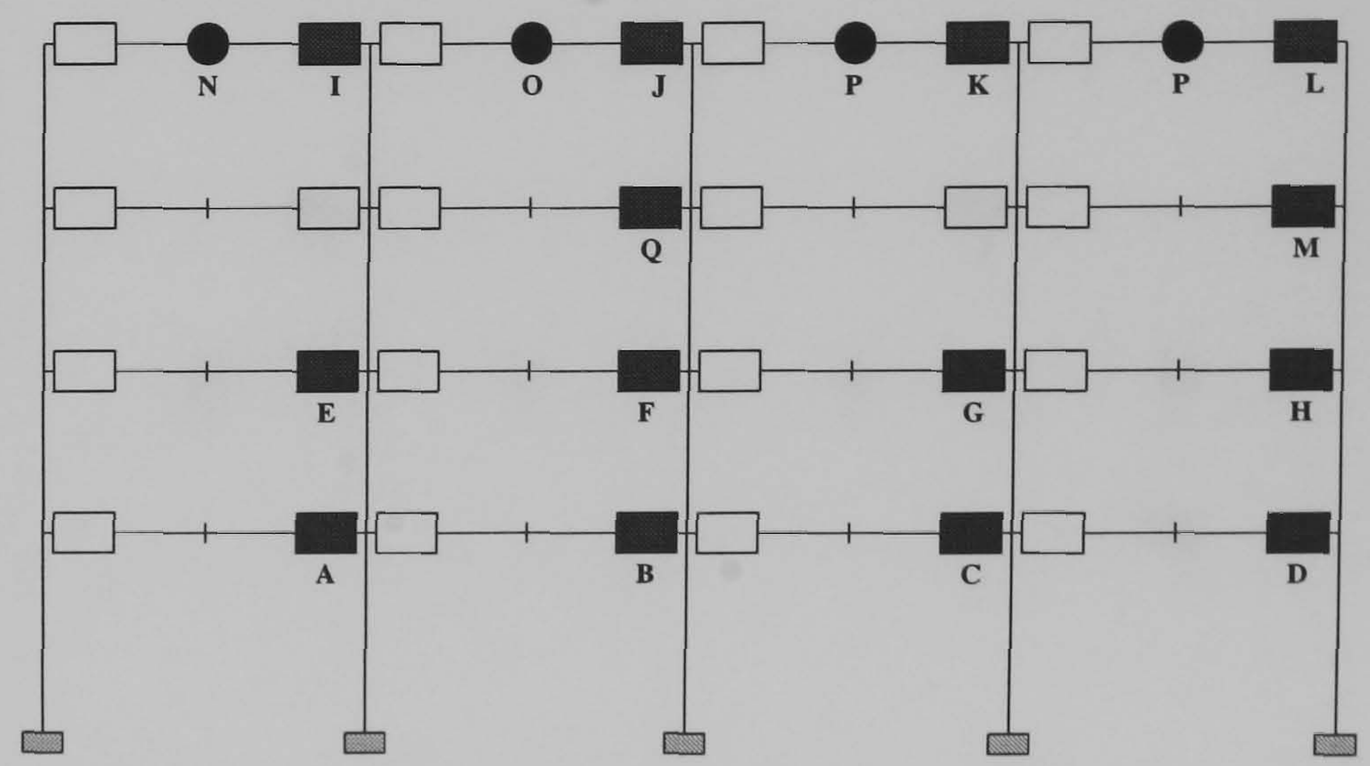

Rigid

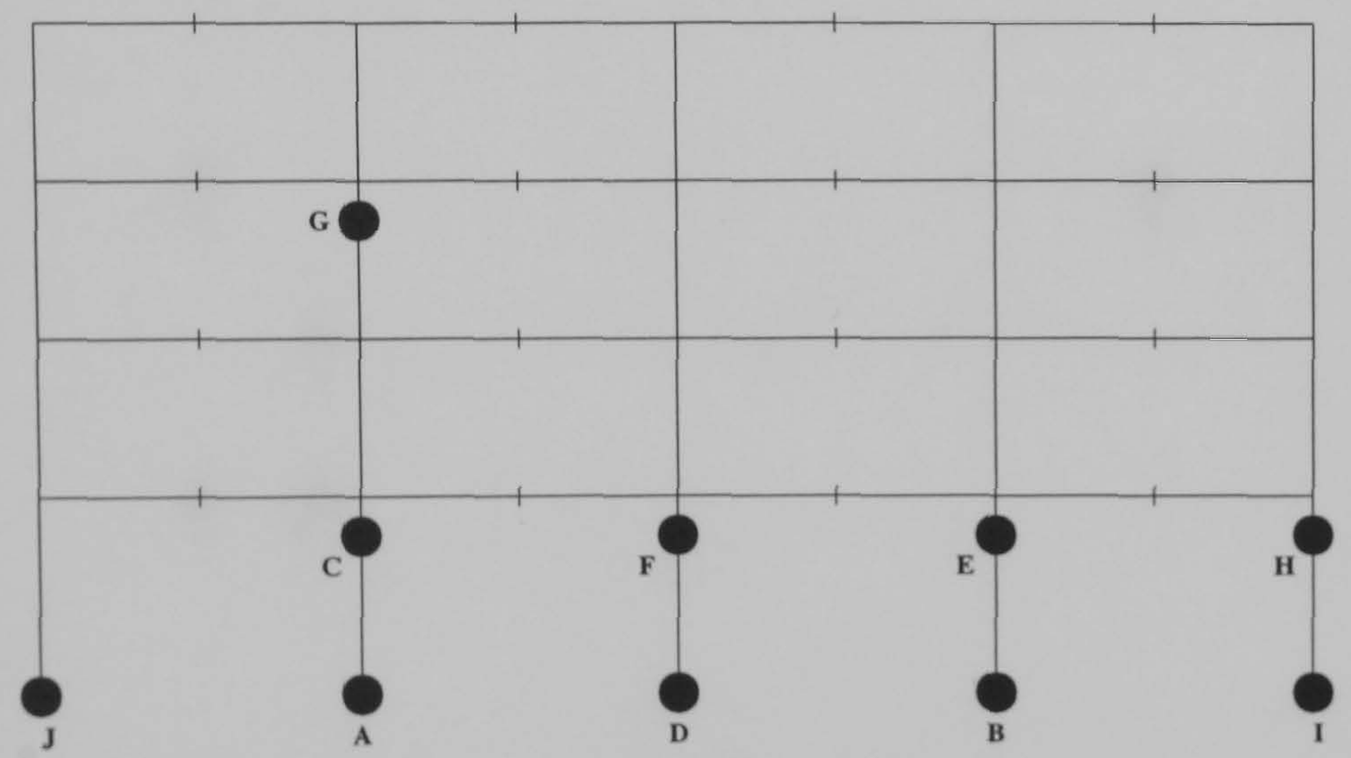

Hinge Location	Load Level at Hinge Formation		
	S-R(1)	S-R(2)	Rigid
A	0.915	1.3225	2.275
B	0.93	1.3325	2.322
C	0.9425	1.335	2.342
D	0.98	1.38	2.357
E	1.0	1.4	2.397
F	1.01	1.4075	2.405
G	1.0325	1.4125	2.425
H	1.0725	1.4225	2.442
I	1.0925	1.495	2.45
J	1.2875	1.525	2.455
K	1.315	1.53	N/A
L	1.3725	1.63	N/A
M	1.43	1.6825	N/A
N	1.6075	1.89	N/A
O	1.6850	1.93	N/A
P	1.88	1.935	N/A
Q	1.94	1.9475	N/A
R	1.945	N/A	N/A

Key :

- Semi-Rigid Connection
- Plastification prior to ULS design load being attained
- Plastification following the attainment of the design load
- Member plastification

FRAME : **f28b24**
Load Case 3

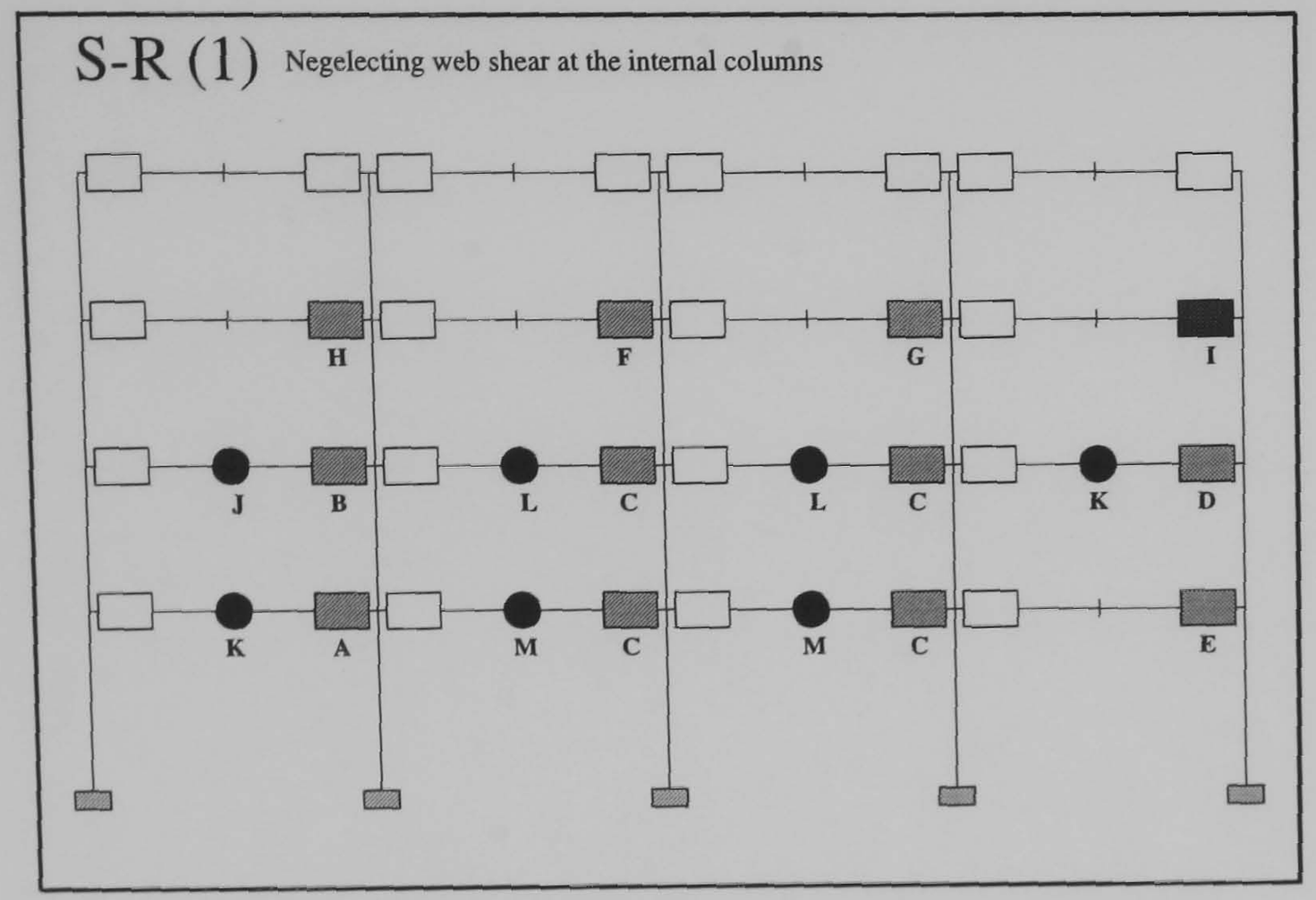

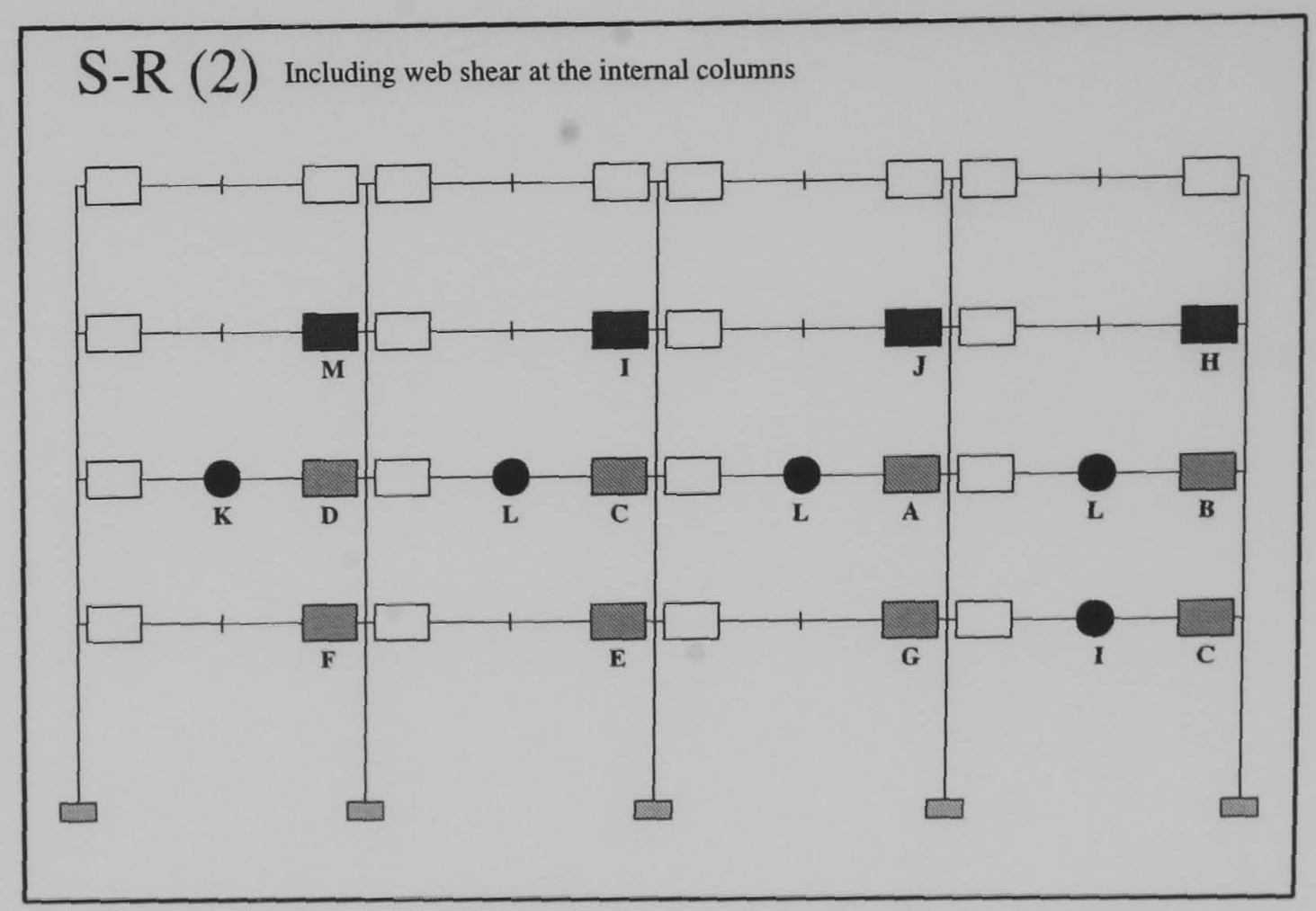

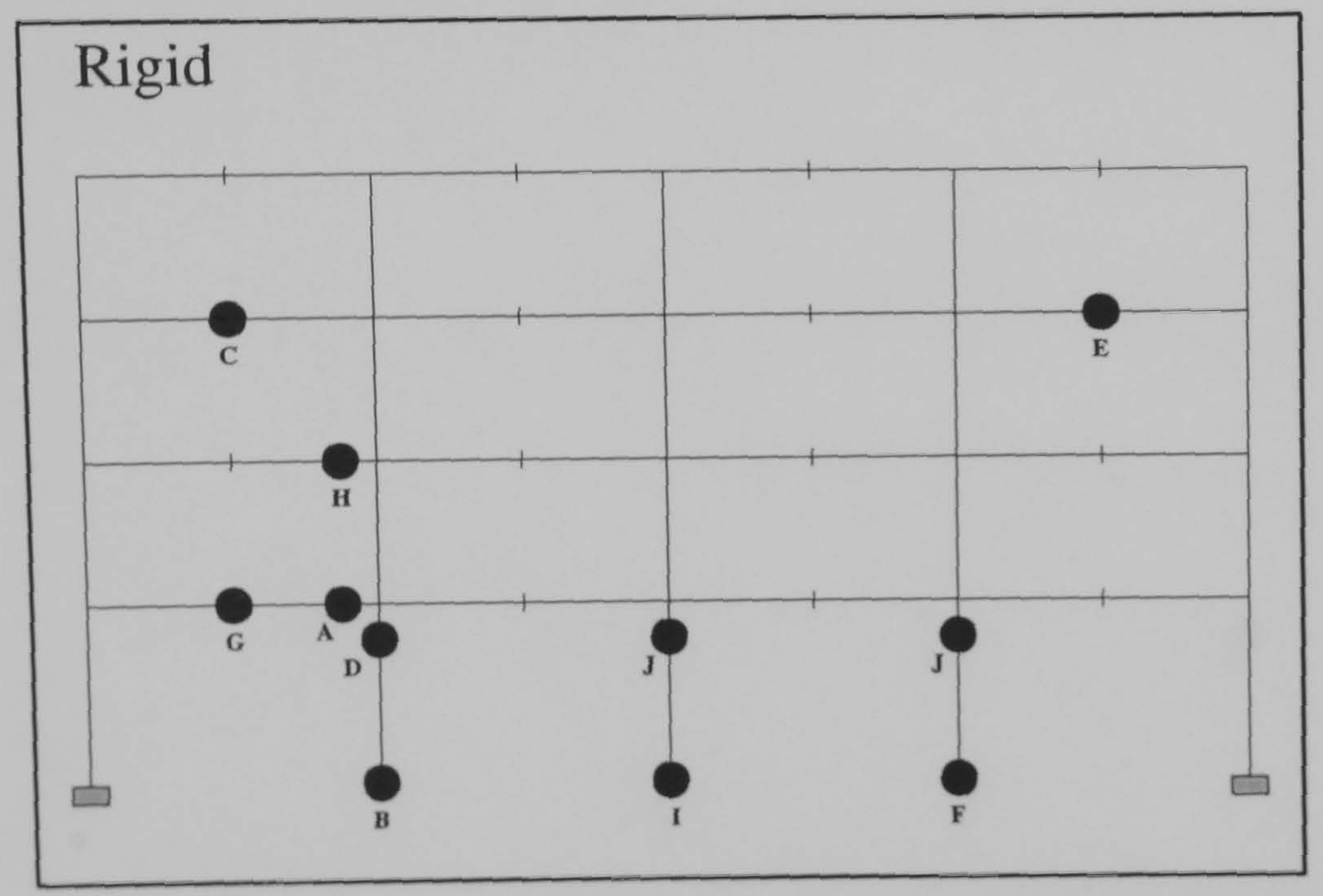

Hinge Location	Load Level at Hinge Formation S-R(1)	S-R(2)	Rigid
A	0.6125	0.79	1.627
B	0.6175	0.7975	1.677
C	0.6225	0.8	1.692
D	0.765	0.8075	1.697
E	0.7825	0.81	1.705
F	0.83	0.8125	1.707
G	0.8325	0.845	1.715
H	0.835	1.01	1.722
I	1.0	1.0975	1.725
J	1.102	1.1025	1.73
K	1.107	1.110	N/A
L	1.11	1.112	N/A
M	1.112	1.1125	N/A

Key :

Semi-Rigid Connection

Plastification prior to ULS design load being attained

Plastification following the attainment of the design load

Member plastification

FRAME : **f29b20**
Load Case 1

S-R (1) Negelecting web shear at the internal columns

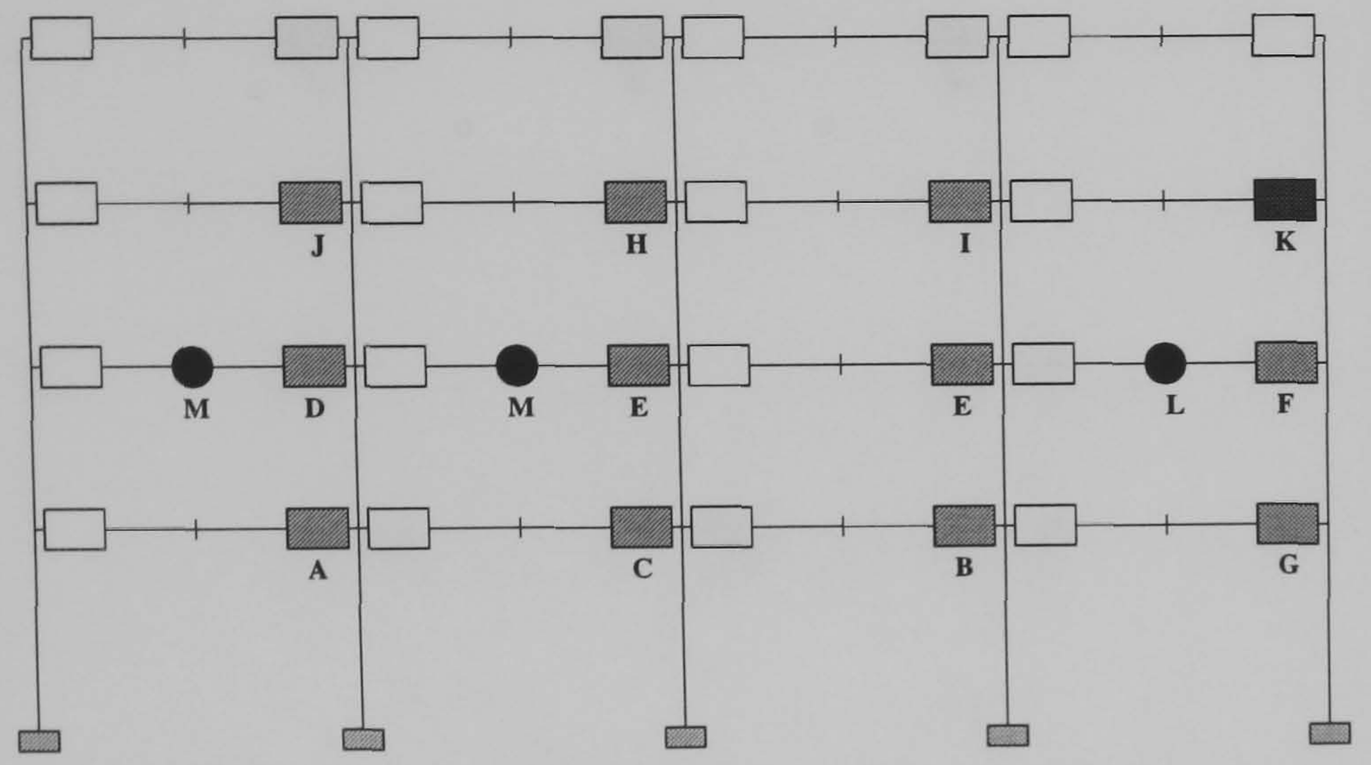

S-R (2) Including web shear at the internal columns

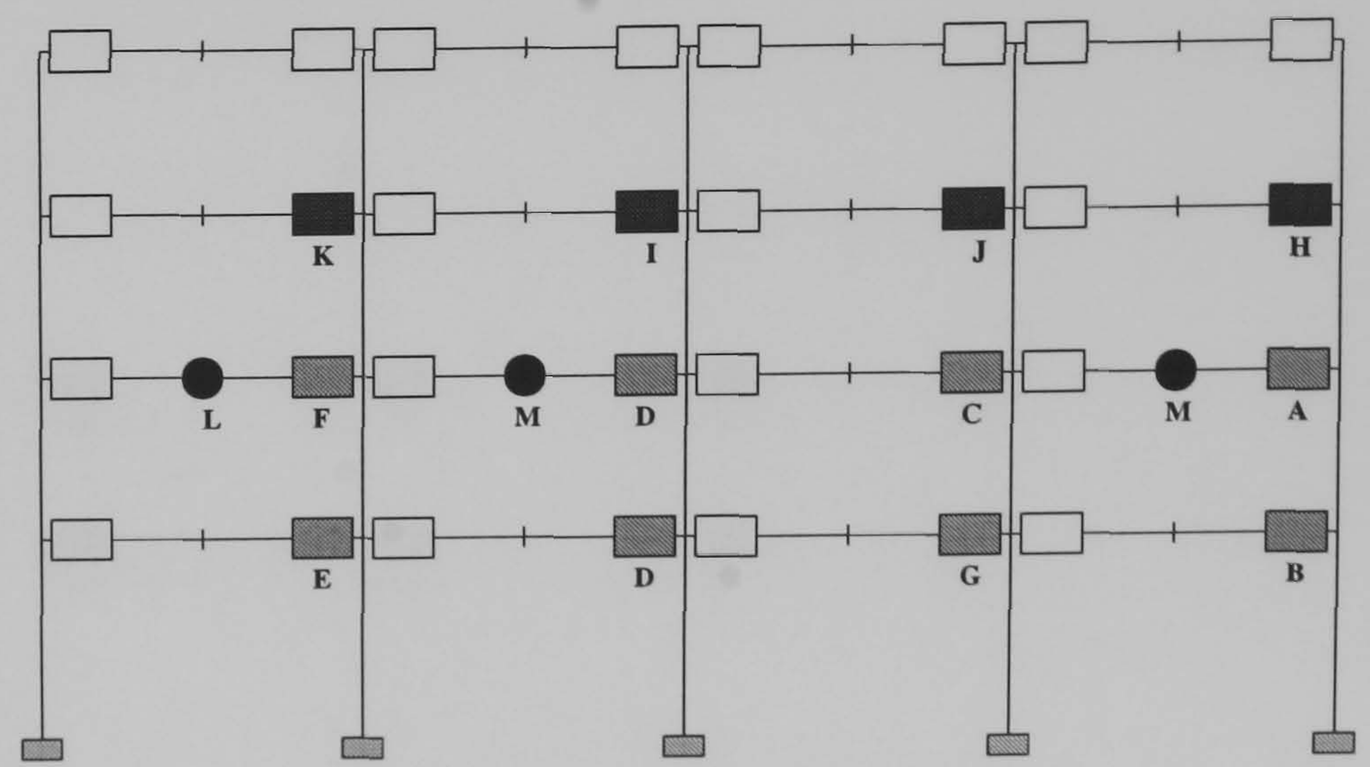

Rigid

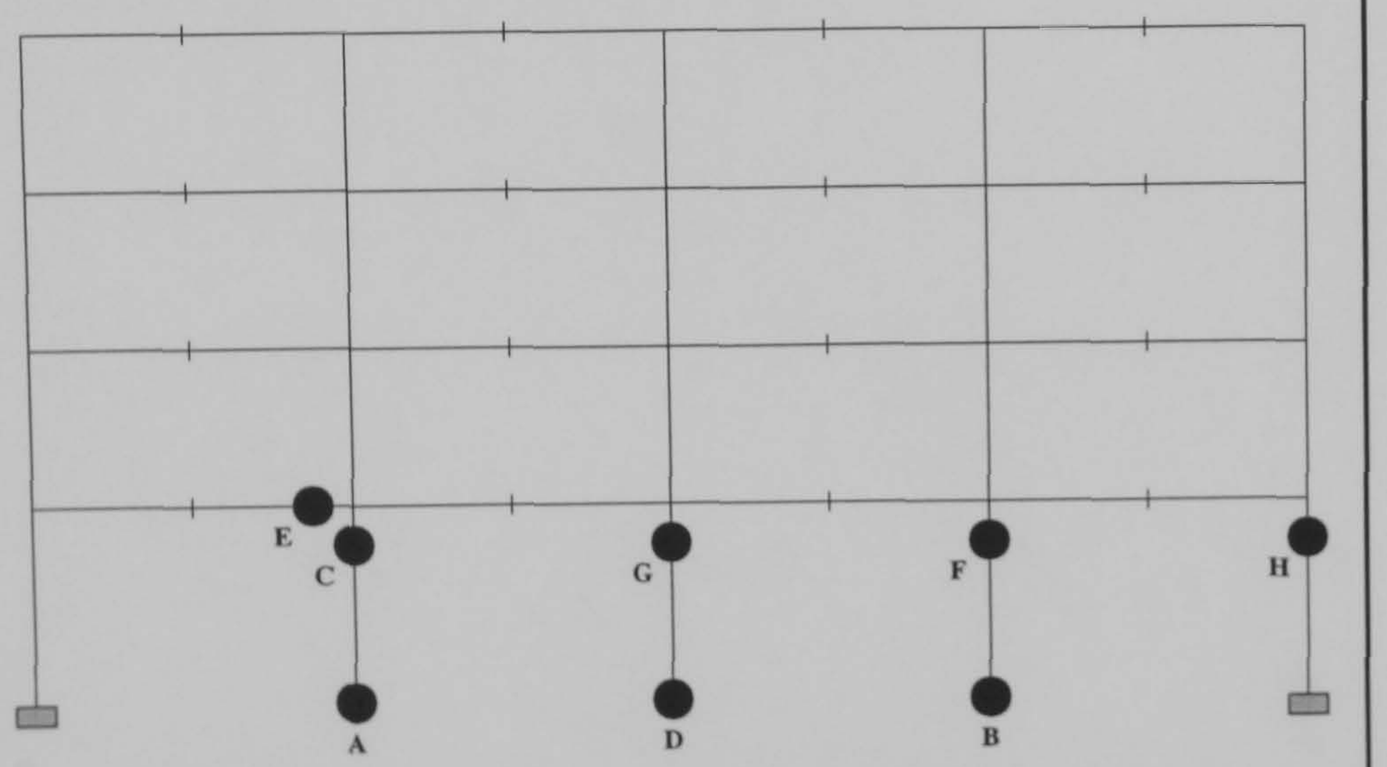

Hinge Location	Load Level at Hinge Formation		
	S-R(1)	S-R(2)	Rigid
A	0.6725	0.835	1.817
B	0.6775	0.845	1.857
C	0.68	0.8525	1.862
D	0.685	0.855	1.880
E	0.69	0.8575	1.882
F	0.83	0.86	1.902
G	0.84	0.8725	1.905
H	0.9325	1.0775	1.917
I	0.9375	1.1975	N/A
J	0.94	1.2025	N/A
K	1.095	1.2125	N/A
L	1.332	1.325	N/A
M	1.335	1.33	N/A

Key :

Semi-Rigid Connection

Plastification prior to ULS design load being attained

Plastification following the attainment of the design load

Member plastification

FRAME : **f29b20**

Load Case 2

S-R (1) Negelecting web shear at the internal columns

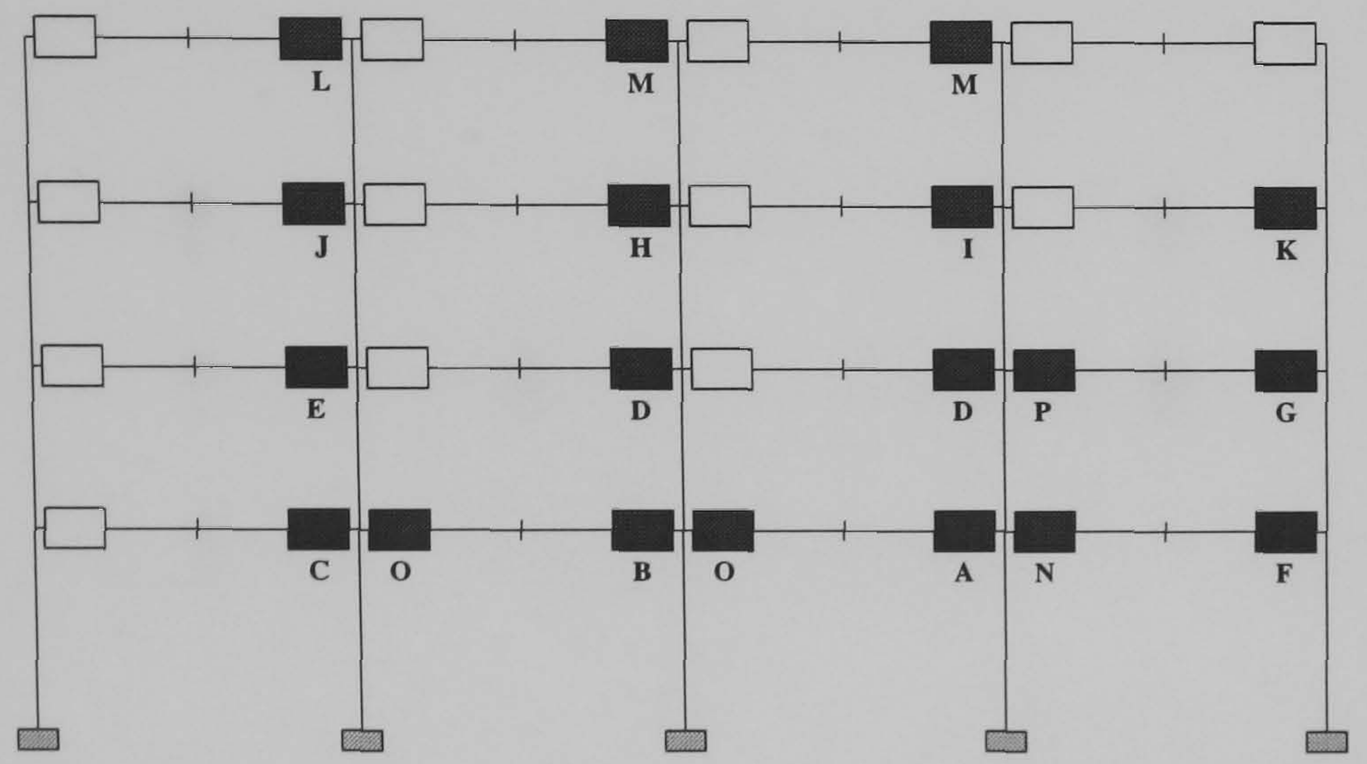

S-R (2) Including web shear at the internal columns

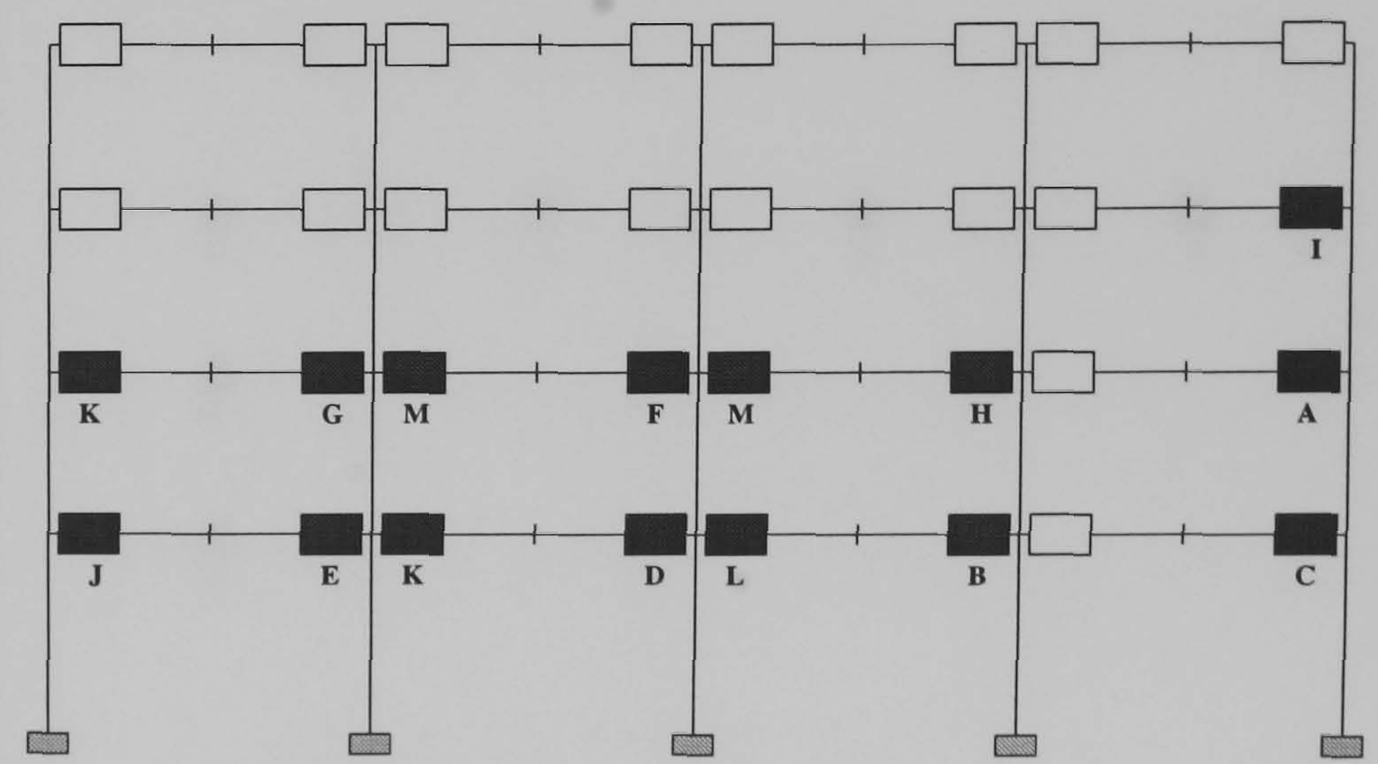

Rigid

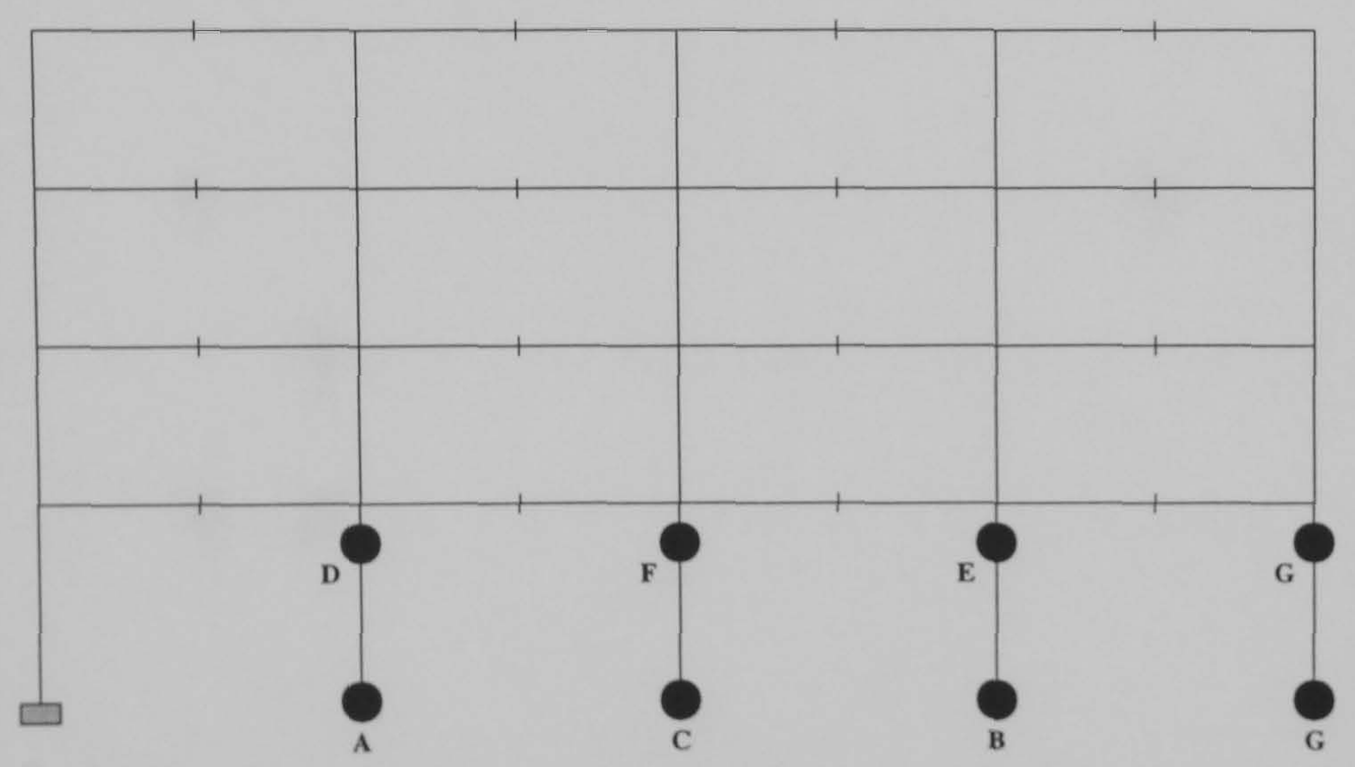

Hinge Location	Load Level at Hinge Formation		
	S-R(1)	S-R(2)	Rigid
A	1.0675	1.245	2.485
B	1.07	1.255	2.527
C	1.0725	1.26	2.547
D	1.12	1.275	2.582
E	1.125	1.2775	2.615
F	1.2825	1.3125	2.62
G	1.3025	1.3175	2.655
H	1.575	1.34	N/A
I	1.585	1.6225	N/A
J	1.595	1.795	N/A
K	1.7275	1.815	N/A
L	1.7325	1.8175	N/A
M	1.745	1.8375	N/A
N	1.8475	N/A	N/A
O	1.86	N/A	N/A
P	1.88	N/A	N/A

Key :

- Semi-Rigid Connection
- Plastification prior to ULS *design load being attained*
- Plastification following the attainment of the design load
- Member plastification

FRAME : **f29b20**
Load Case 3

S-R (1) Negelecting web shear at the internal columns

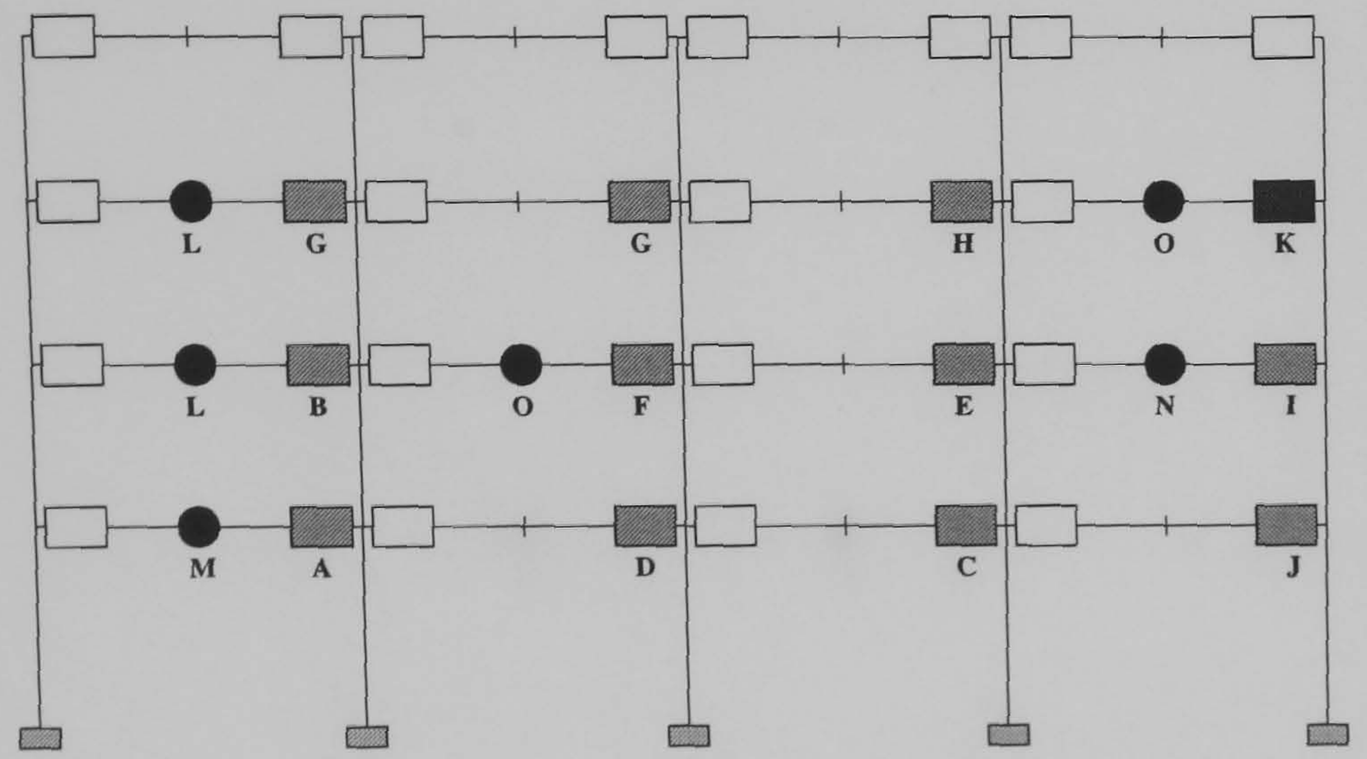

S-R (2) Including web shear at the internal columns

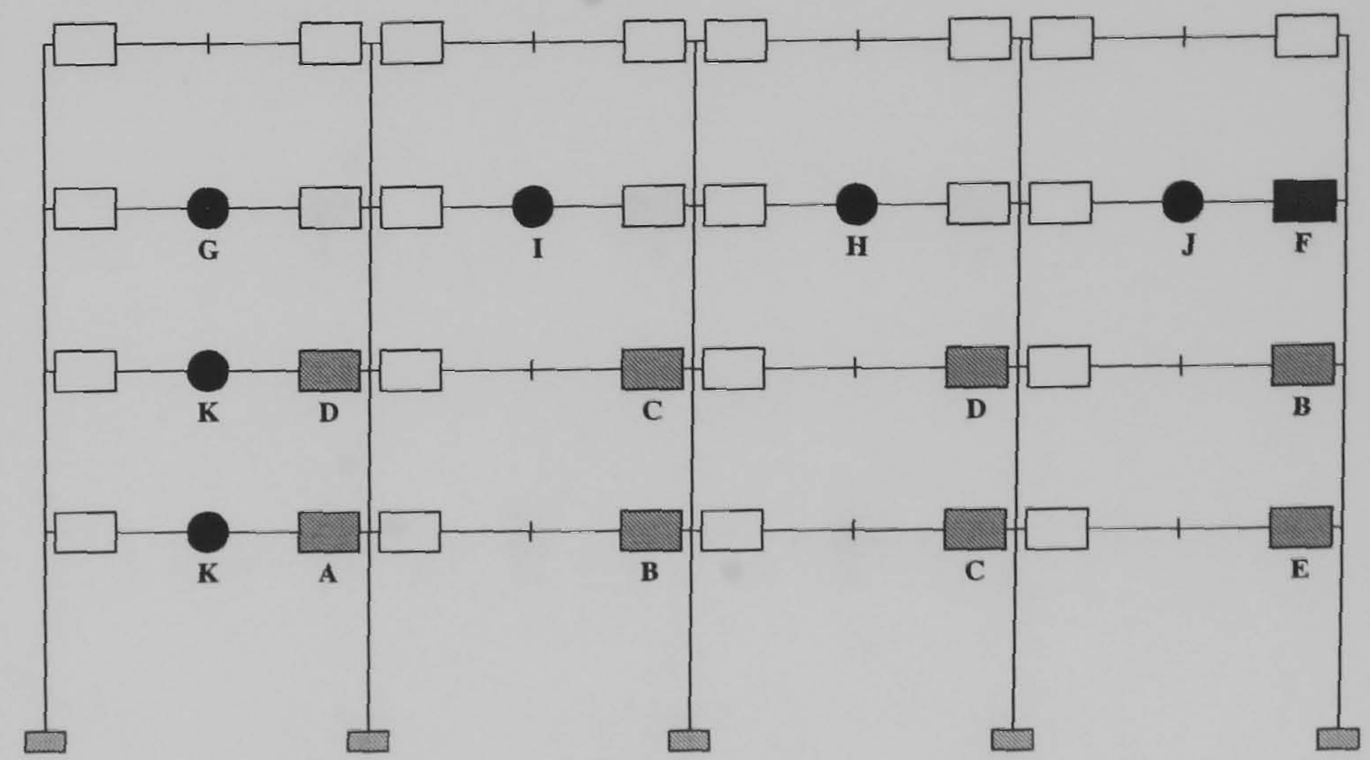

Rigid

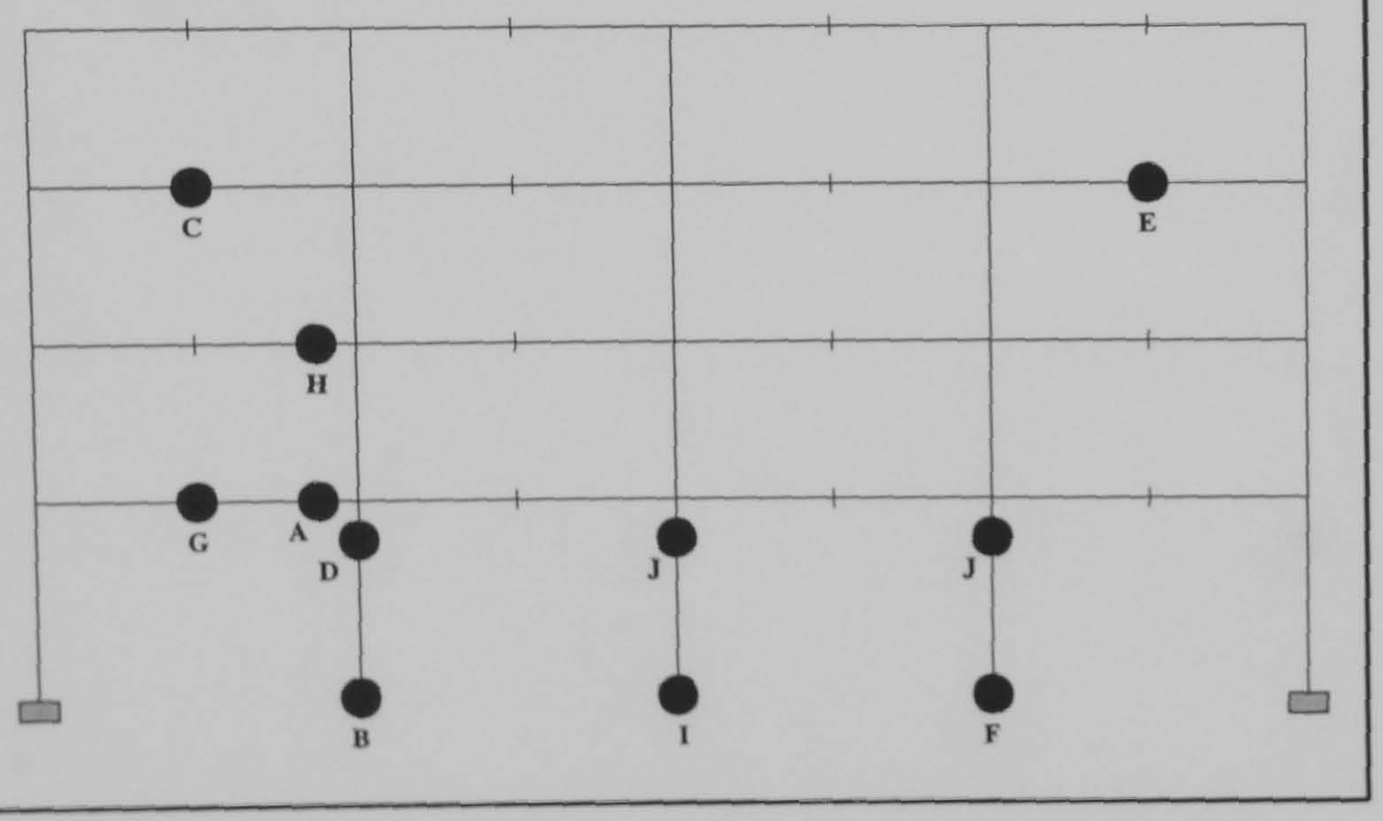

Hinge Location	Load Level at Hinge Formation		
	S-R(1)	S-R(2)	Rigid
A	0.6775	0.965	1.627
B	0.69	0.9675	1.677
C	0.7	0.97	1.692
D	0.705	0.9725	1.697
E	0.7075	0.99	1.705
F	0.71	1.1475	1.707
G	0.8925	1.155	1.715
H	0.895	1.165	1.722
I	0.9325	1.167	1.725
J	0.9475	1.172	1.73
K	1.13	1.175	N/A
L	1.162	N/A	N/A
M	1.165	N/A	N/A
N	1.177	N/A	N/A
O	1.18	N/A	N/A

Key :

- Plastification prior to ULS design load being attained
- Semi-Rigid Connection
- Plastification following the attainment of the design load
- Member plastification

FRAME : **f29b24**
Load Case 1

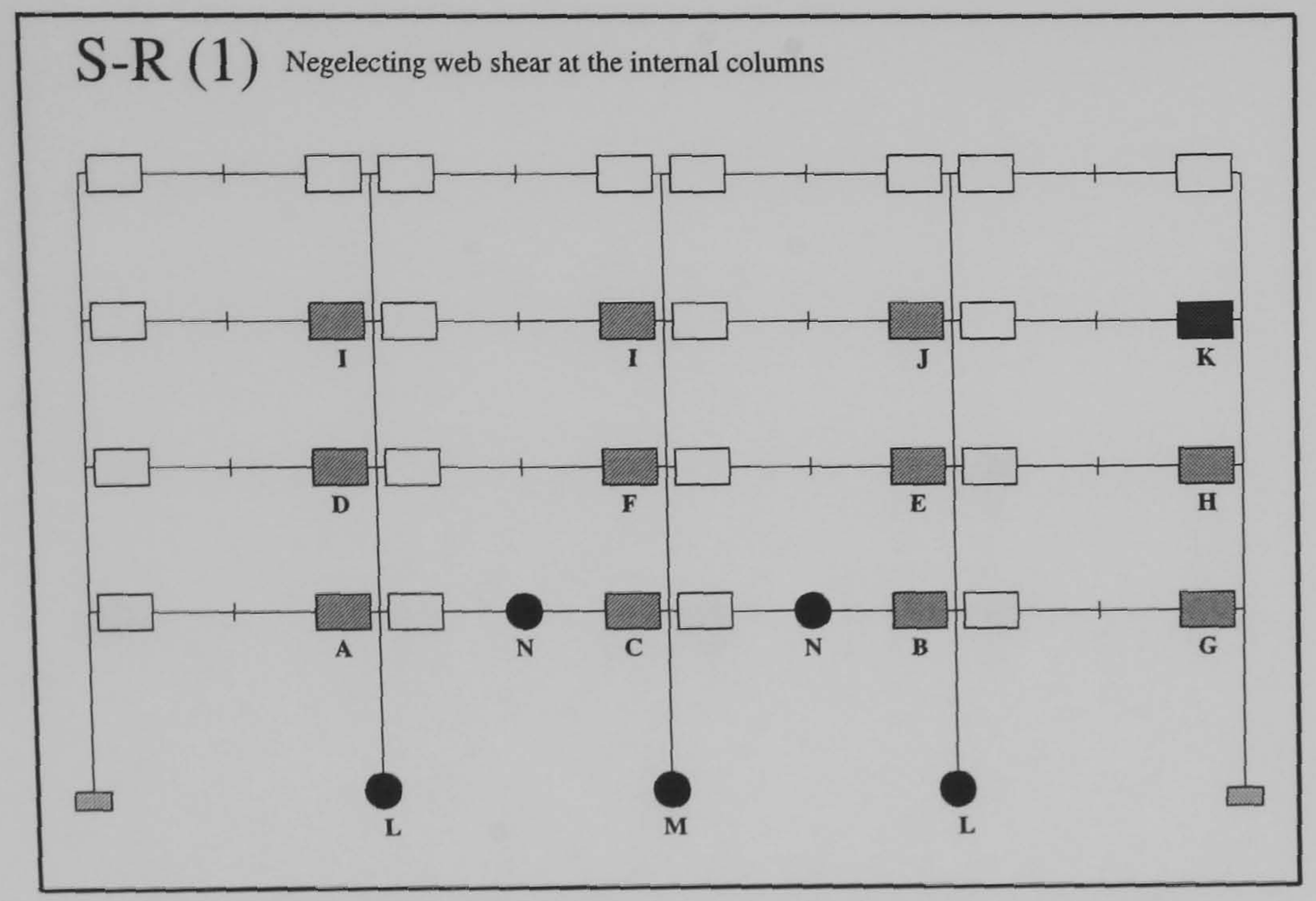

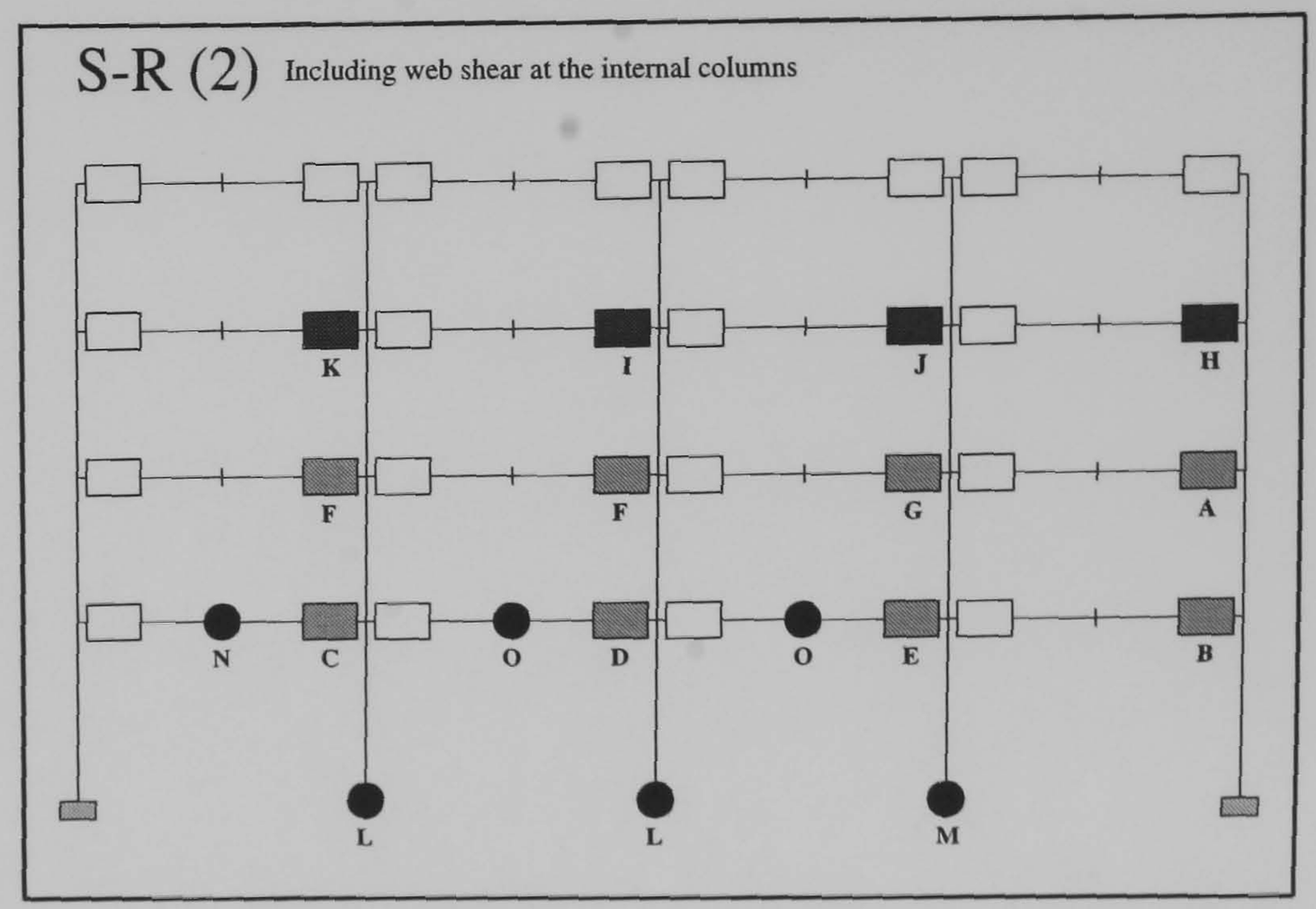

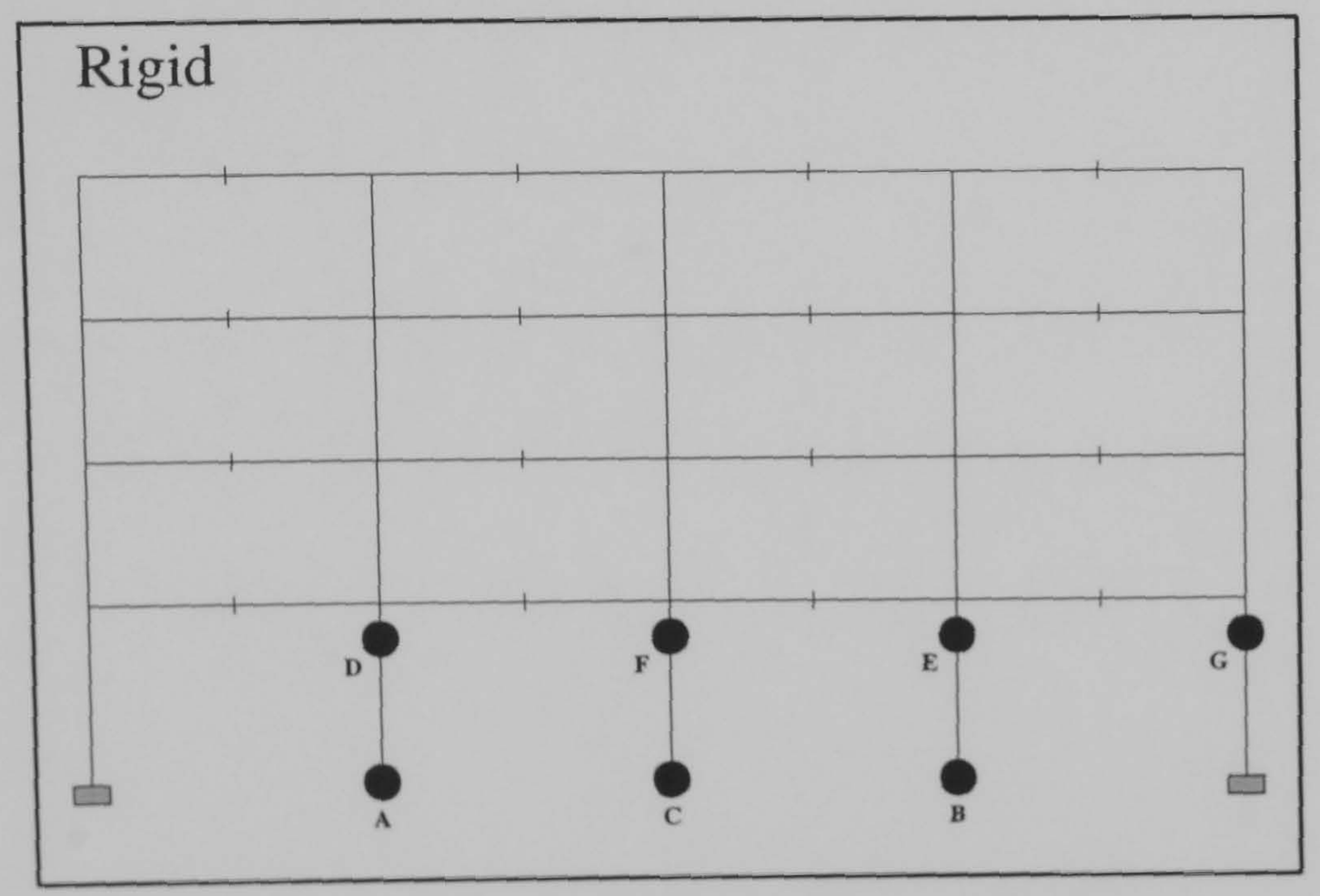

Hinge Location	Load Level at Hinge Formation		
	S-R(1)	S-R(2)	Rigid
A	**0.6725**	**0.89**	**1.577**
B	**0.6825**	**0.895**	**1.61**
C	**0.6875**	**0.9025**	**1.627**
D	**0.7075**	**0.905**	**1.635**
E	**0.715**	**0.9075**	**1.665**
F	**0.7175**	**0.93**	**1.667**
G	**0.895**	**0.9325**	**1.68**
H	**0.9075**	**1.09**	**N/A**
I	**0.9375**	**1.2475**	**N/A**
J	**0.94**	**1.2525**	**N/A**
K	**1.125**	**1.26**	**N/A**
L	**1.295**	**1.282**	**N/A**
M	**1.297**	**1.285**	**N/A**
N	**1.332**	**1.32**	**N/A**
O	**N/A**	**1.327**	**N/A**

Key :

Semi-Rigid Connection

Plastification prior to ULS design load being attained

Plastification following the attainment of the design load

Member plastification

FRAME : **f29b24**

Load Case 2

S-R (1) Negelecting web shear at the internal columns

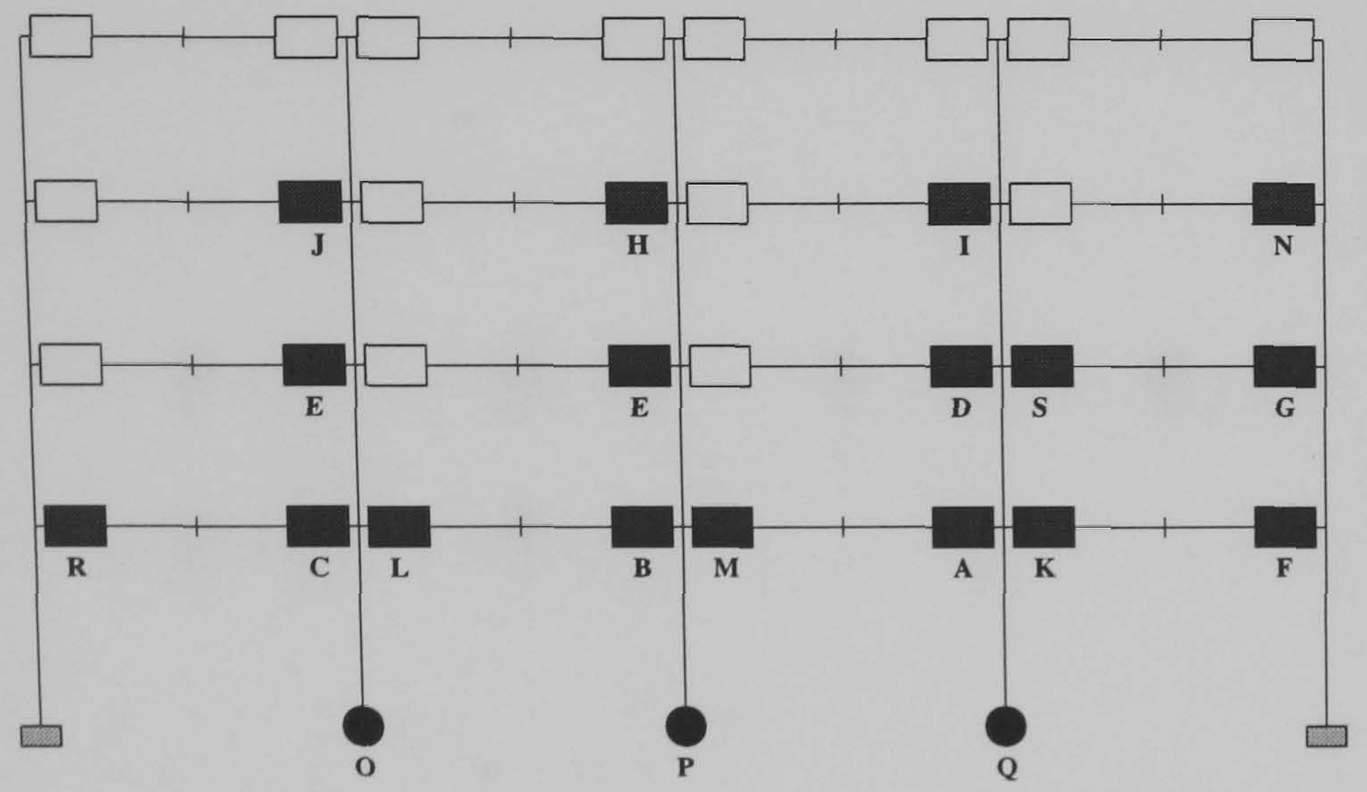

S-R (2) Including web shear at the internal columns

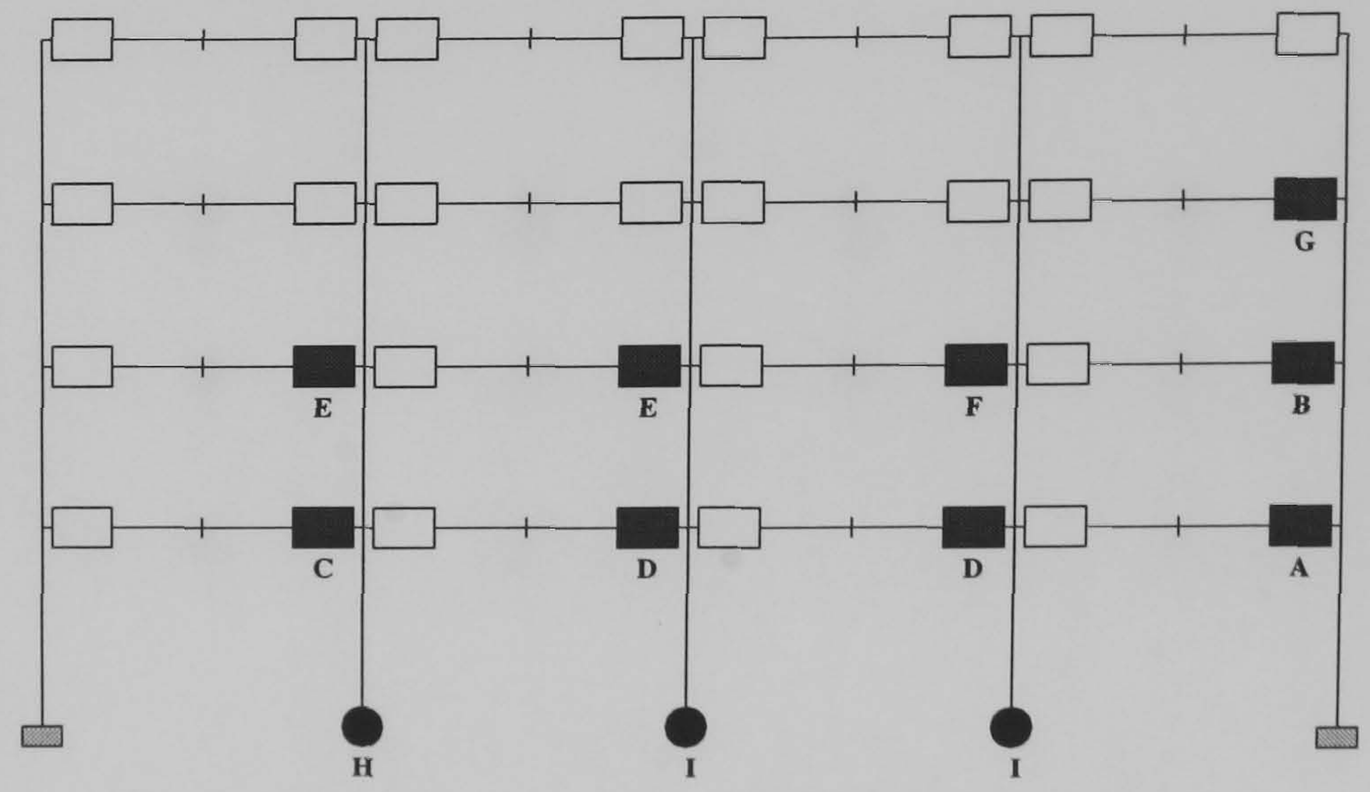

Rigid

Hinge Location	Load Level at Hinge Formation S-R(1)	S-R(2)	Rigid
A	1.0025	1.21	2.012
B	1.0075	1.2475	2.045
C	1.01	1.275	2.057
D	1.0975	1.2775	2.115
E	1.1025	1.3525	2.145
F	1.2675	1.355	2.147
G	1.3275	1.54	2.170
H	1.5025	1.66	2.175
I	1.51	1.665	N/A
J	1.515	N/A	N/A
K	1.655	N/A	N/A
L	1.6625	N/A	N/A
M	1.665	N/A	N/A
N	1.6675	N/A	N/A
O	1.690	N/A	N/A
P	1.692	N/A	N/A
Q	1.695	N/A	N/A
R	1.7075	N/A	N/A
S	1.7125	N/A	N/A

Key :

- Semi-Rigid Connection
- Plastification prior to ULS design load being attained
- Plastification following the attainment of the design load
- Member plastification

FRAME : **f29b24**
Load Case 3

S-R (1) Negelecting web shear at the internal columns

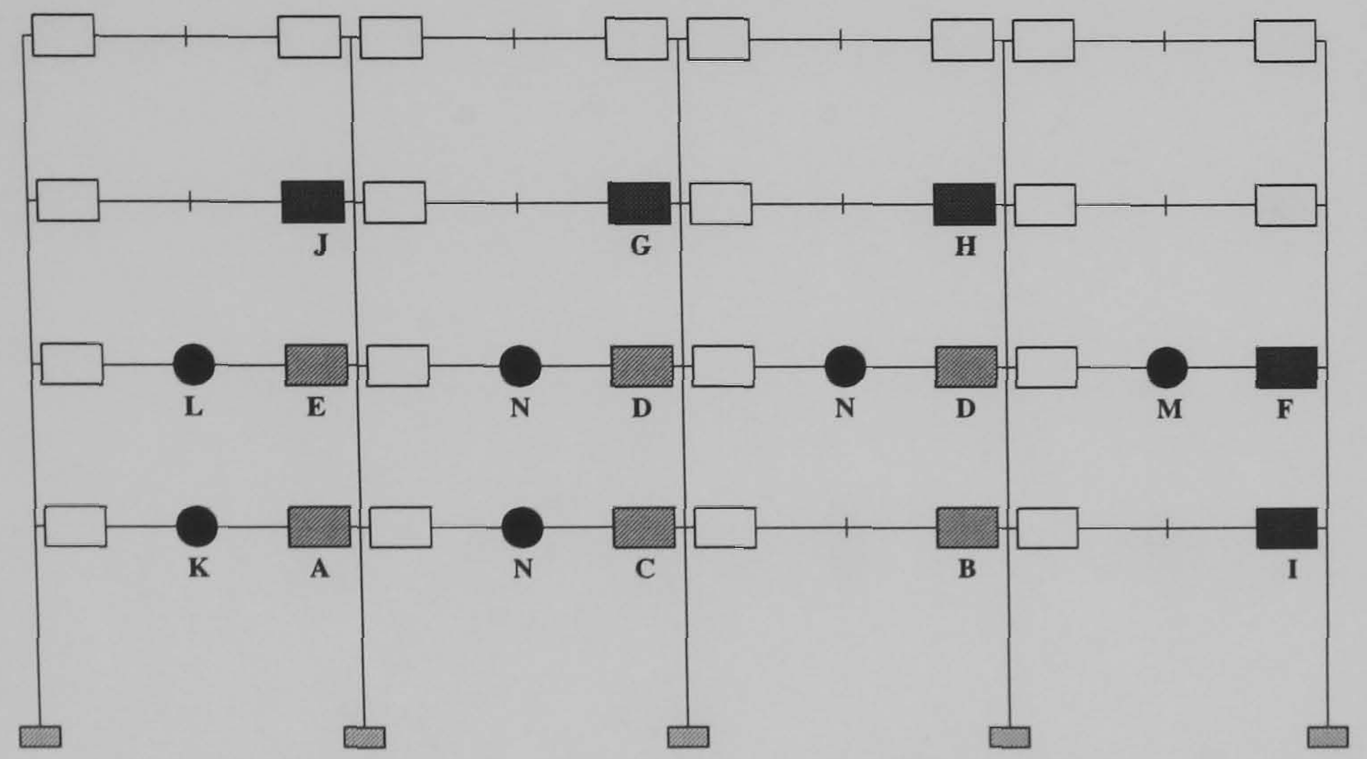

S-R (2) Including web shear at the internal columns

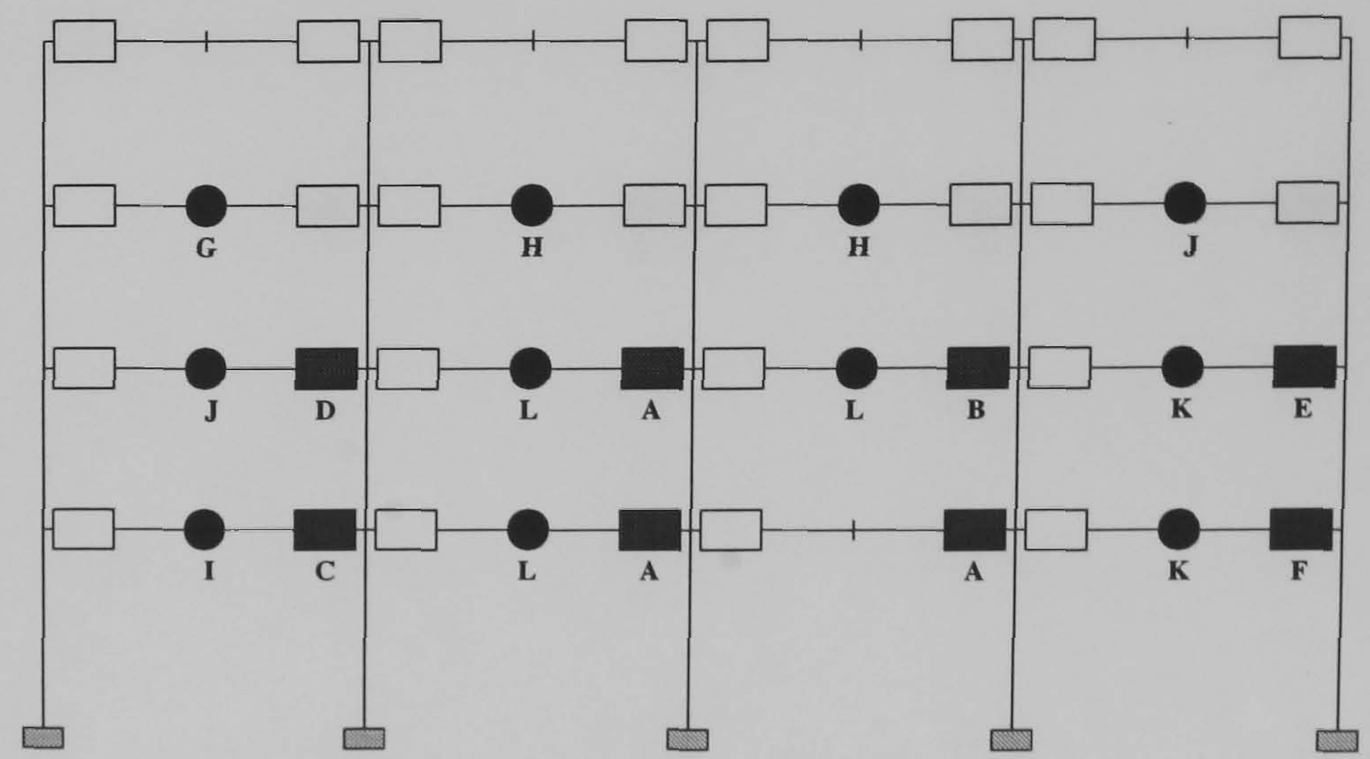

Rigid

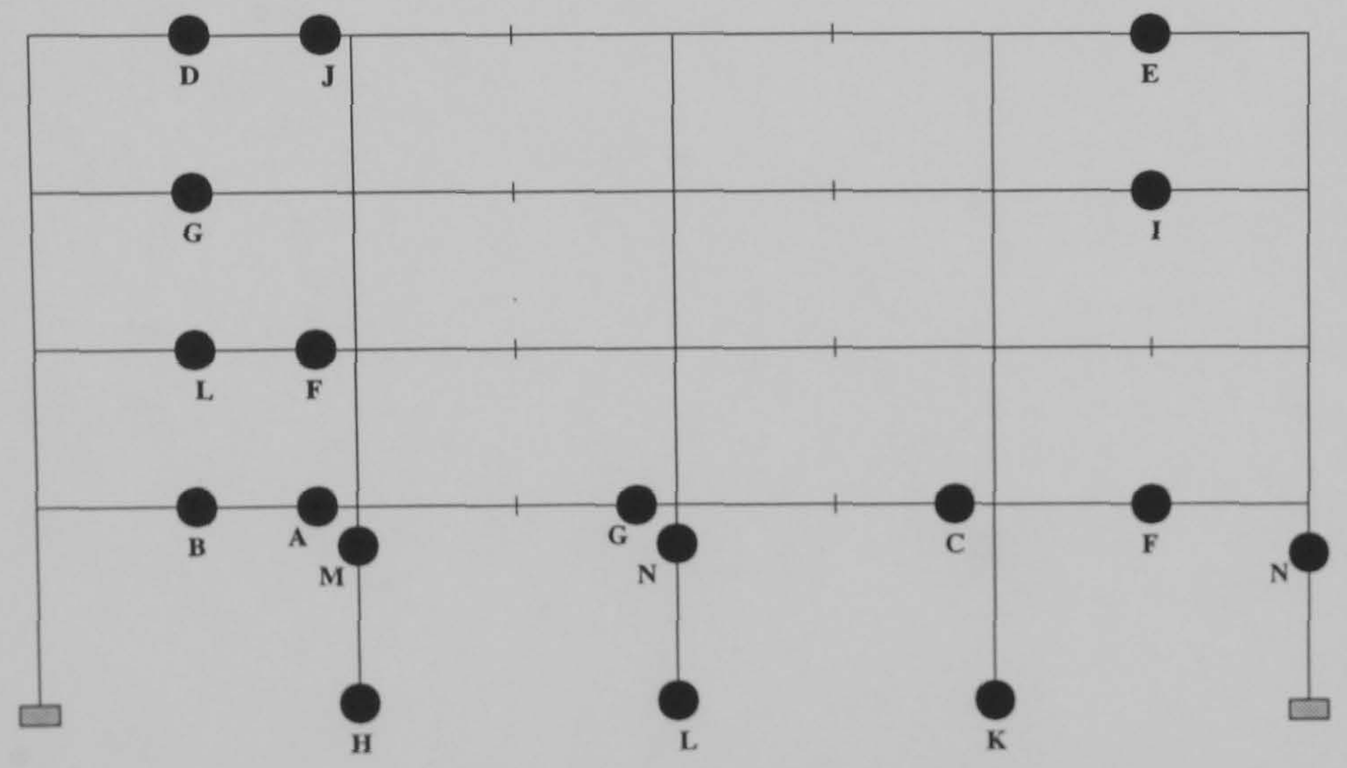

Hinge Location	Load Level at Hinge Formation S-R(1)	S-R(2)	Rigid
A	0.95	1.165	1.712
B	0.955	1.1675	1.827
C	0.9575	1.17	1.835
D	0.9625	1.18	1.857
E	0.965	1.1925	1.862
F	1.18	1.225	1.867
G	1.195	1.23	1.872
H	1.2025	1.235	1.887
I	1.2075	1.24	1.890
J	1.2175	1.245	1.897
K	1.235	1.247	1.90
L	1.24	1.25	1.905
M	1.247	N/A	1.915
N	1.25	N/A	1.917

Key :

- Semi-Rigid Connection
- Plastification prior to ULS design load being attained
- Plastification following the attainment of the design load
- Member plastification

FRAME : **f30b20**
Load Case 1

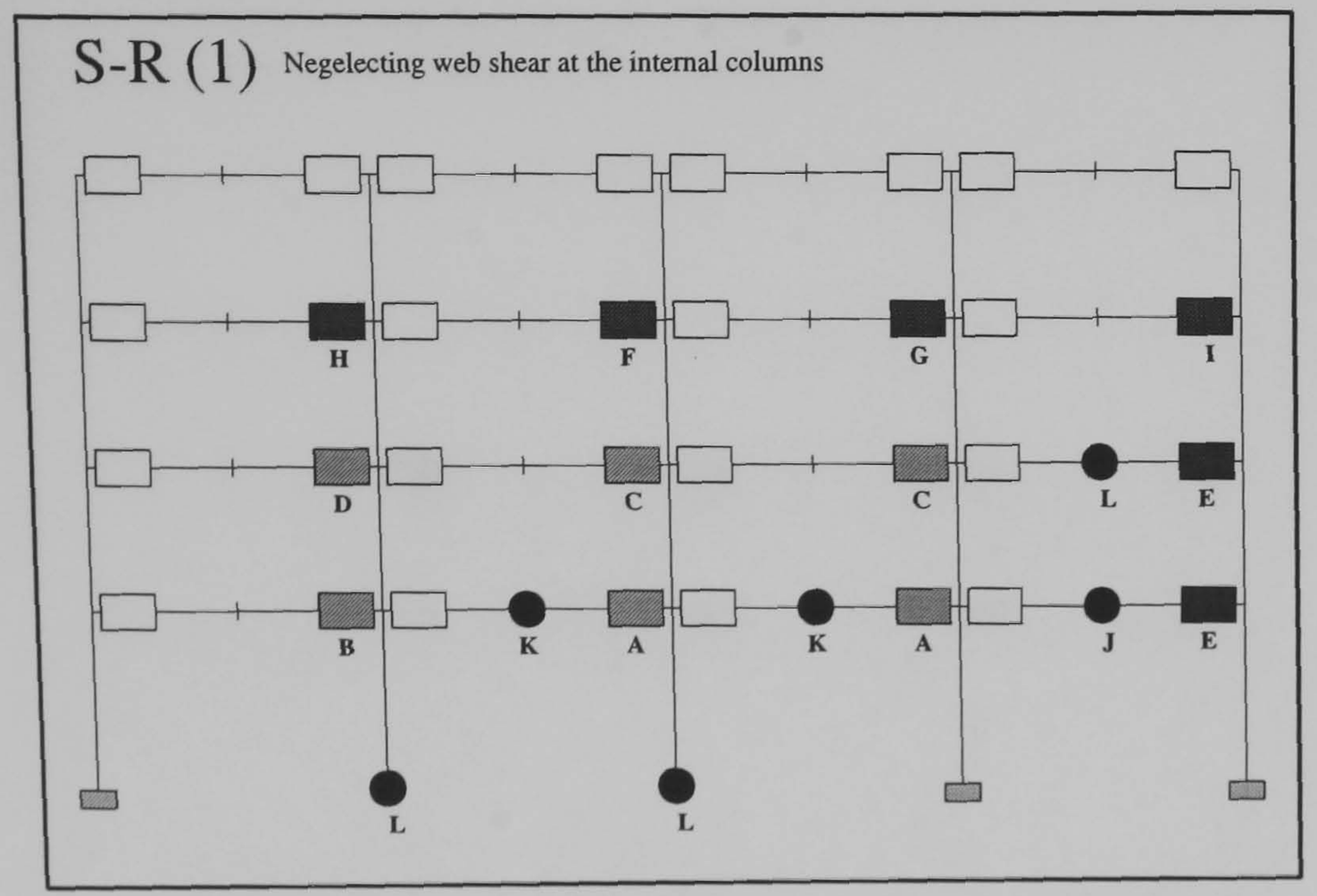

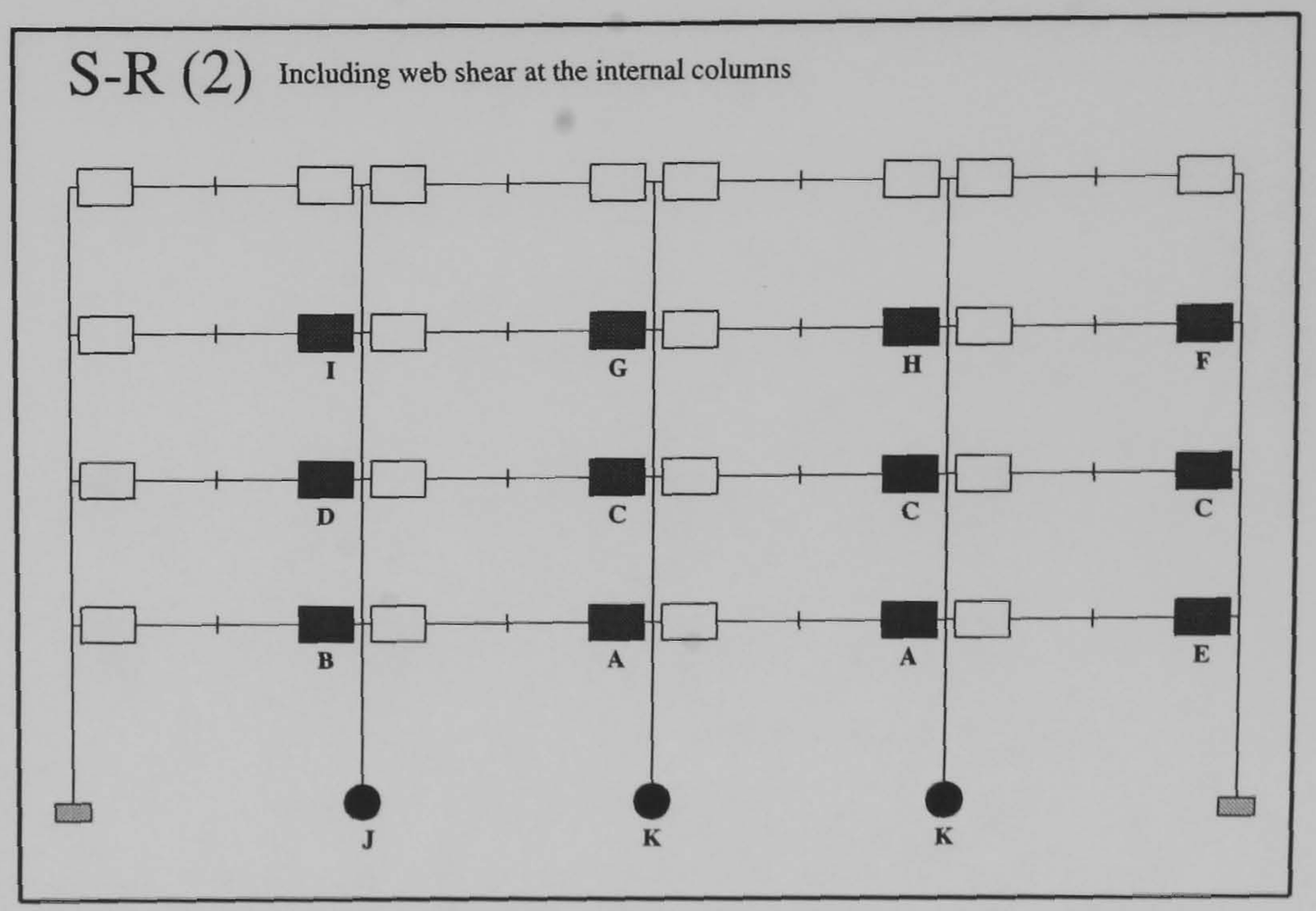

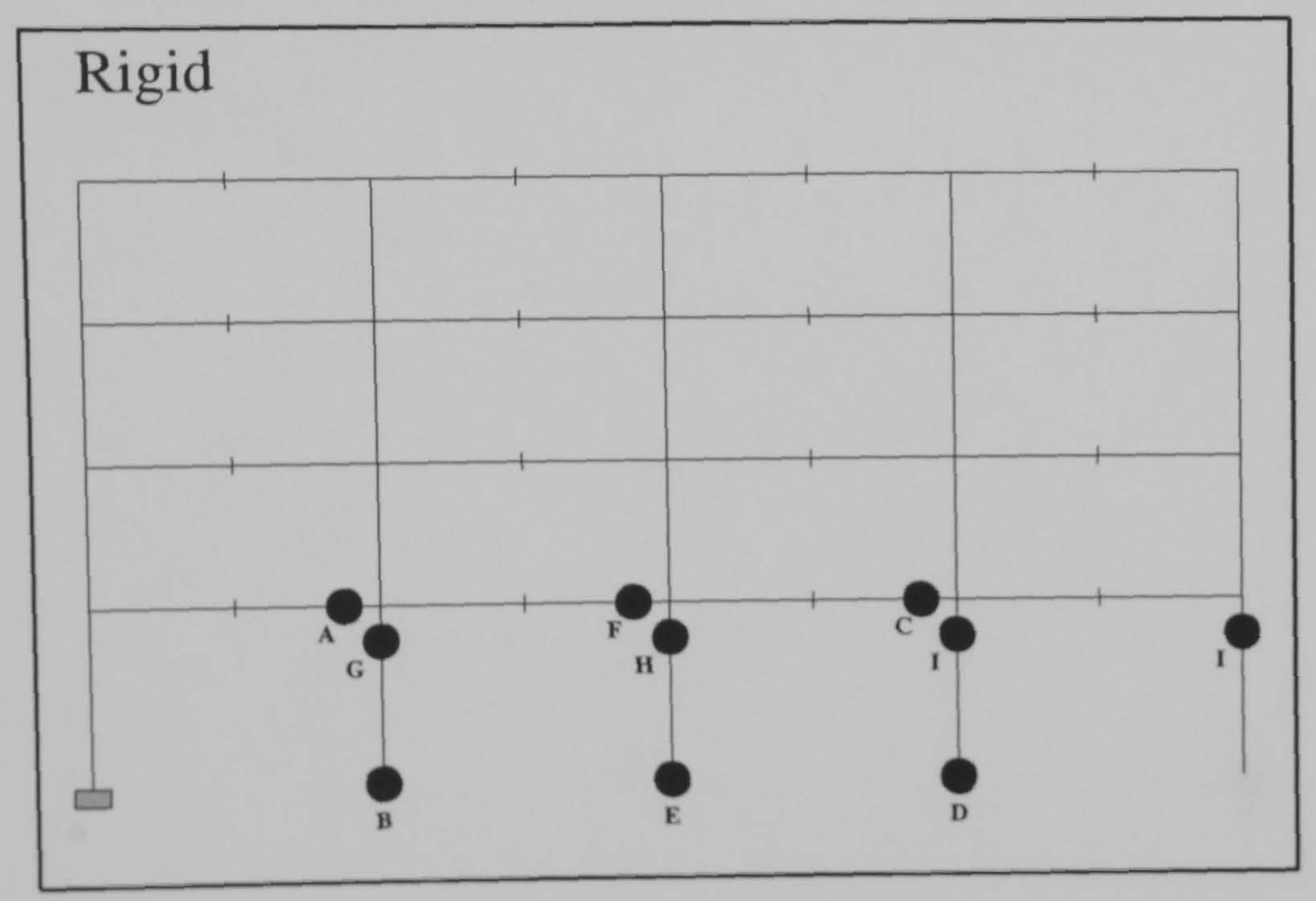

Hinge Location	Load Level at Hinge Formation		
	S-R(1)	S-R(2)	Rigid
A	**0.85**	**1.01**	**1.732**
B	**0.855**	**1.015**	**1.795**
C	**0.88**	**1.0325**	**1.810**
D	**0.8875**	**1.04**	**1.817**
E	**1.06**	**1.0475**	**1.825**
F	**1.15**	**1.195**	**1.842**
G	**1.155**	**1.345**	**1.865**
H	**1.1675**	**1.3475**	**1.875**
I	**1.2525**	**1.36**	**1.877**
J	**1.382**	**1.365**	N/A
K	**1.385**	**1.367**	N/A
L	**1.387**	N/A	N/A

Key :

Semi-Rigid Connection

Plastification prior to ULS design load being attained

Plastification following the attainment of the design load

Member plastification

FRAME : **f30b20**
Load Case 2

S-R (1) Negelecting web shear at the internal columns

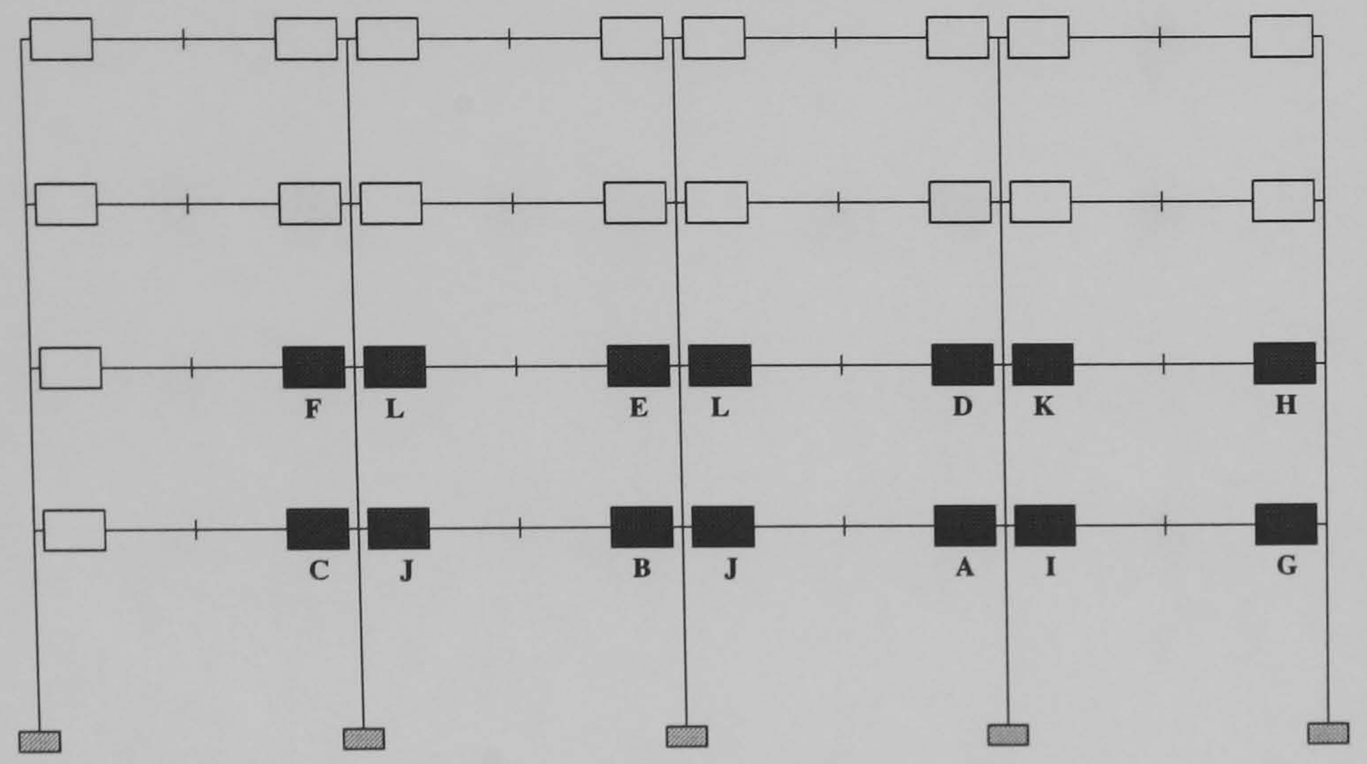

S-R (2) Including web shear at the internal columns

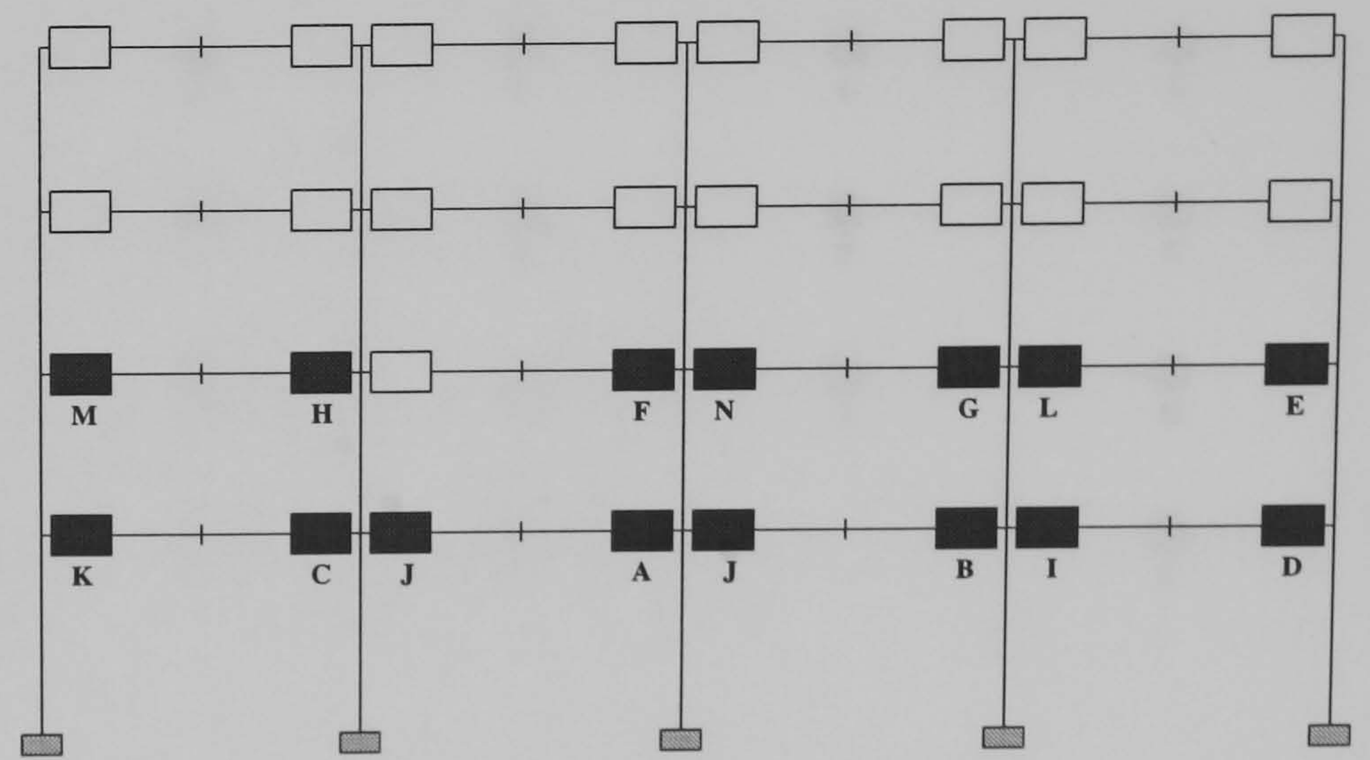

Rigid

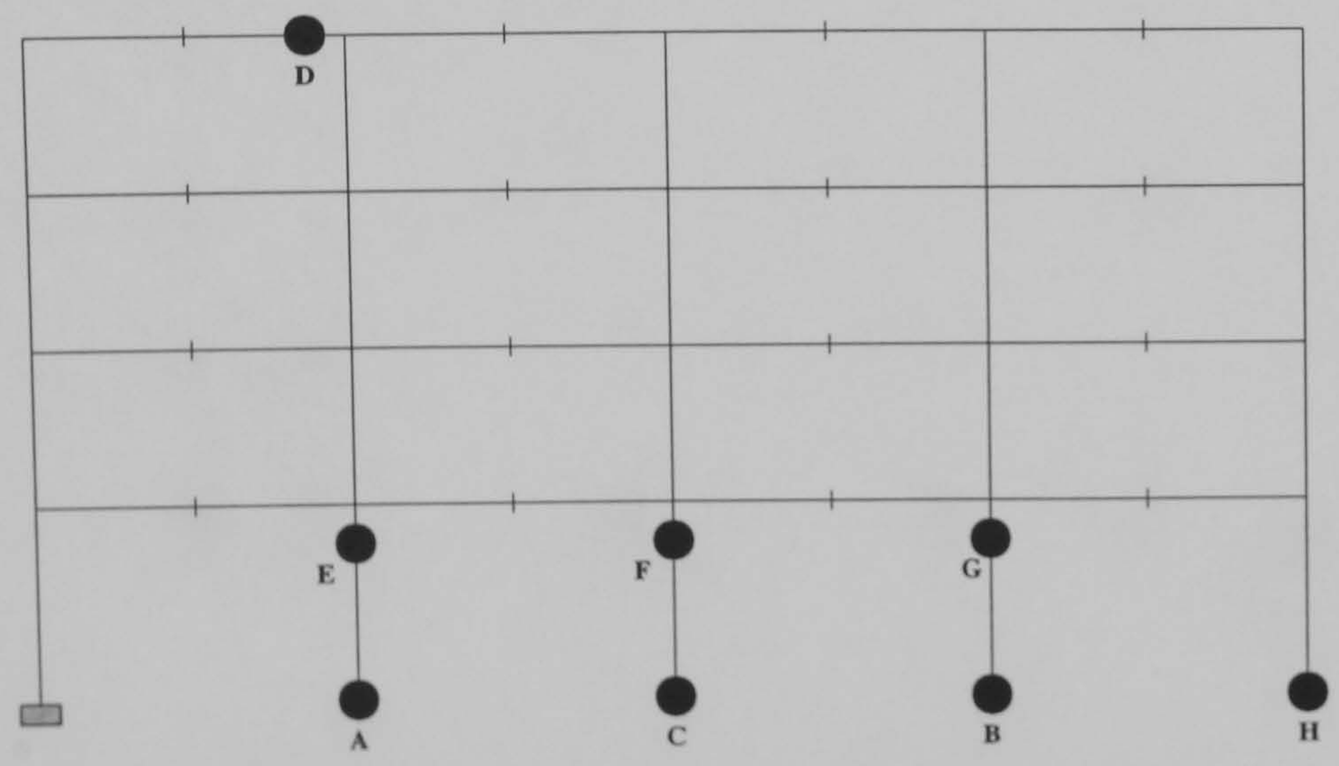

Hinge Location	Load Level at Hinge Formation		
	S-R(1)	S-R(2)	Rigid
A	1.1375	1.325	2.282
B	1.14	1.3275	2.310
C	1.1625	1.34	2.315
D	1.215	1.35	2.352
E	1.2175	1.36	2.4
F	1.24	1.3825	2.417
G	1.4	1.385	2.422
H	1.435	1.395	2.425
I	1.47	1.5075	N/A
J	1.475	1.5125	N/A
K	1.5375	1.5325	N/A
L	1.545	1.5475	N/A
M	N/A	1.55	N/A
N	N/A	1.5525	N/A

Key :

- Semi-Rigid Connection
- Plastification prior to ULS design load being attained
- Plastification following the attainment of the design load
- Member plastification

FRAME : **f30b20**
Load Case 3

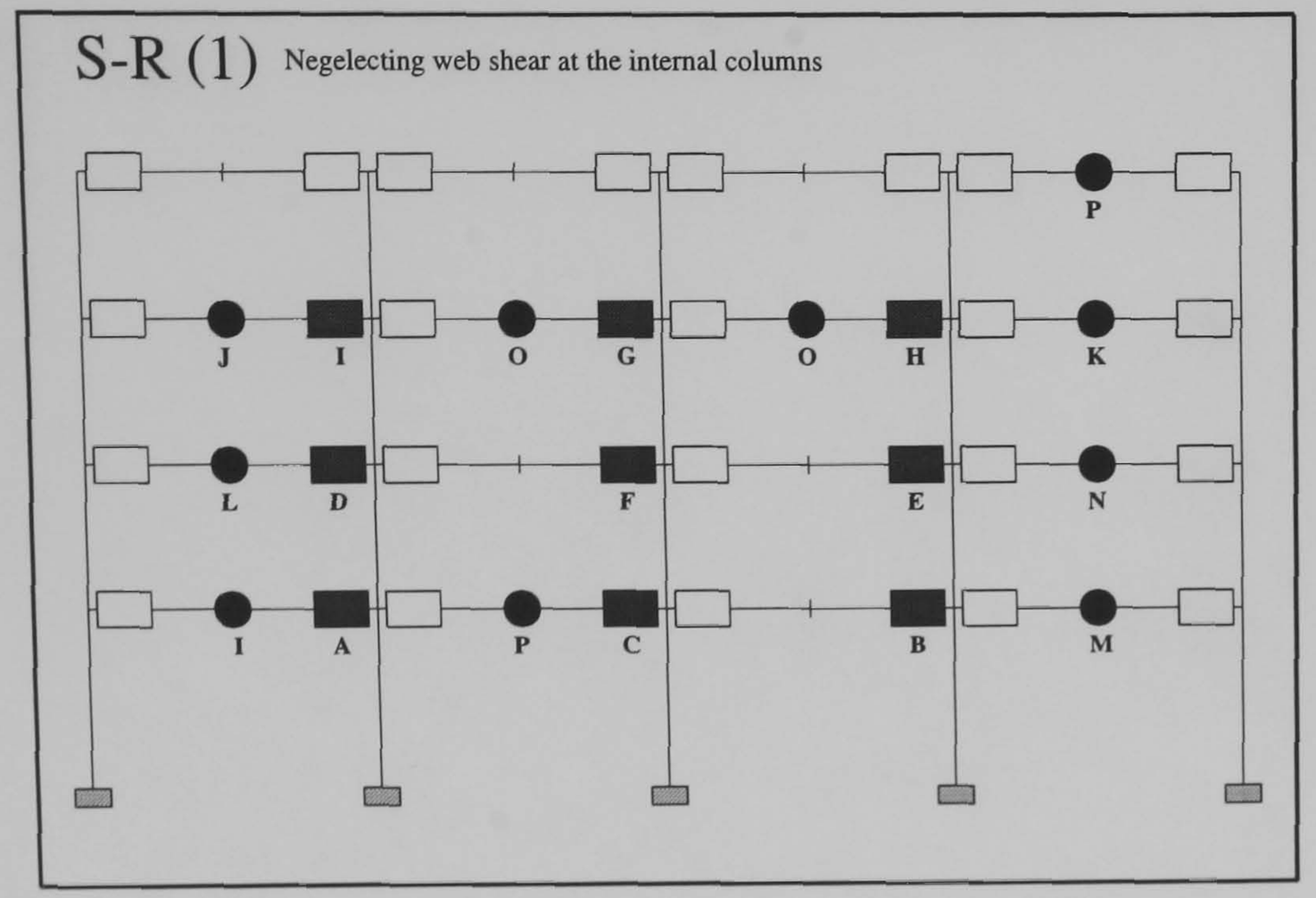

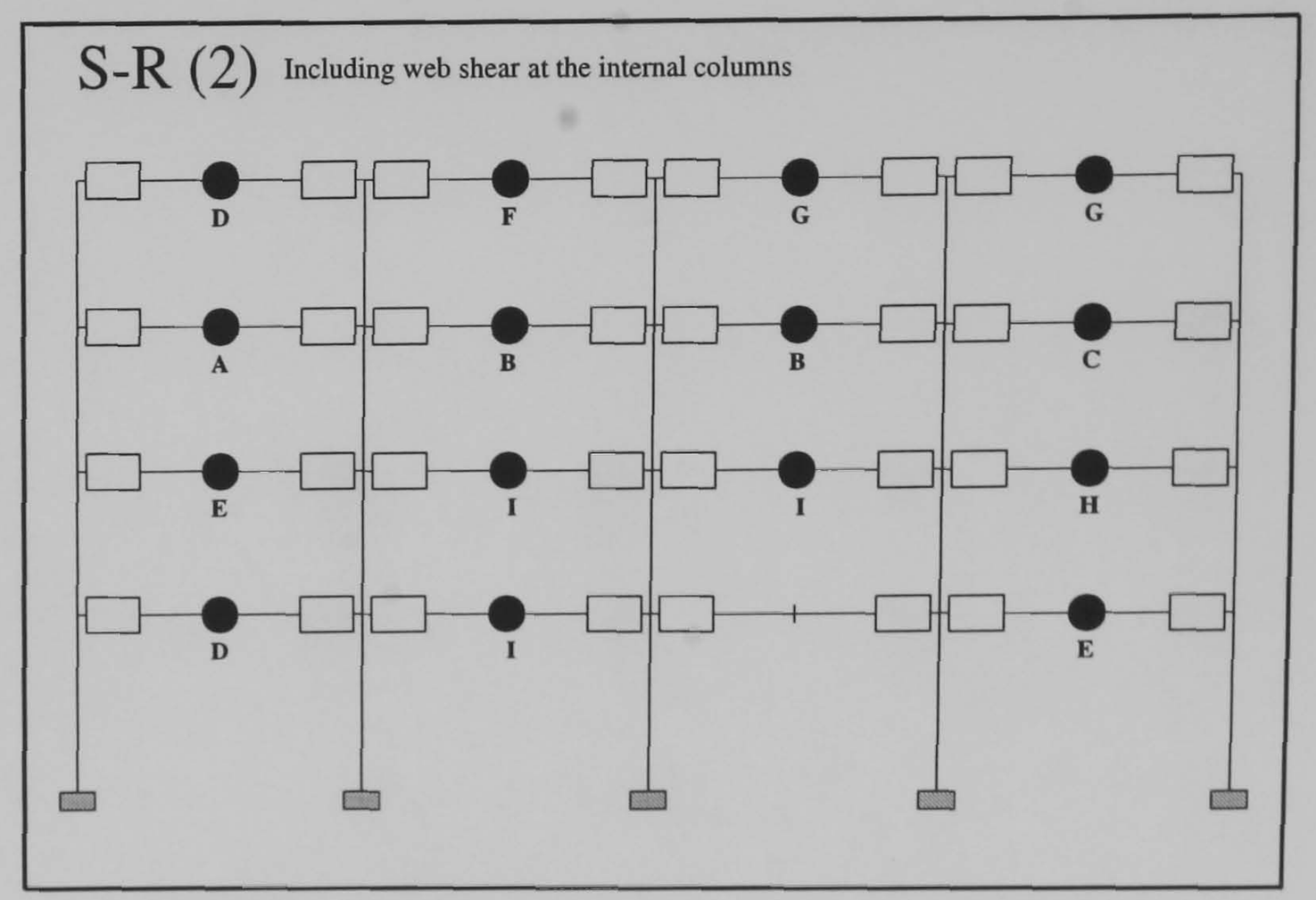

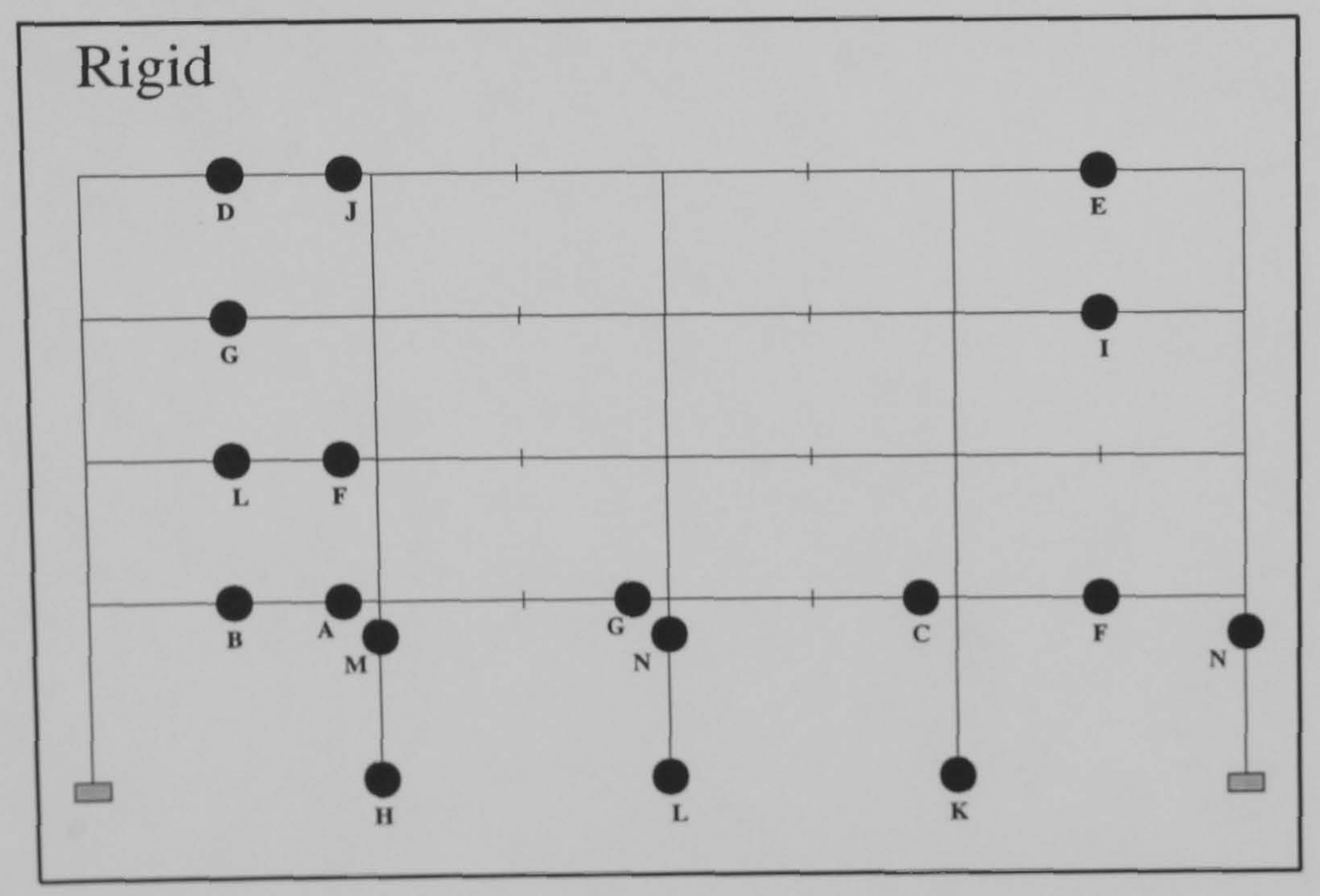

Hinge Location	Load Level at Hinge Formation S-R(1)	S-R(2)	Rigid
A	1.085	1.262	1.712
B	1.1025	1.267	1.827
C	1.11	1.28	1.835
D	1.115	1.302	1.857
E	1.1225	1.307	1.862
F	1.125	1.31	1.867
G	1.295	1.312	1.872
H	1.3025	1.317	1.887
I	1.315	1.332	1.890
J	1.317	N/A	1.897
K	1.32	N/A	1.90
L	1.325	N/A	1.905
M	1.33	N/A	1.915
N	1.337	N/A	1.917
O	1.345	N/A	N/A
P	1.347	N/A	N/A

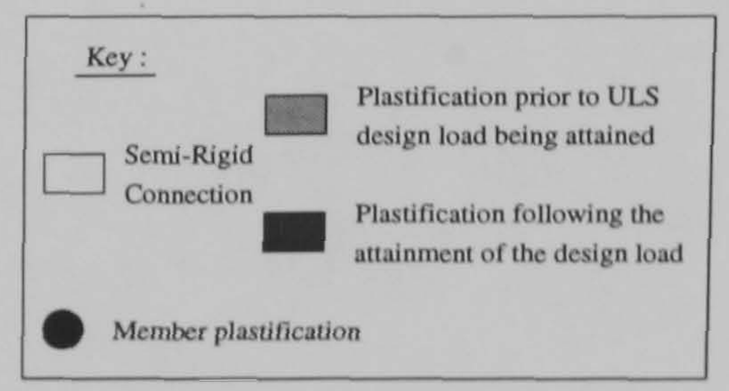

FRAME : **f30b24**
Load Case 1

S-R (1) Negelecting web shear at the internal columns

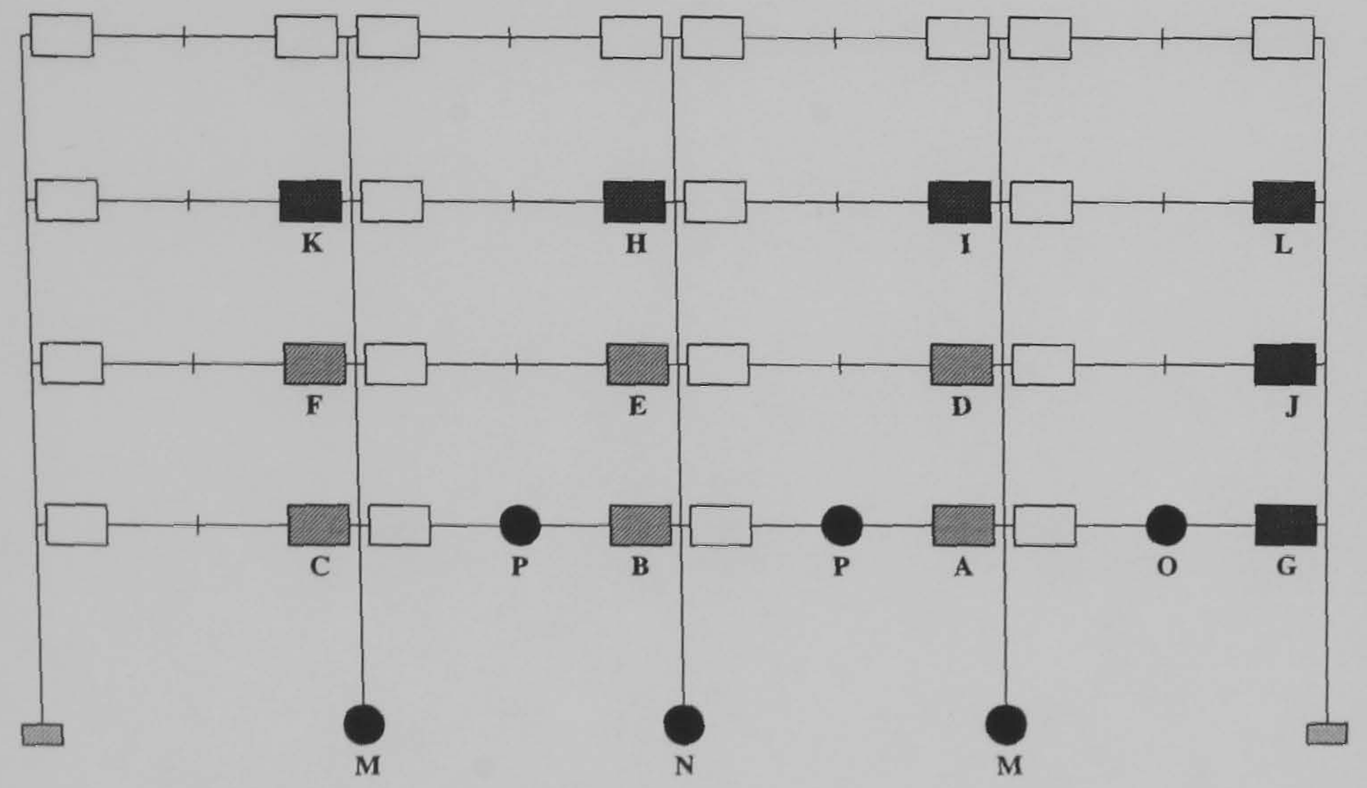

S-R (2) Including web shear at the internal columns

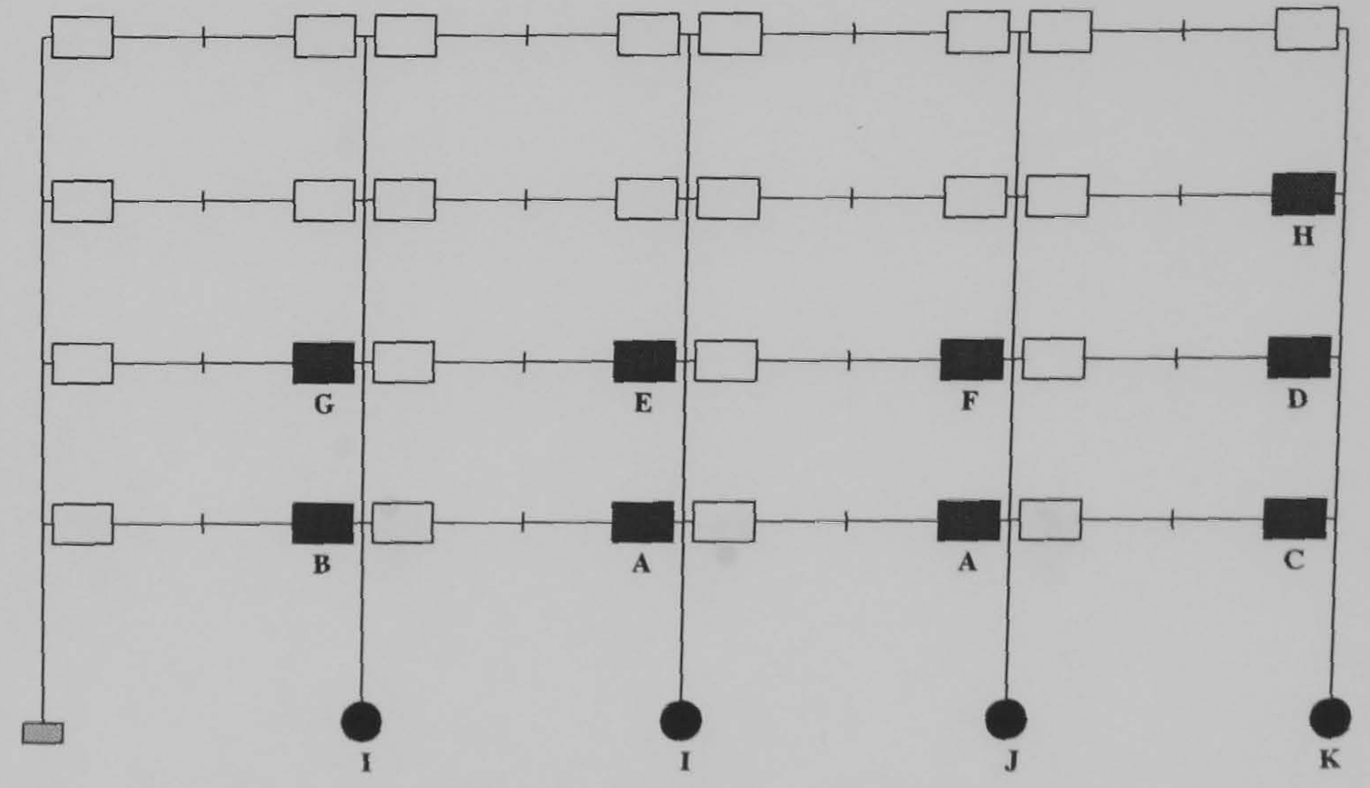

Rigid

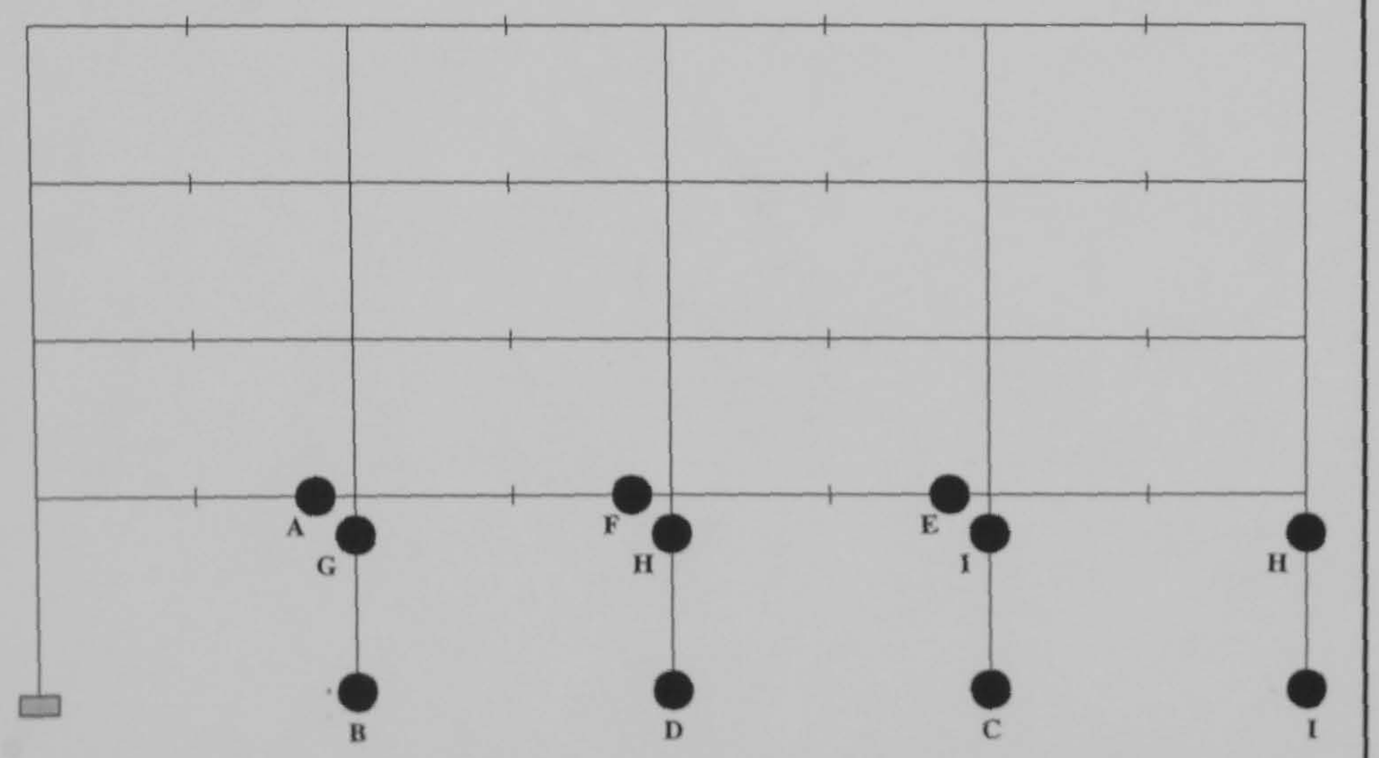

Hinge Location	Load Level at Hinge Formation S-R(1)	S-R(2)	Rigid
A	0.9025	1.12	1.592
B	0.9075	1.1275	1.620
C	0.91	1.155	1.642
D	0.9625	1.1575	1.647
E	0.965	1.17	1.650
F	0.9725	1.1725	1.675
G	1.1775	1.18	1.695
H	1.195	1.2575	1.705
I	1.2	1.322	1.707
J	1.2025	1.325	N/A
K	1.21	1.365	N/A
L	1.33	N/A	N/A
M	1.345	N/A	N/A
N	1.347	N/A	N/A
O	1.39	N/A	N/A
P	1.392	N/A	N/A

Key :

- Plastification prior to ULS design load being attained
- Semi-Rigid Connection
- Plastification following the attainment of the design load
- Member plastification

FRAME : **f30b24**
Load Case 2

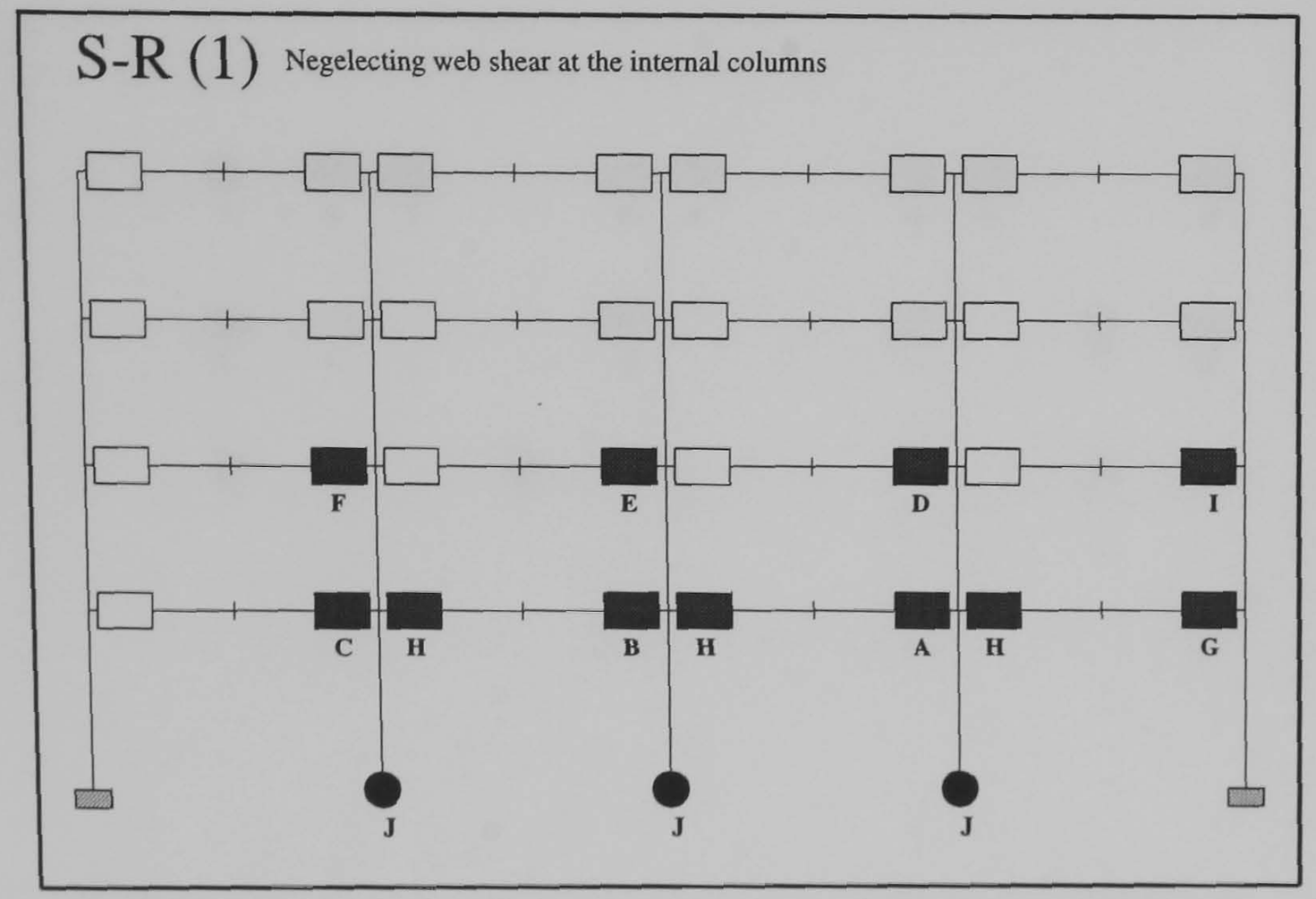

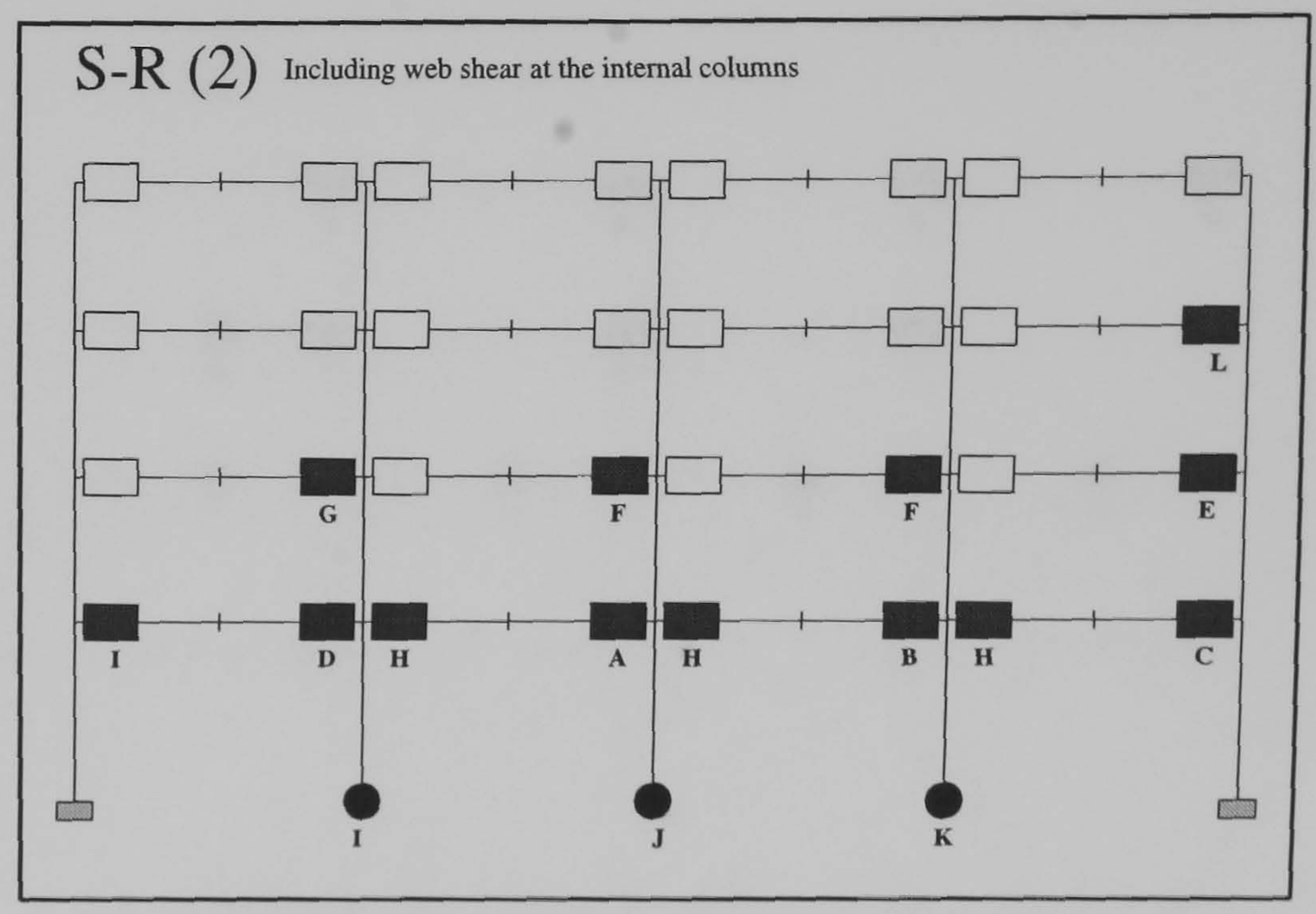

Hinge Location	Load Level at Hinge Formation		
	S-R(1)	S-R(2)	Rigid
A	**1.1725**	**1.425**	**1.98**
B	**1.18**	**1.4275**	**2.002**
C	**1.2075**	**1.435**	**2.005**
D	**1.3**	**1.44**	**2.1**
E	**1.3075**	**1.475**	**2.11**
F	**1.3325**	**1.525**	**2.115**
G	**1.5075**	**1.5375**	**2.117**
H	**1.545**	**1.5975**	**2.12**
I	**1.5775**	**1.61**	**N/A**
J	**1.637**	**1.612**	**N/A**
K	**N/A**	**1.615**	**N/A**
L	**N/A**	**1.62**	**N/A**

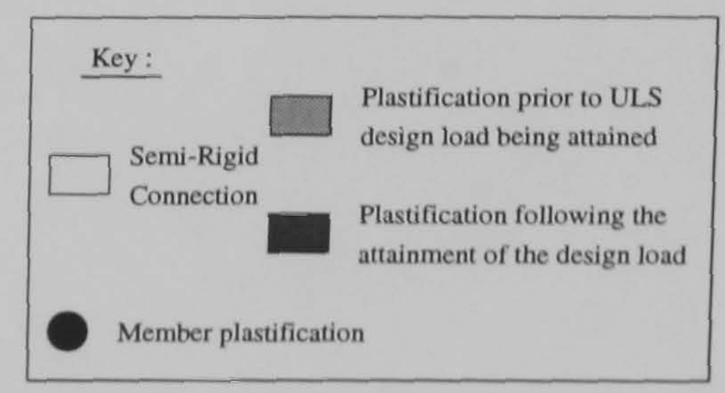

FRAME : **f30b24**
Load Case 3

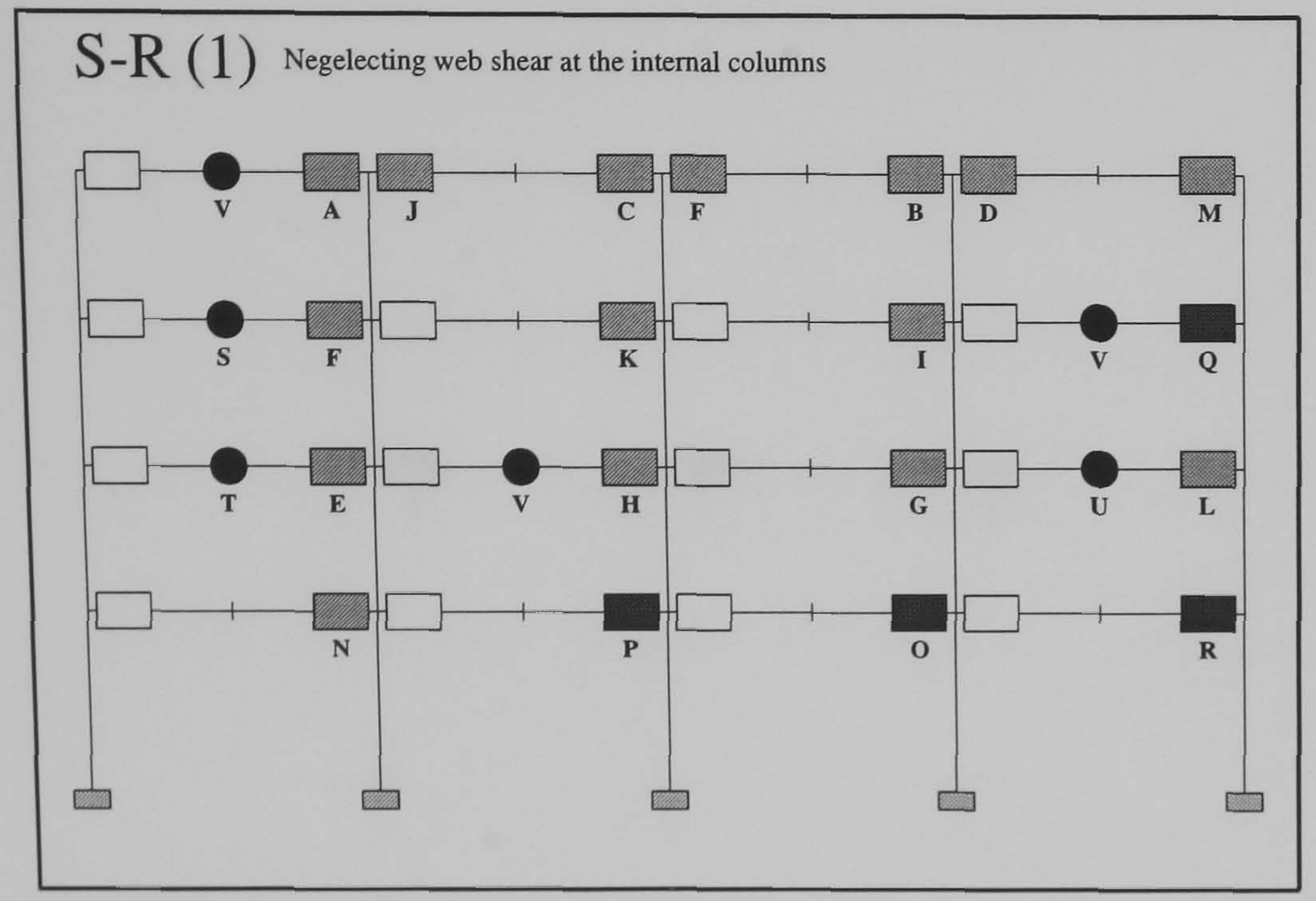

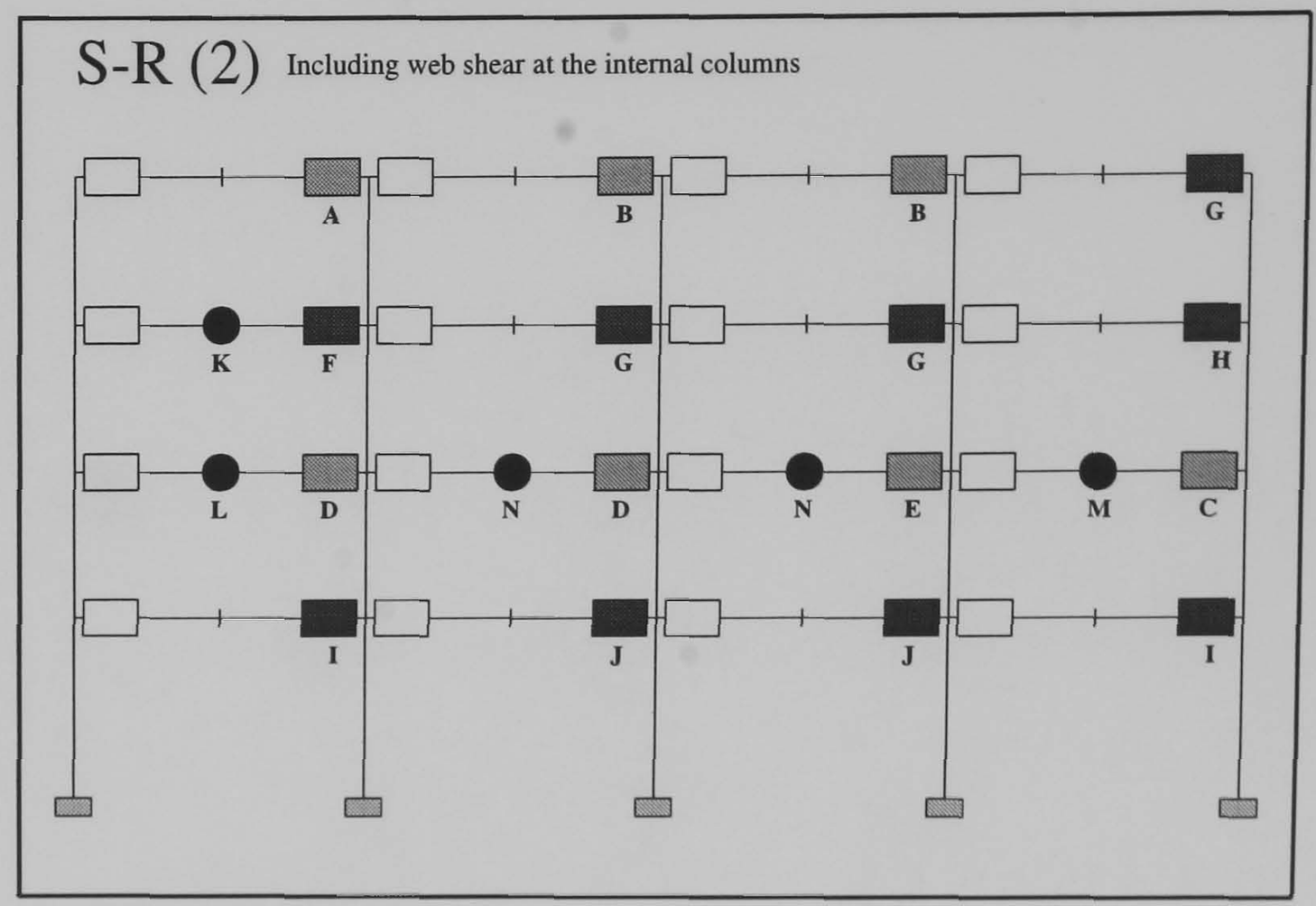

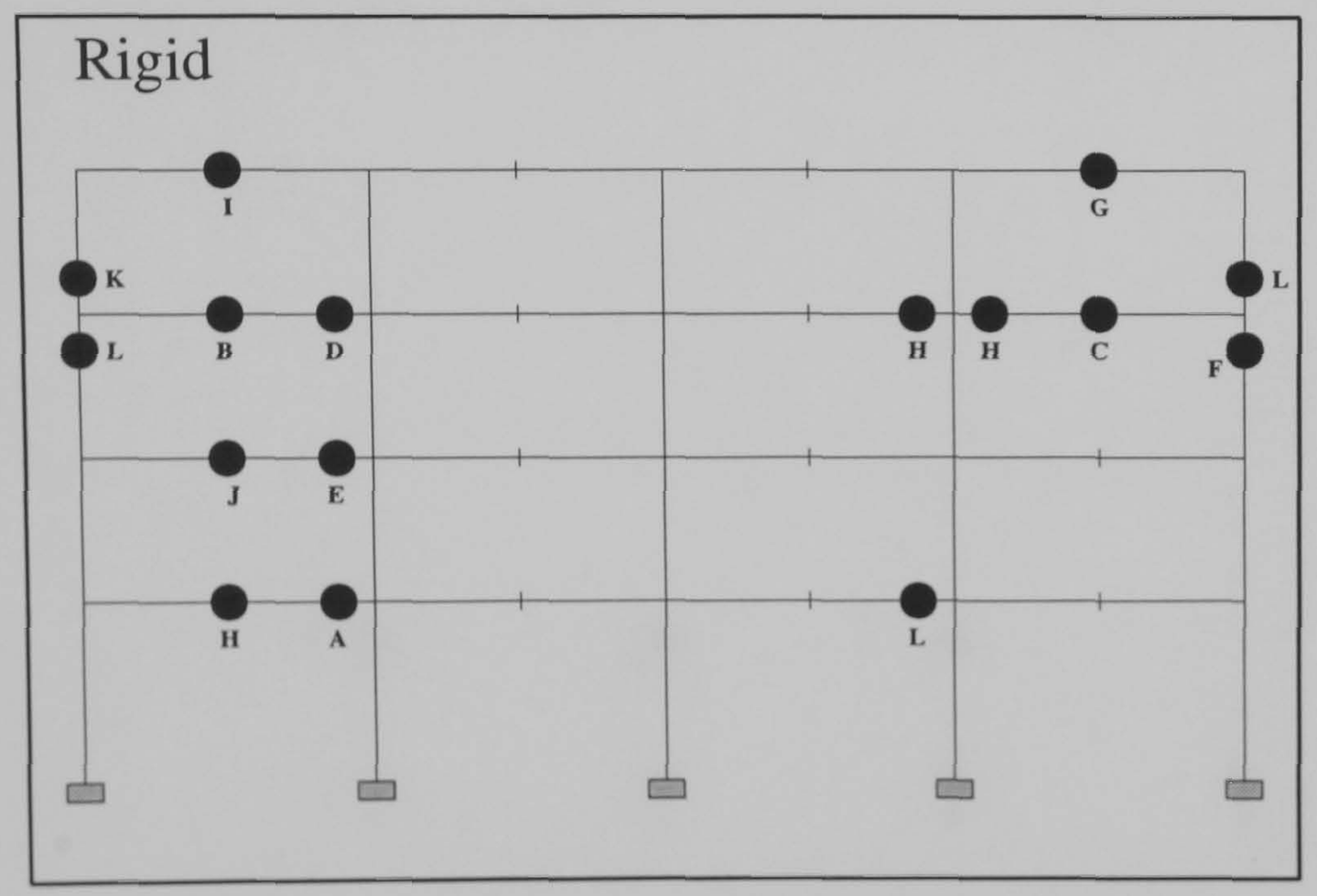

Hinge Location	Load Level at Hinge Formation S-R(1)	S-R(2)	Rigid
A	0.59	0.7875	1.717
B	0.61	0.8	1.752
C	0.6175	0.925	1.760
D	0.635	0.9325	1.762
E	0.73	0.9375	1.770
F	0.74	1.0225	1.807
G	0.7475	1.0325	1.817
H	0.75	1.15	1.820
I	0.7575	1.2025	1.825
J	0.7625	1.2125	1.830
K	0.77	1.215	1.837
L	0.9225	1.225	1.840
M	0.985	1.227	N/A
N	0.9875	1.23	N/A
O	1.0075	N/A	N/A
P	1.0125	N/A	N/A
Q	1.0975	N/A	N/A
R	1.175	N/A	N/A
S	1.197	N/A	N/A
T	1.210	N/A	N/A
U	1.217	N/A	N/A
V	1.22	N/A	N/A

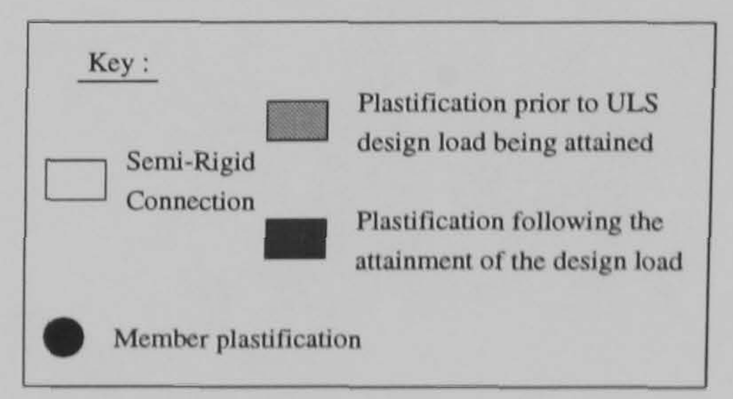

FRAME : **f31 b20**
Load Case 1

S-R (1) Negelecting web shear at the internal columns

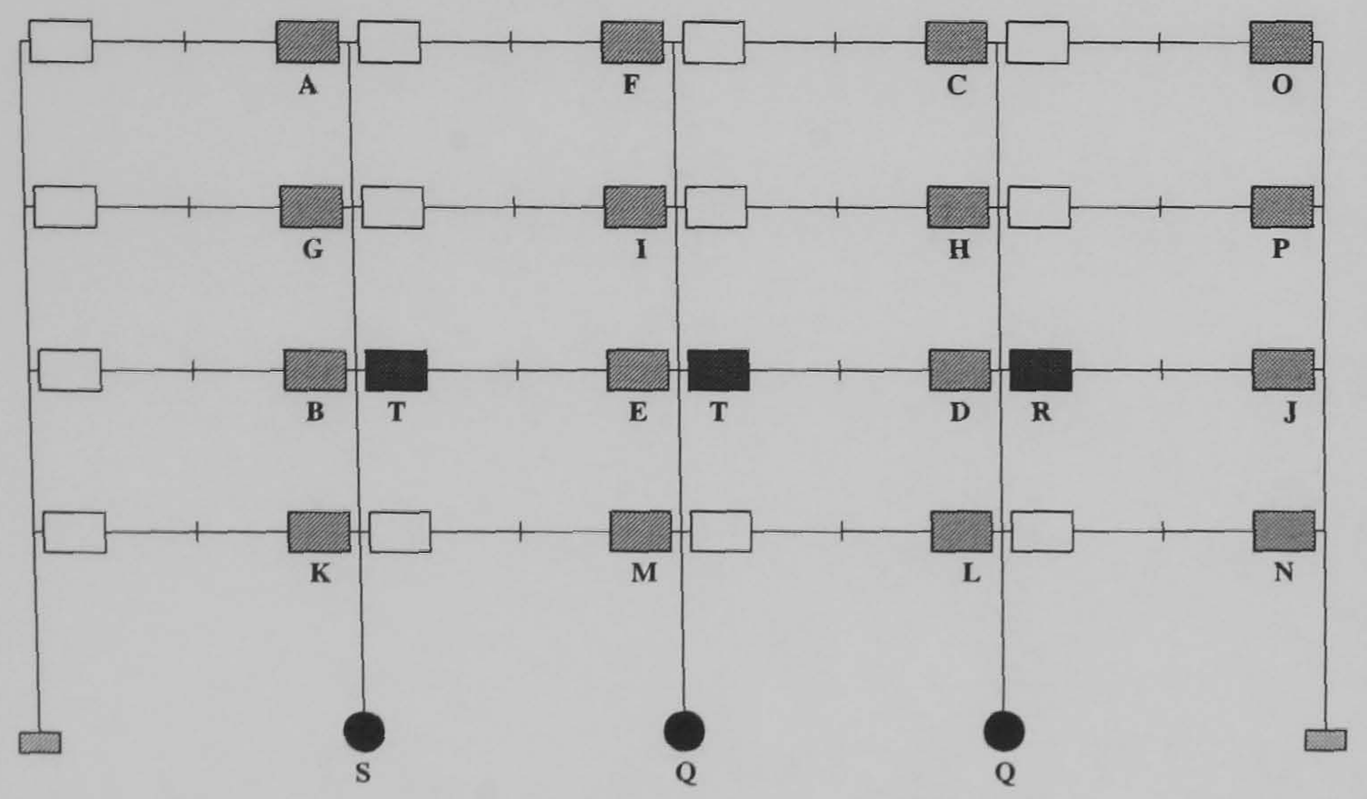

S-R (2) Including web shear at the internal columns

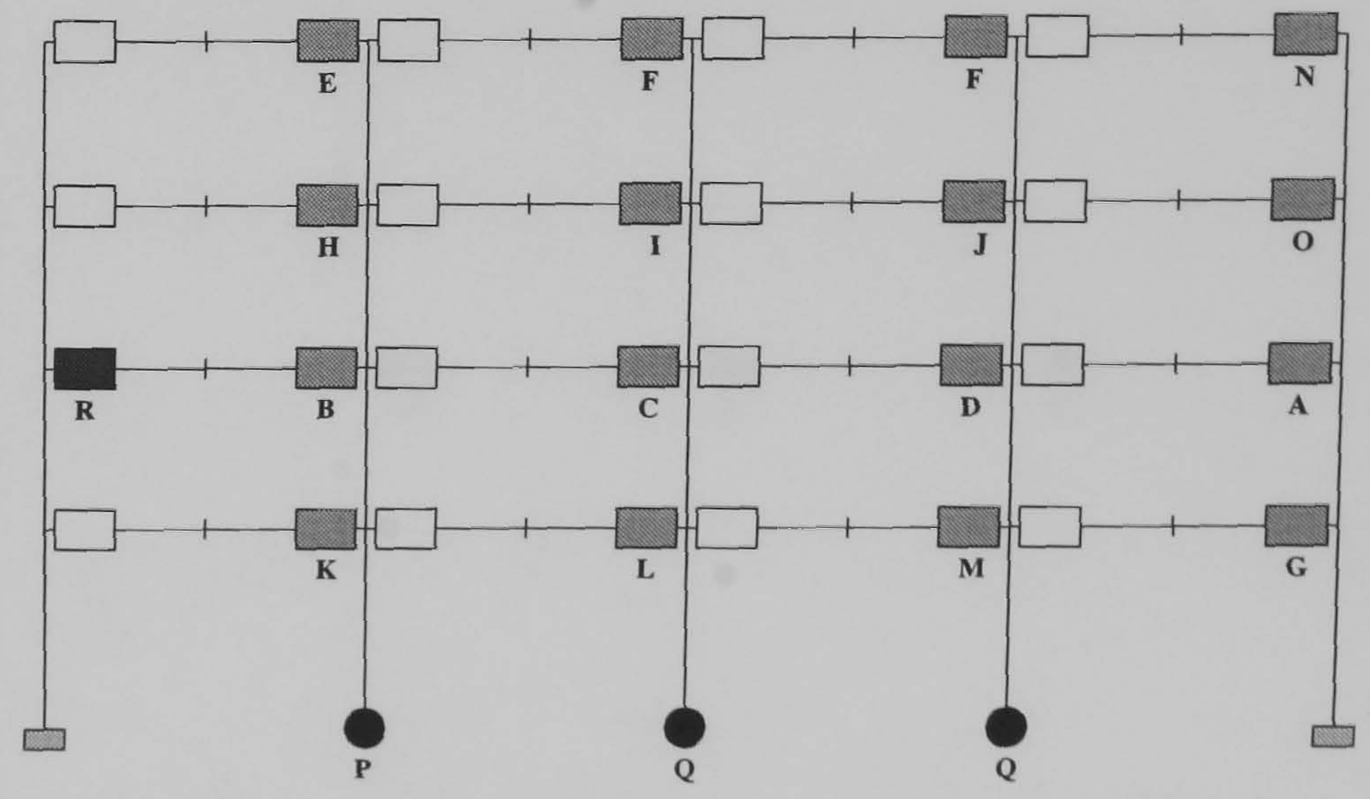

Rigid

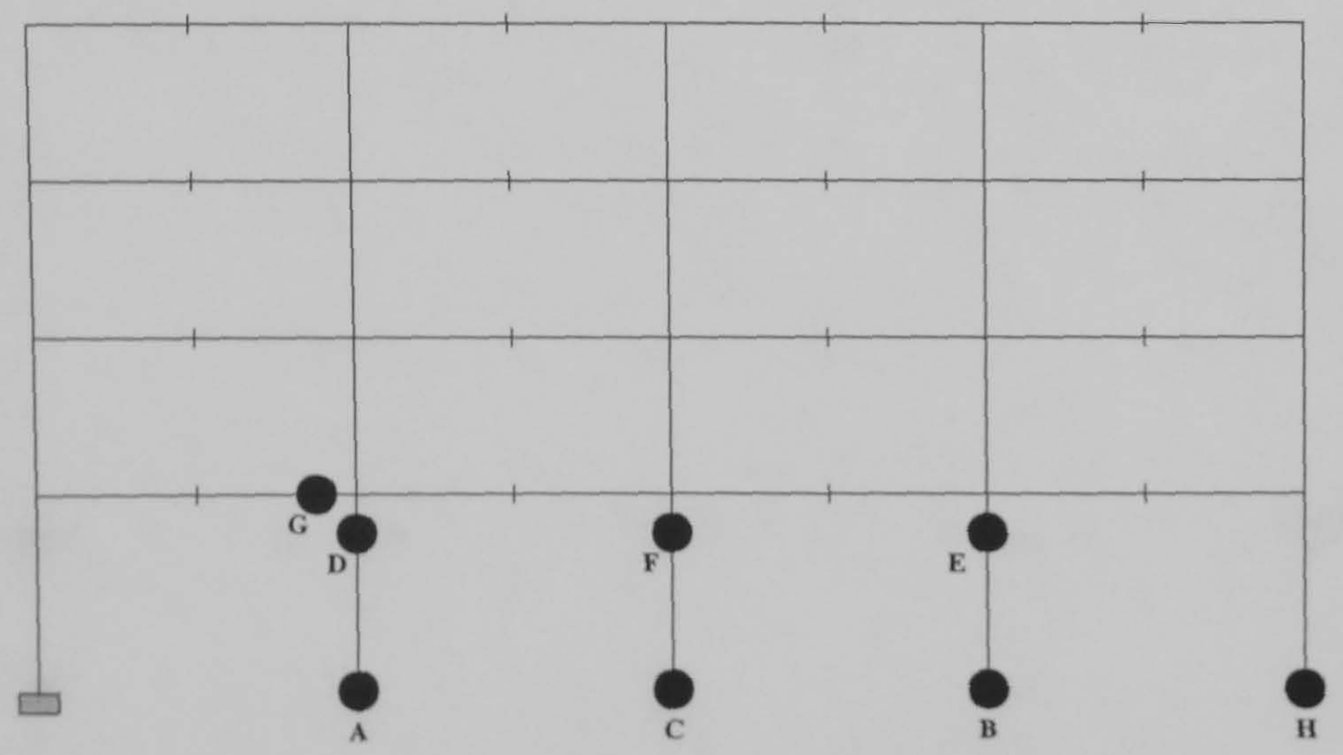

Hinge Location	Load Level at Hinge Formation S-R(1)	S-R(2)	Rigid
A	0.63	0.715	1.41
B	0.64	0.765	1.437
C	0.645	0.7675	1.455
D	0.6475	0.77	1.485
E	0.65	0.8075	1.510
F	0.6525	0.8175	1.517
G	0.7325	0.9175	1.522
H	0.7425	0.9425	1.525
I	0.7525	0.9475	N/A
J	0.76	0.95	N/A
K	0.8225	0.9625	N/A
L	0.83	0.97	N/A
M	0.835	0.9725	N/A
N	0.9375	0.9775	N/A
O	0.965	0.9975	N/A
P	0.995	1.132	N/A
Q	1.147	1.135	N/A
R	1.15	1.15	N/A
S	1.165	N/A	N/A
T	1.17	N/A	N/A

Key :

- Semi-Rigid Connection
- Plastification prior to ULS design load being attained
- Plastification following the attainment of the design load
- Member plastification

FRAME : **f31 b20**
Load Case 2

S-R (1) Negelecting web shear at the internal columns

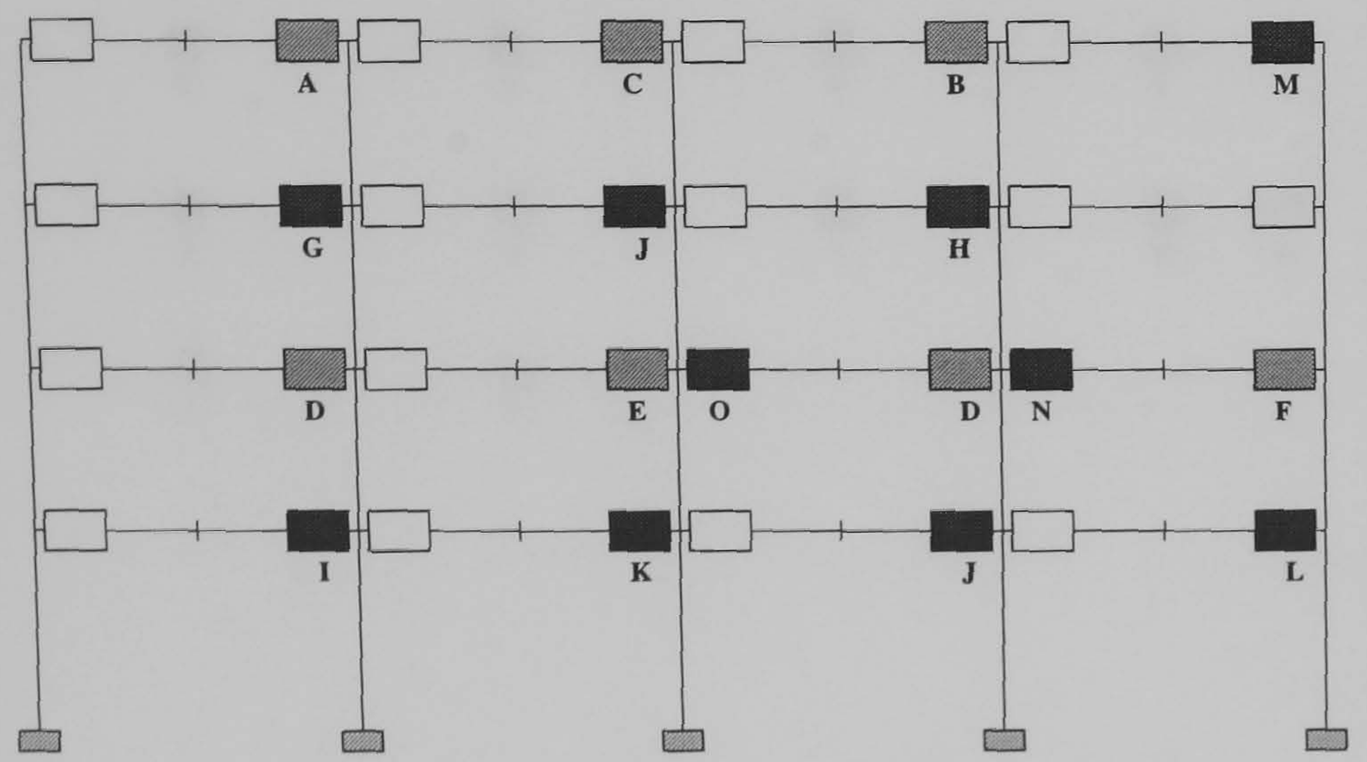

S-R (2) Including web shear at the internal columns

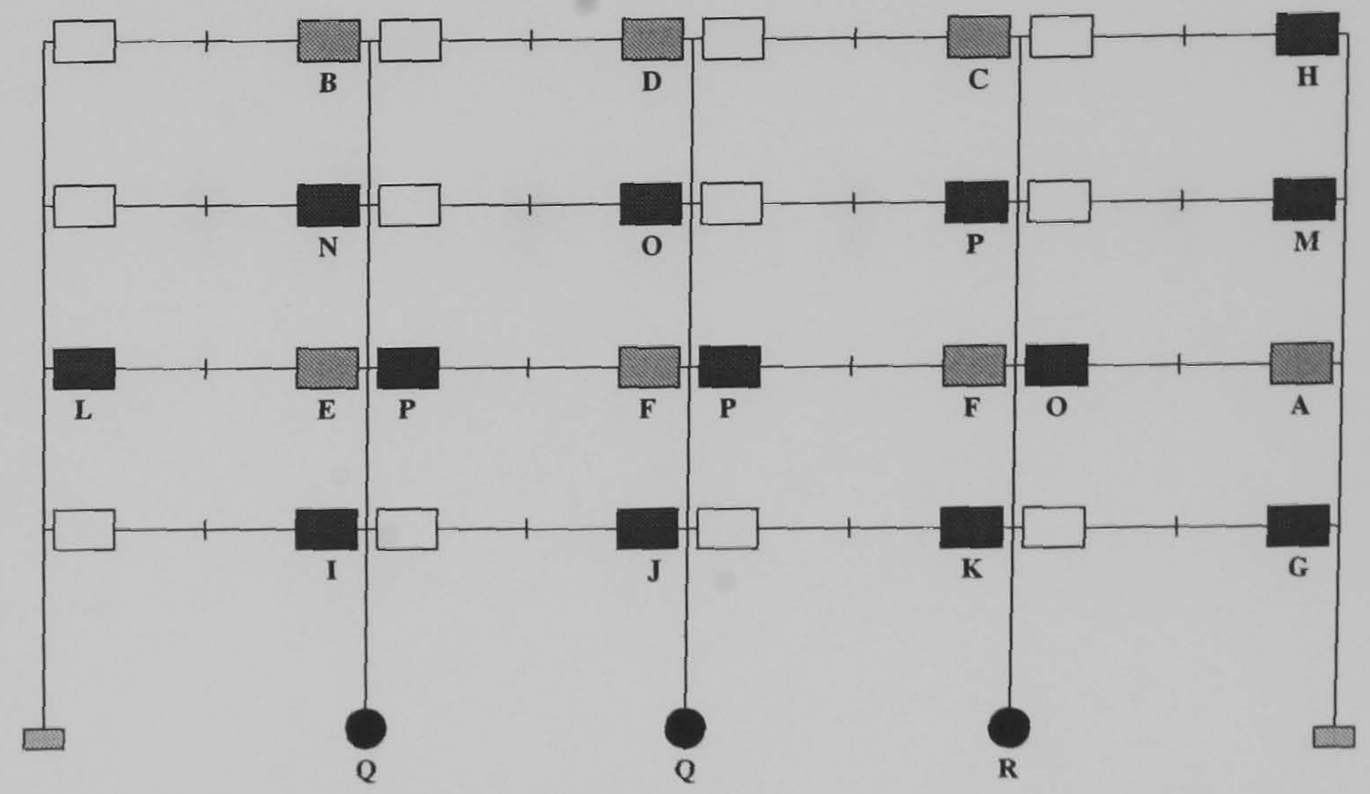

Rigid

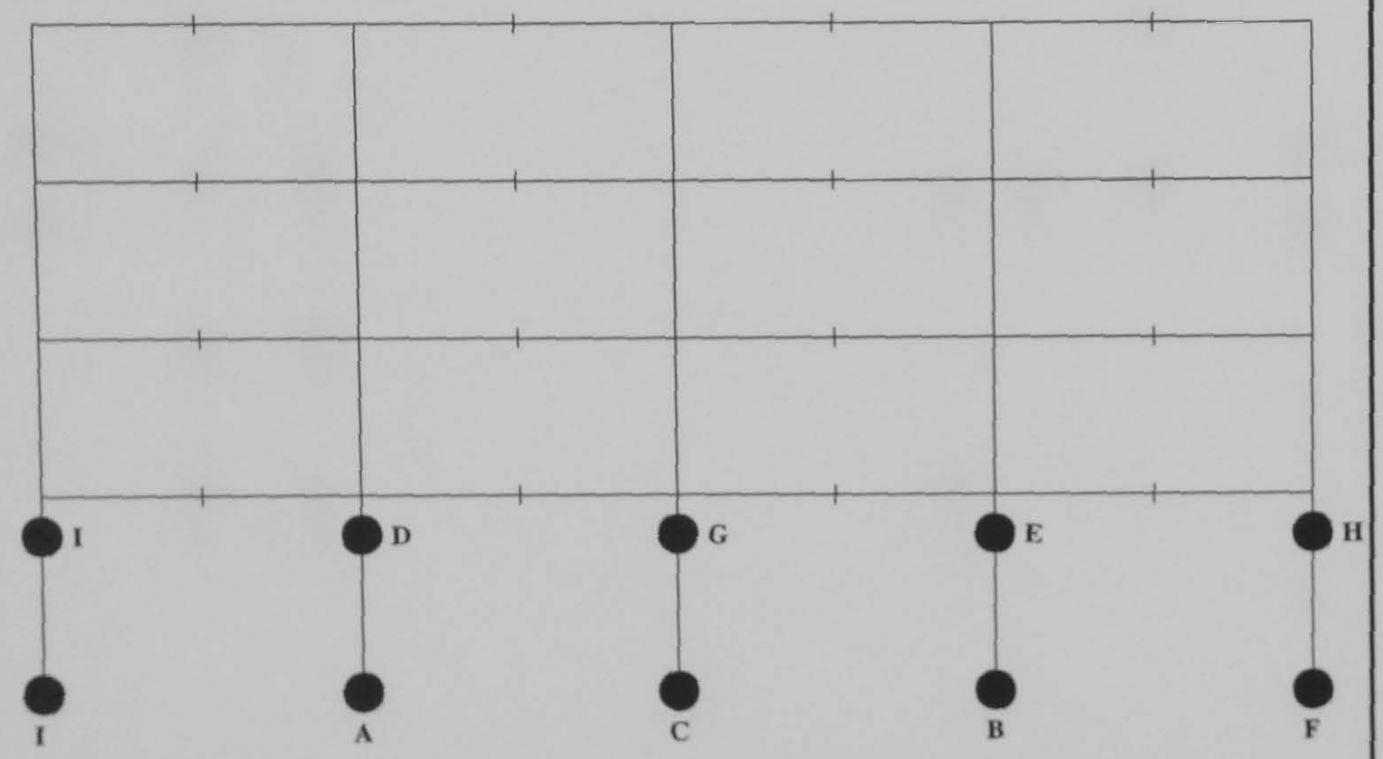

Hinge Location	Load Level at Hinge Formation		
	S-R(1)	S-R(2)	Rigid
A	0.7175	0.8675	1.572
B	0.7325	0.91	1.597
C	0.7475	0.925	1.610
D	0.84	0.9275	1.682
E	0.8425	0.9625	1.705
F	0.95	0.9675	1.712
G	1.0325	1.095	1.715
H	1.035	1.1275	1.725
I	1.0425	1.1825	1.727
J	1.045	1.1925	N/A
K	1.0475	1.195	N/A
L	1.145	1.21	N/A
M	1.155	1.2425	N/A
N	1.24	1.245	N/A
O	1.245	1.2475	N/A
P	N/A	1.2525	N/A
Q	N/A	1.282	N/A
R	N/A	1.285	N/A

Key :

- Semi-Rigid Connection
- Plastification prior to ULS design load being attained
- Plastification following the attainment of the design load
- Member plastification

FRAME : **f31 b20**

Load Case 3

S-R (1) Negelecting web shear at the internal columns

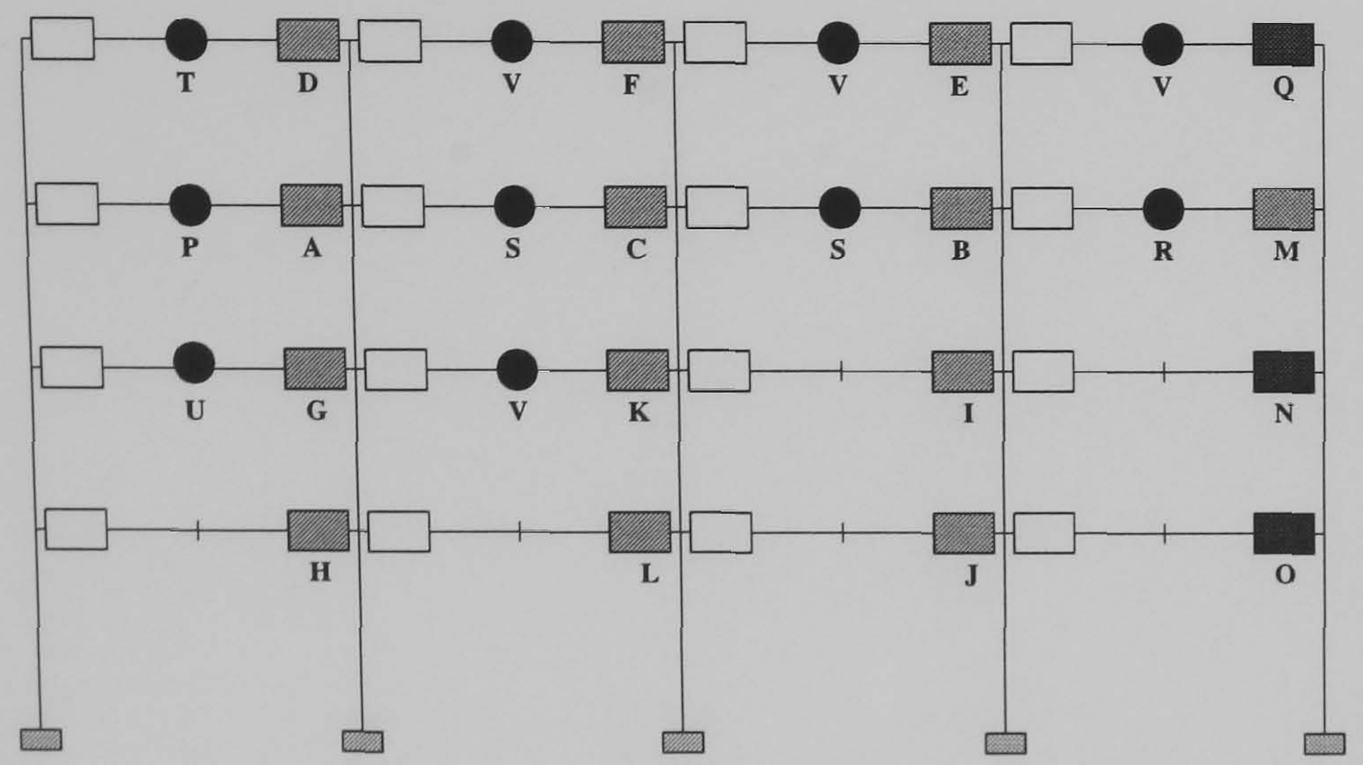

S-R (2) Including web shear at the internal columns

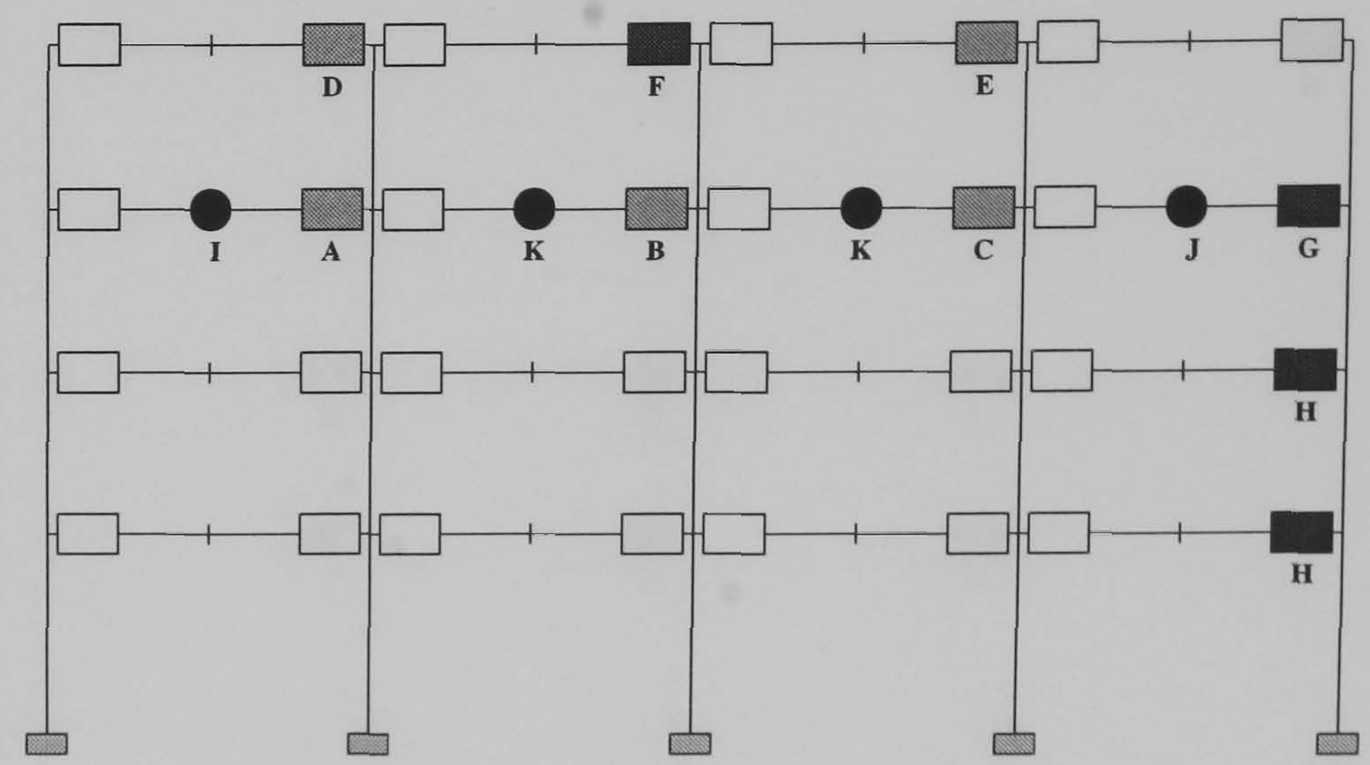

Rigid

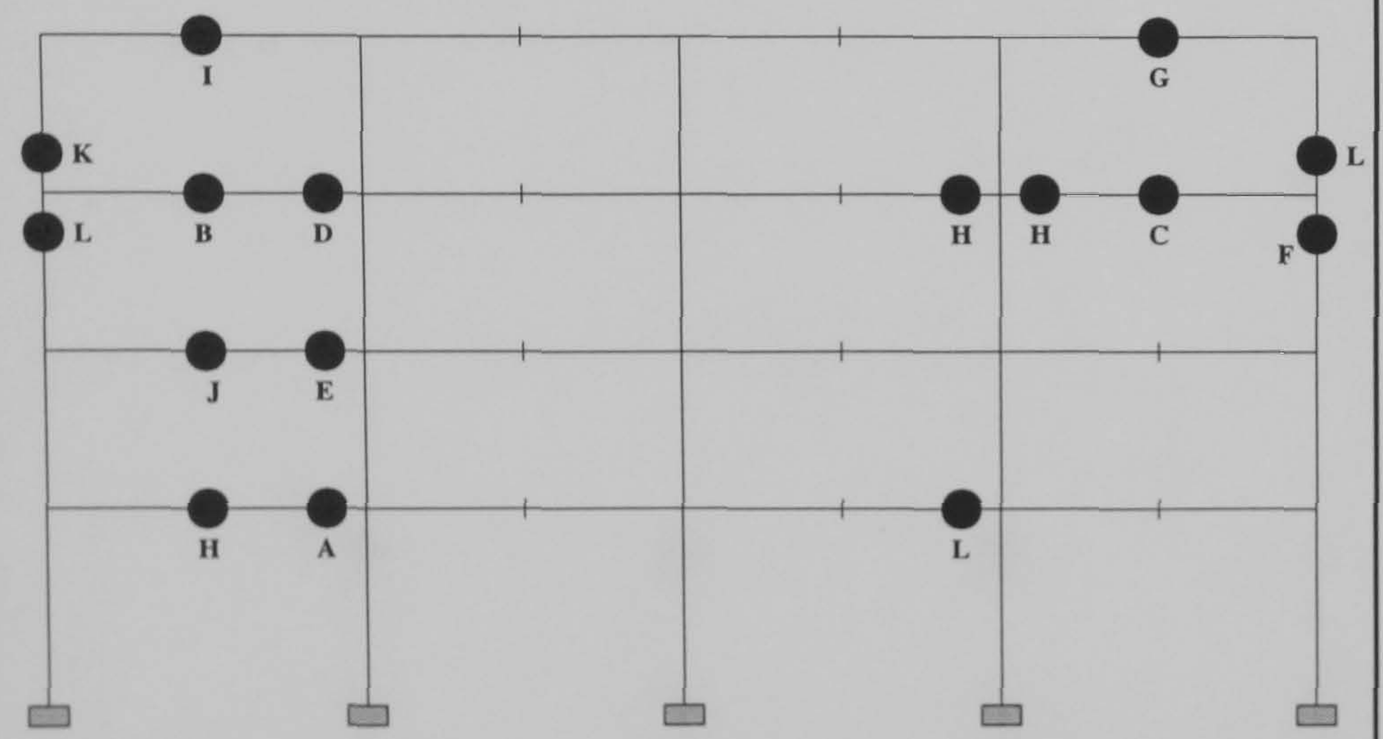

Hinge Location	Load Level at Hinge Formation		
	S-R(1)	S-R(2)	Rigid
A	0.5675	0.8775	1.717
B	0.59	0.885	1.752
C	0.6	0.8875	1.760
D	0.675	0.975	1.762
E	0.7025	0.995	1.770
F	0.7225	1.0025	1.807
G	0.8925	1.0075	1.817
H	0.895	1.1625	1.820
I	0.9225	1.215	1.825
J	0.93	1.227	1.830
K	0.9325	1.232	1.837
L	0.9375	N/A	1.840
M	0.965	N/A	N/A
N	1.14	N/A	N/A
O	1.1525	N/A	N/A
P	1.197	N/A	N/A
Q	1.205	N/A	N/A
R	1.22	N/A	N/A
S	1.225	N/A	N/A
T	1.24	N/A	N/A
U	1.242	N/A	N/A
V	1.245	N/A	N/A

Key :

- Plastification prior to *ULS* design load being attained
- Semi-Rigid Connection
- Plastification following the attainment of the design load
- Member plastification

FRAME : **f31 b24**
Load Case 1

S-R (1) Negelecting web shear at the internal columns

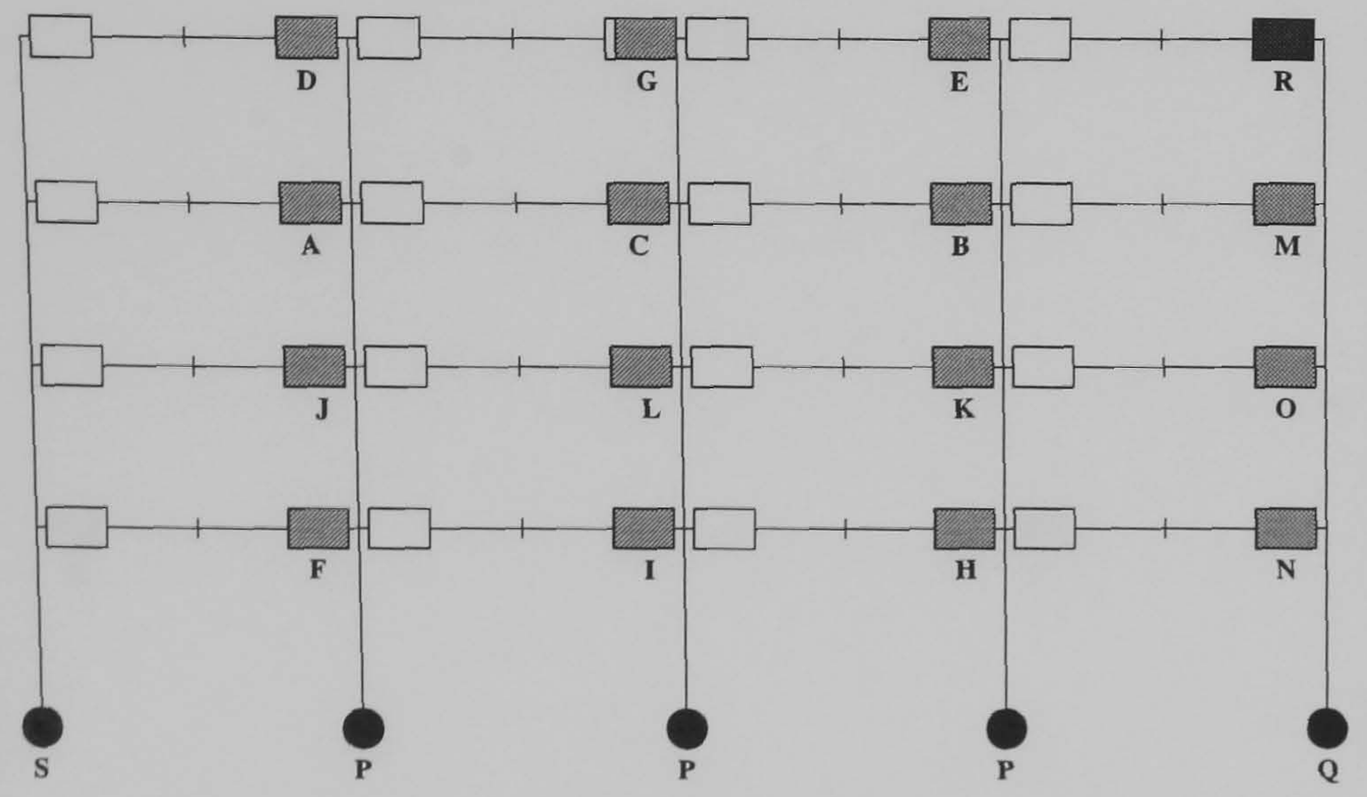

S-R (2) Including web shear at the internal columns

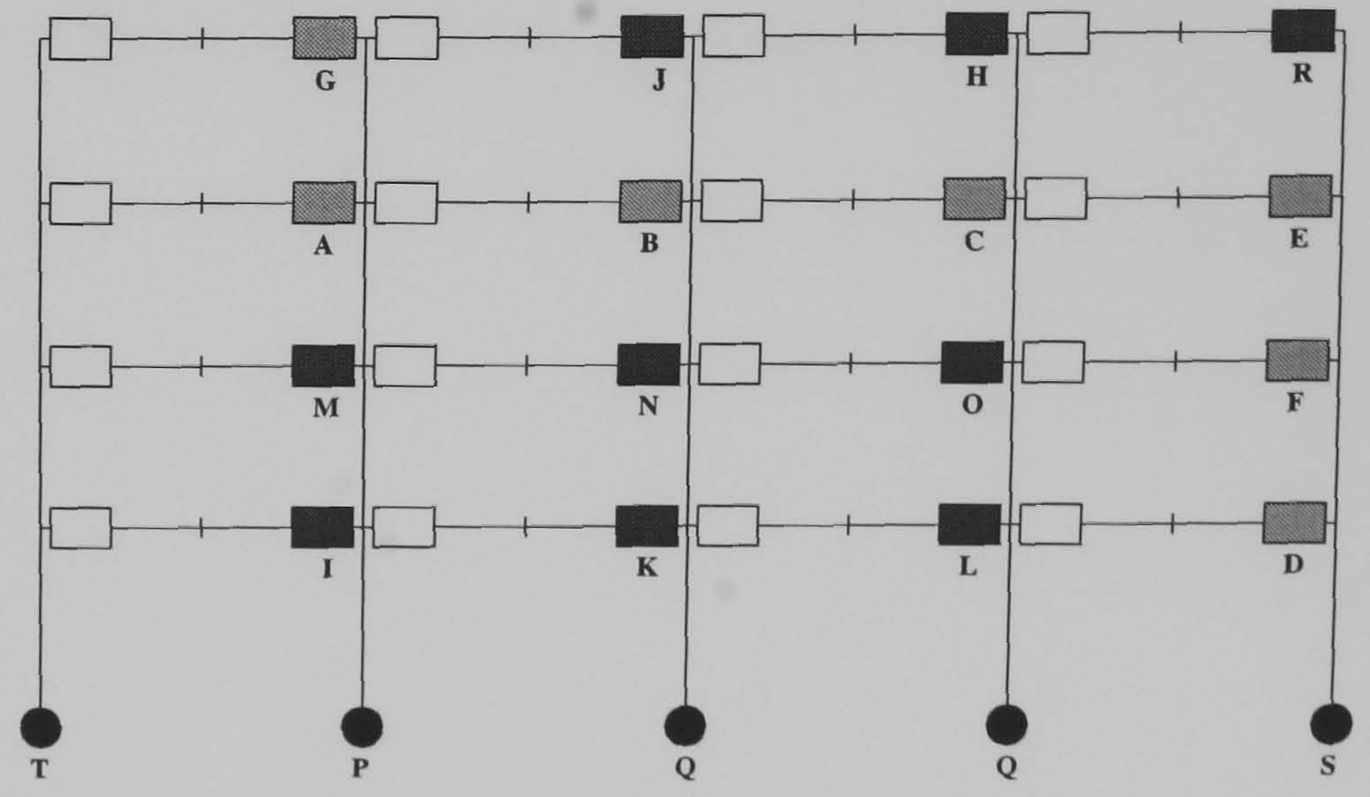

Rigid

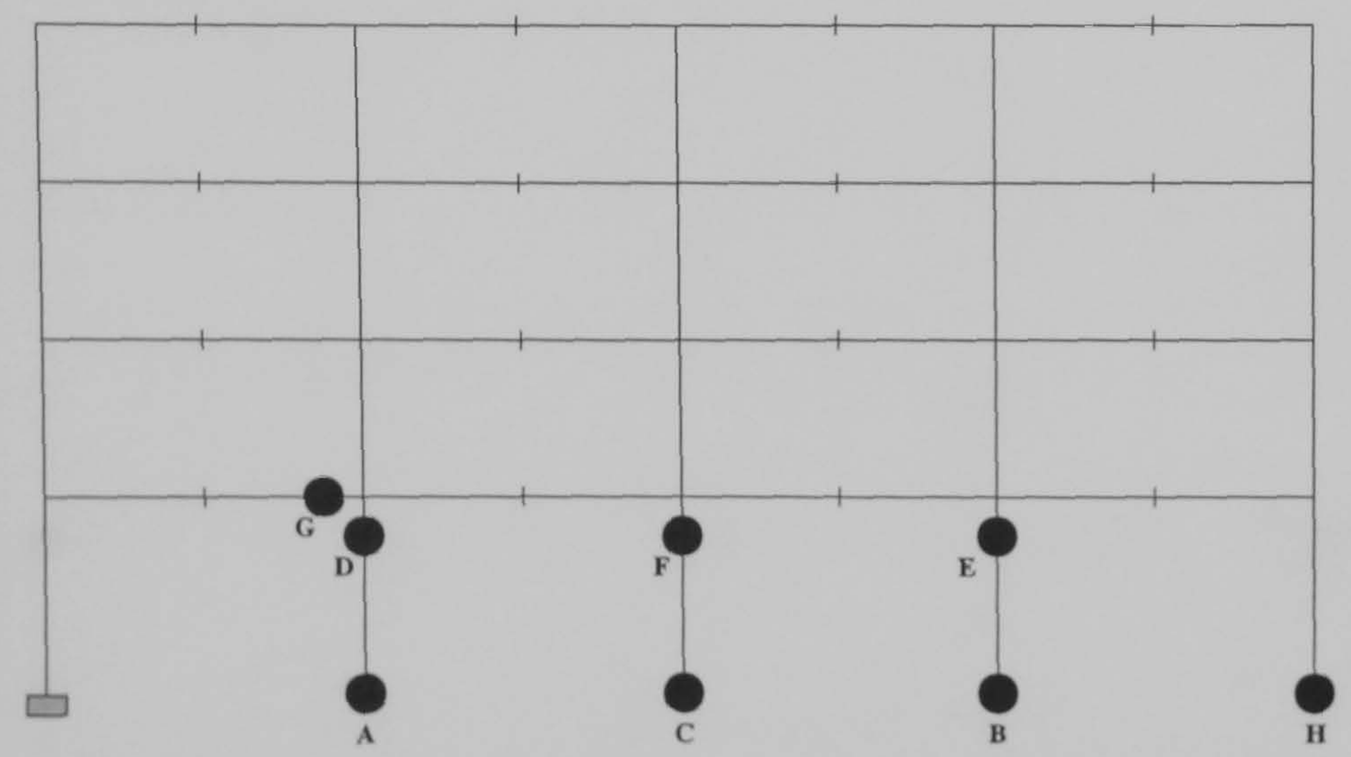

Hinge Location	Load Level at Hinge Formation S-R(1)	S-R(2)	Rigid
A	0.58	0.8275	1.41
B	0.5925	0.8325	1.437
C	0.6025	0.835	1.455
D	0.7325	0.87	1.485
E	0.755	0.8725	1.510
F	0.77	0.925	1.517
G	0.7775	0.9975	1.522
H	0.785	1.015	1.525
I	0.79	1.0175	N/A
J	0.815	1.02	N/A
K	0.83	1.0275	N/A
L	0.835	1.03	N/A
M	0.8875	1.0475	N/A
N	0.9325	1.055	N/A
O	0.9725	1.0575	N/A
P	1.190	1.172	N/A
Q	1.252	1.175	N/A
R	1.2575	1.2225	N/A
S	1.260	1.225	N/A
T	N/A	1.230	N/A

Key :

- Plastification prior to ULS design load being attained
- Semi-Rigid Connection
- Plastification following the attainment of the design load
- Member plastification

FRAME : **f31 b24**
Load Case 2

S-R (1) Negelecting web shear at the internal columns

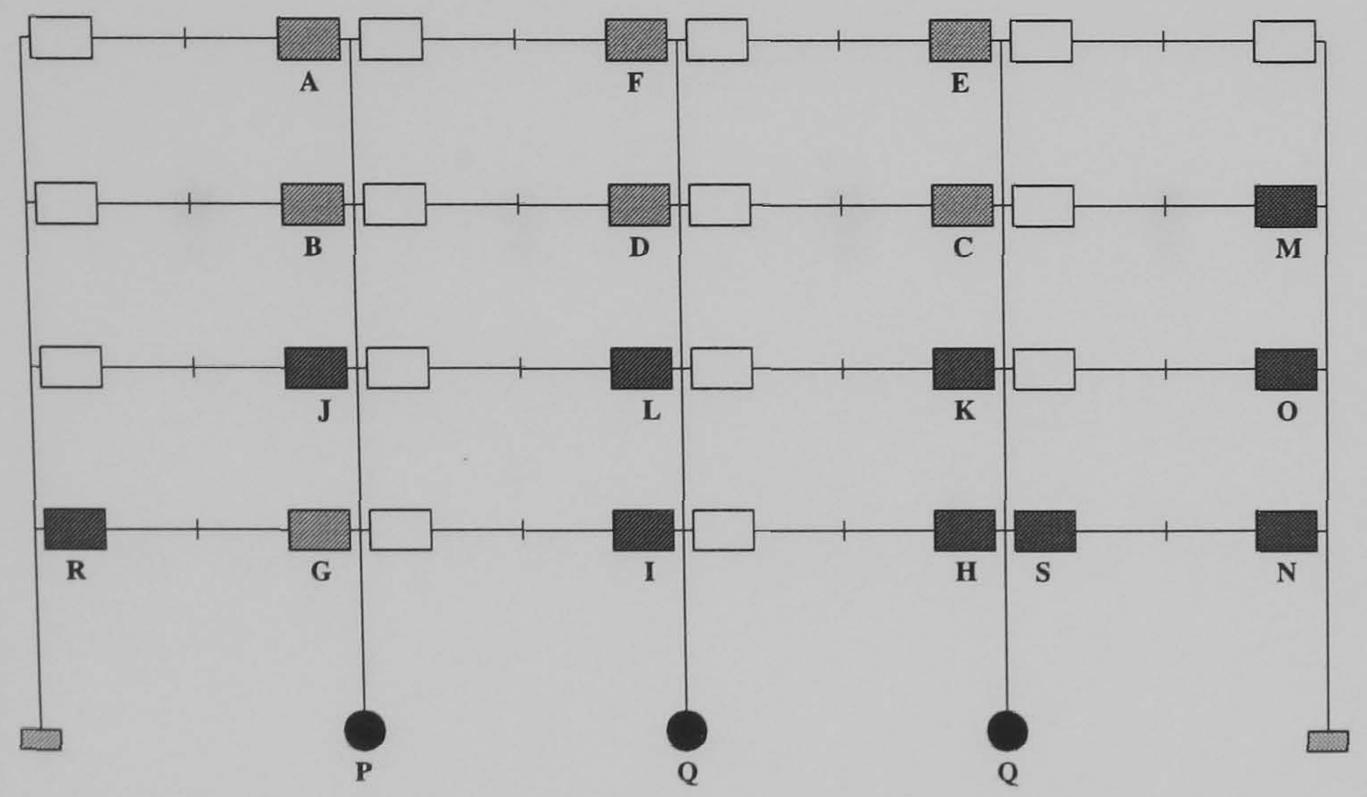

S-R (2) Including web shear at the internal columns

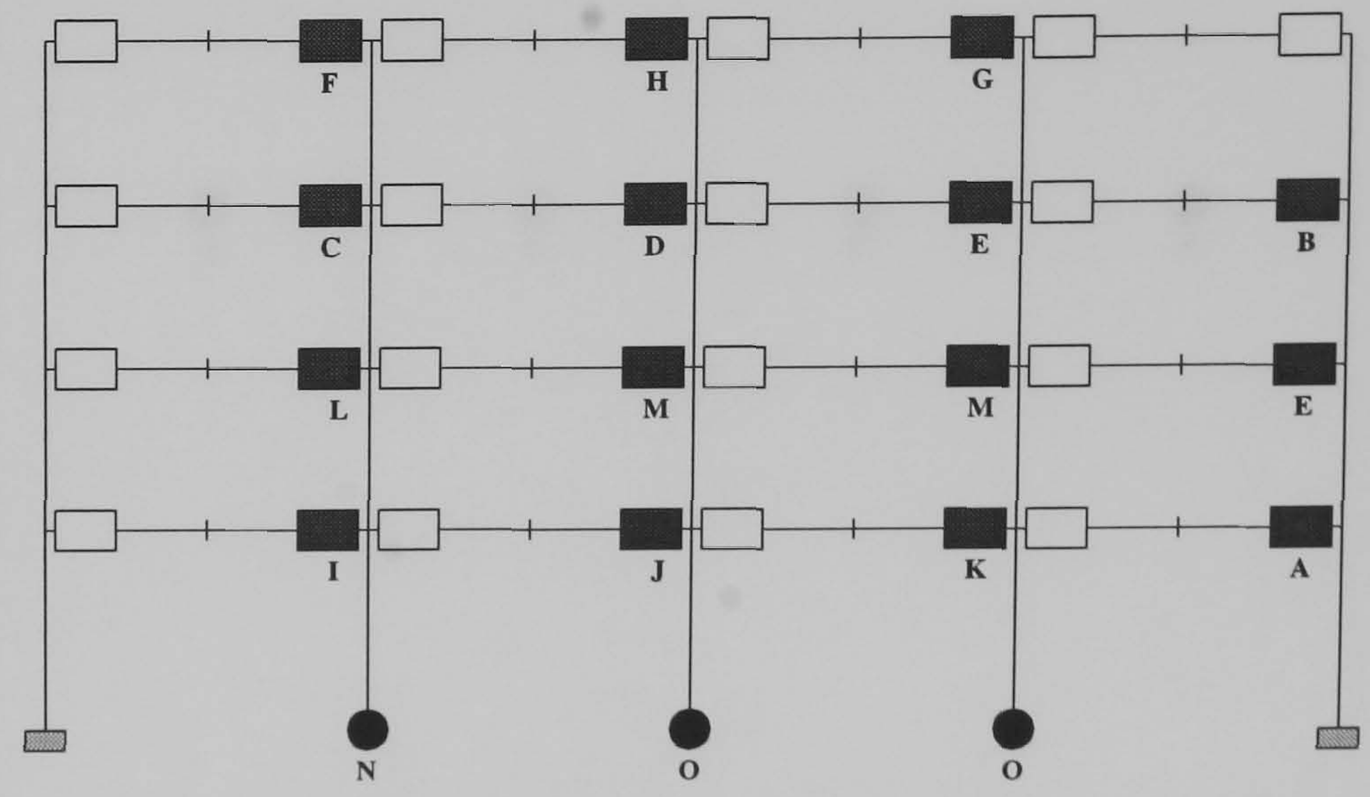

Rigid

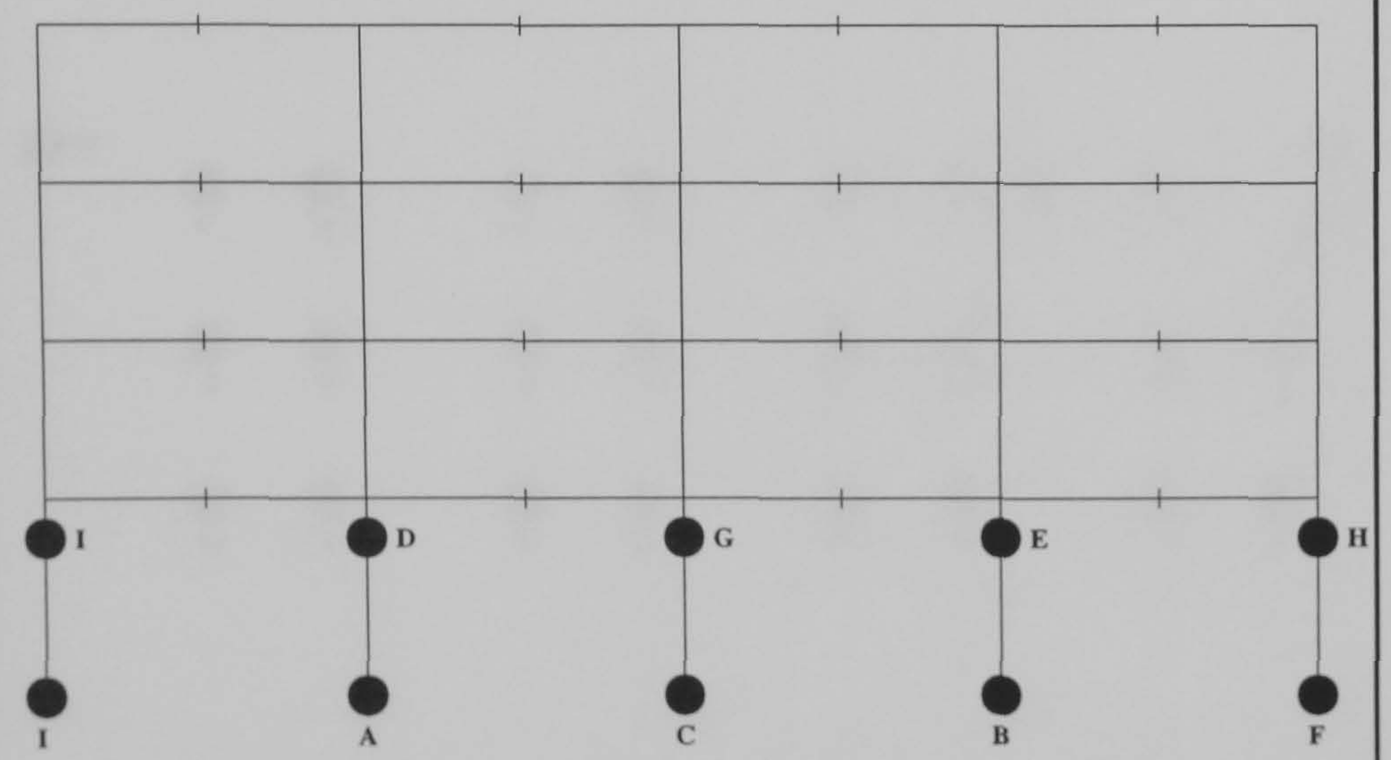

Hinge Location	Load Level at Hinge Formation S-R(1)	S-R(2)	Rigid
A	0.85	1.035	1.572
B	0.855	1.0925	1.597
C	0.8625	1.1325	1.610
D	0.87	1.135	1.682
E	0.875	1.14	1.705
F	0.9025	1.1525	1.712
G	0.995	1.1725	1.715
H	1.0025	1.1825	1.725
I	1.0075	1.2475	1.727
J	1.0925	1.2675	N/A
K	1.0975	1.27	N/A
L	1.105	1.3175	N/A
M	1.1425	1.3325	N/A
N	1.150	1.34	N/A
O	1.245	1.345	N/A
P	1.372	N/A	N/A
Q	1.375	N/A	N/A
R	1.44	N/A	N/A
S	1.445	N/A	N/A

Key :

Semi-Rigid Connection

Plastification prior to ULS design load being attained

Plastification following the attainment of the design load

Member plastification

FRAME : **f31 b24**

Load Case 3

S-R (1) Negelecting web shear at the internal columns

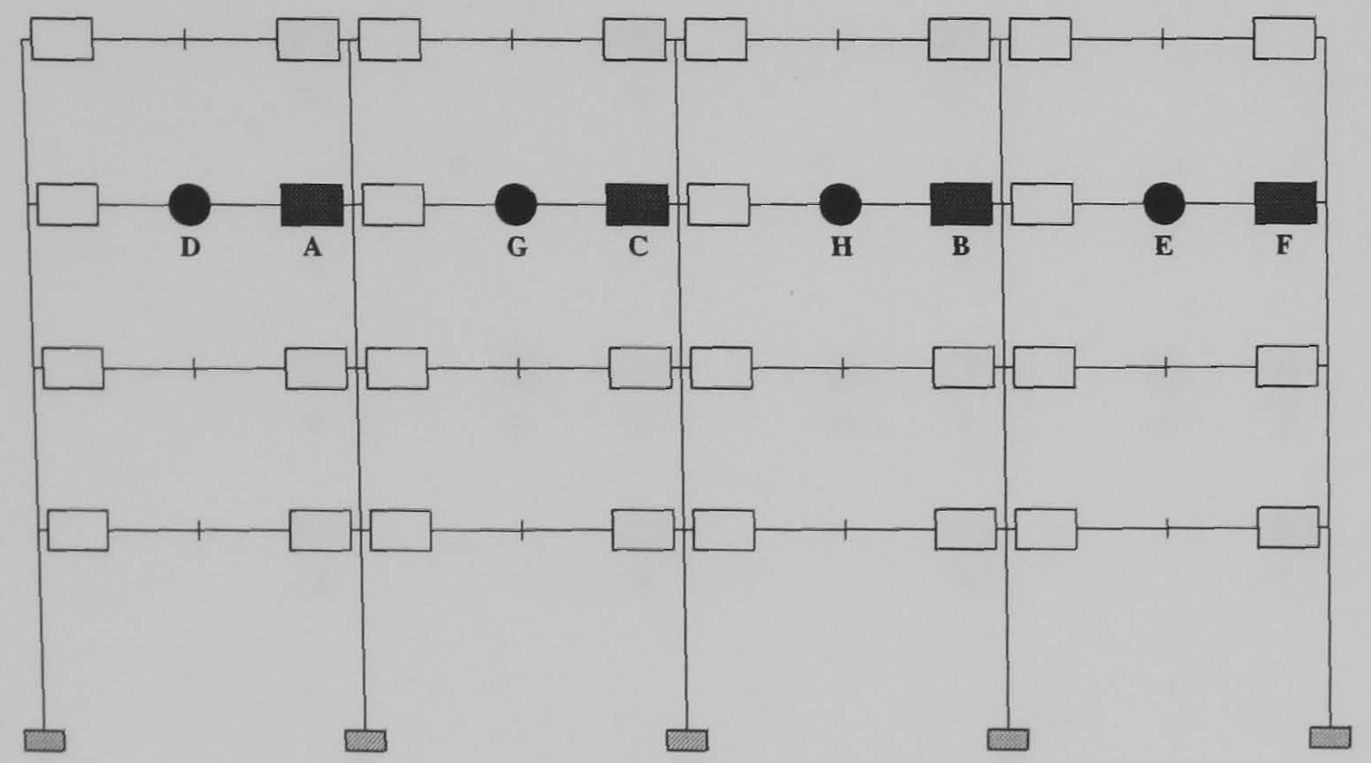

S-R (2) Including web shear at the internal columns

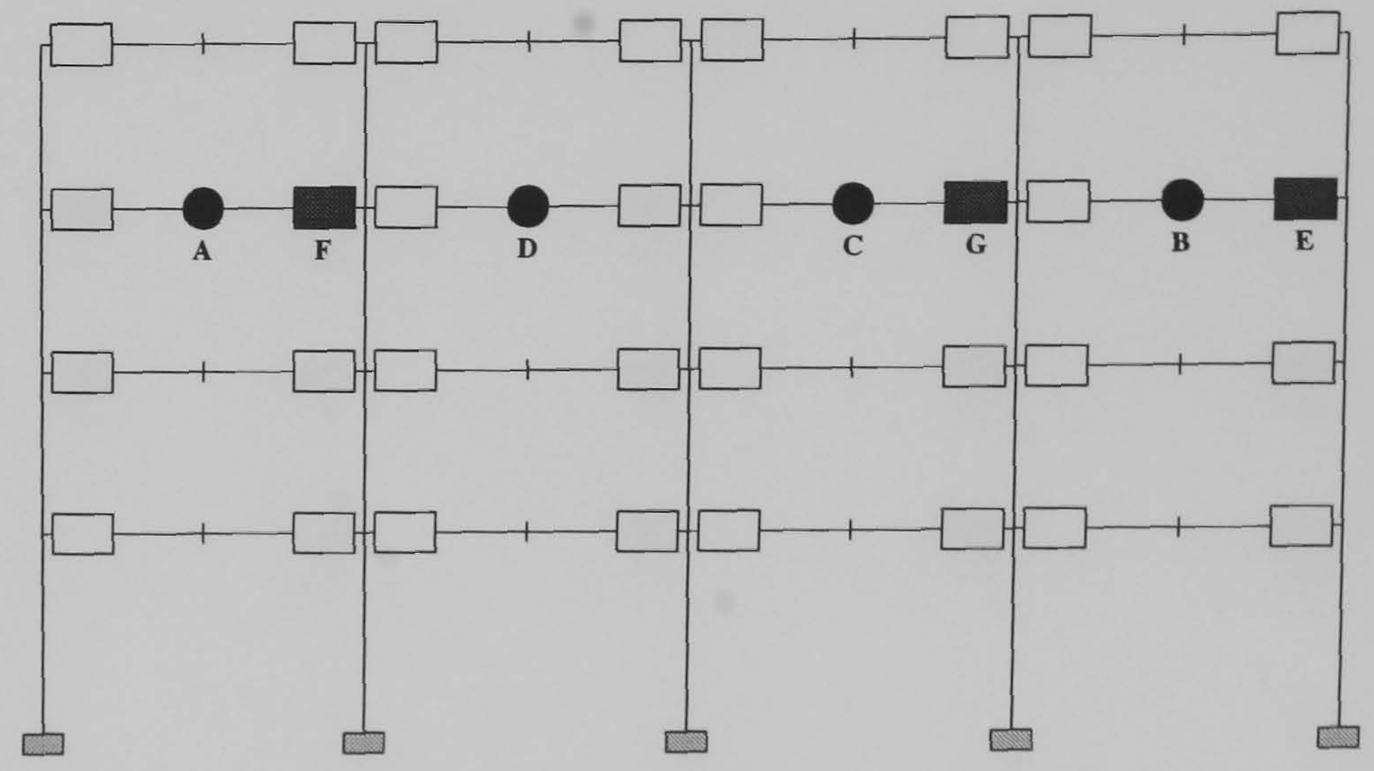

Rigid

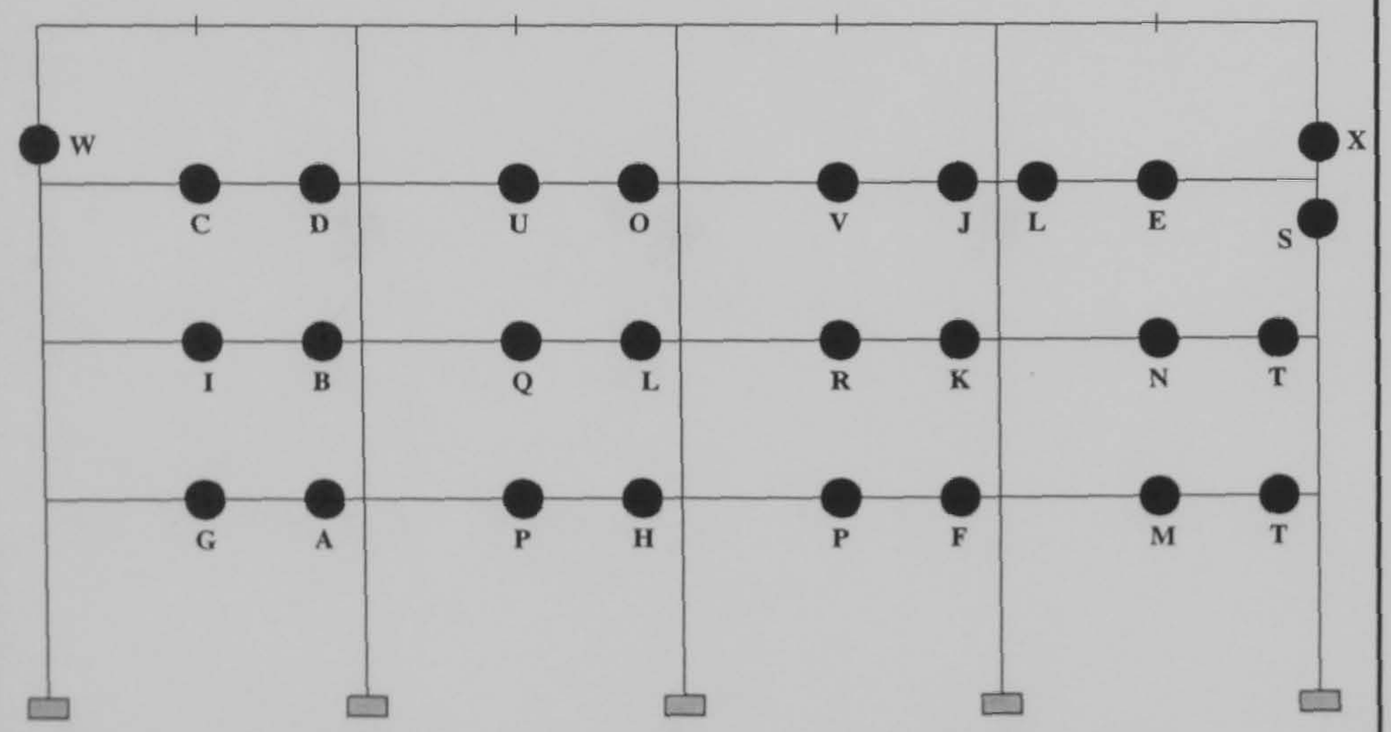

Hinge Location	Load Level at Hinge Formation S-R(1)	S-R(2)	Rigid
A	1.0575	1.247	1.702
B	1.075	1.265	1.760
C	1.08	1.275	1.770
D	1.272	1.277	1.777
E	1.295	1.28	1.785
F	1.305	1.29	1.825
G	1.312	1.3	1.832
H	1.315	N/A	1.840
I	N/A	N/A	1.842
J	N/A	N/A	1.845
K	N/A	N/A	1.862
L	N/A	N/A	1.865
M	N/A	N/A	1.877
N	N/A	N/A	1.880
O	N/A	N/A	1.927
P	N/A	N/A	1.955
Q	N/A	N/A	1.960
R	N/A	N/A	1.962
S	N/A	N/A	1.985
T	N/A	N/A	1.987
U	N/A	N/A	1.990
V	N/A	N/A	1.992
W	N/A	N/A	2.032
X	N/A	N/A	2.047

Key :

Semi-Rigid Connection

Plastification prior to ULS design load being attained

Plastification following the attainment of the design load

Member plastification

FRAME : **f32 b24**
Load Case 1

S-R (1) Negelecting web shear at the internal columns

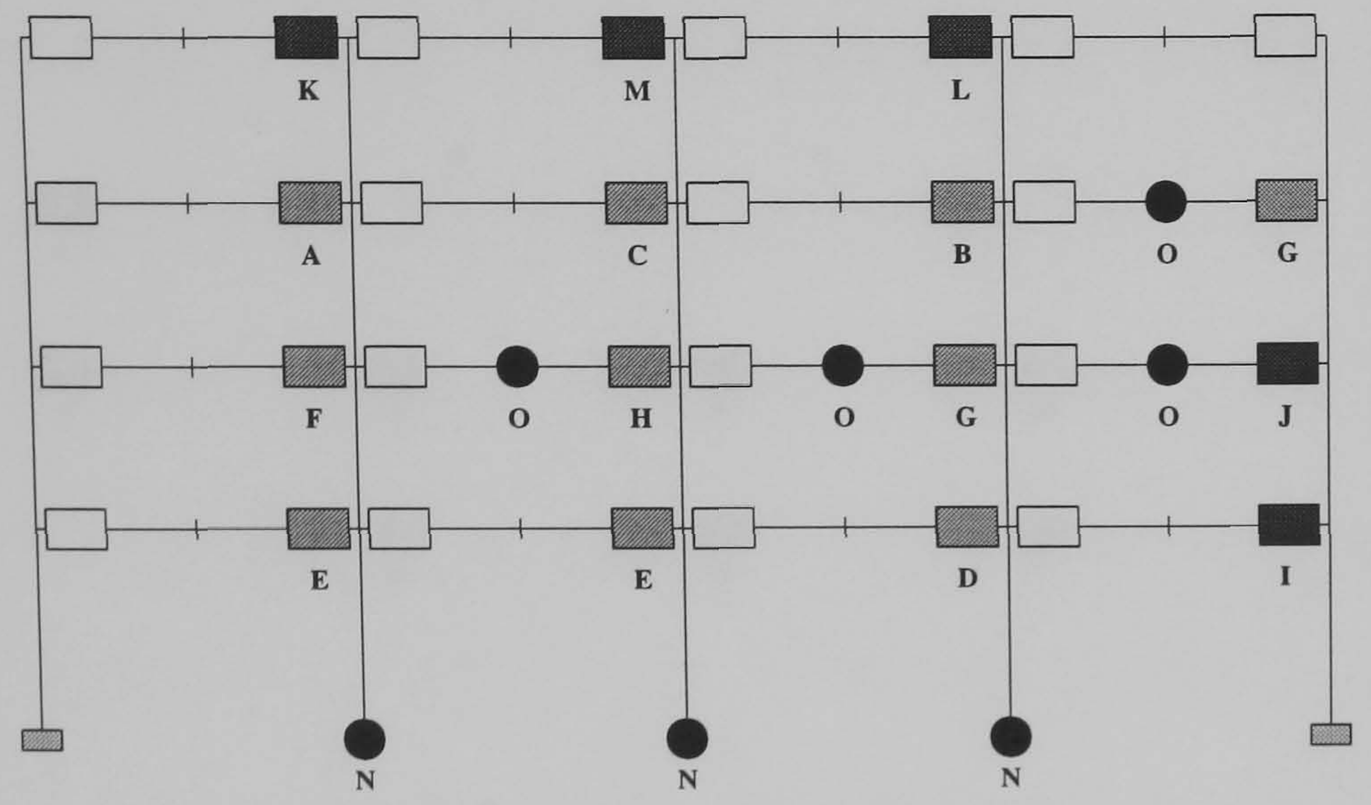

S-R (2) Including web shear at the internal columns

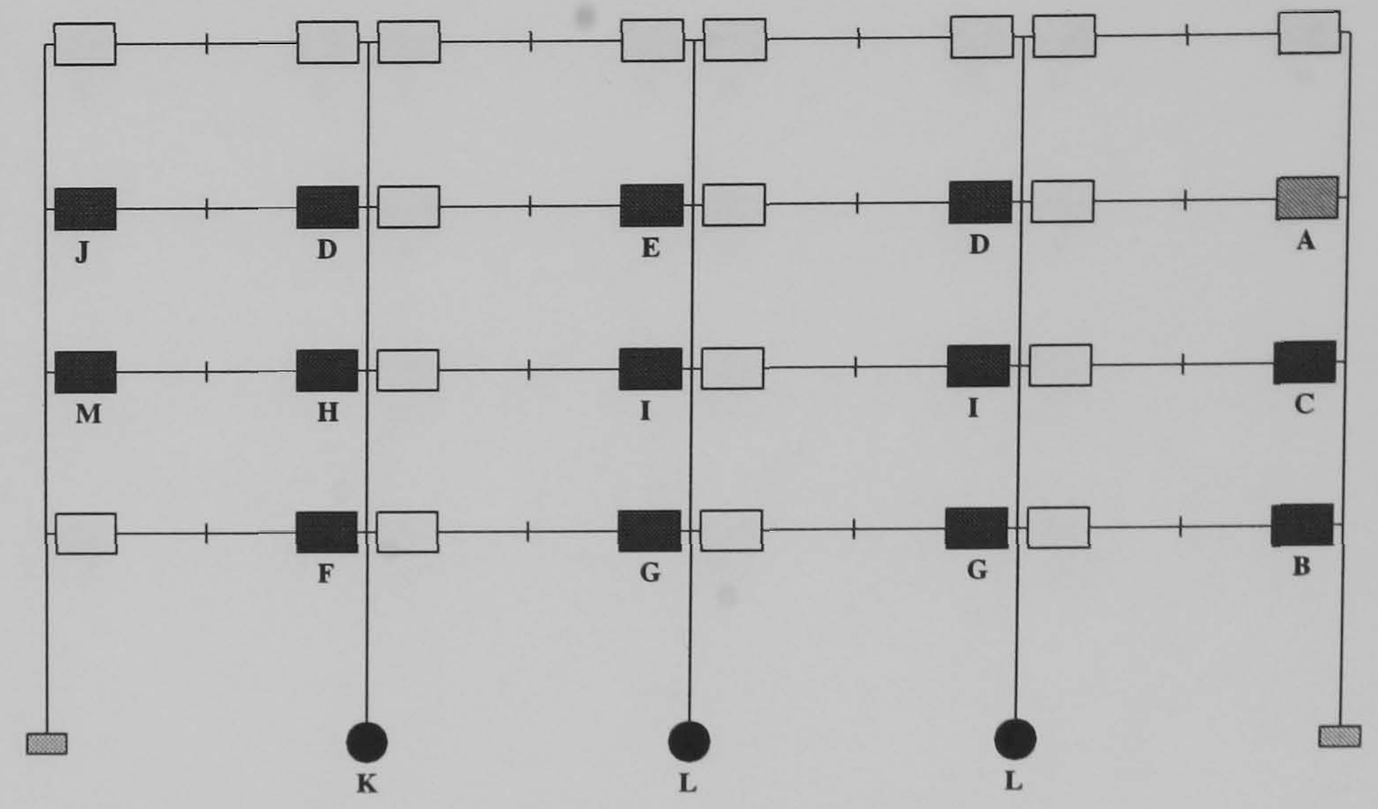

Rigid

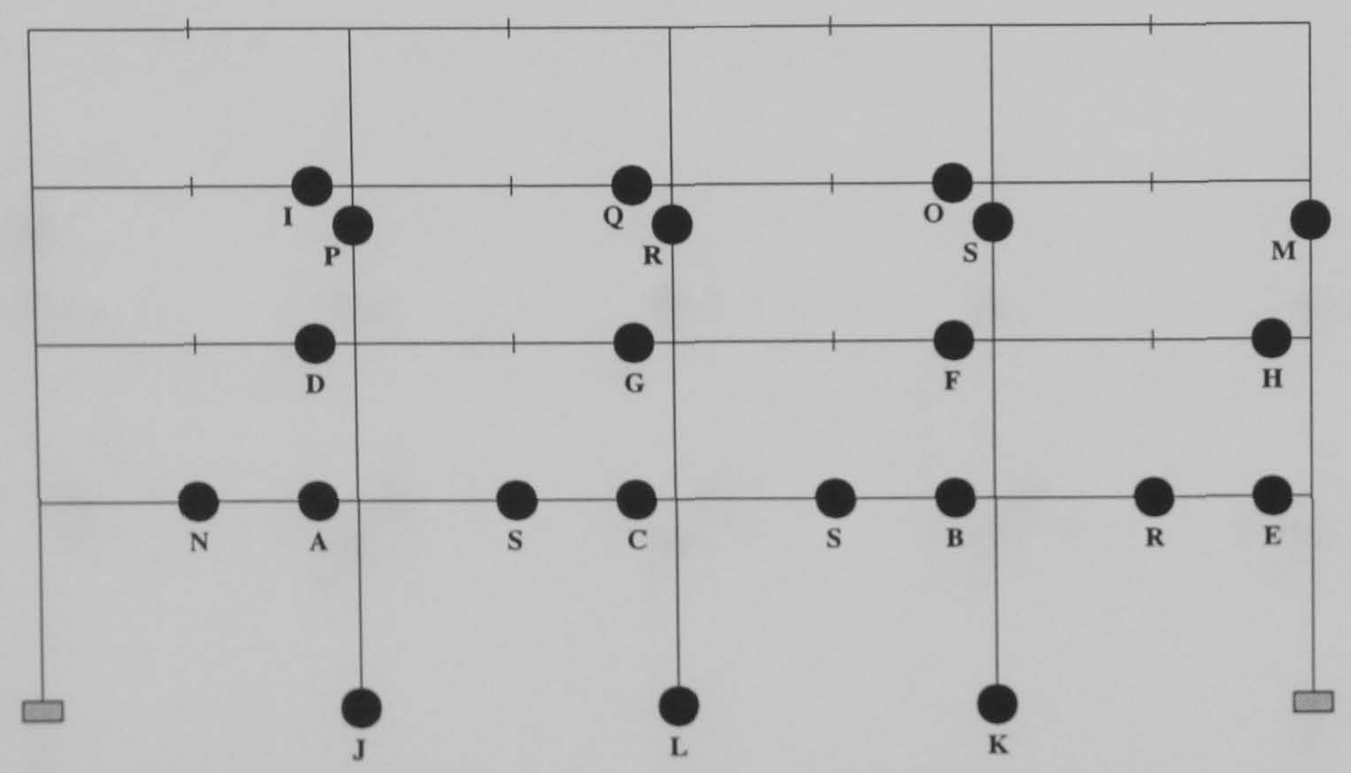

Hinge Location	Load Level at Hinge Formation S-R(1)	S-R(2)	Rigid
A	0.83	0.86	1.217
B	0.8325	1.00	1.262
C	0.8375	1.005	1.267
D	0.8975	1.0125	1.362
E	0.9025	1.015	1.412
F	0.9375	1.035	1.425
G	0.94	1.04	1.427
H	0.9425	1.0475	1.535
I	1.035	1.055	1.637
J	1.0425	1.24	1.690
K	1.2125	1.245	1.697
L	1.2225	1.247	1.707
M	1.2325	1.26	1.747
N	1.272	N/A	1.750
O	1.295	N/A	1.762
P	N/A	N/A	1.770
Q	N/A	N/A	1.780
R	N/A	N/A	1.787
S	N/A	N/A	1.790

Key :

- Plastification prior to ULS design load being attained
- Semi-Rigid Connection
- Plastification following the attainment of the design load
- Member plastification

FRAME : **f32 b24**
Load Case 2

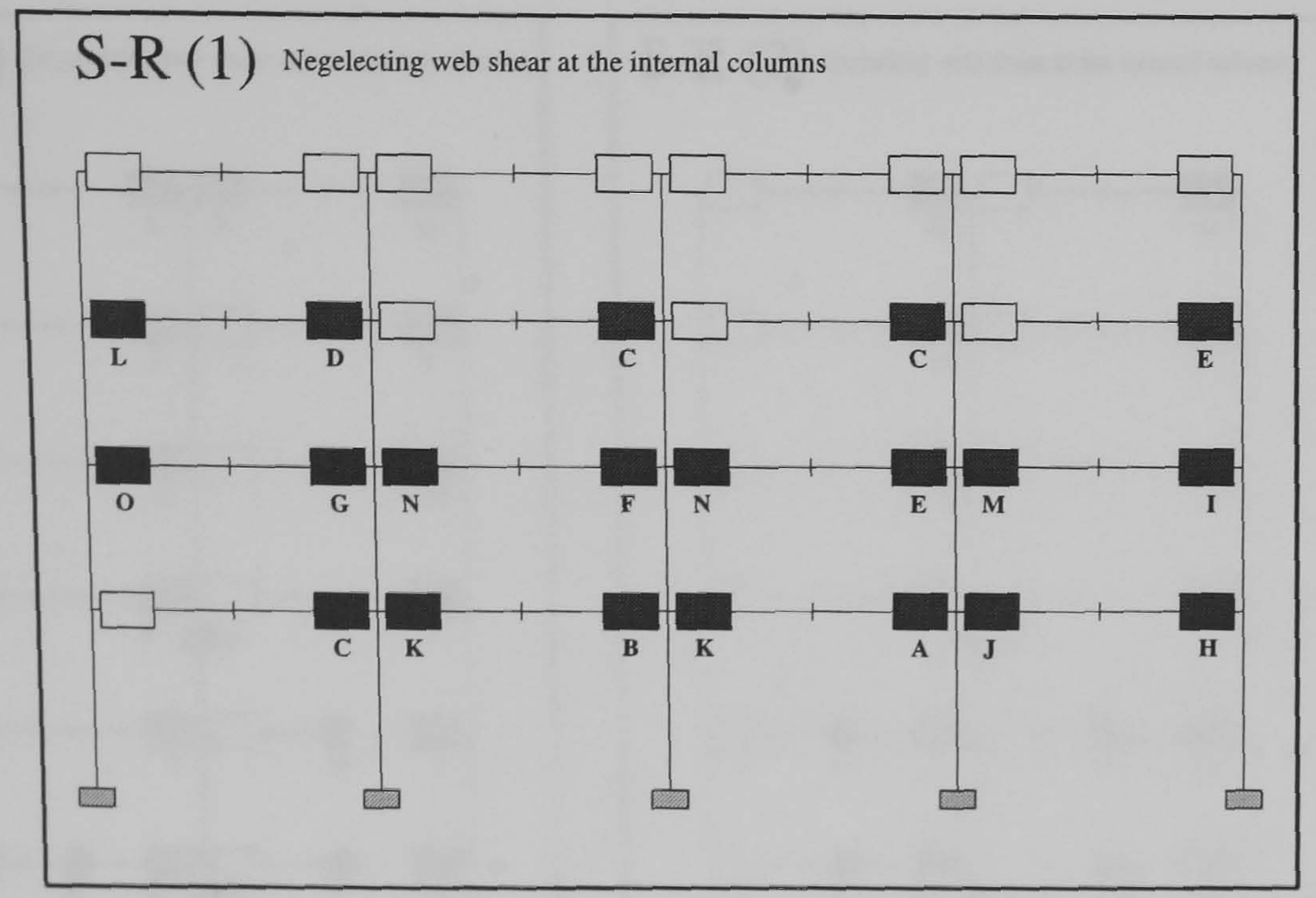

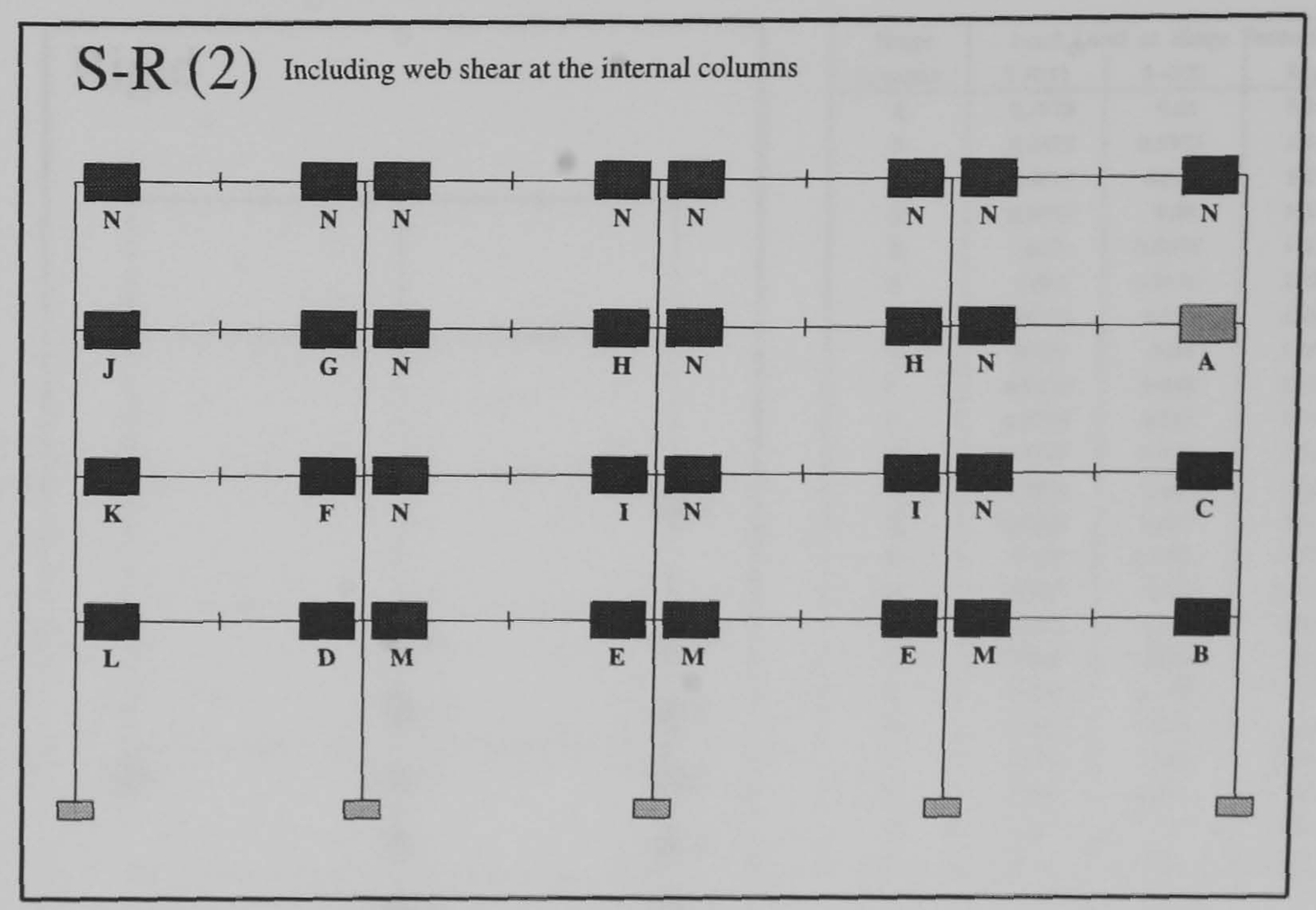

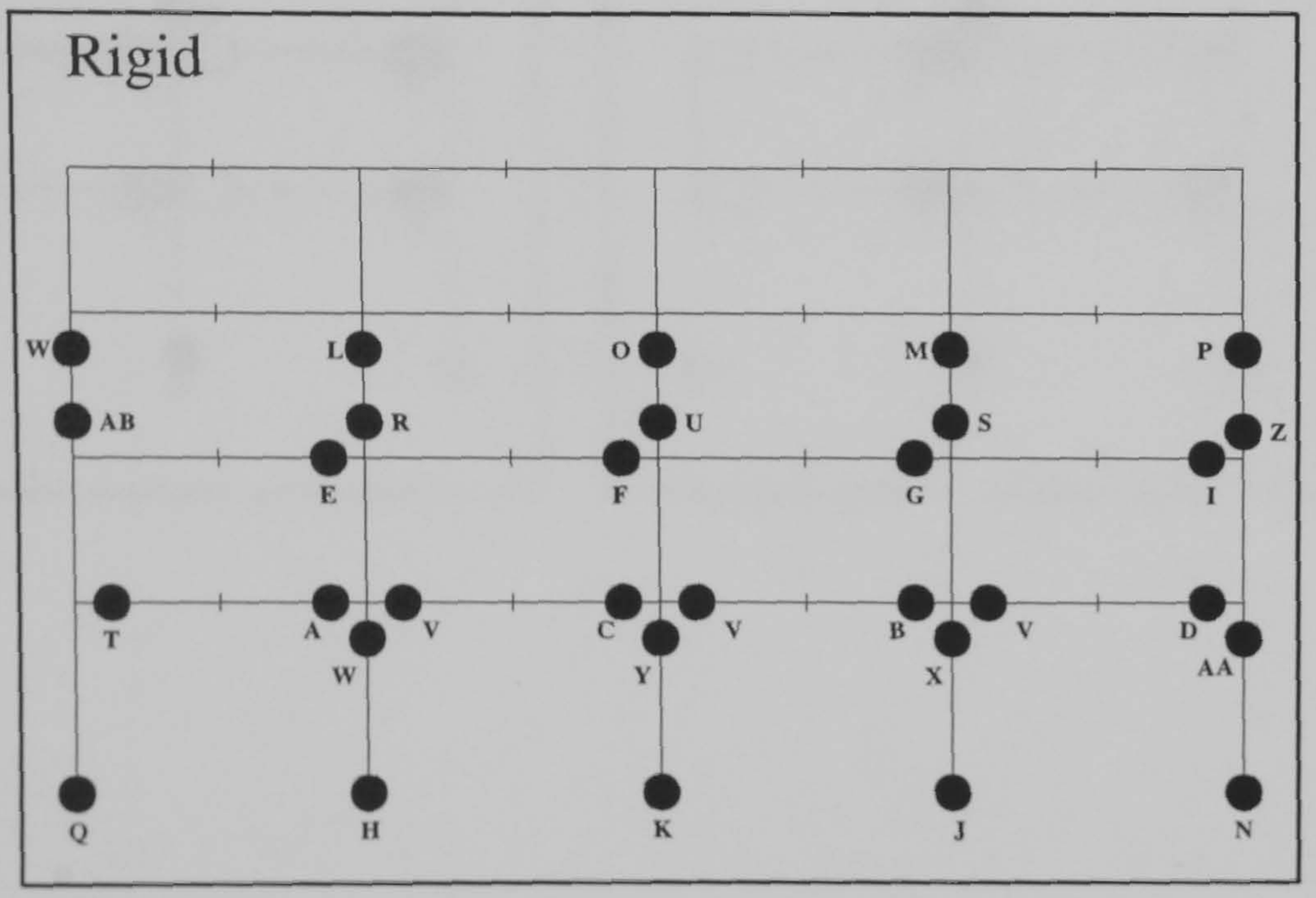

Hinge Location	Load Level at Hinge Formation S-R(1)	S-R(2)	Rigid
A	1.0175	0.975	1.445
B	1.0225	1.1075	1.475
C	1.035	1.1225	1.477
D	1.04	1.1675	1.587
E	1.0925	1.1725	1.675
F	1.0975	1.1975	1.732
G	1.1	1.2025	1.735
H	1.165	1.205	1.792
I	1.195	1.2075	1.795
J	1.285	1.215	1.805
K	1.2875	1.28	1.810
L	1.3075	1.2925	1.867
M	1.3175	1.3125	1.897
N	1.32	1.32	1.907
O	1.3275	N/A	1.917
P	N/A	N/A	1.962
Q	N/A	N/A	1.985
R	N/A	N/A	2.117
S	N/A	N/A	2.125
T	N/A	N/A	2.132
U	N/A	N/A	2.137
V	N/A	N/A	2.152
W	N/A	N/A	2.182
X	N/A	N/A	2.190
Y	N/A	N/A	2.192
Z	N/A	N/A	2.217
AA	N/A	N/A	2.225
AB	N/A	N/A	2.227

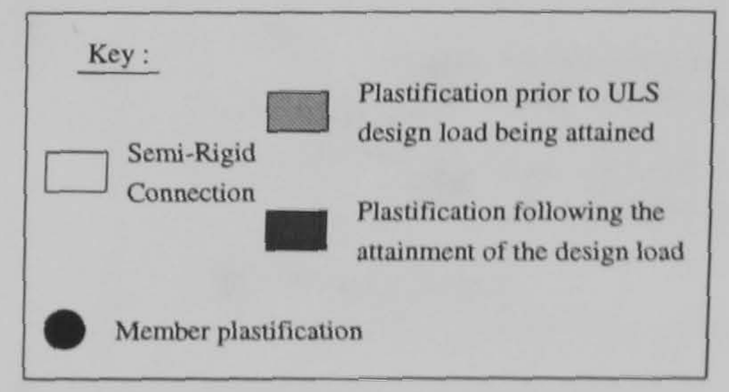

FRAME : **f32 b24**
Load Case 3

S-R (1) Negelecting web shear at the internal columns

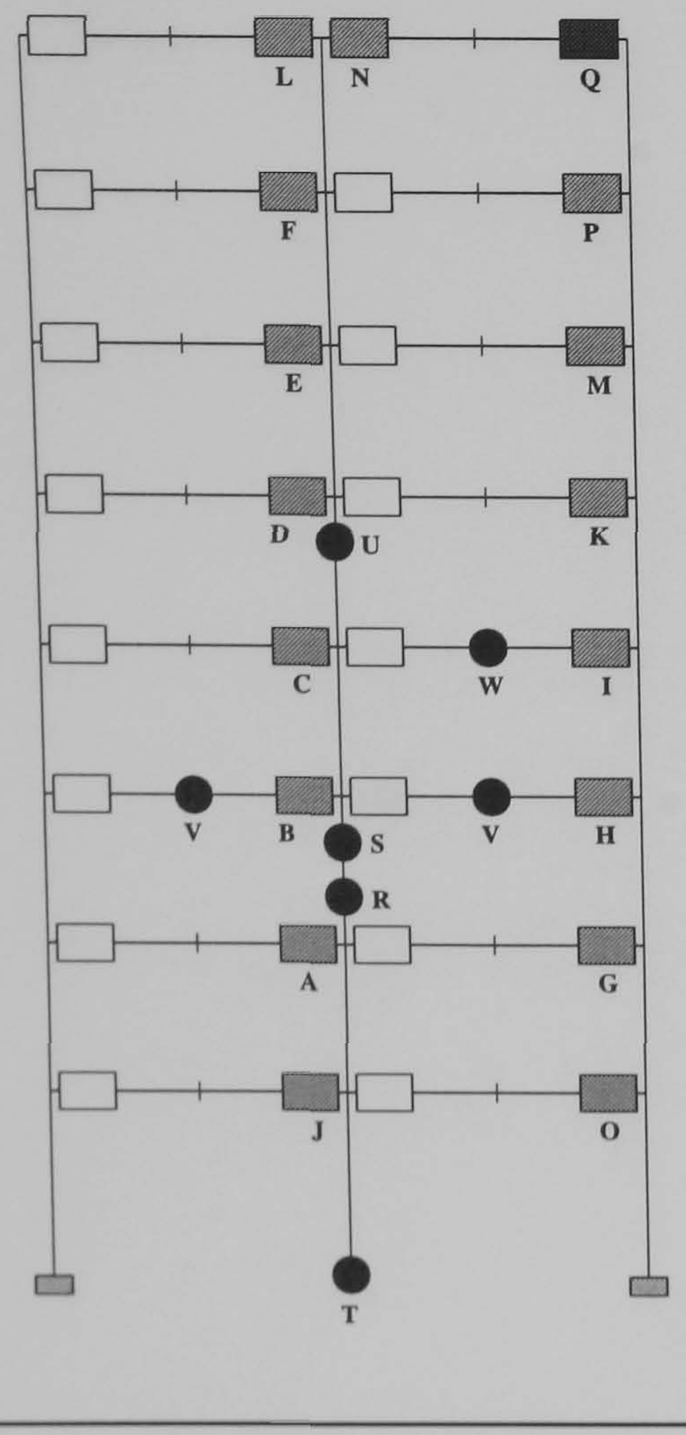

S-R (2) Including web shear at the internal columns

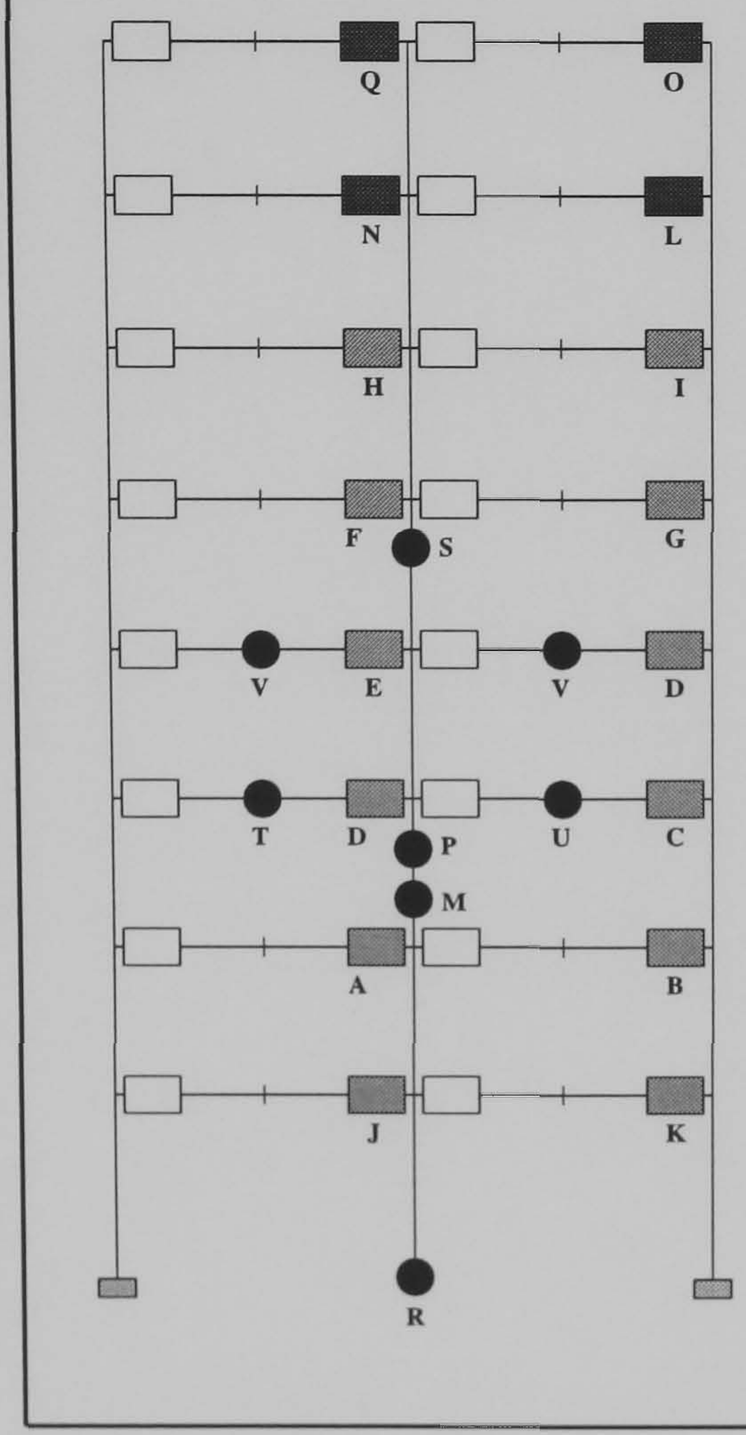

Rigid

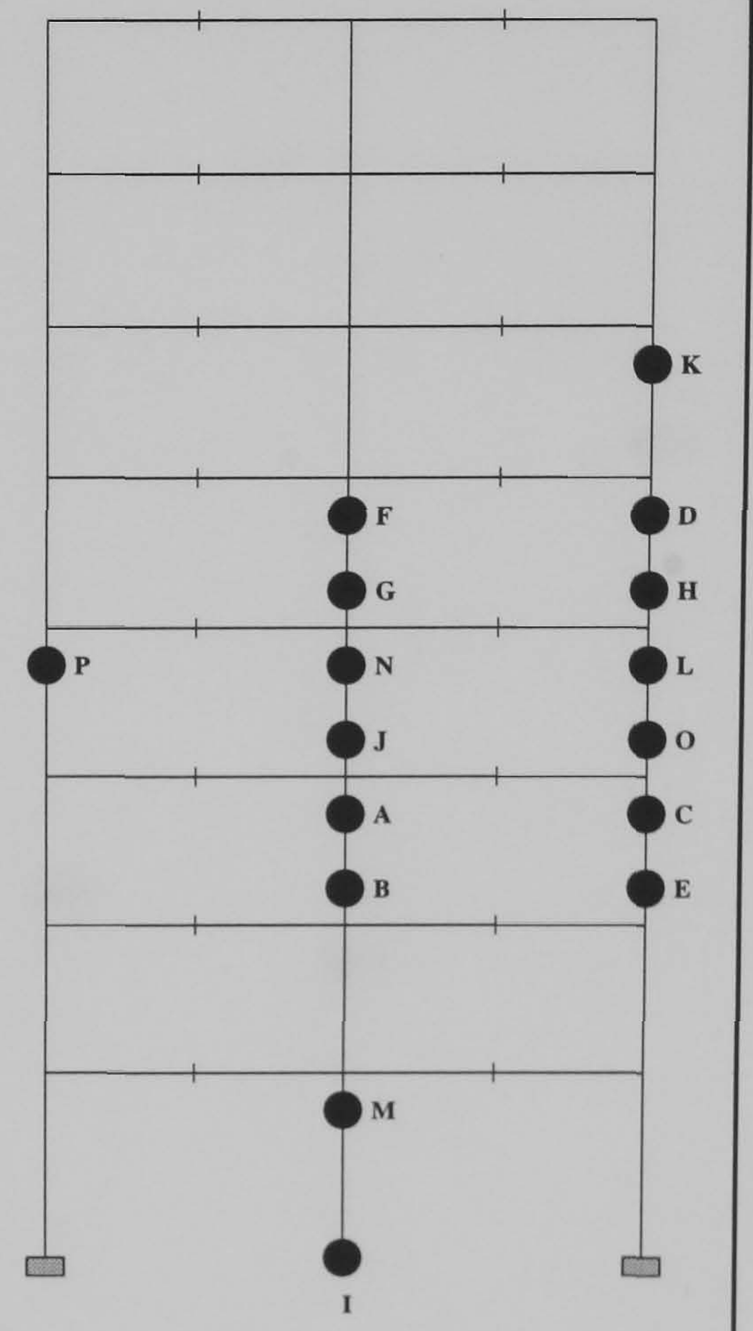

Hinge Location	Load Level at Hinge Formation S-R(1)	S-R(2)	Rigid
A	0.3975	0.56	1.147
B	0.4475	0.5925	1.150
C	0.4575	0.645	1.222
D	0.4925	0.68	1.237
E	0.51	0.6975	1.240
F	0.595	0.7925	1.282
G	0.5975	0.805	1.287
H	0.635	0.84	1.290
I	0.6625	0.875	1.297
J	0.6725	0.915	1.300
K	0.7749	0.975	1.312
L	0.7875	1.015	1.320
M	0.8425	1.097	1.322
N	0.845	1.1275	1.325
O	0.9675	1.14	1.340
P	0.9925	1.155	1.342
Q	1.1075	1.1625	N/A
R	1.097	1.175	N/A
S	1.145	1.177	N/A
T	1.175	1.192	N/A
U	1.185	1.197	N/A
V	1.197	1.2	N/A
W	1.2	N/A	N/A

Key :

- Semi-Rigid *Connection*
- Plastification prior to ULS design load being attained
- Plastification following the attainment of the design load
- Member plastification

FRAME : **f34 b24**
Load Case 1

S-R (1) Negelecting web shear at the internal columns

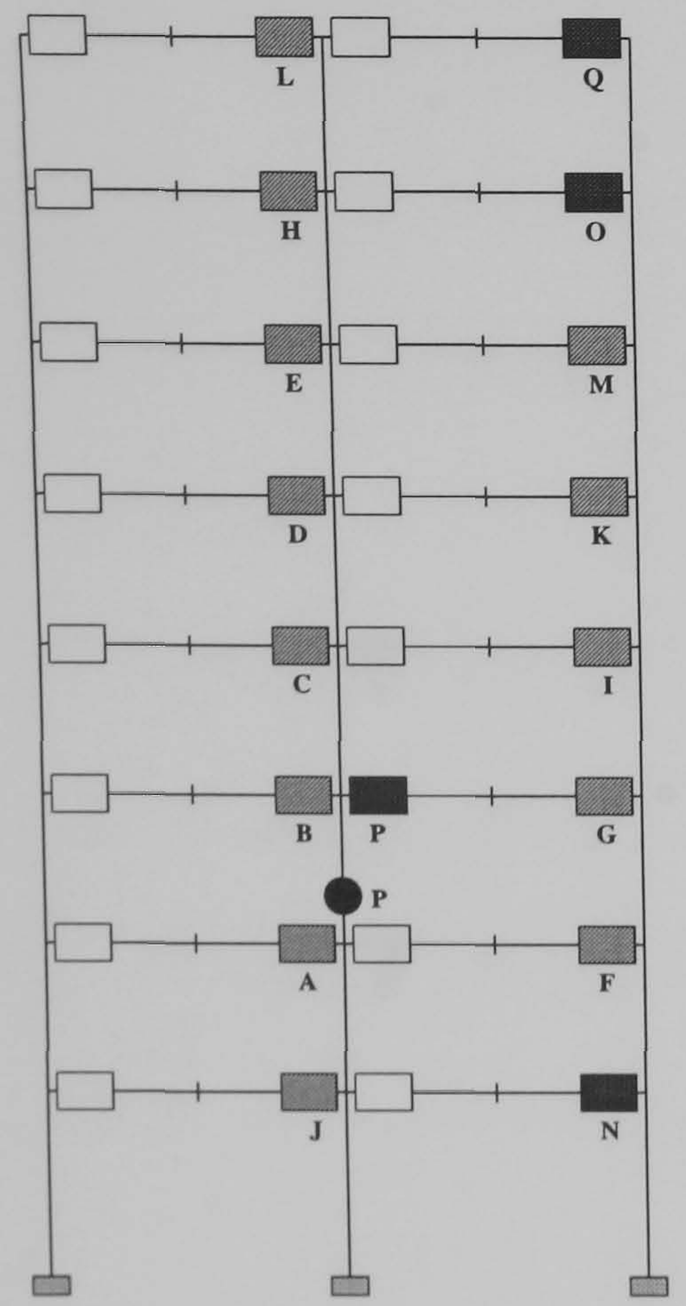

S-R (2) Including web shear at the internal columns

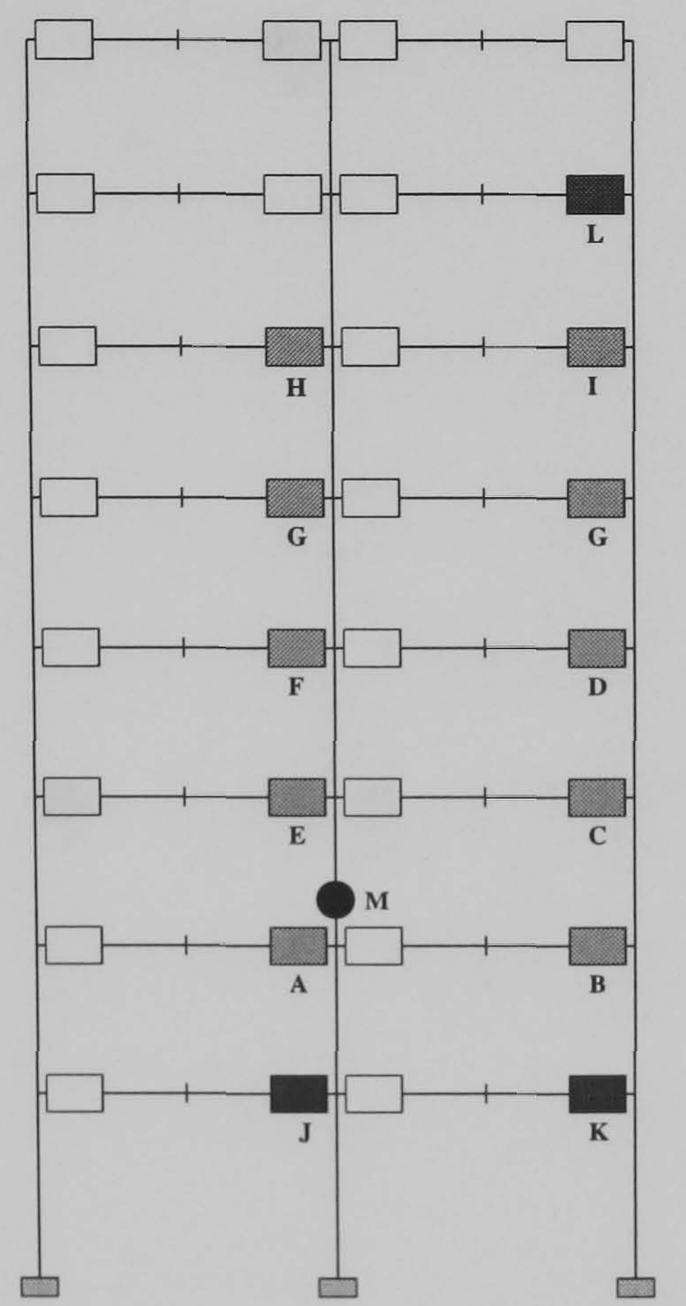

Rigid

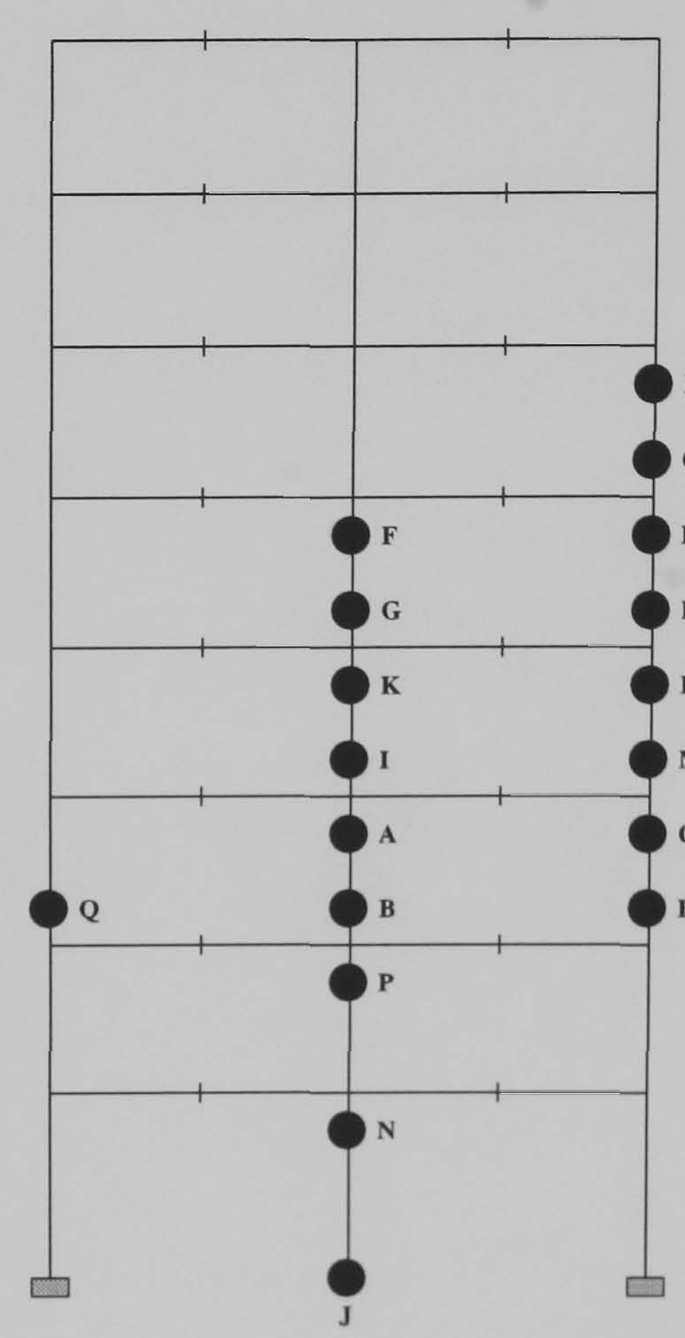

Hinge Location	Load Level at Hinge Formation S-R(1)	S-R(2)	Rigid
A	**0.445**	**0.61**	**1.325**
B	**0.495**	**0.635**	**1.330**
C	**0.51**	**0.6875**	**1.410**
D	**0.555**	**0.72**	**1.412**
E	**0.5875**	**0.7275**	**1.427**
F	**0.65**	**0.75**	**1.450**
G	**0.69**	**0.86**	**1.460**
H	**0.7075**	**0.9275**	**1.462**
I	**0.72**	**0.9425**	**1.490**
J	**0.75**	**1.0025**	**1.492**
K	**0.845**	**1.055**	**1.512**
L	**0.9075**	**1.105**	**1.522**
M	**0.9275**	**1.237**	**1.542**
N	**1.0575**	**N/A**	**1.555**
O	**1.0975**	**N/A**	**1.557**
P	**1.245**	**N/A**	**1.567**
Q	**N/A**	**N/A**	**1.582**

Key :

- Semi-Rigid Connection
- Plastification prior to ULS design load being attained
- Plastification following the attainment of the design load
- Member plastification

FRAME : **f34 b24**
Load Case 2

S-R (1) Negelecting web shear at the internal columns

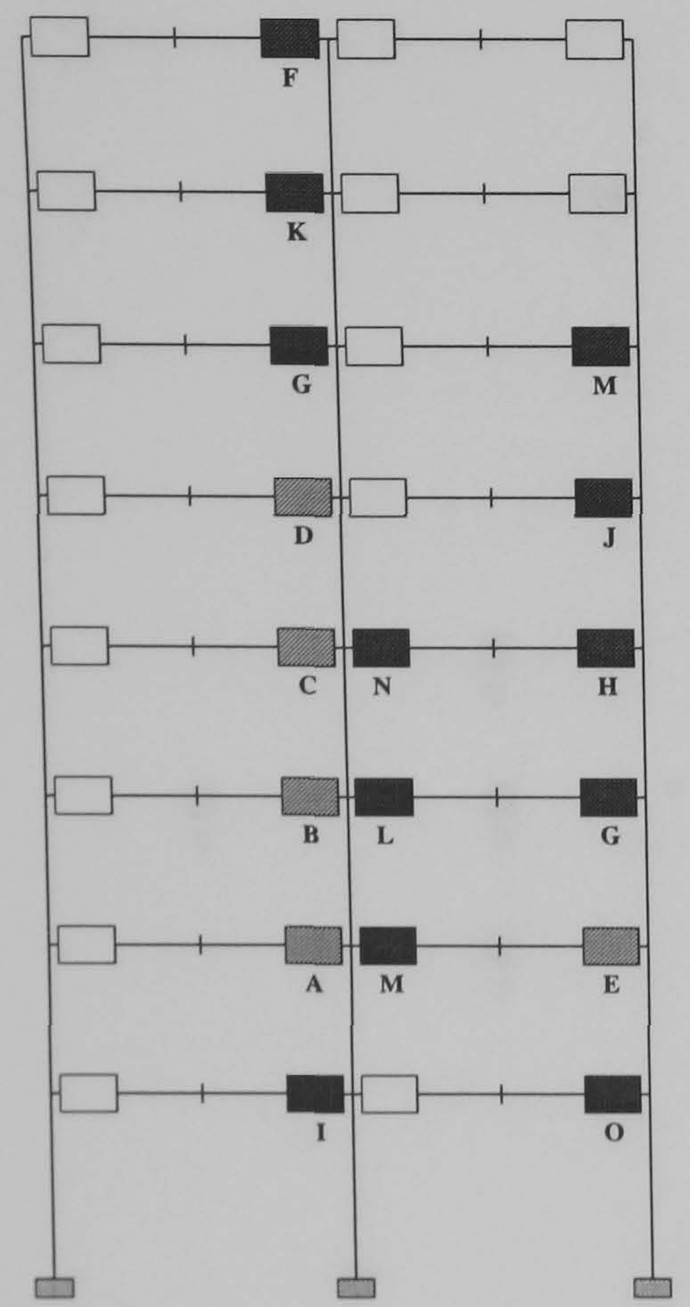

S-R (2) Including web shear at the internal columns

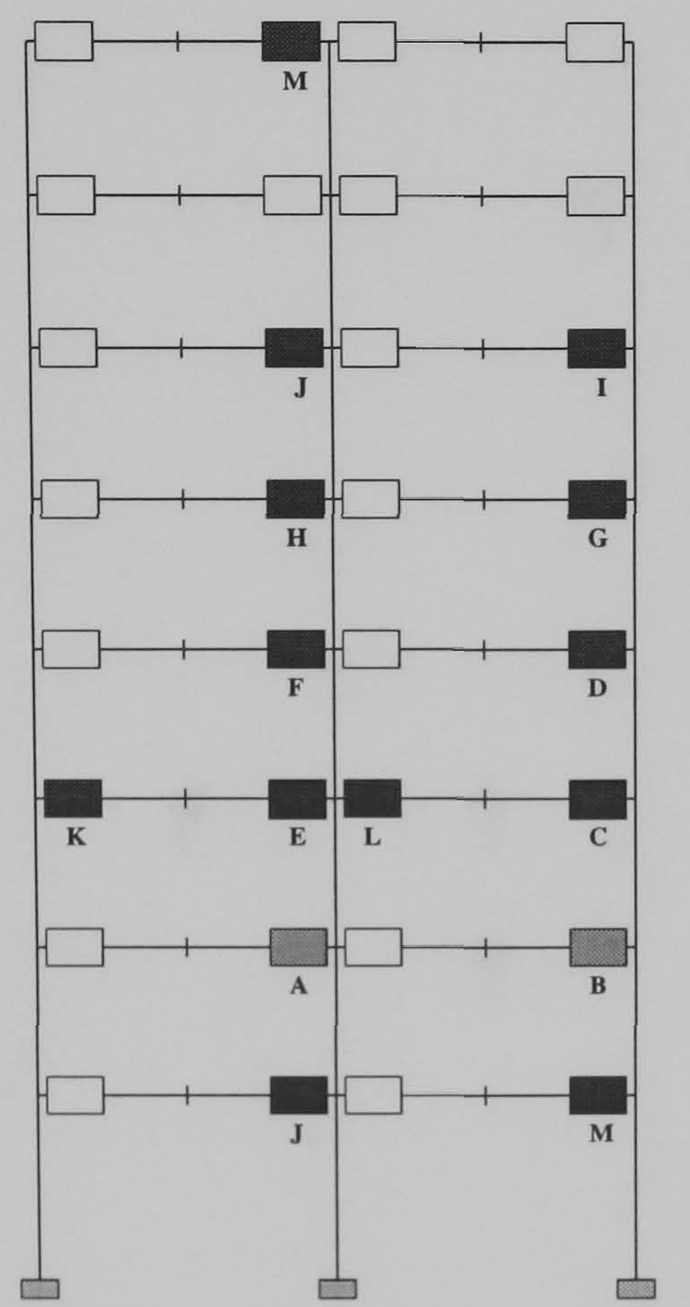

Rigid

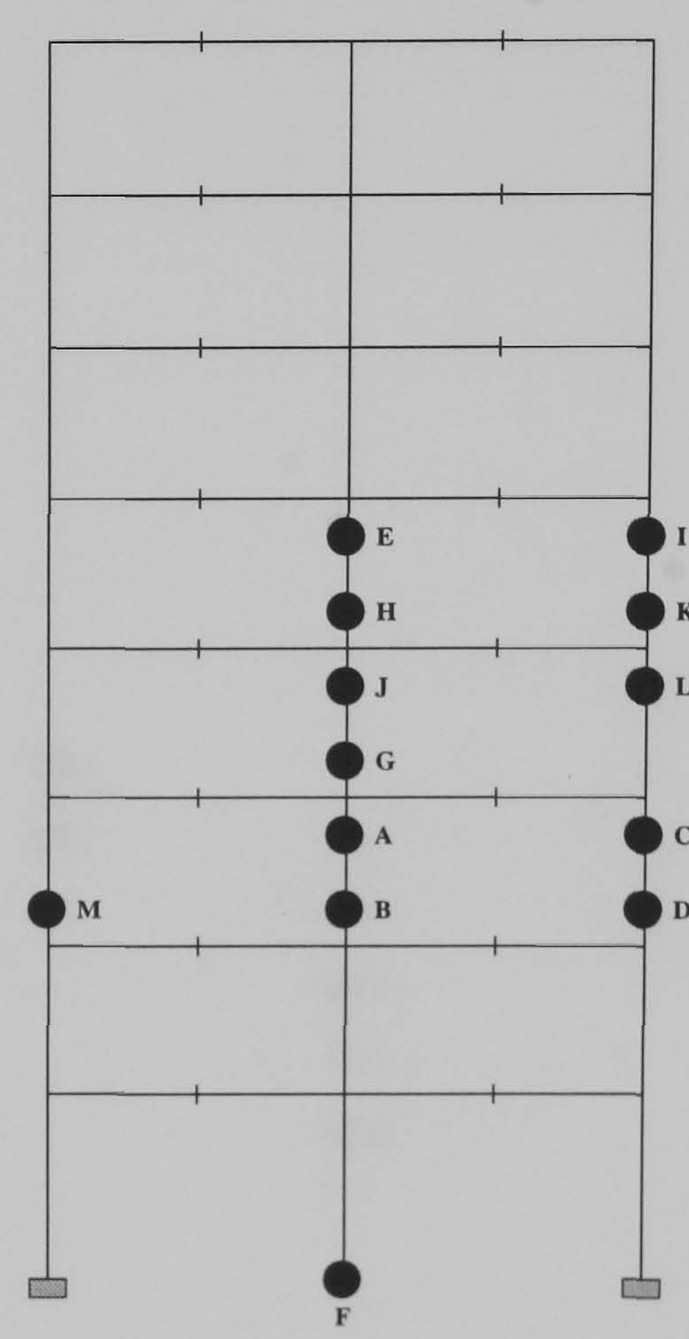

Hinge Location	Load Level at Hinge Formation S-R(1)	S-R(2)	Rigid
A	0.7125	0.935	1.90
B	0.8025	0.9475	1.912
C	0.845	1.0225	2.062
D	0.9475	1.08	2.085
E	0.9875	1.105	2.115
F	1.050	1.155	2.130
G	1.0575	1.31	2.140
H	1.12	1.355	2.142
I	1.195	1.48	2.152
J	1.345	1.53	2.175
K	1.3725	1.5475	2.180
L	1.485	1.555	2.240
M	1.5275	1.565	2.270
N	1.555	N/A	N/A
O	1.5775	N/A	N/A

Key :

- Plastification prior to ULS design load being attained
- Semi-Rigid Connection
- Plastification following the attainment of the design load
- Member plastification

FRAME : **f34 b24**
Load Case 3

S-R (1) Negelecting web shear at the internal columns

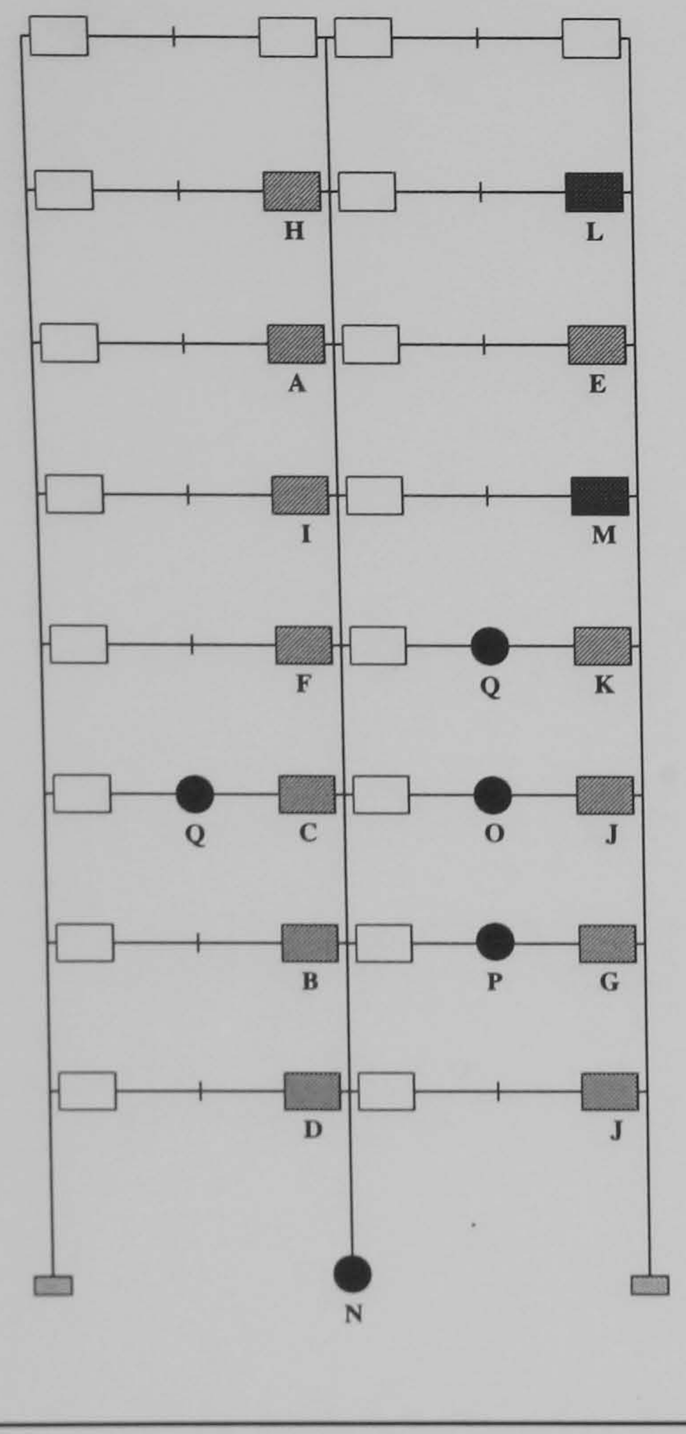

S-R (2) Including web shear at the internal columns

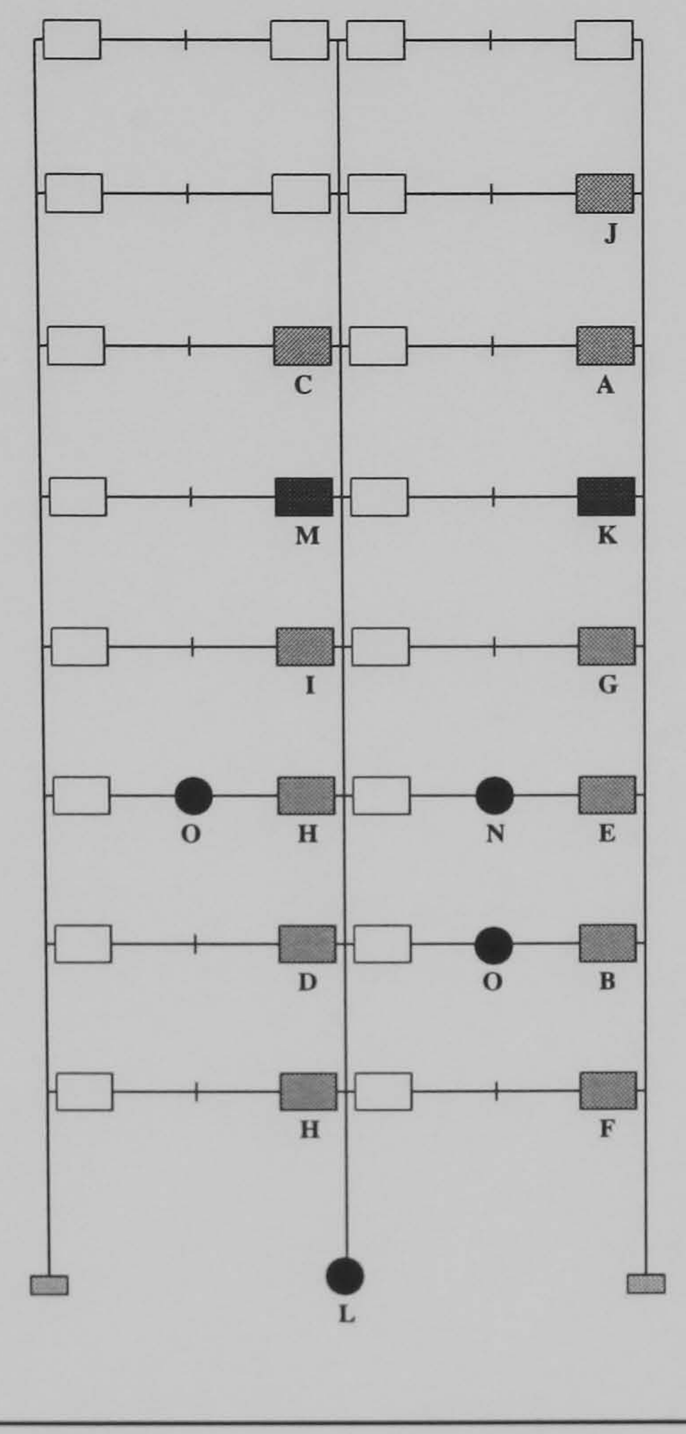

Rigid

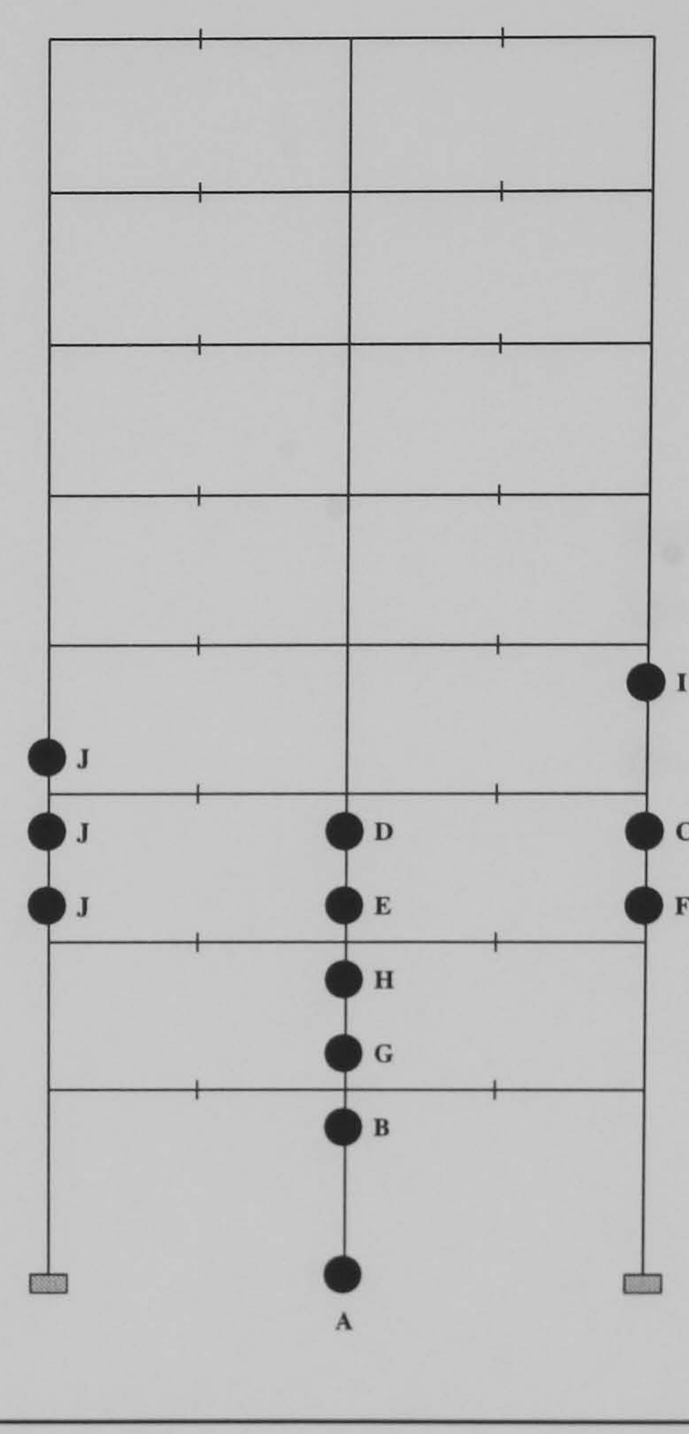

Hinge Location	Load Level at Hinge Formation		
	S-R(1)	S-R(2)	Rigid
A	0.6975	0.7975	1.257
B	0.7725	0.8825	1.302
C	0.8075	0.8925	1.340
D	0.8125	0.9175	1.345
E	0.82	0.935	1.350
F	0.8425	0.94	1.365
G	0.895	0.955	1.385
H	0.91	0.96	1.392
I	0.9125	0.9875	1.400
J	0.94	0.99	1.405
K	0.96	1.025	N/A
L	1.0	1.062	N/A
M	1.03	1.0675	N/A
N	1.065	1.09	N/A
O	1.09	1.092	N/A
P	1.092	N/A	N/A
Q	1.095	N/A	

Key :

- Semi-Rigid Connection
- Plastification prior to ULS design load being attained
- Plastification following the attainment of the design load
- Member plastification

FRAME : **f35 b20**
Load Case 1

S-R (1) Negelecting web shear at the internal columns

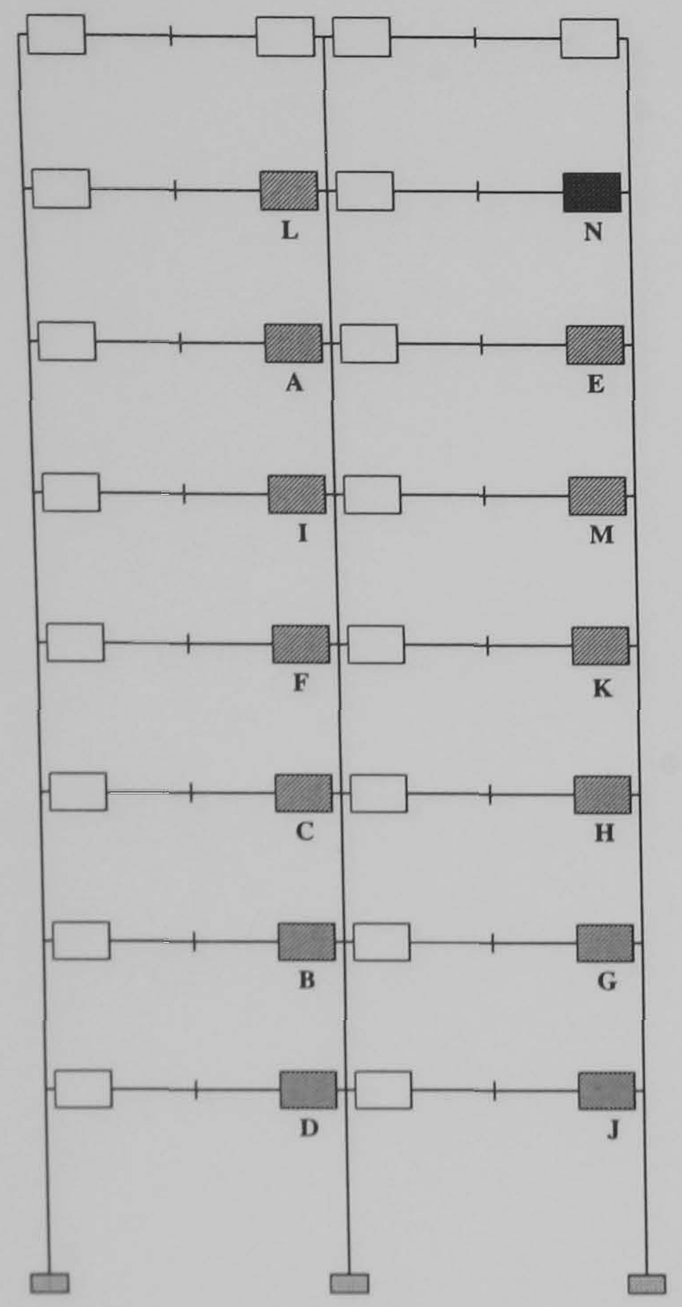

S-R (2) Including web shear at the internal columns

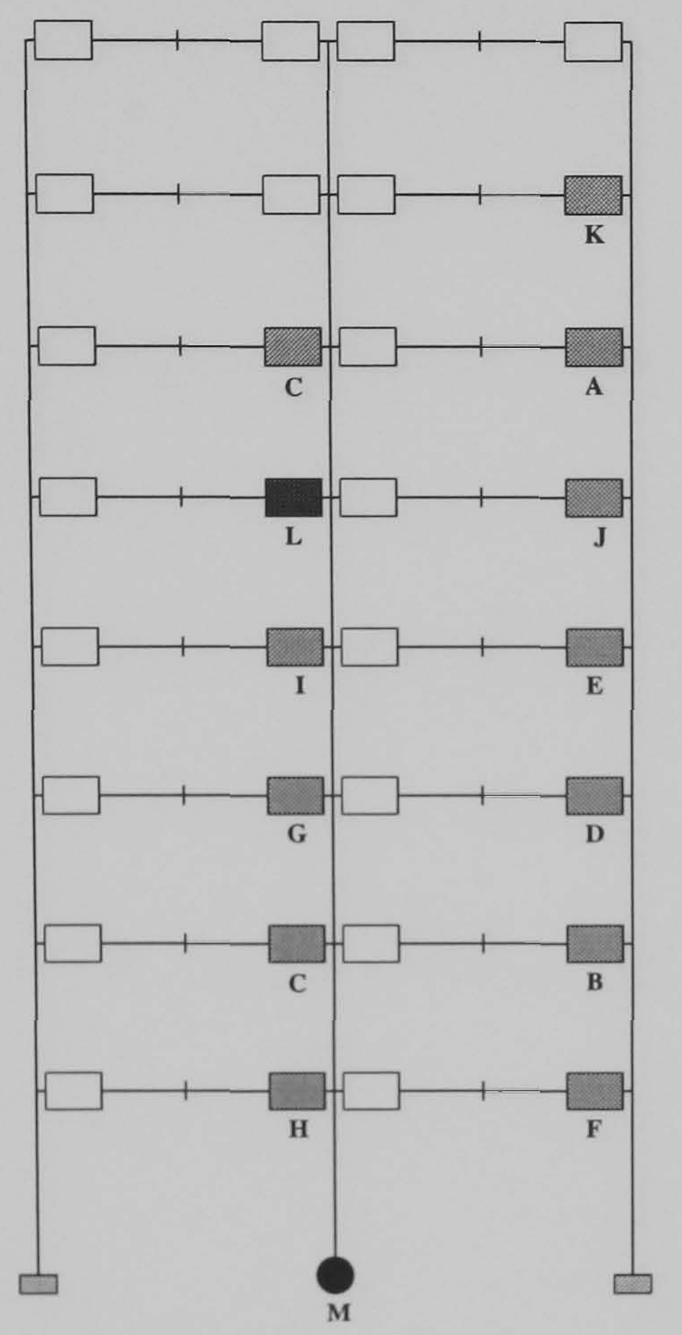

Rigid

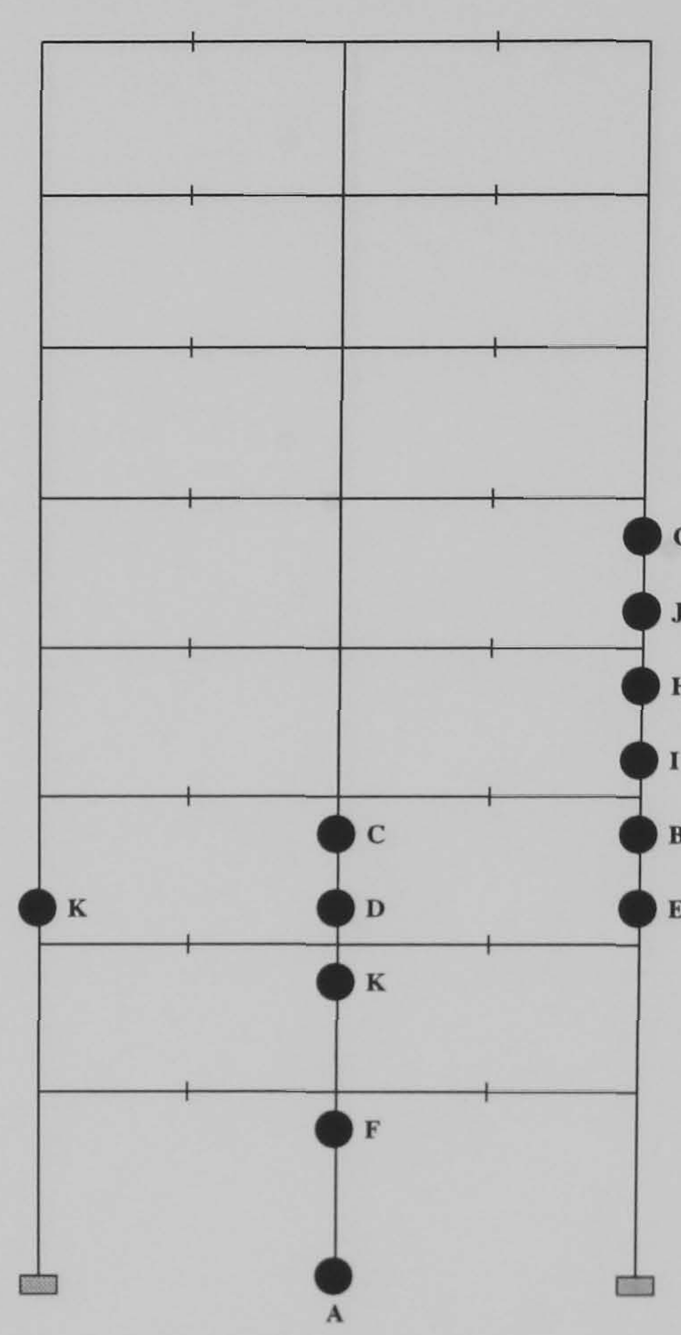

Hinge Location	Load Level at Hinge Formation		
	S-R(1)	S-R(2)	Rigid
A	0.6875	0.7525	1.355
B	0.7325	0.8175	1.412
C	0.7575	0.85	1.432
D	0.78	0.8575	1.435
E	0.79	0.8775	1.452
F	0.7975	0.8825	1.477
G	0.84	0.885	1.500
H	0.8775	0.9075	1.502
I	0.8825	0.9175	1.510
J	0.8925	0.9625	1.520
K	0.905	0.9675	1.522
L	0.9325	1.0175	N/A
M	0.9875	1.062	N/A
N	1.0	N/A	N/A

Key :

Semi-Rigid Connection

Plastification prior to ULS design load being attained

Plastification following the attainment of the design load

Member plastification

FRAME : **f35 b20**

Load Case 2

S-R (1) Negelecting web shear at the internal columns

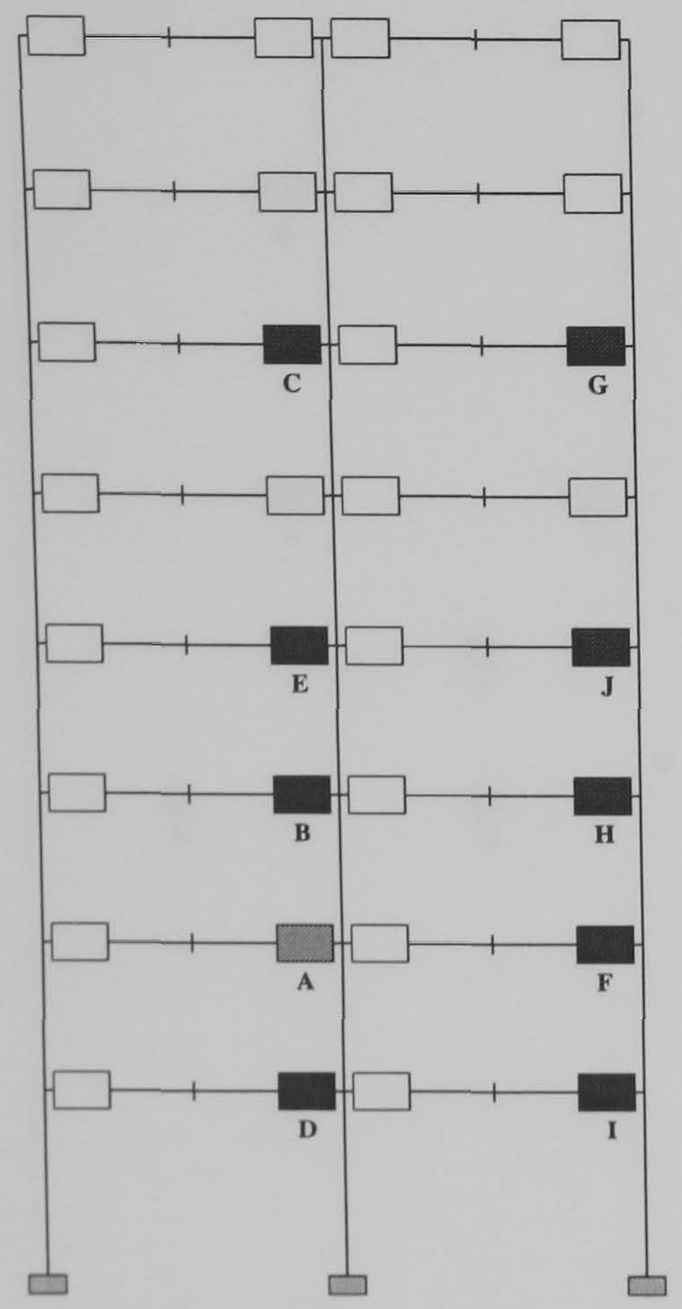

S-R (2) Including web shear at the internal columns

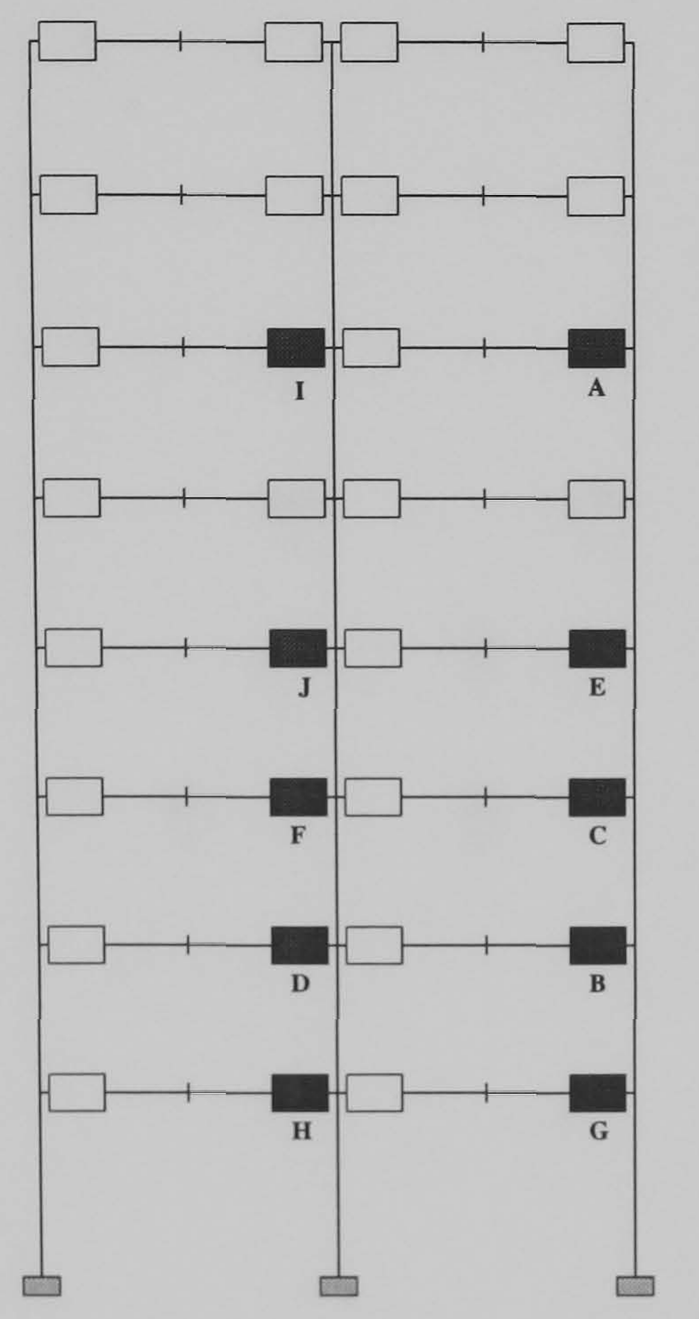

Rigid

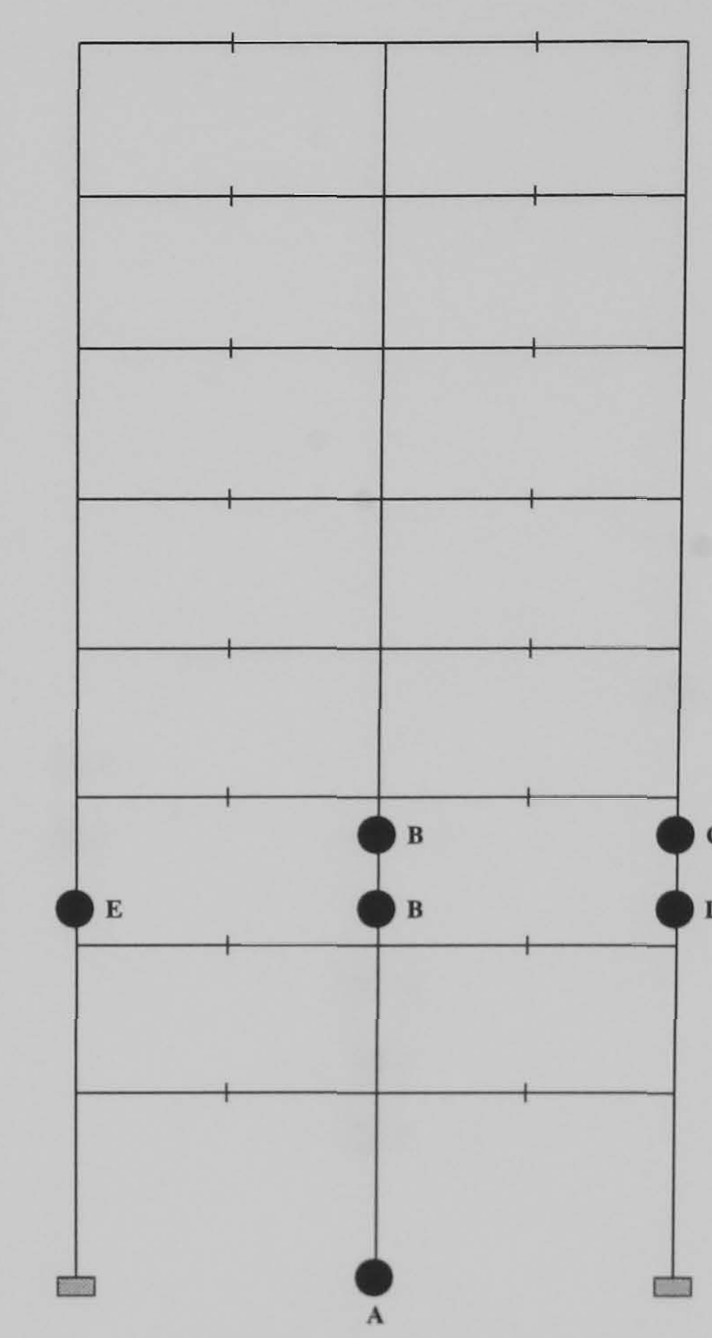

Hinge Location	Load Level at Hinge Formation S-R(1)	S-R(2)	Rigid
A	**0.9825**	**1.0525**	**1.830**
B	**1.02**	**1.0625**	**1.940**
C	**1.035**	**1.11**	**1.945**
D	**1.0625**	**1.115**	**1.975**
E	**1.1**	**1.1575**	**2.065**
F	**1.11**	**1.16**	**N/A**
G	**1.13**	**1.205**	**N/A**
H	**1.16**	**1.215**	**N/A**
I	**1.1875**	**1.225**	**N/A**
J	**1.215**	**N/A**	**N/A**

Key :

- Plastification prior to ULS design load being attained
- Semi-Rigid Connection
- Plastification following the attainment of the design load
- Member plastification

FRAME : **f35 b20**
Load Case 3

S-R (1) Negelecting web shear at the internal columns

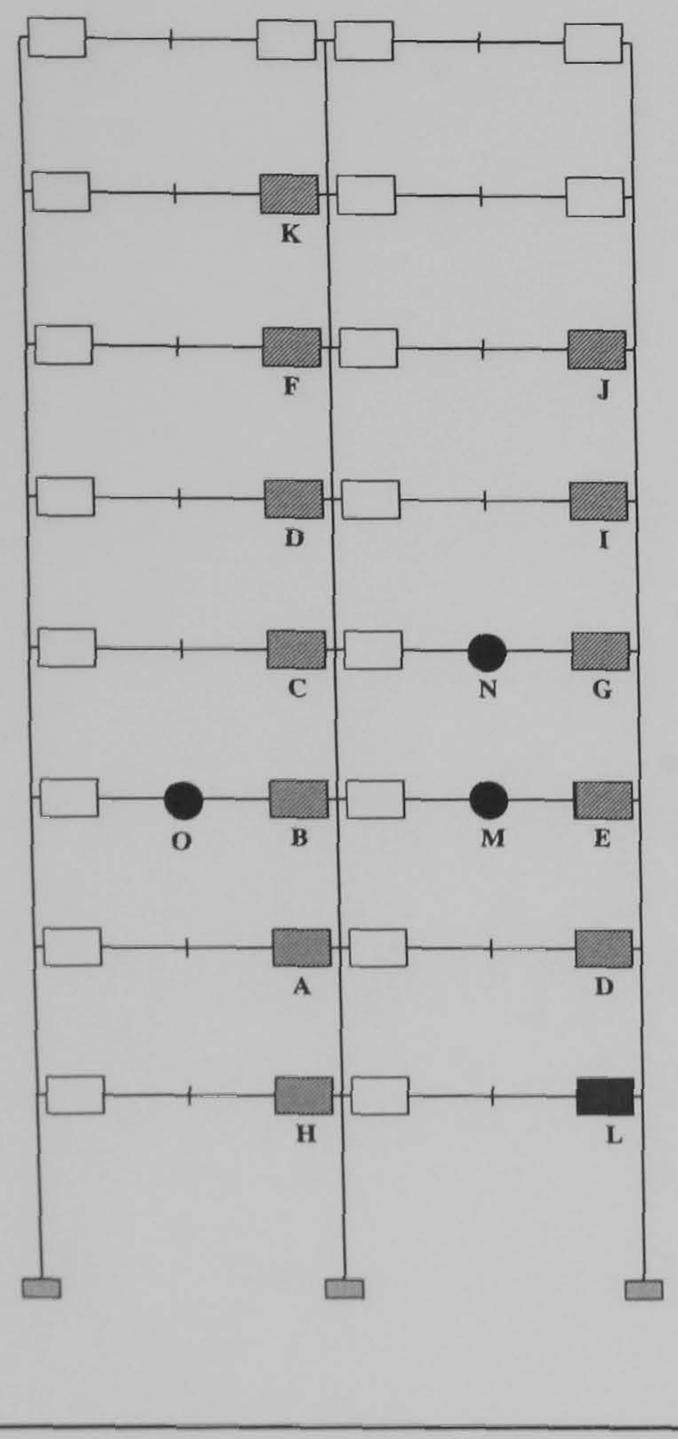

S-R (2) Including web shear at the internal columns

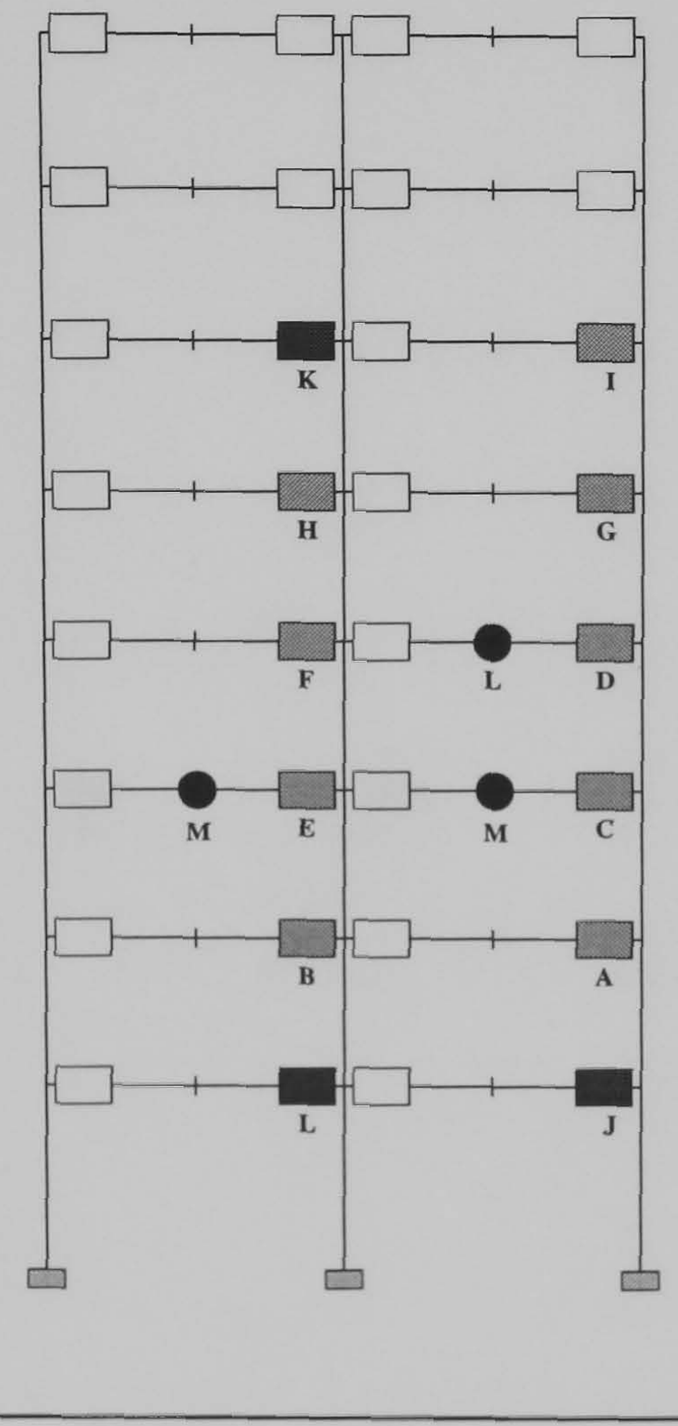

Rigid

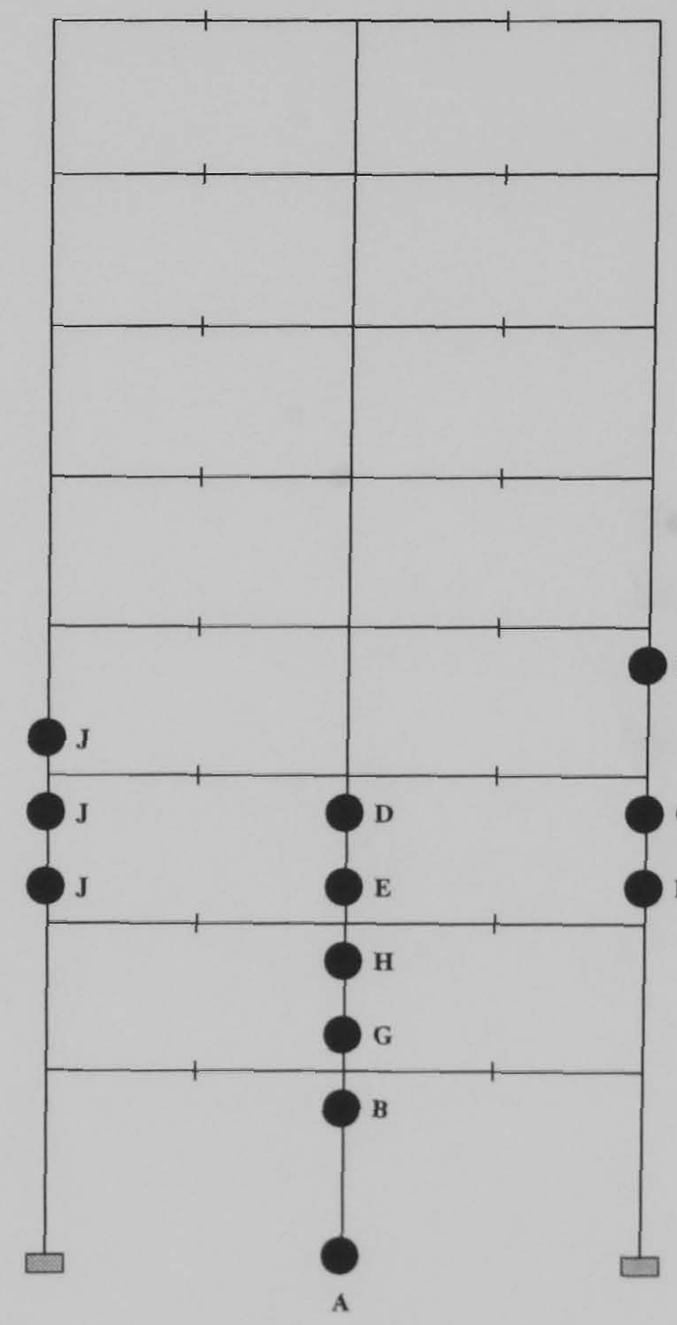

Hinge Location	Load Level at Hinge Formation S-R(1)	S-R(2)	Rigid
A	0.635	0.7525	1.257
B	0.6575	0.79	1.302
C	0.685	0.81	1.340
D	0.7725	0.8275	1.345
E	0.8125	0.8325	1.350
F	0.8275	0.8575	1.365
G	0.8325	0.91	1.385
H	0.91	0.9825	1.392
I	0.92	0.9875	1.400
J	0.9925	1.0475	1.405
K	0.995	1.055	N/A
L	1.055	1.062	N/A
M	1.06	1.067	N/A
N	1.067	N/A	N/A
O	1.07	N/A	N/A

Key :

- Semi-Rigid Connection
- Plastification prior to ULS *design load being attained*
- Plastification following the attainment of the design load
- *Member plastification*

FRAME : **f35 b24**
Load Case 1

S-R (1) Negelecting web shear at the internal columns

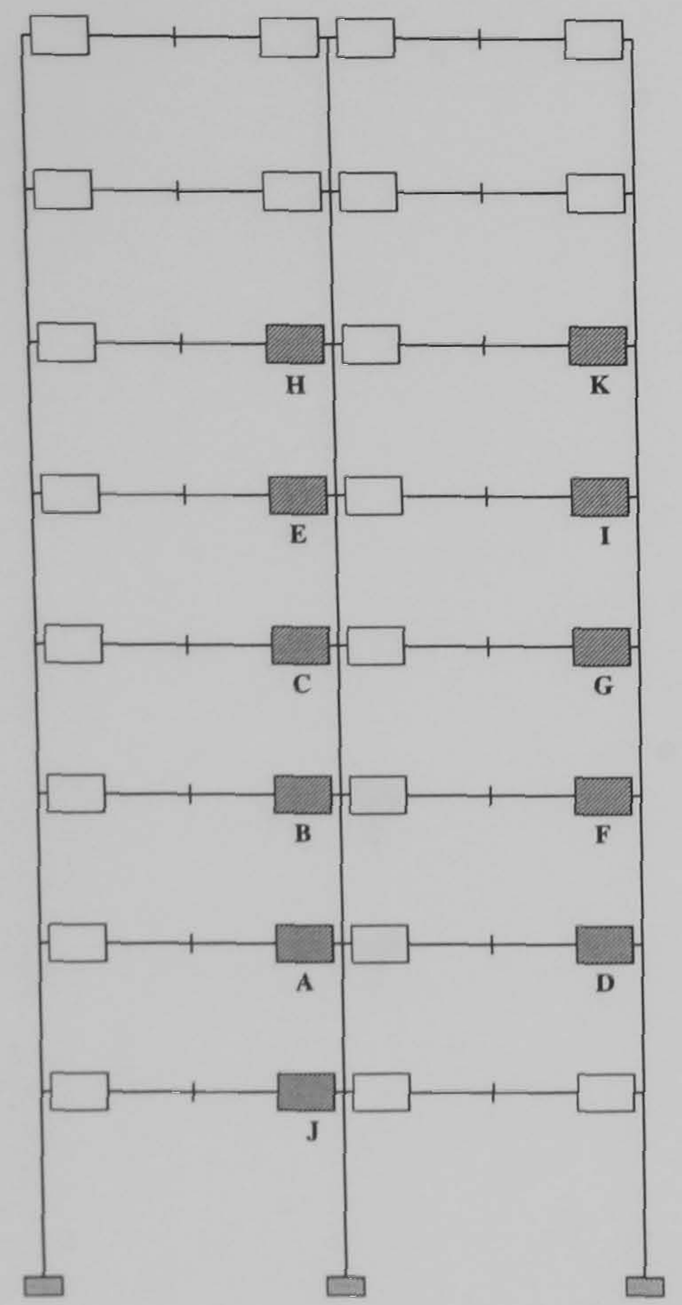

S-R (2) Including web shear at the internal columns

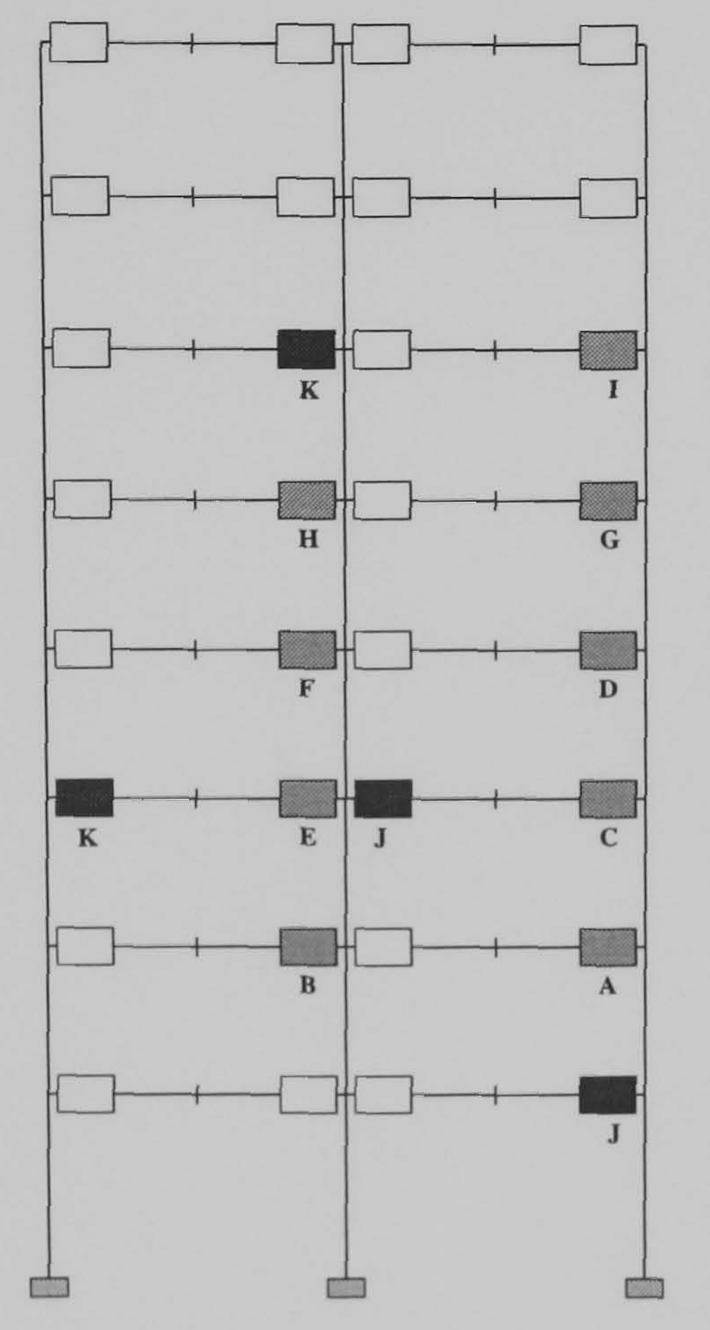

Rigid

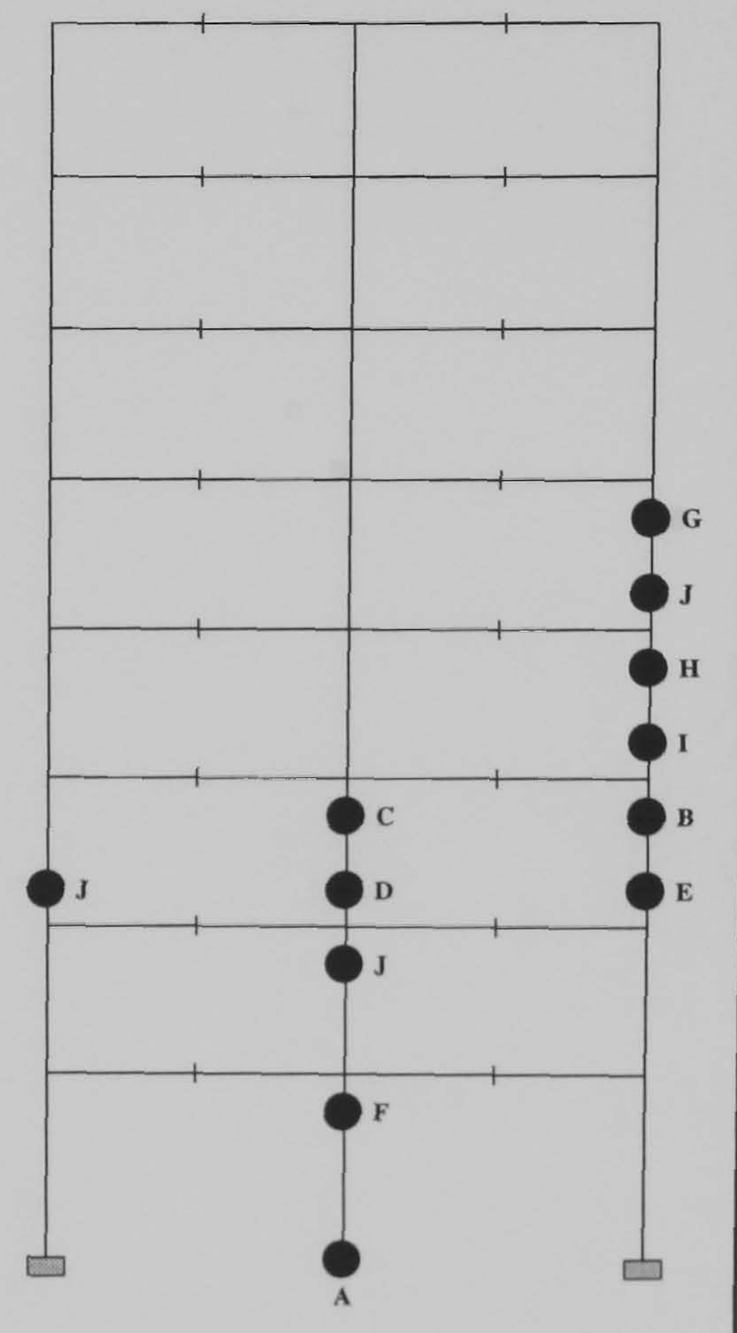

Hinge Location	Load Level at Hinge Formation S-R(1)	S-R(2)	Rigid
A	0.6175	0.715	1.370
B	0.6325	0.75	1.427
C	0.665	0.755	1.447
D	0.7425	0.7725	1.450
E	0.7675	0.78	1.467
F	0.775	0.81	1.487
G	0.7975	0.8675	1.515
H	0.8425	0.945	1.517
I	0.9	0.9575	1.527
J	0.9025	1.025	1.537
K	0.9875	1.04	N/A

Key :

Semi-Rigid Connection

Plastification prior to ULS design load being attained

Plastification following the attainment of the design load

Member plastification

FRAME : **f35 b24**
Load Case 2

S-R (1) Negelecting web shear at the internal columns

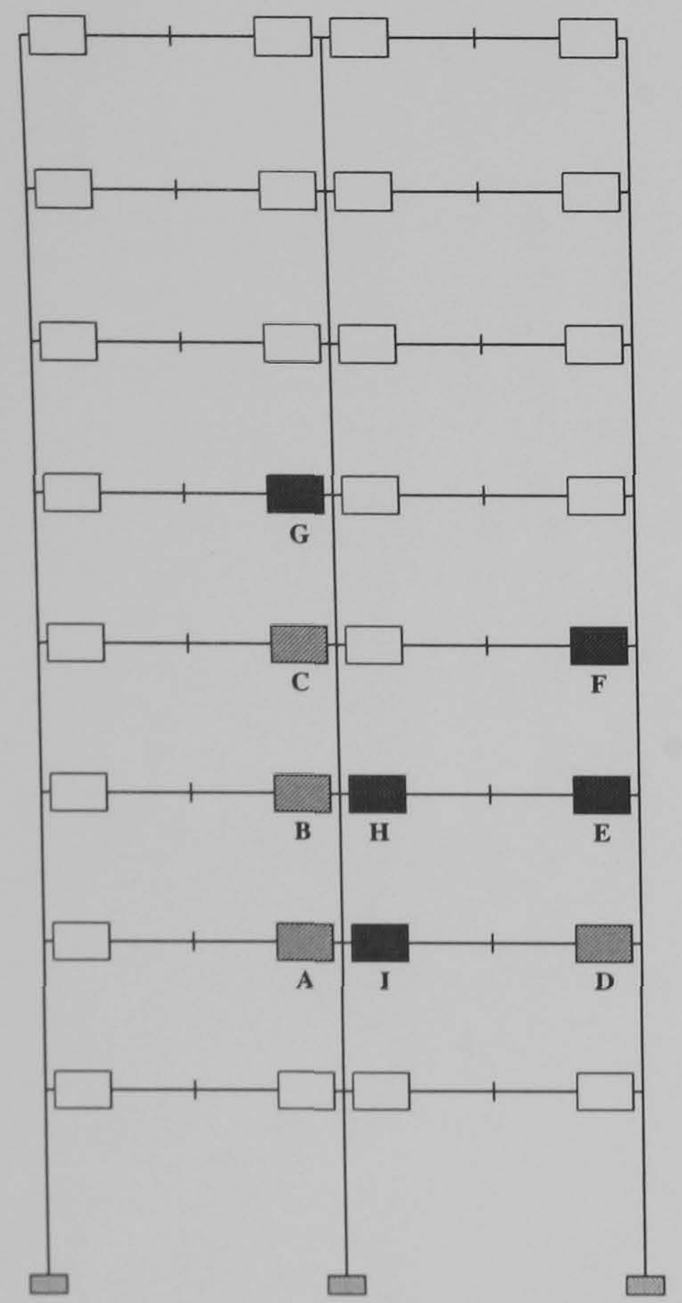

S-R (2) Including web shear at the internal columns

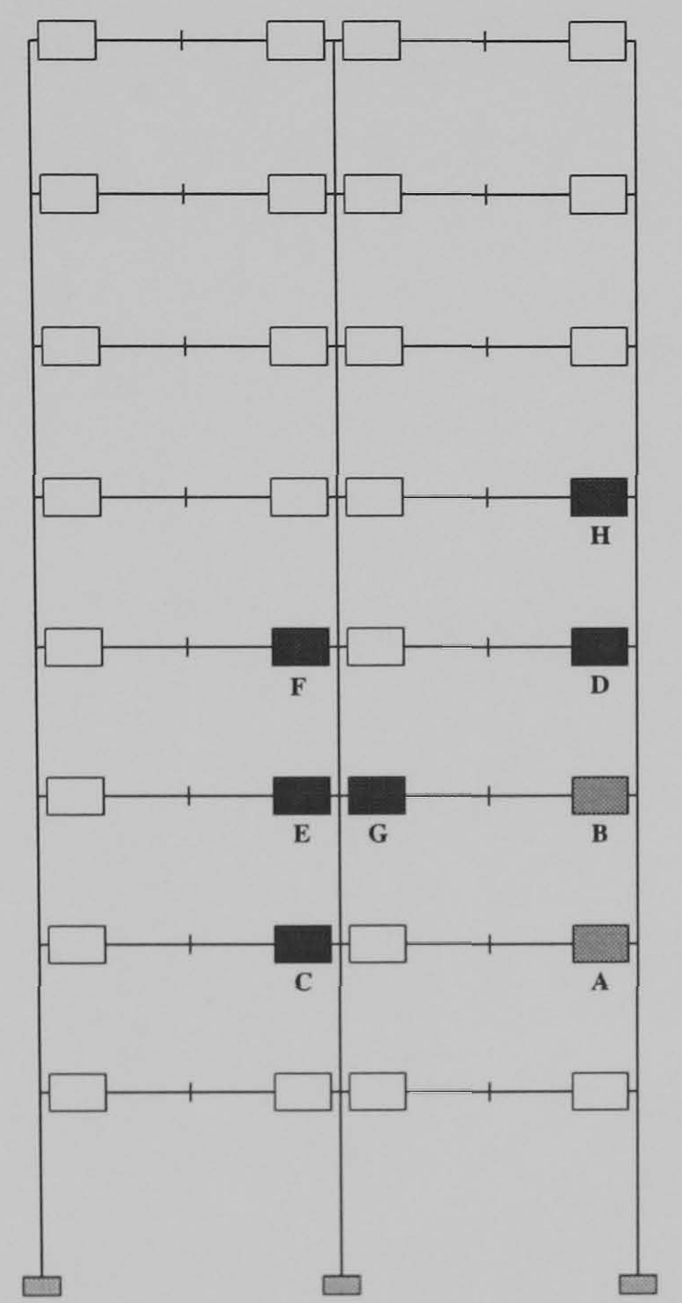

Rigid

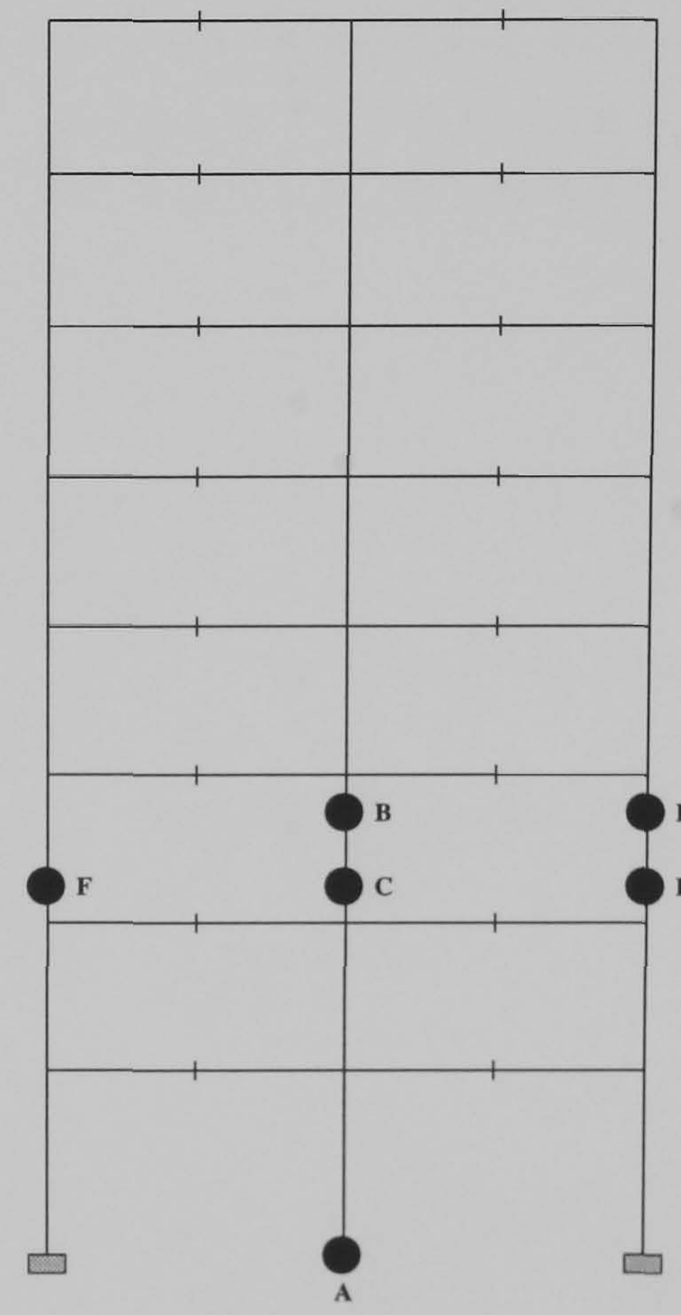

Hinge Location	Load Level at Hinge Formation		
	S-R(1)	S-R(2)	Rigid
A	**0.8475**	**0.945**	**1.860**
B	**0.8725**	**0.9925**	**1.970**
C	**0.9375**	**1.0**	**1.972**
D	**0.995**	**1.03**	**1.977**
E	**1.04**	**1.0375**	**2.007**
F	**1.0875**	**1.0925**	**2.097**
G	**1.1175**	**1.165**	**N/A**
H	**1.14**	**1.1875**	**N/A**
I	**1.1725**	**N/A**	**N/A**

Key :

Plastification prior to ULS design load being attained

Semi-Rigid Connection

Plastification following the attainment of the design load

Member plastification

FRAME : **f35 b24**
Load Case 3

C.5 Sway deflections

The sway deflections presented in this section refer to the horizontal displacement of the top left hand corner of each frame.

	Frame	Fixed Frame		Including Shear at External Columns No Shear at Internal Columns				Including Shear at External Columns Including Shear at Internal Columns			
		1st Order	2nd Order	1st Order	2nd Order	Increase in Frame Drift # 1st Order	2nd Order	1st Order	2nd Order	Increase in Frame Drift 1st Order	2nd Order
2 Storey 1 Bay	f10 b24	14.2* [563]	14.97 [534]					19.34 [414]	20.50 [390]	1.36	1.37
	f11 b20	10.61 [754]	11.25 [711]					18.86 [424]	20.55 [389]	1.78	1.83
	f11 b24	15.89 [503]	16.85 [475]					26.02 [307]	28.19 [284]	1.64	1.67
	f12 b20	13.81 [579]	14.44 [554]					27.44 [292]	29.57 [271]	1.99	2.05
	f12 b24	19.51 [410]	20.40 [392]					34.71 [230]	37.14 [215]	1.78	1.82
	f13 b24	40.78 [270]	42.86 [257]					57.41 [192]	61.17 [180]	1.41	1.43
	f14 b24	37.48 [293]	38.58 [285]					52.99 [208]	55.11 [200]	1.41	1.43
	f15 b24	57.12 [193]	59.07 [186]					85.36 [129]	89.46 [123]	1.49	1.51
2 Storey 4 Bay	f16b24	6.28 [1273]	6.77 [1181]	7.27 [1100]	7.89 [1013]	1.16	1.17	8.12 [985]	8.85 [904]	1.29	1.31
	f17 b20	10.47 [764]	11.46 [698]	15.34 [522]	17.22 [464]	1.47	1.50	16.96 [472]	19.21 [416]	1.62	1.68
	f17 b24			14.22 [583]	15.88 [524]	1.36	1.39	15.89 [503]	17.89 [447]	1.52	1.56
	f18 b20	10.72 [744]	11.51 [695]	17.49 [457]	19.23 [416]	1.63	1.67	19.29 [415]	21.38 [374]	1.80	1.86
	f18 b24			15.79 [506]	17.23 [464]	1.47	1.50	17.67 [453]	19.45 [411]	1.65	1.69
	f19 b20	17.52 [628]	19.06 [577]	22.94 [480]	25.39 [433]	1.31	1.33	25.39 [433]	28.33 [388]	1.45	1.49
	f19 b24			21.74 [506]	23.97 [459]	1.24	1.26	24.53 [448]	27.32 [403]	1.40	1.43
	f20 b20	27.91 [394]	30.57 [360]	37.54 [293]	41.98 [262]	1.35	1.37	40.70 [270]	46.19 [238]	1.46	1.51
	f20 b24			35.90 [306]	40.03 [275]	1.29	1.31	39.89 [276]	44.90 [245]	1.43	1.47
	f21 b20	35.95 [306]	39.35 [280]	53.32 [206]	60.12 [183]	1.48	1.53	57.82 [190]	65.78 [167]	1.61	1.67
	f21 b24			51.54 [213]	58.00 [190]	1.43	1.47	56.92 [193]	64.75 [170]	1.58	1.65

NOTES

* - Horizontal drift of the top left hand corner of the frame (mm)

[ ] - Sway Index

\# - A dimensionless multiplyer to the fixed frame drift, to obtain the corresponding semi-rigid frame drift

▨ - Critical frames where the drift exceeds the allowable tolerance (height/300)

Table C.6: Serviceability sway drifts - 2 storey frames

	Frame	Fixed Frame 1st Order	Fixed Frame 2nd Order	Including Shear at External Columns No Shear at Internal Columns 1st Order	Including Shear at External Columns No Shear at Internal Columns 2nd Order	Increase in Frame Drift # 1st Order	Increase in Frame Drift # 2nd Order	Including Shear at External Columns Including Shear at Internal Columns 1st Order	Including Shear at External Columns Including Shear at Internal Columns 2nd Order	Increase in Frame Drift 1st Order	Increase in Frame Drift 2nd Order
4 Storey 2 Bay	**f22 b24**	**14.99*** **[1001]**	**15.97** **[939]**	**21.04** **[713]**	**22.84** **[657]**	**1.40**	**1.43**	**23.52** **[638]**	**25.77** **[582]**	**1.57**	**1.61**
	f23 b20	**11.58** **[1295]**	**12.55** **[1195]**	**21.52** **[697]**	**24.70** **[607]**	**1.86**	**1.97**	**23.61** **[635]**	**27.48** **[546]**	**2.04**	**2.19**
	f23 b24	**22.76** **[659]**	**24.70** **[607]**	**35.94** **[417]**	**40.39** **[371]**	**1.58**	**1.64**	**40.75** **[368]**	**46.55** **[322]**	**1.79**	**1.88**
	f24 b20	**18.12** **[828]**	**19.65** **[763]**	**37.24** **[403]**	**43.31** **[346]**	**2.06**	**2.20**	**40.00** **[375]**	**46.98** **[319]**	**2.21**	**2.39**
	f24 b24	**26.62** **[563]**	**28.90** **[519]**	**46.85** **[320]**	**53.37** **[281]**	**1.76**	**1.85**	**52.36** **[286]**	**60.56** **[248]**	**1.97**	**2.10**
	f25 b24	**71.21** **[295]**	**76.34** **[275]**	**99.96** **[210]**	**109.96** **[191]**	**1.40**	**1.44**	**108.69** **[193]**	**120.71** **[174]**	**1.53**	**1.58**
4 Storey 4 Bay	**f28 b24**	**11.60** **[1293]**	**12.38** **[1211]**	**15.15** **[990]**	**16.44** **[912]**	**1.31**	**1.33**	**17.93** **[837]**	**19.72** **[761]**	**1.55**	**1.59**
	f29 b20	**12.25** **[1224]**	**13.31** **[1127]**	**21.37** **[702]**	**24.50** **[612]**	**1.74**	**1.84**	**24.61** **[610]**	**28.81** **[521]**	**2.01**	**2.16**
	f29 b24	**20.53** **[731]**	**22.31** **[672]**	**30.88** **[486]**	**34.72** **[432]**	**1.50**	**1.56**	**36.56** **[410]**	**41.96** **[357]**	**1.78**	**1.88**
	f30 b20	**18.41** **[815]**	**19.95** **[752]**	**35.64** **[421]**	**41.18** **[364]**	**1.94**	**2.06**	**40.90** **[367]**	**48.27** **[311]**	**2.22**	**2.42**
	f30 b24	**24.51** **[612]**	**26.56** **[565]**	**40.48** **[371]**	**45.75** **[328]**	**1.65**	**1.72**	**47.87** **[313]**	**55.34** **[271]**	**1.95**	**2.08**
	f31 b20	**54.80** **[383]**	**61.01** **[344]**	**79.81** **[263]**	**92.95** **[226]**	**1.46**	**1.52**	**90.44** **[232]**	**107.47** **[195]**	**1.65**	**1.76**
	f31 b24			**71.83** **[292]**	**82.33** **[255]**	**1.31**	**1.35**	**85.79** **[245]**	**100.97** **[208]**	**1.57**	**1.65**
	f32 b24	**78.00** **[269]**	**86.07** **[244]**	**110.60** **[190]**	**126.81** **[166]**	**1.42**	**1.47**	**126.22** **[166]**	**147.48** **[142]**	**1.62**	**1.71**

NOTES

* - Horizontal drift of the top left hand corner of the frame (mm)

[ ] - Sway Index

\# - A dimensionless multiplyer to the fixed frame drift, to obtain the corressponding semi-rigid frame drift

▨ - Critical frames where the drift exceeds the allowable tolerance (height/300)

Table C.7: Serviceability sway drifts - 4 storey frames

	Frame	Fixed Frame 1st Order	Fixed Frame 2nd Order	Including Shear at External Columns No Shear at Internal Columns 1st Order	Including Shear at External Columns No Shear at Internal Columns 2nd Order	Increase in Frame Drift # 1st Order	Increase in Frame Drift # 2nd Order	Including Shear at External Columns Including Shear at Internal Columns 1st Order	Including Shear at External Columns Including Shear at Internal Columns 2nd Order	Increase in Frame Drift 1st Order	Increase in Frame Drift 2nd Order
8 Storey 2 Bay	**f34 b24**	**20.98*** **[1382]**	**22.50** **[1289]**	**33.45** **[867]**	**37.46** **[774]**	**1.59**	**1.66**	**38.71** **[749]**	**44.20** **[656]**	**1.85**	**1.96**
	f35 b20	**38.05** **[762]**	**42.26** **[686]**	**75.39** **[385]**	**93.53** **[310]**	**1.98**	**2.21**	**83.98** **[345]**	**107.20** **[271]**	**2.21**	**2.54**
	f35 b24	**36.18** **[802]**	**40.18** **[722]**	**66.55** **[436]**	**81.33** **[357]**	**1.84**	**2.02**	**75.58** **[384]**	**95.34** **[304]**	**2.09**	**2.37**

NOTES

* - Horizontal drift of the top left hand corner of the frame (mm)

[ ] - Sway Index

\# - A dimensionless multiplyer to the fixed frame drift, to obtain the corressponding semi-rigid frame drift

▒ - Critical frames where the drift exceeds the allowable tolerance (height/300)

Table C.8: Serviceability sway drifts - 8 storey frames

Appendix D

Material properties and geometrical imperfections

D.1 Scope

The following appendix describes the material properties applicable to the hardened concrete, reinforcement and steel plate samples. In addition, the geometrical imperfections applicable to the structural members are reported.

D.2 Material properties

Test	Compressive strength N/mm^2 7 days	28 days	Test date Compressive strength N/mm^2	Tensile strength
1	Steel only			
2	**36.35**	**42.00**	49 days **45.05**	**3.85**
3	**26.90**	**40.85**	88 days **45.75**	**3.40**
4	**24.35**	**41.20**	31 days **38.90**	**3.60**
5	**33.05**	**49.30**	41 days **47.95**	**3.50**

Figure D.1: Concrete strengths

Bar diameter (mm)	Youngs Modulas kN/mm^2	Yield stress N/mm^2	Ultimate stress N/mm^2	Bar ductility based on % elongation at fracture Test	Average
	Average				
16 (longitudinal)	**200**	**504**	**611**	3 **26** 4 **27** 5 **27**	**26**
6 (A142 mesh)	**197**	**602**	**633**		**12**

Note :
The yield stress was assumed to be the value of the stress when a level of strain equal to 0.2% had been obtained

Figure D.2: Material properties applicable to the reinforcement

Test	Universal column						Universal Beams											
							Connection A						Connection B					
	web			flange			web			flange			web			flange		
	Youngs Modulus kN/mm^2	Yield stress N/mm^2	Ultimate stress N/mm^2	Youngs Modulus kN/mm^2	Yield stress N/mm^2	Ultimate stress N/mm^2	Youngs Modulus kN/mm^2	Yield stress N/mm^2	Ultimate stress N/mm^2	Youngs Modulus kN/mm^2	Yield stress N/mm^2	Ultimate stress N/mm^2	Youngs Modulus kN/mm^2	Yield stress N/mm^2	Ultimate stress N/mm^2	Youngs Modulus kN/mm^2	Yield stress N/mm^2	Ultimate stress N/mm^2
1	**208**	**318**	**502**	**209**	**281**	**484**	**197**	**339**	**489**	**211**	**312**	**489**	**193**	**341**	**492**	**210**	**311**	**488**
2	**194**	**295**	**468**	**215**	**266**	**467**	**198**	**329**	**474**	**194**	**312**	**471**	**200**	**334**	**479**	**196**	**310**	**470**
3	**201**	**289**	**467**	**199**	**276**	**467**	**199**	**331**	**477**	**198**	**293**	**462**	**197**	**329**	**477**	**196**	**306**	**469**
4	**192**	**311**	**510**	**197**	**271**	**466**	**204**	**317**	**454**	**207**	**324**	**455**	**198**	**317**	**453**	**205**	**302**	**449**
5	**196**	**285**	**424**	**222**	**331**	**484**	**202**	**385**	**512**	**207**	**351**	**511**	**200**	**389**	**516**	**206**	**345**	**498**

End plate thickness	Youngs Modulas kN/mm^2	Yield stress N/mm^2	Ultimate stress N/mm^2
10mm	**201**	**350**	**509**
15mm	**215**	**305**	**483**

Note :

The yield stress was assumed to be the value of stress when a level of strain equal to 0.2% had been attained

Figure D.3: Material properties applicable to the plate steel samples

D.3 Geometrical imperfections - structural members

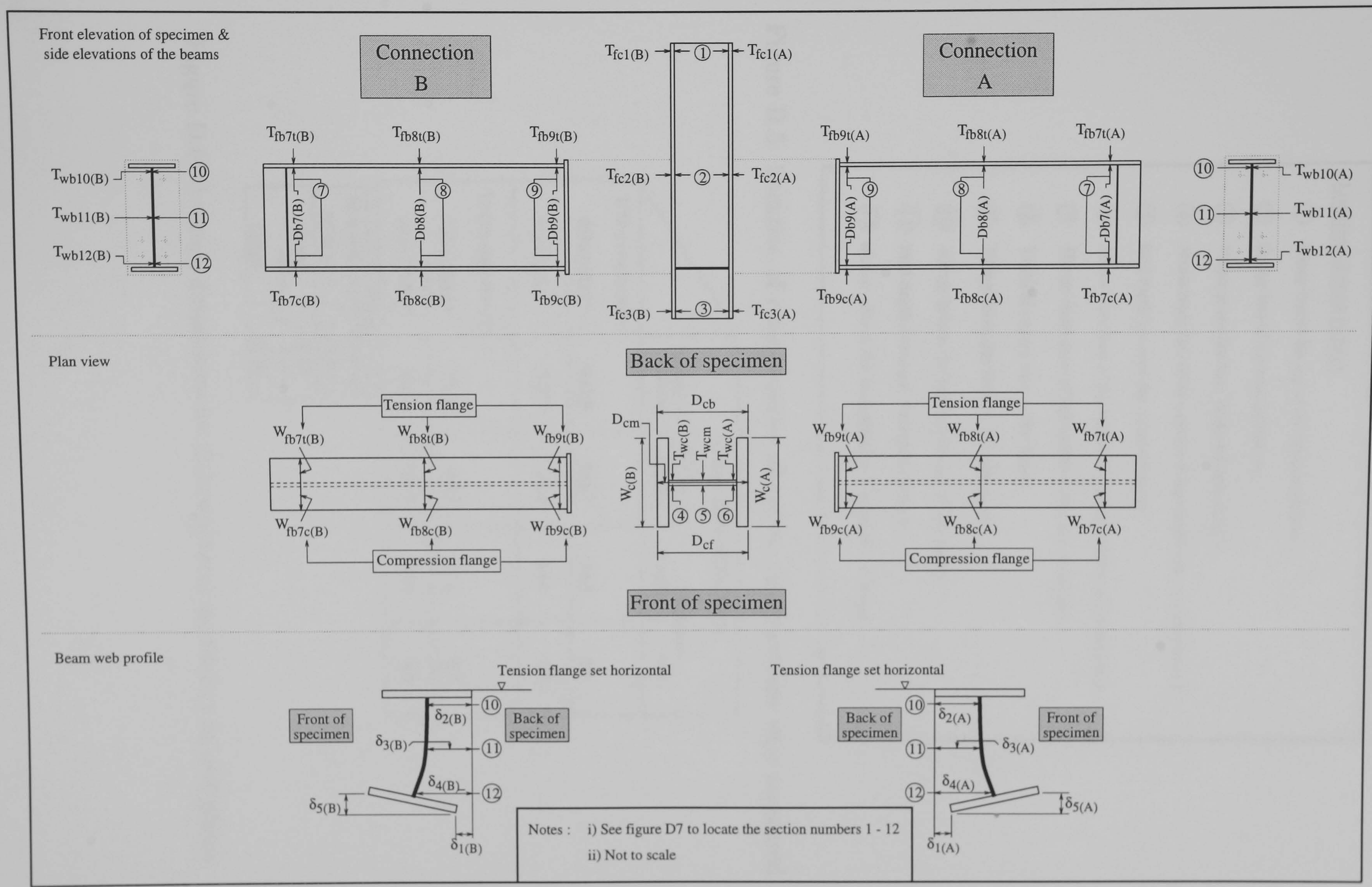

Figure D.4: General arrangement drawing of the imperfections considered

Locations of cross sections

① 10mm below the top of the column section

② Centre line of the tension bolt row

③ 10mm above the base of the column section

④ 30mm from face of the column flange applicable to connection B

⑤ Mid depth between the column flanges

⑥ 30mm from face of the column flange applicable to connection A

⑦ 30mm from face of stiffner towards the end plate

⑧ Vertical centre line of the beam

⑨ 30mm from the face of the end plate

⑩ 40mm below the tension flange of the beam

⑪ Mid depth between the beam flanges

⑫ 40mm above the compression flange of the beam

Figure D.5: Location of cross-sections where the imperfections were measured

	Average dimensions (mm)			
	Depth of section	Width of section	Thickness flange	web
Universal beams				
457x152x52	**447.3**	**154.7**	**10.5**	**8.0**
533x210x82	**527.7**	**210.1**	**13.0**	**9.7**
Universal columns				
203x203x52	**207.3**	**204.3**	**12.4**	**8.1**
254x254x73	**256.7**	**252.7**	**13.4**	**8.4**

End plate thickness (mm)	
nominaly	actual
10mm	**10.05**
15mm	**15.10**

Figure D.6: Average dimensions for the structural members and end plates

Test 1

		Universal beam 457x152x52					
		Reference	Connection B		Reference	Connection A	
			Front	Back		Front	Back
Depth of section (mm)		Db7(B)	**446.0**	**449.0**	Db7(A)	**444.0**	**450.0**
		Db8(B)	**445.0**	**450.0**	Db8(A)	**445.0**	**450.0**
		Db9(B)	**446.0**	**450.0**	Db9(A)	**445.0**	**450.0**
Width of section (mm)	Tension flange	$W_{fb7t(B)}$	**154.5**		$W_{fb7t(A)}$	**154.5**	
		$W_{fb8t(B)}$	**153.9**		$W_{fb8t(A)}$	**154.0**	
		$W_{fb9t(B)}$	**154.0**		$W_{fb9t(A)}$	**154.5**	
	Compression flange	$W_{fb7c(B)}$	**158.9**		$W_{fb7c(A)}$	**154.5**	
		$W_{fb8c(B)}$	**154.0**		$W_{fb8c(A)}$	**154.0**	
		$W_{fb9c(B)}$	**154.0**		$W_{fb9c(A)}$	**154.5**	
Thickness (mm)	Tension flange	$T_{fb7t(B)}$	**10.74**	**10.19**	$T_{fb7t(A)}$	**10.61**	**11.05**
		$T_{fb8t(B)}$	**10.65**	**10.24**	$T_{fb8t(A)}$	**10.70**	**10.84**
		$T_{fb9t(B)}$	**10.90**	**10.20**	$T_{fb9t(A)}$	**10.65**	**10.95**
	Compression flange	$T_{fb7c(B)}$	**10.25**	**10.80**	$T_{fb7c(A)}$	**10.55**	**9.86**
		$T_{fb8c(B)}$	**10.20**	**10.56**	$T_{fb8c(A)}$	**10.65**	**9.85**
		$T_{fb9c(B)}$	**10.30**	**10.64**	$T_{fb9c(A)}$	**10.70**	**9.88**
	Web	$T_{wb10(B)}$	**7.96**		$T_{wb10(A)}$	**8.15**	
		$T_{wb11(B)}$	**7.94**		$T_{wb11(A)}$	**7.91**	
		$T_{wb12(B)}$	**8.00**		$T_{wb12(A)}$	**7.90**	

Figure D.7: Imperfections within the beam section - Test 1

Dimensions in mm	Reference	Beam web profile (457x152x52UB)					
		Connection B			Connection A		
		⑦	⑧	⑨	⑦	⑧	⑨
	$\delta_{1(B)}$	**11.5**	**11.5**	**11.5**			
	$\delta_{2(B)}$	**72.0**	**73.0**	**73.5**			
	$\delta_{3(B)}$	**70.0**	**70.5**	**70.0**			
	$\delta_{4(B)}$	**60.5**	**61.5**	**62.0**			
	$\delta_{5(B)}$	**3.0**	**5.0**	**4.0**			
	$\delta_{1(A)}$				**5.5**	**5.5**	**5.5**
	$\delta_{2(A)}$				**73.0**	**73.5**	**73.5**
	$\delta_{3(A)}$				**71.0**	**71.5**	**71.5**
	$\delta_{4(A)}$				**67.5**	**68.0**	**68.0**
	$\delta_{5(A)}$				**6.0**	**5.0**	**5.0**

Figure D.8: Imperfections within the beam web profile - Test 1

Universal column						
Depth of section (mm)	Reference	Location	Front	Middle	Back	
	D_{cb}	①			**205.5**	
		②			**205.5**	
		③			**205.5**	
	D_{cm}	①		**207.0**		
		②		**N/A**		
		③		**207.0**		
	D_{cf}	①	**207.0**			
		②	**206.5**			
		③	**205.5**			
			Connection B		Connection A	
Width of section (mm)	$W_{c(B)}$	①	**204.5**			
		②	**204.5**			
		③	**204.5**			
	$W_{c(A)}$	①			**204.0**	
		②			**204.0**	
		③			**204.0**	
Thickness (mm)	Flange					
	$T_{fc1(B)}$		**12.95**		**11.84**	
	$T_{fc2(B)}$		**13.00**		**11.86**	
	$T_{fc3(B)}$		**12.86**		**11.90**	
	$T_{fc1(A)}$		**12.80**		**12.35**	
	$T_{fc2(A)}$		**12.85**		**12.35**	
	$T_{fc3(A)}$		**12.75**		**12.35**	
	web					
	$T_{wc(B)}$	①	**7.74**			
		③	**8.02**			
	T_{wcm}	①	**8.39**			
		③	**8.34**			
	$T_{wc(A)}$	①	**7.70**			
		③	**7.95**			

Figure D.9: Imperfections within the column section - Test 1

Test 2

		Universal beam 457x152x52					
		Reference	Connection B		Reference	Connection A	
			Front	Back		Front	Back
Depth of section (mm)		Db7(B)	**445.0**	**449.0**	Db7(A)	**445.0**	**447.5**
		Db8(B)	**444.0**	**450.0**	Db8(A)	**444.0**	**451.0**
		Db9(B)	**445.5**	**450.5**	Db9(A)	**445.0**	**449.0**
Width of section (mm)	Tension flange	$W_{fb7t(B)}$	**155.0**		$W_{fb7t(A)}$	**154.0**	
		$W_{fb8t(B)}$	**155.5**		$W_{fb8t(A)}$	**154.5**	
		$W_{fb9t(B)}$	**155.0**		$W_{fb9t(A)}$	**155.0**	
	Compression flange	$W_{fb7c(B)}$	**154.5**		$W_{fb7c(A)}$	**155.5**	
		$W_{fb8c(B)}$	**155.0**		$W_{fb8c(A)}$	**154.0**	
		$W_{fb9c(B)}$	**155.5**		$W_{fb9c(A)}$	**156.0**	
Thickness (mm)	Tension flange	$T_{fb7t(B)}$	**10.62**	**10.60**	$T_{fb7t(A)}$	**10.91**	**10.70**
		$T_{fb8t(B)}$	**10.65**	**10.67**	$T_{fb8t(A)}$	**10.84**	**10.60**
		$T_{fb9t(B)}$	**10.64**	**10.59**	$T_{fb9t(A)}$	**10.96**	**10.62**
	Compression flange	$T_{fb7c(B)}$	**10.74**	**10.81**	$T_{fb7c(A)}$	**9.90**	**10.60**
		$T_{fb8c(B)}$	**10.30**	**10.80**	$T_{fb8c(A)}$	**9.81**	**10.51**
		$T_{fb9c(B)}$	**10.36**	**10.81**	$T_{fb9c(A)}$	**10.07**	**10.55**
	Web	$T_{wb10(B)}$	**8.80**		$T_{wb10(A)}$	**8.40**	
		$T_{wb11(B)}$	**7.96**		$T_{wb11(A)}$	**8.00**	
		$T_{wb12(B)}$	**7.77**		$T_{wb12(A)}$	**8.21**	

Figure D.10: Imperfections within the beam section - Test 2

Dimensions in mm	Reference	Beam web profile (457x152x52UB) Connection B ⑦	Connection B ⑧	Connection B ⑨	Connection A ⑦	Connection A ⑧	Connection A ⑨
	$\delta_{1(B)}$	**7.0**	**12.0**	**12.0**			
	$\delta_{2(B)}$	**74.0**	**73.0**	**73.0**			
	$\delta_{3(B)}$	**74.0**	**74.0**	**74.0**			
	$\delta_{4(B)}$	**81.0**	**85.0**	**85.0**			
	$\delta_{5(B)}$	**4.0**	**6.0**	**5.0**			
	$\delta_{1(A)}$				**0.0**	**9.0**	**9.0**
	$\delta_{2(A)}$				**72.0**	**73.0**	**73.0**
	$\delta_{3(A)}$				**70.0**	**74.0**	**74.0**
	$\delta_{4(A)}$				**72.0**	**82.0**	**82.0**
	$\delta_{5(A)}$				**2.5**	**6.0**	**4.0**

Figure D.11: Imperfections within the beam web profile - Test 2

Universal column 203x203x52					
	Reference	Location	Front	Middle	Back
Depth of section (mm)	D_{cb}	①			**206.0**
		②			**206.0**
		③			**207.0**
	D_{cm}	①		**206.5**	
		②		**N/A**	
		③		**206.0**	
	D_{cf}	①	**205.5**		
		②	**207.0**		
		③	**206.0**		
Width of section (mm)	$W_{c(B)}$	①	Connection B **203.0**		Connection A
		②	**203.0**		
		③	**203.0**		
	$W_{c(A)}$	①			**204.0**
		②			**203.0**
		③			**203.5**
Thickness (mm) Flange	$T_{fc1(B)}$		**11.88**		**12.91**
	$T_{fc2(B)}$		**11.90**		**13.00**
	$T_{fc3(B)}$		**11.95**		**13.14**
	$T_{fc1(A)}$		**12.16**		**12.56**
	$T_{fc2(A)}$		**12.30**		**12.60**
	$T_{fc3(A)}$		**12.10**		**12.78**
web	$T_{wc(B)}$	①	**8.30**		
		③	**7.75**		
	T_{wcm}	①	**8.40**		
		③	**8.50**		
	$T_{wc(A)}$	①	**7.70**		
		③	**7.81**		

Figure D.12: Imperfections within the column section - Test 2

Test 3

		Universal beam 457x152x52					
		Reference	Connection B		Reference	Connection A	
			Front	Back		Front	Back
Depth of section (mm)		Db7(B)	**445.0**	**449.0**	Db7(A)	**445.0**	**448.5**
		Db8(B)	**445.0**	**449.0**	Db8(A)	**445.0**	**450.0**
		Db9(B)	**445.0**	**448.0**	Db9(A)	**445.0**	**449.0**
Width of section (mm)	Tension flange	$W_{fb7t(B)}$	**155.0**		$W_{fb7t(A)}$	**154.0**	
		$W_{fb8t(B)}$	**154.5**		$W_{fb8t(A)}$	**154.5**	
		$W_{fb9t(B)}$	**154.5**		$W_{fb9t(A)}$	**155.0**	
	Compression flange	$W_{fb7c(B)}$	**155.5**		$W_{fb7c(A)}$	**155.0**	
		$W_{fb8c(B)}$	**155.0**		$W_{fb8c(A)}$	**155.0**	
		$W_{fb9c(B)}$	**156.0**		$W_{fb9c(A)}$	**155.0**	
Thickness (mm)	Tension flange	$T_{fb7t(B)}$	**10.75**	**10.70**	$T_{fb7t(A)}$	**10.75**	**10.53**
		$T_{fb8t(B)}$	**10.75**	**10.64**	$T_{fb8t(A)}$	**10.74**	**10.30**
		$T_{fb9t(B)}$	**10.95**	**10.50**	$T_{fb9t(A)}$	**10.55**	**10.10**
	Compression flange	$T_{fb7c(B)}$	**10.10**	**10.66**	$T_{fb7c(A)}$	**10.52**	**10.48**
		$T_{fb8c(B)}$	**10.00**	**10.67**	$T_{fb8c(A)}$	**10.55**	**10.59**
		$T_{fb9c(B)}$	**10.39**	**10.85**	$T_{fb9c(A)}$	**10.80**	**10.80**
	Web	$T_{wb10(B)}$	**7.90**		$T_{wb10(A)}$	**7.79**	
		$T_{wb11(B)}$	**8.02**		$T_{wb11(A)}$	**8.05**	
		$T_{wb12(B)}$	**8.03**		$T_{wb12(A)}$	**7.95**	

Figure D.13: Imperfections within the beam section - Test 3

Dimensions in mm	Reference	Beam web profile (457x152x52UB)					
		Connection B			Connection A		
		⑦	⑧	⑨	⑦	⑧	⑨
	$\delta_{1(B)}$	**4.0**	**2.0**	**0.0**			
	$\delta_{2(B)}$	**72.0**	**72.0**	**72.0**			
	$\delta_{3(B)}$	**71.0**	**71.0**	**71.0**			
	$\delta_{4(B)}$	**76.0**	**74.0**	**72.0**			
	$\delta_{5(B)}$	**4.0**	**4.0**	**3.0**			
	$\delta_{1(A)}$				**10.0**	**10.0**	**13.0**
	$\delta_{2(A)}$				**74.0**	**74.0**	**74.0**
	$\delta_{3(A)}$				**74.0**	**76.0**	**78.0**
	$\delta_{4(A)}$				**84.0**	**84.0**	**87.0**
	$\delta_{5(A)}$				**3.5**	**5.0**	**4.0**

Figure D.14: Imperfections within the beam web profile - Test 3

Universal column 203x203x52					
	Reference	Location	Front	Middle	Back
Depth of section (mm)	D_{cb}	①			**206.0**
		②			**206.0**
		③			**208.0**
	D_{cm}	①		**207.0**	
		②		**N/A**	
		③		**207.5**	
	D_{cf}	①	**206.5**		
		②	**206.0**		
		③	**207.0**		
Width of section (mm)	$W_{c(B)}$	①	Connection B **204.0**		Connection A
		②	**204.0**		
		③	**204.0**		
	$W_{c(A)}$	①			**204.0**
		②			**205.0**
		③			**204.0**
Thickness (mm) — Flange	$T_{fc1(B)}$		**12.97**		**12.03**
	$T_{fc2(B)}$		**12.90**		**11.87**
	$T_{fc3(B)}$		**13.00**		**12.10**
	$T_{fc1(A)}$		**12.56**		**12.24**
	$T_{fc2(A)}$		**12.85**		**12.08**
	$T_{fc3(A)}$		**12.70**		**12.24**
Thickness (mm) — web	$T_{wc(B)}$	①	**8.12**		
		③	**8.10**		
	T_{wcm}	①	**8.45**		
		③	**8.35**		
	$T_{wc(A)}$	①	**8.34**		
		③	**8.20**		

Figure D.15: Imperfections within the column section - Test 3

Test 4

		Universal beam 457x152x52					
		Reference	Connection B		Reference	Connection A	
			Front	Back		Front	Back
Depth of section (mm)		Db7(B)	**445.0**	**450.0**	Db7(A)	**444.0**	**450.0**
		Db8(B)	**445.0**	**451.0**	Db8(A)	**445.0**	**452.0**
		Db9(B)	**445.0**	**450.1**	Db9(A)	**445.0**	**451.0**
Width of section (mm)	Tension flange	$W_{fb7t(B)}$	**155.0**		$W_{fb7t(A)}$	**155.0**	
		$W_{fb8t(B)}$	**155.0**		$W_{fb8t(A)}$	**155.0**	
		$W_{fb9t(B)}$	**155.0**		$W_{fb9t(A)}$	**155.0**	
	Compression flange	$W_{fb7c(B)}$	**155.0**		$W_{fb7c(A)}$	**155.0**	
		$W_{fb8c(B)}$	**155.0**		$W_{fb8c(A)}$	**155.0**	
		$W_{fb9c(B)}$	**155.0**		$W_{fb9c(A)}$	**155.0**	
Thickness (mm)	Tension flange	$T_{fb7t(B)}$	**10.58**	**10.40**	$T_{fb7t(A)}$	**10.39**	**10.60**
		$T_{fb8t(B)}$	**10.40**	**10.58**	$T_{fb8t(A)}$	**10.36**	**10.54**
		$T_{fb9t(B)}$	**10.52**	**10.40**	$T_{fb9t(A)}$	**10.45**	**10.60**
	Compression flange	$T_{fb7c(B)}$	**10.89**	**10.70**	$T_{fb7c(A)}$	**10.65**	**11.00**
		$T_{fb8c(B)}$	**10.85**	**10.66**	$T_{fb8c(A)}$	**10.56**	**10.90**
		$T_{fb9c(B)}$	**10.71**	**10.60**	$T_{fb9c(A)}$	**10.61**	**10.70**
	Web	$T_{wb10(B)}$	**7.97**		$T_{wb10(A)}$	**8.04**	
		$T_{wb11(B)}$	**7.82**		$T_{wb11(A)}$	**7.76**	
		$T_{wb12(B)}$	**7.90**		$T_{wb12(A)}$	**7.95**	

Figure D.16: Imperfections within the beam section - Test 4

Dimensions in mm	Reference	Beam web profile (457x152x52UB)					
		Connection B			Connection A		
		⑦	⑧	⑨	⑦	⑧	⑨
	$\delta_{1(B)}$	**5.0**	**4.0**	**11.0**			
	$\delta_{2(B)}$	**72.0**	**72.0**	**74.0**			
	$\delta_{3(B)}$	**72.0**	**73.0**	**75.0**			
	$\delta_{4(B)}$	**77.0**	**76.0**	**85.0**			
	$\delta_{5(B)}$	**5.0**	**6.0**	**5.0**			
	$\delta_{1(A)}$				**6.0**	**10.0**	**12.0**
	$\delta_{2(A)}$				**72.0**	**73.0**	**74.0**
	$\delta_{3(A)}$				**72.0**	**73.0**	**75.0**
	$\delta_{4(A)}$				**78.0**	**83.0**	**86.0**
	$\delta_{5(A)}$				**6.0**	**7.0**	**6.0**

Figure D.17: Imperfections within the beam web profile - Test 4

Universal column 203x203x52				
	Reference	Location	Front	Middle	Back
Depth of section (mm)	D_{cb}	①			211.0
		②			210.0
		③			212.0
	D_{cm}	①		210.0	
		②		N/A	
		③		211.0	
	D_{cf}	①	209.0		
		②	209.0		
		③	209.0		
Width of section (mm)	$W_{c(B)}$	①	Connection B 206.0		Connection A
		②	205.0		
		③	205.0		
	$W_{c(A)}$	①			205.0
		②			206.0
		③			206.0
Thickness (mm)	Flange $T_{fc1(B)}$		12.60		12.24
	Flange $T_{fc2(B)}$		12.15		12.55
	Flange $T_{fc3(B)}$		12.24		12.48
	Flange $T_{fc1(A)}$		12.37		12.40
	Flange $T_{fc2(A)}$		12.00		11.90
	Flange $T_{fc3(A)}$		12.35		12.00
	web $T_{wc(B)}$	①	7.92		
		③	7.95		
	web T_{wcm}	①	8.10		
		③	8.00		
	web $T_{wc(A)}$	①	7.90		
		③	7.90		

Figure D.18: Imperfections within the column section - Test 4

Test 5

		Universal beam 533x210x82					
		Reference	Connection B		Reference	Connection A	
			Front	Back		Front	Back
Depth of section (mm)		Db7(B)	526.5	528.5	Db7(A)	526.5	529.0
		Db8(B)	526.5	529.0	Db8(A)	527.0	529.0
		Db9(B)	526.5	529.0	Db9(A)	527.0	529.0
Width of section (mm)	Tension flange	$W_{fb7t(B)}$	209.0		$W_{fb7t(A)}$	212.0	
		$W_{fb8t(B)}$	210.0		$W_{fb8t(A)}$	210.0	
		$W_{fb9t(B)}$	211.0		$W_{fb9t(A)}$	210.0	
	Compression flange	$W_{fb7c(B)}$	210.0		$W_{fb7c(A)}$	209.0	
		$W_{fb8c(B)}$	210.0		$W_{fb8c(A)}$	211.0	
		$W_{fb9c(B)}$	209.0		$W_{fb9c(A)}$	210.0	
Thickness (mm)	Tension flange	$T_{fb7t(B)}$	12.65	13.15	$T_{fb7t(A)}$	13.00	12.54
		$T_{fb8t(B)}$	12.80	12.90	$T_{fb8t(A)}$	13.16	12.64
		$T_{fb9t(B)}$	12.65	13.04	$T_{fb9t(A)}$	13.16	12.70
	Compression flange	$T_{fb7c(B)}$	13.15	13.30	$T_{fb7c(A)}$	13.20	13.05
		$T_{fb8c(B)}$	13.10	13.25	$T_{fb8c(A)}$	13.39	13.11
		$T_{fb9c(B)}$	13.02	13.22	$T_{fb9c(A)}$	13.45	13.15
	Web	$T_{wb10(B)}$	9.41		$T_{wb10(A)}$	9.46	
		$T_{wb11(B)}$	9.84		$T_{wb11(A)}$	9.65	
		$T_{wb12(B)}$	9.82		$T_{wb12(A)}$	10.03	

Figure D.19: Imperfections within the beam section - Test 5

Dimensions in mm	Reference	Beam web profile (533x210x82UB)					
		Connection B			Connection A		
		⑦	⑧	⑨	⑦	⑧	⑨
	$\delta_{1(B)}$	2.00	2.0	2.0			
	$\delta_{2(B)}$	100.5	100.5	100.5			
	$\delta_{3(B)}$	101.0	101.5	101.5			
	$\delta_{4(B)}$	102.5	103.0	103.0			
	$\delta_{5(B)}$	2.0	2.5	2.5			
	$\delta_{1(A)}$				1.5	1.5	1.5
	$\delta_{2(A)}$				100.0	100.0	100.0
	$\delta_{3(A)}$				100.5	100.5	100.5
	$\delta_{4(A)}$				101.5	101.5	101.5
	$\delta_{5(A)}$				2.5	2.0	2.0

Figure D.20: Imperfections within the beam web profile - Test 5

			Universal column 254x254x73		
	Reference	Location	Front	Middle	Back
Depth of section (mm)	D_{cb}	①			256.0
		②			258.0
		③			256.5
	D_{cm}	①		256.0	
		②		N/A	
		③		256.0	
	D_{cf}	①	258.0		
		②	258.0		
		③	256.5		
Width of section (mm)	$W_{c(B)}$	①	Connection B 252.5		Connection A
		②	253.0		
		③	252.0		
	$W_{c(A)}$	①			253.0
		②			254.0
		③			253.0
Thickness (mm) Flange	$T_{fc1(B)}$		13.46		13.35
	$T_{fc2(B)}$		13.52		13.40
	$T_{fc3(B)}$		13.56		13.50
	$T_{fc1(A)}$		13.70		13.09
	$T_{fc2(A)}$		13.70		13.17
	$T_{fc3(A)}$		13.80		13.14
Thickness (mm) web	$T_{wc(B)}$	①	8.35		
		③	8.50		
	T_{wcm}	①	8.45		
		③	8.45		
	$T_{wc(A)}$	①	8.40		
		③	8.50		

Figure D.21: Imperfections within the column section - Test 5